DESIGN of Concrete Structures

Fourteenth Edition in SI Units

Arthur H. Nilson • David Darwin • Charles W. Dolan

DESIGN *of* Concrete Structures

Fourteenth Edition in SI Units

Arthur H. Nilson

Professor Emeritus
College of Engineering
Cornell University

David Darwin

Deane E. Ackers Distinguished Professor
of Civil, Environmental & Architectural Engineering
University of Kansas

Charles W. Dolan

H. T. Person Professor of Engineering
University of Wyoming

Mc Graw Hill

Singapore • Boston • Burr Ridge, IL • Dubuque, IA • Madison, WI • New York • San Francisco
St. Louis • Bangkok • Kuala Lumpur • Lisbon • London • Madrid • Mexico City • Milan
Montreal • New Delhi • Seoul • Sydney • Taipei • Toronto

The McGraw·Hill Companies

Mc Graw Hill Higher Education

DESIGN OF CONCRETE STRUCTURES
Fourteenth Edition in SI Units

Published by McGraw-Hill, a business unit of The McGraw-Hill Companies, Inc., 1221 Avenue of the Americas, New York, NY 10020. Copyright © 2010 by The McGraw-Hill Companies, Inc. All rights reserved. Previous editions © 2004, 1997, and 1991. No part of this publication may be reproduced or distributed in any form or by any means, or stored in a database or retrieval system, without the prior written consent of The McGraw-Hill Companies, Inc., including, but not limited to, in any network or other electronic storage or transmission, or broadcast for distance learning.

Exclusive rights by McGraw-Hill Education (Asia) for adaptation, manufacture, and export. This book cannot be re-exported from the country to which it is sold by McGraw-Hill.

Some ancillaries, including electronic and print components, may not be available to customers outside the United States.

Cover images © iStockphoto.com and Dreamstime.com

10 9 8 7 6 5 4 3 2 1
CTP COS
20 13 12 11

When ordering this title, use **ISBN 978-007-131139-7** or **MHID 007-131139-4**

Printed in Singapore

About the Authors

Arthur H. Nilson was engaged in research, teaching, and consulting relating to structural concrete for over 40 years. He has been a member of the faculty of the College of Engineering at Cornell University since 1956, in charge of undergraduate and graduate courses in the design of reinforced concrete and prestressed concrete structures until his retirement in 1991. He served as Chairman of the Department of Structural Engineering from 1978 to 1985. Dr. Nilson has served on many professional committees, including Building Code Subcommittee 318-D of the American Concrete Institute (ACI). His pioneering work on high-strength concrete has been widely recognized. He was awarded the ACI Wason Medal for materials research in 1974, the ACI Wason Medal for best technical paper in 1986 and 1987, and the ACI Structural Research Award in 1993. Professor Nilson is an Honorary Member of ACI and a Fellow in the American Society of Civil Engineers (ASCE). He has been honored by the civil engineering student body at Cornell for outstanding teaching. He was elected Professor Emeritus in 1991. He has held research appointments or lectureships at the University of Manchester, Salford University, and the Technical University of Milan. He is a registered professional engineer in several states and, prior to entering teaching, was engaged in full-time professional practice. He received the B.S. degree from Stanford University in 1948, the M.S. from Cornell in 1956, and the Ph.D. from the University of California at Berkeley in 1967.

David Darwin has been a member of the faculty at the University of Kansas since 1974 and has been director of the Structural Engineering and Materials Laboratory since 1982. He was appointed the Deane E. Ackers Distinguished Professor of Civil Engineering in 1990. Dr. Darwin served as President of the American Concrete Institute in 2007–2008 and is a member and past chair of ACI Committees 224 on Cracking and 408 on Bond and Development of Reinforcement. He is also a member of ACI Building Code Subcommittee 318-B on Reinforcement and Development and of ACI-ASCE Committee 445 on Shear and Torsion. Dr. Darwin is an acknowledged expert on concrete crack control and bond between steel reinforcement and concrete. He received the ACI Arthur R. Anderson Award in 1992 for his research efforts in plain and reinforced concrete, the ACI Structural Research Award in 1996, and the ACI Joe W. Kelly Award in 2005 for his contributions to teaching and design. He has also received a number of awards from the American Society of Civil Engineers, including the Walter L. Huber Civil Engineering Research Prize in 1985; the Moisseiff Award in 1991; the State-of-the-Art of Civil Engineering Award in 1996 and 2000; the Richard R. Torrens Award in 1997; and the Dennis L. Tewksbury Award in 2008. He has been honored for his teaching by the civil engineering students at the University of Kansas. He is past editor of the ASCE *Journal of Structural Engineering*. Professor Darwin is a Fellow of ACI and ASCE. He is a licensed professional engineer and serves as a consultant in the fields of concrete materials and structures. He was honored with the Distinguished Alumnus Award from the University of Illinois Civil and Environmental Engineering Alumni Association in 2003. Between his M.S. and Ph.D. degrees, he served four years with the U.S. Army Corps of Engineers. He received the B.S. and M.S. degrees from Cornell University in 1967 and 1968 and the Ph.D. from the University of Illinois at Urbana-Champaign in 1974.

Charles W. Dolan has been on the faculty at the University of Wyoming since 1991, serving as Department Head from 1998 to 2001. He was appointed the H. T. Person Professor of Engineering in 2002. He is currently chair of Building Code Subcommittee 318-R of the American Concrete Institute. He has served as chair of the Technical Activities Committee, of ACI Committee 358 on Transit Guideways, and of ACI-ASCE Committee 423 on Prestressed Concrete. In private design practice for nearly 20 years, he was the project engineer on the Walt Disney World Monorail, the Detroit Downtown Peoplemover guideway, and the Dallas–Fort Worth Airport transit system guideway and is responsible for the conceptual design of the Dubai Palm Island monorail. He received the T. Y. Lin Award from ASCE in 1973 for outstanding contributions to the field of prestressed concrete and the Arthur R. Anderson award from ACI in 2005 for advancements in the design of reinforced and prestressed concrete structures. A Fellow in ACI and the Prestressed Concrete Institute (PCI), he is an internationally recognized leader in the development of fiber reinforced polymers for concrete reinforcement. He is a registered professional engineer and a consultant in the design of structural concrete. He received the B.S. from the University of Massachusetts in 1965 and the M.S. and Ph.D. from Cornell University in 1967 and 1989.

Contents

About the Authors v

Preface xv

Chapter 1 **Introduction** **1**
1.1 Concrete, Reinforced Concrete, and Prestressed Concrete 1
1.2 Structural Forms 2
1.3 Loads 8
1.4 Serviceability, Strength, and Structural Safety 12
1.5 Design Basis 15
1.6 Design Codes and Specifications 16
1.7 Safety Provisions of the ACI Code 17
1.8 Fundamental Assumptions for Reinforced Concrete Behavior 19
1.9 Behavior of Members Subject to Axial Loads 20
References 26
Problems 27

Chapter 2 **Materials** **28**
2.1 Introduction 28
2.2 Cement 28
2.3 Aggregates 29
2.4 Proportioning and Mixing Concrete 31
2.5 Conveying, Placing, Compacting, and Curing 33
2.6 Quality Control 34
2.7 Admixtures 38
2.8 Properties in Compression 40
2.9 Properties in Tension 46
2.10 Strength under Combined Stress 48
2.11 Shrinkage and Temperature Effects 49
2.12 High-Strength Concrete 52
2.13 Reinforcing Steels for Concrete 54
2.14 Reinforcing Bars 55
2.15 Welded Wire Reinforcement 61
2.16 Prestressing Steels 61
References 63
Problems 65

Chapter 3 **Flexural Analysis and Design of Beams** **67**
3.1 Introduction 67
3.2 Bending of Homogeneous Beams 67
3.3 Reinforced Concrete Beam Behavior 69
3.4 Design of Tension-Reinforced Rectangular Beams 80
3.5 Design Aids 94
3.6 Practical Considerations in the Design of Beams 97
3.7 Rectangular Beams with Tension and Compression Reinforcement 99
3.8 T Beams 108
References 115
Problems 116

Chapter 4 **Shear and Diagonal Tension in Beams** **120**
4.1 Introduction 120
4.2 Diagonal Tension in Homogeneous Elastic Beams 121
4.3 Reinforced Concrete Beams without Shear Reinforcement 124
4.4 Reinforced Concrete Beams with Web Reinforcement 131
4.5 ACI Code Provisions for Shear Design 136
4.6 Effect of Axial Forces 145
4.7 Beams with Varying Depth 150
4.8 Alternative Models for Shear Analysis and Design 151
4.9 Shear-Friction Design Method 160
References 164
Problems 166

Chapter 5 **Bond, Anchorage, and Development Length** **168**
5.1 Fundamentals of Flexural Bond 168
5.2 Bond Strength and Development Length 172
5.3 ACI Code Provisions for Development of Tension Reinforcement 177
5.4 Anchorage of Tension Bars by Hooks 181
5.5 Anchorage in Tension Using Headed Bars 185
5.6 Anchorage Requirements for Web Reinforcement 189
5.7 Welded Wire Reinforcement 190
5.8 Development of Bars in Compression 191
5.9 Bundled Bars 191
5.10 Bar Cutoff and Bend Points in Beams 192
5.11 Structural Integrity Provisions 199
5.12 Integrated Beam Design Example 200
5.13 Bar Splices 204
References 207
Problems 208

Chapter 6 **Serviceability** **213**
6.1 Introduction 213
6.2 Cracking in Flexural Members 213

6.3 ACI Code Provisions for Crack Control 216
6.4 Control of Deflections 219
6.5 Immediate Deflections 220
6.6 Deflections Due to Long-Term Loads 223
6.7 ACI Code Provisions For Control of Deflections 226
6.8 Deflections Due to Shrinkage and Temperature Changes 232
6.9 Moment vs. Curvature for Reinforced Concrete Sections 234
References 238
Problems 238

Chapter 7 Analysis and Design for Torsion 241
7.1 Introduction 241
7.2 Torsion in Plain Concrete Members 242
7.3 Torsion in Reinforced Concrete Members 245
7.4 Torsion Plus Shear 249
7.5 ACI Code Provisions for Torsion Design 250
References 258
Problems 259

Chapter 8 Short Columns 262
8.1 Introduction: Axial Compression 262
8.2 Lateral Ties and Spirals 265
8.3 Compression Plus Bending of Rectangular Columns 269
8.4 Strain Compatibility Analysis and Interaction Diagrams 270
8.5 Balanced Failure 273
8.6 Distributed Reinforcement 276
8.7 Unsymmetrical Reinforcement 278
8.8 Circular Columns 279
8.9 ACI Code Provisions for Column Design 281
8.10 Design Aids 282
8.11 Biaxial Bending 285
8.12 Load Contour Method 287
8.13 Reciprocal Load Method 288
8.14 Computer Analysis for Biaxial Bending of Columns 291
8.15 Bar Splicing in Columns 292
8.16 Transmission of Column Loads Through Floor Systems 293
References 294
Problems 295

Chapter 9 Slender Columns 299
9.1 Introduction 299
9.2 Concentrically Loaded Columns 300
9.3 Compression Plus Bending 303
9.4 ACI Criteria for Slenderness Effects in Columns 309
9.5 ACI Criteria for Nonsway vs. Sway Structures 310

9.6 ACI Moment Magnifier Method for Nonsway Frames 312
9.7 ACI Moment Magnifier Method for Sway Frames 320
9.8 Second-Order Analysis for Slenderness Effects 325
References 327
Problems 328

Chapter 10 **Strut-and-Tie Models** **332**
10.1 Introduction 332
10.2 Development of Strut-and-Tie Models 332
10.3 Strut-and-Tie Design Methodology 336
10.4 ACI Provisions for Strut-and-Tie Models 342
10.5 Applications 347
References 356
Problems 356

Chapter 11 **Design of Reinforcement at Joints** **358**
11.1 Introduction 358
11.2 Beam-Column Joints 359
11.3 Strut-and-Tie Model for Joint Behavior 371
11.4 Beam-to-Girder Joints 373
11.5 Ledge Girders 374
11.6 Corners and T Joints 377
11.7 Brackets and Corbels 380
References 384
Problems 385

Chapter 12 **Analysis of Indeterminate Beams and Frames** **387**
12.1 Continuity 387
12.2 Loading 389
12.3 Simplifications in Frame Analysis 391
12.4 Methods for Elastic Analysis 393
12.5 Idealization of the Structure 394
12.6 Preliminary Design and Guidelines for Proportioning Members 399
12.7 Approximate Analysis 401
12.8 ACI Moment Coefficients 406
12.9 Limit Analysis 409
12.10 Conclusion 420
References 421
Problems 421

Chapter 13 **Analysis and Design of Slabs** **424**
13.1 Types of Slabs 424
13.2 Design of One-Way Slabs 426
13.3 Temperature and Shrinkage Reinforcement 429
13.4 Behavior of Two-Way Edge-Supported Slabs 432
13.5 Two-Way Column-Supported Slabs 436

13.6 Direct Design Method for Column-Supported Slabs 439
13.7 Flexural Reinforcement for Column-Supported Slabs 445
13.8 Depth Limitations of the ACI Code 447
13.9 Equivalent Frame Method 454
13.10 Shear Design in Flat Plates and Flat Slabs 462
13.11 Transfer of Moments at Columns 477
13.12 Openings in Slabs 480
13.13 Deflection Calculations 482
13.14 Analysis for Horizontal Loads 489
References 490
Problems 492

Chapter 14 **Yield Line Analysis for Slabs** **497**
14.1 Introduction 497
14.2 Upper and Lower Bound Theorems 500
14.3 Rules for Yield Lines 500
14.4 Analysis by Segment Equilibrium 504
14.5 Analysis by Virtual Work 506
14.6 Orthotropic Reinforcement and Skewed Yield Lines 511
14.7 Special Conditions at Edges and Corners 513
14.8 Fan Patterns at Concentrated Loads 515
14.9 Limitations of Yield Line Theory 516
References 517
Problems 517

Chapter 15 **Strip Method for Slabs** **522**
15.1 Introduction 522
15.2 Basic Principles 523
15.3 Choice of Load Distribution 524
15.4 Rectangular Slabs 527
15.5 Fixed Edges and Continuity 529
15.6 Unsupported Edges 534
15.7 Slabs with Holes 542
15.8 Advanced Strip Method 546
15.9 Comparisons of Methods for Slab Analysis and Design 554
References 555
Problems 555

Chapter 16 **Footings and Foundations** **559**
16.1 Types and Functions 559
16.2 Spread Footings 559
16.3 Design Factors 560
16.4 Loads, Bearing Pressures, and Footing Size 561
16.5 Wall Footings 563
16.6 Column Footings 565
16.7 Combined Footings 574
16.8 Two-Column Footings 575
16.9 Strip, Grid, and Mat Foundations 582

16.10 Pile Caps 584
References 587
Problems 587

Chapter 17 **Retaining Walls** **589**
17.1 Function and Types of Retaining Walls 589
17.2 Earth Pressure 589
17.3 Earth Pressure for Common Conditions of Loading 593
17.4 External Stability 594
17.5 Basis of Structural Design 597
17.6 Drainage and Other Details 598
17.7 Example: Design of a Gravity Retaining Wall 599
17.8 Example: Design of a Cantilever Retaining Wall 601
17.9 Counterfort Retaining Walls 608
17.10 Precast Retaining Walls 610
References 611
Problems 611

Chapter 18 **Concrete Building Systems** **613**
18.1 Introduction 613
18.2 Floor and Roof Systems 614
18.3 Panel, Curtain, and Bearing Walls 627
18.4 Shear Walls 628
18.5 Precast Concrete for Buildings 631
18.6 Engineering Drawings for Buildings 646
References 646

Chapter 19 **Prestressed Concrete** **648**
19.1 Introduction 648
19.2 Effects of Prestressing 649
19.3 Sources of Prestress Force 653
19.4 Prestressing Steels 656
19.5 Concrete for Prestressed Construction 658
19.6 Elastic Flexural Analysis 660
19.7 Flexural Strength 666
19.8 Partial Prestressing 670
19.9 Flexural Design Based on Concrete Stress Limits 672
19.10 Shape Selection 682
19.11 Tendon Profiles 683
19.12 Flexural Design Based on Load Balancing 685
19.13 Loss of Prestress 690
19.14 Shear, Diagonal Tension, and Web Reinforcement 694
19.15 Bond Stress, Transfer Length, and Development Length 701
19.16 Anchorage Zone Design 702
19.17 Deflection 706
19.18 Crack Control for Class C Flexural Members 710
References 710
Problems 711

Chapter 20 **Seismic Design** **714**
20.1 Introduction 714
20.2 Structural Response 716
20.3 Seismic Loading Criteria 721
20.4 ACI Provisions for Earthquake-Resistant Structures 726
20.5 ACI Provisions for Special Moment Frames 727
20.6 ACI Provisions for Special Structural Walls, Coupling Beams, Diaphragms, and Trusses 739
20.7 ACI Provisions for Shear Strength 742
20.8 ACI Provisions for Intermediate Moment Frames 747
References 749
Problems 749

Appendix A **Design Aids** **751**

Appendix B **SI Conversion Factors: Inch-Pound Units to SI Units** **785**

Index 787

Preface

The fourteenth edition of *Design of Concrete Structures* has the same dual objectives as the previous work: first to establish a firm understanding of the behavior of structural concrete, then to develop proficiency in the methods used in current design practice. To produce this SI Edition, the text has been updated in accordance with the provisions of the metric version of the 2008 American Concrete Institute (ACI) Building Code (ACI 318M-08).

It is generally recognized that mere training in special design skills and codified procedures is inadequate for successful professional practice. As new research becomes available and new design methods are continually introduced, these procedures are subject to frequent changes. To understand and keep abreast of these rapid developments and to engage safely in innovative design, the engineer needs a thorough grounding in the basic performance of concrete and steel as structural materials, and in the behavior of reinforced concrete members and structures. On the other hand, the main business of the structural engineer is to design structures safely, economically, and efficiently. Consequently, with this basic understanding as a firm foundation, familiarity with current design procedures is essential. This edition, like the preceding ones, addresses both needs.

The text not only presents the basic mechanics of structural concrete and methods for the design of individual members for bending, shear, torsion, and axial forces, but also provides much detail pertaining to applications in the various types of structural systems, including an extensive presentation of slabs, footings, foundations, and retaining walls. The important topic of joint design is included. The chapter on flexural design has been expanded to improve the presentation of both the basic material and the example problems, coverage of seismic design is updated, and an introduction to prestressed concrete is included, as in previous editions.

There have been a number of significant changes in the 2008 ACI Building Code, which governs design practice in most of the United States and serves as a model code in many other countries as well. Among these are a reorganization of the provisions for both slender column and earthquake design, the former with some simplification compared to earlier Codes and the latter with some important additions; and the addition of headed studs for use as shear reinforcement in two-way slabs and headed deformed bars as another option for use in anchoring reinforcement.

In addition to changes in the ACI Code, the text includes the modified compression field theory method of shear design as updated in the 2008 Interim Revisions to the American Association of State Highway and Transportation Officials (AASHTO) *LRFD Bridge Design Specifications*.

A feature of the text is the comprehensive presentation of all aspects of slab design. A chapter covering one-way and two-way edge-supported and column-supported slabs, including the new Code material on headed studs, is followed by chapters on slab analysis and design based on the theory of plasticity covering, respectively, the yield line method for analysis and the strip method for design of slabs, both particularly useful for innovative structures.

A special strength of the text is the analysis chapter, which includes load combinations for use in design, a description of envelope curves for moment and shear, guidelines for proportioning members under both gravity and lateral loads, and procedures for developing preliminary designs of reinforced concrete structures.

Most present-day design is carried out using computer programs, either general-purpose, commercially available software or individual programs written for special needs. Step-by-step procedures are given throughout the book to guide the student and engineer through the increasingly complex methodology of current design, with the emphasis on understanding the design process. Once mastered, these procedures are easily converted into flowcharts to aid in programming. References are given, where appropriate, to the more widely used commercial programs.

The text will be found suitable for either a one or two-semester course in the design of concrete structures. If the curriculum permits only a single course (probably taught in the fourth undergraduate year), the following will provide a good basis: the introduction and treatment of materials found in Chapters 1 and 2, respectively; the material on flexure, shear, and anchorage in Chapters 3, 4, and 5; Chapter 6 on serviceability; Chapter 8 on short columns; and the introduction to one and two-way slabs found in the first four sections of Chapter 13. Time may or may not permit classroom coverage of frame analysis or building systems, Chapters 12 and 18, but these could well be assigned as independent reading, concurrent with the earlier work of the course. In the authors' experience, such complementary outside reading tends to enhance student motivation.

The text is more than adequate for a second course, most likely taught in the first year of graduate study. The authors have found that this is an excellent opportunity to provide students with a more general understanding of reinforced concrete structural design, often beginning with Chapters 12 and 18 and followed by the increasingly important topics of torsion, Chapter 7; slender columns, Chapter 9; the strut-and-tie method, Chapter 10; and the design and detailing of joints, Chapter 11. It should also offer an opportunity for a much expanded study of slabs, including the remaining sections of Chapter 13, plus the methods for slab analysis and design based on plasticity theory found in Chapters 14 and 15, yield line analysis and the strip method of design. Other topics appropriate to a second course include foundations and retaining walls, Chapters 16 and 17, and the introduction to seismic design in Chapter 20. Prestressed concrete is sufficiently important to justify a separate course. If time constraints do not permit this, Chapter 19 provides an introduction and can be used as the text for a one-credit-hour course.

At the end of each chapter, the user will find extensive reference lists, which provide an entry into the literature for those wishing to increase their knowledge through independent study. The Instructor's Solutions Manual is available on a CD for professors.

The authors are especially pleased to provide our readers with a true SI Edition. While the text has always been available worldwide, the presentation has in the past been limited to inch-pound units, which are customary in the United States. Well aware of the lack of applicability of inch-pound units throughout the rest of the world, it has been a goal of the authors to develop a version of the text in SI units based on the metric version of the ACI Code, ACI 318M. With this volume, that goal has been achieved.

A brief historical note may be of interest. This book is the fourteenth edition of a textbook originated in 1923 by Leonard C. Urquhart and Charles E. O'Rourke, both professors of structural engineering at Cornell University at that time. Over its remarkable 86-year history, new editions have kept pace with research, improved materials, and new methods of analysis and design. The second, third, and fourth editions firmly established the work as a leading text for elementary courses in the subject area. Professor George Winter, also of Cornell, collaborated with Urquhart in preparing the fifth and sixth editions. Winter and the present senior author were responsible for the seventh, eighth, and ninth editions, which substantially expanded both the scope and the depth of the presentation. The tenth, eleventh, and twelfth editions were prepared by Professor Nilson subsequent to Professor Winter's passing in 1982, the latter with Professor David Darwin of the University of Kansas serving as a contributor.

Professors Nilson and Darwin were joined by Professor Charles Dolan of the University of Wyoming beginning with the thirteenth edition. All three have been deeply involved in research and teaching in the fields of reinforced and prestressed concrete, as well as professional Code-writing committees, and have spent significant time in professional practice, invaluable in developing the perspective and structural judgement that sets this book apart.

Special thanks are due to reviewers and former students for their many helpful comments and suggestions for this and previous editions. In particular, the authors would like to thank the following reviewers: Paul Barr, Utah State University; Robert N. Emerson, Oklahoma State University; A. Fafitis, Arizona State University; R. Craig Henderson, Tennessee Technological University; Max Porter, Iowa State University; Pizhong Qiao, The University of Akron; Aziz Saber, Louisiana Tech University; and Eric Steinberg, Ohio University. Thanks are also due to the McGraw-Hill project team, notably Debra Hash, Sponsoring Editor; Lorraine Buczek, Developmental Editor; and Melissa Leick, Project Manager.

We gladly acknowledge our indebtedness to the original authors. Although it is safe to say that neither Urquhart nor O'Rourke would recognize very much of the detail, the approach to the subject and the educational philosophy that did so much to account for the success of the early editions would be familiar. We acknowledge with particular gratitude the influence of Professor George Winter in developing a point of view that has shaped the work in the chapters that follow.

Arthur H. Nilson
David Darwin
Charles W. Dolan

SUPPLEMENTS

Instructors using this fourteenth SI edition can obtain the Solutions Manual on an Instructor's Resource CD-ROM. Please contact your local sales representative for more information. For instructors using the U.S. edition, they can access the related Solutions Manual at http://highered.mcgraw-hill.com/sites/0073293490/.

DESIGN *of* Concrete Structures

1 Introduction

1.1 CONCRETE, REINFORCED CONCRETE, AND PRESTRESSED CONCRETE

Concrete is a stonelike material obtained by permitting a carefully proportioned mixture of cement, sand and gravel or other aggregate, and water to harden in forms of the shape and dimensions of the desired structure. The bulk of the material consists of fine and coarse aggregate. Cement and water interact chemically to bind the aggregate particles into a solid mass. Additional water, over and above that needed for this chemical reaction, is necessary to give the mixture the workability that enables it to fill the forms and surround the embedded reinforcing steel prior to hardening. Concretes with a wide range of properties can be obtained by appropriate adjustment of the proportions of the constituent materials. Special cements (such as high early strength cements), special aggregates (such as various lightweight or heavyweight aggregates), admixtures (such as plasticizers, air-entraining agents, silica fume, and fly ash), and special curing methods (such as steam-curing) permit an even wider variety of properties to be obtained.

These properties depend to a very substantial degree on the proportions of the mix, on the thoroughness with which the various constituents are intermixed, and on the conditions of humidity and temperature in which the mix is maintained from the moment it is placed in the forms until it is fully hardened. The process of controlling conditions after placement is known as *curing*. To protect against the unintentional production of substandard concrete, a high degree of skillful control and supervision is necessary throughout the process, from the proportioning by weight of the individual components, through mixing and placing, until the completion of curing.

The factors that make concrete a universal building material are so pronounced that it has been used, in more primitive kinds and ways than at present, for thousands of years, starting with lime mortars from 12,000 to 6000 BCE in Crete, Cyprus, Greece, and the Middle East. The facility with which, while plastic, it can be deposited and made to fill forms or molds of almost any practical shape is one of these factors. Its high fire and weather resistance is an evident advantage. Most of the constituent materials, with the exception of cement and additives, are usually available at low cost locally or at small distances from the construction site. Its compressive strength, like that of natural stones, is high, which makes it suitable for members primarily subject to compression, such as columns and arches. On the other hand, again as in natural stones, it is a relatively brittle material whose tensile strength is small compared with its compressive strength. This prevents its economical use in structural members that are subject to tension either entirely (such as in tie-rods) or over part of their cross sections (such as in beams or other flexural members).

To offset this limitation, it was found possible, in the second half of the nineteenth century, to use steel with its high tensile strength to reinforce concrete, chiefly in those places where its low tensile strength would limit the carrying capacity of the member. The reinforcement, usually round steel rods with appropriate surface deformations to provide interlocking, is placed in the forms in advance of the concrete. When completely surrounded by the hardened concrete mass, it forms an integral part of the member. The resulting combination of two materials, known as *reinforced concrete,* combines many of the advantages of each: the relatively low cost, good weather and fire resistance, good compressive strength, and excellent formability of concrete and the high tensile strength and much greater ductility and toughness of steel. It is this combination that allows the almost unlimited range of uses and possibilities of reinforced concrete in the construction of buildings, bridges, dams, tanks, reservoirs, and a host of other structures.

In more recent times, it has been found possible to produce steels, at relatively low cost, whose yield strength is 3 to 4 times and more that of ordinary reinforcing steels. Likewise, it is possible to produce concrete 4 to 5 times as strong in compression as the more ordinary concretes. These high-strength materials offer many advantages, including smaller member cross sections, reduced dead load, and longer spans. However, there are limits to the strengths of the constituent materials beyond which certain problems arise. To be sure, the strength of such a member would increase roughly in proportion to those of the materials. However, the high strains that result from the high stresses that would otherwise be permissible would lead to large deformations and consequently large deflections of such members under ordinary loading conditions. Equally important, the large strains in such high-strength reinforcing steel would induce large cracks in the surrounding low tensile strength concrete, cracks that not only would be unsightly but also could significantly reduce the durability of the structure. This limits the useful yield strength of high-strength reinforcing steel to 550 MPa according to many codes and specifications; 420 MPa steel is most commonly used.

A special way has been found, however, to use steels and concretes of very high strength in combination. This type of construction is known as *prestressed concrete.* The steel, in the form of wires, strands, or bars, is embedded in the concrete under high tension that is held in equilibrium by compressive stresses in the concrete after hardening. Because of this precompression, the concrete in a flexural member will crack on the tension side at a much larger load than when not so precompressed. Prestressing greatly reduces both the deflections and the tensile cracks at ordinary loads in such structures, and thereby enables these high-strength materials to be used effectively. Prestressed concrete has extended, to a very significant extent, the range of spans of structural concrete and the types of structures for which it is suited.

1.2 STRUCTURAL FORMS

The figures that follow show some of the principal structural forms of reinforced concrete. Pertinent design methods for many of them are discussed later in this volume.

Floor support systems for buildings include the monolithic slab-and-beam floor shown in Fig. 1.1, the one-way joist system of Fig. 1.2, and the flat plate floor, without beams or girders, shown in Fig. 1.3. The flat slab floor of Fig. 1.4, frequently used for more heavily loaded buildings such as warehouses, is similar to the flat plate floor, but makes use of increased slab thickness in the vicinity of the columns, as well

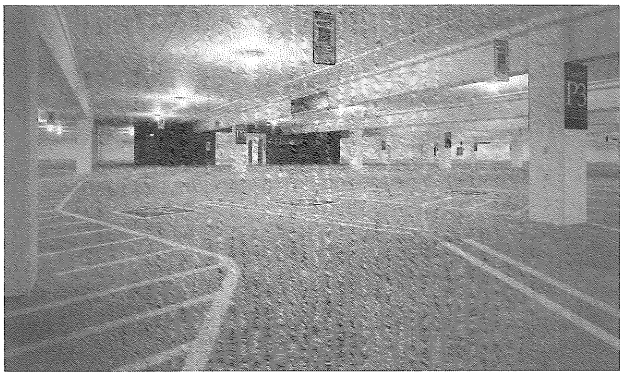

FIGURE 1.1
One-way reinforced concrete floor slab with monolithic supporting beams. (*Portland Cement Association.*)

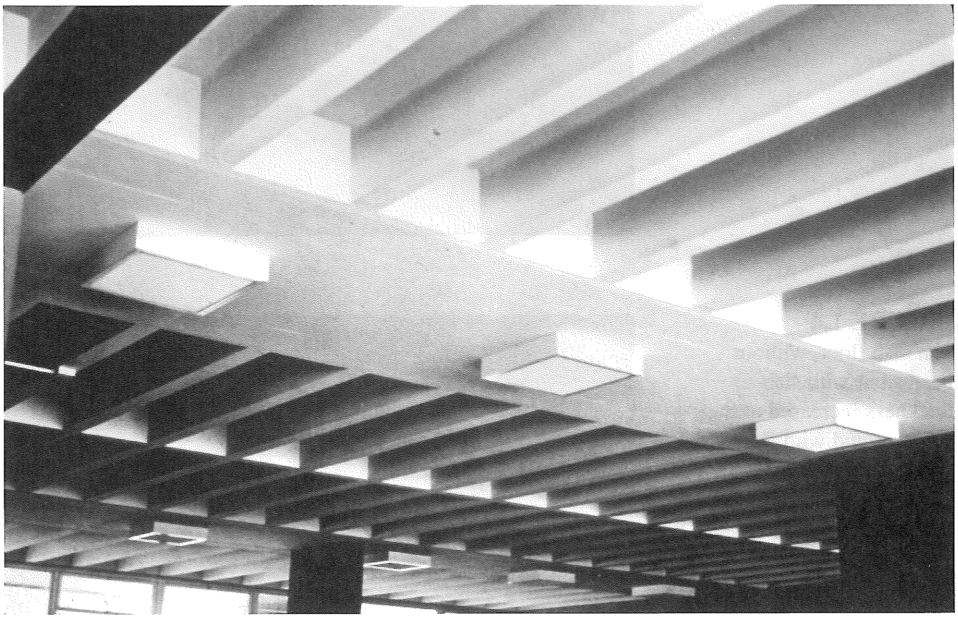

FIGURE 1.2
One-way joist floor system, with closely spaced ribs supported by monolithic concrete beams; transverse ribs provide for lateral distribution of localized loads. (*Portland Cement Association.*)

as flared column tops, to reduce stresses and increase strength in the support region. The choice among these and other systems for floors and roofs depends upon functional requirements, loads, spans, and permissible member depths, as well as on cost and esthetic factors.

Where long clear spans are required for roofs, concrete shells permit use of extremely thin surfaces, often thinner, relatively, than an eggshell. The folded plate roof of Fig. 1.5 is simple to form because it is composed of flat surfaces; such roofs have been employed for spans of 60 m and more. The cylindrical shell of Fig. 1.6 is also relatively easy to form because it has only a single curvature; it is similar to the folded plate in its structural behavior and range of spans and loads. Shells of this type were once quite popular in the United States and remain popular in other parts of the world.

Doubly curved shell surfaces may be generated by simple mathematical curves such as circular arcs, parabolas, and hyperbolas, or they may be composed of complex combinations of shapes. The hyperbolic paraboloid shape, defined by a concave downward parabola moving along a concave upward parabolic path, has been widely

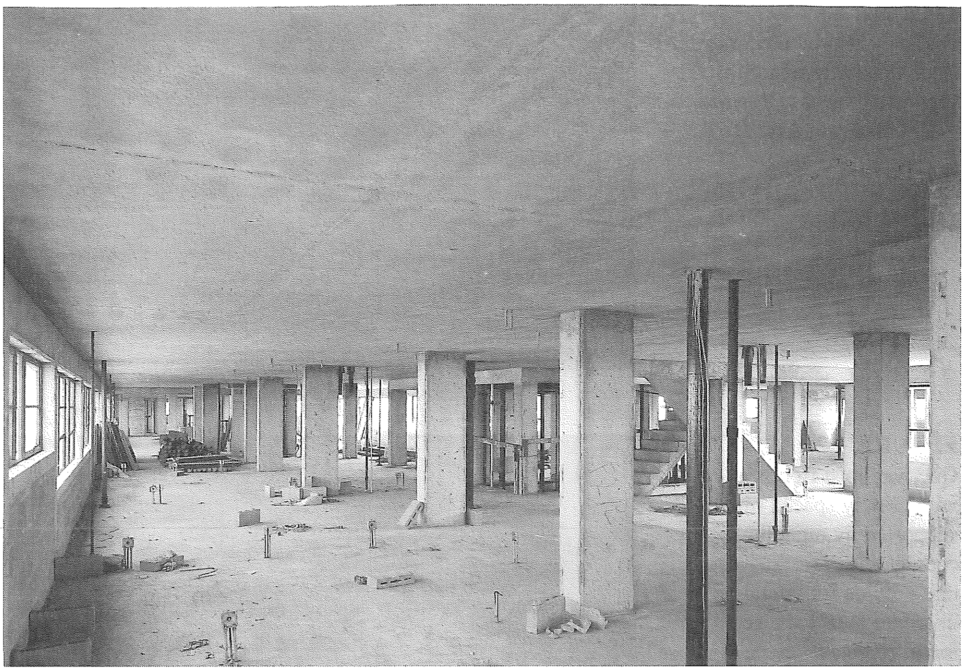

FIGURE 1.3
Flat plate floor slab, carried directly by columns without beams or girders. (*Portland Cement Association.*)

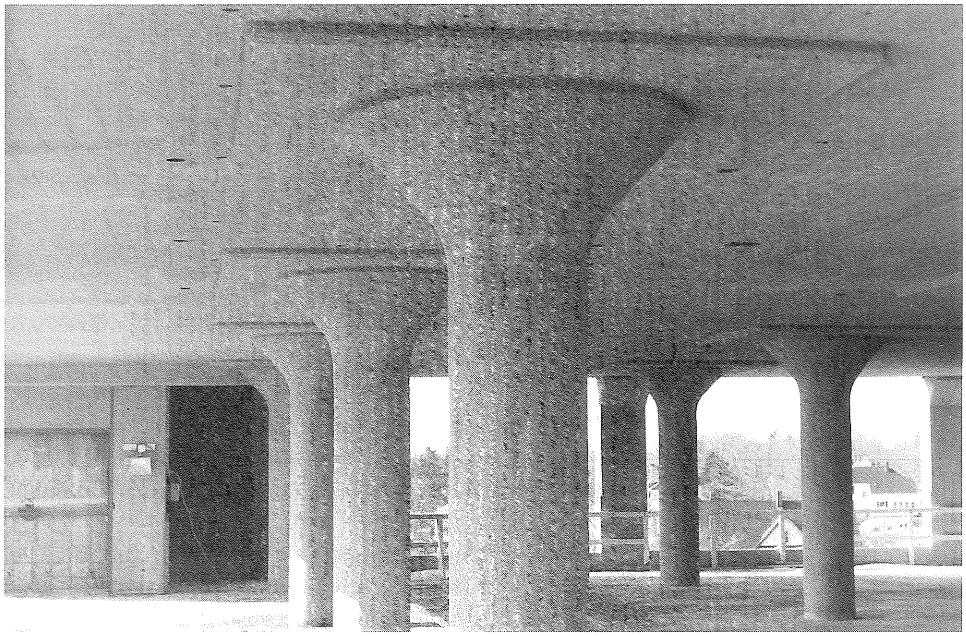

FIGURE 1.4
Flat slab floor, without beams but with slab thickness increased at the columns and with flared column tops to provide for local concentration of forces. (*University of Southern Maine.*)

used. It has the interesting property that the doubly curved surface contains two systems of straight-line generators, permitting straight-form lumber to be used. The complex dome of Fig. 1.7, which provides shelter for performing arts events, consists essentially of a circular dome but includes monolithic, upwardly curved edge surfaces to provide stiffening and strengthening in that critical region.

FIGURE 1.5
Folded plate roof of 38 m span that, in addition to carrying ordinary roof loads, carries the second floor as well from a system of cable hangers; the ground floor is kept free of columns.

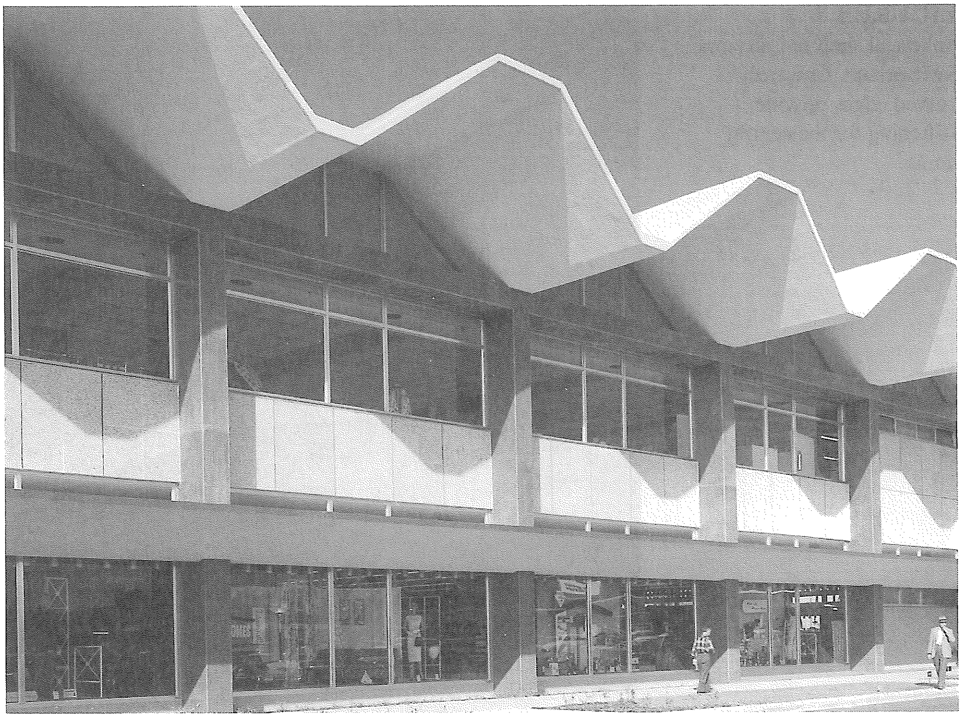

FIGURE 1.6
Cylindrical shell roof providing column-free interior space.

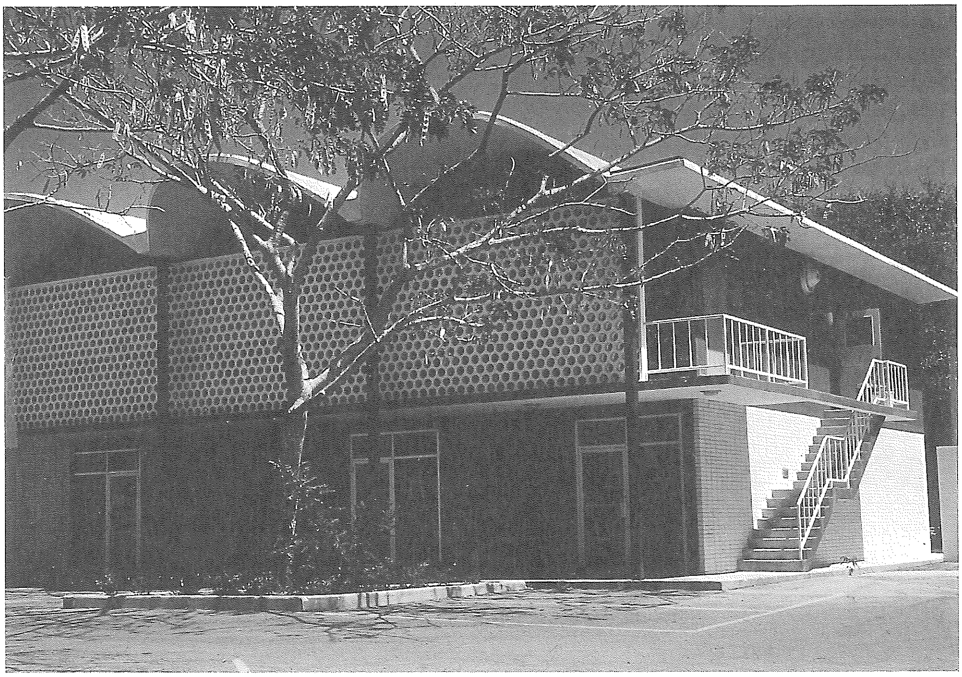

Bridge design has provided the opportunity for some of the most challenging and creative applications of structural engineering. The award-winning Napoleon Bonaparte Broward Bridge, shown in Fig. 1.8, is a six-lane, cable-stayed structure that spans St. John's River at Dame Point, Jacksonville, Florida. Its 396 m center span is the

FIGURE 1.7
Spherical shell in Lausanne, Switzerland. Upwardly curved edges provide stiffening for the central dome.

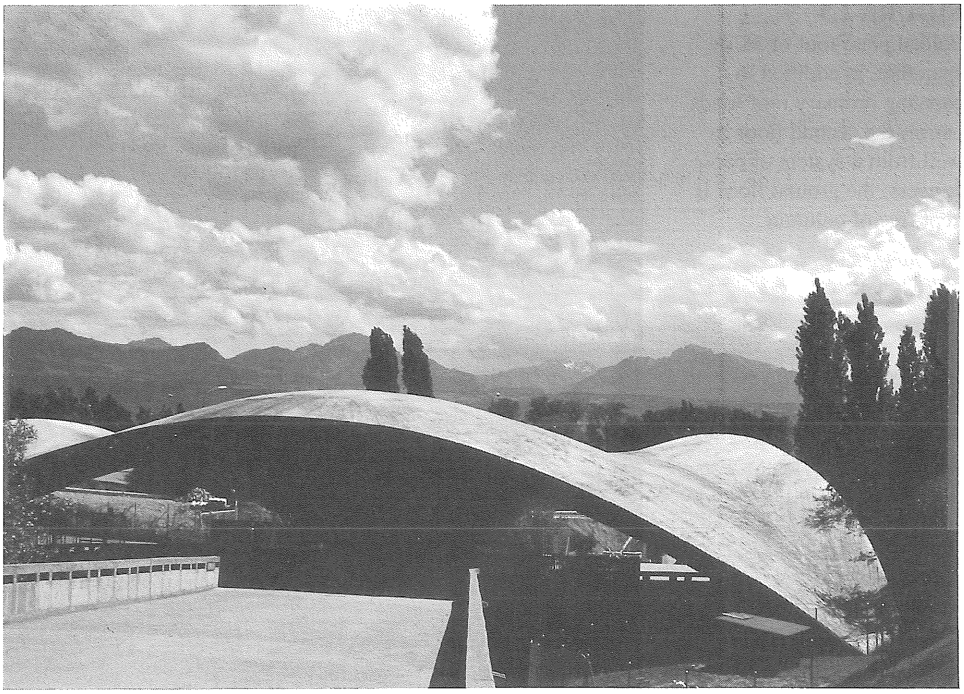

FIGURE 1.8
Napoleon Bonaparte Broward Bridge, with a 396 m center span at Dame Point, Jacksonville, Florida. *(HNTB Corporation, Kansas City, Missouri.)*

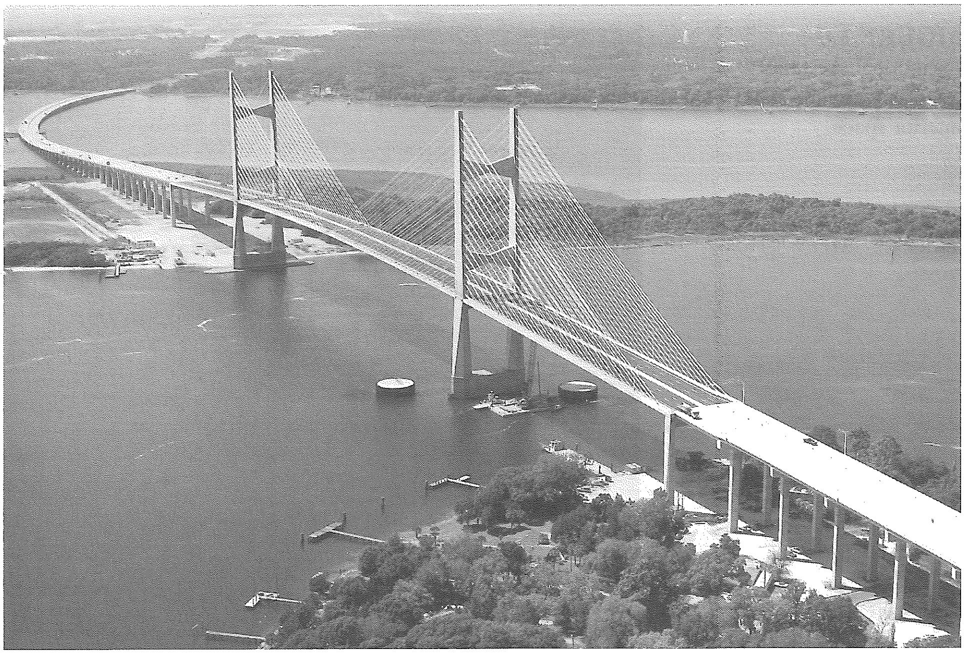

second longest of its type in the western hemisphere. Figure 1.9 shows the Bennett Bay Centennial Bridge, a four-span continuous, segmentally cast-in-place box girder structure. Special attention was given to esthetics in this award-winning design. The spectacular Natchez Trace Parkway Bridge in Fig. 1.10, a two-span arch structure using hollow precast concrete elements, carries a two-lane highway 47 m above the valley

FIGURE 1.9
Bennett Bay Centennial Bridge, Coeur d'Alene, Idaho, a four-span continuous concrete box girder structure of length 527 m. (*HNTB Corporation, Kansas City, Missouri.*)

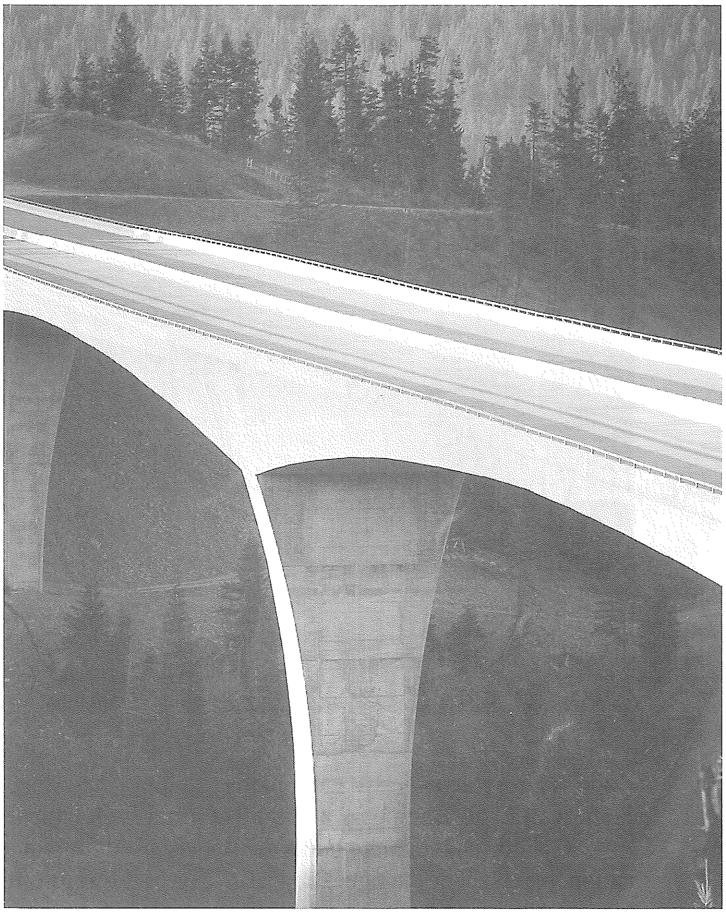

FIGURE 1.10
Natchez Trace Parkway Bridge near Franklin, Tennessee, an award-winning two-span concrete arch structure rising 47 m above the valley floor. (*Figg Engineering Group, Tallahassee, Florida.*)

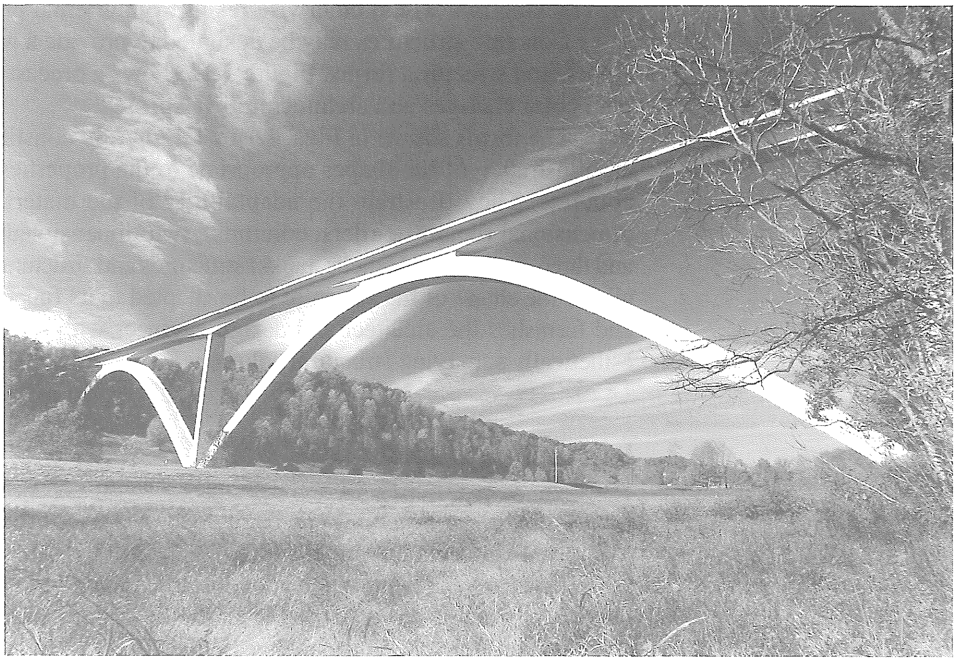

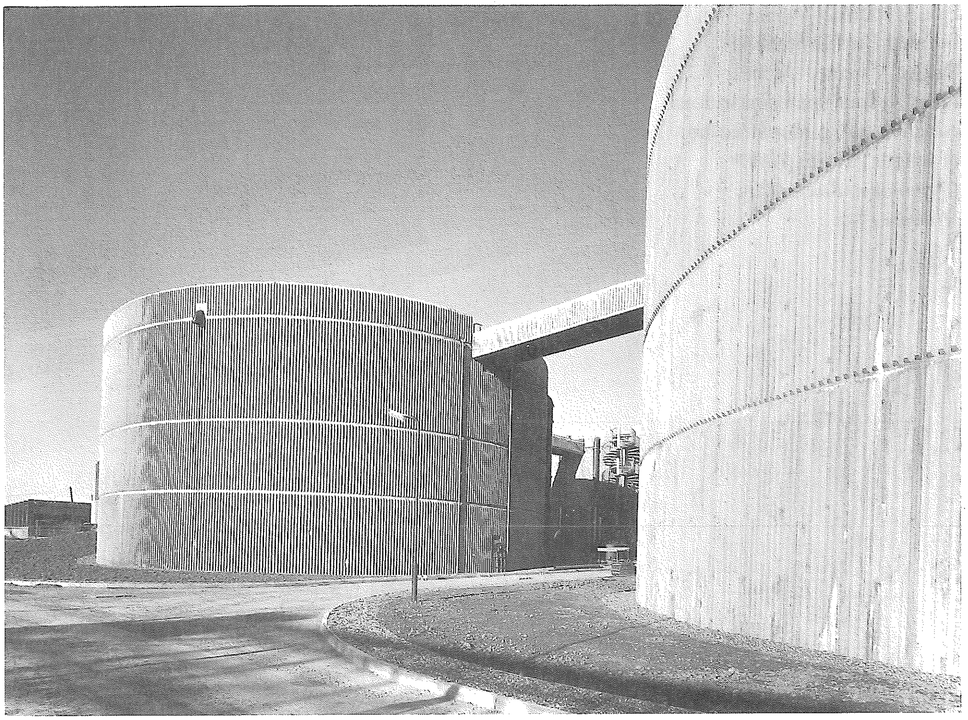

FIGURE 1.11
Circular concrete tanks used as a part of the wastewater purification facility at Howden, England. (*Northumbrian Water Authority with Luder and Jones, Architects.*)

floor. This structure has won many honors, including awards from the American Society of Civil Engineers and the National Endowment for the Arts.

Cylindrical concrete tanks are widely used for storage of water or in waste purification plants. The design shown in Fig. 1.11 is proof that a sanitary engineering facility can be esthetically pleasing as well as functional. Cylindrical tanks are often prestressed circumferentially to maintain compression in the concrete and eliminate the cracking that would otherwise result from internal pressure.

Concrete structures may be designed to provide a wide array of surface textures, colors, and structural forms. Figure 1.12 shows a precast concrete building containing both color changes and architectural finishes.

The forms shown in Figs. 1.1 to 1.12 hardly constitute a complete inventory but are illustrative of the shapes appropriate to the properties of reinforced or prestressed concrete. They illustrate the adaptability of the material to a great variety of one-dimensional (beams, girders, columns), two-dimensional (slabs, arches, rigid frames), and three-dimensional (shells, tanks) structures and structural components. This variability allows the shape of the structure to be adapted to its function in an economical manner, and furnishes the architect and design engineer with a wide variety of possibilities for esthetically satisfying structural solutions.

1.3 LOADS

Loads that act on structures can be divided into three broad categories: dead loads, live loads, and environmental loads.

Dead loads are those that are constant in magnitude and fixed in location throughout the lifetime of the structure. Usually the major part of the dead load is the weight of the structure itself. This can be calculated with good accuracy from the design configuration, dimensions of the structure, and density of the material. For buildings, floor

FIGURE 1.12
Concrete structures can be produced in a wide range of colors, finishes, and architectural detailing.
(*Courtesy of Rocky Mountain Prestress Corp.*)

fill, finish floors, and plastered ceilings are usually included as dead loads, and an allowance is made for suspended loads such as piping and lighting fixtures. For bridges, dead loads may include wearing surfaces, sidewalks, and curbs, and an allowance is made for piping and other suspended loads.

Live loads consist chiefly of occupancy loads in buildings and traffic loads on bridges. They may be either fully or partially in place or not present at all, and may also change in location. Their magnitude and distribution at any given time are uncertain, and even their maximum intensities throughout the lifetime of the structure are not known with precision. The minimum live loads for which the floors and roof of a building should be designed are usually specified in the building code that governs at the site of construction. Representative values of minimum live loads to be used in a wide variety of buildings are found in *Minimum Design Loads for Buildings and Other Structures* (Ref. 1.1), a portion of which is reprinted in Table 1.1. The table gives uniformly distributed live loads for various types of occupancies; these include impact provisions where necessary. These loads are expected maxima and considerably exceed average values.

In addition to these uniformly distributed loads, it is recommended that, as an alternative to the uniform load, floors be designed to support safely certain concentrated loads if these produce a greater stress. For example, according to Ref. 1.1, office floors are to be designed to carry a load of 9 kN distributed over an area 0.75 m square ($0.56\ m^2$), to allow for the weight of a safe or other heavy equipment, and stair treads must safely support a 1.33 kN load applied on the center of the tread. Certain reductions are often permitted in live loads for members supporting large areas, on the premise that it is not likely that the entire area would be fully loaded at one time (Refs. 1.1 and 1.2).

TABLE 1.1
Minimum uniformly distributed live loads

Occupancy or Use	Live Load, kN/m^2	Occupancy or Use	Live Load, kN/m^2
Apartments (see residential)		Dining rooms and restaurants	4.8
Access floor systems		Dwellings (see residential)	
Office use	2.4	Fire escapes	4.8
Computer use	4.8	On single-family dwellings only	1.9
Armories and drill rooms	7.2	Garages (passenger cars only)	1.9
Assembly areas and theaters		Trucks and buses[a]	
Fixed seats (fastened to floor)	2.9	Grandstands (see stadium and arena bleachers)	
Lobbies	4.8	Gymnasiums, main floors and balconies[b]	4.8
Movable seats	4.8	Hospitals	
Platforms (assembly)	4.8	Operating rooms, laboratories	2.9
Stage floors	7.2	Patient rooms	1.9
Balconies (exterior)	4.8	Corridors above first floor	3.8
On one and two-family residences only, and not exceeding 9.3 m^2	2.9	Hotels (see residential)	
		Libraries	
Bowling alleys, poolrooms, and similar recreational areas	3.6	Reading rooms	2.9
		Stack rooms[c]	7.2
Catwalks for maintenance access	1.9	Corridors above first floor	3.8
Corridors		Manufacturing	
First floor	4.8	Light	6.0
Other floors, same as occupancy served except as indicated		Heavy	12.0
		Marquees and canopies	3.6
Dance halls and ballrooms	4.8	Office buildings	
Decks (patio and roof)		File and computer rooms shall be designed for heavier loads based on anticipated occupancy	
Same as area served, or for the type of occupancy accommodated		Lobbies and first-floor corridors	4.8

(*continued*)

Tabulated live loads cannot always be used. The type of occupancy should be considered and the probable loads computed as accurately as possible. Warehouses for heavy storage may be designed for loads as high as 24 kN/m^2 or more; unusually heavy operations in manufacturing buildings may require an increase in the 12 kN/m^2 value specified in Table 1.1; special provisions must be made for all definitely located heavy concentrated loads.

Live loads for highway bridges are specified by the American Association of State Highway and Transportation Officials (AASHTO) in its *LRFD Bridge Design Specifications* (Ref. 1.3). For railway bridges, the American Railway Engineering and Maintenance-of-Way Association (AREMA) has published the *Manual of Railway Engineering* (Ref. 1.4), which specifies traffic loads.

Environmental loads consist mainly of snow loads, wind pressure and suction, earthquake loads (i.e., inertia forces caused by earthquake motions), soil pressures on subsurface portions of structures, loads from possible ponding of rainwater on flat surfaces, and forces caused by temperature differentials. Like live loads, environmental loads at any given time are uncertain in both magnitude and distribution. Reference 1.1 contains much information on environmental loads, which is often modified locally depending, for instance, on local climatic or seismic conditions.

Figure 1.13, from the 1972 edition of Ref. 1.1, gives snow loads for the continental United States and is included here for illustration only. The 2005 edition

TABLE 1.1
(Continued)

Occupancy or Use	Live Load, kN/m^2
Offices	2.4
Corridors above first floor	3.8
Penal institutions	
Cell blocks	1.9
Corridors	4.8
Residential	
Dwellings (one and two-family)	
Uninhabitable attics without storage	0.5
Uninhabitable attics with storage	1.0
Habitable attics and sleeping areas	1.4
All other areas except stairs and balconies	1.9
Hotels and multifamily houses	
Private rooms and corridors serving them	1.9
Public rooms and corridors serving them	4.8
Reviewing stands, grandstands, and bleachers[b]	
Roofs	
Ordinary flat, pitched, and curved roofs	1.0
Roofs used for promenade purposes	2.9
Roofs used for roof gardens or assembly purpose	4.8
Roofs used for other special purposes[e]	
Awnings and canopies	
Fabric construction supported by a lightweight rigid skeleton structure[f]	0.25
All other construction	1.0

Occupancy or Use	Live Load, kN/m^2
Schools	
Classrooms	1.9
Corridors above first floor	3.8
First-floor corridors	4.8
Sidewalks, vehicular driveways, and yards subject to trucking[d]	12.0
Stadiums and arenas	
Bleachers[b]	4.8
Fixed seats (fastened to floor)[b]	2.9
Stairs and exit ways	4.8
One and two-family residences only	1.9
Storage areas above ceilings	1.0
Storage warehouses (shall be designed for heavier loads if required for anticipated storage)	
Light	6.0
Heavy	12.0
Stores	
Retail	
First floor	4.8
Upper floors	3.6
Wholesale, all floors	6.0
Walkways and elevated platforms (other than exitways)	2.9
Yards and terraces, pedestrians	4.8

[a] Garages accommodating trucks and buses shall be designed in accordance with an approved method that contains provisions for truck and bus loadings.

[b] In addition to the vertical live loads, the design shall include horizontal swaying forces applied to each row of seats as follows: 350 N per linear m of seat applied in the direction parallel to each row of seats and 146 N per linear m of seat applied in the direction perpendicular to each row of seats. The parallel and perpendicular horizontal swaying forces need not be applied simultaneously.

[c] The loading applies to stack room floors that support nonmobile, double-faced library bookstacks subject to the following limitations: (a) The nominal bookstack unit height shall not exceed 2.3 m; (b) the nominal shelf depth shall not exceed 0.3 m for each face; and (c) parallel rows of double-faced bookstacks shall be separated by aisles not less than 0.9 m wide.

[d] Other uniform loads in accordance with an approved method that contains provisions for truck loadings shall also be considered where appropriate.

[e] Roofs used for other special purposes shall be designed for appropriate loads as approved by the authority having jurisdiction.

[f] Nonreducible.

Source: From Ref. 1.1. Used by permission of the American Society of Civil Engineers.

of Ref. 1.1 gives much more detailed information. In either case, specified values represent not average values, but expected upper limits. A minimum roof load of 1.0 kN/m^2 is often specified to provide for construction and repair loads and to ensure reasonable stiffness.

Much progress has been made in developing rational methods for predicting horizontal forces on structures due to wind and seismic action. Reference 1.1 summarizes current thinking regarding wind forces and has much information pertaining to earthquake loads as well. Reference 1.5 presents detailed recommendations for lateral forces from earthquakes.

Reference 1.1 specifies design wind pressures per square foot of vertical wall surface. Depending upon locality, these equivalent static forces vary from about 0.5 to 2.4 kN/m^2.

FIGURE 1.13
Snow load in kN/m^2 on the ground, 50-year mean recurrence interval. (*From* Minimum Design Loads for Buildings and Other Structures, *ANSI A58.1–1972, American National Standards Institute, New York, NY, 1972.*)

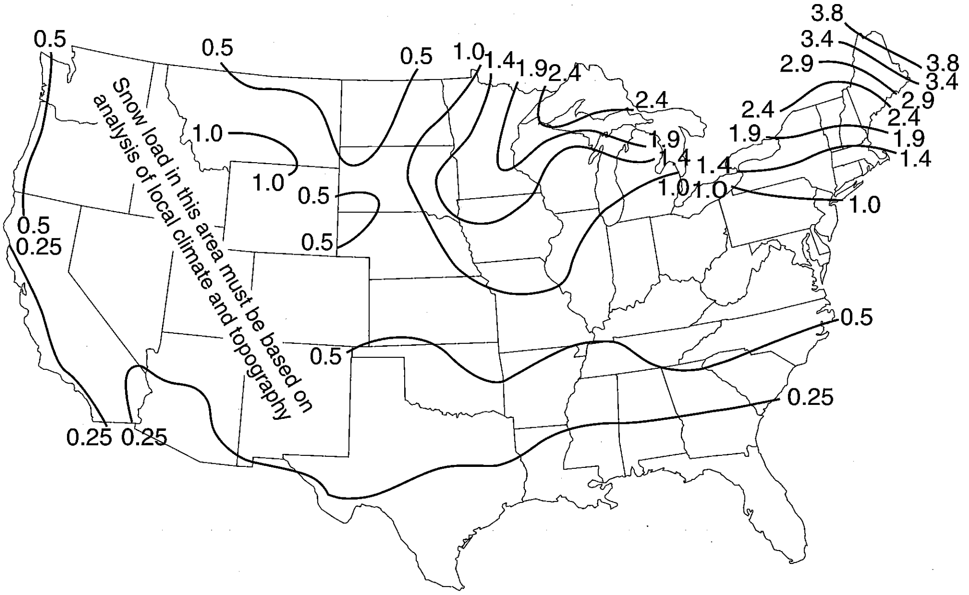

Factors include basic wind speed, exposure (urban vs. open terrain, for example), height of the structure, the importance of the structure (i.e., consequences of failure), and gust effect factors to account for the fluctuating nature of the wind and its interaction with the structure.

Seismic forces may be found for a particular structure by elastic or inelastic dynamic analysis, considering expected ground accelerations and the mass, stiffness, and damping characteristics of the construction. However, often the design is based on equivalent static forces calculated from provisions such as those of Refs. 1.1 and 1.5. The base shear is found by considering such factors as location, type of structure and its occupancy, total dead load, and the particular soil condition. The total lateral force is distributed to floors over the entire height of the structure in such a way as to approximate the distribution of forces obtained from a dynamic analysis.

1.4 SERVICEABILITY, STRENGTH, AND STRUCTURAL SAFETY

To serve its purpose, a structure must be safe against collapse and serviceable in use. Serviceability requires that deflections be adequately small; that cracks, if any, be kept to tolerable limits; that vibrations be minimized; etc. Safety requires that the strength of the structure be adequate for all loads that may foreseeably act on it. If the strength of a structure, built as designed, could be predicted accurately, and if the loads and their internal effects (moments, shears, axial forces) were known accurately, safety could be ensured by providing a carrying capacity just barely in excess of the known loads. However, there are a number of sources of uncertainty in the analysis, design, and construction of reinforced concrete structures. These sources of uncertainty, which require a definite margin of safety, may be listed as follows:

1. Actual loads may differ from those assumed.
2. Actual loads may be distributed in a manner different from that assumed.

3. The assumptions and simplifications inherent in any analysis may result in calculated load effects—moments, shears, etc.—different from those that, in fact, act in the structure.
4. The actual structural behavior may differ from that assumed, owing to imperfect knowledge.
5. Actual member dimensions may differ from those specified.
6. Reinforcement may not be in its proper position.
7. Actual material strength may be different from that specified.

In addition, in the establishment of a safety specification, consideration must be given to the consequences of failure. In some cases, a failure would be merely an inconvenience. In other cases, loss of life and significant loss of property may be involved. A further consideration should be the nature of the failure, should it occur. A gradual failure with ample warning permitting remedial measures is preferable to a sudden, unexpected collapse.

It is evident that the selection of an appropriate margin of safety is not a simple matter. However, progress has been made toward rational safety provisions in design codes (Refs. 1.6 to 1.11).

a. Variability of Loads

Since the maximum load that will occur during the life of a structure is uncertain, it can be considered a random variable. In spite of this uncertainty, the engineer must provide an adequate structure. A probability model for the maximum load can be devised by means of a probability density function for loads, as represented by the frequency curve of Fig. 1.14*a*. The exact form of this distribution curve, for any particular type of loading such as office loads, can be determined only on the basis of statistical data obtained from large-scale load surveys. A number of such surveys have been completed. For types of loads for which such data are scarce, fairly reliable information can be obtained from experience, observation, and judgment.

In such a frequency curve (Fig. 1.14*a*), the area under the curve between two abscissas, such as loads Q_1 and Q_2, represents the probability of occurrence of loads Q of magnitude $Q_1 < Q < Q_2$. A specified service load Q_d for design is selected conservatively in the upper region of Q in the distribution curve, as shown. The probability of occurrence of loads larger than Q_d is then given by the shaded area to the right of Q_d. It is seen that this specified service load is considerably larger than the mean load $\bar{Q}$ acting on the structure. This mean load is much more typical of average load conditions than the design load Q_d.

b. Strength

The strength of a structure depends on the strength of the materials from which it is made. For this purpose, minimum material strengths are specified in standardized ways. Actual material strengths cannot be known precisely and therefore also constitute random variables (see Section 2.6). Structural strength depends, furthermore, on the care with which a structure is built, which in turn reflects the quality of supervision and inspection. Member sizes may differ from specified dimensions, reinforcement may be out of position, poorly placed concrete may show voids, etc.

Strength of the entire structure or of a population of repetitive structures, e.g., highway overpasses, can also be considered a random variable with a probability density function of the type shown in Fig. 1.14*b*. As in the case of loads, the exact form

FIGURE 1.14
Frequency curves for (*a*) loads Q, (*b*) strengths S, and (*c*) safety margin M.

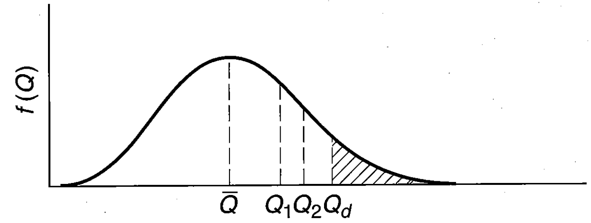

(*a*) Load *Q*

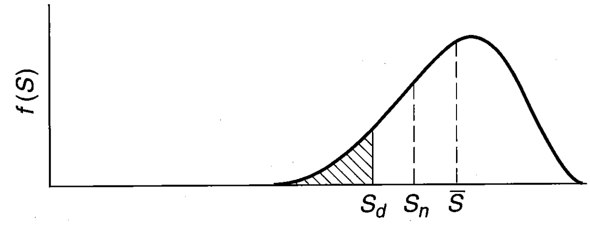

(*b*) Strength *S*

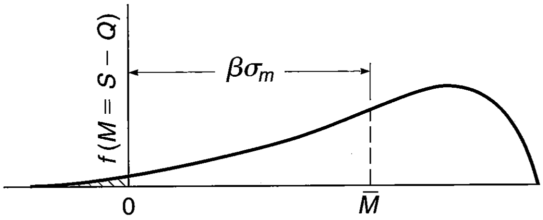

(*c*) Safety margin $M = S - Q$

of this function cannot be known but can be approximated from known data, such as statistics of actual, measured materials and member strengths and similar information. Considerable information of this type has been, or is being, developed and used.

c. Structural Safety

A given structure has a *safety margin M* if

$$M = S - Q > 0 \tag{1.1}$$

i.e., if the strength of the structure is larger than the load acting on it. Since S and Q are random variables, the safety margin $M = S - Q$ is also a random variable. A plot of the probability function of M may appear as in Fig. 1.14*c*. Failure occurs when M is less than zero. Thus, the probability of failure is represented by the shaded area in the figure.

Even though the precise form of the probability density functions for S and Q, and therefore for M, is not known, much can be achieved in the way of a rational approach to structural safety. One such approach is to require that the mean safety margin M be a specified number β of standard deviations σ_m above zero. It can be demonstrated that this results in the requirement that

$$\psi_s\bar{S} \geq \psi_L\bar{Q} \tag{1.2}$$

where ψ_s is a partial safety coefficient smaller than one applied to the mean strength $\bar{S}$ and ψ_L is a partial safety coefficient larger than one applied to the mean load $\bar{Q}$.

The magnitude of each partial safety coefficient depends on the variance of the quantity to which it applies, S or Q, and on the chosen value of β, the reliability index of the structure. As a general guide, a value of the safety index β between 3 and 4 corresponds to a probability of failure of the order of 1:100,000 (Ref. 1.8). The value of β is often established by calibration against well-proved and established designs.

In practice, it is more convenient to introduce partial safety coefficients with respect to code-specified loads which, as already noted, considerably exceed average values, rather than with respect to mean loads as in Eq. (1.2); similarly, the partial safety coefficient for strength is applied to nominal strength generally computed somewhat conservatively, rather than to mean strengths as in Eq. (1.2). A restatement of the safety requirement in these terms is

$$\phi S_n \geq \gamma Q_d \tag{1.3a}$$

in which ϕ is a strength reduction factor applied to nominal strength S_n and γ is a load factor applied to calculated or code-specified design loads Q_d. Furthermore, recognizing the differences in variability between, say, dead loads D and live loads L, it is both reasonable and easy to introduce different load factors for different types of loads. The preceding equation can thus be written

$$\phi S_n \geq \gamma_d D + \gamma_l L \tag{1.3b}$$

in which γ_d is a load factor somewhat greater than 1.0 applied to the calculated dead load D and γ_l is a larger load factor applied to the code-specified live load L. When additional loads, such as the wind load W, are to be considered, the reduced probability that maximum dead, live, and wind or other loads will act simultaneously can be incorporated by using modified load factors such that

$$\phi S_n \geq \gamma_{d_i} D + \gamma_{l_i} L + \gamma_{w_i} W + \cdots \tag{1.3c}$$

Present U.S. design specifications follow the format of Eqs. (1.3*b*) and (1.3*c*).

1.5 DESIGN BASIS

The single most important characteristic of any structural member is its actual strength, which must be large enough to resist, with some margin to spare, all foreseeable loads that may act on it during the life of the structure, without failure or other distress. It is logical, therefore, to proportion members, i.e., to select concrete dimensions and reinforcement, so that member strengths are adequate to resist forces resulting from certain hypothetical overload stages, significantly above loads expected actually to occur in service. This design concept is known as *strength design.*

For reinforced concrete structures at loads close to and at failure, one or both of the materials, concrete and steel, are invariably in their nonlinear inelastic range. That is, concrete in a structural member reaches its maximum strength and subsequent fracture at stresses and strains far beyond the initial elastic range in which stresses and strains are fairly proportional. Similarly, steel close to and at failure of the member is usually stressed beyond its elastic domain into and even beyond the yield region. Consequently, the nominal strength of a member must be calculated on the basis of this inelastic behavior of the materials.

A member designed by the strength method must also perform in a satisfactory way under normal service loading. For example, beam deflections must be limited to acceptable values, and the number and width of flexural cracks at service loads must be controlled. Serviceability limit conditions are an important part of the total design, although attention is focused initially on strength.

Historically, members were proportioned so that stresses in the steel and concrete resulting from normal service loads were within specified limits. These limits, known as *allowable stresses*, were only fractions of the failure stresses of the materials. For members proportioned on such a service load basis, the margin of safety was provided by stipulating allowable stresses under service loads that were appropriately small fractions of the compressive concrete strength and the steel yield stress. We now refer to this basis for design as *service load design*. Allowable stresses, in practice, were set at about one-half the concrete compressive strength and one-half the yield stress of the steel.

Because of the difference in realism and reliability, the strength design method has displaced the older service load design method. However, the older method provides the basis for some serviceability checks and is the design basis for many older structures. Throughout this text, strength design is presented almost exclusively.

1.6 DESIGN CODES AND SPECIFICATIONS

The design of concrete structures such as those of Figs. 1.1 to 1.12 is generally done within the framework of codes giving specific requirements for materials, structural analysis, member proportioning, etc. The International Building Code (Ref. 1.2) is an example of a consensus code governing structural design and is often adopted by local municipalities. The responsibility of preparing material-specific portions of the codes rests with various professional groups, trade associations, and technical institutes. In contrast with many other industrialized nations, the United States does not have an official, government-sanctioned, national code.

The American Concrete Institute (ACI) has long been a leader in such efforts. As one part of its activity, the American Concrete Institute has published the widely recognized *Building Code Requirements for Structural Concrete and Commentary* (Ref. 1.12), which serves as a guide in the design and construction of reinforced concrete buildings. The ACI Code has no official status in itself. However, it is generally regarded as an authoritative statement of current good practice in the field of reinforced concrete. As a result, it has been incorporated into the International Building Code and similar codes, which in turn are adopted by law into municipal and regional building codes that do have legal status. Its provisions thereby attain, in effect, legal standing. Most reinforced concrete buildings and related construction in the United States are designed in accordance with the current ACI Code. It has also served as a model document for many other countries. The commentary incorporated in Ref. 1.12 provides background material and rationale for the Code provisions. The American Concrete Institute also publishes important journals and standards, as well as recommendations for the analysis and design of special types of concrete structures such as the tanks shown in Fig. 1.11.

Most highway bridges in the United States are designed according to the requirements of the AASHTO bridge specifications (Ref. 1.3) which not only contain the provisions relating to loads and load distributions mentioned earlier, but also include detailed provisions for the design and construction of concrete bridges. Many of the provisions follow ACI Code provisions closely, although a number of significant differences will be found.

The design of railway bridges is done according to the specifications of the AREMA *Manual of Railway Engineering* (Ref. 1.4). It, too, is patterned after the ACI

Code in most respects, but it contains much additional material pertaining to railway structures of all types.

No code or design specification can be construed as a substitute for sound engineering judgment in the design of concrete structures. In structural practice, special circumstances are frequently encountered where code provisions can serve only as a guide, and the engineer must rely upon a firm understanding of the basic principles of structural mechanics applied to reinforced or prestressed concrete, and an intimate knowledge of the nature of the materials.

1.7 SAFETY PROVISIONS OF THE ACI CODE

The safety provisions of the ACI Code are given in the form of Eqs. (1.3*b*) and (1.3*c*) using strength reduction factors and load factors. These factors are based to some extent on statistical information but to a larger degree on experience, engineering judgment, and compromise. In words, the design strength ϕS_n of a structure or member must be at least equal to the required strength U calculated from the factored loads, i.e.,

$$\text{Design strength} \geq \text{required strength}$$

or

$$\phi S_n \geq U \tag{1.4}$$

The nominal strength S_n is computed (usually somewhat conservatively) by accepted methods. The required strength U is calculated by applying appropriate load factors to the respective service loads: dead load D, live load L, wind load W, earthquake load E, earth pressure H, fluid pressure F, snow load S, rain load R, and environmental effects T that may include settlement, creep, shrinkage, and temperature change. Loads are defined in a general sense, to include either loads or the related internal effects such as moments, shears, and thrusts. Thus, in specific terms for a member subjected, say, to moment, shear, and axial load

$$\phi M_n \geq M_u \tag{1.5a}$$

$$\phi V_n \geq V_u \tag{1.5b}$$

$$\phi P_n \geq P_u \tag{1.5c}$$

where the subscripts n denote the nominal strengths in flexure, shear, and axial load, respectively, and the subscripts u denote the factored load moment, shear, and axial load. In computing the factored load effects on the right, load factors may be applied either to the service loads themselves or to the internal load effects calculated from the service loads.

The load factors specified in the ACI Code, to be applied to calculated dead loads and those live and environmental loads specified in the appropriate codes or standards, are summarized in Table 1.2. These are consistent with the concepts introduced in Section 1.4 and with SEI/ASCE 7, *Minimum Design Loads for Buildings and Other Structures* (Ref. 1.1), and allow design of composite structures using combinations of structural steel and reinforced concrete. For individual loads, lower factors are used for loads known with greater certainty, e.g., dead load, compared with loads of greater variability, e.g., live loads. Further, for load combinations such as dead plus live loads plus wind forces, reductions are applied to one load or the other that reflect the improbability that an excessively large live load coincides with an unusually high windstorm. The

TABLE 1.2
Factored load combinations for determining required strength *U* in the ACI Code

Condition[a]	Factored Load or Load Effect *U*
Basic[b]	$U = 1.2D + 1.6L$
Dead plus fluid[b]	$U = 1.4(D + F)$
Snow, rain, temperature, and wind	$U = 1.2(D + F + T) + 1.6(L + H) + 0.5(L_r \text{ or } S \text{ or } R)$
	$U = 1.2D + 1.6(L_r \text{ or } S \text{ or } R) + (1.0L \text{ or } 0.8W)$
	$U = 1.2D + 1.6W + 1.0L + 0.5(L_r \text{ or } S \text{ or } R)$
	$U = 0.9D + 1.6W + 1.6H$
Earthquake	$U = 1.2D + 1.0E + 1.0L + 0.2S$
	$U = 0.9D + 1.0E + 1.6H$

[a] Where the following represent the loads or related internal moments or forces resulting from the listed factors: D = dead load; E = earthquake; F = fluids; H = weight or pressure from soil; L = live load; L_r = roof live load; R = rain; S = snow; T = cumulative effects of temperature, creep, shrinkage, and differential settlement; W = wind.

[b] The ACI Code includes F or H loads in the load combinations. The "basic" load condition of $1.2D + 1.6L$ reflects the fact that most buildings have neither F nor H loads present and that $1.4D$ rarely governs design.

factors also reflect, in a general way, uncertainties with which internal load effects are calculated from external loads in systems as complex as highly indeterminate, inelastic reinforced concrete structures which, in addition, consist of variable-section members (because of tension cracking, discontinuous reinforcement, etc.). Finally, the load factors also distinguish between two situations, particularly when horizontal forces are present in addition to gravity, i.e., the situation where the effects of all simultaneous loads are additive, as distinct from that in which various load effects counteract one another. For example, in a retaining wall the soil pressure produces an overturning moment, and the gravity forces produce a counteracting stabilizing moment.

In all cases in Table 1.2, the controlling equation is the one that gives the largest factored load effect U.

The strength reduction factors ϕ in the ACI Code are given different values depending on the state of knowledge, i.e., the accuracy with which various strengths can be calculated. Thus, the value for bending is higher than that for shear or bearing. Also, ϕ values reflect the probable importance, for the survival of the structure, of the particular member and of the probable quality control achievable. For both these reasons, a lower value is used for columns than for beams. Table 1.3 gives the ϕ values specified in the ACI Code.

The joint application of strength reduction factors (Table 1.3) and load factors (Table 1.2) is aimed at producing approximate probabilities of understrength of the order of 1/100 and of overloads of 1/1000. This results in a probability of structural failure of the order of 1/100,000.

In addition to the values given in Table 1.3, ACI Code Appendix B, "Alternative Provisions for Reinforced and Prestressed Concrete Flexural and Compression Members," allows the use of load factors and strength reduction factors from previous editions of the ACI Code. The load factors and strength reduction factors of ACI Code Appendix B are calibrated in conjunction with the detailed requirements of that appendix. Consequently, they may not be interchanged with the provisions of the main body of the Code.

TABLE 1.3
Strength reduction factors in the ACI Code

Strength Condition	Strength Reduction Factor ϕ
Tension-controlled sections[a]	0.90
Compression-controlled sections[b]	
Members with spiral reinforcement	0.75
Other reinforced members	0.65
Shear and torsion	0.75
Bearing on concrete	0.65
Post-tensioned anchorage zones	0.85
Strut-and-tie models[c]	0.75

[a] Chapter 19 discusses reductions in ϕ for pretensioned members where strand embedment is less than the development length.

[b] Chapter 3 contains a discussion of the linear variation of ϕ between tension and compression-controlled sections. Chapter 8 discusses the conditions that allow an increase in ϕ for spirally reinforced columns.

[c] Strut-and-tie models are described in Chapter 10.

1.8 FUNDAMENTAL ASSUMPTIONS FOR REINFORCED CONCRETE BEHAVIOR

The chief task of the structural engineer is the design of structures. *Design* is the determination of the general shape and all specific dimensions of a particular structure so that it will perform the function for which it is created and will safely withstand the influences that will act on it throughout its useful life. These influences are primarily the loads and other forces to which it will be subjected, as well as other detrimental agents, such as temperature fluctuations, foundation settlements, and corrosive influences. *Structural mechanics* is one of the main tools in this process of design. As here understood, it is the body of knowledge that permits one to predict with a good degree of certainty how a structure of given shape and dimensions will behave when acted upon by known forces or other mechanical influences. The chief items of behavior that are of practical interest are (1) the strength of the structure, i.e., that magnitude of loads of a given distribution which will cause the structure to fail, and (2) the deformations, such as deflections and extent of cracking, that the structure will undergo when loaded under service conditions.

The fundamental propositions on which the mechanics of reinforced concrete is based are as follows:

1. The internal forces, such as bending moments, shear forces, and normal and shear stresses, at any section of a member are in equilibrium with the effects of the external loads at that section. This proposition is not an assumption but a fact, because any body or any portion thereof can be at rest only if all forces acting on it are in equilibrium.
2. The strain in an embedded reinforcing bar (unit extension or compression) is the same as that of the surrounding concrete. Expressed differently, it is assumed that perfect bonding exists between concrete and steel at the interface, so that no slip can occur between the two materials. Hence, as the one deforms, so must the other. With modern deformed bars (see Section 2.14), a high degree of mechanical

interlocking is provided in addition to the natural surface adhesion, so this assumption is very close to correct.

3. Cross sections that were plane prior to loading continue to be plane in the member under load. Accurate measurements have shown that when a reinforced concrete member is loaded close to failure, this assumption is not absolutely accurate. However, the deviations are usually minor, and the results of theory based on this assumption check well with extensive test information.
4. In view of the fact that the tensile strength of concrete is only a small fraction of its compressive strength (see Section 2.9), the concrete in that part of a member which is in tension is usually cracked. While these cracks, in well-designed members, are generally so narrow as to be hardly visible (they are known as *hairline* cracks), they evidently render the cracked concrete incapable of resisting tension stress. Correspondingly, it is assumed that concrete is not capable of resisting any tension stress whatever. This assumption is evidently a simplification of the actual situation because, in fact, concrete prior to cracking, as well as the concrete located between cracks, does resist tension stresses of small magnitude. Later in discussions of the resistance of reinforced concrete beams to shear, it will become apparent that under certain conditions this particular assumption is dispensed with and advantage is taken of the modest tensile strength that concrete can develop.
5. The theory is based on the actual stress-strain relationships and strength properties of the two constituent materials (see Sections 2.8 and 2.14) or some reasonable equivalent simplifications thereof. The fact that nonelastic behavior is reflected in modern theory, that concrete is assumed to be ineffective in tension, and that the joint action of the two materials is taken into consideration results in analytical methods which are considerably more complex, and also more challenging, than those that are adequate for members made of a single, substantially elastic material.

These five assumptions permit one to predict by calculation the performance of reinforced concrete members only for some simple situations. Actually, the joint action of two materials as dissimilar and complicated as concrete and steel is so complex that it has not yet lent itself to purely analytical treatment. For this reason, methods of design and analysis, while using these assumptions, are very largely based on the results of extensive and continuing experimental research. They are modified and improved as additional test evidence becomes available.

1.9 BEHAVIOR OF MEMBERS SUBJECT TO AXIAL LOADS

Many of the fundamentals of the behavior of reinforced concrete, through the full range of loading from zero to ultimate, can be illustrated clearly in the context of members subject to simple axial compression or tension. The basic concepts illustrated here will be recognized in later chapters in the analysis and design of beams, slabs, eccentrically loaded columns, and other members subject to more complex loadings.

a. Axial Compression

In members that sustain chiefly or exclusively axial compression loads, such as building columns, it is economical to make the concrete carry most of the load. Still, some steel reinforcement is always provided for various reasons. For one, very few members are truly axially loaded; steel is essential for resisting any bending that may exist. For another, if part of the total load is carried by steel with its much greater strength, the cross-sectional dimensions of the member can be reduced—the more so, the larger the amount of reinforcement.

The two chief forms of reinforced concrete columns are shown in Fig. 1.15. In the square column, the four longitudinal bars serve as main reinforcement. They are held in place by transverse small-diameter steel ties that prevent displacement of the main bars during construction operations and counteract any tendency of the compression-loaded bars to buckle out of the concrete by bursting the thin outer cover. On the left is shown a round column with eight main reinforcing bars. These are surrounded by a closely spaced spiral that serves the same purpose as the more widely spaced ties but also acts to confine the concrete within it, thereby increasing its resistance to axial compression. The discussion that follows applies to tied columns.

When axial load is applied, the compression strain is the same over the entire cross section and, in view of the bonding between concrete and steel, is the same in the two materials (see propositions 2 and 3 in Section 1.8). To illustrate the action of such a member as load is applied, Fig. 1.16 shows two typical stress-strain curves, one for a concrete with compressive strength $f_c' = 28$ MPa and the other for a steel with yield stress $f_y = 420$ MPa. The curves for the two materials are drawn on the same graph using different vertical stress scales. Curve *b* has the shape that would be obtained in a concrete cylinder test. The rate of loading in most structures is considerably slower than that in a cylinder test, and this affects the shape of the curve. Curve *c*, therefore, is drawn as being characteristic of the performance of concrete under slow loading. Under these conditions, tests have shown that the maximum reliable compressive strength of reinforced concrete is about $0.85f_c'$, as shown.

FIGURE 1.15
Reinforced concrete columns.

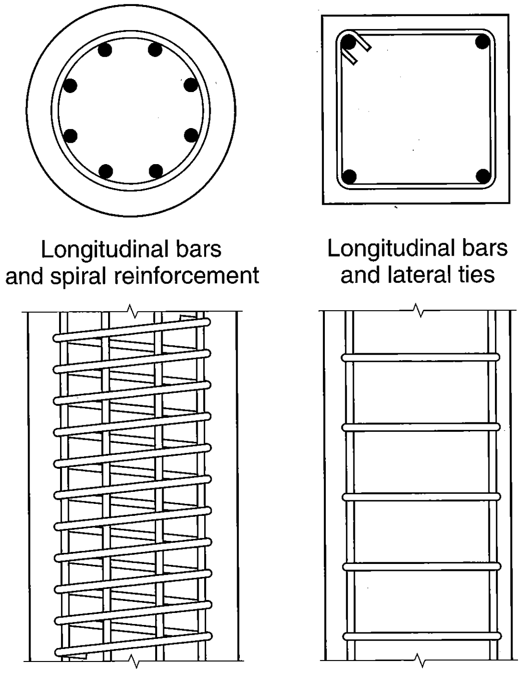

FIGURE 1.16
Concrete and steel stress-strain curves.

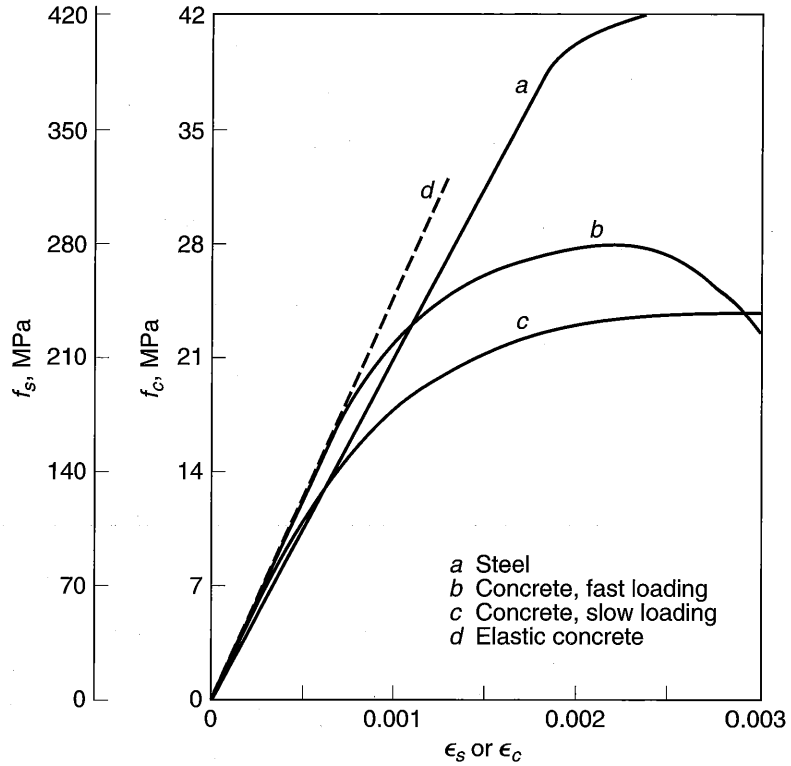

Elastic Behavior At low stresses, up to about $f'_c/2$, the concrete is seen to behave nearly elastically, i.e., stresses and strains are quite closely proportional; the straight line *d* represents this range of behavior with little error for both rates of loading. For the given concrete, the range extends to a strain of about 0.0005. The steel, on the other hand, is seen to be elastic nearly to its yield point of 420 MPa, or to the much greater strain of about 0.002.

Because the compression strain in the concrete, at any given load, is equal to the compression strain in the steel,

$$\epsilon_c = \frac{f_c}{E_c} = \epsilon_s = \frac{f_s}{E_s}$$

from which the relation between the steel stress f_s and the concrete stress f_c is obtained as

$$f_s = \frac{E_s}{E_c} f_c = nf_c \tag{1.6}$$

where $n = E_s/E_c$ is known as the *modular ratio.*

Let

A_c = net area of concrete, i.e., gross area minus area occupied by reinforcing bars
A_g = gross area
A_{st} = total area of reinforcing bars
P = axial load

Then

$$P = f_c A_c + f_s A_{st} = f_c A_c + nf_c A_{st}$$

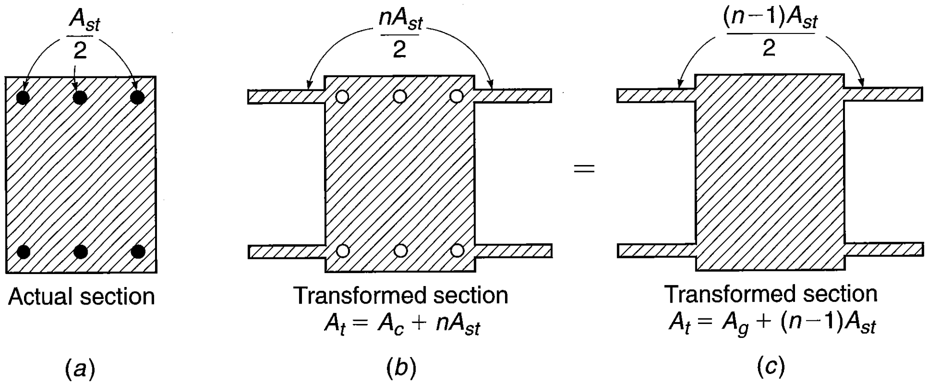

Actual section

(*a*)

Transformed section
$A_t = A_c + nA_{st}$

(*b*)

Transformed section
$A_t = A_g + (n-1)A_{st}$

(*c*)

FIGURE 1.17
Transformed section in axial compression.

or

$$P = f_c(A_c + nA_{st}) \tag{1.7}$$

The term $A_c + nA_{st}$ can be interpreted as the area of a fictitious concrete cross section, the *transformed area*, which when subjected to the particular concrete stress f_c results in the same axial load P as the actual section composed of both steel and concrete. This transformed concrete area is seen to consist of the actual concrete area plus n times the area of the reinforcement. It can be visualized as shown in Fig. 1.17. That is, in Fig. 1.17*b* the three bars along each of the two faces are thought of as being removed and replaced, at the same distance from the axis of the section, with added areas of fictitious concrete of total amount nA_{st}. Alternatively, as shown in Fig. 1.17*c*, one can think of the area of the steel bars as replaced with concrete, in which case one has to add to the gross concrete area A_g so obtained only $(n - 1)A_{st}$ to obtain the same total transformed area. Therefore, alternatively,

$$P = f_c[A_g + (n - 1)A_{st}] \tag{1.8}$$

If load and cross-sectional dimensions are known, the concrete stress can be found by solving Eq. (1.7) or (1.8) for f_c, and the steel stress can be calculated from Eq. (1.6). These relations hold in the range in which the concrete behaves nearly elastically, i.e., up to about 50 to 60 percent of f'_c. For reasons of safety and serviceability, concrete stresses in structures under normal conditions are kept within this range. Therefore, these relations permit one to calculate *service load stresses.*

EXAMPLE 1.1

A column made of the materials defined in Fig. 1.16 has a cross section of 400 × 500 mm and is reinforced by six No. 29 (No. 9) bars, disposed as shown in Fig. 1.17. (See Tables A.1 and A.2 of Appendix A for bar diameters and areas and Section 2.14 for a description of bar size designations.) Determine the axial load that will stress the concrete to 8 MPa. The modular ratio n may be assumed equal to 8. (In view of the scatter inherent in E_c, it is customary and satisfactory to round off the value of n to the nearest integer.)

Solution. One finds $A_g = 400 \times 500 = 200{,}000\ \text{mm}^2$, and from Appendix A, Table A.2, six No. 29 (No. 9) bars provide steel area $A_{st} = 3870\ \text{mm}^2$ or 1.94 percent of the gross area. The load on the column, from Eq. (1.8), is $P = 8[200{,}000 + (8 - 1)3870] = 1{,}816{,}720$ N. Of this total load, the concrete is seen to carry $P_c = f_cA_c = f_c(A_g - A_{st}) = 8(200{,}000 - 3870) = 1{,}569{,}040$ N, and the steel $P_s = f_sA_{st} = (nf_c)A_{st} = 64 \times 3870 = 247{,}680$ N, which is 13.6 percent of the total axial load.

Inelastic Range Inspection of Fig. 1.16 shows that the elastic relationships that have been used so far cannot be applied beyond a strain of about 0.0005 for the given concrete. To obtain information on the behavior of the member at larger strains and, correspondingly, at larger loads, it is therefore necessary to make direct use of the information in Fig. 1.16.

EXAMPLE 1.2

One may want to calculate the magnitude of the axial load that will produce a strain or unit shortening $\epsilon_c = \epsilon_s = 0.0010$ in the column of Example 1.1. At this strain the steel is seen to be still elastic, so that the steel stress $f_s = \epsilon_s E_s = 0.001 \times 200{,}000 = 200$ N/mm^2 (MPa). The concrete is in the inelastic range, so that its stress cannot be directly calculated, but it can be read from the stress-strain curve for the given value of strain.

1. If the member has been loaded at a fast rate, curve *b* holds at the instant when the entire load is applied. The stress for $\epsilon = 0.001$ can be read as $f_c = 22$ MPa. Consequently, the total load can be obtained from

$$P = f_c A_c + f_s A_{st} \tag{1.9}$$

   which applies in the inelastic as well as in the elastic range. Hence, $P = 22(200{,}000 - 3870) + 200 \times 3870 = 4{,}314{,}860 + 774{,}800 = 5090$ kN. Of this total load, the steel is seen to carry 774.8 kN, or 15.2 percent.
2. For slowly applied or sustained loading, curve *c* represents the behavior of the concrete. Its stress at a strain of 0.001 can be read as $f_c = 17$ MPa. Then $P = 17 \times 196{,}130 + 200 \times 3870 = 3{,}334{,}210 + 774{,}800 = 4109$ kN. Of this total load, the steel is seen to carry 18.9 percent.

Comparison of the results for fast and slow loading shows the following. Owing to creep of concrete, a given shortening of the column is produced by a smaller load when slowly applied or sustained over some length of time than when quickly applied. More important, the farther the stress is beyond the proportional limit of the concrete, and the more slowly the load is applied or the longer it is sustained, the smaller the share of the total load carried by the concrete and the larger the share carried by the steel. In the sample column, the steel was seen to carry 13.6 percent of the load in the elastic range, 15.2 percent for a strain of 0.001 under fast loading, and 18.9 percent at the same strain under slow or sustained loading.

Strength The one quantity of chief interest to the structural designer is *strength*, i.e., the maximum load that the structure or member will carry. Information on stresses, strains, and similar quantities serves chiefly as a tool for determining carrying capacity. The performance of the column discussed so far indicates two things: (1) in the range of large stresses and strains that precede attainment of the maximum load and subsequent failure, elastic relationships cannot be used; (2) the member behaves differently under fast and under slow or sustained loading and shows less resistance to the latter than to the former. In usual construction, many types of loads, such as the weight of the structure and any permanent equipment housed therein, are sustained, and others are applied at slow rates. For this reason, to calculate a reliable magnitude of compressive strength, curve *c* of Fig. 1.16 must be used as far as the concrete is concerned.

The steel reaches its tensile strength (peak of the curve) at strains on the order of 0.08 (see Fig. 2.15). Concrete, on the other hand, fails by crushing at the much smaller strain of about 0.003 and, as seen from Fig. 1.16 (curve *c*), reaches its maximum stress in the strain range of 0.002 to 0.003. Because the strains in steel and concrete are equal in axial compression, the load at which the steel begins to yield can be calculated from the information in Fig. 1.16.

If the small knee prior to yielding of the steel is disregarded, i.e., if the steel is assumed to be sharp-yielding, the strain at which it yields is

$$\epsilon_y = \frac{f_y}{E_s} \tag{1.10}$$

or

$$\epsilon_y = \frac{420}{200{,}000} = 0.0021$$

At this strain, curve *c* of Fig. 1.16 indicates a stress of 22 MPa in the concrete; therefore, by Eq. (1.9), the load in the member when the steel starts yielding is $P_y = 22 \times 196{,}130 + 420 \times 3870 = 5940$ kN. At this load the concrete has not yet reached its full strength, which, as mentioned before, can be assumed as $0.85f_c' = 23.8$ MPa for slow or sustained loading, and therefore the load on the member can be further increased. During this stage of loading, the steel keeps yielding at constant stress. Finally, the nominal capacity† of the member is reached when the concrete crushes while the steel yields, i.e.,

$$P_n = 0.85f_c'A_c + f_yA_{st} \tag{1.11}$$

Numerous careful tests have shown the reliability of Eq. (1.11) in predicting the ultimate strength of a concentrically loaded reinforced concrete column, provided its slenderness ratio is small so that buckling will not reduce its strength.

For the particular numerical example, $P_n = 23.8 \times 196{,}130 + 420 \times 3870 = 4{,}667{,}900 + 1{,}625{,}400 = 6{,}293{,}300$ N = 6293 kN. At this stage the steel carries 25.8 percent of the load.

SUMMARY In the elastic range, the steel carries a relatively small portion of the total load of an axially compressed member. As member strength is approached, there occurs a redistribution of the relative shares of the load resisted by concrete and steel, the latter taking an increasing amount. The nominal capacity, at which the member is on the point of failure, consists of the contribution of the steel when it is stressed to the yield point plus that of the concrete when its stress has attained a value of $0.85f_c'$, as reflected in Eq. (1.11).

b. Axial Tension

The tension strength of concrete is only a small fraction of its compressive strength. It follows that reinforced concrete is not well suited for use in tension members because the concrete will contribute little, if anything, to their strength. Still, there are situations in which reinforced concrete is stressed in tension, chiefly in tie-rods in structures such as arches. Such members consist of one or more bars embedded in concrete in a symmetric arrangement similar to compression members (see Figs. 1.15 and 1.17).

When the tension force in the member is small enough for the stress in the concrete to be considerably below its tensile strength, both steel and concrete behave elastically. In this situation, all the expressions derived for elastic behavior in compression in Section 1.9a are identically valid for tension. In particular, Eq. (1.7) becomes

$$P = f_{ct}(A_c + nA_{st}) \tag{1.12}$$

where f_{ct} is the tensile stress in the concrete.

---

† Throughout this book quantities that refer to the strength of members, calculated by accepted analysis methods, are furnished with the subscript *n*, which stands for "nominal." This notation is in agreement with the ACI Code. It is intended to convey that the actual strength of any member is bound to deviate to some extent from its calculated, nominal value because of inevitable variations of dimensions, materials properties, and other parameters. Design in all cases is based on this nominal strength, which represents the best available estimate of the actual member strength.

However, when the load is further increased, the concrete reaches its tensile strength at a stress and strain on the order of one-tenth of what it could sustain in compression. At this stage, the concrete cracks across the entire cross section. When this happens, it ceases to resist any part of the applied tension force, since, evidently, no force can be transmitted across the air gap in the crack. At any load larger than that which caused the concrete to crack, the steel is called upon to resist the entire tension force. Correspondingly, at this stage,

$$P = f_s A_{st} \tag{1.13}$$

With further increased load, the tensile stress f_s in the steel reaches the yield point f_y. When this occurs, the tension members cease to exhibit small, elastic deformations but instead stretch a sizable and permanent amount at substantially constant load. This does not impair the strength of the member. Its elongation, however, becomes so large (on the order of 1 percent or more of its length) as to render it useless. Therefore, the maximum useful strength P_{nt} of a tension member is the force that will just cause the steel stress to reach the yield point. That is,

$$P_{nt} = f_y A_{st} \tag{1.14}$$

To provide adequate safety, the force permitted in a tension member under normal service loads should be limited to about $\frac{1}{2}P_{nt}$. Because the concrete has cracked at loads considerably smaller than this, concrete does not contribute to the carrying capacity of the member in service. It does serve, however, as fire and corrosion protection and often improves the appearance of the structure.

There are situations, though, in which reinforced concrete is used in axial tension under conditions in which the occurrence of tension cracks must be prevented. A case in point is a circular tank (see Fig. 1.11). To provide watertightness, the hoop tension caused by the fluid pressure must be prevented from causing the concrete to crack. In this case, Eq. (1.12) can be used to determine a safe value for the axial tension force P by using, for the concrete tension stress f_{ct}, an appropriate fraction of the tensile strength of the concrete, i.e., of the stress that would cause the concrete to crack.

REFERENCES

1.1. *Minimum Design Loads for Buildings and Other Structures*, ASCE/SEI 7-05, American Society of Civil Engineers, Reston, VA, 2005.

1.2. *International Building Code*, International Code Council, Washington, DC, 2006.

1.3. *AASHTO LRFD Bridge Design Specifications*, 4th ed., American Association of State Highway and Transportation Officials (AASHTO), Washington, DC, 2008.

1.4. *Manual of Railway Engineering*, American Railway Engineering and Maintenance-of-Way Association (AREMA), Landover, MD, 2008.

1.5. *Building Seismic Safety Council NEHRP Recommended Provisions for Seismic Regulations for New Buildings and Other Structures*, 2000 edition, Part 1, "Provisions," FEMA 368, Part 2, "Commentary," FEMA 369, Federal Emergency Management Agency, Washington, DC, March 2001.

1.6. J. G. MacGregor, S. A. Mirza, and B. Ellingwood, "Statistical Analysis of Resistance of Reinforced and Prestressed Concrete Members," *J. ACI*, vol. 80, no. 3, 1983, pp. 167–176.

1.7. J. G. MacGregor, "Load and Resistance Factors for Concrete Design," *J. ACI*, vol. 80, no. 4, 1983, pp. 279–287.

1.8. J. G. MacGregor, "Safety and Limit States Design for Reinforced Concrete," *Can. J. Civ. Eng.*, vol. 3, no. 4, 1976, pp. 484–513.

1.9. G. Winter, "Safety and Serviceability Provisions of the ACI Building Code," ACI-CEB-FIP-PCI Symposium, *ACI Special Publication SP-59*, 1979.

1.10. A. S. Nowak and M. M. Szerszen, "Calibration of Design Code for Buildings (ACI 318): Part 1—Statistical Models for Resistance," *ACI Struct. J.*, vol. 100, no. 3, 2003, pp. 377–382.

1.11 M. M. Szerszen and A. S. Nowak, "Calibration of Design Code for Buildings (ACI 318): Part 2—Reliability Analysis and Resistance Factors," *ACI Struct. J.*, vol. 100, no. 3, 2003, pp. 383–391.

1.12. *Building Code Requirements for Structural Concrete and Commentary* (ACI 318M-08), American Concrete Institute, Farmington Hills, MI, 2008.

PROBLEMS

1.1. A 400 × 500 mm. column is made of the same concrete and reinforced with the same six No. 29 (No. 9) bars as the column in Examples 1.1 and 1.2, except that a steel with yield strength $f_y = 280$ MPa is used. The stress-strain diagram of this reinforcing steel is shown in Fig. 2.15 for $f_y = 280$ MPa. For this column determine (*a*) the axial load that will stress the concrete to 8 MPa; (*b*) the load at which the steel starts yielding; (*c*) the maximum load; and (*d*) the share of the total load carried by the reinforcement at these three stages of loading. Compare results with those calculated in the examples for $f_y = 420$ MPa, keeping in mind, in regard to relative economy, that the price per pound for reinforcing steels with 280 and 420 MPa yield points is about the same.

1.2. The area of steel, expressed as a percentage of gross concrete area, for the column of Problem 1.1 is lower than would often be used in practice. Recalculate the comparisons of Problem 1.1, using f_y of 280 and 420 MPa as before, but for a 400 × 500 mm column reinforced with eight No. 36 (No. 11) bars. Compare your results with those of Problem 1.1.

1.3. A square concrete column with dimensions 560 × 560 mm is reinforced with a total of eight No. 32 (No. 10) bars arranged uniformly around the column perimeter. Material strengths are $f_y = 420$ MPa and $f'_c = 28$ MPa, with stress-strain curves as given by curves *a* and *c* of Fig. 1.16. Calculate the percentages of total load carried by the concrete and by the steel as load is gradually increased from 0 to failure, which is assumed to occur when the concrete strain reaches a limit value of 0.0030. Determine the loads at strain increments of 0.0005 up to the failure strain, and graph your results, plotting load percentages vs. strain. The modular ratio may be assumed at $n = 8$ for these materials.

1.4. A 500 × 600 mm column is made of the same concrete as used in Examples 1.1 and 1.2. It is reinforced with six No. 36 (No. 11) bars with $f_y = 420$ MPa. For this column section, determine (*a*) the axial load that the section will carry at a concrete stress of 9.7 MPa; (*b*) the load on the section when the steel begins to yield; (*c*) the maximum load if the section is loaded slowly; and (*d*) the maximum load if the section is loaded rapidly. The area of one No. 36 (No. 11) bar is 1006 mm^2. Determine the percent of the load carried by the steel and the concrete for each combination.

1.5. A 600 mm diameter column is made of the same concrete as used in Examples 1.1 and 1.2. The area of reinforcement equals 2.1 percent of the gross cross section (that is, $A_s = 0.021A_g$) and $f_y = 420$ MPa. For this column section, determine (*a*) the axial load the section will carry at a concrete stress of 8 MPa; (*b*) the load on the section when the steel begins to yield; (*c*) the maximum load if the section is loaded slowly; (*d*) the maximum load if the section is loaded rapidly; and (*e*) the maximum load if the reinforcement in the column is raised to 6.5 percent of the gross cross section and the column is loaded slowly. Comment on your answer, especially the percent of the load carried by the steel and the concrete for each combination.

2 Materials

2.1 INTRODUCTION

The structures and component members treated in this text are composed of concrete reinforced with steel bars, and in some cases prestressed with steel wire, strand, or alloy bars. An understanding of the materials characteristics and behavior under load is fundamental to understanding the performance of structural concrete, and to safe, economical, and serviceable design of concrete structures. Although prior exposure to the fundamentals of material behavior is assumed, a brief review is presented in this chapter, as well as a description of the types of bar reinforcement and prestressing steels in common use. Numerous references are given as a guide for those seeking more information on any of the topics discussed.

2.2 CEMENT

A cementitious material is one that has the adhesive and cohesive properties necessary to bond inert aggregates into a solid mass of adequate strength and durability. This technologically important category of materials includes not only cements proper but also limes, asphalts, and tars as they are used in road building, and others. For making structural concrete, *hydraulic cements* are used exclusively. Water is needed for the chemical process (hydration) in which the cement powder sets and hardens into one solid mass. Of the various hydraulic cements that have been developed, *portland cement*, which was first patented in England in 1824, is by far the most common.

Portland cement is a finely powdered, grayish material that consists chiefly of calcium and aluminum silicates.[†] The common raw materials from which it is made are limestones, which provide CaO, and clays or shales, which furnish SiO_2 and Al_2O_3. These are ground, blended, fused to clinkers in a kiln, and cooled. Gypsum is added and the mixture is ground to the required fineness. In the United States, the material is shipped in bulk or in bags containing 42.6 kg of cement.

Over the years, five standard types of portland cement have been developed. Type I, *normal* portland cement, is used for over 90 percent of construction in the United States. Concretes made with Type I portland cement generally need one to two weeks to reach sufficient strength so that forms of beams and slabs can be removed and reasonable loads applied; they reach their design strength after 28 days and continue to gain strength thereafter at a decreasing rate. To speed construction when needed, *high early strength cements* such as Type III have been developed. They are costlier than ordinary portland cement, but within 7 to 14 days they reach the strength achieved using Type I at 28 days. Type III portland cement contains the same basic compounds as Type I, but the relative proportions differ and it is ground more finely.

[†] See ASTM C150, "Standard Specification for Portland Cement." This and other ASTM references are published and periodically updated by ASTM International (formerly the American Society for Testing and Materials), West Conshohoken, PA.

When cement is mixed with water to form a soft paste, it gradually stiffens until it becomes a solid. This process is known as *setting* and *hardening*. The cement is said to have set when it has gained sufficient rigidity to support an arbitrarily defined pressure, after which it continues for a long time to harden, i.e., to gain further strength. The water in the paste dissolves material at the surfaces of the cement grains and forms a gel that gradually increases in volume and stiffness. This leads to a rapid stiffening of the paste 2 to 4 hours after water has been added to the cement. *Hydration* continues to proceed deeper into the cement grains, at decreasing speed, with continued stiffening and hardening of the mass. The principal products of hydration are calcium silicate hydrate, which is insoluble, and calcium hydroxide, which is soluble.

In ordinary concrete, the cement is probably never completely hydrated. The gel structure of the hardened paste seems to be the chief reason for the volume changes that are caused in concrete by variations in moisture, such as the shrinkage of concrete as it dries.

For complete hydration of a given amount of cement, an amount of water equal to about 25 percent of that of cement, by weight—i.e., a *water-cement ratio* of 0.25—is needed chemically. An additional amount must be present, however, to provide mobility for the water in the cement paste during the hydration process so that it can reach the cement particles and to provide the necessary workability of the concrete mix. For normal concretes, the water-cement ratio is generally in the range of about 0.40 to 0.60, although for high-strength concretes, ratios as low as 0.21 have been used. In this case, the needed workability is obtained through the use of admixtures.

Any amount of water above that consumed in the chemical reaction produces pores in the cement paste. The strength of the hardened paste decreases in inverse proportion to the fraction of the total volume occupied by pores. Put differently, since only the solids, and not the voids, resist stress, strength increases directly as the fraction of the total volume occupied by the solids. That is why the strength of the cement paste depends primarily on, and decreases directly with, an increasing water-cement ratio.

The chemical process involved in the setting and hardening liberates heat, known as *heat of hydration*. In large concrete masses, such as dams, this heat is dissipated very slowly and results in a temperature rise and volume expansion of the concrete during hydration, with subsequent cooling and contraction. To avoid the serious cracking and weakening that may result from this process, special measures must be taken for its control.

2.3 AGGREGATES

In ordinary structural concretes the aggregates occupy 65 to 75 percent of the volume of the hardened mass. The remainder consists of hardened cement paste, uncombined water (i.e., water not involved in the hydration of the cement), and air voids. The latter two do not contribute to the strength of the concrete. In general, the more densely the aggregate can be packed, the better the durability and economy of the concrete. For this reason the gradation of the particle sizes in the aggregate, to produce close packing, is of considerable importance. It is also important that the aggregate have good strength, durability, and weather resistance; that its surface be free from impurities such as loam, clay, silt, and organic matter that may weaken the bond with cement paste; and that no unfavorable chemical reaction take place between it and the cement.

Natural aggregates are generally classified as fine and coarse. *Fine aggregate* (typically natural sand) is any material that will pass a 4.75 mm sieve, i.e., a sieve with square openings of dimension 4.75 mm. Material coarser than this is classified as *coarse aggregate*. When favorable gradation is desired, aggregates are separated by sieving into two or three size groups of sand and several size groups of coarse aggregate. These can then be combined according to grading charts to result in a densely packed aggregate. The *maximum size of coarse aggregate* in reinforced concrete is governed by the requirement that it shall easily fit into the forms and between the reinforcing bars. For this purpose it should not be larger than one-fifth of the narrowest dimension of the forms or one-third of the depth of slabs, nor three-quarters of the minimum distance between reinforcing bars. Requirements for satisfactory aggregates are found in ASTM C33, "Standard Specification for Concrete Aggregates," and authoritative information on aggregate properties and their influence on concrete properties, as well as guidance in selection, preparation, and handling of aggregate, is found in Ref. 2.1.

The unit weight of *stone concrete*, i.e., concrete with natural stone aggregate, varies from about 2240 to 2430 kg per cubic meter (kg/m^3) and can generally be assumed to be 2320 kg/m^3. For special purposes, lightweight concretes, on one hand, and heavy concretes, on the other, are used.

A variety of *lightweight* aggregates are available. Some unprocessed aggregates, such as pumice or cinders, are suitable for insulating concretes, but for structural lightweight concrete, *processed aggregates* are used because of better control. These consist of expanded shales, clays, slates, slags, or pelletized fly ash. They are light in weight because of the porous, cellular structure of the individual aggregate particle, which is achieved by gas or steam formation in processing the aggregates in rotary kilns at high temperatures (generally in excess of 1100°C). Requirements for satisfactory lightweight aggregates are found in ASTM C330, "Standard Specification for Lightweight Aggregates for Structural Concrete."

Three classes of lightweight concrete are distinguished in Ref. 2.2: low-density concretes, which are chiefly employed for insulation and whose unit weight rarely exceeds 800 kg/m^3; moderate strength concretes, with unit weights from about 960 to 1360 kg/m^3 and compressive strengths of 7 to 17 MPa, which are chiefly used as fill, e.g., over light-gage steel floor panels; and structural concretes, with unit weights from 1440 to 1920 kg/m^3 and compressive strengths comparable to those of stone concretes. Similarities and differences in structural characteristics of lightweight and stone concretes are discussed in Sections 2.8 and 2.9.

Heavyweight concrete is sometimes required for shielding against gamma and X-radiation in nuclear reactors and similar installations, for protective structures, and for special purposes, such as counterweights of lift bridges. Heavy aggregates are used for such concretes. These consist of heavy iron ores or barite (barium sulfate) rock crushed to suitable sizes. Steel in the form of scrap, punchings, or shot (as fines) is also used. Unit weights of heavyweight concretes with natural heavy rock aggregates range from about 3200 to 3680 kg/m^3; if iron punchings are added to high-density ores, weights as high as 4325 kg/m^3 are achieved. The weight may be as high as 5290 kg/m^3 if ores are used for the fines only and steel for the coarse aggregate.

2.4 PROPORTIONING AND MIXING CONCRETE

The various components of a mix are proportioned so that the resulting concrete has adequate strength, proper workability for placing, and low cost. The third calls for use of the minimum amount of cement (the most costly of the components) that will achieve adequate properties. The better the gradation of aggregates, i.e., the smaller the volume of voids, the less cement paste is needed to fill these voids. In addition to the water required for hydration, water is needed for wetting the surface of the aggregate. As water is added, the plasticity and fluidity of the mix increase (i.e., its workability improves), but the strength decreases because of the larger volume of voids created by the free water. To reduce the free water while retaining the workability, cement must be added. Therefore, as for the cement paste, the *water-cement ratio* is the chief factor that controls the strength of the concrete. For a given water-cement ratio, one selects the minimum amount of cement that will secure the desired workability.

Figure 2.1 shows the decisive influence of the water-cement ratio on the compressive strength of concrete. Its influence on the tensile strength, as measured by the nominal flexural strength or modulus of rupture, is seen to be pronounced but much

FIGURE 2.1
Effect of water-cement ratio on 28-day compressive and flexural tensile strength.
(*Adapted from Ref. 2.3.*)

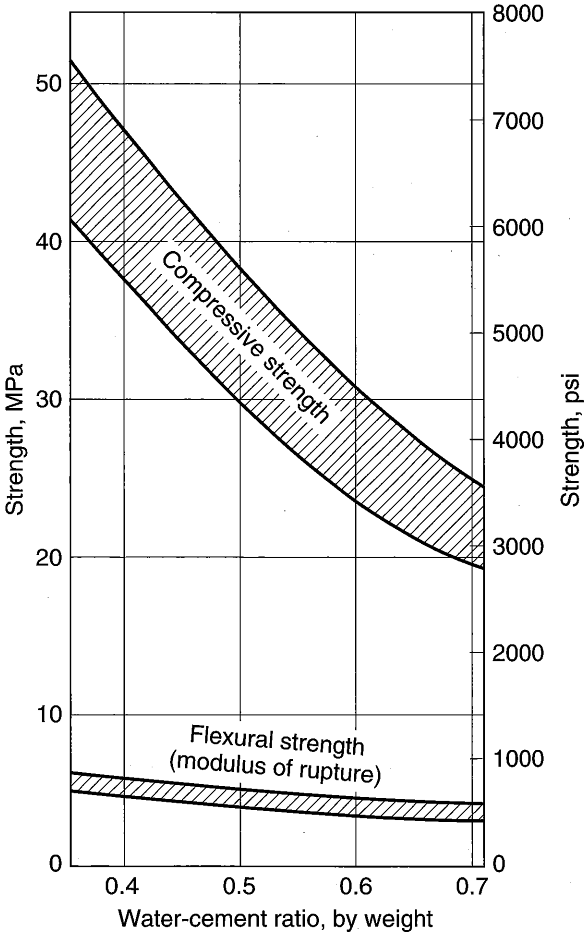

smaller than its effect on the compressive strength. This seems to be so because, in addition to the void ratio, the tensile strength depends strongly on the strength of bond between coarse aggregate and cement mortar (i.e., cement paste plus fine aggregate). According to tests at Cornell University, this bond strength is only slightly affected by the water-cement ratio (Ref. 2.4).

It is customary to define the *proportions* of a concrete mix in terms of the total weight of each component needed to make up 1 m^3 of wet concrete, such as 307 kg of cement, 178 kg of water, 753 kg of sand, and 1551 kg of coarse aggregate, plus the total volume of air, in percent, when air is deliberately *entrained* in the mix (typically 4 to 7 percent). The weights of the fine and coarse aggregates are based on material in the *saturated surface dry condition*, in which, as the description implies, the aggregates are fully saturated but have no water on the exterior of the particles.

Various methods of proportioning are used to obtain mixes of the desired properties from the cements and aggregates at hand. One is the *trial-batch method.* Selecting a water-cement ratio from information such as that in Fig. 2.1, one produces several small trial batches with varying amounts of aggregate to obtain the required strength, consistency, and other properties with a minimum amount of paste. Concrete *consistency* is most frequently measured by the *slump test.* A metal mold in the shape of a truncated cone 300 mm high is filled with fresh concrete in a carefully specified manner. Immediately upon being filled, the mold is lifted off, and the slump of the concrete is measured as the difference in height between the mold and the pile of concrete. The slump is a good measure of the total water content in the mix and should be kept as low as is compatible with workability. Slumps for concretes in building construction generally range from 50 to 130 mm, although higher slumps are used with the aid of chemical admixtures.

The so-called ACI method of proportioning makes use of the slump test in connection with a set of tables that, for a variety of conditions (types of structures, dimensions of members, degree of exposure to weathering, etc.), permit one to estimate proportions that will result in the desired properties (Ref. 2.5). These preliminary selected proportions are checked and adjusted by means of trial batches to result in concrete of the desired quality. Inevitably, strength properties of a concrete of given proportions scatter from batch to batch. It is therefore necessary to select proportions that will furnish an average strength sufficiently greater than the specified design strength for even the accidentally weaker batches to be of adequate quality (for details, see Section 2.6). Discussion in detail of practices for proportioning concrete is beyond the scope of this volume; this topic is treated fully in Refs. 2.5 and 2.6, both for stone concrete and for lightweight aggregate concrete.

If the results of trial batches or field experience are not available, the ACI Code allows concrete to be proportioned based on other experience or information, if approved by the registered design professional overseeing the project. This alternative may not be applied for specified compressive strengths greater than 35 MPa.

On all but the smallest jobs, *batching* is carried out in special batching plants. Separate hoppers contain cement and the various fractions of aggregate. Proportions are controlled, by weight, by means of manually operated or automatic scales connected to the hoppers. The mixing water is batched either by measuring tanks or by water meters.

The principal purpose of *mixing* is to produce an intimate mixture of cement, water, fine and coarse aggregate, and possible admixtures of uniform consistency throughout each batch. This is achieved in machine mixers of the revolving-drum type. Minimum mixing time is 1 min for mixers of not more than 1 m^3 capacity, with an additional 15 sec for each additional 1 m^3. Mixing can be continued for a considerable time without adverse effect. This fact is particularly important in connection with ready mixed concrete.

On large projects, particularly in the open country where ample space is available, movable mixing plants are installed and operated at the site. On the other hand, in construction under congested city conditions, on smaller jobs, and frequently in highway construction, *ready mixed concrete* is used. Such concrete is batched in a stationary plant and then hauled to the site in trucks in one of three ways: (1) mixed completely at the stationary plant and hauled in a truck agitator, (2) transit-mixed, i.e., batched at the plant but mixed in a truck mixer, or (3) partially mixed at the plant with mixing completed in a truck mixer. Concrete should be discharged from the mixer or agitator within a limited time after the water is added to the batch. Although specifications often provide a single value for all conditions, the maximum mixing time should be based on the concrete temperature because higher temperatures lead to increased rates of *slump loss* and rapid setting. Conversely, lower temperatures increase the period during which the concrete remains workable. A good guide for maximum mixing time is to allow 1 hour at a temperature of 24°C, plus (or minus) 15 min for each 2.8°C drop (or rise) in concrete temperature for concrete temperatures between 4 and 32°C. Ten minutes may be used at 35°C, the practical upper limit for normal mixing and placing.

Much information on proportioning and other aspects of design and control of concrete mixtures will be found in Refs. 2.7 and 2.8.

2.5 CONVEYING, PLACING, COMPACTING, AND CURING

Conveying of most building concrete from the mixer or truck to the form is done in bottom-dump buckets or by pumping through steel pipelines. The chief danger during conveying is that of *segregation*. The individual components of concrete tend to segregate because of their dissimilarity. In overly wet concrete standing in containers or forms, the heavier coarse aggregate particles tend to settle, and the lighter materials, particularly water, tend to rise. Lateral movement, such as flow within the forms, tends to separate the coarse gravel from the finer components of the mix.

Placing is the process of transferring the fresh concrete from the conveying device to its final place in the forms. Prior to placing, loose rust must be removed from reinforcement, forms must be cleaned, and hardened surfaces of previous concrete lifts must be cleaned and treated appropriately. Placing and consolidating are critical in their effect on the final quality of the concrete. Proper placement must avoid segregation, displacement of forms or of reinforcement in the forms, and poor bond between successive layers of concrete. Immediately upon placing, the concrete should be *consolidated*, usually by means of vibrators. Consolidation prevents honeycombing, ensures close contact with forms and reinforcement, and serves as a partial remedy to possible prior segregation. Consolidation is achieved by high-frequency, power-driven *vibrators*. These are of the *internal* type, immersed in the concrete, or of the *external* type, attached to the forms. The former are preferable but must be supplemented by the latter where narrow forms or other obstacles make immersion impossible (Ref. 2.9).

Fresh concrete gains strength most rapidly during the first few days and weeks. Structural design is generally based on the *28-day strength*, about 70 percent of which is reached at the end of the first week after placing. The final concrete strength depends greatly on the conditions of moisture and temperature during this initial period. The maintenance of proper conditions during this time is known as *curing*. Thirty percent of the strength or more can be lost by premature drying out of the concrete; similar amounts may be lost by permitting the concrete temperature to drop to 4°C or lower during the first few days unless the concrete is kept continuously moist for a long time thereafter. Freezing of fresh concrete may reduce its strength by 50 percent or more.

To prevent such damage, concrete should be protected from loss of moisture for at least 7 days and, in more sensitive work, up to 14 days. When high early strength cements are used, curing periods can be cut in half. Curing can be achieved by keeping exposed surfaces continually wet through sprinkling, ponding, or covering with plastic film or by the use of sealing compounds, which, when properly used, form evaporation-retarding membranes. In addition to improving strength, proper moist-curing provides better shrinkage control. To protect the concrete against low temperatures during cold weather, the mixing water, and occasionally the aggregates, is heated; temperature insulation is used where possible; and special admixtures are employed. When air temperatures are very low, external heat may have to be supplied in addition to insulation (Refs. 2.7, 2.8, 2.10, and 2.11).

2.6 QUALITY CONTROL

The quality of mill-produced materials, such as structural or reinforcing steel, is ensured by the producer, who must exercise systematic quality controls, usually specified by pertinent ASTM standards. Concrete, in contrast, is produced at or close to the site, and its final qualities are affected by a number of factors, which have been discussed briefly. Thus, systematic quality control must be instituted at the construction site.

The main measure of the structural quality of concrete is its *compressive strength.* Tests for this property are made on cylindrical specimens of height equal to twice the diameter, usually 150 × 300 mm or 100 × 200 mm. Impervious molds of this shape are filled with concrete during the operation of placement as specified by ASTM C172, "Standard Method of Sampling Freshly Mixed Concrete," and ASTM C31, "Standard Practice for Making and Curing Concrete Test Specimens in the Field." The cylinders are moist-cured at about 23°C, generally for 28 days, and then tested in the laboratory at a specified rate of loading. The compressive strength obtained from such tests is known as the *cylinder strength* f'_c and is the main property specified for design purposes.

To provide structural safety, continuous control is necessary to ensure that the strength of the concrete as furnished is in satisfactory agreement with the value called for by the designer. The ACI Code specifies that two 150 × 300 mm or three 100 × 200 mm cylinders must be tested for each 110 m^3 of concrete or for each 460 m^2 of surface area actually placed, but not less than once a day. As mentioned in Section 2.4, the results of strength tests of different batches mixed to identical proportions show inevitable scatter. The scatter can be reduced by closer control, but occasional tests below the cylinder strength specified in the design cannot be avoided.

To ensure adequate concrete strength in spite of such scatter, the ACI Code stipulates that concrete quality is satisfactory if

1. No individual strength test result (the average of two or three cylinder tests depending on cylinder size) falls below the required f'_c by more than 3.5 MPa when f'_c is 35 MPa or less or by more than $0.10f'_c$ when f'_c is more than 35 MPa, and
2. Every arithmetic average of any three consecutive strength tests equals or exceeds f'_c.

It is evident that if concrete were proportioned so that its mean strength were just equal to the required strength f'_c, it would not pass these quality requirements, because about one-half of its strength test results would fall below the required f'_c. It is

FIGURE 2.2
Frequency curves and average strengths for various degrees of control of concretes with specified design strength f_c'. *(Adapted from Ref. 2.12.)*

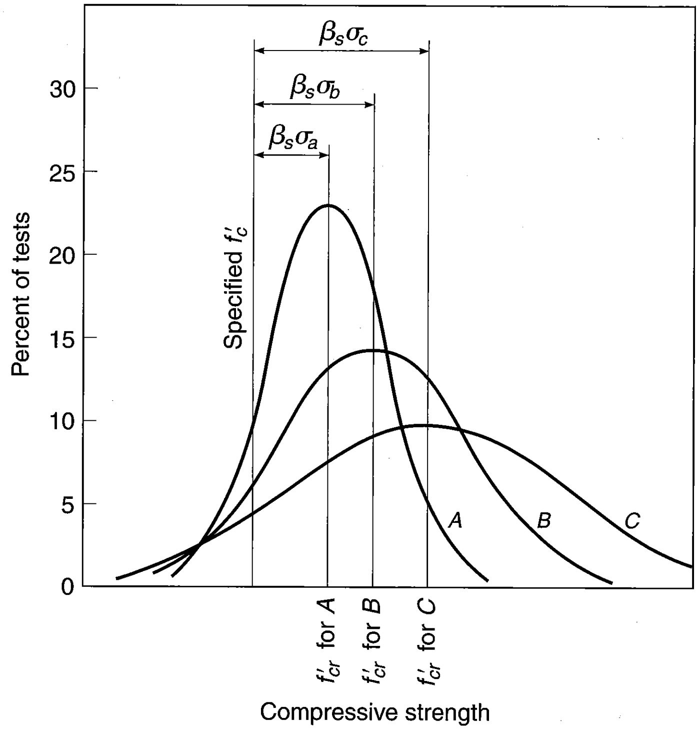

therefore necessary to proportion the concrete so that its mean strength f_{cr}', used as the basis for selection of suitable proportions, exceeds the required design strength f_c' by an amount sufficient to ensure that the two quoted requirements are met. The minimum amount by which the required mean strength must exceed f_c' can be determined only by statistical methods because of the random nature of test scatter. Requirements have been derived, based on statistical analysis, to be used as a guide to proper proportioning of the concrete at the plant so that the probability of strength deficiency at the construction site is acceptably low.

The basis for these requirements is illustrated in Fig. 2.2, which shows three normal frequency curves giving the distribution of strength test results. The specified design strength is f_c'. The curves correspond to three different degrees of quality control, curve A representing the best control, i.e., the least scatter, and curve C the worst control, with the most scatter. The degree of control is measured statistically by the standard deviation σ (σ_a for curve A, σ_b for curve B, and σ_c for curve C), which is relatively small for producer A and relatively large for producer C. All three distributions have the same probability of strength less than the specified value f_c'; i.e., each has the same fractional part of the total area under the curve to the left of f_c'. For any normal distribution curve, that fractional part is defined by the index β_s, a multiplier applied to the standard deviation σ; β_s is the same for all three distributions of Fig. 2.2. It is seen that, to satisfy the requirement that, say, 1 test in 100 will fall below f_c' (with the value of β_s thus determined), for producer A with the best quality control the mean strength f_{cr}' can be much closer to the specified f_c' than for producer C with the most poorly controlled operation.

On the basis of such studies, the ACI Code requires that concrete production facilities maintain records from which the standard deviation achieved in the particular facility can be determined. It then stipulates the minimum amount by which the required average compressive strength f'_{cr}, aimed at when selecting concrete proportions, must exceed the specified compressive strength f'_c. In accordance with ACI Code 5.3.1, the value of f'_{cr} is equal to the larger of the values in Eqs. (2.1) and (2.2).

$$f'_{cr} = f'_c + 1.34 s_s \tag{2.1}$$

or

$$f'_{cr} = \begin{cases} f'_c + 2.33 s_s - 3.5 & \text{for } f'_c \le 35 \text{ MPa} \quad (2.2a) \\ 0.9 f'_c + 2.33 s_s & \text{for } f'_c > 35 \text{ MPa} \quad (2.2b) \end{cases}$$

where s_s is the standard deviation of the test sample.

Equation (2.1) provides a probability of 1 in 100 that averages of three consecutive tests will be below the specified strength f'_c. Equations (2.2*a*) and (2.2*b*) provide a probability of 1 in 100 that an individual strength test will be more than 3.5 MPa below the specified f'_c for f'_c up to 35 MPa or below $0.90 f'_c$ for f'_c over 35 MPa.

To use Eqs. (2.1) and (2.2), ACI Code 5.3.1 requires that a minimum of 30 consecutive test results be available. The tests must represent concrete with (1) a specified compressive strength within 7 MPa of f'_c for the project and (2) materials, quality control, and conditions similar to those expected for the building in question. If fewer than 30 but at least 15 tests are available, the equations may still be used, but s_s must be multiplied by a factor from Table 2.1. If fewer than 15 tests have been made, the average strength must exceed f'_c by at least 7 MPa for f'_c less than or equal to 21 MPa, by at least 8.3 MPa for f'_c between 21 and 35 MPa, and by $0.10 f'_c + 5.0$ MPa for f'_c over 35 MPa, according to the ACI Code.

It is seen that this method of control recognizes the fact that occasional deficient batches are inevitable. The requirements for f'_{cr} ensure (1) a small probability that such strength deficiencies as are bound to occur will be large enough to represent a serious danger and (2) an equally small probability that a sizable portion of the structure, as represented by three consecutive strength tests, will be made of below-par concrete.

Both the requirements described earlier in this section for determining if concrete, as produced, is of satisfactory quality and the process just described of selecting f'_{cr} are based on the same basic considerations but are applied independently, as demonstrated in Examples 2.1 and 2.2.

TABLE 2.1

Modification factors for sample standard deviation s_s when less than 30 tests are available

No. of Tests[†]	Modification Factor for Sample Standard Deviation[‡]
Less than 15	See paragraph following Eqs. (2.1) and (2.2)
15	1.16
20	1.08
25	1.03
30 or more	1.00

[†] Interpolate for intermediate values.

[‡] The sample standard deviation s_s must be multiplied by the modification factor prior to use in Eqs. (2.1) and (2.2).

EXAMPLE 2.1

A building design calls for specified concrete strength f_c' of 28 MPa. Calculate the average required strength f_{cr}' if (*a*) 30 consecutive tests for concrete with similar strength and materials produce a sample standard deviation s_s of 3.7 MPa, (*b*) 15 consecutive tests for concrete with similar strength and materials produce a sample standard deviation s_s of 3.5 MPa, and (*c*) less than 15 tests are available.

Solution. (*a*) 30 tests available. Using $s_s = 3.7$ MPa, Eq. (2.1) gives

$$f_{cr}' = f_c' + 1.34s_s = 28 + 1.34 \times 3.7 = 33.0 \text{ MPa}^{\dagger}$$

Because the specified strength f_c' is less than 35 MPa, Eq. (2.2*a*) must be used.

$$f_{cr}' = f_c' + 2.33s_s - 3.5 = 28 + 2.33 \times 3.7 - 3.5 = 33.1 \text{ MPa}$$

The required average strength f_{cr}' is equal to the larger value, 33.1 MPa.

(*b*) 15 tests available. Because only 15 tests are available, s_s, given as 3.5 MPa, must be multiplied by 1.16, the factor from Table 2.1.

$$1.16 \times s_s = 1.16 \times 3.5 = 4.1 \text{ MPa}$$

Again, using Eqs. (2.1) and (2.2*a*),

$$f_{cr}' = 28 + 1.34 \times 4.1 = 33.5 \text{ MPa}$$

$$f_{cr}' = 28 + 2.33 \times 4.1 - 3.5 = 34.1 \text{ MPa}$$

The larger value, 34.1 MPa, is selected as the required average strength f_{cr}'.

(*c*) Less than 15 tests available. Because f_c' is between 21 and 35 MPa, the required average strength is

$$f_{cr}' = f_c' + 8.3 = 28 + 8.3 = 36.3 \text{ MPa}$$

This example demonstrates that in cases where test data are available, good quality control, represented by a low sample standard deviation s_s, can be used to reduce the required average strength f_{cr}'. The example also demonstrates that a lack of certainty in the value of the standard deviation due to the limited availability of data results in higher values for f_{cr}', as shown in parts (*b*) and (*c*). As additional test results become available, the higher safety margins can be reduced.

EXAMPLE 2.2

The first eight compressive strength test results for the building described in Example 2.1*c* are 32.6, 29.5, 27.2, 30.1, 35.7, 33.5, 34.3, and 33.4 MPa.

(*a*) Are the test results satisfactory, and (*b*) in what fashion, if any, should the mixture proportions of the concrete be altered?

Solution.

(*a*) For concrete to be considered satisfactory, no individual test may fall below $f_c' - 3.5$ MPa and every arithmetic average of any three consecutive tests must equal f_c'. The eight tests meet these criteria. No test is less than $f_c' - 3.5 \text{ MPa} = 28 - 3.5 = 24.5$ MPa, and the average of all sets of three consecutive tests exceeds f_c' [for example, $(32.6 + 29.5 + 27.2)/3 = 29.8$, $(29.5 + 27.2 + 30.1)/3 = 28.9$, etc.].

(*b*) To determine if the mixture proportions must be altered, we note that the solution to Example 2.1*c* requires that f_{cr}' equal or exceed 36.3 MPa. The average of the first eight tests is 32.0 MPa, well below the value of f_{cr}'. Thus, the mixture proportions should be modified by decreasing the water-cement ratio to increase the concrete strength. Once at least 15 tests are available, the value of f_{cr}' can be recalculated using Eqs. (2.1) and (2.2) with the

---

[†] ASTM International specifies that concrete cylinder strengths be recorded to the nearest 0.1 MPa. Hence the values used for test results and f_{cr}' are rounded accordingly.

appropriate factor for s_s from Table 2.1. The mixture proportions can then be adjusted based on the new value of f'_{cr}, the strength of the concrete being produced, and the level of quality control, as represented by the sample standard deviation s_s.

In spite of scientific advances, building in general and concrete making in particular retain some elements of an art; they depend on many skills and imponderables. It is the task of systematic *inspection* to ensure close correspondence between plans and specifications and the finished structure. Inspection during construction should be carried out by a competent engineer, preferably the one who produced the design or one who is responsible to the design engineer. The inspector's main functions in regard to materials quality control are sampling, examination, and field testing of materials; control of concrete proportioning; inspection of batching, mixing, conveying, placing, compacting, and curing; and supervision of the preparation of specimens for laboratory tests. In addition, the inspector must inspect foundations, formwork, placing of reinforcing steel, and other pertinent features of the general progress of work; keep records of all the inspected items; and prepare periodic reports. The importance of thorough inspection to the correctness and adequate quality of the finished structure cannot be emphasized too strongly.

This brief account of concrete technology represents the merest outline of an important subject. Anyone in practice who is actually responsible for any of the phases of producing and placing concrete must be familiar with the details in much greater depth.

2.7 ADMIXTURES

In addition to the main components of concretes, *admixtures* are often used to improve concrete performance. There are admixtures to accelerate or retard setting and hardening, to improve workability, to increase strength, to improve durability, to decrease permeability, and to impart other properties (Ref. 2.13). The beneficial effects of particular admixtures are well established. Chemical admixtures should meet the requirements of ASTM C494, "Standard Specification for Chemical Admixtures for Concrete."

Air-entraining agents are probably the most commonly used admixtures. They cause the entrainment of air in the form of small dispersed bubbles in the concrete. These improve workability and durability (chiefly resistance to freezing and thawing) and reduce segregation during placing. They decrease concrete density because of the increased void ratio and thereby decrease strength; however, this decrease can be partially offset by a reduction of mixing water without loss of workability. The chief use of air-entrained concretes is in pavements, but they are also used for structures, particularly for exposed elements (Ref. 2.14).

Accelerating admixtures are used to reduce setting time and accelerate early strength development. Calcium chloride is the most widely used accelerator because of its cost effectiveness, but it should not be used in prestressed concrete and should be used with caution in reinforced concrete in a moist environment, because of its tendency to promote corrosion of steel. Nonchloride, noncorrosive accelerating admixtures are available, the principal one being calcium nitrite (Ref. 2.13).

Set-retarding admixtures are used primarily to offset the accelerating effect of high ambient temperature and to keep the concrete workable during the entire placing period. This helps to eliminate cracking due to form deflection and also keeps concrete workable long enough that succeeding lifts can be placed without the development of "cold" joints.

Certain organic compounds are used to reduce the water requirement of a concrete mix for a given slump. Such compounds are termed *plasticizers*. Reduction in water demand may result in either a reduction in the water-cement ratio for a given slump and cement content or an increase in slump for the same water-cement ratio and cement content. Plasticizers work by reducing the interparticle forces that exist between cement grains in the fresh paste, thereby increasing the paste fluidity. High-range water-reducing admixtures, or *superplasticizers*, are used to produce high-strength concrete (see Section 2.12) with a very low water-cement ratio while maintaining the higher slumps needed for proper placement and compaction of the concrete. They are also used to produce flowable concrete at conventional water-cement ratios. Superplasticizers differ from conventional water-reducing admixtures in that they do not act as retarders at high dosages; therefore, they can be used at higher dosage rates without severely slowing hydration (Refs. 2.13, 2.15, and 2.16). The specific effects of water-reducing admixtures vary with different cements, changes in water-cement ratio, mixing temperature, ambient temperature, and other job conditions, and trial batches are generally required.

When superplasticizers are combined with *viscosity-modifying admixtures*, they can be used to produce *self-consolidating concrete* (SCC). Self-consolidating concrete is highly fluid and does not require vibration to remove entrapped air. The viscosity modifying agents allow the concrete to remain cohesive even with a very high degree of fluidity. As a result, SCC can be used for members with congested reinforcement, such as beam-column joints in earthquake-resistant structures, and is widely used for precast concrete, especially precast prestressed concrete, a manufactured product (prestressed concrete is discussed in Chapter 19). The high fluidity of the mix, however, has been shown to have a negative impact on the bond strength between the concrete and prestressing steel located in the upper portions of a member, a shortcoming that should be considered in design (Ref. 2.17) but is not currently addressed in the ACI Code, and the composition of SCC mixtures may result in moduli of elasticity, creep, and shrinkage properties that differ from those of more traditional mixtures.

Fly ash and *silica fume* are pozzolans, highly active silicas, that combine with calcium hydroxide, the soluble product of cement hydration (Section 2.2), to form more calcium silicate hydrate, the insoluble product of cement hydration (Refs. 2.18 and 2.19). Pozzolans qualify as *supplementary cementitious materials*, also referred to as *mineral admixtures*, which are used to replace a part of the portland cement in concrete mixes. Fly ash, which is specified under ASTM C618, "Standard Specification for Coal Fly Ash and Raw or Calcified Natural Pozzolan for Use in Concrete," is precipitated electrostatically as a by-product of the exhaust fumes of coal-fired power stations. It is very finely divided and reacts with calcium hydroxide in the presence of moisture to form a cementitious material. It tends to increase the strength of concrete at ages over 28 days. Silica fume, which is specified under ASTM C1240, "Standard Specification for Silica Fume Used in Cementitious Mixtures," is a by-product resulting from the manufacture, in electric-arc furnaces, of ferro-silicon alloys and silicon metal. It is extremely finely divided and is highly cementitious when combined with portland cement. In contrast to fly ash, silica fume contributes mainly to strength gain at early ages, from 3 to 28 days. Both fly ash and silica fume, particularly the latter, have been important in the production of high-strength concrete (see Section 2.12).

Ground granulated blast-furnace slag (GGBFS), which is specified under ASTM C989, "Standard Specification for Ground Granulated Blast-Furnace Slag for Use in Concrete and Mortar," is another supplementary cementitious material. It is produced by water quenching and grinding slag from the production of pig iron, the key ingredient used to make steel (Ref. 2.20). GGBFS consists primarily of calcium silicates, making it very similar to portland cement. As a result of the similarity, slag can be used in higher quantities than fly ash or silica fume, and the resulting material generally has similar or improved properties to those exhibited by concrete made with 100 percent portland cement.

When blast furnace slag, silica fume, fly ash, or a combination is used, it is customary to refer to the *water–cementitious material ratio* rather than the water-cement ratio. This typically may be as low as 0.25 for high-strength concrete, and ratios as low as 0.21 have been used (Refs. 2.21 and 2.22).

Historically, the high durability and high thermal mass of concrete structures have played a key role in *sustainable development*, that is, development that minimizes both its impact on the environment and the resources used both during and after construction. In sustainable development, the "cost" of concrete lies primarily in the manufacture of portland cement. The production of a ton of portland cement requires roughly the energy needed to operate a typical U.S. household for two weeks and generates approximately 0.9 ton of CO_2 (a greenhouse gas). The latter translates to about 150 kg of CO_2 for every cubic meter of concrete that is placed. The energy and greenhouse gases involved in the production of concrete, however, can be viewed as investments because properly designed reinforced concrete structures that take advantage of concrete's thermal mass provide significant reductions in the energy and CO_2 needed for heating and cooling, and concrete's inherent durability results in structures with long service lives. Because by-products, such as the mineral admixtures fly ash and blast furnace slag, involve minimal energy usage or greenhouse gas production, they have the potential to further improve the sustainability of concrete construction when used as a partial replacement for portland cement.

2.8 PROPERTIES IN COMPRESSION

a. Short-Term Loading

Performance of a structure under load depends to a large degree on the stress-strain relationship of the material from which it is made, under the type of stress to which the material is subjected in the structure. Since concrete is used mostly in compression, its compressive stress-strain curve is of primary interest. Such a curve is obtained by appropriate strain measurements in cylinder tests (Section 2.6) or on the compression side in beams. Figure 2.3 shows a typical set of such curves for normal-density concrete, obtained from uniaxial compressive tests performed at normal, moderate testing speeds on concretes that are 28 days old. Figure 2.4 shows corresponding curves for lightweight concretes having a density of 1600 kg/m^3.

All of the curves have somewhat similar character. They consist of an initial relatively straight elastic portion in which stress and strain are closely proportional, then begin to curve to the horizontal, reaching the maximum stress, i.e., the compressive strength, at a strain that ranges from about 0.002 to 0.003 for normal-density concretes, and from about 0.003 to 0.0035 for lightweight concretes (Refs. 2.23 and 2.24), the larger values in each case corresponding to the higher strengths. All curves show a descending branch after the peak stress is reached; however, the characteristics of the curves after peak stress are highly dependent upon the method of testing. If special procedures are followed in testing to ensure a constant strain rate while cylinder resistance is decreasing, long stable descending branches can be obtained (Ref. 2.25). In the absence of special devices, unloading past the point of peak stress

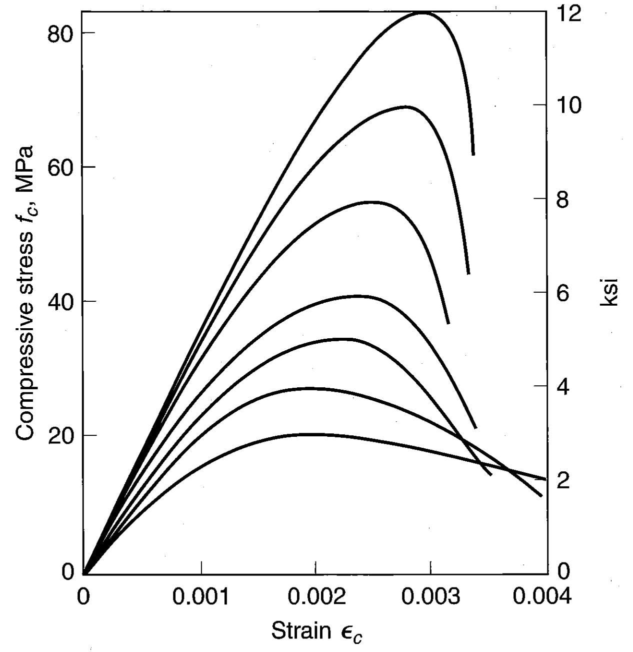

FIGURE 2.3

Typical compressive stress-strain curves for normal-density concrete with $w_c = 2300\ \mathrm{kg/m^3}$. *(Adapted from Refs. 2.23 and 2.24.)*

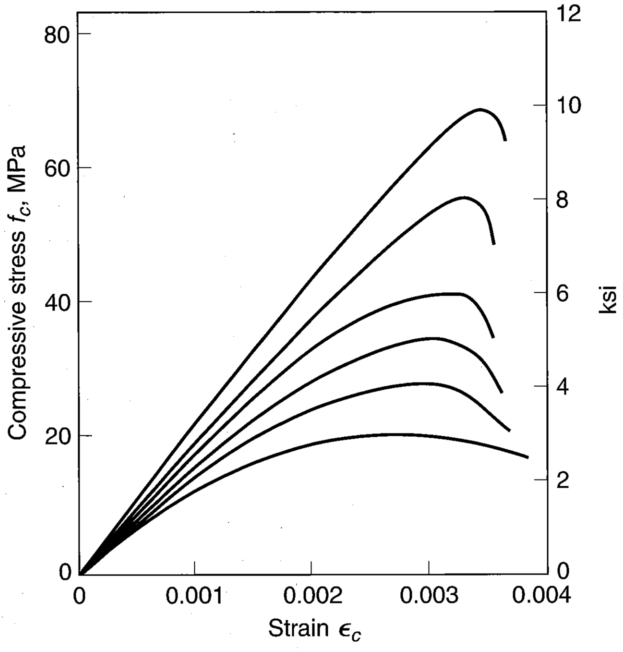

FIGURE 2.4

Typical compressive stress-strain curves for lightweight concrete with $w_c = 1600\ \mathrm{kg/m^3}$. *(Adapted from Refs. 2.23 and 2.24.)*

may be rapid, particularly for the higher-strength concretes, which are generally more brittle than low-strength concrete.

In present practice, the specified compressive strength f'_c is commonly in the range from 21 to 35 MPa for normal-density cast-in-place concrete, and up to about 55 MPa for precast prestressed concrete members. Lightweight concrete strengths are somewhat below these values generally. The high-strength concretes, with f'_c to 100 MPa or more, are used with increasing frequency, particularly for heavily loaded columns in high-rise concrete buildings and for long-span bridges (mostly prestressed) where a significant reduction in dead load may be realized by minimizing member cross section dimensions. (See Section 2.12.)

The *modulus of elasticity* E_c (in MPa), i.e., the slope of the initial straight portion of the stress-strain curve, is seen to be larger as the strength of the concrete increases. For concretes in the strength range to about 42 MPa, it can be computed with reasonable accuracy from the empirical equation found in the ACI Code

$$E_c = 0.043 w_c^{1.5} \sqrt{f'_c} \tag{2.3}$$

where w_c is the unit weight of the hardened concrete in $\mathrm{kg/m^3}$ and f'_c is its strength in MPa. Equation (2.3) was obtained by testing structural concretes with values of w_c from 1440 to 2560 $\mathrm{kg/m^3}$. For normal sand-and-stone concretes, with w_c about 2300 $\mathrm{kg/m^3}$, E_c may be taken as

$$E_c = 4700\sqrt{f'_c} \tag{2.4}$$

For compressive strengths in the range from 42 to 84 MPa, the ACI Code equation may overestimate E_c for both normalweight and lightweight material by as much as 20 percent. Based on research at Cornell University (Refs. 2.23 and 2.24), the following equation is recommended for normal-density concretes with f'_c in the range of 21 to 84 MPa, and for lightweight concretes from 21 to 62 MPa:

$$E_c = (3320\sqrt{f'_c} + 6900)\left(\frac{w_c}{2300}\right)^{1.5} \tag{2.5}$$

where terms and units are as defined above for the ACI Code equations. When coarse aggregates with high moduli of elasticity are used, however, Eq. (2.4) may *underestimate* E_c. Thus, in cases where E_c is a key design criterion, it should be measured, rather than estimated, using Eq. (2.3), (2.4), or (2.5).

Information on concrete strength properties such as those discussed is usually obtained through tests made 28 days after placing. However, cement continues to hydrate, and consequently concrete continues to harden, long after this age, at a decreasing rate. Figure 2.5 shows a typical curve of the gain of concrete strength with age for concrete made using Type I (normal) cement and also Type III (high early strength) cement, each curve normalized with respect to the 28-day compressive strength. High early strength cements produce more rapid strength gain at early ages, although the rate of strength gain at later ages is generally less. Concretes using Type III cement are often used in precasting plants, and often the strength f'_c is specified at 7 days, rather than 28 days.

Note that the shape of the stress-strain curve for various concretes of the same cylinder strength, and even for the same concrete under various conditions of loading, varies considerably. An example of this is shown in Fig. 2.6, where different specimens of the same concrete are loaded at different rates of strain, from one corresponding to a relatively fast loading (0.001 per minute) to one corresponding to an extremely slow application of load (0.001 per 100 days). It is seen that the descending branch of the curve, indicative of internal disintegration of the material, is much more pronounced at fast than at slow rates of loading. It is also seen that the peaks of the curves, i.e., the maximum strengths reached, are somewhat smaller at slower rates of strain.

When compressed in one direction, concrete, like other materials, expands in the direction transverse to that of the applied stress. The ratio of the transverse to the longitudinal strain is known as *Poisson's ratio* and depends somewhat on strength, composition, and other factors. At stresses lower than about $0.7f'_c$, Poisson's ratio for concrete falls within the limits of 0.15 to 0.20.

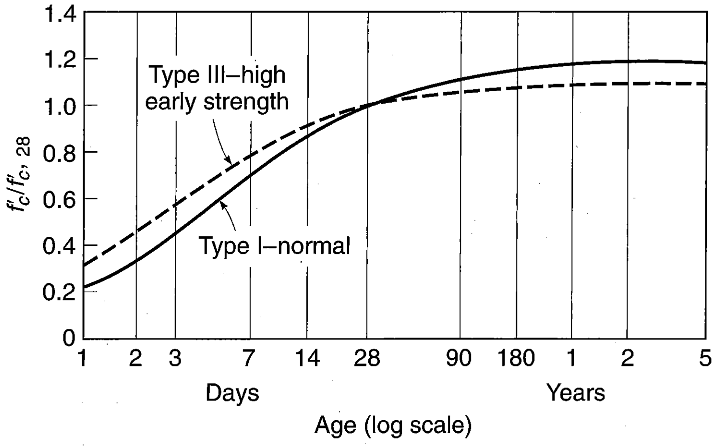

FIGURE 2.5
Effect of age on compressive strength f'_c for moist-cured concrete. (*Adapted from Ref. 2.26.*)

FIGURE 2.6
Stress-strain curves at various strain rates, concentric compression. (*Adapted from Ref. 2.27.*)

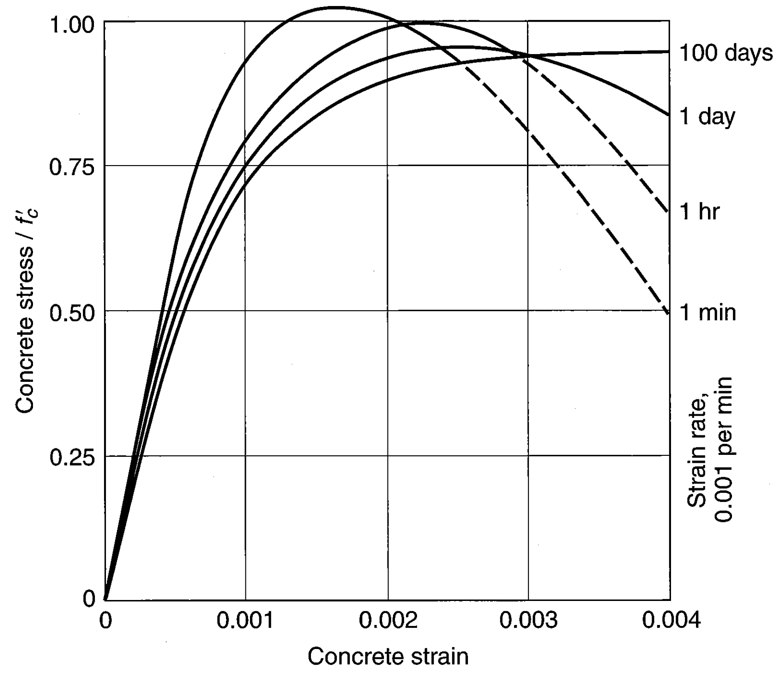

b. Long-Term Loading

In some engineering materials, such as steel, strength and the stress-strain relationships are independent of rate and duration of loading, at least within the usual ranges of rate of stress, temperature, and other variables. In contrast, Fig. 2.6 illustrates the fact that the influence of time, in this case of rate of loading, on the behavior of concrete under load is pronounced. The main reason is that concrete creeps under load, while steel does not exhibit creep under conditions prevailing in buildings, bridges, and similar structures.

Creep is the slow deformation of a material over considerable lengths of time at constant stress or load. The nature of the creep process is shown schematically in Fig. 2.7. This particular concrete was loaded after 28 days with resulting instantaneous strain ϵ_{inst}. The load was then maintained for 230 days, during which time creep was seen to have increased the total deformation to almost 3 times its instantaneous value. If the load were maintained, the deformation would follow the solid curve. If the load is removed, as shown by the dashed curve, most of the elastic instantaneous strain ϵ_{inst} is recovered, and some creep recovery is seen to occur. If the concrete is reloaded at some later date, instantaneous and creep deformations develop again, as shown.

Creep deformations for a given concrete are practically proportional to the magnitude of the applied stress; at any given stress, and even at the same ratio of stress to compressive strength, high-strength concretes show less creep than lower-strength concretes (Ref. 2.28). As seen in Fig. 2.7, with elapsing time, creep proceeds at a decreasing rate and ceases after 2 to 5 years at a final value which, depending on concrete strength and other factors, is about 1.2 to 3 times the magnitude of the instantaneous strain. If, instead of being applied quickly and thereafter kept constant, the load is increased slowly and gradually, as is the case in many structures during and after construction, then instantaneous and creep deformations proceed simultaneously.

FIGURE 2.7
Typical creep curve (concrete loaded to 4.1 MPa at age 28 days).

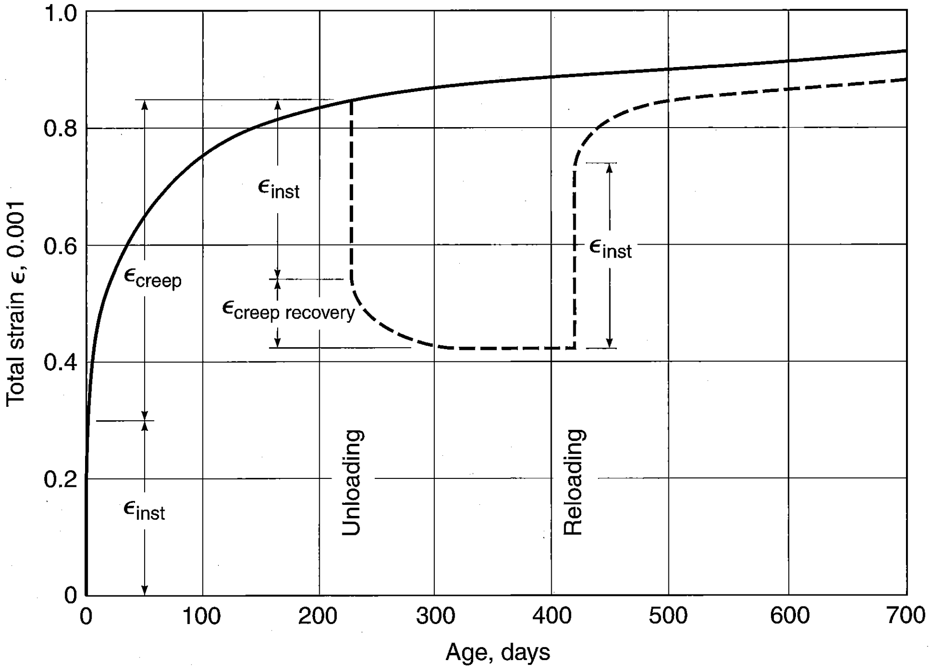

The effect is shown in Fig. 2.6; i.e., the previously discussed difference in the shape of the stress-strain curve for various rates of loading is chiefly the result of the creep deformation of concrete.

For stresses not exceeding about one-half the cylinder strength, creep strains are approximately proportional to stress. Because initial elastic strains are also proportional to stress in this range, this permits definition of the *creep coefficient*

$$C_{cu} = \frac{\epsilon_{cu}}{\epsilon_{ci}} \tag{2.6}$$

where ϵ_{cu} is the final asymptotic value of the additional creep strain and ϵ_{ci} is the initial, instantaneous strain when the load is first applied. Creep may also be expressed in terms of the *specific creep* δ_{cu}, defined as the additional time-dependent strain per MPa stress. It can easily be shown that

$$C_{cu} = E_c \delta_{cu} \tag{2.7}$$

In addition to the stress level, creep depends on the average ambient relative humidity, being more than twice as large for 50 percent as for 100 percent humidity (Ref. 2.8). This is so because part of the reduction in volume under sustained load is caused by outward migration of free pore water, which evaporates into the surrounding atmosphere. Other factors of importance include the type of cement and aggregate, age of the concrete when first loaded, and concrete strength (Ref. 2.8). The creep coefficient for high-strength concrete is much less than that for low-strength concrete. However, sustained load stresses are apt to be higher so that the creep *deformation* may be as great for high-strength concrete, even though the creep coefficient is less.

The values of Table 2.2, quoted from Ref. 2.29 and extended for high-strength concrete based on research at Cornell University, are typical values for average humidity conditions, for concretes loaded at the age of 7 days.

TABLE 2.2
Typical creep parameters

Compressive Strength		Specific Creep δ_{cu}		
MPa	psi	10^{-6} per MPa	10^{-6} per psi	Creep coefficient C_{cu}
21	3,000	145	1.00	3.1
28	4,000	116	0.80	2.9
41	6,000	80	0.55	2.4
55	8,000	58	0.40	2.0
69	10,000	41	0.28	1.6
83	12,000	33	0.22	1.4

To illustrate, if the concrete in a column with $f_c' = 28$ MPa is subject to a long-time load that causes sustained stress of 8.3 MPa, then after several years under load the final value of the creep strain will be about $8.3 \times 116 \times 10^{-6} = 0.00096$. Thus, if the column were 6 m long, creep would shorten it by about 6 mm.

The creep coefficient at any time C_{ct} can be related to the ultimate creep coefficient C_{cu}. In Ref. 2.26, Branson suggests the equation

$$C_{ct} = \frac{t^{0.60}}{10 + t^{0.60}} C_{cu} \tag{2.8}$$

where t = time in days after loading.

In many special situations, e.g., slender members or frames, or in prestressed construction, the designer must take account of the combined effects of creep and shrinkage (Section 2.11). In such cases, rather than rely on the sample values of Table 2.2, more accurate information on creep parameters should be obtained, such as from Ref. 2.26 or 2.29.

Sustained loads affect not only the deformation but also the strength of concrete. The cylinder strength f_c' is determined at normal rates of test loading (about 0.25 MPa/sec). Tests by Rüsch (Ref. 2.27) and at Cornell University (Refs. 2.30 and 2.31) have shown that, for concentrically loaded unreinforced concrete prisms and cylinders, the *strength under sustained load* is significantly smaller than f_c', on the order of 75 percent of f_c' for loads maintained for a year or more. Thus, a member subjected to a sustained overload causing compressive stress of over 75 percent of f_c' may fail after a period of time, even though the load is not increased.

c. Fatigue

When concrete is subject to fluctuating rather than sustained loading, its *fatigue strength*, as for all other materials, is considerably smaller than its static strength. When plain concrete in compression is stressed cyclically from zero to maximum stress, its fatigue limit is from 50 to 60 percent of the static compressive strength, for 2,000,000 cycles. A reasonable estimate can be made for other stress ranges using the modified Goodman diagram (see Ref. 2.29). For other types of applied stress, such as flexural compressive stress in reinforced concrete beams or flexural tension in unreinforced beams or on the tension side of reinforced beams, the fatigue limit likewise appears to be about 55 percent of the corresponding static strength. These figures, however, are for general guidance only. It is known that the fatigue strength of concrete depends not only on its static strength but also on moisture condition, age, and rate of loading (see Ref. 2.32).

2.9 PROPERTIES IN TENSION

While concrete is best employed in a manner that uses its favorable compressive strength, its behavior in tension is also important. The conditions under which cracks form and propagate on the tension side of reinforced concrete flexural members depend strongly on both the tensile strength and the fracture properties of the concrete, the latter dealing with the ease with which a crack progresses once it has formed. Concrete tensile stresses also occur as a result of shear, torsion, and other actions, and in most cases member behavior changes upon cracking. Thus, it is important to be able to predict, with reasonable accuracy, the tensile strength of concrete and to understand the factors that control crack propagation.

a. Tensile Strength

There are considerable experimental difficulties in determining the true tensile strength of concrete. In *direct tension* tests, minor misalignments and stress concentrations in the gripping devices are apt to mar the results. For many years, tensile strength has been measured in terms of the *modulus of rupture* f_r, the computed flexural tensile stress at which a test beam of plain concrete fractures. Because this nominal stress is computed on the assumption that concrete is an elastic material, and because this bending stress is localized at the outermost surface, it is apt to be larger than the strength of concrete in uniform axial tension. It is thus a measure of, but not identical with, the real axial tensile strength.

More recently the result of the *split-cylinder test* has established itself as a measure of the tensile strength of concrete. A concrete cylinder, the same as is used for compressive tests, is inserted in a compression testing machine in the horizontal position, so that compression is applied uniformly along two opposite generators. Pads are inserted between the compression platens of the machine and the cylinder to equalize and distribute the pressure. It can be shown that in an elastic cylinder so loaded, a nearly uniform tensile stress of magnitude $2P/(\pi dL)$ exists at right angles to the plane of load application. Correspondingly, such cylinders, when tested, split into two halves along that plane, at a stress f_{ct} that can be computed from the above expression. P is the applied compressive load at failure, and d and L are the diameter and length of the cylinder, respectively. Because of local stress conditions at the load lines and the presence of stresses at right angles to the aforementioned tension stresses, the results of the split-cylinder tests likewise are not identical with (but are believed to be a good measure of) the true axial tensile strength. The results of all types of tensile tests show considerably more scatter than those of compression tests.

Tensile strength, however determined, does not correlate well with the compressive strength f_c'. It appears that for sand-and-gravel concrete, the tensile strength depends primarily on the strength of bond between hardened cement paste and aggregate, whereas for lightweight concretes it depends largely on the tensile strength of the porous aggregate. The compressive strength, on the other hand, is much less determined by these particular characteristics.

Better correlation is found between the various measures of tensile strength and the square root of the compressive strength. The direct tensile strength, for example, ranges from about 0.25 to $0.58\sqrt{f_c'}$ for normal-density concretes, and from about 0.17 to $0.25\sqrt{f_c'}$ for all-lightweight concrete. Typical ranges of values for direct tensile strength, split-cylinder strength, and modulus of rupture are summarized in Table 2.3. In these expressions, f_c' is expressed in MPa, and the resulting tensile strengths are obtained in MPa.

These approximate expressions show that tensile and compressive strengths are by no means proportional, and that any increase in compressive strength, such as that achieved by lowering the water-cement ratio, is accompanied by a much smaller percentage increase in tensile strength.

The ACI Code recommends that the modulus of rupture f_r be taken to equal $0.62\sqrt{f_c'}$ for normalweight concrete, and that this value be multiplied by 0.85 for "sand-lightweight" and 0.75 for "all-lightweight" concretes, giving values of $0.53\sqrt{f_c'}$ and $0.46\sqrt{f_c'}$, respectively, for those materials.

b. Tensile Fracture

The failure of concrete in tension involves both the formation and the propagation of cracks. The field of fracture mechanics deals with the latter. While reinforced concrete structures have been successfully designed and built for over 150 years without the use of fracture mechanics, the brittle response of high-strength concretes (Section 2.12), in tension as well as compression, increases the importance of the fracture properties of the material as distinct from tensile strength. Research dealing with the shear strength of high-strength concrete beams and the bond between reinforcing steel and high-strength concrete indicates relatively low increases in these structural properties with increases in concrete compressive strength (Refs. 2.33 and 2.34). While shear and bond strength are associated with the $\sqrt{f_c'}$ for normal-strength concrete, tests of high-strength concrete indicate that increases in shear and bond strengths are well below values predicted using $\sqrt{f_c'}$, indicating that concrete tensile strength alone is not the governing factor. An explanation for this behavior is provided by research at the University of Kansas and elsewhere (Refs. 2.35 and 2.36) that demonstrates that the energy required to fully open a crack (i.e., after the crack has started to grow) is largely independent of compressive strength, water-cement ratio, and age. Design expressions reflecting this research are not yet available. The behavior is, however, recognized in the ACI Code by limitations on the maximum value of $\sqrt{f_c'}$ that may be used to calculate shear and bond strength, as will be discussed in Chapters 4 and 5.

TABLE 2.3
Approximate range of tensile strengths of concrete

	Normalweight Concrete, MPa	Lightweight Concrete, MPa
Direct tensile strength f_t'	0.25 to $0.58\sqrt{f_c'}$	0.17 to $0.25\sqrt{f_c'}$
Split-cylinder strength f_{ct}	0.50 to $0.66\sqrt{f_c'}$	0.33 to $0.50\sqrt{f_c'}$
Modulus of rupture f_r	0.66 to $1.00\sqrt{f_c'}$	0.50 to $0.66\sqrt{f_c'}$

2.10 STRENGTH UNDER COMBINED STRESS

In many structural situations, concrete is subjected simultaneously to various stresses acting in various directions. For instance, in beams much of the concrete is subject simultaneously to compression and shear stresses, and in slabs and footings to compression in two perpendicular directions plus shear. By methods well known from the study of engineering mechanics, any state of combined stress, no matter how complex, can be reduced to three principal stresses acting at right angles to one another on an appropriately oriented elementary cube in the material. Any or all of the principal stresses can be either tension or compression. If any one of them is zero, a state of *biaxial* stress is said to exist; if two of them are zero, the state of stress is *uniaxial*, either simple compression or simple tension. In most cases, only the uniaxial strength properties of a material are known from simple tests, such as the cylinder strength f_c' and the tensile strength f_t'. For predicting the strengths of structures in which concrete is subject to biaxial or triaxial stress, it would be desirable to be able to calculate the strength of concrete in such states of stress, knowing from tests only either f_c' or f_c' and f_t'.

In spite of extensive and continuing research, no general theory of the strength of concrete under combined stress has yet emerged. Modifications of various strength theories, such as maximum stress, maximum strain, the Mohr-Coulomb, and the octahedral shear stress theories, all of which are discussed in structural mechanics texts, have been adapted with varying partial success to concrete. At present, none of these theories has been generally accepted, and many have obvious internal contradictions. The main difficulty in developing an adequate general strength theory lies in the highly nonhomogeneous nature of concrete, and in the degree to which its behavior at high stresses and at fracture is influenced by microcracking and other discontinuity phenomena (Refs. 2.8 and 2.37).

However, the strength of concrete has been well established by tests, at least for the biaxial stress state (Refs. 2.38 and 2.39). Results may be presented in the form of an interaction diagram such as Fig. 2.8, which shows the strength in direction 1 as a function of the stress applied in direction 2. All stresses are normalized in terms of the uniaxial compressive strength f_c'. It is seen that in the quadrant representing biaxial compression a strength increase as great as about 20 percent over the uniaxial compressive strength is attained, the amount of increase depending upon the ratio of f_2 to f_1. In the biaxial tension quadrant, the strength in direction 1 is almost independent of stress in direction 2. When tension in direction 2 is combined with compression in direction 1, the compressive strength is reduced almost linearly, and vice versa. For example, lateral compression of about one-half the uniaxial compressive strength will reduce the tensile strength by almost one-half compared with its uniaxial value. This fact is of great importance in predicting diagonal tension cracking in deep beams or shear walls, for example.

Experimental investigations into the triaxial strength of concrete have been few, due mainly to the practical difficulty of applying load in three directions simultaneously without introducing significant restraint from the loading equipment (Ref. 2.40). From information now available, the following conclusions can be drawn relative to the triaxial strength of concrete: (1) in a state of equal triaxial compression, concrete strength may be an order of magnitude larger than the uniaxial compressive strength; (2) for equal biaxial compression combined with a smaller value of compression in the third direction, a strength increase greater than 20 percent can be expected; and (3) for stress states including compression combined with tension in at least one other direction, the intermediate principal stress is of little consequence, and the compressive strength can be predicted safely based on Fig. 2.8.

FIGURE 2.8
Strength of concrete in biaxial stress. (*Adapted from Ref. 2.39.*)

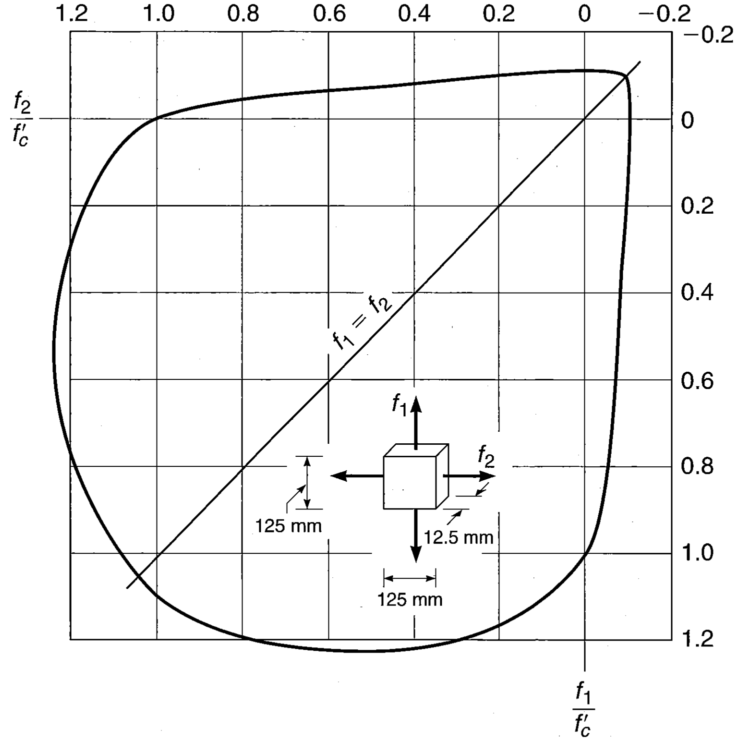

In fact, the strength of concrete under combined stress cannot yet be calculated rationally, and, equally important, in many situations in concrete structures it is nearly impossible to calculate all of the acting stresses and their directions; these are two of the main reasons for continued reliance on tests. Because of this, the design of reinforced concrete structures continues to be based more on extensive experimental information than on consistent analytical theory, particularly in the many situations where combined stresses occur.

2.11 SHRINKAGE AND TEMPERATURE EFFECTS

The deformations discussed in Section 2.8 were induced by stresses caused by external loads. Influences of a different nature cause concrete, even when free of any external loading, to undergo deformations and volume changes. The most important of these are shrinkage and the effects of temperature variations.

a. Shrinkage

As discussed in Sections 2.2 and 2.4, any workable concrete mix contains more water than is needed for hydration. If the concrete is exposed to air, the larger part of this free water evaporates in time, the rate and completeness of drying depending on ambient temperature and humidity conditions. As the concrete dries, it shrinks in volume, due initially to the capillary tension that develops in the water remaining in the concrete (Ref. 2.8). Conversely, if dry concrete is immersed in water, it expands, regaining much of the volume loss from prior shrinkage. Shrinkage, which continues at a decreasing rate for several months, depending on the configuration of the member, is a detrimental property of concrete in several respects. When not adequately controlled, it will cause unsightly and often deleterious cracks, as in slabs, walls, etc. In structures that are statically indeterminate (and most concrete structures are), it can cause large and harmful stresses. In prestressed concrete it leads to partial loss of initial prestress. For these reasons it is essential that shrinkage be minimized and controlled.

As is clear from the nature of the process, a key factor in determining the amount of final shrinkage is the unit water content of the fresh concrete. This is illustrated in Fig. 2.9, which shows the amount of shrinkage for varying amounts of mixing water. The same aggregates were used for all tests, but in addition to and independently of the water content, the amount of cement was also varied from 223 to 613 kg/m^3 of concrete. This very large variation of cement content causes a 20 to 30 percent variation in shrinkage strain for water contents between 150 to 210 kg/m^3, the range used for most structural concretes. Increasing the cement content increases the cement paste constituent of the concrete, where the shrinkage actually takes place, while reducing the aggregate content. Since most aggregates do not contribute to shrinkage, an increase in aggregate content can significantly decrease shrinkage. This is shown in Fig. 2.10, which compares the shrinkage of concretes with various aggregate contents with the shrinkage obtained for neat cement paste (cement and water alone). For example, increasing the aggregate content from 71 to 74 percent (at the same water-cement ratio) results in a 20 percent reduction in shrinkage (Ref. 2.29). Increased aggregate content may be obtained through the use of (1) a larger maximum size coarse aggregate (which also reduces the water content required for a given workability), (2) a concrete with lower workability, and (3) chemical admixtures to increase

FIGURE 2.9
Effect of water content on drying shrinkage. (*From Ref. 2.3.*)

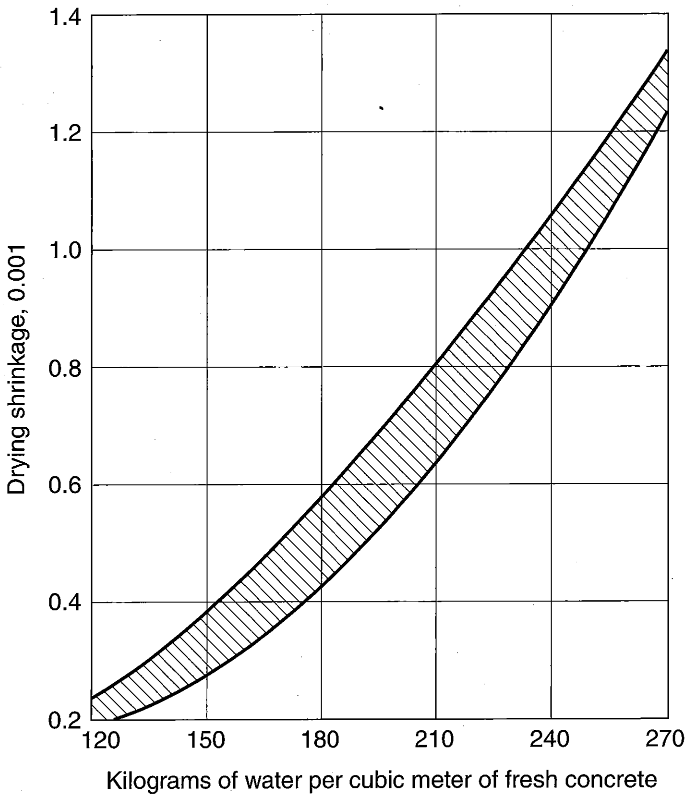

FIGURE 2.10
Influence of aggregate content in concrete (by volume) on the ratio of the shrinkage of concrete to the shrinkage of neat cement paste. (*Adapted from Ref. 2.29, based on data in Ref. 2.41.*)

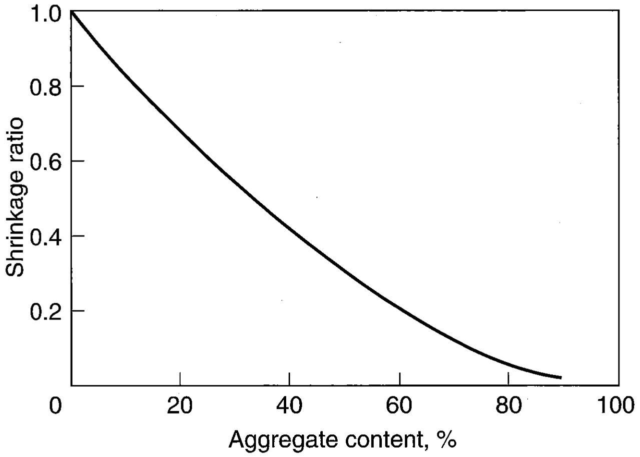

workability at lower water contents. It is evident that an effective means of reducing shrinkage involves both a reduction in water content and an increase in aggregate content. In addition, prolonged and careful curing is beneficial for shrinkage control.

Values of final shrinkage for ordinary concretes are generally on the order of 400×10^{-6} to 800×10^{-6}, depending on the initial water content, ambient temperature and humidity conditions, and the nature of the aggregate. Highly absorptive aggregates with low moduli of elasticity, such as some sandstones and slates, result in shrinkage values 2 or more times those obtained with less absorptive materials, such as granites and some limestones. Some lightweight aggregates, in view of their great porosity, easily result in much larger shrinkage values than ordinary concretes.

For some purposes, such as predicting the time-dependent loss of force in prestressed concrete beams, it is important to estimate the amount of shrinkage as a function of time. Long-term studies (Ref. 2.26) show that, for moist-cured concrete at any time t after the initial 7 days, shrinkage can be predicted satisfactorily by the equation

$$\epsilon_{sh,t} = \frac{t}{35 + t}\epsilon_{sh,u} \tag{2.9}$$

where $\epsilon_{sh,t}$ is the unit shrinkage strain at time t in days and $\epsilon_{sh,u}$ is the ultimate value after a long period of time. Equation (2.9) pertains to "standard" conditions, defined in Ref. 2.26 to exist for humidity not in excess of 40 percent and for an average thickness of member of 150 mm, and it applies both for normalweight and lightweight concretes. Modification factors are applied for nonstandard conditions, and separate equations are given for steam-cured members.

For structures in which a reduction in cracking is of particular importance, such as bridge decks, pavement slabs, and liquid storage tanks, the use of *expansive cement concrete* is appropriate. Shrinkage-compensating cement is constituted and proportioned such that the concrete will increase in volume after setting and during hardening. When the concrete is restrained by reinforcement or other means, the tendency to expand will result in compression. With subsequent drying, the shrinkage so produced, instead of causing a tension stress in the concrete that would result in cracking, merely reduces or relieves the expansive strains caused by the initial expansion (Ref. 2.42). Expansive cement is produced by adding a source of reactive aluminate to ordinary portland cement; approximately 90 percent of shrinkage-compensating cement is made up of the constituents of conventional portland cement.

Of the three main types of expansive cements produced, only type K is commercially available in the United States; it is about 20 percent more expensive than ordinary portland cement (Ref. 2.43). Requirements for expansive cement are given in ASTM C845, "Standard Specification for Expansive Hydraulic Cement." The usual admixtures can be used in shrinkage-compensating concrete, but trial mixes are necessary because some admixtures, particularly air-entraining agents, are not compatible with certain expansive cements.

b. Effect of Temperature Change

Like most other materials, concrete expands with increasing temperature and contracts with decreasing temperature. The effects of such volume changes are similar to those caused by shrinkage; i.e., temperature contraction can lead to objectionable cracking, particularly when superimposed on shrinkage. In indeterminate structures, deformations due to temperature changes can cause large and occasionally harmful stresses.

The coefficient of thermal expansion and contraction varies somewhat, depending upon the type of aggregate and richness of the mix. It is generally within the range of 7×10^{-6} to 12.5×10^{-6} per °C. A value of 9.9×10^{-6} is generally accepted as satisfactory for calculating stresses and deformations caused by temperature changes (Ref. 2.8).

2.12 HIGH-STRENGTH CONCRETE

There are a number of applications in which *high-strength concrete* will provide improved structural performance. Although the exact definition is arbitrary, the term generally refers to concrete having uniaxial compressive strength in the range of about 56 to 138 MPa or higher. Such concretes can be made using carefully selected but widely available cements, sands, and stone; certain admixtures including high-range water-reducing superplasticizers, fly ash, and silica fume; plus very careful quality control during production (Refs. 2.44 and 2.45). In addition to higher strength in compression, most other engineering properties are improved, leading to use of the alternative term *high-performance concrete.*

The most common application of high-strength concretes has been in the columns of tall concrete buildings, where normal concrete would result in unacceptably large cross sections, with loss of valuable floor space. It has been shown that the use of the more expensive high-strength concrete mixes in columns not only saves floor area but also is more economical than increasing the amount of steel reinforcement. Concrete of up to138 MPa was specified for the lower-story columns of 311 South Wacker Drive in Chicago (see Fig. 2.11), a pioneering structure with a total height of 288 m. Formerly holding the height record, it has been superseded by taller buildings; the present record is held by the tallest building and the tallest structure of any type in the world, the Burj Khalifa in Dubai, United Arab Emirates, shown in Fig. 18.2, which has a total height in excess of 790 m.

For bridges, too, smaller cross sections bring significant advantages, and the resulting reduction in dead load permits longer spans. The higher elastic modulus and lower creep coefficient result in reduced initial and long-term deflections, and in the case of prestressed concrete bridges, initial and time-dependent losses of prestress force are less. Other recent applications of high-strength concrete include offshore oil structures, parking garages, bridge deck overlays, dam spillways, warehouses, and heavy industrial slabs (Ref. 2.46).

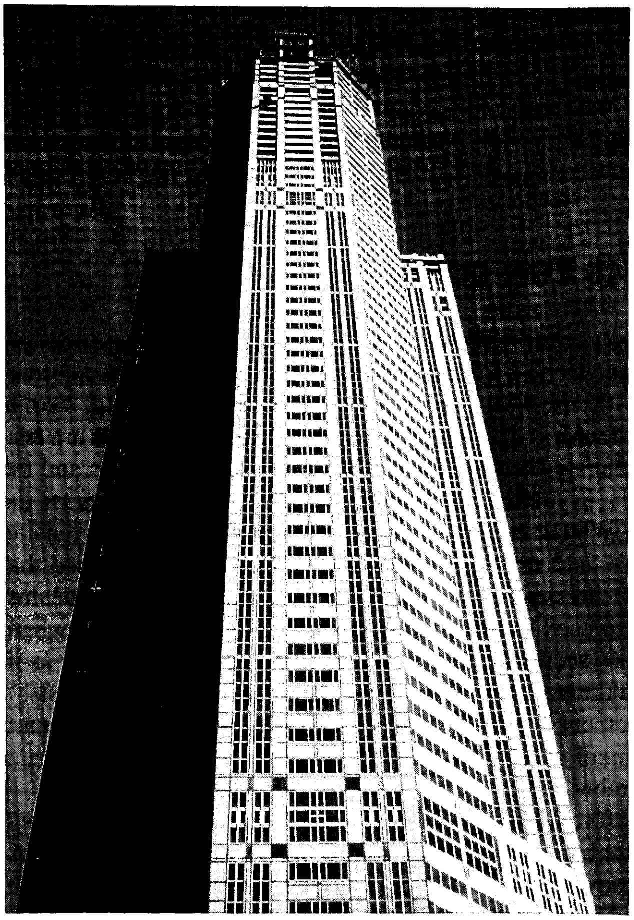

FIGURE 2.11
311 South Wacker Drive, Chicago, which is among the world's tallest buildings. High-strength concrete with $f_c' =$ 84 MPa was used in the lower stories. (*Courtesy of Portland Cement Association.*)

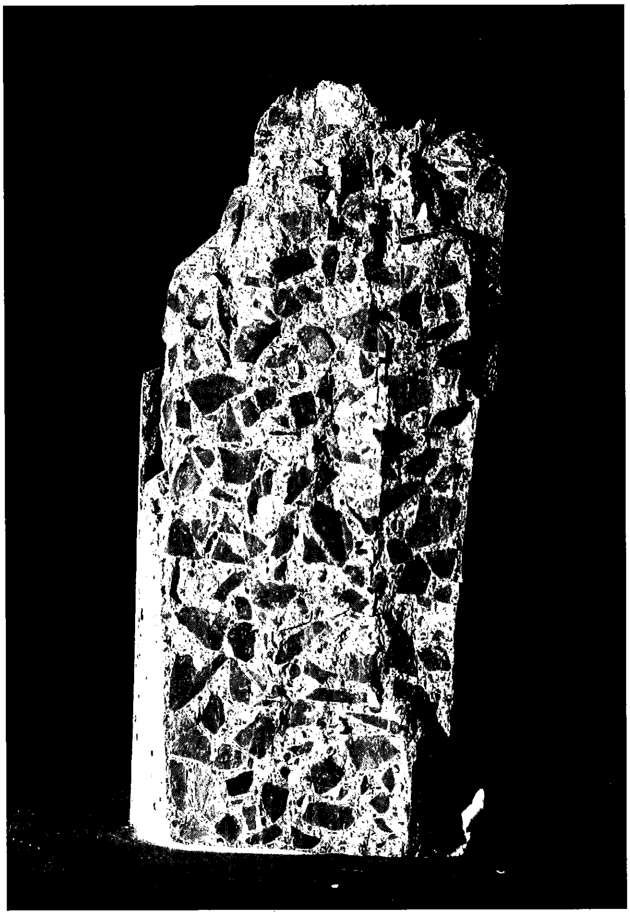

FIGURE 2.12
High-strength concrete test cylinder after uniaxial loading to failure; note the typically smooth fracture surface, with little aggregate interlock.

An essential requirement for high-strength concrete is a low water–cementitious material ratio. For normal concretes, this usually falls in the range from about 0.40 to 0.60 by weight, but for high-strength mixes it may be 0.25 or even lower. To permit proper placement of what would otherwise be a zero slump mix, high-range water-reducing admixtures, or superplasticizers, are essential and may increase slumps to as much as 150 or 200 mm. Other additives include fly ash and, most notably, silica fume (see Section 2.7).

Much research in recent years has been devoted to establishing the fundamental and engineering properties of high-strength concretes, as well as the engineering characteristics of structural members made with the material (Refs. 2.33, 2.34, and 2.47 to 2.53). A large body of information is now available, permitting the engineer to use high-strength concrete with confidence when its advantages justify the higher cost. The compressive strength curves in Figs. 2.3 and 2.4 illustrate important differences compared with normal concrete, including a higher elastic modulus and an extended range of linear elastic response. Creep coefficients are reduced, as indicated in Table 2.2. Disadvantages include brittle behavior in compression (see Fig. 2.12), somewhat reduced ultimate strain capacity, and an increased tendency to crack when drying shrinkage is restrained (Ref. 2.54), the latter resulting from the lower creep exhibited by the material. Strength under sustained load is a higher fraction of standard cylinder strength (Refs. 2.30 and 2.31), and high-strength concrete exhibits improved durability and abrasion resistance (Refs. 2.51 and 2.55). As broader experience is gained in practical applications, and as design codes are gradually updated to recognize the special properties of higher-strength concretes now available, much wider use can be expected.

2.13 REINFORCING STEELS FOR CONCRETE

The useful strength of ordinary reinforcing steels in tension as well as compression, i.e., the yield strength, is about 15 times the compressive strength of common structural concrete and well over 100 times its tensile strength. On the other hand, steel is a high-cost material compared with concrete. It follows that the two materials are best used in combination if the concrete is made to resist the compressive stresses and the steel the tensile stresses. Thus, in reinforced concrete beams, the concrete resists the compressive force, longitudinal steel reinforcing bars are located close to the tension face to resist the tension force, and usually additional steel bars are so disposed that they resist the inclined tension stresses that are caused by the shear force in the beams. However, reinforcement is also used for resisting compressive forces primarily where it is desired to reduce the cross-sectional dimensions of compression members, as in the lower-floor columns of multistory buildings. Even if no such necessity exists, a minimum amount of reinforcement is placed in all compression members to safeguard them against the effects of small accidental bending moments that might crack and even fail an unreinforced member.

For most effective reinforcing action, it is essential that steel and concrete deform together, i.e., that there be a sufficiently strong *bond* between the two materials to ensure that no relative movements of the steel bars and the surrounding concrete occur. This bond is provided by the relatively large *chemical adhesion* that develops at the steel-concrete interface, by the *natural roughness* of the mill scale of hot-rolled reinforcing bars and by the closely spaced rib-shaped *surface deformations* with which reinforcing bars are furnished to provide a high degree of interlocking of the two materials.

Additional features that make for the satisfactory joint performance of steel and concrete are the following:

1. The *thermal expansion coefficients* of the two materials, about 11.7×10^{-6} for steel vs. an average of 9.9×10^{-6} for concrete, are sufficiently close to forestall cracking and other undesirable effects of differential thermal deformations.
2. While the *corrosion resistance* of bare steel is poor, the concrete that surrounds the steel reinforcement provides excellent corrosion protection, minimizing corrosion problems and corresponding maintenance costs.
3. The *fire resistance* of unprotected steel is impaired by its high thermal conductivity and by the fact that its strength decreases sizably at high temperatures. Conversely, the thermal conductivity of concrete is relatively low. Thus, damage caused by even prolonged fire exposure, if any, is generally limited to the outer layer of concrete, and a moderate amount of concrete cover provides sufficient thermal insulation for the embedded reinforcement.

Steel is used in two different ways in concrete structures: as reinforcing steel and as prestressing steel. Reinforcing steel is placed in the forms prior to casting of the concrete. Stresses in the steel, as in the hardened concrete, are caused only by the loads on the structure, except for possible parasitic stresses from shrinkage or similar causes. In contrast, in prestressed concrete structures, large tension forces are applied to the reinforcement prior to letting it act jointly with the concrete in resisting external loads. The steels for these two uses are very different and will be discussed separately.

2.14 REINFORCING BARS

The most common type of reinforcing steel (as distinct from prestressing steel) is in the form of round bars, often called *rebars*, available in a large range of diameters from about 9.5 to 36 mm for ordinary applications and in two heavy bar sizes of about 43 and 57 mm. These bars are furnished with surface deformations for the purpose of increasing resistance to slip between steel and concrete. Minimum requirements for these deformations (spacing, projection, etc.) have been developed in experimental research. Different bar producers use different patterns, all of which satisfy these requirements. Figure 2.13 shows a variety of current types of deformations.

For many years, bar sizes have been designated by numbers, Nos. 3 to 11 being commonly used and Nos. 14 and 18 representing the two special large-sized bars previously mentioned. Designation by number, instead of by diameter, was introduced because the surface deformations make it impossible to define a single easily measured value of the diameter. The numbers are so arranged that the unit in the number designation corresponds closely to the number of $\frac{1}{8}$ in. of diameter size. A No. 5 bar, for example, has a nominal diameter of $\frac{5}{8}$ in. Bar sizes are rolled into the surface of the bars for easy identification.

For a number of years, however, ASTM standards have included a second designation for bar size, the International System of Units (SI), with the size being identified using the nominal diameter in millimeters. To limit the number of bar designations, reinforcing bar producers in the United States have converted to SI for marking the bars. Thus, Nos. 3 to 11 bars are marked with Nos. 10 to 36, and Nos. 14 and 18 bars with Nos. 43 and 57. Both systems are still used in the ASTM standards, and the

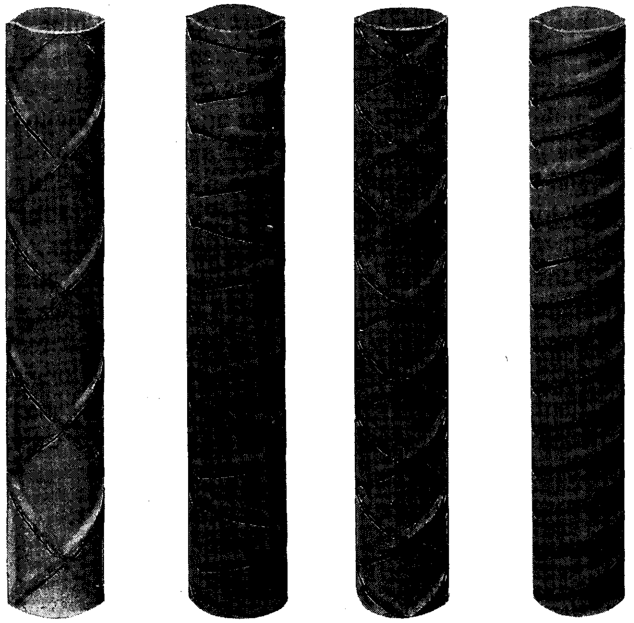

FIGURE 2.13
Types of deformed reinforcing bars.

older, customary system is used in the 2008 ACI Code, while the SI system is used in the SI version of the Code, ACI 318M. To recognize the dual system of identifying and marking the bars, the SI designation system is used throughout this text, followed by the inch-pound designations in parentheses, such as No. 19 (No. 6). Table A.1 of Appendix A gives areas and masses of standard bars. Tables A.2 and A.3 give similar information for groups of bars.

a. Grades and Strengths

In reinforced concrete, a long-term trend is evident toward the use of higher-strength materials, both steel and concrete. Reinforcing bars with 280 MPa yield stress, once standard, have largely been replaced by bars with 420 MPa yield stress, both because they are more economical and because their use tends to reduce steel congestion in the forms. Bars with a yield stress of 520 MPa are often used in columns, and bars with a yield stress of 690 MPa are allowed to be used as confining reinforcement. Table 2.4 lists all presently available reinforcing steels, their grade designations, the ASTM specifications that define their properties (including deformations) in detail, and their two main minimum specified strength values. Grade 280 bars are no longer available in sizes larger than No. 19 (No. 6) and Grade 350 bars are available in sizes up to No. 25 (No. 8).[†]

Welding of reinforcing bars in making splices, or for convenience in fabricating reinforcing cages for placement in the forms, may result in metallurgical changes that reduce both strength and ductility, and special restrictions must be placed both on the type of steel used and the welding procedures. The provisions of ASTM A706 relate specifically to welding.

The ACI Code permits reinforcing steels up to $f_y = 550$ MPa for most applications. Such high-strength steels usually yield gradually but have no yield plateau (see Fig. 2.15). In this situation it is required that at the specified minimum yield strength the total strain not exceed 0.0035. This is necessary to make current design methods, which were developed for sharp-yielding steels with a yield plateau, applicable to such higher-strength steels. Under special circumstances, steel in this higher-strength range has its place, e.g., in lower-story columns of high-rise buildings.

To allow bars of various grades and sizes to be easily distinguished, which is necessary to avoid accidental use of lower-strength or smaller-size bars than called for in the design, all deformed bars are furnished with rolled-in markings. These identify the producing mill (usually with an initial), the bar size (Nos. 10 to 57 under the SI and Nos. 3 to 18 under the inch-pound system), the type of steel (*S* for carbon steel, *W* for low-alloy steel, a rail sign for rail steel, *A* for axle steel, and *CS* for low-carbon chromium steel, corresponding, respectively, to ASTM Specifications A615, A706, A996 for both rail and axle steel, and A1035), and an additional marking to identify higher-strength steels. Grade 420 (60) bars have either one longitudinal line or the number 4 (60); Grade 520 (75) bars have either two longitudinal lines or the number 5 (75); Grade 690 (100) bars have either three longitudinal bars or the number 6 (100). The identification marks are shown in Fig. 2.14. As mentioned earlier, SI markings are used exclusively for bars rolled by mills in the United States.

[†] In practice, very little Grade 350 reinforcement is produced.

TABLE 2.4
Summary of minimum ASTM strength requirements

Product	ASTM Specification	Designation	Minimum Yield Strength, MPa (psi)	Minimum Tensile Strength, MPa (psi)
Reinforcing bars	A615	Grade 280	280 (40,000)	420 (60,000)
		Grade 420	420 (60,000)	620 (90,000)
		Grade 520	520 (75,000)	690 (100,000)
	A706	Grade 420	420 (60,000) [540 (78,000) maximum]	550 (80,000)[a]
	A996	Grade 280	280 (40,000)	420 (60,000)
		Grade 350	350 (50,000)	550 (80,000)
		Grade 420	420 (60,000)	620 (90,000)
	A1035	Grade 690	690 (100,000)	1030 (150,000)
Deformed bar mats	A184	Same as reinforcing bars		
Zinc-coated bars	A767	Same as reinforcing bars		
Epoxy-coated bars	A775, A934	Same as reinforcing bars		
Stainless-steel bars[b]	A955	Same as reinforcing bars		
Wire				
Plain	A82		480 (70,000)	550 (80,000)
Deformed	A496		515 (75,000)	585 (85,000)
Welded wire reinforcement				
Plain	A185			
W1.2 and larger			450 (65,000)	515 (75,000)
Smaller than W1.2			385 (56,000)	485 (70,000)
Deformed	A497		480 (70,000)	550 (80,000)
Prestressing tendons				
Seven-wire strand	A416	Grade 1725 (stress-relieved)	1465 (212,500)	1725 (250,000)
		Grade 1725 (low-relaxation)	1555 (225,000)	1725 (250,000)
		Grade 1860 (stress-relieved)	1580 (229,500)	1860 (270,000)
		Grade 1860 (low-relaxation)	1675 (243,000)	1860 (270,000)
Wire	A421	Stress-relieved	1375 (199,750) to 1465 (212,500)[c]	1620 (235,000) to 1725 (250,000)[c]
		Low-relaxation	1455 (211,500) to 1550 (225,000)[c]	1620 (235,000) to 1725 (250,000)[c]
Bars	A722	Type I (plain)	800 (127,500)	1035 (150,000)
		Type II (deformed)	825 (120,000)	1035 (150,000)
Compacted strand[b]	A779	Type 1700	1480 (241,900)	1700 (247,000)
		Type 1800	1575 (228,800)	1810 (263,000)
		Type 1860	1620 (234,900)	1860 (270,000)

[a] But not less than 1.25 times the actual yield strength.

[b] Not listed in ACI 318.

[c] Minimum strength depends on wire size.

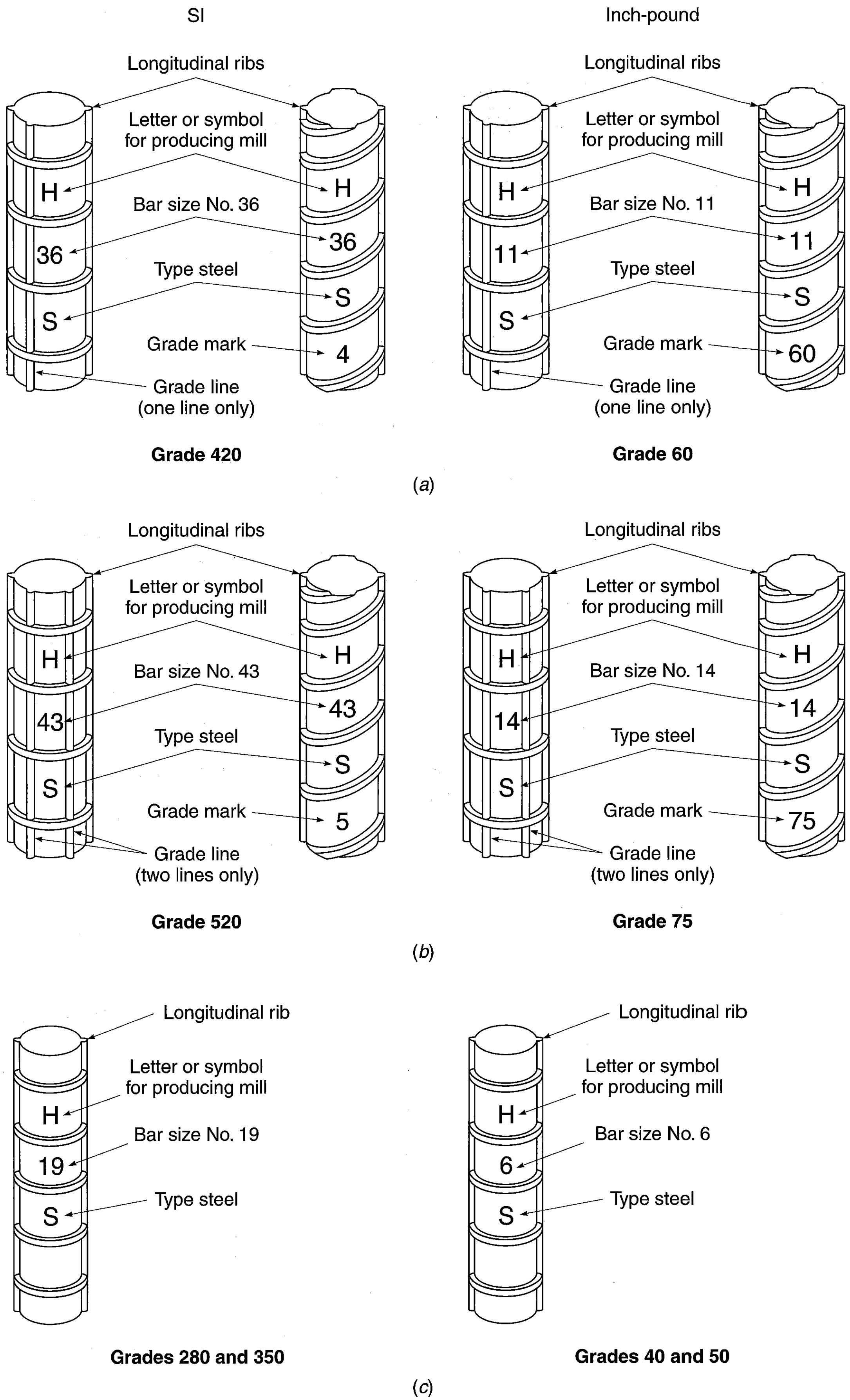
SI
Inch-pound
Longitudinal ribs
Letter or symbol for producing mill
Bar size No. 36
Type steel
Grade mark
Grade line (one line only)
H
36
S
4
Grade 420
Longitudinal ribs
Letter or symbol for producing mill
Bar size No. 11
Type steel
Grade mark
Grade line (one line only)
H
11
S
60
Grade 60
(a)
Longitudinal ribs
Letter or symbol for producing mill
Bar size No. 43
Type steel
Grade mark
Grade line (two lines only)
H
43
S
5
Grade 520
Longitudinal ribs
Letter or symbol for producing mill
Bar size No. 14
Type steel
Grade mark
Grade line (two lines only)
H
14
S
75
Grade 75
(b)
Longitudinal rib
Letter or symbol for producing mill
Bar size No. 19
Type steel
H
19
S
Grades 280 and 350
Longitudinal rib
Letter or symbol for producing mill
Bar size No. 6
Type steel
H
6
S
Grades 40 and 50
(c)

FIGURE 2.14
Marking system for reinforcing bars meeting ASTM Specifications A615, A706, and A996: (*a*) Grades 420 and 60; (*b*) Grades 520 and 75; (*c*) Grades 280, 350, 40, and 50. (*Adapted from Ref. 2.56.*) (Facing page.)

b. Stress-Strain Curves

The two chief numerical characteristics that determine the character of bar reinforcement are its *yield point* (generally identical in tension and compression) and its *modulus of elasticity* E_s. The latter is practically the same for all reinforcing steels (but not for prestressing steels) and is taken as $E_s = 200{,}000$ MPa.

In addition, however, the shape of the stress-strain curve, and particularly of its initial portion, has significant influence on the performance of reinforced concrete members. Typical stress-strain curves for U.S. reinforcing steels are shown in Fig. 2.15. The complete stress-strain curves are shown in the left part of the figure; the right part gives the initial portions of the curves magnified 10 times.

Low-carbon steels, typified by the Grade 280 curve, show an elastic portion followed by a *yield plateau*, i.e., a horizontal portion of the curve where strain continues to increase at constant stress. For such steels, the yield point is that stress at which the yield plateau establishes itself. With further strains, the stress begins to increase again, though at a slower rate, a process that is known as *strain-hardening*. The curve flattens out when the *tensile strength* is reached; it then turns down until fracture occurs. Higher-strength carbon steels, e.g., those with 420 MPa yield stress or higher, either have a yield plateau of much shorter length or enter strain-hardening immediately without any continued yielding at constant stress. In the latter case, the ACI Code specifies that the yield stress f_y be the stress corresponding to a strain of 0.0035, as shown in Fig. 2.15. Low-alloy, high-strength steels rarely show any yield plateau and usually enter strain-hardening immediately upon beginning to yield.

c. Fatigue Strength

In highway bridges and some other situations, both steel and concrete are subject to large numbers of stress fluctuations. Under such conditions, steel, just like concrete (Section 2.8c), is subject to *fatigue*. In metal fatigue, one or more microscopic cracks form after cyclic stress has been applied a significant number of times. These fatigue

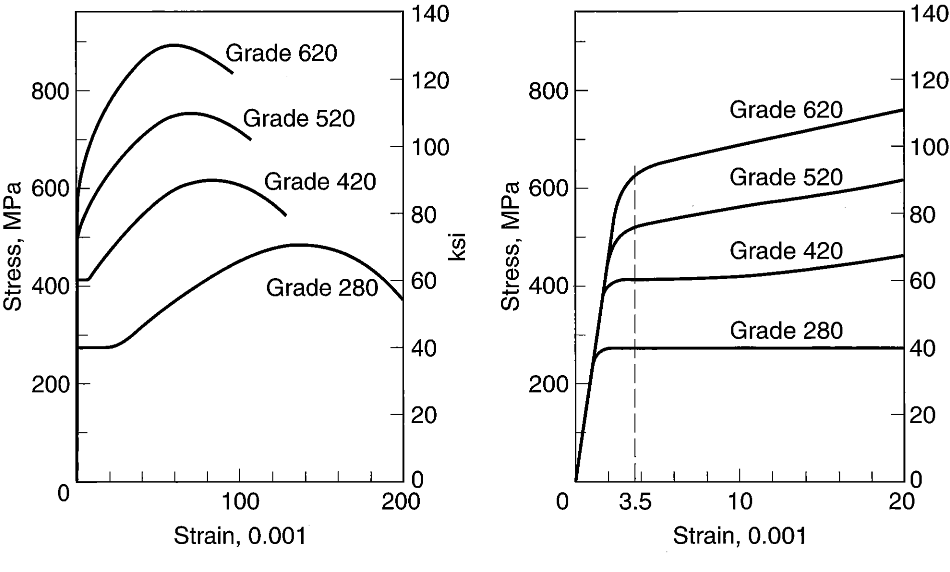

FIGURE 2.15
Typical stress-strain curves for reinforcing bars.

cracks occur at points of stress concentrations or other discontinuities and gradually increase with increasing numbers of stress fluctuations. This reduces the remaining uncracked cross-sectional area of the bar until it becomes too small to resist the applied force. At this point the bar fails in a sudden, brittle manner.

For reinforcing bars it has been found (Refs. 2.32 and 2.57) that the fatigue strength, i.e., the stress at which a given stress fluctuation between $f_{\max}$ and $f_{\min}$ can be applied 2 million times or more without causing failure, is practically independent of the grade of steel. It has also been found that the stress range, i.e., the algebraic difference between maximum and minimum stress, $f_1 = f_{\max} - f_{\min}$, that can be sustained without fatigue failure depends on $f_{\min}$. Further, in deformed bars the degree of stress concentration at the location where the deformation joins the main cylindrical body of the bar tends to reduce the safe stress range. This stress concentration depends on the ratio r/h, where r is the base radius of the deformation and h its height. The radius r is the transition radius from the surface of the bar to that of the deformation; it is a fairly uncertain quantity that changes with roll wear as bars are being rolled.

On the basis of extensive tests (Ref. 2.57), the following formula has been developed for design:

$$f_r = 145 - 0.33 f_{\min} + 55 \frac{r}{h} \tag{2.10}$$

where f_r = safe stress range, MPa
$f_{\min}$ = minimum stress; positive if tension, negative if compression
r/h = ratio of base radius to height of rolled-on deformation (in the common situation where r/h is not known, a value of 0.3 may be used)

Where bars are exposed to fatigue regimes, stress concentrations such as welds or sharp bends should be avoided since they may impair fatigue strength.

d. Coated Reinforcing Bars

Galvanized or epoxy-coated reinforcing bars are often specified to minimize corrosion of reinforcement and consequent spalling of concrete under severe environmental conditions, such as in bridge decks or parking garages subject to deicing chemicals, port and marine structures, and wastewater treatment plants.

ASTM A767, "Standard Specification for Zinc-Coated (Galvanized) Steel Bars for Concrete Reinforcement," includes requirements for the zinc coating material, the galvanizing process, the class or weight of coating, finish and adherence of coating, and the method of fabrication. Bars are usually galvanized after cutting and bending. Supplementary requirements pertain to coating of sheared ends and repair of damaged coating if bars are fabricated after galvanizing.

Epoxy-coated bars, presently more widely used than galvanized bars, are governed by ASTM A775, "Standard Specification for Epoxy-Coated Reinforcing Steel Bars," which includes requirements for the coating material, surface preparation prior to coating, method of application, and limits on coating thickness, and by ASTM A934, "Standard Specification for Epoxy-Coated Prefabricated Steel Reinforcing Bars." Under ASTM A775, the coating is applied to straight bars in a production-line operation, and the bars are cut and bent after coating. Under ASTM A934, bars are bent to final shape prior to coating. Cut ends and small spots of damaged coating are suitably repaired after fabrication. Extra care is required in the field to ensure that the coating is not damaged during shipment and placing and that repairs are made if necessary.

2.15 WELDED WIRE REINFORCEMENT

Apart from single reinforcing bars, *welded wire reinforcement* (also described as *welded wire fabric*) is often used for reinforcing slabs and other surfaces, such as shells, and for shear reinforcement in thin beam webs, particularly in prestressed beams. Welded wire reinforcement consists of sets of longitudinal and transverse cold-drawn steel wires at right angles to each other and welded together at all points of intersection. The size and spacing of wires may be the same in both directions or may be different, depending on the requirements of the design.

The notation used to describe the type and size of welded wire fabric involves a letter-number combination. ASTM uses the letters "MW" to designate smooth wire and letters "MD" to describe deformed wire. The number following the letter gives the cross-sectional area of the wire in square millimeters. For example, a MW30 wire is a smooth wire with a cross-sectional area of 30 mm^2. An MW35 wire has a cross-sectional area of 35 mm^2. MD50 indicates a deformed wire with a cross-sectional area of 50 mm^2. Welded wire fabric having a designation $100 \times 100 - \text{MW30} \times \text{MW30}$ has wire spacings 100 mm in each way with smooth wire of cross-sectional area 30 mm^2 in each direction. Sizes and spacings for common types of welded wire fabric and cross-sectional areas of steel per meter, as well as weight per 100 m^2, are shown in Table A.12 of Appendix A.

ASTM Specifications A185 and A497 pertain to smooth and deformed welded wire reinforcement, respectively, as shown in Table 2.4. Because the yield stresses shown are specified at a strain of 0.005, the ACI Code requires that f_y be taken equal to 420 MPa unless the stress at a strain of 0.0035 is used.

2.16 PRESTRESSING STEELS

Prestressing steel is used in three forms: round wires, stranded cable, and alloy steel bars. Prestressing wire ranges in diameter from 4.88 to 7.01 mm. It is made by cold-drawing high-carbon steel after which the wire is stress-relieved by heat treatment to produce the prescribed mechanical properties. Wires are normally bundled in groups of up to about 50 individual wires to produce prestressing tendons of the required strength. Stranded cable, more common than wire in U.S. practice, is fabricated with six wires wound around a seventh of slightly larger diameter. The pitch of the spiral winding is between 12 and 16 times the nominal diameter of the strand. Strand diameters range from 6.4 to 17.8 mm. Alloy steel bars for prestressing are available in diameters from 19 to 35 mm as plain round bars and from 15 to 65 mm as deformed bars. Specific requirements for prestressing steels are found in ASTM A421, "Standard Specification for Uncoated Stress-Relieved Steel Wire for Prestressed Concrete"; ASTM A416, "Standard Specification for Steel Strand, Uncoated Seven-Wire Stress-Relieved for Prestressed Concrete"; and ASTM A722, "Standard Specification for Uncoated High-Strength Steel Bar for Prestressing Concrete." Table A.15 of Appendix A provides design information for U.S. prestressing steels.

a. Grades and Strengths

The tensile strengths of prestressing steels range from about 2.5 to 6 times the yield strengths of commonly used reinforcing bars. The grade designations correspond to the minimum specified tensile strength in MPa. For the widely used seven-wire strand, three grades are available: Grade 1725 (f_{pu} = 1725 MPa), Grade 1860, and Grade 2070, although the last is not yet recognized in ASTM A421. Grade 1860 strand is used most often. For alloy steel bars, two grades are used: the regular Grade 1035 is most common, but special Grade 1100 bars may be ordered. Round wires may be obtained in Grades 1620, 1655, and 1725, depending on diameter.

b. Stress-Strain Curves

Figure 2.16 shows stress-strain curves for prestressing wires, strand, and alloy bars of various grades. For comparison, the stress-strain curve for a Grade 420 reinforcing bar is also shown. It is seen that, in contrast to reinforcing bars, prestressing steels do not show a sharp yield point or yield plateau; i.e., they do not yield at constant or nearly constant stress. Yielding develops gradually, and in the inelastic range the curve continues to rise smoothly until the tensile strength is reached. Because well-defined yielding is not observed in these steels, the yield strength is somewhat arbitrarily defined as the stress at a total elongation of 1 percent for strand and wire and at 0.7 percent for alloy steel bars. Figure 2.16 shows that the yield strengths so defined represent a good limit below which stress and strain are fairly proportional, and above which strain increases much more rapidly with increasing stress. It is also seen that the spread between tensile strength and yield strength is smaller in prestressing steels than in reinforcing steels. It may further be noted that prestressing steels have significantly less ductility.

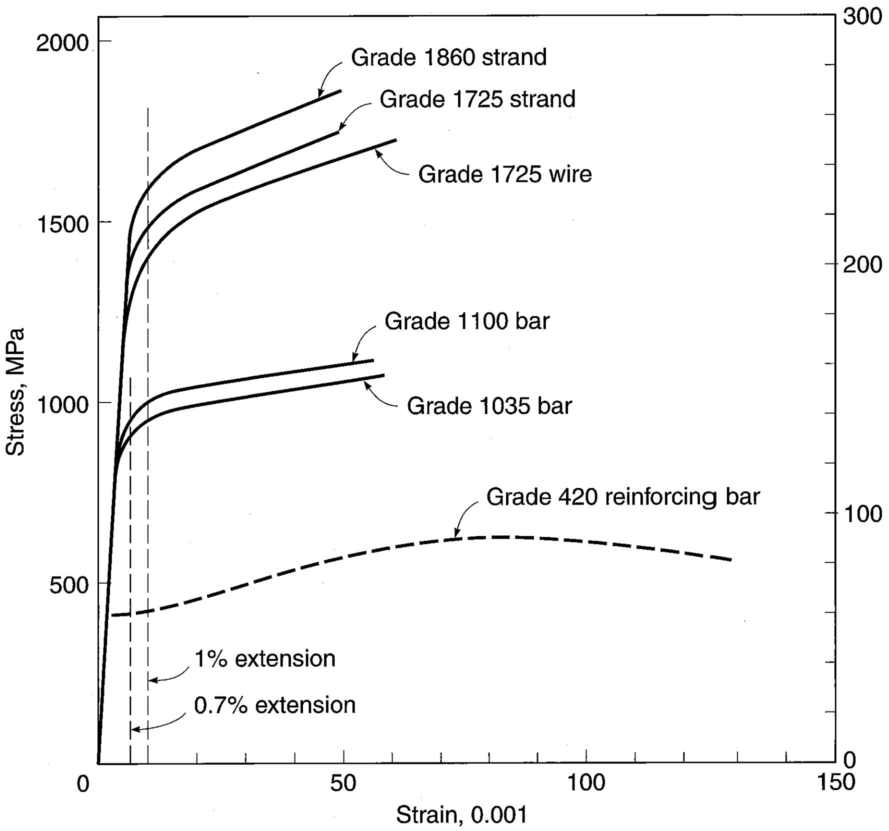

FIGURE 2.16
Typical stress-strain curves for prestressing steels.

While the modulus of elasticity E_s for bar reinforcement is taken as 200,000 MPa, the effective modulus of prestressing steel varies, depending on the type of steel (e.g., strand vs. wire or bars) and type of use, and is best determined by test or supplied by the manufacturer. For unbonded strand (i.e., strand not embedded in concrete), the modulus may be as low as 179,000 MPa. For bonded strand, E_s is usually about 186,000 MPa, while for smooth round wires E_s is about 200,000 MPa, the same as for reinforcing bars. The elastic modulus of alloy steel bars is usually taken as $E_s = 186{,}000$ MPa.

c. Relaxation

When prestressing steel is stressed to the levels that are customary during initial tensioning and at service loads, it exhibits a property known as *relaxation*. Relaxation is defined as the loss of stress in stressed material held at constant length. (The same basic phenomenon is known as creep when defined in terms of change in strain of a material under constant stress.) To be specific, if a length of prestressing steel is stressed to a sizable fraction of its yield strength f_{py} (say, 80 to 90 percent) and held at a constant strain between fixed points such as the ends of a beam, the steel stress f_p will gradually decrease from its initial value f_{pi}. In prestressed concrete members this stress relaxation is important because it modifies the internal stresses in the concrete and changes the deflections of the beam some time after initial prestress was applied.

The amount of relaxation varies, depending on the type and grade of steel, the time under load, and the initial stress level. A satisfactory estimate for ordinary stress-relieved strand and wires can be obtained from Eq. (2.11), which was derived from more than 400 relaxation tests of up to 9 years' duration:

$$\frac{f_p}{f_{pi}} = 1 - \frac{\log t}{10}\left(\frac{f_{pi}}{f_{py}} - 0.55\right) \tag{2.11}$$

where f_p is the final stress after t hours, f_{pi} is the initial stress, and f_{py} is the nominal yield stress (Ref. 2.58). In Eq. (2.11), log t is to the base 10, and f_{pi}/f_{py} not less than 0.55; below that value essentially no relaxation occurs.

The tests on which Eq. (2.11) is based were carried out on round, stress-relieved wires and are equally applicable to stress-relieved strand. In the absence of other information, results may be applied to alloy steel bars as well.

Low-relaxation strand has replaced stress-relieved strand as the industry standard. According to ASTM A416, such steel must exhibit relaxation after 1000 hours of not more than 2.5 percent when initially stressed to 70 percent of specified tensile strength and not more than 3.5 percent when loaded to 80 percent of tensile strength. For low-relaxation strand, Eq. (2.11) is replaced by

$$\frac{f_p}{f_{pi}} = 1 - \frac{\log t}{45}\left(\frac{f_{pi}}{f_{py}} - 0.55\right) \tag{2.12}$$

REFERENCES

2.1. "Guide for Use of Normal Weight and Heavyweight Aggregate in Concrete," ACI Committee 221, *ACI Manual of Concrete Practice*, Part 1, 2009.

2.2. "Guide for Structural Lightweight Aggregate Concrete," ACI Committee 213, *ACI Manual of Concrete Practice*, Part 1, 2009.

2.3. G. E. Troxell, H. E. Davis, and J. W. Kelly, *Composition and Properties of Concrete*, 2nd ed., McGraw-Hill, New York, 1968.

2.4. T. T. C. Hsu and F. O. Slate, "Tensile Bond Strength between Aggregate and Cement Paste or Mortar," *J. ACI*, vol. 60, no. 4, 1963, pp. 465–486.

2.5. "Standard Practice for Selecting Proportions for Normal, Heavyweight, and Mass Concrete," ACI Committee 211, *ACI Manual of Concrete Practice*, Part 1, 2009.

2.6. "Standard Practice for Selecting Proportions for Structural Lightweight Concrete," ACI Committee 211, *ACI Manual of Concrete Practice*, Part 1, 2009.

2.7. S. A. Kosmatka, B. Kerkhoff, and W. C. Panarese, *Design and Control of Concrete Mixtures*, 14th ed., Portland Cement Association, Skokie, IL, 2003.

2.8. S. Mindess, J. F. Young, and D. Darwin, *Concrete*, 2nd ed., Prentice-Hall, Upper Saddle River, NJ, 2003.

2.9. "Guide for Consolidation of Concrete," ACI Committee 309, *ACI Manual of Concrete Practice*, Part 2, 2009.

2.10. "Guide for Measuring, Transporting, and Placing Concrete," ACI Committee 304, *ACI Manual of Concrete Practice*, Part 2, 2009.

2.11. "Cold Weather Concreting," ACI Committee 306, *ACI Manual of Concrete Practice*, Part 2, 2009.

2.12. "Recommended Practice for Evaluation of Strength Test Results of Concrete," ACI Committee 214, *ACI Manual of Concrete Practice*, Part 1, 2009.

2.13. "Chemical Admixtures for Concrete," ACI Committee 212, *ACI Manual of Concrete Practice*, Part 1, 2009.

2.14. K. C. Hover, "Why Is There Air in Concrete?" *Concr. Construction*, vol. 38, no. 1, 1993, pp. 11–15.

2.15. "Guide for the Use of High-Range Water-Reducing Admixtures (Superplasticizers) in Concrete," ACI Committee 212, *ACI Manual of Concrete Practice*, Part 1, 2009.

2.16. A. A. Ramezanianpour, V. Sivasundaram, and V. M. Malhotra, "Superplasticizers: Their Effect on the Strength Properties of Concrete," *Concr. Intl.*, vol. 17, no. 4, 1995, pp. 30–35.

2.17. R. J. Peterman, "The Effects of As-Cast Depth and Concrete Fluidity on Strand Bond," *PCI J.*, vol. 52, no. 3, 2007, pp. 72–101.

2.18. "Use of Fly Ash in Concrete," ACI Committee 232, *ACI Manual of Concrete Practice*, Part 1, 2009.

2.19. "Guide for the Use of Silica Fume in Concrete," ACI Committee 234, *ACI Manual of Concrete Practice*, Part 1, 2009.

2.20. "Guide to Use of Slag Cement in Concrete and Mortar," ACI Committee 233, *ACI Manual of Concrete Practice*, Part 1, 2009.

2.21. V. M. Malhotra, "Fly Ash, Silica Fume, and Rice-Husk Ash in Concrete: A Review," *Concr. Intl.*, vol. 15, no. 4, 1993, pp. 23–28.

2.22. G. Detwiler, "High-Strength Silica Fume Concrete—Chicago Style," *Concr. Intl.*, vol. 14, no. 10, 1992, pp. 32–36.

2.23. R. L. Carrasquillo, A. H. Nilson, and F. O. Slate, "Properties of High Strength Concrete Subject to Short Term Loads," *J. ACI*, vol. 78, no. 3, 1981, pp. 171–178.

2.24. F. O. Slate, A. H. Nilson, and S. Martinez, "Mechanical Properties of High-Strength Lightweight Concrete," *J. ACI*, vol. 83, no. 4, 1986, pp. 606–613.

2.25. P. T. Wang, S. P. Shah, and A. E. Naaman, "Stress-Strain Curves of Normal and Lightweight Concrete in Compression," *J. ACI*, vol. 75, no. 11, 1978, pp. 603–611.

2.26. D. E. Branson, *Deformation of Concrete Structures*, McGraw-Hill, New York, 1977.

2.27. H. Rüsch, "Researches toward a General Flexural Theory for Structural Concrete," *J. ACI*, vol. 32, no. 1, 1960, pp. 1–28.

2.28. A. S. Ngab, A. H. Nilson, and F. O. Slate, "Shrinkage and Creep of High-Strength Concrete," *J. ACI*, vol. 78, no. 4, 1981, pp. 255–261.

2.29. A. M. Neville, *Properties of Concrete*, 4th ed., John Wiley & Sons, Inc., New York, 1996.

2.30. M. M. Smadi, F. O. Slate, and A. H. Nilson, "High, Medium, and Low-Strength Concretes Subject to Sustained Overloads," *J. ACI*, vol. 82, no. 5, 1985, pp. 657–664.

2.31. M. M. Smadi, F. O. Slate, and A. H. Nilson, "Shrinkage and Creep of High, Medium, and Low-Strength Concretes, Including Overloads," *ACI Mater. J.*, vol. 84, no. 3, 1987, pp. 224–234.

2.32. "Fatigue of Concrete Structures," Special Publication SP-75, American Concrete Institute, Detroit, MI, 1982.

2.33. M. P. Collins and D. Kuchma, "How Safe Are Our Large, Lightly Reinforced Concrete Beams, Slabs, and Footings?" *ACI Struct. J.*, vol. 96, no. 4, 1999, pp. 482–490.

2.34. J. Zuo and D. Darwin, "Splice Strength of Conventional and High Relative Rib Area Bars in Normal and High Strength Concrete," *ACI Struct. J.*, vol. 97, no. 4, 2000, pp. 630–641.

2.35. D. Darwin, S. Barham, R. Kozul, and S. Luan, "Fracture Energy of High-Strength Concrete," *ACI Mater. J.*, vol. 98, no. 5, 2001, pp. 410–417.

2.36. E. A. Jensen and W. Hansen, "Fracture Energy Test for Highway Concrete—Determining the Effect of Coarse Aggregate on Crack Propagation Resistance," *Transp. Res. Rec. 1730*, 2001, pp. 10–16.
2.37. T. T. C. Hsu, F. O. Slate, G. M. Sturman, and G. Winter, "Microcracking of Plain Concrete and the Shape of the Stress-Strain Curve," *J. ACI*, vol. 60, no. 2, 1963, pp. 209–224.
2.38. H. Kupfer, H. K. Hilsdorf, and H. Rüsch, "Behavior of Concrete under Biaxial Stresses," *J. ACI*, vol. 66, no. 8, 1969, pp. 656–666.
2.39. M. E. Tasuji, F. O. Slate, and A. H. Nilson, "Stress-Strain Response and Fracture of Concrete in Biaxial Loading," *J. ACI*, vol. 75, no. 7, 1978, pp. 306–312.
2.40. K. H. Gerstle et al., "Strength of Concrete under Multiaxial Stress States," *Proc. Douglas McHenry International Symposium on Concrete and Concrete Structures*, ACI Special Publication SP-55, American Concrete Institute, 1978, pp. 103–131.
2.41. G. Pickett, "Effect of Aggregate on Shrinkage of Concrete and Hypothesis Concerning Shrinkage," *J. ACI*, vol. 52, no. 6, 1956, pp. 581–589.
2.42. "Standard Practice for the Use of Shrinkage-Compensating Cements," ACI Committee 223, *ACI Manual of Concrete Practice*, Part 1, 2009.
2.43. A. Neville, "Whither Expansive Cement," *Concr. Intl.*, vol. 16, no. 9, 1994, pp. 34–35.
2.44. "State-of-the-Art Report on High-Strength Concrete," ACI Committee 363, *ACI Manual of Concrete Practice*, Part 5, 2002.
2.45. S. P. Shah and S. H. Ahmad (eds.), *High-Performance Concrete: Properties and Applications*, McGraw-Hill, New York, 1994.
2.46. H. G. Russell, S. H. Gebler, and D. Whiting, "High-Strength Concrete: Weighing the Benefits," *Civ. Eng.*, vol. 59, no. 11, 1989, pp. 59–61.
2.47. A. H. Nilson, "High-Strength Concrete—An Overview of Cornell Research," *Proc. of Symposium on Utilization of High-Strength Concrete*, Stavanger, Norway, 1987, pp. 27–38.
2.48. A. H. Nilson, "Properties and Performance of High-Strength Concrete," *Proc. of IABSE Symposium on Concrete Structures for the Future*, Paris-Versailles, 1987, pp. 389–394.
2.49. A. H. Nilson, "Design Implications of Current Research on High-Strength Concrete," *High-Strength Concrete*, Special Publication SP-87, American Concrete Institute, Detroit, MI, 1985, pp. 85–118.
2.50. K. A. Paulson, A. H. Nilson, and K. C. Hover, "Long-Term Deflection of High-Strength Concrete Beams," *ACI Mater. J.*, vol. 88, no. 2, 1991, pp. 197–206.
2.51. A. E. Fiorato, "PCA Research on High-Strength Concrete," *Concr. Intl.*, vol. 11, no. 4, 1989, pp. 44–50.
2.52. N. J. Carino and J. R. Clifton, "High-Performance Concrete: Research Needs to Enhance Its Use," *Concr. Intl.*, vol. 13, no. 9, 1991, pp. 70–76.
2.53. A. Azizinamini, R. Pavel, E. Hatfield, and S. K. Ghosh, "Behavior of Spliced Reinforcing Bars Embedded in High-Strength Concrete," *ACI Struct. J.*, vol. 96, no. 5, 1999, pp. 826–835.
2.54 D. Darwin, J. Browning, and W. D. Lindquist, "Control of Cracking in Bridge Decks: Observations from the Field," *Cement, Concrete and Aggregates*, ASTM International, vol. 26, no. 2, 2004, pp. 148–154.
2.55. D. Whiting, "Durability of High-Strength Concrete," *Proc. of Katharine and Bryant Mather International Conference*, Special Publication SP-100, American Concrete Institute, Detroit, MI, 1987, pp. 169–186.
2.56. *Manual of Standard Practice*, 28th ed., Concrete Reinforcing Steel Institute, Schaumburg, IL, 2009.
2.57. W. G. Corley, J. M. Hanson, and T. Helgason, "Design of Reinforced Concrete for Fatigue," *J. Struct. Div., ASCE*, vol. 104, no. ST6, 1978, pp. 921–932.
2.58. W. G. Corley, M. A. Sozen, and C. P. Siess, "Time-Dependent Deflections of Prestressed Concrete Beams," *Highway Res. Board Bull. No. 307*, 1961, pp. 1–25.

PROBLEMS

2.1. The specified concrete strength f_c' for a new building is 42 MPa. Calculate the required average strength f_c' for the concrete (*a*) if there are no prior test results for concrete with a compressive strength within 7 MPa of f_c' made with similar materials, (*b*) if 20 test results for concrete with $f_c' = 35$ MPa made with similar materials produce a sample standard deviation s_s of 4.0 MPa, and (*c*) if 30 tests with $f_c' = 38$ MPa made with similar materials produce a sample standard deviation s_s of 4.1 MPa.

2.2. Ten consecutive strength tests are available for a new concrete mixture with $f_c' = 28$ MPa: 31.7, 32.8, 36.4, 29.0, 30.8, 28.8, 25.9, 35.2, 32.0, and 28.8 MPa.

(*a*) Do the strength results represent concrete of satisfactory quality? Explain your reasoning.

(*b*) If f'_{cr} has been selected based on 30 consecutive test results from an earlier project with a sample standard deviation s_s of 3.5 MPa, must the mixture proportions be adjusted? Explain.

3

Flexural Analysis and Design of Beams

3.1 INTRODUCTION

The fundamental assumptions upon which the analysis and design of reinforced concrete members are based were introduced in Section 1.8, and the application of those assumptions to the simple case of axial loading was developed in Section 1.9. The student should review Sections 1.8 and 1.9 at this time. In developing methods for the analysis and design of beams in this chapter, the same assumptions apply, and identical concepts will be used. This chapter will include analysis and design for flexure, including the dimensioning of the concrete cross section and the selection and placement of reinforcing steel. Other important aspects of beam design including shear reinforcement, bond, and anchorage of reinforcing bars, and the important questions of serviceability (e.g., limiting deflections and controlling concrete cracking) will be treated in Chapters 4, 5, and 6.

3.2 BENDING OF HOMOGENEOUS BEAMS

Reinforced concrete beams are nonhomogeneous in that they are made of two entirely different materials. The methods used in the analysis of reinforced concrete beams are therefore different from those used in the design or investigation of beams composed entirely of steel, wood, or any other structural material. The fundamental principles involved are, however, essentially the same. Briefly, these principles are as follows.

At any cross section there exist internal forces that can be resolved into components normal and tangential to the section. Those components that are normal to the section are the *bending* stresses (tension on one side of the neutral axis and compression on the other). Their function is to resist the bending moment at the section. The tangential components are known as the *shear* stresses, and they resist the transverse or shear forces.

Fundamental assumptions relating to flexure and flexural shear are as follows:

1. A cross section that was plane before loading remains plane under load. This means that the unit strains in a beam above and below the neutral axis are proportional to the distance from that axis.
2. The bending stress f at any point depends on the strain at that point in a manner given by the stress-strain diagram of the material. If the beam is made of a homogeneous material whose stress-strain diagram in tension and compression is that of Fig. 3.1*a*, the following holds. If the maximum strain at the outer fibers is smaller than the strain ϵ_p up to which stress and strain are proportional for the

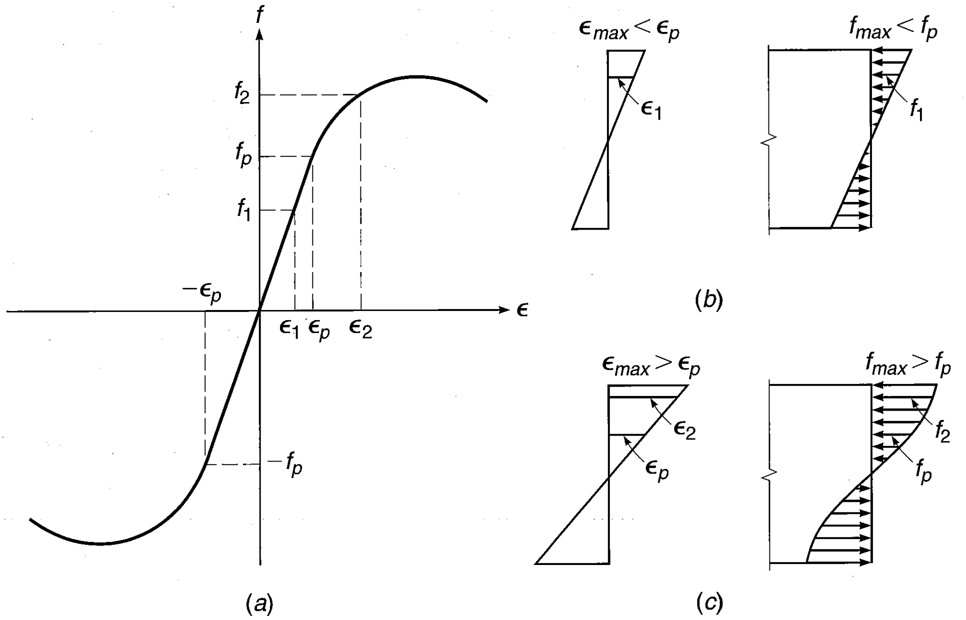

FIGURE 3.1
Elastic and inelastic stress distributions in homogeneous beams.

given material, then the compression and tension stresses on either side of the axis are proportional to the distance from the axis, as shown in Fig. 3.1*b*. However, if the maximum strain at the outer fibers is larger than ϵ_p, this is no longer true. The situation that then occurs is shown in Fig. 3.1*c*; i.e., in the outer portions of the beam, where $\epsilon > \epsilon_p$, stresses and strains are no longer proportional. In these regions, the magnitude of stress at any level, such as f_2 in Fig. 3.1*c*, depends on the strain ϵ_2 at that level in the manner given by the stress-strain diagram of the material. In other words, for a given strain in the beam, the stress at a point is the same as that given by the stress-strain diagram for the same strain.

3. The distribution of the shear stresses v over the depth of the section depends on the shape of the cross section and of the stress-strain diagram. These shear stresses are largest at the neutral axis and equal to zero at the outer fibers. The shear stresses on horizontal and vertical planes through any point are equal.
4. Owing to the combined action of shear stresses (horizontal and vertical) and flexure stresses, at any point in a beam there are inclined stresses of tension and compression, the largest of which form an angle of 90° with each other. The intensity of the inclined maximum or principal stress at any point is given by

$$t = \frac{f}{2} \pm \sqrt{\frac{f^2}{4} + v^2} \tag{3.1}$$

where f = intensity of normal fiber stress
v = intensity of tangential shearing stress

The inclined stress makes an angle α with the horizontal such that $\tan 2\alpha = 2v/f$.

5. Since the horizontal and vertical shearing stresses are equal and the flexural stresses are zero at the neutral plane, the inclined tensile and compressive stresses at any point in that plane form an angle of 45° with the horizontal, the intensity of each being equal to the unit shear at the point.

6. When the stresses in the outer fibers are smaller than the proportional limit f_p, the beam behaves *elastically*, as shown in Fig. 3.1*b*. In this case the following pertains:

(a) The neutral axis passes through the center of gravity of the cross section.

(b) The intensity of the bending stress normal to the section increases directly with the distance from the neutral axis and is a maximum at the extreme fibers. The stress at any given point in the cross section is represented by the equation

$$f = \frac{My}{I} \tag{3.2}$$

where f = bending stress at a distance y from neutral axis
M = external bending moment at section
I = moment of inertia of cross section about neutral axis

The maximum bending stress occurs at the outer fibers and is equal to

$$f_{\max} = \frac{Mc}{I} = \frac{M}{S} \tag{3.3}$$

where c = distance from neutral axis to outer fiber
$S = I/c$ = section modulus of cross section

(c) The shear stress (horizontal equals vertical) v at any point in the cross section is given by

$$v = \frac{VQ}{Ib} \tag{3.4}$$

where V = total shear at section
Q = statical moment about neutral axis of that portion of cross section lying between a line through point in question parallel to neutral axis and nearest face (upper or lower) of beam
I = moment of inertia of cross section about neutral axis
b = width of beam at a given point

(d) The intensity of shear along a vertical cross section in a rectangular beam varies as the ordinates of a parabola, the intensity being zero at the outer fibers of the beam and a maximum at the neutral axis. For a total depth h, the maximum is $\frac{3}{2}V/bh$, since at the neutral axis $Q = bh^2/8$ and $I = bh^3/12$ in Eq. (3.4).

The remainder of this chapter deals only with bending stresses and their effects on reinforced concrete beams. Shear stresses and their effects are discussed separately in Chapter 4.

3.3 REINFORCED CONCRETE BEAM BEHAVIOR

Plain concrete beams are inefficient as flexural members because the tensile strength in bending (modulus of rupture, see Section 2.9) is a small fraction of the compressive strength. As a consequence, such beams fail on the tension side at low loads long before the strength of the concrete on the compression side has been fully utilized. For this reason, steel reinforcing bars are placed on the tension side as close to the extreme tension fiber as is compatible with proper fire and corrosion protection of the steel. In such a reinforced concrete beam, the tension caused by the bending moments is chiefly

FIGURE 3.2
Behavior of reinforced concrete beam under increasing load.

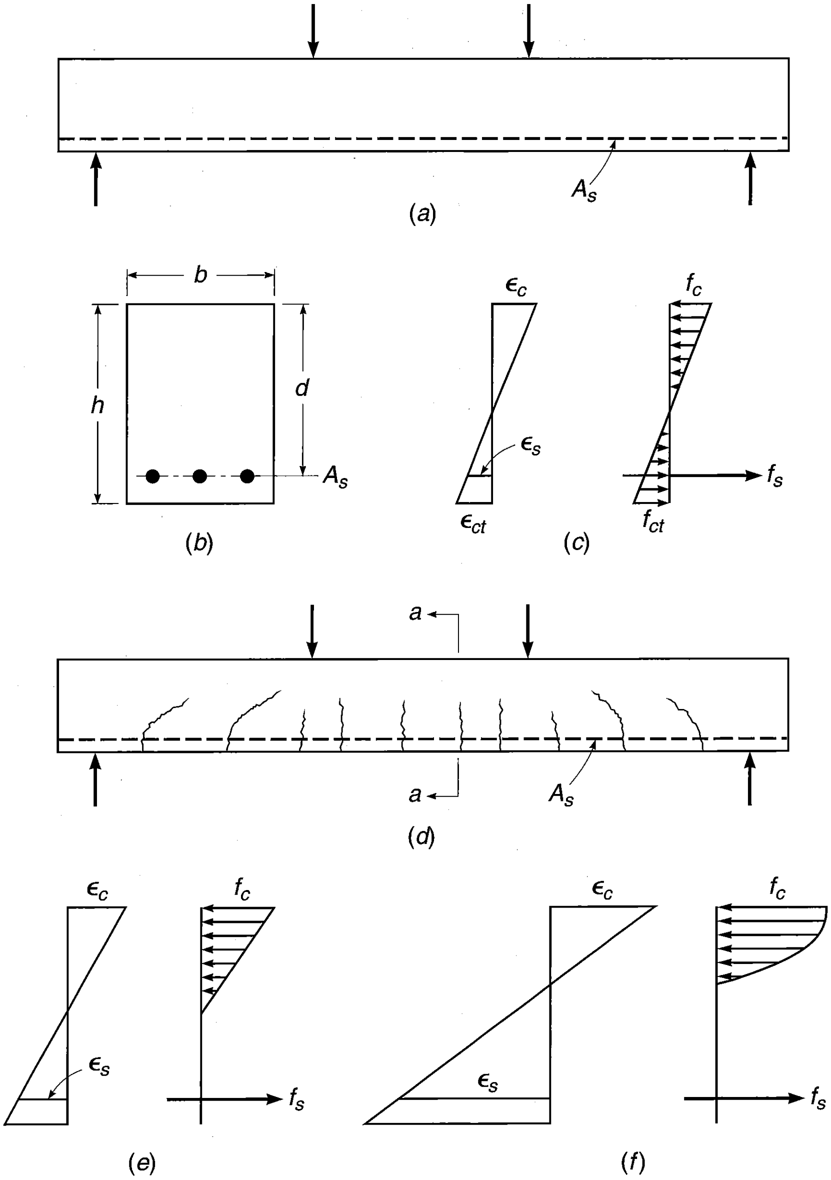
A_s
(a)
b
h
d
A_s
(b)
ϵ_c
ϵ_s
ϵ_{ct}
f_c
f_s
f_{ct}
(c)
a
a
A_s
(d)
ϵ_c
ϵ_s
f_c
f_s
(e)
ϵ_c
ϵ_s
f_c
f_s
(f)

resisted by the steel reinforcement, while the concrete alone is usually capable of resisting the corresponding compression. Such joint action of the two materials is ensured if relative slip is prevented. This is achieved by using deformed bars with their high bond strength at the steel-concrete interface (see Section 2.14) and, if necessary, by special anchorage of the ends of the bars. A simple example of such a beam, with the customary designations for the cross-sectional dimensions, is shown in Fig. 3.2. For simplicity, the discussion that follows will deal with beams of rectangular cross section, even though members of other shapes are very common in most concrete structures.

When the load on such a beam is gradually increased from zero to the magnitude that will cause the beam to fail, several different stages of behavior can be clearly distinguished. At low loads, as long as the maximum tensile stress in the concrete is smaller than the modulus of rupture, the entire concrete is effective in resisting stress, in compression on one side and in tension on the other side of the neutral axis. In addition, the reinforcement, deforming the same amount as the adjacent concrete, is also subject to tensile stresses. At this stage, all stresses in the concrete are of small magnitude and are proportional to strains. The distribution of strains and stresses in concrete and steel over the depth of the section is shown in Fig. 3.2*c*.

When the load is further increased, the tensile strength of the concrete is soon reached, and at this stage tension cracks develop. These propagate quickly upward to or close to the level of the neutral plane, which in turn shifts upward with progressive cracking. The general shape and distribution of these tension cracks is shown in Fig. 3.2*d*. In well-designed beams, the width of these cracks is so small (hairline cracks) that they are not objectionable from the viewpoint of either corrosion protection or appearance. Their presence, however, profoundly affects the behavior of the beam under load. Evidently, in a cracked section, i.e., in a cross section located at a crack such as *a-a* in Fig. 3.2*d*, the concrete does not transmit any tensile stresses. Hence, just as in tension members (Section 1.9b), the steel is called upon to resist the entire tension. At moderate loads, if the concrete stresses do not exceed approximately $f'_c/2$, stresses and strains continue to be closely proportional (see Fig. 1.16). The distribution of strains and stresses at or near a cracked section is then that shown in Fig. 3.2*e*. When the load is still further increased, stresses and strains rise correspondingly and are no longer proportional. The ensuing nonlinear relation between stresses and strains is that given by the concrete stress-strain curve. Therefore, just as in homogeneous beams (see Fig. 3.1), the distribution of concrete stresses on the compression side of the beam is of the same shape as the stress-strain curve. Figure 3.2*f* shows the distribution of strains and stresses close to the ultimate load.

Eventually, the carrying capacity of the beam is reached. Failure can be caused in one of two ways. When relatively moderate amounts of reinforcement are employed, at some value of the load the steel will reach its yield point. At that stress, the reinforcement yields suddenly and stretches a large amount (see Fig. 2.15), and the tension cracks in the concrete widen visibly and propagate upward, with simultaneous significant deflection of the beam. When this happens, the strains in the remaining compression zone of the concrete increase to such a degree that crushing of the concrete, the *secondary compression failure*, ensues at a load only slightly larger than that which caused the steel to yield. Effectively, therefore, attainment of the yield point in the steel determines the carrying capacity of moderately reinforced beams. Such yield failure is gradual and is preceded by visible signs of distress, such as the widening and lengthening of cracks and the marked increase in deflection.

On the other hand, if large amounts of reinforcement or normal amounts of steel of very high strength are employed, the compressive strength of the concrete may be exhausted before the steel starts yielding. Concrete fails by crushing when strains become so large that they disrupt the integrity of the concrete. Exact criteria for this occurrence have yet to be established, but it has been observed that rectangular beams fail in compression when the concrete strains reach values of about 0.003 to 0.004. Compression failure through crushing of the concrete is sudden, of an almost explosive nature, and occurs without warning. For this reason it is good practice to dimension beams in such a manner that should they be overloaded, failure would be initiated by yielding of the steel rather than by crushing of the concrete.

The analysis of stresses and strength in the different stages just described will be discussed in the next several sections.

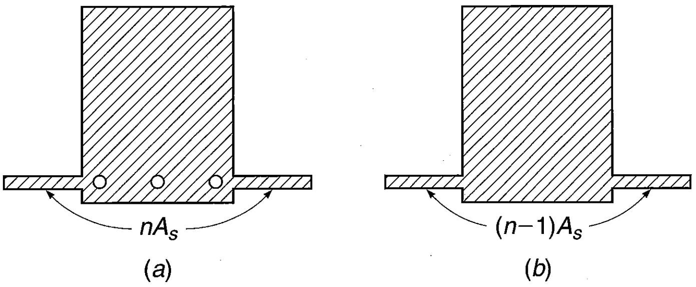

FIGURE 3.3
Uncracked transformed beam section.

a. Stresses Elastic and Section Uncracked

As long as the tensile stress in the concrete is smaller than the modulus of rupture, so that no tension cracks develop, the strain and stress distribution as shown in Fig. 3.2*c* is essentially the same as in an elastic, homogeneous beam (Fig. 3.1*b*). The only difference is the presence of another material, the steel reinforcement. As shown in Section 1.9a, in the elastic range, for any given value of strain, the stress in the steel is n times that of the concrete [Eq. (1.6)]. In the same section, it was shown that one can take account of this fact in calculations by replacing the actual steel-and-concrete cross section with a fictitious section thought of as consisting of concrete only. In this "transformed section," the actual area of the reinforcement is replaced with an equivalent concrete area equal to nA_s located at the level of the steel. The transformed, uncracked section pertaining to the beam of Fig. 3.2*b* is shown in Fig. 3.3.

Once the transformed section has been obtained, the usual methods of analysis of elastic homogeneous beams apply. That is, the section properties (location of neutral axis, moment of inertia, section modulus, etc.) are calculated in the usual manner, and, in particular, stresses are computed with Eqs. (3.2) to (3.4).

EXAMPLE 3.1 A rectangular beam has the dimensions (see Fig. 3.2*b*) $b = 250$ mm, $h = 650$ mm, and $d = 600$ mm and is reinforced with three No. 25 (No. 8) bars so that $A_s = 1530$ mm^2. The concrete cylinder strength f'_c is 28 MPa, and the tensile strength in bending (modulus of rupture) is 3.27 MPa. The yield point of the steel f_y is 420 MPa, the stress-strain curves of the materials being those of Fig. 1.16. Determine the stresses caused by a bending moment $M = 61$ kN-m.

Solution. With a value $n = E_s/E_c = 200{,}000/24{,}800 = 8$, one has to add to the rectangular outline an area $(n - 1)A_s = 7 \times 1530 = 10{,}710$ mm^2, disposed as shown on Fig. 3.4, to obtain the uncracked, transformed section. Conventional calculations show that the location of the neutral axis of this section is given by $\bar{y} = 342$ mm from the top of the section, and its moment of inertia about this axis is 6,481,000,000 mm^4. For $M = 61$ kN-m $= 61{,}000{,}000$ N-mm, the concrete compression stress at the top fiber is, from Eq. (3.3),

$$f_c = \frac{M\bar{y}}{I} = \frac{61{,}000{,}000 \times 342}{6{,}481{,}000{,}000} = 3.22 \text{ MPa}$$

and, similarly, the concrete tension stress at the bottom fiber, 308 mm from the neutral axis, is

$$f_{ct} = \frac{61{,}000{,}000 \times 308}{6{,}481{,}000{,}000} = 2.90 \text{ MPa}$$

FIGURE 3.4
Transformed beam section of Example 3.1.

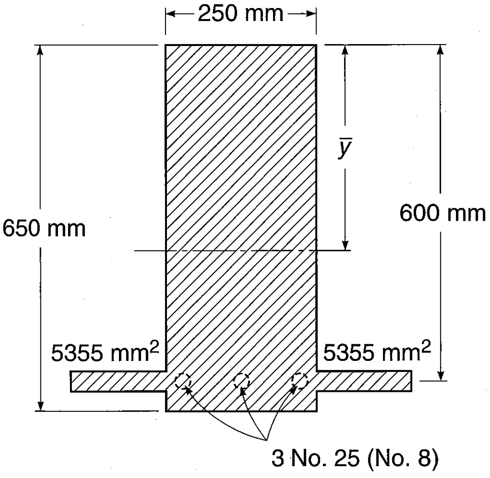

Since this value is below the given tensile bending strength of the concrete, 3.27 MPa, no tension cracks will form, and calculation by the uncracked, transformed section is justified. The stress in the steel, from Eqs. (1.6) and (3.2), is

$$f_s = n\frac{My}{I} = 8\left(\frac{61{,}000{,}000 \times 258}{6{,}481{,}000{,}000}\right) = 19.43 \text{ MPa}$$

By comparing f_c and f_s with the concrete cylinder strength and the yield point, respectively, it is seen that at this stage the actual stresses are quite small compared with the available strengths of the two materials.

b. Stresses Elastic and Section Cracked

When the tensile stress f_{ct} exceeds the modulus of rupture, cracks form, as shown in Fig. 3.2*d*. If the concrete compressive stress is less than approximately $\frac{1}{2}f_c'$ and the steel stress has not reached the yield point, both materials continue to behave elastically, or very nearly so. This situation generally occurs in structures under normal service conditions and loads, since at these loads the stresses are generally of the order of magnitude just discussed. At this stage, for simplicity and with little if any error, it is assumed that tension cracks have progressed all the way to the neutral axis and that sections plane before bending are plane in the deformed member. The situation with regard to strain and stress distribution is that shown in Fig. 3.2*e*.

To compute stresses, and strains if desired, the device of the transformed section can still be used. One need only take account of the fact that all of the concrete that is stressed in tension is assumed cracked, and therefore effectively absent. As shown in Fig. 3.5*a*, the transformed section then consists of the concrete in compression on one side of the axis and n times the steel area on the other. The distance to the neutral axis, in this stage, is conventionally expressed as a fraction kd of the effective depth d. (Once the concrete is cracked, any material located below the steel is ineffective, which is why d is the effective depth of the beam.) To determine the location of the

FIGURE 3.5
Cracked transformed section.

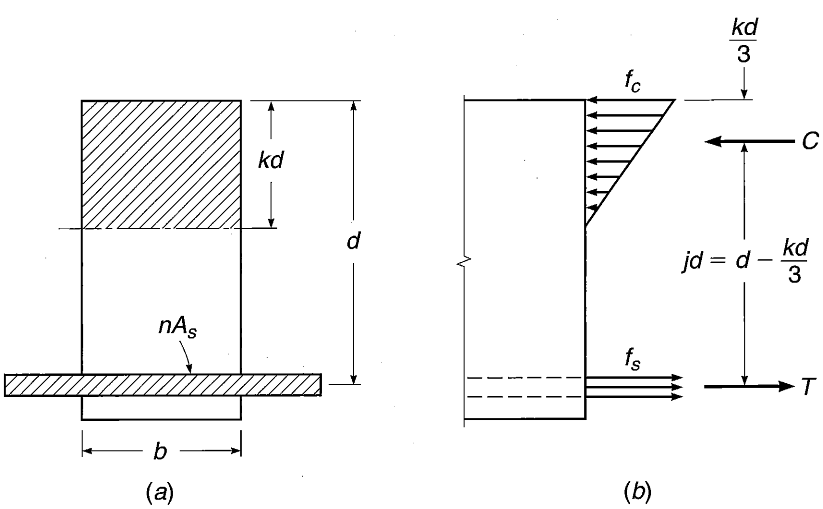

neutral axis, the moment of the tension area about the axis is set equal to the moment of the compression area, which gives

$$b\frac{(kd)^2}{2} - nA_s(d - kd) = 0 \tag{3.5}$$

Having obtained *kd* by solving this quadratic equation, one can determine the moment of inertia and other properties of the transformed section as in the preceding case. Alternatively, one can proceed from basic principles by accounting directly for the forces that act on the cross section. These are shown in Fig. 3.5*b*. The concrete stress, with maximum value f_c at the outer edge, is distributed linearly as shown. The entire steel area A_s is subject to the stress f_s. Correspondingly, the total compression force *C* and the total tension force *T* are

$$C = \frac{f_c}{2}bkd \qquad \text{and} \qquad T = A_s f_s \tag{3.6}$$

The requirement that these two forces be equal numerically has been taken care of by the manner in which the location of the neutral axis has been determined.

Equilibrium requires that the couple constituted by the two forces *C* and *T* be equal numerically to the external bending moment *M*. Hence, taking moments about *C* gives

$$M = Tjd = A_s f_s jd \tag{3.7}$$

where *jd* is the internal lever arm between *C* and *T*. From Eq. (3.7), the steel stress is

$$f_s = \frac{M}{A_s jd} \tag{3.8}$$

Conversely, taking moments about *T* gives

$$M = Cjd = \frac{f_c}{2}bkdjd = \frac{f_c}{2}kjbd^2 \tag{3.9}$$

from which the concrete stress is

$$f_c = \frac{2M}{kjbd^2} \tag{3.10}$$

In using Eqs. (3.6) through (3.10), it is convenient to have equations by which k and j may be found directly, to establish the neutral axis distance kd and the internal lever arm jd. First defining the *reinforcement ratio* as

$$\rho = \frac{A_s}{bd} \tag{3.11}$$

then substituting $A_s = \rho bd$ into Eq. (3.5) and solving for k, one obtains

$$k = \sqrt{(\rho n)^2 + 2\rho n} - \rho n \tag{3.12}$$

From Fig. 3.5*b* it is seen that $jd = d - kd/3$, or

$$j = 1 - \frac{k}{3} \tag{3.13}$$

Values of k and j for elastic cracked section analysis, for common reinforcement ratios and modular ratios, are found in Table A.6 of Appendix A.

EXAMPLE 3.2 The beam of Example 3.1 is subject to a bending moment $M = 122$ kN-m (rather than 61 kN-m as previously). Calculate the relevant properties and stresses.

Solution. If the section were to remain uncracked, the tensile stress in the concrete would now be twice its previous value, that is, 6.44 MPa. Since this exceeds by far the modulus of rupture of the given concrete (3.27 MPa), cracks will have formed and the analysis must be adapted consistent with Fig. 3.5. Equation (3.5), with the known quantities b, n, and A_s inserted, gives the distance to the neutral axis $kd = 198$ mm, or $k = 198/600 = 0.33$. From Eq. (3.13), $j = 1 - 0.33/3 = 0.89$. With these values the steel stress is obtained from Eq. (3.8) as $f_s = 153.6$ MPa, and the maximum concrete stress from Eq. (3.10) as $f_c = 9.58$ MPa.

Comparing the results with the pertinent values for the same beam when subject to one-half the moment, as previously calculated, one notices that (1) the neutral plane has migrated upward so that its distance from the top fiber has changed from 308 to 198 mm; (2) even though the bending moment has only been doubled, the steel stress has increased from 19.43 to 153.6 MPa, or about 7.9 times, and the concrete compression stress has increased from 3.22 to 9.58 MPa, or 3 times; (3) the moment of inertia of the cracked transformed section is easily computed to be 2,625,000,000 mm^4, compared with 6,481,000,000 mm^4 for the uncracked section. This affects the magnitude of the deflection, as discussed in Chapter 6. Thus, it is seen how radical is the influence of the formation of tension cracks on the behavior of reinforced concrete beams.

---

c. Flexural Strength

It is of interest in structural practice to calculate those stresses and deformations that occur in a structure in service under design load. For reinforced concrete beams, this can be done by the methods just presented, which assume elastic behavior of both materials. It is equally, if not more, important that the structural engineer be able to predict with satisfactory accuracy the strength of a structure or structural member. By making this strength larger by an appropriate amount than the largest loads that can be expected during the lifetime of the structure, an adequate margin of safety is ensured. In the past, methods based on elastic analysis, like those just presented or variations thereof, have been used for this purpose. It is clear, however, that at or near the ultimate load, stresses are no longer proportional to strains. In regard to axial compression, this has been discussed in detail in Section 1.9, and in regard to bending, it has been pointed out that at high loads, close to failure, the distribution of stresses and strains is that of Fig. 3.2*f* rather than the elastic distribution of Fig. 3.2*e*. More realistic methods of analysis, based on actual inelastic rather than assumed elastic behavior of the materials and on results of extremely extensive experimental research, have been developed to predict the member strength. They are now used almost exclusively in structural design practice.

If the distribution of concrete compressive stresses at or near ultimate load (Fig. 3.2*f*) had a well-defined and invariable shape—parabolic, trapezoidal, or otherwise—it would be possible to derive a completely rational theory of bending strength, just as the theory of elastic bending with its known triangular shape of stress distribution (Figs. 3.1*b* and 3.2*c* and *e*) is straightforward and rational. Actually, inspection of Figs. 2.3, 2.4, and 2.6, and of many more concrete stress-strain curves that have been published, shows that the geometric shape of the stress distribution is quite varied and depends on a number of factors, such as the cylinder strength and the rate and duration of loading. For this and other reasons, a wholly rational flexural theory for reinforced concrete has not yet been developed (Refs. 3.1 to 3.3). Present methods of analysis, therefore, are based in part on known laws of mechanics and are supplemented, where needed, by extensive test information.

Let Fig. 3.6 represent the distribution of internal stresses and strains when the beam is about to fail. One desires a method to calculate that moment M_n (nominal moment) at which the beam will fail either by tension yielding of the steel or by crushing of the concrete in the outer compression fiber. For the first mode of failure, the criterion is that the steel stress equal the yield point, $f_s = f_y$. It has been mentioned before that an exact criterion for concrete compression failure is not yet known, but that for rectangular beams, strains of 0.003 to 0.004 have been measured immediately preceding failure. If one assumes, usually slightly conservatively, that the concrete is about to crush when the maximum strain reaches $\epsilon_u = 0.003$, comparison with a great many tests of beams and columns of a considerable variety of shapes and conditions of loading shows that a satisfactorily accurate and safe strength prediction can be

FIGURE 3.6
Stress distribution at ultimate load.

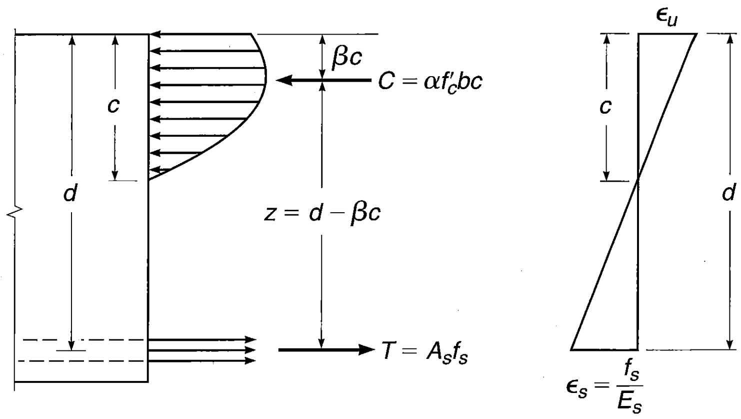

made (Ref. 3.4). In addition to these two criteria (yielding of the steel at a stress of f_y and crushing of the concrete at a strain of 0.003), it is not really necessary to know the exact shape of the concrete stress distribution in Fig. 3.6. What is necessary is to know, for a given distance c of the neutral axis, (1) the total resultant compression force C in the concrete and (2) its vertical location, i.e., its distance from the outer compression fiber.

In a rectangular beam, the area that is in compression is bc, and the total compression force on this area can be expressed as $C = f_{\mathrm{av}} bc$, where f_{av} is the average compression stress on the area bc. Evidently, the average compressive stress that can be developed before failure occurs becomes larger, the higher the cylinder strength f'_c of the particular concrete. Let

$$\alpha = \frac{f_{\mathrm{av}}}{f'_c} \tag{3.14}$$

Then

$$C = \alpha f'_c bc \tag{3.15}$$

For a given distance c to the neutral axis, the location of C can be defined as some fraction β of this distance. Thus, as indicated in Fig. 3.6, for a concrete of given strength it is necessary to know only α and β to completely define the effect of the concrete compressive stresses.

Extensive direct measurements, as well as indirect evaluations of numerous beam tests, have shown that the following values for α and β are satisfactorily accurate (see Ref. 3.5, where α is designated as k_1k_3 and β as k_2):

α equals 0.72 for $f'_c \leq 28$ MPa and decreases by 0.04 for every 7 MPa above 28 up to 56 MPa. For $f'_c > 56$ MPa, $\alpha = 0.56$.

β equals 0.425 for $f'_c \leq 28$ MPa and decreases by 0.025 for every 7 MPa above 28 up to 56 MPa. For $f'_c > 56$ MPa, $\beta = 0.325$.

The decrease in α and β for high-strength concretes is related to the fact that such concretes are more brittle; i.e., they show a more sharply curved stress-strain plot with a smaller near-horizontal portion (see Figs. 2.3 and 2.4). Figure 3.7 shows these simple relations.

If this experimental information is accepted, the maximum moment can be calculated from the laws of equilibrium and from the assumption that plane cross sections remain plane. Equilibrium requires that

$$C = T \qquad \text{or} \qquad \alpha f'_c bc = A_s f_s \tag{3.16}$$

Also, the bending moment, being the couple of the forces C and T, can be written as either

$$M = Tz = A_s f_s (d - \beta c) \tag{3.17}$$

or

$$M = Cz = \alpha f'_c bc (d - \beta c) \tag{3.18}$$

For failure initiated by yielding of the tension steel, $f_s = f_y$. Substituting this value in Eq. (3.16), one obtains the distance to the neutral axis

$$c = \frac{A_s f_y}{\alpha f'_c b} \tag{3.19a}$$

FIGURE 3.7
Variation of α and β with concrete strength f'_c.

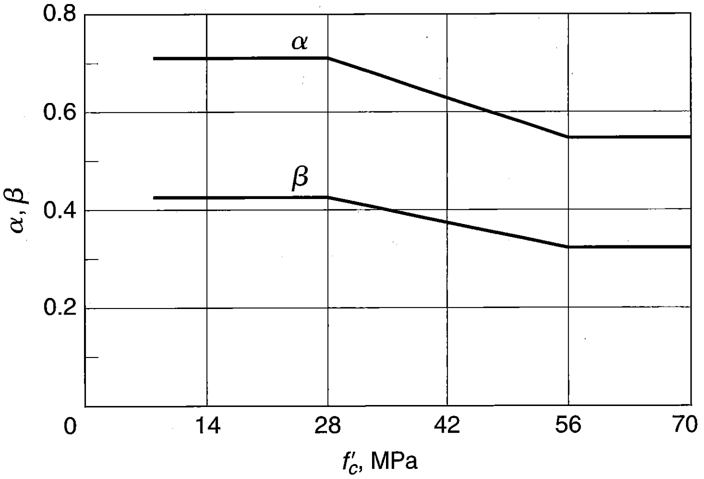

Alternatively, using $A_s = \rho bd$, the neutral axis distance is

$$c = \frac{\rho f_y d}{\alpha f'_c} \tag{3.19b}$$

giving the distance to the neutral axis when tension failure occurs. The nominal moment M_n is then obtained from Eq. (3.17) with the value for c just determined, and $f_s = f_y$; that is,

$$M_n = \rho f_y b d^2 \left(1 - \frac{\beta f_y \rho}{\alpha f'_c}\right) \tag{3.20a}$$

With the specific, experimentally obtained values for α and β given previously, this becomes

$$M_n = \rho f_y b d^2 \left(1 - 0.59 \frac{\rho f_y}{f'_c}\right) \tag{3.20b}$$

If, for larger reinforcement ratios, the steel does not reach yield at failure, then the strain in the concrete becomes $\epsilon_u = 0.003$, as previously discussed. The steel stress f_s, not having reached the yield point, is proportional to the steel strain ϵ_s; i.e., according to Hooke's law,

$$f_s = \epsilon_s E_s$$

From the strain distribution of Fig. 3.6, the steel strain ϵ_s can be expressed in terms of the distance c by evaluating similar triangles, after which it is seen that

$$f_s = \epsilon_u E_s \frac{d - c}{c} \tag{3.21}$$

Then, from Eq. (3.16),

$$\alpha f'_c bc = A_s \epsilon_u E_s \frac{d - c}{c} \tag{3.22}$$

and this quadratic may be solved for c, the only unknown for the given beam. With both c and f_s known, the nominal moment of the beam, so heavily reinforced that failure occurs by crushing of the concrete, may be found from either Eq. (3.17) or Eq. (3.18).

Whether or not the steel has yielded at failure can be determined by comparing the actual reinforcement ratio with the *balanced reinforcement ratio* ρ_b, representing that amount of reinforcement necessary for the beam to fail by crushing of the concrete at the same load that causes the steel to yield. This means that the neutral axis must be so located that at the load at which the steel starts yielding, the concrete reaches its compressive strain limit ϵ_u. Correspondingly, setting $f_s = f_y$ in Eq. (3.21) and substituting the yield strain ϵ_y for f_y/E_s, one obtains the value of c defining the unique position of the neutral axis corresponding to simultaneous crushing of the concrete and initiation of yielding in the steel

$$c = \frac{\epsilon_u}{\epsilon_u + \epsilon_y} d \tag{3.23}$$

Substituting that value of c into Eq. (3.16), with $A_s f_s = \rho b d f_y$, one obtains for the balanced reinforcement ratio

$$\rho_b = \frac{\alpha f'_c}{f_y} \frac{\epsilon_u}{\epsilon_u + \epsilon_y} \tag{3.24}$$

EXAMPLE 3.3 Determine the nominal moment M_n at which the beam of Examples 3.1 and 3.2 will fail.

Solution. For this beam the reinforcement ratio $\rho = A_s/(bd) = 1530/(250 \times 600) = 0.0102$. The balanced reinforcement ratio is found from Eq. (3.24) to be 0.0284. Since the amount of steel in the beam is less than that which would cause failure by crushing of the concrete, the beam will fail in tension by yielding of the steel. Its nominal moment, from Eq. (3.20*b*), is

$$\begin{aligned} M_n &= 0.0102 \times 420 \times 250 \times 600^2 \left(1 - 0.59 \frac{0.0102 \times 420}{28} \right) \\ &= 350{,}800{,}000 \text{ N-mm} = 350.8 \text{ kN-m} \end{aligned}$$

When the beam reaches M_n, the distance to its neutral axis, from Eq. (3.19*b*), is

$$c = \frac{0.0102 \times 420 \times 600}{0.72 \times 28} = 127.5 \text{ mm}$$

It is informative to compare this result with those of Examples 3.1 and 3.2. In the previous calculations, it was found that at low loads, when the concrete had not yet cracked in tension, the neutral axis was located at a distance of 342 mm from the compression edge; at higher loads, when the tension concrete was cracked but stresses were still sufficiently small to be elastic, this distance was 198 mm. Immediately before the beam fails, as has just been shown, this distance has further decreased to 127.5 mm. For these same stages of loading, the stress in the steel increased from 19.43 MPa in the uncracked section, to 153.6 MPa in the cracked elastic section, and to 420 MPa at the nominal moment capacity. This migration of the neutral axis toward the compression edge and the increase in steel stress as load is increased is a graphic illustration of the differences between the various stages of behavior through which a reinforced concrete beam passes as its load is increased from zero to the value that causes it to fail. The examples also illustrate the fact that nominal moments cannot be determined accurately by elastic calculations.

3.4 DESIGN OF TENSION-REINFORCED RECTANGULAR BEAMS

For reasons that were explained in Chapter 1, the present design of reinforced concrete structures is based on the concept of providing sufficient strength to resist hypothetical overloads. The *nominal strength* of a proposed member is calculated based on the best current knowledge of member and material behavior. That nominal strength is modified by a *strength reduction factor* ϕ, less than unity, to obtain the *design strength*. The *required strength*, should the hypothetical overload stage actually be realized, is found by applying *load factors* γ, greater than unity, to the loads actually expected. These expected *service loads* include the calculated dead load, the calculated or legally specified live load, and environmental loads such as those due to wind, seismic action, or temperature. Thus reinforced concrete members are proportioned so that, as shown in Eq. (1.5),

$$M_u \leq \phi M_n$$

$$P_u \leq \phi P_n$$

$$V_u \leq \phi V_n$$

where the subscripts n denote the nominal strengths in flexure, thrust, and shear, respectively, and the subscripts u denote the factored load moment, thrust, and shear. The strength reduction factors ϕ normally differ, depending upon the type of strength to be calculated, the importance of the member in the structure, and other considerations discussed in detail in Chapter 1.

A member proportioned on the basis of adequate strength at a hypothetical overload stage must also perform in a satisfactory way under normal service load conditions. In specific terms, the deflection must be limited to an acceptable value, and concrete tensile cracks, which inevitably occur, must be of narrow width and well distributed throughout the tensile zone. Therefore, after proportioning for adequate strength, deflections are calculated and compared against limiting values (or otherwise controlled), and crack widths limited by specific means. This approach to design, referred to in Europe, and to some extent in U.S. practice, as *limit states design*, is the basis of the 2008 ACI Code, and it is the approach that will be followed in this and later chapters.

a. Equivalent Rectangular Stress Distribution

The method presented in Section 3.3c for calculating the flexural strength of reinforced concrete beams, derived from basic concepts of structural mechanics and pertinent experimental research information, also applies to situations other than the case of rectangular beams reinforced on the tension side. It can be used and gives valid answers for beams of other cross-sectional shapes, reinforced in other manners, and for members subject not only to simple bending but also to the simultaneous action of bending and axial force (compression or tension). However, the pertinent equations for these more complex cases become increasingly cumbersome and lengthy. What is more important, it becomes increasingly difficult for the designer to visualize the physical basis for the design methods and formulas; this could lead to a blind reliance on formulas, with a resulting lack of actual understanding. This is not only undesirable on general grounds but also, practically, is more likely to lead to numerical errors in design work than when the designer at all times has a clear picture of the physical situation in the member being dimensioned or analyzed. Fortunately, it is possible, essentially by a conceptual trick, to formulate the strength analysis of reinforced concrete members in a different manner, which gives the same answers as the general analysis just developed but which is much more easily visualized and much more easily applied to cases of greater complexity than that of the simple rectangular beam. Its consistency is shown, and its application to more complex cases has been checked against the results of a vast number of tests on a great variety of types of members and conditions of loading (Ref. 3.4).

It was noted in the preceding section that the actual geometric shape of the concrete compressive stress distribution varies considerably and that, in fact, one need not know this shape exactly, provided one does know two things: (1) the magnitude C of the resultant of the concrete compressive stresses and (2) the location of this resultant. Information on these two quantities was obtained from the results of experimental research and expressed in the two parameters α and β.

Evidently, then, one can think of the actual complex stress distribution as replaced by a fictitious one of some simple geometric shape, provided that this fictitious distribution results in the same total compression force C applied at the same location as in the actual member when it is on the point of failure. Historically, a number of simplified, fictitious equivalent stress distributions have been proposed by investigators in various countries. The one generally accepted in this country, and increasingly abroad, was first proposed by C. S. Whitney (Ref. 3.4) and was subsequently elaborated and checked experimentally by others (see, for example, Refs. 3.5 and 3.6). The actual stress distribution immediately before failure and the fictitious equivalent distribution are shown in Fig. 3.8.

It is seen that the actual stress distribution is replaced by an equivalent one of simple rectangular outline. The intensity $\gamma f'_c$ of this equivalent constant stress and its depth $a = \beta_1 c$ are easily calculated from the two conditions that (1) the total compression force C and (2) its location, i.e., distance from the top fiber, must be the same in the equivalent rectangular as in the actual stress distribution. From Fig. 3.8*a* and *b* the first condition gives

$$C = \alpha f'_c cb = \gamma f'_c ab \qquad \text{from which} \qquad \gamma = \alpha \frac{c}{a}$$

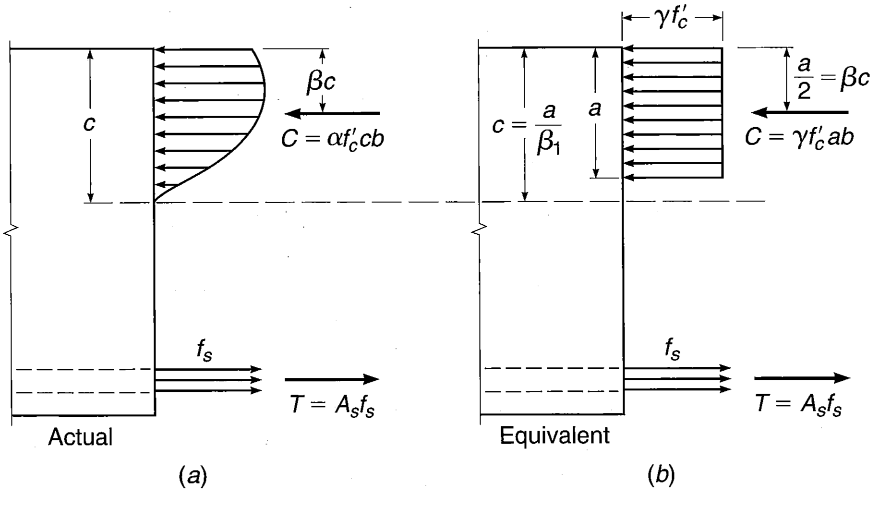

FIGURE 3.8
Actual and equivalent rectangular stress distributions at ultimate load.

TABLE 3.1
Concrete stress block parameters

	f'_c, MPa				
	≤ 28	35	42	49	≥ 56
α	0.72	0.68	0.64	0.60	0.56
β	0.425	0.400	0.375	0.350	0.325
$\beta_1 = 2\beta$	0.85	0.80	0.75	0.70	0.65
$\gamma = \alpha/\beta_1$	0.85	0.85	0.85	0.86	0.86

With $a = \beta_1 c$, this gives $\gamma = \alpha/\beta_1$. The second condition simply requires that in the equivalent rectangular stress block, the force C be located at the same distance βc from the top fiber as in the actual distribution. It follows that $\beta_1 = 2\beta$.

To supply the details, the upper two lines of Table 3.1 present the experimental evidence of Fig. 3.7 in tabular form. The lower two lines give the just-derived parameters β_1 and γ for the rectangular stress block. It is seen that the stress intensity factor γ is essentially independent of f'_c and can be taken as 0.85 throughout. Hence, regardless of f'_c, the concrete compression force at failure in a rectangular beam of width b is

$$C = 0.85 f'_c ab \tag{3.25}$$

Also, for the common concretes with $f'_c \le 28$ MPa, the depth of the rectangular stress block is $a = 0.85c$, with c being the distance to the neutral axis. For higher-strength concretes, this distance is $a = \beta_1 c$, with the β_1 values shown in Table 3.1. This is expressed in ACI Code 10.2.7.3 as follows: For f'_c between 17 and 28 MPa, β_1 shall be taken as 0.85; for f'_c above 28 MPa, β_1 shall be reduced linearly at a rate of 0.05 for each 7 MPa of strength in excess of 28 MPa, but β_1 shall not be taken as less than 0.65. In mathematical terms, the relationship between β_1 and f'_c can be expressed as

$$\beta_1 = 0.85 - 0.05\frac{f'_c - 28}{7} \qquad \text{and} \qquad 0.65 \le \beta_1 \le 0.85 \tag{3.26}$$

The equivalent rectangular stress distribution can be used for deriving the equations that have been developed in Section 3.3c. The failure criteria, of course, are the same as before: yielding of the steel at $f_s = f_y$ or crushing of the concrete at $\epsilon_u = 0.003$. Because the rectangular stress block is easily visualized and its geometric properties are extremely simple, many calculations are carried out directly without reference to formally derived equations, as will be seen in the following sections.

b. Balanced Strain Condition

A reinforcement ratio ρ_b producing balanced strain conditions can be established based on the condition that, at balanced failure, the steel strain is exactly equal to ϵ_y when the strain in the concrete simultaneously reaches the crushing strain of $\epsilon_u = 0.003$. Referring to Fig. 3.6,

$$c = \frac{\epsilon_u}{\epsilon_u + \epsilon_y} d \tag{3.27}$$

which is seen to be identical to Eq. (3.23). Then from the equilibrium requirement that $C = T$

$$\rho_b f_y bd = 0.85 f_c' ab = 0.85 \beta_1 f_c' bc$$

from which

$$\rho_b = 0.85 \beta_1 \frac{f_c'}{f_y} \frac{\epsilon_u}{\epsilon_u + \epsilon_y} \tag{3.28}$$

This is easily shown to be equivalent to Eq. (3.24).

c. Underreinforced Beams

A compression failure in flexure, should it occur, gives little if any warning of distress, while a tension failure, initiated by yielding of the steel, typically is gradual. Distress is obvious from observing the large deflections and widening of concrete cracks associated with yielding of the steel reinforcement, and measures can be taken to avoid total collapse. In addition, most beams for which failure initiates by yielding possess substantial strength based on strain-hardening of the reinforcing steel, which is not accounted for in the calculations of M_n.

Because of these differences in behavior, it is prudent to require that beams be designed such that failure, if it occurs, will be by yielding of the steel, not by crushing of the concrete. This can be done, theoretically, by requiring that the reinforcement ratio ρ be less than the balance ratio ρ_b given by Eq. (3.28).

In actual practice, the upper limit on ρ should be below ρ_b for the following reasons: (1) for a beam with ρ exactly equal to ρ_b, the compressive strain limit of the concrete would be reached, theoretically, at precisely the same moment that the steel reaches its yield stress, without significant yielding before failure; (2) material properties are never known precisely; (3) strain-hardening of the reinforcing steel, not accounted for in design, may lead to a brittle concrete compression failure even though ρ may be somewhat less than ρ_b; (4) the actual steel area provided, considering standard reinforcing bar sizes, will always be equal to or larger than required, based on selected reinforcement ratio ρ, tending toward overreinforcement; and (5) the extra ductility provided by beams with lower values of ρ increases the deflection capability substantially and thus provides warning prior to failure.

d. ACI Code Provisions for Underreinforced Beams

While the nominal strength of a member may be computed based on principles of mechanics, the mechanics alone cannot establish safe limits for maximum reinforcement ratios. These limits are defined by the ACI Code. The limitations take two forms. First, the Code addresses the minimum tensile reinforcement strain allowed at nominal strength in the design of beams. Second, the Code defines strength reduction factors that may depend on the tensile strain at nominal strength. Both limitations are based on the *net tensile strain* ϵ_t of the reinforcement farthest from the compression face of the concrete at the depth d_t. The net tensile strain is exclusive of prestress, temperature, and shrinkage effects. For beams with a single layer of reinforcement, the depth to the centroid of the steel d is the same as d_t. For beams with multiple layers of reinforcement, d_t is greater than the depth to the centroid of the reinforcement d. Substituting d_t for d and ϵ_t for ϵ_y in Eq. (3.27), the net tensile strain may be represented as

$$\epsilon_t = \epsilon_u \frac{d_t - c}{c} \tag{3.29}$$

Then based on Eq. (3.28), the reinforcement ratio to produce a selected value of net tensile strain is

$$\rho = 0.85\beta_1 \frac{f'_c}{f_y} \frac{d_t}{d} \frac{\epsilon_u}{\epsilon_u + \epsilon_t} \tag{3.30a}$$

or somewhat conservatively

$$\rho = 0.85\beta_1 \frac{f'_c}{f_y} \frac{\epsilon_u}{\epsilon_u + \epsilon_t} \tag{3.30b}$$

To ensure underreinforced behavior, ACI Code 10.3.5 establishes a minimum net tensile strain ϵ_t at the nominal member strength of 0.004 for members subjected to axial loads less than $0.10f'_cA_g$, where A_g is the gross area of the cross section. By way of comparison ϵ_y, the steel strain at the balanced condition, is 0.00210 for $f_y = 420$ MPa and 0.00260 for $f_y = 520$ MPa.

Using $\epsilon_t = 0.004$ in Eq. (3.30*b*) provides the maximum reinforcement ratio allowed by the ACI Code for beams

$$\rho_{\max} = 0.85\beta_1 \frac{f'_c}{f_y} \frac{\epsilon_u}{\epsilon_u + 0.004} \tag{3.30c}$$

The ACI Code further encourages the use of lower reinforcement ratios by allowing higher strength reduction factors in such beams. The Code defines a *tension-controlled member* as one with a net tensile strain greater than or equal to 0.005. The corresponding strength reduction factor is $\phi = 0.9$.[†] The Code additionally defines a *compression-controlled member* as having a net tensile strain of less than 0.002. The strength reduction factor for compression-controlled members is 0.65. A value of 0.75 may be used if the members are spirally reinforced. A value of $\epsilon_t = 0.002$ corresponds approximately to the yield strain for steel with $f_y = 420$ MPa yield strength. Between net tensile strains of 0.002 and 0.005, the strength reduction factor varies linearly, and the ACI Code allows a linear interpolation of ϕ based on ϵ_t, as shown in Fig. 3.9. Based on Eq. (3.30*b*), the maximum reinforcement ratio for a tension-controlled beam is

$$\rho_{0.005} = 0.85\beta_1 \frac{f'_c}{f_y} \frac{\epsilon_u}{\epsilon_u + 0.005} \tag{3.30d}$$

A comparison of Eqs. (3.30*c*) and (3.30*d*) shows that, for a given concrete cross section, using $\epsilon_t = 0.004$ will result in a higher reinforcement ratio, and thus a higher nominal flexural strength, than using $\epsilon_t = 0.005$. This higher strength, however, cannot be used to full advantage in design because the increase in flexural strength is canceled by the drop in ϕ as ϵ_t decreases from 0.005 to 0.004. As a result, the maximum practical reinforcement ratio for beams is attained at a net tensile strain of 0.005. Values of ϵ_t below 0.005 are not recommended for the design of members with low axial loads.

[†] The selection of a net tensile strain of 0.005 is intended to encompass the yield strain of all reinforcing steel including high-strength bars and prestressing tendons.

FIGURE 3.9
Variation of strength reduction factor with net tensile strain in the steel.

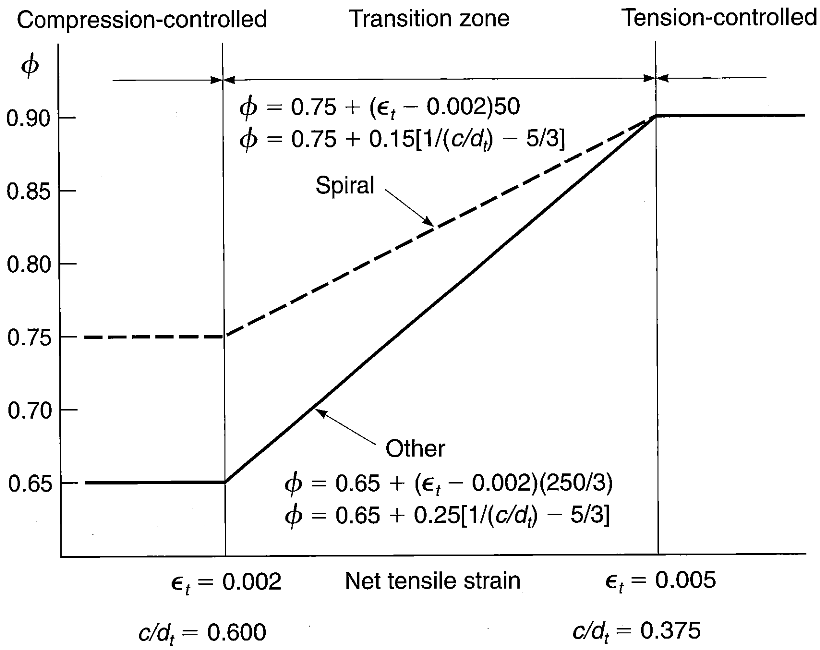

Calculation of the nominal moment capacity frequently involves determination of the depth of the equivalent rectangular stress block a. Since $c = a/\beta_1$, it is sometimes more convenient to compute c/d_t ratios than either ρ or the net tensile strain. The assumption that plane sections remain plane ensures a direct correlation between net tensile strain and the c/d_t ratio, as shown in Fig. 3.10. The maximum value of c/d_t for $\epsilon_t \geq 0.005$ is 0.375.

Comparing Eqs. (3.30*a*) and (3.30*b*), it can be seen that the maximum reinforcement ratios in Eqs. (3.30*c*) and (3.30*d*) are exact for beams with a single layer of reinforcement and slightly conservative for beams with multiple layers of reinforcement, where d_t is greater than d. Because $\epsilon_t \geq 0.004$ (better yet $\epsilon_t \geq 0.005$) ensures

FIGURE 3.10
Net tensile strain and c/d_t ratios.

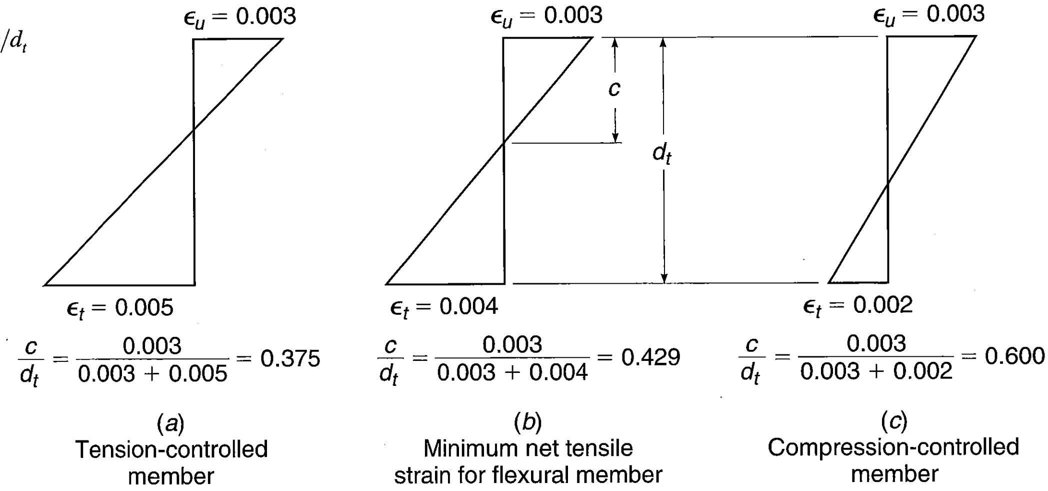
$\epsilon_u = 0.003$
$\epsilon_u = 0.003$
$\epsilon_u = 0.003$
c
d_t
$\epsilon_t = 0.005$
$\epsilon_t = 0.004$
$\epsilon_t = 0.002$
$\frac{c}{d_t} = \frac{0.003}{0.003 + 0.005} = 0.375$
$\frac{c}{d_t} = \frac{0.003}{0.003 + 0.004} = 0.429$
$\frac{c}{d_t} = \frac{0.003}{0.003 + 0.002} = 0.600$

(*a*) Tension-controlled member

(*b*) Minimum net tensile strain for flexural member

(*c*) Compression-controlled member

FIGURE 3.11
Singly reinforced rectangular beam.

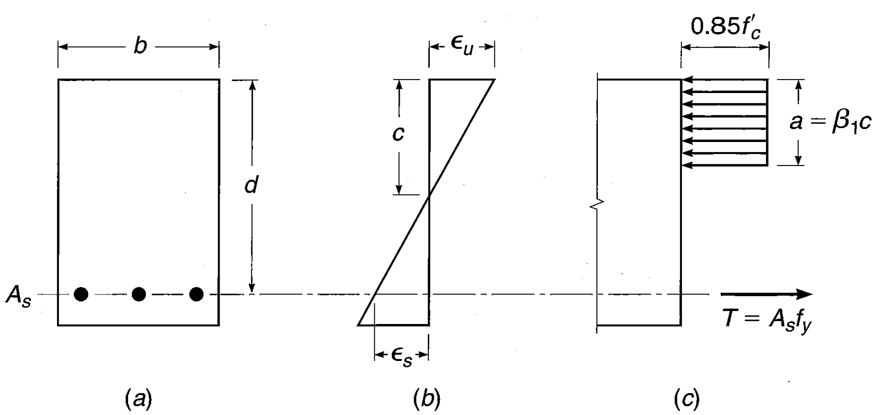

that steel is yielding in tension, $f_s = f_y$ at failure, and the nominal flexural strength (referring to Fig. 3.11) is given by

$$M_n = A_s f_y \left(d - \frac{a}{2} \right) \tag{3.31}$$

where

$$a = \frac{A_s f_y}{0.85 f'_c b} \tag{3.32}$$

EXAMPLE 3.4

Using the equivalent rectangular stress distribution, directly calculate the nominal strength of the beam previously analyzed in Example 3.3. Recall that $b = 250$ mm, $d = 600$ mm, $A_s = 1530$ mm^2, $f'_c = 28$ MPa, $f_y = 420$ MPa, and $\beta_1 = 0.85$.

Solution. The distribution of stresses, internal forces, and strains is shown in Fig. 3.11. The maximum practical reinforcement ratio is calculated from Eq. (3.30*d*) as

$$\rho_{0.005} = 0.85 \times 0.85 \frac{28}{420} \frac{0.003}{0.003 + 0.005} = 0.0181$$

and comparison with the actual reinforcement ratio of 0.0102 confirms that the member is underreinforced and will fail by yielding of the steel. Alternatively, recalling that $c = 127.5$ mm,

$$\frac{c}{d_t} = \frac{c}{d} = \frac{127.5}{600} = 0.213$$

which is less than 0.375, the value of c/d_t corresponding to $\epsilon_t = 0.005$, also confirming that the member is underreinforced. The depth of the equivalent stress block is found from the equilibrium condition that $C = T$. Hence $0.85f'_c ab = A_s f_y$, or $a = 1530 \times 420/(0.85 \times 28 \times 250) = 108$ mm. The nominal moment is

$$M_n = A_s f_y \left(d - \frac{a}{2} \right) = 1530 \times 420 \left(600 - \frac{108}{2} \right) = 350.9 \times 10^6 \text{ N-mm} = 350.9 \text{ kN-m}$$

The results of this simple and direct numerical analysis, based on the equivalent rectangular stress distribution, are identical with those previously determined from the general strength analysis described in Section 3.3c.

It is convenient for everyday design to combine Eqs. (3.31) and (3.32) as follows. Noting that $A_s = \rho bd$, Eq. (3.32) can be rewritten as

$$a = \frac{\rho f_y d}{0.85 f'_c} \tag{3.33}$$

This is then substituted into Eq. (3.31) to obtain

$$M_n = \rho f_y bd^2 \left(1 - 0.59 \frac{\rho f_y}{f'_c}\right) \tag{3.34}$$

which is identical to Eq. (3.20*b*) derived in Section 3.3c. This basic equation can be simplified further as follows:

$$M_n = Rbd^2 \tag{3.35}$$

in which

$$R = \rho f_y \left(1 - 0.59 \frac{\rho f_y}{f'_c}\right) \tag{3.36}$$

The *flexural resistance factor R* depends only on the reinforcement ratio and the strengths of the materials and is easily tabulated. Tables A.5a and A.5b of Appendix A give R values for ordinary combinations of steel and concrete and the full practical range of reinforcement ratios.

In accordance with the safety provisions of the ACI Code, the nominal flexural strength M_n is reduced by imposing the strength reduction factor ϕ to obtain the *design strength*

$$\phi M_n = \phi A_s f_y \left(d - \frac{a}{2}\right) \tag{3.37}$$

or, alternatively,

$$\phi M_n = \phi \rho f_y bd^2 \left(1 - 0.59 \frac{\rho f_y}{f'_c}\right) \tag{3.38}$$

or

$$\phi M_n = \phi Rbd^2 \tag{3.39}$$

EXAMPLE 3.4 (*continued*) Calculate the design moment capacity ϕM_n for the beam analyzed earlier in Example 3.4.

SOLUTION. Comparing ρ with $\rho_{0.005}$ or c/d_t for the beam with the value of c/d_t corresponding to $\epsilon_t = 0.005$ demonstrates that $\epsilon_t > 0.005$. Therefore, $\phi = 0.90$ and the design capacity is

$$\phi M_n = 0.9 \times 350.9 = 315.8 \text{ kN-m}$$

---

e. Minimum Reinforcement Ratio

Another mode of failure may occur in very lightly reinforced beams. If the flexural strength of the cracked section is less than the moment that produced cracking of the previously uncracked section, the beam will fail immediately and without warning of distress upon formation of the first flexural crack. To ensure against this type of failure, a *lower limit* can be established for the reinforcement ratio by equating the cracking moment, computed from the concrete modulus of rupture (Section 2.9), to the strength of the cracked section.

For a rectangular section having width b, total depth h, and effective depth d (see Fig. 3.2*b*), the section modulus with respect to the tension fiber is $bh^2/6$. For typical cross sections, it is satisfactory to assume that $h/d = 1.1$ and that the internal lever arm at flexural failure is $0.95d$. If the modulus of rupture is taken as $f_r = 0.625\sqrt{f'_c}$, as usual, then an analysis equating the cracking moment to the flexural strength results in

$$A_{s,\min} = \frac{0.13\sqrt{f'_c}}{f_y} bd \tag{3.40a}$$

This development can be generalized to apply to beams having a T cross section (see Section 3.8 and Fig. 3.16). The corresponding equations depend on the proportions of the cross section and on whether the beam is bent with the flange (slab) in tension or in compression. For T beams of typical proportions that are bent with the flange in compression, analysis will confirm that the minimum steel area should be

$$A_{s,\min} = \frac{0.22\sqrt{f'_c}}{f_y} b_w d \tag{3.40b}$$

where b_w is the width of the web, or stem, projecting below the slab. For T beams that are bent with the flange in tension, from a similar analysis, the minimum steel area is

$$A_{s,\min} = \frac{0.51\sqrt{f'_c}}{f_y} b_w d \tag{3.40c}$$

The ACI Code requirements for minimum steel area are based on the results just discussed, but there are some differences. According to ACI Code 10.5, at any section where tensile reinforcement is required by analysis, with some exceptions as noted below, the area A_s provided must not be less than

$$A_{s,\min} = \frac{0.25\sqrt{f'_c}}{f_y} b_w d \geq \frac{1.4 b_w d}{f_y} \tag{3.41}$$

This applies to both positive and negative bending sections. The inclusion of the additional limit of $1.4b_w d/f_y$ is merely for historical reasons; it happens to give the same minimum reinforcement ratio of 0.005 that was imposed in earlier codes for then-common material strengths. Note that in Eq. (3.41) the section width b_w is used; it is understood that for rectangular sections $b_w = b$. Note further that the ACI coefficient of 0.25 is a conservatively rounded value compared with 0.22 in Eq. (3.40*b*) for T beams with the flange in compression, and is very conservative when applied to rectangular beam sections, for which a rational analysis gives 0.13 in Eq. (3.40*a*). This probably reflects the view that the minimum steel for the negative bending sections of a continuous T beam (which are, in effect, rectangular sections, as discussed in Section 3.8c) should be no less than for the positive bending sections, where the moment is generally smaller.

ACI Code 10.5 treats *statically determinate* T beams with the flange in *tension* as a special case, for which the minimum steel area is equal to or greater than the value given by Eq. (3.41) with b_w replaced by either $2b_w$ or the width of the *flange*, whichever is smaller.

Note that ACI Code Eq. (3.41) is conveniently expressed in terms of a *minimum tensile reinforcement ratio* $\rho_{\min}$ by dividing both sides by $b_w d$.

According to ACI Code 10.5, the requirements of Eq. (3.41) need not be imposed if, at every section, the area of tensile reinforcement provided is at least one-third greater than that required by analysis. This provides sufficient reinforcement for large members such as grade beams, where the usual equations would require excessive amounts of steel.

For structural slabs and footings of uniform thickness, the minimum area of tensile reinforcement in the direction of the span is that required for shrinkage and temperature steel (see Section 13.3 and Table 13.2), and the above minimums need not be imposed. The maximum spacing of such steel is the smaller of 3 times the total slab thickness or 450 mm.

f. Examples of Rectangular Beam Analysis and Design

Flexural problems can be classified broadly as *analysis problems* or *design problems*. In analysis problems, the section dimensions, reinforcement, and material strengths are known, and the moment capacity is required. In the case of design problems, the required moment capacity is given, as are the material strengths, and it is required to find the section dimensions and reinforcement. Examples 3.5 and 3.6 illustrate analysis and design, respectively.

EXAMPLE 3.5

Flexural strength of a given member. A rectangular beam has width 300 mm and effective depth 440 mm. It is reinforced with four No. 29 (No. 9) bars in one row. If f_y = 420 MPa and f'_c = 28 MPa, what is the nominal flexural strength, and what is the maximum moment that can be utilized in design, according to the ACI Code?

Solution. From Table A.2 of Appendix A, the area of four No. 29 (No. 9) bars is 2580 mm^2. Assuming that the beam is underreinforced and using Eq. (3.32),

$$a = \frac{2580 \times 420}{0.85 \times 28 \times 300} = 151.8 \text{ mm}$$

The depth of the neutral axis is $c = a/\beta_1 = 151.8/0.85 = 178.5$ mm, giving

$$\frac{c}{d_t} = \frac{178.5}{440} = 0.406$$

which is between 0.429 and 0.375, the values corresponding, respectively, to $\epsilon_t = 0.004$ and $\epsilon_t = 0.005$, as shown in Fig. 3.10. Thus, the beam is, as assumed, underreinforced, and from Eq. (3.31)

$$M_n = 2580 \times 420\left(440 - \frac{151.8}{2}\right) = 394.5 \times 10^6 \text{ N-mm} = 394.5 \text{ kN-m}$$

The fact that the beam is unreinforced could also have been established by calculating $\rho = 2580/(300 \times 440) = 0.0195$, which just exceeds $\rho_{0.005}$, which is calculated using Eq. (3.30*d*).

$$\rho_{0.005} = 0.85 \times 0.85\left(\frac{28}{420}\right)\left(\frac{0.003}{0.003 + 0.005}\right) = 0.0181$$

Because the net tensile strain ϵ_t is between 0.004 and 0.005, ϕ must be calculated: $\epsilon_t = \epsilon_u(d - c)/c = 0.003(440 - 178.5)/178.5 = 0.00439$. Using linear interpolation from Fig. 3.9, $\phi = 0.85$, and the design strength is taken as

$$\phi M_n = 0.85 \times 394.5 = 335.3 \text{ kN-m}$$

The ACI Code limits on the reinforcement ratio

$$\rho_{\max} = 0.0206$$

$$\rho_{\min} = \frac{0.25\sqrt{28}}{420} \geq \frac{1.4}{420} = 0.0033$$

are satisfied for this beam.

EXAMPLE 3.6 **Concrete dimensions and steel area to resist a given moment.** Find the concrete cross section and the steel area required for a simply supported rectangular beam with a span of 4.5 m that is to carry a computed dead load of 20 kN/m and a service live load of 31 kN/m, as shown in Fig. 3.12. Material strengths are $f'_c = 28$ MPa and $f_y = 420$ MPa.

SOLUTION. Load factors are first applied to the given service loads to obtain the factored load for which the beam is to be designed, and the corresponding moment:

$$w_u = 1.2 \times 20 + 1.6 \times 31 = 73.6 \text{ kN/m}$$

$$M_u = \frac{1}{8} \times 73.6 \times 4.5^2 = 186.3 \text{ kN-m}$$

The concrete dimensions will depend on the designer's choice of reinforcement ratio. To minimize the concrete section, it is desirable to select the maximum permissible reinforcement ratio. To maintain $\phi = 0.9$, the maximum reinforcement ratio corresponding to a net tensile strain of 0.005 will be selected (see Fig. 3.9). Then, from Eq. (3.30*d*)

$$\rho_{0.005} = 0.85\beta_1 \frac{f'_c}{f_y} \frac{\epsilon_u}{\epsilon_u + 0.005} = 0.85 \times 0.85 \left(\frac{28}{420}\right)\left(\frac{0.003}{0.003 + 0.005}\right) = 0.0181$$

Using Eq. (3.30*c*) gives $\rho_{\max} = 0.0206$, but would require a lower strength reduction factor. Setting the required flexural strength equal to the design strength from Eq. (3.38), and substituting the selected values for ρ and material strengths,

$$M_u = \phi M_n$$

$$186.3 \times 10^6 = 0.90 \times 0.0181 \times 420bd^2\left(1 - 0.59\,\frac{0.0181 \times 420}{28}\right)$$

from which

$$bd^2 = 32{,}420{,}000 \text{ mm}^3$$

A beam with width $b = 250$ mm and $d = 360$ mm will satisfy this requirement. The required steel area is found by applying the chosen reinforcement ratio to the required concrete dimensions:

$$A_s = 0.0181 \times 250 \times 360 = 1630 \text{ mm}^2$$

Two No. 32 (No. 10) bars provide 1638 mm^2, which provides the required area.

Assuming 65 mm concrete cover from the centroid of the bars, the required total depth is $h = 425$ mm. In actual practice, however, the concrete dimensions b and h are always rounded up to the nearest 25 mm, and often to the nearest multiple of 50 mm (see Section 3.5).

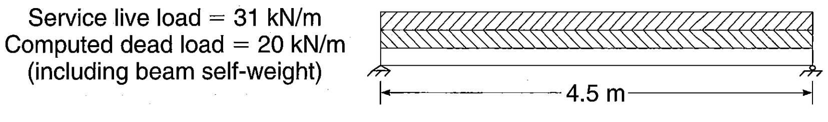
Service live load = 31 kN/m
Computed dead load = 20 kN/m
(including beam self-weight)
4.5 m

FIGURE 3.12
Structural loads for Example 3.6.

The actual d is then found by subtracting the required concrete cover dimension from h. For the present example, $b = 250$ mm and $h = 450$ mm will be selected, resulting in effective depth $d = 385$ mm. Improved economy then may be possible, refining the steel area based on the actual, larger, effective depth. One can obtain the revised steel requirement directly by solving Eq. (3.38) for ρ, with $\phi M_n = M_u$. A quicker solution can be obtained by iteration. First a reasonable value of a is assumed, and A_s is found from Eq. (3.37). From Eq. (3.32) a revised estimate of a is obtained, and A_s is revised. This method converges very rapidly. For example, assume $a = 125$ mm. Then

$$A_s = \frac{186.3 \times 10^6}{0.90 \times 420(385 - 120/2)} = 1516 \text{ mm}^2$$

Checking the assumed a gives

$$a = \frac{1516 \times 420}{0.85 \times 28 \times 250} = 107 \text{ mm}$$

This is close enough to the assumed value that no further calculation is required. The required steel area of 1516 mm^2 could be provided using three No. 25 (No. 8) bars, but for simplicity of construction, two No. 32 (No. 10) bars will be used as before.

A somewhat larger beam cross section using less steel may be more economical, and will tend to reduce deflections. As an alternative solution, the beam will be redesigned with a lower reinforcement ratio of $\rho = 0.60\rho_{\max} = 0.60 \times 0.0206 = 0.0124$. Setting the required strength equal to the design strength [Eq. (3.38)] as before,

$$186.3 \times 10^6 = 0.90 \times 0.0124 \times 420bd^2\left(1 - 0.59\,\frac{0.0124 \times 420}{28}\right)$$

and

$$bd^2 = 44{,}650{,}000 \text{ mm}^3$$

A beam with $b = 250$ mm and $d = 423$ mm will meet the requirement, for which

$$A_s = 0.0124 \times 250 \times 423 = 1311 \text{ mm}^2$$

Two No. 29 (No. 9) bars are almost sufficient, providing an area of 1290 mm^2. If the total concrete height is rounded up to 500 mm, a 435 mm effective depth results, reducing the required steel area to 1260 mm^2. Two No. 29 (No. 9) bars remain the best choice.

It is apparent that an infinite number of solutions to the stated problem are possible, depending upon the reinforcement ratio selected. That ratio may vary from an upper limit of $\rho_{\max}$ to a lower limit of $0.25\sqrt{f_c'}/f_y \geq 1.4/f_y$ for beams, according to the ACI Code. To compare the two solutions (using the theoretical dimensions, unrounded for the comparison, and assuming h is 65 mm greater than d in each case), increasing the concrete section area by 14 percent achieves a steel saving of 20 percent. The second solution would certainly be more economical and would be preferred, unless beam dimensions must be minimized for architectural or functional reasons. Economical designs will typically have reinforcement ratios between $0.50\rho_{0.005}$ and $0.75\rho_{0.005}$.

There is a type of problem, occurring frequently, that does not fall strictly into either the analysis or the design category. The concrete dimensions are given and are known to be adequate to carry the required moment, and it is necessary only to find the steel area. Typically, this is the situation at critical design sections of continuous beams, in which the concrete dimensions are often kept constant, although the steel reinforcement varies along the span according to the required flexural resistance. Dimensions b, d, and h are determined at the maximum moment section, usually at one of the supports. At other supports, and at midspan locations, where moments are usually smaller, the concrete dimensions are known to be adequate and only the tensile steel remains to be found. An identical situation was encountered in the design problem of Example 3.6, in which concrete dimensions were rounded up from the minimum required values, and the required steel area was to be found. In either case, the iterative approach demonstrated in Example 3.6 is convenient.

EXAMPLE 3.7

Determination of steel area. Using the same concrete dimensions as were used for the second solution of Example 3.6 ($b = 250$ mm, $d = 435$ mm, and $h = 500$ mm) and the same material strengths, find the steel area required to resist a moment M_u of 150 kN-m.

Solution. Assume $a = 100$ mm. Then

$$A_s = \frac{150 \times 10^6}{0.90 \times 420(435 - 50)} = 1031 \text{ mm}^2$$

Checking the assumed a gives

$$a = \frac{1031 \times 420}{0.85 \times 28 \times 250} = 72.8 \text{ mm}$$

Next assume $a = 70$ mm and recalculate A_s:

$$A_s = \frac{150 \times 10^6}{0.90 \times 420(435 - 35)} = 992 \text{ mm}^2$$

No further iteration is required. Use $A_s = 992 \text{ mm}^2$. Two No. 25 (No. 8) bars, $A_s = 1.080 \text{ mm}^2$, will be used. A check of the reinforcement ratio shows $\rho < \rho_{0.005}$ and $\phi = 0.9$.

As seen in Example 3.5, the strength reduction factor becomes a variable at high reinforcement ratios. Example 3.8 demonstrates how the variation in strength reduction factor affects the design process.

EXAMPLE 3.8

Determination of steel area and variable strength reduction factor. Architectural considerations limit the height of a 6 m long simple span beam to 400 mm and the width to 300 mm. The following loads and material properties are given: $w_d = 11$ kN/m, $w_l = 24$ kN/m, $f'_c = 35$ MPa, and $f_y = 420$ MPa. Determine the reinforcement for the beam.

Solution. Calculating the factored loads gives

$$w_u = 1.2 \times 11 + 1.6 \times 24 = 51.6 \text{ kN/m}$$

$$M_u = 51.6 \times \frac{6^2}{8} = 232.2 \text{ kN-m}$$

Assume $a = 100$ mm and $\phi = 0.90$. The structural depth is $(400 - 60)$ mm $= 340$ mm. Calculating A_s gives

$$A_s = \frac{M_u}{\phi f_y(d - a/2)} = \frac{232.2 \times 10^6}{0.9 \times 420(335 - 50)} = 2156 \text{ mm}^2$$

Try two No. 32 (No. 10) and one No. 29 (No. 9) bar, $A_s = 2283 \text{ mm}^2$.

Check $a = 2283 \times 420/(0.85 \times 35 \times 300) = 107.4$ mm from Eq. (3.32). This is more than assumed; therefore, continue to check the moment capacity.

$$M_n = 2283 \times 420(335 - 107.4/2) \times 10^{-6} = 269.7 \text{ kN-m}$$

Using a ϕ of 0.90 gives $\phi M_n = 242.7$ kN-m, which is adequate; however, the net tensile strain must be checked to validate the selection of $\phi = 0.9$. In this case $c = a/\beta_1 = 107.4/0.80 = 134.3$ mm. The c/d ratio is $0.401 > 0.375$, so $\epsilon_t > 0.005$ is not satisfied. The corresponding net tensile strain is

$$\epsilon_t = 0.003\,\frac{335 - 134.3}{134.3} = 0.00448$$

A value of $\epsilon_t = 0.00448$ is allowed by the ACI Code, but only if the strength reduction factor is adjusted. A linear interpolation from Fig. 3.9 gives $\phi = 0.86$ and $M_u = \phi M_n = 231.9$ kN-m, which is less than the required capacity. Try increasing the reinforcement to three No. 32 (No. 10) bars, $A_s = 2457\ \text{mm}^2$. Repeating the calculations,

$$a = \frac{2457 \times 420}{0.85 \times 35 \times 300} = 115.6\ \text{mm}$$

$$c = \frac{115.6}{0.80} = 144.5\ \text{mm}$$

$$M_n = 2457 \times 420\left(335 - \frac{115.6}{2}\right) \times 10^{-6} = 286.1\ \text{kN-m}$$

$$\epsilon_t = \frac{0.003(335 - 144.5)}{144.5} = 0.00400$$

$$\phi = 0.65 + (0.00400 - 0.002)(250/3) = 0.817$$

$$M_u = \phi M_n = 0.817 \times 286.1 = 233.7\ \text{kN-m}$$

which meets the design requirements.

In actuality, the first solution deviates less than 1 percent from the desired value and would likely be acceptable. The remaining portion of the example demonstrates the design implications of requiring a variable strength reduction factor when the net tensile strain falls between 0.005 and 0.004. In this example, the reinforcement increased nearly 8 percent, yet the design moment capacity ϕM_n only increased 0.5 percent due to the decreasing strength reduction factor. For this reason, designs with $\rho < \rho_{0.005}$ are desirable.

In solving these examples, the basic equations have been used to develop familiarity with them. In actual practice, however, design aids such as Table A.4 of Appendix A, giving values of maximum and minimum reinforcement ratios, and Table A.5, providing values of flexural resistance factor R, are more convenient. The example problems will be repeated in Section 3.5 to demonstrate use of these aids.

g. Overreinforced Beams

According to the ACI Code, all beams are to be designed for yielding of the tension steel with ϵ_t not less than 0.004 and thus $\rho \le \rho_{\max}$. Occasionally, however, such as when analyzing the capacity of existing construction, it may be necessary to calculate the flexural strength of an overreinforced compression-controlled member, for which f_s is less than f_y at flexural failure.

In this case, the steel strain, in Fig. 3.11*b*, will be less than the yield strain, but can be expressed in terms of the concrete strain ϵ_u and the still-unknown distance c to the neutral axis:

$$\epsilon_s = \epsilon_u\,\frac{d - c}{c} \tag{3.42}$$

From the equilibrium requirement that $C = T$, one can write

$$0.85\beta_1 f_c' bc = \rho\epsilon_s E_s bd$$

Substituting the steel strain from Eq. (3.42) in the last equation, and defining $k_u = c/d$, one obtains a quadratic equation in k_u as follows:

$$k_u^2 + m\rho k_u - m\rho = 0$$

Here, $\rho = A_s/bd$ as usual, and m is a material parameter given by

$$m = \frac{E_s\epsilon_u}{0.85\beta_1 f_c'} \tag{3.43}$$

Solving the quadratic equation for k_u,

$$k_u = \sqrt{m\rho + \left(\frac{m\rho}{2}\right)^2} - \frac{m\rho}{2} \tag{3.44}$$

The neutral axis depth for the overreinforced beam can then easily be found from $c = k_u d$, after which the stress-block depth $a = \beta_1 c$. With steel strain ϵ_s then computed from Eq. (3.42), and with $f_s = E_s\epsilon_s$, the nominal flexural strength is

$$M_n = A_s f_s\left(d - \frac{a}{2}\right) \tag{3.45}$$

The strength reduction factor ϕ will equal 0.65 for beams in this range.

3.5 DESIGN AIDS

Basic equations were developed in Section 3.4 for the analysis and design of reinforced concrete beams, and these were used directly in the examples. In practice, the design of beams and other reinforced concrete members is greatly facilitated by the use of aids such as those in Appendix A of this text and in Refs. 3.7 through 3.9. Tables A.1, A.2, A.4 through A.7, and Graph A.1 of Appendix A relate directly to this chapter, and the student can scan this material to become familiar with the coverage. Other aids will be discussed, and their use demonstrated, in later chapters.

Equation (3.39) gives the flexural design strength ϕM_n of an underreinforced rectangular beam with a reinforcement ratio at or below $\rho_{\max}$. The flexural resistance factor R, from Eq. (3.36), is given in Table A.5a for lower reinforcement ratios or Table A.5b for higher reinforcement ratios. Alternatively, R can be obtained from Graph A.1. For *analysis* of the capacity of a section with known concrete dimensions b and d, having known reinforcement ratio ρ, and with known materials strengths, the design strength ϕM_n can be obtained directly by Eq. (3.39).

For *design* purposes, where concrete dimensions and reinforcement are to be found and the factored load moment M_u is to be resisted, there are two possible approaches. One starts with selecting the optimum reinforcement ratio and then calculating concrete dimensions, as follows:

1. Set the required strength M_u equal to the design strength ϕM_n from Eq. (3.39):

$$M_u = \phi R b d^2$$

2. With the aid of Table A.4, select an appropriate reinforcement ratio between ρ_{max} and ρ_{min}. Often a ratio of about $0.60\rho_{max}$ will be an economical and practical choice. Selection of $\rho \leq \rho_{0.005}$ ($\epsilon_t \geq 0.005$) ensures that ϕ will remain equal to 0.90. For $\rho_{0.005} < \rho < \rho_{max}$ an iterative solution will be necessary.
3. From Table A.5, for the specified material strengths and selected reinforcement ratio, find the flexural resistance factor R. Then

$$bd^2 = \frac{M_u}{\phi R}$$

4. Choose b and d to meet that requirement. Unless construction depth must be limited or other constraints exist (see Section 12.6), an effective depth about 2 to 3 times the width is often appropriate.
5. Calculate the required steel area

$$A_s = \rho bd$$

Then, referring to Table A.2, choose the size and number of bars, giving preference to the larger bar sizes to minimize placement costs.

6. Refer to Table A.7 to ensure that the selected beam width will provide room for the bars chosen, with adequate concrete cover and spacing. (These points will be discussed further in Section 3.6.)

The alternative approach starts with selecting concrete dimensions (see Section 12.6 for practical guidelines), after which the required reinforcement is found, as follows:

1. Select beam width b and effective depth d. Then calculate the required R:

$$R = \frac{M_u}{\phi bd^2}$$

2. Using Table A.5 for specified material strengths, find the reinforcement ratio $\rho < \rho_{max}$ that will provide the required value of R and verify the selected value of ϕ.
3. Calculate the required steel area

$$A_s = \rho bd$$

and from Table A.2 select the size and number of bars.

4. Using Table A.7, confirm that the beam width is sufficient to contain the selected reinforcement.

Use of design aids to solve the example problems of Section 3.4 will be illustrated as follows.

EXAMPLE 3.9

Flexural strength of a given member. Find the nominal flexural strength and design strength of the beam in Example 3.5, which has b = 300 mm and d = 440 mm and is reinforced with four No. 29 (No. 9) bars. Make use of the design aids of Appendix A. Material strengths are f'_c = 28 MPa and f_y = 420 MPa.

Solution. From Table A.2, four No. 29 (No. 9) bars provide $A_s = 2580 \text{ mm}^2$, and with b = 300 mm and d = 440 mm, the reinforcement ratio is $\rho = 2580/(300 \times 440) = 0.0195$. According to Table A.4, this is below $\rho_{max} = 0.0206$ and above $\rho_{min} = 0.0033$. Then from

Table A.5b, with $f_c' = 28$ MPa, $f_y = 420$ MPa, and $\rho = 0.0195$, the value $R = 6.79$ MPa is found. The nominal and design strengths are (with $\phi = 0.85$ from Example 3.5), respectively,

$$M_n = Rbd^2 = 6.79 \times 300 \times 440^2 = 394.4 \times 10^6 \text{ N-mm} = 394.4 \text{ kN-m}$$

$$\phi M_n = 0.85 \times 394.4 = 335.2 \text{ kN-m}$$

as before.

EXAMPLE 3.10

Concrete dimensions and steel area to resist a given moment. Find the cross section of concrete and the area of steel required for the beam in Example 3.6, making use of the design aids of Appendix A. $M_u = 186.3$ kN-m, $f_c' = 28$ MPa, and $f_y = 420$ MPa. Use a reinforcement ratio of $0.60\rho_{\max}$.

Solution. From Table A.4, the maximum reinforcement ratio is $\rho_{\max} = 0.0206$. For economy, a value of $\rho = 0.60\rho_{\max} = 0.0124$ will be used. For that value, by interpolation from Table A.5a, the required value of R is 4.63. Then

$$bd^2 = \frac{M_u}{\phi R} = \frac{186.3 \times 10^6}{0.9 \times 4.63} = 44.71 \times 10^6 \text{ mm}^3$$

Concrete dimensions $b = 250$ mm and $d = 422.9$ mm will satisfy this, but the depth will be increased to 435 mm to provide a total beam depth of 500 mm. It follows that

$$R = \frac{M_u}{\phi bd^2} = \frac{186.3 \times 10^6}{0.9 \times 250 \times 435^2} = 4.38 \text{ MPa}$$

and from Table A.5a, by interpolation, $\rho = 0.0116$. This leads to a steel requirement of $A_s = 0.0116 \times 250 \times 435 = 1262 \text{ mm}^2$ as before.

EXAMPLE 3.11

Determination of steel area. Find the steel area required for the beam in Example 3.7, with concrete dimensions $b = 250$ mm and $d = 440$ mm known to be adequate to carry the factored load moment of 150 kN-m. Material strengths are $f_c' = 28$ MPa and $f_y = 420$ MPa.

Solution. Note that in cases in which the concrete dimensions are known to be adequate and only the reinforcement must be found, the iterative method used earlier is not required. The necessary flexural resistance factor is

$$R = \frac{M_u}{\phi bd^2} = \frac{150 \times 10^6}{0.9 \times 250 \times 435^2} = 3.52 \text{ MPa}$$

According to Table A.5a, with the specified material strengths, this corresponds to a reinforcement ratio of $\rho = 0.0091$, giving a steel area of

$$A_s = 0.0091 \times 250 \times 435 = 990 \text{ mm}^2$$

as before. Two No. 25 (No. 8) bars will be used.

The tables and graphs of Appendix A give basic information and are used extensively throughout this text for illustrative purposes. The reader should be aware, however, of the greatly expanded versions of these tables, plus many other useful aids, that are found in Refs. 3.7 through 3.9 and in commercial design software.

3.6 PRACTICAL CONSIDERATIONS IN THE DESIGN OF BEAMS

To focus attention initially on the basic aspects of flexural design, the preceding examples were carried out with only minimum regard for certain practical considerations that always influence the actual design of beams. These relate to optimal concrete proportions for beams, rounding of dimensions, standardization of dimensions, required cover for main and auxiliary reinforcement, and selection of bar combinations. Good judgment on the part of the design engineer is particularly important in translating from theoretical requirements to practical design. Several of the more important aspects are discussed here; much additional guidance is provided by the publications of ACI (Refs. 3.7 and 3.8) and CRSI (Refs. 3.9 to 3.11).

a. Concrete Protection for Reinforcement

To provide the steel with adequate concrete protection against fire and corrosion, the designer must maintain a certain minimum thickness of concrete cover outside of the outermost steel. The thickness required will vary, depending upon the type of member and conditions of exposure. According to ACI Code 7.7, for cast-in-place concrete, concrete protection at surfaces not exposed directly to the ground or weather should be not less than 20 mm for slabs and walls and 40 mm for beams and columns. If the concrete surface is to be exposed to the weather or in contact with the ground, a protective covering of at least 50 mm is required [40 mm for No. 16 (No. 5) and smaller bars], except that if the concrete is cast in direct contact with the ground without the use of forms, a cover of at least 75 mm must be furnished.

In general, the centers of main flexural bars in beams should be placed 65 mm to 75 mm from the top or bottom surface of the beam to furnish at least 40 mm of clear cover for the bars and the stirrups (see Fig. 3.13). In slabs, 25 mm to the center of the bar is ordinarily sufficient to give the required 20 mm cover.

To simplify construction and thereby to reduce costs, the overall concrete dimensions of beams, b and h, are almost always rounded up to the nearest 25 mm, and often to the next multiple of 50 mm. As a result, the actual effective depth d, found by subtracting the sum of cover distance, stirrup diameter, and one-half the main

FIGURE 3.13
Requirements for concrete cover in beams and slabs.

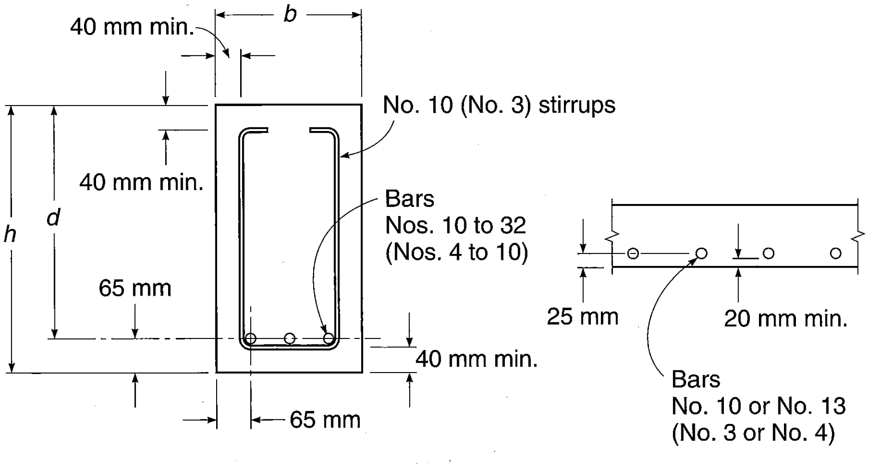

(*a*) Beam with stirrups (*b*) Slab

reinforcing bar diameter from the total depth h, is seldom an even dimension. For slabs, the total depth is generally rounded up to the nearest 10 mm. The differences between h and d shown in Fig. 3.13 are not exact, but are satisfactory for design purposes for beams with No. 10 (No. 3) stirrups and No. 32 (No. 10) longitudinal bars or smaller, and for slabs using No. 13 (No. 4) or smaller bars. If larger bars are used for the main flexural reinforcement or for the stirrups, as is frequently the case, the corresponding dimensions are easily calculated.

Recognizing the closer tolerances that can be maintained under plant-control conditions, ACI Code 7.7.3 permits some reduction in concrete protection for reinforcement in precast concrete.

b. Concrete Proportions

Reinforced concrete beams may be wide and shallow, or relatively narrow and deep. Consideration of maximum material economy often leads to proportions with effective depth d in the range from about 2 to 3 times the width b (or web width b_w for T beams). However, constraints may dictate other choices, and as will be discussed in Section 12.6, maximum material economy may not translate to maximum structural economy. For example, with one-way concrete joists supported by monolithic beams (see Chapter 18), use of beams and joists with the same total depth will permit use of a single flat-bottom form, resulting in fast, economical construction and permitting level ceilings. The beams will generally be wide and shallow, with heavier reinforcement than otherwise, but the result will be an overall saving in construction cost. In other cases, it may be necessary to limit the total depth of floor or roof construction for architectural or other reasons. An advantage of reinforced concrete is its adaptability to such special needs.

c. Selection of Bars and Bar Spacing

As noted in Section 2.14, common reinforcing bar sizes range from No. 10 to No. 36 (No. 3 to No. 11), the bar number corresponding closely to the number of millimeters (eighth-inches) of bar diameter. The two larger sizes, No. 43 (No. 14) (43.0 mm diameter) and No. 57 (No. 18) (57.3 mm diameter) are used mainly in columns.

It is often desirable to mix bar sizes to meet steel area requirements more closely. In general, mixed bars should be of comparable diameter, for practical as well as theoretical reasons, and generally should be arranged symmetrically about the vertical centerline. Many designers limit the variation in diameter of bars in a single layer to two bar sizes, using, say, No. 32 and No. 25 (No. 10 and No. 8) bars together, but not Nos. 36 and 19 (Nos. 11 and 6). There is some practical advantage to minimizing the number of different bar sizes used for a given structure.

Normally, it is necessary to maintain a certain minimum distance between adjacent bars to ensure proper placement of concrete around them. Air pockets below the steel are to be avoided, and full surface contact between the bars and the concrete is desirable to optimize bond strength. ACI Code 7.6 specifies that the minimum clear distance between adjacent bars not be less than the nominal diameter of the bars, or 25 mm. (For columns, these requirements are increased to $1\frac{1}{2}$ bar diameters and 40 mm) Where beam reinforcement is placed in two or more layers, the clear distance between layers must not be less than 25 mm, and the bars in the upper layer should be placed directly above those in the bottom layer.

The maximum number of bars that can be placed in a beam of given width is limited by bar diameter and spacing requirements and is also influenced by stirrup diameter, by concrete cover requirement, and by the maximum size of concrete aggregate specified. Table A.7 of Appendix A gives the maximum number of bars that can be placed in a single layer in beams, assuming 40 mm concrete cover and the use of No. 13 (No. 4) stirrups. When using the minimum bar spacing in conjunction with a large number of bars in a single plane of reinforcement, the designer should be aware that problems may arise in the placement and consolidation of concrete, especially when multiple layers of bars are used or when the bar spacing is smaller than the size of the vibrator head.

There are also restrictions on the *minimum* number of bars that can be placed in a single layer, based on requirements for the distribution of reinforcement to control the width of flexural cracks (see Section 6.3). Table A.8 gives the minimum number of bars that will satisfy ACI Code requirements, which will be discussed in Chapter 6.

In large girders and columns, it is sometimes advantageous to "bundle" tensile or compressive reinforcement with two, three, or four bars in contact to provide for better deposition of concrete around and between adjacent bundles. These bars may be assumed to act as a unit, with not more than four bars in any bundle, provided that stirrups or ties enclose the bundle. No more than two bars should be bundled in one plane; typical bundle shapes are triangular, square, or L-shaped patterns. Individual bars in a bundle, cut off within the span of flexural members, should terminate at different points. ACI Code 7.6.6 requires at least 40 bar diameters stagger between points of cutoff. Where spacing limitations and minimum concrete cover requirements are based on bar diameter, a unit of bundled bars is treated as a single bar with a diameter that provides the same total area.

ACI Code 7.6.6 states that bars larger than No. 36 (No. 11) shall not be bundled in beams, although the AASHTO Specifications permit bundling of No. 43 and No. 57 (No. 14 and No. 18) bars in highway bridges.

3.7 RECTANGULAR BEAMS WITH TENSION AND COMPRESSION REINFORCEMENT

If a beam cross section is limited because of architectural or other considerations, it may happen that the concrete cannot develop the compression force required to resist the given bending moment. In this case, reinforcement is added in the compression zone, resulting in a *doubly reinforced* beam, i.e., one with compression as well as tension reinforcement (see Fig. 3.14). The use of compression reinforcement has decreased markedly with the use of strength design methods, which account for the full-strength potential of the concrete on the compressive side of the neutral axis. However, there are situations in which compressive reinforcement is used for reasons other than strength. It has been found that the inclusion of some compression steel will reduce the long-term deflections of members (see Section 6.5). In addition, in some cases, bars will be placed in the compression zone for minimum-moment loading (see Section 12.2) or as stirrup support bars continuous throughout the beam span (see Chapter 4). It may be desirable to account for the presence of such reinforcement in flexural design, although in many cases they are neglected in flexural calculations.

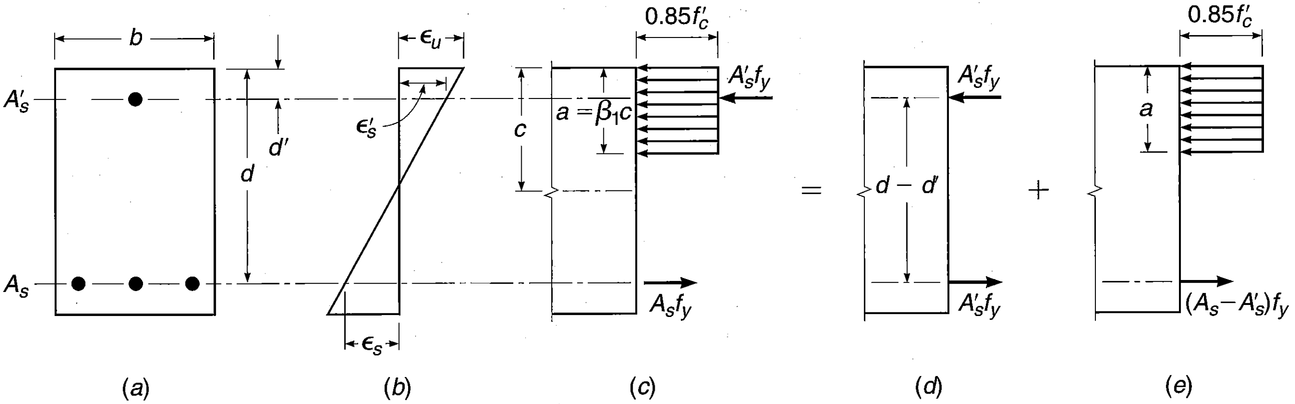

FIGURE 3.14
Doubly reinforced rectangular beam.

a. Tension and Compression Steel Both at Yield Stress

If, in a doubly reinforced beam, the tensile reinforcement ratio ρ is less than or equal to ρ_b, the strength of the beam may be approximated within acceptable limits by disregarding the compression bars. The strength of such a beam will be controlled by tensile yielding, and the lever arm of the resisting moment will ordinarily be little affected by the presence of the compression bars.

If the tensile reinforcement ratio is larger than ρ_b, a somewhat more elaborate analysis is required. In Fig. 3.14*a*, a rectangular beam cross section is shown with compression steel A_s' placed a distance d' from the compression face and with tensile steel A_s at effective depth d. It is assumed initially that both A_s' and A_s are stressed to f_y at failure. The total resisting moment can be thought of as the sum of two parts. The first part, M_{n1}, is provided by the couple consisting of the force in the compression steel A_s' and the force in an equal area of tension steel

$$M_{n1} = A_s'f_y(d - d') \tag{3.46a}$$

as shown in Fig. 3.14*d*. The second part, M_{n2}, is the contribution of the remaining tension steel $A_s - A_s'$ acting with the compression concrete:

$$M_{n2} = (A_s - A_s')f_y\left(d - \frac{a}{2}\right) \tag{3.46b}$$

as shown in Fig. 3.14*e*, where the depth of the stress block is

$$a = \frac{(A_s - A_s')f_y}{0.85f_c'b} \tag{3.47a}$$

With the definitions $\rho = A_s/bd$ and $\rho' = A_s'/bd$, this can be written

$$a = \frac{(\rho - \rho')f_yd}{0.85f_c'} \tag{3.47b}$$

The total nominal resisting moment is then

$$M_n = M_{n1} + M_{n2} = A_s'f_y(d - d') + (A_s - A_s')f_y\left(d - \frac{a}{2}\right) \tag{3.48}$$

In accordance with the safety provisions of the ACI Code, the net tensile strain is checked; and if $\epsilon_t \geq 0.005$, this nominal capacity is reduced by the factor $\phi = 0.90$ to obtain the design strength. For ϵ_t between 0.005 and 0.004, ϕ must be adjusted, as discussed earlier.

It is highly desirable, for reasons given earlier, that failure, should it occur, be precipitated by tensile yielding rather than crushing of the concrete. This can be ensured by setting an *upper limit* on the tensile reinforcement ratio. By setting the tensile steel strain in Fig. 3.14*b* equal to ϵ_y to establish the location of the neutral axis for the failure condition and then summing horizontal forces shown in Fig. 3.14*c* (still assuming the compressive steel to be at the yield stress at failure), it is easily shown that the balanced reinforcement ratio $\bar{\rho}_b$ for a doubly reinforced beam is

$$\bar{\rho}_b = \rho_b + \rho' \tag{3.49}$$

where ρ_b is the balanced reinforcement ratio for the corresponding singly reinforced beam and is calculated from Eq. (3.28). The ACI Code limits the net tensile strain, not the reinforcement ratio. To provide the same margin against brittle failure as for singly reinforced beams, the maximum reinforcement ratio should be limited to

$$\bar{\rho}_{\max} = \rho_{\max} + \rho' \tag{3.50a}$$

Because $\rho_{\max}$ establishes the location of the neutral axis, the limitation in Eq. (3.50*a*) will provide acceptable net tensile strains. A check of ϵ_t is required to determine the strength reduction factor ϕ and to verify net tensile strain requirements are satisfied. Substituting $\rho_{0.005}$ for $\rho_{\max}$ in Eq. (3.50*a*) will give the maximum reinforcement ratio for $\phi = 0.90$.

$$\bar{\rho}_{0.005} = \rho_{0.005} + \rho' \tag{3.50b}$$

b. Compression Steel below Yield Stress

The preceding equations, through which the fundamental analysis of doubly reinforced beams is developed clearly and concisely, are valid *only* if the compression steel has yielded when the beam reached its nominal capacity. In many cases, such as for wide, shallow beams, beams with more than the usual concrete cover over the compression bars, beams with high yield strength steel, or beams with relatively small amounts of tensile reinforcement, the compression bars will be below the yield stress at failure. It is necessary, therefore, to develop more generally applicable equations to account for the possibility that the compression reinforcement has not yielded when the doubly reinforced beam fails in flexure.

Whether or not the compression steel will have yielded at failure can be determined as follows. Referring to Fig. 3.14*b*, and taking as the limiting case $\epsilon_s' = \epsilon_y$, one obtains, from geometry,

$$\frac{c}{d'} = \frac{\epsilon_u}{\epsilon_u - \epsilon_y} \qquad \text{or} \qquad c = \frac{\epsilon_u}{\epsilon_u - \epsilon_y} d'$$

Summing forces in the horizontal direction (Fig. 3.14*c*) gives the *minimum* tensile reinforcement ratio $\bar{\rho}_{cy}$ that will ensure yielding of the compression steel at failure:

$$\bar{\rho}_{cy} = 0.85\beta_1 \frac{f_c'}{f_y} \frac{d'}{d} \frac{\epsilon_u}{\epsilon_u - \epsilon_y} + \rho' \tag{3.51}$$

If the *tensile reinforcement ratio* is *less than* this limiting value, the neutral axis is sufficiently high that the compression steel stress at failure is less than the yield stress. In this case, it can easily be shown on the basis of Fig. 3.14*b* and *c* that the balanced reinforcement ratio is

$$\bar{\rho}_b = \rho_b + \rho' \frac{f'_s}{f_y} \tag{3.52}$$

where

$$f'_s = E_s \epsilon'_s = E_s \left[\epsilon_u - \frac{d'}{d}(\epsilon_u + \epsilon_y) \right] \le f_y \tag{3.53a}$$

To determine $\rho_{\max}$, $\epsilon_t = 0.004$ is substituted for ϵ_y in Eq. (3.53*a*), giving

$$f'_s = E_s \left[\epsilon_u - \frac{d'}{d}(\epsilon_u + 0.004) \right] \le f_y \tag{3.53b}$$

Likewise, for $\epsilon_t = 0.005$,

$$f'_s = E_s \left[\epsilon_u - \frac{d'}{d}(\epsilon_u + 0.005) \right] \le f_y \tag{3.53c}$$

Hence, the maximum reinforcement ratio permitted by the ACI Code is

$$\bar{\rho}_{\max} = \rho_{\max} + \rho' \frac{f'_s}{f_y} \tag{3.54a}$$

and the maximum reinforcement ratio for $\phi = 0.90$ is

$$\bar{\rho}_{0.005} = \rho_{0.005} + \rho' \frac{f'_s}{f_y} \tag{3.54b}$$

where f'_s is given in Eq. (3.53*b*). A simple comparison shows that Eqs. (3.52), (3.54*a*), and (3.54*b*), with f'_s given by Eqs. (3.53*a*), (3.53*b*), and (3.53*c*), respectively, are the generalized forms of Eqs. (3.49), (3.50*a*), and (3.50*b*).

It should be emphasized that Eqs. (3.53*a*), (3.53*b*), and (3.53*c*) for compression steel stress apply *only for beams with exact strain values in the extreme tensile steel of* ϵ_y, $\epsilon_t = 0.004$, *or* $\epsilon_t = 0.005$.

If the tensile reinforcement ratio is less than $\bar{\rho}_b$, as given by Eq. (3.52), and less than $\bar{\rho}_{cy}$, as given by Eq. (3.51), then the tensile steel is at the yield stress at failure but the compression steel is not, and new equations must be developed for compression steel stress and flexural strength. The compression steel stress can be expressed in terms of the still-unknown neutral axis depth as

$$f'_s = \epsilon_u E_s \frac{c - d'}{c} \tag{3.55}$$

Consideration of horizontal force equilibrium (Fig. 3.14*c* with compression steel stress equal to f'_s) then gives

$$A_s f_y = 0.85\beta_1 f'_c bc + A'_s \epsilon_u E_s \frac{c - d'}{c} \tag{3.56}$$

This is a quadratic equation in c, the only unknown, and is easily solved for c. The nominal flexural strength is found using the value of f'_s from Eq. (3.55), and $a = \beta_1 c$ in the expression

$$M_n = 0.85 f'_c ab \left(d - \frac{a}{2} \right) + A'_s f'_s (d - d') \tag{3.57}$$

TABLE 3.2
Minimum beam depths for compression reinforcement to yield

	$\epsilon_t = 0.004$		$\epsilon_t = 0.005$	
f_y, psi	Maximum d'/d	Minimum d for $d' = 65$ mm, mm	Maximum d'/d	Minimum d for $d' = 65$ mm, mm
40,000	0.23	282	0.20	325
60,000	0.13	500	0.12	542
75,000	0.06	1083	0.05	1300

This nominal capacity is reduced by the strength reduction factor ϕ to obtain the design strength.

If compression bars are used in a flexural member, precautions must be taken to ensure that these bars will not buckle outward under load, spalling off the outer concrete. ACI Code 7.11.1 imposes the requirement that such bars be anchored in the same way that compression bars in columns are anchored by lateral ties (Section 8.2). Such ties must be used throughout the distance where the compression reinforcement is required.

For the compression steel to yield, the reinforcement ratio must lie below $\bar{\rho}_{\max}$ and above $\bar{\rho}_{cy}$. The ratio between d' and the steel centroidal depth d to allow yielding of the compression reinforcement can be found by equating $\bar{\rho}_{cy}$ to $\bar{\rho}_{\max}$ (or $\bar{\rho}_{0.005}$) and solving for d'/d. Furthermore, if d' is assumed to be 65 mm, as is often the case, the minimum depth of beam necessary for the compression steel to yield may be found for each grade of steel. The ratios and minimum beam depths are summarized in Table 3.2. Values are included for $\epsilon_t = 0.004$, the minimum tensile yield strain permitted for flexural members, and $\epsilon_t = 0.005$, the net tensile strain needed to ensure that $\phi = 0.90$. For beams with less than the minimum depth, the compression reinforcement cannot yield unless the tensile reinforcement exceeds $\rho_{\max}$. The compression reinforcement may yield in beams that exceed the minimum depth in Table 3.2, depending on the relative distribution of the tensile and compressive reinforcement.

c. Examples of Analysis and Design of Beams with Tension and Compression Steel

As was the case for beams with only tension reinforcement, doubly reinforced beam problems can be placed in one of two categories: analysis problems or design problems. For *analysis*, in which the concrete dimensions, reinforcement, and material strengths are given, one can find the flexural strength directly from the equations in Section 3.7a or 3.7b. First, it must be confirmed that the tensile reinforcement ratio is less than $\bar{\rho}_b$ given by Eq. (3.52), with compression steel stress from Eq. (3.53*a*). Once it is established that the tensile steel has yielded, the tensile reinforcement ratio defining compression steel yielding is calculated from Eq. (3.51), and the actual tensile reinforcement ratio is compared. If it is greater than $\bar{\rho}_{cy}$, then $f_s' = f_y$, and M_n is found from Eq. (3.48). If it is less than $\bar{\rho}_{cy}$, then $f_s' < f_y$. In this case, c is calculated by solving Eq. (3.56), f_s' comes from Eq. (3.55), and M_n is found from Eq. (3.57).

For the *design* case, in which the factored load moment M_u to be resisted is known and the section dimensions and reinforcement are to be found, a direct solution is impossible. The steel areas to be provided depend on the steel stresses, which are not known before the section is proportioned. It can be assumed that the compression steel stress is equal to the yield stress, but this must be confirmed; if it has not yielded, the design must be adjusted. The design procedure can be outlined as follows:

1. Calculate the maximum moment that can be resisted by the underreinforced section with $\rho = \rho_{\max}$, or $\rho_{0.005}$ to ensure that $\phi = 0.90$. The corresponding tensile steel area is $A_s = \rho bd$, and, as usual,

$$M_n = A_s f_y \left(d - \frac{a}{2} \right)$$

with

$$a = \frac{A_s f_y}{0.85 f'_c b}$$

2. Find the excess moment, if any, that must be resisted, and set $M_2 = M_n$, as calculated in step 1.

$$M_1 = \frac{M_u}{\phi} - M_2$$

Now A_s from step 1 is defined as A_{s2}, i.e., that part of the tension steel area in the doubly reinforced beam that works with the compression force in the concrete. In Fig. 3.14*e*, $A_s - A'_s = A_{s2}$.

3. Tentatively assume that $f'_s = f_y$. Then

$$A'_s = \frac{M_1}{f_y(d - d')}$$

Alternatively, if from Table 3.2 the compression reinforcement is known not to yield, go to step 6.

4. Add an additional amount of tensile steel $A_{s1} = A'_s$. Thus, the total tensile steel area A_s is A_{s2} from step 2 plus A_{s1}.
5. Analyze the doubly reinforced beam to see if $f'_s = f_y$; that is, check the tensile reinforcement ratio against $\bar{\rho}_{cy}$.
6. If $\rho < \bar{\rho}_{cy}$, then the compression steel stress is less than f_y and the compression steel area must be increased to provide the needed force. This can be done as follows. The stress block depth is found from the requirement of horizontal equilibrium (Fig. 3.14*e*),

$$a = \frac{(A_s - A'_s) f_y}{0.85 f'_c b} \qquad \text{or} \qquad a = \frac{\left[A_s - A'_s \, (f'_s / f_y) \right] f_y}{0.85 f'_c b}$$

and the neutral axis depth is $c = a/\beta_1$. From Eq. (3.55),

$$f'_s = \epsilon_u E_s \frac{c - d'}{c}$$

The revised compression steel area, acting at f'_s, must provide the same force as the trial steel area that was assumed to act at f_y. Therefore,

$$A'_{s,\text{revised}} = A'_{s,\text{trial}} \frac{f_y}{f'_s}$$

The tensile steel area need not be revised, because it acts at f_y as assumed.

EXAMPLE 3.12

Flexural strength of a given member. A rectangular beam, shown in Fig. 3.15, has a width of 300 mm and an effective depth to the centroid of the tension reinforcement of 600 mm. The tension reinforcement consists of six No. 32 (No. 10) bars in two rows. Compression reinforcement consisting of two No. 25 (No. 8) bars is placed 65 mm from the compression face of the beam. If $f_y = 420$ MPa and $f'_c = 35$ MPa, what is the design moment capacity of the beam?

Solution. The steel areas and ratios are

$$A_s = 4914 \text{ mm}^2 \qquad \rho = \frac{4914}{300 \times 600} = 0.0273$$

$$A'_s = 1020 \text{ mm}^2 \qquad \rho' = \frac{1020}{300 \times 600} = 0.0057$$

Check the beam first as a singly reinforced beam to see if the compression bars can be disregarded,

$$\rho_{\max} = 0.0243 \qquad \text{from Table A.4 or Eq. (3.30}c\text{)}$$

The actual $\rho = 0.0273$ is larger than $\rho_{\max}$, so the beam must be analyzed as doubly reinforced. From Eq. (3.51), with $\beta_1 = 0.80$,

$$\bar{\rho}_{cy} = 0.85 \times 0.80 \times \frac{35}{420} \times \frac{65}{600} \times \frac{0.003}{0.003 - 0.0021} + 0.0057 = 0.0262$$

The tensile reinforcement ratio is greater than this, so the compression bars will yield when the beam fails. The maximum reinforcement ratio thus can be found from Eq. (3.50),

$$\bar{\rho}_{\max} = 0.0243 + 0.0057 = 0.0300$$

The actual tensile reinforcement ratio is below the maximum value, as required. Then, from Eq. (3.47*a*),

$$a = \frac{(4914 - 1020)420}{0.85 \times 35 \times 300} = 183.2 \text{ mm}$$

$$c = a/\beta_1 = \frac{183.2}{0.80} = 229 \text{ mm}$$

$$\epsilon_t = 0.003\left(\frac{600 - 229}{229}\right) = 0.0049$$

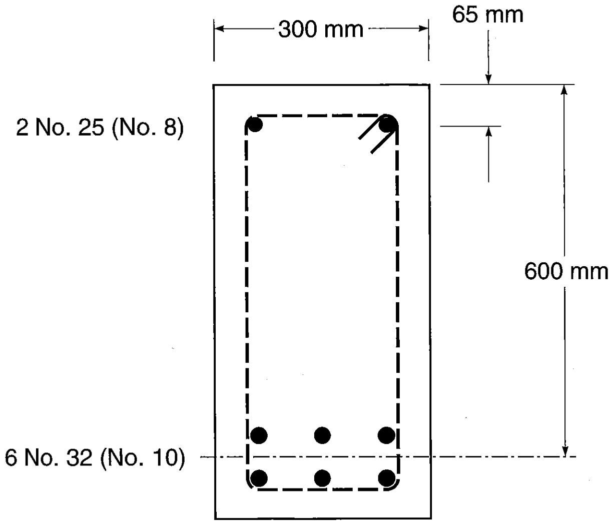

FIGURE 3.15
Doubly reinforced beam of Example 3.12.

and because $\epsilon_t = 0.0049$,

$$\phi = 0.89$$

and from Eq. (3.48),

$$M_n = \left[1020 \times 420(600 - 65) + 3894 \times 420\left(600 - \frac{183.2}{2}\right)\right] \times 10^{-6} = 1061 \text{ kN-m}$$

The design strength is

$$\phi M_n = 0.89 \times 1061 = 954 \text{ kN-m}$$

EXAMPLE 3.13 **Design of a doubly reinforced beam.** A rectangular beam that must carry a service live load of 36 kN/m and a calculated dead load of 15.3 kN/m on a 5.5 m simple span is limited in cross section for architectural reasons to 250 mm width and 500 mm total depth. If $f_y = 420$ MPa and $f'_c = 28$ MPa, what steel area(s) must be provided?

Solution. The service loads are first increased by load factors to obtain the factored load of $1.2 \times 15.3 + 1.6 \times 36 = 75.96$ kN/m. Then $M_u = 75.96 \times 5.5^2/8 = 287.2$ kN-m. To satisfy spacing and cover requirements (see Section 3.6), assume that the tension steel centroid will be 100 mm above the bottom face of the beam and that compression steel, if required, will be placed 65 mm below the beam's top surface. Then $d = 400$ mm and $d' = 65$ mm.

First, check the capacity of the section if singly reinforced. Table A.4 shows that $\rho_{0.005}$, the maximum value of ρ for $\phi = 0.90$, to be 0.0181. While the maximum reinforcement ratio is slightly higher, Example 3.8 demonstrated there was no economic efficiency of using $\epsilon_t \leq 0.005$. So $A_s = 250 \times 400 \times 0.0181 = 1810$ mm^2. Then with

$$a = \frac{1810 \times 420}{0.85 \times 28 \times 250} = 127.8 \text{ mm}$$

$c = a/\beta_1 = 127.8/0.85 = 150.3$ mm, and the maximum nominal moment that can be developed is

$$M_n = 1810 \times 420\left(400 - \frac{127.8}{2}\right)10^{-6} = 255.5 \text{ kN-m}$$

Alternatively, using $R = 6.39$ from Table A.5b, the nominal moment is $M_n = 6.39 \times 250 \times 400^2 \times 10^{-6} = 255.5$ kN-m. Because the corresponding design moment $\phi M_n = 230.0$ kN-m is less than the required capacity 287.2 kN-m, compression steel is needed as well as additional tension steel.

The remaining moment to be carried by the compression steel couple is

$$M_1 = \frac{287.2}{0.90} - 230 = 89.1 \text{ kN-m}$$

As d is less than the value required to develop the compression reinforcement yield stress (Table 3.2), a reduced stress in the compression reinforcement will be used. Using the strain distribution in Fig. 3.14b, ϵ'_s and f'_c can be computed as

$$\epsilon'_s = 0.003 \frac{150.3 - 65}{150.3} = 0.00170 \qquad \text{and} \qquad f'_s = 0.00170 \times 200{,}000 = 340 \text{ MPa}$$

Try $f'_s = 340$ MPa for the compression reinforcement to obtain the required area of compression steel.

$$A'_s = \frac{89.1 \times 10^6}{340(400 - 65)} = 781 \text{ mm}^2$$

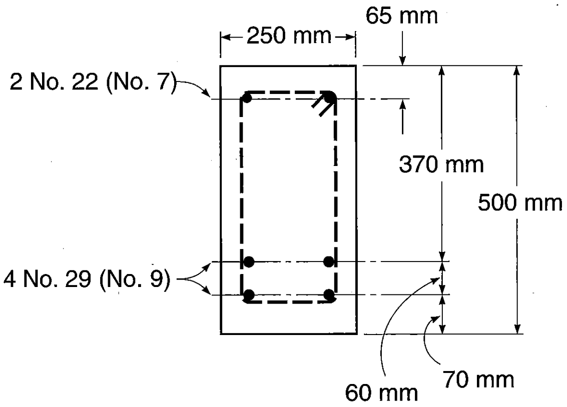

FIGURE 3.16
Doubly reinforced beam of Example 3.13.

The total area of tensile reinforcement at 420 MPa is

$$A_s = 1810 + 781\left(\frac{340}{420}\right) = 2443 \text{ mm}^2$$

Two No. 22 (No. 7) bars will be used for the compression reinforcement and four No. 29 (No. 9) bars will provide the tensile steel area, as shown in Fig. 3.16. To place the tension bars in a 250 mm beam width, two rows of two bars each are used.

A final check is made to ensure that the selection of reinforcement does not create a compressive stress lower than the assumed 340 MPa.

$$A_s - A_s'\left(\frac{f_s'}{f_y}\right) = 2580 - 774\left(\frac{340}{420}\right) = 1953 \text{ mm}^2$$

which is greater than 1810 mm^2 for $\epsilon_t = 0.005$, so ϕ may be less than 0.90.

$$a = \frac{1953 \times 420}{0.85 \times 28 \times 250} = 137.9 \text{ mm}$$

$$c = \frac{137.9}{0.85} = 162.2 \text{ mm}$$

$$\epsilon_s' = 0.003\,\frac{162.2 - 65}{162.2} = 0.0018$$

$$f_s' = 200{,}000 \times 0.0018 = 360 \text{ MPa}$$

which is greater than assumed. Check ϕ, using $d_t = 430$ mm from the strain distribution in Fig. 3.14*b*, and compute the revised M_u. For simplicity, the area of tensile reinforcement is not modified.

$$\epsilon_t = 0.003\,\frac{430 - 162.2}{162.2} = 0.0050$$

for which $\phi = 0.90$. Then

$$\phi M_n = 0.90\left[1953 \times 420\left(400 - \frac{137.9}{2}\right) + 774 \times 360(400 - 65)\right] \times 10^{-6}$$
$$= 328.4 \text{ kN-m}$$

This is greater than M_u, so no further refinement is necessary.

d. Tensile Steel below the Yield Stress

All doubly reinforced beams designed according to the ACI Code must be underreinforced, in the sense that the tensile reinforcement ratio is limited to ensure yielding at beam failure. Two cases were considered in Sections 3.7a and 3.7b, respectively: (a) both tension steel and compression steel yield and (b) tension steel yields but compression steel does not. Two other combinations may be encountered in analyzing the capacity of existing beams: (c) tension steel does not yield, but compression steel does, and (d) neither tension steel nor compression steel yields. The last two cases are unusual, and in fact, it would be difficult to place sufficient tension reinforcement to create such conditions, but it is possible. The solution in such cases is obtained as a simple extension of the treatment of Section 3.7b. An equation for horizontal equilibrium is written, in which both tension and compression steel stress are expressed in terms of the unknown neutral axis depth c. The resulting quadratic equation is solved for c, after which steel stresses can be calculated and the nominal flexural strength determined.

3.8 T BEAMS

With the exception of precast systems, reinforced concrete floors, roofs, decks, etc., are almost always monolithic. Forms are built for beam soffits and sides and for the underside of slabs, and the entire construction is cast at once, from the bottom of the deepest beam to the top of the slab. Beam stirrups and bent bars extend up into the slab. It is evident, therefore, that a part of the slab will act with the upper part of the beam to resist longitudinal compression. The resulting beam cross section is T-shaped rather than rectangular. The slab forms the beam flange, while the part of the beam projecting below the slab forms what is called the *web* or *stem*. The upper part of such a T beam is stressed laterally due to slab action in that direction. Although transverse compression at the level of the bottom of the slab may increase the longitudinal compressive strength by as much as 25 percent, transverse tension at the top surface reduces the longitudinal compressive strength (see Section 2.10). Neither effect is usually taken into account in design.

a. Effective Flange Width

The next issue to be resolved is that of the effective width of flange. In Fig. 3.17*a*, it is evident that if the flange is but little wider than the stem width, the entire flange can be considered effective in resisting compression. For the floor system shown in Fig. 3.17*b*, however, it may be equally obvious that elements of the flange midway between the beam stems are less highly stressed in longitudinal compression than those elements directly over the stem. This is so because of shearing deformation of the flange, which relieves the more remote elements of some compressive stress.

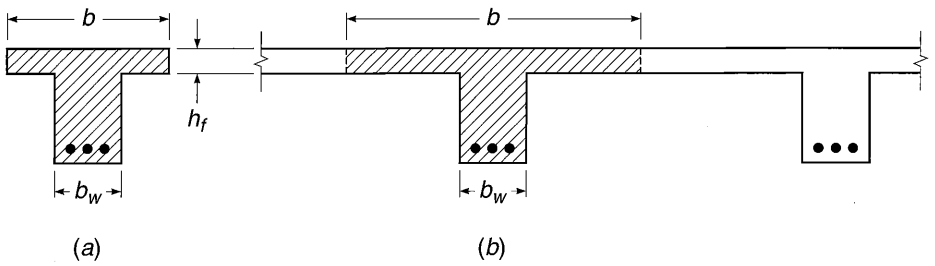

FIGURE 3.17
Effective flange width of T beams.

Although the actual longitudinal compression varies because of this effect, it is convenient in design to make use of an *effective flange width*, which may be smaller than the actual flange width but is considered to be uniformly stressed at the maximum value. This effective width has been found to depend primarily on the beam span and on the relative thickness of the slab.

The criteria for effective width given in ACI Code 8.12 are as follows:

1. For symmetric T beams, the effective width b shall not exceed one-fourth the span length of the beam. The overhanging slab width on either side of the beam web shall not exceed 8 times the thickness of the slab or go beyond one-half the clear distance to the next beam.
2. For beams having a slab on one side only, the effective overhanging slab width shall not exceed one-twelfth the span length of the beam, 6 times the slab thickness, or one-half the clear distance to the next beam.
3. For isolated beams in which the flange is used only for the purpose of providing additional compressive area, the flange thickness shall not be less than one-half the width of the web, and the total flange width shall not be more than 4 times the web width.

b. Strength Analysis

The neutral axis of a T beam may be either in the flange or in the web, depending upon the proportions of the cross section, the amount of tensile steel, and the strengths of the materials. If the calculated depth to the neutral axis is less than or equal to the flange thickness h_f, the beam can be analyzed as if it were a rectangular beam of width equal to b, the effective flange width. The reason is illustrated in Fig. 3.18*a*, which shows a T beam with the neutral axis in the flange. The compressive area is indicated by the shaded portion of the figure. If the additional concrete indicated by areas 1 and 2 had been added when the beam was cast, the physical cross section would have been rectangular with a width b. No bending strength would have been added because areas 1 and 2 are entirely in the tension zone, and tension concrete is disregarded in flexural calculations. The original T beam and the rectangular beam are equal in flexural strength, and rectangular beam analysis for flexure applies.

When the neutral axis is in the web, as in Fig. 3.18*b*, the preceding argument is no longer valid. In this case, methods must be developed to account for the actual T-shaped compressive zone.

In treating T beams, it is convenient to adopt the same equivalent stress distribution that is used for beams of rectangular cross section. The rectangular stress block, having a uniform compressive-stress intensity $0.85f'_c$, was devised originally on the

FIGURE 3.18
Effective cross sections of T beams.

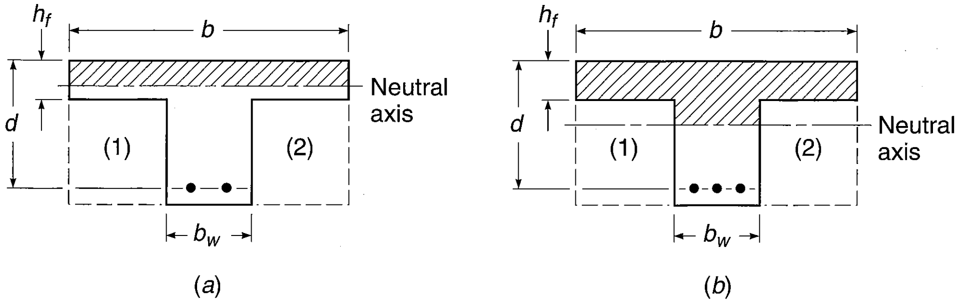

FIGURE 3.19
Strain and equivalent stress distributions for T beams.

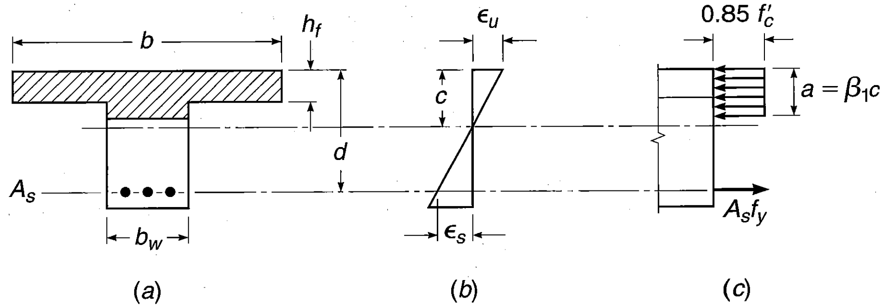

basis of tests of rectangular beams (see Section 3.4a), and its suitability for T beams may be questioned. However, extensive calculations based on actual stress-strain curves (reported in Ref. 3.12) indicate that its use for T beams, as well as for beams of circular or triangular cross section, introduces only minor error and is fully justified.

Accordingly, a T beam may be treated as a rectangular beam if the depth of the equivalent stress block is less than or equal to the flange thickness. Figure 3.19 shows a tensile-reinforced T beam with effective flange width b, web width b_w, effective depth to the steel centroid d, and flange thickness h_f. If for trial purposes the stress block is assumed to be completely within the flange,

$$a = \frac{A_s f_y}{0.85 f_c' b} = \frac{\rho f_y d}{0.85 f_c'} \tag{3.58}$$

where $\rho = A_s/bd$. If a is less than or equal to the flange thickness h_f, the member may be treated as a rectangular beam of width b and depth d. If a is greater than h_f, a T beam analysis is required as follows.

It will be assumed that the strength of the T beam is controlled by yielding of the tensile steel. This will nearly always be the case because of the large compressive concrete area provided by the flange. In addition, an upper limit can be established for the reinforcement ratio to ensure that this is so, as will be shown.

As a computational device, it is convenient to divide the total tensile steel into two parts, as shown in Fig. 3.20. The first part, A_{sf}, represents the steel area that, when stressed to f_y, is required to balance the longitudinal compressive force in the overhanging portions of the flange that are stressed uniformly at $0.85 f_c'$ (Fig. 3.20*b*). Thus,

$$A_{sf} = \frac{0.85 f_c' (b - b_w) h_f}{f_y} \tag{3.59}$$

FIGURE 3.20
Computational model for design and analysis of T beams.

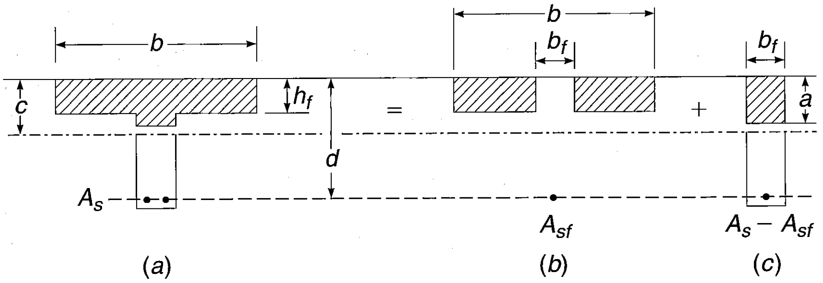

The force $A_{sf}f_y$ and the equal and opposite force $0.85\,f'_c(b - b_w)h_f$ act with a lever arm $d - h_f/2$ to provide the nominal resisting moment

$$M_{n1} = A_{sf}f_y\left(d - \frac{h_f}{2}\right) \tag{3.60}$$

The remaining steel area $A_s - A_{sf}$, at a stress f_y, is balanced by the compression in the rectangular portion of the beam (Fig. 3.20*c*). The depth of the equivalent rectangular stress block in this zone is found from horizontal equilibrium.

$$a = \frac{(A_s - A_{sf})f_y}{0.85f'_c\, b_w} \tag{3.61}$$

An additional moment M_{n2} is thus provided by the forces $(A_s - A_{sf})f_y$ and $0.85f'_c ab_w$ acting at the lever arm $d - a/2$.

$$M_{n2} = (A_s - A_{sf})f_y\left(d - \frac{a}{2}\right) \tag{3.62}$$

and the total nominal resisting moment is the sum of the parts:

$$M_n = M_{n1} + M_{n2} = A_{sf}f_y\left(d - \frac{h_f}{2}\right) + (A_s - A_{sf})f_y\left(d - \frac{a}{2}\right) \tag{3.63}$$

This moment is reduced by the strength reduction factor ϕ in accordance with the safety provisions of the ACI Code to obtain the design strength.

As for rectangular beams, the tensile steel should yield prior to sudden crushing of the compression concrete, as assumed in the preceding development. Yielding of the tensile reinforcement and Code compliance are ensured if the net tensile strain is greater than 0.004. From the geometry of the section,

$$\frac{c}{d_t} \le \frac{\epsilon_u}{\epsilon_u + \epsilon_t} \tag{3.64}$$

Setting $\epsilon_u = 0.003$ and $\epsilon_t = 0.004$ provides a maximum c/d_t ratio of 0.429, as seen in Fig. 3.10. Thus, as long as the depth to the neutral axis is less than $0.429d_t$, the net tensile strain requirements are satisfied, as they are for rectangular beam sections. This will occur if $\rho_w = A_s/b_wd$ is less than

$$\rho_{w,\max} = \rho_{\max} + \rho_f \tag{3.65}$$

where $\rho_f = A_{sf}/b_wd$ and $\rho_{\max}$ is as previously defined for a rectangular cross section [Eq. (3.30*c*)]. For c/d_t ratios between 0.429 and 0.375, equivalent to ρ_w between the $\rho_{w,\max}$ from Eq. (3.65) and $\rho_{w,0.005}$, calculated by substituting $\rho_{0.005}$ from Eq. (3.30*d*) for $\rho_{\max}$ in Eq. (3.65), the strength reduction factor ϕ must be adjusted for ϵ_t, as shown in Fig. 3.9. For $\rho_w \le \rho_{w,0.005}$ or $c/d_t \le 0.375$, $\phi = 0.90$.

The practical result of applying Eq. (3.65) is that the stress block of T beams will almost always be within the flange, except for unusual geometry or combinations of material strength. Consequently, rectangular beam equations may be applied in most cases.

The ACI Code restriction that the tensile reinforcement ratio for beams not be less than $\rho_{\min} = 0.25\sqrt{f'_c}/f_y$ and $\ge 1.4/f_y$ (see Section 3.4d) applies to T beams as well as rectangular beams. For T beams, the ratio ρ should be computed for this purpose based on the web width b_w.

c. Proportions of Cross Section

When designing T beams, in contrast to analyzing the capacity of a given section, normally the slab dimensions and beam spacing will have been established by transverse flexural requirements. Consequently, the only additional section dimensions that must be determined from flexural considerations are the width and depth of the web and the area of the tensile steel.

If the stem dimensions were selected on the basis of concrete stress capacity in compression, they would be very small because of the large compression flange width furnished by the presence of the slab. Such a design would not represent the optimum solution because of the large tensile steel requirement resulting from the small effective depth, because of the excessive web reinforcement that would be required for shear, and because of large deflections associated with such a shallow member. It is better practice to select the proportions of the web (1) so as to keep an arbitrarily low web reinforcement ratio ρ_w or (2) so as to keep web-shear stress at desirably low limits (Chapter 4) or (3) for continuous T beams, on the basis of the flexural requirements at the supports, where the effective cross section is rectangular and of width b_w.

In addition to the main reinforcement calculated according to the preceding requirements, it is necessary to ensure the integrity of the compressive flange of T beams by providing steel in the flange in the direction transverse to the main span. In typical construction, the slab steel serves this purpose. In other cases, additional bars must be added to permit the overhanging flanges to carry, as cantilever beams, the loads directly applied. According to ACI Code 8.12.5, the spacing of such bars must not exceed 5 times the thickness of the flange or in any case exceed 450 mm.

d. Examples of Analysis and Design of T Beams

For *analyzing* the capacity of a T beam with known concrete dimensions and tensile steel area, it is reasonable to start with the assumption that the stress block depth a does not exceed the flange thickness h_f. In that case, all ordinary rectangular beam equations (see Section 3.4) apply, with beam width taken equal to the effective width of the flange. If, upon checking that assumption, a proves to exceed h_f, then T beam analysis must be applied. Equations (3.59) through (3.63) can be used, in sequence, to obtain the nominal flexural strength, after which the design strength is easily calculated.

For *design*, the following sequence of calculations may be followed:

1. Establish flange thickness h_f based on flexural requirements of the slab, which normally spans transversely between parallel T beams.
2. Determine the effective flange width b according to ACI limits.
3. Choose web dimensions b_w and d based on either of the following:
   (a) Negative bending requirements at the supports, if a continuous T beam
   (b) Shear requirements, setting a reasonable upper limit on the nominal unit shear stress v_u in the beam web (see Chapter 4)
4. With all concrete dimensions thus established, calculate a trial value of A_s, assuming that a does not exceed h_f, with beam width equal to flange width b. Use ordinary rectangular beam design methods.
5. For the trial A_s, check the depth of stress block a to confirm that it does not exceed h_f. If it should exceed that value, revise A_s, using the T beam equations.
6. Check to ensure that $\epsilon_t \geq 0.005$ or $c/d \leq 0.375$ to ensure that $\phi = 0.90$. (This will almost invariably be the case.)
7. Check to ensure that $\rho_w \geq \rho_{w,\min}$.

EXAMPLE 3.14

Moment capacity of a given section. The isolated T beam shown in Fig. 3.21 is composed of a flange 700 mm wide and 150 mm deep cast monolithically with a web of 250 mm width that extends 600 mm below the bottom surface of the flange to produce a beam of 750 mm total depth. Tensile reinforcement consists of six No. 32 (No. 10) bars placed in two horizontal rows separated by 25 mm clear spacing. The centroid of the bar group is 650 mm from the top of the beam. The concrete has a strength of 21 MPa, and the yield strength of the steel is 420 MPa. What is the design moment capacity of the beam?

Solution. It is easily confirmed that the flange dimensions are satisfactory according to the ACI Code for an isolated beam. The entire flange can be considered effective. For six No. 32 (No. 10) bars, $A_s = 4914\ \text{mm}^2$. First check the location of the neutral axis, on the assumption that rectangular beam equations may be applied. Using Eq. (3.32)

$$a = \frac{4914 \times 420}{0.85 \times 21 \times 700} = 165.2\ \text{mm}$$

This exceeds the flange thickness, and so a T beam analysis is required. From Eq. (3.59) and Fig. 3.19*b*,

$$A_{sf} = 0.85 \times \frac{21}{420}(700 - 250) \times 150 = 2869\ \text{mm}^2$$

Then, from Eq. (3.60),

$$M_{n1} = 2869 \times 420(650 - 150/2) \times 10^{-6} = 692.8\ \text{kN-m}$$

Then, from Fig. 3.19*c*,

$$A_s - A_{sf} = 4914 - 2869 = 2045\ \text{mm}^2$$

and from Eqs. (3.58) and (3.59)

$$a = \frac{2045 \times 420}{0.85 \times 21 \times 250} = 192.5\ \text{mm}$$

$$M_{n2} = 2045 \times 420\left(650 - \frac{192.5}{2}\right) \times 10^{-6} = 475.6\ \text{kN-m}$$

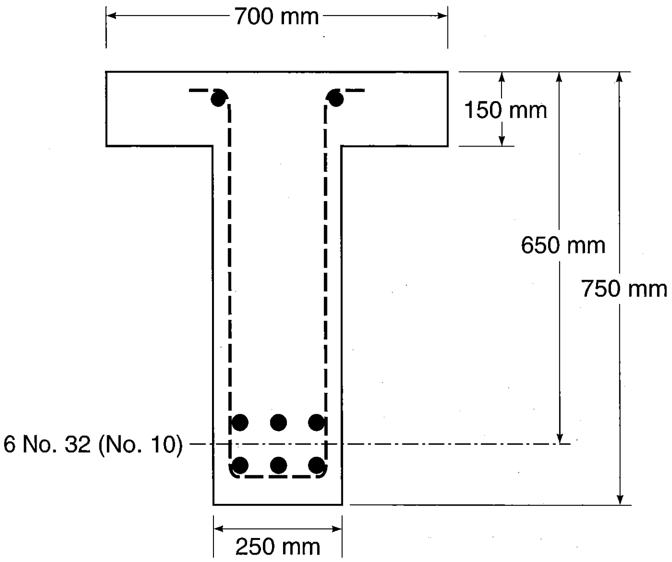

FIGURE 3.21
T beam of Example 3.14.

The depth to the neutral axis is $c = a/\beta_1 = 192.5/0.85 = 226.5$ and $d_t = 685$ mm to the lowest bar. The c/d_t ratio is $\frac{226.5}{685} = 0.331 < 0.375$, so the $\epsilon_t > 0.005$ requirement is met and $\phi = 0.90$. When the ACI strength reduction factor is incorporated, the design strength is

$$\phi M_n = 0.90(692.9 + 475.6) = 1052 \text{ kN-m}$$

EXAMPLE 3.15

Determination of steel area for a given moment. A floor system, shown in Fig. 3.22, consists of a 75 mm concrete slab supported by continuous T beams with a 7.5 m span, 1.2 m on centers. Web dimensions, as determined by negative-moment requirements at the supports, are $b_w = 275$ mm and $d = 500$ mm. What tensile steel area is required at midspan to resist a factored moment of 725 kN-m if $f_y = 420$ MPa and $f'_c = 21$ MPa?

Solution. First determining the effective flange width,

$$16h_f + b_w = 16 \times 75 + 275 = 1475 \text{ mm} = 1.475 \text{ m}$$

$$\frac{\text{Span}}{4} = \frac{7.5}{4} = 1.875 \text{ m}$$

$$\text{Centerline beam spacing} = 1.2 \text{ m}$$

The centerline T beam spacing controls in this case, and $b = 1.2$ m. The concrete dimensions b_w and d are known to be adequate in this case, since they have been selected for the larger negative support moment applied to the effective rectangular section $b_w d$. The tensile steel at midspan is most conveniently found by trial. Assuming the stress-block depth a is equal to the flange thickness of $h_f = 75$ mm, one gets

$$d - \frac{a}{2} = 500 - 37.5 = 462.5 \text{ mm}$$

Trial:

$$A_s = \frac{M_u}{\phi f_y(d - a/2)} = \frac{725 \times 10^6}{0.90 \times 420 \times 462.5} = 4147 \text{ mm}^2$$

Checking the assumed value for a,

$$a = \frac{A_s f_y}{0.85 f'_c b} = \frac{4147 \times 420}{0.85 \times 21 \times 1200} = 81.3 \text{ mm}$$

Since a is greater than h_f, a T beam design is required and $\phi = 0.90$ is assumed.

$$A_{sf} = \frac{0.85 f'_c (b - b_w) h_f}{f_y} = \frac{0.85 \times 21 \times 925 \times 75}{420} = 2948 \text{ mm}^2$$

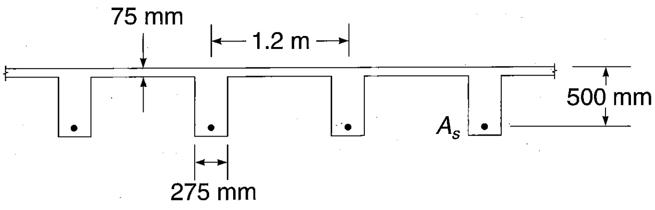

FIGURE 3.22
T beam of Example 3.15.

$$\phi M_{n1} = \phi A_{sf} f_y \left(d - \frac{h_f}{2} \right) = 0.90 \times 2948 \times 420 \times (500 - 75/2) \times 10^{-6} = 515.4 \text{ kN-m}$$

$$\phi M_{n2} = M_u - \phi M_{n1} = 725 - 515.4 = 209.6 \text{ kN-m}$$

Assume $a = 100$ mm

$$A_s - A_{sf} = \frac{\phi M_{n2}}{\phi f_y (d - a/2)} = \frac{209.6 \times 10^6}{0.90 \times 420 \times (500 - 100/2)} = 1232 \text{ mm}^2$$

Check:

$$a = \frac{(A_s - A_{sf}) f_y}{0.85 f'_c b_w} = \frac{1232 \times 420}{0.85 \times 21 \times 275} = 105.4 \text{ mm}$$

This is satisfactorily close to the assumed value of 100 mm. Then

$$A_s = A_{sf} + A_s - A_{sf} = 2948 + 1232 = 4181$$

Checking to ensure that the net tensile strain of 0.005 is met to allow $\phi = 0.90$,

$$c = \frac{a}{\beta_1} = \frac{105.4}{0.85} = 124 \text{ mm}$$

$$\frac{c}{d_t} = \frac{124}{500} = 0.248 < 0.325$$

indicating that the design is satisfactory.

The close agreement should be noted between the approximate tensile steel area of 4147 mm^2 found by assuming the stress-block depth equal to the flange thickness and the more exact value of 4180 mm^2 found by T beam analysis. The approximate solution would be satisfactory in most cases.

REFERENCES

3.1. H. Rusch, "Researches toward a General Flexural Theory of Structural Concrete," *J. ACI*, vol. 32, no. 1, 1960, pp. 1–28.

3.2. L. B. Kriz, "Ultimate Strength Criteria for Reinforced Concrete," *J. Eng. Mech. Div. ASCE*, vol. 85, no. EM3, 1959, pp. 95–110.

3.3. L. B. Kriz and S. L. Lee, "Ultimate Strength of Overreinforced Beams," *Proc. ASCE*, vol. 86, no. EM3, 1960, pp. 95–106.

3.4. C. S. Whitney, "Design of Reinforced Concrete Members under Flexure or Combined Flexure and Direct Compression," *J. ACI*, vol. 33, Mar-Apr. 1937, pp. 483–498.

3.5. A. H. Mattock, L. B. Kriz, and E. Hogenstad, "Rectangular Concrete Stress Distribution in Ultimate Strength Design," *J. ACI*, vol. 32, no. 8, 1961, pp. 875–928.

3.6. P. H. Kaar, N. W. Hanson, and H. T. Capell, "Stress-Strain Curves and Stress Block Coefficients for High-Strength Concrete," *Proc. Douglas McHenry Symposium*, ACI Special Publication SP-55, 1978.

3.7. *ACI Design Handbook: Beams, One-Way Slabs, Brackets, Footings, Pile Caps, Columns, Two-Way Slabs, and Seismic Design in Accordance with the Strength Design Method of 318-95*, SP-17, American Concrete Institute, Farmington Hills, MI, 1997.

3.8. *ACI Detailing Manual*, ACI Special Publication SP-66, American Concrete Institute, Farmington Hills, MI, 2004.

3.9. *CRSI Design Handbook*, 9th ed., Concrete Reinforcing Steel Institute, Schaumburg, IL, 2008.

3.10. *Economical Concrete Construction*, Engineering Data Report No. 30, Concrete Reinforcing Steel Institute, Schaumburg, IL, 1988.

3.11. *Manual of Standard Practice*, 27th ed., Concrete Reinforcing Steel Institute, Schaumburg, IL, 2001.

3.12. C. W. Dolan, *Ultimate Capacity of Reinforced Concrete Sections Using a Continuous Stress-Strain Function*, M.S. Thesis, Cornell University, Ithaca, NY, June 1967.

PROBLEMS

3.1. A rectangular beam made using concrete with $f_c' = 42$ MPa and steel with $f_y = 420$ MPa has a width $b = 500$ mm, an effective depth of $d = 440$ mm, and a total depth of $h = 500$ mm. The concrete modulus of rupture $f_r = 3.6$ MPa. The elastic moduli of the concrete and steel are, respectively, $E_c = 28{,}000$ MPa and $E_s = 200{,}000$ MPa. The tensile steel consists of four No. 36 (No. 11) bars.

(*a*) Find the maximum service load moment that can be resisted without stressing the concrete above $0.45f_c'$ or the steel above $0.40f_y$.

(*b*) Determine whether the beam will crack before reaching the service load.

(*c*) Compute the nominal flexural strength of the beam.

(*d*) Compute the ratio of the nominal flexural strength of the beam to the maximum service load moment, and compare your findings to the ACI load factors and strength reduction factor.

3.2. A rectangular, tension-reinforced beam is to be designed for dead load of 7.3 kN/m plus self-weight and service live load of 17.5 kN/m, with a 6.70 m simple span. Material strengths will be $f_y = 420$ MPa and $f_c' = 21$ MPa for steel and concrete, respectively. The total beam depth must not exceed 400 mm. Calculate the required beam width and tensile steel requirement, using a reinforcement ratio of $0.60\rho_{\max}$. Use ACI load factors and strength reduction factors. The effective depth may be assumed to be 60 mm less than the total depth.

3.3. A beam with a 6 m simple span has cross-sectional dimensions $b = 300$ mm, $d = 440$ mm, and $h = 500$ mm (see Fig. 3.2*b* for notation). It carries a uniform service load of 36 kN/m in addition to its own weight. Material strengths are $f_c' = 28$ MPa and $f_y = 420$ MPa. Assume a weight of 24 kN/m^3 for reinforced concrete.

(*a*) Check whether this beam, if reinforced with three No. 29 (No. 9) bars, is adequate to carry this load with a minimum factor of safety against flexural failure of 1.85. If this requirement is not met, select a three-bar reinforcement of diameter or diameters adequate to provide this safety.

(*b*) Determine the maximum stress in the steel and in the concrete under service load, i.e., when the beam carries its own weight and the specified uniform load.

(*c*) Will the beam show hairline cracks on the tension side under service load?

3.4. A rectangular reinforced concrete beam with dimensions $b = 350$ mm, $d = 500$ mm, and $h = 700$ mm is reinforced with three No. 32 (No. 10) bars. Material strengths are $f_y = 420$ MPa and $f_c' = 35$ MPa.

(*a*) Find the moment that will produce the first cracking at the bottom surface of the beam, basing your calculation on I_g, the moment of inertia of the gross concrete section.

(*b*) Repeat the calculation, using I_{ut}, the moment of inertia of the uncracked transformed section.

(*c*) Determine the maximum moment that can be carried without stressing the concrete beyond $0.45f_c'$ or the steel beyond $0.60f_y$.

(*d*) Find the nominal flexural strength of this beam.

(*e*) Compute the ratio of the flexural strength from part (*d*) to the service capacity from part (*c*).

(*f*) Comment on your results, paying particular attention to comparing parts (*a*) and (*b*) and comparing the result in part (*e*) with the load factors in the ACI Code.

3.5. A tensile-reinforced beam has $b = 300$ mm and $d = 500$ mm to the center of the bars, which are placed all in one row. If $f_y = 420$ MPa and $f'_c = 35$ MPa, find the nominal flexural strength M_n for (*a*) A_s = two No. 25 (No. 8) bars, (*b*) A_s = two No. 32 (No. 10) bars, (*c*) A_s = three No. 32 (No. 10) bars.

3.6. A singly reinforced rectangular beam is to be designed, with effective depth approximately 1.5 times the width, to carry a service live load of 30 kN/m in addition to its own weight, on a 7.5 m simple span. The ACI Code load factors are to be applied as usual. With $f_y = 420$ MPa and $f'_c = 28$ MPa, determine the required concrete dimensions b, d, and h, and steel reinforcing bars (*a*) for $\rho = 0.60\rho_{\max}$ and (*b*) for $\rho = \rho_{0.005}$. Include a sketch of each cross section drawn to scale. Allow for No. 13 (No. 4) stirrups. Comment on your results.

3.7. A four-span continuous beam of constant rectangular cross section is supported at A, B, C, D, and E. The factored moments resulting from analysis are as follows:

At Supports, kN-m	At Midspan, kN-m
$M_a = 188$	$M_{ab} = 215$
$M_b = 300$	$M_{bc} = 188$
$M_c = 270$	$M_{cd} = 188$
$M_d = 300$	$M_{de} = 215$
$M_e = 188$	

Determine the required final concrete dimensions for this beam, using $d = 1.75b$, and determine the reinforcement requirements at each critical moment section. Your final reinforcement ratio should not exceed $= 0.6\rho_{0.005}$. Use $f_y = 420$ MPa and $f'_c = 42$ MPa.

3.8. A two-span continuous concrete beam is to be supported by three concrete walls spaced 10 m on centers. A service live load of 20 kN/m is to be carried in addition to the self-weight of the beam. Use pattern loading; i.e., consider two loading conditions: (1) live load on both spans and (2) live load on a single span. A constant rectangular cross section is to be used with $d = 2b$, but reinforcement is to be varied according to requirements. Find the required concrete dimensions and reinforcement at all critical sections. Allow for No. 10 (No. 3) stirrups. Use a span-to-depth ratio of 15 as the first estimate of the depth. Adjust the depth if the reinforcement ratio is too high. Include sketches, drawn to scale, of the critical cross sections. Use $f_y = 420$ MPa and $f'_c = 42$ MPa.

3.9. A rectangular concrete beam measures 300 mm wide and has an effective depth of 450 mm. Compression steel consisting of two No. 25 (No. 8) bars is located 65 mm from the compression face of the beam. If $f'_c = 28$ MPa and $f_y = 420$ MPa, what is the design moment capacity of the beam, according to the ACI Code, for the following alternative tensile steel areas? (*a*) A_s = three No. 32 (No. 10) bars in one layer, (*b*) A_s = four No. 32 (No. 10) bars in two layers, (*c*) A_s = six No. 29 (No. 9) bars in two layers. (*Note*: Check for yielding of compression steel in each case.) Plot M_n versus ρ and comment on your findings.

3.10. A rectangular concrete beam of width $b = 600$ mm is limited by architectural considerations to a maximum total depth $h = 400$ mm. It must carry a total factored load moment $M_u = 540$ kN-m. Design the flexural reinforcement for this member, using compression steel if necessary. Allow 75 mm to the center of the bars from the compression or tension face of the beam. Material strengths are $f_y = 420$ MPa and $f'_c = 28$ MPa. Select reinforcement to provide the needed areas, and show a sketch of your final design, including provision for No. 13 (No. 4) stirrups.

3.11. For the beam with the triangular cross section shown in Fig. P3.11, determine (*a*) the balanced reinforcement ratio and (*b*) the maximum reinforcement ratio if $\epsilon_t = 0.005$. The dimensions of the triangle are such that the width of the triangle equals the distance from the apex. Thus, the width at the effective depth b equals the effective depth d. Express the reinforcement ratio ρ in terms of b and d. Draw the strain distribution, and stress distribution, and define your notation.

FIGURE P3.11

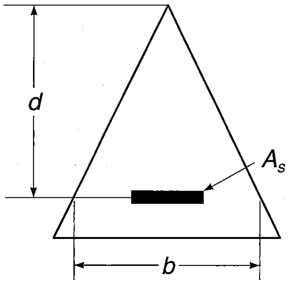

3.12. Develop a design table and graph for the moment capacity of rectangular concrete beams based on the use of the flexural resistance factor R. (See Table A.5a and Graph A.1a for examples.) Material strengths are $f_y = 420$ MPa and $f'_c = 56$ MPa. The table and graph should begin with $\rho_{\min}$ and end at $\rho_{\max}$. Your work must show how the maximum and minimum values of ρ were computed. You may use Excel or MathCAD to perform your calculations. Your submittal must include a table, a graph, and commentary on how you checked the work.

3.13. A rectangular beam made using concrete with $f'_c = 35$ MPa and steel with $f_y = 420$ MPa has a width $b = 450$ mm, an effective depth $d = 540$ mm and a total depth $h = 600$ mm. The beam is reinforced with four No. 29 (No. 9) bars. Compute the nominal moment capacity, assuming (*a*) an equivalent rectangular stress block, (*b*) a triangular stress block with a peak value of f'_c, and (*c*) a parabolic stress block with a peak value of f'_c (see Fig. P3.13). Compare and comment on your results, knowing that the rectangular stress block correlates within 4 percent with test results.

FIGURE P3.13

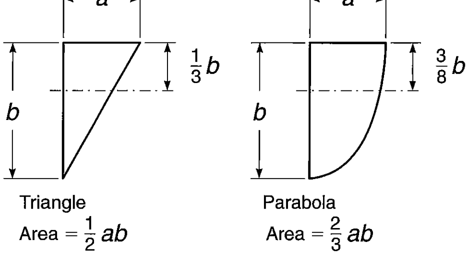

3.14. A precast T beam is to be used as a bridge over a small roadway. Concrete dimensions are $b = 1.2$ m, $b_w = 400$ mm, $h_f = 125$ mm, and $h = 650$ mm. The effective depth $d = 590$ mm. Concrete and steel strengths are 42 MPa and

420 MPa, respectively. Using approximately one-half the maximum tensile reinforcement permitted by the ACI Code (select the actual size of bar and number to be used), determine the design moment capacity of the girder. If the beam is used on a 10 m simple span, and if in addition to its own weight it must support railings, curbs, and suspended loads totaling 7.0 kN/m, what uniform service live load limit should be posted?

3.15. A rectangular beam with a width of 200 mm, an effective depth of 240 mm, and a total depth of 300 mm is reinforced with a single fiberglass reinforcing bar that has a cross-sectional area of 290 mm^2. The bar has a nominal tensile strength of 950 MPa, a linear stress-strain curve to failure, and a strain at failure of 1.8 percent. The concrete strength $f'_c = 42$ MPa. Determine the nominal flexural strength of the section if $E_{\text{glass}} = 50{,}000$ MPa.

3.16. Compute the maximum and minimum reinforcement ratios for reinforcement with a 550 MPa yield point and $f'_c = 28$ to 56 MPa in 7 MPa increments, similar to those shown in Table A.4. Using the maximum and minimum reinforcement ratios, develop resistance factors and design graphs similar to Table A.5b and Graph A.1a.

4 Shear and Diagonal Tension in Beams

4.1 INTRODUCTION

Chapter 3 dealt with the flexural behavior and flexural strength of beams. Beams must also have an adequate safety margin against other types of failure, some of which may be more dangerous than flexural failure. This may be so because of greater uncertainty in predicting certain other modes of collapse, or because of the catastrophic nature of some other types of failure, should they occur.

Shear failure of reinforced concrete, more properly called *diagonal tension failure*, is one example. Shear failure is difficult to predict accurately. In spite of many decades of experimental research (Refs. 4.1 to 4.6) and the use of highly sophisticated analytical tools (Refs. 4.7 and 4.8), it is not yet fully understood. Furthermore, if a beam without properly designed shear reinforcement is overloaded to failure, shear collapse is likely to occur suddenly, with no advance warning of distress. This is in strong contrast with the nature of flexural failure. For typically underreinforced beams, flexural failure is initiated by gradual yielding of the tension steel, accompanied by obvious cracking of the concrete and large deflections, giving ample warning and providing the opportunity to take corrective measures. Because of these differences in behavior, reinforced concrete beams are generally provided with special *shear reinforcement* to ensure that flexural failure would occur before shear failure if the member were severely overloaded.

Figure 4.1 shows a shear-critical beam tested under third point loading. With no shear reinforcement provided, the member failed immediately upon formation of the critical crack in the high-shear region near the right support.

It is important to realize that shear analysis and design are not really concerned with shear as such. The shear stresses in most beams are far below the direct shear strength of the concrete. The real concern is with *diagonal tension stress*, resulting from the combination of shear stress and longitudinal flexural stress. Most of this chapter deals with analysis and design for diagonal tension, and it provides background for understanding and using the shear provisions of the 2008 ACI Code. Members without web reinforcement are studied first to establish the location and orientation of cracks and the diagonal cracking load. Methods are then developed for the design of shear reinforcement according to the present ACI Code, both in ordinary beams and in special types of members, such as deep beams.

Over the years, alternative methods of shear design have been proposed, based on variable angle truss models and diagonal compression field theory (Refs. 4.9 and 4.10). These approaches will be reviewed briefly later in this chapter, with one such approach, the modified compression field theory, presented in detail.

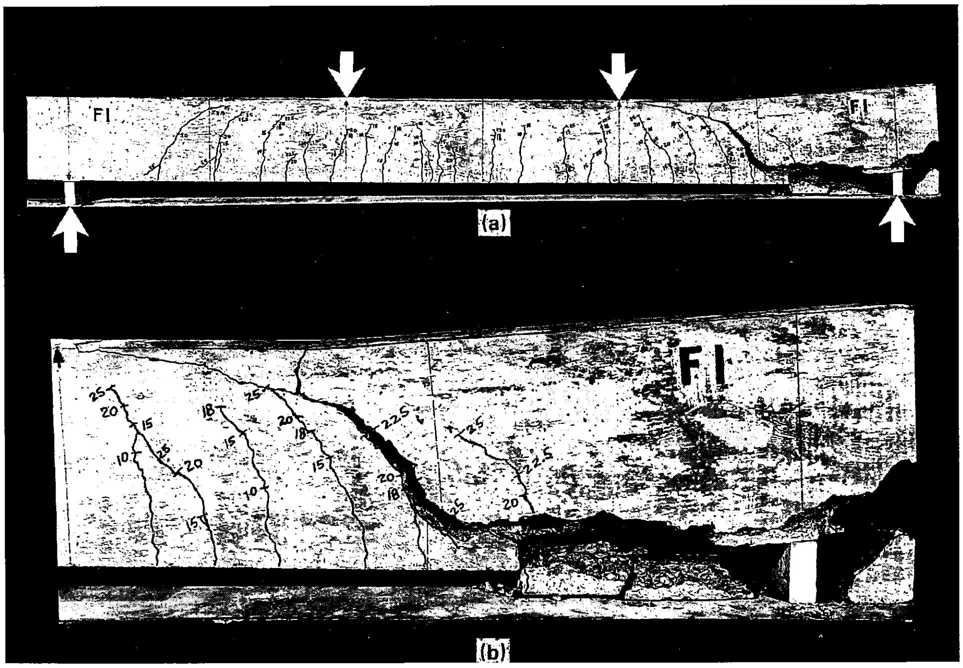

FIGURE 4.1
Shear failure of reinforced concrete beam: (*a*) overall view, (*b*) detail near right support.

Finally, there are some circumstances in which consideration of direct shear is appropriate. One example is in the design of composite members combining precast beams with a cast-in-place top slab. Horizontal shear stresses on the interface between components are important. The shear-friction theory, useful in this and other cases, will be presented following development of methods for the analysis and design of beams for diagonal tension.

4.2 DIAGONAL TENSION IN HOMOGENEOUS ELASTIC BEAMS

The stresses acting in homogeneous beams were briefly reviewed in Section 3.2. It was pointed out that when the material is elastic (stresses proportional to strains), shear stresses

$$v = \frac{VQ}{Ib} \tag{3.4}$$

act at any section in addition to the bending stresses

$$f = \frac{My}{I} \tag{3.2}$$

except for those locations at which the shear force V happens to be zero.

The role of shear stresses is easily visualized by the performance under load of the laminated beam of Fig. 4.2; it consists of two rectangular pieces bonded together along the contact surface. If the adhesive is strong enough, the member will deform as one single beam, as shown in Fig. 4.2*a*. On the other hand, if the adhesive is weak, the two pieces will separate and slide relative to each other, as shown in Fig. 4.2*b*.

FIGURE 4.2
Shear in homogeneous rectangular beams.

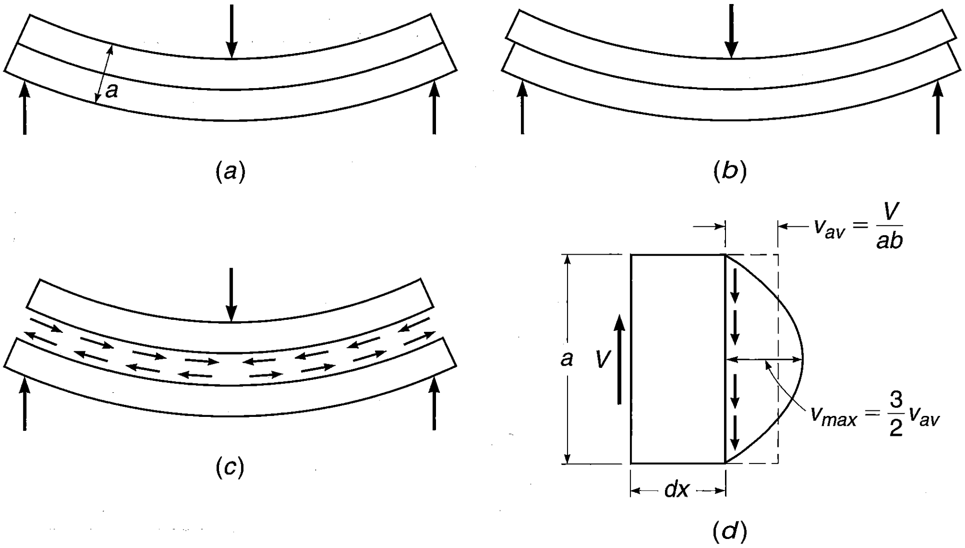

Evidently, then, when the adhesive is effective, there are forces or stresses acting in it that prevent this sliding or shearing. These horizontal shear stresses are shown in Fig. 4.2*c* as they act, separately, on the top and bottom pieces. The same stresses occur in horizontal planes in single-piece beams; they are different in intensity at different distances from the neutral axis.

Figure 4.2*d* shows a differential length of a single-piece rectangular beam acted upon by a shear force of magnitude V. Upward translation is prevented; i.e., vertical equilibrium is provided by the vertical shear stresses v. Their average value is equal to the shear force divided by the cross-sectional area $v_{av} = V/ab$, but their intensity varies over the depth of the section. As is easily computed from Eq. (3.4), the shear stress is zero at the outer fibers and has a maximum of $1.5v_{av}$ at the neutral axis, the variation being parabolic as shown. Other values and distributions are found for other shapes of the cross section, the shear stress always being zero at the outer fibers and of maximum value at the neutral axis. If a small square element located at the neutral axis of such a beam is isolated, as shown in Fig. 4.3*b*, the vertical shear stresses on it, equal and opposite on the two faces for reasons of equilibrium, act as shown. However, if these were the only stresses present, the element would not be in equilibrium; it would spin. Therefore, on the two horizontal faces there exist equilibrating horizontal shear stresses of the same magnitude. That is, at any point within the beam, the horizontal shear stresses of Fig. 4.3*b* are equal in magnitude to the vertical shear stresses of Fig. 4.2*d*.

It is proved in any strength-of-materials text that on an element cut at 45° these shear stresses combine in such a manner that their effect is as shown in Fig. 4.3*c*. That is, the action of the two pairs of shear stresses on the vertical and horizontal faces is the same as that of two pairs of normal stresses, one tensile and one compressive, acting on the 45° faces and of numerical value equal to that of the shear stresses. If an element of the beam is considered that is located neither at the neutral axis nor at the outer edges, its vertical faces are subject not only to the shear stresses but also to the familiar bending stresses whose magnitude is given by Eq. (3.2) (Fig. 4.3*d*). The six stresses that now act on the element can again be combined into a pair of inclined

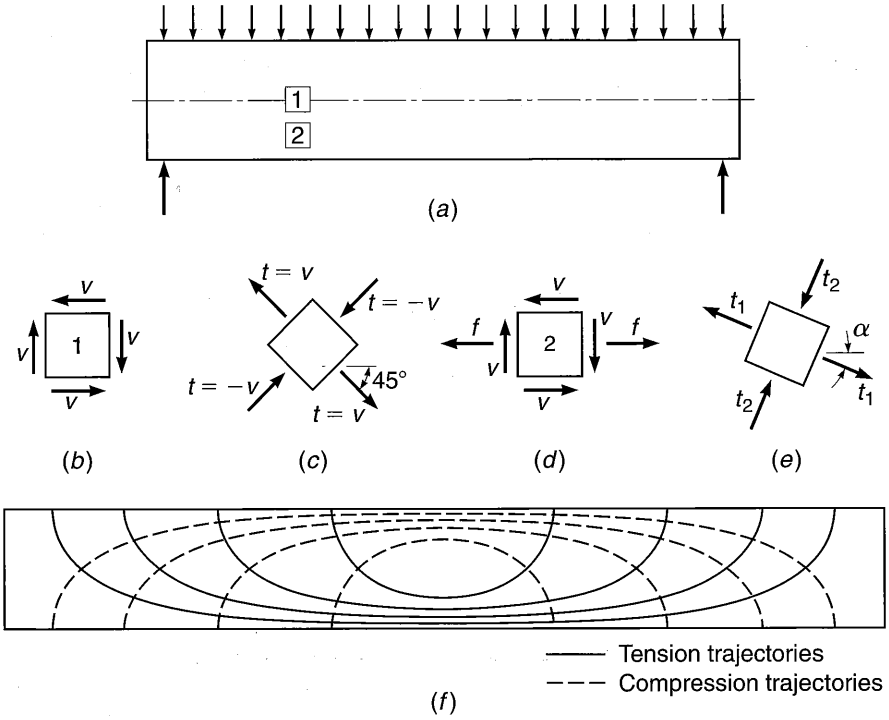

FIGURE 4.3
Stress trajectories in homogeneous rectangular beam.

compressive stresses and a pair of inclined tensile stresses that act at right angles to each other. They are known as *principal stresses* (Fig. 4.3*e*). Their value, as mentioned in Section 3.2, is given by

$$t = \frac{f}{2} \pm \sqrt{\frac{f^2}{4} + v^2} \tag{3.1}$$

and their inclination α by $\tan 2\alpha = 2v/f$.

Since the magnitudes of the shear stresses v and the bending stresses f change both along the beam and vertically with distance from the neutral axis, the inclinations as well as the magnitudes of the resulting principal stresses t also vary from one place to another. Figure 4.3*f* shows the inclinations of these principal stresses for a rectangular beam uniformly loaded. That is, these stress trajectories are lines which, at any point, are drawn in that direction in which the particular principal stress, tension or compression, acts at that point. It is seen that at the neutral axis the principal stresses in a beam are always inclined at 45° to the axis. In the vicinity of the outer fibers they are horizontal near midspan.

An important point follows from this discussion. Tensile stresses, which are of particular concern in view of the low tensile strength of the concrete, are not confined to the horizontal bending stresses f that are caused by bending alone. Tensile stresses of various inclinations and magnitudes, resulting from shear alone (at the neutral axis) or from the combined action of shear and bending, exist in all parts of a beam and can impair its integrity if not adequately provided for. It is for this reason that the inclined tensile stresses, known as *diagonal tension*, must be carefully considered in reinforced concrete design.

4.3 REINFORCED CONCRETE BEAMS WITHOUT SHEAR REINFORCEMENT

The discussion of shear in a homogeneous elastic beam applies very closely to a plain concrete beam *without* reinforcement. As the load is increased in such a beam, a tension crack will form where the tensile stresses are largest and will immediately cause the beam to fail. Except for beams of very unusual proportions, the largest tensile stresses are those caused at the outer fiber by bending alone, at the section of maximum bending moment. In this case, shear has little, if any, influence on the strength of a beam.

However, when tension reinforcement is provided, the situation is quite different. Even though tension cracks form in the concrete, the required flexural tension strength is furnished by the steel, and much higher loads can be carried. Shear stresses increase proportionally to the loads. In consequence, diagonal tension stresses of significant intensity are created in regions of high shear forces, chiefly close to the supports. The longitudinal tension reinforcement has been so calculated and placed that it is chiefly effective in resisting longitudinal tension near the tension face. It does not reinforce the tensionally weak concrete against the diagonal tension stresses that occur elsewhere, caused by shear alone or by the combined effect of shear and flexure. Eventually, these stresses attain magnitudes sufficient to open additional tension cracks in a direction perpendicular to the local tension stress. These are known as *diagonal* cracks, in distinction to the vertical flexural cracks. The latter occur in regions of large moments, the former in regions in which the shear forces are high. In beams in which no reinforcement is provided to counteract the formation of large diagonal tension cracks, their appearance has far-reaching and detrimental effects. For this reason, methods of predicting the loads at which these cracks will form are desired.

a. Criteria for Formation of Diagonal Cracks

It is seen from Eq. (3.1) that the diagonal tension stresses t represent the combined effect of the shear stresses v and the bending stresses f. These in turn are, respectively, proportional to the shear force V and the bending moment M at the particular location in the beam [Eqs. (3.2) and (3.4)]. Depending on configuration, support conditions, and load distribution, a given location in a beam may have a large moment combined with a small shear force, or the reverse, or large or small values for both shear and moment. Evidently, the relative values of M and V will affect the magnitude as well as the direction of the diagonal tension stresses. Figure 4.4 shows a few typical beams and their moment and shear diagrams and draws attention to locations at which various combinations of high or low V and M occur.

At a location of large shear force V and small bending moment M, there will be little flexural cracking, if any, prior to the development of a diagonal tension crack. Consequently, the average shear stress prior to crack formation is

$$v = \frac{V}{bd} \tag{4.1}$$

The exact distribution of these shear stresses over the depth of the cross section is not known. It cannot be computed from Eq. (3.4) because this equation does not account for the influence of the reinforcement and because concrete is not an elastic homogeneous material. The value computed from Eq. (4.1) must therefore be regarded merely as a measure of the average intensity of shear stresses in the section. The maximum

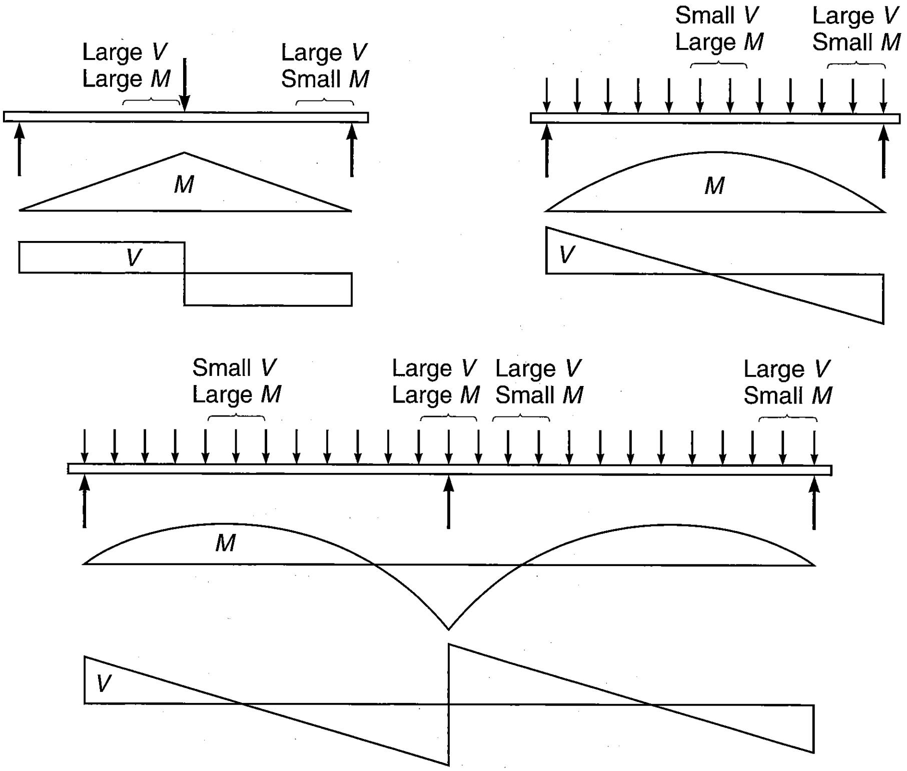

FIGURE 4.4
Typical locations of critical combinations of shear and moment.

value, which occurs at the neutral axis, will exceed this average by an unknown but moderate amount.

If flexural stresses are negligibly small at the particular location, the diagonal tensile stresses, as in Fig. 4.3*b* and *c*, are inclined at about 45° and are numerically equal to the shear stresses, with a maximum at the neutral axis. Consequently, diagonal cracks form mostly at or near the neutral axis and propagate from that location, as shown in Fig. 4.5*a*. These *web-shear* cracks can be expected to form when the diagonal tension stress in the vicinity of the neutral axis becomes equal to the tensile strength of the concrete. The former, as was indicated, is of the order of, and somewhat larger than, $v = V/bd$; the latter, as discussed in Section 2.9, varies from about $0.25\sqrt{f'_c}$ to about $0.58\sqrt{f'_c}$. An evaluation of a very large number of beam tests is in fair agreement with this reasoning (Ref. 4.1). It was found that in regions with large shear and small moment, diagonal tension cracks form at an average or nominal shear stress v_{cr} of about $0.29\sqrt{f'_c}$, that is,

$$v_{cr} = \frac{V_{cr}}{bd} = 0.29\sqrt{f'_c} \tag{4.2a}$$

where V_{cr} is that shear force at which the formation of the crack was observed.[†] Web-shear cracking is relatively rare and occurs chiefly near supports of deep, thin-webbed beams or at inflection points of continuous beams.

[†] Actually, diagonal tension cracks form at places where a compressive stress acts in addition to and perpendicular to the diagonal tension stress, as shown in Fig. 4.3*d* and *e*. The crack, therefore, occurs at a location of biaxial stress rather than uniaxial tension. However, the effect of this simultaneous compressive stress on the cracking strength appears to be small, in agreement with the information in Fig. 2.8.

FIGURE 4.5
Diagonal tension cracking in reinforced concrete beams.

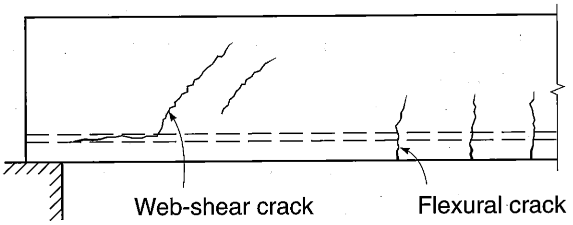

(*a*) Web-shear cracking

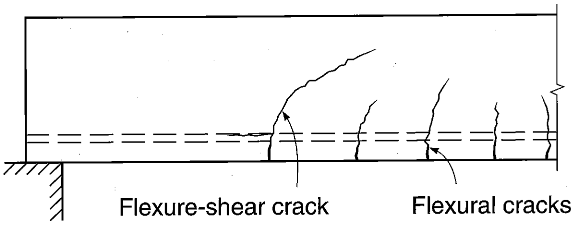

(*b*) Flexure-shear cracking

The situation is different when both the shear force and the bending moment have large values. At such locations, in a well-proportioned and reinforced beam, flexural tension cracks form first. Their width and length are well controlled and kept small by the presence of longitudinal reinforcement. However, when the diagonal tension stress at the upper end of one or more of these cracks exceeds the tensile strength of the concrete, the crack bends in a diagonal direction and continues to grow in length and width (see Fig. 4.5*b*). These cracks are known as *flexure-shear* cracks and are more common than web-shear cracks.

It is evident that at the instant at which a diagonal tension crack of this type develops, the average shear stress is larger than that given by Eq. (4.1). This is so because the preexisting tension crack has reduced the area of uncracked concrete that is available to resist shear to a value smaller than that of the uncracked area bd used in Eq. (4.1). The amount of this reduction will vary, depending on the unpredictable length of the preexisting flexural tension crack. Furthermore, the simultaneous bending stress f combines with the shear stress v to increase the diagonal tension stress t further [see Eq. (3.1)]. No way has been found to calculate reliable values of the diagonal tension stress under these conditions, and recourse must be made to test results.

A large number of beam tests have been evaluated for this purpose (Ref. 4.1). They show that in the presence of large moments (for which adequate longitudinal reinforcement has been provided) the nominal shear stress at which diagonal tension cracks form and propagate is, in most cases, conservatively given by

$$v_{cr} = \frac{V_{cr}}{bd} = 0.16\sqrt{f'_c} \tag{4.2b}$$

Comparison with Eq. (4.2*a*) shows that large bending moments can reduce the shear force at which diagonal cracks form to roughly one-half the value at which they would form if the moment were zero or nearly so. This is in qualitative agreement with the discussion just given.

It is evident, then, that the shear at which diagonal cracks develop depends on the ratio of shear force to bending moment, or, more precisely, on the ratio of shear stress v to bending stress f near the top of the flexural crack. Neither of these can be accurately calculated. It is clear, though, that $v = K_1(V/bd)$, where, by comparison with Eq. (4.1), constant K_1 depends chiefly on the depth of penetration of the flexural crack. On the other hand [see Eq. (3.10)], $f = K_2(V/bd^2)$, where K_2 also depends on crack configuration. Hence, the ratio

$$\frac{v}{f} = \frac{K_1}{K_2}\frac{Vd}{M}$$

must be expected to affect that load at which flexural cracks develop into flexure-shear cracks, the unknown quantity K_1/K_2 to be explored by tests. Equation (4.2*a*) gives the cracking shear for very large values of Vd/M, and Eq. (4.2*b*) for very small values. Moderate values of Vd/M result in magnitudes of v_{cr} intermediate between these extremes. Again, from evaluations of large numbers of tests (Ref. 4.1), it has been found that the nominal shear stress at which diagonal flexure-shear cracking develops can be predicted from

$$v_{cr} = \frac{V_{cr}}{bd} = 0.16\sqrt{f'_c} + 17\,\frac{\rho V d}{M} \leq 0.29\sqrt{f'_c} \tag{4.3a}$$

where

$$V_{cr} = v_{cr}\,bd$$

and $\rho = A_s/bd$, as before, and 17 is an empirical constant in MPa. A graph of this relation and comparison with test data are given in Fig. 4.6.

FIGURE 4.6
Correlation of Eq. (4.3*a*) with test results.

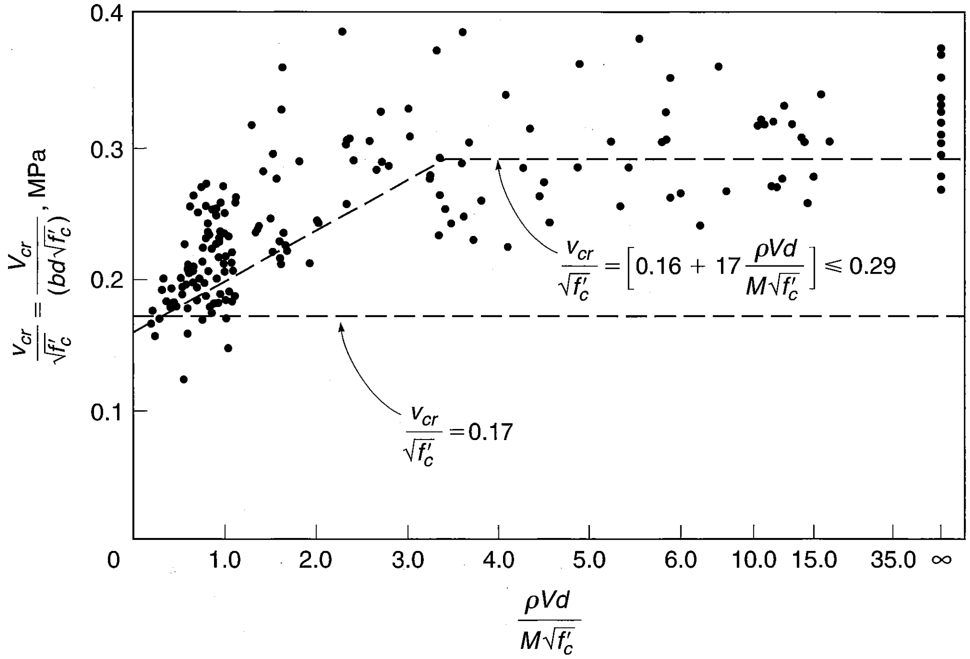

Apart from the influence of Vd/M, it is seen from Eq. (4.3*a*) that increasing amounts of tension reinforcement, i.e., increasing values of the reinforcement ratio ρ, have a beneficial effect in that they increase the shear at which diagonal cracks develop. This is so because larger amounts of longitudinal steel result in smaller and narrower flexural tension cracks prior to the formation of diagonal cracking, leaving a larger area of uncracked concrete available to resist shear. [For more details on the development of Eq. (4.3*a*), see Ref. 4.1.]

A brief study of Fig. 4.6 will show that although Eq. (4.3*a*) captures the overall effects of the controlling variables on v_{cr}, the match with actual data is far from perfect. Of particular concern is the tendency of Eq. (4.3*a*) to overestimate the shear strength of beams with reinforcement ratios $\rho < 1.0$ percent, values that are commonly used in practice. The cracking stress predicted in Eq. (4.3*a*) becomes progressively less conservative as f'_c increases above 35 MPa and as beam depth d increases above 500 mm. On the other hand, Eq. (4.3*a*) underestimates the effect of Vd/M on v_{cr} and ignores the positive effect of flanges (present on most reinforced concrete beams) on shear strength. The conservatism of Eq. (4.3*a*) increases as both flange thickness and web width increase (Ref. 4.3), although these factors have less of an effect than f'_c, ρ, or Vd/M on v_{cr}.

Considering the three main variables, an improved match with test results is obtained with the empirical relationship (Ref. 4.11)

$$v_{cr} = \frac{V_{cr}}{bd} = 2.1\left(f'_c\rho\frac{Vd}{M}\right)^{1/3} \tag{4.3b}$$

Equation (4.3*b*) was calibrated based on beams with $d \approx 300$ mm. It can be modified to account for the lower average shear cracking stress exhibited by deeper beams with the addition of one term.

$$v_{cr} = \frac{V_{cr}}{bd} = 2.1\left(\frac{300}{d}\right)^{1/4}\left(f'_c\rho\frac{Vd}{M}\right)^{1/3} \tag{4.3c}$$

b. Behavior of Diagonally Cracked Beams

In regard to flexural cracks, as distinct from diagonal tension cracks, it was explained in Section 3.3 that cracks on the tension side of a beam are permitted to occur and are in no way detrimental to the strength of the member. One might expect a similar situation in regard to diagonal cracking caused chiefly by shear. The analogy, however, is not that simple. Flexural tension cracks are harmless only because adequate longitudinal reinforcement has been provided to resist the flexural tension stresses that the cracked concrete is no longer able to transmit. In contrast, the beams now being discussed, although furnished with the usual longitudinal reinforcement, are not equipped with any other reinforcement to offset the effects of diagonal cracking. This makes the diagonal cracks much more decisive in subsequent performance and strength of the beam than the flexural cracks.

Two types of behavior have been observed in the many tests on which present knowledge is based:

1. The diagonal crack, once formed, spreads either immediately or at only slightly higher load, traversing the entire beam from the tension reinforcement to the compression face, splitting it in two and failing the beam. This process is sudden and without warning and occurs chiefly in the shallower beams, i.e., beams with

span-depth ratios of about 8 or more. Beams in this range of dimensions are very common. Complete absence of shear reinforcement would make them very vulnerable to accidental large overloads, which would result in catastrophic failures without warning. For this reason it is good practice to provide a minimum amount of shear reinforcement even if calculation does not require it, because such reinforcement restrains growth of diagonal cracks, thereby increasing ductility and providing warning in advance of actual failure. Only in situations where an unusually large safety factor against inclined cracking is provided, i.e., where actual shear stresses are very small compared with v_{cr}, as in some slabs and most footings, is it permissible to omit shear reinforcement.

2. Alternatively, the diagonal crack, once formed, spreads toward and partially into the compression zone but stops short of penetrating to the compression face. In this case no sudden collapse occurs, and the failure load may be significantly higher than that at which the diagonal crack first formed. This behavior is chiefly observed in the deeper beams with smaller span-depth ratios and will be analyzed now.

Figure 4.7*a* shows a portion of a beam, arbitrarily loaded, in which a diagonal tension crack has formed. Consider the part of the beam to the left of the crack, shown in solid lines. There is an external upward shear force $V_{\text{ext}} = R_l - P_1$ acting on this portion.

Once a crack is formed, no tension force perpendicular to the crack can be transmitted across it. However, as long as the crack is narrow, it can still transmit forces in its own plane through interlocking of the surface roughnesses. Sizable interlock forces V_i of this kind have in fact been measured, amounting to one-third and more of the total shear force. The components V_{ix} and V_{iy} of V_i are shown in Fig. 4.7*a*. The other

FIGURE 4.7
Forces at a diagonal crack in a beam without web reinforcement.

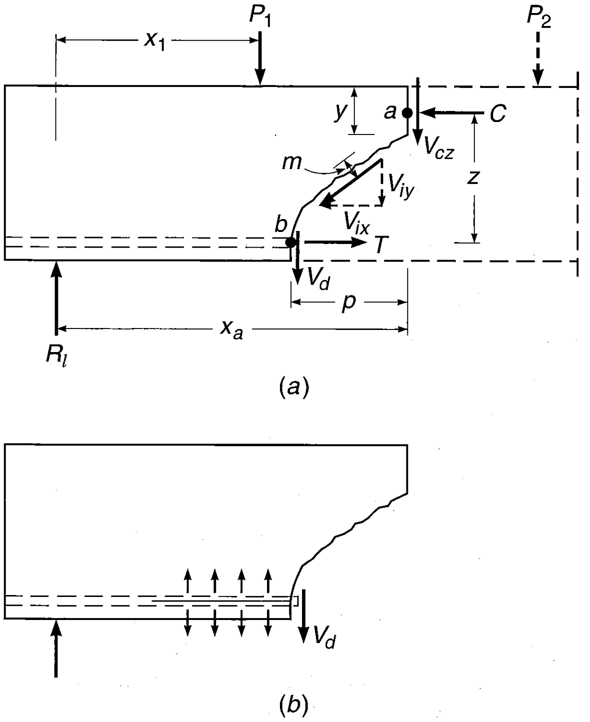

internal vertical forces are those in the uncracked portion of the concrete V_{cz} and across the longitudinal steel, acting as a dowel, V_d. Thus, the internal shear force is

$$V_{\text{int}} = V_{cz} + V_d + V_{iy}$$

Equilibrium requires that $V_{\text{int}} = V_{\text{ext}}$ so that the part of the shear resisted by the uncracked concrete is

$$V_{cz} = V_{\text{ext}} - V_d - V_{iy} \tag{4.4}$$

In a beam provided with longitudinal reinforcement only, the portion of the shear force resisted by the steel in dowel action is usually quite small. In fact, the reinforcing bars on which the dowel force V_d acts are supported against vertical displacement chiefly by the thin concrete layer below. The bearing pressure caused by V_d creates, in this concrete, vertical tension stresses as shown in Fig. 4.7*b*. Because of these stresses, diagonal cracks often result in splitting of the concrete along the tension reinforcement, as shown. (See also Fig. 4.1.) This reduces the dowel force V_d and also permits the diagonal crack to widen. This, in turn, reduces the interface force V_i and frequently leads to immediate failure.

Next consider moments about point *a* at the intersection of V_{cz} and *C*; the external moment $M_{\text{ext},a}$ acts at *a* and happens to be $R_l x_a - P_1(x_a - x_1)$ for the loading shown. The internal moment is

$$M_{\text{int},a} = T_b z + V_d p - V_i m$$

Here *p* is the horizontal projection of the diagonal crack and *m* is the moment arm of the force V_i with respect to point *a*. The designation T_b for *T* is meant to emphasize that this force in the steel acts at point *b* rather than vertically below point *a*. Equilibrium requires that $M_{\text{int},a} = M_{\text{ext},a}$ so that the longitudinal tension in the steel at *b* is

$$T_b = \frac{M_{\text{ext},a} - V_d p + V_i m}{z} \tag{4.5}$$

Neglecting the forces V_d and V_i, which decrease with increasing crack opening, one has, with very little error,

$$T_b = \frac{M_{\text{ext},a}}{z} \tag{4.6}$$

The formation of the diagonal crack, then, is seen to produce the following redistribution of internal forces and stresses:

1. At the vertical section through point *a*, the average shear stress before crack formation was V_{ext}/bd. After crack formation, the shear force is resisted by a combination of the dowel shear, the interface shear, and the shear force on the much smaller area *by* of the remaining uncracked concrete. As tension splitting develops along the longitudinal bars, V_d and V_i decrease; this, in turn, increases the shear force and the resulting shear stress on the remaining uncracked concrete area.
2. The diagonal crack, as described previously, usually rises above the neutral axis and traverses some part of the compression zone before it is arrested by the compression stresses. Consequently, the compression force *C* also acts on an area *by* smaller than that on which it acted before the crack was formed. Correspondingly, formation of the crack has increased the compression stresses in the remaining uncracked concrete.
3. Prior to diagonal cracking, the tension force in the steel at point *b* was caused by, and was proportional to, the bending moment in a vertical section through the

same point b. As a consequence of the diagonal crack, however, Eq. (4.6) shows that the tension in the steel at b is now caused by, and is proportional to, the bending moment at a. Since the moment at a is evidently larger than that at b, formation of the crack has caused a sudden increase in the steel stress at b.

If the two materials are capable of resisting these increased stresses, equilibrium will establish itself after internal redistribution and further load can be applied before failure occurs. Such failure can then develop in various ways. For one, if only enough steel has been provided at b to resist the moment at that section, the increase of the steel force, described in item 3, will cause the steel to yield because of the larger moment at a, thus failing the beam. If the beam is properly designed to prevent this occurrence, it is usually the concrete at the head of the crack that will eventually crush. This concrete is subject simultaneously to large compression and shear stresses, and this biaxial stress combination is conducive to earlier failure than would take place if either of these stresses were acting alone. Finally, if there is splitting along the reinforcement, it will cause the bond between steel and concrete to weaken to such a degree that the reinforcement may pull loose. This either may be the cause of failure of the beam or may occur simultaneously with crushing of the remaining uncracked concrete.

It was noted earlier that relatively deep beams will usually show continued and increasing resistance after formation of a critical diagonal tension crack, but relatively shallow beams will fail almost immediately upon formation of the crack. The amount of reserve strength, if any, was found to be erratic. In fact, in several test series in which two specimens as identical as one can make them were tested, one failed immediately upon formation of a diagonal crack, while the other reached equilibrium under the described redistribution and failed at a higher load.

For this reason, this reserve strength is discounted in modern design procedures. As previously mentioned, most beams are furnished with at least a minimum of web reinforcement. For those flexural members that are not, such as slabs, footings, and others, design is based on that shear force V_{cr} or shear stress v_{cr} at which formation of inclined cracks must be expected. Thus, Eq. (4.3a), or some equivalent of it, has become the design criterion for such members.

4.4 REINFORCED CONCRETE BEAMS WITH WEB REINFORCEMENT

Economy of design demands, in most cases, that a flexural member be capable of developing its full moment capacity rather than having its strength limited by premature shear failure. This is also desirable because structures, if overloaded, should not fail in the sudden and explosive manner characteristic of many shear failures, but should show adequate ductility and warning of impending distress. The latter, as pointed out earlier, is typical of flexural failure caused by yielding of the longitudinal bars, which is preceded by gradual excessively large deflections and noticeable widening of cracks. Therefore, if a fairly large safety margin relative to the available shear strength as given by Eq. (4.3a) or its equivalent does not exist, special shear reinforcement, known as *web reinforcement*, is used to increase this strength.

a. Types of Web Reinforcement

Typically, web reinforcement is provided in the form of vertical *stirrups*, spaced at varying intervals along the axis of the beam depending on requirements, as shown in Fig. 4.8a. Relatively small bars are used, generally Nos. 10 to 16 (Nos. 3 to 5). Simple

FIGURE 4.8
Types of web reinforcement.

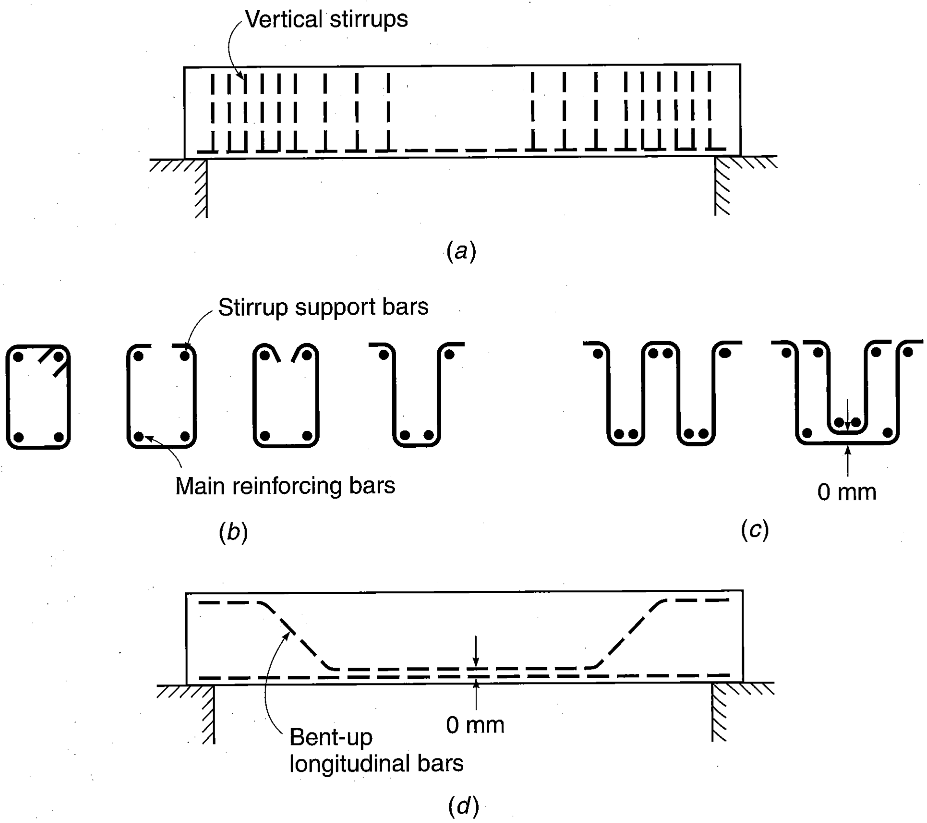

U-shaped bars similar to Fig. 4.8*b* are most common, although multiple-leg stirrups such as shown in Fig. 4.8*c* are sometimes necessary. Stirrups are formed to fit around the main longitudinal bars at the bottom and hooked or bent around longitudinal bars at the top of the member to improve anchorage and provide support during construction. Detailed requirements for anchorage of stirrups will be discussed in Chapter 5.

Alternatively, shear reinforcement may be provided by bending up a part of the longitudinal steel where it is no longer needed to resist flexural tension, as suggested by Fig. 4.8*d*. In continuous beams, these bent-up bars may also provide all or part of the necessary reinforcement for negative moments. The requirements for longitudinal flexural reinforcement often conflict with those for diagonal tension, and because the savings in steel resulting from use of the capacity of bent bars as shear resistance is small, most designers prefer to include vertical stirrups to provide for all the shear requirement, counting on the bent part of the longitudinal bars, if bent bars are used, only to increase the overall safety against diagonal tension failure.

Welded wire reinforcement is also used for shear reinforcement, particularly for small, lightly loaded members with thin webs, and for certain types of precast, prestressed beams.

b. Behavior of Web-Reinforced Concrete Beams

Web reinforcement has no noticeable effect prior to the formation of diagonal cracks. In fact, measurements show that the web steel is practically free of stress prior to crack formation. After diagonal cracks have developed, web reinforcement augments the shear resistance of a beam in four separate ways:

1. Part of the shear force is resisted by the bars that traverse a particular crack. The mechanism of this added resistance is discussed below.
2. The presence of these same bars restricts the growth of diagonal cracks and reduces their penetration into the compression zone. This leaves more uncracked concrete available at the head of the crack for resisting the combined action of shear and compression, already discussed.
3. The stirrups also counteract the widening of the cracks, so that the two crack faces stay in close contact. This makes for a significant and reliable interface force V_i (see Fig. 4.7).
4. As shown in Fig. 4.8, the stirrups are arranged so that they tie the longitudinal reinforcement into the main bulk of the concrete. This provides some measure of restraint against the splitting of concrete along the longitudinal reinforcement, shown in Figs. 4.1 and 4.7*b*, and increases the share of the shear force resisted by dowel action.

From this it is clear that failure will be imminent when the stirrups start yielding. This not only exhausts their own resistance but also permits a wider crack opening with consequent reduction of the beneficial restraining effects, points 2 to 4, above.

It becomes clear from this description that member behavior, once a crack is formed, is quite complex and dependent in its details on the particulars of crack configuration (length, inclination, and location of the main or critical crack). The latter, in turn, is quite erratic and has so far defied purely analytical prediction. For this reason, the concepts that underlie present design practice are not wholly rational. They are based partly on rational analysis, partly on test evidence, and partly on successful long-time experience with structures in which certain procedures for designing web reinforcement have resulted in satisfactory performance.

Beams with Vertical Stirrups. Since web reinforcement is ineffective in the uncracked beam, the magnitude of the shear force or stress that causes cracking to occur is the same as in a beam without web reinforcement and is approximated by Eq. (4.3*a*). Most frequently, web reinforcement consists of *vertical stirrups*; the forces acting on the portion of such a beam between the crack and the nearby support are shown in Fig. 4.9. They are the same as those of Fig. 4.7, except that each stirrup traversing the crack exerts a force $A_v f_v$ on the given portion of the beam. Here A_v is the cross-sectional area of the stirrup (in the case of the U-shaped stirrup of Fig. 4.8*b* it is

FIGURE 4.9
Forces at a diagonal crack in a beam with vertical stirrups.

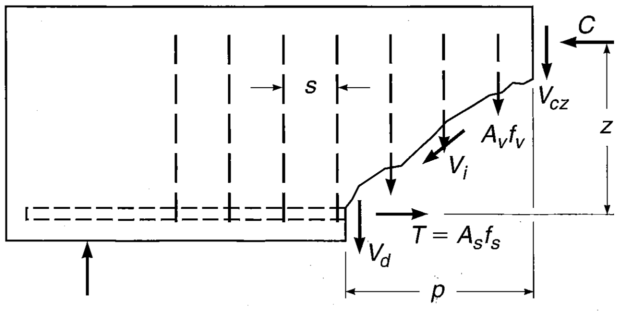

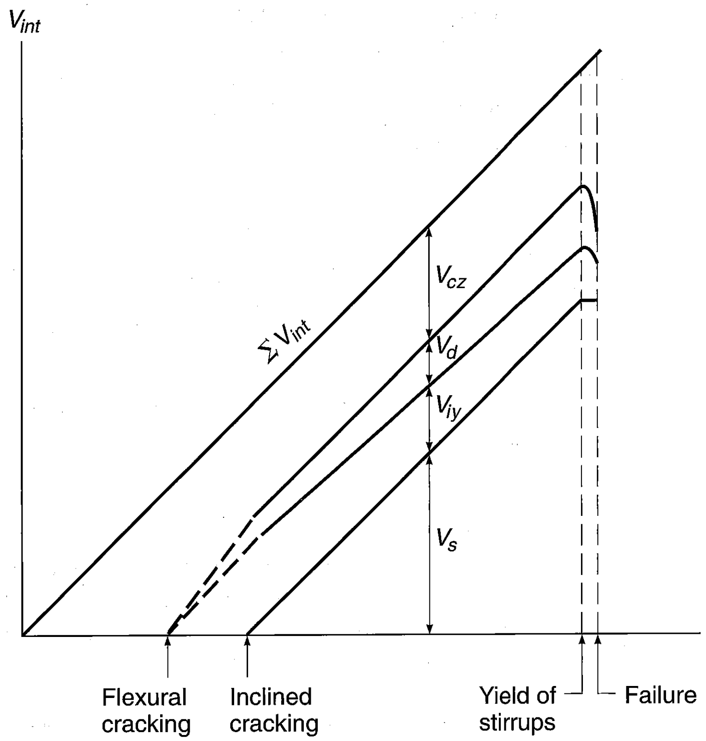

FIGURE 4.10
Redistribution of internal shear forces in a beam with stirrups. (*Adapted from Ref. 4.3.*)

twice the area of one bar), and f_v is the tensile stress in the stirrup. Equilibrium in the vertical direction requires

$$V_{\text{ext}} = V_{cz} + V_d + V_{iy} + V_s \qquad (a)$$

where $V_s = nA_v f_v$ is the vertical force in the stirrups, n being the number of stirrups traversing the crack. If s is the stirrup spacing and p the horizontal projection of the crack, as shown, then $n = p/s$.

The approximate distribution of the four components of the internal shear force with increasing external shear V_{ext} is shown schematically in Fig. 4.10. It is seen that after inclined cracking, the portion of the shear $V_s = nA_v f_v$ carried by the stirrups increases linearly, while the sum of the three other components, $V_{cz} + V_d + V_{iy}$, stays nearly constant. When the stirrups yield, their contribution remains constant at the yield value $V_s = nA_v f_{yt}$, where f_{yt} represents the yield strength of the stirrup (or transverse) reinforcement. However, because of widening of the inclined cracks and longitudinal splitting, V_{iy} and V_d fall off rapidly. This overloads the remaining uncracked concrete and very soon precipitates failure.

While total shear carried by the stirrups at yielding is known, the individual magnitudes of the three other components are not. Limited amounts of test evidence have led to the conservative assumption in present-day methods that just prior to failure of a web-reinforced beam, the sum of these three internal shear components is equal to the cracking shear V_{cr}, as given by Eq. (4.3*a*). This sum is generally (somewhat loosely) referred to as the *contribution of the concrete* to the total shear resistance and is denoted V_c. Thus $V_c = V_{cr}$ and

$$V_c = V_{cz} + V_d + V_{iy} \qquad (b)$$

The number of stirrups n spaced a distance s apart was seen to depend on the length p of the horizontal projection of the diagonal crack. This length is conservatively assumed to be equal to the effective depth of the beam; thus $n = d/s$, implying a crack somewhat flatter than 45°. Then, at failure, when $V_{\text{ext}} = V_n$, Eqs. (*a*) and (*b*) yield for the nominal shear strength

$$V_n = V_c + \frac{A_v f_{yt} d}{s} \tag{4.7a}$$

where V_c is taken equal to the cracking shear V_{cr} given by Eq. (4.3*a*); that is,

$$V_c = \left(0.16\sqrt{f_c'} + 17\frac{\rho V d}{M}\right) bd \le 0.29\sqrt{f_c'}\, bd \tag{4.3a}$$

Dividing both sides of Eq. (4.7*a*) by bd, the same relation is expressed in terms of the nominal shear stress:

$$v_n = \frac{V_n}{bd} = v_c + \frac{A_v f_{yt}}{bs} \tag{4.7b}$$

In Ref. 4.1, the results of 166 beam tests are compared with Eq. (4.7*b*). It is shown that the equation predicts the actual shear strength quite conservatively, the observed strength being on average 45 percent larger than predicted; a very few of the individual test beams developed strength just slightly below that of Eq. (4.7*b*).

Beams with Inclined Bars. The function of *inclined web reinforcement* (Fig. 4.8*d*) can be discussed in very similar terms. Figure 4.11 again indicates the forces that act on the portion of the beam to one side of the diagonal crack that results in eventual failure. The crack with horizontal projection p and inclined length $i = p/\cos\theta$ is crossed by inclined bars horizontally spaced a distance s apart. The inclination of the bars is α and that of the crack θ, as shown. The distance between bars measured parallel to the direction of the crack is seen from the irregular triangle to be

$$a = \frac{s}{\sin\theta(\cot\theta + \cot\alpha)} \tag{a}$$

The number of bars crossing the crack $n = i/a$, after some transformation, is

$$n = \frac{p}{s}(1 + \cot\alpha\tan\theta) \tag{b}$$

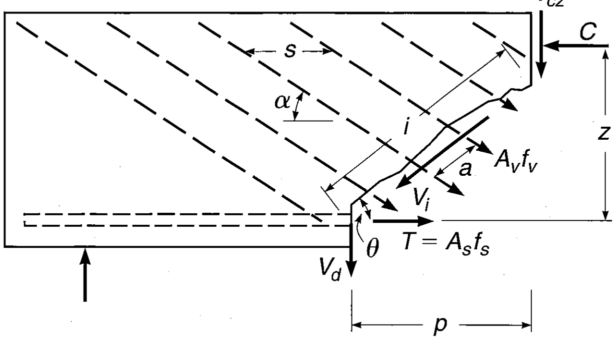

FIGURE 4.11
Forces at a diagonal crack in a beam with inclined web reinforcement.

The vertical component of the force in one bar or stirrup is $A_v f_v \sin \alpha$, so that the total vertical component of the forces in all bars that cross the crack is

$$V_s = nA_v f_v \sin \alpha = A_v f_v \frac{p}{s}(\sin \alpha + \cos \alpha \tan \theta) \tag{4.8}$$

As in the case of vertical stirrups, shear failure occurs when the stress in the web reinforcement reaches the yield point. Also, the same assumptions are made as in the case of stirrups, namely, that the horizontal projection of the diagonal crack is equal to the effective depth d, and that $V_{cz} + V_d + V_{iy}$ is equal to V_c. Lastly, the inclination θ of the diagonal crack, which varies somewhat depending on various influences, is generally assumed to be 45°. On this basis, when failure is caused by shear, the nominal strength is

$$V_n = V_c + \frac{A_v f_{yt} d(\sin \alpha + \cos \alpha)}{s} \tag{4.9}$$

It is seen that Eq. (4.7*a*), developed for vertical stirrups, is only a special case, for $\alpha = 90°$, of the more general expression (4.9).

Note that Eqs. (4.7) and (4.9) apply only if web reinforcement is so spaced that any conceivable diagonal crack is traversed by at least one stirrup or inclined bar. Otherwise web reinforcement would not contribute to the shear strength of the beam, because diagonal cracks that could form between widely spaced web reinforcement would fail the beam at the load at which it would fail if no web reinforcement were present. This imposes upper limits on the permissible spacing s to ensure that the web reinforcement is actually effective as calculated.

To summarize, at this time the nature and mechanism of diagonal tension failure are clearly understood qualitatively, but some of the quantitative assumptions that have been made in the preceding development cannot be proved by rational analysis. However, the calculated results are in acceptable and generally conservative agreement with a very large body of empirical data, and structures designed on this basis have proved satisfactory. Newer methods, introduced in Section 4.8, provide alternatives that are slowly being incorporated into the ACI Code and the AASHTO Bridge Specifications (Ref. 4.12). Chapter 10 presents a detailed description of one such alternative, the so-called strut-and-tie model, which appears in Appendix A of the 2008 ACI Code.

4.5 ACI CODE PROVISIONS FOR SHEAR DESIGN

According to ACI Code 11.1.1, the design of beams for shear is to be based on the relation

$$V_u \le \phi V_n \tag{4.10}$$

where V_u is the total shear force applied at a given section of the beam due to factored loads and $V_n = V_c + V_s$ is the nominal shear strength, equal to the sum of the contributions of the concrete and the web steel if present. Thus for vertical stirrups

$$V_u \le \phi V_c + \frac{\phi A_v f_{yt} d}{s} \tag{4.11a}$$

and for inclined bars

$$V_u \le \phi V_c + \frac{\phi A_v f_{yt} d(\sin \alpha + \cos \alpha)}{s} \tag{4.11b}$$

FIGURE 4.12
Location of critical section for shear design: (*a*) end-supported beam; (*b*) beam supported by columns; (*c*) concentrated load within *d* of the face of the support; (*d*) member loaded near the bottom; (*e*) beam supported by girder of similar depth; (*f*) beam supported by monolithic vertical element.

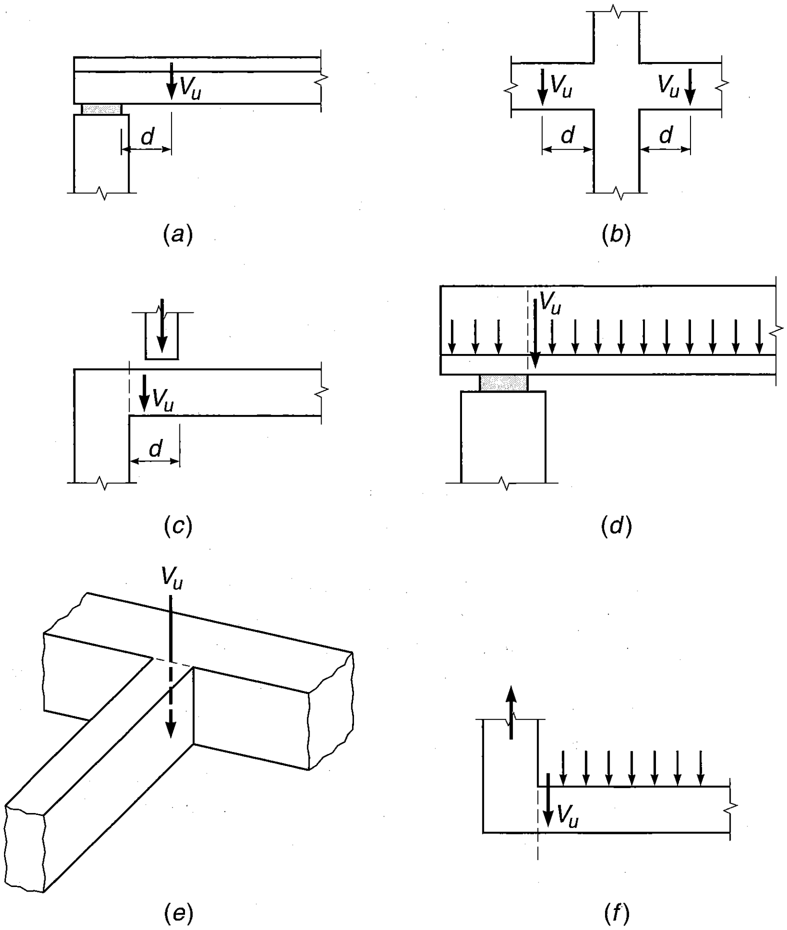

where all terms are as previously defined. The strength reduction factor ϕ is to be taken equal to 0.75 for shear. The additional conservatism, compared with the value of $\phi = 0.90$ for bending for typical beam designs, reflects both the sudden nature of diagonal tension failure and the large scatter of test results.

For typical support conditions, where the reaction from the support surface or from a monolithic column introduces vertical compression at the end of the beam, sections located less than a distance *d* from the face of the support may be designed for the same shear V_u as that computed at a distance *d*, as shown in Fig. 4.12*a* and *b*. However, the critical design section should be taken at the face of the support if concentrated loads act within that distance (Fig. 4.12*c*), if the beam is loaded near its bottom edge (as may occur for an inverted T beam, as shown in Fig. 4.12*d*), or if the reaction causes vertical tension rather than compression [e.g., if the beam is supported by a girder of similar depth (Fig. 4.12*e*) or at the end of a monolithic vertical element (Fig. 4.12*f*)].

a. Shear Strength Provided by the Concrete

The nominal shear strength contribution of the concrete (including the contributions from aggregate interlock, dowel action of the main reinforcing bars, and that of the uncracked concrete) is basically the same as Eq. (4.3*a*) with slight notational changes.

To permit application of Eq. (4.3*a*) to T beams having web width b_w, the rectangular beam width b is replaced by b_w with the understanding that for rectangular beams b is used for b_w. For T beams with a tapered web width, such as typical concrete joists, the average web width is used, unless the narrowest part of the web is in compression, in which case b_w is taken as the minimum width. Further, in Eq. (4.3*a*), the shear V and moment M are designated V_u and M_u to emphasize that they are the values computed at factored loads. Thus, for members subject to shear and flexure, according to ACI Code 11.2.2, the concrete contribution to shear strength is

$$V_c = \left(0.16\lambda\sqrt{f_c'} + 17\,\frac{\rho_w V_u d}{M_u}\right) b_w d \le 0.29\lambda\sqrt{f_c'}\,b_w d \qquad (4.12a)$$

where ρ_w = longitudinal reinforcement ratio $A_s/b_w d$ or A_s/bd. With the section dimension b_w and d in mm and $V_u d$ and M_u in consistent units, V_c is expressed in N. In Eq. (4.12*a*), the quantity $V_u d/M_u$ is not to be taken greater than 1.0.

The term λ in Eq. (4.12*a*) is a modification factor reflecting the lower tensile strength of lightweight concrete compared with normalweight concrete of the same compressive strength (see Table 2.2 and Ref. 4.13). Lightweight aggregate concretes having densities from 1440 to 1920 kg/m^3 are used widely, particularly for precast elements. In accordance with ACI Code 8.6.1, $\lambda = 0.85$ for "sand-lightweight" concrete and 0.75 for "all-lightweight" concrete. Linear interpolation between 0.75 and 0.85, based on volumetric fractions, is permitted when a portion of the lightweight fine aggregate is replaced by normalweight fine aggregate. Linear interpolation between 0.85 and 1.0 is also permitted for concretes containing normalweight fine aggregate and a blend of lightweight and normalweight coarse aggregate. If the average split-cylinder strength of lightweight concrete (a good measure of its direct tensile strength) is specified, $\lambda = f_{ct}/(0.56\sqrt{f_c'}) \le 1.0$. For normalweight concert, $\lambda = 1.0$.

While Eq. (4.12*a*) is perfectly well suited to computerized design or for research, for manual calculations its use is tedious because ρ_w, V_u, and M_u generally change along the span, requiring that V_c be calculated at frequent intervals. For this reason, an alternative equation for V_c is permitted by ACI Code 11.2.1:

$$V_c = 0.17\lambda\sqrt{f_c'}\,b_w d \qquad (4.12b)$$

Referring to Fig. 4.6, it is clear that Eq. (4.12*b*) is very conservative in regions where the shear-moment ratio is high, such as near the ends of simple spans or near the inflection points of continuous spans; however, because of its simplicity, it is often used in practice.

For members with a circular cross section, ACI Code 11.2.3 provides that the area used to calculate V_c in Eqs. (4.12*a*) and (4.12*b*) be the product of the diameter and the effective depth. The latter may be taken as 0.8 times the diameter of the member.

The tests on which Eqs. (4.12*a*) and (4.12*b*) are based used beams with concrete compressive strength mostly in the range of 21 to 35 MPa. More recent experimental results (Refs. 4.14 to 4.17) have shown that in beams constructed using high-strength concrete (see Section 2.12) with f_c' above 42 MPa, the concrete contribution to shear strength V_c is less than predicted by those equations. Differences become increasingly significant, the higher the concrete strength. For this reason, ACI Code 11.1.2 places an upper limit of 8.3 MPa on the value of $\sqrt{f_c'}$ to be used in Eqs. (4.12*a*) and (4.12*b*), *as well as in all other ACI Code shear provisions*. However, values of $\sqrt{f_c'}$ greater than 8.3 MPa may be used in computing V_c if a minimum amount of web reinforcement is used (see Section 4.5b).

b. Minimum Web Reinforcement

If V_u, the shear force at factored loads, is no larger than ϕV_c, calculated by Eq. (4.12*a*) or alternatively by Eq. (4.12*b*), then theoretically no web reinforcement is required. Even in such a case, however, ACI Code 11.4.6 requires provision of at least a minimum area of web reinforcement equal to

$$A_{v,\min} = 0.062\sqrt{f'_c}\,\frac{b_w s}{f_{yt}} \geq 0.35\,\frac{b_w s}{f_{yt}} \tag{4.13}$$

where s = longitudinal spacing of web reinforcement, mm
f_{yt} = yield strength of web steel, MPa
$A_{v,\min}$ = total cross-sectional area of web steel within distance s, mm^2

This provision holds unless V_u is one-half or less of the design shear strength provided by the concrete ϕV_c. Specific exceptions to this requirement for minimum web steel are made for slabs and footings; for concrete joist floor construction; for beams with total depth h not greater than 250 mm; and for beams integral with slabs with h not greater than 600 mm and not greater than the larger of 2.5 times the thickness of the flange and 0.5 times the thickness of the web. These members are excluded because of their capacity to redistribute internal forces before diagonal tension failure, as confirmed by both tests and successful design experience. In addition, beams constructed of steel fiber reinforced, normalweight concrete with f'_c not exceeding 42 MPa, total depth h not greater than 600 mm, and V_u not greater than $\phi\, 0.17\sqrt{f'_c}\, b_w d$ are not required to meet the requirements for minimum web reinforcement because beams meeting these requirements have been shown to have shear strength in excess of $0.29\sqrt{f'_c}\, b_w d$ (Ref. 4.18).[†]

For high-strength concrete beams, the limitation of 8.3 MPa imposed on the value of $\sqrt{f'_c}$ used in calculating V_c by Eq. (4.12*a*) or (4.12*b*) is waived by ACI Code 11.1.2.1 if such beams are designed with minimum web reinforcement equal to the amount required by Eq. (4.13). In this case, the concrete contribution to shear strength may be calculated based on the full concrete compressive strength. Tests described in Refs. 4.14 and 4.17 indicate that for beams with concrete strength above about 42 MPa, the concrete contribution V_c was significantly less than predicted by the ACI Code equations, although the steel contribution V_s was higher. The total nominal shear strength V_n was greater than predicted by ACI Code methods in all cases. The use of minimum web steel for high-strength concrete beams is intended to enhance the post-cracking capacity, thus resulting in safe designs even though the concrete contribution to shear strength is overestimated.[‡]

EXAMPLE 4.1 **Beam without web reinforcement.** A rectangular beam is to be designed to carry a shear force V_u of 120 kN. No web reinforcement is to be used, and f'_c is 28 MPa. What is the minimum cross section if controlled by shear?

[†] To qualify, the fiber-reinforced concrete must conform to requirements in ACI Code 5.6.6.2 that specify a minimum deformed steel fiber content of 60 kg/m^3 and minimum residual flexural strength values when the concrete is tested in accordance with ASTM C1609, "*Standard Test Method for Flexural Performance of Fiber-Reinforced Concrete (Using Beam with Third-Point Loading).*"

[‡] The shortcomings of the ACI Code "$V_c + V_s$" approach to shear design, particularly the provisions relating to the concrete contribution V_c, have provided motivation for the development of more rational procedures, as will be discussed in Section 4.8.

SOLUTION. If no web reinforcement is to be used, the cross-sectional dimensions must be selected so that the applied shear V_u is no larger than one-half the design shear strength ϕV_c. The calculations will be based on Eq. (4.12*b*). Thus,

$$V_u = \frac{1}{2}\,\phi(0.17\lambda\sqrt{f'_c}\,b_w d)$$

$$b_w d = \frac{120{,}000}{0.75 \times 0.085 \times 1.0\sqrt{28}} = 355{,}700 \text{ mm}^2$$

A beam with $b_w = 450$ mm and $d = 800$ mm is required. Alternately, if the minimum amount of web reinforcement given by Eq. (4.13) is used, the concrete shear resistance may be taken at its full value ϕV_c, and it is easily confirmed that a beam with $b_w = 300$ mm and $d = 600$ mm will be sufficient.

c. Region in Which Web Reinforcement Is Required

If the required shear strength V_u is greater than the design shear strength ϕV_c provided by the concrete in any portion of a beam, there is a theoretical requirement for web reinforcement. Elsewhere in the span, web steel at least equal to the amount given by Eq. (4.13) must be provided, unless the factored shear force is less than $\frac{1}{2}\phi V_c$.

The portion of any span through which web reinforcement is theoretically necessary can be found from the shear diagram for the span, superimposing a plot of the shear strength of the concrete. Where the shear force V_u exceeds ϕV_c, shear reinforcement must provide for the excess. The additional length through which at least the minimum web steel is needed can be found by superimposing a plot of $\phi V_c/2$.

EXAMPLE 4.2 **Limits of web reinforcement.** A simply supported rectangular beam 400 mm wide having an effective depth of 550 mm carries a total factored load of 137 kN/m on a 6 m clear span. It is reinforced with 4914 mm^2 of tensile steel, which continues uninterrupted into the supports. If $f'_c = 28$ MPa, throughout what part of the beam is web reinforcement required?

SOLUTION. The maximum external shear force occurs at the ends of the span, where $V_u = 137 \times 6/2 = 411$ kN. At the critical section for shear, a distance d from the support, $V_u = 411 - 137 \times 0.55 = 336$ kN. The shear force varies linearly to zero at midspan. The variation of V_u is shown in Fig. 4.13*a*. Adopting Eq. (4.12*b*) gives

$$V_c = 0.17\lambda\sqrt{f'_c}\,b_w d = 0.17 \times 1.0\sqrt{28} \times 400 \times 550 = 197{,}900 \text{ N}$$

Hence $\phi V_c = 0.75 \times 197.9 = 148.4$ kN. This value is superimposed on the shear diagram, and, from geometry, the point at which web reinforcement theoretically is no longer required is

$$3\left(\frac{411 - 148.4}{411}\right) = 1.92 \text{ m}$$

from the support face. However, according to the ACI Code, at least a minimum amount of web reinforcement is required wherever the shear force exceeds $\phi V_c/2$, or 74.2 kN in this case. As seen from Fig. 4.13*a*, this applies to a distance

$$3\left(\frac{411 - 74.2}{411}\right) = 2.46 \text{ m}$$

from the support face. To summarize, at least the minimum web steel must be provided within a distance of 2.46 m from the supports, and within 1.92 m the web steel must provide for the shear force corresponding to the shaded area.

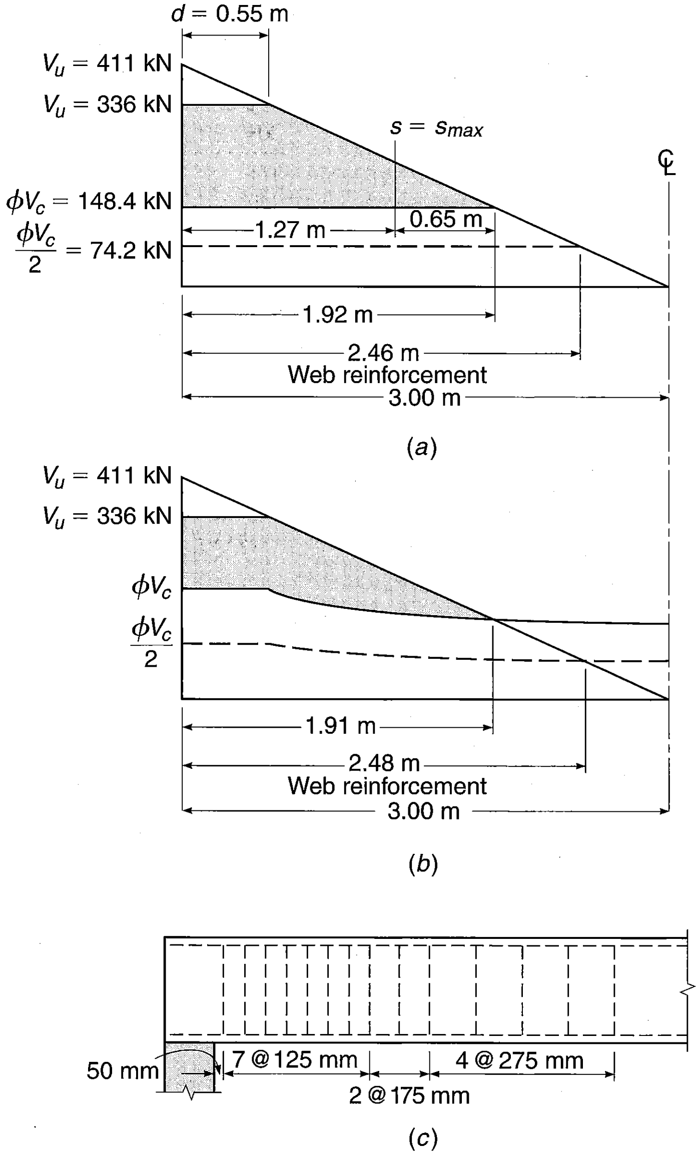
d = 0.55 m
V_u = 411 kN
V_u = 336 kN
s = smax
℄
ϕV_c = 148.4 kN
$\frac{\phi V_c}{2}$ = 74.2 kN
1.27 m
0.65 m
1.92 m
2.46 m
Web reinforcement
3.00 m
(a)
V_u = 411 kN
V_u = 336 kN
ϕV_c
$\frac{\phi V_c}{2}$
1.91 m
2.48 m
Web reinforcement
3.00 m
(b)
50 mm
7 @ 125 mm
4 @ 275 mm
2 @ 175 mm
(c)

FIGURE 4.13
Shear design example.

If the alternative Eq. (4.12*a*) is used, the variation along the span of ρ_w, V_u, and M_u must be known so that V_c can be calculated. This is shown in tabular form in Table 4.1.

The factored shear V_u and the design shear capacity ϕV_c are plotted in Fig. 4.13*b*. From the graph it is found that stirrups are theoretically no longer required 1.91 m from the support face. However, from the plot of $\phi V_c/2$ it is found that at least the minimum web steel is to be provided within a distance of 2.48 m.

When Figs. 4.13*a* and *b* are compared, it is evident that the length over which web reinforcement is needed is nearly the same for this example whether Eq. (4.12*a*) or (4.12*b*) is used. However, the smaller shaded area of Fig. 4.13*b* indicates that substantially less web-steel area would be needed within that required distance if the more accurate Eq. (4.12*a*) were adopted.

TABLE 4.1
Shear design example

Distance from support, m	M_u, kN-m	V_u, kN	V_c^a	ϕV_c
0.0	0	411	270	202
0.3	117	370	270	202
0.6	222	329	254	191
0.9	314	288	228	171
1.2	395	247	215	161
1.5	462	206	207	155
1.8	518	164	201	151
2.1	561	123	196	147
2.4	592	82	193	144
2.7	610	41	189	142
3.0	617	0	186	140

[a] $V_c = (0.16\lambda\sqrt{f_c'} + 17\rho_w V_u d/M_u)b_w d \leq 0.29\lambda\sqrt{f_c'}\, b_w d$ and $V_u d/M_u \leq 1.0$

d. Design of Web Reinforcement

The design of web reinforcement, under the provisions of the ACI Code, is based on Eq. (4.11*a*) for vertical stirrups and Eq. (4.11*b*) for inclined stirrups or bent bars. In design, it is usually convenient to select a trial web-steel area A_v based on standard stirrup sizes [usually in the range from No. 10 to 16 (No. 3 to 5) for stirrups, and according to the longitudinal bar size for bent-up bars], for which the required spacing s can be found. Equating the design strength ϕV_n to the required strength V_u and transposing Eqs. (4.11*a*) and (4.11*b*) accordingly, one finds that the required spacing of web reinforcement is, for vertical stirrups,

$$s = \frac{\phi A_v f_{yt} d}{V_u - \phi V_c} \tag{4.14a}$$

and for bent bars

$$s = \frac{\phi A_v f_{yt} d(\sin\alpha + \cos\alpha)}{V_u - \phi V_c} \tag{4.14b}$$

It should be emphasized that when conventional U stirrups such as in Fig. 4.8*b* are used, the web area A_v provided by each stirrup is *twice* the cross-sectional area of the bar; for stirrups such as those of Fig. 4.8*c*, A_v is 4 times the area of the bar used. Equation (4.14*a*) is applicable to members with circular, as well as rectangular, cross sections. For circular members, d is taken as the effective depth, as defined earlier in Section 4.5a, and A_v is taken as 2 times the area of the bar, hoop, or spiral.

While the ACI Code requires only that the inclined part of a bent bar make an angle of at least 30° with the longitudinal part, bars are usually bent at a 45° angle. Only the center three-fourths of the inclined part of any bar is to be considered effective as web reinforcement.

It is undesirable to space vertical stirrups closer than about 100 mm; the size of the stirrups should be chosen to avoid a closer spacing. When vertical stirrups are required over a comparatively short distance, it is good practice to space them uniformly over the entire distance, the spacing being calculated for the point of greatest

FIGURE 4.14
Maximum spacing of web reinforcement as governed by diagonal crack interception.

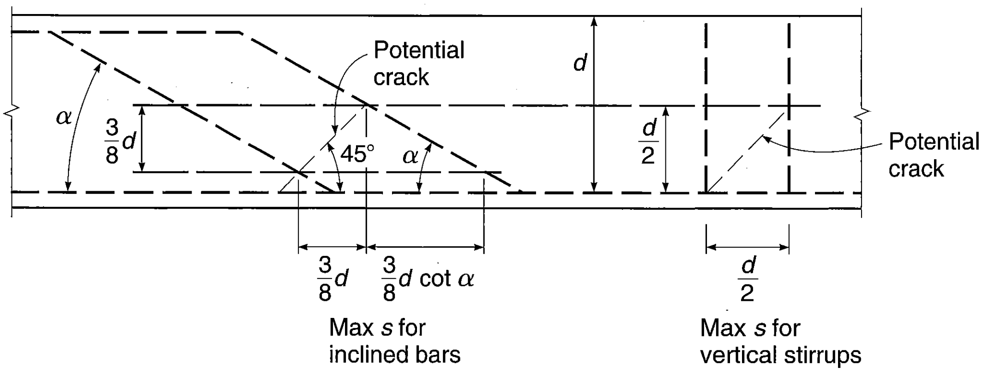

shear (minimum spacing). If the web reinforcement is required over a long distance, and if the shear varies materially throughout this distance, it is more economical to compute the spacings required at several sections and to place the stirrups accordingly, in groups of varying spacing.

Where web reinforcement is needed, the Code requires it to be spaced so that every 45° line, representing a potential diagonal crack and extending from the middepth $d/2$ of the member to the longitudinal tension bars, is crossed by at least one line of web reinforcement; in addition, the Code specifies a maximum spacing of 600 mm. When V_s exceeds $0.33\sqrt{f'_c}b_w d$, these maximum spacings are halved. These limitations are shown in Fig. 4.14 for both vertical stirrups and inclined bars, for situations in which the excess shear does not exceed the stated limit.

For design purposes, Eq. (4.13) giving the minimum web-steel area A_v is more conveniently inverted to permit calculation of maximum spacing s for the selected A_v. Thus, for the usual case of vertical stirrups, with $V_s \leq 0.33\sqrt{f'_c}b_w d$, the maximum spacing of stirrups is the smallest of

$$s_{\max} = \frac{A_v f_{yt}}{0.062\sqrt{f'_c}\,b_w} \leq \frac{A_v f_{yt}}{0.35 b_w} \tag{4.15a}$$

$$s_{\max} = \frac{d}{2} \tag{4.15b}$$

$$s_{\max} = 600 \text{ mm} \tag{4.15c}$$

For longitudinal bars bent at 45°, Eq. (4.15*b*) is replaced by $s_{\max} = 3d/4$, as confirmed by Fig. 4.14.

To avoid excessive crack width in beam webs, the ACI Code limits the yield strength of the reinforcement to $f_{yt} = 420$ MPa or less for reinforcing bars and 550 MPa or less for welded wire reinforcement. In no case, according to the ACI Code, is V_s to exceed $0.66\sqrt{f'_c}\,b_w d$, regardless of the amount of web steel used.

EXAMPLE 4.3

Design of web reinforcement. Using vertical U stirrups with $f_{yt} = 420$ MPa, design the web reinforcement for the beam in Example 4.2.

Solution. The solution will be based on the shear diagram in Fig. 4.13*a*. The stirrups must be designed to resist that part of the shear shown shaded. With No. 10 (No. 3) stirrups used for trial, the three maximum spacing criteria are first applied. For $\phi V_s = V_u - \phi V_c = 187{,}600$ N, which is less than $0.33\phi\sqrt{f_c'}b_wd = 288{,}100$ N, the maximum spacing must exceed neither $d/2 = 275$ mm nor 600 mm. Also, from Eq. (4.15*a*),

$$s_{\max} = \frac{A_v f_{yt}}{0.062\sqrt{f_c'}\,b_w} = \frac{142 \times 420}{0.062\sqrt{28} \times 400} = 454 \text{ mm}$$

$$\leq \frac{A_v f_{yt}}{0.35 b_w} = \frac{142 \times 420}{0.35 \times 400} = 426 \text{ mm}$$

The first criterion controls in this case, and a maximum spacing of 275 mm is imposed. From the support to a distance *d* from the support, the excess shear $V_u - \phi V_c$ is 187,600 N. In this region, the required spacing is

$$s = \frac{\phi A_v f_{yt} d}{V_u - \phi V_c} = \frac{0.75 \times 142 \times 420 \times 550}{187{,}600} = 131 \text{ mm}$$

A value of 125 mm will be used. This is neither so small that placement problems would result nor so large that maximum spacing criteria would control, and the choice of No. 10 (No. 3) stirrups is confirmed. Solving Eq. (4.14*a*) for the excess shear at which the maximum spacing can be used gives

$$V_u - \phi V_c = \frac{\phi A_v f_{yt} d}{s} = \frac{0.75 \times 142 \times 420 \times 550}{275} = 18{,}460 \text{ N}$$

With reference to Fig. 4.13*a*, this is attained at a distance x_1 from the point of zero excess shear, where $x_1 = 1.92 \times 89{,}460/262{,}600 = 0.65$ m. This is 1.27 m from the support face. With this information, a satisfactory spacing pattern can be selected. The first stirrup is usually placed at a distance $s/2$ from the support. The following spacing pattern is satisfactory:

1 space at 50 mm = 50 mm
7 spaces at 125 mm = 875 mm
2 spaces at 175 mm = 350 mm
4 spaces at 275 mm = 1100 mm
Total = 2375 mm = 2.375 m

The resulting stirrup pattern is shown in Fig. 4.13*c*. As an alternative solution, it is possible to plot a curve showing required spacing as a function of distance from the support. Once the required spacing at some reference section, say at the support, is determined,

$$s_0 = \frac{0.75 \times 142 \times 420 \times 550}{411{,}000 - 148{,}400} = 93.7 \text{ mm}$$

it is easy to obtain the required spacings elsewhere. In Eq. (4.14*a*), only $V_u - \phi V_c$ changes with distance from the support. For uniform load, this quantity is a linear function of distance from the point of zero excess shear, 1.92 m from the support face. Hence, at 300 mm intervals,

$$s_1 = 93.7 \times 1.92/1.62 = 111 \text{ mm}$$

$$s_2 = 93.7 \times 1.92/1.32 = 136 \text{ mm}$$

$$s_3 = 93.7 \times 1.92/1.02 = 176 \text{ mm}$$

$$s_4 = 93.7 \times 1.92/0.72 = 250 \text{ mm}$$

$$s_5 = 93.7 \times 1.92/0.42 = 428 \text{ mm}$$

This is plotted in Fig. 4.15 together with the maximum spacing of 275 mm, and a practical spacing pattern is selected. The spacing at a distance *d* from the support face is selected as the

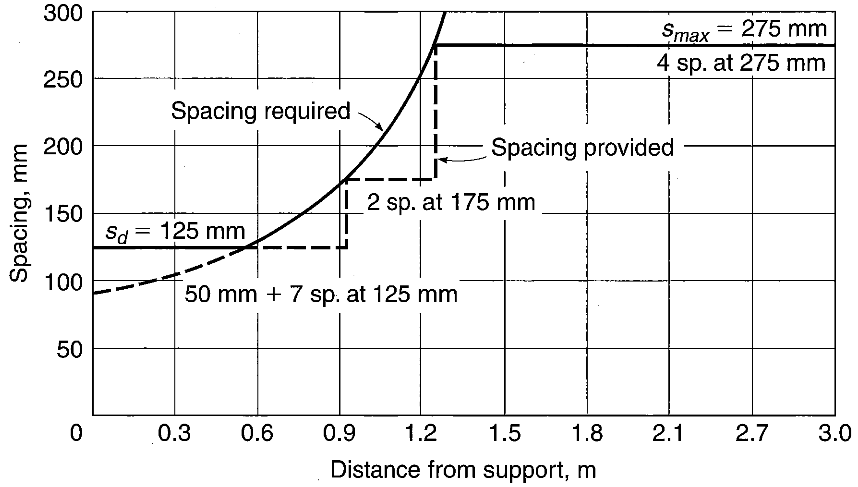

FIGURE 4.15
Required stirrup spacings for Example 4.3.

minimum requirement, in accordance with the ACI Code. The pattern of No. 10 (No. 3) U-shaped stirrups selected (shown on the graph) is identical with the previous solution. In most cases, the experienced designer would find it unnecessary actually to plot the spacing diagram of Fig. 4.15 and would select a spacing pattern directly after calculating the required spacing at intervals along the beam.

If the web steel were to be designed on the basis of the excess-shear diagram in Fig. 4.13*b*, the second approach illustrated above would necessarily be selected, and spacings would be calculated at intervals along the span. In this particular case, a spacing of 183 mm is calculated up to 525 mm from the face of the support. The calculated spacing drops to 175 mm at *d* from the face of the support, and then increases to 275 mm, the maximum permissible spacing, 1.2 m from the support. The following practical spacing could be used:

$$\begin{aligned} 1 \text{ space at } 75 \text{ mm} &= 75 \text{ mm} \\ 6 \text{ spaces at } 175 \text{ mm} &= 1050 \text{ mm} \\ 4 \text{ spaces at } 275 \text{ mm} &= \underline{1100 \text{ mm}} \\ \text{Total} &= 2225 \text{ mm} = 2.225 \text{ m} \end{aligned}$$

Thus, 11 No. 10 (No. 3) stirrups would be used, rather than the 14 previously calculated, in each half of the span.

The number of stirrups just calculated represents the minimum for each of the two expressions for V_c. Although not required by the ACI Code, it is good design practice to continue the stirrups (at maximum spacing) through the middle region of the beam, even though the calculated shear is low. Doing so satisfies the dual purposes of providing continuing support for the top longitudinal reinforcement that is required wherever stirrups are used and providing additional shear capacity in the region to handle load cases not considered in developing the shear diagram. If this were done, the number of stirrups would increase from 14 and 11 to $16\frac{1}{2}$ and $13\frac{1}{2}$ per half-span (i.e., one stirrup at midspan), respectively.

4.6 EFFECT OF AXIAL FORCES

The beams considered in the preceding sections were subjected to shear and flexure only. Reinforced concrete beams may also be subjected to axial forces, acting simultaneously with shear and flexure, due to a variety of causes. These include external axial loads, longitudinal prestressing, and restraint forces introduced as a result of shrinkage of the concrete or temperature changes. Beams may have their strength in shear significantly modified in the presence of axial tension or compression, as is evident from a review of Sections 4.1 through 4.4.

Prestressed concrete members are treated by somewhat specialized methods, according to present practice, based largely on results of testing prestressed concrete beams. They will be considered separately in Chapter 19, and only nonprestressed reinforced concrete beams will be treated here.

The main effect of axial load is to modify the diagonal cracking load of the member. It was shown in Section 4.3 that diagonal tension cracking will occur when the principal tensile stress in the web of a beam, resulting from combined action of shear and bending, reaches the tensile strength of the concrete. It is clear that the introduction of longitudinal force, which modifies the magnitude and direction of the principal tensile stresses, may significantly alter the diagonal cracking load. Axial compression will increase the cracking load, while axial tension will decrease it.

For members carrying only flexural and shear loading, the shear force at which diagonal cracking occurs V_{cr} is predicted by Eq. (4.3*a*), based on a combination of theory and experimental evidence. Furthermore, for reasons that were explained in Section 4.4b, in beams with web reinforcement, the contribution of the concrete to shear strength V_c is taken equal to the diagonal cracking load V_{cr}. Thus, according to the ACI Code, the concrete contribution is calculated by Eq. (4.12*a*) or (4.12*b*). For members carrying flexural and shear loading plus axial loads, V_c can be calculated by suitable modifications of these equations as follows.

a. Axial Compression

In developing Eq. (4.3*a*) for V_{cr}, it was pointed out that the diagonal cracking load depends on the ratio of shear stress v to bending stress f at the top of the flexural crack. While these stresses were never actually determined, they were conveniently expressed as

$$v = K_1\left(\frac{V}{bd}\right) \tag{a}$$

and

$$f = K_2\left(\frac{M}{bd^2}\right) \tag{b}$$

Equation (*a*) relates the concrete shear stress at the top of the flexural crack to the average shear stress; Eq. (*b*) can be used to relate the flexural tension in the concrete at the top of the crack to the tension in the flexural steel, through the modular ratio $n = E_s/E_c$, as follows:

$$f = K_0\frac{f_s}{n} = K_0\frac{M}{nA_sjd}$$

or

$$f = K_0\frac{M}{n\rho jbd^2} \tag{c}$$

where jd is the internal lever arm between C and T, and K_0 is an unknown constant. Thus, the previous constant K_2 is equal to $K_0/n\rho j$.

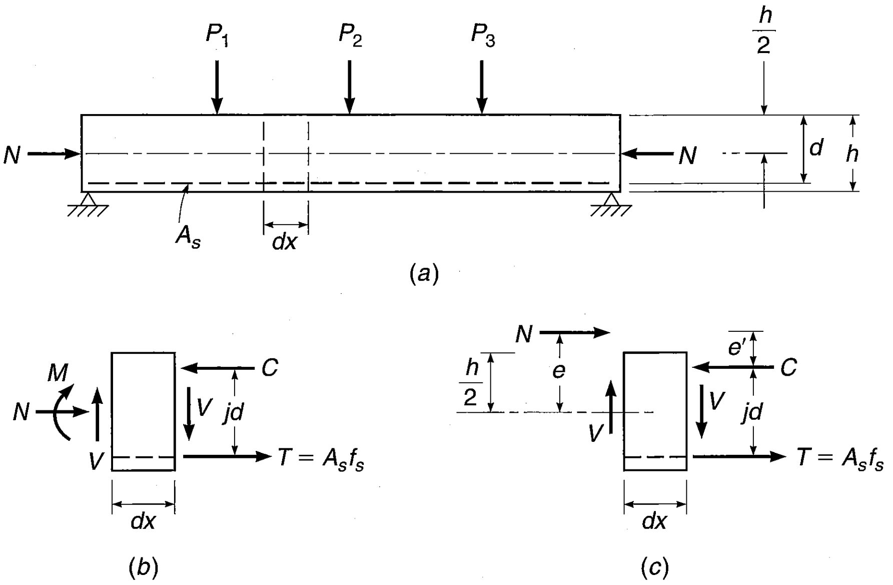

FIGURE 4.16
Beams subject to axial compression plus bending and shear loads.

Now consider a beam subject to axial compression N as well as M and V, as shown in Fig. 4.16*a*. In Fig. 4.16*b*, the external moment, shear, and thrust acting on the left side of a small element of the beam, having length dx, are equilibrated by the internal stress resultants T, C, and V acting on the right. It is convenient to replace the external loads M and N with the statically equivalent load N acting at eccentricity $e = M/N$ from the middepth, as shown in Fig. 4.16*c*. The lever arm of the eccentric force N with respect to the compressive resultant C is

$$e' = e + d - \frac{h}{2} - jd \qquad (d)$$

The steel stress f_s can now be found taking moments about the point of application of C.

$$f_s = \frac{Ne'}{A_s jd}$$

from which

$$f_s = \frac{M + N(d - h/2 - jd)}{A_s jd}$$

Noting that j is very close to $\frac{7}{8}$ for loads up to that producing diagonal cracking, the term in parentheses in the last equation above can be written as $(d - 4h)/8$. Then with $f = K_0 f_s/n$ as before, the concrete tensile stress at the head of the flexural crack is

$$f = K_0 \frac{M - N(4h - d)/8}{npjbd^2} = K_2 \frac{M - N(4h - d)/8}{bd^2} \qquad (e)$$

Comparing Eq. (*e*) with Eqs. (*c*) and (*b*) makes it clear that the previous derivation for flexural tension f holds for the present case including axial loads if a modified moment $M - N(4h - d)/8$ is substituted for M. It follows that Eq. (4.3*a*) can be used to calculate V_{cr} with the same substitution of modified for actual moment.

The ACI Code provisions are based on this development. The concrete contribution to shear strength V_c is taken equal to V_{cr} and is given by Eq. (4.12*a*) as before:

$$V_c = \left(0.16\lambda\sqrt{f'_c} + 17\,\frac{\rho_w V_u d}{M_u}\right) b_w d \tag{4.12a}$$

except that the modified moment

$$M_m = M_u - N_u\,\frac{4h - d}{8} \tag{4.16}$$

is to be substituted for M_u and $V_u d/M_u$ need not be limited to 1.0 as before. The thrust N_u is to be taken positive for compression. For beams with axial compression, the upper limit of $0.29\lambda\sqrt{f'_c}\,b_w d$ is replaced by

$$V_c = 0.29\lambda\sqrt{f'_c}\,b_w d\sqrt{1 + \frac{0.29N_u}{A_g}} \tag{4.17}$$

where A_g is the gross area of the concrete and N_u/A_g is expressed in MPa.

As an alternative to the rather complicated determination of V_c using Eqs. (4.12*a*), (4.16), and (4.17), ACI Code 11.2.1.2 permits the use of an alternative simplified expression:

$$V_c = 0.17\left(1 + \frac{N_u}{14A_g}\right)\lambda\sqrt{f'_c}\,b_w d \tag{4.18}$$

Figure 4.17 shows a comparison of V_c calculated by the more complex and simplified expressions for beams with compression load. Equation (4.18) is seen to be generally quite conservative, particularly for higher values of N_u/A_g. However, because of its simplicity, it is widely used in practice.

FIGURE 4.17
Comparison of equations for V_c for members subject to axial loads.

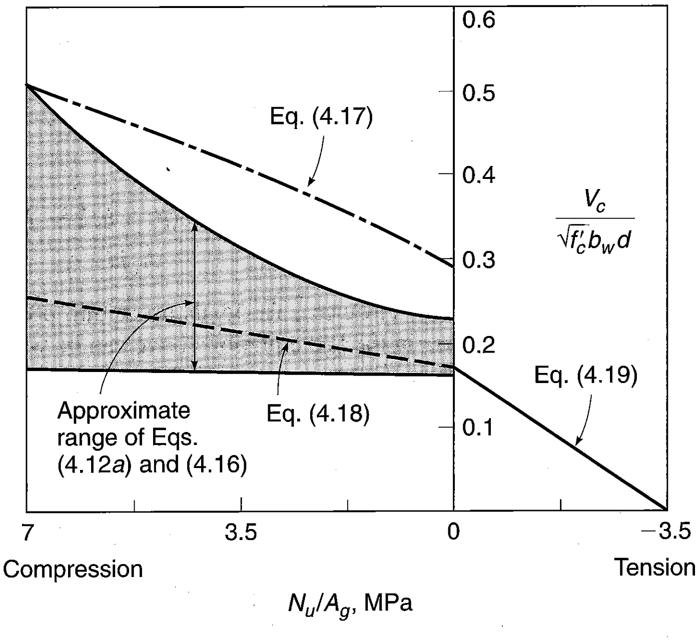

b. Axial Tension

The approach developed above for beams with axial compression does not correlate well with experimental evidence for beams subject to axial tension, and often predicts strengths V_c higher than actually measured. For this reason, the ACI Code provides that, for members carrying significant axial tension as well as bending and shear, the contribution of the concrete be taken as

$$V_c = 0.17\left(1 + \frac{0.29\,N_u}{A_g}\right)\lambda\sqrt{f'_c}\,b_w d \qquad (4.19)$$

but not less than zero, where N_u is negative for tension. As a simplifying alternative, the Commentary to the Code suggests that, for beams carrying axial tension, V_c be taken equal to zero and the shear reinforcement be required to carry the total shear. The variation of V_c with N_u/A_g for beams with tension is shown in Fig. 4.17 also.

EXAMPLE 4.4

Effect of axial forces on V_c. A beam with dimensions b = 300 mm, d = 600 mm, and h = 700 mm, with 28 MPa, carries a single concentrated factored load of 440 kN at midspan. Find the maximum shear strength of the concrete V_c at the first critical section for shear at a distance d from the support (*a*) if no axial forces are present, (*b*) if axial compression of 270 kN acts, and (*c*) if axial tension of 270 kN acts. In each case, compute V_c by both the more complex and simplified expressions of the ACI Code. Neglect the self-weight of the beam. At the section considered, tensile reinforcement consists of three No. 32 (No. 10) bars with a total area of 2457 mm^2.

Solution. At the critical section, V_u = 220 kN and $M_u = 220 \times 0.6 = 132$ kN-m, while $\rho = 2457/(300 \times 600) = 0.0137$.

(*a*) If $N_u = 0$, Eq. (4.12*a*) predicts

$$V_c = \left(0.16 \times 1.0\sqrt{28} + 17\,\frac{0.0137 \times 220 \times 600}{132{,}000}\right)300 \times \frac{600}{1000} = 194.3 \text{ kN}$$

not to exceed the value of

$$V_c = 0.29 \times 1.0\sqrt{28} \times 300 \times \frac{600}{1000} = 276.2 \text{ kN}$$

If the simplified Eq. (4.12*b*) is used,

$$V_c = 0.17 \times 1.0\sqrt{28} \times 300 \times \frac{600}{1000} = 276.2 \text{ kN}$$

which is about 17 percent below the more exact value of Eq. (4.12*a*).

(*b*) With a compression of 270 kN introduced, the modified moment is found from Eq. (4.16) to be

$$M_m = 132 - 270\,\frac{4 \times 0.7 - 0.6}{8} = 57.8 \text{ kN-m}$$

After introduction of that value into Eq. (4.12*a*) in place of M_u, the concrete shear strength is

$$V_c = \left(0.16 \times 1.0\sqrt{28} + 17\,\frac{0.0137 \times 220 \times 600}{57{,}800}\right)300 \times \frac{600}{1000} = 248.1 \text{ kN}$$

and, according to Eq. (4.17), should not exceed

$$V_c = 276.6\sqrt{1 + \frac{0.29 \times 270{,}000}{300 \times 700}} = 324.1 \text{ kN}$$

If the simplified Eq. (4.18) is used,

$$V_c = 0.17\left(1 + \frac{270{,}000}{14 \times 300 \times 700}\right) \times 1.0\sqrt{28} \times 300 \times \frac{600}{1000} = 176.8 \text{ kN}$$

Comparing the results of the more exact calculation for (*a*) and (*b*), one sees that the introduction of an axial compressive stress of 270,000/(300 × 700) = 1.29 MPa increases the concrete shear V_c by about 27 percent.

(*c*) With an axial tension of 270 kN acting, the reduced V_c is found from Eq. (4.19) to be

$$V_c = 2\left(1 - \frac{0.29 \times 270{,}000}{300 \times 700}\right) \times 1.0\sqrt{28} \times 300 \times \frac{600}{1000} = 101.5 \text{ kN}$$

a reduction of almost 50 percent from the value for $N_u = 0$. The alternative of using Eq. (4.19) for this case, according to the ACI Commentary, would be to set $V_c = 0$.

In all cases above, the strength reduction factor $\phi = 0.75$ would be applied to V_c to obtain the design strength.

4.7 BEAMS WITH VARYING DEPTH

Reinforced concrete members having varying depth are frequently used in the form of haunched beams for bridges or portal frames, as shown in Fig. 4.18*a*, as precast roof girders such as shown in Fig. 4.18*b*, or as cantilever slabs. Generally the depth increases in the direction of increasing moments. For beams with varying depth, the inclination of the internal compressive and tensile stress resultants may significantly affect the shear for which the beam should be designed. In addition, the shear resistance of such members may differ from that of prismatic beams.

Figure 4.18*c* shows a cantilever beam, with fixed support at the left end, carrying a single concentrated load *P* at the right. The depth increases linearly in the direction

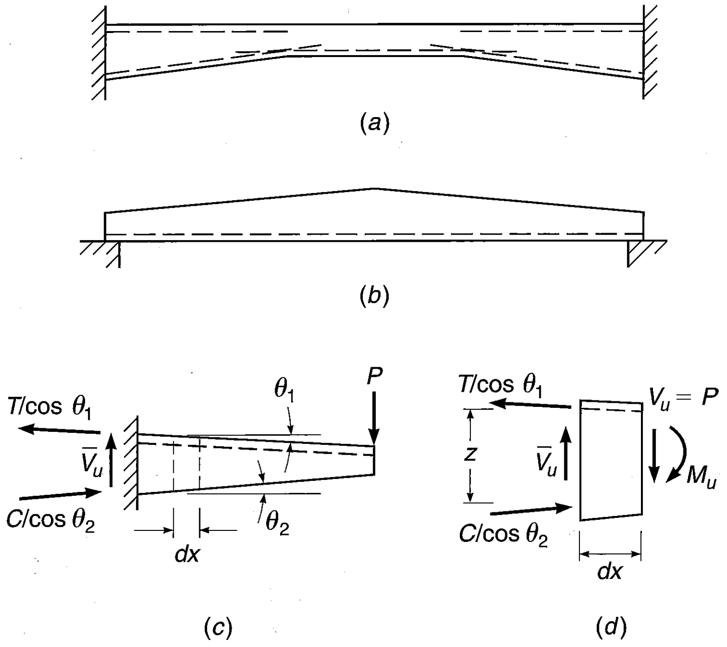

FIGURE 4.18
Effect of varying beam depth on shear.

of increasing moment. In such cases, the internal tension in the steel and the compressive stress resultant in the concrete are inclined, and introduce components transverse to the axis of the member. With reference to Fig. 4.18*d*, showing a short length dx of the beam, if the slope of the top surface is θ_1 and that of the bottom is θ_2, the net shear force $\overline{V}_u$ for which the beam should be designed is very nearly equal to

$$\overline{V}_u = V_u - T \tan \theta_1 - C \tan \theta_2$$

where V_u is the external shear force equal to the load P here, and $C = T = M_u/z$. The internal lever arm $z = d - a/2$ as usual. Thus, in a case for which the beam depth increases in the direction of increasing moment, the shear for which the member should be designed is approximately

$$\overline{V}_u = V_u - \frac{M_u}{z} (\tan \theta_1 + \tan \theta_2) \tag{4.20a}$$

For the infrequent case in which the member depth decreases in the direction of increasing moment, it is easily confirmed that the corresponding equation is

$$\overline{V}_u = V_u + \frac{M_u}{z} (\tan \theta_1 + \tan \theta_2) \tag{4.20b}$$

These equations are approximate because the direction of the internal forces is not exactly as assumed; however, the equations may be used without significant error provided the slope angles do not exceed about 30°.

There has been very little research studying the shear strength of beams having varying depth. Tests reported in Ref. 4.19 on simple span beams with haunches at slopes up to about 15° and with depths both increasing and decreasing in the direction of increasing moments indicate no appreciable change in the cracking load V_{cr} compared with that for prismatic members. Furthermore, the strength of the haunched beams, which contained vertical stirrups as web reinforcement, was not significantly decreased or increased, regardless of the direction of decreasing depth. Based on this information, *it appears safe to design beams with varying depth for shear using equations for* V_c *and* V_s *developed for prismatic members*, provided the actual depth d at the section under consideration is used in the calculations.

4.8 ALTERNATIVE MODELS FOR SHEAR ANALYSIS AND DESIGN

The ACI Code method of design for shear and diagonal tension in beams, presented in preceding sections of this chapter, is essentially empirical. While generally leading to safe designs, the ACI Code "$V_c + V_s$" approach lacks a physical model for the behavior of beams subject to shear combined with bending, and its shortcomings are now generally recognized. The "concrete contribution" V_c is generally considered to be some combination of force transfer by dowel action of the main steel, aggregate interlock along a diagonal crack, and shear in the uncracked concrete beyond the end of the crack. The values of each contribution are not identified. A rather vague rationalization is followed in adopting the diagonal cracking load of a member *without* web steel as the concrete contribution to the shear strength of an otherwise identical beam *with* web steel (see Section 4.4). Furthermore, as discussed in Section 4.3, Eqs. (4.3*a*) and (4.12*a*), used to predict the diagonal cracking load, overestimate concrete shear strength for beams with low reinforcement ratios ($\rho < 1.0$ percent), overestimate the gain in shear strength resulting from the use of high-strength concrete (Refs. 4.14 to 4.17), and underestimate the influence of $V_u d/M_u$ (Ref. 4.3). The expressions also ignore the fact that shear strength decreases as member size increases (Refs. 4.20 to 4.21).

Ad hoc procedures are built into the ACI Code to adjust for some of these deficiencies, but it follows that it is necessary to include equations, also empirically developed for the most part, for specific classes of members (e.g., deep beams vs. normal beams, beams with axial loads, prestressed vs. nonprestressed beams, high-strength concrete beams)—with restrictions on the range of applicability of such equations. And it is necessary to incorporate seemingly arbitrary provisions for the maximum nominal shear stress and for the extension of flexural reinforcement past the theoretical point of need. The end result is that the number of ACI Code equations for shear design has grown from 4 prior to 1963 to 38 in 2008.

With this as background, attention has been given to the development of design approaches based on rational behavioral models, generally applicable, rather than on empirical evidence alone (Ref. 4.6).

The *truss model* was originally introduced by Ritter (Ref. 4.22) and Morsch (Ref. 4.23) at the turn of the last century. A simplified version has long provided the basis for the ACI Code design of shear steel. The essential features of the truss model are reviewed with reference to Fig. 4.19*a*, which shows one-half the span of a simply supported, uniformly loaded beam. The combined action of flexure and shear produces the pattern of cracking shown. Reinforcement consists of the main flexural steel near the tension face and vertical stirrups distributed over the span.

The structural action can be represented by the truss of Fig. 4.19*b*, with the main steel providing the tension chord, the concrete top flange acting as the compression chord, the stirrups providing the vertical tension web members, and the concrete between inclined cracks acting as 45° compression diagonals. The truss is formed by lumping all the stirrups cut by section *a-a* into one vertical member and all the diagonal concrete struts cut by section *b-b* into one compression diagonal. Experience shows that for typical cases, the results of the model described are quite conservative, particularly for beams with small amounts of web reinforcement. As noted above, in the ACI Code the observed excess shear capacity is taken equal to the shear at the commencement of diagonal cracking and is referred to as the *concrete contribution* V_c.

Over the past 25 years, the truss concept has been greatly extended by the work of Schlaich, Marti, Collins, MacGregor, and others (Refs. 4.6, 4.24 to 4.29). It was realized that the angle of inclination of the concrete struts is generally not 45° but may range between about 25° and 65°, depending to a large extent on the arrangement of reinforcement. This led to what has become known as the *variable-angle truss model*, shown in Fig. 4.19*c*, which illustrates the five basic components of the improved model: (*a*) struts, or concrete compression members uniaxially loaded; (*b*) ties, or steel tension members; (*c*) joints at the intersection of truss members, assumed to be pin-connected; (*d*) compression fans, which form at "disturbed" regions, such as at the supports or under concentrated loads, transmitting the forces into the beam; and (*e*) diagonal compression fields, occurring where parallel compression struts transmit force from one stirrup to another. As in the ACI Code development, stirrups are typically assumed to reach yield stress at failure. With the force in all the verticals known and equal to $A_v f_{yt}$, the truss of Fig. 4.19*c* becomes statically determinate. Direct design equations can be based on the variable-angle truss model for ordinary cases. The model also permits direct numerical solution for the required reinforcement for special cases. The truss model does not include components of the shear failure mechanism such as aggregate interlock and friction, dowel action of the longitudinal steel, and shear carried across uncracked concrete. Furthermore, in the format originally proposed, the truss

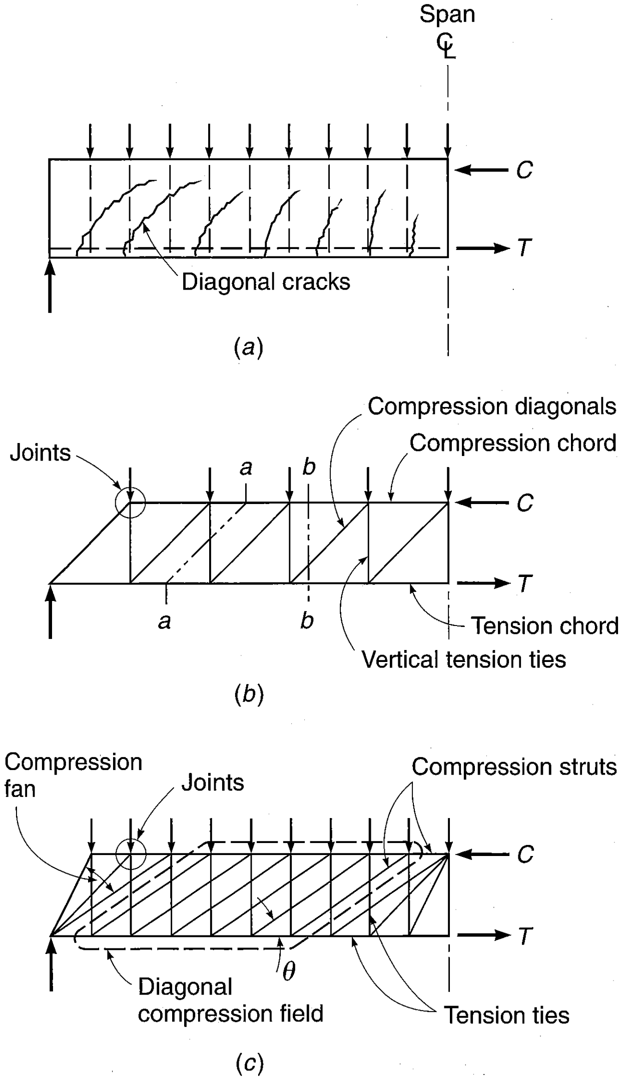
Span
℄
C
T
Diagonal cracks
(a)
Compression diagonals
Compression chord
Joints
a
b
C
T
a
b
Tension chord
Vertical tension ties
(b)
Compression fan
Joints
Compression struts
C
T
θ
Diagonal compression field
Tension ties
(c)

FIGURE 4.19
Truss model for beams with web reinforcement:
(*a*) uniformly loaded beam;
(*b*) simple truss model;
(*c*) more realistic model.

model does not account for compatibility requirements; i.e., it is based on *plasticity theory*. One form of the truss model is incorporated in Appendix A of the ACI Code; strut-and-tie models are discussed in detail in Chapter 10.

a. Compression Field Theory

The Canadian National Standard for reinforced concrete (Ref. 4.30) includes a method of shear design that is essentially the same as the present ACI method but also includes an alternative "general method" based on the variable-angle truss and the *compression field theory* (Refs. 4.27 and 4.31). The latter is incorporated in *AASHTO LRFD Bridge Design Specifications* (Ref. 4.12), where its use is mandatory for shear design. In its complete form, known as the *modified compression field theory*, it accounts for requirements of compatibility as well as equilibrium and incorporates stress-strain characteristics of both materials. Thus, it is capable of predicting not only the failure

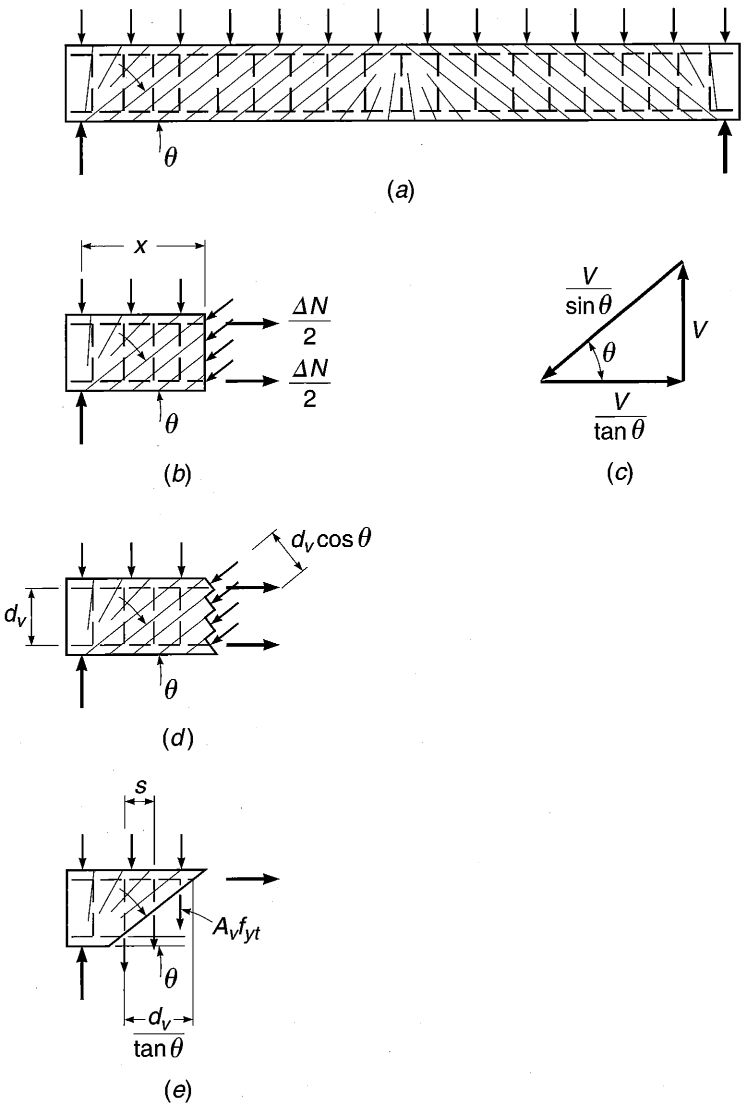

FIGURE 4.20
Basis of compression field theory for shear: (*a*) beam with shear and longitudinal steel; (*b*) tension in horizontal bars due to shear; (*c*) diagonal compression on beam web; (*d*) vertical tension in stirrups; (*e*) equilibrium diagram of forces due to shear. (*Adapted from Ref. 4.27.*)

load but also the complete load-deformation response. The most basic elements of the compression field theory, applied to members carrying combined flexure and shear, will be clear from Fig. 4.20. Figure 4.20*a* shows a simple-span concrete beam, reinforced with longitudinal bars and transverse stirrups, and carrying a uniformly distributed loading along the top face. The light diagonal lines are an idealized representation of potential tensile cracking in the concrete.

Figure 4.20*b* illustrates that the net shear V at a section a distance x from the support is resisted by the vertical component of the diagonal compression force in the concrete struts. The horizontal component of the compression in the struts must be equilibrated by the total tension force ΔN in the longitudinal steel. Thus, with reference to Fig. 4.20*b* and *c*, the magnitude of the longitudinal tension resulting from shear is

$$\Delta N = \frac{V}{\tan\theta} = V\cot\theta \tag{4.21}$$

where θ is the angle of inclination of the diagonal struts. These forces superimpose on the longitudinal forces owing to flexure, not shown in Fig. 4.20*b*.

The effective depth for shear calculations, according to this method, is taken at the distance between longitudinal force resultants d_v. Thus, from Fig. 4.20*d*, the diagonal compressive stress in a web having width b_v is

$$f_d = \frac{V}{b_v d_v \sin\theta \cos\theta} \tag{4.22}$$

The tensile force in the vertical stirrups, each having area A_v and assumed to act at the yield stress f_{yt}, can be found from the free body of Fig. 4.20*e*. With stirrups assumed to be at uniform spacing s,

$$A_v f_{yt} = \frac{Vs\tan\theta}{d_v} \tag{4.23}$$

Note, with reference to the free-body diagram, that the transverse reinforcement within the length $d_v/\tan\theta$ can be designed to resist the lowest shear that occurs within this length, i.e., the shear at the right end.

In the ACI Code method developed in Section 4.4, it was assumed that the angle θ was 45°. With that assumption, and if d is substituted for d_v, Eq. (4.23) is identical to that used earlier for the design of vertical stirrups. It is generally recognized, however, that the slope angle of the compression struts is not necessarily 45°, and following Refs. 4.12 and 4.30 that angle can range from 20 to 75°, provided the same value of θ is used in satisfying all requirements at a section. It is evident from Eqs. (4.21) and (4.23) that if a lower slope angle is selected, less vertical reinforcement but more horizontal reinforcement will be required. In addition, the compression in the concrete diagonals will be increased. Conversely, if a higher slope angle is used, more vertical steel but less horizontal steel will be needed, and the diagonal thrust will be less. It is generally economical to use a slope angle θ somewhat less than 45°, with the limitation that the concrete diagonal struts not be overstressed in compression.

In addition to providing an improved basis for the design of reinforcement for shear, the variable angle truss model gives important insights into detailing needs. For example, it becomes clear from the above that the increase in longitudinal steel tension resulting from the diagonal compression in the struts requires that flexural steel be extended beyond the point at which it is theoretically not needed for flexure, to account for the increased horizontal tensile force resulting from the thrust in the compression diagonals. This is not recognized explicitly in the ACI Code method for beam design. (However, the ACI Code does contain the arbitrary requirement that the flexural steel be extended a distance d or 12 bar diameters beyond the point indicated by flexural requirements.) Also, it is clear from the basic concept of the truss model that stirrups must be capable of developing their full tensile strength throughout the entire stirrup height. For wide beams, focus on truss action indicates that special attention should be given to lateral distribution of web reinforcement. It is often the practice to use conventional U stirrups for wide beams, with the vertical tension from the stirrups concentrated around the outermost bars. According to the discussion above, diagonal compression struts transmit forces only at the joints. Lack of stirrup joints at the interior of the wide-beam web would force joints to form only at the exterior longitudinal bars, which would concentrate the diagonal compression at the outer faces of the beam and possibly result in premature failure. It is best to form a truss joint at each of the longitudinal bars, and multiple leg stirrups should always be used in wide beams (see Fig. 4.8*c*).

References 4.12 and 4.30 incorporate a refined version of the approach just described, known as the modified compression field theory (MCFT), in which the cracked concrete is treated as a new material with its own stress-strain characteristics, including the ability to carry tension following crack formation. The compressive strength and the stress-strain curve of the concrete in the diagonal compression struts decrease as the diagonal tensile strain in the concrete increases. Equilibrium, compatibility, and constitutive relationships are formulated in terms of average stresses and average strains. Variability in the angle of inclination of the compression struts and stress-strain softening effects in the response of the concrete are taken into account. Consideration is also given to local stress conditions at crack locations. The method is capable of accurately predicting the response of complex elements such as shear walls, diaphragms, and membrane elements subjected to in-plane shear and axial loads through the full range of loading, from zero load to failure (Refs. 4.28 and 4.29). The version of the method adopted in Ref. 4.12 has been simplified to allow its use for routine design.

b. Design Provisions

The version of the MCFT adopted in the *AASHTO LRFD Bridge Design Specifications* (Ref. 4.12) is, like the shear provisions in the ACI Code, based on nominal shear capacity, with V_n equal to the lesser of

$$V_n = V_c + V_s \tag{4.24}$$

$$V_n = 0.25f_c' b_v d_v \tag{4.25}$$

where b_v = web width (the same as b_w in the ACI Code) and d_v = effective depth in shear, taken as equal to the flexural lever arm (the distance between the centroids of the tensile and compressive forces), but not less than the greater of $0.9d$ or $0.72h$.

The values of V_c and V_s differ from those used by the ACI, with

$$V_c = 0.083\beta\sqrt{f_c'}\,b_v d_v \tag{4.26}$$

and

$$V_s = \frac{A_v f_{yt} d_v(\cot\theta + \cot\alpha)\sin\alpha}{s} \tag{4.27}$$

where A_v, f_{yt}, s, α, and θ are as defined before. β is the *concrete tensile stress factor* and is based on the ability of diagonally cracked concrete to resist tension, which also controls the angle of the diagonal tension crack θ. In Ref. 4.12, the values of β and θ are determined based on the strain in the longitudinal tension reinforcement, which can be approximated by[†]

$$\epsilon_s = \frac{|M_u|/d_v - 0.5N_u + |V_u|}{E_s A_s} \le 0.006 \tag{4.28}$$

The sign convention for N_u is the same as used in Section 4.6 and the ACI Code: compression is positive and tension is negative (the opposite sign convention is used in Ref. 4.12). M_u should not be taken less than $V_u d_v$; when calculating A_s, the area of bars terminated less than their development length (see Chapter 5) from the section under consideration should be reduced in proportion to the decreased development; ϵ_s should be taken as zero if the value calculated in Eq. (4.28) is negative; and ϵ_s should be doubled if N_u is high enough to cause cracking to the flexural compression face of the member. For sections closer than d_v to the face of the support, ϵ_s calculated at d_v from the face of the support may be used to determine β and θ.

[†] Equation (4.28) is a simplification of $\epsilon_s = \dfrac{|M_u/d_v| - 0.5N_u + 0.5\,|V_u|\cot\theta}{E_s A_s}$, with $0.5|V_u|\cot\theta$ approximated by $|V_u|$. The simplification eliminates the need for an iterative solution between ϵ_s and θ.

For members with at least the minimum shear reinforcement, the concrete tensile stress factor is given by

$$\beta = \frac{4.8}{1+750\epsilon_s} \tag{4.29}$$

The angle θ, in degrees, is given by

$$\theta = 29 + 3500\epsilon_s \tag{4.30}$$

As shown in Eq. (4.21), the strength of the *longitudinal* reinforcement must be adequate to carry the additional forces induced by shear. Referring to Fig. 4.21, this leads to

$$A_s f_y \geq T = \frac{|M_u|}{\phi_f} - \frac{0.5N_u}{\phi_c} + \left(\frac{|V_u|}{\phi_v} - 0.5V_s\right)\cot\theta \tag{4.31}$$

where ϕ_f, ϕ_c, and ϕ_v are, respectively, the capacity reduction factors for flexure, axial load (tension or compression), and shear. V_s need not be taken greater than V_u/ϕ. Since the inclination of the compression struts changes, tension in the longitudinal reinforcement does not exceed that required to resist the maximum moment alone.

For members with less than the minimum transverse reinforcement, the angle θ is given by Eq. (4.30), while the value of β becomes a function of ϵ_s and a crack spacing parameter s_{xe}.

$$\beta = \frac{4.8}{1 + 750\epsilon_s} \; \frac{1295}{991 + s_{xe}} \tag{4.32}$$

The crack spacing parameter is

$$s_{xe} = s_x \frac{35}{a_g + 16} \tag{4.33}$$

FIGURE 4.21
Equilibrium diagram for calculating tensile force in reinforcement. (*Adapted from Ref. 4.12.*)

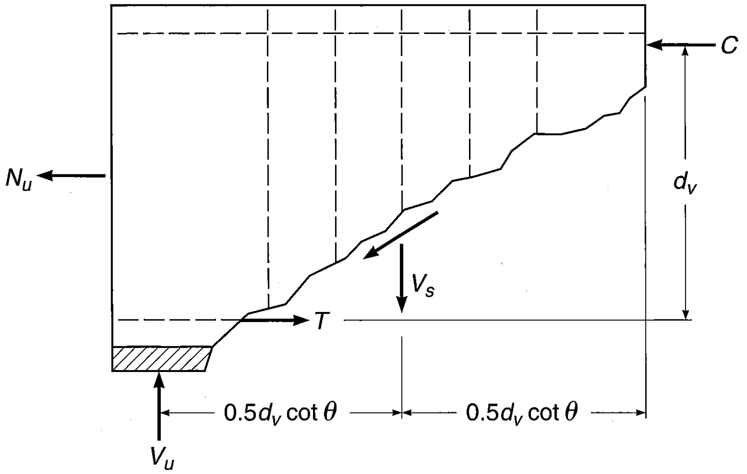

where 300 mm $\leq s_{xe} \leq$ 2000 mm, s_x = lesser of the shear depth d_v or the spacing between layers of longitudinal crack control reinforcement, each layer with an area of steel of at least $0.003b_v s_x$, and a_g = maximum size of the coarse aggregate. Note that $s_{xe} = s_x$ for 19-mm coarse aggregate.

Since θ is not, in general, equal to 45°, the critical section might appropriately be taken as $d_v \cot \theta$ from the face of the support if all the load were applied to the upper surface of the member. For simplicity, however, the critical section is taken a distance d_v from the face of the support when the reaction introduces compression into the end region of the member, similar to the loading cases shown in Fig. 4.12*a* and *b*. For all other cases, the crucial section is taken at the face of the support, as shown in Fig. 4.12*c* to *f*.

AASHTO requires a minimum amount of transverse reinforcement $A_v = 0.083\sqrt{f'_c}\,b_v s/f_{yt}$ (compared to $0.062\sqrt{f'_c}\,b_w s/f_{yt}$ for ACI), when $V_u > 0.5\phi V_c$, and specifies maximum spacings of transverse reinforcement of $s \leq 0.8d_v \leq 600$ mm when $v_u < 0.125f'_c$ and $s \leq 0.4d_v \leq 300$ mm when $v_u \geq 0.125f'_c$. Because the predictions obtained with the MCFT are generally more accurate than those obtained with the ACI method, AASHTO allows the use of $\phi = 0.90$ for shear, the same as for flexure.

EXAMPLE 4.5

Design by modified compression field approach. Re-solve the problem given in Examples 4.2 and 4.3 based on the MCFT. Use ACI load factors and $\phi = 0.9$ for shear, as used in *AASHTO LRFD Bridge Design Specifications* (Ref. 4.12). Assume an aggregate size a_g of 19 mm.

Solution. For simplicity, the effective depth for shear d_v will be set at the minimum allowable value $= 0.9d = 0.9 \times 500 = 495$ mm. Both M_u and V_u are as tabulated previously in Table 4.1.

The critical section for shear is located a distance $d_v = 0.495$ m from the support where $V_u = 411 - 137 \times 0.495 = 343.2$ kN. Calculating $0.125f'_c b_v d_v = 0.125 \times 28 \times 400 \times 550/1000 = 6160$ kN leads to maximum spacing criteria for No. 10 (No. 3) stirrups equal to the smaller of $0.8d_v = 0.8 \times 495 = 396$ mm, 600 mm, or

$$s_{\max} = \frac{A_v f_{yt}}{\sqrt{f'_c}\,b_v} = \frac{142 \times 420}{0.083\sqrt{28} \times 400} = 339 \text{ mm}$$

Using Eq. (4.28), the strain in the longitudinal tension steel is approximated as

$$\epsilon_s = \frac{|M_u|/495 + |V_u|}{200{,}000 \times 4914}$$

with M_u and V_u in N-mm and N, respectively.

The values of ϵ_s are tabulated along with M_u and V_u in Table 4.2. These values are used to calculate θ using Eq. (4.30) and β using Eqs. (4.29) and (4.32) for sections with and without minimum stirrups, respectively. Where the section meets the minimum stirrup criterion, the values of β are used to calculate the values of V_c, which are then used, along with the values of θ, to calculate V_s and the required stirrup spacing s (see Table 4.2).

For transverse reinforcement less than the minimum, the values of β are based on ϵ_s and s_x. The latter may be taken as the lesser of d_v or the spacing of longitudinal crack control reinforcement. In this case, $d_v = 495$ mm controls since crack control reinforcement is not used. The equivalent crack spacing parameter $s_{xe} = s_x$ because $a_g = 19$ mm. These values of β are used to determine the point where $\phi V_c/2 \geq V_u$, the point at which stirrups may be terminated (Table 4.2). The values of V_u, ϕV_c with at least minimum stirrups, and $\phi V_c/2$ for less than minimum stirrups are plotted in Fig. 4.22*a*. The following stirrup spacings can be used for this case:

1 space at 150 mm = 150 mm
6 spaces at 330 mm = 1980 mm
Total = 2130 mm = 2.13 m

TABLE 4.2
Modified compression field design example using $\phi = 0.9$ for shear

					ϕV_c for at Least Minimum Stirrups				ϕV_c for Less Than Minimum Stirrups		
Distance from Support, m	M_u, kN-m	V_u, kN	$\epsilon_x \times 1000$	θ	β	ϕV_c, kN	V_s, kN	s, mm	β	ϕV_c, kN	$\phi V_c/2$, kN
0.0	0	411	0.84	31.9	2.95	231	200	237	2.57	201	101
0.3	117	370	0.75	31.6	3.07	240	144	332	2.67	209	105
0.495†	187	343	0.73	31.6	3.10	242	112	429	2.70	211	106
0.6	222	329	0.79	31.8	3.01	236	103	461	2.63	206	103
0.9	314	288	0.94	32.3	2.82	220	75	625	2.45	192	96
1.2	395	247	1.06	32.7	2.67	209	42	1103	2.33	182	91
1.5	462	206	1.16	33.1	2.57	201	5	8933	2.24	175	88
1.8	518	164	1.23	33.3	2.50	195	—	—	2.17	170	85
2.1	561	123	1.28	33.5	2.45	192	—	—	2.14	167	84
2.4	592	82	1.30	33.6	2.43	190	—	—	2.12	166	83
2.7	610	41	1.30	33.5	2.43	190	—	—	2.12	166	83
3.0	617	0	1.27	33.4	2.46	193	—	—	2.14	168	84

† d_v from face of support.

For this example, V_s is selected based on V_u at each point, not the minimum V_u on a crack with angle θ. This simplifies the design procedure and results in a somewhat more conservative design. Even so, only 7 No. 10 (No. 3) stirrups are needed, or 9 stirrups if the stirrups are continued at the maximum spacing through the middle region of the beam. These values compare favorably with the minimum number of stirrups per half-span, 11 and 14, previously

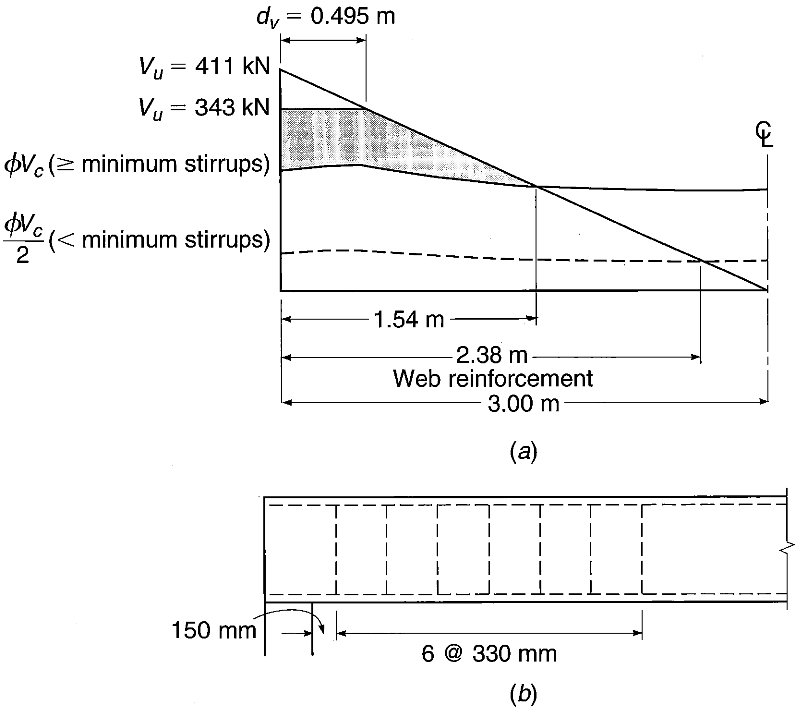

FIGURE 4.22
Modified compression field design for Example 4.5.

calculated (Example 4.3) using the two methods required by the ACI Code. The resulting stirrup pattern is shown in Fig. 4.22*b*.

By way of comparison, had $\phi_{\text{shear}} = 0.75$ been used in this example, the stirrup spacing would have been

$$\begin{aligned} 1 \text{ space at } 100 \text{ mm} &= 100 \text{ mm} \\ 3 \text{ spaces at } 250 \text{ mm} &= 750 \text{ mm} \\ 4 \text{ spaces at } 330 \text{ mm} &= \underline{1320 \text{ mm}} \\ \text{Total} &= 2170 \text{ mm} = 2.17 \text{ m} \end{aligned}$$

for a total of 8 stirrups.

The MCFT recognizes that shear increases the force in the flexural steel, although, as explained earlier, the maximum tensile force in the steel is not affected. Equation (4.31) should be used to calculate the tensile force T along the span, which will then govern the locations where tensile steel may be terminated. This will be discussed further in Chapter 5.

The MCFT is not included in the 2008 ACI Code. ACI Code 1.4, however, permits the use of "any system of design or construction . . . , the adequacy of which has been shown by successful use or by analysis or test," if approved by the appropriate building official. The application of the MCFT in Canada and in U.S. bridge practice provides the evidence needed to demonstrate "successful use."

4.9 SHEAR-FRICTION DESIGN METHOD

Generally, in reinforced concrete design, shear is used merely as a convenient measure of diagonal tension, which is the real concern. In contrast, there are circumstances such that direct shear may cause failure of reinforced concrete members. Such situations occur commonly in precast concrete structures, particularly in the vicinity of connections, as well as in composite construction combining cast-in-place concrete with either precast concrete or structural steel elements. Potential failure planes can be established for such cases along which direct shear stresses are high, and failure to provide adequate reinforcement across such planes may produce disastrous results.

The necessary reinforcement may be determined on the basis of the *shear-friction method* of design (Refs. 4.32 to 4.38). The basic approach is to assume that the concrete may crack in an unfavorable manner, or that slip may occur along a predetermined plane of weakness. Reinforcement must be provided crossing the potential or actual crack or shear plane to prevent direct shear failure.

The shear-friction theory is very simple, and the behavior is easily visualized. Figure 4.23*a* shows a cracked block of concrete, with the crack crossed by reinforcement. A shear force V_n acts parallel to the crack, and the resulting tendency for the upper block to slip relative to the lower is resisted largely by friction along the concrete interface at the crack. Since the crack surface is naturally rough and irregular, the effective coefficient of friction may be quite high. In addition, the irregular surface will cause the two blocks of concrete to separate slightly, as shown in Fig. 4.23*b*.

If reinforcement is present normal to the crack, then slippage and subsequent separation of the concrete will stress the steel in tension. Tests have confirmed that well-anchored steel will be stressed to its yield strength when shear failure is obtained (Ref. 4.34). The resulting tensile force sets up an equal and opposite pressure between the concrete faces on either side of the crack. It is clear from the free body of Fig. 4.23*c* that the maximum value of this interface pressure is $A_{vf}f_y$, where A_{vf} is the total area of steel crossing the crack and f_y is its yield strength.

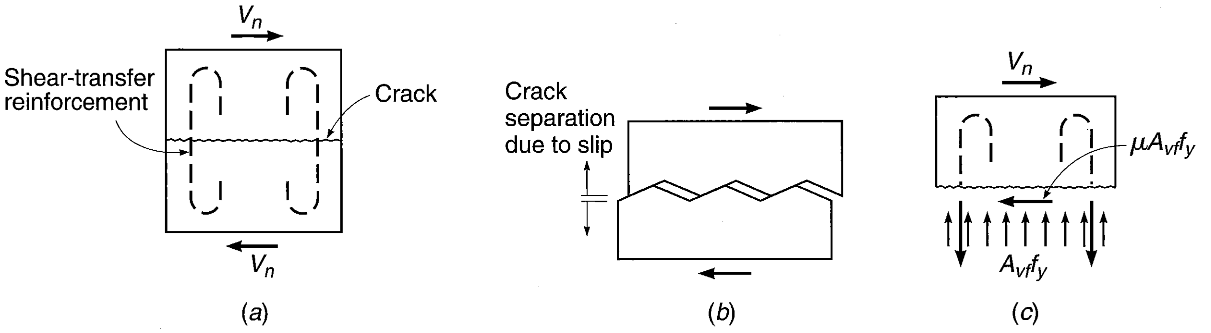

FIGURE 4.23
Basis of shear-friction design method: (*a*) applied shear; (*b*) enlarged representation of crack surface; (*c*) free-body sketch of concrete above crack.

The concrete resistance to sliding may be expressed in terms of the normal force times a coefficient of friction μ. By setting the summation of horizontal forces equal to zero

$$V_n = \mu A_{vf} f_y \tag{4.34}$$

Based on tests, μ may be taken as 1.4 for cracks in monolithic concrete, but V_n should not be assumed to be greater than $0.2 f'_c A_c$, $(480 + 0.08 f'_c)A_c$, or $1600A_c$ (Refs. 4.32, 4.37, and 4.38).

The relative movement of the concrete on opposite sides of the crack also subjects the individual reinforcing bars to shearing action, and the dowel resistance of the bars to this shearing action contributes to shear resistance. However, it is customary to neglect the dowel effect for simplicity in design and to compensate for this by using an artificially high value of the friction coefficient.

The provisions of ACI Code 11.6 are based on Eq. (4.34). The design strength is equal to ϕV_n, where $\phi = 0.75$ for shear-friction design, and V_n must not exceed the smallest of $0.2 f'_c A_c$, $(3.3 + 0.08 f'_c)A_c$, and $11A_c$ for monolithic or intentionally roughened normalweight concrete or the smaller of $0.2 f'_c A_c$ and $5.5A_c$ N for other cases. When concretes of different strengths are cast against each other, V_n should be based on the lower value of f'_c. Recommendations for friction factor μ are as follows:

Concrete placed monolithically	1.4λ
Concrete placed against hardened concrete with surface intentionally roughened	1.0λ
Concrete placed against hardened concrete not intentionally roughened	0.6λ
Concrete anchored to as-rolled structural steel by headed studs or reinforcing bars	0.7λ

where λ is 1.0 for normalweight concrete and 0.75 for both sand-lightweight and all-lightweight concrete. In other cases, λ is determined based on volumetric proportions of lightweight and normalweight aggregates, as described in Section 4.5a and specified in ACI Code 8.6.1, but not greater than 0.85. The yield strength of the reinforcement f_y may not exceed 420 MPa. Direct tension across the shear plane, if present, must be carried by additional reinforcement, and permanent net compression across the shear plane may be taken as additive to the force in the shear-friction reinforcement $A_{vf} f_y$ when calculating the required A_{vf}.

FIGURE 4.24
Shear-friction reinforcement inclined with respect to crack face.

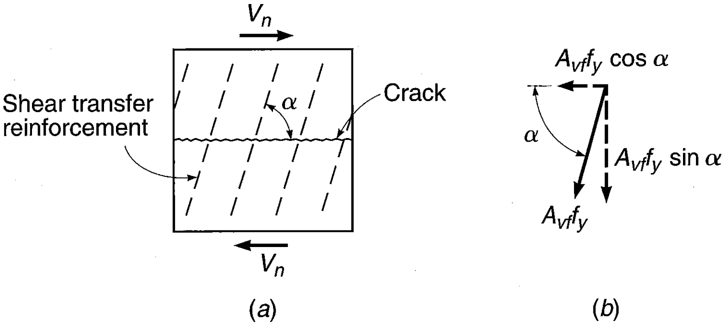

When shear is transferred between concrete newly placed against hardened concrete, the surface roughness is an important variable; an intentionally roughened surface is defined to have a full amplitude of approximately 6 mm. In any case, the old surface must be clean and free of laitance. When shear is to be transferred between as-rolled steel and concrete, the steel must be clean and without paint, according to ACI Code 11.6.

If V_u is the shear force to be resisted at factored loads, then with $V_u = \phi V_n$, the required steel area is found by transposition of Eq. (4.34):

$$A_{vf} = \frac{V_u}{\phi \mu f_y} \tag{4.35}$$

In some cases, the shear-friction reinforcement may not cross the shear plane at 90° as described in the preceding paragraphs. If the shear-friction reinforcement is inclined to the shear plane so that the shear force is applied in the direction to increase tension in the steel, as in Fig. 4.24*a*, then the component of that tension parallel to the shear plane, shown in Fig. 4.24*b*, contributes to the resistance to slip. Then the shear strength may be computed from

$$V_n = A_{vf} f_y (\mu \sin\alpha + \cos\alpha) \tag{4.36}$$

in lieu of Eq. (4.34). Here α is the angle between the shear-friction reinforcement and the shear plane. If α is larger than 90°, i.e., if the inclination of the steel is such that the tension in the bars tends to be reduced by the shear force, then the assumption that the steel stress equals f_y is not valid, and a better arrangement of bars should be made.

Certain precautions should be observed in applying the shear-friction method of design. Reinforcement, of whatever type, should be well anchored to develop the yield strength of the steel, by the full development length or by hooks or bends, in the case of reinforcing bars, or by proper heads and welding, in the case of studs joining concrete to structural steel. The concrete should be well confined, and the liberal use of hoops has been recommended (Ref. 4.32). Care must be taken to consider all possible failure planes and to provide sufficient well-anchored steel across these planes.

EXAMPLE 4.6

Design of beam bearing detail. A precast beam must be designed to resist a support reaction, at factored loads, of $V_u = 445$ kN applied to a 75 × 75 mm steel angle, as shown in Fig. 4.25. In lieu of a calculated value, a horizontal force N_u, owing to restrained volume change, will be assumed to be 20 percent of the vertical reaction, or 89 kN. Determine the required auxiliary reinforcement, using steel of yield strength $f_y = 420$ MPa. Concrete strength $f'_c = 35$ MPa.

FIGURE 4.25
Design of beam bearing shoe: (*a*) diagonal crack; (*b*) horizontal crack; (*c*) reinforcement; (*d*) cross section.

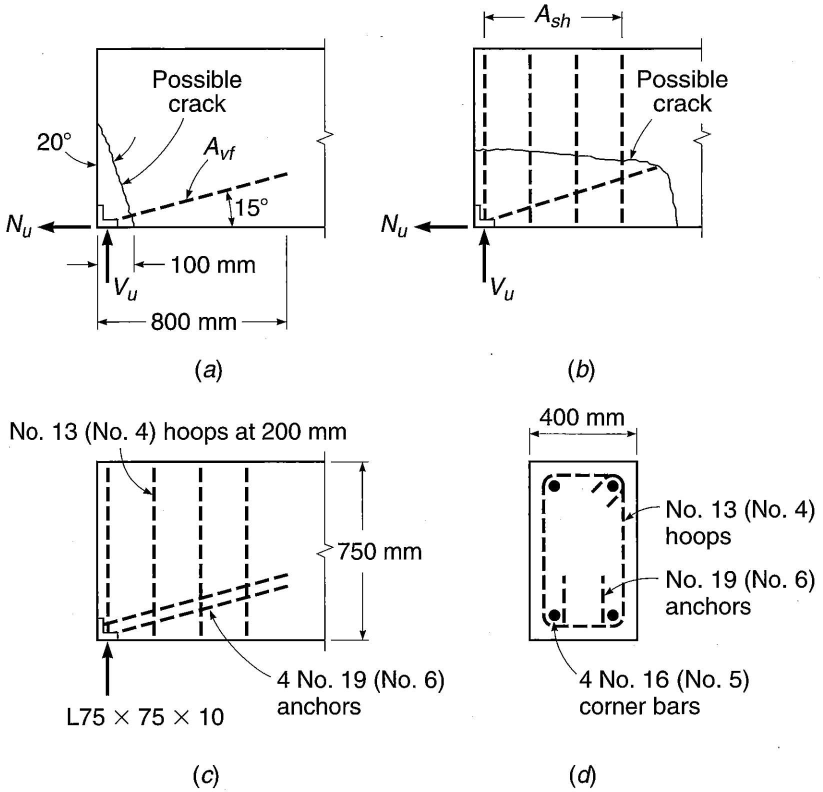
Possible crack
20°
A_{vf}
15°
N_u
V_u
100 mm
800 mm
(a)
A_{sh}
Possible crack
N_u
V_u
(b)
No. 13 (No. 4) hoops at 200 mm
750 mm
4 No. 19 (No. 6) anchors
L75 × 75 × 10
(c)
400 mm
No. 13 (No. 4) hoops
No. 19 (No. 6) anchors
4 No. 16 (No. 5) corner bars
(d)

Solution. A potential crack will be assumed at 20°, initiating at a point 100 mm from the end of the beam, as shown in Fig. 4.25*a*. The total required steel A_{vf} is the sum of that required to resist the resultant of V_u and N_u acting parallel to the cracks $= V_u \cos 20° + N_u \sin 20°$. Equation (4.35) is modified accordingly:

$$
\begin{aligned}
A_{vf} &= \frac{V_u \cos 20° + N_u \sin 20°}{\phi \mu f_y} \\
&= \frac{(445 \times 0.940 + 89 \times 0.340) \times 1000}{0.75 \times 1.4 \times 420} = \frac{449{,}000\text{ N}}{441\text{ MPa}} \\
&= 1018\text{ mm}^2
\end{aligned}
$$

The net compression normal to the potential crack would be no less than $V_u \sin 20° - N_u \cos 20° = 67.6$ kN. This could be counted upon to reduce the required shear-friction steel, according to the ACI Code, but it will be discounted conservatively here. Four No. 19 (No. 6) bars will be used, providing an area of 1136 mm^2. They will be welded to the 75 × 75 mm angle and will extend into the beam a sufficient distance to develop the yield strength of the bars. According to the ACI Code, the development length for a No. 19 (No. 6) bar is 646 mm, 798 mm without the ψ_s factor (see Chapter 5). Considering the uncertainty of the exact crack location, the bars will be extended 800 mm into the beam as shown in Fig. 4.25*a*. The bars will be placed at an angle of 15° with the bottom face of the member. For the crack oriented at an angle of 20°, as assumed, the area of the crack is

$$
A_c = 400\left(\frac{100}{\sin 20°}\right) = 117{,}650\text{ mm}^2
$$

Thus, according to the ACI Code, the maximum nominal shear strength of the surface is not to exceed $V_n = 0.2f'_c A_c = 824$ kN, $V_n = (3.3 + 0.08f'_c)A_c = 718$ kN, or $V_n = 11A_c = 1294$ kN. The maximum design strength to be used is $\phi V_n = 0.75 \times 718 = 539$ kN. As calculated earlier, the applied shear on the interface at factored loads is

$$V_u = 445 \cos 20° + 89 \sin 20° = 449 \text{ kN}$$

and so the design is judged satisfactory to this point.

A second possible crack must be considered, as shown in Fig. 4.25*b*, resulting from the tendency of the entire anchorage weldment to pull horizontally out of the beam.

The required steel area A_{sh} and the concrete shear stress will be calculated based on the development of the full yield tension in the bars A_{vf}. (Note that the factor ϕ need not be used here because it has already been introduced in computing A_{vf}.)

$$\begin{aligned} A_{sh} &= \frac{A_{vf} f_y \cos 15°}{\mu f_y} \\ &= \frac{1136 \times 0.966}{1.4} \\ &= 784 \text{ mm}^2 \end{aligned}$$

Four No. 13 (No. 4) hoops will be used, providing an area of 1032 mm^2.

The maximum shear force that can be transferred, according to the ACI Code limits, will be based conservatively on a horizontal plane 800 mm long. No strength reduction factor need be included in the calculation of this maximum value because it was already introduced in determining the steel area A_{vf} by which the shear force is applied. Accordingly,

$$V_n \leq (3.3 + 0.08f'_c) \times 400 \times 800/1000 = 1952 \text{ kN}$$

The maximum shear force that could be applied in the given instance is the value used to calculate A_{sh},

$$V_u = 1136 \times 420 \cos 15° = 461 \text{ kN}$$

which is well below the specified maximum.

The first hoop will be placed 50 mm from the end of the member, with the others spaced at 200 mm, as shown in Fig. 4.25*c*. Also shown in Fig. 4.25*d* are four No. 16 (No. 5) bars that will provide anchorage for the hoop steel.

REFERENCES

4.1. "Shear and Diagonal Tension," pt. 2, ACI-ASCE Committee 326, *J. ACI*, vol. 59, no. 2, 1962, pp. 277–333.

4.2. B. Bresler and J. G. MacGregor, "Review of Concrete Beams Failing in Shear," *J. Struct. Div.*, ASCE, vol. 93, no. ST1, 1967, pp. 343–372.

4.3. "The Shear Strength of Reinforced Concrete Members," ASCE-ACI Committee 426, *Proc. ASCE*, vol. 99, no. ST6, 1973, pp. 1091–1187 (with extensive bibliography).

4.4. "The Shear Strength of Reinforced Concrete Members—Slabs," ASCE-ACI Task Committee 426, *Proc. ASCE*, vol. 100, no. ST8, 1974, pp. 1543–1591.

4.5. *Shear in Reinforced Concrete*, vols. 1 and 2, *Special Publication* SP-42, American Concrete Institute, Detroit, 1974.

4.6. "Recent Approaches to Shear Design of Structural Concrete," ASCE-ACI Committee 445, *J. Struct. Eng.*, ASCE, vol. 124, no. 12, 1998, pp. 1375–1417.

4.7. A. H. Nilson (ed.), *Finite Element Analysis of Reinforced Concrete*, American Society of Civil Engineers, New York, 1982.

4.8. J. Isenberg (ed.), *Finite Element Analysis of Reinforced Concrete Structures II*, American Society of Civil Engineers, New York, 1993, pp. 203–232.

4.9. M. P. Collins, "Toward a Rational Theory for RC Members in Shear," *J. Struct. Div.*, ASCE, vol. 104, no. ST4, April 1978, pp. 649–666.

4.10. T. T. C. Hsu, *Unified Theory of Reinforced Concrete*, CRC Press, Inc., Boca Raton, FL, 1993.

4.11. T. C. Zsutty, "Shear Strength Prediction for Separate Categories of Simple Beam Tests," *J. ACI*, vol. 68, no. 2, 1971, pp. 138–143.

4.12. *AASHTO LRFD Bridge Design Specifications,* 4th ed., American Association of State Highway and Transportation Officials (AASHTO), Washington, DC, 2007, with interim update 2008.

4.13. S. Martinez, A. H. Nilson, and F. O. Slate, "Short-Term Mechanical Properties of High-Strength Lightweight Concrete," *Research Report No. 82–9*, Department of Structural Engineering, Cornell University, August 1982.

4.14. A. H. Elzanaty, A. H. Nilson, and F. O. Slate, "Shear Capacity of Reinforced Concrete Beams Using High-Strength Concrete," *J. ACI*, vol. 83, no. 2, 1986, pp. 290–296.

4.15. J. J. Roller and H. G. Russell, "Shear Strength of High-Strength Concrete Beams with Web Reinforcement," *ACI Struct. J.*, vol. 87, no. 2, 1990, pp. 191–198.

4.16. S. H. Ahmad, A. R. Khaloo, and A. Proveda, "Shear Capacity of Reinforced High-Strength Concrete Beams," *J. ACI*, vol. 83, no. 2, 1986, pp. 297–305.

4.17. M. P. Collins and D. Kuchma, "How Safe Are Our Large, Lightly Reinforced Concrete Beams, Slabs, and Footings?" *ACI Struct. J.*, vol. 96, no. 4, 1999, pp. 282–290.

4.18. G. J. Parra-Montesinos, "Shear Strength of Beams with Deformed Steel Fibers," *Concr. Int.*, vol. 28, no. 11, 2006, pp. 57–66.

4.19. S. Y. Debaiky and E. I. Elmiema, "Behavior and Strength of Reinforced Concrete Haunched Beams in Shear," *J. ACI*, vol. 79, no. 3, 1982, pp. 184–194.

4.20. G. N. J. Kani, "How Safe Are Our Large Reinforced Concrete Beams?" *J. ACI*, vol. 64, no. 3, 1967, pp. 128–141.

4.21. T. Shioya, M. Iguro, Y. Akiayma, and T. Okada, "Shear Strength of Large Reinforced Concrete Beams, Fracture Mechanics: Application to Concrete," *Special Publication* SP-118, American Concrete Institute, Detroit, 1989, pp. 259–279.

4.22. W. Ritter, "Die Bauweise Hennebique" (The Hennebique System), *Schweizerische Bauzeitung*, XXXIII, no. 7, 1899.

4.23. E. Morsch, *Der Eisenbetonbau, seine Theorie und Anwendung* (Reinforced Concrete Theory and Application), Verlag Konrad Wittner, Stuttgart, 1912.

4.24. J. Schlaich, K. Schafer, and M. Jennewein, "Toward a Consistent Design of Structural Concrete," *J. Prestressed Concr. Inst.*, vol. 32, no. 3, 1987, pp. 74–150.

4.25. P. Marti, "Truss Models in Detailing," *Concr. Int.*, vol. 7, no. 12, 1985, pp. 66–73. (See also P. Marti, "Basic Tools of Reinforced Concrete Beam Design," *J. ACI*, vol. 82, no. 1, 1985, pp. 46–56.)

4.26. J. G. MacGregor and J. K. Wight, *Reinforced Concrete*, 4th ed., Prentice-Hall, Englewood Cliffs, NJ, 2005.

4.27. M. P. Collins and D. Mitchell, *Prestressed Concrete Structures*, Prentice-Hall, Englewood Cliffs, NJ, 1991.

4.28. F. J. Vecchio and M. P. Collins, "Modified Compression Field Theory for Reinforced Concrete Elements Subjected to Shear," *J. ACI*, vol. 83, no. 2, 1986, pp. 219–231.

4.29. F. J. Vecchio and M. P. Collins, "Predicting the Response of Reinforced Concrete Beams Subjected to Shear Using the Modified Compression Field Theory," *J. ACI*, vol. 85, no. 3, 1988, pp. 258–268.

4.30. CSA Committee A23.3, *Design of Concrete Structures*, Canadian Standards Association, Etobicoke, Ontario, 2004.

4.31. M. P. Collins, D. Mitchell, P. Adebar, and F. J. Vecchio, "A General Shear Design Method," *ACI Struct. J.*, vol. 93, no. 1, 1996, pp. 36–45.

4.32. P. W. Birkeland and H. W. Birkeland, "Connections in Precast Concrete Construction," *J. ACI*, vol. 63, no. 3, 1966, pp. 345–368.

4.33. R. F. Mast, "Auxiliary Reinforcement in Precast Concrete Connections," *J. Struct. Div.,* ASCE, vol. 94, no. ST6, June 1968, pp. 1485–1504.

4.34. A. H. Mattock and N. M. Hawkins, "Shear Transfer in Reinforced Concrete—Recent Research," *J. Prestressed Concr. Inst.*, vol. 17, no. 2, 1972, pp. 55–75.

4.35. A. H. Mattock, "Shear Transfer in Concrete Having Reinforcement at an Angle to the Shear Plane," *Special Publication* SP-42, American Concrete Institute, Detroit, 1974.

4.36. *PCI Design Handbook*, 6th ed., Precast Prestressed Concrete Institute, Chicago, 2004.

4.37. L. F. Kahn and A. D. Mitchell, "Shear Friction Tests with High-Strength Concrete," *ACI Struct. J.*, vol. 99, no. 1, 2002, pp. 98–103.

4.38. A. H. Mattock, "Shear Friction and High-Strength Concrete," *ACI Struct. J.*, vol. 98, no. 1, 2001, pp. 50–59.

PROBLEMS

4.1. A beam is to be designed for loads causing a maximum factored shear of 270 kN, using concrete with f'_c = 35 MPa. Proceeding on the basis that the concrete dimensions will be determined by diagonal tension, select the appropriate width and effective depth (*a*) for a beam in which no web reinforcement is to be used, (*b*) for a beam in which only the minimum web reinforcement is provided, as given by Eq. (4.13), and (*c*) for a beam in which web reinforcement provides shear strength $V_s = 2V_c$. Follow the ACI Code requirements, and let $d = 2b$ in each case. Calculations may be based on the more approximate value of V_c given by Eq. (4.12*b*).

4.2. A rectangular beam having b = 250 mm and d = 450 mm spans 4.5 m face to face of simple supports. It is reinforced for flexure with three No. 29 (No. 9) bars that continue uninterrupted to the ends of the span. It is to carry service dead load D = 18.5 kN/m (including self-weight) and service live load L = 54.0 kN/m, both uniformly distributed along the span. Design the shear reinforcement, using No. 10 (No. 3) vertical U stirrups. The more approximate Eq. (4.12*b*) for V_c may be used. Material strengths are f'_c = 28 MPa and f_y = 420 MPa.

4.3. Redesign the shear reinforcement for the beam of Problem 4.2, basing V_c on the more accurate Eq. (4.12*a*). Comment on your results, with respect to design time and probable construction cost difference.

4.4. Design the shear reinforcement, using No. 13 (No. 4) vertical U stirrups for the independent T beam shown in Fig. P4.4. The beam spans 7 m face to face between simple supports, has an effective depth d = 775 mm, and is reinforced for flexure with six No. 32 (No. 10) bars in two layers that continue uninterrupted to the ends of the span. It is to carry service dead load D = 39 kN/m (including self-weight) and service live load L = 78 kN/m, both uniformly distributed along the span. The more approximate Eq. (4.12*b*) for V_c may be used. Material strengths are f'_c = 35 MPa and f_y = 420 MPa.

FIGURE P4.4

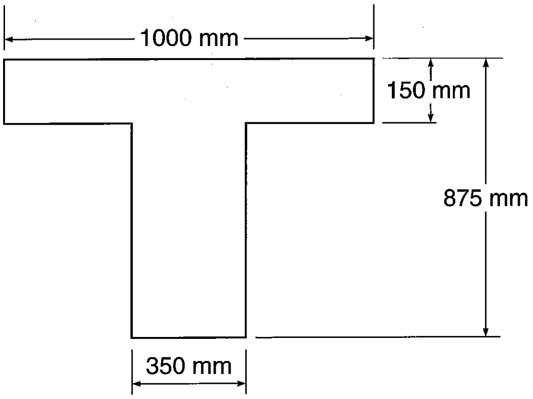

4.5. A beam of 280 mm width and effective depth of 400 mm carries a factored uniformly distributed load of 77 kN/m, including its own weight, in addition to a central, concentrated factored load of 53 kN. It spans 5.5 m, and restraining end moments at full factored load are 185 kN-m at each support. It is reinforced with three No. 29 (No. 9) bars for both positive and negative bending. If f'_c = 28 MPa, through what part of the beam is web reinforcement theoretically required (*a*) if Eq. (4.12*b*) is used and (*b*) if Eq. (4.12*a*) is used? Comment.

4.6. What effect would an additional clockwise moment of 239 kN-m at the right support have on the requirement for shear reinforcement determined in part (*a*) of Problem 4.5?

4.7. Design the web reinforcement for the beam of Problem 4.5, with V_c determined by the more approximate ACI equation, using No. 10 (No. 3) vertical stirrups with $f_y = 420$ MPa.

4.8. Design the web reinforcement for the beam of Problem 4.6, with V_c determined by the more approximate ACI equation, using No. 10 (No. 3) vertical stirrups with $f_y = 420$ MPa.

4.9. The beam of Problem 4.2 will be subjected to a factored axial compression load of 390 kN on the 250×500 mm gross cross section, in addition to the loads described earlier. What is the effect on concrete shear strength V_c (*a*) by the more accurate ACI equation and (*b*) by the more approximate ACI equation?

4.10. The beam of Problem 4.2 will be subjected to a factored axial tension load of 195 kN on the 250×500 mm gross cross section, in addition to the loads described earlier. What is the effect on concrete shear strength V_c (*a*) by the more accurate ACI equation and (*b*) by the more conservative ACI approach?

4.11. Redesign the shear reinforcement for the beam of Problem 4.2, using the modified compression field theory with (*a*) $\phi_{\text{shear}} = 0.90$ and (*b*) $\phi_{\text{shear}} = 0.75$.

4.12. Redesign the shear reinforcement for the beam of Problem 4.4, using the modified compression field theory with (*a*) $\phi_{\text{shear}} = 0.90$ and (*b*) $\phi_{\text{shear}} = 0.75$.

4.13. A precast concrete beam having cross-sectional dimensions $b = 250$ mm and $h = 600$ mm is designed to act in a composite sense with a cast-in-place top slab having depth $h_f = 250$ mm and width 1200 mm. At factored loads, the maximum compressive stress in the flange at midspan is 16.5 MPa; at the supports of the 8.5 m simple span the flange force must be zero. Vertical U stirrups provided for flexural shear will be extended into the slab and suitably anchored to provide also for transfer of the flange force by shear friction. Find the minimum number of No. 13 (No. 4) stirrups that must be provided, based on shear-friction requirements. Concrete in both precast and cast-in-place parts will have $f'_c = 28$ MPa and $f_y = 420$ MPa. The top surface of the precast web will be intentionally roughened according to the ACI Code definition.

4.14. Redesign the beam-end reinforcement of Example 4.6, given that a roller support will be provided so that $N_u = 0$.

5

Bond, Anchorage, and Development Length

5.1 FUNDAMENTALS OF FLEXURAL BOND

If the reinforced concrete beam of Fig. 5.1*a* were constructed using plain round reinforcing bars, and, furthermore, if those bars were to be greased or otherwise lubricated before the concrete were cast, the beam would be very little stronger than if it were built of plain concrete, without reinforcement. If a load were applied, as shown in Fig. 5.1*b*, the bars would tend to maintain their original length as the beam deflected. The bars would slip longitudinally with respect to the adjacent concrete, which would experience tensile strain due to flexure. Proposition 2 of Section 1.8, the assumption that the strain in an embedded reinforcing bar is the same as that in the surrounding concrete, would not be valid. For reinforced concrete to behave as intended, it is essential that *bond forces* be developed on the interface between concrete and steel, such as to prevent significant slip from occurring at that interface.

Figure 5.1*c* shows the bond forces that act on the concrete at the interface as a result of bending, while Fig. 5.1*d* shows the equal and opposite bond forces acting on the reinforcement. It is through the action of these interface bond forces that the slip indicated in Fig. 5.1*b* is prevented.

Some years ago, when plain bars without surface deformations were used, initial bond strength was provided only by the relatively weak chemical adhesion and mechanical friction between steel and concrete. Once adhesion and static friction were overcome at larger loads, small amounts of slip led to interlocking of the natural roughness of the bar with the concrete. However, this natural bond strength is so low that in beams reinforced with plain bars, the bond between steel and concrete was frequently broken. Such a beam will collapse as the bar is pulled through the concrete. To prevent this, end anchorage was provided, chiefly in the form of hooks, as in Fig. 5.2. If the anchorage is adequate, such a beam will not collapse, even if the bond is broken over the entire length between anchorages. This is so because the member acts as a tied arch, as shown in Fig. 5.2, with the uncracked concrete shown shaded representing the arch and the anchored bars the tie-rod. In this case, over the length in which the bond is broken, bond forces are zero. This means that over the entire unbonded length the force in the steel is constant and equal to $T = M_{\max}/jd$. As a consequence, the total steel elongation in such beams is larger than in beams in which bond is preserved, resulting in larger deflections and greater crack widths.

To improve this situation, deformed bars are now universally used in the United States and many other countries (see Section 2.14). With such bars, the shoulders of the projecting deformations bear on the surrounding concrete and result in greatly increased bond strength. It is then possible in most cases to dispense with special anchorage devices such as hooks. In addition, crack widths as well as deflections are reduced.

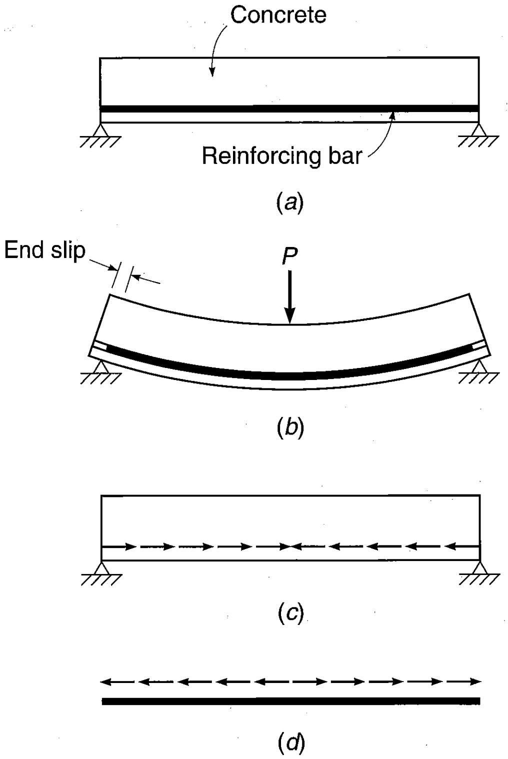

FIGURE 5.1
Bond forces due to flexure: (*a*) beam before loading; (*b*) unrestrained slip between concrete and steel; (*c*) bond forces acting on concrete; (*d*) bond forces acting on steel.

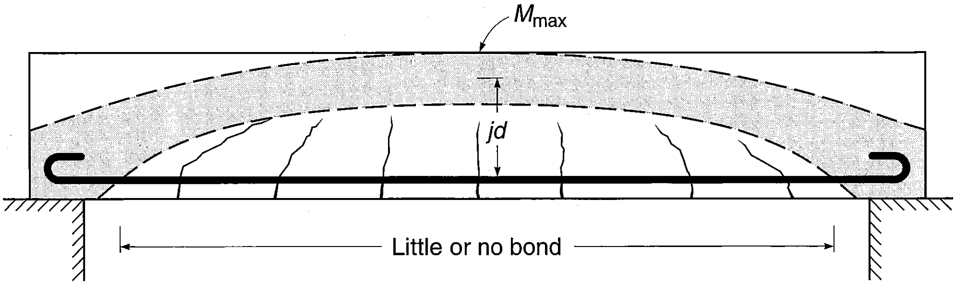

FIGURE 5.2
Tied-arch action in a beam with little or no bond.

a. Bond Force Based on Simple Cracked Section Analysis

In a short piece of a beam of length *dx*, such as shown in Fig. 5.3*a*, the moment at one end will generally differ from that at the other end by a small amount *dM*. If this piece is isolated, and if one assumes that, after cracking, the concrete does not resist any tension stresses, the internal forces are those shown in Fig. 5.3*a*. The change in bending moment *dM* produces a change in the bar force

$$dT = \frac{dM}{jd} \tag{a}$$

where *jd* is the internal lever arm between tensile and compressive force resultants. Since the bar or bars must be in equilibrium, this change in bar force is resisted at the contact surface between steel and concrete by an equal and opposite force produced by bond, as indicated by Fig. 5.3*b*.

FIGURE 5.3
Forces acting on elemental length of beam: (*a*) free-body sketch of reinforced concrete element; (*b*) free-body sketch of steel element.

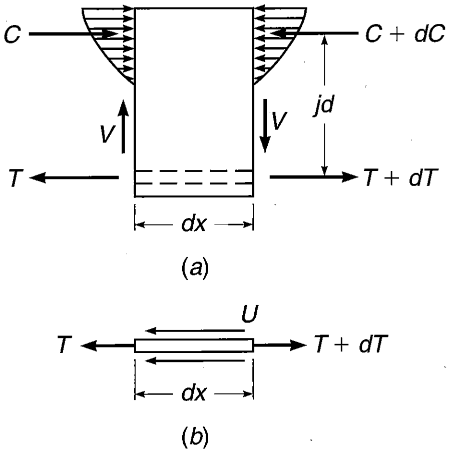

If U is the magnitude of the local bond force per unit length of bar, then, by summing horizontal forces

$$U\,dx = dT \tag{b}$$

Thus

$$U = \frac{dT}{dx} \tag{5.1}$$

indicating that the local unit bond force is proportional to the rate of change of bar force along the span. Alternatively, substituting Eq. (*a*) in Eq. (5.1), the unit bond force can be written as

$$U = \frac{1}{jd}\frac{dM}{dx} \tag{c}$$

from which

$$U = \frac{V}{jd} \tag{5.2}$$

Equation (5.2) is the "elastic cracked section equation" for flexural bond force, and it indicates that the bond force per unit length is proportional to the shear at a particular section, i.e., to the rate of change of bending moment.

Note that Eq. (5.2) applies to the *tension* bars in a concrete zone that is assumed to be fully cracked, with the concrete resisting no tension. It applies, therefore, to the tensile bars in simple spans, or, in continuous spans, either to the bottom bars in the positive bending region between inflection points or to the top bars in the negative bending region between the inflection points and the supports. It does not apply to compression reinforcement, for which it can be shown that the flexural bond forces are very low.

b. Actual Distribution of Flexural Bond Force

The actual distribution of bond force along deformed reinforcing bars is much more complex than that represented by Eq. (5.2), and Eq. (5.1) provides a better basis for understanding beam behavior. Figure 5.4 shows a beam segment subject to pure

FIGURE 5.4
Variation of steel and bond forces in a reinforced concrete member subject to pure bending: (*a*) cracked concrete segment; (*b*) bond forces acting on reinforcing bar; (*c*) variation of tensile force in steel; (*d*) variation of bond force along steel.

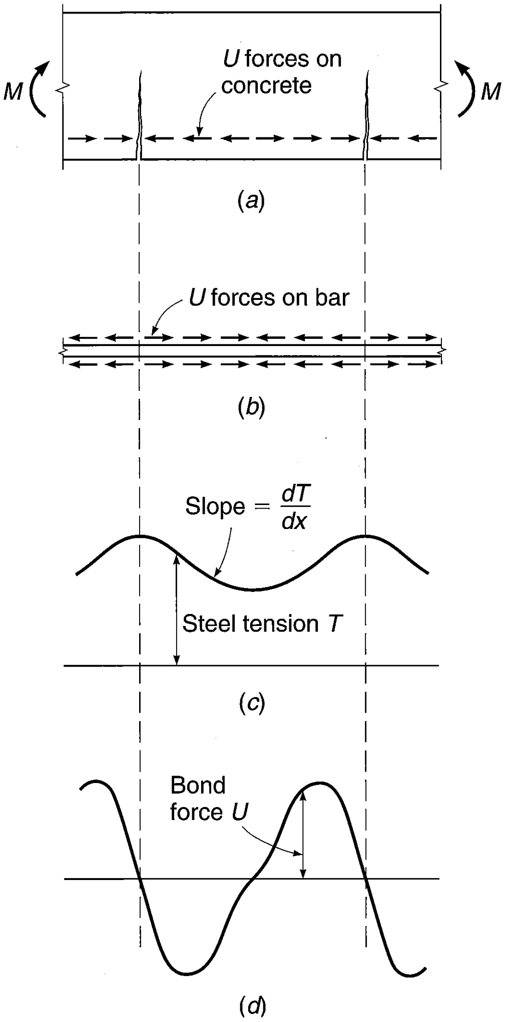

bending. The concrete fails to resist tensile stresses only where the actual crack is located; there the steel tension is maximum and has the value predicted by simple theory: $T = M/jd$. Between cracks, the concrete *does* resist moderate amounts of tension, introduced by bond forces acting along the interface in the direction shown in Fig. 5.4*a*. This reduces the tensile force in the steel, as illustrated by Fig. 5.4*c*. From Eq. (5.1), it is clear that U is proportional to the rate of change of bar force, and thus will vary as shown in Fig. 5.4*d*; unit bond forces are highest where the slope of the steel force curve is greatest and are zero where the slope is zero. Very high local bond forces adjacent to cracks have been measured in tests (Refs. 5.1 and 5.2). They are so high that inevitably some slip occurs between concrete and steel adjacent to each crack.

Beams are seldom subject to pure bending moment; they generally carry transverse loads producing shear and moment that vary along the span. Figure 5.5*a* shows a beam carrying a distributed load. The cracking indicated is typical. The steel force T predicted by simple cracked section analysis is proportional to the moment diagram and is as shown by the dashed line in Fig. 5.5*b*. However, the actual value of

FIGURE 5.5
Effect of flexural cracks on bond forces in beam: (*a*) beam with flexural cracks; (*b*) variation of tensile force T in steel along span; (*c*) variation of bond force per unit length U along span.

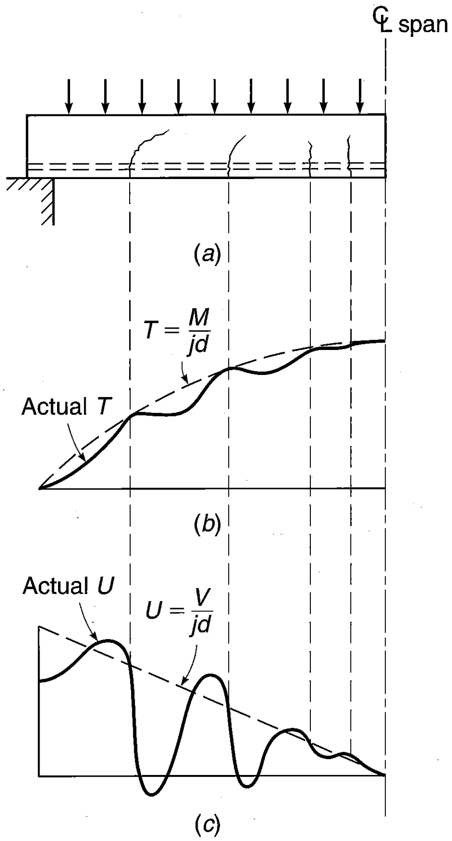

T is less than that predicted by the simple analysis everywhere except at the actual crack locations. The actual variation of T is shown by the solid line of Fig. 5.5*b*. In Fig. 5.5*c*, the bond forces predicted by the simplified theory are shown by the dashed line, and the actual variation is shown by the solid line. Note that the value of U is equal to that given by Eq. (5.2) only at those locations where the slope of the steel force diagram equals that of the simple theory. Elsewhere, if the slope is greater than assumed, the local bond force is greater; if the slope is less, local bond force is less. Just to the left of the cracks, for the present example, U is much higher than predicted by Eq. (5.2), and in all probability will result in local bond failure. Just to the right of the cracks, U is much lower than predicted and in fact is generally negative very close to the crack; i.e., the bond forces act in the reverse direction.

It is evident that actual bond forces in beams bear very little relation to those predicted by Eq. (5.2), except in the general sense that they are highest in the regions of high shear.

5.2 BOND STRENGTH AND DEVELOPMENT LENGTH

For reinforcing bars in tension, two types of bond failure have been observed. The first is *direct pullout* of the bar, which occurs when ample confinement is provided by the surrounding concrete. This could be expected when relatively small-diameter bars are used with sufficiently large concrete cover distances and bar spacing. The second type of failure is *splitting* of the concrete along the bar when cover, confinement, or bar spacing is insufficient to resist the lateral concrete tension resulting from the wedging effect of the bar deformations. Present-day design methods require that both possible failure modes be accounted for.

a. Bond Strength

If the bar is sufficiently confined by a mass of surrounding concrete, then as the tensile force on the bar is increased, adhesive bond and friction are overcome, the concrete eventually crushes locally ahead of the bar deformations, and bar pullout results. The surrounding concrete remains intact, except for the crushing that takes place ahead of the ribs immediately adjacent to the bar interface. For modern deformed bars, adhesion and friction are much less important than the mechanical interlock of the deformations with the surrounding concrete.

Bond failure resulting from splitting of the concrete is more common in beams than direct pullout. Such splitting comes mainly from wedging action when the ribs of the deformed bars bear against the concrete (Refs. 5.3 and 5.4). It may occur either in a vertical plane as in Fig. 5.6*a* or horizontally in the plane of the bars as in Fig. 5.6*b*. The horizontal type of splitting of Fig 5.6*b* frequently begins at a diagonal crack. In this case, as discussed in connection with Fig. 4.7*b* and shown in Fig. 4.1, dowel action increases the tendency toward splitting. This indicates that shear and bond failures are often intricately interrelated.

When pullout resistance is overcome or when splitting has spread all the way to the end of an unanchored bar, complete bond failure occurs. Sliding of the steel relative to the concrete leads to immediate collapse of the beam.

If one considers the large local variations of bond force caused by flexural and diagonal cracks (see Figs. 5.4 and 5.5), it becomes clear that local bond failures immediately adjacent to cracks will often occur at loads considerably below the failure load of the beam. These local failures result in small local slips and some widening of cracks and increase of deflections, but will be harmless as long as failure does not propagate all along the bar, with resultant total slip. In fact, as discussed in connection with Fig. 5.2, when end anchorage is reliable, bond can be severed along the entire length of the bar, excluding the anchorages, without endangering the carrying capacity of the beam. End anchorage can be provided by hooks as suggested by Fig. 5.2 or,

FIGURE 5.6
Splitting of concrete along reinforcement.

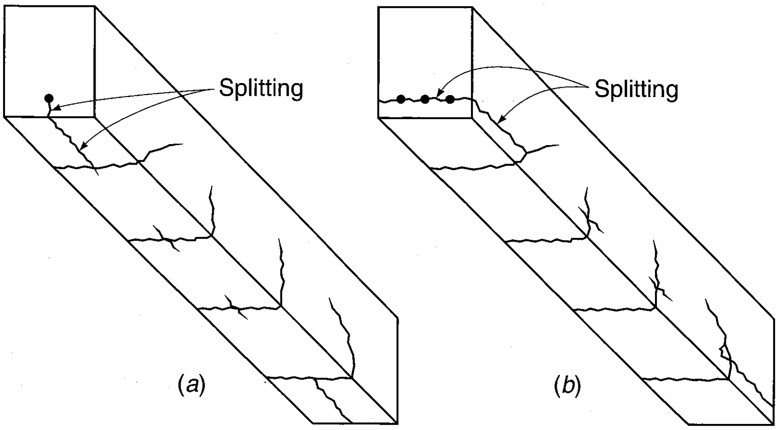

FIGURE 5.7
Development length.

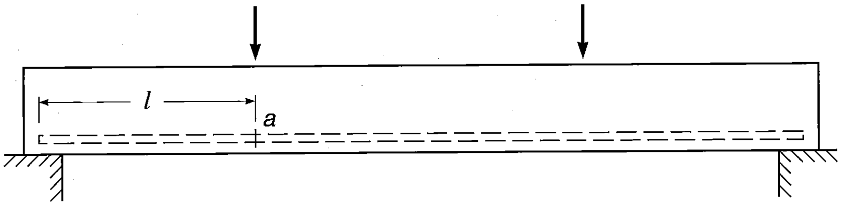

much more commonly, by extending the straight bar a sufficient distance from the point of maximum stress.

Extensive testing (Refs. 5.5 to 5.11), using beam specimens, has established limiting values of bond strength. This testing provides the basis for current design requirements.

b. Development Length

The preceding discussion suggests the concept of *development length* of a reinforcing bar. The development length is defined as that length of embedment necessary to develop the full tensile strength of the bar, controlled by either pullout or splitting. With reference to Fig. 5.7, the moment, and therefore the steel stress, is evidentally maximum at point a (neglecting the weight of the beam) and zero at the supports. If the bar stress is f_s at a, then the total tension force $A_b f_s$ must be transferred from the bar to the concrete in the distance l by bond forces. To fully develop the strength of the bar $A_b f_y$, the distance l must be at least equal to the development length of the bar, established by tests. In the beam of Fig. 5.7, if the actual length l is equal to or greater than the development length l_d, no premature bond failure will occur. That is, the beam will fail in bending or shear rather than by bond failure. This will be so even if in the vicinity of cracks local slip may have occurred over small regions along the beam.

It is seen that the main requirement for safety against bond failure is this: the length of the bar, from any point of given steel stress (f_s or at most f_y) to its nearby free end, must be at least equal to its development length. If this requirement is satisfied, the magnitude of the nominal flexural bond force along the beam, as given by Eq. (5.2), is of only secondary importance, since the integrity of the member is ensured even in the face of possible minor local bond failures. However, if the actual available length is inadequate for full development, special anchorage, such as by hooks, must be provided.

c. Factors Influencing Development Length

Experimental research has identified the factors that influence development length, and analysis of the test data has resulted in the empirical equations used in present design practice. The most basic factors will be clear from review of the preceding paragraphs and include concrete tensile strength, cover distance, spacing of the reinforcing bars, and the presence of transverse steel reinforcement.

Clearly, the *tensile strength* of the concrete is important because the most common type of bond failure in beams is the type of splitting shown in Fig. 5.6. Although tensile strength does not appear explicitly in experimentally derived equations for development length (see Section 5.3), the term $\sqrt{f'_c}$ appears in the denominator of those equations and reflects the influence of concrete tensile strength.

As discussed in Section 2.9, the fracture energy of concrete plays an important role in bond failure because a splitting crack must propagate after it has formed. Since fracture energy is largely independent of compressive strength, bond strength increases more slowly than $\sqrt{f'_c}$, and as data for higher-strength concretes have become available, $f'^{1/4}_c$ has been shown to provide a better representation of the effect of concrete strength on bond than $\sqrt{f'_c}$ (Refs. 5.12 to 5.14). This point is recognized by ACI Committee 408, Bond and Development of Reinforcement (Ref. 5.15), in proposed design expressions based on $f'^{1/4}_c$ and within the ACI Code, which sets an upper limit on the value of $\sqrt{f'_c}$ for use in design.

For lightweight concretes, the tensile strength is usually less than for normal-density concrete having the same compressive strength; accordingly, if lightweight concrete is used, development lengths must be increased. Alternatively, if split-cylinder strength is known or specified for lightweight concrete, it can be incorporated in development length equations as follows. For normal concrete, the split-cylinder tensile strength f_{ct} is generally taken as $f_{ct} = 0.56\sqrt{f'_c}$. If the split-cylinder strength f_{ct} is known for a particular lightweight concrete, then $\sqrt{f'_c}$ in the development length equations can be replaced by $f_{ct}/0.56 = 1.79\,f_{ct}$.

Cover distance—conventionally measured from the *center* of the bar to the nearest concrete face and measured either in the plane of the bars or perpendicular to that plane—also influences splitting. Clearly, if the vertical or horizontal cover is increased, more concrete is available to resist the tension resulting from the wedging effect of the deformed bars, resistance to splitting is improved, and development length is less.

Similarly, Fig. 5.6*b* illustrates that if the *bar spacing* is increased (e.g., if only two instead of three bars are used), more concrete per bar will be available to resist horizontal splitting (Ref. 5.16). In beams, bars are typically spaced about one or two bar diameters apart. On the other hand, for slabs, footings, and certain other types of member, bar spacings are typically much greater, and the required development length is reduced.

Transverse reinforcement, such as that provided by stirrups of the types shown in Fig. 4.8, improves the resistance of tensile bars to both vertical or horizontal splitting failure because the tensile force in the transverse steel tends to prevent opening of the actual or potential crack. The effectiveness of such transverse reinforcement depends on its cross-sectional area and spacing along the development length. Its effectiveness does not depend on its yield strength f_{yt}, because transverse reinforcement rarely yields during a bond failure (Refs. 5.12 to 5.15). The yield strength of the transverse steel f_{yt}, however, is presently used in the bond provisions of the ACI Code.

Based on the results of a statistical analysis of test data (Ref. 5.10), with appropriate simplifications, the length l_d needed to develop stress f_s in a reinforcing bar may be expressed as

$$l_d = \left(\frac{f_s}{1.1\sqrt{f'_c}\left(\dfrac{c + K_{tr}}{d_b}\right)} \right) d_b \tag{5.3}$$

where d_b = bar diameter

c = smaller of minimum cover or one-half of bar spacing *measured to center of bar*

$K_{tr} = 40A_{tr}/sn$, which represents effect of confining reinforcement

A_{tr} = area of transverse reinforcement normal to plane of splitting through the bars being developed
s = spacing of transverse reinforcement
n = number of bars developed or spliced at same location

Equation (5.3) captures the effects of concrete strength, concrete cover, and transverse reinforcement on l_d and serves as the basis for design in the 2008 ACI Code. For full development of the bar, f_s is set equal to f_y.

In addition to the factors just discussed, other influences have been identified. The vertical location of horizondal bars relative to beam depth has been found to have an effect (Ref. 5.17). If bars are placed in the forms during construction such that a substantial *depth of concrete is placed below those bars*, there is a tendency for excess water, often used in the mix for workability, and for entrapped air to rise to the top of the concrete during consolidation. Air and water tend to accumulate on the underside of the bars. Tests have shown a significant loss in bond strength for bars with more than 300 mm of fresh concrete cast beneath them, and accordingly the development length must be increased. This effect increases as the slump of the concrete increases and is greatest for bars cast near the upper surface of a concrete placement (Ref. 5.18).

Epoxy-coated reinforcing bars are used regularly in projects where the structure may be subjected to corrosive environmental conditions or deicing chemicals, such as for highway bridge decks and parking garages. Studies have shown that bond strength is reduced because the epoxy coating reduces the friction between the concrete and the bar, and the required development length must be increased substantially (Refs. 5.19 to 5.23). Early evidence showed that if cover and bar spacing were large, the effect of the epoxy coating would not be so pronounced, and as a result, a smaller increase was felt justified under these conditions (Ref. 5.20). Although later research (Ref. 5.12) does not support this conclusion, provisions to allow for a smaller increase remain in the ACI Code. Since the bond strength of epoxy-coated bars is already reduced because of lack of adhesion, an upper limit has been established for the product of development length factors accounting for the depth of concrete cast below horizontal bars and epoxy coating.

Not infrequently, tensile reinforcement somewhat in excess of the calculated requirement will be provided, e.g., as a result of upward rounding A_s when bars are selected or when minimum steel requirements govern. Logically, in this case, the required development length may be reduced by the ratio of steel area required to steel area actually provided. The modification for *excess reinforcement* should be applied only where anchorage or development for the full yield strength of the bar is not required.

Finally, based on bars with very short development lengths (most with values of $l_d/d_b < 15$), it was observed that *smaller-diameter bars* required lower development lengths than predicted by Eq. (5.3). As a result, the required development lengths for No. 19 (No. 6) and smaller bars were reduced below the values required by Eq. (5.3).[†]

Reference 5.15 presents a detailed discussion of the factors that control the bond and development of reinforcing bars in tension. Except as noted, these influences are accounted for in the basic equation for development length in the 2008 ACI Code.

[†] The use of Eq. (5.3) for low values of l_d/d_b greatly underestimates the actual value of bond strength and makes it appear that a lower value of l_d can be used safely. An evaluation of test results for small bars with more realistic development lengths ($l_d/d_b \geq 16$), however, has shown that the special provision in the ACI Code for smaller bars is not justified (Refs. 5.14, 5.15, and 5.24). Because of the unconservative nature of the small bar provision, ACI Committee 408 (Ref. 5.15) recommends that it not be applied in design.

All modification factors for development length are defined explicitly in the Code, with appropriate restrictions. Details are given next.

5.3 ACI CODE PROVISIONS FOR DEVELOPMENT OF TENSION REINFORCEMENT

The approach to bond strength incorporated in the ACI Code follows from the discussion presented in Section 5.2. The fundamental requirement is that the calculated force in the reinforcement at each section of a reinforced concrete member be developed on each side of that section by adequate embedment length, hooks, mechanical anchorage, or a combination of these, to ensure against pullout. Local high bond forces, such as are known to exist adjacent to cracks in beams, are not considered to be significant. Generally, the force to be developed is calculated based on the yield stress in the reinforcement; i.e., the bar strength is to be fully developed.

In the ACI Code, the required development length for deformed bars in tension is based on Eq. (5.3). A single basic equation is given that includes *all* the influences discussed in Section 5.2 and thus appears highly complex because of its inclusiveness. However, it does permit the designer to see the effects of all the controlling variables and allows more rigorous calculation of the required development length when it is critical. The ACI Code also includes simplified equations that can be used for most cases in ordinary design, provided that some restrictions are accepted on bar spacing, cover values, and minimum transverse reinforcement. These alternative equations can be further simplified for normal-density concrete and uncoated bars.†

In the following presentation of development length, the basic ACI equation is given first and its terms are defined and discussed. After this, the alternative equations, also part of the ACI Code, are presented. Note that, in any case, development length l_d must not be less than 300 mm.

a. Basic Equation for Development of Tension Bars

According to ACI Code 12.2.3, for deformed bars or deformed wires,

$$l_d = \left(\frac{f_y}{1.1\,\lambda\sqrt{f'_c}} \frac{\psi_t\,\psi_e\,\psi_s}{\left(\dfrac{c_b + K_{tr}}{d_b}\right)} \right) d_b \tag{5.4}$$

in which the term $(c + K_{tr})/d_b$ shall not be taken greater than 2.5. In Eq. (5.4), terms are defined and values established as follows.

ψ_t = reinforcement location factor	
Horizontal reinforcement so placed that more than 300 mm of fresh concrete is cast in the member below the development length or splice:	1.3
Other situations:	1.0

---

† This two-tier approach to development length corresponds exactly to the ACI Code treatment for V_c, the contribution of concrete in shear calculations. The more detailed calculation by Eq. (4.12*a*) is useful for computerized design or research but is tedious for manual calculations because of the need to recalculate the governing variables at close intervals along the span. For ordinary design, recognizing that overall economy is but little affected, the simpler but more approximate and more conservative Eq. (4.12*b*) is used.

ψ_e = coating factor	
Epoxy-coated bars or wires with cover less than $3d_b$ or clear spacing less than $6d_b$:	1.5
All other epoxy-coated bars or wires:	1.2
Uncoated and zinc-coated (galvanized) reinforcement:	1.0
However, the product of $\psi_t\psi_e$ need not be taken greater than 1.7.	
ψ_s = reinforcement size factor	
No. 19 (No. 6) and smaller bars and deformed wires:	$0.8^{\dagger}$
No. 22 (No. 7) and larger bars:	1.0
λ = lightweight aggregate concrete factor	
When lightweight aggregate concrete is used:	0.75
However, when f_{ct} is specified, $\lambda = f_{ct}/(0.56\sqrt{f_c'}) \leq 1.0$.	
When normalweight concrete is used:	1.0

c = spacing or cover dimension, mm
Use the smaller of either the distance from the center of the bar to the nearest concrete surface or one-half the center-to-center spacing of the bars being developed.

K_{tr} = transverse reinforcement index: $40A_{tr}/sn$
where A_{tr} = total cross-sectional area of all transverse reinforcement that is within the spacing s and that crosses the potential plane of splitting through the reinforcement being developed, mm^2
s = maximum spacing of transverse reinforcement within l_d center to center, mm
n = number of bars or wires being developed along the plane of splitting

As a simplification, the designer is permitted to use $K_{tr} = 0$ even if transverse reinforcement is present.

The limit of 2.5 on $(c + K_{tr})/d_b$ is imposed to avoid pullout failure. With that term taken equal to its limit of 2.5, evaluation of Eq. (5.4) results in $l_d = 0.36d_bf_y/\sqrt{f_c'}$, the experimentally derived limit found in earlier ACI Codes when pullout failure controls. Note that in Eq. (5.4) and in all other ACI Code equations relating to the development length and splices of reinforcement, *values of* $\sqrt{f_c'}$ *are not to be taken greater than 8.3 MPa* because of the lack of experimental evidence on bond strengths obtainable with concretes having compressive strength in excess of 69 MPa at the time that Eqs. (5.3) and (5.4) were formulated. More recent tests with concrete with values of f_c' to 110 MPa justify this limitation.

b. Simplified Equations for Development Length

Calculation of required development length (in terms of bar diameter) by Eq. (5.4) requires that the term $(c + K_{tr})/d_b$ be calculated for each particular combination of cover, spacing, and transverse reinforcement. Alternatively, according to the Code, a simplified form of Eq. (5.4) may be used in which $(c + K_{tr})/d_b$ is set equal to 1.5, provided that certain restrictions are placed on cover, spacing, and transverse reinforcement. Two cases of practical importance are:

1. Minimum clear cover of $1.0d_b$, minimum clear spacing of $1.0d_b$, and at least the Code required minimum stirrups or ties (see Section 4.5b) throughout l_d
2. Minimum clear cover of $1.0d_b$ and minimum clear spacing of $2d_b$

[†] ACI Committee 408 recommends a value of 1.0 for all bar sizes based on experimental evidence. The ACI Code value of 0.8, however, will be used in what follows.

TABLE 5.1
Simplified tension development length in bar diameters according to the ACI Code

	No. 19 (No. 6) and Smaller Bars and Deformed Wires†	No. 22 (No. 7) and Larger Bars
Clear spacing of bars being developed or spliced $\geq d_b$, clear cover $\geq d_b$, and stirrups or ties throughout l_d not less than the Code minimum	$l_d = \left(\dfrac{f_y \psi_t \psi_e}{2.1\lambda\sqrt{f'_c}}\right) d_b$	$l_d = \left(\dfrac{f_y \psi_t \psi_e}{1.7\lambda\sqrt{f'_c}}\right) d_b$
Clear spacing of bars being developed or spliced $\geq 2d_b$, and clear cover $\geq d_b$	Same as above	Same as above
Other cases	$l_d = \left(\dfrac{3f_y \psi_t \psi_e}{1.4\lambda\sqrt{f'_c}}\right) d_b$	$l_d = \left(\dfrac{3f_y \psi_t \psi_e}{1.1\lambda\sqrt{f'_c}}\right) d_b$

† For reasons discussed in Section 5.3a, ACI Committee 408 recommends that l_d for No. 22 (No. 7) and larger bars be used for all bar sizes.

For either of these common cases, it is easily confirmed from Eq. (5.4) that for No. 22 (No. 7) and larger bars

$$l_d = \left(\frac{f_y \psi_t \psi_e}{1.7\lambda\sqrt{f'_c}}\right) d_b \tag{5.5a}$$

and for No. 19 (No. 6) bars and smaller (with $\gamma = 0.8$)

$$l_d = \left(\frac{f_y \psi_t \psi_e}{2.1\lambda\sqrt{f'_c}}\right) d_b \tag{5.5b}$$

If these restrictions on spacing are not met, then, provided that Code-imposed minimum spacing requirements are met (see Section 3.6c), the term $(c + K_{tr})/d_b$ will have a value not less than 1.0 (rather than 1.5 as before) whether or not transverse steel is used. The values given by Eqs. (5.5*a*) and (5.5*b*) are then multiplied by the factor 1.5/1.0.

Thus if the designer accepts certain restrictions on bar cover, spacing, and transverse reinforcement, simplified calculation of development requirements is possible. The simplified equations are summarized in Table 5.1.

Further simplification is possible for the most common condition of normal-density concrete and uncoated reinforcement. Then λ and ψ_e in Table 5.1 take the value 1.0, and the development lengths, in terms of bar diameters, are simply a function of f_y, f'_c, and the bar location factor ψ_t. Thus development lengths are easily tabulated for the usual combinations of material strengths and bottom or top bars and for the restrictions on bar spacing, cover, and transverse steel defined.† Results are given in Table A.10 of Appendix A.

Regardless of whether development length is calculated using the basic Eq. (5.4) or the more approximate Eqs. (5.5*a*) and (5.5*b*), development length may be reduced where reinforcement in a flexural member is in excess of that required by analysis, except where anchorage or development for f_y is specifically required or the reinforcement is designed for a region of high seismic risk. According to the ACI Code, the reduction is made according to the ratio (A_s required/A_s provided).

---

† Note that, for convenient reference, the term top bar is used for any horizontal reinforcing bar placed with more than 300 mm of fresh concrete cast below the development length or splice. This definition may require that bars relatively near the bottom of a deep member be treated as top bars.

EXAMPLE 5.1 **Development length in tension.** Figure 5.8 shows a beam-column joint in a continuous building frame. Based on frame analysis, the negative steel required at the end of the beam is 1870 mm^2; two No. 36 (No. 11) bars are used, providing $A_s = 2012$ mm^2. Beam dimensions are $b = 250$ mm, $d = 450$ mm, and $h = 530$ mm. The design will include No. 10 (No. 3) stirrups spaced four at 75 mm followed by a constant 125 mm spacing in the region of the support, with 40 mm clear cover. Normalweight concrete is to be used, with $f'_c = 28$ MPa, and reinforcing bars have $f_y = 420$ MPa. Find the minimum distance l_d at which the negative bars can be cut off, based on development of the required steel area at the face of the column, (*a*) using the simplified equations of Table 5.1, (*b*) using Table A.10, of Appendix A, and (*c*) using the basic Eq. (5.4).

SOLUTION. Checking for lateral spacing in the No. 36 (No. 11) bars determines that the clear distance between the bars is $250 - 2(40 + 9.5 + 35.8) = 79$ mm, or 2.22 times the bar diameter d_b. The clear cover of the No. 36 (No. 11) bars to the side face of the beam is $40 + 9.5 = 49.5$ mm, or 1.38 bar diameters, and that to the top of the beam is $80 - 35.8/2 = 62.1$ mm, or 1.78 bar diameters. These dimensions meet the restrictions stated in the second row of Table 5.1. Then for top bars, uncoated, and with normal-density concrete, we have the values of $\psi_t = 1.3$, $\psi_e = 1.0$, and $\lambda = 1.0$. From Table 5.1,

$$l_d = \frac{420 \times 1.3 \times 1.0}{1.7 \times 1.0\sqrt{28}} 35.8 = 61 \times 35.8 = 2180 \text{ mm}$$

This can be reduced by the ratio of steel required to that provided, so that the final development length is $2180 \times 1870/2012 = 2030$ mm.

Alternatively, from the lower portion of Table A.10, $l_d/d_b = 61$. The required length to point of cutoff is $61 \times 35.8 \times 1870/2012 = 2030$ mm, as before.

The more accurate Eq. (5.4) will now be used. The center-to-center spacing of the No. 36 (No. 11) bars is $250 - 2(40 + 9.5 + 35.8/2) = 115$ mm, one-half of which is 57.5 mm. The side cover to bar centerline is $40 + 9.5 + 35.8/2 = 67$ mm, and the top cover is 80 mm. The smallest of these three distances controls, and $c = 57.5$ mm. Potential splitting would be in the

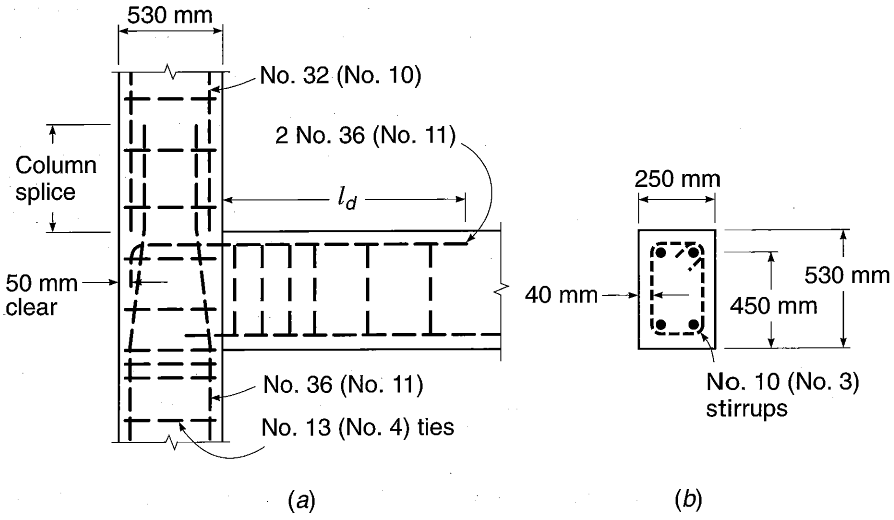

FIGURE 5.8
Bar details at beam-column joint for bar development examples.

horizontal plane of the bars, and in calculating A_{tr} two times the stirrup bar area is used.[†] Based on the No. 10 (No. 3) stirrups at 125 mm spacing:

$$K_{tr} = \frac{40 \times 71 \times 2}{125 \times 2} = 22.7 \qquad \text{and} \qquad \frac{c + K_{tr}}{d_b} = \frac{57.5 + 22.7}{35.8} = 2.24$$

This is less than the limit value of 2.5. Then from Eq. (5.4)

$$l_d = \frac{420 \times 1.3}{1.1 \times 1.0\sqrt{28} \times 2.24} 35.8 = 42 \times 35.8 = 1500 \text{ mm}$$

and the required development length is $1500 \times 1870/2012 = 1395$ mm rather than 2180 mm as before. Clearly, the use of the more accurate Eq. (5.4) permits a considerable reduction in development length. Even though its use requires much more time and effort, it is justified if the design is to be repeated many times in a structure.

5.4 ANCHORAGE OF TENSION BARS BY HOOKS

a. Standard Dimensions

In the event that the desired tensile stress in a bar cannot be developed by bond alone, it is necessary to provide special anchorage at the ends of the bar, usually by means of a 90° or a 180° hook or a headed bar (the latter is discussed in Section 5.5). The dimensions and bend radii for hooks have been standardized in ACI Code 7.1 as follows (see Fig. 5.9):

1. A 180° bend plus an extension of at least 4 bar diameters, but not less than 65 mm at the free end of the bar, or
2. A 90° bend plus an extension of at least 12 bar diameters at the free end of the bar, or
3. For stirrup and tie anchorage only:
   (*a*) For No. 16 (No. 5) bars and smaller, a 90° bend plus an extension of at least 6 bar diameters at the free end of the bar, or
   (*b*) For Nos. 19, 22, and 25 (Nos. 6, 7, and 8) bars, a 90° bend plus an extension of at least 12 bar diameters at the free end of the bar, or
   (*c*) For No. 25 (No. 8) bars and smaller, a 135° bend plus an extension of at least 6 bar diameters at the free end of the bar.

The minimum diameter of bend, measured on the inside of the bar, for standard hooks other than for stirrups or ties in sizes Nos. 10 through 16 (Nos. 3 through 5), should be not less than the values shown in Table 5.2. For stirrup and tie hooks, for bar sizes No. 16 (No. 5) and smaller, the inside diameter of bend should not be less than 4 bar diameters, according to the ACI Code.

When welded wire reinforcement (smooth or deformed wires) is used for stirrups or ties, the inside diameter of bend should not be less than 4 wire diameters for deformed wire larger than MD 40 and 2 wire diameters for all other wires. Bends with an inside diameter of less than 8 wire diameters should not be less than 4 wire diameters from the nearest welded intersection.

[†] If the top cover had controlled, the potential splitting plane would be vertical and one times the stirrup bar area would be used in calculating A_{tr}.

FIGURE 5.9
Standard bar hooks: (*a*) main reinforcement; (*b*) stirrups and ties.

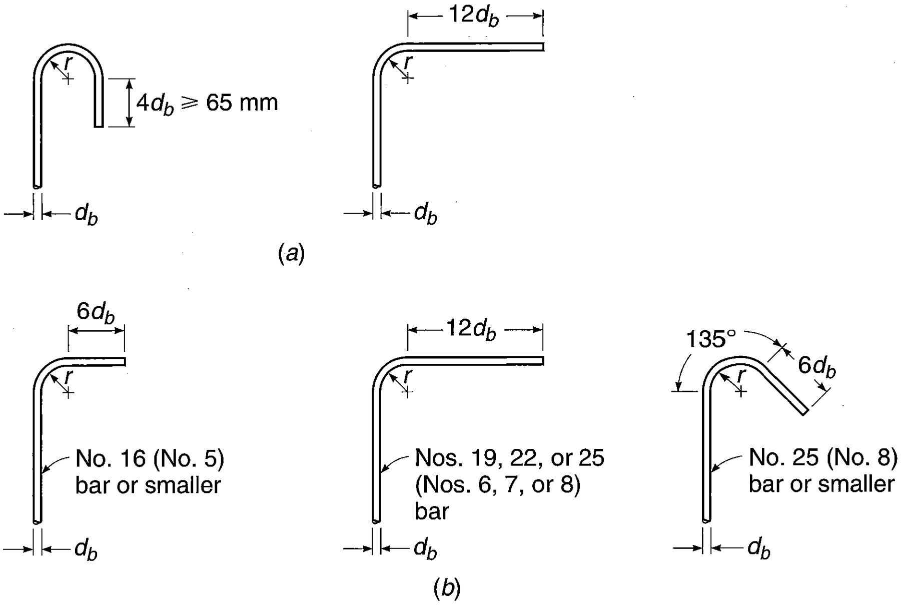
12d_b
r
4d_b ≥ 65 mm
d_b
d_b
(a)
6d_b
r
No. 16 (No. 5) bar or smaller
d_b
12d_b
r
Nos. 19, 22, or 25 (Nos. 6, 7, or 8) bar
d_b
135°
6d_b
r
No. 25 (No. 8) bar or smaller
d_b
(b)

TABLE 5.2
Minimum diameters of bend for standard hooks

Bar Size	Minimum Diameter
Nos. 10 through 25 (Nos. 3 through 8)	6 bar diameters
Nos. 29, 32, and 36 (Nos. 9, 10, and 11)	8 bar diameters
Nos. 43 and 57 (Nos. 14 and 18)	10 bar diameters

b. Development Length and Modification Factors for Hooked Bars

Hooked bars resist pullout by the combined actions of bond along the straight length of bar leading to the hook and anchorage provided by the hook. Tests indicate that the main cause of failure of hooked bars in tension is splitting of the concrete in the plane of the hook. This splitting is due to the very high stresses in the concrete inside of the hook; these stresses are influenced mainly by the bar diameter d_b for a given tensile force, and the radius of bar bend. Resistance to splitting has been found to depend on the concrete cover for the hooked bar, measured laterally from the edge of the member to the bar perpendicular to the plane of the hook, and measured to the top (or bottom) of the member from the point where the hook starts, parallel to the plane of the hook. If these distances must be small, the strength of the anchorage can be substantially increased by providing confinement steel in the form of closed stirrups or ties.

ACI Code 12.5 provisions for hooked bars in tension are based on research summarized in Refs. 5.8 and 5.9. The Code requirements account for the combined contribution of bond along the straight bar leading to the hook, plus the hooked anchorage. A total development length l_{dh} is defined as shown in Fig. 5.10 and is

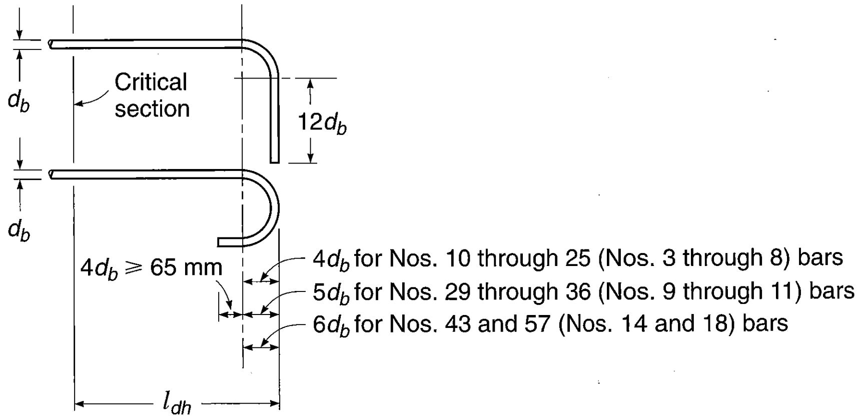

d_b
Critical section
$12d_b$
d_b
$4d_b \geqslant 65$ mm
$4d_b$ for Nos. 10 through 25 (Nos. 3 through 8) bars
$5d_b$ for Nos. 29 through 36 (Nos. 9 through 11) bars
$6d_b$ for Nos. 43 and 57 (Nos. 14 and 18) bars
l_{dh}

FIGURE 5.10
Bar details for development of standard hooks.

measured from the critical section to the farthest point on the bar, parallel to the straight part of the bar. For standard hooks, as shown in Fig. 5.9, the development length is

$$l_{dh} = \left(\frac{0.24\, \psi_e f_y}{\lambda \sqrt{f_c'}} \right) d_b \tag{5.6}$$

with $\psi_e = 1.2$ for epoxy-coated reinforcement and $\lambda = 0.75$ for lightweight aggregate concrete. For other cases, ψ_e and λ are taken as 1.0.

The development length l_{dh} should be multiplied by certain applicable modifying factors, summarized in Table 5.3. These factors are combined as appropriate; e.g., if side cover of at least 65 mm is provided for a 180° hook and if, in addition, ties are provided, the development length is multiplied by the product of 0.7 and 0.8. In any case, the length l_{dh} is not to be less than 8 bar diameters and not less than 150 mm.

Transverse confinement steel is essential if the full bar strength must be developed with minimum concrete confinement, such as when hooks may be required at the ends of a simply supported beam or where a beam in a continuous structure frames into an end column and does not extend past the column or when bars must be anchored in a short cantilever, as shown in Fig. 5.11 (Ref. 5.11). According to ACI Code 12.5.4, for bars hooked at the discontinuous ends of members with both side

FIGURE 5.11
Transverse reinforcement requirements at discontinuous ends of members with small cover distances.

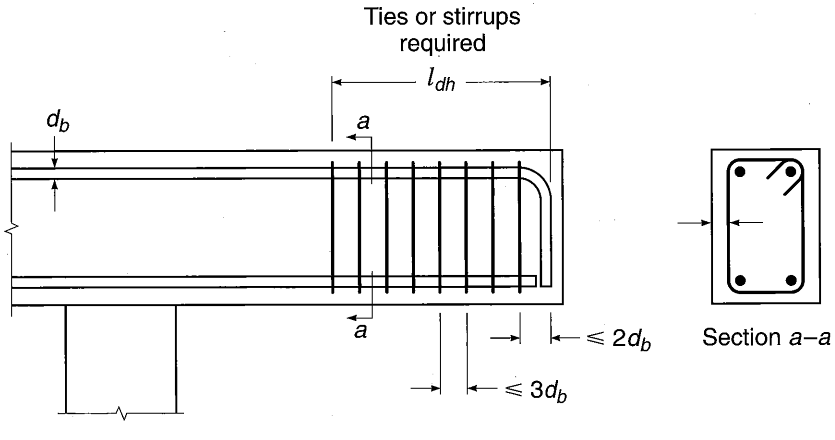

Ties or stirrups required
l_{dh}
d_b
a
a
$\leqslant 2d_b$
$\leqslant 3d_b$
Section a–a

TABLE 5.3
Development lengths for hooked deformed bars in tension

A. Development length l_{dh} for hooked bars	$\left(\dfrac{0.24\psi_e f_y}{\lambda\sqrt{f_c'}}\right) d_b$
B. Modification factors applied to l_{dh}	
For No. 36 (No. 11) and smaller bar hooks with side cover (normal to plane of hook) not less than 65 mm, and for 90° hooks with cover on bar extension beyond hook not less than 50 mm	0.7
For 90° hooks of No. 36 (No. 11) and smaller bars that are either enclosed within ties or stirrups perpendicular to the bar being developed, spaced not greater than $3d_b$ along the development length l_{dh} of the hook; or enclosed within ties or stirrups parallel to the bar being developed, spaced not greater than $3d_b$ along the length of the tail extension of the hook plus bend	0.8
For 180° hooks of No. 36 (No. 11) and smaller bars that are enclosed within ties or stirrups perpendicular to the bar being developed, spaced not greater than $3d_b$ along the development length l_{dh} of the hook	0.8
Where anchorage or development for f_y is not specifically required, reinforcement in excess of that required by analysis	$\dfrac{A_s \text{ required}}{A_s \text{ provided}}$
ψ_e:	
For epoxy-coated bars	1.2
For other bars	1.0
λ:	
For lightweight concrete	0.75
For normalweight concrete	1.0

cover and top or bottom cover less than 65 mm, hooks *must* be enclosed with closed stirrups or ties along the full development length, as shown in Fig. 5.11. The spacing of the confinement steel must not exceed 3 times the diameter of the hooked bar d_b, and the first stirrup or tie must enclose the bent portion of the hook within a distance equal to $2d_b$ of the outside of the bend. In such cases, the factor 0.8 of Table 5.3 does not apply.

EXAMPLE 5.2 **Development of hooked bars in tension.** Referring to the beam-column joint shown in Fig. 5.8, the No. 36 (No. 11) negative bars are to be extended into the column and terminated in a standard 90° hook, keeping 50 mm clear to the outside face of the column. The column width in the direction of beam width is 400 mm. Find the minimum length of embedment of the hook past the column face, and specify the hook details.

SOLUTION. The development length for hooked bars, measured from the critical section along the bar to the far side of the vertical hook, is given by Eq. (5.6):

$$l_{dh} = \frac{0.24 \times 1.0 \times 420}{1.0 \times \sqrt{28}} 35.8 = 680 \text{ mm}$$

In this case, side cover for the No. 36 (No. 11) bars exceeds 65 mm and cover beyond the bent bar is adequate, so a modifying factor of 0.7 can be applied. The only other factor applicable is for excess reinforcement, which is 0.93 as for Example 5.1. Accordingly, the minimum development length for the hooked bars is

$$l_{dh} = 680 \times 0.7 \times 0.93 = 440 \text{ mm}$$

With $530 - 50 = 480$ mm available, the required length is contained within the column. The hook will be bent to a minimum diameter of $8 \times 35.8 = 286$ mm. The bar will continue for 12 bar diameters, or 430 mm past the end of the bend in the vertical direction.

5.5 ANCHORAGE IN TENSION USING HEADED BARS

a. Requirements for Headed Bars

Headed bars provide an alternative to hooks when the desired tensile stress in the bar cannot be developed by bond alone. ACI Code 3.5.9 requires that headed deformed bars conform to ASTM A970 and, in addition, that obstructions or interruptions of the bar deformations not extend more than 2 bar diameters from the bearing face of the head, as shown in Fig. 5.12. While heads come in many configurations and sizes, ACI Code 12.6.1 requires that the bearing area of the head A_{brg} be equal to at least 4 times the area of the bar A_b.

Obstructions, such as shown in Fig. 5.12, are not counted as part of the bearing area according to the Commentary to ACI Code 3.5.9, and thus, the net bearing area of the head may be less than the gross area of the head minus the area of the bar.

b. Development Length and Modification Factors for Headed Bars

Differences between the mode of failure of headed bars loaded in tension and those exhibited by straight bars and hooks, coupled with the fact that only limited test data are available for headed bars, have resulted in the ACI Code adding restrictions to the design criteria for headed bars.

The bond strength of headed bars results from a combination of bond along the length of the bar and bearing at the face of the head. Prior to failure, the bond force along the bar increases and then decreases as slip occurs, while the bearing force on

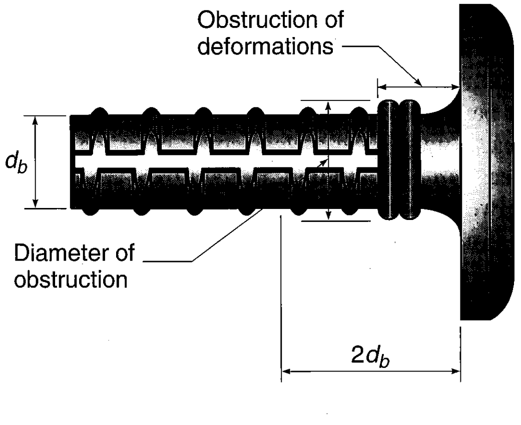

FIGURE 5.12
Headed deformed reinforcing bar with an obstruction of the deformations that extends less than 2 bar diameters from the bearing face of the head.

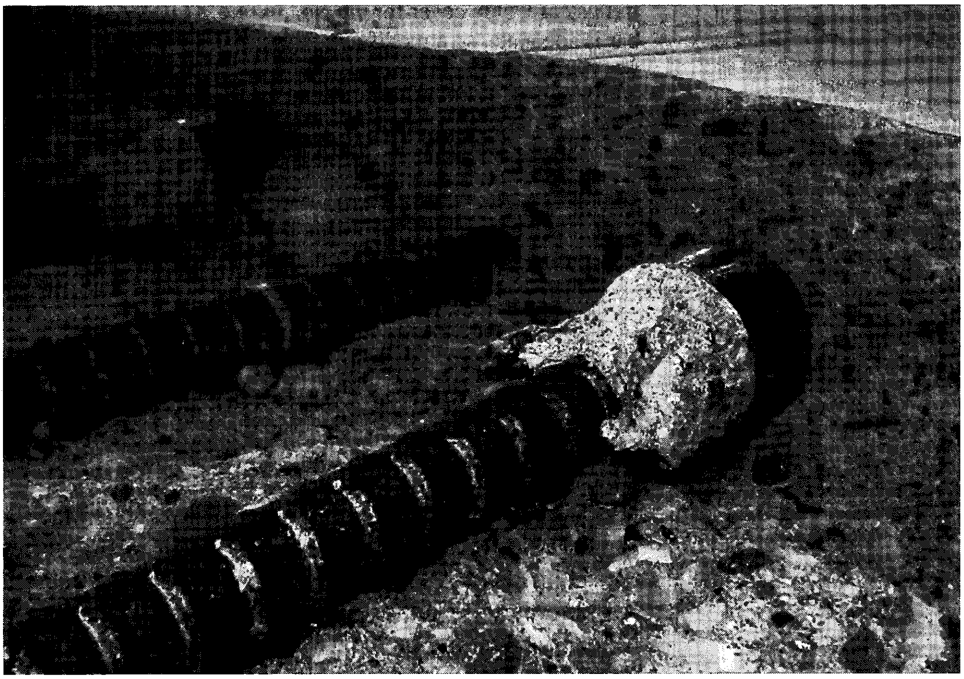

FIGURE 5.13
Headed deformed bars showing conical concrete wedges. (*Photograph courtesy of Michael Keith Thompson.*)

the head increases. In some cases, the contribution of bond along the length of the bar may become negligible prior to failure. Unlike straight reinforcing bars, which tend to fail in bond due to the formation of splitting cracks between bars or between the bar and the surface of the concrete, and hooks, which tend to fail in bond by cracking in the plane of the hook, headed bars fail in bond due to the formation of a conical wedge, as shown in Fig. 5.13, which causes radial splitting cracks in the concrete. In addition to radial splitting, failure can also occur due to the formation of a flat concrete cone near the surface (shallow pullout), if the development is relatively short, or a breakout cone, if the development length is long, and due to spalling or side-face blowout, if the side cover is low (Refs. 5.25 to 5.28). Transverse confining reinforcement, such as stirrups and ties, which increase the bond strength of both straight and hooked bars, provides little additional capacity to headed bars and is, thus, not considered when calculating the development length of headed bars. Because transverse reinforcement limits the width of splitting cracks, however, its use is still recommended when headed bars are used.

Because test data are not available for a wide range of concrete properties, bar sizes, and member geometries, the design provisions are restricted to No. 36 (No. 11) and smaller bars with yield strengths not greater than 420 MPa. The bars, as distinct from the heads, must have a clear cover of at least $2d_b$ and a clear spacing between bars of at least $4d_b$. In addition, headed bars are restricted by ACI Code 12.6 to use with normalweight concrete, and the value of f'_c used to calculate the development length l_{dt} is limited to 42 MPa. The development length for headed deformed bars in tension is

$$l_{dt} = \left(\frac{0.19\psi_e f_y}{\sqrt{f'_c}}\right)d_b \tag{5.7}$$

where $\psi_e = 1.2$ for epoxy-coated reinforcement and 1.0 for other cases.

TABLE 5.4
Development lengths for headed deformed bars in tension

A. Development length l_{dt} for headed bars	$\left(\dfrac{0.19\psi_e f_y}{\sqrt{f'_c}}\right) d_b$
B. Modification factors applied to l_{dt}	
Where anchorage or development for f_y is not specifically required, reinforcement in excess of that required by analysis	$\dfrac{A_s \text{ required}}{A_s \text{ provided}}$
ψ_e	
For epoxy-coated bars	1.2
For other bars	1.0

Where the reinforcement provided exceeds that required by analysis, except when development of the yield strength f_y is specifically required, the value of l_{dt} in Eq. (5.7) may be multiplied by the factor (A_s required)/(A_s provided). Under any circumstances, l_{dt} may not be less than 8 bar diameters or less than 150 mm. Calculation of the development length l_{dt} and the applicable modifying factors are summarized in Table 5.4.

The development length l_{dt} should be measured from the bearing face of the head to the critical section, as shown in Fig. 5.14. When headed bars from a flexural member, such as a beam or a slab, terminate in a supporting member, such as the column shown in Fig. 5.15, the commentary to ACI Code 12.6 recommends that the bar be extended "through the joint to the far face of the confined core of the supporting member, allowing for cover and avoidance of interference with column reinforcement," even if the resulting anchorage length is greater than l_{dt}. Doing so helps to adequately anchor

FIGURE 5.14
Development length of headed deformed bars.

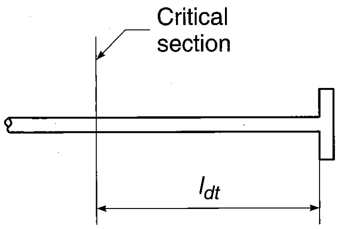

FIGURE 5.15
Headed deformed bar extended to far side of column with anchorage length that exceeds l_{dt}.

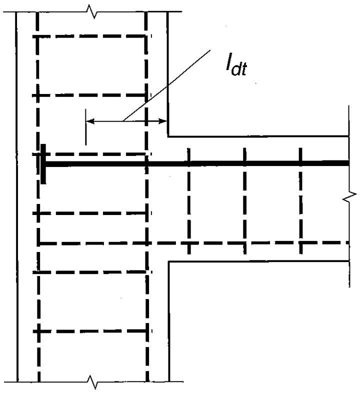

the compressive forces that are developed at the face of the head and improves the performance of the beam-column connection.

c. Mechanical Anchorage

In cases where headed bars do not meet the requirements specified in Section 12.6 or in cases where bars are terminated by mechanisms such as welded plates or other manufactured devices, ACI Code 12.6.4 allows such devices to be used to develop the reinforcement if the adequacy of the devices is established by tests. In such cases, the development of the reinforcement may consist of the combined contributions of bond along the length of the bar leading to the critical section, plus that of the mechanical anchorage, much in the way that the total resistance of headed bars is provided.

EXAMPLE 5.3

Development of headed deformed bars in tension. Three No. 22 (No. 7) bars serve as top reinforcement for a bracket framing into a 400 × 400 mm column (Fig. 5.16). The bracket projects 375 mm from the column and is the same width as the column. The top cover to the center of the bars is 75 mm, and the side cover to the center of the bars is 90 mm. The bars are spaced laterally at 115 mm. These dimensions are inadequate for straight development length or for standard hooks. Based on other reinforcement, cover requirements, and head thickness, total development lengths for headed bars of 300 mm in the column and 315 mm in the bracket are available. The reinforcing bars have $f_y = 420$ MPa, and the concrete is normalweight with $f'_c = 35$ MPa. Determine if a bar with heads at both ends can be used in this application.

SOLUTION. The minimum head size is $A_{brg} = 4A_b = 1550\ \text{mm}^2$. The smaller available anchorage length in the column governs. Assuming that the bars will be used at the full yield strength, the development length l_{dt} calculated using Eq. (5.7) is

$$l_{dt} = \left(\frac{0.19\psi_e f_y}{\sqrt{f'_c}}\right)d_b = \left(\frac{0.19 \times 1.0 \times 420}{\sqrt{35}}\right)22.2 = 299\ \text{mm}$$

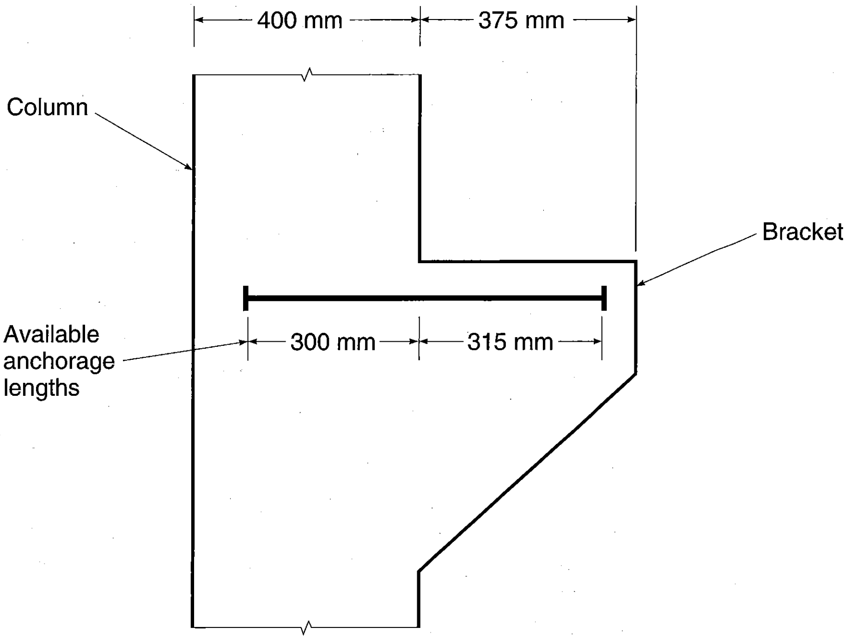

FIGURE 5.16
Column and bracket for headed deformed bar development example.

which must be checked against the minimum values for l_{dt}, which are

$$l_{dt} \geq 8d_b = 178 \text{ mm}$$
$$l_{dt} \geq 150 \text{ mm}$$

Thus, the value of l_{dt} obtained using Eq. (5.7) governs and is less than the available anchorage length. Thus, a bar with heads at both ends can be used, with a distance between heads of 615 mm, as shown in Fig. 5.16.

5.6 ANCHORAGE REQUIREMENTS FOR WEB REINFORCEMENT

Stirrups should be carried as close as possible to the compression and tension faces of a beam, and special attention must be given to proper anchorage. The truss model (see Section 4.8 and Fig. 4.19) for design of shear reinforcement indicates the development of diagonal compressive struts, the thrust from which is equilibrated, near the top and bottom of the beam, by the tension web members (i.e., the stirrups). Thus, at the factored load, the tensile strength of the stirrups must be developed for almost their full height. Clearly, it is impossible to do this by development length. For this reason, stirrups normally are provided with 90° or 135° hooks at their upper end (see Fig. 5.9*b* for standard hook details) and at their lower end are bent 90° to pass around the longitudinal reinforcement. In simple spans, or in the positive bending region of continuous spans, where no top bars are required for flexure, stirrup support bars must be used. These are usually about the same diameter as the stirrups themselves, and they not only provide improved anchorage of the hooks but also facilitate fabrication of the reinforcement cage, holding the stirrups in position during placement of the concrete.

ACI Code 12.13 includes special provisions for anchorage of web reinforcement. The ends of single-leg, simple-U, or multiple-U stirrups are to be anchored by one of the following means:

1. For No. 16 (No. 5) bars and smaller, and for Nos. 19, 22, and 25 (Nos. 6, 7, and 8) bars with f_{yt} of 280 MPa or less, a standard hook around longitudinal reinforcement, as shown in Fig. 5.17*a*.
2. For Nos. 19, 22, and 25 (Nos. 6, 7, and 8) stirrups with f_{yt} greater than 280 MPa, a standard hook around a longitudinal bar, plus an embedment between midheight of the member and the outside end of the hook equal to or greater than $0.17 d_b f_{yt}/\lambda\sqrt{f_c'}$ mm, as shown in Fig. 5.17*b*.

ACI Code 12.13 specifies further that, between anchored ends, each bend in the continuous portion of a simple-U or multiple-U stirrup shall enclose a longitudinal bar, as in Fig. 5.17*c*. Longitudinal bars bent to act as shear reinforcement, if extended into a region of tension, shall be continuous with longitudinal reinforcement and, if extended into a region of compression, shall be anchored beyond middepth $d/2$ as specified for development length. Pairs of U stirrups or ties so placed as to form a closed unit shall be considered properly spliced when length of laps are $1.3l_d$ as in Fig. 5.17*d*. In members at least 450 mm deep, such splices are considered adequate if $A_b f_{yt} \leq 40$ kN and the stirrup legs extend the full depth of the member. As will be discussed in Section 5.11, pairs of U stirrups may not be used in perimeter beams.

Other provisions are contained in the ACI Code relating to the use of welded wire reinforcement, which is sometimes used for web reinforcement in precast and prestressed concrete beams.

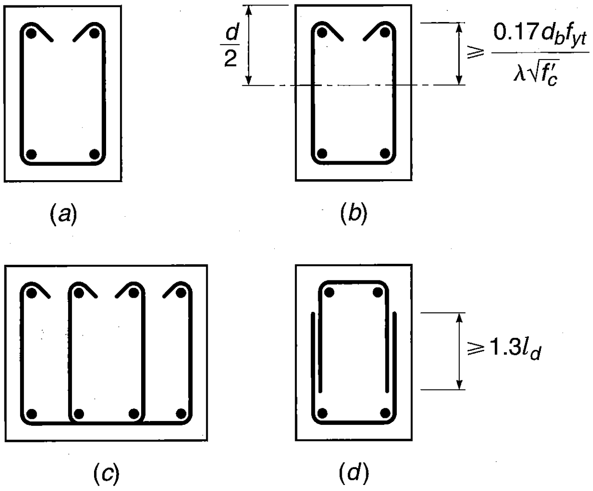

FIGURE 5.17
ACI requirements for stirrup anchorage: (*a*) No. 16 (No. 5) stirrups and smaller, and Nos. 19, 22, and 25 (Nos. 6, 7, and 8) stirrups with yield stress not exceeding 280 MPa; (*b*) Nos. 19, 22, and 25 (Nos. 6, 7, and 8) stirrups with yield stress exceeding 280 MPa; (*c*) wide beam with multiple-leg U stirrups; (*d*) pairs of U stirrups forming a closed unit. See Fig. 5.9 for alternative standard hook details.

5.7 WELDED WIRE REINFORCEMENT

Tensile steel consisting of welded wire reinforcement (often referred to as welded wire fabric), with either deformed or smooth wires, is commonly used in one-way and two-way slabs and certain other types of members (see Section 2.15). For *deformed* wire reinforcement, some of the development is assigned to the welded cross wires and some to the embedded length of the deformed wire. According to ACI Code 12.7, the development length of welded deformed wire reinforcement measured from the point of the critical section to the end of the wire is computed as the product of the development length l_d from Table 5.1 or from the more accurate Eq. (5.4) and the appropriate modification factor or factors related to those equations, except that the development length is not to be less than 200 mm. For welded deformed wire reinforcement with at least one cross wire within the development length and not less than 50 mm from the point of the critical section, a *deformed wire factor* ψ_w equal to the greater of

$$\frac{f_y - 240}{f_y} \tag{5.8a}$$

or

$$\frac{5d_b}{s} \tag{5.8b}$$

is applied, where s is the lateral spacing of the wires being developed; but this factor need not exceed 1.0. When ψ_w from Eq. (5.8*a*) or (5.8*b*) is used, the epoxy coating factor ψ_e is taken as 1.0. For welded wire deformed reinforcement with no cross wires within the development length or with a single cross wire less than 50 mm from the point of the critical section, the wire fabric factor is taken to be equal to 1.0 and the development length determined as for the deformed wire.

For welded *plain* wire reinforcement, development is considered to be provided by embedment of two cross wires, with the closer wire not less than 50 mm from the critical section. However, the development length measured from the critical section to the outermost cross wire is not to be less than

$$l_d = 3.3 \frac{A_b}{s} \frac{f_y}{\lambda \sqrt{f'_c}} \tag{5.9}$$

according to ACI Code 12.8, where A_b is the cross-sectional area of an individual wire to be developed or spliced. The modification factor for excess reinforcement may be applied, but l_d is not to be less than 150 mm for the welded plain wire reinforcement.[†]

5.8 DEVELOPMENT OF BARS IN COMPRESSION

Reinforcement may be required to develop its compressive strength by embedment under various circumstances, e.g., where bars transfer their share of column loads to a supporting footing or where lap splices are made of compression bars in column (see Section 5.13). In the case of bars in compression, a part of the total force is transferred by bond along the embedded length, and a part is transferred by end bearing of the bars on the concrete. Because the surrounding concrete is relatively free of cracks and because of the beneficial effect of end bearing, shorter basic development lengths are permissible for compression bars than for tension bars. If transverse confinement steel is present, such as spiral column reinforcement or special spiral steel around an individual bar, the required development length is further reduced. Hooks and heads such as are shown in Figs. 5.9 and 5.12 are *not* effective in transferring compression from bars to concrete, and, if present for other reasons, should be disregarded in determining required embedment length.

According to ACI Code 12.3, the development length in compression is the greater of

$$l_{dc} = \left(\frac{0.24 f_y}{\lambda \sqrt{f'_c}} \right) d_b \tag{5.10a}$$

and

$$l_{dc} = 0.043 f_y d_b \tag{5.10b}$$

Modification factors summarized in part *B* of Table 5.5, as applicable, are applied to the development length in compression to obtain the value of development length l_{dc} to be used in design. In no case is l_d to be less than 200 mm, according to the ACI Code. Basic and modified compressive development lengths are given in Table A.11 of Appendix A.

5.9 BUNDLED BARS

It was pointed out in Section 3.6c that it is sometimes advantageous to "bundle" tensile reinforcement in large beams, with two, three, or four bars in contact, to provide for improved placement of concrete around and between bundles of bars. Bar bundles are typically triangular or L-shaped for three bars, and square for four. When bars are cut off in a bundled group, the cutoff points must be staggered at least 40 diameters.

[†] The ACI Code offers no explanation as to why $l_{d,\min} = 150$ mm for welded plain wire reinforcement, but 200 mm for welded deformed wire reinforcement.

TABLE 5.5
Development lengths for deformed bars in compression

A. Basic development length l_{dc}	$\begin{cases} \geq \left(\dfrac{0.24 f_y}{\lambda \sqrt{f_c'}}\right) d_b \\ \geq 0.043 f_y d_b \end{cases}$
B. Modification factors to be applied to l_{dc}	
Reinforcement in excess of that required by analysis	$\dfrac{A_s \text{ required}}{A_s \text{ provided}}$
Reinforcement enclosed within spiral reinforcement not less than 6 mm diameter and not more than 100 mm pitch or within No. 13 (No. 4) ties spaced at not more than 100 mm on centers	0.75

According to ACI Code 12.4, the development length of individual bars within a bundle, for both tension and compression, is that of the individual bar increased by 20 percent for a three-bar bundle and by 33 percent for a four-bar bundle, to account for the probable deficiency of bond at the inside of the bar group.

For bundled bars, to determine the appropriate spacing and cover values (1) for use in Table 5.1, (2) when calculating the confinement term K_{tr} in Eq. (5.4), or (3) when selecting the epoxy coating factor ψ_e, the unit of bundled bars is treated as a single bar with a diameter derived from the equivalent total area and having a centroid that coincides with that of the bar group.

5.10 BAR CUTOFF AND BEND POINTS IN BEAMS

Chapter 3 dealt with moments, flexural stresses, concrete dimensions, and longitudinal bar areas at the critical moment sections of beams. These critical moment sections are generally at the face of the supports (negative bending) and near the middle of the span (positive bending). Occasionally, haunched members having variable depth or width are used so that the concrete flexural capacity will agree more closely with the variation of bending moment along a span or series of spans. Usually, however, prismatic beams with constant concrete cross-sectional dimensions are used to simplify formwork and thus to reduce cost.

The steel requirement, on the other hand, is easily varied in accordance with requirements for flexure, and it is common practice either to cut off bars where they are no longer needed to resist stress or, sometimes in the case of continuous beams, to bend up the bottom steel (usually at 45°) so that it provides tensile reinforcement at the top of the beam over the supports.

a. Theoretical Points of Cutoff or Bend

The tensile force to be resisted by the reinforcement at any cross section is

$$T = A_s f_s = \frac{M}{z}$$

where M is the value of bending moment at that section and z is the internal lever arm of the resisting moment. The lever arm z varies only within narrow limits and is never

FIGURE 5.18
Bar cutoff points from moment diagrams.

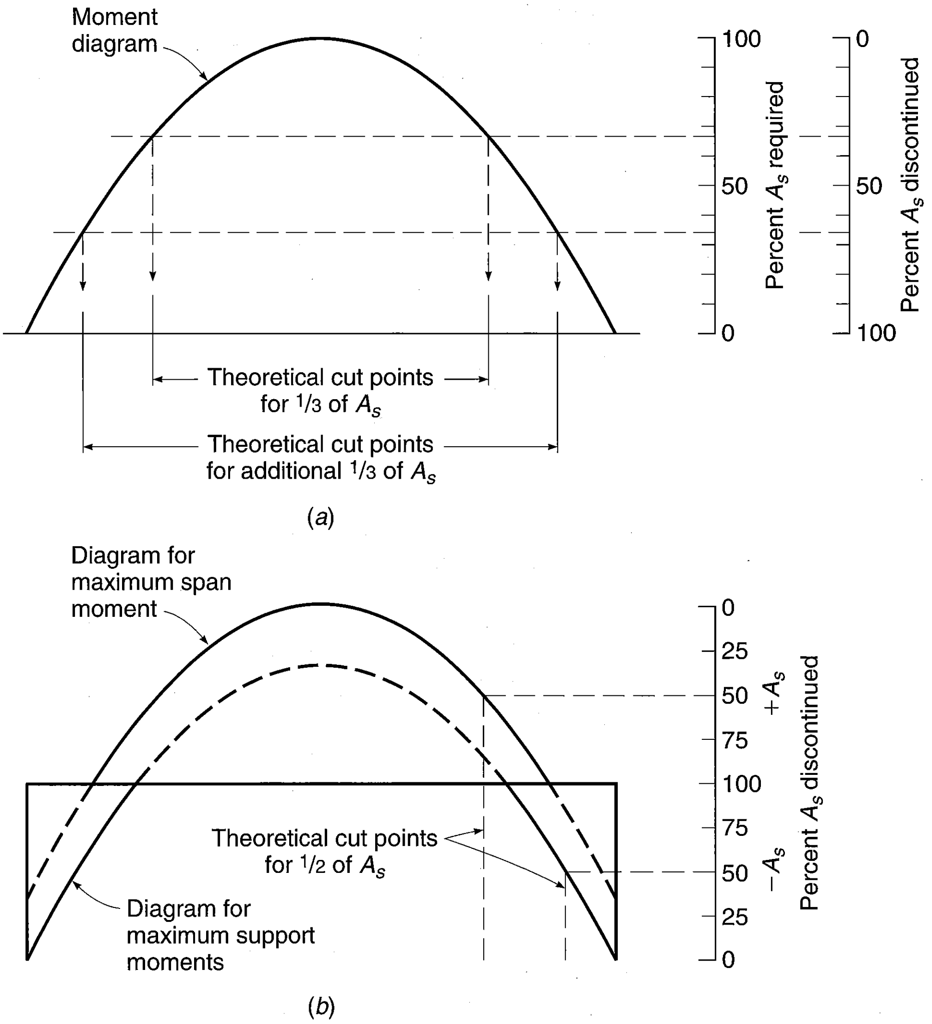
Moment diagram
100
50
0
Percent A_s required
0
50
100
Percent A_s discontinued
Theoretical cut points for 1/3 of A_s
Theoretical cut points for additional 1/3 of A_s
(a)
Diagram for maximum span moment
0
25
50
75
100
75
50
25
0
$+A_s$
$-A_s$
Percent A_s discontinued
Theoretical cut points for 1/2 of A_s
Diagram for maximum support moments
(b)

less than the value at the maximum-moment section. Consequently, the tensile force can be taken with good accuracy directly proportional to the bending moment. Since it is desirable to design so that the steel everywhere in the beam is as nearly fully stressed as possible, it follows that the required steel area is very nearly proportional to the bending moment.

To illustrate, the moment diagram for a uniformly loaded simple-span beam shown in Fig. 5.18*a* can be used as a steel requirement diagram. At the maximum-moment section, 100 percent of the tensile steel is required (0 percent can be discontinued or bent), while at the supports, 0 percent of the steel is theoretically required (100 percent can be discontinued or bent). The percentage of bars that could be discontinued elsewhere along the span is obtainable directly from the moment diagram, drawn to scale. To facilitate the determination of cutoff or bend points for simple spans, Graph A.2 of Appendix A has been prepared. It represents a half-moment diagram for a uniformly loaded simple span.

To determine cutoff or bend points for continuous beams, the moment diagrams resulting from loading for maximum span moment and maximum support moment are drawn. A moment envelope results that defines the range of values of moment at any section. Cutoff or bend points can be found from the appropriate moment curve as for simple spans. Figure 5.18*b* illustrates, for example, a continuous beam with moment envelope resulting from alternate loadings to produce maximum span and maximum support moments. The locations of the points at which 50 percent of the bottom and top steel may theoretically be discontinued are shown.

According to ACI Code 8.3, uniformly loaded, continuous reinforced concrete beams of fairly regular span may be designed using moment coefficients (see Table 12.1). These coefficients, analogous to the numerical constant in the expression $\frac{1}{8}wL^2$ for simple-beam bending moment, give a conservative approximation of span and support moments for continuous beams. When such coefficients are used in design, cutoff and bend points may conveniently be found from Graph A.3 of Appendix A. Moment curves corresponding to the various span and support-moment coefficients are given at the top and bottom of the chart, respectively.

Alternatively, if moments are found by frame analysis rather than from ACI moment coefficients, the location along the span where bending moment reduces to any particular value (e.g., as determined by the bar group after some bars are cut off), or to zero, is easily computed by statics.

b. Practical Considerations and ACI Code Requirements

Actually, in no case should the tensile steel be discontinued exactly at the theoretically described points. As described in Section 4.3 and shown in Fig. 4.7, when diagonal tension cracks form, an internal redistribution of forces occurs in a beam. Prior to cracking, the steel tensile force at any point is proportional to the moment at a vertical section passing through the point. However, after the crack has formed, the tensile force in the steel at the crack is governed by the moment at a section nearer midspan, which may be much larger. Furthermore, the actual moment diagram may differ from that used as a design basis, due to approximation of the real loads, approximations in the analysis, or the superimposed effect of settlement or lateral loads. In recognition of these facts, ACI Code 12.10 requires that every bar be continued at least a distance equal to the effective depth of the beam or 12 bar diameters (whichever is larger) beyond the point at which it is theoretically no longer required to resist stress, except at supports of simple spans and at the free end of cantilevers.

In addition, it is necessary that the calculated stress in the steel at each section be developed by adequate embedded length or end anchorage, or a combination of the two. For the usual case, with no special end anchorage, this means that the full development length l_d must be provided beyond critical sections at which peak stress exists in the bars. These critical sections are located at points of maximum moment and at points where adjacent terminated reinforcement is no longer needed to resist bending.[†]

Further reflecting the possible change in peak stress location, ACI Code 12.11 requires that at least one-third of the positive-moment steel (one-fourth in continuous spans) be continued uninterrupted along the same face of the beam a distance at least 150 mm into the support. When a flexural member is a part of a primary lateral load resisting system, positive-moment reinforcement required to be extended into the support must be anchored to develop the yield strength of the bars at the face of support to account for

---

[†] The ACI Code is ambiguous as to whether or not the extension length d or $12d_b$ is to be added to the required development length l_d. The Code Commentary presents the view that these requirements need not be superimposed, and Fig. 5.19 has been prepared on that basis. However, the argument just presented regarding possible shifts in moment curves or steel stress distribution curves leads to the conclusion that these requirements should be superimposed. In such cases, each bar should be continued a distance l_d plus the greater of d or $12d_b$ beyond the peak stress location.

FIGURE 5.19
Bar cutoff requirements of the ACI Code.

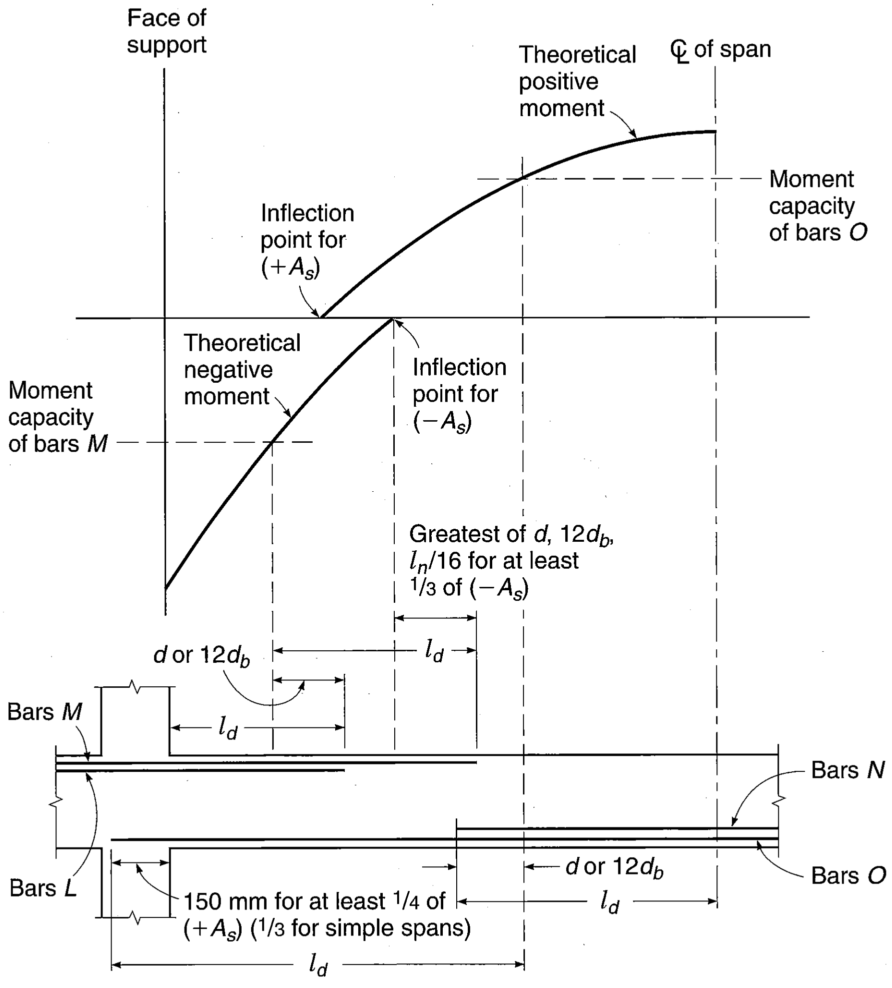
Face of support
Theoretical positive moment
℄ of span
Moment capacity of bars O
Inflection point for (+A_s)
Theoretical negative moment
Moment capacity of bars M
Inflection point for (−A_s)
Greatest of d, $12d_b$, $l_n/16$ for at least 1/3 of (−A_s)
d or $12d_b$
l_d
l_d
Bars M
Bars N
Bars L
Bars O
150 mm for at least 1/4 of (+A_s) (1/3 for simple spans)
d or $12d_b$
l_d
l_d

the possibility of reversal of moment at the supports. According to ACI Code 12.12, at least one-third of the total reinforcement provided for negative moment at the support must be extended beyond the extreme position of the point of inflection a distance not less than one-sixteenth the clear span, or d, or $12d_b$, whichever is greatest.

Requirements for bar cutoff or bend point locations are summarized in Fig. 5.19. If negative bars L are to be cut off, they must extend a full development length l_d beyond the face of the support. In addition, they must extend a distance d or $12d_b$ beyond the theoretical point of cutoff defined by the moment diagram. The remaining negative bars M (at least one-third of the total negative area) must extend at least l_d beyond the theoretical point of cutoff of bars L and in addition must extend d, $12d_b$, or $l_n/16$ (whichever is greatest) past the point of inflection of the negative-moment diagram.

If the positive bars N are to be cut off, they must project l_d past the point of theoretical maximum moment, as well as d or $12d_b$ beyond the cutoff point from the positive-moment diagram. The remaining positive bars O must extend l_d past the theoretical point of cutoff of bars N and must extend at least 150 mm into the face of the support.

When bars are cut off in a tension zone, there is a tendency toward the formation of premature flexural and diagonal tension cracks in the vicinity of the cut end. This may result in a reduction of shear capacity and a loss in overall ductility of the beam.

ACI Code 12.10 requires special precautions, specifying that no flexural bar shall be terminated in a tension zone unless *one* of the following conditions is satisfied:

1. The shear is not over two-thirds of the design strength ϕV_n.
2. Stirrups in excess of those normally required are provided over a distance along each terminated bar from the point of cutoff equal to $\frac{3}{4}d$. These "binder" stirrups shall provide an area $A_v \geq 0.41 b_w s/f_{yt}$. In addition, the stirrup spacing shall not exceed $d/8\beta_b$, where β_b is the ratio of the area of bars cut off to the total area of bars at the section.
3. The continuing bars, if No. 36 (No. 11) or smaller, provide twice the area required for flexure at that point, and the shear does not exceed three-quarters of the design strength ϕV_n.

As an alternative to cutting off the steel, tension bars may be anchored by bending them across the web and making them continuous with the reinforcement on the opposite face. Although this leads to some complication in detailing and placing the steel, thus adding to construction cost, some engineers prefer the arrangement because added insurance is provided against the spread of diagonal tension cracks. In some cases, particularly for relatively deep beams in which a large percentage of the total bottom steel is to be bent, it may be impossible to locate the bend-up point for bottom bars far enough from the support for the same bars to meet the requirements for top steel. The theoretical points of bend should be checked carefully for both bottom and top steel.

Because the determination of cutoff or bend points may be rather tedious, particularly for frames that have been analyzed by elastic methods rather than by moment coefficients, many designers specify that bars be cut off or bent at more or less arbitrarily defined points that experience has proved to be safe. For nearly equal spans, uniformly loaded, in which not more than about one-half the tensile steel is to be cut off or bent, the locations shown in Fig. 5.20 are satisfactory. Note, in Fig. 5.20, that the beam at the exterior support at the left is shown to be simply supported. If the beam is monolithic with exterior columns or with a concrete wall at that end, details for a typical interior span could be used for the end span as well.

c. Special Requirements near the Point of Zero Moment

While the basic requirement for flexural tensile reinforcement is that a full development length l_d be provided beyond the point where the bar is assumed fully stressed to f_y, this requirement may *not* be sufficient to ensure safety against bond distress. Figure 5.21 shows the moment and shear diagram representative of a uniformly loaded continuous beam. Positive bars provided to resist the maximum moment at *c* are required to have a full development length beyond the point *c*, measured in the direction of decreasing moment. Thus l_d in the limiting case could be exactly equal to the distance from point *c* to the point of inflection. However, if that requirement were exactly met, then at point *b*, halfway from *c* to the point of inflection, those bars would have only one-half their development length remaining, whereas the moment would be three-quarters of that at point *c*, and three-quarters of the bar force must yet be developed. This situation arises whenever the moments over the development length are greater than those corresponding to a linear reduction to zero. Therefore, the problem is a concern in the positive-moment region of continuous uniformly loaded spans, but not in the negative-moment region.

FIGURE 5.20
Cutoff or bend points for bars in approximately equal spans with uniformly distributed loads.

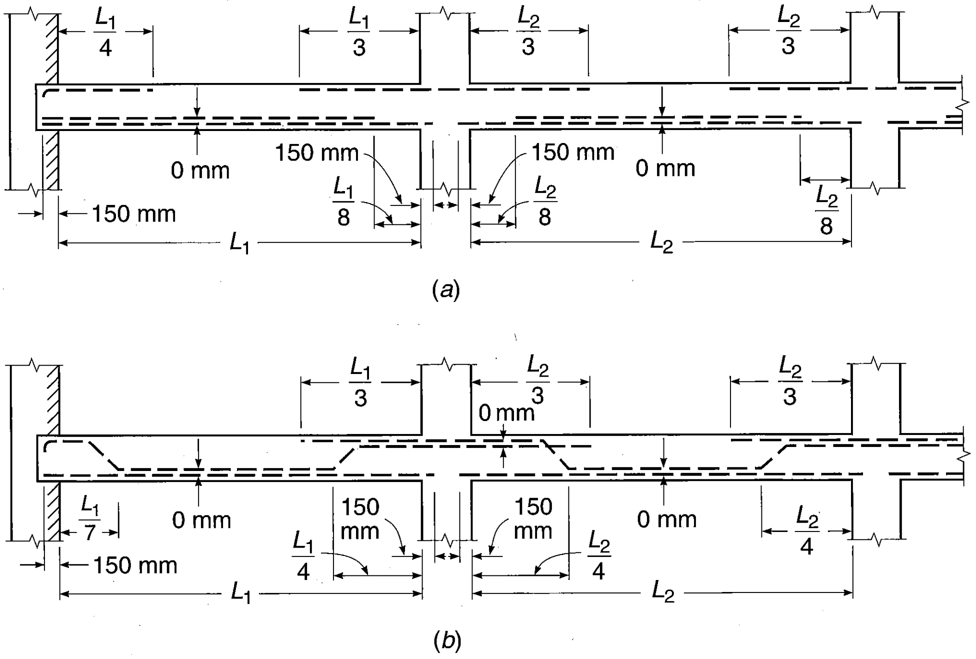
$\frac{L_1}{4}$
$\frac{L_1}{3}$
$\frac{L_2}{3}$
$\frac{L_2}{3}$
0 mm
150 mm
150 mm
0 mm
$\frac{L_1}{8}$
$\frac{L_2}{8}$
$\frac{L_2}{8}$
150 mm
L_1
L_2
(a)
$\frac{L_1}{3}$
$\frac{L_2}{3}$
0 mm
$\frac{L_2}{3}$
$\frac{L_1}{7}$
0 mm
150 mm
150 mm
0 mm
$\frac{L_1}{4}$
$\frac{L_2}{4}$
$\frac{L_2}{4}$
150 mm
L_1
L_2
(b)

FIGURE 5.21
Development length requirement at point of inflection.

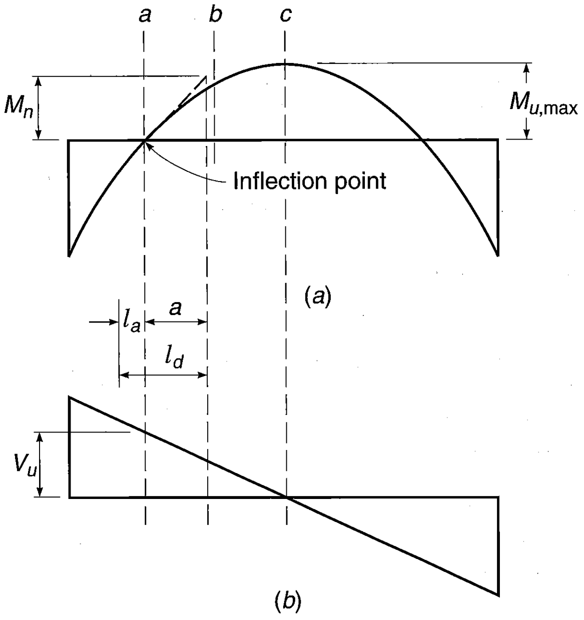
a
b
c
M_n
$M_{u,\max}$
Inflection point
(a)
l_a
a
l_d
V_u
(b)

The bond force U per unit length along the tensile reinforcement in a beam is $U = dT/dx$, where dT is the change in bar tension in the length dx. Since $dT = dM/z$, this can be written

$$U = \frac{dM}{z\,dx} \qquad (a)$$

that is, the bond force per unit length of bar, generated by bending, is proportional to the slope of the moment diagram. In reference to Fig. 5.21*a*, the maximum bond force U in the positive-moment region would therefore be at the point of inflection, and U would gradually diminish along the beam toward point c. Clearly, a conservative approach in evaluating adequacy in bond for those bars that are continued as far as the point of inflection (not necessarily the full A_s provided for M_u at point c) would be to require that the bond resistance, which is assumed to increase linearly along the bar from its end, be governed by the maximum rate of moment increase, i.e., the maximum slope dM/dx of the moment diagram, which for positive bending is seen to occur at the inflection point.

From elementary mechanics, it is known that the slope of the moment diagram at any point is equal to the value of the shear force at that point. Therefore, with reference to Fig. 5.21, the slope of the moment diagram at the point of inflection is V_u. A dashed line may therefore be drawn tangent to the moment curve at the point of inflection having the slope equal to the value of shear force V_u. Then if M_n is the nominal flexural strength provided by those bars that extend to the point of inflection, and if the moment diagram were conservatively assumed to vary linearly along the dashed line tangent to the actual moment curve, from the basic relation that $M_n/a = V_u$, a distance a is established:

$$a = \frac{M_n}{V_u} \tag{b}$$

If the bars in question were fully stressed at a distance a to the right of the point of inflection, and if the moments diminished linearly to the point of inflection, as suggested by the dashed line, then bond failure would not occur if the development length l_d did not exceed the distance a. The actual moments are less than indicated by the dashed line, so the requirement is on the safe side.

If the bars extend past the point of inflection toward the support, as is always required, then the extension can be counted as contributing toward satisfying the requirement for embedded length. Arbitrarily, according to ACI Code 12.11, a length past the point of inflection not greater than the larger of the beam depth d or 12 times the bar diameter d_b may be counted toward satisfying the requirement. Thus, the requirement for tensile bars at the point of inflection is that

$$l_d \le \frac{M_n}{V_u} + l_a \tag{5.11}$$

where M_n = nominal flexural strength assuming all reinforcement at section to be stressed to f_y
V_u = factored shear force at section
l_a = embedded length of bar past point of zero moment, but not to exceed the greater of d or $12d_b$

A corresponding situation occurs near the supports of simple spans carrying uniform loads, and similar requirements must be imposed. However, because of the beneficial effect of vertical compression in the concrete at the end of a simply supported span, which tends to prevent splitting and bond failure along the bars, the value M_n/V_u may be increased 30 percent for such cases, according to ACI Code 12.11. Thus, at the ends of a simply supported span, the requirement for tension reinforcement is

$$l_d \le 1.3\frac{M_n}{V_u} + l_a \tag{5.12}$$

The consequence of these special requirements at the point of zero moment is that, in some cases, smaller bar sizes must be used to obtain smaller l_d, even though requirements for development past the point of maximum stress are met.

It may be evident from review of Sections 5.10b and 5.10c that the determination of cutoff or bend points in flexural members is complicated and can be extremely time-consuming in design. It is important to keep the matter in perspective and to recognize that the overall cost of construction will be increased very little if some bars are slightly longer than absolutely necessary, according to calculation, or as dictated by ACI Code provisions. In addition, simplicity in construction is a desired goal, and can, in itself, produce compensating cost savings. Accordingly, many engineers in practice continue *all* positive reinforcement into the face of the supports the required 150 mm and extend *all* negative reinforcement the required distance past the points of inflection, rather than using staggered cutoff points.

5.11 STRUCTURAL INTEGRITY PROVISIONS

Experience with structures that have been subjected to damage to a major supporting element, such as a column, owing to accident or abnormal loading has indicated that total collapse can be prevented through relatively minor changes in bar detailing. If some reinforcement, properly confined, is carried continuously through a support, then even if that support is damaged or destroyed, catenary action of the beams can prevent total collapse. In general, if beams have bottom and top steel meeting or exceeding the requirements summarized in Sections 5.10b and 5.10c, and if binding steel is provided in the form of properly detailed stirrups, then that catenary action can usually be ensured.

According to ACI Code 7.13.2, beams at the perimeter of the structure (spandrel beams) must have continuous reinforcement passing through the region bounded by the longitudinal reinforcement of the columns consisting of at least one-sixth of the tension reinforcement required for negative moment at the support, but not less than two bars, and at least one-quarter of the tension reinforcement required for positive moment at midspan, but not less than two bars. At noncontinuous supports, the reinforcement must be anchored using a standard hook or a headed deformed bar to develop f_y at the face of the support. The continuous reinforcement must be enclosed by closed stirrups or closed ties perpendicular to the axis of the member, a closed cage of welded wire reinforcement with transverse wires perpendicular to the axis of the member, or spiral reinforcement (see Fig. 1.15). This transverse reinforcement must be anchored by a 135° standard hook (Fig. 5.9*b*) or a seismic hook (see Section 20.4) around a longitudinal bar, or where the concrete surrounding the anchorage is restrained against spalling by a flange or slab, by either a 90° or 135° standard hook around a longitudinal bar, as shown in Fig. 5.17*a* and *b*.

Figure 5.22 shows a two-piece stirrup that meets the requirements of ACI Code 7.13.2. Although the spacing of these stirrups is not specified, the requirements for minimum shear steel given in Section 4.5b provide guidance in regions where shear does not require closer spacing. The stirrups need not be extended through the joints. Overlapping pairs of U stirrups of the type shown in Fig. 5.17*d* are not permitted in perimeter beams because damage to the side cover concrete may cause both the stirrups and top longitudinal reinforcement to tear out of the concrete, thus preventing the longitudinal reinforcement from acting as a catenary.

FIGURE 5.22
Two-piece stirrup meeting the requirements of ACI Code 7.13.2 for confinement of longitudinal integrity reinforcement in perimeter beams. The 90 degree hook must be placed adjacent to the slab.

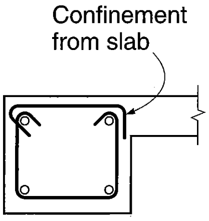

The required continuity of longitudinal steel can be provided using top reinforcement spliced at midspan and bottom reinforcement spliced at or near the supports using Class B tension splices, or mechanical or welded splices (see Section 5.13).

In other than perimeter beams, when stirrups of the type shown in Fig. 5.22 are not provided, at least one-quarter of the positive-moment reinforcement required at midspan, but not less than two bars, must pass through the columns' longitudinal reinforcement and must be continuous. The requirements for anchoring this longitudinal reinforcement at noncontinuous supports and for splicing the bars to provide continuity are the same as for perimeter beams.

Note that these provisions require very little additional steel in the structure. At least one-quarter of the bottom bars must be extended 150 mm into the support by other ACI Code provisions; the structural integrity provisions merely require that these bars be made continuous or spliced. Similarly, other ACI Code provisions require that at least one-third of the negative bars be extended a certain minimum distance past the point of inflection; the structural integrity provisions for perimeter beams require only that one-half of those bars be further extended and spliced at midspan.

5.12 INTEGRATED BEAM DESIGN EXAMPLE

In this and in the preceding chapters, the several aspects of the design of reinforced concrete beams have been studied more or less separately: first the flexural design, then design for shear, and finally for bond and anchorage. The following example is presented to show how the various requirements for beams, which are often in some respects conflicting, are satisfied in the overall design of a representative member.

EXAMPLE 5.4

Integrated design of T beam. A floor system consists of single-span T beams 2.4 m on centers, supported by 300 mm masonry walls spaced at 7.5 m between inside faces. The general arrangement is shown in Fig. 5.23*a*. A 125 mm monolithic slab carries a uniformly distributed service live load of 7.9 kN/m^2. The T beams, in addition to the slab load and their own weight, must carry two 71 kN equipment loads applied over the stem of the T beam 0.9 m from the span centerline as shown. A complete design is to be provided for the T beams, using concrete of 28 MPa strength and bars with 420 MPa yield stress. (*Note*: Because normalweight concrete is used, $\lambda = 1.0$ and, as such, will be dropped from the calculations for shear and bond.)

Solution. According to the ACI Code, the span length is to be taken as the clear span plus the beam depth, but need not exceed the distance between the centers of supports. The latter

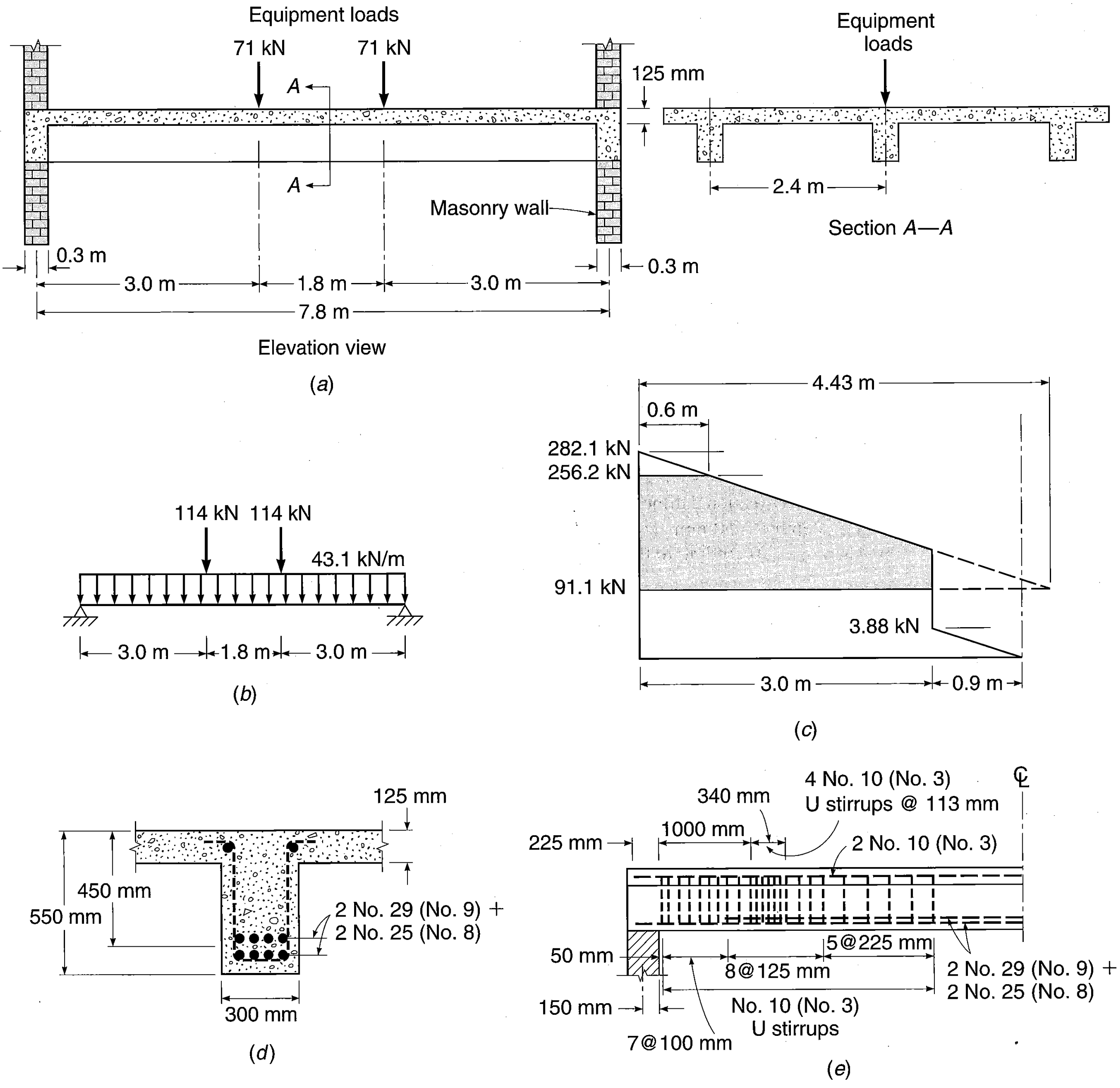
Equipment loads
71 kN
71 kN
A
A
125 mm
Masonry wall
0.3 m
3.0 m
1.8 m
3.0 m
0.3 m
7.8 m
Elevation view
(a)
Equipment loads
2.4 m
Section A—A
114 kN 114 kN
43.1 kN/m
3.0 m
1.8 m
3.0 m
(b)
4.43 m
0.6 m
282.1 kN
256.2 kN
91.1 kN
3.88 kN
3.0 m
0.9 m
(c)
125 mm
450 mm
550 mm
2 No. 29 (No. 9) +
2 No. 25 (No. 8)
300 mm
(d)
4 No. 10 (No. 3)
U stirrups @ 113 mm
340 mm
1000 mm
225 mm
2 No. 10 (No. 3)
℄
5@225 mm
50 mm
8@125 mm
2 No. 29 (No. 9) +
2 No. 25 (No. 8)
150 mm
No. 10 (No. 3)
U stirrups
7@100 mm
(e)

FIGURE 5.23
T beam design for Example 5.4.

provision controls in this case, and the effective span is 7.8 m. Estimating the beam web dimensions to be 300 × 600 mm, the calculated and factored dead loads[†] are as follows:

Slab:

$$0.125 \times 2.1 \times 24 = 6.3 \text{ kN/m}$$

[†] Normalweight concrete exerts a load of approximately 24 kN/m^3.

Beam:

$$0.3 \times 0.6 \times 24 = 4.3 \text{ kN/m}$$

$$w_d = 10.6 \text{ kN/m}$$

$$1.2w_d = 12.7 \text{ kN/m}$$

The uniformly distributed live load is

$$w_l = 7.9 \times 2.4 = 19.0 \text{ kN/m}^2$$

$$1.6w_l = 30.4 \text{ kN/m}^2$$

Live load overload factors are applied to the two concentrated loads to obtain $P_u = 71 \times 1.6 = 114$ kN. Factored loads are summarized in Fig. 5.23*b*.

In lieu of other controlling criteria, the beam web dimensions will be selected on the basis of shear. The left and right reactions under factored load are $114 \times 43.1 \times 3.9 = 282.1$ kN. With the effective beam depth estimated to be 500 mm, the maximum shear that need be considered in design is $282.1 - 43.1(0.150 + 0.500) = 254.1$ kN. Although the ACI Code permits V_s as high as $0.66\sqrt{f_c'}\,b_w d$, this would require very heavy web reinforcement. A lower limit of $0.33\sqrt{f_c'}\,b_w d$ will be adopted. With $V_c = 0.17\sqrt{f_c'}\,b_w d$ this results in a maximum $V_n = 0.50\sqrt{f_c'}\,b_w d$. Then $b_w d = V_u/(0.50\phi\sqrt{f_c'}) = 254.1/(0.5 \times 0.75\sqrt{28}) = 128{,}000 \text{ mm}^2$. Cross-sectional dimensions $b_w = 300$ mm and $d = 450$ mm are selected, providing a total beam depth of 550 mm. The assumed dead load of the beam need not be revised.

According to the Code, the effective flange width b is the smallest of the three quantities

$$\frac{L}{4} = \frac{7800}{4} = 1950 \text{ mm}$$

$$16h_f + b_w = 2000 + 300 = 2300 \text{ mm}$$

$$\text{Centerline spacing} = 2400 \text{ mm}$$

The first controls in this case. The maximum moment is at midspan, where

$$M_u = \frac{1}{8} \times 43.1 \times 7.8^2 + 114 \times 3 = 670 \text{ kN-m}$$

Assuming for trial that the stress-block depth will equal the slab thickness leads to

$$A_s = \frac{M_u}{\phi f_y(d - a/2)} = \frac{670 \times 10^6}{0.90 \times 420 \times 387.5} = 4574 \text{ mm}^2$$

Then

$$a = \frac{A_s f_y}{0.85 f_c' b} = \frac{4574 \times 420}{0.85 \times 28 \times 1950} = 41.4 \text{ mm}$$

The stress-block depth is seen to be less than the slab depth; rectangular beam equations are valid. An improved determination of A_s is

$$A_s = \frac{670 \times 10^6}{0.90 \times 420 \times 429.3} = 4129 \text{ mm}^2$$

A check confirms that this is well below the maximum permitted reinforcement ratio. Four No. 29 (No. 9) plus four No. 25 (No. 8) bars will be used, providing a total area of 4620 mm². They will be arranged in two rows, as shown in Fig. 5.23*d*, with No. 29 (No. 9) bars at the outer end of each row. Beam width b_w is adequate for this bar arrangement.

While the ACI Code permits discontinuation of two-thirds of the longitudinal reinforcement for simple spans, in the present case it is convenient to discontinue only the upper layer of steel, consisting of one-half of the total area. The moment capacity of the member after the upper layer of bars has been discontinued is then found:

$$a = \frac{23.0 \times 420}{0.85 \times 28 \times 1950} = 20.9 \text{ mm}$$

$$\phi M_n = \phi A_s f_y \left(d - \frac{a}{2} \right) = 0.90 \times 2310 \times 420 \times 466.4/10^6 = 0.9 \times 452 = 407 \text{ kN-m}$$

For the present case, with a moment diagram resulting from combined distributed and concentrated loads, the point at which the applied moment is equal to this amount must be calculated. (In the case of uniformly loaded beams, Graphs A.2 and A.3 in Appendix A are helpful.) If x is the distance from the support centerline to the point at which the moment is 407 kN-m, then

$$282.1x - \frac{43.1x^2}{2} = 407$$

$$x = 1.65 \text{ m}$$

The upper bars must be continued at least $d = 0.450$ m or $12d_b = 0.344$ m beyond this theoretical point of cutoff. In addition, the full development length l_d must be provided past the maximum-moment section at which the stress in the bars to be cut is assumed to be f_y. Because of the heavy concentrated loads near the midspan, the point of peak stress will be assumed to be at the concentrated load rather than at midspan. For the four upper bars, assuming 40 mm clear cover to the outside of the No. 10 (No. 3) stirrups, the clear side cover is $40 + 9.5 = 49.5$ mm, or $1.72d_b$. Assuming equal clear spacing between all four bars, that clear spacing is $[300 - 2 \times (40 + 9.5 + 28.7 + 25.4)]/3 = 30.9$ mm, or $1.08d_b$. Noting that the ACI Code requirements for minimum stirrups are met, it is clear that all restrictions for the use of the simplified equation for development length are met. From Table 5.1 (Section 5.3), the required development length is

$$l_d = \frac{420}{1.7\sqrt{28}} 28.7 = 47 \times 28.7 = 1350 \text{ mm}$$

Thus, the bars must be continued at least $0.90 + 1.35 = 2.25$ m past the midspan point, but in addition they must continue to a point $1.65 - 0.45 = 1.20$ m from the support centerline. The second requirement controls and the upper layer of the bars will be terminated, as shown in Fig. 5.23*e*, 1.05 m from the support face. The bottom layer of bars will be extended to a point 75 mm from the end of the beam, providing 1.73 m embedment past the critical section for cutoff of the upper bars. This exceeds the development length of the lower set of bars, confirming that cutoff and extension requirements are met.

Note that a simpler design, using very little extra steel, would result from extending all eight positive bars into the support. Whether or not the more elaborate calculations and more complicated placement are justified would depend largely on the number of repetitions of the design in the total structure.

Checking by Eq. (5.12) to ensure that the continued steel is of sufficiently small diameter determines that

$$l_d \leq 1.3 \frac{452{,}000}{282.1} + 75 = 1677 \text{ mm}$$

The actual l_d of 1350 mm meets this restriction.

Since the cut bars are located in the tension zone, special binding stirrups will be used to control cracking; these will be selected after the normal shear reinforcement has been determined.

The shear diagram resulting from application of factored loads is shown in Fig. 5.23*c*. The shear contribution of the concrete is

$$\phi V_c = 0.75 \times 0.17\sqrt{28} \times 300 \times 450/1000 = 91.1 \text{ kN}$$

Thus web reinforcement must be provided for that part of the shear diagram shown shaded.

No. 10 (No. 3) stirrups will be selected. The maximum spacings must not exceed $d/2 = 225$ mm, 600 mm, or $A_v f_{yt}/(0.062\sqrt{f'_c}\, b_w) = 142 \times 420/(0.062\sqrt{28} \times 300) = 606 \text{ mm} \leq A_v f_{yt}/50b_w = 142 \times 420/(0.35 \times 300) = 568$ mm. The first criterion controls here. For reference, from Eq. (4.14*a*) the hypothetical stirrup spacing at the support is

$$s_0 = \frac{0.75 \times 142 \times 420 \times 450}{(282.1 - 91.1) \times 10^3} = 105 \text{ mm}$$

and at 600 mm intervals along the span,

$$s_2 = 121 \text{ mm}$$
$$s_4 = 144 \text{ mm}$$
$$s_6 = 176 \text{ mm}$$
$$s_8 = 229 \text{ mm}$$
$$s_{10} = 325 \text{ mm}$$

The spacing need not be closer than that required 600 mm from the support centerline. In addition, stirrups are not required past the point of application of concentrated load, since beyond that point the shear is less than one-half of ϕV_c. The final spacing of vertical stirrups selected is

1 space at 50 mm = 50 mm
7 spaces at 100 mm = 700 mm
8 spaces at 125 mm = 1000 mm
5 spaces at 225 mm = 1125 mm
Total = 2875 mm = 2.875 m from the face of the support (3.025 m from the support centerline)

Two No. 10 (No. 3) longitudinal bars will be added to meet anchorage requirements and fix the top of the stirrups.

In addition to the shear reinforcement just specified, it is necessary to provide extra web reinforcement over a distance equal to $\frac{3}{4}d$, or 340 mm, from the cut ends of the discontinued steel. The spacing of this extra web reinforcement must not exceed $d/8\beta_b = 450/(8 \times \frac{1}{2}) = 113$ mm. In addition, the area of added steel within the distance s must not be less than $0.41 b_w s/f_{yt} = 0.41 \times 300 \times 100/420 = 29 \text{ mm}^2$. For convenience, No. 10 (No. 3) stirrups will be used for this purpose also, providing an area of 142 mm^2 in the distance s. The placement of the four extra stirrups is shown in Fig. 5.23*e*.

5.13 BAR SPLICES

In general, reinforcing bars are stocked by suppliers in lengths of 18 m for bars from No. 16 to No. 57 (No. 5 to No. 18) and in 6 or 12 m lengths for smaller sizes. For this reason, and because it is often more convenient to work with shorter bar lengths, it is frequently necessary to splice bars in the field. Splices in reinforcement at points of maximum stress should be avoided, and when splices are used, they should be staggered, although neither condition is practical, for example, in compression splices in columns.

Splices for No. 36 (No. 11) bars and smaller are usually made simply by lapping the bars a sufficient distance to transfer stress by bond from one bar to the other. The lapped bars are usually placed in contact and lightly wired so that they stay in position as the concrete is placed. Alternatively, splicing may be accomplished by welding or by sleeves or mechanical devices. ACI Code 12.14.2 prohibits use of lapped splices for bars larger than No. 36 (No. 11), except that No. 43 and No. 57 (No. 14 and No. 18) bars may be lapped in compression with No. 36 (No. 11) and smaller bars per ACI Code 12.16.2 and 15.8.2.3. For bars that will carry only compression, it is possible to transfer load by end bearing of square cut ends, if the bars are accurately held in position by a sleeve or other device.

Lap splices of bars in bundles are based on the lap splice length required for individual bars within the bundle but must be increased in length by 20 percent for three-bar bundles and by 33 percent for four-bar bundles because of the reduced effective perimeter. Individual bar splices within a bundle should not overlap, and entire bundles must not be lap-spliced.

According to ACI Code 12.14.3, welded splices must develop at least 125 percent of the specified yield strength of the bar. The same requirement applies to full mechanical connections. This ensures that an overloaded spliced bar would fail by ductile yielding in the region away from the splice, rather than at the splice where brittle failure is likely. Mechanical connections of No. 16 (No. 5) and smaller bars not meeting this requirement may be used at points of less than maximum stress, in accordance with ACI Code 12.15.5.

a. Lap Splices in Tension

The required length of lap for tension splices is stated in terms of the development length l_d. In the process of calculating l_d, the usual modification factors are applied except that the reduction factor for excess reinforcement should not be applied because that factor is already accounted for in the splice specification.

Two different classifications of lap splices are established, corresponding to the minimum length of lap required: a Class A splice requires a lap of $1.0l_d$, and a Class B splice requires a lap of $1.3l_d$. In either case, a minimum length of 300 mm applies. For Class B splices, the 300 mm minimum applies to $1.3l_d$, not to the value of l_d used to calculate the lap length. Lap splices, in general, must be Class B splices, according to ACI Code 12.15.2, except that Class A splices are allowed when the area of reinforcement provided is at least twice that required by analysis over the entire length of the splice *and* when one-half or less of the total reinforcement is spliced within the required lap length. The effect of these requirements is to encourage designers to locate splices away from regions of maximum stress, to a location where the actual steel area is at least twice that required by analysis, and to stagger splices.

Spiral reinforcement is spliced with a lap of $48d_b$ for uncoated bars and $72d_b$ for epoxy-coated bars, in accordance with ACI Code 7.10.4.5. The lap for epoxy-coated bars is reduced to $48d_b$ if the bars are anchored with a standard stirrup or tie hook.

b. Compression Splices

Reinforcing bars in compression are spliced mainly in columns, where bars are most often terminated just above each floor or every other floor. This is done partly for construction convenience, to avoid handling and supporting very long column bars, but it is also done to permit column steel area to be reduced in steps, as loads become lighter at higher floors.

Compression bars may be spliced by lapping, by direct end bearing, or by welding or mechanical devices that provide positive connection. The minimum length of lap for compression splices is set according to ACI Code 12.16:

For bars with $f_y \leq 420$ MPa $\quad 0.071 f_y d_b$

For bars with $f_y > 420$ MPa $\quad (0.13 f_y - 24) d_b$

but not less than 300 mm. For f'_c less than 21 MPa, the required lap is increased by one-third. When bars of different size are lap-spliced in compression, the splice length is to be the larger of the development length of the larger bar and the splice length of the smaller bar. In exception to the usual restriction on lap splices for large-diameter bars, No. 43 and No. 57 (No. 14 and No. 18) bars *may* be lap-spliced to No. 36 (No. 11) and smaller bars.

Direct end bearing of the bars has been found by test and experience to be an effective means for transmitting compression. In such a case, the bars must be held in proper alignment by a suitable device. The bar ends must terminate in flat surfaces within 1.5° of a right angle, and the bars must be fitted within 3° of full bearing after assembly, according to ACI Code 12.16.4. Ties, closed stirrups, or spirals must be used.

c. Column Splices

Lap splices, butt-welded splices, mechanical connections, or end-bearing splices may be used in columns, with certain restrictions. Reinforcing bars in columns may be subjected to compression or tension, or, for different load combinations, both tension and compression. Accordingly, column splices must conform in some cases to the requirements for compression splices only or tension splices only or to requirements for both. ACI Code 12.17 requires that a minimum tension capacity be provided in each face of all columns, even where analysis indicates compression only. Ordinary compressive lap splices provide sufficient tensile resistance, but end-bearing splices may require additional bars for tension, unless the splices are staggered.

For lap splices, where the bar stress due to factored loads is compression, column lap splices must conform to the requirements presented in Section 5.13b for compression splices. Where the stress is tension and does not exceed $0.5f_y$, lap splices must be Class B if more than one-half the bars are spliced at any section, or Class A if one-half or fewer are spliced and alternate lap splices are staggered by l_d. If the stress is tension and exceeds $0.5f_y$, then lap splices must be Class B, according to ACI Code.

If lateral ties are used throughout the splice length having an area of at least $0.0015hs$ in both directions, where s is the spacing of ties and h is the overall thickness of the member, the required splice length may be multiplied by 0.83 but must not be less than 300 mm. If spiral reinforcement confines the splice, the length required may be multiplied by 0.75 but again must not be less than 300 mm.

End-bearing splices, as described above, may be used for column bars stressed in compression, if the splices are staggered or additional bars are provided at splice locations. The continuing bars in each face must have a tensile strength of not less than $0.25f_y$ times the area of reinforcement in that face.

As mentioned in Section 5.13b, column splices are commonly made just above a floor. However, for frames subjected to lateral loads, a better location is within the center half of the column height, where the moments due to lateral loads are much lower than at floor level. Such placement is mandatory for columns in "special moment frames" designed for seismic loads, as will be discussed in Chapter 20.

EXAMPLE 5.5

Compression splice of column reinforcement. In reference to Fig. 5.8, four No. 36 (No. 11) column bars from the floor below are to be lap-spliced with four No. 32 (No. 10) column bars from above, and the splice is to be made just above a construction joint at floor level. The column, measuring 300 mm × 530 mm in cross section, will be subject to compression only for all load combinations. Transverse reinforcement consists of No. 13 (No. 4) ties at 400 mm spacing. All vertical bars may be assumed to be fully stressed. Calculate the required splice length. Material strengths are $f_y = 420$ MPa and $f_c' = 28$ MPa.

Solution. The length of the splice must be the larger of the development length of the No. 36 (No. 11) bars and the splice length of the No. 32 (No. 10) bars. For the No. 36 (No. 11) bars, the development length is equal to the larger of the values obtained with Eqs. (5.10*a*) and (5.10*b*):

$$l_{dc} = \frac{0.24 \times 420}{\sqrt{28}} 35.8 = 682 \text{ mm}$$

$$l_{dc} = 0.043 \times 420 \times 35.8 = 647 \text{ mm}$$

The first criterion controls. No modification factors apply. For the No. 32 (No. 10) bars, the compression splice length is $0.071 \times 420 \times 32.3 = 963$ mm. In the check for use of the modification factor for tied columns, the critical column dimension is 530 mm, and the required effective tie area is thus $0.0015 \times 530 \times 400 = 318 \text{ mm}^2$. The No. 13 (No. 4) ties provide an area of only $129 \times 2 = 258 \text{ mm}^2$, so the reduction factor of 0.83 cannot be applied to the splice length. Thus the compression splice length of 963 mm, which exceeds the development length of 682 mm for the No. 36 (No. 11) bars, controls here, and a lap splice of 963 mm is required. Note that if the spacing of the ties at the splice were reduced to 324 mm or less (say 300 mm), the required lap would be reduced to $963 \times 0.83 = 799$ mm. This would save steel, and, although placement cost would increase slightly, would probably represent the more economical design.

REFERENCES

5.1. R. M. Mains, "Measurement of the Distribution of Tensile and Bond Stresses along Reinforcing Bars," *J. ACI*, vol. 23, no. 3, 1951, pp. 225–252.

5.2. A. H. Nilson, "Internal Measurement of Bond Slip," *J. ACI*, vol. 69, no. 7, 1972, pp. 439–441.

5.3. Y. Goto, "Cracks Formed in Concrete around Deformed Tension Bars," *J. ACI*, vol. 68, no. 4, 1971, pp. 244–251.

5.4. L. A. Lutz and P. Gergely, "Mechanics of Bond and Slip of Deformed Bars in Concrete," *J. ACI*, vol. 64, no. 11, 1967, pp. 711–721.

5.5. P. M. Ferguson and J. N. Thompson, "Development Length of High Strength Reinforcing Bars in Bond," *J. ACI*, vol. 59, no. 7, 1962, pp. 887–922.

5.6. R. G. Mathey and D. Watstein, "Investigation of Bond in Beam and Pullout Specimens with High-Strength Reinforcing Bars," *J. ACI*, vol. 32, no. 9, 1961, pp. 1071–1090.

5.7. ACI Committee 408, "Bond Stress—The State of the Art," *J. ACI*, vol. 63, no. 11, 1966, pp. 1161–1190.

5.8. ACI Committee 408, "Suggested Development, Splice, and Standard Hook Provisions for Deformed Bars in Tension," *Concr. Intl.*, vol. 1, no. 7, 1979, pp. 44–46.

5.9. J. O. Jirsa, L. A. Lutz, and P. Gergely, "Rationale for Suggested Development, Splice, and Standard Hook Provisions for Deformed Bars in Tension," *Concr. Intl.*, vol. 1, no. 7, 1979, pp. 47–61.

5.10. C. O. Orangun, J. O. Jirsa, and J. E. Breen, "A Reevaluation of the Test Data on Development Length and Splices," *J. ACI*, vol. 74, no. 3, 1977, pp. 114–122.

5.11. L. A. Lutz, S. A. Mirza, and N. K. Gosain, "Changes to and Applications of Development and Lap Splice Length Provisions for Bars in Tension," *ACI Struct. J.*, vol. 90, no. 4, 1993, pp. 393–406.

5.12. D. Darwin, M. L. Tholen, E. K. Idun, and J. Zuo, "Splice Strength of High Relative Rib Area Reinforcing Bars," *ACI Struct. J.*, vol. 93, no. 1, 1996, pp. 95–107.

5.13. D. Darwin, J. Zuo, M. L. Tholen, and E. K. Idun, "Development Length Criteria for Conventional and High Relative Rib Area Reinforcing Bars," *ACI Struct. J.*, vol. 93, no. 3, 1996, pp. 347–359.

5.14. J. Zuo and D. Darwin, "Splice Strength of Conventional and High Relative Rib Area Bars in Normal and High Strength Concrete," *ACI Struct. J.*, vol. 97, no. 4, 2000, pp. 630–641.

5.15. ACI Committee 408, *Bond and Development of Straight Reinforcement in Tension*, ACI 408R-03, American Concrete Institute, Farmington Hills, MI, 2003.

5.16. P. M. Ferguson, "Small Bar Spacing or Cover—A Bond Problem for the Designer," *J. ACI*, vol. 74, no. 9, 1977, pp. 435–439.

5.17. P. R. Jeanty, D. Mitchell, and M. S. Mirza, "Investigation of Top Bar Effects in Beams," *ACI Struct. J.*, vol. 85, no. 3, 1988, pp. 251–257.

5.18. B. B. Brettmann, D. Darwin, and R. C. Donahey, "Bond of Reinforcement to Superplasticized Concrete," *J. ACI*, vol. 83, no. 1, 1986, pp. 98–107.

5.19. R. G. Mathey and J. R. Clifton, "Bond of Coated Reinforcing Bars in Concrete," *J. Struct. Div.*, ASCE, vol. 102, no. ST1, 1976, pp. 215–228.

5.20. R. A. Treece and J. O. Jirsa, "Bond Strength of Epoxy-Coated Reinforcing Bars," *ACI Matls. J.*, vol. 86, no. 2, 1989, pp. 167–174.

5.21. B. S. Hamad, J. O. Jirsa, and N. I. dePaulo, "Anchorage Strength of Epoxy-Coated Hooked Bars," *ACI Struct. J.*, vol. 90, no. 2, 1993, pp. 210–217.

5.22. H. H. Ghaffari, O. C. Choi, D. Darwin, and S. L. McCabe, "Bond of Epoxy-Coated Reinforcement: Cover, Casting Position, Slump, and Consolidation," *ACI Struct. J.*, vol. 91, no. 1, 1994, pp. 59–68.

5.23. C. J. Hester, S. Salamizavaregh, D. Darwin, and S. L. McCabe, "Bond of Epoxy-Coated Reinforcement: Splices," *ACI Struct. J.*, vol. 90, no. 1, 1993, pp. 89–102.

5.24. D. Darwin and J. Zuo, "Discussion of Proposed Changes to ACI 318 in *ACI 318-02 Discussion and Closure*," *Concr. Intl.*, vol. 24, no. 1, 2002, pp. 91, 93, 97–101.

5.25. M. K. Thompson, "The Anchorage Behavior of Headed Reinforcement in CCT Nodes and Lap Splices," Ph.D. Thesis, University of Texas at Austin, 2002.

5.26. M. K. Thompson, A. Ledesma, J. O. Jirsa, and J. E. Breen, "Lap Splices Anchored by Headed Bars," *ACI Struct. J.*, vol. 103, no. 2, 2006, pp. 271–279.

5.27. M. K. Thompson, J. O. Jirsa, and J. E. Breen, "CCT Nodes Anchored by Headed Bars—Part 2: Capacity of Nodes," *ACI Struct. J.*, vol. 103, no. 1, 2006, pp. 65–73.

5.28. M. K. Thompson, M. Ziehl, J. O. Jirsa, and J. E. Breen, "CCT Nodes Anchored by Headed Bars—Part 1: Behavior of Nodes," *ACI Struct. J.*, vol. 103, no. 6, 2006, pp. 808–815.

PROBLEMS

5.1. The short beam shown in Fig. P5.1 cantilevers from a supporting column at the left. It must carry a calculated dead load of 29 kN/m including its own weight and a service live load of 38 kN/m. Tensile flexural reinforcement consists of two No. 36 (No. 11) bars at a 525 mm effective depth. Transverse No. 10 (No. 3) U stirrups with 40 mm cover are provided at the following spacings from the face of the column: 100 mm, 3 at 200 mm, 5 at 260 mm.

(*a*) If the flexural and shear steel use $f_y = 420$ MPa and if the beam uses lightweight concrete having $f'_c = 28$ MPa, check to see if proper development length can be provided for the No. 36 (No. 11) bars. Use the simplified development length equations.

(*b*) Recalculate the required development length for the beam bars using the basic Eq. (5.4). Comment on your results.

FIGURE P5.1

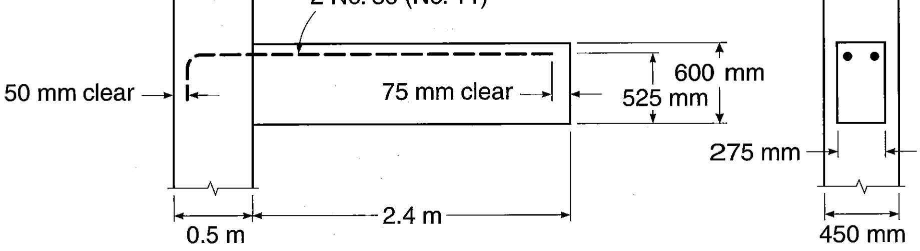

(*c*) If the column material strengths are f_y = 420 MPa and f'_c = 35 MPa (normalweight concrete), check to see if adequate embedment can be provided within the column for the No. 36 (No. 11) bars. If hooks are required, specify detailed dimensions.

5.2. The beam shown in Fig. P5.2 is simply supported with a clear span of 8 m and is to carry a distributed dead load of 15.3 kN/m including its own weight and live load of 23.6 kN/m, unfactored, in service. The reinforcement consists of five No. 32 (No. 10) bars at a 400 mm effective depth, two of which are to be discontinued where no longer needed. Material strengths specified are f_y = 420 MPa and f'_c = 35 MPa. No. 10 (No. 3) stirrups are used with a cover of 40 mm at spacing less than ACI Code maximum.

(*a*) Calculate the point where two bars can be discontinued.

(*b*) Check to be sure that adequate embedded length is provided for continued and discontinued bars.

(*c*) Check special requirements at the support, where M_u = 0.

(*d*) If No. 10 (No. 3) bars are used for transverse reinforcement, specify special reinforcing details in the vicinity where the No. 32 (No. 10) bar is cut off.

(*e*) Comment on the practical aspects of the proposed design. Would you recommend cutting off the steel as suggested? Could three bars be discontinued rather than two?

FIGURE P5.2

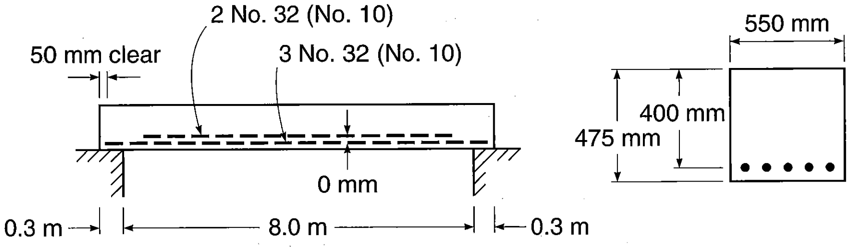

5.3. Figure P5.3 shows the column reinforcement for a 400 mm diameter concrete column, with f_y = 520 MPa and f'_c = 56 MPa. Analysis of the building frame indicates a required A_s = 4710 mm^2 in the lower column and 3742 mm^2 in the upper column. Spiral reinforcement consists of a No. 10 (No. 3) bar with a 50 mm pitch. Column bars are to be spliced just above the construction joint at the floor level, as shown in the sketch. Calculate the minimum permitted length of splice.

FIGURE P5.3

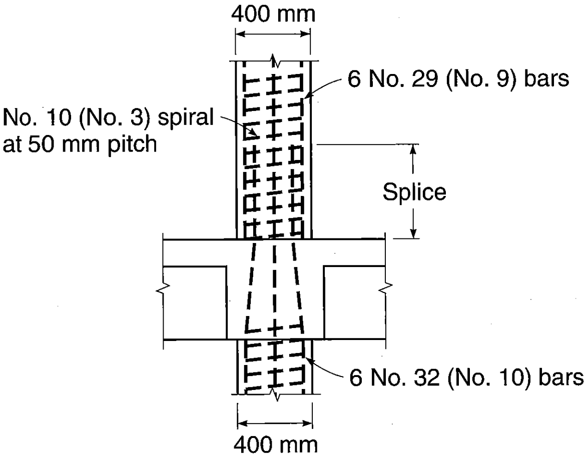

5.4. The short cantilever shown in Fig. P5.4 carries a heavy concentrated load 150 mm from its outer end. Flexural analysis indicates that three No. 25 (No. 8) bars are required, suitably anchored in the supporting wall and extending to a point no closer than 50 mm from the free end. The bars will be fully stressed to f_y at the fixed support. Investigate the need for hooks and transverse confinement steel at the right end of the member. Material strengths are f_y = 420 MPa and f'_c = 28 MPa. If hooks and transverse steel are required, show details in a sketch.

FIGURE P5.4

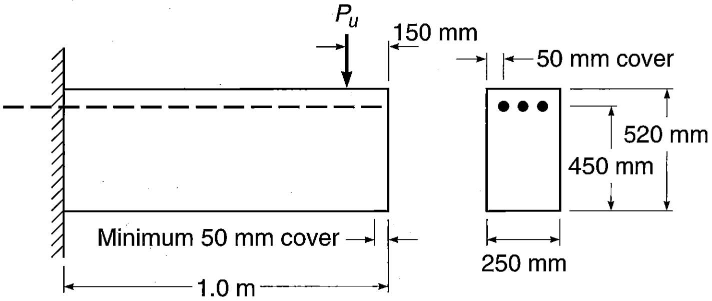

5.5. A continuous-strip wall footing is shown in cross section in Fig. P5.5. It is proposed that tensile reinforcement be provided using No. 25 (No. 8) bars at 400 mm spacing along the length of the wall, to provide a bar area of 1275 mm^2/m. The bars have strength f_y = 420 MPa, and the footing concrete has f'_c = 28 MPa. The critical section for bending is assumed to be at the face of the supported wall, and the effective depth to the tensile steel is 300 mm. Check to ensure that sufficient development length is available for the No. 25 (No. 8) bars, and if hooks are required, sketch details of the hooks, giving dimensions.

Note: If hooks are required for the No. 25 (No. 8) bars, prepare an alternate design using bars having the same area per foot but of smaller diameter such that hooks could be eliminated; use the largest bar size possible to minimize the cost of steel placement.

FIGURE P5.5

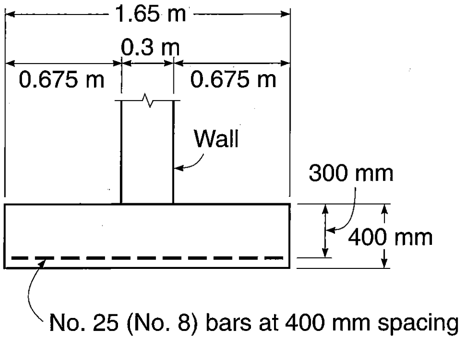

5.6. A closure strip is to be used between two precast slabs (Fig. P5.6). The slabs contain No. 16 (No. 5) bars spaced at 250 mm. Determine the minimum width of the closure strip for use with headed bars spliced within the strip. A_{brg} = $4A_b$. Material strengths are f_y = 420 MPa and f'_c = 35 MPa. The maximum size aggregate = 19 mm. Assume head thickness = 13 mm.

FIGURE P5.6

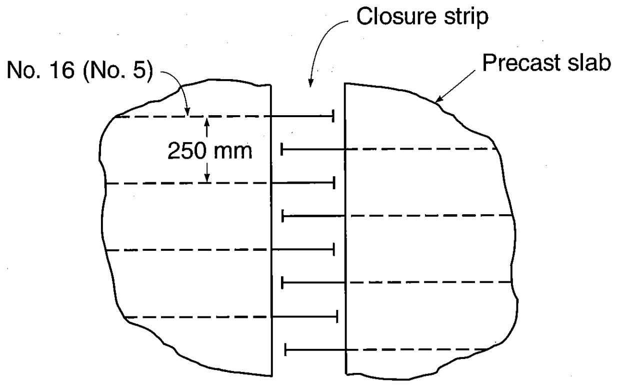

5.7. The continuous beam shown in Fig. P5.7 has been designed to carry a service dead load of 32.8 kN/m including self-weight and service live load of 47.4 kN/m. Flexural design has been based on ACI moment coefficients of $\frac{1}{11}$ and $\frac{1}{16}$ at the face of support and midspan, respectively, resulting in a concrete section with $b = 350$ mm and $d = 550$ mm. Negative reinforcement at the support face is provided by four No. 32 (No. 10) bars, which will be cut off in pairs where no longer required by the ACI Code. Positive bars consist of four No. 25 (No. 8) bars, which will also be cut off in pairs. Specify the exact point of cutoff for all negative and positive steel. Specify also any supplementary web reinforcement that may be required. Check for satisfaction of ACI Code requirements at the point of inflection, and suggest modifications of reinforcement if appropriate. Material strengths are $f_y = 420$ MPa and $f'_c = 28$ MPa.

FIGURE P5.7

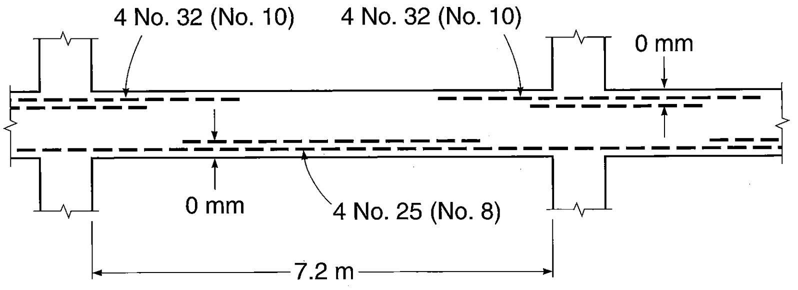

5.8. Figure P5.8 shows a deep transfer girder that carries two heavy column loads at its outer ends from a high-rise concrete building. Ground-floor columns must be offset 2.4 m as shown. The loading produces an essentially constant moment (neglect self-weight of girder) calling for a concrete section with $b = 550$ mm and $b = 1250$ mm, with main tensile reinforcement at the top of the girder comprised of 12 No. 36 (No. 11) bars in three layers of four bars each. The maximum available bar length is 18 m, so tensile splices must be provided. Design and detail all splices, following ACI Code provisions. Splices will be

FIGURE P5.8

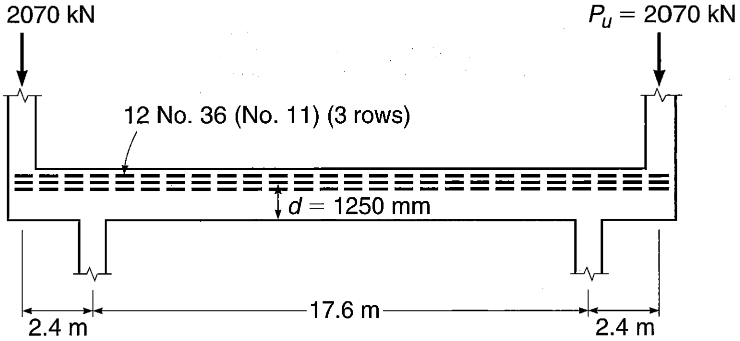
P_u = 2070 kN
P_u = 2070 kN
12 No. 36 (No. 11) (3 rows)
d = 1250 mm
2.4 m
17.6 m
2.4 m

staggered, with no more than four bars spliced at any section. Also, investigate the need for special anchorage at the outer ends of main reinforcement, and specify details of special anchorage if required. Material strengths are f_y = 420 MPa and f'_c = 28 MPa.

6 Serviceability

6.1 INTRODUCTION

Chapters 3, 4, and 5 have dealt mainly with the strength design of reinforced concrete beams. Methods have been developed to ensure that beams will have a proper safety margin against failure in flexure or shear, or due to inadequate bond and anchorage of the reinforcement. The member has been assumed to be at a hypothetical overload state for this purpose.

It is also important that member performance in normal service be satisfactory, when loads are those actually expected to act, i.e., when load factors are 1.0. This is not guaranteed simply by providing adequate strength. Service load deflections under full load may be excessively large, or long-term deflections due to sustained loads may cause damage. Tension cracks in beams may be wide enough to be visually disturbing, and in some cases may reduce the durability of the structure. These and other questions, such as vibration or fatigue, require consideration.

Serviceability studies are carried out based on elastic theory, with stresses in both concrete and steel assumed to be proportional to strain. The concrete on the tension side of the neutral axis may be assumed uncracked, partially cracked, or fully cracked, depending on the loads and material strengths (see Section 3.3).

In early reinforced concrete designs, questions of serviceability were dealt with indirectly, by limiting the stresses in concrete and steel at service loads to the rather conservative values that had resulted in satisfactory performance. In contrast, with current design methods that permit more slender members through more accurate assessment of capacity, and with higher-strength materials further contributing to the trend toward smaller member sizes, such indirect methods no longer work. The current approach is to investigate service load cracking and deflections specifically, after proportioning members based on strength requirements.

In this chapter, methods will be developed to ensure that the cracks associated with flexure of reinforced concrete beams are narrow and well distributed, and that short and long-term deflections at loads up to the full service load are not objectionably large.

6.2 CRACKING IN FLEXURAL MEMBERS

All reinforced concrete beams crack, generally starting at loads well below service level, and possibly even prior to loading due to restrained shrinkage. Flexural cracking due to loads is not only inevitable, but actually necessary for the reinforcement to be used effectively. Prior to the formation of flexural cracks, the steel stress is no more than n times the stress in the adjacent concrete, where n is the modular ratio E_s/E_c. For materials common in current practice, n is approximately 8. Thus, when the concrete is close to its modulus of rupture of about 3.5 MPa, the steel stress will be only $8 \times 3.5 = 28$ MPa, far too low to be very effective as reinforcement. At normal service loads, steel stresses 8 or 9 times that value can be expected.

In a well-designed beam, flexural cracks are fine, so-called hairline cracks, almost invisible to the casual observer, and they permit little if any corrosion of the reinforcement. As loads are gradually increased above the cracking load, both the number and the width of cracks increase, and at service load level a maximum width of crack of about 0.4 mm is typical. If loads are further increased, crack widths increase further, although the number of cracks is more or less stable.

Cracking of concrete is a random process, highly variable and influenced by many factors. Because of the complexity of the problem, present methods for predicting crack widths are based primarily on test observations. Most equations that have been developed predict the *probable maximum crack width*, which usually means that about 90 percent of the crack widths in the member are below the calculated value. However, isolated cracks exceeding twice the computed width can sometimes occur (Ref. 6.1).

a. Variables Affecting Width of Cracks

In the discussion of the importance of a good bond between steel and concrete in Section 5.1, it was pointed out that if proper end anchorage is provided, a beam will not fail prematurely, even though the bond is destroyed along the entire span. However, crack widths will be greater than for an otherwise identical beam in which good resistance to slip is provided along the length of the span. In general, beams with smooth round bars will display a relatively small number of rather wide cracks in service, while beams with good slip resistance ensured by proper surface deformations on the bars will show a larger number of very fine, almost invisible cracks. Because of this improvement, reinforcing bars in current practice are always provided with surface deformations, the maximum spacing and minimum height of which are established by ASTM Specifications A615, A706, and A996.

A second variable of importance is the stress in the reinforcement. Studies by Gergely and Lutz and others (Refs. 6.2 to 6.4) have confirmed that crack width is proportional to f_s^n, where f_s is the steel stress and n is an exponent that varies in the range from about 1.0 to 1.4. For steel stresses in the range of practical interest, say from 140 to 250 MPa, n may be taken equal to 1.0. The steel stress is easily computed based on elastic cracked-section analysis (Section 3.3b). Alternatively, f_s may be taken equal to $\frac{2}{3}f_y$ according to ACI Code 10.6.4.

Experiments by Broms (Ref. 6.5) and others have shown that both crack spacing and crack width are related to the concrete cover distance d_c, measured from the center of the bar to the face of the concrete. In general, increasing the cover increases the spacing of cracks and also increases crack width. Furthermore, the distribution of the reinforcement in the tension zone of the beam is important. Generally, to control cracking, it is better to use a larger number of smaller-diameter bars to provide the required A_s than to use the minimum number of larger bars, and the bars should be well distributed over the tensile zone of the concrete. For deep flexural members, this includes additional reinforcement on the sides of the web to prevent excessive surface crack widths above or below the level of the main flexural reinforcement.

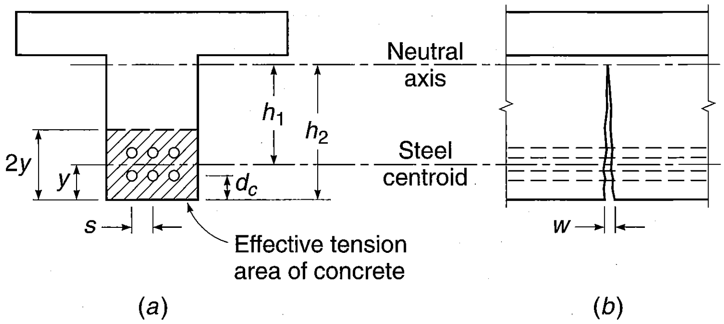

FIGURE 6.1
Geometric basis of crack width calculations.

b. Equations for Crack Width

A number of expressions for maximum crack width have been developed based on the statistical analysis of experimental data. Two expressions that have figured prominently in the development of the crack control provisions in the ACI Code are those developed by Gergely and Lutz (Ref. 6.2) and Frosch (Ref. 6.4) for the maximum crack width at the tension face of a beam. They are, respectively,

$$w = 1.1\beta f_s \sqrt[3]{d_c A} \times 10^{-5} \tag{6.1}$$

and

$$w = 2\frac{f_s}{E_s}\beta\sqrt{d_c^2 + \left(\frac{s}{2}\right)^2} \tag{6.2}$$

where w = maximum width of crack, mm
f_s = steel stress at load for which crack width is to be determined, MPa
E_s = modulus of elasticity of steel, MPa

The geometric parameters are shown in Fig. 6.1 and are as follows:

d_c = thickness of concrete cover measured from tension face to center of bar closest to that face, mm
β = ratio of distances from tension face and from steel centroid to neutral axis, equal to h_2/h_1
A = concrete area surrounding one bar, equal to total effective tension area of concrete surrounding reinforcement and having same centroid, divided by number of bars, mm^2
s = maximum bar spacing, mm

Equations (6.1) and (6.2), which apply only to beams in which deformed bars are used, include all the factors just named as having an important influence on the width of cracks: steel stress, concrete cover, and the distribution of the reinforcement in the concrete tensile zone. In addition, the factor β is added to account for the increase in crack width with distance from the neutral axis (see Fig. 6.1*b*).

c. Cyclic and Sustained Load Effects

Both cyclic and sustained loading account for increasing crack width. While there is a large amount of scatter in test data, results of fatigue tests and sustained loading tests indicate that a doubling of crack width can be expected with time (Ref. 6.1). Under most conditions, the spacing of cracks does not change with time at constant levels of sustained stress or cyclic stress range.

6.3 ACI CODE PROVISIONS FOR CRACK CONTROL

In view of the random nature of cracking and the wide scatter of crack width measurements, even under laboratory conditions, crack width is controlled in the ACI Code by establishing a maximum center-to-center spacing s for the reinforcement closest to the surface of a tension member as a function of the bar stress under service conditions f_s (in MPa) and the *clear cover* from the nearest surface in tension to the surface of the flexural tension reinforcement c_c.

$$s = 380\left(\frac{280}{f_s}\right) - 2.5c_c \leq 300\left(\frac{280}{f_s}\right) \tag{6.3}$$

The choice of clear cover c_c, rather than the cover to the center of the bar d_c, was made to simplify design, since this allows s to be independent of bar size. As a consequence, maximum crack widths will be somewhat greater for larger bars than for smaller bars.

As shown in Eq. (6.3), the ACI Code sets an upper limit on s of $300(280/f_s)$. The stress f_s is calculated by dividing the service load moment by the product of the area of reinforcement and the internal moment arm, as shown in Eq. (3.8). Alternatively, the ACI Code permits f_s to be taken as two-thirds of the specified yield strength f_y. For members with only a single bar, s is taken as the width of the extreme tension face.

Figure 6.2*a* compares the values of spacing s obtained using Eqs. (6.1) and (6.2) for a beam containing No. 25 (No. 8) reinforcing bars, for $f_s = 280$ MPa, $\beta = 1.2$, and a maximum crack width $w = 0.4$ mm to the values calculated using Eq. (6.3). Equations (6.1) and (6.2) give identical spacings for two values of clear cover, but significantly different spacings for other values of c_c. Equation (6.3) provides a practical compromise between the values of s that are calculated using the two experimentally based expressions. The equation is plotted in Fig. 6.2*b* for $f_s = 186.7$, 280, and 346.7 MPa, corresponding to $\frac{2}{3}f_y$ for Grade 280, 420 and 520 bars, respectively.

ACI Code 10.6.5 points out that the limitation on s in Eq. (6.3) is not sufficient for structures subject to very aggressive exposure or designed to be watertight. In such cases "special investigations or precautions" are required. These include the use of expressions such as Eqs. (6.1) and (6.2) to determine the probable maximum crack width. Further guidance is given in Ref. 6.1.

When concrete T beam flanges are in tension, as in the negative-moment region of continuous T beams, concentration of the reinforcement over the web may result in excessive crack width in the overhanging slab, even though cracks directly over the web are fine and well distributed. To prevent this, the tensile reinforcement should be distributed over the width of the flange, rather than concentrated. However, because of shear lag, the outer bars in such a distribution would be considerably less highly stressed than those directly over the web, producing an uneconomical design. As a reasonable compromise, ACI Code 10.6.6 requires that the tension reinforcement in such cases be distributed over the effective flange width or a width equal to one-tenth the span, whichever is smaller. If the effective flange width exceeds one-tenth of the span, some longitudinal reinforcement must be provided in the outer portions of the flange. The amount of such additional reinforcement is left to the discretion of the designer; it should at least be the equivalent of temperature reinforcement for the slab (see Section 13.3), and is often taken as twice that amount.

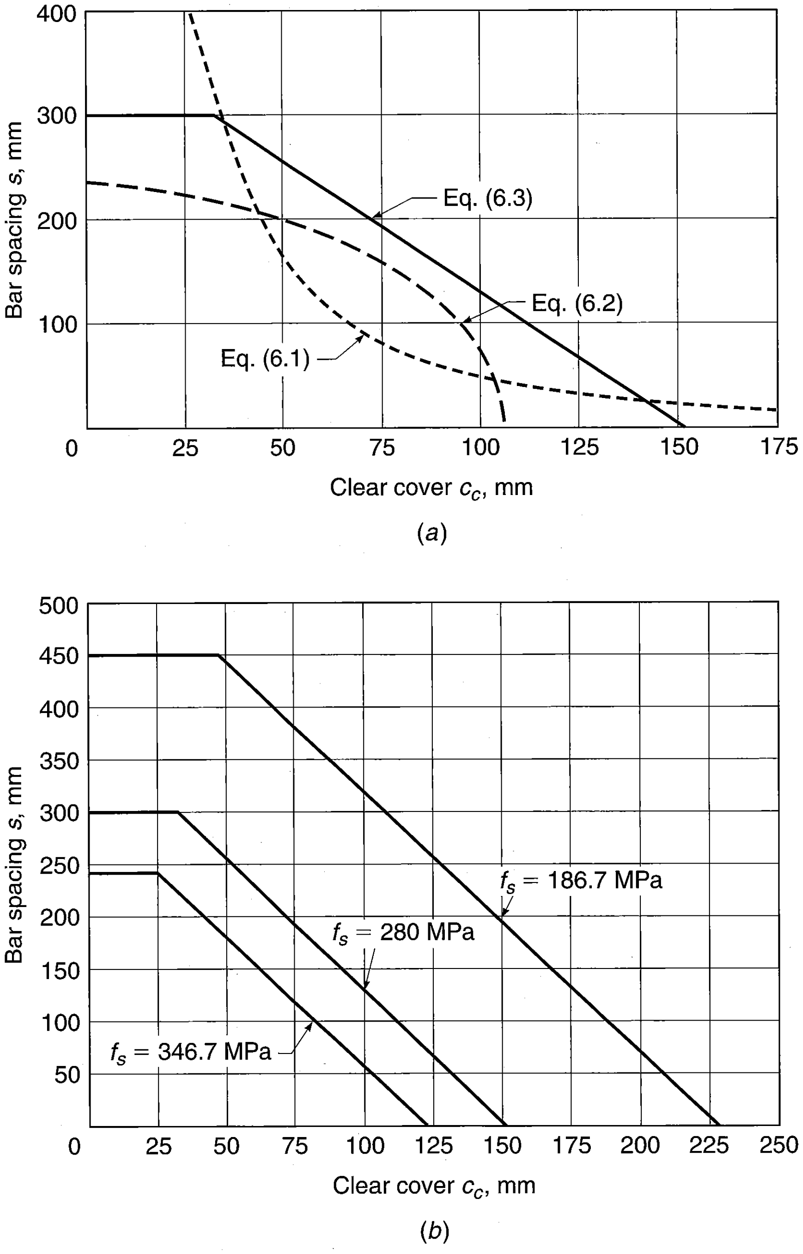

FIGURE 6.2
Maximum bar spacing versus clear cover: (*a*) Comparison of Eqs. (6.1), (6.2), and (6.3) for $w_c = 0.4$ mm, $f_s =$ 280 MPa, $\beta = 1.2$, bar size = No. 25 (No. 8); (*b*) Eq. (6.3) for f_s = 186.7, 280, and 346.7 MPa, corresponding to $\frac{2}{3}f_y$ for Grades 280, 420, and 520 reinforcement, respectively. [*Part* (*a*) *after Ref. 6.6.*]

For beams with relatively deep webs, some reinforcement should be placed near the vertical faces of the web to control the width of cracks in the concrete tension zone above the level of the main reinforcement. Without such steel, crack widths in the web wider than those at the level of the main bars have been observed. According to ACI Code 10.6.7, if the total depth of the beam h exceeds 900 mm, longitudinal "skin" reinforcement must be uniformly distributed along both side faces of the member for a distance $h/2$ nearest the flexural tension steel, as shown in Fig. 6.3. The spacing s between longitudinal bars or wires is as specified in Eq. (6.3). The size of the bars or

FIGURE 6.3
Skin reinforcement for flexural members with total depth h greater than 900 mm.

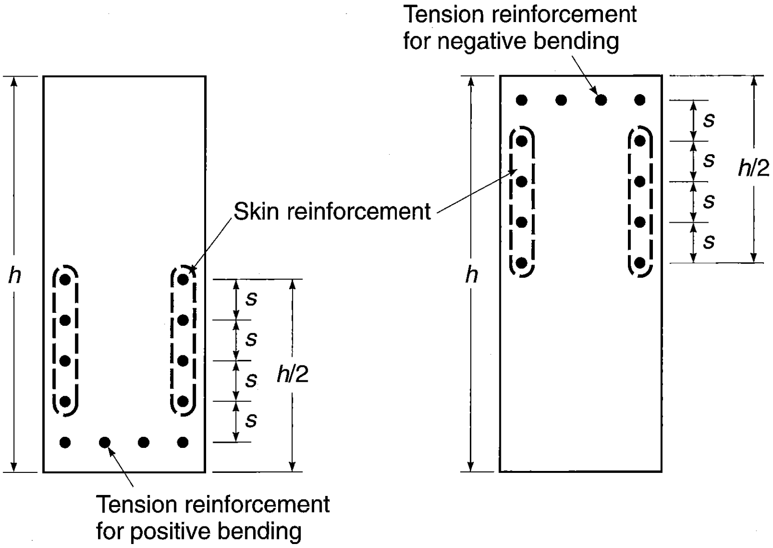
Tension reinforcement for negative bending
Skin reinforcement
h
s
s
s
s
h/2
h
s
s
s
s
h/2
Tension reinforcement for positive bending

wires is not specified, but as indicated in ACI Commentary 10.6.7, No. 10 to No. 16 (No. 3 to No. 5) bars or welded wire reinforcement with a minimum area of 210 mm^2 per meter of depth are typically used. The contribution of the skin steel to flexural strength is usually disregarded, although it may be included in the strength calculations if a strain compatibility analysis is used to establish the stress in the skin steel at the flexural failure load.

Figure 6.2*b* provides a convenient design aid for determining the maximum center-to-center bar spacing as a function of clear cover for the usual case used in design, $f_s = \frac{2}{3}f_y$. From a practical point of view, it is even more helpful to know the minimum number of bars across the width of a beam stem that is needed to satisfy the ACI Code requirements for crack control. That number depends on side cover, as well as clear cover to the tension face, and is dependent on bar size. Table A.8 in Appendix A gives the minimum number of bars across a beam stem for two common cases, 50 mm clear cover on the sides and bottom, which corresponds to using No. 10 or No. 13 (No. 3 or No. 4) stirrups, and 40 mm clear cover on the sides and bottom, representing beams in which no stirrups are used.

EXAMPLE 6.1

Check crack control criteria. Figure 6.4 shows the main flexural reinforcement at midspan for a T girder in a high-rise building that carries a service load moment of 975 kN-m. The clear cover on the side and bottom of the beam stem is 60 mm. Determine if the beam meets the crack control criteria in the ACI Code.

SOLUTION. Since the depth of the beam equals but does not exceed 900 mm, skin reinforcement is not needed. To check the bar spacing criteria, the steel stress can be estimated closely by taking the internal lever arm equal to the distance $d - h_f/2$:

$$f_s = \frac{M_s}{A_s(d - h_f/2)} = \frac{975 \times 10^6}{5100 \times 725} = 263 \text{ MPa}$$

(Alternately, the ACI Code permits using $f_s = \frac{2}{3}f_y$, giving 280 MPa.)

FIGURE 6.4
T beam for crack width determination in Example 6.1.

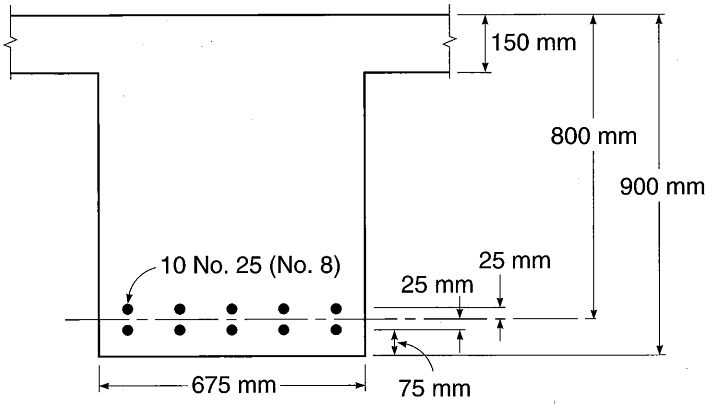

Using f_s in Eq. (6.3) gives

$$s = 380\left(\frac{280}{f_s}\right) - 2.5c_c = 380\left(\frac{280}{263}\right) - 2.5 \times 60 = 255 \text{ mm}$$

By inspection, it is clear that this requirement is satisfied for the beam. If the results had been unfavorable, a redesign using a larger number of smaller-diameter bars would have been indicated.

6.4 CONTROL OF DEFLECTIONS

In addition to limitations on cracking, described in the preceding sections, it is usually necessary to impose certain controls on deflections of beams to ensure serviceability. Excessive deflections can lead to cracking of supported walls and partitions, ill-fitting doors and windows, poor roof drainage, misalignment of sensitive machinery and equipment, or visually offensive sag. It is important, therefore, to maintain control of deflections, in one way or another, so that members designed mainly for strength at prescribed overloads will also perform well in normal service.

There are presently two approaches to deflection control. The first is indirect and consists in setting suitable upper limits on the span-depth ratio. This is simple, and it is satisfactory in many cases where spans, loads and load distributions, and member sizes and proportions fall in the usual ranges. Otherwise, it is essential to calculate deflections and to compare those predicted values with specific limitations that may be imposed by codes or by special requirements.

It will become clear, in the sections that follow, that calculations can, at best, provide a guide to probable actual deflections. This is so because of uncertainties regarding material properties, effects of cracking, and load history for the member under consideration. Extreme precision in the calculations, therefore, is never justified, because highly accurate results are unlikely. However, it is generally sufficient to know, for example, that the deflection under load will be about 10 mm rather than 50 mm, while it is relatively unimportant to know whether it will actually be 15 mm rather than 10 mm.

The deflections of concern are generally those that occur during the normal service life of the member. In service, a member sustains the full dead load, plus some fraction or all of the specified service live load. Safety provisions of the ACI Code and similar design specifications ensure that, under loads up to the full service load, stresses in both steel and concrete remain within the elastic ranges. Consequently, deflections that occur at once upon application of load, the *immediate deflections*, can be calculated based on the properties of the uncracked elastic member, the cracked elastic member, or some combination of these (see Section 3.3).

It was pointed out in Sections 2.8 and 2.11, however, that in addition to concrete deformations that occur immediately when load is applied, there are other deformations that take place gradually over an extended time. These time-dependent deformations are chiefly due to concrete creep and shrinkage. As a result of these influences, reinforced concrete members continue to deflect with the passage of time. Long-term deflections continue over a period of several years, and may eventually be 2 or more times the initial elastic deflections. Clearly, methods for predicting both instantaneous and time-dependent deflections are essential.

6.5 IMMEDIATE DEFLECTIONS

Elastic deflections can be expressed in the general form

$$\Delta = \frac{f(\text{loads, spans, supports})}{EI}$$

where EI is the flexural rigidity and f(loads, spans, supports) is a function of the particular load, span, and support arrangement. For instance, the deflection of a uniformly loaded simple beam is $5wl^4/384EI$, so that $f = 5wl^4/384$. Similar deflection equations have been tabulated or can easily be computed for many other loadings and span arrangements, simple, fixed, or continuous, and the corresponding f functions can be determined. The particular problem in reinforced concrete structures is therefore the determination of the appropriate flexural rigidity EI for a member consisting of two materials with properties and behavior as widely different as steel and concrete.

If the maximum moment in a flexural member is so small that the tensile stress in the concrete does not exceed the modulus of rupture f_r, no flexural tension cracks will occur. The full, uncracked section is then available for resisting stress and providing rigidity. This stage of loading has been analyzed in Section 3.3a. In agreement with this analysis, the effective moment of inertia for this low range of loads is that of the uncracked transformed section I_{ut}, and E is the modulus of concrete E_c as given by Eq. (2.3). Correspondingly, for this load range,

$$\Delta_{iu} = \frac{f}{E_c I_{ut}} \tag{a}$$

At higher loads, flexural tension cracks are formed. In addition, if shear stresses exceed v_{cr} [see Eq. (4.3)] and web reinforcement is employed to resist them, diagonal cracks can exist at service loads. In the region of flexural cracks, the position of the neutral axis varies: directly at each crack it is located at the level calculated for the cracked transformed section (see Section 3.3b); midway between cracks it dips to a location closer to that calculated for the uncracked transformed section. Correspondingly, flexural-tension cracking causes the effective moment of inertia to be that of the cracked transformed section in the immediate neighborhood of flexural-tension cracks, and closer to that of the uncracked transformed section midway between cracks, with a gradual transition between these extremes.

The value of the local moment of inertia varies in those portions of the beam in which the bending moment exceeds the cracking moment of the section

$$M_{cr} = \frac{f_r I_{ut}}{y_t} \tag{6.4}$$

where y_t is the distance from the neutral axis to the tension face and f_r is the modulus of rupture. The exact variation of I depends on the shape of the moment diagram and on the crack pattern, and is difficult to determine. This makes an exact deflection calculation impossible.

However, extensively documented studies (Ref. 6.7) have shown that deflections Δ_{ic} occurring in a beam after the maximum moment M_a has reached and exceeded the cracking moment M_{cr} can be calculated by using an effective moment of inertia I_e; that is,

$$\Delta_{ic} = \frac{f}{E_c I_e} \tag{b}$$

where

$$I_e = \left(\frac{M_{cr}}{M_a}\right)^3 I_{ut} + \left[1 - \left(\frac{M_{cr}}{M_a}\right)^3\right] I_{cr} \leq I_{ut} \tag{6.5}$$

and I_{cr} is the moment of inertia of the cracked transformed section.

In Fig. 6.5, the effective moment of inertia, given by Eq. (6.5), is plotted as a function of the ratio M_a/M_{cr} (the reciprocal of the moment ratio used in the equation). It is seen that, for values of maximum moment M_a less than the cracking moment M_{cr}, that is, M_a/M_{cr} less than 1.0, $I_e = I_{ut}$. With increasing values of M_a, I_e approaches I_{cr}; and for values of M_a/M_{cr} of 3 or more, I_e is almost the same as I_{cr}. Typical values of M_a/M_{cr} at full service load range from about 1.5 to 3.

Figure 6.6 shows the growth of deflections with increasing moment for a simple-span beam and illustrates the use of Eq. (6.5). For moments no larger than M_{cr}, deflections are practically proportional to moments, and the deflection at which cracking

FIGURE 6.5
Variation of I_e with moment ratio.

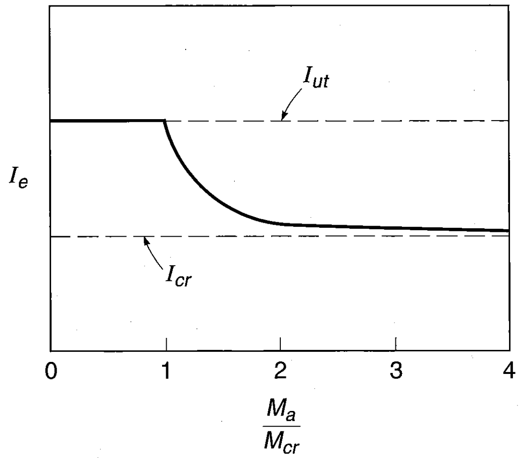

FIGURE 6.6
Deflection of a reinforced concrete beam.

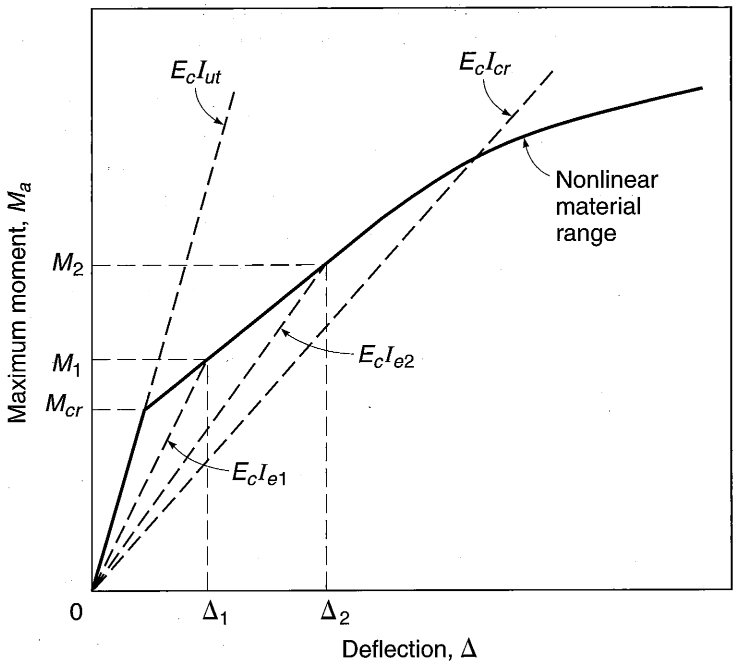

begins is obtained from Eq. (*a*) with $M = M_{cr}$. At larger moments, the effective moment of inertia I_e becomes progressively smaller, according to Eq. (6.5), and deflections are found by Eq. (*b*) for the load level of interest. The moment M_2 might correspond to the full service load, for example, while the moment M_1 would represent the dead load moment for a typical case. A moment-deflection curve corresponding to the line E_cI_{cr} represents an upper bound for deflections, consistent with Fig. 6.5, except that at loads somewhat beyond the service load, the nonlinear response of steel or concrete or both causes a further nonlinear increase in deflections.

Note that to calculate the increment of deflection due to live load, causing a moment increase $M_2 - M_1$, a two-step computation is required: the first for deflection Δ_2 due to live and dead load, and the second for deflection Δ_1 due to dead load alone, each with the appropriate value of I_e. Then the deflection increment due to live load is found, equal to $\Delta_2 - \Delta_1$.

Most reinforced concrete spans are continuous, not simply supported. The concepts just introduced for simple spans can be applied, but the moment diagram for a given span will include both negative and positive regions, reflecting the rotational restraint provided at the ends of the spans by continuous frame action. The effective moment of inertia for a continuous span can be found by a simple averaging procedure, according to the ACI Code, that will be described in Section 6.7c.

A fundamental problem for continuous spans is that although the deflections are based on the moment diagram, that moment diagram depends, in turn, on the flexural rigidity *EI* for each member of the frame. The flexural rigidity depends on the extent of cracking, as has been demonstrated. Cracking, in turn, depends on the moments, which are to be found. The circular nature of the problem is evident.

One could use an iterative procedure, initially basing the frame analysis on uncracked concrete members, determining the moments, calculating effective *EI* terms for all members, then recalculating moments, adjusting the *EI* values, etc. The process could be continued for as many iterations as needed, until changes are not significant. However, such an approach would be expensive and time-consuming, even with computer use.

Usually, a very approximate approach is adopted. Member flexural stiffnesses for the frame analysis are based simply on properties of uncracked rectangular concrete cross sections. This can be defended by noting that the moments in a continuous frame depend only on the *relative* values of *EI* in its members, not the *absolute* values. Hence, if a consistent assumption, i.e., uncracked section, is used for all members, the results should be valid. Although cracking is certainly more prevalent in beams than in columns, thus reducing the relative *EI* for the beams, this is compensated to a large extent, in typical cases, by the stiffening effect of the flanges in the positive bending regions of continuous T beam construction. This subject is discussed at greater length in Section 12.5.

6.6 DEFLECTIONS DUE TO LONG-TERM LOADS

Initial deflections are increased significantly if loads are sustained over a long period of time, due to the effects of shrinkage and creep. These two effects are usually combined in deflection calculations. Creep generally dominates, but for some types of members, shrinkage deflections are large and should be considered separately (see Section 6.8).

It was pointed out in Section 2.8 that creep deformations of concrete are directly proportional to the compressive stress up to and beyond the usual service load range. They increase asymptotically with time and, for the same stress, are larger for low-strength than for high-strength concretes. The ratio of additional time-dependent strain to initial elastic strain is given by the creep coefficient C_{cu} (see Table 2.2).

For a reinforced concrete beam, the long-term deformation is much more complicated than for an axially loaded cylinder, because while the concrete creeps under sustained load, the steel does not. The situation in a reinforced concrete beam is illustrated by Fig. 6.7. Under sustained load, the initial strain ϵ_i at the top face of the beam increases, due to creep, by the amount ϵ_t, while the strain ϵ_s in the steel is essentially unchanged. Because the rotation of the strain distribution diagram is therefore about a point at the level of the steel, rather than about the cracked elastic neutral axis, the neutral axis moves down as a result of creep, and

$$\frac{\phi_t}{\phi_i} < \frac{\epsilon_t}{\epsilon_i} \qquad (a)$$

demonstrating that the usual creep coefficients cannot be applied to initial curvatures to obtain creep curvatures (hence deflections).

The situation is further complicated. Due to the lowering of the neutral axis associated with creep (see Fig. 6.7*b*) and the resulting increase in compression area, the compressive stress required to produce a given resultant C to equilibrate $T = A_s f_s$ is less than before, in contrast to the situation in a creep test of a compressed cylinder, because the beam creep occurs at a gradually diminishing stress. On the other hand, with the new lower neutral axis, the internal lever arm between compressive and tensile resultant forces is less, calling for an increase in both resultants for a constant moment. This, in turn, will require a small increase in stress, and hence strain, in the steel; thus, ϵ_s is not constant as assumed originally.

Because of such complexities, it is necessary in practice to calculate additional, time-dependent deflections of beams due to creep (and shrinkage) using a simplified,

FIGURE 6.7
Effect of concrete creep on curvature: (*a*) beam cross section; (*b*) strains; (*c*) stresses and forces. (*Adapted from Ref. 6.8.*)

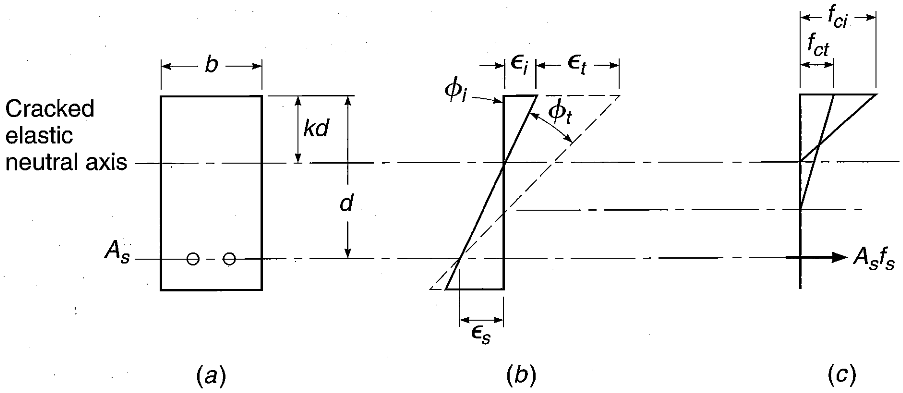

empirical approach by which the initial elastic deflections are multiplied by a factor λ_Δ to obtain the additional long-time deflections. Values of λ_Δ for use in design are based on long-term deflection data for reinforced concrete beams (Refs. 6.8 to 6.11). Thus

$$\Delta_t = \lambda_\Delta \Delta_i \tag{6.6}$$

where Δ_t is the *additional* long-term deflection due to the combined effect of creep and shrinkage and Δ_i is the initial elastic deflection calculated by the methods described in Section 6.5.

The coefficient λ_Δ depends on the duration of the sustained load. It also depends on whether the beam has only reinforcement A_s on the tension side, or whether additional longitudinal reinforcement A'_s is provided on the compression side. In the latter case, the long-term deflections are much reduced. This is so because when no compression reinforcement is provided, the compression concrete is subject to unrestrained creep and shrinkage. On the other hand, since steel is not subject to creep, if additional bars are located close to the compression face, they will resist and thereby reduce the amount of creep and shrinkage and the corresponding deflection (Ref. 6.11). Compression steel may be included for this reason alone. Specific values of λ_Δ, used to account for the influence of creep and compression reinforcement, will be given in Section 6.7.

If a beam carries a certain sustained load *W* (e.g., the dead load plus the average traffic load on a bridge) and is subject to a short-term heavy live load *P* (e.g., the weight of an unusually heavy vehicle), the maximum total deflection under this combined loading is obtained as follows:

1. Calculate the instantaneous deflection Δ_{iw} caused by the sustained load *W* by methods given in Section 6.5.
2. Calculate the additional long-term deflection caused by *W*, that is,

$$\Delta_{tw} = \lambda_\Delta \Delta_{iw}$$

3. Then the total deflection caused by the sustained part of the load is

$$\Delta_w = \Delta_{iw} + \Delta_{tw}$$

4. In calculating the additional instantaneous deflection caused by the short-term load *P*, account must be taken of the fact that the load-deflection relation after cracking is nonlinear, as illustrated by Fig. 6.6. Hence

$$\Delta_{ip} = \Delta_{i(w+p)} - \Delta_{iw}$$

where $\Delta_{i(w+p)}$ is the total instantaneous deflection that would be obtained if W and P were applied simultaneously, calculated by using I_e determined for the moment caused by $W + P$.

5. Then the total deflection under the sustained load plus heavy short-term load is

$$\Delta = \Delta_w + \Delta_{ip}$$

In calculations of deflections, careful attention must be paid to the load history, i.e., the time sequence in which loads are applied, as well as to the magnitude of the loads. The short-term peak load on the bridge girder just described might be applied early in the life of the member, before time-dependent deflections had taken place. Similarly, for buildings, heavy loads such as stacked material are often placed during construction. These temporary loads may be equal to, or even greater than, the design live load. The state of cracking will correspond to the *maximum load* that was carried, and the sustained load deflection, on which the long-term effects are based, would correspond to that cracked condition. I_e for the maximum load reached should be used to recalculate the sustained load deflection before calculating long-term effects.

This will be illustrated referring to Fig. 6.8, showing the load-deflection plot for a building girder that is designed to carry a specified dead and live load. Assume first that the dead and live loads increase monotonically. As the full dead load W_d is applied, the load deflection curve follows the path 0-1, and the dead load deflection Δ_d is found using I_{e1} calculated from Eq. (6.5), with $M_a = M_d$. The time-dependent effect of the dead load would be $\lambda_\Delta \Delta_d$. As live load is then applied, path 1-2 would be followed. Live load deflection Δ_l would be found in two steps, as described in Section 6.5, first finding Δ_{d+l} based on I_{e2}, with M_a in Eq. (6.5) equal to M_{d+l}, and then subtracting dead load deflection Δ_d.

If, on the other hand, short-term construction loads were applied, then removed, the deflection path 1-2-3 would be followed. Then, under dead load only,

FIGURE 6.8
Effect of load history on deflection of a building girder.

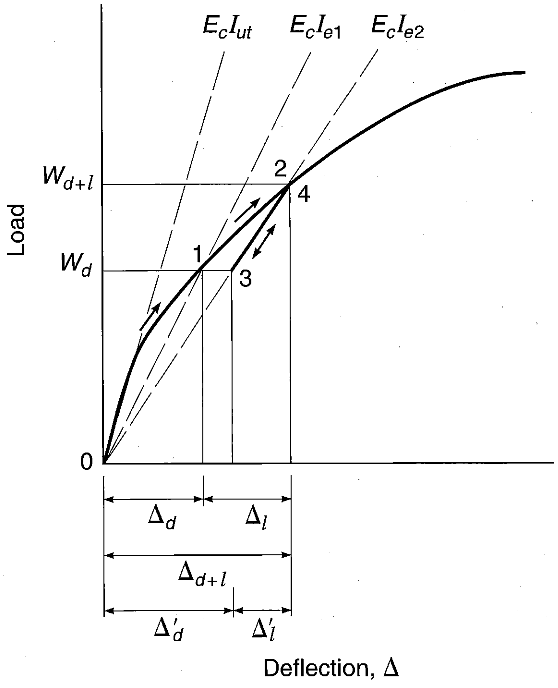

the resulting deflection would be Δ'_d. Note that this deflection can be found in one step using W_d, but with I_{e2} corresponding to the maximum load reached. The long-term deflection now would be $\lambda_\Delta \Delta'_d$, significantly *larger* than before. Should the full design *live* load then be applied, the deflection would follow path 3-4, and the live load deflection would be *less* than for the first case. It, too, can be calculated by a simple one-step calculation using W_l alone, in this case, and with moment of inertia equal to I_{e2}.

Clearly, in calculating deflections, the engineer must anticipate, as nearly as possible, both the magnitude and time sequence of the loadings. Although long-term deflections are often calculated assuming monotonic loading, with both immediate and long-term effects of dead load occurring before application of live load, in many cases this is not realistic.

6.7 ACI CODE PROVISIONS FOR CONTROL OF DEFLECTIONS

a. Minimum Depth-Span Ratios

As pointed out in Section 6.4, two approaches to deflection control are in current use, both acceptable under the provisions of the ACI Code, within prescribed limits. The simpler of these is to impose restrictions on the minimum member depth h, relative to the span l, to ensure that the beam will be sufficiently stiff that deflections are unlikely to cause problems in service. Deflections are greatly influenced by support conditions (e.g., a simply supported uniformly loaded beam will deflect 5 times as much as an otherwise identical beam with fixed supports), so minimum depths must vary depending on conditions of restraint at the ends of the spans.

According to ACI Code 9.5.2, the minimum depths of Table 6.1 apply to one-way construction *not* supporting or attached to partitions or other construction likely to be damaged by large deflections, unless computation of deflections indicates a lesser depth can be used without adverse effects. Values given in Table 6.1 are to be used directly for normalweight concrete with $w_c = 2315$ kg/m^3 and reinforcement with $f_y = 420$ MPa. For members using lightweight concrete with density in the range from 1440 to 1840 kg/m^3, the values of Table 6.1 should be multiplied by $1.65 - 0.0003w_c \geq 1.09$. For yield strengths other than 420 MPa, the values should be multiplied by $0.4 + f_y/700$.

TABLE 6.1

Minimum thickness of nonprestressed beams or one-way slabs unless deflections are computed

Member	Minimum Thickness h			
	Simply Supported	One End Continuous	Both Ends Continuous	Cantilever
	Members Not Supporting or Attached to Partitions or Other Construction Likely to Be Damaged by Large Deflections			
Solid one-way slabs	$l/20$	$l/24$	$l/28$	$l/10$
Beams or ribbed one-way slabs	$l/16$	$l/18.5$	$l/21$	$l/8$

b. Calculation of Immediate Deflections

When there is need to use member depths shallower than are permitted by Table 6.1, or when members support construction that is likely to be damaged by large deflections, or for prestressed members, deflections must be calculated and compared with limiting values (see Section 6.7e). The calculation of deflections, when required, proceeds along the lines described in Sections 6.5 and 6.6. For design purposes, the moment of the uncracked transformed section I_{ut} can be replaced by that of the gross concrete section I_g, neglecting reinforcement, without serious error. With this simplification, Eqs. (6.4) and (6.5) are replaced by the following:

$$M_{cr} = \frac{f_r I_g}{y_t} \tag{6.7}$$

and

$$I_e = \left(\frac{M_{cr}}{M_a}\right)^3 I_g + \left[1 - \left(\frac{M_{cr}}{M_a}\right)^3\right] I_{cr} \le I_g \tag{6.8}$$

The modulus of rupture is to be taken equal to

$$f_r = 0.62\lambda\sqrt{f'_c} \tag{6.9a}$$

As explained in Section 4.5a, in accordance with ACI Code 8.6.1, $\lambda = 1.0$ for normalweight concrete, 0.85 for sand-lightweight concrete, and 0.75 for all-lightweight concrete. If the splitting tensile strength of the concrete f_{ct} is known, $\lambda = f_{ct}/(0.56\sqrt{f'_c}) \le 1.0$, and Eq. (6.9*a*) becomes

$$f_r = 0.62\frac{f_{ct}}{0.50} = 1.11 f_{ct} \tag{6.9b}$$

c. Continuous Spans

For continuous spans, ACI Code 9.5.2 calls for a simple average of values obtained from Eq. (6.8) for the critical positive and negative-moment sections, i.e.,

$$I_e = 0.50 I_{em} + 0.25(I_{e1} + I_{e2}) \tag{6.10a}$$

where I_{em} is the effective moment of inertia for the midspan section and I_{e1} and I_{e2} are those for the negative-moment sections at the respective beam ends, each calculated from Eq. (6.8) using the applicable value of M_a. It is shown in Ref. 6.12 that a somewhat improved result can be had for continuous prismatic members using a weighted average for beams with both ends continuous of

$$I_e = 0.70 I_{em} + 0.15(I_{e1} + I_{e2}) \tag{6.10b}$$

and for beams with one end continuous and the other simply supported of

$$I_e = 0.85 I_{em} + 0.15 I_{e1} \tag{6.10c}$$

where I_{e1} is the effective moment of inertia at the continuous end. The ACI Code, as an option, also permits use of I_e for continuous prismatic beams to be taken equal to the value obtained from Eq. (6.8) at midspan; for cantilevers, I_e calculated at the support section may be used.

After I_e is found, deflections may be computed with due regard for rotations of the tangent to the elastic curve at the supports. In general, in computing the maximum deflection, the loading producing the maximum positive moment may be used, and the

FIGURE 6.9
Time variation of ξ for long-term deflections.

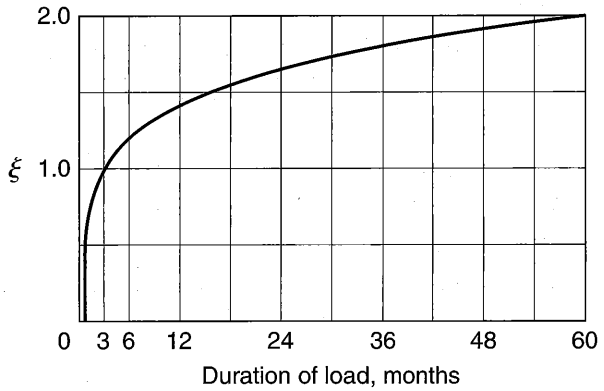

midspan deflection may normally be used as an acceptable approximation of the maximum deflection. Coefficients for deflection calculation such as derived by Branson in Ref. 6.7 are helpful. For members where supports may be considered fully fixed or hinged, handbook equations for deflections may be used.

d. Long-Term Deflection Multipliers

On the basis of empirical studies (Refs. 6.7, 6.9, and 6.11), ACI Code 9.5.2 specifies that *additional* long-term deflections Δ_t due to the combined effects of creep and shrinkage be calculated by multiplying the immediate deflection Δ_i by the factor

$$\lambda_\Delta = \frac{\xi}{1 + 50\rho'} \tag{6.11}$$

where $\rho' = A_s'/bd$ and ξ is a time-dependent coefficient that varies as shown in Fig. 6.9. In Eq. (6.11), the quantity $1/(1 + 50\rho')$ is a reduction factor that is essentially a section property, reflecting the beneficial effect of compression reinforcement A_s' in reducing long-term deflections, whereas ξ is a material property depending on creep and shrinkage characteristics. For simple and continuous spans, the value of ρ' used in Eq. (6.11) should be that at the midspan section, according to the ACI Code, or that at the support for cantilevers. Equation (6.11) and the values of ξ given by Fig. 6.9 apply to both normalweight and lightweight concrete beams. The additional, time-dependent deflections are thus found using values of λ_Δ from Eq. (6.11) in Eq. (6.6).

Values of ξ given in the ACI Code and Commentary are satisfactory for ordinary beams and one-way slabs, but may result in underestimation of time-dependent deflections of two-way slabs, for which Branson has suggested a 5-year value of $\xi = 3.0$ (Ref. 6.7).

Research by Paulson, Nilson, and Hover indicates that Eq. (6.11) does not properly reflect the reduced creep that is characteristic of higher-strength concretes (Ref. 6.13). As indicated in Table 2.2, the creep coefficient for high-strength concrete may be as low as one-half the value for normal concrete. Clearly, the long-term deflection of high-strength concrete beams under sustained load, expressed as a ratio of immediate elastic deflection, correspondingly will be less. This suggests a lower value of the material modifier ξ in Eq. (6.11) and Fig. 6.9. On the other hand, in high-strength concrete beams, the influence of compression

TABLE 6.2
Maximum allowable computed deflections

Type of Member	Deflection to Be Considered	Deflection Limitation
Flat roofs not supporting or attached to nonstructural elements likely to be damaged by large deflections	Immediate deflection due to the live load L	$\dfrac{l}{180}$
Floors not supporting or attached to nonstructural elements likely to be damaged by large deflections	Immediate deflection due to the live load L	$\dfrac{l}{360}$
Roof or floor construction supporting or attached to nonstructural elements likely to be damaged by large deflections	That part of the total deflection occurring after attachment of the nonstructural elements (sum of the long-time deflection due to all sustained loads and the immediate deflection due to any additional live load)	$\dfrac{l}{480}$
Roof or floor construction supporting or attached to nonstructural elements not likely to be damaged by large deflections		$\dfrac{l}{240}$

steel in reducing creep deflections is less pronounced, requiring an adjustment in the section modifier $1/(1 + 50\rho')$ in that equation.

Based on long-term tests involving six experimental programs, the following modified form of Eq. (6.11) is recommended (Ref. 6.13):

$$\lambda_\Delta = \frac{\mu\xi}{1 + 50\,\mu\rho'} \tag{6.12}$$

in which

$$\mu = 1.4 - f_c'/700$$

$$0.4 \leq \mu \leq 1.0 \tag{6.13}$$

The proposed equation gives results identical to Eq. (6.11) for concrete strengths of 28 MPa and below, and much improved predictions for concrete strengths between 28 and 84 MPa.

e. Permissible Deflections

To ensure satisfactory performance in service, ACI Code 9.5.2 imposes certain limits on deflections calculated according to the procedures just described. These limits are given in Table 6.2. Limits depend on whether or not the member supports or is attached to other nonstructural elements, and whether or not those nonstructural elements are likely to be damaged by large deflections. When long-term deflections are computed, that part of the deflection that occurs before attachment of the nonstructural elements may be deducted; information from Fig. 6.9 is useful for this purpose. The last two limits of Table 6.2 may be exceeded under certain conditions, according to the ACI Code.

EXAMPLE 6.2 **Deflection calculation.** The beam shown in Fig. 6.10 is a part of the floor system of an apartment house and is designed to carry calculated dead load w_d of 24 kN/m and a service live load w_l of 48 kN/m. Of the total live load, 20 percent is sustained in nature, while 80 percent will be applied only intermittently over the life of the structure. Under full dead and live load, the moment diagram is as shown in Fig. 6.10*c*. The beam will support nonstructural partitions that would be damaged if large deflections were to occur. They will be installed shortly after construction shoring is removed and dead loads take effect, but before significant creep occurs. Calculate that part of the total deflection that would adversely affect the partitions, i.e., the sum of long-time deflection due to dead and partial live load plus the immediate deflection due to the nonsustained part of the live load. Material strengths are $f'_c = 28$ MPa and $f_y = 420$ MPa.

SOLUTION. For the specified materials, $E_c = 4700\sqrt{28} = 24{,}870$ MPa, and with $E_s = 200{,}000$ MPa, the modular ratio $n = 8$. The modulus of rupture $f_r = 0.62 \times 1\sqrt{28} = 3.28$ MPa. The effective moment of inertia will be calculated for the moment diagram shown in Fig. 6.10*c* corresponding to the full service load, on the basis that the extent of cracking will be governed by the full service load, even though that load is intermittent. In the positive-moment region, the

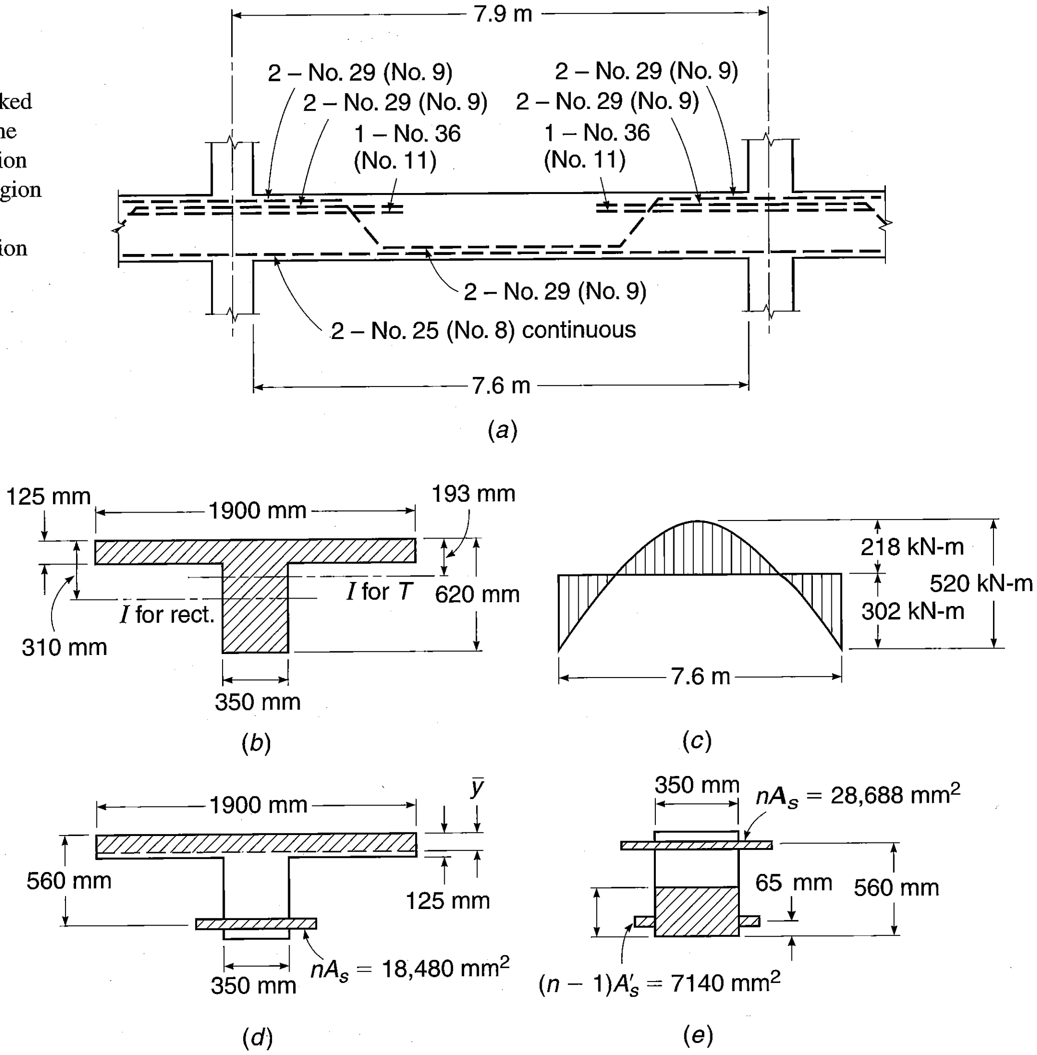
7.9 m
2 – No. 29 (No. 9)
2 – No. 29 (No. 9)
1 – No. 36 (No. 11)
2 – No. 29 (No. 9)
2 – No. 29 (No. 9)
1 – No. 36 (No. 11)
2 – No. 29 (No. 9)
2 – No. 25 (No. 8) continuous
7.6 m
(a)
125 mm
1900 mm
193 mm
I for T
620 mm
I for rect.
310 mm
350 mm
(b)
218 kN-m
520 kN-m
302 kN-m
7.6 m
(c)
1900 mm
ȳ
560 mm
125 mm
350 mm
nA_s = 18,480 mm²
(d)
350 mm
nA_s = 28,688 mm²
65 mm
560 mm
(n – 1)A'_s = 7140 mm²
(e)

FIGURE 6.10
Continuous T beam for deflection calculations in Example 6.2. The uncracked section is shown in (*b*), the cracked transformed section in the positive moment region is shown in (*d*), and the cracked transformed section in the negative moment region is shown in (*e*).

centroidal axis of the uncracked T section of Fig. 6.10*b* is found by taking moments about the top surface, to be at 193 mm depth, and $I_g = 1.347 \times 10^{10}$ mm^4. By similar means, the centroidal axis of the cracked transformed T section shown in Fig. 6.10*d* is located 95.7 mm below the top of the slab and $I_{cr} = 4.539 \times 10^9$ mm^4. The cracking moment is then found by means of Eq. (6.7):

$$M_{cr} = 3.28 \times \frac{1.347 \times 10^{10}}{427} \times \frac{1}{10^6} = 104 \text{ kN-m}$$

With $M_{cr}/M_a = 104/218 = 0.477$, the effective moment of inertia in the positive bending region is found from Eq. (6.8) to be

$$I_e = 0.477^3 \times 1.347 \times 10^{10} + (1 - 477^3) \times 4.539 \times 10^9 = 5.508 \times 10^9 \text{ mm}^4$$

In the negative bending region, the gross moment of inertia will be based on a rectangular section with a width equal to 350 mm and a depth equal to 620 mm. For this area, the centroid is 310 mm from the top surface and $I_g = 6.951 \times 109$ mm^4. For the cracked transformed section shown in Fig. 6.10*e*, the centroidal axis is found, taking moments about the bottom surface, to be 222 mm from that level, and $I_{cr} = 4.730 \times 10^9$ mm^4. Then

$$M_{cr} = 3.28 \times \frac{6.951 \times 10^9}{310} \times \frac{1}{10^6} = 73.5 \text{ kN-m}$$

giving $M_{cr}/M_a = 73.5/302 = 0.243$. Thus, for the negative-moment regions,

$$I_e = 0.243^3 \times 6.951 \times 10^9 + (1 - 0.243^3) \times 4.730 \times 10^9 = 4.762 \times 10^9 \text{ mm}^4$$

The average value of I_e to be used in calculation of deflection is

$$I_{e,av} = \frac{1}{2}(5.508 \times 10^9 + 4.792 \times 10^9) = 5.15 \times 10^9 \text{ mm}^4$$

It is next necessary to find the sustained-load deflection multiplier given by Eq. (6.11) and Fig. 6.9. For the positive bending zone, with no compression reinforcement, $\lambda_{\Delta\text{pos}} = 2.00$.

For convenient reference, the deflection of the member under full dead plus live load of 72 kN/m, corresponding to the moment diagram of Fig. 6.10*c*, will be found. Making use of the moment-area principles,

$$\Delta_{d+l} = \frac{1}{EI}\left[\left(\frac{2}{3} \times 520 \times 3.8 \times \frac{5}{8} \times 3.8\right) - (302 \times 3.8 \times 1.9)\right] = \frac{948}{EI}$$

$$= \frac{948 \times 10^{12}}{24{,}870 \times 5.15 \times 10^9} = 7.40 \text{ mm}$$

Using this figure as a basis, the time-dependent portion of dead load deflection (the only part of the total that would affect the partitions) is

$$\Delta_d = 7.40 \times \frac{24}{72} \times 2.00 = 4.93 \text{ mm}$$

while the sum of the immediate and time-dependent deflection due to the sustained portion of the live load is

$$\Delta_{0.20l} = 7.40 \times \frac{48}{72} \times 0.20 \times 3.00 = 2.96 \text{ mm}$$

and the instantaneous deflection due to application of the short-term portion of the live load is

$$\Delta_{0.80l} = 7.40 \times \frac{48}{72} \times 0.80 = 3.95 \text{ mm}$$

Thus the total deflection that would adversely affect the partitions, from the time they are installed until all long-time and subsequent instantaneous deflections have occurred, is

$$\Delta = 4.93 + 2.96 + 3.95 = 11.8 \text{ mm}$$

For comparison, as shown in Table 6.2, the limitation imposed by the ACI Code in such circumstances is $l/480 = 7900/480 = 16.5$ mm, indicating that the stiffness of the proposed member is sufficient.

Note that relatively little error would have been introduced in the above solution if the cracked-section moment of inertia had been used for both positive and negative sections rather than I_e. Significant savings in computational effort would have resulted. If M_{cr}/M_a is less than $\frac{1}{3}$, use of I_{cr} would almost always be acceptable. Note further that computation of the moment of inertia for both uncracked and cracked sections is greatly facilitated by design aids like those included in Ref. 6.14.

6.8 DEFLECTIONS DUE TO SHRINKAGE AND TEMPERATURE CHANGES

Concrete shrinkage will produce compressive stress in the longitudinal reinforcement in beams and slabs and equilibrating tensile stress in the concrete. If, as usual, the reinforcement is not symmetrically placed with respect to the concrete centroid, then shrinkage will produce curvature and corresponding deflection. The deflections will be in the same direction as those produced by the loads, if the reinforcement is mainly on the side of the member subject to flexural tension.

Shrinkage deflection is not usually calculated separately, but is combined with creep deflection, according to ACI Code procedures (see Section 6.7d). However, there are circumstances where a separate and more accurate estimation of shrinkage deflection may be necessary, particularly for thin, lightly loaded slabs. Compression steel, while it has only a small effect in reducing immediate elastic deflections, contributes significantly in reducing deflections due to shrinkage (as well as creep), and is sometimes added for this reason.

Curvatures due to shrinkage of concrete in an unsymmetrically reinforced concrete member can be found by the fictitious tensile force method (Ref. 6.7). Figure 6.11*a* shows the member cross section, with compression steel area A_s' and tensile steel area A_s, at depths d' and d, respectively, from the top surface. In Fig. 6.11*b*, the concrete and steel are imagined to be temporarily separated, so that the concrete can assume its free shrinkage strain ϵ_{sh}. Then a fictitious compressive force $T_{sh} = (A_s + A_s')\epsilon_{sh}E_s$ is applied to the steel, at the centroid of all the bars, a distance e below the concrete centroid, such that the steel shortening will exactly equal the free shrinkage strain of the concrete. The equilibrating tension force T_{sh} is then applied to the recombined section, as in Fig. 6.11*c*. This produces a moment $T_{sh}e$, and the corresponding shrinkage curvature is

$$\phi_{sh} = \frac{T_{sh}e}{EI}$$

The effects of concrete cracking and creep complicate the analysis, but comparisons with experimental data (Ref. 6.7) indicate that good results can be obtained using e_g and I_g for the uncracked gross concrete section and by using a reduced modulus E_{ct} equal to $\frac{1}{2}E_c$ to account for creep. Thus

$$\phi_{sh} = \frac{2T_{sh}e_g}{E_cI_g} \qquad (6.14)$$

where E_c is the usual value of concrete modulus given by Eq. (2.3).

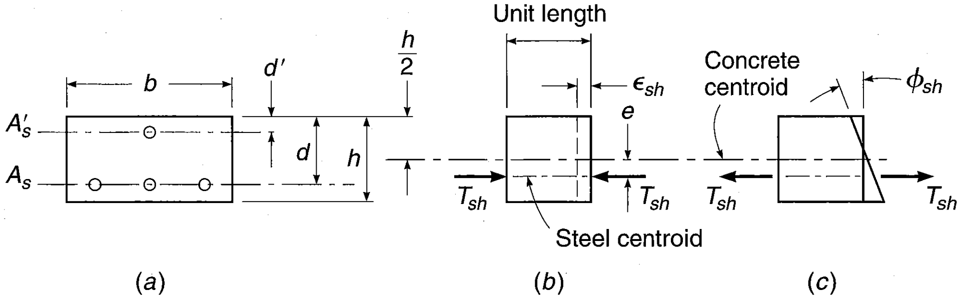

FIGURE 6.11
Shrinkage curvature of a reinforced concrete beam or slab: (*a*) cross section; (*b*) free shrinkage strain; (*c*) shrinkage curvature.

Empirical methods are also used, in place of the fictitious tensile force method, to calculate shrinkage curvatures. These methods are based on the simple but reasonable proposition that the shrinkage curvature is a direct function of the free shrinkage and steel percentage, and an inverse function of the section depth (Ref. 6.7). Branson suggests that for steel percentage $p - p' \leq 3$ percent (where $p = 100A_s/bd$ and $p' = 100A_s'/bd$),

$$\phi_{sh} = 0.7\frac{\epsilon_{sh}}{h}(p - p')^{1/3}\left(\frac{p - p'}{p}\right)^{1/2} \tag{6.15a}$$

and for $p - p' > 3$ percent,

$$\phi_{sh} = \frac{\epsilon_{sh}}{h} \tag{6.15b}$$

With shrinkage curvature calculated by either method, the corresponding member deflection can be determined by any convenient means such as the moment-area or conjugate-beam method. If steel percentages and eccentricities are constant along the span, the deflection ϵ_{sh} resulting from the shrinkage curvature can be determined from

$$\Delta_{sh} = K_{sh}\phi_{sh}l^2 \tag{6.16}$$

where K_{sh} is a coefficient equal to 0.500 for cantilevers, 0.125 for simple spans, 0.065 for interior spans of continuous beams, and 0.090 for end spans of continuous beams (Ref. 6.7).

EXAMPLE 6.3

Shrinkage deflection. Calculate the midspan deflection of a simply supported beam of 6 m span due to shrinkage of the concrete for which $\epsilon_{sh} = 780 \times 10^{-6}$. With reference to Fig. 6.11*a*, $b = 250$ mm, $d = 440$ mm, $h = 500$ mm, $A_s = 1935$ mm^2, and $A_s' = 0$. The elastic moduli are $E_c = 25{,}000$ MPa and $E_s = 200{,}000$ MPa.

Solution. By the fictitious tensile force method,

$$T_{sh} = 1935 \times 780 \times 10^{-6} \times 200{,}000 = 301{,}860\ \text{N}$$

and from Eq. (6.14) with $I_g = 2.60 \times 10^9$ mm^4,

$$\phi_{sh} = \frac{2 \times 301{,}860 \times 190}{25{,}000 \times 2.60 \times 10^9} = 1.76 \times 10^{-6}\ \text{mm}^{-1}$$

while from Eq. (6.16) with $K_{sh} = 0.125$ for the simple span,

$$\Delta_{sh} = 0.125 \times 1.76 \times 10^{-6} \times 6000^2 = 7.92\ \text{mm}$$

Alternatively, by Branson's approximate Eq. (6.15*a*) with $p = 100 \times 1935/110{,}000 = 1.76$ percent and $p' = 0$,

$$\phi_{sh} = \frac{0.7 \times 780 \times 10^{-6}}{500}(1.76)^{1/3} = 1.32 \times 10^{-6}$$

compared with 1.76×10^{-6} obtained by the equivalent tensile force method. Considering the uncertainties such as the effects of cracking and creep, the approximate approach can usually be considered satisfactory.

Deflections will be produced as a result of differential temperatures varying from top to bottom of a member also. Such variation will result in a strain variation with member depth that may usually be assumed to be linear. For such cases, the deflection due to differential temperature can be calculated using Eq. (6.16) in which ϕ_{sh} is replaced by $\alpha \Delta T/h$, where the thermal coefficient α for concrete may be taken as 9.9×10^{-6} per °C and ΔT is the temperature differential in degrees Celsius from one side to the other. The presence of the reinforcement has little influence on curvatures and deflections resulting from differential temperatures, because the thermal coefficient for the steel (11.7×10^{-6}) is very close to that for concrete.

6.9 MOMENT VS. CURVATURE FOR REINFORCED CONCRETE SECTIONS

Although it is not needed explicitly in ordinary design and is not a part of ACI Code procedures, the relation between moment applied to a given beam section and the resulting curvature, through the full range of loading to failure, is important in several contexts. It is basic to the study of member ductility, understanding the development of plastic hinges, and accounting for the redistribution of elastic moments that occurs in most reinforced concrete structures before collapse (see Section 12.9).

It will be recalled, with reference to Fig. 6.12, that curvature is defined as the angle change per unit length at any given location along the axis of a member subjected to bending loads:

$$\psi = \frac{1}{r} \tag{6.17}$$

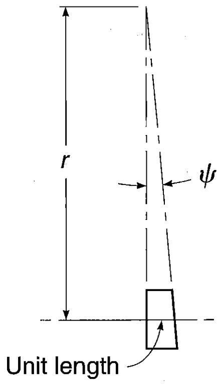

FIGURE 6.12
Unit curvature resulting from bending of beam section.

where ψ = unit curvature and r = radius of curvature. With the stress-strain relationships for steel and concrete, represented in idealized form in Fig. 6.13*a* and *b*, respectively, and the usual assumptions regarding perfect bond and plane sections, it is possible to calculate the relation between moment and curvature for a typical underreinforced concrete beam section, subject to flexural cracking, as follows.

Figure 6.14*a* shows the transformed cross section of a rectangular, tensile-reinforced beam in the uncracked elastic stage of loading, with steel represented by the equivalent concrete area nA_s, i.e., with area $(n - 1)A_s$ added outside of the rectangular concrete section.† The neutral axis, a distance c_1 below the top surface of the beam, is easily found (see Section 3.3a). In the limiting case, the concrete stress at the tension face is just equal to the modulus of rupture f_r and the strain is $\epsilon_r = f_r/E_c$.

---

† Note that compression reinforcement, or multiple layers of tension reinforcement, can easily be included in the analysis with no essential complication.

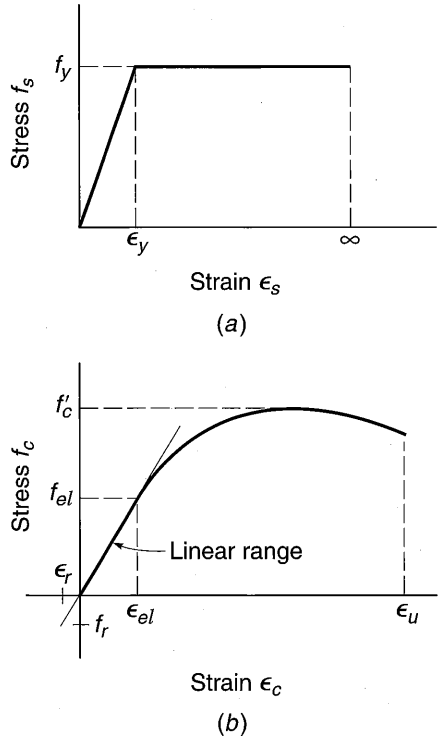

FIGURE 6.13
Idealized stress-strain curves: (*a*) steel; (*b*) concrete.

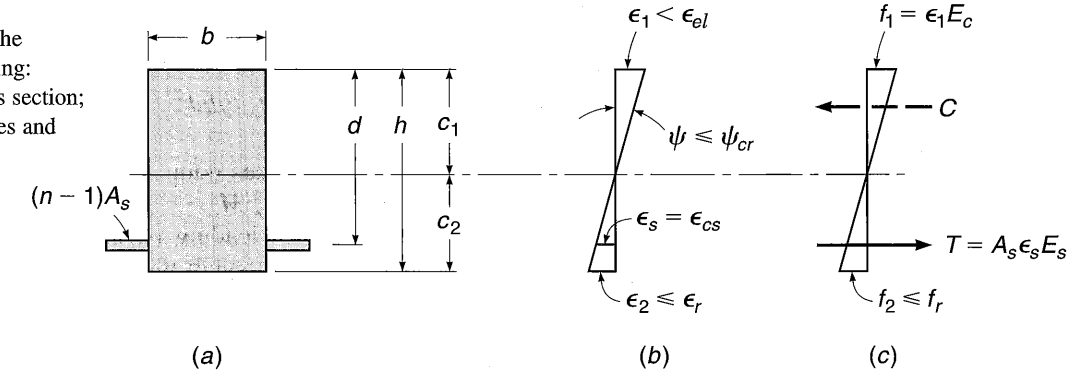
b
d
h
c_1
c_2
$(n-1)A_s$
$\epsilon_1 < \epsilon_{el}$
$\psi \leq \psi_{cr}$
$\epsilon_s = \epsilon_{cs}$
$\epsilon_2 \leq \epsilon_r$
$f_1 = \epsilon_1 E_c$
C
$T = A_s \epsilon_s E_s$
$f_2 \leq f_r$
(a)
(b)
(c)

FIGURE 6.14
Uncracked beam in the elastic range of loading: (*a*) transformed cross section; (*b*) strains; (*c*) stresses and forces.

The steel is well below yield at this stage, which can be confirmed by computing, from the strain diagram, the steel strain $\epsilon_s = \epsilon_{cs}$, where ϵ_{cs} is the concrete strain at the level of the steel. It is easily confirmed, also, that the maximum concrete compressive stress will be well below the proportional limit. The curvature is seen, in Fig. 6.14*b*, to be

$$\psi_{cr} = \frac{\epsilon_1}{c_1} = \frac{\epsilon_r}{c_2} \tag{6.18}$$

and the corresponding moment is

$$M_{cr} = \frac{f_r I_{ut}}{c_2} \tag{6.19}$$

FIGURE 6.15
Cracked beam in the elastic range of material response: (*a*) transformed cross section; (*b*) strains; (*c*) stresses and forces.

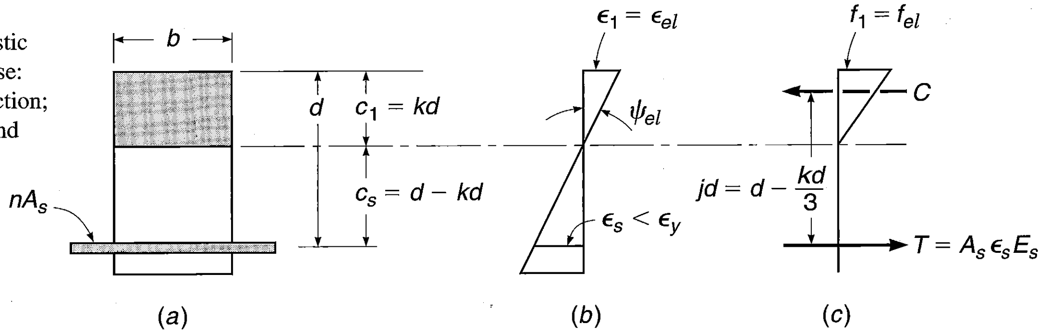

where I_{ut} is the moment of inertia of the uncracked transformed section. Equations (6.18) and (6.19) provide the information needed to plot point 1 of the moment-curvature graph of Fig. 6.17*a*.

When tensile cracking occurs at the section, the stiffness is immediately reduced, and curvature increases to point 2 in Fig. 6.17 with no increase in moment. The analysis now is based on the cracked transformed section of Fig. 6.15*a*, with steel represented by the transformed area nA_s and tension concrete deleted. The cracked, elastic neutral axis distance $c_1 = kd$ is easily found by the usual methods (see Section 3.3b). In the limiting case, the concrete strain just reaches the proportional limit, as shown in Fig. 6.15*b*, and typically the steel is still below the yield strain. The curvature is easily computed by

$$\psi_{el} = \frac{\epsilon_1}{c_1} = \frac{\epsilon_{el}}{c_1} \tag{6.20}$$

and the corresponding moment is

$$M_{el} = \frac{1}{2} f_{el} kjbd^2 \tag{6.21}$$

as was derived in Section 3.3b. This provides point 3 in Fig. 6.17. The curvature at point 2 can now be found from the ratio M_{cr}/M_{el}.

Next, the cracked, inelastic stage of loading is shown in Fig. 6.16. Here the concrete is well into the inelastic range, although the steel has not yet yielded. The neutral axis depth c_1 is less than the elastic *kd* and is changing with increasing load as the shape of the concrete stress distribution changes and the steel stress changes.

It is now convenient to adopt a numerical representation of the concrete compressive stress distribution, to find both the total concrete compressive force *C* and the location of its centroid, for any arbitrarily selected value of maximum concrete strain ϵ_1 in this range. The compressive strain diagram is divided into an arbitrary number of steps (e.g., four, in Fig. 6.16*b*), and the corresponding compressive stresses for each strain are read from the stress-strain curve of Fig. 6.13*b*. The stepwise representation of the actual continuous stress block is integrated numerically to find *C*, and its point of application is located, taking moments of the concrete forces about the top of the section. The basic equilibrium requirement $C = T$ then can be used to find the correct location of the neutral axis, for the particular compressive strain selected, following an iterative procedure.

The entire process can be summarized as follows:

1. Select any top face concrete strain ϵ_1 in the inelastic range, i.e., between ϵ_{el} and ϵ_u.
2. Assume the neutral axis depth, a distance c_1 below the top face.
3. From the strain diagram geometry, determine $\epsilon_s = \epsilon_{cs}$.

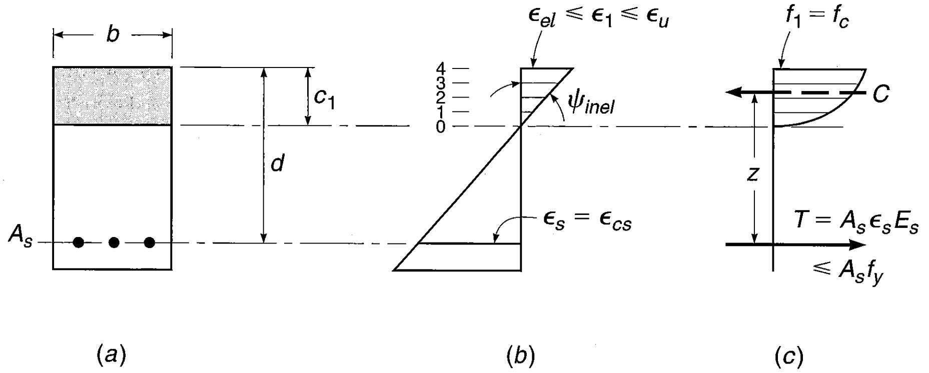

FIGURE 6.16
Cracked beam with concrete in the inelastic range of loading: (*a*) cross section; (*b*) strains; (*c*) stresses and forces.

4. Compute $f_s = \epsilon_s E_s \leq f_y$ and $T = A_s f_s$.
5. Determine C by integrating numerically under the concrete stress distribution curve.
6. Check to see if $C = T$. If not, the neutral axis must be adjusted upward or downward, for the particular concrete strain that was selected in step 1, until equilibrium is satisfied. This determines the correct value of c_1.

Curvature can then be found from

$$\psi_{inel} = \frac{\epsilon_1}{c_1} \tag{6.22}$$

The internal lever arm z from the centroid of the concrete stress distribution to the tensile resultant, Fig. 6.16*c*, is calculated, after which

$$M_{inel} = Cz = Tz \tag{6.23}$$

The sequence of steps 1 through 6 is then repeated for newly selected values of concrete strain ϵ_1. The end result will be a series of points, such as 4, 5, 6, and 7 in Fig. 6.17. The limit of the moment-curvature plot is reached when the concrete top face strain equals ϵ_u, corresponding to point 7. The steel would be well past the yield strain at this loading, and at the yield stress.

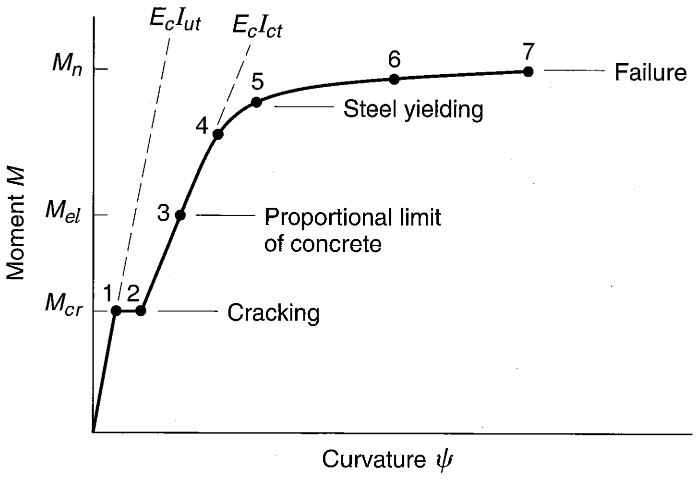

FIGURE 6.17
Moment-curvature relation for tensile-reinforced beam.

It is important to be aware of the difference between a moment-unit curvature plot, such as Fig. 6.17, and a moment-rotation diagram for the hinging region of a reinforced concrete beam. The hinging region normally includes a number of discrete cracks, but between those cracks, the uncracked concrete reduces the steel strain, leading to what is termed the *tension stiffening* effect. The result is that the total rotation at the hinge is much less than would be calculated by multiplying the curvature per unit length at the cracked section by the observed or assumed length of the hinging region. Furthermore, the sharp increase in unit curvature shown in Fig. 6.17 at cracking would not be seen on the moment-rotation plot, only a small, but progressive, reduction of the slope of the diagram.

REFERENCES

6.1. ACI Committee 224, "Control of Cracking in Concrete Structures (ACI 224R-01)," *ACI Manual of Concrete Practice*, Part 1, American Concrete Institute, Farmington Hills, MI, 2008.

6.2. P. Gergely and L. A. Lutz, "Maximum Crack Width in Reinforced Concrete Flexural Members," in *Causes, Mechanisms, and Control of Cracking in Concrete*, SP-20, American Concrete Institute, Detroit, MI, 1968, pp. 1–17.

6.3. P. H. Kaar and A. H. Mattock, "High-Strength Bars as Concrete Reinforcement—Part 4: Control of Cracking," *Journal*, PCA Research and Development Laboratories, vol. 5, no. 1, 1963, pp. 15–38.

6.4. R. J. Frosch, "Another Look at Cracking and Crack Control in Reinforced Concrete," *ACI Struct. J.*, vol. 96, no. 3, 1999, pp. 437–442.

6.5. B. B. Broms, "Crack Width and Crack Spacing in Reinforced Concrete Members," *J. ACI*, vol. 62, no. 10, 1965, pp. 1237–1256.

6.6. ACI Committee 318, "Discussion of Proposed Revisions to Building Code Requirements for Structural Concrete (ACI 318-95) and Commentary (ACI 318R-95)," *Concr. Intl.*, vol. 21, no. 5, 1999, pp. 318-1–318-49.

6.7. D. E. Branson, *Deformation of Concrete Structures*, McGraw-Hill, New York, 1977.

6.8. ACI Committee 435, "Control of Deflection in Concrete Structures (ACI 435R-95)," *ACI Manual of Concrete Practice*, Part 5, American Concrete Institute, Farmington Hills, MI, 2003.

6.9. W. W. Yu and G. Winter, "Instantaneous and Long-Time Deflections of Reinforced Concrete Beams under Working Loads," *J. ACI*, vol. 57, no. 1, 1960, pp. 29–50.

6.10. ACI Committee 209, "Prediction of Creep, Shrinkage and Temperature Effects in Concrete Structures (ACI 209R-92)," *ACI Manual of Concrete Practice*, Part 1, 2003.

6.11. D. E. Branson, "Compression Steel Effect on Long-Time Deflections," *J. ACI*, vol. 68, no. 8, 1971, pp. 555–559.

6.12. ACI Committee 435, "Proposed Revisions by Committee 435 to ACI Building Code and Commentary Provisions on Deflections," *J. ACI*, vol. 75, no. 6, June 1978, pp. 229–238.

6.13. K. Paulson, A. H. Nilson, and K. C. Hover, "Long-Term Deflection of High-Strength Concrete Beams," *ACI Mater. J.*, vol. 88, no. 2, 1991, pp. 197–206.

6.14. *CRSI Handbook*, 10th ed., Concrete Reinforcing Steel Institute, Schaumburg, IL, 2008.

PROBLEMS

6.1. A rectangular beam of width $b = 380$ mm, effective depth $d = 520$ mm, and total depth $h = 580$ mm spans 5.6 m between simple supports. It will carry a computed dead load of 15.8 kN/m including self-weight, plus a service live load of 33.4 kN/m. Reinforcement consists of four evenly spaced No. 22 (No. 7) bars in one row. The clear cover on the sides is 50 mm. Material strengths are $f_y = 420$ MPa and $f'_c = 28$ MPa.

(*a*) Compute the stress in the steel at full service load, and using the Gergely-Lutz equation, estimate the maximum crack width.

(*b*) Confirm the suitability of the proposed design based on Eq. (6.3).

6.2. To save steel-handling costs, an alternative design is proposed for the beam in Problem 6.1, using two No. 29 (No. 9) Grade 520 bars to provide approximately the same steel strength as the originally proposed four No. 22 (No. 7)

Grade 420 bars. Check to determine if the redesigned beam is satisfactory with respect to cracking according to the ACI Code. What modification could you suggest that would minimize the number of bars to reduce cost, yet satisfy requirements of crack control?

6.3. For the beam in Problem 6.1:

(*a*) Calculate the increment of deflection resulting from the first application of the short-term live load.

(*b*) Find the creep portion of the sustained load deflection plus the immediate deflection due to live load.

(*c*) Compare your results with the limitations imposed by the ACI Code, as summarized in Table 6.2.

Assume that the beam is a part of a floor system and supports cinder block partitions susceptible to cracking if deflections are excessive.

6.4. A beam having $b = 300$ mm, $d = 530$ mm, and $h = 600$ mm is reinforced with three No. 36 (No. 11) bars. Material strengths are $f_y = 420$ MPa and $f_c' = 28$ MPa. It is used on a 8.5 m simple span to carry a total service load of 35 kN/m. For this member, the sustained loads include self-weight of the beam plus additional superimposed dead load of 7.4 kN/m, plus 5.8 kN/m representing that part of the live load that acts more or less continuously, such as furniture, equipment, and time-average occupancy load. The remaining 17.8 kN/m live load consists of short-duration loads, such as the brief peak load in the corridors of an office building at the end of a workday.

(*a*) Find the increment of deflection under sustained loads due to creep.

(*b*) Find the additional deflection increment due to the intermittent part of the live load.

In your calculations, you may assume that the peak load is applied almost immediately after the building is placed in service, then reapplied intermittently. Compare with ACI Code limits from Table 6.2. Assume that, for this long-span floor beam, construction details are provided that will avoid damage to supported elements due to deflections. If ACI Code limitations are not met, what changes would you recommend to improve the design?

6.5. A reinforced concrete beam is continuous over two equal 6.7 m spans, simply supported at the two exterior supports, and fully continuous at the interior support. Concrete cross-sectional dimensions are $b = 250$ mm, $h = 550$ mm, and $d = 480$ mm for both positive and negative bending regions. Positive reinforcement in each span consists of two No. 29 (No. 9) bars, and negative reinforcement at the interior support is made up of three No. 32 (No. 10) bars. No compression steel is used. Material strengths are $f_y = 420$ MPa and $f_c' = 35$ MPa. The beam will carry a service live load, applied early in the life of the member, of 26.0 kN/m distributed uniformly over both spans; 20 percent of this load will be sustained more or less permanently, while the rest is intermittent. The total service dead load is 14.6 kN/m including self-weight.

(*a*) Find the immediate deflection when shores are removed and the full dead load is applied.

(*b*) Find the long-term deflection under sustained load.

(*c*) Find the increment of deflection when the short-term part of the live load is applied.

Compare with ACI Code deflection limits; piping and brittle conduits are carried that would be damaged by large deflections. Note that midspan deflection may be used as a close approximation of maximum deflection.

6.6. Recalculate the deflections of Problem 6.5 based on the assumption that 20 percent of the live load represents the normal service condition of loading and is sustained more or less continuously, while the remaining 80 percent is a short-term peak loading that would probably not be applied until most creep deflections have occurred. Compare with your earlier results.

6.7. The tensile-reinforced rectangular beam shown in Fig. P6.7 is made using steel with $f_y = 420$ MPa and $E_s = 200{,}000$ MPa. A perfectly plastic response after yielding can be assumed. The concrete has a stress-strain curve in compression that may be approximated by the parabola $f_c = f'_c[2\epsilon_c/\epsilon_0 - (\epsilon_c/\epsilon_0)^2]$, where f_c and ϵ_c are the stress and strain in the concrete. The variable ϵ_0 is the strain at the peak stress $= 0.002$, and $f'_c = 28$ MPa. The ultimate strain in the concrete is 0.003. The concrete responds elastically in tension up to the modulus of rupture $f_r = 3.3$ MPa. Based on this information, plot a curve relating applied moment to unit curvature at a section subjected to flexural cracking. Label points corresponding to first cracking, first yielding of steel, and peak moment.

FIGURE P6.7

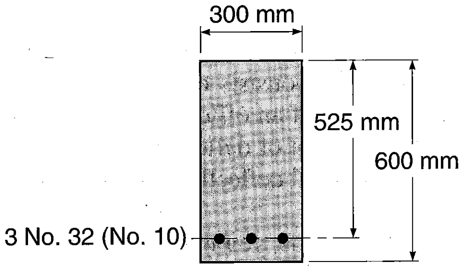

7

Analysis and Design for Torsion

7.1 INTRODUCTION

Reinforced concrete members are commonly subjected to bending moments, to transverse shears associated with those bending moments, and, in the case of columns, to axial forces often combined with bending and shear. In addition, torsional forces may act, tending to twist a member about its longitudinal axis. Such torsional forces seldom act alone and are almost always concurrent with bending moment and transverse shear, and sometimes with axial force as well.

For many years, torsion was regarded as a secondary effect and was not considered explicitly in design, its influence being absorbed in the overall factor of safety of rather conservatively designed structures. Current methods of analysis and design, however, have resulted in less conservatism, leading to somewhat smaller members that, in many cases, must be reinforced to increase torsional strength. In addition, there is increasing use of structural members for which torsion is a central feature of behavior; examples include curved bridge girders, eccentrically loaded box beams, and helical stairway slabs. The design procedures in the ACI Code were first proposed in Switzerland (Refs. 7.1 and 7.2) and are also included in the European and Canadian model codes (Refs. 7.3 and 7.4).

It is useful in considering torsion to distinguish between primary and secondary torsion in reinforced concrete structures. *Primary torsion*, sometimes called *equilibrium torsion* or *statically determinate torsion*, exists when the external load has no alternative load path but must be supported by torsion. For such cases, the torsion required to maintain static equilibrium can be uniquely determined. An example is the cantilevered slab of Fig. 7.1*a*. Loads applied to the slab surface cause twisting moments m_t to act along the length of the supporting beam. These are equilibrated by the resisting torque T provided at the columns. Without the torsional moments, the structure will collapse.

In contrast to this condition, *secondary torsion*, also called *compatibility torsion* or *statically indeterminate torsion*, arises from the requirements of continuity, i.e., compatibility of deformation between adjacent parts of a structure. For this case, the torsional moments cannot be found based on static equilibrium alone. Disregard of continuity in the design will often lead to extensive cracking, but generally will not cause collapse. An internal readjustment of forces is usually possible and an alternative equilibrium of forces found. An example of secondary torsion is found in the spandrel or edge beam supporting a monolithic concrete slab, shown in Fig. 7.1*b*. If the spandrel beam is torsionally stiff and suitably reinforced, and if the columns can provide the necessary resisting torque T, then the slab moments will approximate those for a rigid exterior support as shown in Fig. 7.1*c*. However, if the beam has little torsional stiffness

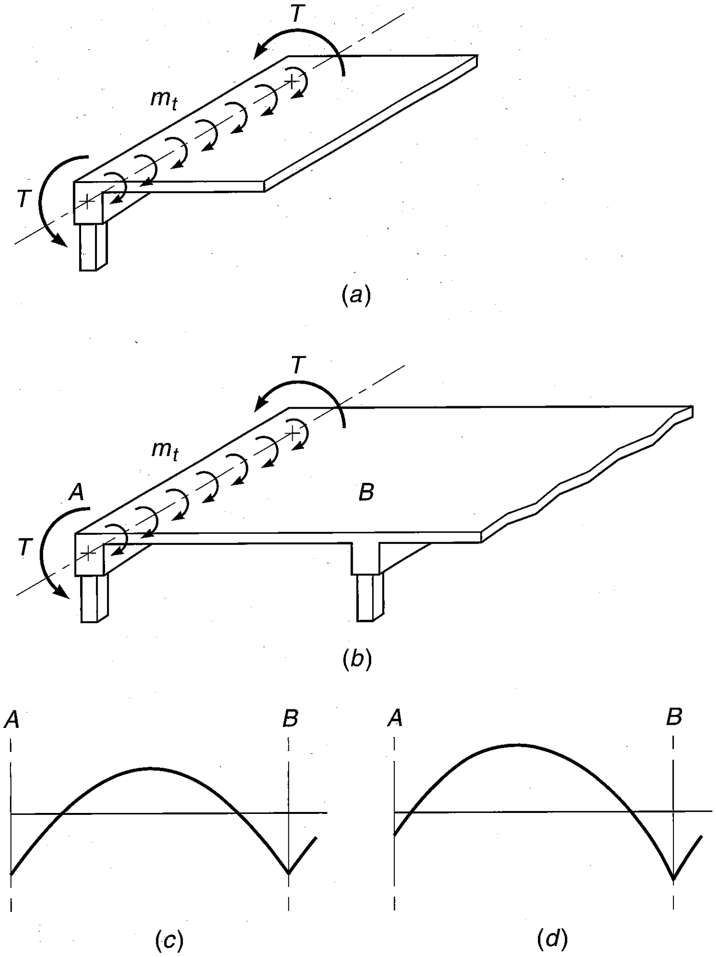

FIGURE 7.1
Torsional effects in reinforced concrete: (*a*) primary or equilibrium torsion at a cantilevered slab; (*b*) secondary or compatibility torsion at an edge beam; (*c*) slab moments if edge beam is stiff torsionally; (*d*) slab moments if edge beam is flexible torsionally.

and inadequate torsional reinforcement, cracking will occur to further reduce its torsional stiffness, and the slab moments will approximate those for a hinged edge, as shown in Fig. 7.1*d*. If the slab is designed to resist the altered moment diagram, collapse will not occur (see discussion in Section 12.10).

Although current techniques for analysis permit the realistic evaluation of torsional moments for statically indeterminate conditions as well as determinate, designers often neglect secondary torsional effects when torsional stresses are low and alternative equilibrium states are possible. This is permitted according to the ACI Code and many other design specifications. On the other hand, when torsional strength is an essential feature of the design, such as for the bridge shown in Fig. 7.2, special analysis and special torsional reinforcement are required, as described in the remainder of this chapter.

7.2 TORSION IN PLAIN CONCRETE MEMBERS

Figure 7.3 shows a portion of a prismatic member subjected to equal and opposite torques *T* at the ends. If the material is elastic, St. Venant's torsion theory indicates that

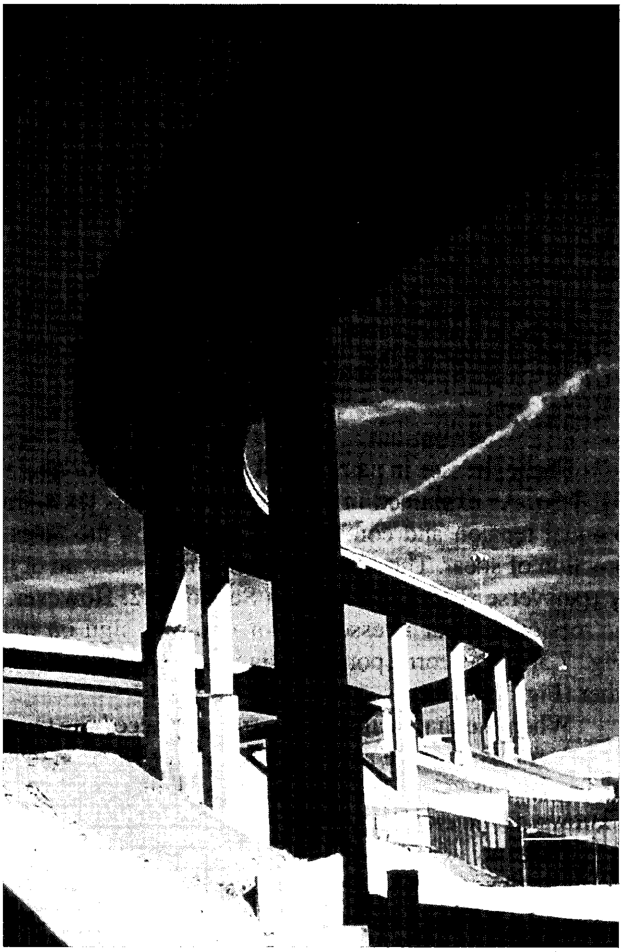

FIGURE 7.2
Curved continuous beam bridge, Las Vegas, Nevada, designed for torsional effects. (*Courtesy of Portland Cement Association.*)

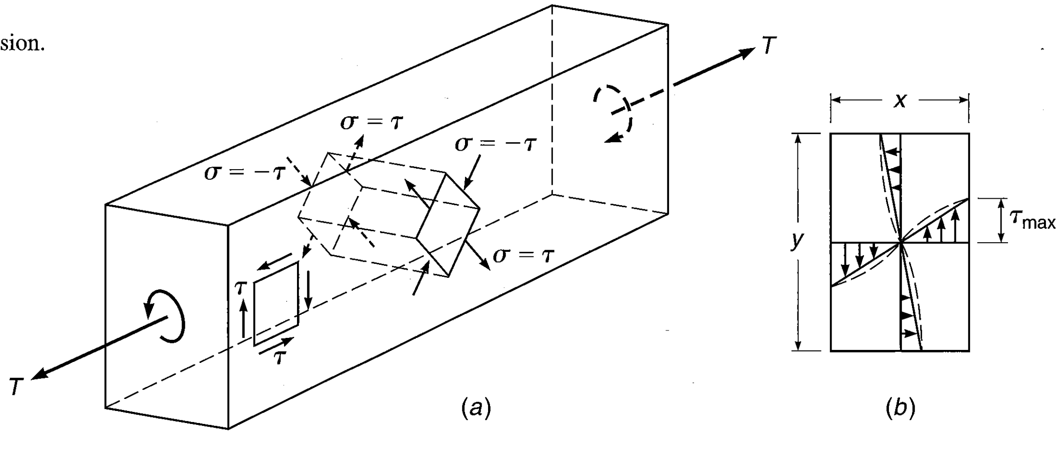
$\sigma = \tau$
$\sigma = -\tau$
$\sigma = -\tau$
$\sigma = \tau$
τ
τ
T
T
x
y
$\tau_{\max}$
(*a*)
(*b*)

FIGURE 7.3
Stresses caused by torsion.

torsional shear stresses are distributed over the cross section, as shown in Fig. 7.3*b*. The largest shear stresses occur at the middle of the wide faces. If the material deforms inelastically, as expected for concrete, the stress distribution is closer to that shown by the dashed line.

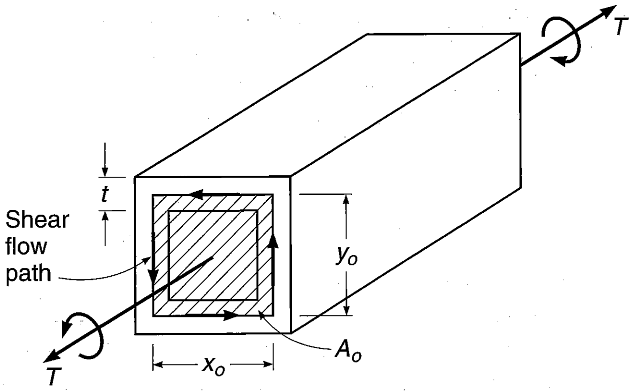

FIGURE 7.4
Thin-walled tube under torsion.

Shear stresses in pairs act on an element at or near the wide surface, as shown in Fig. 7.3*a*. As explained in strength of materials texts, this state of stress corresponds to equal tension and compression stresses on the faces of an element at 45° to the direction of shear. These inclined tension stresses are of the same kind as those caused by transverse shear, discussed in Section 4.2. However, in the case of torsion, since the torsional shear stresses are of opposite sign on opposing sides of the member (Fig. 7.3*b*), the corresponding diagonal tension stresses are at right angles to each other (Fig. 7.3*a*).

When the diagonal tension stresses exceed the tensile resistance of the concrete, a crack forms at some accidentally weaker location and spreads immediately across the beam. The value of torque corresponding to the formation of this diagonal crack is known as the *cracking torque* T_{cr}.

There are several ways of analyzing members subjected to torsion. The nonlinear stress distribution shown by the dotted lines in Fig. 7.3*b* lends itself to the use of the *thin-walled tube, space truss analogy*. Using this analogy, the shear stresses are treated as constant over a finite thickness t around the periphery of the member, allowing the beam to be represented by an equivalent tube, as shown in Fig. 7.4. Within the walls of the tube, torque is resisted by the shear flow q, which has units of force per unit length. In the analogy, q is treated as a constant around the perimeter of the tube. As shown in Fig. 7.4, the resultants of the individual components of shear flow are located within the walls of the tube and act along lengths y_o in the vertical walls and along lengths x_o in the horizontal walls, with y_o and x_o measured at the center of the walls.

The relationship between the applied torque and the shear flow can be obtained by summing the moments about the axial centerline of the tube, giving

$$T = 2qx_oy_o/2 + 2qy_ox_o/2 \qquad (a)$$

where the two terms on the right-hand side represent the contributions of the horizontal and vertical walls to the resting torque, respectively. Thus,

$$T = 2qx_oy_o \qquad (b)$$

The product x_oy_o represents the area enclosed by the shear flow path A_o, giving

$$T = 2qA_o \qquad (c)$$

and

$$q = \frac{T}{2A_o} \qquad (d)$$

Note that although A_o is an area, it derives from the moment calculation shown in Eq. (*a*) above. Thus, A_o is applicable for hollow box sections, as well as solid sections, and in such case includes the area of the central void.

For a tube wall thickness t, the unit shear stress acting within the walls of the tube is

$$\tau = \frac{q}{t} = \frac{T}{2A_o t} \tag{7.1}$$

As shown in Fig. 7.3*a*, the principal tensile stress $\sigma = \tau$. Thus, the concrete will crack only when $\tau = \sigma = f_t'$, the tensile strength of concrete. Considering that concrete is under biaxial tension and compression, f_t' can be conservatively represented by $0.33\sqrt{f_c'}$ rather than the value typically used for the modulus of rupture of concrete, which is taken as $f_r = 0.62\sqrt{f_c'}$ for normal-density concrete. Substituting $\tau = \tau_{cr} = 0.33\sqrt{f_c'}$ in Eq. (7.1) and solving for T give the value of the cracking torque:

$$T_{cr} = 0.33\sqrt{f_c'}(2A_o t) \tag{7.2}$$

Remembering that A_o represents the area enclosed by the shear flow path, A_o must be some fraction of the area enclosed by the outside perimeter of the full concrete cross section A_{cp}. The value of t can, in general, be approximated as a fraction of the ratio A_{cp}/p_{cp}, where p_{cp} is the perimeter of the cross section. For solid members with rectangular cross sections, t is typically one-sixth to one-fourth of the minimum width. Using a value of one-fourth for a member with a width-to-depth ratio of 0.5 yields a value of A_o approximately equal to $\frac{2}{3}A_{cp}$. For the same member, $t = \frac{3}{4}A_{cp}/p_{cp}$. Using these values for A_o and t in Eq. (7.2) gives

$$T_{cr} = 0.33\sqrt{f_c'}\frac{A_{cp}^2}{p_{cp}} \qquad \text{kN-m} \tag{7.3}$$

It has been found that Eq. (7.3) gives a reasonable estimate of the cracking torque of solid reinforced concrete members regardless of the cross-sectional shape. For hollow sections, T_{cr} in Eq. (7.3) should be reduced by the ratio A_g/A_{cp}, where A_g is the gross cross section of the concrete, i.e., not including the area of the voids (Ref. 7.5).

7.3 TORSION IN REINFORCED CONCRETE MEMBERS

To resist torsion for values of T above T_{cr}, reinforcement must consist of closely spaced stirrups and longitudinal bars. Tests have shown that longitudinal bars alone hardly increase the torsional strength, with test results showing an improvement of at most 15 percent (Ref. 7.5). This is understandable because the only way in which longitudinal steel can directly contribute to torsional strength is by dowel action, which is particularly weak and unreliable if longitudinal splitting along bars is not restrained by transverse reinforcement. Thus, the torsional strength of members reinforced only with longitudinal steel is satisfactorily, and somewhat conservatively, predicted by Eqs. (7.2) and (7.3).

When members are adequately reinforced, as in Fig. 7.5*a*, the concrete cracks at a torque that is equal to or only somewhat larger than in an unreinforced member, as given by Eq. (7.3). The cracks form a spiral pattern, as shown in Fig. 7.5*b*. Upon cracking, the torsional resistance of the concrete drops to about one-half of that of the uncracked member, the remainder being now resisted by reinforcement. This redistribution of internal resistance is reflected in the torque-twist curve (Fig. 7.6), which at

FIGURE 7.5
Reinforced concrete beam in torsion: (*a*) torsional reinforcement; (*b*) torsional cracks.

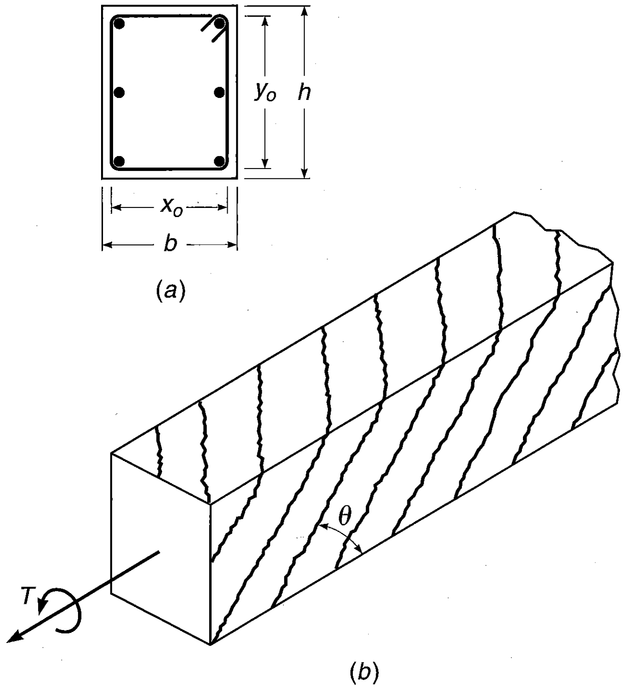

FIGURE 7.6
Torque-twist curve in reinforced concrete member.

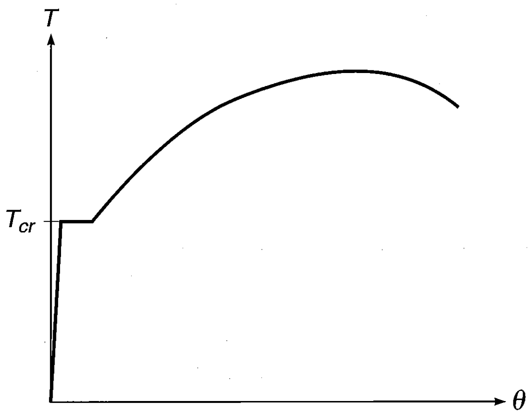

the cracking torque shows continued twist at constant torque until the internal forces have been redistributed from the concrete to the steel. As the section approaches the ultimate load, the concrete outside the reinforcing cage cracks and begins to spall off, contributing progressively less to the torsional capacity of the member.

Tests show that, after cracking, the area enclosed by the shear path is defined by the dimensions x_o and y_o measured to the centerline of the outermost closed transverse reinforcement, rather than to the center of the tube walls as before. These dimensions define the gross area $A_{oh} = x_o y_o$ and the shear perimeter $p_h = 2(x_o + y_o)$ measured at the steel centerline.

Analysis of the torsional resistance of the member is aided by treating the member as a space truss consisting of spiral *concrete diagonals* that are able to take load parallel but not perpendicular to the torsional cracks, transverse *tension tie members*

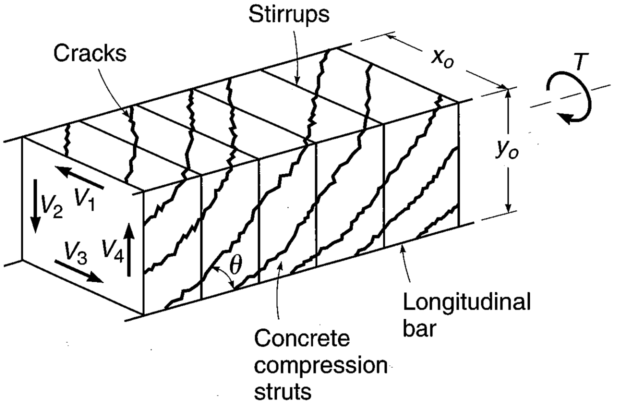

FIGURE 7.7
Space truss analogy.

that are provided by closed stirrups or ties, and *tension chords* that are provided by longitudinal reinforcement. The hollow-tube, space truss analogy represents a simplification of actual behavior, since, as will be demonstrated, the calculated torsional strength is controlled by the strength of the transverse reinforcement, independent of concrete strength. Such a simplification will be used here because it aids understanding, although it greatly underestimates torsional capacity and does not reflect the higher torsional capacities obtained with higher concrete strengths (Refs. 7.6 and 7.7).

With reference to Fig. 7.7, the torsional resistance provided by a member with a rectangular cross section can be represented as the sum of the contributions of the shears in each of the four walls of the equivalent hollow tube. The contribution of the shear acting in the right-hand vertical wall of the tube to the torsional resistance, for example, is

$$T_4 = \frac{V_4 x_o}{2} \qquad (a)$$

Following a procedure similar to that used for analyzing the variable-angle truss shear model discussed in Section 4.8 and shown in Figs. 4.19 and 4.20, the equilibrium of a section of the vertical wall—with one edge parallel to a torsional crack with angle θ—can be evaluated using Fig. 7.8*a*. Assuming that the stirrups crossing the crack are yielding, the shear in the wall under consideration is

$$V_4 = A_t f_{yt} n \qquad (b)$$

where A_t = area of one leg of a closed stirrup
f_{yt} = yield strength of transverse reinforcement
n = number of stirrups intercepted by torsional crack

Since the horizontal projection of the crack is $y_o \cot \theta$ and $n = y_o \cot \theta / s$ where θ is the slope angle of the strut and s is the spacing of the stirrups,

$$V_4 = \frac{A_t f_{yt} y_o}{s} \cot \theta \qquad (c)$$

Combining Eqs. (*c*) and (*a*) gives

$$T_4 = \frac{A_t f_{yt} y_o x_o}{2s} \cot \theta \qquad (d)$$

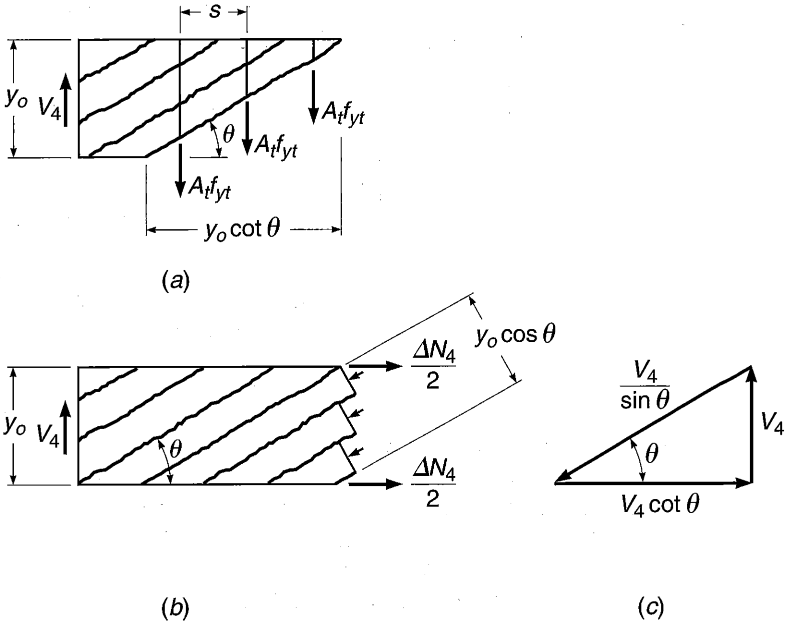

FIGURE 7.8
Basis for torsional design: (*a*) vertical tension in stirrups; (*b*) diagonal compression in vertical wall of beam; (*c*) equilibrium diagram of forces due to shear in vertical wall.

It is easily shown that an identical expression is obtained for each horizontal and vertical wall. Thus, summing over all four sides, the nominal capacity of the section is

$$T_n = \sum_{i=1}^{4} T_i = \frac{2A_t f_{yt} y_o x_o}{s} \cot\theta \tag{e}$$

Noting that $y_o x_o = A_{oh}$ and rearranging slightly give

$$T_n = \frac{2A_{oh} A_t f_{yt}}{s} \cot\theta \tag{7.4}$$

The diagonal compression struts that form parallel to the torsional cracks are necessary for the equilibrium of the cross section. As shown in Fig. 7.8*b* and *c*, the horizontal component of compression in the struts in the vertical wall must be equilibrated by an axial tensile force ΔN_4. Based on the assumed uniform distribution of shear flow around the perimeter of the member, the diagonal stresses in the struts must be uniformly distributed, resulting in a line of action of the resultant axial force that coincides with the midheight of the wall. Referring to Fig. 7.8*c*, the total contribution of the right-hand vertical wall to the change in axial force of the member due to the presence of torsion is

$$\Delta N_4 = V_4 \cot\theta = \frac{A_t f_{yt} y_o}{s} \cot^2\theta$$

Again, summing over all four sides, the total increase in axial force for the member is

$$\Delta N = \sum_{i=1}^{4} \Delta N_i = \frac{A_t f_{yt}}{s} 2(x_o + y_o) \cot^2\theta \tag{7.5a}$$

$$\Delta N = \frac{A_t f_{yt} p_h}{s} \cot^2\theta \tag{7.5b}$$

where p_h is the perimeter of the centerline of the closed stirrups.

Longitudinal reinforcement must be provided to carry the added axial force ΔN. If that steel is designed to yield, then

$$A_l f_y = \frac{A_t f_{yt} p_h}{s} \cot^2 \theta \tag{7.6}$$

and

$$A_l = \frac{A_t}{s} p_h \frac{f_{yt}}{f_y} \cot^2 \theta \tag{7.7}$$

where A_l = total area of longitudinal reinforcement to resist torsion, mm^2
f_y = yield strength of longitudinal torsional reinforcement, MPa

It has been found experimentally that, after cracking, the effective area enclosed by the shear flow path is somewhat less than the value of A_{oh} used in the previous development. It is recommended in Ref. 7.7 that the reduced value be taken as $A_o = 0.85A_{oh}$, where, it will be recalled, A_{oh} is the area enclosed by the centerline of the transverse reinforcement. This recommendation is incorporated in the ACI Code (see Section 7.5) and in a modified form of Eq. (7.4) with A_o substituted for A_{oh}. It has further been found experimentally that the thickness of the equivalent tube at loads near ultimate is closely approximated by $t = A_{oh}/p_h$, where p_h is the perimeter of A_{oh}.

7.4 TORSION PLUS SHEAR

Members are rarely subjected to torsion alone. The prevalent situation is that of a beam subject to the usual flexural moments and shear forces, which, in addition, must resist torsional moments. In an uncracked member, shear forces as well as torque produce shear stresses. In a cracked member, both shear and torsion increase the forces in the diagonal struts (Figs. 4.20*d* and 7.8*b*), they increase the width of diagonal cracks, and they increase the forces required in the transverse reinforcement (Figs. 4.20*e* and 7.8*a*).

Using the usual representation for reinforced concrete, the nominal shear stress caused by an applied shear force V is $\tau_v = V/b_w d$. The shear stress caused by torsion, given in Eq. (7.1), is $\tau_t = T/(2A_o t)$. As shown in Fig 7.9*a* for *hollow sections*, these stresses are directly additive on one side of the member. Thus, for a cracked concrete cross section with $A_o = 0.85A_{oh}$ and $t = A_{oh}/p_h$, the maximum shear stress can be expressed as

$$\tau = \tau_v + \tau_t = \frac{V}{b_w d} + \frac{T p_h}{1.7A_{oh}^2} \tag{7.8}$$

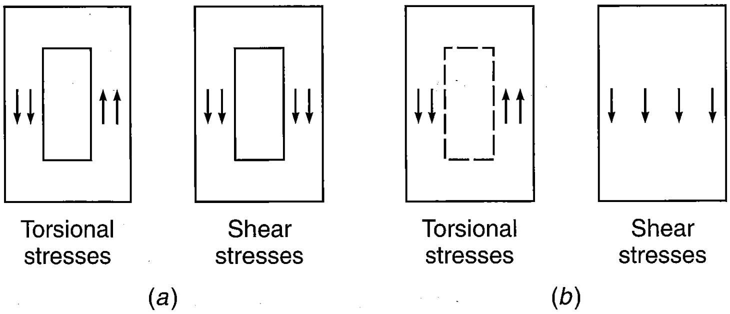

FIGURE 7.9
Addition of torsional and shear stresses: (*a*) hollow section; (*b*) solid section. (*Adapted from Ref. 7.7.*)

For a member with a *solid section*, Fig. 7.9*b*, τ_t is predominately distributed around the perimeter, as represented by the hollow tube analogy, but the full cross section contributes to carrying τ_v. Comparisons with experimental results show that Eq. (7.8) is somewhat overconservative for solid sections and that a better representation for maximum shear stress is provided by the square root of the sum of the squares of the nominal shear stresses:

$$\tau = \sqrt{\left(\frac{V}{b_w d}\right)^2 + \left(\frac{T p_h}{1.7 A_{oh}^2}\right)^2} \tag{7.9}$$

Equations (7.8) and (7.9) serve as a measure of the shear stresses in the concrete under both service and ultimate loading.

7.5 ACI CODE PROVISIONS FOR TORSION DESIGN

The basic principles upon which ACI Code design provisions are based have been presented in the preceding sections. ACI Code 11.5.3.5 safety provisions require that

$$T_u \leq \phi T_n \tag{7.10}$$

where T_u = required torsional strength at factored loads
T_n = nominal torsional strength of member

The strength reduction factor $\phi = 0.75$ applies for torsion. Strength T_n is based on Eq. (7.4) with A_o substituted for A_{oh}, thus

$$T_n = \frac{2A_o A_t f_{yt}}{s} \cot\theta \tag{7.11}$$

In accordance with ACI Code 11.5.2, sections located less than a distance *d* from the face of a support may be designed for the same torsional moment T_u as that computed at a distance *d*, recognizing the beneficial effects of support compression. However, if a concentrated torque is applied within this distance, the critical section must be taken at the face of the support. These provisions parallel those used in shear design. For beams supporting slabs such as are shown in Fig. 7.1, the torsional loading from the slab may be treated as being uniformly distributed along the beam.

a. T Beams and Box Sections

For T beams, a portion of the overhanging flange contributes to the cracking torsional capacity and, if reinforced with closed stirrups, to the torsional strength. According to ACI Code 11.5.1, the contributing width of the overhanging flange on either side of the web is equal to the smaller of (1) the projection of the beam above or below the slab, whichever is greater, and (2) 4 times the slab thickness. These criteria are the same as those used for two-way slabs with beams, illustrated in Fig. 13.10. As with solid sections, A_{cp} for box sections, with or without flanges, represents the area enclosed by the outside perimeter of the concrete section.

After torsional cracking, the applied torque is resisted by the portion of the section represented by A_{oh}, the area enclosed by the centerline of the outermost closed transverse torsional reinforcement. For rectangular, box, and T sections A_{oh} is illustrated in Fig. 7.10. For sections with flanges, the Code does not require that the section used to establish A_{cp} coincide with that used to establish A_{oh}.

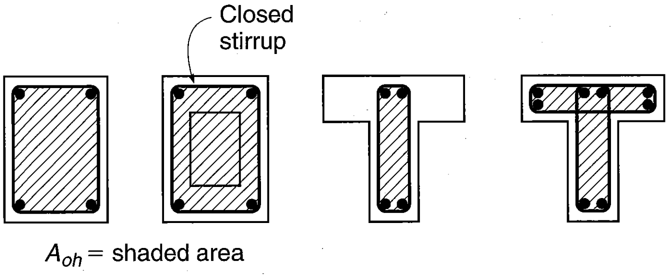

FIGURE 7.10
Definition of A_{oh}. *(Adapted from Ref. 7.7.)*

b. Minimal Torsion

If the factored torsional moment T_u does not exceed $\phi 0.083\lambda\sqrt{f_c'}\,(A_{cp}^2/p_{cp})$, torsional effects may be neglected, according to ACI Code 11.5.1. This lower limit is 25 percent of the cracking torque, given by Eq. (7.3), reduced by the factor ϕ, as usual, for design purposes. The presence of torsional moment at or below this limit will have a negligible effect on the flexural and shear strength of the member. The value of λ is as specified in ACI Code 8.6.1 and previously described in Section 4.5a, with $\lambda = 0.85$, 0.75, and 1.0 for sand-lightweight, all-lightweight, and normalweight concrete, respectively. Linear interpolation between values is permitted for concretes containing blends of lightweight and normalweight aggregates, and λ may be taken as $f_{ct}/(0.56\sqrt{f_c'})$ if the average split-cylinder strength of lightweight concrete is specified.

For members subjected to an axial load N_u (positive in compression), torsional effects may be neglected when T_u does not exceed $\phi 0.083\lambda\sqrt{f_c'}\,(A_{cp}^2/p_{cp}) \times \sqrt{1 + N_u/(0.33A_g\lambda\sqrt{f_c'})}$. For hollow sections (with or without axial load), A_{cp} must be replaced by the gross area of the concrete A_g to determine if torsional effects may be neglected. This has the effect of multiplying 25 percent of the cracking torque by the ratio A_g/A_{cp} twice—once to account for the reduction in cracking torque for hollow sections from the value shown in Eq. (7.3) and a second time to account for the transition from the circular interaction of combined shear and torsion stresses in Eq. (7.9) to the linear interaction represented by Eq. (7.8).

c. Equilibrium vs. Compatibility Torsion

A distinction is made in the ACI Code between equilibrium (primary) torsion and compatibility (secondary) torsion. For the first condition, described earlier with reference to Fig. 7.1*a*, the supporting member *must* be designed to provide the torsional resistance required by static equilibrium. For secondary torsion resulting from compatibility requirements, shown in Fig. 7.1*b*, it is assumed that cracking will result in a redistribution of internal forces; and according to ACI Code 11.5.2, the maximum torsional moment T_u may be reduced to $\phi 0.33\lambda\sqrt{f_c'}\,(A_{cp}^2/p_{cp})$ or $\phi 0.33\lambda\sqrt{f_c'}\,(A_{cp}^2/p_{cp})\,\sqrt{1 + N_u/(0.33A_g\lambda\sqrt{f_c'})}$ for members subjected to axial load. In the case of hollow sections, A_{cp} is *not* replaced by A_g. The design moments and shears in the supported member must be adjusted accordingly. The reduced value of T_u permitted by the ACI Code is intended to approximate the torsional cracking strength of the supporting beam, for combined torsional and flexural loading. The large rotations that occur at essentially constant torsional load would result in significant redistribution of internal forces, justifying use of the reduced value for design of the torsional member and the supported elements.

d. Limitations on Shear Stress

Based largely on empirical observations, the width of diagonal cracks caused by combined shear and torsion under *service loads* can be limited by limiting the calculated shear stress under *factored shear and torsion* (Ref. 7.4) so that

$$v_{\max} \leq \phi\left(\frac{V_c}{b_w d} + 0.66\sqrt{f_c'}\right) \tag{7.12}$$

where $v_{\max}$ in Eq. (7.12) corresponds to the upper limits on shear capacity described in Section 4.5d. Combining Eq. (7.12) with Eq. (7.8) provides limits on the cross-sectional dimensions of *hollow sections*, in accordance with ACI Code 11.5.3.

$$\frac{V_u}{b_w d} + \frac{T_u p_h}{1.7A_{oh}^2} \leq \phi\left(\frac{V_c}{b_w d} + 0.66\sqrt{f_c'}\right) \tag{7.13}$$

Likewise, for *solid sections*, combining Eq. (7.12) with Eq. (7.9) gives

$$\sqrt{\left(\frac{V_u}{b_w d}\right)^2 + \left(\frac{T_u p_h}{1.7A_{oh}^2}\right)^2} \leq \phi\left(\frac{V_c}{b_w d} + 0.66\sqrt{f_c'}\right) \tag{7.14}$$

Either member dimensions or concrete strength must be increased if the criteria in Eq. (7.13) or (7.14) are not satisfied.

ACI Code 11.5.3 requires that if the wall thickness varies around the perimeter of a hollow section, Eq. (7.13) be evaluated at the location where the left-hand side of the expression is a maximum. If the wall thickness is less than the assumed value of t used in the development of Eq. (7.8) A_{oh}/p_h, the actual value of t must be used in the calculation of torsional shear stress. As a result, the second term on the left-hand side of Eq. (7.13) must be taken as

$$\frac{T_u}{1.7A_{oh}t}$$

where t is the thickness of the wall of the hollow section at the location where the stresses are being checked.

e. Reinforcement for Torsion

The nominal torsional strength is given by Eq. (7.11).

$$T_n = \frac{2A_o A_t f_{yt}}{s}\cot\theta \tag{7.11}$$

According to ACI Code 11.5.3, the angle θ may assume any value between 30 and 60°, with a value of $\theta = 45°$ suggested. The area enclosed by the shear flow A_o may be determined by analysis using procedures such as suggested in Ref. 7.8, or A_o may be taken as equal to $0.85A_{oh}$. Combining Eq. (7.11) with Eq. (7.10), the required cross-sectional area of one stirrup leg for torsion is

$$A_t = \frac{T_u s}{2\phi A_o f_{yt}\cot\theta} \tag{7.15}$$

The Code limits f_{yt} to a maximum of 420 MPa for reasons of crack control.

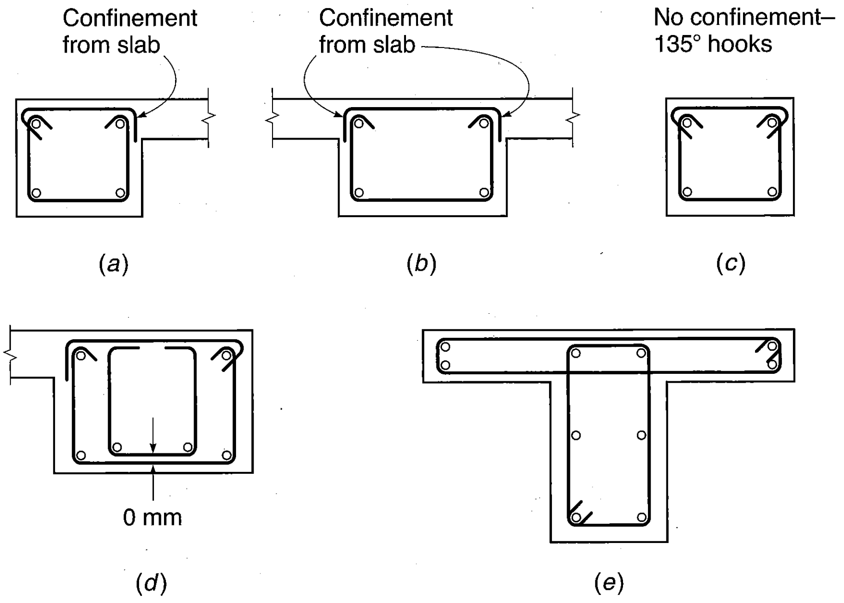

FIGURE 7.11
Stirrup-ties and longitudinal reinforcement for torsion: (*a*) spandrel beam with flanges on one side; (*b*) interior beam; (*c*) isolated rectangular beam; (*d*) wide spandrel beam; (*e*) T beam with torsional reinforcement in flanges.

The reinforcement provided for torsion must be combined with that required for shear. Based on the typical two-leg stirrup, this may be expressed as

$$\frac{A_{v+t}}{s} = \frac{A_v}{s} + 2\frac{A_t}{s} \tag{7.16}$$

As described in Section 7.3, the transverse stirrups used for torsional reinforcement must be of a closed form to provide the required tensile capacity across the diagonal cracks of all faces of the beam. U-shaped stirrups commonly used for transverse shear reinforcement are not suitable for torsional reinforcement. On the other hand, one-piece closed stirrups make field assembly of beam reinforcement difficult, and for practical reasons torsional stirrups are generally two-piece stirrup-ties, as shown in Fig. 7.11. A U-shaped stirrup is combined with a horizontal top bar, suitably anchored.

Because concrete outside the reinforcing cage tends to spall off when the member is subjected to high torque, transverse torsional reinforcement must be anchored within the concrete core (Ref. 7.9). ACI Code 11.5.4 requires that stirrups or ties used for transverse longitudinal reinforcement be anchored with a 135° standard hook or a seismic hook (described in section 20.4) around a longitudinal bar, unless the concrete surrounding the anchorage is restrained against spalling by a flange or a slab, in which case 90° standard hooks may be used, as shown in Fig. 7.11*a*, *b*, and *d*. Overlapping U-shaped stirrups, such as shown in Fig. 5.12*d*, may not be used. If flanges are included in the computation of torsional strength for T or L-shaped beams, closed torsional stirrups must be provided in the flanges, as shown in Fig. 7.11*e*.

The required spacing of closed stirrups, satisfying Eq. (7.16), is selected for the trial design based on standard bar sizes.

To control spiral cracking, the maximum spacing of torsional stirrups should not exceed $p_h/8$ or 300 mm, whichever is smaller. In addition, for members requiring both shear and torsion reinforcement, the minimum area of closed stirrups is equal to

$$A_v + 2A_t = 0.062\sqrt{f_c'}\,\frac{b_w s}{f_{yt}} \geq 0.35\,\frac{b_w s}{f_{yt}} \tag{7.17}$$

according to ACI Code 11.5.5.

The area of longitudinal bar reinforcement A_l required to resist torsion is given by Eq. (7.7), where θ must have the same value used to calculate A_t. The term A_t/s in Eq. (7.7) should be taken as the value calculated using Eq. (7.15), not modified based on minimum transverse steel requirements. ACI Code 11.5.3 permits the portion of A_l in the flexural compression zone to be reduced by an amount equal to $M_u/(0.9df_y)$, where M_u is the factored moment acting at the section in combination with T_u.

Based on an evaluation of the performance of reinforced concrete beam torsional test specimens, ACI Code 11.5.5 requires that A_l not be less than

$$A_{l,\min} = \frac{0.42\sqrt{f_c'}\,A_{cp}}{f_y} - \left(\frac{A_t}{s}\right)p_h\frac{f_{yt}}{f_y} \tag{7.18}$$

where $A_t/s \geq 0.175b_w/f_{yt}$, with f_{yt} in MPa.

The spacing of the longitudinal bars should not exceed 300 mm, and they should be distributed around the perimeter of the cross section to control cracking. The bars may not be less than No. 10 (No. 3) in size or have a diameter less than 0.042 times the spacing of the transverse stirrups. At least one longitudinal bar must be placed at each corner of the stirrups. Careful attention must be paid to the anchorage of longitudinal torsional reinforcement so that it is able to develop its yield strength at the face of the supporting columns, where torsional moments are often maximum.

Reinforcement required for torsion may be combined with that required for other forces, provided that the area furnished is the sum of the individually required areas and that the most restrictive requirements of spacing and placement are met. According to ACI Code 11.5.6, torsional reinforcement must be provided at least a distance $b_t + d$ beyond the point theoretically required, where b_t is the width of that part of the cross section containing the closed stirrups resisting torsion. According to the provisions of the ACI Code, the point at which the torsional reinforcement is no longer required is the point at which $T_u < \phi 0.083\lambda\sqrt{f_c'}(A_{cp}^2/p_{cp})$, or $T_u < \phi 0.083\lambda\sqrt{f_c'}(A_{cp}^2/p_{cp})\sqrt{1 + N_u/(0.33A_g\lambda\sqrt{f_c'})}$ for members subjected to axial load. The value is 25 percent of the cracking torque, reduced by the factor ϕ, as given in Section 7.5b.

The subject of torsional design of prestressed concrete is not treated here, but as presented in ACI Code 11.5, it differs only in certain details from the above presentation for nonprestressed reinforced concrete beams.

f. Design for Torsion

Designing a reinforced concrete flexural member for torsion involves a series of steps. The following sequence ensures that each is covered:

1. Determine if the factored torque is less than $\phi 0.083\lambda\sqrt{f_c'}(A_{cp}^2/p_{cp})$, or $\phi 0.083\lambda\sqrt{f_c'}(A_{cp}^2/p_{cp})\sqrt{1 + N_u/(0.33\,A_g\lambda\sqrt{f_c'})}$ for members subjected to axial load. If so, torsion may be neglected. If not, proceed with the design. Note that in this step, portions of over-hanging flanges, as defined in Section 7.5a, must be included in the calculation of A_{cp} and p_{cp}.
2. If the torsion is compatibility torsion, rather than equilibrium torsion, as described in Sections 7.1 and 7.5c, the maximum factored torque may be reduced to $\phi 0.33\lambda\sqrt{f_c'}(A_{cp}^2/p_{cp})$, or $\phi 0.33\lambda\sqrt{f_c'}(A_{cp}^2/p_{cp})\sqrt{1 + N_u/(0.33\,A_g\lambda\sqrt{f_c'})}$ for members subjected to axial load, with the moments and shears in the supported members adjusted accordingly. Equilibrium torsion cannot be adjusted.
3. Check the shear stresses in the section under combined torsion and shear, using the criteria of Section 7.5d.
4. Calculate the required transverse reinforcement for torsion using Eq. (7.15) and shear using Eq. (4.14*a*). Combine A_t and A_v using Eq. (7.16).

5. Check that the minimum transverse reinforcement requirements are met for both torsion and shear. These include the maximum spacing, as described in Sections 7.5e and 4.5d, and minimum area, as given in Eq. (7.17).
6. Calculate the required longitudinal torsional reinforcement A_l, using the larger of the values given in Eqs. (7.7) and (7.18), and satisfy the spacing and bar size requirements given in Section 7.5e. The portion of A_l in the flexural compression zone may be reduced by $M_u/(0.9df_y)$, providing that Eq. (7.18) and the spacing and bar size requirements are satisfied.
7. Continue torsional reinforcement $b_t + d$ past the point where T_u is less than $\phi 0.083\lambda\sqrt{f_c'}(A_{cp}^2/p_{cp})$, or $\phi 0.083\lambda\sqrt{f_c'}(A_{cp}^2/p_{cp})\sqrt{1 + N_u/(0.33A_g\lambda\sqrt{f_c'})}$ for members subjected to axial load.

EXAMPLE 7.1

Design for torsion with shear. The 8.5 m span beam shown in Fig. 7.12*a* and *b* carries a monolithic slab cantilevering 1.8 m past the beam centerline. The resulting L beam supports a live load of 13 kN/m along the beam centerline plus 2.4 kN/m² uniformly distributed over the upper slab surface. The effective depth to the flexural steel centroid is 535 mm, and the distance from the beam surfaces to the centroid of stirrup steel is 45 mm. Material strengths are $f_c' = 35$ MPa and $f_y = 420$ MPa. Design the torsional and shear reinforcement for the beam.

Solution. Applying ACI load factors gives the slab load as

$$
\begin{aligned}
1.2w_d &= 1.2 \times 0.150 \times 24 \times 1.65 = 7.13\ \text{kN/m}\\
1.6w_l &= 1.6 \times 2.4 \times 1.65 = \underline{6.34\ \text{kN/m}}\\
\text{Total} &= 13.47\ \text{kN-m at } 0.975\ \text{m eccentricity}
\end{aligned}
$$

while the beam carries directly

$$
\begin{aligned}
1.2w_d &= 1.2 \times 0.6 \times 0.3 \times 24 = 5.18\ \text{kN/m}\\
1.6w_l &= 1.6(13.0 + 2.4 \times 0.3) = \underline{21.95\ \text{kN/m}}\\
\text{Total} &= 27.13\ \text{kN/m}
\end{aligned}
$$

Thus, the uniformly distributed load on the beam is 40.6 kN/m, acting together with a uniformly distributed torque of 13.47 × 0.975 = 13.13 kN-m/m. At the face of the column, the design shear force is $V_u = 40.6 \times 8/2 = 162.4$ kN. At the same location, the design torsional moment is $T_u = 13.13 \times 8/2 = 52.5$ kN-m.

The variation of V_u and T_u with distance from the face of the supporting column is given by Fig. 7.12*c* and *d*, respectively. The values of V_u and T_u at the critical design section, a distance d from the column face, are

$$V_u = 162.4 \times \frac{3.465}{4} = 140.7\ \text{kN}$$

$$T_u = 52.5 \times \frac{3.465}{4} = 45.5\ \text{kN-m}$$

For the effective beam, $A_{cp} = 300 \times 600 + 150 \times 450 = 247{,}500\ \text{mm}^2$ and $p_{cp} = 2 \times 600 + 2 \times 750 = 2700$ mm. According to the ACI Code, torsion may be neglected for normalweight concrete ($\lambda = 1.0$) if $T_u \le 0.75 \times 0.083 \times 1.0\sqrt{35}(247{,}500^2/2700) \times 10^{-6} = 8.36$ kN-m. Torsion must clearly be considered in the present case. Since the torsional resistance of the beam is required for equilibrium, no reduction in T_u may be made.

Before designing the torsional reinforcement, the section will be checked for adequacy in accordance with Eq. (7.14). Although A_{cp} was calculated considering the flange to check if torsion could be neglected (as required by ACI Code 11.5.1), subsequent calculations for

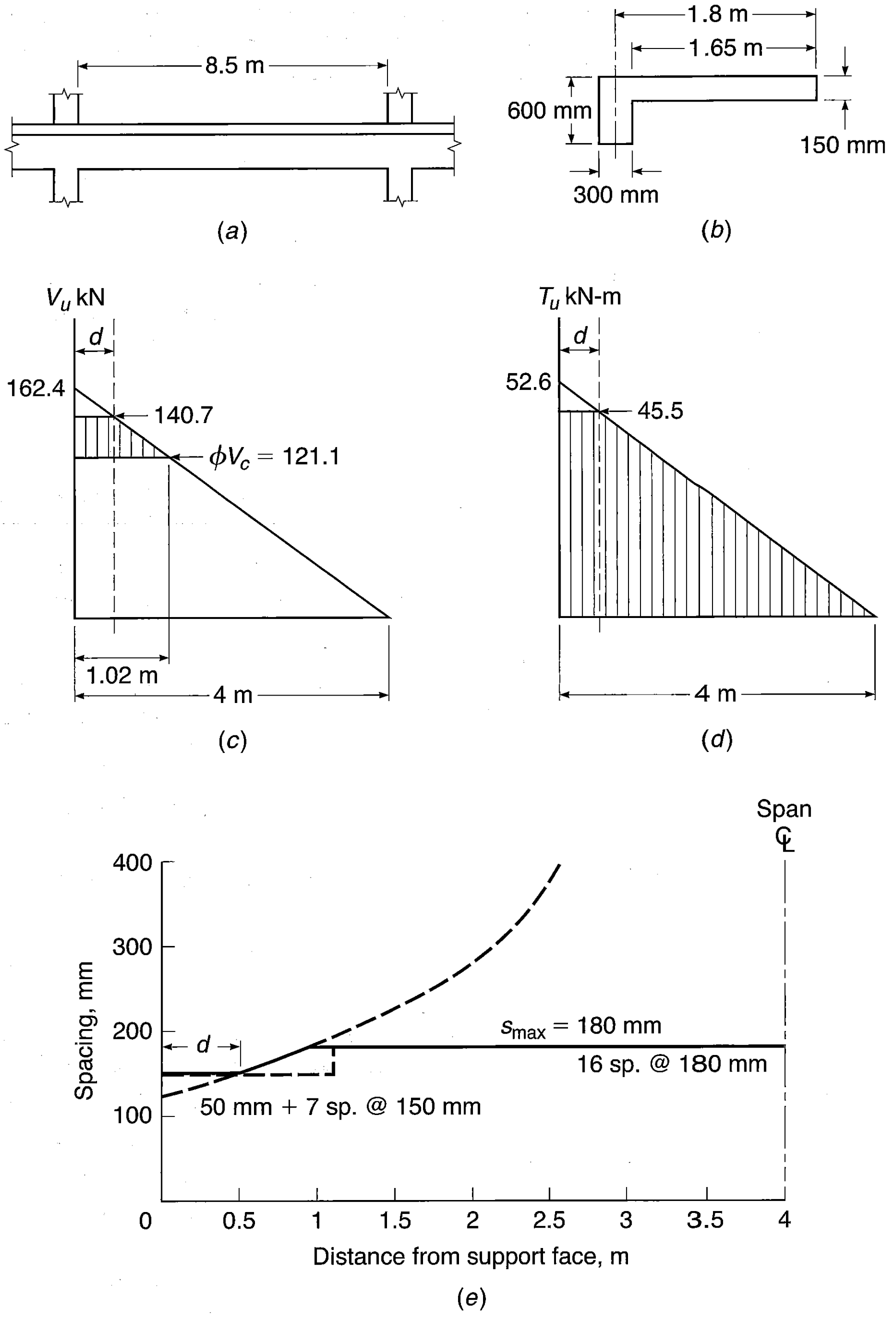

FIGURE 7.12
Shear and torsion design example.

8.5 m
(a)
1.8 m
1.65 m
600 mm
150 mm
300 mm
(b)
V_u kN
d
162.4
140.7
ϕV_c = 121.1
1.02 m
4 m
(c)
T_u kN-m
d
52.6
45.5
4 m
(d)
Span ℄
400
300
200
100
Spacing, mm
d
s_{max} = 180 mm
16 sp. @ 180 mm
50 mm + 7 sp. @ 150 mm
0
0.5
1
1.5
2
2.5
3
3.5
4
Distance from support face, m
(e)

serviceability and strength will neglect the flange and no torsional reinforcement will be provided in the flange. For reference, $b_wd = 300 \times 535 = 160{,}500\ \text{mm}^2$. With 45 mm cover to the center of the stirrup bars from all faces, $x_o = 300 - 90 = 210$ mm and $y_o = 600 - 90 = 510$ mm. Thus, $A_{oh} = 210 \times 510 = 107{,}100\ \text{mm}^2$, $A_o = 0.85 \times 107{,}100 = 91{,}000\ \text{mm}^2$, and $p_h = 2(210 + 510) = 1440$ mm. Using Eq. (7.14),

$$\sqrt{\left(\frac{140.7 \times 10^3}{160{,}500}\right)^2 + \left(\frac{45.5 \times 10^6 \times 1440}{1.7 \times 107{,}100^2}\right)^2} \le 0.75\left(0.17\sqrt{35} + 0.66\sqrt{35}\right)$$

$$3.47\ \text{MPa} \le 3.69\ \text{MPa}$$

Therefore, the cross section is of adequate size for the given concrete strength.

The values of A_t and A_v will now be calculated at the column face (for reference only). Using Eq. (7.15) and choosing $\theta = 45°$,

$$A_t = \frac{T_u s}{2\phi A_o f_{yt} \cot \theta}$$

$$= \frac{52.5 \times 10^6 s}{2 \times 0.75 \times 91{,}000 \times 420 \times 1} = 0.916s$$

for one leg of a closed vertical stirrup, or 1.832s for two legs.

The shear capacity of the concrete alone, obtained using Eq. (4.12b), is

$$\phi V_c = 0.75 \times 0.17\lambda\sqrt{f_c'}\, b_w d$$

$$= \frac{0.75 \times 0.17 \times 1.0\sqrt{35} \times 160{,}500}{1000} = 121.1 \text{ kN}$$

From Eq. (4.14a), the web reinforcement for transverse shear, again computed at the column face, is

$$A_v = \frac{(V_u - \phi V_c)s}{\phi f_{yt} d} = \frac{(162.4 - 121.1)10^3 s}{0.75 \times 420 \times 535} = 0.245s$$

to be provided in two vertical legs.

The calculated value of A_t will decrease linearly to zero at the midspan, and the calculated value of A_v will decrease linearly to zero 1.02 m from the face of the support, the point at which $V_u = \phi V_c$. Thus, the total area to be provided by the two vertical legs is

$$2A_t + A_v = 1.832s\left(1 - \frac{x}{4}\right) + 0.245s\left(1 - \frac{x}{1.02}\right)$$

for $0 \leq x \leq 1.02$ m, where x is the distance from the face of the support, and

$$2A_t + A_v = 1.832s\left(1 - \frac{x}{4}\right)$$

for $1.02 \leq x \leq 4$ m.

No. 13 (No. 4) closed stirrups will provide a total area in the two legs of 258 mm^2. For $2A_t + A_v = 258$ mm^2, the required spacing at d and at 0.5 m intervals along the span can be found using the given relationships between stirrup area and spacing:

$$\begin{aligned} s_d &= 151 \text{ mm} \\ s_1 &= 187 \text{ mm} \\ s_{1.5} &= 225 \text{ mm} \\ s_2 &= 282 \text{ mm} \\ s_{2.5} &= 376 \text{ mm} \\ s_3 &= 563 \text{ mm} \end{aligned}$$

These values of s are plotted in Fig. 7.12e. ACI provisions for maximum spacing should now be checked. For torsion reinforcement, the maximum spacing is the smaller of

$$\frac{p_h}{8} = \frac{1440}{8} = 180 \text{ mm}$$

or 300 mm, whereas for shear reinforcement, the maximum spacing is $d/2 = 268$ mm $\leq$ 600 mm. The most restrictive provision is the first, and the maximum spacing of 180 mm is plotted in Fig. 7.12e. Stirrups between the face of the support and the distance d can be spaced at s_d. The resulting spacing requirements are shown by the solid line in the figure. These requirements are met in a practical way by No. 13 (No. 4) closed stirrups, the first placed 50 mm from the face of the column, followed by 7 at 150 mm. spacing and 16 at 180 mm spacing. According to the ACI Code, stirrups may be discontinued at the point where $V_u < \phi V_c/2$ (1.49 m from the span centerline) or $b_t + d = 0.835$ m past the point at which $T_u < \phi 0.083\lambda\sqrt{f'_c}(A_{cp}^2/p_{cp})$. The latter point is past the centerline of the member; therefore, minimum stirrups are required throughout the span. The minimum web steel provided, 258 mm^2, satisfies the ACI Code minimum $= 0.062\sqrt{f'_c}\,b_w s/f_{yt} = 0.062\sqrt{35}\,(300) \times 180/420 = 47 \text{ mm}^2 \geq 0.35 b_w s/f_{yt} = 0.35 \times 300 \times 180/420 = 45 \text{ mm}^2$.

The longitudinal steel required for torsion at a distance d from the column face is computed next. At that location

$$\frac{A_t}{s} = 0.916\left(1 - \frac{0.535}{4}\right) = 0.794$$

and from Eq. (7.7)

$$A_l = 0.794 \times 1440 \times \frac{420}{420} \times 1^2 = 1143 \text{ mm}^2$$

with a total not less than given by Eq. (7.18), in which A_t/s is not to be taken less than $0.175 \times 300/420 = 0.125$.

$$A_{l,\min} = \frac{0.42\sqrt{35} \times 247{,}500}{420} - 0.794 \times 1440 \times \frac{420}{420} = 321 \text{ mm}^2$$

According to the ACI Code, the spacing must not exceed 300 mm, and the bars may not be less than No. 10 (No. 3) in size or have a diameter less than $0.042s = 7.6$ mm. Reinforcement will be placed at the top, middepth, and bottom of the member—each level to provide not less than $1143/3 = 381$ mm^2. Two No. 19 (No. 6) bars will be used at middepth, and reinforcement to be placed for flexure will be increased by 381 mm^2 at the top and bottom of the member.

Although A_l reduces in direct proportion to A_t and, hence, decreases linearly starting at d from the face of the column to the midspan, for simplicity of construction the added bars and the increment in the flexural steel will be maintained throughout the length of the member. Although ACI Code 11.5.3 states that A_l may be decreased in flexural compression zones by an amount equal to $M_u/(0.9df_y)$, that reduction will not be made here. Adequate embedment must be provided past the face of the column to fully develop f_y in the bars at that location.

REFERENCES

7.1. P. Lampert and B. Thurlimann, "Ultimate Strength and Design of Reinforced Concrete Beams in Torsion and Bending," *Int. Assoc. Bridge and Struct. Eng.* Publ. 31-I, Zurich, 1971, pp. 107–131.

7.2. B. Thurlimann, "Torsional Strength of Reinforced and Prestressed Beams—CEB Approach," in *Concrete Design: U.S. and European Practices*, SP-59, 1979, American Concrete Institute, Detroit, MI, pp. 117–143.

7.3. *CEB-FIP Model Code 1990*, Thomas Telford, London, 1991.

7.4. CSA Committee A23.3, *Design of Concrete Structures*, Canadian Standards Association, Etobicoke, Ontario, 2004.

7.5. T. T. C. Hsu, "Torsion of Structural Concrete—Behavior of Reinforced Concrete Rectangular Members," in *Torsion of Structural Concrete*, SP-18, 1968, American Concrete Institute, Detroit, MI, pp. 261–306.

7.6. A. H. Mattock, Disc. of "Design of Torsion" by J. G. MacGregor and M. G. Ghoneim (Ref 7.7), *ACI Struct. J.*, vol. 93, no. 1, 1996, pp. 142–143.

7.7. J. G. MacGregor and M. G. Ghoneim, "Design of Torsion," *ACI Struct. J.*, vol. 92, no. 2, 1995, pp. 218–221.

7.8. T. T. C. Hsu, "Shear Flow Zone in Torsion of Reinforced Concrete," *J. Struct. Eng.*, vol. 116, no. 11, 1990, pp. 3206–3226.

7.9. D. Mitchell and M. P. Collins, "Detailing for Torsion," *J. ACI*, vol. 73, no. 9, 1976, pp. 506–511.

PROBLEMS

7.1. A beam of rectangular cross section having $b = 550$ mm and $h = 375$ mm is to carry a total factored load of 51 kN/m uniformly distributed over its 7.9 m span, and in addition the beam will be subjected to a uniformly distributed torsion of 7.8 kN-m/m at factored loads. Closed stirrup-ties will be used to provide for flexural shear and torsion, placed with the stirrup steel centroid 45 mm from each concrete face. The corresponding flexural effective depth will be approximately 310 mm. Design the transverse reinforcement for this beam and calculate the increment of longitudinal steel area needed to provide for torsion, using $f'_c = 28$ MPa and $f_y = 420$ MPa.

7.2. Architectural and clearance requirements call for the use of a transfer girder, shown in Fig. P7.2, spanning 6 m between supporting column faces. The girder must carry from above a concentrated column load of 78 kN at midspan, applied with eccentricity 600 mm from the girder centerline. (Load factors are already included, as is an allowance for girder self-weight.) The member is to have dimensions $b = 250$ mm, $h = 500$ mm, $x_o = 160$ mm, $y_o = 410$ mm, and $d = 425$ mm. Supporting columns provide full torsional rigidity; flexural rigidity at the ends of the span can be assumed to develop 40 percent of the maximum moment that would be obtained if the girder were simply supported. Design both transverse and longitudinal steel for the beam. Material strengths are $f'_c = 35$ MPa and $f_y = 420$ MPa.

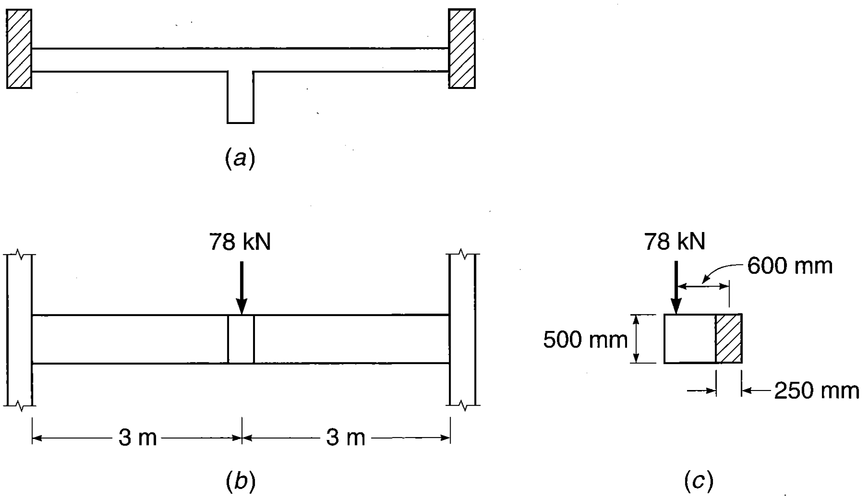

FIGURE P7.2
Transfer girder: (*a*) top view; (*b*) front view; (*c*) side view.

7.3. The beam shown in cross section in Fig. P7.3 is a typical interior member of a continuous building frame, with span 9 m between support faces. At factored loads, it will carry a uniformly distributed vertical load of 45 kN/m, acting simultaneously with a uniformly distributed torsion of 11.5 kN-m/m. Transverse reinforcement for shear and torsion will consist of No. 13 (No. 4) stirrup-ties, as shown, with 40 mm clear to all concrete faces. The effective depth to flexural steel is taken equal to 560 mm for both negative and positive bending regions. Design the transverse reinforcement for shear and torsion, and calculate the longitudinal steel to be added to the flexural

FIGURE P7.3

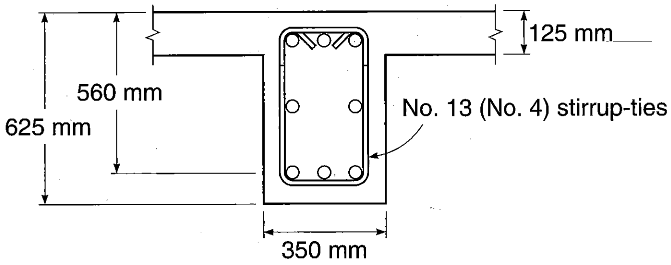

requirements to provide for torsion. Torsional reinforcement will be provided only in the web, not in the flanges. Material strengths are $f_c' = 28$ MPa and $f_y = 420$ MPa.

7.4. The single-span T beam bridge described in Problem 3.14 is reinforced for flexure with four No. 32 (No. 10) bars in two layers, which continue uninterrupted into the supports, permitting a service live load of 21.9 kN/m to be carried, in addition to the dead load of 13.5 kN/m, including self-weight. Assume now that only one-half of that live load acts but that it is applied over only one-half the width of the member, entirely to the right of the section centerline. Design the transverse reinforcement for shear and torsion, and calculate the modified longitudinal steel needed for this eccentric load condition. Torsional reinforcement can be provided in the slab if needed, as well as in the web. Stirrup-ties will be No. 10 or No. 13 (No. 3 or No. 4) bars, with 40 mm clear to all concrete faces. Supports provide no restraint against flexural rotations but do provide full restraint against twist. Show a sketch of your final design, detailing all reinforcement. Material strengths are as given for Problem 3.14.

7.5. Design a spandrel (edge) girder for shear and torsion that is loaded with a uniform factored load of 16 kN/m. In addition, beams framing into the girder apply concentrated factored vertical loads F_{u1} and F_{u2} and torsional moments T_{u1} and T_{u2}, as shown in Fig. P7.5. Girder dimensions are $h = 800$ mm and $b_w = 700$ mm, and slab thickness (one side of girder only) = 150 mm. An analysis of various loading combinations indicates the following results:

Case 1	$F_{u1} = F_{u2} = 350$ kN $T_{u1} = T_{u2} = 210$ kN-m
Case 2	$F_{u1} = 360$ kN; $F_{u2} = 98$ kN $T_{u1} = 210$ kN-m; $T_{u2} = 72$ kN-m
Case 3	$F_{u1} = 98$ kN; $F_{u2} = 360$ kN $T_{u1} = 72$ kN-m; $T_{u2} = 210$ kN-m

FIGURE P7.5

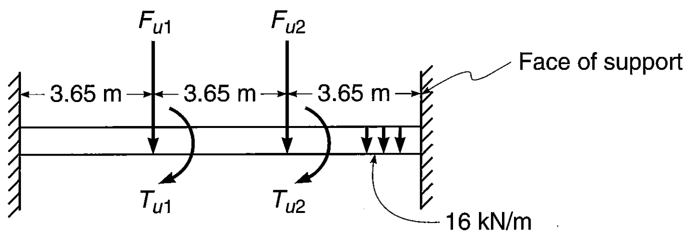

To calculate reactions, treat the ends of the girder as fixed. Use $f_y = 420$ MPa and $f_c' = 28$ MPa. Provide design drawings showing the transverse steel and the longitudinal steel required in addition to the flexural steel.

7.6. A 6 m long rectangular beam, free-standing except for being fixed at each end against rotation, must carry a midspan live load of 150 kN. The load can be as much as 300 mm off the axis of the beam. Beam dimensions are $b = 300$ mm, $d = 500$ mm, and $h = 580$ mm. Use $f_y = 420$ MPa and $f_c' = 28$ MPa. Design the shear and torsion reinforcement.

8

Short Columns

8.1 INTRODUCTION: AXIAL COMPRESSION

Columns are defined as members that carry loads chiefly in compression. Usually columns carry bending moments as well, about one or both axes of the cross section, and the bending action may produce tensile forces over a part of the cross section. Even in such cases, columns are generally referred to as compression members, because the compression forces dominate their behavior. In addition to the most common type of compression member, i.e., vertical elements in structures, compression members include arch ribs; rigid frame members inclined or otherwise; compression elements in trusses, shells, or portions thereof that carry axial compression; and other forms. In this chapter the term *column* will be used interchangeably with the term *compression member*, for brevity and in conformity with general usage.

Three types of reinforced concrete compression members are in use:

1. Members reinforced with longitudinal bars and lateral ties.
2. Members reinforced with longitudinal bars and continuous spirals.
3. Composite compression members reinforced longitudinally with structural steel shapes, pipe, or tubing, with or without additional longitudinal bars, and various types of lateral reinforcement.

Types 1 and 2 are by far the most common, and most of the discussion in this chapter will refer to them.

The main reinforcement in columns is longitudinal, parallel to the direction of the load, and consists of bars arranged in a square, rectangular, or circular pattern, as was shown in Fig. 1.15. Figure 8.1 shows an ironworker tightening splices for the main reinforcing steel during construction of the 60-story Bank of America Corporate Center in Charlotte, North Carolina. The ratio of longitudinal steel area A_{st} to gross concrete cross section A_g is in the range from 0.01 to 0.08, according to ACI Code 10.9.1. The lower limit is necessary to ensure resistance to bending moments not accounted for in the analysis and to reduce the effects of creep and shrinkage of the concrete under sustained compression. Ratios higher than 0.08 not only are uneconomical, but also would cause difficulty owing to congestion of the reinforcement, particularly where the steel must be spliced. Most columns are designed with ratios below 0.04. Larger-diameter bars are used to reduce placement costs and to avoid unnecessary congestion. The special large-diameter No. 43 and No. 57 (No. 14 and No. 18) bars are produced mainly for use in columns. According to ACI Code 10.9.2, a minimum of four longitudinal bars is required when the bars are enclosed by spaced rectangular or circular ties, and a minimum of six bars must be used when the longitudinal bars are enclosed by a continuous spiral.

FIGURE 8.1
Reinforcement for primary column of 60-story Bank of America Corporate Center in Charlotte, North Carolina. (*Courtesy of Walter P. Moore and Associates.*)

Columns may be divided into two broad categories: *short columns*, for which the strength is governed by the strength of the materials and the geometry of the cross section, and *slender columns*, for which the strength may be significantly reduced by lateral deflections. A number of years ago, an ACI-ASCE survey indicated that 90 percent of columns braced against sidesway and 40 percent of unbraced columns could be designed as short columns. Effective lateral bracing, which prevents relative lateral movement of the two ends of a column, is commonly provided by shear walls, elevator and stairwell shafts, diagonal bracing, or a combination of these. Although slender columns are more common now because of the wider use of high-strength materials and improved methods of dimensioning members, it is still true that most columns in ordinary practice can be considered short columns. Only short columns will be discussed in this chapter; the effects of slenderness in reducing column strength will be covered in Chapter 9.

The behavior of short, axially loaded compression members was discussed in Section 1.9 in introducing the basic aspects of reinforced concrete. It is suggested that the earlier material be reviewed at this point. In Section 1.9, it was demonstrated that, for lower loads at which both materials remain elastic, the steel carries a relatively small portion of the total load. The steel stress f_s is equal to n times the concrete stress:

$$f_s = nf_c \tag{8.1}$$

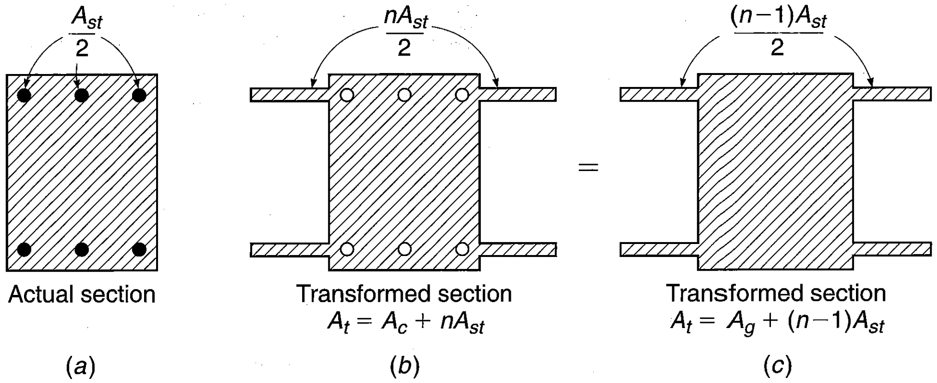

FIGURE 8.2
Transformed section in axial compression.

where $n = E_s/E_c$ is the modular ratio. In this range the axial load P is given by

$$P = f_c[A_g + (n-1)A_{st}] \tag{8.2}$$

where A_g is the gross area of the cross section, A_{st} is the total area of the reinforcing steel, and the term in brackets is the area of the transformed section (see Fig. 8.2). Equations (8.2) and (8.1) can be used to find concrete and steel stresses, respectively, for given loads, provided both materials remain elastic. Example 1.1 demonstrated the use of these equations.

In Section 1.9, it was further shown that the nominal strength of an axially loaded column can be found, recognizing the nonlinear response of both materials, by

$$P_n = 0.85f_c'A_c + A_{st}f_y \tag{8.3a}$$

where A_c = net area of concrete, or

$$P_n = 0.85f_c'(A_g - A_{st}) + A_{st}f_y \tag{8.3b}$$

i.e., by summing the strength contributions of the two components of the column. At this stage, the steel carries a significantly larger fraction of the load than was the case at lower total load.

The calculation of the nominal strength of an axially loaded column was demonstrated in Section 1.9.

According to ACI Code 10.3.6, the *design strength* of an axially loaded column is to be found based on Eq. (8.3*b*) with the introduction of certain strength reduction factors. The ACI factors are lower for columns than for beams, reflecting their greater importance in a structure. A beam failure would normally affect only a local region, whereas a column failure could result in the collapse of the entire structure. In addition, these factors reflect differences in the behavior of tied columns and spirally reinforced columns that will be discussed in Section 8.2. A basic ϕ factor of 0.75 is used for spirally reinforced columns and 0.65 for tied columns, vs. $\phi = 0.90$ for most beams.

A further limitation on column strength is imposed by ACI Code 10.3.6 to allow for accidental eccentricities of loading not considered in the analysis. This is done by imposing an upper limit on the axial load that is less than the calculated design strength. This upper limit is taken as 0.85 times the design strength for spirally reinforced columns and 0.80 times the calculated strength for tied columns. Thus, according to ACI Code 10.3.6, for spirally reinforced columns

$$\phi P_{n(\max)} = 0.85\phi[0.85f_c'(A_g - A_{st}) + f_y A_{st}] \tag{8.4a}$$

with $\phi = 0.75$. For tied columns

$$\phi P_{n(\max)} = 0.80\phi[0.85f_c'(A_g - A_{st}) + f_y A_{st}] \tag{8.4b}$$

with $\phi = 0.65$.

8.2 LATERAL TIES AND SPIRALS

Figure 1.15 shows cross sections of the simplest types of columns, spirally reinforced or provided with lateral ties. Other cross sections frequently found in buildings and bridges are shown in Fig. 8.3. In general, in members with large axial forces and small moments, longitudinal bars are spaced more or less uniformly around the perimeter (Fig. 8.3*a* to *d*). When bending moments are large, much of the longitudinal steel is concentrated at the faces of highest compression or tension, i.e., at maximum distances from the axis of bending (Fig. 8.3*e* to *h*). Specific recommended patterns for many combinations and arrangements of bars are found in Refs. 8.1 and 8.2. In heavily loaded columns with large steel percentages, the result of a large number of bars, each of them positioned and held individually by ties, is steel congestion in the forms and

FIGURE 8.3
Tie arrangements for square and rectangular columns.

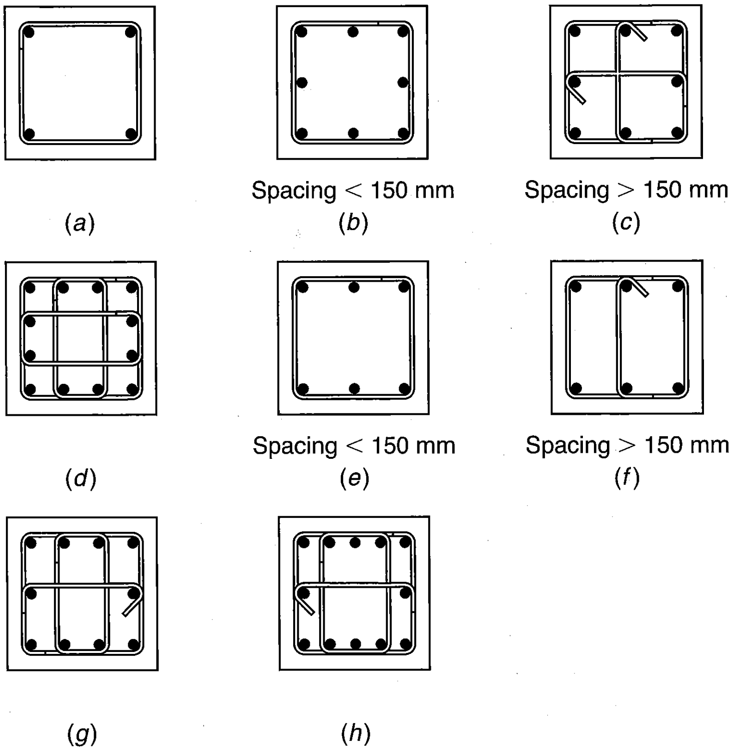
(*a*)

Spacing < 150 mm
(*b*)

Spacing > 150 mm
(*c*)

(*d*)

Spacing < 150 mm
(*e*)

Spacing > 150 mm
(*f*)

(*g*)

(*h*)

difficulties in placing the concrete. In such cases, bundled bars are frequently employed. Bundles consist of three or four bars tied in direct contact, wired, or otherwise fastened together. These are usually placed in the corners. Tests have shown that adequately bundled bars act as one unit; i.e., they are detailed as if a bundle constituted a single round bar of area equal to the sum of the bundled bars.

Lateral reinforcement, in the form of individual relatively widely spaced ties or a continuous closely spaced spiral, serves several functions. For one, such reinforcement is needed to hold the longitudinal bars in position in the forms while the concrete is being placed. For this purpose, longitudinal and transverse steel is wired together to form cages, which are then moved into the forms and properly positioned before placing the concrete. For another, transverse reinforcement is needed to prevent the highly stressed, slender longitudinal bars from buckling outward by bursting the thin concrete cover.

Closely spaced spirals serve these two functions. Ties, which can be arranged and spaced in various ways, must be so designed that these two requirements are met. This means that the spacing must be sufficiently small to prevent buckling between ties and that, in any tie plane, a sufficient number of ties must be provided to position and hold all bars. On the other hand, in columns with many longitudinal bars, if the column section is crisscrossed by too many ties, they interfere with the placement of concrete in the forms. To achieve adequate tying yet hold the number of ties to a minimum, ACI Code 7.10.5 gives the following rules for tie arrangement:

> All bars of tied columns shall be enclosed by *lateral ties*, at least No. 10 (No. 3) in size for longitudinal bars up to No. 32 (No. 10), and at least No. 13 (No. 4) in size for Nos. 36, 43, and 57 (Nos. 11, 14, and 18) and bundled longitudinal bars. The spacing of the ties shall not exceed 16 diameters of longitudinal bars, 48 diameters of tie bars, nor the least dimension of the column. The ties shall be so arranged that every corner and alternate longitudinal bar shall have lateral support provided by the corner of a tie having an included angle of not more than 135°, and no bar shall be farther than 150 mm clear on either side from such a laterally supported bar. Deformed wire or welded wire fabric of equivalent area may be used instead of ties. Where the bars are located around the periphery of a circle, complete circular ties may be used.

For spirally reinforced columns ACI Code 7.10.4 requirements for lateral reinforcement may be summarized as follows:

> Spirals shall consist of a continuous bar or wire not less than 10 mm in diameter, and the clear spacing between turns of the spiral must not exceed 75 mm nor be less than 25 mm.

In addition, a minimum ratio of spiral steel is imposed such that the structural performance of the column is significantly improved, with respect to both ultimate load and the type of failure, compared with an otherwise identical tied column.

The structural effect of a spiral is easily visualized by considering as a model a steel drum filled with sand (Fig. 8.4). When a load is placed on the sand, a lateral pressure is exerted by the sand on the drum, which causes hoop tension in the steel wall. The load on the sand can be increased until the hoop tension becomes large enough to burst the drum. The sand pile alone, if not confined in the drum, would have been able to support hardly any load. A cylindrical concrete column, to be sure, does have a definite strength without any lateral confinement. As it is being loaded, it shortens longitudinally and expands laterally, depending on Poisson's ratio. A closely spaced spiral confining the column counteracts the expansion, as

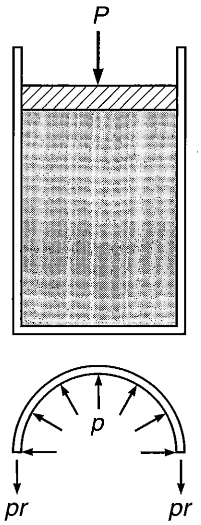

FIGURE 8.4
Model for action of a spiral.

did the steel drum in the model. This causes hoop tension in the spiral, while the carrying capacity of the confined concrete in the core is greatly increased. Failure occurs only when the spiral steel yields, which greatly reduces its confining effect, or when it fractures.

A tied column fails at the load given by Eq. (8.3*a* or *b*). At this load the concrete fails by crushing and shearing outward along inclined planes, and the longitudinal steel by buckling outward between ties (Fig. 8.5). In a spirally reinforced column, when the same load is reached, the longitudinal steel and the concrete within the core are prevented from moving outward by the spiral. The concrete in the outer shell, however, not being so confined, does fail; i.e., the outer shell spalls off when the load P_n is reached. It is at this stage that the confining action of the spiral has a significant effect, and if sizable spiral steel is provided, the load that will ultimately fail the column by causing the spiral steel to yield or fracture can be much larger than that at which the shell spalled off. Furthermore, the axial strain limit when the column fails will be much greater than otherwise; the toughness of the column has been much increased.

In contrast to the practice in some foreign countries, it is reasoned in the United States that any excess capacity beyond the spalling load of the shell is wasted because the member, although not actually failed, would no longer be considered serviceable. For this reason, the ACI Code provides a minimum spiral reinforcement of such an amount that its contribution to the carrying capacity is just slightly larger than that of the concrete in the shell. The situation is best understood from Fig. 8.6, which compares the performance of a tied column with that of a spiral column whose spalling load is equal to the ultimate load of the tied column. The failure of the tied column is abrupt and complete. This is true, to almost the same degree, of a spiral column with a spiral so light that its strength contribution is considerably less than the strength lost in the spalled shell. With a heavy spiral the reverse is true, and with considerable prior deformation the spalled column would fail at a higher load. The "ACI spiral," its strength contribution about compensating for that lost in the spalled shell, hardly increases the ultimate load. However, by preventing instantaneous crushing of concrete and buckling of steel, it produces a more gradual and ductile failure, i.e., a tougher column.

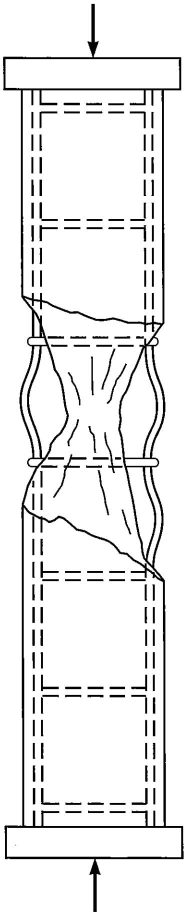

FIGURE 8.5
Failure of a tied column.

FIGURE 8.6
Behavior of spirally reinforced and tied columns.

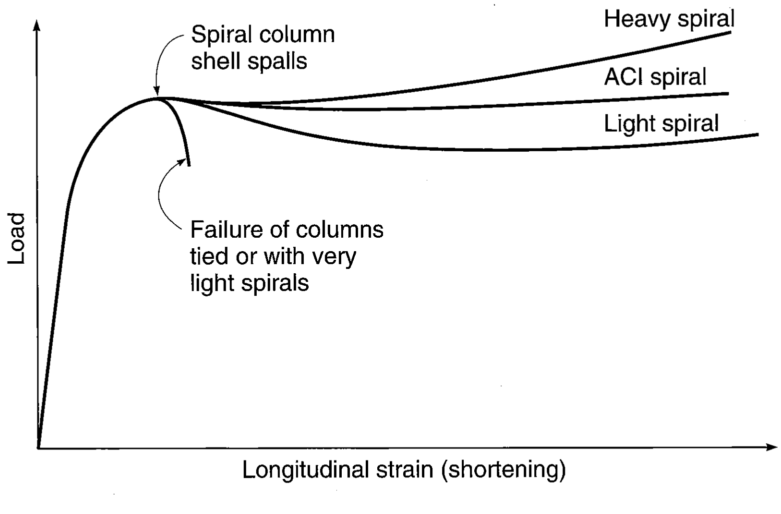

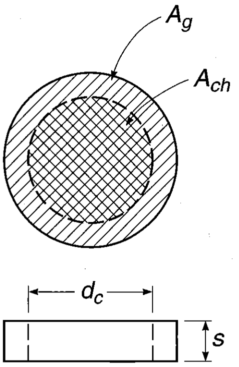

FIGURE 8.7
Confinement of core concrete due to hoop tension.

It has been found experimentally (Refs. 8.3 to 8.5) that the increase in compressive strength of the core concrete in a column provided through the confining effect of spiral steel is closely represented by the equation

$$f_c^* - 0.85f_c' = 4.0f_2' \tag{a}$$

where f_c^* = compressive strength of spirally confined core concrete
$0.85f_c'$ = compressive strength of concrete if unconfined
f_2' = lateral confinement stress in core concrete produced by spiral

The confinement stress f_2' is calculated assuming that the spiral steel reaches its yield stress f_y when the column eventually fails. With reference to Fig. 8.7, a hoop tension analysis of an idealized model of a short segment of column confined by one turn of lateral steel shows that

$$f_2' = \frac{2A_{sp}f_{yt}}{d_c s} \tag{b}$$

where A_{sp} = cross-sectional area of spiral wire
f_{yt} = yield strength of spiral steel
d_c = outside diameter of spiral
s = spacing or pitch of spiral wire

A *volumetric ratio* is defined as the ratio of the volume of spiral steel to the volume of core concrete:

$$\rho_s = \frac{2\pi d_c A_{sp}}{2}\,\frac{4}{\pi d_c^2 s}$$

from which

$$A_{sp} = \frac{\rho_s d_c s}{4} \tag{c}$$

Substituting the value of A_{sp} from Eq. (*c*) into Eq. (*b*) results in

$$f_2' = \frac{\rho_s f_{yt}}{2} \tag{d}$$

To find the right amount of spiral steel, one calculates

$$\text{Strength contribution of the shell} = 0.85f_c'(A_g - A_{ch}) \tag{e}$$

where A_g and A_c are, respectively, the gross and core concrete areas. Then substituting the confinement stress from Eq. (*d*) into Eq. (*a*) and multiplying by the core concrete area, one finds

$$\text{Strength provided by spiral} = 2\rho_s f_{yt} A_{ch} \tag{f}$$

The basis for the design of the spiral is that the strength gain provided by the spiral should be at least equal to that lost when the shell spalls, so combining Eqs. (*e*) and (*f*) yields

$$0.85f_c'(A_g - A_{ch}) = 2\rho_s f_{yt} A_{ch}$$

from which

$$\rho_s = 0.425\left(\frac{A_g}{A_{ch}} - 1\right)\frac{f_c'}{f_{yt}} \tag{g}$$

According to the ACI Code, this result is rounded upward slightly, and ACI Code 10.9.3 states that the ratio of spiral reinforcement shall not be less than

$$\rho_s = 0.45\left(\frac{A_g}{A_{ch}} - 1\right)\frac{f'_c}{f_{yt}} \tag{8.5}$$

It is further stipulated in the ACI Code that f_{yt} not be taken greater than 700 MPa and that spiral reinforcement not be spliced if f_{yt} is greater than 420 MPa.

It follows from this development that two concentrically loaded columns designed in accordance with the ACI Code, one tied and one with spiral but otherwise identical, will fail at about the same load, the former in a sudden and brittle manner, the latter gradually with prior spalling of the shell and with more ductile behavior. This advantage of the spiral column is much less pronounced if the load is applied with significant eccentricity or when bending from other sources is present simultaneously with axial load. For this reason, while the ACI Code permits somewhat larger design loads on spiral than on tied columns when the moments are small or zero ($\phi = 0.75$ for spirally reinforced columns vs. $\phi = 0.65$ for tied), the difference is not large, and it is even further reduced for large eccentricities, for which ϕ approaches 0.90 for both.

The design of spiral reinforcement according to the ACI Code provisions is easily reduced to tabular form, as in Table A.14 of Appendix A.

8.3 COMPRESSION PLUS BENDING OF RECTANGULAR COLUMNS

Members that are axially, i.e., concentrically, compressed occur rarely, if ever, in buildings and other structures. Components such as columns and arches chiefly carry loads in compression, but simultaneous bending is almost always present. Bending moments are caused by continuity, i.e., by the fact that building columns are parts of monolithic frames in which the support moments of the girders are partly resisted by the abutting columns, by transverse loads such as wind forces, by loads carried eccentrically on column brackets, or in arches when the arch axis does not coincide with the pressure line. Even when design calculations show a member to be loaded purely axially, inevitable imperfections of construction will introduce eccentricities and consequent bending in the member as built. For this reason members that must be designed for simultaneous compression and bending are very frequent in almost all types of concrete structures.

When a member is subjected to combined axial compression P and moment M, such as in Fig. 8.8*a*, it is usually convenient to replace the axial load and moment with an equal load P applied at eccentricity $e = M/P$, as in Fig. 8.8*b*. The two loadings are statically equivalent. All columns may then be classified in terms of the equivalent eccentricity. Those having relatively small e are generally characterized by compression over the entire concrete section, and if overloaded, will fail by crushing of the concrete accompanied by yielding of the steel in compression on the more heavily loaded side. Columns with large eccentricity are subject to tension over at least a part of the section, and if overloaded, may fail due to tensile yielding of the steel on the side farthest from the load.

For columns, load stages below the ultimate are generally not important. Cracking of concrete, even for columns with large eccentricity, is usually not a serious problem, and lateral deflections at service load levels are seldom, if ever, a factor. Design of

FIGURE 8.8
Equivalent eccentricity of column load.

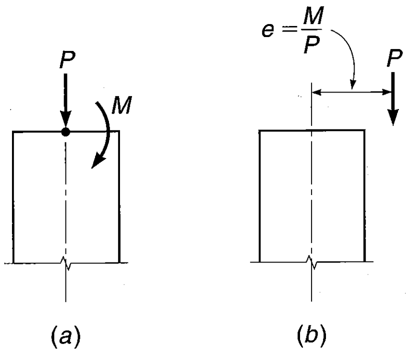

columns is therefore based on the factored load, which must not exceed the design strength, as usual, i.e.,

$$\phi M_n \geq M_u \tag{8.6a}$$

$$\phi P_n \geq P_u \tag{8.6b}$$

8.4 STRAIN COMPATIBILITY ANALYSIS AND INTERACTION DIAGRAMS

Figure 8.9*a* shows a member loaded parallel to its axis by a compressive force P_n at an eccentricity e measured from the centerline. The distribution of strains at a section *a-a* along its length, at incipient failure, is shown in Fig. 8.9*b*. With plane sections assumed to remain plane, concrete strains vary linearly with distance from the neutral axis, which is located a distance c from the more heavily loaded side of the member. With full compatibility of deformations, the steel strains at any location are the same as the strains in the adjacent concrete; thus, if the ultimate concrete strain is ϵ_u, the strain in the bars nearest the load is ϵ_s', while that in the tension bars at the far side is ϵ_s. Compression steel with area A_s' and tension steel with area A_s are located at distances d' and d, respectively, from the compression face.

The corresponding stresses and forces are shown in Fig. 8.9*c*. Just as for simple bending, the actual concrete compressive stress distribution is replaced by an equivalent rectangular distribution having depth $a = \beta_1 c$. A large number of tests on columns with a variety of shapes have shown that the strengths computed on this basis are in satisfactory agreement with test results (Ref. 8.6).

Equilibrium between external and internal axial forces shown in Fig. 8.9*c* requires that

$$P_n = 0.85 f_c' ab + A_s' f_s' - A_s f_s \tag{8.7}$$

Also, the moment about the centerline of the section of the internal stresses and forces must be equal and opposite to the moment of the external force P_n, so that

$$M_n = P_n e = 0.85 f_c' ab \left(\frac{h}{2} - \frac{a}{2} \right) + A_s' f_s' \left(\frac{h}{2} - d' \right) + A_s f_s \left(d - \frac{h}{2} \right) \tag{8.8}$$

These are the two basic equilibrium relations for rectangular eccentrically compressed members.

FIGURE 8.9
Column subject to eccentric compression: (*a*) loaded column; (*b*) strain distribution at section *a-a*; (*c*) stresses and forces at nominal strength.

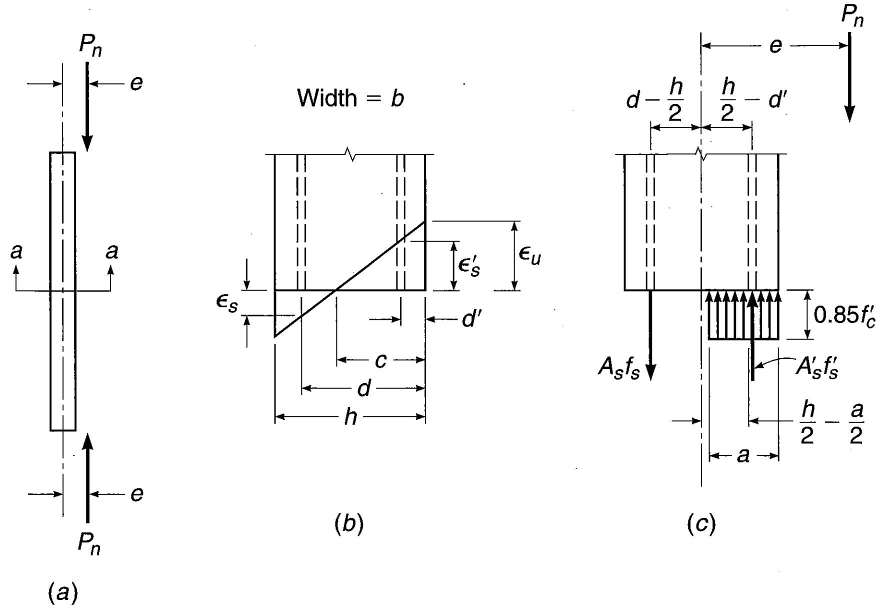

The fact that the presence of the compression reinforcement A'_s has displaced a corresponding amount of concrete of area A'_s is neglected in writing these equations. If necessary, particularly for large reinforcement ratios, one can account for this very simply. Evidently, in the above equations a nonexistent concrete compression force of amount $A'_s(0.85f'_c)$ has been included as acting in the displaced concrete at the level of the compression steel. This excess force can be removed in both equations by multiplying A'_s by $f'_s - 0.85f'_c$ rather than by f'_s.

For large eccentricities, failure is initiated by yielding of the tension steel A_s. Hence, for this case, $f_s = f_y$. When the concrete reaches its ultimate strain ϵ_u, the compression steel may or may not have yielded; this must be determined based on compatibility of strains. For small eccentricities the concrete will reach its limit strain ϵ_u before the tension steel starts yielding; in fact, the bars on the side of the column farther from the load may be in compression, not tension. For small eccentricities, too, the analysis must be based on compatibility of strains between the steel and the adjacent concrete.

For a given eccentricity determined from the frame analysis (i.e., $e = M_u/P_u$) it is possible to solve Eqs. (8.7) and (8.8) for the load P_n and moment M_n that would result in failure as follows. In both equations, f'_s, f_s, and a can be expressed in terms of a single unknown c, the distance to the neutral axis. This is easily done based on the geometry of the strain diagram, with ϵ_u taken equal to 0.003 as usual, and using the stress-strain curve of the reinforcement. The result is that the two equations contain only two unknowns, P_n and c, and can be solved for those values simultaneously. However, to do so in practice would be complicated algebraically, particularly because of the need to incorporate the limit f_y on both f'_s and f_s.

A better approach, providing the basis for practical design, is to construct a *strength interaction diagram* defining the failure load and failure moment for a given column for the full range of eccentricities from zero to infinity. For any eccentricity, there is a unique pair of values of P_n and M_n that will produce the state of incipient failure. That pair of values can be plotted as a point on a graph relating P_n and M_n,

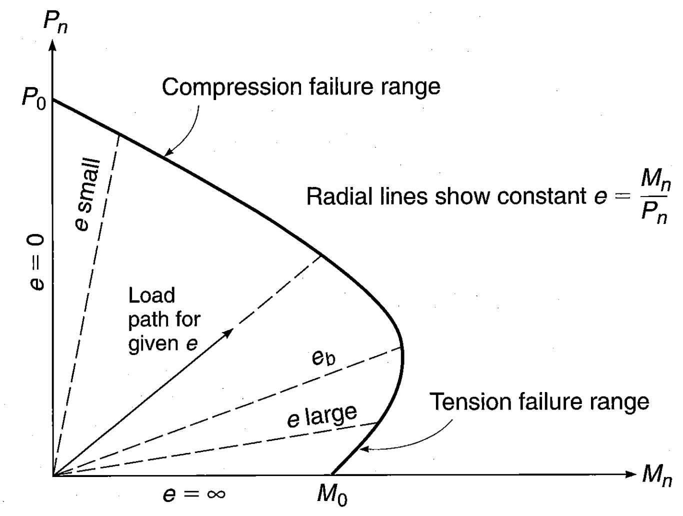

FIGURE 8.10
Interaction diagram for nominal column strength in combined bending and axial load.

such as shown in Fig. 8.10. A series of such calculations, each corresponding to a different eccentricity, will result in a curve having a shape typically as shown in Fig. 8.10. On such a diagram, any radial line represents a particular eccentricity $e = M/P$. For that eccentricity, gradually increasing the load will define a load path as shown, and when that load path reaches the limit curve, failure will result. Note that the vertical axis corresponds to $e = 0$, and P_0 is the capacity of the column if concentrically loaded, as given by Eq. (8.3*b*). The horizontal axis corresponds to an infinite value of e, i.e., pure bending at moment capacity M_0. Small eccentricities will produce failure governed by concrete compression, while large eccentricities give a failure triggered by yielding of the tension steel.

For a given column, selected for trial, the interaction diagram is most easily constructed by selecting successive choices of neutral axis distance c, from infinity (axial load with eccentricity 0) to a very small value found by trial to give $P_n = 0$ (pure bending). For each selected value of c, the steel strains and stresses and the concrete force are easily calculated as follows. For the tension steel,

$$\epsilon_s = \epsilon_u \frac{d - c}{c} \tag{8.9}$$

$$f_s = \epsilon_u E_s \frac{d - c}{c} \leq f_y \tag{8.10}$$

while for the compression steel,

$$\epsilon_s' = \epsilon_u \frac{c - d'}{c} \tag{8.11}$$

$$f_s' = \epsilon_u E_s \frac{c - d'}{c} \leq f_y \tag{8.12}$$

The concrete stress block has depth

$$a = \beta_1 c \leq h \tag{8.13}$$

and consequently the concrete compressive resultant is

$$C = 0.85 f_c' ab \tag{8.14}$$

The nominal axial force P_n and nominal moment M_n corresponding to the selected neutral axis location can then be calculated from Eqs. (8.7) and (8.8), respectively, and thus a single point on the strength interaction diagram is established. The calculations are then repeated for successive choices of neutral axis to establish the curve defining the strength limits, such as Fig. 8.10. The calculations, of a repetitive nature, are easily programmed for the computer or performed using a spreadsheet.

8.5 BALANCED FAILURE

As already noted, the interaction curve is divided into a compression failure range and a tension failure range.[†] It is useful to define what is termed a *balanced failure mode* and corresponding eccentricity e_b with the load P_b and moment M_b acting in combination to produce failure, with the concrete reaching its limit strain ϵ_u at precisely the same instant that the tensile steel on the far side of the column reaches yield strain. This point on the interaction diagram is the dividing point between compression failure (small eccentricities) and tension failure (large eccentricities).

The values of P_b and M_b are easily computed with reference to Fig. 8.9. For balanced failure,

$$c = c_b = d\frac{\epsilon_u}{\epsilon_u + \epsilon_y} \tag{8.15}$$

and

$$a = a_b = \beta_1 c_b \tag{8.16}$$

Equations (8.9) through (8.14) are then used to obtain the steel stresses and the compressive resultant, after which P_b and M_b are found from Eqs. (8.7) and (8.8).

Note that, in contrast to beam design, one cannot restrict column designs such that yielding failure rather than crushing failure would always be the result of overloading. The type of failure for a column depends on the value of eccentricity e, which in turn is defined by the load analysis of the building or other structure.

It is important to observe, in Fig. 8.10, that in the region of compression failure the larger the axial load P_n, the smaller the moment M_n that the section is able to sustain before failing. However, in the region of tension failure, the reverse is true; the larger the axial load, the larger the simultaneous moment capacity. This is easily understood. In the compression failure region, failure occurs through overstraining of the concrete. The larger the concrete compressive strain caused by the axial load alone, the smaller the margin of additional strain available for the added compression caused by bending. On the other hand, in the tension failure region, yielding of the steel initiates failure. If the member is loaded in simple bending to the point at which yielding begins in the tension steel, and if an axial compression load is then added, the steel compressive stresses caused by this load will superimpose on the previous tensile stresses. This reduces the total steel stress to a value below its yield strength. Consequently, an additional moment can now be sustained of such magnitude that the combination of the steel stress from the axial load and the increased moment again reaches the yield strength.

[†] The terms *compression failure range* and *tension failure range* are used for the purpose of general description and are distinct from *tension-controlled* and *compression-controlled* failures, as described in Chapter 3 and Section 8.9.

The typical shape of a column interaction diagram shown in Fig. 8.10 has important design implications. In the range of tension failure, a *reduction in axial load* may produce failure for a given moment. In carrying out a frame analysis, the designer must consider all combinations of loading that may occur, including that which would produce minimum axial load paired with a given moment (the specific load combinations are specified in ACI Code 8.10 and described in Section 12.3). Only that amount of compression that is certain to be present should be used in calculating the capacity of a column subject to a given moment.

EXAMPLE 8.1

Column strength interaction diagram. A 300 × 500 mm column is reinforced with four No. 29 (No. 9) bars of area 645 mm^2 each, one in each corner as shown in Fig. 8.11*a*. The concrete cylinder strength is $f_c' = 28$ MPa and the steel yield strength is 420 MPa. Determine (*a*) the load P_b, moment M_b, and corresponding eccentricity e_b for balanced failure; (*b*) the load and moment for a representative point in the tension failure region of the interaction curve; (*c*) the load and moment for a representative point in the compression failure region; (*d*) the axial load strength for zero eccentricity. Then (*e*) sketch the strength interaction diagram for this column. Finally, (*f*) design the transverse reinforcement, based on ACI Code provisions.

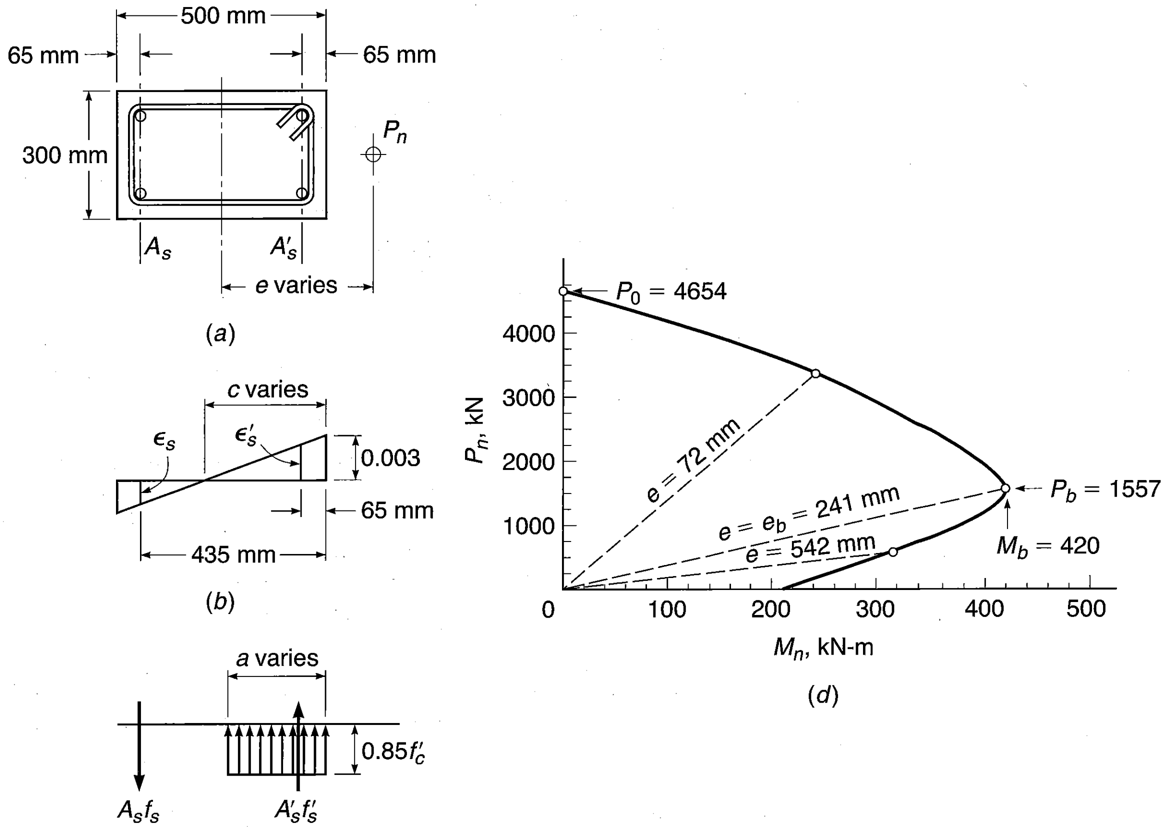
500 mm
65 mm
65 mm
300 mm
P_n
A_s
A_s'
e varies
(a)
c varies
ϵ_s
ϵ_s'
0.003
65 mm
435 mm
(b)
a varies
0.85f_c'
A_sf_s
$A_s'f_s'$
(c)
P_0 = 4654
P_n, kN
4000
3000
2000
1000
0
100
200
300
400
500
M_n, kN-m
e = 72 mm
e = e_b = 241 mm
e = 542 mm
P_b = 1557
M_b = 420
(d)

FIGURE 8.11

Column interaction diagram for Example 8.1: (*a*) cross section; (*b*) strain distribution; (*c*) stresses and forces; (*d*) strength interaction diagram.

SOLUTION.

(*a*) The neutral axis for the balanced failure condition is easily found from Eq. (8.15) with $\epsilon_u = 0.003$ and $\epsilon_y = 420/200{,}000 = 0.0021$

$$c_b = 435 \times \frac{0.003}{0.0051} = 256 \text{ mm}$$

giving a stress-block depth $a = 0.85 \times 256 = 218$ mm. For the balanced failure condition, by definition, $f_s = f_y$. The compressive steel stress is found from Eq. (8.12):

$$f'_s = 0.003 \times 200{,}000 \frac{256 - 65}{256} = 448 \text{ MPa} \qquad \text{but} \qquad \leq 420 \text{ MPa}$$

confirming that the compression steel, too, is at the yield. The concrete compressive resultant is

$$C = 0.85 \times 28 \times 218 \times 300 \times 10^{-3} = 1557 \text{ kN}$$

The balanced load P_b is then found from Eq. (8.7) to be

$$P_b = 1557 + 1290 \times 420 \times 10^{-3} - 1290 \times 420 \times 10^{-3} = 1557 \text{ kN}$$

and the balanced moment from Eq. (8.8) is

$$M_b = 1557(250 - 109) + 1290 \times 420(250 - 65) + 1290 \times 420(435 - 250)$$
$$= 420 \times 10^3 \text{ kN-mm} = 420 \text{ kN-m}$$

The corresponding eccentricity of load is $e_b = 241$ mm.

(*b*) Any choice of c *smaller than* $c_b = 256$ mm will give a point in the tension failure region of the interaction curve, with eccentricity larger than e_b. For example, choose $c = 125$ mm. By definition, $f_s = f_y$. The compressive steel stress is found to be

$$f'_s = 0.003 \times 200{,}000 \frac{125 - 65}{125} = 288 \text{ MPa}$$

With the stress-block depth $a = 0.85 \times 125 = 106$, the compressive resultant is $C = 0.85 \times 28 \times 106 \times 300 \times 10^{-3} = 757$ kN. Then from Eq. (8.7), the thrust is

$$P_n = 757 + 1290 \times 288 \times 10^{-3} - 1290 \times 420 \times 10^{-3}$$
$$= 587 \text{ kN}$$

and the moment capacity from Eq. (8.8) is

$$M_n = 757(250 - 53) + 1290 \times 288(250 - 65) + 1290 \times 420(435 - 250)$$
$$= 318 \times 10^3 \text{ kN-mm} = 318 \text{ kN-m}$$

giving eccentricity $e = 318{,}000/587 = 542$ mm, well above the balanced value.

(*c*) Now selecting a c value *larger than* c_b to demonstrate a compression failure point on the interaction curve, choose $c = 460$ mm, for which $a = 0.85 \times 460 = 391$ mm. The compressive concrete resultant is $C = 0.85 \times 28 \times 391 \times 300 \times 10^{-3} = 2792$ kN. From Eq. (8.10) the stress in the steel at the left side of the column is

$$f_s = 0.003 \times 200{,}000 \frac{435 - 460}{460} = -33 \text{ MPa}$$

Note that the negative value of f_s indicates correctly that A_s is in compression if c is greater than d, as in the present case. The compressive steel stress is found from Eq. (8.12) to be

$$f'_s = 0.003 \times 200{,}000 \frac{460 - 65}{460} = 515 \text{ MPa} \quad \text{but} \quad \leq 420 \text{ MPa}$$

Then the column capacity is

$$P_n = 2792 + 1290 \times 420 \times 10^{-3} + 1290 \times 33 \times 10^{-3} = 3376 \text{ kN}$$
$$M_n = 2792(250 - 196) + 1290 \times 420(250 - 65) - 1290 \times 33(435 - 250)$$
$$= 243 \times 10^3 \text{ kN-mm} = 243 \text{ kN-m}$$

giving eccentricity $e = 243{,}000/3376 = 72$ mm.

(*d*) The axial strength of the column if concentrically loaded corresponds to $c = \infty$ and $e = 0$. For this case,

$$P_n = 0.85 \times 28 \times 300 \times 500 \times 10^{-3} + 2580 \times 420 \times 10^{-3} = 4654 \text{ kN}$$

Note that, for this as well as the preceding calculations, subtraction of the concrete displaced by the steel has been neglected. For comparison, if the deduction were made in the last calculation,

$$P_n = 0.85 \times 28(300 \times 500 - 2580) \times 10^{-3} + (2580 \times 420) \times 10^{-3} = 4592 \text{ kN}$$

The error in neglecting this deduction is only 1 percent in this case; the difference generally can be neglected, except perhaps for columns with reinforcement ratios close to the maximum of 8 percent. In the case of design aids, however, such as those presented in Refs. 8.2 and 8.7 and discussed in Section 8.10, the deduction is usually included for all reinforcement ratios.

(*e*) From the calculations just completed, plus similar repetitive calculations that will not be given here, the strength interaction curve of Fig. 8.11*d* is constructed. Note the characteristic shape, described earlier, the location of the balanced failure point as well as the "small eccentricity" and "large eccentricity" points just found, and the axial load capacity. In the process of developing a strength interaction curve, it is possible to select the values of steel strain ϵ_s, as done in step *a*, for use in steps *b* and *c*. Selecting ϵ_s uniquely establishes the neutral axis depth *c*, as shown by Eqs. (8.9) and (8.15), and is useful in determining M_n and P_n for values of steel strain that correspond to changes in the strength reduction factor ϕ, as will be discussed in Section 8.9.

(*f*) The design of the column ties will be carried out following the ACI Code restrictions. For the minimum permitted tie, a No. 10 (No. 3) bar having a diameter of 9.5 mm, used with No. 29 (No. 9) longitudinal bars having a diameter of 28.7 mm in a column the least dimension of which is 300 mm, the tie spacing is not to exceed

$$48 \times 9.5 = 456 \text{ mm}$$
$$16 \times 28.7 = 459 \text{ mm}$$
$$b = 300 \text{ mm}$$

The last restriction controls in this case, and No. 10 (No. 3) ties will be used at 300 mm spacing, detailed as shown in Fig. 8.11*a*. Note that the permitted spacing as controlled by the first and second criteria, 456 mm, must be reduced because of the 300 mm column dimension.

8.6 DISTRIBUTED REINFORCEMENT

When large bending moments are present, it is most economical to concentrate all or most of the steel along the outer faces parallel to the axis of bending. Such arrangements are shown in Fig. 8.3*e* to *h*. On the other hand, with small eccentricities so that axial compression is predominant, and when a small cross section is desired, it is often advantageous to place the steel more uniformly around the perimeter, as in Fig. 8.3*a* to *d*. In this case, special attention must be paid to the intermediate bars, i.e., those that are not placed along the two faces that are most highly stressed. This is so because when the ultimate load is reached, the stresses in these intermediate bars are usually below the yield point, even though the bars along one or both extreme faces may be yielding. This situation can be analyzed by a simple and obvious extension of the previous analysis based on compatibility of strains. A strength interaction diagram may be constructed just as before. A sequence of choices of neutral axis location results in a set of paired values of P_n and M_n, each corresponding to a particular eccentricity of load.

EXAMPLE 8.2

Analysis of eccentrically loaded column with distributed reinforcement. The column in Fig. 8.12*a* is reinforced with ten No. 36 (No. 11) bars distributed around the perimeter as shown. Load P_n will be applied with eccentricity e about the strong axis. Material strengths are $f_c' = 42$ MPa and $f_y = 550$ MPa. Find the load and moment corresponding to a failure point with neutral axis $c = 460$ mm from the right face.

Solution. When the concrete reaches its limit strain of 0.003, the strain distribution is that shown in Fig. 8.12*b*, the strains at the locations of the four bar groups are found from similar triangles, after which the stresses are found by multiplying strains by $E_s = 200{,}000$ MPa applying the limit value f_y:

$\epsilon_{s1} = 0.00258$ $\quad f_{s1} = 516$ MPa compression
$\epsilon_{s2} = 0.00140$ $\quad f_{s2} = 280$ MPa compression
$\epsilon_{s3} = 0.00023$ $\quad f_{s3} = 46$ MPa compression
$\epsilon_{s4} = 0.00095$ $\quad f_{s4} = 190$ MPa tension

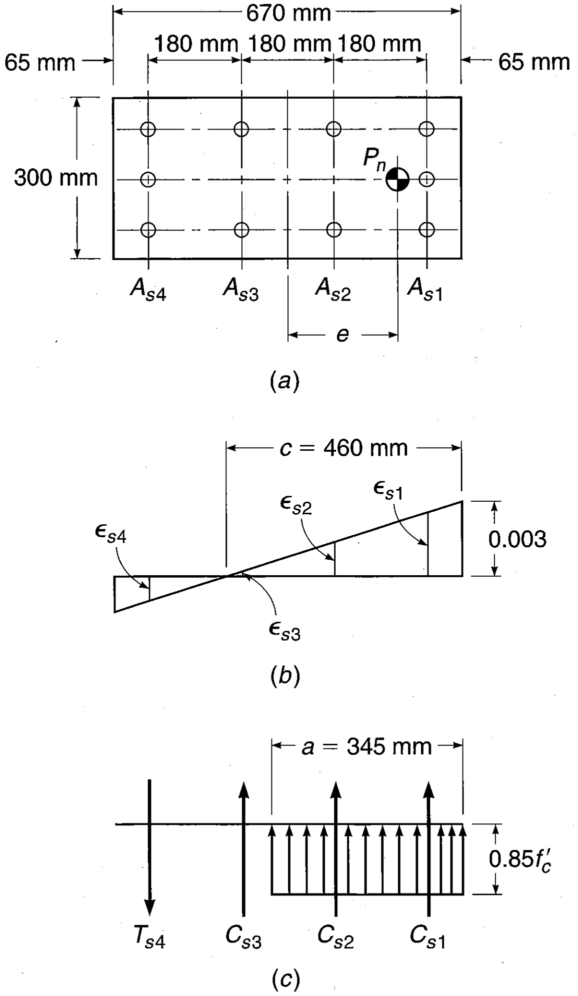
670 mm
180 mm
180 mm
180 mm
65 mm
65 mm
300 mm
P_n
A_{s4}
A_{s3}
A_{s2}
A_{s1}
e
(a)
$c = 460$ mm
ϵ_{s1}
ϵ_{s2}
ϵ_{s4}
0.003
ϵ_{s3}
(b)
$a = 345$ mm
$0.85f_c'$
T_{s4}
C_{s3}
C_{s2}
C_{s1}
(c)

FIGURE 8.12
Column in Example 8.2: (*a*) cross section; (*b*) strain distribution; (*c*) stresses and forces.

For $f'_c = 42$ MPa, $\beta_1 = 0.75$ and the depth of the equivalent rectangular stress block is $a = 0.75 \times 460 = 345$ mm. The concrete compressive resultant is $C = 0.85 \times 42 \times 345 \times 300 \times 10^{-3} = 3608$ kN, and the respective steel forces in Fig. 8.12*c* are

$$
\begin{aligned}
C_{s1} &= 3018 \times 516 \times 10^{-3} = 1557 \text{ kN} \\
C_{s2} &= 2012 \times 280 \times 10^{-3} = 563 \text{ kN} \\
C_{s3} &= 2012 \times 46 \times 10^{-3} = 92 \text{ kN} \\
T_{s4} &= 3018 \times 190 \times 10^{-3} = 573 \text{ kN}
\end{aligned}
$$

The axial load and moment that would produce failure for a neutral axis 460 mm from the right face are found by the obvious extensions of Eqs. (8.7) and (8.8):

$$
\begin{aligned}
P_n &= 3608 + 1557 + 563 + 90 - 573 = 5245 \text{ kN} \\
M_n &= 3608(335 - 172.5) + 1557(335 - 65) + 565(335 - 245) - 90(335 - 245) \\
&\quad + 573(335 - 65) \\
&= 1{,}204{,}000 \text{ kN-mm} \\
&= 1204 \text{ kN-m}
\end{aligned}
$$

The corresponding eccentricity is $e = 1{,}204{,}000/5245 = 230$ mm. Other points on the interaction diagram can be computed in a similar way.

Two general conclusions can be made from this example:

1. Even with the relatively small eccentricity of about one-third of the depth of the section, only the bars of group 1 just barely reached their yield strain, and consequently their yield stress. All other bar groups of the relatively high-strength steel that was used are stressed far below their yield strength, which would also have been true for group 1 for a slightly larger eccentricity. It follows that the use of the more expensive high-strength steel is economical in symmetrically reinforced columns only for very small eccentricities, e.g., in the lower stories of tall buildings.
2. The contribution of the intermediate bars of groups 2 and 3 to both P_n and M_n is quite small because of their low stresses. Again, intermediate bars, except as they are needed to hold ties in place, are economical only for columns with very small eccentricities.

8.7 UNSYMMETRICAL REINFORCEMENT

Most reinforced concrete columns are symmetrically reinforced about the axis of bending. However, for some cases, such as the columns of rigid portal frames in which the moments are uniaxial and the eccentricity is large, it is more economical to use an unsymmetrical pattern of bars, with most of the bars on the tension side such as shown in Fig. 8.13. Such columns can be analyzed by the same strain compatibility approach as described above. However, for an unsymmetrically reinforced column to be loaded concentrically, the load must pass through a point known as the *plastic centroid.* The plastic centroid is defined as the point of application of the resultant force for the column cross section (including concrete and steel forces) if the column is compressed uniformly to the failure strain $\epsilon_u = 0.003$ over its entire cross section. Eccentricity of the applied load must be measured with respect to the plastic centroid, because only then will $e = 0$ correspond to an axial load with no moment. The location of the plastic

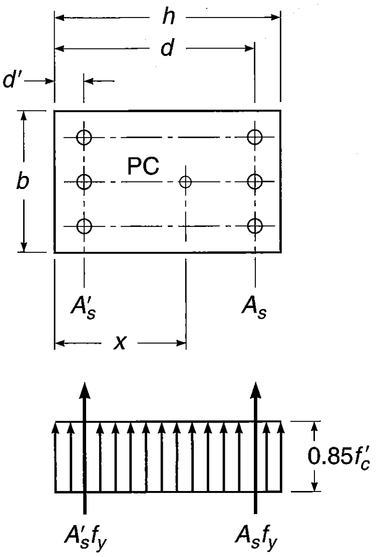

FIGURE 8.13
Plastic centroid of an unsymmetrically reinforced column.

centroid for the column of Fig. 8.13 is the resultant of the three internal forces to be accounted for. Its distance from the left face is

$$x = \frac{0.85f'_c bh^2/2 + A_s f_y d + A'_s f_y d'}{0.85f'_c bh + A_s f_y + A'_s f_y} \tag{8.17}$$

Clearly, in a symmetrically reinforced cross section, the plastic centroid and the geometric center coincide.

8.8 CIRCULAR COLUMNS

It was mentioned in Section 8.2 that when load eccentricities are small, spirally reinforced columns show greater toughness, i.e., greater ductility, than tied columns, although this difference fades out as the eccentricity is increased. For this reason, as discussed in Section 8.2, the ACI Code provides a more favorable reduction factor $\phi = 0.75$ for spiral columns, compared with $\phi = 0.65$ for tied columns. Also, the maximum stipulated design load for entirely or nearly axially loaded members is larger for spirally reinforced members than for comparable tied members (see Section 8.9). It follows that spirally reinforced columns permit a somewhat more economical utilization of the materials, particularly for small calculated eccentricities. A further advantage lies in the fact that the circular shape is frequently desired by the architect.

Figure 8.14 shows the cross section of a spirally reinforced column. Six or more longitudinal bars of equal size are provided for longitudinal reinforcement, depending on column diameter. The strain distribution at the instant at which the ultimate load is reached is shown in Fig. 8.14*b*. Bar groups 2 and 3 are seen to be strained to much smaller values than groups 1 and 4. The stresses in the four bar groups are easily found. For any of the bars with strains in excess of yield strain $\epsilon_y = f_y/E_s$, the stress at failure is evidently the yield stress of the bar. For bars with smaller strains, the stress is found from $f_s = \epsilon_s E_s$.

FIGURE 8.14
Circular column with compression plus bending.

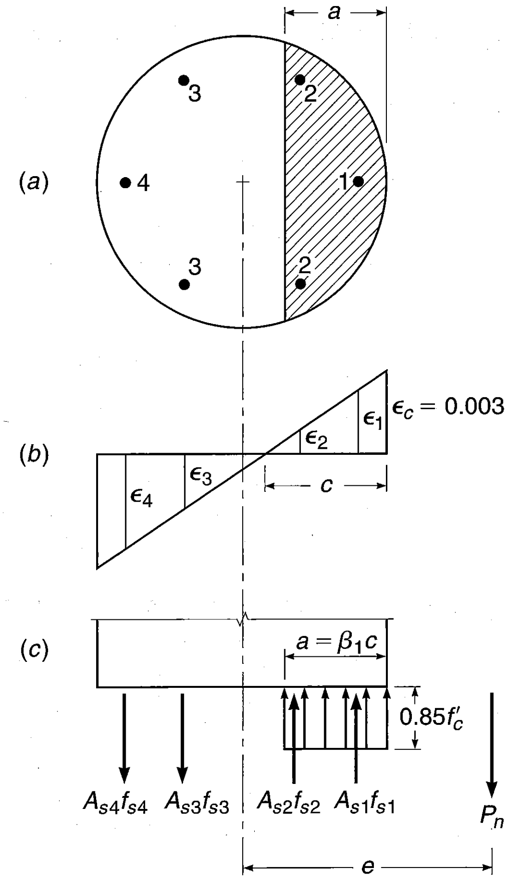

One then has the internal forces shown in Fig. 8.14*c*. They must be in force and moment equilibrium with the nominal strength P_n. Note that the situation is analogous to that discussed in Sections 8.4 to 8.6 for rectangular columns. Calculations can be carried out exactly as in Example 8.1, except that for circular columns the concrete compression zone subject to the equivalent rectangular stress distribution has the shape of a segment of a circle, shown shaded in Fig. 8.14*a*.

Although the shape of the compression zone and the strain variation in the different groups of bars make longhand calculations awkward, no new principles are involved and computer solutions are easily developed.

Design or analysis of spirally reinforced columns is usually carried out by means of design aids, such as Graphs A.13 to A.16 of Appendix A. Additional tables and graphs are available, e.g., in Ref. 8.7. In developing such design aids, the entire steel area is often assumed to be arranged in a uniform, concentric ring, rather than being concentrated in the actual bar locations; this simplifies calculations without noticeably affecting results if the column contains at least eight longitudinal bars. When fewer bars are used, the interaction curve should be calculated based on the weakest orientation in bending.

Note that to qualify for the more favorable safety provisions for spiral columns, the reinforcement ratio of the spiral must be at least equal to that given by Eq. (8.5) for reasons discussed in Section 8.2.

8.9 ACI CODE PROVISIONS FOR COLUMN DESIGN

For columns, as for all members designed according to the ACI Code, adequate safety margins are established by applying load factors to the service loads and strength reduction factors to the nominal strengths. Thus, for columns, $\phi P_n \geq P_u$ and $\phi M_n \geq M_u$ are the basic safety criteria. For most members subject to axial compression or compression plus flexure (compression-controlled members, as described in Chapter 3), the ACI Code provides basic reduction factors:

$$\phi = 0.65 \text{ for tied columns}$$

$$\phi = 0.75 \text{ for spirally reinforced columns}$$

The spread between these two values reflects the added safety furnished by the greater toughness of spirally reinforced columns.

There are various reasons why the ϕ values for columns are lower than those for flexure or shear (0.90 and 0.75, respectively). One is that the strength of underreinforced flexural members is not much affected by variations in concrete strength, since it depends primarily on the yield strength of the steel, while the strength of axially loaded members depends strongly on the concrete compressive strength. Because the cylinder strength of concrete under site conditions is less closely controlled than the yield strength of mill-produced steel, a larger occasional strength deficiency must be allowed for. This is particularly true for columns, in which concrete, being placed from the top down in a long, narrow form, is more subject to segregation than in horizontally cast beams. Moreover, electrical and other conduits are frequently located in building columns; this reduces their effective cross sections, often to an extent unknown to the designer, even though this is poor practice and restricted by the ACI Code. Finally, the consequences of a column failure, say in a lower story, would be more catastrophic than those of a single beam failure in the same building.

For high eccentricities, as the eccentricity increases from e_b to infinity (pure bending), the ACI Code recognizes that the member behaves progressively more like a flexural member and less like a column. As described in Chapter 3, this is acknowledged in ACI Code 9.3.2 by providing a linear transition in ϕ from values of 0.65 and 0.75 to 0.90 as the net tensile strain in the extreme tensile steel ϵ_t increases from f_y/E_s (which may be taken as 0.002 for Grade 420 reinforcement) to 0.005.

At the other extreme, for columns with very small or zero calculated eccentricities, the ACI Code recognizes that accidental construction misalignments and other unforeseen factors may produce actual eccentricities in excess of these small design values. Also, the concrete strength under high, sustained axial loads may be somewhat smaller than the short-term cylinder strength. Therefore, regardless of the magnitude of the calculated eccentricity, ACI Code 10.3.6 limits the maximum design strength to $0.80\phi P_0$ for tied columns (with $\phi = 0.65$) and to $0.85\phi P_0$ for spirally reinforced columns (with $\phi = 0.75$), where P_0 is the nominal strength of the axially loaded column with zero eccentricity [see Eq. (8.4)].

The effects of the safety provisions of the ACI Code are shown in Fig. 8.15. The solid curve labeled "nominal strength" is the same as Fig. 8.10 and represents the actual carrying capacity, as nearly as can be predicted. The smooth curve shown partially dashed, then solid, then dashed, represents the basic design strength obtained by reducing the nominal strengths P_n and M_n, for each eccentricity, by $\phi = 0.65$ for tied columns and $\phi = 0.75$ for spiral columns. The horizontal cutoff at $\alpha\phi P_0$ represents the maximum design load stipulated in the ACI Code for small eccentricities,

FIGURE 8.15
ACI safety provisions superimposed on column strength interaction diagram.

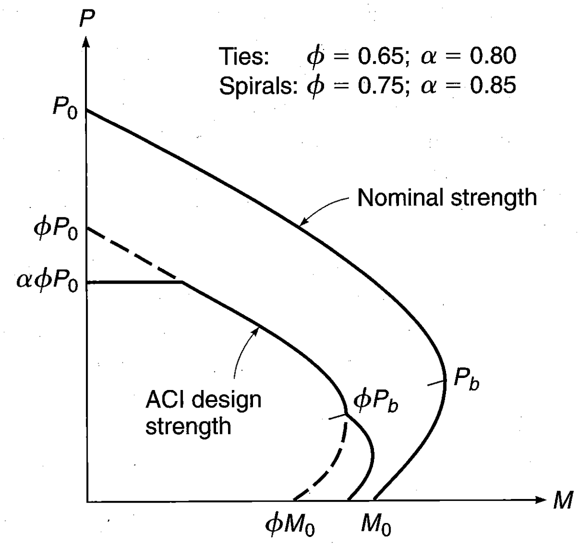

i.e., large axial loads, as just discussed. At the other end, for large eccentricities, i.e., small axial loads, the ACI Code permits a linear transition of ϕ from 0.65 or 0.75, applicable for $\epsilon_t \leq f_y/E_s$ (or 0.002 for Grade 420 reinforcement) to 0.90 at $\epsilon_t = 0.005$. By definition, $\epsilon_t = f_y/E_s$ at the balanced condition. The effect of the transition in ϕ is shown at the lower right end of the design strength curve.[†]

8.10 DESIGN AIDS

The design of eccentrically loaded columns using the strain compatibility method of analysis described requires that a trial column be selected. The trial column is then investigated to determine if it is adequate to carry any combination of P_u and M_u that may act on it should the structure be overloaded, i.e., to see if P_u and M_u from the analysis of the structure, when plotted on a strength interaction diagram such as Fig. 8.15, fall within the region bounded by the curve labeled "ACI design strength." Furthermore, economical design requires that the controlling combination of P_u and M_u be close to the limit curve. If these conditions are not met, a new column must be selected for trial.

While a simple computer program or spreadsheet can be developed, based on the strain compatibility analysis, to calculate points on the design strength curve, and even to plot the curve, for any trial column, in practice design aids are used such as are available in handbooks and special volumes published by the American Concrete Institute (Ref. 8.7) and the Concrete Reinforcing Steel Institute (Ref. 8.2). They cover the most frequent practical cases, such as symmetrically reinforced rectangular and square columns and circular spirally reinforced columns. There are also a number of commercially available computer programs (e.g., pcaCOLUMN, Portland Cement Association, Skokie, Illinois).

[†] While the general intent of the ACI Code safety provisions relating to eccentric columns is clear and fundamentally sound, the end result is a set of strangely shaped column design curves following no discernible physical law, as is demonstrated in Fig. 8.15. Improved column safety provisions, resulting in a smooth design curve appropriately related to the strength curve, would be simpler to use and more rational as well.

Graphs A.5 through A.16 of Appendix A are representative of column design charts (such as found in Ref. 8.7), in this case for concrete with $f'_c = 28$ MPa and steel with yield strength $f_y = 420$ MPa, for varying cover distances.[†] Reference 8.7 includes charts for a broad range of material strengths. Graphs A.5 through A.8 are drawn for rectangular columns with reinforcement distributed around the column perimeter; Graphs A.9 through A.12 are for rectangular columns with reinforcement along two opposite faces. Circular columns with bars in a circular pattern are shown in Graphs A.13 through A.16.

The graphs are seen to consist of nominal strength interaction curves of the type shown in Fig. 8.15. However, instead of plotting P_n versus M_n, corresponding parameters have been used to make the charts more generally applicable, i.e., load is plotted as $K_n = P_n/(f'_c A_g)$, while moment is expressed as $R_n = P_n e/(f'_c A_g h)$. Families of curves are drawn for various values of $\rho_g = A_{st}/A_g$ between 0.01 and 0.08. The graphs also include radial lines representing different eccentricity ratios e/h, as well as lines representing different ratios of stress f_s/f_y or values of strain $\epsilon_t = 0.002$ and 0.005 in the extreme tension steel.

Charts such as these permit the direct design of eccentrically loaded columns throughout the common range of strength and geometric variables. They may be used in one of two ways as follows. For a given factored load P_u and equivalent eccentricity $e = M_u/P_u$:

1. **(a)** Select trial cross-sectional dimensions b and h (refer to Fig. 8.9).
   (b) Calculate the ratio γ based on required cover distances to the bar centroids, and select the corresponding column design chart.
   (c) Calculate $K_n = P_u/(\phi f'_c A_g)$ and $R_n = P_u e/(\phi f'_c A_g h)$, where $A_g = bh$.
   (d) From the graph, for the values found in **(c)**, read the required reinforcement ratio ρ_g.
   (e) Calculate the total steel area $A_{st} = \rho_g bh$.
2. **(a)** Select the reinforcement ratio ρ_g.
   (b) Choose a trial value of h and calculate e/h and γ.
   (c) From the corresponding graph, read $K_n = P_u/(\phi f'_c A_g)$ and calculate the required A_g.
   (d) Calculate $b = A_g/h$.
   (e) Revise the trial value of h if necessary to obtain a well-proportioned section.
   (f) Calculate the total steel area $A_{st} = \rho_g bh$.

Use of the column design charts will be illustrated in Examples 8.3 and 8.4.

Other design aids pertaining to ties and spirals, as well as recommendations for standard practice, will be found in Refs. 8.2 and 8.7.

988

EXAMPLE 8.3 **Selection of reinforcement for column of given size.** In a three-story structure, an exterior column is to be designed for a service dead load of ~~998~~ kN, maximum live load of 1320 kN, dead load moment of 180 kN-m, and live load moment of 260 kN-m. The minimum live load compatible with the full live load moment is 738 kN, obtained when no live load is placed on the roof but a full live load is placed on the second floor. Architectural considerations require that a rectangular column be used, with dimensions $b = 500$ mm and $h = 625$ mm.

[†] Graphs A.5 through A.16 were developed for the specific bar configurations shown on the graphs. The curves exhibit changes in curvature, especially apparent near the balanced load, that result when bars within the cross section yield. The values provided in the graphs, however, are largely insensitive to the exact number of bars in the cross section and may be used for columns with similar bar configurations, but with smaller or larger numbers of bars.

(*a*) Find the required column reinforcement for the condition that the full live load acts.
(*b*) Check to ensure that the column is adequate for the condition of no live load on the roof.
Material strengths are $f'_c = 28$ MPa and $f_y = 420$ MPa.

SOLUTION.

(*a*) The column will be designed initially for full load, then checked for adequacy when live load is partially removed. According to the ACI safety provisions, the column must be designed for a factored load $P_u = 1.2 \times 988 + 1.6 \times 1320 = 3298$ kN and a factored moment $M_u = 1.2 \times 180 + 1.6 \times 260 = 632$ kN-m. A column 500 × 625 mm is specified, and reinforcement distributed around the column perimeter will be used. Bar cover is estimated to be 62.5 mm from the column face to the steel centerline for each bar. The column parameters (assuming bending about the strong axis) are

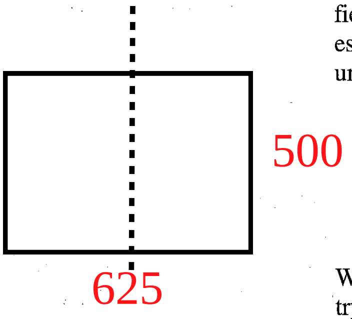

$$K_n = \frac{P_u}{\phi f'_c A_g} = \frac{3298 \times 10^3}{0.65 \times 28 \times 312{,}500} = 0.580$$

$$R_n = \frac{M_u}{\phi f'_c A_g h} = \frac{632 \times 10^6}{0.65 \times 28 \times 312{,}500 \times 625} = 0.177$$

With 62.5 mm cover, the parameter $\gamma = (625 - 125)/625 = 0.80$. For this column geometry and material strengths, Graph A.7 of Appendix A applies. From that figure, with the calculated values of K_n and R_n, $\rho_g = 0.024$. Thus, the required reinforcement is $A_{st} = 0.024 \times 312{,}500 = 7500$ mm^2. Twelve No. 29 (No. 9) bars will be used, one at each corner and two evenly spaced along each face of the column, providing $A_{st} = 7740$ mm^2.

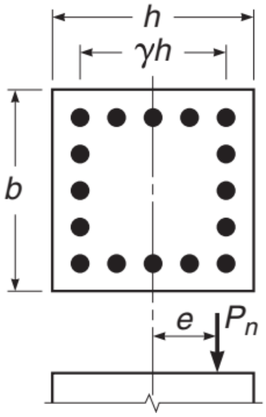

(*b*) With the roof live load absent, the column will carry a factored load $P_u = 1.2 \times 988 + 1.6 \times 738 = 2366$ kN and factored moment $M_u = 632$ kN-m, as before. Thus, the column parameters for this condition are

$$K_n = \frac{P_u}{\phi f'_c A_g} = \frac{2366 \times 10^3}{0.65 \times 28 \times 312{,}500} = 0.416$$

$$R_n = \frac{M_u}{\phi f'_c A_g h} = \frac{632 \times 10^6}{0.65 \times 28 \times 312{,}500 \times 625} = 0.177$$

and $\gamma = 0.80$ as before. From Graph A.7 it is found that a reinforcement ratio of $\rho_g = 0.018$ is sufficient for this condition, less than that required in part (*a*), so no modification is required.

Selecting No. 10 (No. 3) ties for trial, the maximum tie spacing must not exceed 48 × 9.5 = 456 mm, 16 × 28.7 = 459 mm, or 500 mm. Spacing is controlled by the diameter of the ties, and No. 10 (No. 3) ties will be used at 450 mm spacing, in the pattern shown in Fig. 8.3*d*.

EXAMPLE 8.4 **Selection of column size for a given reinforcement ratio.** A column is to be designed to carry a factored load $P_u = 2140$ kN and factored moment $M_u = 665$ kN-m. Material strengths $f_y = 420$ MPa and $f'_c = 28$ MPa are specified. Cost studies for the particular location indicate that a reinforcement ratio ρ_g of about 0.03 is optimum. Find the required dimensions *b* and *h* of the column. Bending will be about the strong axis, and an arrangement of steel with bars concentrated in two layers, adjacent to the outer faces of the column and parallel to the axis of bending, will be used.

SOLUTION. It is convenient to select a trial column dimension *h*, perpendicular to the axis of bending; a value of $h = 625$ mm will be selected, and assuming a concrete cover of 62.5 mm to the bar centers, the parameter $\gamma = 0.80$. Graph A.11 of Appendix A applies. For the stated loads the eccentricity is $e = 665/2140 = 0.311$ m = 311 mm, and $e/h = 311/625 = 0.50$. From

Graph A.11 with $e/h = 0.50$ and $\rho_g = 0.03$, $K_n = P_w/\phi f_c' A_g = 0.505$. For the trial dimension $h = 625$ mm, the required column width is

$$b = \frac{P_u}{\phi f_c' K_n h} = \frac{2140 \times 10^3}{0.65 \times 28 \times 0.505 \times 625} = 373 \text{ mm}$$

A column 375 × 625 mm will be used, for which the required steel area is $A_{st} = 0.03 \times 375 \times 625 = 7031$ mm. Eight No. 36 (No. 11) bars will be used, providing $A_{st} = 8048 \text{ mm}^2$, arranged in two layers of four bars each, similar to the sketch shown in Graph A.11.

8.11 BIAXIAL BENDING

The methods discussed in the preceding sections permit rectangular or square columns to be designed if bending is present about only one of the principal axes. There are situations, by no means exceptional, in which axial compression is accompanied by simultaneous bending about both principal axes of the section. Such is the case, for instance, in corner columns of buildings where beams and girders frame into the columns in the directions of both walls and transfer their end moments into the columns in two perpendicular planes. Similar loading may occur at interior columns, particularly if the column layout is irregular.

The situation with respect to strength of biaxially loaded columns is shown in Fig. 8.16. Let X and Y denote the directions of the principal axes of the cross section. In Fig. 8.16*a*, the section is shown subject to bending about the Y axis only, with load

FIGURE 8.16
Interaction diagram for compression plus biaxial bending: (*a*) uniaxial bending about Y axis; (*b*) uniaxial bending about X axis; (*c*) biaxial bending about diagonal axis; (*d*) interaction surface.

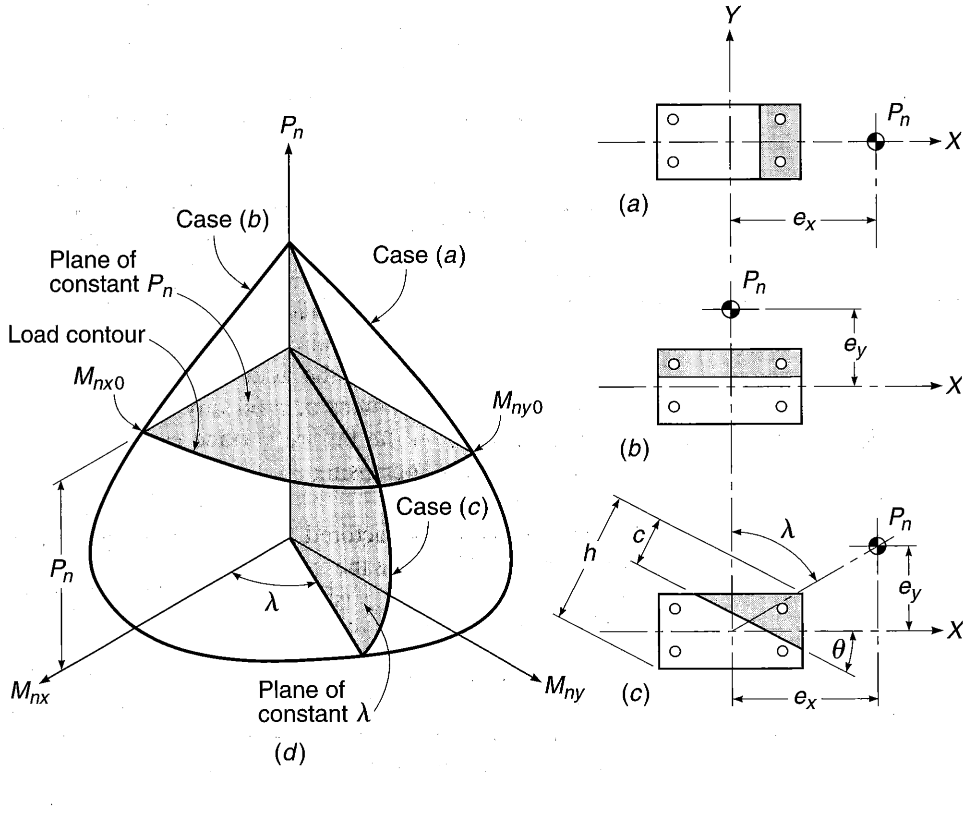

eccentricity e_x measured in the X direction. The corresponding strength interaction curve is shown as case (*a*) in the three-dimensional sketch in Fig. 8.16*d* and is drawn in the plane defined by the axes P_n and M_{ny}. Such a curve can be established by the usual methods for uniaxial bending. Similarly, Fig. 8.16*b* shows bending about the X axis only, with eccentricity e_y measured in the Y direction. The corresponding interaction curve is shown as case (*b*) in the plane of P_n and M_{nx} in Fig. 8.16*d*. For case (*c*), which combines X and Y axis bending, the orientation of the resultant eccentricity is defined by the angle λ:

$$\lambda = \arctan \frac{e_x}{e_y} = \arctan \frac{M_{ny}}{M_{nx}}$$

Bending for this case is about an axis defined by the angle θ with respect to the X axis. The angle λ in Fig. 8.16*c* establishes a plane in Fig. 8.16*d*, passing through the vertical P_n axis and making an angle λ with the M_{nx} axis, as shown. In that plane, column strength is defined by the interaction curve labeled case (*c*). For other values of λ, similar curves are obtained to define a *failure surface* for axial load plus biaxial bending, such as shown in Fig. 8.16*d*. The surface is exactly analogous to the *interaction curve* for axial load plus uniaxial bending. Any combination of P_u, M_{ux}, and M_{uy} falling inside the surface can be applied safely, but any point falling outside the surface would represent failure. Note that the failure surface can be described either by a set of curves defined by radial planes passing through the P_n axis, such as shown by case (*c*), or by a set of curves defined by horizontal plane intersections, each for a constant P_n, defining load contours.

Constructing such an interaction surface for a given column would appear to be an obvious extension of uniaxial bending analysis. In Fig. 8.16*c*, for a selected value of θ, successive choices of neutral axis distance c could be taken. For each, using strain compatibility and stress-strain relations to establish bar forces and the concrete compressive resultant, then using the equilibrium equations to find P_n, M_{nx}, and M_{ny}, one can determine a single point on the interaction surface. Repetitive calculations, easily done by computer, then establish sufficient points to define the surface. The triangular or trapezoidal compression zone, such as shown in Fig. 8.16*c*, is a complication, and in general the strain in each reinforcing bar will be different, but these features can be incorporated.

The main difficulty, however, is that the neutral axis will not, in general, be perpendicular to the resultant eccentricity, drawn from the column center to the load P_n. For each successive choice of neutral axis, there are unique values of P_n, M_{nx}, and M_{ny}, and only for special cases will the ratio of M_{ny}/M_{nx} be such that the eccentricity is perpendicular to the neutral axis chosen for the calculation. The result is that, for successive choices of c for any given θ, the value of λ in Fig. 8.16*c* and *d* will vary. Points on the failure surface established in this way will wander up the failure surface for increasing P_n, not representing a plane intersection, as shown for case (*c*) in Fig. 8.16*d*.

In practice, the factored load P_u and the factored moments M_{ux} and M_{uy} to be resisted are known from the frame analysis of the structure. Therefore, the actual value of $\lambda = \arctan(M_{uy}/M_{ux})$ is established, and one needs only the curve of case (*c*), Fig. 8.16*d*, to test the adequacy of the trial column. An iterative computer method to establish the interaction line for the particular value of λ that applies will be described in Section 8.14.

Alternatively, simple approximate methods are widely used. These will be described in Sections 8.12 and 8.13.

8.12 LOAD CONTOUR METHOD

The load contour method is based on representing the failure surface of Fig. 8.16*d* by a family of curves corresponding to constant values of P_n (Ref. 8.8). The general form of these curves can be approximated by a nondimensional interaction equation

$$\left(\frac{M_{nx}}{M_{nx0}}\right)^{\alpha 1} + \left(\frac{M_{ny}}{M_{ny0}}\right)^{\alpha 2} = 1.0 \tag{8.18}$$

where

$$M_{nx} = P_n e_y$$

$$M_{nx0} = M_{nx} \qquad \text{when } M_{ny} = 0$$

$$M_{ny} = P_n e_x$$

$$M_{ny0} = M_{ny} \qquad \text{when } M_{nx} = 0$$

and α_1 and α_2 are exponents depending on column dimensions, amount and distribution of steel reinforcement, stress-strain characteristics of steel and concrete, amount of concrete cover, and size of lateral ties or spiral. When $\alpha_1 = \alpha_2 = \alpha$, the shapes of such interaction contours are as shown in Fig. 8.17 for specific α values.

Calculations reported by Bresler in Ref. 8.9 indicate that α falls in the range from 1.15 to 1.55 for square and rectangular columns. Values near the lower end of that range are the more conservative. Methods and design aids permitting a more defined estimation of α are found in Ref. 8.7.

In practice, the values of P_u, M_{ux}, and M_{uy} are known from the analysis of the structure. For a trial column section, the values of M_{nx0} and M_{ny0} corresponding to the load P_u/ϕ can easily be found by the usual methods for uniaxial bending. Then replacing M_{nx} with M_{ux}/ϕ and M_{ny} with M_{uy}/ϕ and using $\alpha_1 = \alpha_2 = \alpha$ in Eq. (8.18), or alternatively by plotting $(M_{nx}/\phi)/M_{nx0}$ and $(M_{ny}/\phi)/M_{ny0}$ in Fig. 8.17, it can be confirmed that a

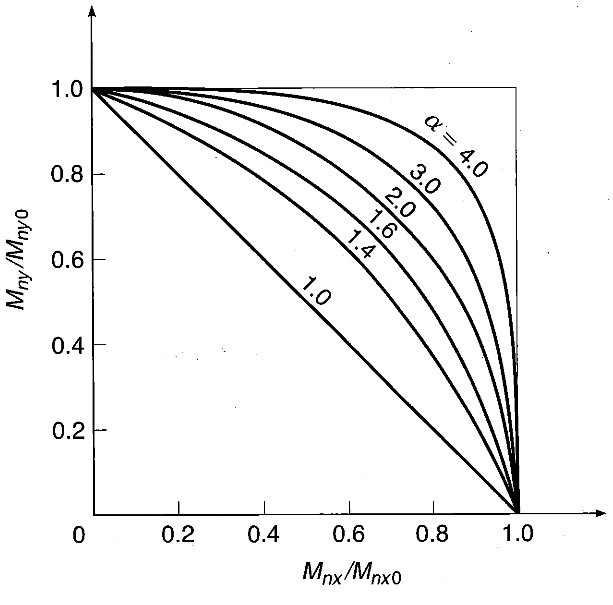

FIGURE 8.17
Interaction contours at constant P_n for varying α. (*Adapted from Ref. 8.8.*)

particular combination of factored moments falls within the load contour (safe design) or outside the contour (failure), and the design modified if necessary.

An approximate approach to the load contour method, in which the curved load contour is represented by a bilinear approximation, will be found in Ref. 8.10. It leads to a method of *trial design* in which the biaxial bending moments are represented by an equivalent uniaxial bending moment. Design charts based on this approximate approach will be found in the *ACI Design Handbook* (Ref. 8.7). Trial designs arrived at in this way should be checked for adequacy by the load contour method, described above, or by the method of reciprocal loads that follows.

8.13 RECIPROCAL LOAD METHOD

A simple, approximate design method developed by Bresler (Ref. 8.9) has been satisfactorily verified by comparison with results of extensive tests and accurate calculations (Ref. 8.11). It is noted that the column interaction surface in Fig. 8.16*d* can, alternatively, be plotted as a function of the axial load P_n and eccentricities $e_x = M_{ny}/P_n$ and $e_y = M_{nx}/P_n$, as is shown in Fig. 8.18*a*. The surface S_1 of Fig. 8.18*a* can be transformed into an equivalent failure surface S_2, as shown in Fig. 8.18*b*, where e_x and e_y are plotted against $1/P_n$ rather than P_n. Thus, $e_x = e_y = 0$ corresponds to the inverse of the capacity of the column if it were concentrically loaded P_0, and this is plotted as point C. For $e_y = 0$ and any given value of e_x, there is a load P_{ny0} (corresponding to moment M_{ny0}) that would result in failure. The reciprocal of this load is plotted as point A. Similarly, for $e_x = 0$ and any given value of e_y, there is a certain load P_{nx0} (corresponding to moment M_{nx0}) that would cause failure, the reciprocal of which is point B. The values of P_{nx0} and P_{ny0} are easily established, for known eccentricities of loading applied to a given column, using the methods already established for uniaxial bending, or using design charts for uniaxial bending.

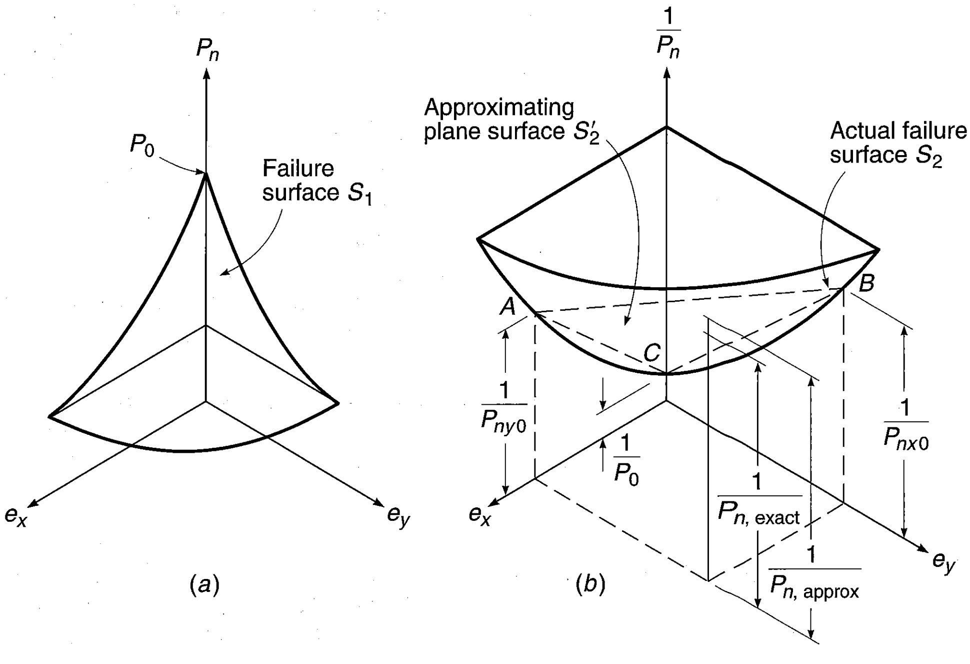

FIGURE 8.18
Interaction surfaces for the reciprocal load method.

An oblique plane S_2' is defined by the three points: A, B, and C. This plane is used as an approximation of the actual failure surface S_2. Note that, for any point on the surface S_2 (i.e., for any given combination of e_x and e_y), there is a corresponding plane S_2'. Thus, the approximation of the true failure surface S_2 involves an infinite number of planes S_2' determined by particular pairs of values of e_x and e_y, i.e., by particular points A, B, and C.

The vertical ordinate $1/P_{n,\text{exact}}$ to the true failure surface will always be conservatively estimated by the distance $1/P_{n,\text{approx}}$ to the oblique plane ABC (extended), because of the concave upward eggshell shape of the true failure surface. In other words, $1/P_{n,\text{approx}}$ is always greater than $1/P_{n,\text{exact}}$, which means that $P_{n,\text{approx}}$ is always less than $P_{n,\text{exact}}$.

Bresler's reciprocal load equation derives from the geometry of the approximating plane. It can be shown that

$$\frac{1}{P_n} = \frac{1}{P_{nx0}} + \frac{1}{P_{ny0}} - \frac{1}{P_0} \tag{8.19}$$

where P_n = approximate value of nominal load in biaxial bending with eccentricities e_x and e_y

P_{ny0} = nominal load when only eccentricity e_x is present ($e_y = 0$)

P_{nx0} = nominal load when only eccentricity e_y is present ($e_x = 0$)

P_0 = nominal load for concentrically loaded column

Equation (8.19) has been found to be acceptably accurate for design purposes provided $P_n \geq 0.10P_0$. It is not reliable where biaxial bending is prevalent and accompanied by an axial force smaller than $P_0/10$. In the case of such strongly prevalent bending, failure is initiated by yielding of the steel in tension, and the situation corresponds to the lowest tenth of the interaction diagram of Fig. 8.16*d*. In this range, it is conservative and accurate enough to neglect the axial force entirely and to calculate the section for biaxial bending only.

Over most of the range for which the Bresler method is applicable, above $0.10P_0$, ϕ is constant, although for very small eccentricities the ACI Code imposes an upper limit on the maximum design strength that has the effect of flattening the upper part of the column strength interaction curve (see Section 8.9 and Graphs A.5 through A.16 of Appendix A). When using the Bresler method for biaxial bending, it is necessary to use the uniaxial strength curve *without* the horizontal cutoff (as shown by the lighter lines in the graphs of Appendix A) in obtaining values for use in Eq. (8.19). The value of ϕP_n obtained in this way should then be subject to the restriction, as for uniaxial bending, that it must not exceed $0.80\phi P_0$ for tied columns and $0.85\phi P_0$ for spirally reinforced columns.

In a typical design situation, given the size and reinforcement of the trial column and the load eccentricities e_y and e_x, one finds by computation or from design charts the nominal loads P_{nx0} and P_{ny0} for uniaxial bending around the X and Y axes, respectively, and the nominal load P_0 for concentric loading. Then $1/P_n$ is computed from Eq. (8.19), and from that P_n is calculated. The design requirement is that the factored load P_u not exceed ϕP_n, as modified by the horizontal cutoff mentioned above, if applicable.

EXAMPLE 8.5

Design of column for biaxial bending. The 300 × 500 mm column shown in Fig. 8.19 is reinforced with eight No. 29 (No. 9) bars arranged around the column perimeter, providing an area $A_{st} = 5160\ \text{mm}^2$. A factored load P_u of 110 kN is to be applied with eccentricities $e_y = 75$ mm and

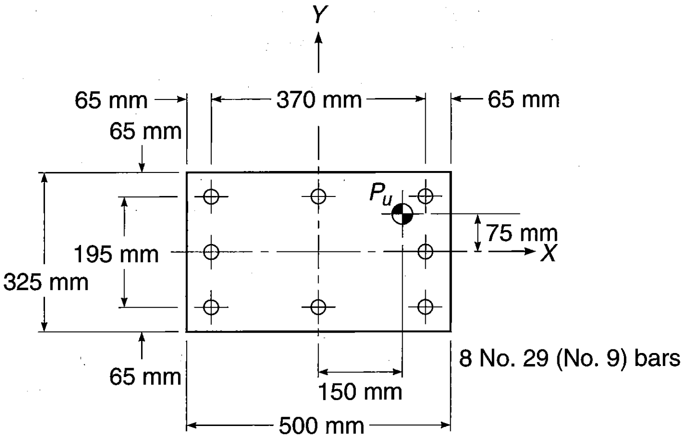

FIGURE 8.19
Column cross section for Example 8.5.

$e_x = 150$ mm, as shown. Material strengths are $f'_c = 28$ MPa and $f_y = 420$ MPa. Check the adequacy of the trial design (*a*) using the reciprocal load method and (*b*) using the load contour method.

SOLUTION.

(*a*) By the reciprocal load method, first considering bending about the *Y* axis, $\gamma = 370/500 = 0.74$, and $e/h = 150/500 = 0.30$. With the reinforcement ratio of $A_{st}/bh = 5160/(325 \times 500) = 0.0318$, using the weighted average of Graphs A.6 ($\gamma = 0.70$) and A.7 ($\gamma = 0.80$),

$$\frac{P_{ny0}}{f'_c A_g}\ (\text{avg}) = 0.6 \times 0.62 + 0.4 \times 0.65 = 0.63$$

$$P_{ny0} = 0.63 \times 28 \times 162{,}500 \times 10^{-3} = 2867 \text{ kN}$$

$$\frac{P_0}{f'_c A_g} = 1.30 \qquad P_0 = 1.30 \times 28 \times 162{,}500 \times 10^{-3} = 5915 \text{ kN}$$

Then for bending about the *X* axis, $\gamma = 195/325 = 0.60$, and $e/h = 75/325 = 0.23$. Graph A.5 of Appendix A gives

$$\frac{P_{nx0}}{f'_c A_g} = 0.70 \qquad P_{nx0} = 0.70 \times 28 \times 162{,}500 \times 10^{-3} = 3185 \text{ kN}$$

$$\frac{P_0}{f'_c A_g} = 1.30 \qquad P_0 = 1.30 \times 28 \times 162{,}500 \times 10^{-3} = 5915 \text{ kN}$$

Substituting these values in Eq. (8.19) results in

$$\frac{1}{P_n} = \frac{1}{3185} + \frac{1}{2867} - \frac{1}{5915} = 0.000494$$

from which $P_n = 2025$ kN. Thus, according to the Bresler method, the design load of $P_u = 0.65 \times 2025 = 1317$ kN can be applied safely.

(*b*) By the load contour method, for *Y* axis bending with $P_u/(\phi f'_c A_g) = 1100/(0.65 \times 28 \times 162{,}500 \times 10^{-3}) = 0.37$. The weighted average from Graphs A.6 and A.7 of Appendix A is

$$\frac{M_{ny0}}{f'_c A_g h}\ (\text{avg}) = 0.6 \times 0.215 + 0.4 \times 0.235 = 0.223$$

Hence, $M_{ny0} = 0.223 \times 28 \times 162{,}500 \times 500 \times 10^{-6} = 507$ kN-m. Then for *X* axis bending, with $P_u/(\phi f'_c A_g) = 0.37$, as before, from Graph A.5,

$$\frac{M_{nx0}}{f'_c A_g h} = 0.185$$

So $M_{nx0} = 0.185 \times 28 \times 162{,}500 \times 325 \times 10^{-6} = 274$ kN-m. The factored load moments about the Y and X axes, respectively, are

$$M_{uy} = 1100 \times 150 \times 10^{-3} = 165 \text{ kN-m}$$

$$M_{ux} = 1100 \times 75 \times 10^{-3} = 82.5 \text{ kN-m}$$

Adequacy of the trial design will now be checked using Eq. (8.18) with an exponent α conservatively taken equal to 1.15. Then with $M_{nx} = M_{ux}/\phi$ and $M_{ny} = M_{uy}/\phi$, that equation indicates

$$\left(\frac{82.5/0.65}{274}\right)^{1.15} + \left(\frac{165/0.65}{507}\right)^{1.15} = 0.413 + 0.451 = 0.864$$

Thus, according to the load contour method, the design is also considered to be safe.

In actual practice, the values of α used in Eq. (8.18) should be checked, for the specific column, because predictions of that equation are quite sensitive to changes in α. In Ref. 8.10, it is shown that $\alpha = \log 0.5/\log \beta$, where values of β can be tabulated for specific column geometries, material strengths, and load ranges (see Ref. 8.7). For the present example, it can be confirmed from Ref. 8.7 that $\beta = 0.56$ and hence $\alpha = 1.19$, approximately as chosen.

One observes that, in Example 8.5*a*, an eccentricity in the Y direction equal to 50 percent of that in the X direction causes a reduction in nominal capacity of 29 percent, i.e., from 2867 to 2025 kN. For cases in which the ratio of eccentricities is smaller, there is some justification for the frequent practice in framed structures of neglecting the bending moments in the direction of the smaller eccentricity. *In general, biaxial bending should be taken into account when the estimated eccentricity ratio approaches or exceeds 0.2.*

8.14 COMPUTER ANALYSIS FOR BIAXIAL BENDING OF COLUMNS

Although the load contour method and the reciprocal load method are widely used in practice, each has serious shortcomings. With the load contour method, selection of the appropriate value of the exponent α is made difficult by a number of factors relating to column shape and bar distribution. For many cases, the usual assumption that $\alpha_1 = \alpha_2$ is a poor approximation. Design aids are available, but they introduce further approximations, e.g., the use of a bilinear representation of the load contour. The reciprocal load method is very simple to use, but the representation of the curved failure surface by an approximating plane is not reliable in the range of large eccentricities, where failure is initiated by steel yielding.

With the general availability and wide use of computers, it is better to use simpler methods to obtain faster, and more exact, solutions to the biaxial column problem. Such a method is that developed by Ehsani (Ref. 8.12). A column strength interaction curve is established for a trial column, exactly analogous to the curve for axial load plus uniaxial bending, as described in Sections 8.3 to 8.7. However, the curve is generated for the particular value of the eccentricity angle that applies, as determined by the ratio of M_{uy}/M_{ux} from the structural frame analysis [see case (*c*) of Fig. 8.16*d*]. This is done by taking successive choices of neutral axis distance, measured in this case along one face of the column from the most heavily compressed corner, from very small (large eccentricity) to very large (small eccentricity), then calculating the axial force P_n and moments M_{nx} and M_{ny}. For each neutral axis distance, iteration is performed with successive values of the orientation angle θ, Fig. 8.16*c*, until $\lambda = \arctan (M_{ny}/M_{nx})$ is in agreement with the value of $\lambda = \arctan (M_{uy}/M_{ux})$ from the structural frame analysis. Thus, one point on curve (*c*) of Fig. 8.16*d* is established. The sequence of calculations is repeated: another choice of neutral axis distance is made, a value of θ is selected, the axial force and moments are calculated, λ is found, and the value of θ is iterated until λ is correct. Thus, the next point is established, and so on, until the complete strength interaction curve for that particular value of λ is complete. ACI Code safety provisions may then be imposed in the usual way, and the adequacy of the proposed design tested, for the known load and moments, against the design strength curve for the trial column.

The method is obviously impractical for manual calculation, but the iterative steps are easily and quickly performed by computer, which can also provide a graphical presentation of results. Full details will be found in Ref. 8.12.

A number of computer programs for biaxial bending are available commercially, such as pcaCOLUMN (Portland Cement Association, Skokie, Illinois).

8.15 BAR SPLICING IN COLUMNS

The main vertical reinforcement in columns is usually spliced just above each floor, or sometimes at alternate floors. This permits the column steel area to be reduced progressively at the higher levels in a building, where loads are smaller, and in addition avoids handling and supporting very long column bars. Column steel may be spliced by lapping, by butt welding, by various types of mechanical connections, or by direct end bearing, using special devices to ensure proper alignment of bars.

Special attention must be given to the problem of bar congestion at splices. Lapping the bars, for example, effectively doubles the steel area in the column cross section at the level of the splice and can result in problems placing concrete and meeting the ACI Code requirement for minimum lateral spacing of bars ($1.5d_b$ or 40 mm). To avoid difficulty, column steel percentages are often limited in practice to not more than about 4 percent, or the bars are extended two stories and staggered splices are used.

The most common method of splicing column steel is the simple lapped bar splice, with the bars in contact throughout the lapped length. It is standard practice to offset the lower bars, as shown in Fig. 8.20, to permit the proper positioning of the upper bars. To prevent outward buckling of the bars at the bottom bend point of such an offset, with spalling of the concrete cover, it is necessary to provide special lateral reinforcement in the form of extra ties. According to ACI Code 7.8.1, the slope of the inclined part of an offset bar must not exceed 1 in 6, and lateral steel must be provided to resist $1\frac{1}{2}$ times the horizontal component of the computed force in the inclined part of the offset bar. This special reinforcement must be placed not more than 150 mm from the point of bend, as shown in Fig. 8.20. Elsewhere in the column, above and below the floor, the usual spacing requirements described in Section 8.2 apply, except that ties must be located not more than one-half the normal spacing s above the floor. Where beams frame from four directions into a joint, as shown in Fig. 8.20, ties may be terminated not more than 75 mm below the lowest reinforcement in the shallowest of such beams, according to ACI Code 7.10.5. If beams are not present on four sides, such as for exterior columns, ties must be placed vertically at the usual spacing through the depth of the joint to a level not more than one-half the usual spacing s below the lowest reinforcement in the slab.

FIGURE 8.20
Splice details at typical interior column.

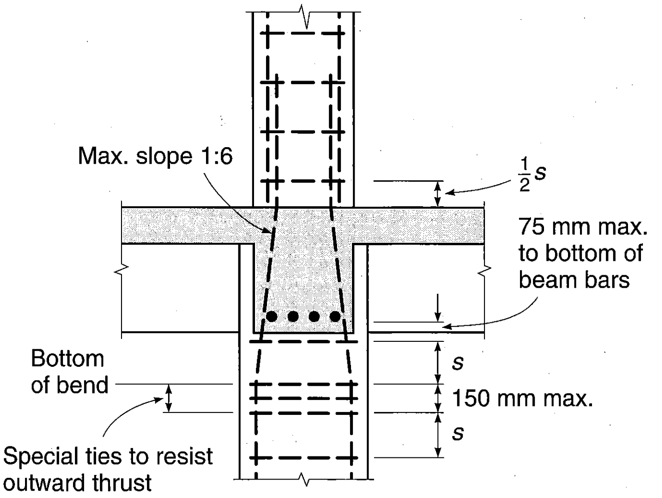
Max. slope 1:6
$\frac{1}{2}s$
75 mm max. to bottom of beam bars
Bottom of bend
s
150 mm max.
s
Special ties to resist outward thrust

Analogous requirements are found in ACI Code 7.10.4 and are illustrated in Ref. 8.1 for spirally reinforced columns.

As discussed in Section 5.11, in frames subjected to lateral loading, a viable alternative to splicing bars just above the floor is to splice them in the center half of the column height, where the moment due to lateral loading is much lower than at floor level. Splicing near midheight is mandatory in "special moment frames" designed for seismic loading (Chapter 20). The use of midheight splices removes the requirement for the special ties shown in Fig. 8.20 because bent bars are not used.

Column splices are mainly compression splices, although load combinations producing moderate to large eccentricity require that splices transmit tension as well. ACI Code 12.17 permits splicing by lapping, butt welding, mechanical connectors, or end bearing. As discussed in Section 5.13, the length of compression lap splices may be reduced in cases where ties or spiral reinforcement throughout the lap length meets specific requirements. If the column bars are in tension, Class A tension lap splices are permitted if the tensile stress does not exceed $0.5f_y$ and less than one-half of the bars are spliced at any section. Class B tension splices are required if the tensile stresses are higher than $0.5f_y$ under factored loads or where more than one-half of the reinforcement is spliced at one location. When end bearing splices are used, they must be staggered or additional reinforcement must be added so that the continuing bars on each column face possess a tensile strength not less than $0.25f_y$ times the area of the vertical reinforcement on that face.

Full requirements for both compression and tension lap splices are discussed in Section 5.13, and the design of a compression splice in a typical column is illustrated in Example 5.5.

8.16 TRANSMISSION OF COLUMN LOADS THROUGH FLOOR SYSTEMS

Quite often, the specified compressive strength of the concrete in columns will exceed that of the floor system. This is especially true for the lower stories in high-rise buildings, where high-strength concrete is used to minimize the cross-sectional area of the columns and thus maximize the usable floor space. High-strength concrete, however, is not needed for the beams and slabs that make up the floor system.

Floor systems and columns must be cast in separate placements. This not only is good construction practice to allow the concrete in the columns to settle prior to placement of the floor system, but also is required by ACI Code 6.4.6 to prevent cracking at the interface between the floor and the column that would occur if the floor and supporting members were cast at the same time. This standard practice, however, opens the possibility for placement of lower-strength concrete within the portion of a floor system that directly supports the columns above, which would, in turn, significantly reduce their capacity. The high lateral confinement provided by the floor system to the concrete in the vicinity of the column does have a mitigating effect because it places that region in triaxial compression and thus increases its usable compressive strength, as explained in Section 2.10.

To address the effects on performance of using concretes with significantly different compressive strengths in the columns and floor system, ACI Code 10.12 specifies that if f_c' of the column exceeds 1.4 times that of the floor system, one of three requirements must be met:

1. At the time of concrete placement in the floor system, concrete with the strength specified for the column must be placed in the floor at the column location. The concrete must extend 600 mm into the surrounding slab from the face of the column and be well integrated with the floor concrete.
2. The strength of the column through the floor system must be based on the lower compressive strength of the floor concrete. Additional reinforcement may be required.
3. For columns that are laterally supported on four sides by beams of approximately the same depth or by slabs, the strength of the column may be based on a compressive strength equal to 75 percent of the column concrete strength plus 35 percent of the floor concrete strength. The ratio of the column concrete strength to the slab concrete strength may not be taken greater than 2.5 for use in design.

REFERENCES

8.1. *ACI Detailing Manual*, SP-66, American Concrete Institute, Farmington Hills, MI, 2004.

8.2. *CRSI Design Handbook*, 10th ed., Concrete Reinforcing Steel Institute, Schaumburg, IL, 2008.

8.3. F. E. Richart, A. Brandtzaeg, and R. L. Brown, "A Study of the Failure of Concrete under Combined Compressive Stresses," *Univ. Ill. Eng. Exp. Stn. Bull.* 185, 1928.

8.4. F. E. Richart, A. Brandtzaeg, and R. L. Brown, "The Failure of Plain and Spirally Reinforced Concrete in Compression," *Univ. Ill. Eng. Exp. Stn. Bull.* 190, 1929.

8.5. S. Martinez, A. H. Nilson, and F. O. Slate, "Spirally Reinforced High Strength Concrete Columns," *J. ACI*, vol. 81, no. 5, 1984, pp. 431–442.

8.6. A. H. Mattock, L. B. Kriz, and E. Hognestad, "Rectangular Concrete Stress Distribution in Ultimate Strength Design," *J. ACI*, vol. 32, no. 8, 1961, pp. 875–928.

8.7. *ACI Design Handbook*, SP-17, American Concrete Institute, Farmington Hills, MI, 1997.

8.8. F. N. Pannell, "Failure Surfaces for Members in Compression and Biaxial Bending," *J. ACI*, vol. 60, no. 1, 1963, pp. 129–140.

8.9. B. Bresler, "Design Criteria for Reinforced Columns under Axial Load and Biaxial Bending," *J. ACI*, vol. 32, no. 5, 1960, pp. 481–490.

8.10. A. L. Parme, J. M. Nieves, and A. Gouwens, "Capacity of Reinforced Concrete Rectangular Members Subject to Biaxial Bending," *J. ACI*, vol. 63, no. 9, 1966, pp. 911–923.

8.11. L. N. Ramamurthy, "Investigation of the Ultimate Strength of Square and Rectangular Columns under Biaxially Eccentric Loads," in *Symp. Reinforced Concrete Columns*, SP-13, American Concrete Institute, Detroit, MI, 1966, pp. 263–298.

8.12. M. R. Ehsani, "CAD for Columns," *Concr. Intl.*, vol. 8, no. 9, 1986, pp. 43–47.

PROBLEMS

8.1. A 400 mm square column is reinforced with four No. 43 (No. 14) bars, one in each corner, with cover distances 75 mm to the steel center in each direction. Material strengths are $f'_c = 35$ MPa and $f_y = 420$ MPa. Construct the interaction diagram relating axial strength P_n and flexural strength M_n. Bending will be about an axis parallel to one face. Calculate the coordinates for P_o, P_b, and at least three other representative points on the curve.

8.2. Starting with the column in Problem 8.1, perform enough additional calculations to determine the effects of increasing f'_c from 35 to 56 MPa on column capacity at both high and low axial loads. Assuming that a compressive strength of 56 MPa is appropriate for the lower stories of a high-rise structure, would you recommend using concrete with $f'_c = 56$ MPa for the columns supporting all stories within the building? Use your analysis to support your answer.

8.3. Plot the design strength curve relating ϕP_n and ϕM_n for the column of Problem 8.1. Design and detail the tie steel required by the ACI Code. Is the column a good choice to resist a load $P_u = 2300$ kN applied with an eccentricity $e = 110$ mm?

8.4. The short column shown in Fig. P8.4 will be subjected to an eccentric load causing uniaxial bending about the Y axis. Material strengths are $f_y = 420$ MPa and $f'_c = 28$ MPa.

(*a*) Construct the nominal strength interaction curve for this column, calculating no fewer than five points, including those corresponding to pure bending, pure axial thrust, and balanced failure.

(*b*) Compare the calculated values with those obtained using Graph A.10 in Appendix A.

(*c*) Show on the same drawing the design strength curve obtained through introduction of the ACI ϕ factors.

(*d*) Design the lateral reinforcement for the column, giving key dimensions for ties.

FIGURE P8.4

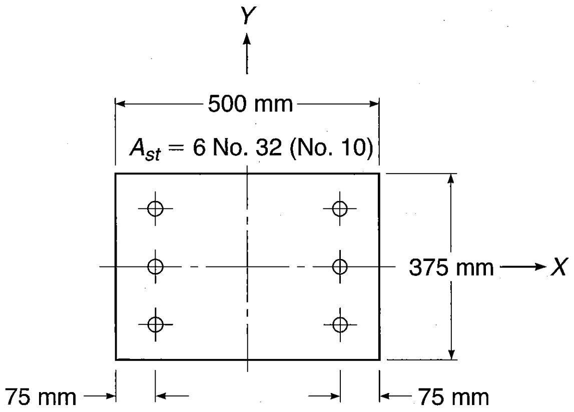

8.5. The column shown in Fig. P8.5 is subjected to axial load and bending moment, causing bending about an axis parallel to that of the rows of bars. What moment M_n would cause the column to fail if the axial load P_n applied simultaneously was 550 kN? Material strengths are $f'_c = 28$ MPa and $f_y = 420$ MPa.

FIGURE P8.5

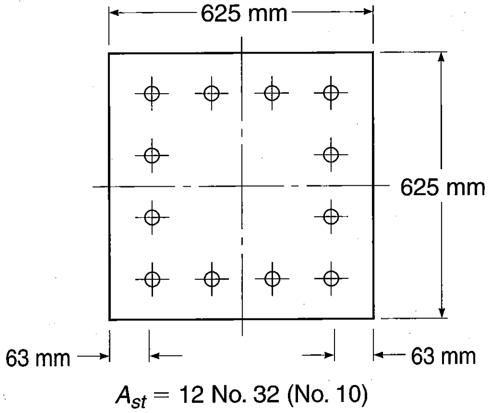

8.6. What is the strength M_n of the column of Problem 8.5 if it was loaded in pure bending (axial force = 0) about one principal axis?

8.7. Construct the interaction diagram relating P_n to M_n for the building column shown in Fig. P8.7. Bending will be about the axis *a-a*. Calculate specific coordinates for concentric loading ($e = 0$), for P_b, and at least three other points, well chosen, on the curve. Material strengths are $f'_c = 56$ MPa and $f_y = 420$ MPa.

FIGURE P8.7

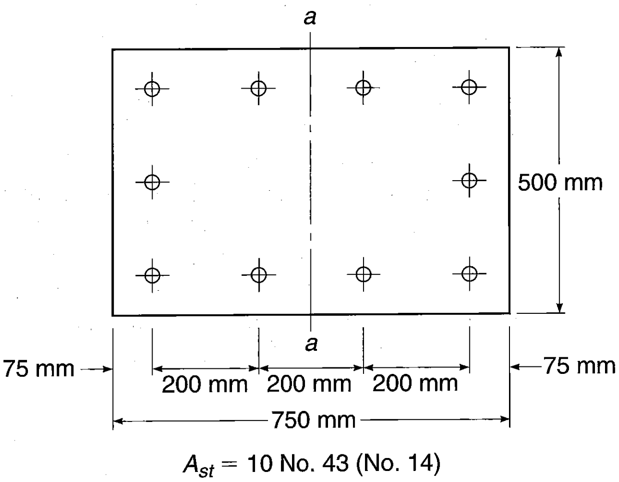

8.8. A short rectangular reinforced concrete column shown in Fig. P8.8 is to be a part of a long-span rigid frame and will be subjected to high bending moments combined with relatively low axial loads, causing bending about the strong axis. Because of the high eccentricity, steel is placed unsymmetrically as shown, with three No. 43 (No. 14) bars near the tension face and two No. 36 (No. 11) bars near the compression face. Material strengths are $f'_c = 42$ MPa and $f_y = 520$ MPa. Construct the complete strength interaction diagram, plotting P_n vs. M_n, relating eccentricities to the plastic centroid of the column (not the geometric center).

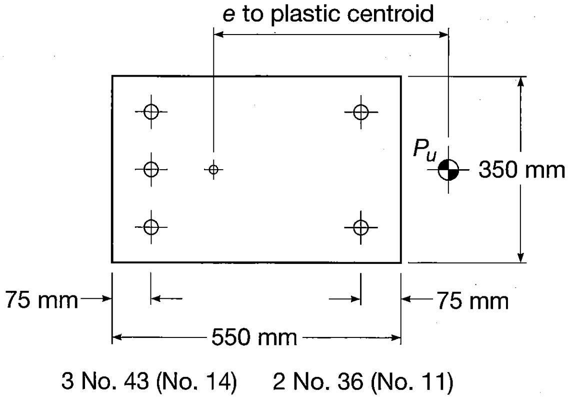
e to plastic centroid
P_u
350 mm
75 mm
75 mm
550 mm
3 No. 43 (No. 14)
2 No. 36 (No. 11)

FIGURE P8.8

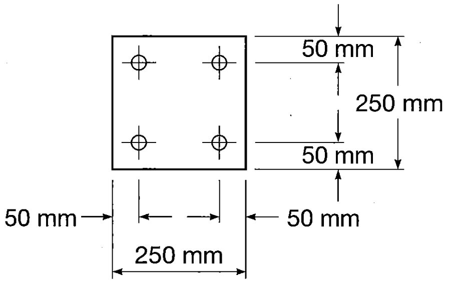
50 mm
250 mm
50 mm
50 mm
50 mm
250 mm

FIGURE P8.9

8.9. The square column shown in Fig. P8.9 must be designed for a factored axial load of 560 kN. Material strengths are $f'_c = 28$ MPa and $f_y = 420$ MPa.

(*a*) Select the longitudinal and transverse reinforcement for an eccentricity $e_y = 66$ mm

(*b*) Select the longitudinal and transverse reinforcement for the same axial load with $e_x = e_y = 66$ mm

(*c*) Construct the strength interaction diagram and design strength curves for the column designed in part (*b*), given that the column will be subjected to biaxial bending with equal eccentricities about both principal axes.

8.10. The square column shown in Fig. P8.10 is a corner column subject to axial load and biaxial bending. Material strengths are $f_y = 420$ MPa and $f'_c = 28$ MPa

(*a*) Find the unique combination of P_n, M_{nx}, and M_{ny} that will produce incipient failure with the neutral axis located as in the figure. The compressive zone is shown shaded. Note that the actual neutral axis is shown, not the equivalent rectangular stress block limit; however, the rectangular stress block may be used as the basis of calculations.

(*b*) Find the angle between the neutral axis and the eccentricity axis, the latter defined as the line from the column center to the point of load.

FIGURE P8.10

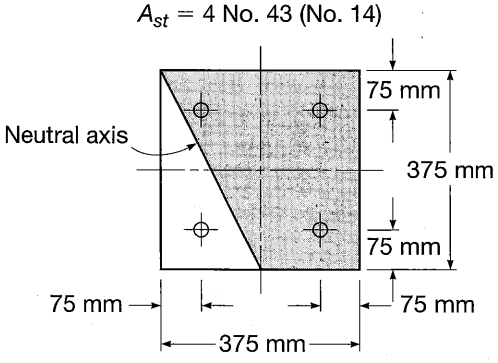
A_{st} = 4 No. 43 (No. 14)
Neutral axis
75 mm
375 mm
75 mm
75 mm
75 mm
375 mm

8.11. For the axial load P_n found in Problem 8.10, and for the same column, with the same eccentricity ratio e_y/e_x, find the values of M_{nx} and M_{ny} that would produce incipient failure, using the load contour method. Compare with the results of Problem 8.10. Take $\alpha = 1.30$, and use the graphs in Appendix A, as appropriate.

8.12. For the eccentricities e_x and e_y found in Problem 8.10, find the value of axial load P_n that would produce incipient failure, using the reciprocal load (Bresler) method. Use the graphs in Appendix A, as appropriate. Compare with the results of Problems 8.10 and 8.11.

8.13. A 500 mm square lower-story interior building column must be designed for maximum and minimum factored axial loads P_u of 3800 and 2380 kN, respectively. For both values of P_u, the column will be subjected to simultaneous factored bending moments M_u of 400 and 32 kN-m about the Y and X axes, respectively (Fig. P8.13). Material strengths are $f_y = 420$ MPa and $f'_c = 28$ MPa. Using equal reinforcement on all sides, design the longitudinal and transverse reinforcement for this column.

FIGURE P8.13

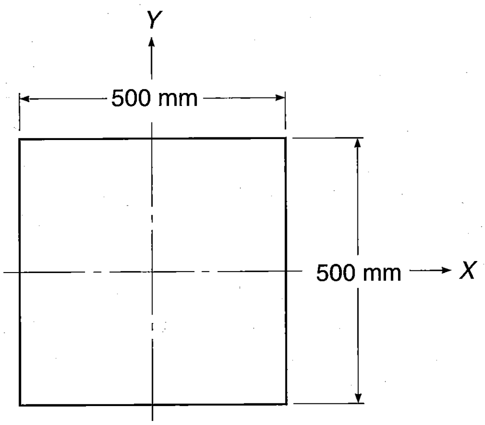

8.14. A 400 mm square lower-story corner column in the building described in Problem 8.13 will be subjected to maximum and minimum factored axial loads P_u of 901 and 560 kN, respectively. For both values of P_u, the columns must be designed for simultaneous factored bending moments M_u of 149 and 140 kN-m about the Y and X axes, respectively. Using equal reinforcement on all sides, design the longitudinal and transverse reinforcement for this column.

9

Slender Columns

9.1 INTRODUCTION

The material presented in Chapter 8 pertained to concentrically or eccentrically loaded *short columns*, for which the strength is governed entirely by the strength of the materials and the geometry of the cross section. Most columns in present-day practice fall in that category. However, with the increasing use of high-strength materials and improved methods of dimensioning members, it is now possible, for a given value of axial load, with or without simultaneous bending, to design a much smaller cross section than in the past. This clearly makes for more slender members. It is because of this, together with the use of more innovative structural concepts, that rational and reliable design procedures for slender columns have become increasingly important.

A column is said to be *slender* if its cross-sectional dimensions are small compared with its length. The degree of slenderness is generally expressed in terms of the slenderness ratio l/r, where l is the unsupported length of the member and r is the radius of gyration of its cross section, equal to $\sqrt{I/A}$. For square or circular members, the value of r is the same about either axis; for other shapes r is smallest about the minor principal axis, and it is generally this value that must be used in determining the slenderness ratio of a freestanding column.

It has long been known that a member of great slenderness will collapse under a smaller compression load than a stocky member with the same cross-sectional dimensions. When a stocky member, say with $l/r = 10$ (e.g., a square column of length equal to about 3 times its cross-sectional dimension h), is loaded in axial compression, it will fail at the load given by Eq. (8.3), because at that load both concrete and steel are stressed to their maximum carrying capacity and give way, respectively, by crushing and by yielding. If a member with the same cross section has a slenderness ratio $l/r = 100$ (e.g., a square column hinged at both ends and of length equal to about 30 times its section dimension), it may fail under an axial load equal to one-half or less of that given by Eq. (8.3). In this case, collapse is caused by buckling, i.e., by sudden lateral displacement of the member between its ends, with consequent overstressing of steel and concrete by the bending stresses that are superimposed on the axial compressive stresses.

Most columns in practice are subjected to bending moments as well as axial loads, as was made clear in Chapter 8. These moments produce lateral deflection of a member between its ends and may also result in relative lateral displacement of joints. Associated with these lateral displacements are *secondary moments* that add to the primary moments and that may become very large for slender columns, leading to failure. A practical definition of a slender column is one for which there is a significant reduction in axial load capacity because of these secondary moments. In the development of ACI Code column provisions, for example, any reduction greater than about 5 percent is considered significant, requiring consideration of slenderness effects.

The ACI Code and Commentary contain detailed provisions governing the design of slender columns. ACI Code 10.10.5, 10.10.6, and 10.10.7 present approximate methods for accounting for slenderness through the use of *moment magnification factors*. The provisions are quite similar to those used for many years for steel columns designed under the American Institute of Steel Construction (AISC) Specification. Alternatively, in ACI Code 10.10.3 and 10.10.4, a more fundamental approach is endorsed, in which the effect of lateral displacements is accounted for directly in the frame analysis. The latter approach, known as *second-order analysis*, is often incorporated as a feature in commercially available structural analysis software.

As noted, most columns in practice continue to be short columns. Simple expressions are included in the ACI Code to determine whether slenderness effects must be considered. These will be presented in Section 9.4 following the development of background information in Sections 9.2 and 9.3 relating to column buckling and slenderness effects.

9.2 CONCENTRICALLY LOADED COLUMNS

The basic information on the behavior of straight, concentrically loaded slender columns was developed by Euler more than 200 years ago. In generalized form, it states that such a member will fail by buckling at the critical load

$$P_c = \frac{\pi^2 E_t I}{(kl)^2} \tag{9.1}$$

It is seen that the buckling load decreases rapidly with increasing *slenderness ratio* kl/r (Ref. 9.1).

For the simplest case of a column hinged at both ends and made of elastic material, E_t simply becomes Young's modulus and kl is equal to the actual length l of the column. At the load given by Eq. (9.1), the originally straight member buckles into a half sine wave, as shown in Fig. 9.1*a*. In this bent configuration, bending moments Py act at any section such as a; y is the deflection at that section. These deflections continue to increase until the bending stress caused by the increasing moment, together with the original compression stress, overstresses and fails the member.

If the stress-strain curve of a short piece of the given member has the shape shown in Fig. 9.2*a*, as it would be for reinforced concrete columns, E_t is equal to Young's modulus, provided that the buckling stress P_c/A is below the proportional limit f_p. If the strain is larger than f_p, buckling occurs in the inelastic range. In this case, in Eq. (9.1), E_t is the tangent modulus, i.e., the slope of the tangent to the stress-strain curve. As the stress increases, E_t decreases. A plot of the buckling load vs. the slenderness ratio, the so-called column curve, therefore has the shape given in Fig. 9.2*b*, which shows the reduction in buckling strength with increasing slenderness. For very stocky columns, the value of the buckling load, calculated from Eq. (9.1), exceeds the direct crushing strength of the stocky column P_n, given by Eq. (8.3). This is also shown in Fig. 9.2*b*. Correspondingly, there is a limiting slenderness ratio $(kl/r)_{\text{lim}}$. For values smaller than this, failure occurs by simple crushing, regardless of

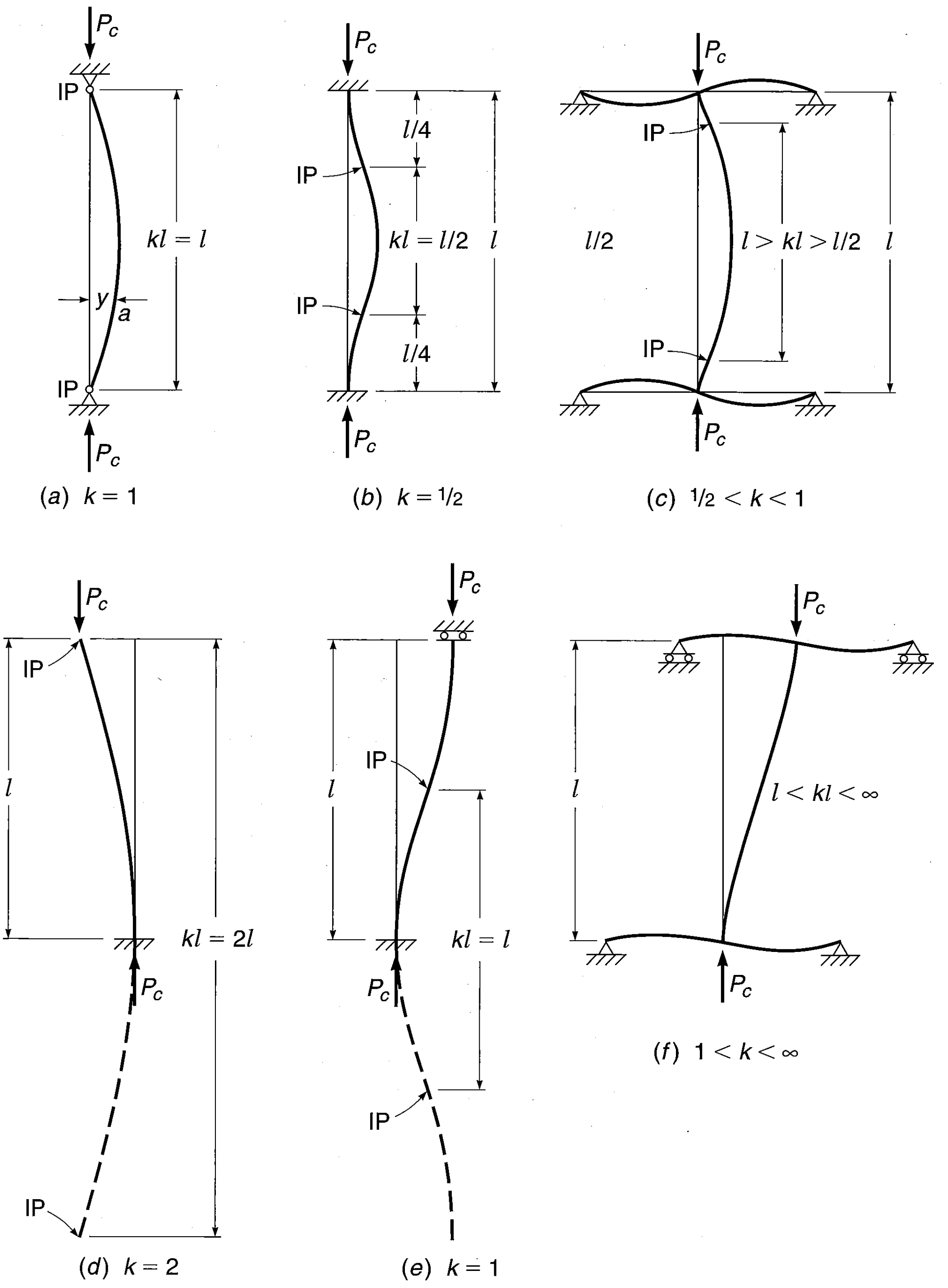

(a) $k = 1$ (b) $k = 1/2$ (c) $1/2 < k < 1$

(d) $k = 2$ (e) $k = 1$ (f) $1 < k < \infty$

FIGURE 9.1
Buckling and effective length of axially loaded columns.

kl/r; for values larger than $(kl/r)_{\text{lim}}$, failure occurs by buckling, the buckling load or stress decreasing for greater slenderness.

If a member is fixed against rotation at both ends, it buckles in the shape of Fig. 9.1*b*, with inflection points (IPs) as shown. The portion between the inflection points is in precisely the same situation as the hinge-ended column of Fig. 9.1*a*, and thus, the *effective length kl* of the fixed-fixed column, i.e., the distance between inflection points, is seen to be $kl = l/2$. Equation (9.1) shows that an elastic column fixed at both ends will carry 4 times as much load as when hinged.

FIGURE 9.2
Effect of slenderness on strength of axially loaded columns.

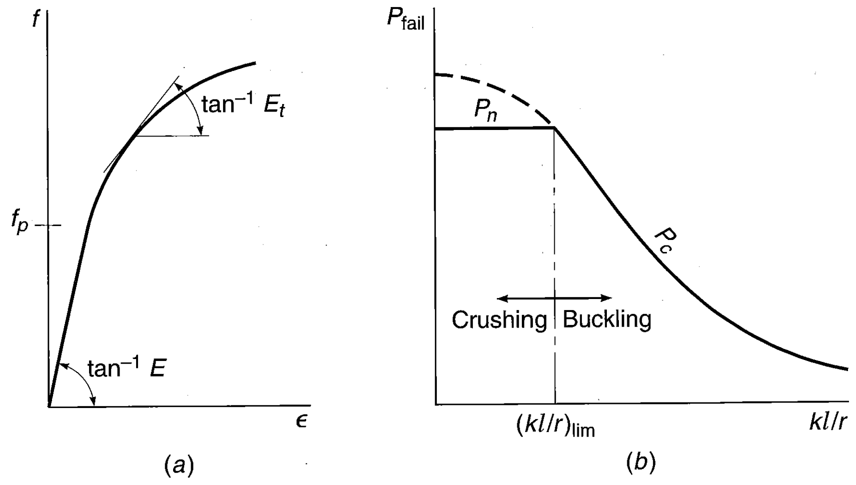

Columns in real structures are rarely either hinged or fixed but have ends partially restrained against rotation by abutting members. This is shown schematically in Fig. 9.1*c*, from which it is seen that for such members the effective length kl, i.e., the distance between inflection points, has a value between l and $l/2$. The precise value depends on the degree of end restraint, i.e., on the ratio of the stiffness EI/l of the column to the sum of stiffnesses EI/l of the restraining members at both ends.

In the columns of Fig. 9.1*a* to *c*, it was assumed that one end was prevented from moving laterally relative to the other end, by horizontal bracing or otherwise. In this case, it is seen that the effective length kl is always smaller than (or at most it is equal to) the real length l.

If a column is fixed at one end and entirely free at the other (cantilever column or flagpole), it buckles as shown in Fig. 9.1*d*. That is, the upper end moves laterally with respect to the lower, a kind of deformation known as *sidesway*. It buckles into a quarter of a sine wave and is therefore analogous to the upper half of the hinged column in Fig. 9.1*a*. The inflection points, one at the end of the actual column and the other at the imaginary extension of the sine wave, are a distance $2l$ apart, so that the effective length is $kl = 2l$.

If the column is rotationally fixed at both ends but one end can move laterally with respect to the other, it buckles as shown in Fig. 9.1*e*, with an effective length $kl = l$. If one compares this column, fixed at both ends but free to sidesway, with a fixed-fixed column that is braced against sidesway (Fig. 9.1*b*), one sees that the effective length of the former is twice that of the latter. By Eq. (9.1), this means that the buckling strength of an elastic fixed-fixed column that is free to sidesway is only one-quarter that of the same column when braced against sidesway. This is an illustration of the general fact that *compression members free to buckle in a sidesway mode are always considerably weaker than when braced against sidesway.*

Again, the ends of columns in actual structures are rarely hinged, fixed, or entirely free but are usually restrained by abutting members. If sidesway is not prevented, buckling occurs as shown in Fig. 9.1*f*, and the effective length, as before, depends on the degree of restraint. If the cross beams are very rigid compared with the column, the case of Fig. 9.1*e* is approached and kl is only slightly larger than l. On the other hand, if the restraining members are extremely flexible, a hinged condition is approached at both ends. Evidently, a column hinged at both ends and free to sidesway is unstable. It will simply topple, being unable to carry any load whatever.

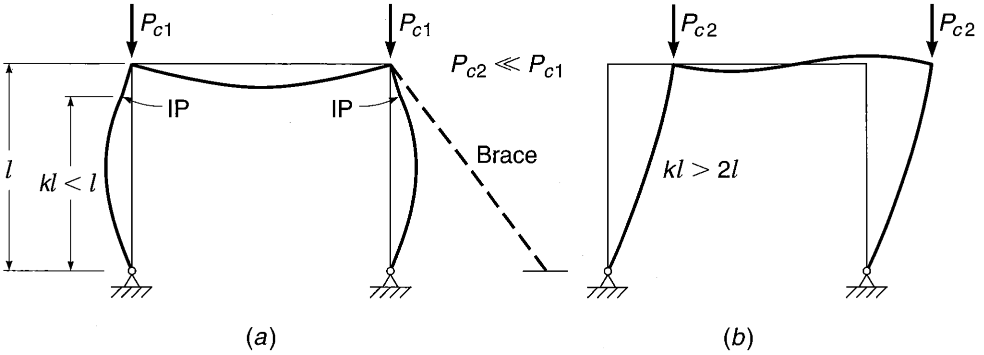

FIGURE 9.3
Rigid-frame buckling: (*a*) laterally braced; (*b*) unbraced.

In reinforced concrete structures, one is rarely concerned with single members but rather with rigid frames of various configurations. The manner in which the relationships just described affect the buckling behavior of frames is illustrated by the simple portal frame shown in Fig. 9.3, with loads applied concentrically to the columns. If sidesway is prevented, as indicated schematically by the brace in Fig. 9.3*a*, the buckling configuration will be as shown. The buckled shape of the column corresponds to that in Fig. 9.1*c*, except that the lower end is hinged. It is seen that the effective length kl is smaller than l. On the other hand, if no sidesway bracing is provided to an otherwise identical frame, buckling occurs as shown in Fig. 9.3*b*. The column is in a situation similar to that shown in Fig. 9.1*d*, upside down, except that the upper end is not fixed but only partially restrained by the girder. It is seen that the effective length kl exceeds $2l$ by an amount depending on the degree of restraint. The buckling strength depends on kl/r in the manner shown in Fig. 9.2*b*. As a consequence, even though they are dimensionally identical, the unbraced frame will buckle at a radically smaller load than the braced frame.

In summary, the following can be noted:

1. The strength of concentrically loaded columns decreases with increasing slenderness ratio kl/r.
2. In columns that are *braced against sidesway* or that are parts of frames braced against sidesway, the effective length kl, i.e., the distance between inflection points, falls between $l/2$ and l, depending on the degree of end restraint.
3. The effective lengths of columns that are *not braced against sidesway* or that are parts of frames not so braced are always larger than l, the more so the smaller the end restraint. In consequence, the buckling load of a frame not braced against sidesway is always substantially smaller than that of the same frame when braced.

9.3 COMPRESSION PLUS BENDING

Most reinforced concrete compression members are also subject to simultaneous flexure, caused by transverse loads or by end moments owing to continuity. The behavior of members subject to such combined loading also depends greatly on their slenderness.

Figure 9.4*a* shows such a member, axially loaded by P and bent by equal end moments M_e. If no axial load were present, the moment M_0 in the member would be constant throughout and equal to the end moments M_e. This is shown in Fig. 9.4*b*. In this situation, i.e., in simple bending without axial compression, the member deflects as shown by the dashed curve of Fig. 9.4*a*, where y_0 represents the deflection at any

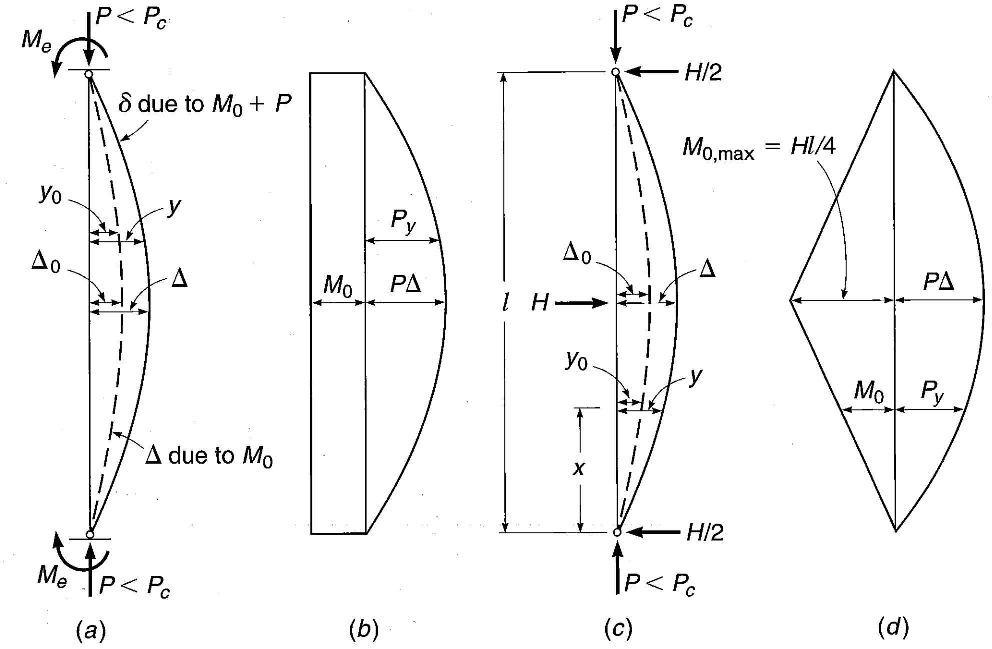

FIGURE 9.4
Moments in slender members with compression plus bending, bent in single curvature.

point caused by bending only. When P is applied, the moment at any point increases by an amount equal to P times its lever arm. The increased moments cause additional deflections, so that the deflection curve under the simultaneous action of P and M_0 is the solid curve of Fig. 9.4*a*. At any point, then, the total moment is now

$$M = M_0 + Py \tag{9.2}$$

i.e., the total moment consists of the moment M_0 that acts in the presence of P and the additional moment caused by P, equal to P times the deflection. This is one illustration of the so-called P-Δ effect.

A similar situation is shown in Fig. 9.4*c*, where bending is caused by the transverse load H. When P is absent, the moment at any point x is $M_0 = Hx/2$, with a maximum value at midspan equal to $Hl/4$. The corresponding M_0 diagram is shown in Fig. 9.4*d*. When P is applied, additional moments Py are caused again, distributed as shown, and the total moment at any point in the member consists of the same two parts as in Eq. (9.2).

The deflections y of elastic columns of the type shown in Fig. 9.4 can be calculated from the deflections y_0, that is, from the deflections of the corresponding beam without axial load, using the following expression (see, for example, Ref. 9.1).

$$y = y_0 \frac{1}{1 - P/P_c} \tag{9.3}$$

If Δ is the deflection at the point of maximum moment $M_{\max}$, as shown in Fig. 9.4, $M_{\max}$ can be calculated using Eqs. (9.2) and (9.3).

$$M_{\max} = M_0 + P\Delta = M_0 + P\Delta_0 \frac{1}{1 - P/P_c} \tag{9.4}$$

It can be shown (Ref. 9.2) that Eq. (9.4) can be written

$$M_{\max} = M_0 \frac{1 + \psi P/P_c}{1 - P/P_c} \tag{9.5}$$

where ψ is a coefficient that depends on the type of loading and varies between about ± 0.20 for most practical cases. Because P/P_c is always significantly smaller than 1, the second term in the numerator of Eq. (9.5) is small enough to be neglected. Doing so, one obtains the simplified design equation

$$M_{\max} = M_0 \frac{1}{1 - P/P_c} \tag{9.6}$$

where $1/(1 - P/P_c)$ is known as the *moment magnification factor*, which reflects the amount by which the moment M_0 is magnified by the presence of a simultaneous axial force P.

Since P_c decreases with increasing slenderness ratio, it is seen from Eq. (9.6) that the moment M in the member increases with the slenderness ratio kl/r. The situation is shown schematically in Fig. 9.5. It indicates that, for a given transverse loading (i.e., a given value of M_0), an axial force P causes a larger additional moment in a slender member than in a stocky member.

In the two members in Fig. 9.4, the largest moment caused by P, namely $P\Delta$, adds directly to the maximum value of M_0; for example,

$$M_0 = \frac{Hl}{4}$$

in Fig. 9.4*d*. As P increases, the maximum moment at midspan increases at a rate faster than that of P in the manner given by Eqs. (9.2) and (9.6) and shown in Fig. 9.6. The member will fail when the simultaneous values of P and M become equal to P_n and M_n, the nominal strength of the cross section at the location of maximum moment.

This direct addition of the maximum moment caused by P to the maximum moment caused by the transverse load, clearly the most unfavorable situation, does not result for all types of deformations. For instance, the member in Fig. 9.7*a*, with equal and opposite end moments, has the M_0 diagram shown in Fig. 9.7*b*. The deflections caused by M_0 alone are again magnified when an axial load P is applied.

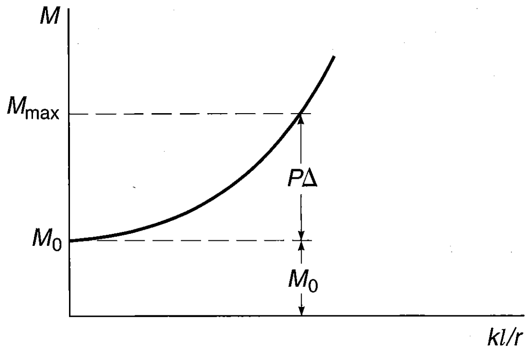

FIGURE 9.5
Effect of slenderness on column moments.

FIGURE 9.6
Effect of axial load on column moments.

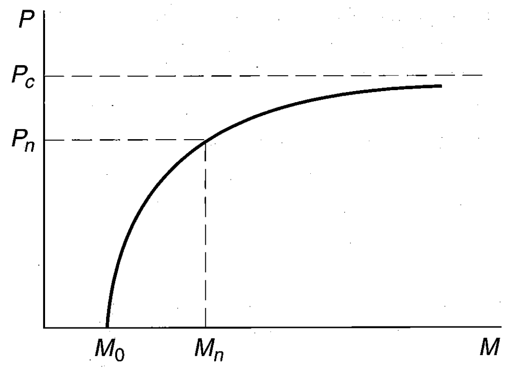

In this case, these deflections under simultaneous bending and compression can be approximated by (Ref. 9.1)

$$y = y_0 \frac{1}{1 - P/4P_c} \tag{9.7}$$

By comparison with Eq. (9.3) it is seen that the deflection magnification here is much smaller.

The additional moments Py caused by the axial load are distributed as shown in Fig. 9.7*c*. Although the M_0 moments are largest at the ends, the Py moments are seen to be largest at some distance from the ends. Depending on their relative magnitudes, the total moments $M = M_0 + Py$ are distributed as shown in either Fig. 9.7*d* or *e*. In the former case, the maximum moment continues to act at the end and to be equal to M_e; the presence of the axial force, then, does not result in any increase in the maximum moment. Alternatively, in the case of Fig. 9.7*e*, the maximum moment is

FIGURE 9.7
Moments in slender members with compression plus bending, bent in double curvature.

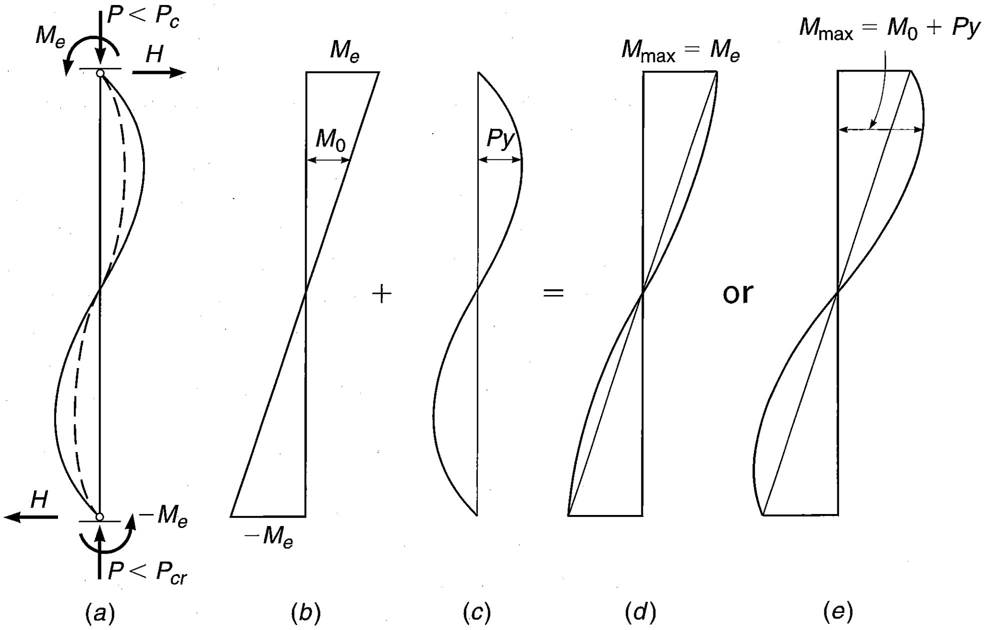

located at some distance from the end; at that location M_0 is significantly smaller than its maximum value M_e, and for this reason the added moment Py increases the maximum moment to a value only moderately greater than M_e.

Comparing Figs. 9.4 and 9.7, one can generalize as follows. The moment M_0 will be magnified most strongly when the location where M_0 is largest coincides with that where the deflection y_0 is largest. This occurs in members bent into single curvature by symmetrical loads or equal end moments. If the two end moments of Fig. 9.4*a* are unequal but of the same sign, i.e., producing single curvature, M_0 will still be strongly magnified, though not quite so much as for equal end moments. On the other hand, as evident from Fig. 9.7, there will be little or possibly no magnification if the end moments are of opposite sign and produce an inflection point along the member.

It can be shown (Ref. 9.2) that the way in which moment magnification depends on the relative magnitude of the two end moments (as in Figs. 9.4*a* and 9.7*a*) can be expressed by a modification of Eq. (9.6):

$$M_{\max} = M_0 \frac{C_m}{1 - P/P_c} \tag{9.8}$$

where

$$C_m = 0.6 + 0.4 \frac{M_1}{M_2} \geq 0.4 \tag{9.9}$$

Here M_1 is the numerically smaller and M_2 the numerically larger of the two end moments; hence, by definition, $M_0 = M_2$. The fraction M_1/M_2 is defined as positive if the end moments produce single curvature and negative if they produce double curvature. It is seen that when $M_1 = M_2$, as in Fig. 9.4*a*, $C_m = 1$, so that Eq. (9.8) becomes Eq. (9.6), as it should. Note that Eq. (9.9) *applies only to members braced against sidesway*. As will become apparent from the discussion that follows, for members not braced against sidesway, maximum moment magnification usually occurs, that is, $C_m = 1$.

Members that are braced against sidesway include columns that are parts of structures in which sidesway is prevented in one of various ways: by walls sufficiently strong and rigid in their own planes to effectively prevent horizontal displacement; by special bracing in vertical planes; in buildings by designing the utility core to resist horizontal loads and furnish bracing to the frames; or by bracing the frame against some other essentially immovable support.

If no such bracing is provided, *sidesway can occur only for the entire frame simultaneously*, not for individual columns in the frame. If this is the case, the combined effect of bending and axial load is somewhat different from that in braced columns. As an illustration, consider the simple portal frame of Fig. 9.8*a* subject to a horizontal load H, such as a wind load, and compression forces P, such as from gravity loads. The moments M_0 caused by H alone, in the absence of P, are shown in Fig. 9.8*b*; the corresponding deformation of the frame is given in dashed curves. When P is added, horizontal moments are caused that result in the magnified deformations shown in solid curves and in the moment diagram of Fig. 9.8*d*. It is seen that the maximum values of M_0, both positive and negative, and the maximum values of the additional moments M_P of the same sign occur at the same locations, namely, at the ends of the columns. They are therefore fully additive, leading to a large moment magnification. In contrast, if the frame in Fig. 9.8 is laterally braced and vertically loaded, Fig. 9.9 shows that the maximum values of the two different moments occur in different locations; the moment magnification, if any, is therefore much smaller, as correctly expressed by C_m.

FIGURE 9.8
Fixed portal frame, laterally unbraced.

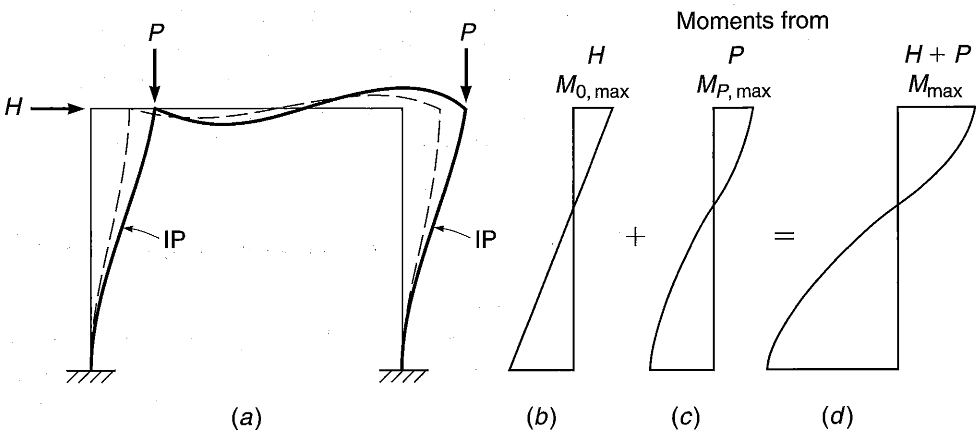

FIGURE 9.9
Fixed portal frame, laterally braced.

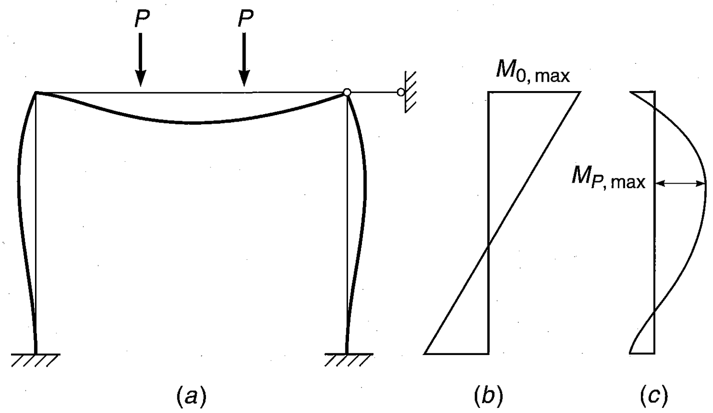

The moments that cause a frame to sidesway need not be caused by horizontal loads as in Fig. 9.8. Asymmetries, of either frame configuration or vertical loading or both, also result in sidesway displacements. In this case, the presence of axial column loads again results in the increased deflection and moment magnification.

In summary, it can be stated as follows:

1. In flexural members, the presence of axial compression causes additional deflections and additional moments Py. Other things being equal, the additional moments increase with increasing slenderness ratio kl/r.
2. In *members braced against sidesway* and bent in single curvature, the maxima of both types of moments, M_0 and Py, occur at the same or at nearby locations and are fully additive; this leads to large moment magnifications. If the M_0 moments result in double curvature (i.e., in the occurrence of an inflection point), the opposite is true and less or no moment magnification occurs.
3. In *members in frames not braced against sidesway*, the maximum moments of both kinds, M_0 and Py, almost always occur at the same locations, the ends of the columns; they are fully additive, regardless of the presence or absence of an inflection point. Here, too, other things being equal, the additional deflections and the corresponding moments increase with increasing kl/r.

This discussion is a simplified presentation of a fairly complex subject. The provisions of the ACI Code regarding slender columns are based on the behavior and the corresponding equations that have just been presented. They take account, in an approximate manner, of the additional complexities that arise from the fact that concrete is not an elastic material, that tension cracking changes the moment of inertia of a member, and that under sustained load, creep increases the short-term deflections and, thereby, the moments caused by these deflections.

9.4 ACI CRITERIA FOR SLENDERNESS EFFECTS IN COLUMNS

The procedure of designing slender columns is inevitably lengthy, particularly because it involves a trial-and-error process. At the same time, studies have shown that most columns in existing buildings are sufficiently stocky that slenderness effects reduce their capacity only a few percent. As stated in Chapter 8, an ACI-ASCE survey indicated that 90 percent of columns braced against sway, and 40 percent of unbraced columns, could be designed as short columns; i.e., they could develop essentially the full cross-sectional strength with little or no reduction from slenderness (Ref. 9.3). Furthermore, lateral bracing is usually provided by shear walls, elevator shafts, stairwells, or other elements for which resistance to lateral deflection is much greater than for the columns of the building frame. It can be concluded that in most cases in reinforced concrete buildings, slenderness effects may be neglected.

To permit the designer to dispense with the complicated analysis required for slender column design for these ordinary cases, ACI Code 10.10.1 provides limits below which the effects of slenderness are insignificant and may be neglected. These limits are adjusted to result in a maximum unaccounted reduction in column capacity of no more than 5 percent. Separate limits are applied to braced and unbraced structures, alternately described in the ACI Code as *nonsway* and *sway* frames, respectively. For the purpose of determining if slenderness effects may be neglected, ACI Code 10.10.1 permits compression members to be considered as braced against sidesway if the total stiffness of the bracing elements resisting lateral movement of a story is at least 12 times the stiffness of all columns in that story. The Code provisions are as follows:

1. For compression members braced against sidesway (i.e., in nonsway structures), the effects of slenderness may be neglected when $kl_u/r \leq 34 - 12M_1/M_2$, where $34 - 12M_1/M_2$ is not taken greater than 40.
2. For compression members not braced against sidesway (i.e., in sway structures), the effects of slenderness may be neglected when kl_u/r is less than 22.

In these provisions, k is the effective length factor (see Section 9.2); l_u is the unsupported length, taken as the clear distance between floor slabs, beams, or other members providing lateral support; M_1 is the smaller factored end moment on the compression member, positive if the member is bent in single curvature and negative if bent in double curvature; and M_2 is the larger factored end moment on the compression member, always positive.

The radius of gyration r for rectangular columns may be taken as $0.30h$, where h is the overall cross-sectional dimension in the direction in which stability is being considered. For circular members, it may be taken as 0.25 times the diameter. For other shapes, r may be computed for the gross concrete section.

The effective length factor k may be conservatively taken as 1.0 for compression members that are braced against sidesway if a more accurate value is not determined by analysis. By necessity, k must be determined by analysis for compression members that are not braced against sidesway. The ACI criteria for determining k for both braced and unbraced columns are discussed in Section 9.6.

If slenderness effects must be considered, ACI Code 10.10.2 requires that the design of columns, beams restraining those columns, and other supporting members in the structure be based on a second-order analysis. The analysis may be nonlinear (ACI Code 10.10.3) or linear (ACI Code 10.10.4), or may be in accordance with the ACI moment magnifier procedure (ACI Code 10.10.5). To limit the potential for excessive moment magnification, the total moment including second-order effects in compression members may not exceed 1.4 times the moment due to first-order effects. In addition, second-order effects must be considered along the length of a member to cover cases in which the maximum moment may occur away from the ends. If a second-order analysis program is used, checking along the length of a member will require subdividing the member when it is modeled. In lieu of doing so, the ACI moment magnification method may be used. ACI Code 10.10.2 requires that the dimensions of all members used in the analysis be within 10 percent of the final dimensions. If not, the structure must be reanalyzed.

Nonlinear and linear second-order analyses, which are covered in ACI Code 10.10.3 and 10.10.4, are discussed in Section 10.8. The ACI moment magnification method of second-order analysis is discussed next.

9.5 ACI CRITERIA FOR NONSWAY VS. SWAY STRUCTURES

The discussion of Section 9.3 clearly shows important differences in the behavior of slender columns in nonsway (braced) structures and corresponding columns in sway (unbraced) structures. ACI Code provisions and Commentary guidelines for the approximate design of slender columns reflect this, and there are separate provisions in each relating to the important parameters in nonsway vs. sway structures, including moment magnification factors and effective length factors.

In practice, a structure is seldom either completely braced or completely unbraced. It is necessary, therefore, to determine in advance if bracing provided by shear walls, elevator and utility shafts, stairwells, or other elements is adequate to restrain the structure against significant sway effects. Both the ACI Code and Commentary provide guidance.

As suggested in ACI Commentary 10.10.5, a compression member can be assumed braced if it is located in a story in which the bracing elements (shear walls, etc.) have a stiffness substantial enough to limit lateral deflection to the extent that the column strength is not substantially affected. Such a determination can often be made by inspection. If not, ACI Code 10.10.5 provides two alternate criteria for determining if columns and stories are treated as nonsway or sway.

To be considered as a nonsway or braced column, the first criterion requires that the increase in column end moment due to second-order effects not exceed 5 percent of the first-order end moments. The designer is free to select the method for such a determination.

As an alternative, the Code allows a story to be considered nonsway when the *stability index*

$$Q = \frac{\Sigma P_u \Delta_o}{V_{us} l_c} \tag{9.10}$$

for a story is not greater than 0.05, where ΣP_u and V_{us} are the total factored vertical load and story shear, respectively, for the story; Δ_o is the first-order relative deflection between the top and the bottom of the story due to V_{us}; and l_c is the length of the compressive member measured center to center of the joints in the frame. ACI

Commentary 10.10.5 provides the guidance that ΣP_u should be based on the lateral loading that maximizes the value of ΣP_u; the case of $V_{us} = 0$ is not included. In most cases, this calculation involves the combinations of load factors in Table 1.2 for wind, earthquake, or soil pressure (e.g., $1.2D + 1.6W + 1.0L + 0.5L_r$).

As shown in Refs. 9.3 and 9.4, for Q not greater than 0.6, the stability index closely approximates the ratio P/P_c used in the calculation of the moment magnification factor, so that $1/(1 - P/P_c)$ can be replaced by $1/(1 - Q)$. Thus, for $Q = 0.05$, $M_{\max} \approx 1.05M_0$.[†]

The section properties of the frame members used to calculate Q need to account for the effects of axial loads, cracked regions along the length of the member, and the duration of the loads. ACI Code 10.10.4 provides useful guidance that is appropriate for first-order as well as second-order analysis. According to ACI Code 10.10.4, section properties may be represented using the modulus of elasticity E_c given in Eq. (2.3) and the following section properties:

Moments of inertia	
Beams	$0.35I_g$
Columns	$0.70I_g$
Walls—uncracked	$0.70I_g$
—cracked	$0.35I_g$
Flat plates and flat slabs	$0.25I_g$
Area	$1.0A_g$

where I_g and A_g are based on the gross concrete cross section, neglecting reinforcement. As discussed in Section 12.5, I_g for T beams can be closely approximated as 2 times I_g for the web. The reduced values of I given above take into account the effect of nonlinear material behavior on the effective stiffness of the members. Reference 9.3 shows that these values for moments of inertia underestimate the true moments of inertia and conservatively overestimate second-order effects by 20 to 25 percent for reinforced concrete frames.

Based on work described in Refs. 9.5 and 9.6, ACI Code 10.10.4 indicates that the moments of inertia I of compression members and flexural members may also be computed using alternative expressions. For compression members,

$$I = \left(0.80 + 25\frac{A_{st}}{A_g}\right)\left(1 - \frac{M_u}{P_u h} - 0.5\frac{P_u}{P_o}\right)I_g \leq 0.875I_g \tag{9.11}$$

where P_u and M_u are based on the load combination under consideration, or the combination of P_u and M_u resulting in the smallest value of I. The value of I calculated using Eq. (9.11) need not be taken less than $0.35I_g$.

For flexural members,

$$I = (0.10 + 25\,\rho)\left(1.2 - 0.2\frac{b_w}{d}\right)I_g \leq 0.5I_g \tag{9.12}$$

The value of I calculated using Eq. (9.12) need not be taken less than $0.25I_g$. For continuous flexural members, I may be taken as the average value of I calculated at critical positive and negative moment locations along the length of the beam. The Code requires that the member dimensions and reinforcement ratios used in Eqs. (9.11) and (9.12) be within 10 percent of the final values.

[†] The near equivalence of Q to P/P_{cr} for reinforced concrete columns can be demonstrated using a single-sway column with ends fixed against rotation, as shown in Fig. 9.1*e*. For this column, $Q = P_u\Delta_o/V_{us}l_c$. Since V_{us}/Δ_o = the lateral stiffness of the column $= 12EI/l_c^3$, the stability index can be expressed as $Q = P_u/(12EI/l_c^2)$. For an unsupported length of the column (the length used to calculate P_c) $l_u = 0.9l_c$ and $P = P_u$, $Q = P_u/(9.72EI/l_u^2)$ compared to $P/P_c = P_u/(\pi^2EI/l_u^2) = P_u/(9.87EI/l_u^2)$.

To account for the effects of creep on Δ_o in Eq. (9.10) when sustained lateral loads act, the moments of inertia for compression members must be divided by $1 + \beta_{ds}$, where β_{ds} is the ratio of the maximum factored sustained shear within a story to the maximum factored shear in that story associated with the same load combination, but not greater than 1.0.

9.6 ACI MOMENT MAGNIFIER METHOD FOR NONSWAY FRAMES

A slender reinforced concrete column reaches the limit of its strength when the combination of P and M at the most highly stressed section causes that section to fail. In general, P is essentially constant along the length of the member. This means that the column approaches failure when, at the most highly stressed section, the axial force P combines with a moment $M = M_{\max}$, as given by Eq. (9.8), so that this combination becomes equal to P_n and M_n, which will cause the section to fail. This is easily visualized by means of Fig. 9.10.

For a column of given cross section, Fig. 9.10 presents a typical interaction diagram. For simplicity, suppose that the column is bent in single curvature with equal eccentricities at both ends. For this eccentricity, the strength of the cross section is given by point A on the interaction curve. If the column is stocky enough for the moment magnification to be negligibly small, then $P_{n,\text{stocky}}$ at point A represents the member strength of the column under the simultaneous moment $M_{n,\text{stocky}} = e_0 P_{n,\text{stocky}}$.

On the other hand, if the same column is sufficiently slender, significant moment magnification will occur with increasing P. Then the moment at the most highly stressed section is $M_{\max}$, as given by Eq. (9.8), with $C_m = 1$ because of equal end eccentricities. The solid curve in Fig. 9.10 shows the nonlinear increase of $M_{\max}$ as

FIGURE 9.10
Effect of slenderness on carrying capacity.

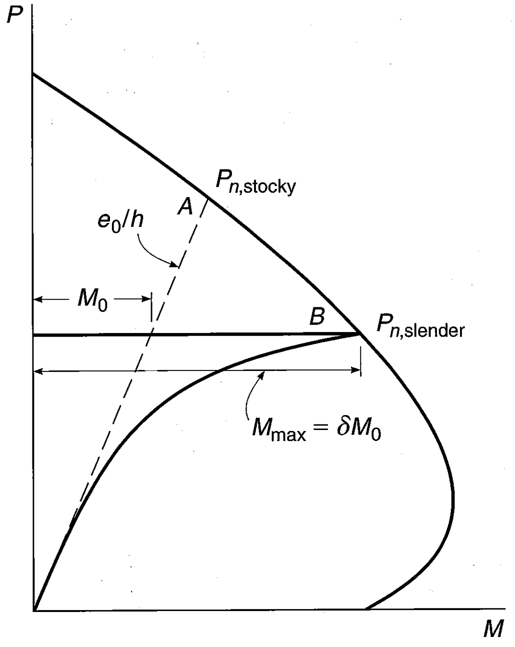

P increases. The point where this curve intersects the interaction curve, i.e., point B, defines the member strength $P_{n,\text{slender}}$ of the slender column, combined with the simultaneously applied end moments $M_0 = e_0 P_{n,\text{slender}}$. If end moments are unequal, the factor C_m will be less than 1, as discussed in Section 9.3.

For slender column design, the axial load and end moments in a column are first determined using conventional frame analysis (see Chapter 12), typically using the section properties given in Section 9.5. The member is then designed for that axial load and a simultaneous magnified column moment.

For a nonsway frame, the ACI Code equation for magnified moment, acting with the factored axial load P_u, is written as

$$M_c = \delta_{ns} M_2 \tag{9.13}$$

where the moment magnification factor is

$$\delta_{ns} = \frac{C_m}{1 - P_u/0.75P_c} \geq 1 \tag{9.14}$$

In Eqs. (9.13) and (9.14), the subscript *ns* denotes a nonsway frame. The 0.75 term in Eq. (9.14) is a *stiffness reduction factor*, designed to provide a conservative estimate of P_c. The critical load P_c, in accordance with Eq. (9.1), is given as

$$P_c = \frac{\pi^2 EI}{(kl_u)^2} \tag{9.15}$$

where l_u is defined as the unsupported length of the compression member. The value of k in Eq. (9.15) should be set equal to 1.0, unless calculated using the values of E_c and I given in Section 9.5 and procedures described later in this section.

In Eq. (9.14), the value of C_m is as previously given in Eq. (9.9):

$$C_m = 0.6 + 0.4\frac{M_1}{M_2} \geq 0.4 \tag{9.9}$$

for members braced against sidesway and without transverse loads between supports. Here M_2 is the larger of the two end moments, and M_1/M_2 is positive when the end moments produce single curvature and negative when they produce double curvature. The variation of C_m with M_1/M_2 is shown in Fig. 9.11. In Eq. (9.14), when the calculated value of δ_{ns} is smaller than 1, it indicates that the larger of the two end moments, M_2, is the largest moment in the column, a situation depicted in Fig. 9.7*d*.

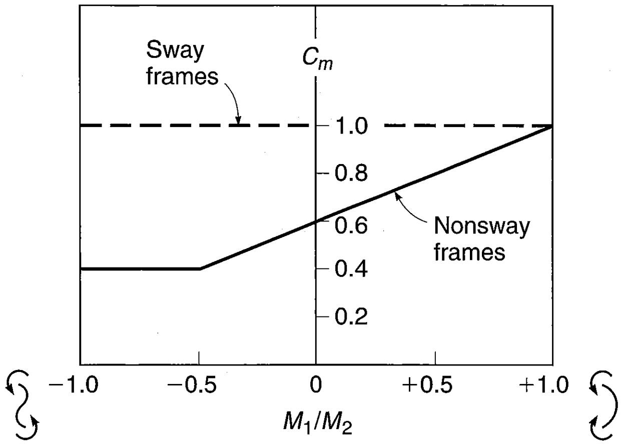

FIGURE 9.11
Values of C_m for slender columns in sway and nonsway frames.

In this way, the ACI Code provides for the capacity-reducing effects of slenderness in nonsway frames by means of the moment magnification factor δ_{ns}. However, it is well known that for columns with no or very small applied moments, i.e., axially or nearly axially loaded columns, increasing slenderness also reduces the column strength. For this situation, ACI Code 10.10.6.5 provides that the factored moment M_2 in Eq. (9.13) not be taken less than

$$M_{2,\min} = P_u(15 + 0.03h) \tag{9.16}$$

about each axis separately, where 0.6 and h are in mm. For members in which $M_{2,\min}$ exceeds M_2, the value of C_m in Eq. (9.9) is taken equal to 1.0 or is based on the ratio of the computed end moments M_1 and M_2.

The value of EI used in Eq. (9.15) to calculate P_c for an individual member must be both accurate and reasonably conservative to account for the greater variability inherent in the properties of individual columns, as compared to the properties of the reinforced concrete frame, as a whole. The values of EI provided in Section 9.5 are adequate for general frame analysis but not for establishing P_c for individual columns.

In homogeneous elastic members, such as steel columns, EI is easily obtained from Young's modulus and the usual moment of inertia. Reinforced concrete columns, however, are nonhomogeneous, since they consist of both steel and concrete. Whereas steel is substantially elastic, concrete is not and is, in addition, subject to creep and to cracking if tension occurs on the convex side of the column. All these factors affect the effective value of EI for a reinforced concrete member. It is possible by computer methods to calculate fairly realistic effective section properties, taking account of these factors. Even these calculations are no more accurate than the assumptions on which they are based. On the basis of elaborate studies, both analytical and experimental (Ref. 9.7), the ACI Code requires that EI be determined by either

$$EI = \frac{0.2E_cI_g + E_sI_{se}}{1 + \beta_{dns}} \tag{9.17}$$

or by the simpler expression

$$EI = \frac{0.4E_cI_g}{1 + \beta_{dns}} \tag{9.18}$$

where E_c = modulus of elasticity of concrete, MPa
I_g = moment of inertia of gross section of column, mm^4
E_s = modulus of elasticity of steel = 200,000 MPa
I_{se} = moment of inertia of reinforcement about centroidal axis of member cross section, mm^4
β_{dns} = ratio of maximum factored axial sustained load to maximum factored axial load associated with same load combination, but not greater than 1.0 (this definition differs from that used in Section 9.5 to calculate Δ_o)

The factor β_{dns} accounts approximately for the effects of creep. That is, the larger the sustained loads, the larger are the creep deformations and corresponding curvatures. Consequently, the larger the sustained loads relative to the temporary loads, the smaller the effective rigidity, as correctly reflected in Eqs. (9.17) and (9.18). Because, of the two materials, only concrete is subject to creep, and reinforcing steel as ordinarily used is not, the argument can be made that the creep parameter $1 + \beta_{dns}$ should be applied only to the term $0.2E_cI_g$ in Eq. (9.17). However, as explained in ACI Commentary 10.10.6.2, the creep parameter is applied to both terms because of the potential for premature yielding of steel in columns under sustained loading.

Both Eqs. (9.17) and (9.18) are conservative lower limits for large numbers of actual members (Ref. 9.3). The simpler but more conservative Eq. (9.18) is not unreasonable for lightly reinforced members, but it greatly underestimates the effect of reinforcement for more heavily reinforced members, i.e., for the range of higher ρ values. Equation (9.17) is more reliable for the entire range of ρ and definitely preferable for medium and high ρ values (Ref. 9.8).

An accurate determination of the effective length factor k is essential in connection with Eqs. (9.13) and (9.15). In Section 9.2, it was shown that, for frames braced against sidesway (nonsway frames), k varies from $\frac{1}{2}$ to 1, whereas for laterally unbraced frames (sway frames), it varies from 1 to ∞, depending on the degree of rotational restraint at both ends. This was illustrated in Fig. 9.1. For frames, it is seen that this degree of rotational restraint depends on whether the stiffnesses of the beams framing into the column at top and bottom are large or small compared with the stiffness of the column itself. An approximate but generally satisfactory way of determining k is by means of *alignment charts* based on isolating the given column plus all members framing into it at top and bottom, as shown in Fig. 9.12. The *degree of end restraint* at each end is $\psi = \Sigma(EI/l_c$ of columns) $\div$ $\Sigma(EI/l$ of floor members). Only floor members that are in a plane at either end of the column are to be included. The value of k can be read directly from the chart of Fig. 9.13, as illustrated by the dashed lines.[†]

It is seen that k must be known before a column in a frame can be dimensioned. Yet k depends on the stiffness EI/l of the members to be dimensioned, as well as on that of the abutting members. Thus, the dimensioning process necessarily involves iteration; i.e., one assumes member sizes, calculates member stiffnesses and corresponding k values, and then calculates the critical buckling load and more accurate member sizes on the basis of these k values until assumed and final member sizes coincide or are satisfactorily close. The stiffness EI/l should be calculated based on the values of E_c and I given in Section 9.5, and the span lengths of the members l_c and l should be measured center to center of the joints.

An outline of the separate steps in the analysis/design procedure for nonsway stories or frames follows along these lines:

1. Select a trial column section to carry the factored axial load P_u and moment $M_u = M_2$ from the elastic first-order frame analysis, assuming short column behavior and following the procedures of Chapter 8.
2. Determine if the frame should be considered as nonsway or sway, using the criteria of Section 9.5.
3. Find the unsupported length l_u.
4. For the trial column, check for consideration of slenderness effects, using the criteria of Section 9.4 with $k = 1.0$.
5. If slenderness is tentatively found to be important, refine the calculation of k based on the alignment chart in Fig. 9.13*a*, with member stiffnesses EI/l (Section 9.5)

[†] Equations for the determination of effective length factors k, more convenient than charts for developing computer solutions, are presented in Refs. 9.9 through 9.12. The expressions in Ref. 9.12 are the most accurate.

FIGURE 9.12
Section of rigid frame including column to be designed.

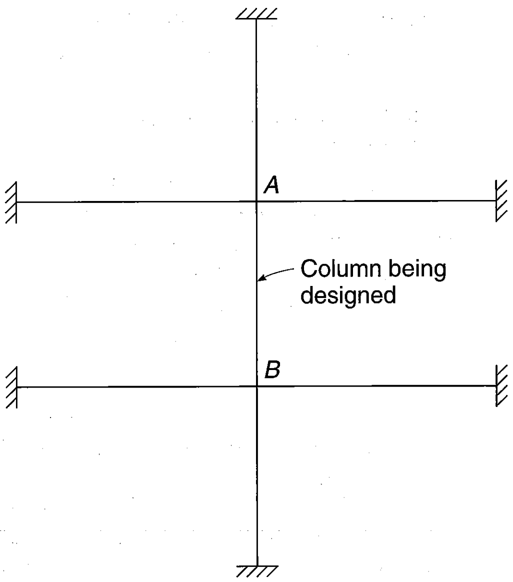

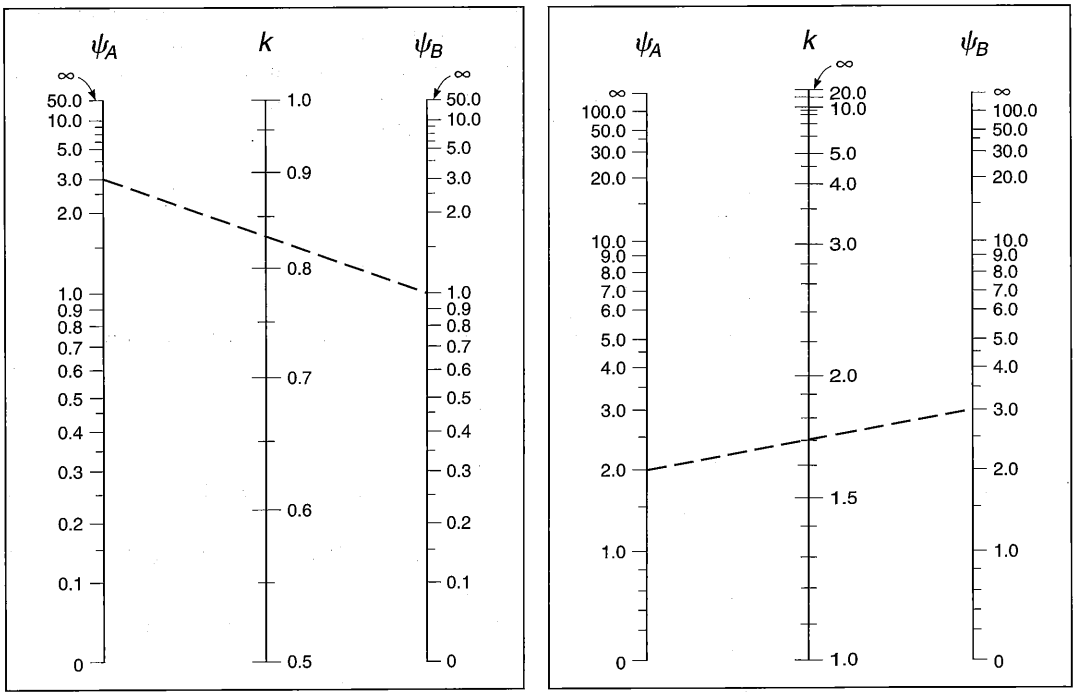

(*a*) Nonsway frames (*b*) Sway frames

FIGURE 9.13
Alignment charts for effective length factors *k*.

and rotational restraint factors ψ based on trial member sizes. Recheck against the slenderness criteria.

6. If moments from the frame analysis are small, check to determine if the minimum moment from Eq. (9.16) controls.

7. Calculate the equivalent uniform moment factor C_m from Eq. (9.9).
8. Calculate β_{dns}, EI from Eq. (9.17) or (9.18), and P_c from Eq. (9.15) for the trial column.
9. Calculate the moment magnification factor δ_{ns} from Eq. (9.14) and magnified moment M_c from Eq. (9.13).
10. Check the adequacy of the column to resist axial load and magnified moment, using the column design charts of Appendix A in the usual way. Revise the column section and reinforcement if necessary.
11. If column dimensions are altered, repeat the calculations for k, ψ, and P_c based on the new cross section. Determine the revised moment magnification factor and check the adequacy of the new design.

EXAMPLE 9.1

Design of a slender column in a nonsway frame. Figure 9.14 shows an elevation view of a multistory concrete frame building, with 1200 mm wide × 300 mm deep beams on all column lines, carrying two-way slab floors and roof. The clear height of the columns is 3.95 m. Interior columns are tentatively dimensioned at 450 × 450 mm, and exterior columns at 400 × 400 mm. The frame is effectively braced against sway by stair and elevator shafts having concrete walls that are monolithic with the floors, located in the building corners (not shown in the figure). The structure will be subjected to vertical dead and live loads. Trial calculations by first-order analysis indicate that the pattern of live loading shown in Fig. 9.14, with full load distribution on roof and upper floors and a checkerboard pattern adjacent to column $C3$, produces maximum moments with single curvature in that column, at nearly maximum axial load. Dead loads act on all spans. Service load values of dead and live load axial force and moments for the typical interior column $C3$ are as follows:

Dead load	*Live load*
$P = 990$ kN	$P = 745$ kN
$M_2 = 3$ kN-m	$M_2 = 146$ kN-m
$M_1 = -3$ kN-m	$M_1 = 135$ kN-m

The column is subjected to double curvature under dead load alone and single curvature under live load.

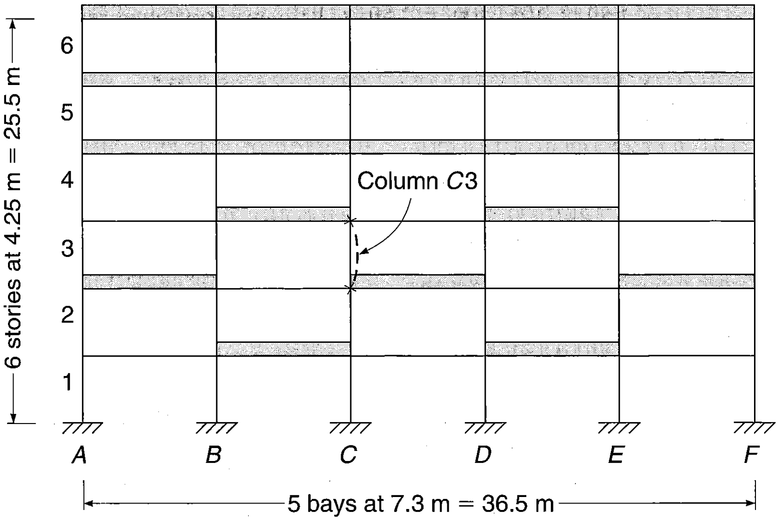

FIGURE 9.14
Concrete building frame for Example 9.1.

Design column $C3$, using the ACI moment magnifier method. Use $f_c' = 28$ MPa and $f_y = 420$ MPa.

Solution. The column will first be designed as a short column, assuming no slenderness effect. With the application of the usual load factors,

$$P_u = 1.2 \times 990 + 1.6 \times 745 = 2380 \text{ kN}$$

$$M_u = 1.2 \times 3 + 1.6 \times 146 = 237 \text{ kN}$$

For a 450 × 450 mm column, with the 40 mm clear to the outside steel, No. 10 (No. 3) stirrups, and (assumed) No. 32 (No. 10) longitudinal steel:

$$\gamma = (450 - 2 \times 40 - 2 \times 9.5 - 32.3)/450 = 0.71$$

Graph A.6 for $\gamma = 0.70$, with bars arranged around the column perimeter, will be used. Then

$$\frac{P_u}{\phi f_c' A_g} = \frac{2380 \times 10^3}{0.65 \times 28 \times 202{,}500} = 0.646$$

$$\frac{M_u}{\phi f_c' A_g h} = \frac{237 \times 10^6}{0.65 \times 28 \times 202{,}500 \times 450} = 0.143$$

and from the graph $\rho_g = 0.02$. This is low enough that an increase in steel area could be made, if necessary, to allow for slenderness, and the 450 × 450 mm concrete dimensions will be retained.

For an initial check on slenderness, an effective length factor $k = 1.0$ will be used. Then

$$\frac{kl_u}{r} = \frac{1.0 \times 3950}{0.3 \times 450} = 29.3$$

For a braced frame, the upper limit for short column behavior is

$$34 - 12\frac{M_1}{M_2} = 34 - 12\frac{1.2 \times (-3) + 1.6 \times 135}{1.2 \times 3 + 1.6 \times 146} = 23.3$$

The calculated value of 29.3 exceeds this, so slenderness must be considered in the design. A more refined calculation of the effective length factor k is thus called for.

Because E_c is the same for column and beams, it will be canceled in the stiffness calculations. For this step, the column moment of inertia will be taken as $0.7I_g = 0.7 \times 450 \times 450^3/12 = 2.39 \times 10^9$ mm^4, giving $I/l_c = 2.39 \times 10^9/4250 = 5.62 \times 10^5$ mm^3. For the beams, the moment of inertia will be taken as $0.35I_g$, where I_g is taken as 2 times the gross moment of inertia of the web. Thus, $0.35I_g = 0.35 \times 2 \times 1200 \times 300^3/12 = 1.89 \times 10^9$ mm^4, and $I/l = 1.89 \times 10^9/7300 = 2.59 \times 10^5$ mm^3. Rotational restraint factors at the top and bottom of column $C3$ are the same and are

$$\psi_a = \psi_b = \frac{5.62 \times 10^5 + 5.62 \times 10^5}{2.59 \times 10^5 + 2.59 \times 10^5} = 2.17$$

From Fig. 9.13*a* for the braced frame, the value of k is 0.87, rather than 1.0 as used previously. Consequently,

$$\frac{kl_u}{r} = \frac{0.87 \times 3950}{0.3 \times 450} = 25.5$$

This is still above the limit value of 23.3, confirming that slenderness must be considered.

A check will now be made of minimum moment. According to Eq. (9.16), $M_{2,\min} = 2380(15 + 0.03 \times 450) \times 10^{-3} = 67.8$ kN-m. It is seen that this does not control.

The coefficient C_m can now be found from Eq. (9.9) with $M_1 = 1.2 \times (-3) + 1.6 \times 135 = 212$ kN-m and $M_2 = 1.2 \times 3 + 1.6 \times 146 = 237$ kN-m:

$$C_m = 0.6 + 0.4\frac{212}{237} = 0.96$$

FIGURE 9.15
Cross section of column $C3$, Example 9.1.

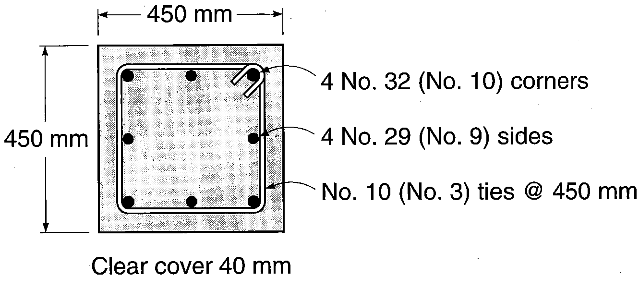

Next the factor β_{dns} will be found based on the ratio of the maximum factored sustained axial load (the factored dead load in this case) to the maximum factored axial load:

$$\beta_{dns} = \frac{1.2 \times 990}{1.2 \times 990 + 1.6 \times 745} = 0.50$$

For a relatively low reinforcement ratio, one estimated to be in the range of 0.02 to 0.03, the more approximate Eq. (9.18) for EI will be used, and

$$EI = \frac{0.4\,E_c I_g}{1 + \beta_{dns}} = \frac{0.4 \times 4700\sqrt{28} \times 450 \times 450^3/12}{1 + 0.50}$$
$$= 2.266 \times 10^{13}\text{ N-mm}^2 = 2.266 \times 10^{10}\text{ kN-mm}^2$$

The critical buckling load is found from Eq. (9.15) to be

$$P_c = \frac{\pi^2 EI}{(kl_u)^2} = \frac{\pi^2 \times 2.266 \times 10^{10}}{(0.87 \times 3950)^2} = 1.89 \times 10^4\text{ kN}$$

The moment magnification factor can now be found from Eq. (9.14).

$$\delta_{ns} = \frac{C_m}{1 - P_u/0.75P_c} = \frac{0.96}{1 - 2380/(0.75 \times 18{,}900)} = 1.15$$

Thus, the required axial strength of the column is $P_u = 2380$ kN (as before), while the magnified design moment is $M_c = \delta_{ns} M_2 = 1.15 \times 237 = 273$ kN-m. As described in Section 9.5, ACI Code 10.10.2 limits the magnified moment to 1.4 times the moment due to first-order effects. This limitation is clearly satisfied. With reference again to the column design chart A.6 with

$$\frac{P_u}{\phi f_c' A_g} = \frac{2380 \times 10^3}{0.65 \times 28 \times 202{,}500} \doteq 0.646$$

$$\frac{M_u}{\phi f_c' A_g h} = \frac{273 \times 10^6}{0.65 \times 28 \times 202{,}500 \times 450} = 0.165$$

it is seen that the required reinforcement ratio is increased from 0.020 to 0.027 because of slenderness. The steel area now required is

$$A_{st} = 0.027 \times 202{,}500 = 5468\text{ mm}^2$$

which can be provided using four No. 32 (No. 10) and four No. 29 (No. 9) bars ($A_{st} = 5856\text{ mm}^2$), arranged as shown in Fig. 9.15. No. 10 (No. 3) ties will be used at a spacing not to exceed the least dimension of the column (450 mm), 48 tie diameters (456 mm), or 16 bar diameters (459 mm). Single ties at 450 mm spacing, as shown in the figure, will meet requirements of the ACI Code.

Further refinements in the design could, of course, be made by recalculating the critical buckling load using Eq. (9.17). This extra step is not justified here because the column slenderness is barely above the upper limit for short column behavior and the moment magnification is not great.

9.7 ACI MOMENT MAGNIFIER METHOD FOR SWAY FRAMES

The important differences in behavior between columns braced against sidesway and columns for which sidesway is possible were discussed in Sections 9.2 and 9.3. The critical load for a column P_c depends on the effective length kl_u, and although the effective length factor k falls between 0.5 and 1.0 for braced columns, it is between 1.0 and ∞ for columns that are unbraced (see Figs. 9.1 and 9.13). Consequently, an unbraced column will buckle at a much smaller load than will a braced column that is otherwise identical.

Columns subject to sidesway do not normally stand alone but are part of a structural system including floors and roof. A floor or roof is normally very stiff in its own plane. Consequently, all columns at a given story level in a structure are subject to essentially identical sway displacements; i.e., sidesway of a particular story can occur only by simultaneous lateral motion of all columns of that story. Clearly, all columns at a given level must be considered together in evaluating slenderness effects relating to sidesway.

On the other hand, it is also possible for a single column in a sway frame to buckle individually under gravity loads, the ends of the column being held against relative lateral movement by other, stiffer columns at the same floor level. This possibility, resulting in magnification of nonsway moments due to gravity loads, must also be considered in the analysis and design of slender columns in unbraced frames.

The ACI moment magnifier approach can still be used for frames subject to sidesway, but it is necessary, according to ACI Code 10.10.7, to separate the loads acting on a structure into two categories: loads that result in no appreciable sidesway and loads that result in appreciable sidesway. Clearly two separate frame analyses are required, one for loads of each type. In general, gravity loads acting on reasonably symmetrical frames produce little sway, and the effects of gravity load may therefore be placed in the first category. This is confirmed by tests and analyses in Ref. 9.13 that show that the sway magnification of gravity moments by the sway multiplier is unwarranted.

The maximum magnified moments caused by sway loading occur at the ends of the column, but those due to gravity loads may occur somewhere in the midheight of the column, the exact location of the latter varying depending on the end moments. Because magnified gravity moments and magnified sway moments do not occur at the same location, the argument can be made that, in most cases, no magnification should be applied to the nonsway moments when sway moments are considered; that is, it is unlikely that the actual maximum moment will exceed the sum of the nonmagnified gravity moment and the magnified sway moment. Consequently, for cases involving sidesway, Eq. (9.13) is replaced by

$$M_1 = M_{1ns} + \delta_s M_{1s} \tag{9.19}$$

$$M_2 = M_{2ns} + \delta_s M_{2s} \tag{9.20}$$

where M_1 = smaller factored end moment on compression member
M_2 = larger factored end moment on compression member
M_{1ns} = factored end moment on compression member at end at which M_1 acts, due to loads that cause no appreciable sidesway, calculated using a first-order elastic frame analysis
M_{2ns} = factored end moment on compression member at end at which M_2 acts, due to loads that cause no appreciable sidesway, calculated using a first-order elastic frame analysis

M_{1s} = factored end moment on compression member at end at which M_1 acts, due to loads that cause appreciable sidesway, calculated using a first-order elastic frame analysis

M_{2s} = factored end moment on compression member at end at which M_2 acts, due to loads that cause appreciable sidesway, calculated using a first-order elastic frame analysis

δ_s = moment magnification factor for frames not braced against sidesway, to reflect lateral drift resulting from lateral (and sometimes gravity) loads

ACI Code 10.10.7 provides two alternate methods for calculating the moment magnification factor for frames not braced against sidesway δ_s.

With the first alternative, the moment magnification factor is calculated as

$$\delta_s = \frac{1}{1 - Q} \geq 1 \tag{9.21}$$

where Q is the stability index calculated using Eq. (9.10). The ACI Code limits application of Eq. (9.21) to values of $\delta_s = 1/(1 - Q) \leq 1.5$. An elastic second-order analysis, as described in ACI Code 10.10.4, or the second alternative described in ACI Code 10.10.7 must be used for higher values of δ_s.

For the second alternative, the moment magnification factor is calculated as

$$\delta_s = \frac{1}{1 - \Sigma P_u / 0.75 \Sigma P_c} \geq 1 \tag{9.22}$$

in which ΣP_u is the total axial load on all columns and ΣP_c is the total critical buckling load for all columns in the story under consideration. As with Eq. (9.14), the 0.75 factor in Eq. (9.22) is a stiffness reduction factor to provide a conservative estimate of the critical buckling loads P_c. The individual values of P_c are calculated using Eq. (9.15) with effective length factors k for unbraced frames (Fig. 9.13*b*) and values of EI from Eq. (9.17) or (9.18).

When calculating δ_s, the factor β_{ds} is defined differently than β_{dns} is for nonsway frames. As described earlier, in Section 9.5, β_{ds} is the ratio of the maximum factored sustained shear within a story to the maximum factored shear in that story. Thus, for most applications, $\beta_{ds} = 0$ for the purpose of calculating δ_s. In unusual situations, $\beta_{ds} \neq 0$ will occur, such as a building located on a sloping site that is subjected to soil pressure on a single side (Refs. 9.14 and 9.15).

The sequence of design steps for slender columns in sway frames is similar to that outlined in Section 9.6 for nonsway frames, except for the requirement that loads be separated into gravity loads, which are assumed to produce no sway, and horizontal loads producing sway. Separate frame analyses are required, and different equivalent length factors k and creep coefficients β_{dns} and β_{ds} must be applied. Note that according to ACI Code 9.2 (see also Table 1.2 of Chapter 1), if wind effects W are included in the design, four possible factored load combinations are to be applied:

$$U = 1.2D + 1.6L$$

$$U = 1.2D + 1.6(L_r \text{ or } S \text{ or } R) + 0.8W$$

$$U = 1.2D + 1.6W + 1.0L + 0.5(L_r \text{ or } S \text{ or } R)$$

$$U = 0.9D + 1.6W$$

Similar provisions are included for cases where earthquake loads are to be considered. This represents a significant complication in the sway frame analysis; however, the factored loads can be separated into gravity effects and sway effects, as required, and a separate analysis can be performed for each.

It is important to realize that, for sway frames, *the beams must be designed for the total magnified end moments of the compression members at the joint.* Even though the columns may be very rigid, if plastic hinges were to form in the restraining beams adjacent to the joints, the effective column length would be greatly increased and the critical column load much reduced.

The choice of which of the methods to use for calculating δ_s depends upon the desired level of accuracy and the available analytical tools.

Second-order analysis (discussed in greater detail in Section 9.8) provides the most accurate estimate of the magnified sway moments but requires more sophisticated techniques. The extra effort required for second-order analysis, however, usually produces a superior design. The first alternative, Eq. (9.21), will in most cases be the easiest to apply, since matrix analysis is used for virtually all frames to determine member forces under gravity and lateral loading. Such an analysis automatically generates the value of Δ_o, the first-order relative deflection within a story, allowing Q to be calculated for each story within a structure. The second alternative, Eq. (9.22), is retained with minor modifications from previous versions of the ACI Code. As will be demonstrated in the following example, calculations using Eq. (9.22) are more tedious than those needed for Eq. (9.21) but do not require knowledge of Δ_o. Application of Eq. (9.21) is limited by the Code to values of $\delta_s \leq 1.5$. For $\delta_s > 1.5$, application of Eq. (9.22) is mandatory if a second-order analysis is not used.

EXAMPLE 9.2

Design of a slender column in a sway frame. Consider now that the concrete building frame of Example 9.1 acts as a *sway frame*, without the stairwells or elevator shafts described earlier. An initial evaluation is carried out using the member dimensions and reinforcement given in Example 9.1. The reinforcement for the interior 450 × 450 mm columns, shown in Fig. 9.15, consists of four No. 32 (No. 10) bars at the corners and four No. 29 (No. 9) bars at the center of each side. Reinforcement for the exterior 400 × 400 mm columns consists of eight No. 25 (No. 8) bars distributed in a manner similar to that shown for the longitudinal reinforcement in Fig. 9.15. The building will be subjected to gravity dead and live loads and horizontal wind loads. Elastic first-order analysis of the frame at service loads (all load factors = 1.0) using the values of E and I defined in Section 9.5 gives the following results at the third story:

	Cols. A3 *and* F3	*Cols.* B3 *and* E3	*Cols.* C3 *and* D3
P_{dead}	496 kN	990 kN	990 kN
P_{live}	388 kN	745 kN	745 kN
P_{wind}	±129 kN	±78 kN	±26 kN
V_{wind}	24 kN	48 kN	48 kN
$M_{2,\text{dead}}$			3 kN-m
$M_{2,\text{live}}$			146 kN-m
$M_{2,\text{wind}}$			±102 kN-m
$M_{1,\text{dead}}$			−3 kN-m
$M_{1,\text{live}}$			135 kN-m
$M_{1,\text{wind}}$			±92 kN-m

To simplify the analysis in this example, roof loads will not be considered. The relative lateral deflection for the third story under total wind shear $V_{\text{wind}} = 240$ kN is 20 mm.

Column *C*3 is to be designed for the critical loading condition, using $f'_c = 28$ MPa and $f_y = 420$ MPa as before.

Solution. The column size and reinforcement must satisfy requirements for each of the four load conditions noted above.

Initially, a check is made to see if a sway frame analysis is required. The factored shear $V_{us} = 1.6 \times V_{\text{wind}} = 1.6 \times 240 = 384$ kN. The corresponding deflection $\Delta_o = 1.6 \times 20 = 32$ mm. The total factored axial force on the story is obtained using the load table.

Columns $A3$ and $F3$: $P_u = 1.2 \times 496 + 1.0 \times 388 = 983$ kN

Columns $B3$, $C3$, $D3$, and $E3$: $P_u = 1.2 \times 990 + 1.0 \times 745 = 1933$ kN

Note that in this case the values of P_{wind} in the columns are not considered since they cancel out for the floor as a whole, i.e., $\Sigma P_{\text{wind}} = 0$. Thus, $\Sigma P_u = 2 \times 983 + 4 \times 1933 = 9698$ kN, and the stability index is

$$Q = \frac{\Sigma P_u \Delta_o}{V_{us} l_c} = \frac{9698 \times 32}{384 \times 4250} = 0.19$$

Since $Q > 0.05$, sway frame analysis is required for this story.

(a) Gravity loads only. All columns in sway frames must first be considered as braced columns under gravity loads acting alone, i.e., for $U = 1.2D + 1.6L$. This check has already been made for column $C3$ in Example 9.1.

(b) Gravity plus wind loads. Three additional load combinations must be considered when wind effects are included: $U = 1.2D + 1.6(L_r \text{ or } S \text{ or } R) + 0.8W$, $U = 1.2D + 1.6W + 1.0L + 0.5(L_r \text{ or } S \text{ or } R)$, and $U = 0.9D + 1.6W$. By inspection, the second combination will control for this case, and the others will not be considered further. From Example 9.1, $\psi_a = \psi_b = 2.17$. With reference to the alignment chart in Fig. 9.13*b*, the effective length factor for an unbraced frame $k = 1.64$ and

$$\frac{kl_u}{r} = \frac{1.64 \times 3950}{0.3 \times 450} = 48.0$$

This is much above the limit value of 22 for short column behavior in an unbraced frame. (This should be no surprise since $kl_u/r = 25.1$ for column $C3$ in the braced condition.) For sway frame analysis, the loads must be separated into gravity loads and sway loads, and the appropriate magnification factor must be computed and applied to the sway moments. The factored end moments resulting from the nonsway loads on column $C3$ are

$$M_{1ns} = 1.2 \times (-3) + 1.0 \times 135 = 131 \text{ kN-m}$$

$$M_{2ns} = 1.2 \times 3 + 1.0 \times 146 = 150 \text{ kN-m}$$

The sway effects will amplify the moments:

$$M_{1s} = 1.6(-92) = -147 \text{ kN-m}$$

$$M_{2s} = 1.6 \times 102 = 163 \text{ kN-m}$$

For the purposes of comparison, the magnified sway moments will be calculated based on both Q [Eq. (9.21)] and $\Sigma P_u/\Sigma P_c$ [Eq. (9.22)].

Using Eq. (9.21),

$$\delta_s = \frac{1}{1 - Q} = \frac{1}{1 - 0.19} = 1.23$$

giving

$$\delta_s M_{1s} = 1.23 \times (-147) = -181 \text{ kN-m}$$

$$\delta_s M_{2s} = 1.23 \times 163 = 200 \text{ kN-m}$$

To use Eq. (9.22), the critical loads must be calculated for each of the columns as follows. For columns $A3$ and $F3$,

Columns: $I = 0.7I_g = 0.7 \times 400 \times 400^3/12 = 1.493 \times 10^9 \text{ mm}^4$
and $I/l_c = 1.493 \times 10^9/4250 = 3.51 \times 10^5 \text{ mm}^3$

Beams: $I = 1.89 \times 10^9 \text{ mm}^4$ and $I/l_c = 2.59 \times 10^5 \text{ mm}^3$

Rotational restraint factors for this case, with two columns and one beam framing into the joint, are

$$\psi_a = \psi_b = \frac{3.51 \times 10^5 + 3.51 \times 10^5}{2.59 \times 10^5} = 2.71$$

which, with reference to the alignment chart for unbraced frames, gives $k = 1.77$. For wind load, $\beta_{ds} = 0$. Since reinforcement has been initially selected for one column, EI will be calculated using Eq. (9.17).

$$EI = 0.2E_cI_g + E_sI_{se} = 0.2 \times 4700\sqrt{28} \times 400 \times 400^3/12 + 200{,}000 \times 6 \times 510 \times 138^2$$

$$= 2.23 \times 10^{13}\ \text{N-mm}^2 = 2.23 \times 10^{10}\ \text{kN-mm}^2$$

Then the critical load is

$$P_c = \frac{\pi^2 \times 2.23 \times 10^{10}}{(1.77 \times 3950)^2} = 4503\ \text{kN}$$

For columns $B3$, $C3$, $D3$, and $E3$, from earlier calculations for column $C3$, $k = 1.64$ for the sway loading case. For these columns,

$$EI = 0.2 \times 4700\sqrt{28} \times 450 \times 450^3/12 + 200{,}000(4 \times 819 \times 159^2 + 2 \times 645 \times 161^2)$$

$$= 4.02 \times 10^{13}\ \text{N-mm}^2 = 4.02 \times 10^{10}\ \text{kN-mm}^2$$

$$P_c = \frac{\pi^2 \times 4.02 \times 10^{10}}{(1.64 \times 3950)^2} = 9455\ \text{kN}$$

Thus, for all the columns at this level of the structure,

$$\Sigma P_c = 2 \times 4503 + 4 \times 9455 = 46{,}826\ \text{kN}$$

The sway moment magnification factor is

$$\delta_s = \frac{1}{1 - \Sigma P_u/0.75\Sigma P_c} = \frac{1}{1 - 9698/(0.75 \times 46{,}826)} = 1.38$$

and the magnified sway moments for the top and bottom of column $C3$ are

$$\delta_s M_{1s} = 1.38 \times (-147) = -203\ \text{kN-m}$$

$$\delta_s M_{2s} = 1.38 \times 163 = 225\ \text{kN-m}$$

The values of $\delta_s M_s$ are higher based on $\Sigma P_u/\Sigma P_c$ than they are based on Q (225 kN-m vs. 200 kN-m for $\delta_s M_{2s}$), emphasizing the conservative nature of the moment magnifier approach based on Eq. (9.22). The design will proceed using the less conservative value of $\delta_s M_s$.

The total magnified moments are

$$M_1 = 131 - 181 = -50\ \text{kN-m}$$

$$M_2 = 150 + 200 = 350\ \text{kN-m}$$

The values do not exceed the upper limit of 1.4 times the moments due to first-order effects and will now be combined with factored axial load $P_u = 1975$ kN (now including $1.6P_{\text{wind}}$). In reference to Graph A.6 with column parameters

$$\frac{P_u}{\phi f'_c A_g} = \frac{1975 \times 10^3}{0.65 \times 28 \times 202{,}500} = 0.536$$

$$\frac{M_u}{\phi f'_c A_g h} = \frac{350 \times 10^6}{0.65 \times 28 \times 202{,}500 \times 450} = 0.211$$

it is seen that $\rho_g = 0.037$. This is considerably higher than the value of 0.026 required for column $C3$ in a braced frame. The required steel area of

$$A_{st} = 0.037 \times 202{,}500 = 7493\ \text{mm}^2$$

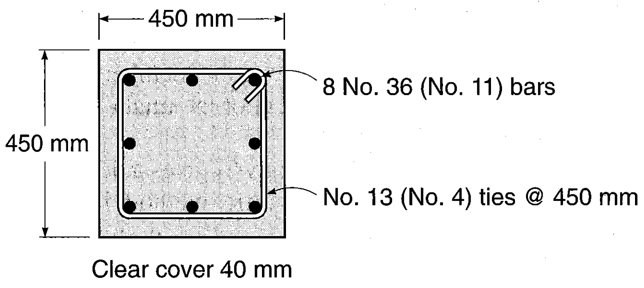

FIGURE 9.16
Cross section of column *C*3, Example 9.2.

will be provided using eight No. 36 (No. 11) bars, arranged as shown in Fig. 9.16. Spacing of No. 13 (No. 4) ties must not exceed the least dimension of the column, 48 tie diameters, or 16 main bar diameters. The first criterion controls, and No. 13 (No. 4) ties at 450 mm spacing will be used in the pattern shown in Fig. 9.16.

9.8 SECOND-ORDER ANALYSIS FOR SLENDERNESS EFFECTS

It may be evident from the preceding examples that although the ACI moment magnifier method works well enough for nonsway frames, its application to sway frames is complicated, with many opportunities for error, especially when Eq. (9.22) is used to calculate δ_s.

With the universal availability of computers in design offices, and because of the complexity of the moment magnifier method, it is advantageous to apply rational second-order frame analysis, or P-Δ analysis, in which the effects of lateral deflection on moments, axial forces, and, in turn, lateral deflections are computed directly. The resulting moments and deflections include the effects of slenderness, and so the problem is strictly nonlinear, whether the model used for the analysis is nonlinear (ACI Code 10.10.3) or elastic (ACI Code 10.10.4).

Nonlinear second-order analysis in accordance with ACI Code 10.10.3 must account for the effects of material nonlinearity, member curvature and lateral drift, load duration, shrinkage and creep, and the interaction between the frame and the supporting foundation. ACI Code 10.10.3 requires that the second-order analysis procedure be one that provides a strength prediction that is in "substantial agreement" with test results for reinforced concrete columns in statically indeterminate frames. ACI Commentary 10.10.3 suggests that a prediction within 15 percent of the test results is satisfactory. It also suggests that a stiffness reduction factor ϕ_K of 0.80 be used to account for variations in actual member properties and for consistency with elastic second-order analysis under ACI Code 10.10.4.

Elastic second-order analysis in accordance with ACI Code 10.10.4 must consider the effects of axial loads, cracked regions within the members, and load duration, and although elastic models are simpler to implement than nonlinear models, as pointed out in Ref. 9.16, the key requirement for EI values for second-order frame analysis, whether elastic of nonlinear, is that they be representative of member stiffness just prior to failure. The values of E and I in Section 9.5, which are taken from ACI Code 10.10.4, meet that requirement and include a stiffness reduction factor of 0.875 (Ref. 9.16). The value of the stiffness reduction factor and the moments of inertia in Section 9.5 are higher than the factor 0.75 in Eqs. (9.14) and (9.21) and the effective values of I in

Eqs. (9.17) and (9.18), respectively, because of the inherently lower variability in the total stiffness of a frame compared to that of an individual member.

As pointed out in Section 9.5, the member dimensions used in any second-order analysis must be within 10 percent of the final dimensions. Otherwise, the frame must be reanalyzed.

A rational second-order analysis gives a better approximation of actual moments and forces than the moment magnifier method. Differences are particularly significant for irregular frames, for frames subject to significant sway forces, and for lightly braced frames. There may be important economies in the resulting design.

Practical methods for performing a full second-order analysis are described in the literature (Refs. 9.3, 9.17, 9.18, 9.19, and 9.20 to name a few), and general-purpose programs that perform a full nonlinear analysis including sway effects are commercially available. Linear first-order analysis programs are also available, but must include an iterative approach to produce acceptable results. This iterative approach can be summarized as follows.

Figure 9.17*a* shows a simple frame subject to lateral loads H and vertical loads P. The lateral deflection Δ is calculated by ordinary first-order analysis. As the frame is displaced laterally, the column end moments must equilibrate the lateral loads and a moment equal to $(\Sigma P)\Delta$:

$$\Sigma (M_{\text{top}} + M_{\text{bot}}) = Hl_c + \Sigma P \Delta \tag{9.23}$$

where Δ is the lateral deflection of the top of the frame with respect to the bottom, and ΣP is the sum of the vertical forces acting. The moment $\Sigma P \Delta$ in a given story can be represented by equivalent shear forces $(\Sigma P)\Delta/l_c$, where l_c is the story height, as shown in Fig. 9.17*b*. These shears give an overturning moment equal to that of the loads P acting at a displacement Δ.

Figure 9.17*c* shows the story shears acting in a three-story frame. The algebraic sum of the story shears from the columns above and below a given floor corresponds in effect to a sway force dH acting on that floor. For example, at the second floor the sway force is

$$dH_2 = \frac{\Sigma P_1 \Delta_1}{l_1} - \frac{\Sigma P_2 \Delta_2}{l_2} \tag{9.24}$$

The sway forces must be added to the applied lateral force H at any story level, and the structure is then reanalyzed, giving new deflections and increased moments. If the lateral deflections increase significantly (say more than 5 percent), new dH sway forces are computed, and the structure is reanalyzed for the sum of the applied lateral forces and the new sway forces. Iteration is continued until changes are insignificant. Generally one or two cycles of iteration are adequate for structures of reasonable lateral stiffness (Ref. 9.3).

It is noted in Ref. 9.17 that a correction must be made in the analysis to account for the differences in shape between the $P\Delta$ moment diagram that has the same shape as the deflected column, and the moment diagram associated with the $P\Delta/l$ forces, which is linear between the joints at the column ends. The area of the actual $P\Delta$ moment diagram is larger than the linear equivalent representation, and consequently lateral deflections will be larger. The difference will vary depending on the relative stiffnesses of the column and the beams framing into the joints. In Ref. 9.17, it is suggested that the increased deflection can be accounted for by taking the sway forces dH as 15 percent greater than the calculated value for each iteration. Iteration and the

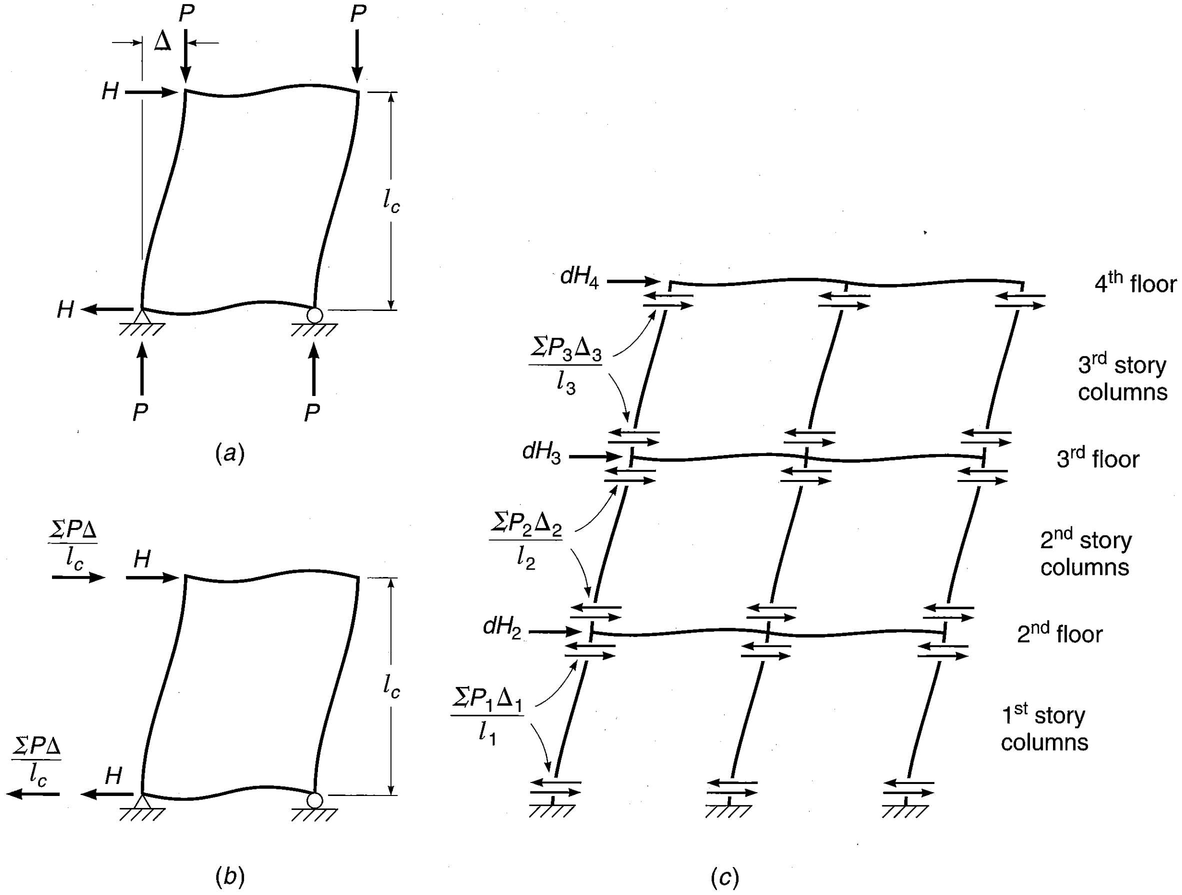
P
P
Δ
H
H
l_c
P
P
$\frac{\Sigma P\Delta}{l_c}$
H
$\frac{\Sigma P\Delta}{l_c}$
H
l_c
dH_4
$\frac{\Sigma P_3\Delta_3}{l_3}$
dH_3
$\frac{\Sigma P_2\Delta_2}{l_2}$
dH_2
$\frac{\Sigma P_1\Delta_1}{l_1}$
4th floor
3rd story columns
3rd floor
2nd story columns
2nd floor
1st story columns

(*a*)

(*b*) (*c*)

FIGURE 9.17

Basis for iterative P-Δ analysis: (*a*) vertical and lateral loads on rectangular frame; (*b*) real lateral forces H and fictitious sway forces dH; (*c*) three-story frame subject to sway forces. (*Adapted from Ref. 9.17.*)

15 percent increase in deflection are not required if the program performs a full nonlinear geometric analysis, since the $P\Delta$ moments are calculated in full.

The accuracy of the results of a P-Δ analysis will be strongly influenced by the values of member stiffness used, by foundation rotations, if any, and by the effects of concrete creep. In connection with creep effects, lateral loads causing significant sway are usually wind or earthquake loads of short duration, so creep effects are minimal. In general, the use of sway frames to resist *sustained* lateral loads, e.g., from earth or liquid pressures, is not recommended, and it would be preferable to include shear walls or other elements to resist these loads.

REFERENCES

9.1. S. P. Timoshenko and J. M. Gere, *Theory of Elastic Stability*, 3d ed., McGraw-Hill, New York, 1969.

9.2. T. V. Galambos (ed.), *Guide to Stability Design Criteria for Metal Structures*, 5th ed., John Wiley & Sons, New York, 1998.

9.3. J. G. MacGregor and S. E. Hage, "Stability Analysis and Design of Concrete Frames," *J. Struct. Div.*, ASCE, vol. 103, no. ST10, 1977, pp. 1953–1977.

9.4. S.-M. A. Lai and J. G. MacGregor, "Geometric Nonlinearities in Unbraced Multistory Frames," *J. Struct. Eng.*, ASCE, vol. 109, no. 11, 1983, pp. 2528–2545.

9.5. M. Khuntia and S. K. Ghosh, "Flexural Stiffness of Reinforced Concrete Columns and Beams: Analytical Approach," *ACI Struct. J.*, vol. 101, no. 3, 2004, pp. 351–363.

9.6. M. Khuntia and S. K. Ghosh, "Flexural Stiffness of Reinforced Concrete Columns and Beams: Experimental Verification," *ACI Struct. J.*, vol. 101, no. 3, 2004, pp. 364–374.

9.7. J. G. MacGregor, J. E. Breen, and E. O. Pfrang, "Design of Slender Concrete Columns," *J. ACI*, vol. 67, no. 1, 1970, pp. 6–28.

9.8. J. G. MacGregor, V. H. Oelhafen, and S. E. Hage, "A Reexamination of the *EI* Value for Slender Columns," *Reinforced Concrete Columns*, American Concrete Institute, Detroit, MI, 1975, pp. 1–40.

9.9. *Code of Practice for the Structural Use of Concrete*, Part 1, "Design Materials and Workmanship," (CP110: Part 1, 1972), British Standards Institution, London, 1972.

9.10. W. B. Cranston, "Analysis and Design of Reinforced Concrete Columns," *Research Report* No. 20, Paper 41.020, Cement and Concrete Association, London, 1972.

9.11. R. W. Furlong, "Column Slenderness and Charts for Design," *J. ACI*, vol. 68, no. 1, 1971, pp. 9–18.

9.12. M. Valley and P. Dumonteil, Disc. of "*K*-Factor Equation to Alignment Charts for Column Design," by L. Duan, W.-S. King, and W.-F. Chen, *ACI Struct. J.*, vol. 91, no. 2, Mar.-Apr. 1994, pp. 229–230.

9.13. J. S. Ford, D. C. Chang, and J. E. Breen, "Design Indications from Tests of Unbraced Multipanel Concrete Frames," *Concr. Intl.*, vol. 3, no. 3, 1981, pp. 37–47.

9.14. *Building Code Requirements for Structural Concrete*, ACI 318-02, American Concrete Institute, Farmington Hills, MI, 2002.

9.15. *Commentary on Building Code Requirements for Structural Concrete*, ACI 318R-02, American Concrete Institute, Farmington Hills, MI, 2002 (published as part of Ref. 9.14).

9.16. J. G. MacGregor, "Design of Slender Concrete Columns —Revisited," *ACI Struct. J.*, vol. 90, no. 3, 1993, pp. 302–309.

9.17. J. G. MacGregor, *Reinforced Concrete*, 3d ed., Prentice-Hall, Upper Saddle River, NJ, 1997.

9.18. B. R. Wood, D. Beaulieu, and P. F. Adams, "Column Design by *P*-Delta Model," *Proc. ASCE*, vol. 102, no. ST2, 1976, pp. 487–500.

9.19. B. R. Wood, D. Beaulieu, and P. F. Adams, "Further Aspects of Design by *P*-Delta Model," *J. Struct. Div.*, ASCE, vol. 102, no. ST3, 1976, pp. 487–500.

9.20. R. W. Furlong, "Rational Analysis of Multistory Concrete Structures," *Concr. Intl.*, vol. 3, no. 6, 1981, pp. 29–35.

PROBLEMS

9.1. The 375 × 375 mm column shown in Fig. P9.1 must extend from footing level to the second floor of a braced frame structure with an unsupported length of 6.15 m. Exterior exposure requires 50 mm clear cover for the outermost steel. Analysis indicates the critical loading corresponds with the following

FIGURE P9.1

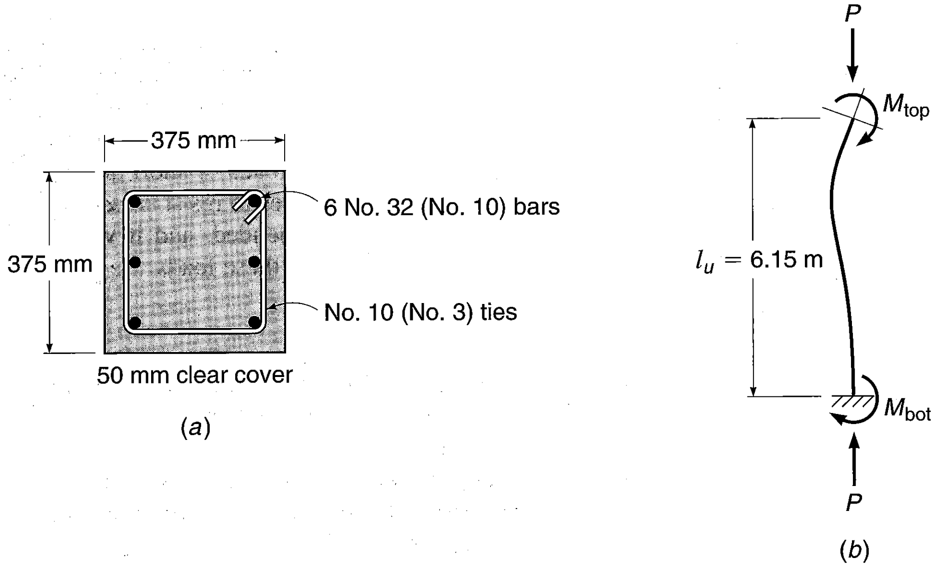

service loads: (*a*) from dead loads, $P = 733$ kN, $M_{\text{top}} = 39$ kN-m, $M_{\text{bot}} = 19.5$ kN-m; (*b*) from live loads, $P = 430$ kN, $M_{\text{top}} = 67.5$ kN-m, $M_{\text{bot}} = 33.5$ kN-m, with the column bent in double curvature as shown. The effective length factor k determined using Fig. 9.13*a* is 0.90. Material strengths are $f'_c = 28$ MPa and $f_y = 420$ MPa. Using the ACI moment magnifier method, determine whether the column is adequate to resist these loads.

9.2. The structure shown in Fig. P9.2*a* requires tall slender columns at the left side. It is fully braced by shear walls on the right. All columns are 400 × 400 mm, as shown in Fig. P9.2*b*, and all beams are 600 × 450 mm with 150 mm monolithic floor slab, as in Fig. P9.2*c*. Trial calculations call for column reinforcement as shown. Alternate load analysis indicates the critical condition with column *AB* bent in single curvature, and service loads and moments as follows: from dead loads, $P = 600$ kN, $M_{\text{top}} = 81$ kN-m, $M_{\text{bot}} = 55$ kN-m; from live load, $P = 401$ kN, $M_{\text{top}} = 55$ kN-m, $M_{\text{bot}} = 36$ kN-m. Material strengths are $f'_c = 28$ MPa and $f_y = 420$ MPa. Is the proposed column, reinforced as shown, satisfactory for this load condition? Use Eq. (9.18) to calculate *EI* for the column.

FIGURE P9.2

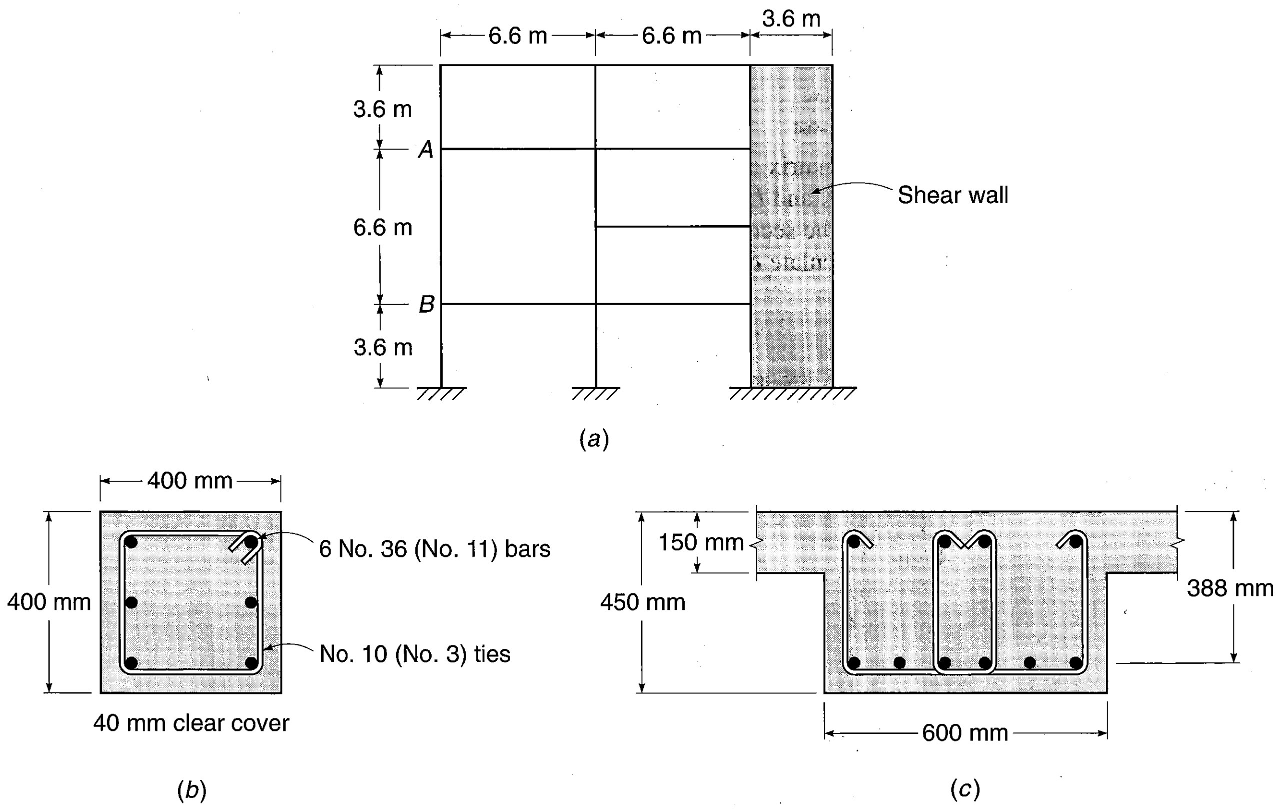

9.3. Refine the calculations of Problem 9.2, using Eq. (9.17) to calculate *EI* for the column. The reinforcement will be as given in Problem 9.2. Comment on your results.

9.4. An interior column in a braced frame has an unsupported length of 6 m and carries the following service load forces and moments: (*a*) from dead loads, $P = 775$ kN, $M_{\text{top}} = 38$ kN-m, $M_{\text{bot}} = -38$ kN-m; (*b*) from live loads,

$P = 950$ kN, $M_{\text{top}} = 151$ kN-m, $M_{\text{bot}} = 151$ kN-m, with the signs of the moments representing double curvature under dead load and single curvature under live load. Rotational restraint factors at the top and bottom may be taken equal to 1.0. Design a square tied column to resist these loads, with a reinforcement ratio of about 0.02. Use $f_c' = 28$ MPa and $f_y = 420$ MPa.

9.5. The first three floors of a multistory building are shown in Fig. P9.5. The lateral load resisting frame consists of 500 × 500 mm exterior columns, 600 × 600 mm interior columns, and 900 mm wide × 600 mm deep girders. The center-to-center column height is 4.8 m. For the second-story columns, the service gravity dead and live loads and the horizontal wind loads based on an elastic first-order analysis of the frame are:

	Cols. A2 *and* E2	*Cols.* B2 *and* D2	*Col.* C2
P_{dead}	1501 kN	3266 kN	2968 kN
P_{live}	591 kN	1324 kN	1272 kN
P_{wind}	±82 kN	±39 kN	0 kN
V_{wind}	29 kN	60 kN	60 kN
$M_{2,\text{dead}}$		177 kN-m	
$M_{2,\text{live}}$		218 kN-m	
$M_{2,\text{wind}}$		142 kN-m	
$M_{1,\text{dead}}$		−46 kN-m	
$M_{1,\text{live}}$		140 kN-m	
$M_{1,\text{wind}}$		−133 kN-m	

A matrix analysis for the total unfactored wind shear of 238 kN, using values of E and I specified in Section 9.5, indicates that the relative lateral deflection of the second story is 6.1 mm. Design columns $B2$ and $D2$ using Eq. (9.21) to calculate δ_s. Material strengths are $f_c' = 28$ MPa and $f_y = 420$ MPa.

FIGURE P9.5

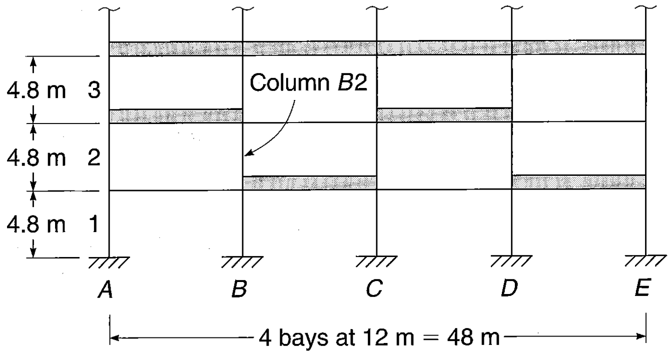

9.6. Repeat Problem 9.5, using Eq. (9.22) to calculate δ_s. Comment on your results.

9.7. Redesign column $C3$ from Example 9.2 for a story height of 4.8 m, a column unsupported length of 4.5 m, and a relative lateral displacement of the third story of 28 mm. Loads and other dimensions remain unchanged.

9.8. The first four floors of a multistory building are shown in Fig. P9.8. The lateral load-resisting frame consists of 550 × 550 mm exterior columns, 650 × 650 mm interior columns, and 825 mm wide × 450 mm deep girders. The foundation is at ground level, supported on drilled piers, and may be considered as fully fixed against rotation. The first-story columns have a clear height to the girder soffit of 6.45 m, giving a floor-to-floor height of 6.9 m. The upper floors have a center-to-center spacing of 3.9 m. For the first-story columns, the service gravity dead and live loads plus the horizontal and vertical wind loads based on an elastic first-order analysis of the frame are:

	Cols. A*1 and* F*1*	*Cols.* B*1 and* E*1*	*Cols.* C*1 and* D*1*
P_{dead}	2136 kN	4703 kN	4267 kN
P_{live}	427 kN	888 kN	811 kN
P_{wind}	±138 kN	±82 kN	±26 kN
V_{wind}	49 kN	98 kN	98 kN
$M_{2,\text{dead}}$		5 kN-m	
$M_{2,\text{live}}$		95 kN-m	
$M_{2,\text{wind}}$		325 kN-m	
$M_{1,\text{dead}}$		−3 kN-m	
$M_{1,\text{live}}$		−47 kN-m	
$M_{1,\text{wind}}$		−325 kN-m	

A matrix analysis for the total unfactored wind shear of 490 kN, using values of E and I specified in Section 9.5, indicates that the relative lateral deflection of the second story is 10.2 mm. Design columns $B1$ and $E1$, using Eq. (9.21) to calculate δ_s. Material strengths are $f_c' = 28$ MPa and $f_y = 420$ MPa.

FIGURE P9.8

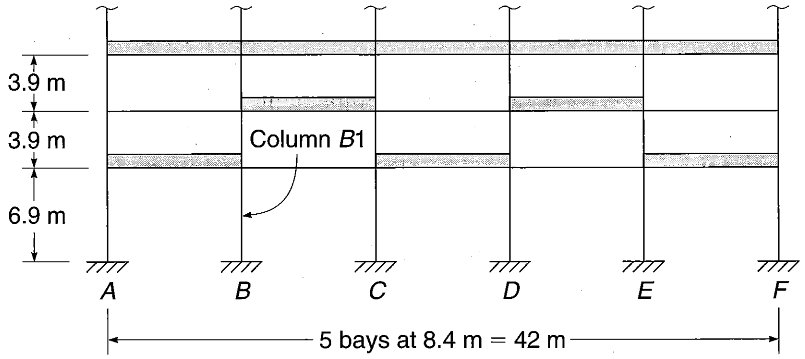

9.9. Repeat Problem 9.8, using Eq. (9.22) to calculate δ_s. Comment on your results.

10

Strut-and-Tie Models

10.1 INTRODUCTION

Reinforced concrete beam theory is based on equilibrium, compatibility, and the constitutive behavior of the materials, steel and concrete. Of particular importance is the assumption that strain varies linearly through the depth of a member and that, as a result, plane sections remain plane. This assumption is validated by St. Venant's principle, which stipulates that strains induced by discontinuities in load or in member cross section vary in an approximately linear fashion at distances greater than or equal to the greatest cross-sectional dimension h from the point of load application. St. Venant's principle underlies the development of beam theory as presented in Chapters 1 and 3.

St. Venant's principle, however, does not apply at points closer than the distance h to discontinuities in applied load or geometry. This leads to the identification of *discontinuity regions* within reinforced concrete members near concentrated loads, openings, or changes in cross section. Because of their geometry, the full volume of deep beams and column brackets qualify as discontinuity regions. Thus, reinforced concrete structures may be divided into regions where beam theory is valid, often referred to as *B-regions*, and regions where discontinuities affect member behavior, known as *D-regions*. A number of D-regions are illustrated in Fig. 10.1.

At low stresses, when the concrete is elastic and uncracked, the stresses within D-regions may be computed using finite element analysis or elasticity theory. When concrete cracks, the strain field is disrupted, causing a redistribution of the internal forces. Once this happens, it is possible to represent the internal forces within discontinuity regions using a statically determinate truss, referred to as a *strut-and-tie model*. This allows a complex design problem to be greatly simplified, producing a safe solution that satisfies statics. As shown in Fig. 10.2, strut-and-tie models consist of concrete compression *struts*, steel tension *ties*, and joints that are referred to as *nodal zones* (for consistency of presentation, struts are represented by dashed lines and ties are represented by solid lines).

10.2 DEVELOPMENT OF STRUT-AND-TIE MODELS

Strut-and-tie models evolved in the early 1980s in Europe (Refs. 10.1 to 10.4). Their use is permitted by ACI Code 8.3.4 and defined in Appendix A of the Code (Ref. 10.5). As defined, strut-and-tie models divide members into D-regions and B-regions. A D-region is that portion of a member that is within a distance equal to the member

FIGURE 10.1
Geometric and load discontinuities for D-regions.

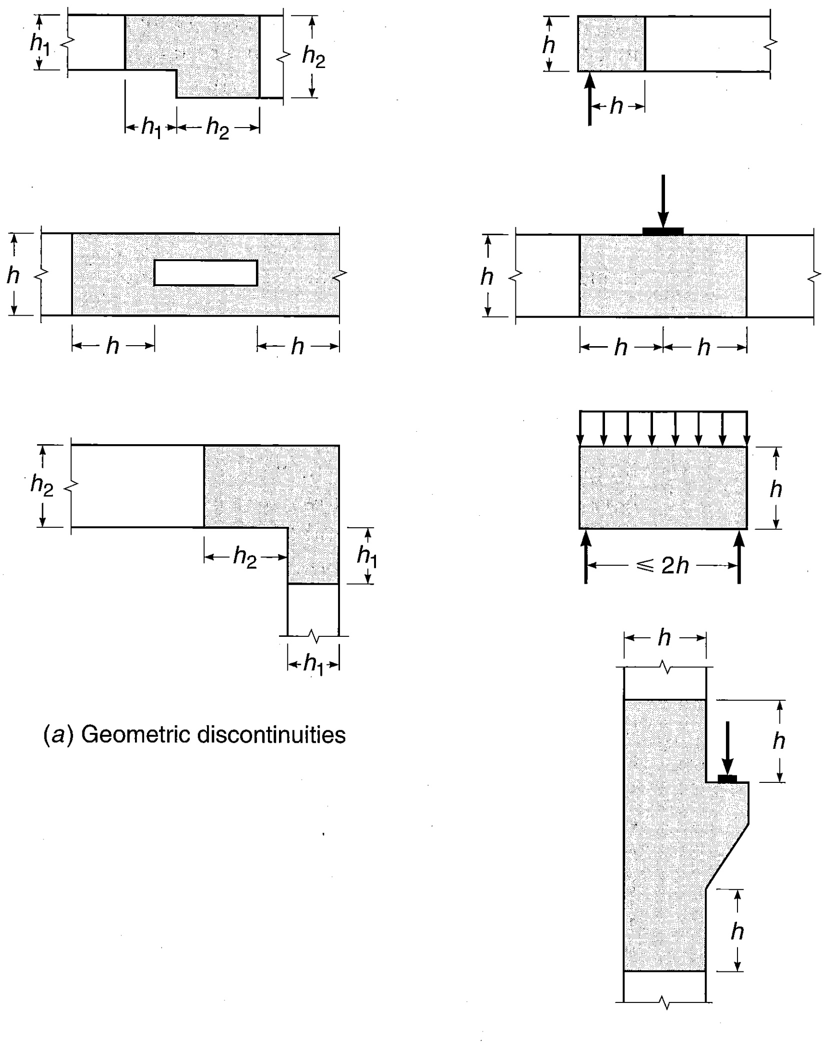
h_1
h_2
h_1
h_2
h
h
h
h
h
h
h
h
h_2
h_2
h_1
h_1
h
$\leqslant 2h$
h
h
h

(*a*) Geometric discontinuities

(*b*) Loading discontinuities

FIGURE 10.2
Strut-and-tie model.

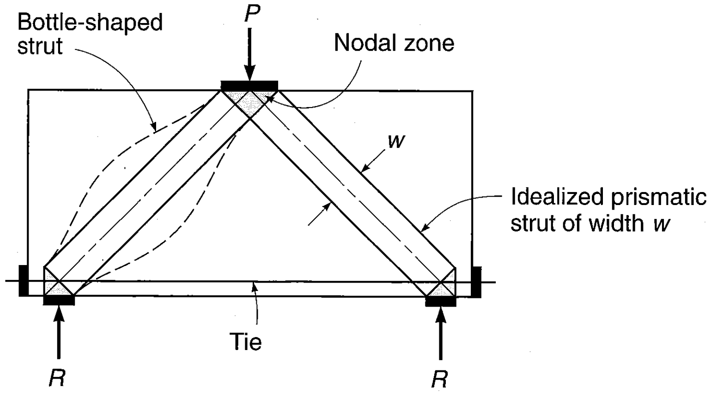
Bottle-shaped strut
P
Nodal zone
w
Idealized prismatic strut of width w
Tie
R
R

height h[†] from a force or geometric discontinuity, as shown in Fig. 10.1. B-regions are, in general, any portions of a member outside of D-regions. The assumption is that within B-regions strain varies linearly through the member cross section and plane sections remain plane.

Strut-and-tie models are applied within D-regions. Models consist of struts and ties connected at nodal zones that are capable of transferring loads to the supports or adjacent B-regions. The cross-sectional dimensions of the struts and ties are designated as thickness and width. Thickness b is perpendicular to the plane of the truss model, and width w is measured in the plane of the model, as shown in Fig. 10.2.

a. Struts

A strut is an internal compression member. It may consist of a single element, parallel elements, or a fan-shaped compression field. Along its length, a strut may be rectangular or *bottle-shaped,* in which case the compression field spreads laterally between nodal zones, as shown in Fig. 10.3. For design purposes, a strut is typically idealized as a prismatic member between two nodes. While not preferred, a strut can also be idealized as a uniformly tapered compression member if the design criteria require different widths at the two ends of the strut. The dimensions of the cross section of the strut are established by the contact area between the strut and the nodal zone. Bottle-shaped struts are wider at the center than at the ends and form when the surrounding concrete permits the compression field to spread laterally. As the compression zone spreads along the length of bottle-shaped struts, tensile stresses perpendicular to the axis of the strut may result in longitudinal cracking. For simplicity in design, bottle-shaped struts are idealized as having linearly tapered ends and uniform center sections. The linear taper is taken at a slope of 1:2 to the axis of the compression force, as shown in Fig. 10.3*b*. The capacity of a strut is a function of the effective concrete compressive strength, which is affected by lateral stresses within the struts. Because of longitudinal splitting, bottle-shaped struts are weaker than rectangular struts, even though they possess a larger cross section at midlength. Transverse reinforcement is designed to control longitudinal splitting and proportioned using a strut-and-tie model that forms within the strut element, as shown in Fig. 10.3*b*.

FIGURE 10.3
Bottle-shaped strut.

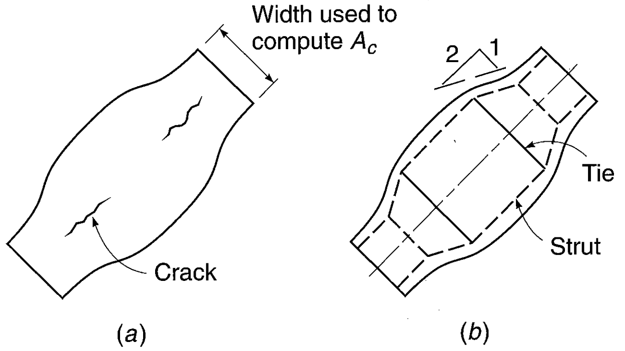

[†] The ACI Code defines a D-region based on the member height h or effective depth d. No guidance is provided when to use h or d. The member height h is used in this text because it is conservative, always defining a larger D-region than that defined by the effective depth d.

b. Ties

A tie is a tension member within a strut-and-tie model. Ties consist of reinforcement (prestressed or nonprestressed) plus a portion of the concrete that is concentric with and surrounds the axis of the tie. The surrounding concrete defines the tie area and the region available to anchor the tie. For design purposes, it is assumed that the concrete within the tie does not carry any tensile force. Even though the tensile capacity of the concrete is not used in design, it assists in reducing tie deformation at service load.

c. Nodal Zones

Nodes are points within strut-and-tie models where the axes of struts, ties, and concentrated loads intersect. A nodal zone is the volume of concrete around a node where force transfer occurs. A nodal zone may be treated as a single region or may be subdivided into two smaller zones to equilibrate forces. For example, the nodal zone shown in Fig. 10.4*a* is subdivided, as shown in Fig. 10.4*b*, where two reactions R_1 and R_2 equilibrate the vertical components of strut forces C_1 and C_2.

For equilibrium, at least three forces must act on a node. Nodes are classified by the sign of these forces (Fig. 10.5). Thus, a *C-C-C* node resists three compressive forces, and a *C-C-T* node resists two compressive forces and one tensile force. Both tensile and compressive forces place nodes in compression because tensile forces are treated as if they pass through the node and apply a compressive force on the far side, or anchorage face. Thus, within the plane of a strut-and-tie model truss, nodal zones

FIGURE 10.4
Subdivision of nodal zones.

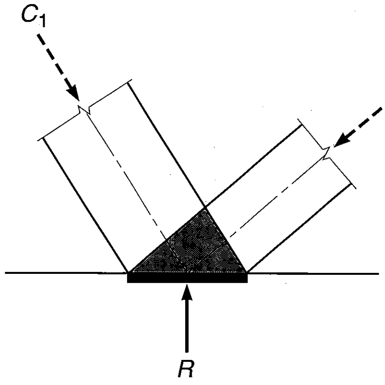

(*a*) Nodal zone

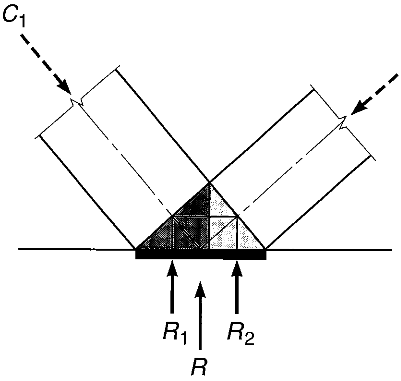

(*b*) Subdivided nodal zone

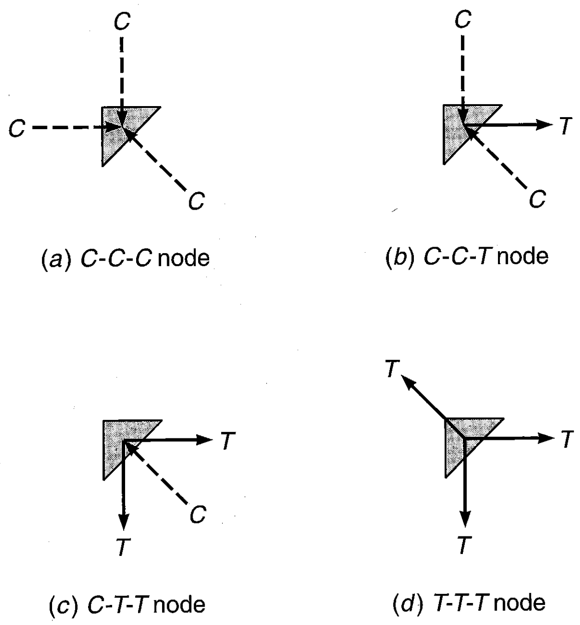

(*a*) *C*-*C*-*C* node

(*b*) *C*-*C*-*T* node

(*c*) *C*-*T*-*T* node

(*d*) *T*-*T*-*T* node

FIGURE 10.5
Classification of nodes.

are considered to be in compression, as shown in Fig. 10.6*a*. If the nodal zone dimensions w_{n1}, w_{n2}, and w_{n3} are proportional to the applied compressive forces, the state of stress becomes one of *hydrostatic* compression. The dimension of one side of a nodal zone is often determined based on the contact area of the load, e.g., by a bearing plate, column base, or beam support. If a hydrostatic state of stress is desired, the dimensions of the remaining sides are selected to maintain a constant level of stress p within the node. By selecting nodal zone dimensions that are proportional to the applied loads, the stresses on the faces of the nodal zone are equal.† If, instead, the dimensions are determined based on preselected strut dimensions, e.g., minimum width, the state of stress will no longer be hydrostatic. The decision to use a hydrostatic or a nonhydrostatic state of stress is made by the designer, with the former being more typical because the latter results in a more complex design.

The length of a hydrostatic zone is often not adequate to allow for anchorage of tie reinforcement. For this reason, an *extended nodal zone*, defined by the intersection of the nodal zone and the associated strut (shown in light shading in Fig. 10.6*b* and *c*), is used. An extended nodal zone may be regarded as that portion of the overlap region between struts and ties that is not already counted as part of a primary node. It increases the length within which the tensile force from the tie can be transferred to the concrete and, thus, defines the available anchorage length for ties. Ties may be developed outside of the nodal and extended nodal zones if needed, as shown to the left of the node in Fig. 10.6*c*.

10.3 STRUT-AND-TIE DESIGN METHODOLOGY

Strut-and-tie models are used in several ways during the design process. At the *conceptual* design level, sketching a strut-and-tie model provides insight into structural behavior and detailing requirements. Examples of conceptual design can be seen in the

---

† The state of stress within a nodal zone is not truly hydrostatic since out-of-plane stresses are not considered.

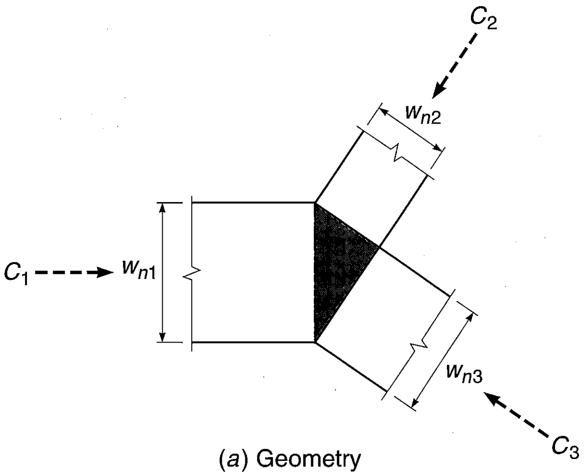
C_2
w_{n2}
C_1
w_{n1}
w_{n3}
C_3

(*a*) Geometry

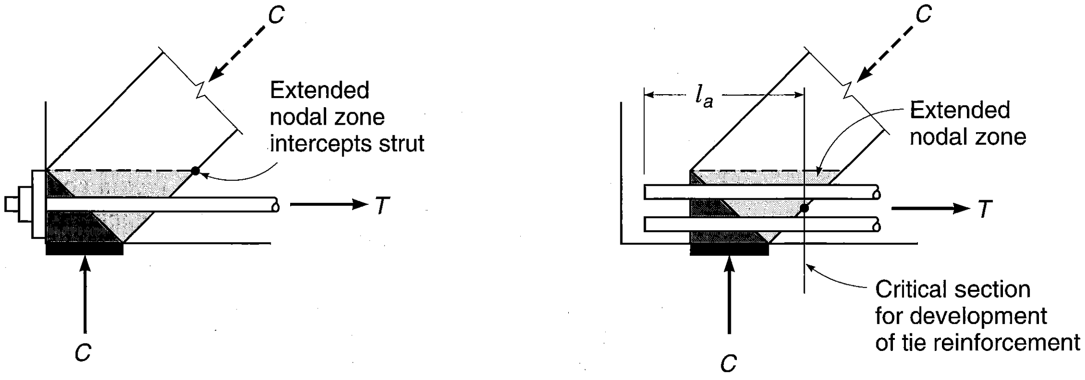
C
Extended nodal zone intercepts strut
T
C
C
l_a
Extended nodal zone
T
Critical section for development of tie reinforcement
C

(*b*) Tension force anchored by plate

(*c*) Tension force anchored by bond

FIGURE 10.6
Nodal zones and extended nodal zones.

development of connection details in Chapter 11. Strut-and-tie models may be used to *validate* design details, such as for special reinforcement configurations. Finally, strut-and-tie models may form the basis for *detailed* design of a member.

Application of a detailed strut-and-tie model involves completion of the following steps.

a. Define and isolate the D-regions.
b. Compute the force resultants on each D-region boundary.
c. Select a truss model to transfer the forces across a D-region.
d. Select dimensions for strut-and-tie nodal zones.
e. Verify the capacity of the node and the strut, the latter both at midlength and at the nodal interface.
f. Design the ties and the tie anchorage.
g. Prepare design details and check minimum reinforcement requirements.

As will be described shortly, the design process requires interaction between these steps.

According to ACI Code A.2.6, design using a strut-and-tie model requires that

$$\phi F_n \geq F_u \tag{10.1}$$

where F_u = factored force acting in strut, tie, bearing area, or nodal zone
F_n = nominal capacity of strut, tie, or nodal zone
ϕ = strength reduction factor

In addition to strength criteria, service level performance must be considered in design because strut-and-tie models, which are based on strength, do not necessarily satisfy serviceability requirements. To this end, the spacing of reinforcement within ties should be checked using Eq. (6.3). ACI Code 11.8.3 limits the nominal shear strength of deep beams to $0.83\sqrt{f_c'}b_w d$. This limit applies to strut-and-tie models and should be checked prior to beginning a detailed design, as described in Section 10.4d.

a. D-region

A D-region extends on both sides of a discontinuity by a distance equal to the member height h. At geometric discontinuities, a D-region may have different dimensions on either side of the discontinuity, as shown in Fig. 10.1.

b. Force Resultants on D-region Boundaries

Once the D-region is defined, the next step involves determining the magnitude, location, and direction of the resultant forces acting on the D-region boundaries. These forces serve as input for the strut-and-tie model and assist in establishing the geometry of the truss model. When one face of a D-region is loaded with a uniform or linearly varying stress field, or when a face is loaded by bending of a concrete section, it may be necessary to subdivide the boundary into segments corresponding to struts or ties and then to compute the resultant force on each segment, as shown in Fig. 10.7. For example, in Fig. 10.7*a*, the distributed load along the top of the deep beam is represented by four concentrated loads, and the stresses at the beam-column interface are represented by concentrated reactions. In Fig. 10.7*b*, the moments at the faces of the beam-column joint are represented by couples consisting of tensile and compressive forces acting at the interfaces between the members and the joint.

c. The Truss Model

The truss representing the strut-and-tie model must fit within the envelope defined by the D-region. The selection of struts and ties is made at the discretion of the designer, and, therefore, multiple solutions are possible. The axes of the truss members are chosen to coincide with the centroids of the tension and compression fields, and the geometry so established is used to compute the forces in the members. The layout of a truss model is constrained by the geometric requirement that struts must intersect only at nodal zones. Ties may cross struts. An effective model will represent a minimum energy distribution through the D-region (Refs. 10.1 and 10.4); i.e., within the model, forces should follow the stiffest load path. Because struts are typically much stiffer than ties, a model with a minimum number of tension ties is generally preferred. Alternative truss models for a deep beam are compared in Fig. 10.8. Figure 10.8*a* shows a deep beam subjected to a concentrated load at midspan. Figure 10.8*b* shows the preferred strut-and-tie model for this beam and loading condition. In this case, struts carry the load directly to nodal regions at the supports, which are, in turn, connected by

FIGURE 10.7
Resolution of forces in a D-region.

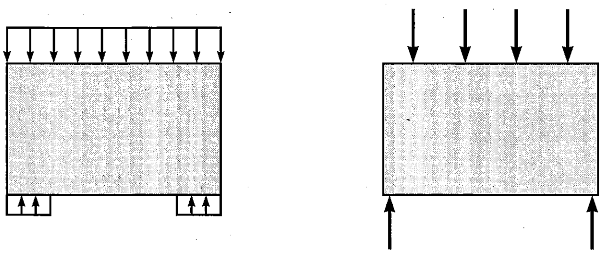

Applied load

Force resultants

(*a*) Distributed load applied to a deep beam

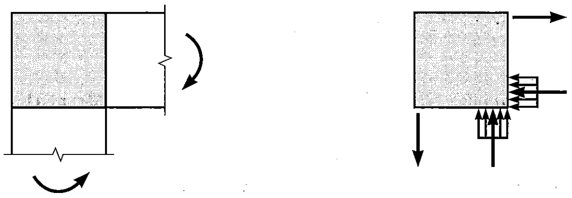

Applied load

Force resultants

(*b*) Moment resisting corner

FIGURE 10.8
Alternatives for a deep beam truss model.

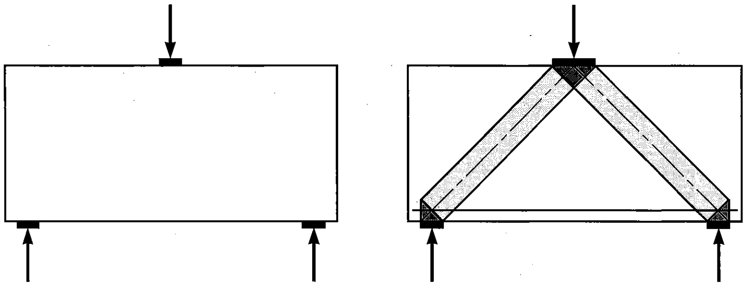

(*a*) Loading

(*b*) Preferred model

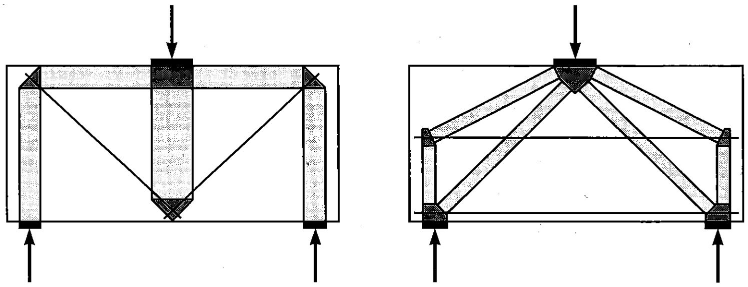

(*c*) Inefficient load path

(*d*) Incompatible load path

a single tension tie. The model in Fig. 10.8*c* shows an ineffective load path, with a single strut carrying the load to a node at the bottom of the beam that is supported by two diagonal tension ties, which are, in turn, supported by vertical struts over the supports. In this instance, the number of transfer points and tension ties is greater, as is the flexibility of the truss, indicating a solution that is much less effective than that shown in Fig. 10.8*b*. Lastly, Fig. 10.8*d* illustrates a model with multiple struts and ties. This particular layout not only is unduly complex, but also includes an upper tension tie that will be effective only after extensive yielding and possible failure of the lower tension tie.

Theoretically, there may be a unique minimum energy solution for a strut-and-tie model. Practically, any model that satisfies equilibrium and pays attention to structural stiffness will prove satisfactory. Using the rationale just discussed allows the designer to select a logical model that effectively mobilizes ties and minimizes the potential for excessive cracking. Finite element analyses and solutions based on the theory of elasticity for the full structure can provide an indication of where maximum stresses occur. A truss model that provides struts in regions of high compression and ties in regions of high tension based on these analyses will, in general, provide an efficient load path.

d. Selecting Dimensions for Struts and Nodal Zones

The struts, ties, and nodal zones within the truss that represents a strut-and-tie model have finite widths that must be considered when selecting the dimensions of the truss. The width of each truss member depends on the magnitude of the forces and the dimensions of the adjoining elements. An external element, such as a bearing plate or column, can serve to define a nodal zone. If the bearing area is too small, a high hydrostatic pressure results, and the corresponding width of the node or struts will not be sufficient to carry the applied load. The solution in this case is to increase the size of the bearing surface and, thus, reduce the contact pressures. Some designers intentionally select struts and nodes that are large enough to keep the compressive stresses low; in this case, only the tension ties require detailed design. To minimize cracking and to reduce complications that may result from incompatibility in the deformations due to struts shortening and ties elongating in nearly the same plane, the angle between struts and ties at a node should be greater than 25°.

The design of nodal zones is based on the assumption that the principal stresses within the intersecting struts and ties are parallel to the axes of these truss members. The widths of the struts and ties are, in general, proportional to the magnitude of the force in the elements. If two or more struts converge on the same face, such as shown in Fig. 10.9*a* and *b*, it is generally necessary to resolve the forces into a single force and to orient the face of the nodal zone so that it is perpendicular to the combined force, as shown in Fig. 10.9*c* and *d*. Some geometric arrangements preclude establishing a purely hydrostatic node. In these cases, the width of the strut is determined by the geometry of the bearing plate or tension tie, as shown in Fig. 10.10*a*.

The thickness of the strut, tie, and nodal zone is typically equal to the thickness of the member. If the thickness of the bearing area is less than the thickness of the member, it may be necessary to add reinforcement perpendicular to the principal plane of the member to add confinement and prevent splitting parallel to the plane of the truss. In this instance, a strut-and-tie model may be used to determine the requirements for transverse reinforcement in a manner that is similar to that used to reinforce bottle-shaped struts.

e. Capacity of Struts

Strut capacity is based on both the strength of the strut itself and the strength of the nodal zone. If a strut does not have sufficient capacity, the design must be revised by providing compression reinforcement or by increasing the size of the nodal zone. This may, in turn, affect the size of the bearing plate or column.

FIGURE 10.9
Resolution of forces in nodal zones.

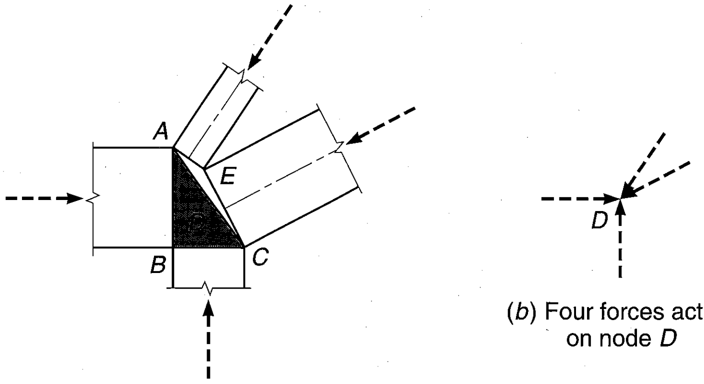

(*a*) Struts *AE* and *EC* may be replaced by *AC*

(*b*) Four forces acting on node *D*

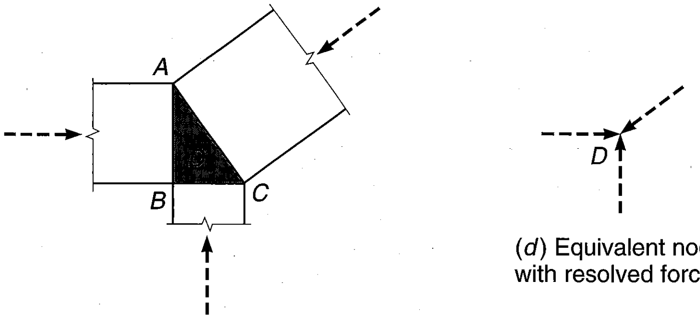

(*c*) Equivalent node

(*d*) Equivalent node with resolved forces

FIGURE 10.10
Extended nodal zone definition.

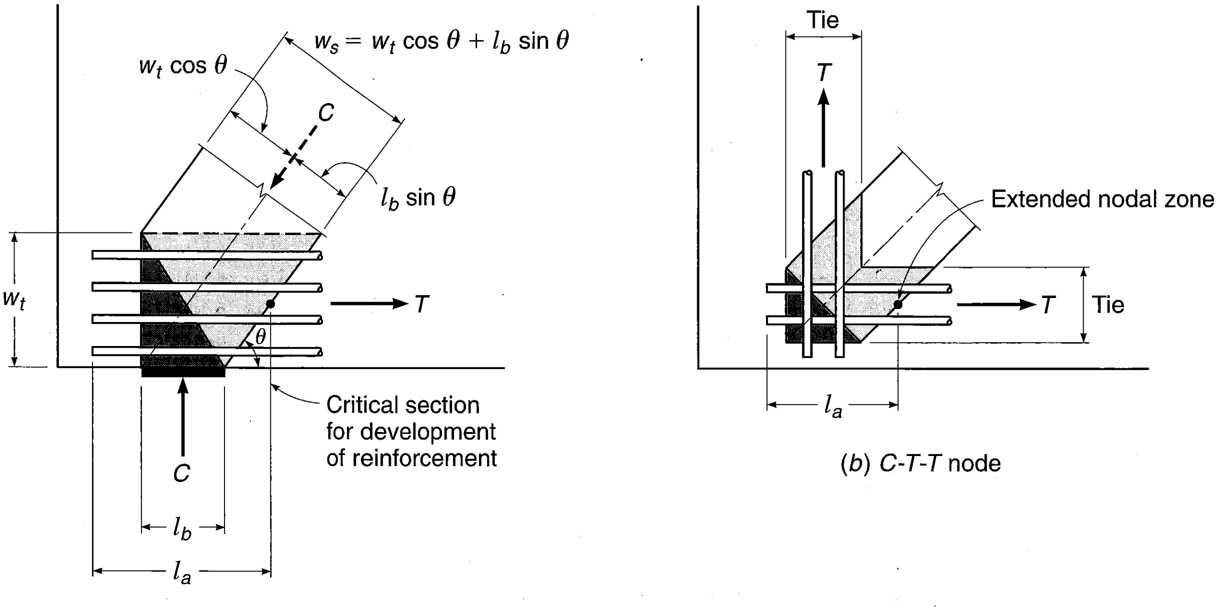
$w_s = w_t \cos\theta + l_b \sin\theta$
$w_t \cos\theta$
C
$l_b \sin\theta$
w_t
T
θ
Critical section for development of reinforcement
C
l_b
l_a
Tie
T
Extended nodal zone
T
Tie
l_a

(*a*) *C-C-T* node with eccentric strut

(*b*) *C-T-T* node

f. Design of Ties and Anchorage

To control cracking in a D-region, ties are designed so that the stress in the reinforcement is below yield at service loads. The geometry of the tie must be selected so that the reinforcement fits within the tie dimensions and is fully anchored.

Anchorage for ties is provided within the nodal and extended nodal zones plus regions on the far side of the node that may be available based on the geometry of the member. Figure 10.10*a* illustrates an extended nodal zone and the length available for anchorage of ties l_a. In this case, the tie is extended to the left of the nodal zone to allow for full development of the reinforcement. The shape of the extended nodal zone is a function of the strut angle θ and the width of the tie w_t. Figure 10.10*a* illustrates the geometry and dimensions of a *C-C-T* node with a tension tie that contains multiple layers of reinforcement. Figure 10.10*b* shows a *C-T-T* nodal zone. If insufficient length is available to anchor the reinforcement within the nodal and extended nodal zones, the reinforcement must extend beyond the node or a hook or headed bar must be used to fully develop the reinforcement.

g. Design Details and Minimum Reinforcement Requirements

A complete design includes verification that (1) tie reinforcement can be placed in the section, (2) nodal zones are confined by compressive forces or tension ties, and (3) minimum reinforcement requirements are satisfied. Reinforcement within ties must meet the ACI Code requirements for bar spacing (see Section 3.6c) and fit within the overall width and thickness of the tie. Tie details should be reviewed to ensure that ties are adequately developed on the far side of nodes by tension development length, hooks, headed bars, or other mechanical anchorage. Shear reinforcement requirements are satisfied by ensuring that the factored shear is less than the ACI Code maximum, as described in Chapter 4, longitudinal cracking of bottle-shaped struts is controlled, or the minimum reinforcement requirements described in Section 10.4d are met.

10.4 ACI PROVISIONS FOR STRUT-AND-TIE MODELS

ACI Code Appendix A provides guidance for sizing struts, nodes, and ties. It addresses the performance of highly stressed compression zones that may be adjacent to or crossed by cracks in a member, the effect of stresses in nodal zones, and the requirements for bond and anchorage of ties. The effective compressive strength of concrete $0.85f'_c$ is modified by a factor β to account for the effects of cracks (caused by spreading compressive resultants) and confining reinforcement in struts and the anchorage of ties in nodal zones.

The balance of this section describes the steps needed to calculate the capacity of struts, verify nodal zones, and design ties and tie anchorage. A strength reduction factor $\phi = 0.75$ is used for struts, ties, nodal zones, and bearing areas.

a. Strength of Struts

The strength of a strut is limited based on the strength of the concrete in the strut and the strength of the nodal zones at the ends of the strut. The nominal compressive strength of a strut F_{ns} is given as

$$F_{ns} = f_{ce}A_{cs} \tag{10.2}$$

TABLE 10.1
β_s values for strut strength

Condition	β_s
Strut with uniform cross section over its entire length	1.0
Strut with the width at midsection larger than the width at the nodes (bottle-shaped strut) and with reinforcement satisfying transverse requirements	0.75
Strut with the width at midsection larger than the width at the nodes (bottle-shaped strut) and reinforcement not satisfying transverse requirements	$0.60\lambda^{\dagger}$
Struts in tension members or in the tension flange of members	0.40
All other cases, Fig. 10.11	0.60λ

[†] λ equals 1.0 for normalweight concrete, 0.85 for sand-lightweight concrete, and 0.75 for all-lightweight concrete.

where f_{ce} is the effective compressive strength of the concrete in a strut or nodal zone and A_{cs} is the cross-sectional area at one end of the strut, which is equal to the product of the strut thickness and the strut width. The effective strength of concrete in a strut is

$$f_{ce} = 0.85\beta_s f'_c \tag{10.3}$$

where β_s is a factor that accounts for the effects of cracking and confining reinforcement within the strut, with values ranging from 1.0 for a strut with a uniform cross-sectional area over its length to 0.4 for struts in tension members or the tension flanges of members (Table 10.1). Intermediate values include 0.75 for struts with a width at midsection that is larger than the width at the nodes (bottle-shaped struts) and crossed by transverse reinforcement to resist the transverse tensile force resulting from the compressive force spreading in the strut and 0.60λ for bottle-shaped struts without the required transverse reinforcement, where λ is the correction factor related to the unit weight of concrete: 1.0 for normalweight concrete, 0.85 for sand-lightweight concrete, and 0.75 for all-lightweight concrete. $\beta_s = 0.60\lambda$ for all other cases, as when parallel diagonal cracks divide the web struts or when diagonal cracks are likely to turn and cross a strut, as shown in Fig. 10.11.

Compression steel may be added to increase the strength of a strut, so that

$$F_{ns} = f_{ce}A_{cs} + A'_s f'_s \tag{10.4}$$

where f'_s is based on the strain in the concrete at peak stress. For Grades 280 and 420 reinforcement, $f'_s = f_y$. In accordance with ACI Code A.3.5, compression reinforcement must be properly anchored, oriented parallel to the axis of the strut, located within the strut, and enclosed by ties or spirals, as required for columns (see Section 8.2).

To design transverse reinforcement for bottle-shaped struts, ACI Code A.3.3 permits the assumption that the compressive force in the struts spreads at a slope of two longitudinal to one transverse along the axis of the strut, as shown in Fig. 10.3*b*. For $f'_c \leq 42$ MPa, the ACI Code considers the transverse reinforcement requirement to be satisfied if the strut is crossed by layers of reinforcement that satisfy

$$\sum \frac{A_{si}}{b_s s_i} \sin \alpha_i \geq 0.003 \tag{10.5}$$

where A_{si} is the total area of reinforcement at spacing s_i in a layer of reinforcement with bars at an angle α_i to the axis of the strut and b_s is the thickness of the strut. The

FIGURE 10.11
Beam cracking conditions for $\beta_s = 0.6\lambda$.

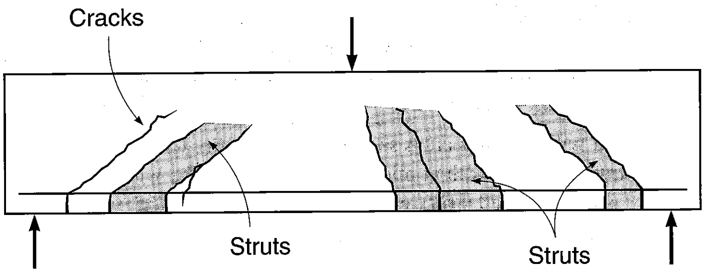
Cracks
Struts
Struts

(*a*) Struts in beam with inclined cracks parallel to strut

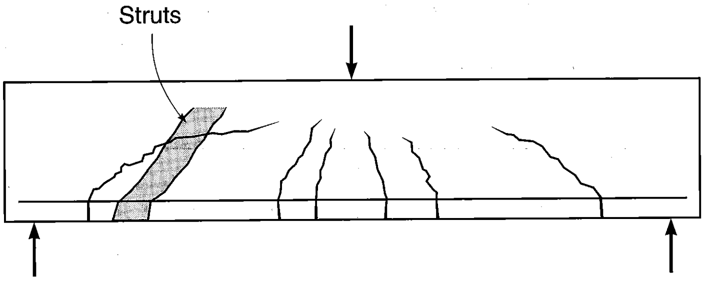

(*b*) Struts crossed by skew cracks

reinforcement may be perpendicular to the strut axis or may be placed in an orthogonal grid pattern. The subscript i denotes the layer of reinforcement. The values s_i and α_i are shown in Fig. 10.12. The minimum reinforcement requirements described for deep beams in Section 10.4d provide additional guidance for selection of reinforcement to satisfy Eq. (10.5).

The ACI Code provides no clear guidance to indicate when a strut should be considered as rectangular or bottle-shaped. Some researchers suggest that horizontal

FIGURE 10.12
Details of reinforcement crossing a strut.

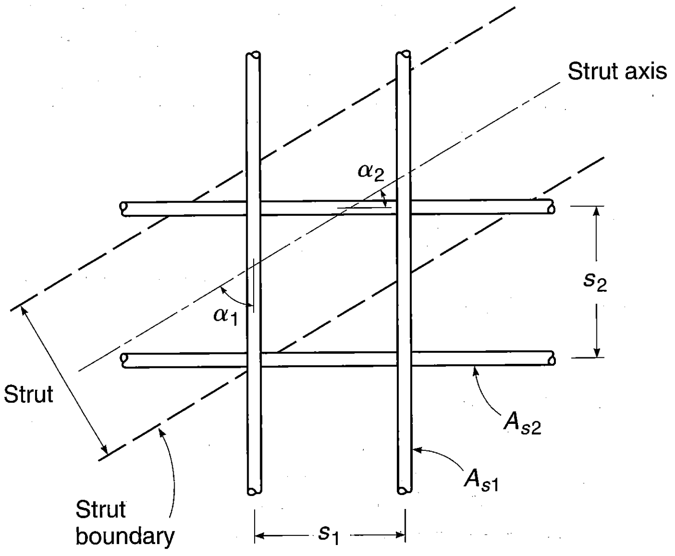
Strut axis
α_2
s_2
α_1
Strut
A_{s2}
A_{s1}
Strut boundary
s_1

TABLE 10.2
β_n values for node strength

Nodal Zone Condition	Classification	β_n
Bounded by struts or bearing area	*C-C-C*	1.0
Anchoring one tie	*C-C-T*	0.80
Anchoring two or more ties	*C-T-T* or *T-T-T*	0.60

struts be represented as rectangular and inclined struts represented as bottle-shaped (Ref. 10.6). Others simply assume a bottle-shaped strut will develop and use the lower values of β_s for design (Ref. 10.7). Examples in this text use rectangular horizontal struts and bottle-shaped inclined struts.

b. Strength of Nodal Zones

The nominal compressive strength of a nodal zone is

$$F_{nn} = f_{ce} A_{nz} \tag{10.6}$$

where f_{ce} is the effective strength of the concrete in the nodal zone and A_{nz} is (1) the area of the face of the nodal zone taken perpendicular to the line of action of the force from the strut or tie or (2) the area of a section through the nodal zone taken perpendicular to the line of action of the resultant force on the section. The latter condition occurs when multiple struts intersect a node, as shown in Fig. 10.9.

The effective concrete strength in a nodal zone is

$$f_{ce} = 0.85\beta_n f'_c \tag{10.7}$$

where f'_c is the compressive strength of the concrete in the nodal zone and β_n is a factor that reflects the degree of disruption in nodal zones due to the incompatibility of tensile strains in ties with compressive strains in struts. $\beta_n = 1.0$ for *C-C-C* nodes, 0.80 for *C-C-T* nodes, and 0.60 for *C-T-T* or *T-T-T* nodes. Values of β_n are summarized in Table 10.2. ACI Code A.5.2 permits the strength of a node to be increased above the value given in Eq. (10.7) if the node contains confining reinforcement and the effect of that reinforcement is demonstrated by tests and analysis.

Unless compression reinforcement is used in the struts, the lower value of f_{ce} from Eqs. (10.3) and (10.7) governs and should be used to design both the node and the adjoining struts.

c. Strength of Ties

The nominal strength of ties F_{nt} is the sum of the strengths of the reinforcing steel and prestressing steel within the tie.

$$F_{nt} = A_{ts} f_y + A_{tp}(f_{pe} + \Delta f_p) \tag{10.8}$$

where A_{ts} = area of reinforcing steel
f_y = yield strength of reinforcing steel
A_{tp} = area of prestressing steel, if any
f_{pe} = effective stress in prestressing steel
Δf_p = increase in prestressing steel stress due to factored load

The sum $f_{pe} + \Delta f_p$ must be less than or equal to the yield stress of the prestressing reinforcement f_{py}, and A_{tp} is zero for nonprestressed members. The value of Δf_p may be found by analysis; or, in lieu of formal analysis, ACI Code A.4.1 allows a value 420 MPa to be used for bonded tendons and 70 MPa to be used for unbonded tendons.

The effective width of a tie w_t depends on the distribution of the tie reinforcement. If the reinforcement in a tie is placed in a single layer, the effective width of a tie may be taken as the diameter of the largest bars in the tie plus twice the cover to the surface of the bars. Alternatively, the width of a tie may be taken as the width of the anchor plates. The practical upper limit for tie width $w_{t,\max}$ is equal to the width corresponding to the width of a hydrostatic nodal zone, given as

$$w_{t,\max} = \frac{F_{nt}}{b_s f_{ce}} \tag{10.9}$$

where f_{ce} is the effective nodal zone compressive stress given in Eq. (10.7) and b_s is the thickness of the strut.

Ties must be anchored before they leave the extended nodal zone at a point defined by the centroid of the bars in the tie and the extension of the outlines of either the strut or the bearing area, as shown in Fig. 10.10. If the combined lengths of the nodal zone and extended nodal zone are inadequate to provide for development of the reinforcement, additional anchorage may be obtained by extending the reinforcement beyond the nodal zone, using 90° hooks, or by using a mechanical anchor. If the tie is anchored with a 90° hook, the hooks should be confined by reinforcement extending into the beam from supporting members to avoid splitting of the concrete within the anchorage region.

d. ACI Shear Requirements for Deep Beams

Beams with clear spans less than or equal to 4 times the total member depth or with concentrated loads placed within twice the member depth of a support are classified as deep beams, according to ACI Code 11.7.[†] Examples of deep beams are shown in Fig. 10.13. ACI Code 11.7.2 allows such members to be designed either by using a nonlinear analysis or by applying the strut-and-tie method of ACI Code Appendix A. While solutions based on nonlinear strain distributions are available (Ref. 10.8), the strut-and-tie approach allows a rational design solution.

ACI Code 11.8.3 specifies that the nominal shear in a deep beam may not exceed $0.83\sqrt{f_c'}b_w d$, where b_w is the width of the web and d is the effective depth. ACI Code 11.7.4 and 11.7.5 provide minimum steel requirements for horizontal and vertical reinforcement within a deep beam. The minimum reinforcement perpendicular to a span is

$$A_v \geq 0.0025 b_w s \tag{10.10}$$

where s is the spacing of the reinforcement. The minimum reinforcement parallel to a span is

$$A_{vh} \geq 0.0015 b_w s_2 \tag{10.11}$$

where s_2 is the spacing of the reinforcement perpendicular to the longitudinal reinforcement. Spacings s and s_2 may not exceed $d/5$ or 300 mm. ACI Code 11.7.6 allows Eq. (10.5) to be used in lieu of Eqs. (10.10) and (10.11). For strut-and-tie models, b_w equals the thickness of the element b.

[†] The ACI Code does not specify the magnitude of the concentrated load at a beam end needed to invoke the deep beam provisions of Section 11.7. A level of professional judgment is required if a low-magnitude concentrated load is placed at the end of a beam. Deep beam design may not be required in this situation.

FIGURE 10.13
Deep beam D-regions.

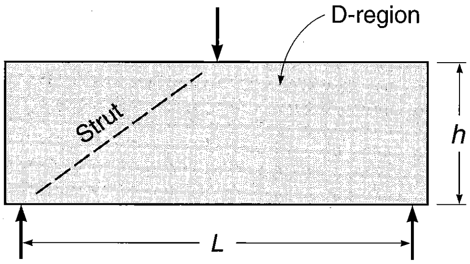

(a) Deep beam with $L \leqslant 4h$

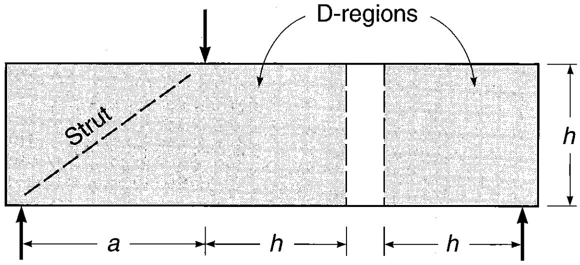

(b) Deep beam with $a \leqslant 2h$

10.5 APPLICATIONS

While there are a number of possible applications for a strut-and-tie model, ACI Code 11.7 and 11.8 specifically allow deep beam and column bracket design to be completed with this method. The following examples examine the details of deep beams and dapped beam end design by the strut-and-tie method. Additional examples of strut-and-tie modeling may be found in Chapter 11 and in Refs. 10.9 through 10.12.

a. Deep Beams

Deep beams represent one of the principal applications of strut-and-tie models, since the alternative under ACI Code 11.7 is a nonlinear analysis. Two examples of deep beam design are presented next, one that includes the application of concentrated loads at the upper surface of a transfer girder and a second that addresses design for distributed as well as concentrated loads.

EXAMPLE 10.1

Deep beam. A transfer girder is to carry two 600 mm square columns, each with factored loads of 5000 kN located at the third points of its 11 m span, as shown in Fig. 10.14*a*. The beam has a thickness of 600 mm and a total height of 3.6 m. Design the beam for the given loads, ignoring the self-weight, using $f'_c = 35$ MPa and $f_y = 420$ MPa.

Solution. The span-to-depth ratio for the beam is 3, thereby qualifying it as a deep beam. A strut-and-tie solution will be used.

Definition of D-region
All of the supports and loads are within *h* of each other or the supports, so the entire structure may be characterized as a D-region. The thickness of the struts and ties is equal to the thickness

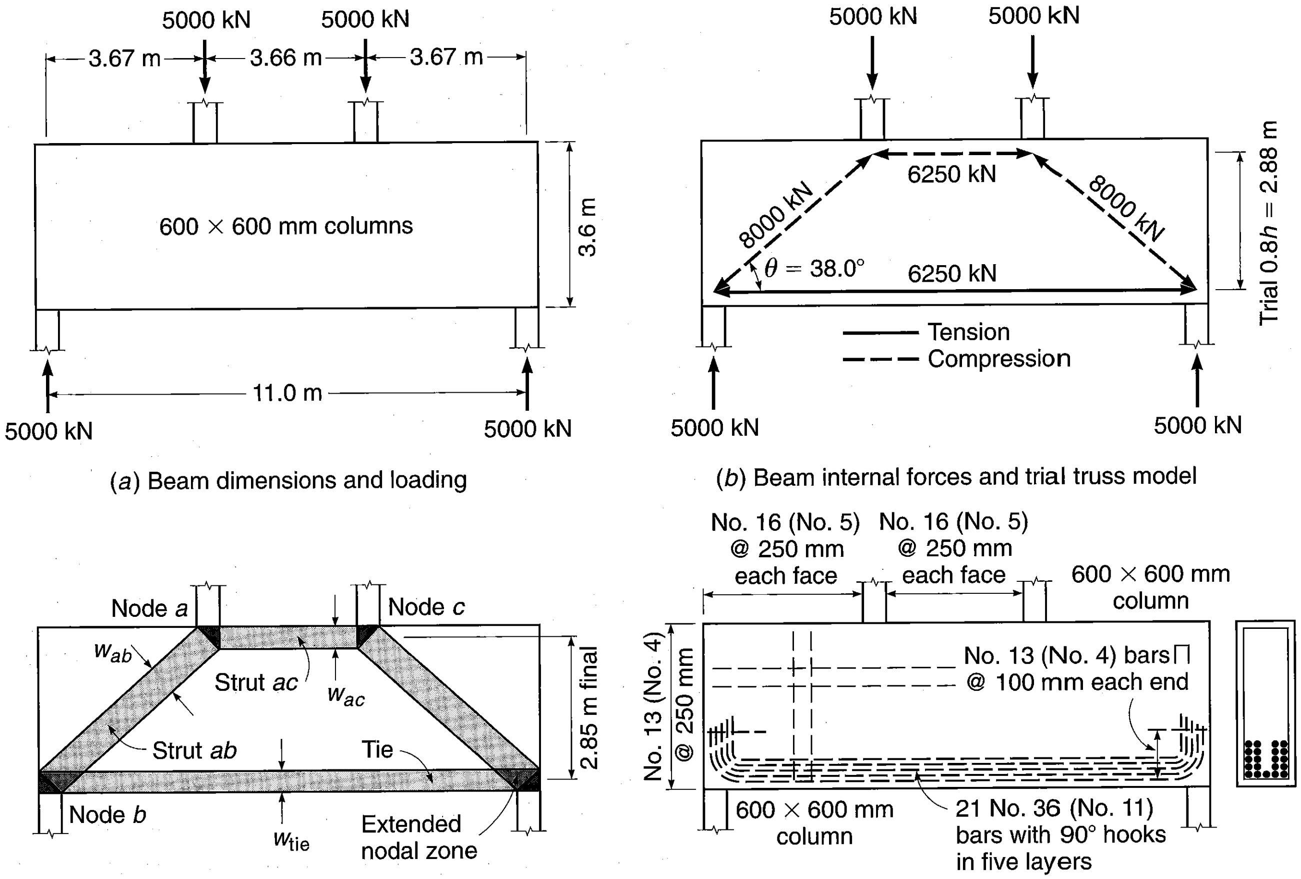
5000 kN
5000 kN
3.67 m
3.66 m
3.67 m
600 × 600 mm columns
3.6 m
11.0 m
5000 kN
5000 kN
5000 kN
5000 kN
6250 kN
8000 kN
8000 kN
θ = 38.0°
6250 kN
Tension
Compression
Trial 0.8h = 2.88 m
5000 kN
5000 kN
Node a
Node c
w_{ab}
Strut ac
w_{ac}
Strut ab
Tie
2.85 m final
Node b
w_{tie}
Extended nodal zone
No. 16 (No. 5) @ 250 mm each face
No. 16 (No. 5) @ 250 mm each face
600 × 600 mm column
No. 13 (No. 4) @ 250 mm
No. 13 (No. 4) bars @ 100 mm each end
600 × 600 mm column
21 No. 36 (No. 11) bars with 90° hooks in five layers

(*a*) Beam dimensions and loading

(*b*) Beam internal forces and trial truss model

(*c*) Schematic showing widths of struts, ties, and nodes in final truss model

(*d*) Reinforcement details

FIGURE 10.14
Deep beam design for Example 10.1.

of the beam $b = 600$ mm. Assuming an effective depth $d = 0.9h = 0.9 \times 3.6 = 2.88$ m in the middle third of the beam, the maximum design shear capacity of the beam is $\phi V_n = \phi\, 0.83\sqrt{f'_c}\, b_w d = 0.75 \times 0.83\sqrt{35} \times 600 \times 2880 = 6364$ kN. This is greater than $V_u = 5000$ kN. Thus, the design may continue.

Force resultants on D-region boundaries

The 5000 kN column loads on the upper face of the beam are equilibrated by 5000 kN reactions at the supports, as shown in Fig. 10.14*b*. Based on an assumed center-to-center distance between the horizontal strut and the tie of 0.8*h*, the trial diagonal struts form at an angle $\theta = 38.66°$ and carry a load of 8000 kN. A horizontal 6250 kN compression strut runs between the two column loads, and a 6250 kN tension tie runs between the bottom nodes.

The truss model

Based on the beam geometry and loading, a single truss is sufficient to carry the column loads, as shown in Fig. 10.14*c*. The truss has a trapezoidal shape. This is an acceptable solution since the nodes are not true pins and instability within the plane of the truss is not a concern in a strut-and-tie model. The truss geometry is established by the assumed intersection of the struts and ties and used to determine θ.

Selecting dimensions for strut and nodal zones

As mentioned in Section 10.2c, two approaches are used to select strut and nodal zone sizes: selection based on the geometry of the load-bearing transfer elements to maintain a constant level of stress p and selection based on the minimum strut width w. For this example, the first approach will be used. The nodal stress p is determined by the average stress under the columns. Thus, $p = 5000/(600 \times 600) = 13.9$ MPa. Because this is a *C-C-C* node, β_n is 1.0, and the design strength of the node is $\phi f_{ce} = \phi 0.85\beta_n f_c' = 0.75 \times 0.85 \times 1.0 \times 35 = 22.3$ MPa, which is greater than the demand from the column. This result implies that smaller truss member sizes may be possible, a point that is discussed at the end of this example. The width of strut *ac*, found using p, is

$$w_{ac} = F_{ac}/(b_s \times p) = 6250 \times 10^3/(600 \times 13.9) = 749 \text{ mm}$$

Similarly, $w_{ab} = 959$ mm and $w_{\text{tie}} = 749$ mm. The center-to-center distance between the horizontal strut *ac* and the tie is $3.600 - 0.749 = 2.851$ m, or $0.79h$. The angle θ between the diagonal strut *ab* and the tie is thus 38.3°. Using an angle of 38.0° gives a revised force in strut *ab* of 8121 kN. Similarly, the revised force in strut *ac* and the tie is 6345 kN, while the widths are revised to $w_{ab} = 974$ mm, and w_{ac} and $w_{\text{tie}} = 761$ mm. (*Note*: After iteration, the actual angle becomes 38.2°. The value of 38.0° is conservative and is, thus, retained.)

Capacity of struts

The horizontal strut *ac* will be assumed to have a uniform cross section, while the diagonal struts will be considered as bottle-shaped because of the greater width available. Strut capacity is given in Eqs. (10.2) and (10.3), which, when combined, give $\phi F_{ns} = \phi 0.85\beta_s f_c' w_i b_s$, where w_i is the width of the strut and β_s is 1.0 for a rectangular strut. For strut *ac*,

$$\phi F_{ns} = 0.75 \times 0.85 \times 1.0 \times 35 \times 761 \times 600 \times 10^{-3} = 10{,}190 \text{ kN} > 6345 \text{ kN}$$

Therefore, strut *ac* is adequate. Similarly, for strut *ab*,

$$\phi F_{ns} = 0.75 \times 0.85 \times 0.75 \times 35 \times 974 \times 600 \times 10^{-3} = 9780 \text{ kN} > 8121 \text{ kN}$$

From Eqs. (10.6) and (10.7), the capacity of the nodal zone is $\phi F_{nn} = \phi 0.85\beta_n f_c' w_i b_s$. At *a*, a *C-C-C* node, $\beta_n = 1.0$, and at *b*, a *C-C-T* node, $\beta_n = 0.80$. Thus, the capacity of strut *ab* is established at node *b* with $\beta_n = 0.80$ and

$$\phi F_{nn} = 0.75 \times 0.85 \times 0.80 \times 35 \times 974 \times 600 \times 10^{-3} = 10{,}430 \text{ kN} \geq 8121 \text{ kN}$$

Similarly, the nodal end capacity of strut *ac* is 10,190 kN with $\beta_n = 1.0$. The capacity at the end of the struts and at the nodes exceeds the factored loads, and thus, the struts are adequate.

Design ties and anchorage

The tie design consists of three steps: selection of the area of steel, design of the anchorage, and validation that the tie fits within the available tie width. The steel area is computed as $A_{ts} = F_{tu}/\phi f_y = 6345 \times 10^3/(0.75 \times 420) = 20{,}140$ mm². This is satisfied by using 21 No. 36 (No. 11) bars, having a total area of $A_{ts} = 20{,}120$ mm². Placing the bars in one layer of five bars and four layers, while allowing for 60 mm clear cover to the bottom of the beam and 112 mm clear spacing between layers, results in a total tie width of $5 \times 35.8 + 4 \times 112 + 2 \times 60 = 747$ mm, closely matching the tie dimension.

The anchorage length l_d for No. 36 (No. 11) bars (from Table A.10 in Appendix A) is $42d_b = 1.617$ m. The length of the nodal zone and extended nodal zone is $600 + 0.5 \times 761 \cot 38.0° = 1.087$ m, which is less than l_d. The beam geometry does not allow the tie reinforcement to extend linearly beyond the node; therefore, 90° hooks or mechanical anchors are required on the No. 36 (No. 11) bars. Placement details are covered in the next section. Allowing 40 mm cover on the sides, No. 16 (No. 5) transverse and horizontal reinforcement, and 65 mm spacing between No. 36 (No. 11) bars, five No. 36 (No. 11) bars require a total thickness of $b_{\text{reqd}} = 2 \times 40 + 4 \times 15.9 + 4$ spaces @ $65 + 5$ bars $\times\ 35.8 = 582.6$ mm, which fits within the 600 mm beam thickness.

Design details and minimum reinforcement requirements

ACI Code 11.8.6 requires that shear reinforcement in deep beams satisfy (1) both Eqs. (10.10) and (10.11) or (2) Eq. (10.5). Using Eq. (10.10), the minimum required vertical steel is $A_v \geq 0.0025 b_w s = 0.0025 \times 600 \times 1000 = 1500$ mm²/m. This is satisfied by No. 16 (No. 5) bars at 250 mm placed on each face, giving a total area of reinforcement equal to 1592 mm²/m. Similarly, using Eq. (10.11), the horizontal reinforcement is $A_{vh} \geq 0.0015 b_w s_2 = 0.0015 \times 600 \times 1000 = 900$ mm²/m, which is satisfied using No. 13 (No. 4) bars at 250 mm placed on each face, giving 1032 mm²/m.

Equation (10.5) produces similar steel requirements. Using the reinforcement selected using Eqs. (10.10) and (10.11), two No. 16 (No. 5) bars ($\gamma = 38.0°$) give $A_v = 398$ mm² and two No. 13 (No. 4) bars ($\alpha = 52.0°$) give $A_{vh} = 258$ mm². Equation (10.5) becomes

$$\sum \frac{A_{si}}{b_s s_i} sin\ \alpha_i = \frac{398 \sin 52.0° + 258 \sin 38.0°}{600 \times 250} = 0.00315 > 0.003 \text{ req'd.}$$

This ensures that sufficient reinforcement is present to control longitudinal splitting in the bottle-shaped struts as well as to satisfy minimum reinforcement requirements.

The large number of No. 36 (No. 11) bars will require either the use of mechanical anchorage or staggering the location of the hooks. Heads require less space than hooks and would be preferable for concrete placement, but because they require a clear spacing of $4d_b$ (see Section 5.5), headed bars will not work in this case. Figure 10.14*d* shows staggered hooks for the final design. In addition, horizontal U-shaped No. 13 (No. 4) bars are placed at 100 mm ($3d_b = 3 \times 35.8$ mm $= 107.4$ mm) across the end of the beam to confine the No. 36 (No. 11) hooks. The final beam details are given in Fig. 10.14*d*.

Because the ACI Code does not require that hydrostatic pressure be maintained within the nodes, alternate solutions are possible. For example, a bottle-shaped strut ($\beta_s = 0.75$) can carry a maximum stress that is higher than p. Using the design compressive strength ϕf_{ce}, the width of the strut can be reduced to

$$w_{ab} = F_{ab}/(b_s \times \phi 0.85 \beta_s f'_c) = 8000 \times 10^3/(600 \times 0.75 \times 0.85 \times 0.70 \times 35) = 854 \text{ mm}$$

compared with the width of 959 mm used in this example. Using this reduction would lead to smaller nodes, but also increased complexity in nodal geometry. Such complexity, however, may be warranted if it is necessary to fit a truss into a more confined area.

EXAMPLE 10.2

Deep beam with distributed loads. In addition to the concentrated loads, the transfer girder from Example 10.1 carries a distributed factored load of 60 kN/m applied along its top edge, as shown in Fig. 10.15*a*. Design for the given loads, plus the self-weight, using $f'_c = 35$ MPa and $f_y = 420$ MPa.

SOLUTION. The factored self-weight of the beam is 1.2(3.6 m × 0.6 m × 23.7 kN/m³) = 61.4 kN/m. Thus, the total factored distributed load is 61.4 + 60.0 = 120.4 kN/m, resulting in a total factored load of 120.4 kN/m × 11.6 m = 1397 kN, approximately 14 percent of the column loads. The solution follows Example 10.1 and accounts for the distributed loads. For this example, the self-weight of the beam is combined with the superimposed dead load. A more conservative solution could place the self-weight at the bottom of the beam and correspondingly increase the vertical tension tie requirements to transfer the load to the top flange. The top placement is used in this case because the self-weight is a small percentage of the total load and the concentrated forces are moved slightly toward the center of the beam for a conservative placement.

Definition of D-region

The entire beam is a D-region, as shown in Fig. 10.15*a*. The maximum factored shear in the beam is $V_u = 5000 + 1397/2 = 5698$ kN $< \phi\, 0.83\sqrt{f'_c} b_w d = 6298$ kN, the maximum design shear using $d = 2.88$ m. Thus, the design can continue.

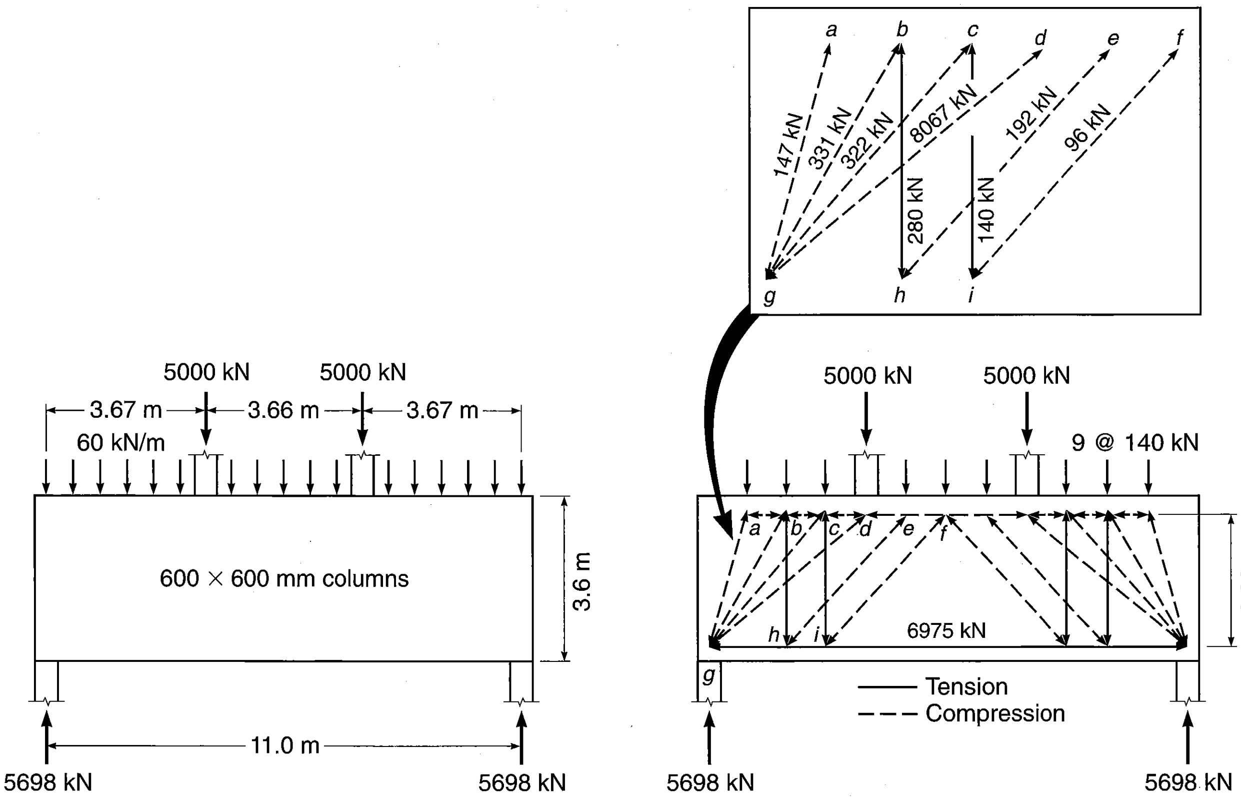
5000 kN
5000 kN
3.67 m
3.66 m
3.67 m
60 kN/m
600 × 600 mm columns
3.6 m
11.0 m
5698 kN
5698 kN
a
b
c
d
e
f
147 kN
331 kN
322 kN
8067 kN
192 kN
96 kN
280 kN
140 kN
g
h
i
5000 kN
5000 kN
9 @ 140 kN
a
b
c
d
e
f
h
i
6975 kN
2.90 m
g
Tension
Compression
5698 kN
5698 kN

(*a*) Beam dimensions and loading

(*b*) Beam internal forces and truss model

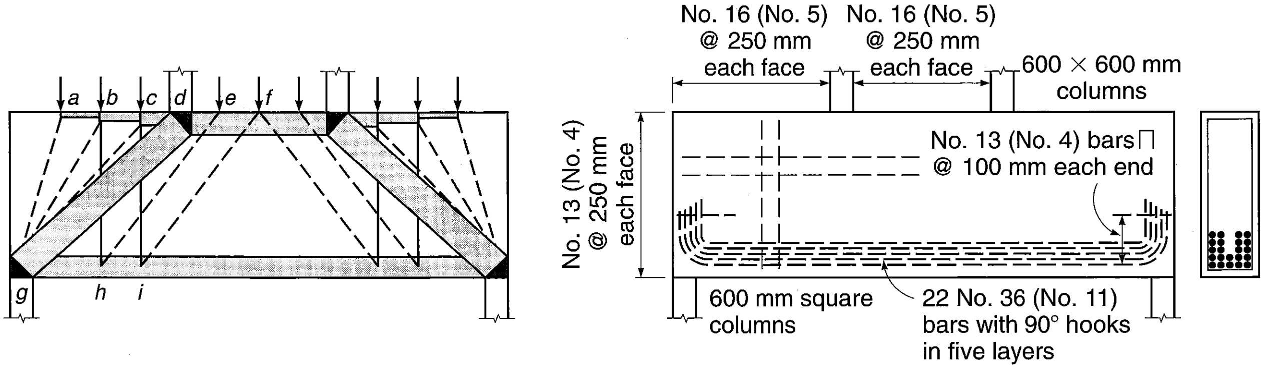
a
b
c
d
e
f
g
h
i
No. 16 (No. 5) @ 250 mm each face
No. 16 (No. 5) @ 250 mm each face
600 × 600 mm columns
No. 13 (No. 4) @ 250 mm each face
No. 13 (No. 4) bars ⊓ @ 100 mm each end
600 mm square columns
22 No. 36 (No. 11) bars with 90° hooks in five layers

(*c*) Struts, ties, and nodes

(*d*) Reinforcement details

FIGURE 10.15
Deep beam with distributed loads for Example 10.2.

Force resultants on D-region boundaries

The 5000 kN column loads are the same as in Example 10.1; however, the lower column reactions are equal to 5698 kN. Maintaining the same lower column size gives a stress at the beam-column interface of $p = 5698 \times 10^3/(600 \times 600) = 15.83$ MPa.

The stress on the column node cannot exceed the effective concrete strength. For a *C-C-T* node,

$$p \le \phi f_{ce} = \phi 0.85 \beta_n f_c' = 0.75 \times 0.85 \times 0.80 \times 35 = 17.85 \text{ MPa}$$

Therefore, the bottom column of 600 × 600 mm, giving $p = 5698 \times 10^3/(600 \times 600) = 15.83$ MPa $<$ 17.85 MPa is adequate. As in Example 10.1, the center-to-center distance between the horizontal strut and the horizontal tie at midspan is taken as 2.90 m to compute the slope of the strut *dg* as $\theta = 38.0°$. The vertical dimension for struts *ag*, *bg*, and *cg* is assumed to be 3.20 m because they are anchored closer to the top edge of the beam.

The total distributed load of 1397 kN is represented by nine 140 kN concentrated loads placed at 0.91 m centers, as shown in Fig. 10.15*b*. Distributed loads can be grouped at the discretion of the designer. It would be equally satisfactory to group them into 12 loads, placed at 0.36 m, or combine some load with the column loads. The loads are not combined with the column loads in this example to illustrate design for distributed loads. Using the geometric layout of the loads, strut-and-tie forces are computed and summarized in Fig. 10.15*b* and Table 10.3.

The truss model

In addition to the struts and ties needed to carry the column loads, struts and ties to carry the distributed loads are now included in the truss. The distributed loads between the columns are carried by struts to the bottom chord; tension ties then transfer the vertical component of the load to the top chord, while the horizontal component is transferred to the bottom tie. The geometry of the struts is selected to allow tension ties to be placed vertically. The loads at nodes *a*, *b*, and *c* between the column and the support create a fan of compression struts to node *g*, as shown in Fig. 10.15*b* and *c*.

Selecting dimensions for strut and nodal zones

The forces in the "fan" struts are based on the geometry of the struts. The widths of struts *ag*, *bg*, and *cg* are computed based on the contact area at node *g*, because the capacity of a *C-C-T* node (at the lower end) is lower than that of a *C-C-C* node (at the upper end). The stress on the column at node *g* is $p = 15.83$ MPa. To maintain constant stress in the node, strut *ag* has a width $w_{ag} = F_u/pb_s = 147 \times 10^3/(15.83 \times 600) = 15.5$ mm. The dimensions of struts *eh* and *fi*, with no concentrated loads acting directly on either end, are governed by the nodal capacity, since the nodes *h* and *i* are *C-T-T* nodes, with $\beta_n = 0.60$ (Table 10.2). For example, for strut *eh*, $p = \phi f_{ce} = 0.75 \times 0.85 \times 0.60 \times 35 = 13.39$ MPa and width $w_{eh} = F_u/pb_s = 192 \times 10^3/(13.39 \times 600) = 23.9$ mm. In this case, the design capacity will exactly equal the factored load. The remaining strut widths, geometries, and loads are summarized in Table 10.3.

Capacity of struts

By inspection, the stresses in the fan struts *ag*, *bg*, and *cg* will be critical as bottle-shaped struts. Using $\beta_n = 0.75$ for a *C-C-T* node and $\phi = 0.75$, strut *ag* has a design capacity $\phi F_{ns,ag} = \phi 0.85\beta_s f'_c w_{ab} b_s = 0.75 \times 0.85 \times 0.75 \times 35 \times 15.5 \times 600 \times 10^{-3} = 156$ kN, which is greater than the applied load of 147 kN. The strut capacities are summarized in Table 10.3. In all cases, the design strength ϕF_{ns} exceeds the applied forces and the struts are adequate.

TABLE 10.3
Diagonal strut properties and forces for Example 10.2

Strut	Vertical Load, kN	Slope, deg	Axial Load, kN	w_i, mm	β_s	β_n	Strut End Capacity, kN	Horizontal Force, kN
dg	5000	38.3	8067	849.0	0.75	0.8	11,370	6331.0
ag	140	72.0	147	15.5	0.75	0.8	156	45.5
bg	279	57.4	331	34.8	0.75	0.8	466	178.4
cg	233	46.4	322	33.9	0.75	0.8	454	221.9
eh	140	46.7	192	23.9	0.75	0.6	216	131.9
fi	70	46.7	96	10.1	0.75	0.6	108	66.0
Total tie force								6975.0

Design ties and anchorage

Tie design is similar to that in Example 10.1, except that the additional horizontal thrust from the distributed loads increases the force to 6975 kN. The required area of steel for the tie is $A_{ts} = F_{tu}/\phi f_y = 6975 \times 10^3/(0.75 \times 420) = 22{,}140\ \text{mm}^2$ or 22 No. 36 (No. 11) bars. As in Example 10.1, 90° hooks will be required to anchor the tie. The steel will be placed in two layers of five bars and three layers of four bars. Example 10.1 validated that the reinforcement will fit in the available space.

The vertical tie *bh* carries 280 kN. The required area of steel for this tie is $A_{ts} = F_{tu}/\phi f_y = 280 \times 10^3/(0.75 \times 420) = 889\ \text{mm}^2$. Distributed steel is selected for vertical ties because the placement of the struts was arbitrary due to the assumptions made in modeling the distributed load. Thus, the 889 mm^2 is distributed over 910 mm, the center-to-center spacing used for the distributed load. The minimum reinforcement in Example 10.1, No. 16 (No. 5) bars at 250 mm on each face, provides the required steel.

Design details and minimum reinforcement requirements

The minimum reinforcement requirements from Example 10.1 remain unchanged. The final details are shown in Fig. 10.15*d*.

A comparison of Examples 10.1 and 10.2 demonstrates the sensitivity of the design to the applied loading. The addition of the distributed load resulted in an increase in the horizontal tie reinforcement, although the vertical reinforcement, which in the case of Example 10.2 serves as the vertical tie steel, remains unchanged.

Examples 10.1 and 10.2 illustrate that the limiting size of the struts and nodes is determined by the element with the lowest strength, i.e., the lowest value of f_{ce}. Examination of the β_s and β_n values in Tables 10.3 and 10.4 shows the variation in strength. Recognizing that using the lowest value of β (and f_{ce}) will establish the minimum usable strut and node dimensions allows the designer to minimize the number of iterations needed to construct the truss model.

b. Dapped beam ends

Precast and prestressed concrete beams often have *dapped* or notched ends, such as shown in Fig. 10.16, to reduce the floor-to-floor height of buildings. The recess allows structural overlap between the main beams and the floor beams. While the dapped end is advantageous in controlling building floor-to-floor height, it creates two structural problems. First, the shear at the end of the beam must be carried by a much smaller section, and second, the mechanism of load transfer through the notched zone is difficult to represent using conventional design techniques. As a result, dapped-end beams lend themselves to strut-and-tie design methods.

EXAMPLE 10.3 **Design of a dapped beam end.** A 600 mm deep precast concrete T beam has a 250 mm thick web that carries factored end reactions of 290 kN in the vertical direction and 58 kN in the horizontal direction, as shown in Fig. 10.16*a*. The beam end is notched 250 mm vertically and 200 mm along the beam axis. The load is transferred to the support through a 100 × 250 mm bearing plate. Design the end reinforcement, using $f_c' = 35$ MPa and $f_y = 420$ MPa.

Solution. The combination of the concentrated load and the geometric discontinuity suggest the use of a strut-and-tie solution.

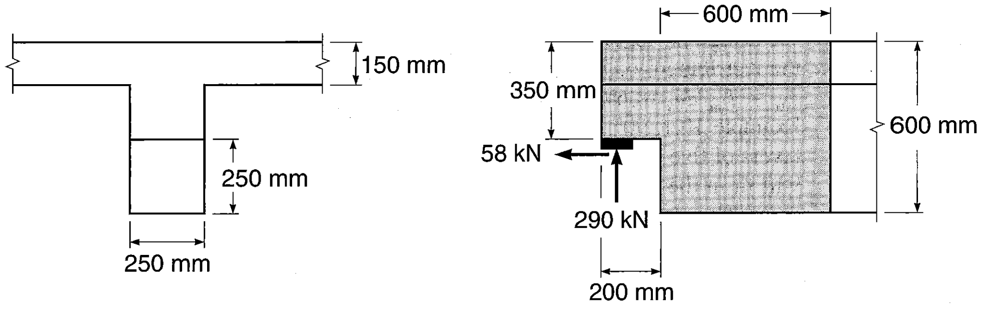
150 mm
250 mm
250 mm
600 mm
350 mm
58 kN
290 kN
600 mm
200 mm

(*a*) Beam section and loads

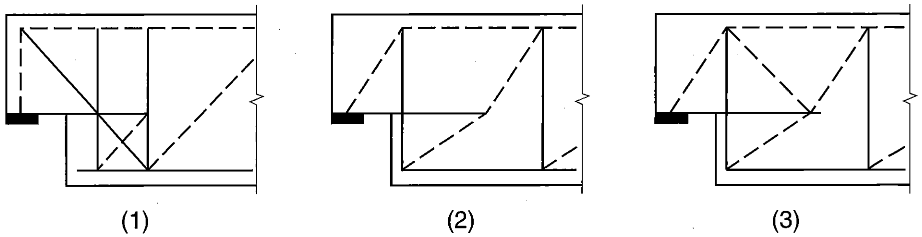

(*b*) Alternative truss models

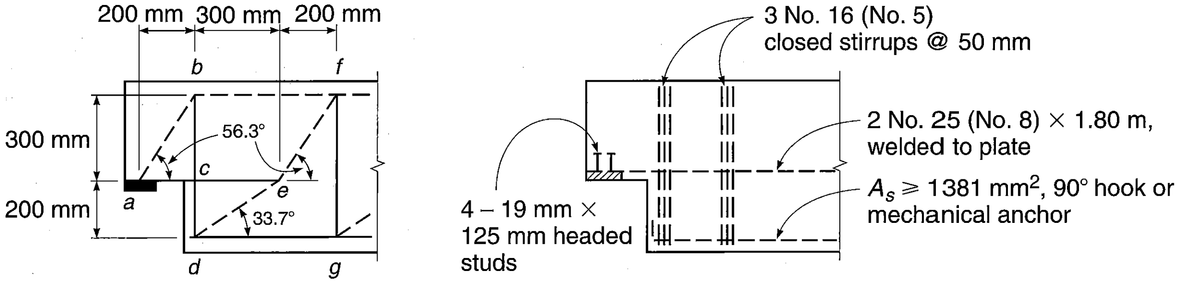
200 mm
300 mm
200 mm
b
f
300 mm
56.3°
c
e
200 mm
a
33.7°
d
g
3 No. 16 (No. 5)
closed stirrups @ 50 mm
2 No. 25 (No. 8) × 1.80 m,
welded to plate
$A_s \geq 1381$ mm^2, 90° hook or
mechanical anchor
4 – 19 mm ×
125 mm headed
studs

(*c*) Truss geometry and loads (*d*) Final end design

FIGURE 10.16
Dapped beam end design for Example 10.3.

Definition of D-region

The D-region for this beam is approximately one structural depth in from the end of the notch. The bearing plate will have longitudinal reinforcement welded to it to allow for load transfer. Therefore, the effective depth at the notch is taken as 325 mm. The maximum allowable shear capacity is $V_u = \phi V_n = \phi 0.83\sqrt{f'_c}\,b_w d = 0.75 \times 0.83\sqrt{35} \times 250 \times 325 \times 10^{-3} = 299$ kN. This exceeds the 290 kN applied load, so the section is adequate to proceed with the design.

Force resultants on D-region boundaries and the truss model

Three possible truss layouts are considered, as shown in Fig. 10.16*b*. Option 1 includes a vertical strut and a diagonal tension tie to the lower chord of the beam. The presence of several tension ties in this model suggests that this is not a minimum energy solution. Option 2 includes a diagonal compressive strut and a vertical hanger to transfer the load to the bottom chord of the beam. The compression strut below the dapped end transfers the tensile reaction to the main longitudinal steel. Option 3 includes an internal triangular truss to balance the reaction within the interior of the beam. Balancing nodal forces at an indeterminate interior four-member joint

TABLE 10.4
Strut and tie properties and forces for Example 10.3

Member Type	Member	β_s	β_n	Force, kN	w_i, mm	Capacity, kN	A_s Required, mm^2	A_s Provided, mm^2	Reinforcement
Strut	*ab*	0.75	0.8	354	122	510			
	bf	1.0	0.8	196	68	285			
	de	0.75	0.8	523	180	753			
	ef	0.75	0.8	354	122	510			
Tie	*ae*			251	88		798	1020	2 No. 25 (No. 8)
	bd[†]			290	100		920	1194	3 No. 16 (No. 5)
	dg[‡]			435	150		1381	1530	3 No. 25 (No. 8)
	fg[†]			290	100		920	1194	3 No. 16 (No. 5)

[†] For ties *bd* and *fg*, use three No. 16 (No. 5) stirrups with two legs each, $A_s = 3$ stirrups $\times$ 2 legs $\times$ 199 mm^2 = 1194 mm^2

[‡] Tie *dg* is an extension of the main longitudinal reinforcement and must have an area $\geq$ 1381 mm^2 and a 90° hook or mechanical anchor at node *d*. If the main reinforcement is insufficient, auxiliary reinforcement may be added.

poses difficulties in joint detailing, but may be desirable if concentrated loads are applied to the top flange. Option 2 is selected as the design choice based on its simplicity and limited number of tension ties. The dimensions of the truss are shown in Fig. 10.16*c*, and the truss forces are summarized in Table 10.4.

Selecting dimensions for strut and nodal zones

The nodal zone stress is established at the bearing plate. The stress is $p = V_u/A_b = 290{,}000/(100 \times 250) = 11.60$ MPa. The calculations for strut *ab* follow, and the remaining strut-and-tie widths and capacities are given in Table 10.4. $F_{u,ab} = V_u/\sin\theta = 290/\sin 56.3° = 354$ kN. The strut width is $w_{ab} = F_{u,ab}/(p \times 250) = 122$ mm.

Capacity of struts

The strut design capacity is based on the strength of a bottle-shaped strut ($\beta_s = 0.75$). For strut *ab*, $\phi F_{ns,ab} = \phi 0.85\beta_s f_c'\, w_{ab} b_s = 0.75 \times 0.85 \times 0.75 \times 35 \times 122 \times 250 \times 10^{-3} = 510$ kN. This exceeds the applied load of 354 kN, so the strut is adequate. The remaining strut design capacities are summarized in Table 10.4. All exceed the applied forces, as would be expected with the low nodal stress used in this design.

Design ties and anchorage

For tie *bd*, $A_{ts} = F_{u,bd}/\phi f_y = 290 \times 10^3/(0.75 \times 420) = 921$ mm^2. Three No. 16 (No. 5) stirrups provide 1194 mm^2 of steel. The maximum width for tie *bd* is $w_{bd} = F_{u,bd}/pb = 290 \times 10^3/(11.60 \times 250) = 100$ mm. Three No. 16 (No. 5) stirrups may be placed within a total width of 68 mm and, thus, fit within the maximum tie width for *bd*. Tie *ae* carries both the horizontal component of strut *ab* and the 58 kN horizontal reaction. Therefore, $F_{u,ae} = 290 \times 200/300 + 58 = 251$ kN, requiring an area of steel equal to 798 mm^2, which is provided by two No. 25 (No. 8) bars. The anchorage length of the ties exceeds the available nodal dimensions. Therefore, tie *ae* is welded to the plate at node *a* and has a full development length to the right of node *f*. Ties *bd* and *fg* are detailed as closed stirrups. The area of steel and the selected bar sizes for the ties are tabulated in Table 10.4. Stirrups for tie *bd* are grouped together and should be added to any normal shear reinforcement from the B-region of the beam.

Design details and minimum reinforcement requirements

Strut *ab* transfers a horizontal thrust to node *a*. Welding the reinforcement for tie *ae* to the plate anchors the tie, but it is not sufficient to ensure that the horizontal component of the strut force is transferred to the tie. Two solutions are possible. First, the plate at node *a* may be replaced with a steel angle. An 88 mm tall leg is needed to confine the nodal zone width. Second, a more common practice in the precast industry, headed studs are welded to the plate and the connection is designed by the shear-friction principles described in Section 4.9. Headed studs have a yield stress of 350 MPa and a coefficient of friction μ between concrete and steel of 0.7. Thus, the area of studs required to resist the horizontal components of strut *ab* is $A_{vf} = V_{uf}/\phi f_y \mu = 290 \times 10^3 \times (200/300)/(0.75 \times 350 \times 0.7) = 1052\ \text{mm}^2$. Four 19 mm diameter × 125 mm long headed studs will be used to provide 1134 mm^2. The 125 mm length places the head of the stud outside of the nodal zone width.

Tie *dg* is an extension of the main longitudinal reinforcement. An area of Grade 60 steel $\geq$ 1381 mm^2 is needed to provide the force in the tie, which should also be checked against the reinforcement requirements for moment in the B-region. A 90° hook or mechanical anchor is required at node *d* to provide full development of the force in tie *dg*. If the beam is prestressed, the prestressing steel and the accompanying compression in the concrete provide an equivalent anchorage.

Minimum reinforcement in the dapped end is $A_{v,\min} = 0.0025 b_w s = 0.0025 \times 250 \times 1000 = 625\ \text{mm}^2/\text{m}$. This is satisfied by No. 13 (No. 4) bars at 300 mm. Since the steel in tie *bd* exceeds this, no further reinforcement is needed. The final connection is detailed in Fig. 10.16*d*.

The examples in this section illustrate both the methodology of strut-and-tie design and the importance of understanding the detailing requirements needed to transfer forces at nodes. Failure to appreciate the need to provide anchorage for the tie in Example 10.1 or to supply thrust resistance for the struts in Example 10.3 can lead to failure. In the examples, the contact area was used to establish the hydrostatic nodal pressure. As discussed, an equally acceptable solution would have been to select the maximum stress for one of the struts. The remaining strut and tie widths would then be adjusted accordingly.

REFERENCES

10.1. J. Schlaich, K. Schäfer, and M. Jennewein, "Toward a Consistent Design of Structural Concrete," *J. PCI*, vol. 32, no. 3, May-June 1987, pp. 74–150.
10.2. P. Marti, "Truss Models in Detailing," *Concr. Intl.*, vol. 7, no. 12, 1985, pp. 66–73.
10.3. P. Marti, "Basic Tools for Reinforced Concrete Design," *J. ACI*, vol. 82, no. 1, 1985, pp. 46–56.
10.4. J. Schlaich and K. Schäfer, "Design and Detailing of Structural Concrete Using Strut-and-Tie Models," *Struct. Eng.*, vol. 69, no. 6, March 1991, 13 pp.
10.5. *Building Code Requirements for Structural Concrete and Commentary*, Appendix A, ACI 318-08, American Concrete Institute, Farmington Hills, MI, 2008.
10.6. C. M. Uribe and S. Alcocer, "Example 1a: Deep Beam Design in Accordance with ACI 318-2002," *Examples for the Design of Structural Concrete with Strut-and-Tie Models*, ACI SP 208, Karl-Heinz Reineck (ed.), American Concrete Institute, Farmington Hills, MI, 2002, pp. 65–80.
10.7. L. C. Nowak and H. Sprenger, "Example 5: Deep Beam with Opening," *Examples for the Design of Structural Concrete with Strut-and-Tie Models*, ACI SP 208, Karl-Heinz Reineck (ed.), American Concrete Institute, Farmington Hills, MI, 2002, pp. 129–144.
10.8. L. Chow, H. Conway, and G. Winter, "Stresses in Deep Beams," *Trans. ASCE*, vol. 118, 1953, p. 686.
10.9. *Examples for the Design of Structural Concrete with Strut-and-Tie Models*, ACI SP 208, Karl-Heinz Reineck (ed.), American Concrete Institute, Farmington Hills, MI, 2002.
10.10. J. MacGregor, *Reinforced Concrete, Mechanics and Design*, 3rd ed., Prentice-Hall, Upper Saddle River, NJ, 1997.
10.11. J. K. Wight and G. J. Parra-Montesinos, "Strut-and-Tie Model for Deep Beam Design," *Concr. Intl.*, vol. 25, no. 5, 2003, pp. 63–70.
10.12. G. J. Klein, "Curved-Bar Nodes," *Concr. Intl.*, vol. 30, no. 9, 2008, pp. 43–47.

PROBLEMS

10.1. A deep beam with the dimensions and material properties given in Example 10.1 carries a single 600 × 600 mm column with a factored load of 7000 kN located 3.67 m from the left end. Design the beam using a strut-and-tie solution that includes the self-weight of the beam. In your solution, include (*a*) a sketch of the load path and truss layout, (*b*) the sizes and geometry of the struts, ties, and nodal zones, and (*c*) a complete sketch of the final design.

10.2. Redesign the column bracket shown in Example 11.5 using the strut-and-tie method. Your strut-and-tie model may be based on Fig. 11.23. Material properties remain the same as in Example 11.5.

10.3. A 1 m deep single T beam with a dapped end has a web thickness of 150 mm. The factored end reactions are 370 kN in the vertical direction and 80 kN in the horizontal direction. The horizontal force places the beam in tension. The beam end is notched 300 mm high by 250 mm along the beam axis. Design the end connection using a bearing plate that is 75 mm wide with a thickness equal to that of the web. Adjust the bearing plate size if necessary. Specified material strengths are $f_c' = 42$ MPa and $f_y = 420$ MPa.

10.4. A transfer girder has an overall depth of 3.4 m and spans 6.8 m between column supports. In addition to its own weight, it will pick up a uniformly distributed factored load of 55 kN/m from the floor above and will carry a 350 × 350 mm column delivering a concentrated factored load of 4500 kN from floors above at midspan. The girder width must be equal to or less than 400 mm. Design the beam for the given loads. Find the girder width and the area and geometry of tie steel, and specify the placement details. Material strengths are $f_c' = 35$ MPa and $f_y = 420$ MPa.

10.5. A column transfers a factored load of 3000 kN to the 3 m square spread footing shown in Fig. P10.5, resulting in a factored uniform soil pressure of 333 kN/m^2. Design the footing reinforcement using strut-and-tie methods. Material strengths are $f_c' = 28$ MPa and $f_y = 420$ MPa. Because footings typically contain no shear reinforcement, your design should be based on unreinforced bottle-shaped struts.

FIGURE P10.5

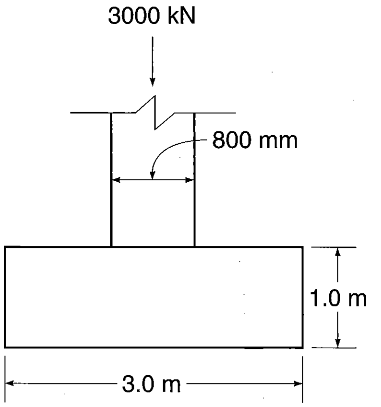

10.6. Redesign the footing in Problem 10.5 using traditional flexure and shear methods, as described in Chapter 16. Compare your solution to the solution for Problem 10.5, and comment on your results.

11

Design of Reinforcement at Joints

11.1 INTRODUCTION

Most reinforced concrete failures occur not because of any inadequacies in analysis of the structure or in design of the members but because of inadequate attention to the detailing of reinforcement. Most often, the problem is at the connections of main structural elements (Ref. 11.1).

There is an increasing tendency in modern structural practice for the engineer to rely upon a detailer, employed by the reinforcing bar fabricator, to provide the joint design. Certainly, in many cases, standard details such as those found in the ACI Detailing Manual (Ref. 11.2) can be followed, but only the design engineer, with the complete results of analysis of the structure at hand, can make this judgment. In many other cases, special requirements for force transfer require that joint details be fully specified on the engineering drawings, including bend configurations and cutoff points for main bars and provision of supplementary reinforcement.

The basic requirement at joints is that all of the forces existing at the ends of the members must be transmitted through the joint to the supporting members. Complex stress states exist at the junction of beams and columns, for example, that must be recognized in designing the reinforcement. Sharp discontinuities occur in the direction of internal forces, and it is essential to place reinforcing bars, properly anchored, to resist the resulting tension. Some frequently used connection details, when tested, have been found to provide as little as 30 percent of the strength required (Refs. 11.1 and 11.3).

Over the years, important research has been directed toward establishing an improved basis for joint design (Refs. 11.4 and 11.5). Full-scale tests of beam-column joints have led to improved design methods such as those described in *Recommendations for Design of Beam-Column Joints in Monolithic Reinforced Concrete Structures,* reported by ACI-ASCE Committee 352 (Ref. 11.6). Although they are not a part of the ACI Code, such recommendations provide a basis for the safe design of beam-column joints both for ordinary construction and for buildings subject to seismic forces. Other tests have given valuable insight into the behavior of beam-girder joints, wall junctions, and other joint configurations, thus providing a sound basis for design.

The practicality of the joint design should not be overlooked. Beam reinforcement entering a beam-column joint must clear the vertical column bars, and timely consideration of this fact in selecting member widths and bar size and spacing can avoid costly delays in the field. Similarly, beam steel and girder steel, intersecting at right angles at a typical beam-girder-column joint, cannot be in the same horizontal plane as they enter the joint. Figure 11.1 illustrates the congestion of reinforcing bars at such an intersection. Concrete placement in such a region is difficult at best, but is assisted with the use of plasticizer admixtures.

FIGURE 11.1
Steel congestion at beam-girder-column joint.

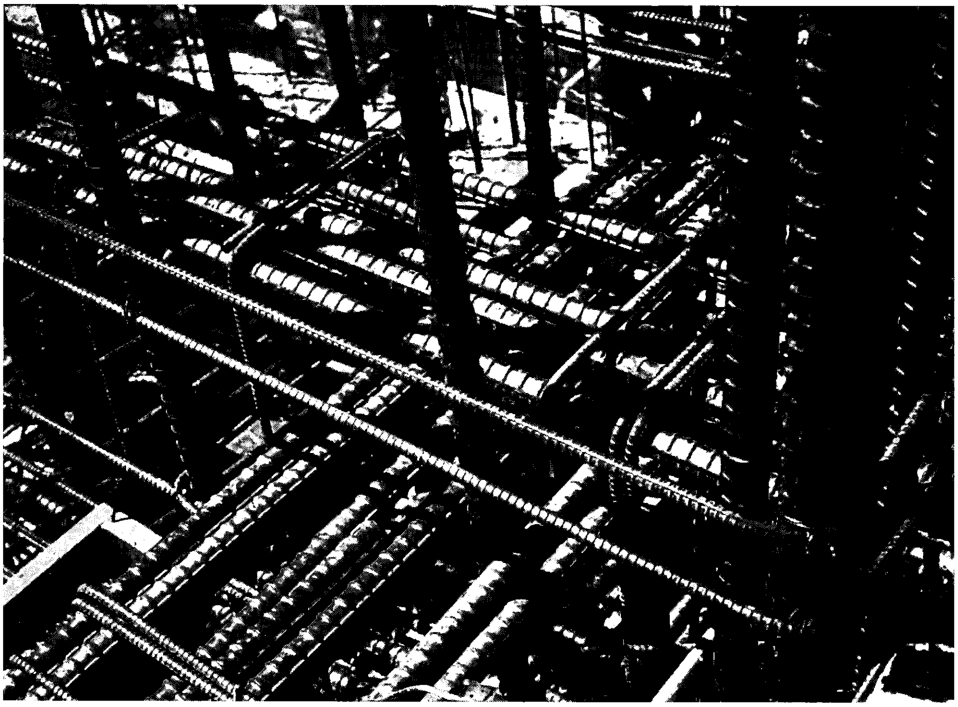

Most of this chapter treats the design of joint regions for typical continuous-frame monolithic structures that are designed according to the strength requirements of the ACI Code for gravity loads or normal wind loads. Joints connecting members that must sustain strength under reversals of deformation into the inelastic range, as in earthquakes, represent a separate category and are covered in Chapter 20. Brackets and corbels, although they are most often a part of precast buildings rather than monolithic construction, have features in common with monolithic joints, and these will be covered here.

11.2 BEAM-COLUMN JOINTS

A *beam-column joint* is defined as the portion of a column within the depth of the beams that frame into it. Formerly, the design of monolithic joints was limited to providing adequate anchorage for the reinforcement. However, the increasing use of high-strength concrete, resulting in smaller member cross sections, and the use of larger-diameter and higher-strength reinforcing bars now require that greater attention be given to joint design and detailing. Although very little guidance is provided by the ACI Code, the ACI-ASCE Committee 352 report *Recommendations for Design of Beam-Column Joints in Monolithic Reinforced Concrete Structures* (Ref. 11.6) provides a basis for the design of joints in both ordinary structures and structures required to resist heavy cyclic loading into the inelastic range.

a. Classification of Joints

Reference 11.6 classifies structural joints into two categories. A *Type 1* joint connects members in an ordinary structure designed on the basis of strength, according to the

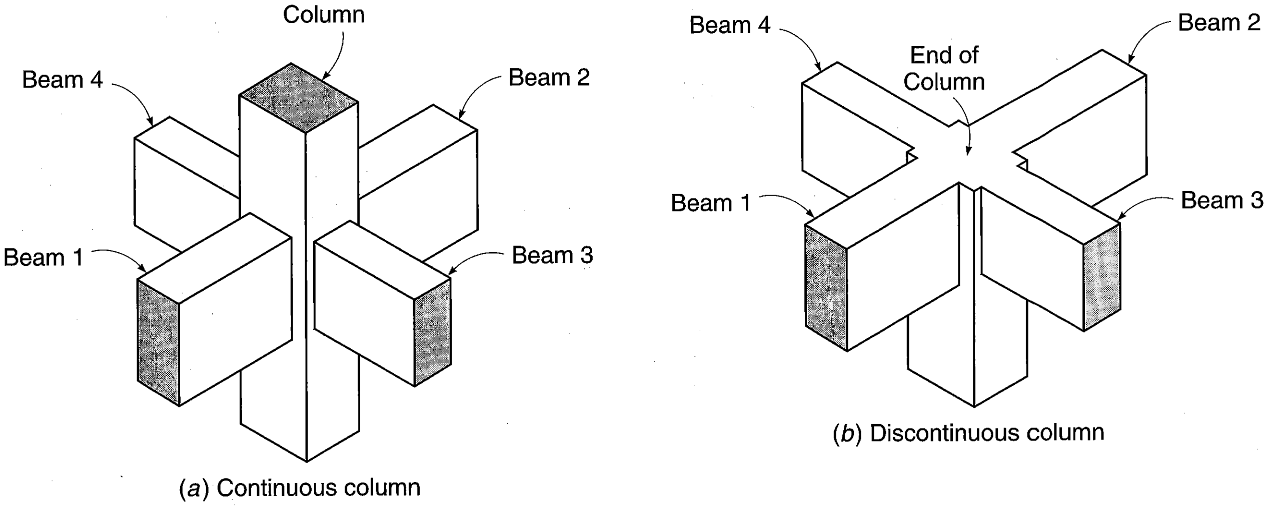

(*a*) Continuous column

(*b*) Discontinuous column

FIGURE 11.2
Typical monolithic interior beam-column joint.

main body of the ACI Code, to resist gravity and normal wind load. A *Type 2* joint connects members designed to have sustained strength under deformation reversals into the inelastic range, such as members in a structure designed for earthquake motions, very high winds, or blast effects. Only Type 1 joints will be considered in this chapter.

Figure 11.2*a* shows typical *interior joints* in a monolithic reinforced concrete frame, with beams 1 and 2 framing into opposite faces of the column and beams 3 and 4 framing into the column faces in the perpendicular direction. An *exterior joint* would include beams 1, 2, and 3, or in some cases only beams 1 and 2. A *corner joint* would include only beams 1 and 3, or occasionally only a single beam 1. A joint may have beams framing into it from two perpendicular directions as shown, but for purposes of analysis and design each direction can be considered separately. Joint confinement is further affected if the column is discontinuous, as illustrated in Fig. 11.2*b*.

b. Joint Loads and Resulting Forces

The joint region must be designed to resist forces that the beams and column transfer to the joint, including axial loads, bending, torsion, and shear. Figure 11.3*a* shows joint loads acting on the free body of a typical joint of a frame subject to gravity loads, with moments M_1 and M_2 acting on opposite faces, in the opposing sense. In general, these moments will be unequal, with their difference equilibrated by the sum of the column moments M_3 and M_4. Figure 11.3*b* shows the resulting forces to be transmitted through the joint. Similarly, Fig. 11.4*a* shows the loads on a joint in a structure subjected to sidesway loading. The corresponding joint forces are shown in Fig. 11.4*b*. Only for very heavy lateral loading, such as from seismic forces, would the moments acting on opposite faces of the joint act in the same sense, as shown here, producing very high horizontal shears within the joint.

According to the recommendations by Committee 352, the forces to be considered in designing joint regions are not those determined from the conventional frame analysis; rather, they are calculated based on the *nominal strengths of the members*.

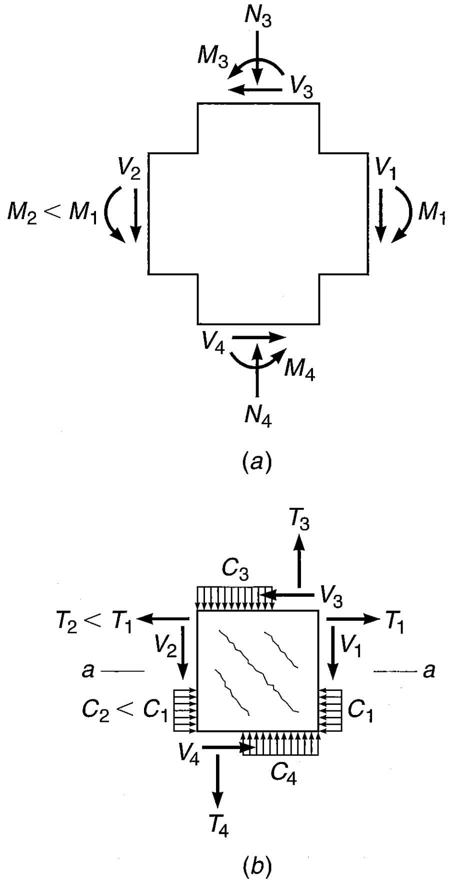

FIGURE 11.3
Joint loads and forces resulting from gravity loads: (*a*) forces and moments on the free body of a joint region; (*b*) resulting internal forces.

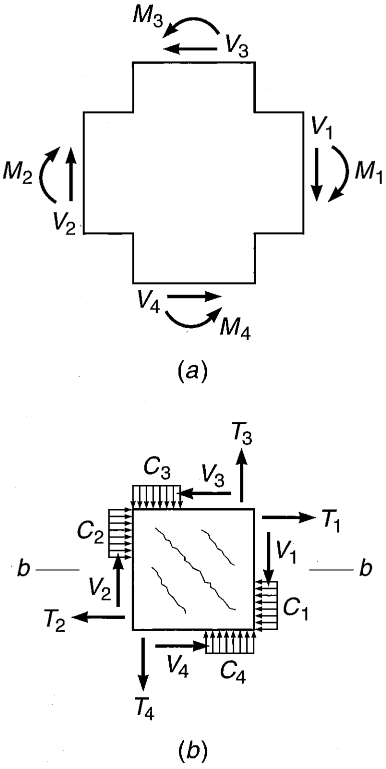

FIGURE 11.4
Joint loads and forces resulting from lateral loads: (*a*) forces and moments on the free body of a joint; (*b*) resulting internal forces.

Where a typical underreinforced beam meets the column face, the tension force from the negative moment reinforcement at the top of the beam is to be taken as $T = A_s f_y$, and the compression force at the face is from equilibrium $C = T$, not the nominal compressive capacity of the concrete. The design moment applied at the joint face is that corresponding to these maximum forces, $M_u = M_n = A_s f_y(d - a/2)$, rather than that from the overall analysis of the frame. Note that the inclusion of the usual strength reduction factor ϕ would be unconservative in the present case because it would reduce the forces for which the joint is to be designed; it is therefore not included in this calculation.

With the moment applied to each joint face found in this way, the corresponding column forces for joint design are those forces required to keep the connection in equilibrium. To illustrate, the column shears V_3 and V_4 of Figs. 11.3*a* and 11.4*a* are calculated based on the free body of the column between inflection points, as shown in Fig. 11.5. The inflection points generally can be assumed at column midheight, as shown.

FIGURE 11.5
Free-body diagram of an interior column and joint region.

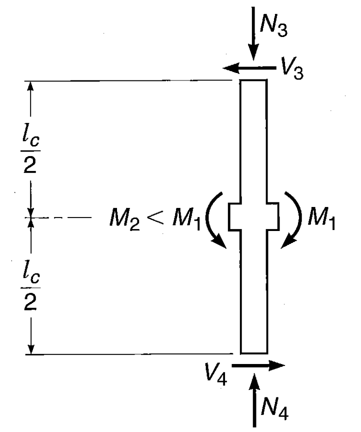

c. Shear Strength of a Joint

A joint subject to the forces shown in Fig. 11.3*b* or 11.4*b* will develop a pattern of diagonal cracking owing to the diagonal tensile stresses that result from the normal forces and shears, as indicated by those figures. The approach used by Committee 352 is to limit the shear force on a horizontal plane through the joint to a value established by tests. The design basis is

$$V_u \le \phi V_n \tag{11.1}$$

where V_u is the applied shear force, V_n is the nominal shear strength of the joint, and ϕ is taken equal to 0.75.

The shear force V_u is to be calculated on a horizontal plane at midheight of the joint, such as plane *a-a* of Fig. 11.3*b* or plane *b-b* of Fig. 11.4*b*, by summing horizontal forces acting on the joint above that plane. For example, in Fig. 11.3*b* the joint shear on plane *a-a* is

$$V_u = T_1 - T_2 - V_3$$

and in Fig. 11.4*b*, the joint shear on plane *b-b* is

$$\begin{aligned} V_u &= T_1 + C_2 - V_3 \\ &= T_1 + T_2 - V_3 \end{aligned}$$

The nominal shear strength V_n is given by the equation

$$V_n = \gamma \sqrt{f_c'}\, b_j h_c \tag{11.2}$$

where b_j is the effective joint width in mm, h_c is the thickness in mm of the column in the direction of the load being considered, and $\sqrt{f_c'}$ is expressed in MPa units. According to Committee 352, Eq. (11.2) is conservative for concretes with strengths up to 105 MPa. As discussed in Chapter 20, ACI Code 21.7 follows similar procedures for the design of joints in moment resistant frames, the only difference being that lower values for the coefficient γ are recommended.

The coefficient γ in Eq. (11.2) depends on the confinement of the joint provided by the beams framing into it and whether the column is continuous or terminates at the level under consideration, as shown in Table 11.1.

TABLE 11.1

Values of γ for beam-to-column connections

	Continuous Columns		Discontinuous Columns	
Joint	Gravity Frames (Type 1)	Moment Resisting Frames (Type 2)	Gravity Frames (Type 1)	Moment Resisting Frames (Type 2)
Interior	2.0	1.7	1.7	1.25
Exterior	1.7	1.25	1.25	1.0
Column	1.25	1.0	1.0	0.7

The definitions of interior, exterior, and corner joints were discussed in Section 11.2a. However, there are restrictions to be applied for purposes of determining γ as follows:

1. An *interior joint* has beams framing into all four sides of the joint. However, to be classified as an interior joint, the beams should cover at least $\frac{3}{4}$ the width of the column, and the total depth of the shallowest beam should not be less than $\frac{3}{4}$ the total depth of the deepest beam. Interior joints that do not satisfy this requirement should be classified as *exterior joints*.
2. An *exterior joint* has at least two beams framing into opposite sides of the joint. However, to be classified as an exterior joint, the widths of the beams on the two opposite faces of the joint should cover at least $\frac{3}{4}$ the width of the column, and the depths of these two beams should be not less than $\frac{3}{4}$ the total depth of the deepest beam framing into the joint. Joints that do not satisfy this requirement should be classified as *corner joints*.

For joints with beams framing in from two perpendicular directions, as for a typical interior joint, the horizontal shear should be checked independently in each direction. Although such a joint is designed to resist shear in two directions, only one classification is made for the joint in this case (i.e., only one value of γ is selected based on the joint classification, and that value is used to compute V_n when checking the design shear capacity in each direction).

According to Committee 352 recommendations, the effective joint width b_j to be used in Eq. (11.2) depends on the transverse width of the beams that frame into the column as well as the transverse width of the column. With regard to the beam width b_b, if there is a single beam framing into the column in the load direction, then b_b is the width of that beam. If there are two beams in the direction of shear, one framing into each column face, then b_b is the average of the two beam widths. In reference to Fig. 11.6*a*, when the beam width is less than the column width, the effective joint width is equal to the smaller of the average of the beam width and column width,

$$b_j = \frac{b_b + b_c}{2} \tag{11.3}$$

and

$$b_j = b_b + \sum \frac{mh_c}{2} \tag{11.4}$$

FIGURE 11.6
Determination of effective joint width b_j: (*a*) beams narrower than column; (*b*) eccentricity between beam centerline and column centroid; (*c*) beam wider than column. (*Parts a and b adapted from Ref. 11.6.*)

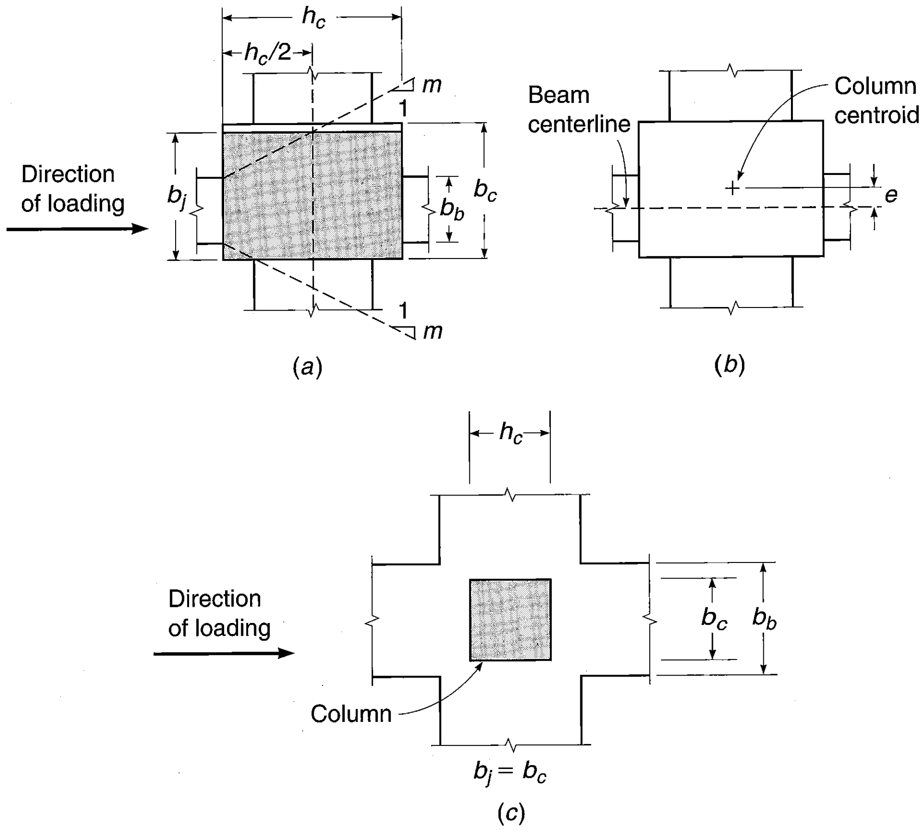

where m is a slope that depends on the eccentricity e of the beam centerline with respect to the column centroid (Fig. 11.6*b*). If e is greater than $b_c/8$, $m = 0.3$; otherwise, $m = 0.5$. As shown in Fig, 11.6*a*, the slope m defines a width at the centroid of the column. According to Committee 352, $mh_c/2$ should not be taken as greater than the extension of the column edge beyond the edge of the beam.

If the beam width b_b *exceeds* the column width, the effective joint width b_j is equal to the column width b_c, as shown in Fig. 11.6*c*.

d. Confinement and Transverse Joint Reinforcement

The successful performance of a beam-column joint depends strongly on the lateral confinement of the joint. Confinement has two benefits: (1) the core concrete is strengthened and its strain capacity improved, and (2) the vertical column bars are prevented from buckling outward. Confinement can be provided either by the beams that frame into the joint or by special column ties provided within the joint region.

Confinement by beams is illustrated in Fig. 11.7. According to Committee 352 recommendations, if beams frame into four sides of the joint, as in Fig. 11.7*a*, adequate confinement is provided if each beam width is at least $\frac{3}{4}$ the width of the intersected column face and if no more than 100 mm of column face is exposed on either side of the beam. Where beams frame into only two sides of the joint, as in Fig. 11.7*b*, adequate confinement can be assumed *in the direction of the beams* if the beam widths are at least $\frac{3}{4}$ the column width and no more than 100 mm of concrete is exposed on either

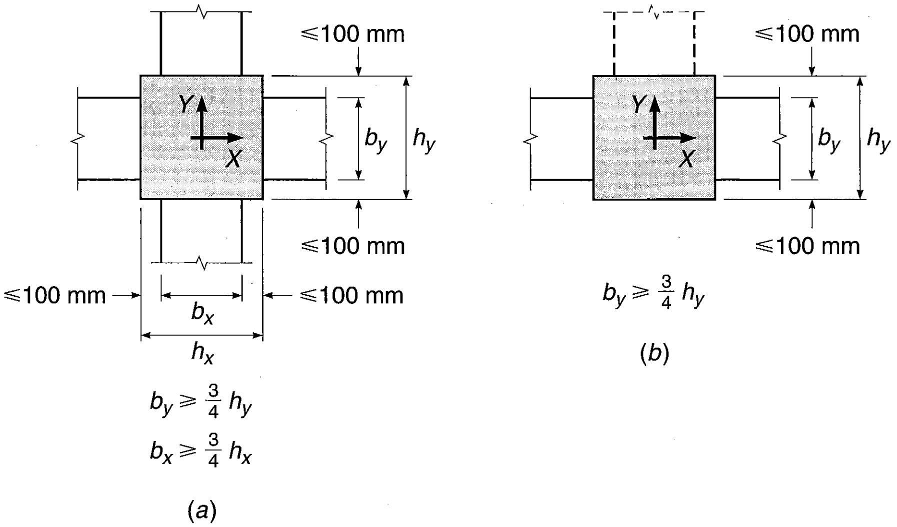

FIGURE 11.7
Confinement of joint concrete by beams: (*a*) confinement in *X* and *Y* directions; (*b*) confinement in *X* direction only.

side of the beams. In the other direction, transverse reinforcement must be provided for confinement. The presence of a third beam, but not a fourth, in the perpendicular direction does not modify the requirement for transverse reinforcement.

If adequate confinement is not provided by beams according to these criteria, then transverse reinforcement must be provided. If confinement steel is needed, it must meet all the usual requirements for column ties (see Section 8.2). In addition, there must be at least two layers of ties between the top and bottom flexural steel in the beams at the joint, and the vertical center-to-center spacing of these ties must not exceed 300 mm. If the beam-column joint is part of the primary system for resisting nonseismic lateral loads, this maximum spacing is reduced to 150 mm. For joints that are not confined by beams on four sides, ACI Code 11.10 requires that the ties satisfy Eq. (4.13).

e. Anchorage and Development of Beam Reinforcement

For interior joints, normally the flexural reinforcement in a beam entering one face of the joint is continued through the joint to become the flexural steel for the beam entering the opposite face. Therefore, for loadings associated with Type 1 joints, pullout is unlikely, and no special recommendations are made. However, for exterior or corner joints, where one or more of the beams do not continue beyond the joint, a problem of bar anchorage exists. The critical section for development of the yield strength of the beam steel is at the face of the column. Column dimensions seldom permit development of the steel entering the joint by straight embedment alone, and hooks are usually needed for the negative beam reinforcement. Headed bars or ninety degree hooks are used, with the hook extending toward and beyond the middepth of the joint. If the bottom bars entering the joint need to develop their strength $A_s f_y$ at the face of the joint, as they do if the beam is a part of a primary lateral load-resisting system, they should also be anchored with 90° hooks, in this case turned upward to extend toward the middepth of the joint, or headed bars. Requirements for development of hooked bars given in Chapter 5 are applicable in both cases, including modification factors for concrete cover and for enclosure with ties or stirrups.

EXAMPLE 11.1 **Design of exterior Type 1 joint.** The exterior joint shown in Fig. 11.8 is a part of a continuous, monolithic, reinforced concrete frame designed to resist gravity loads only. Member section dimensions $b \times h$ and reinforcements are as shown. The frame story height is 3.6 m. Material strengths are $f'_c = 28$ MPa and $f_y = 420$ MPa. Design the joint, following the recommendations of the Committee 352 report.

Solution. First the joint geometry must be carefully laid out, to be sure that beam bars and column bars do not interfere with one another and that placement and vibration of the concrete are practical. In this case, bar layout is simplified by making the column 100 mm wider than the beams. Column steel is placed with the usual 40 mm of concrete outside of the No. 13 (No. 4) ties. Beam top and bottom bars are placed just inside the outer column bars. The slight offset of the center top beam bars to avoid the center column bars is of no concern. Top bars of the spandrel beams are placed just under the top normal beam bars, except for the outer spandrel bar, which is above the hook shown in Fig. 11.8*b*. Bottom bars enter the joint at different levels without interference.

No anchorage problems exist for the spandrel beam top reinforcement, which is continuous through the joint. However, the normal beam top steel must be provided with hooks to develop its yield strength at the face of the column. Referring to Table 5.3, the basic development length for No. 32 (No. 10) hooked bars is

$$l_{dh} = \left(\frac{0.24\psi_e f_y}{\lambda\sqrt{f'_c}}\right) d_b = \left(\frac{0.24 \times 1 \times 420}{1 \times \sqrt{28}}\right) 32.3 = 615 \text{ mm}$$

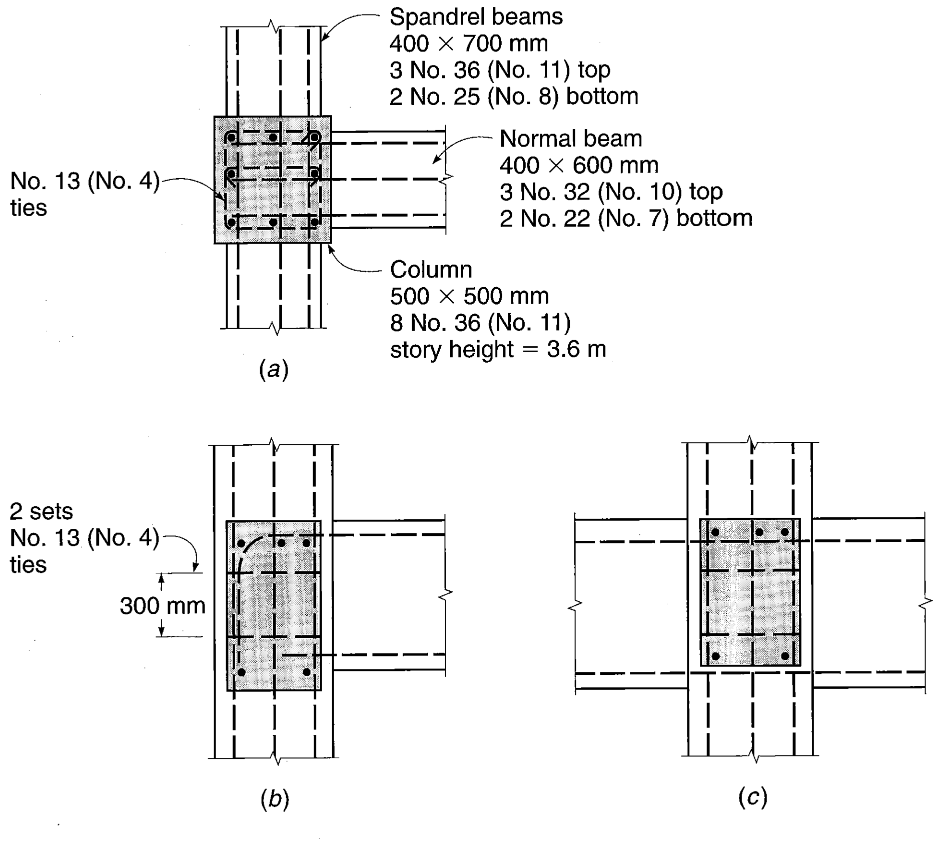

FIGURE 11.8
Exterior beam-column joint for Example 11.1: (*a*) plan view; (*b*) cross section through spandrel beam; (*c*) cross section through normal beam. Note that beam stirrups and column ties outside of the joint are not shown.

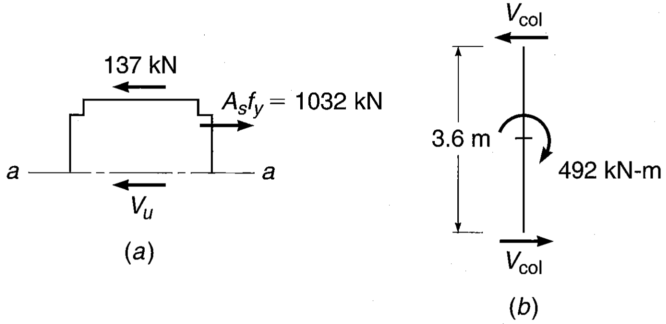

FIGURE 11.9
Basis of column shear for Example 11.1: (*a*) horizontal forces on joint free-body sketch; (*b*) free-body sketch of column between inflection points.

Being inside the column bars, the beam top bars have side cover of 40 + 12.7 + 35.8 = 88.5 mm. This exceeds 65 mm, so a modification factor of 0.7 is applicable, and the required hook development length is

$$l_{dh} = 615 \times 0.7 = 431 \text{ mm}$$

If the hooked bars are carried down just inside the column ties, the actual embedded length is 500 − 40 − 12.7 = 477 mm, exceeding 431 mm, so development is ensured. None of the beams are a part of the primary, lateral load–resisting system of the frame, so the bottom bars simply can be carried 150 mm into the face of the joint and stopped.

Next the shear strength of the joint must be checked. In the direction of the spandrel beams, moments applied to the joint will be about the same and acting in the opposite sense, so very little joint shear is expected in that direction. However, the normal beam will subject the joint to horizontal shears. In reference to Fig. 11.9*a*, which shows a free-body sketch of the top half of the joint, the maximum force from the beam top steel is

$$A_sf_y = 3 \times 819 \times 420 = 1032 \text{ kN}$$

The joint moment is calculated based on this tensile force. The normal beam effective depth is $d = 600 - 40 - 12.7 - 32.3/2 = 531$ mm and with stress block depth $a = A_sf_y/0.85f'_cb_w = 1032/(0.85 \times 28 \times 400) = 108$ mm, the design moment is

$$M_u = M_n = A_sf_y\left(d - \frac{a}{2}\right) = 1032\left(531 - \frac{108}{2}\right) \times 10^{-3} = 492 \text{ kN-m}$$

Column shears corresponding to this joint moment are found based on the free body of the column between assumed midheight inflection points, as shown in Fig. 11.9*b*: $V_{col} = 492/3.6 = 137$ kN. Then summing horizontal forces on the joint above the middepth plane *a-a*, the joint shear in the direction of the normal beam is

$$V_u = 1032 - 137 = 895 \text{ kN}$$

For purposes of calculating the joint shear strength, the joint can be classified as exterior, because the 400 mm width of the spandrel beams exceeds $\frac{3}{4}$ the column width of 375 mm, and the spandrels are the deepest beams framing into the joint. Thus, $\gamma = 1.7$. The effective joint width is the smaller of

$$b_j = \frac{b_b + b_c}{2} = \frac{400 + 500}{2} = 450 \text{ mm}$$

and

$$b_j = b_b + \sum \frac{mh_c}{2} = 400 + 2\left(\frac{0.5 \times 500}{2}\right) = 650 \text{ mm}$$

In the latter case, limiting $mh_c/2$ to be no greater than the extension of the column edge beyond the edge of the beam results in $b_j = b_c = 500$ mm.

Using $b_j = 450$ mm, the nominal and design shear strengths of the joint are, respectively,

$$V_n = \gamma\sqrt{f_c'}\, b_j h = 1.7\sqrt{28} \times 450 \times 500 = 1988 \text{ kN}$$

$$\phi V_n = 0.75 \times 1988 = 1491 \text{ kN}$$

The applied shear $V_u = 895$ kN does not exceed the design strength, so shear is satisfactory.

Confinement is provided in the direction of the spandrel beams by the beams themselves because the spandrel width of 400 mm exceeds $\frac{3}{4}$ the column width and no more than 100 mm of column face is exposed on either side. However, in the direction of the normal beam, confinement must be provided by column ties within the joint. Two sets of No. 13 (No. 4) ties will be provided, as shown in Fig. 11.8*a* and *b*. The clear distance between column bars is 144 mm here, less than 150 mm, so strictly speaking the single-leg crosstie is not required. However, it will improve the joint confinement, guard against outward buckling of the central No. 36 (No. 11) column bar, and add little to the cost of construction, so crossties will be specified, as shown in Fig. 11.8*a*. The ties satisfy Eq. (4.13) several times over. Note that a 90° hook at one end, rather than the 135° bend shown, will meet ACI Code tie anchorage requirements and facilitate steel fabrication as well.

EXAMPLE 11.2 **Design of interior Type 1 joint.** Figure 11.10 shows a proposed interior joint of a reinforced concrete building, with beam and column dimensions and reinforcement as indicated. The building frame is to carry gravity loads and normal wind loads. Design and detail the joint reinforcement.

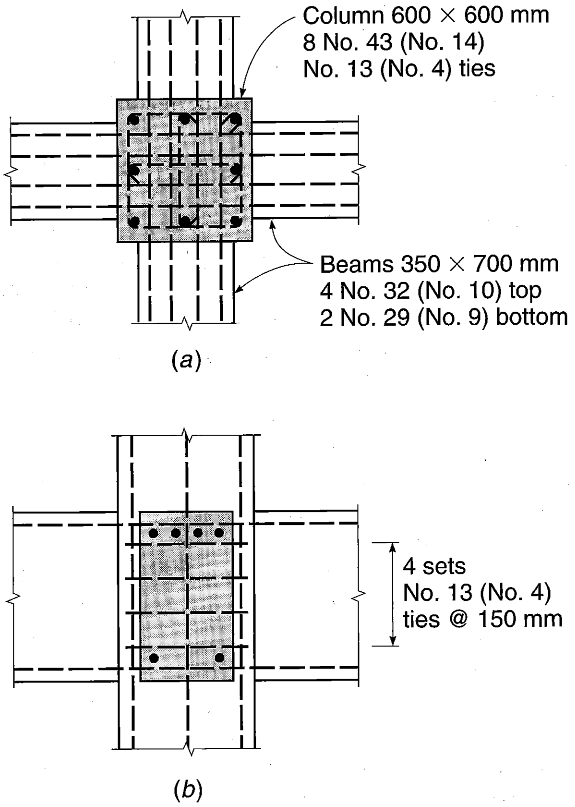

FIGURE 11.10
Interior beam-column joint for Example 11.2: (*a*) plan view; (*b*) section through beam.

SOLUTION. Because the joint is to be a part of the primary, lateral load–resisting system, beam bottom bars as well as top bars are carried straight through the joint for anchorage. In such cases, it is usually convenient to lap splice the bottom steel near the point of inflection of the beams.

In Fig. 11.10*a* and *b*, top and bottom beam bars entering the joint in one direction must pass, respectively, under and over the corresponding bars in the perpendicular direction. It will be assumed that this has been recognized by adjusting the effective depths in designing the beams. Because the column is 250 mm wider than the beams, the outer beam bars can be passed inside the corner column bars without interference. Four bars are used for the beam top steel in order to avoid interference with the center column bar.

Even the combination of normal wind loading with gravity loads should not produce large unbalanced moment on opposite faces of this interior column, and it can be safely assumed that joint shear will not be critical. However, confinement of the joint region by the beams is considered inadequate because (1) the beam width of 350 mm is less than $\frac{3}{4}$ the column width of 600 mm and (2) the exposed column face outside the beam is $(600 - 350)/2 = 125$ mm, which exceeds the 100 mm limit. Consequently, transverse column ties must be added within the joint for confinement. For the 600 mm square column, the spacing between the vertical bars exceeds 150 mm, so it is necessary, according to the ACI Code, to provide ties to support the intermediate bars as well as the corner bars. Three ties are used per set, as shown in Fig. 11.10*a*. Since the joint is a part of the lateral load–resisting system, the maximum vertical spacing of these tie sets is 150 mm. Four sets within the joint, as indicated in Fig. 11.10*b*, are adequate to satisfy this requirement.

f. Wide-Beam Joints

In multistory buildings, to reduce the construction depth of each floor and to reduce the overall building height, wide shallow beams are sometimes used. Joint design in cases where the beams are wider than the column introduces some important concepts not addressed in the Committee 352 report. It is important to equilibrate all of the forces applied to the joint. The tension from the top bars in the usual case, with beam width no greater than the column, will be equilibrated by the horizontal component of a diagonal compression strut within the joint. The diagonal compression at the ends of the strut, in turn, is equilibrated by the beam compression and the thrust from the column. (See Section 11.3 for a more complete description of the strut-and-tie model.) If the outer bars of the normal beam pass *outside* of the column, as they often do in wide-beam designs, the diagonal strut will also be outside of the column, with no equilibrating vertical compression at its upper and lower ends. The outer parts of the beam would tend to shear off, resulting in premature failure. The problem is of special concern for Type 2 connections.

To minimize the problem, Committee 352 suggests that satisfactory performance of Type 2 connections with wide beams will result if, to provide satisfactory bond, the reinforcement passing outside the joint core is selected so that the ratio of the column depth h_c to the bar diameter d_b is greater than or equal to 24 and that at least one-third of the steel passes through or is anchored in the column between the vertical bars. In the event that these restrictions cannot be met, two possibilities exist to improve performance. The first solution requires that all of the beam top steel be placed within the width of the column, and preferably inside the outer column bars. If the normal beam bars are carried outside the joint, the second solution is to provide vertical stirrups through the joint region to carry the vertical component of thrust from the compression strut. In addition, Type 2 exterior beams must be designed for equilibrium torsion per ACI Code 11.5, which may require additional transverse reinforcement.

In extreme but not unusual cases, very wide beams are used, several times wider than the column, with beam depth only about 2 times the slab depth. In such cases, a safe basis for joint design is to treat the wide beam as a slab and follow the recommendations for slab-column connections contained in Chapter 13.

EXAMPLE 11.3

Design of exterior Type 1 joint with wide beams. Figure 11.11 shows a typical exterior joint in the floor of a wide-beam structure, designed to resist gravity loads. Here the beams in each direction are 200 mm wider than the corresponding column dimension. Check the proposed joint geometry and shear strength, and design the transverse joint reinforcement. Material strengths are $f_c' = 28$ MPa and $f_y = 420$ MPa. Story height is 3.6 m.

Solution. For the present case, all normal beam top steel is passed inside the core of the joint, terminating in 90° hooks at the outside of the column. Top steel in the spandrel beams is continuous through the joint but is also carried inside the joint core. Bottom beam bars, in each case, can be spread across the width of the beam, and they are carried only 150 mm into the joint for the normal beam because the joint is not a part of the primary, lateral load–resisting system. The bottom spandrel beam bars are continued to provide structural integrity (ACI Code 7.13). Beam stirrups outside of the joint, not shown in Fig. 11.11, would be carried outside of the outer bottom bars and bent up. They would require small-diameter horizontal bars inside the hooks for proper anchorage at the upper ends of their vertical legs.

FIGURE 11.11
Exterior beam-column joint for Example 11.3: (*a*) plan view; (*b*) section through spandrel beam; (*c*) section through normal beam.

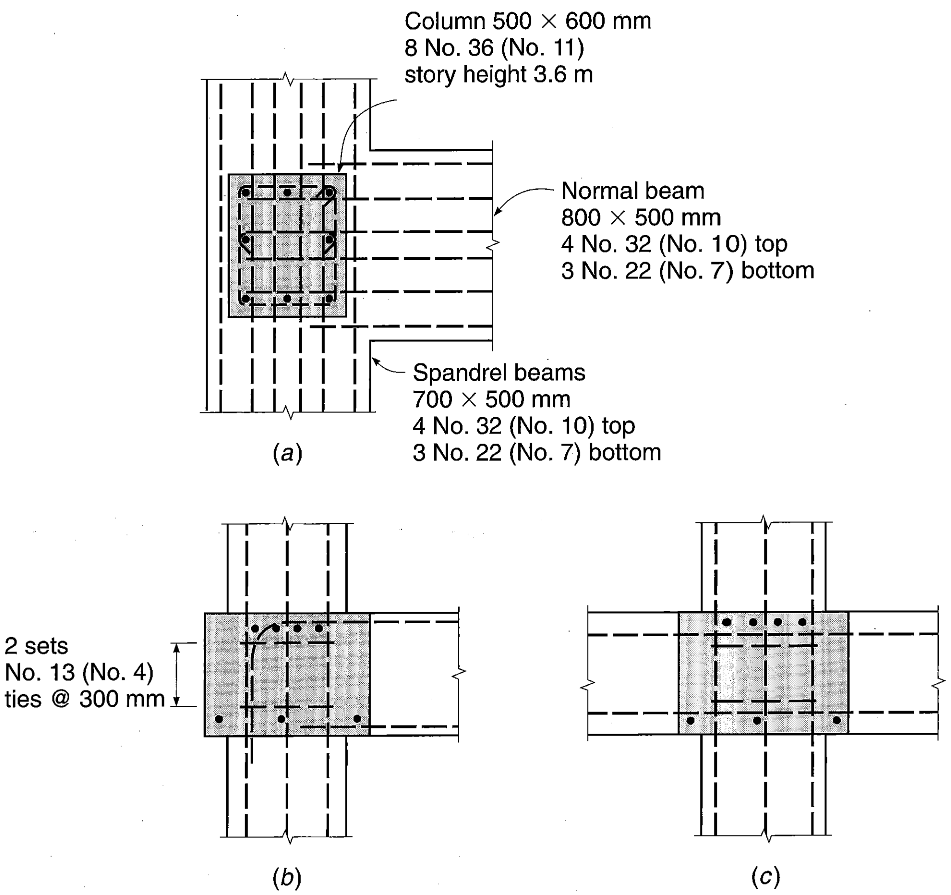

Checking the required development length of the No. 32 (No. 10) top bars of the normal beam gives

$$l_{dh} = \left(\frac{0.24\psi_e f_y}{\lambda\sqrt{f'_c}}\right) d_b = \left(\frac{0.24 \times 1 \times 420}{1 \times \sqrt{28}}\right) 32.3 = 615 \text{ mm}$$

With lateral cover well in excess of 65 mm, a modification factor of 0.7 is applicable, and the necessary hook development length is

$$l_{dh} = 6.5 \times 0.7 = 431 \text{ mm}$$

If the hooks are carried down in the plane of the outer column bars, the available embedment is $500 - 40 - 12.7 = 447$ mm, exceeding the minimum required embedment.

Moments from the spandrels on either side of the joint will be about equal, so no joint shear problem exists in that direction. In the direction of the normal beam, shear must be checked. The tensile force applied by the top bars is $A_s f_y = 4 \times 819 \times 420 \times 10^{-3} = 1376$ kN. The normal beam effective depth is $500 - 40 - 12.7 - 32.3/2 = 431$ mm, the depth of the compressive stress block is $a = A_s f_y / 0.85 f'_c b_w = 1376 \times 10^3/(0.85 \times 28 \times 800) = 72.3$ mm, and the corresponding moment is

$$M_u = M_n = A_s f_y\left(d - \frac{a}{2}\right) = 1376\left(431 - \frac{72.3}{2}\right) \times 10^{-3} = 543 \text{ kN-m}$$

Column shears are based on a free body corresponding to that of Fig. 11.9*b*, and are equal to $V_{\text{col}} = 543/3.6 = 150$ kN. Thus, the joint shear at middepth is $V_u = 1376 - 150 = 1226$ kN.

The spandrel beams provide full-width joint confinement in their direction, and the joint can be classed as exterior, so $\gamma = 1.7$. In the perpendicular direction, when the beam width exceeds the column width, the joint width b_j is to be taken equal to the column width (600 mm in the present case). The nominal and design shear strengths are, respectively,

$$V_n = \gamma\sqrt{f'_c}\, b_j h = 1.7\sqrt{28} \times 600 \times 500 \times 10^{-3} = 2699 \text{ kN}$$

$$\phi V_n = 0.75 \times 2699 = 2024 \text{ kN}$$

Because the design strength is well above the applied shear of 1226 kN, the shear requirement is met.

Transverse confinement steel must be provided in the direction of the normal beam, between the top and bottom bars of the normal beam, with spacing not to exceed 300 mm. Two sets of No. 13 (No. 4) column ties will be used, as shown in Fig. 11.11. In addition to the hoop around the outside bars, a single-leg crosstie is required for the middle column bars because the clear distance between column bars exceeds 150 mm. The ties satisfy Eq. (4.13).

11.3 STRUT-AND-TIE MODEL FOR JOINT BEHAVIOR

Although the Committee 352 report (Ref. 11.6) is an important contribution to the safe design of joints of certain standard configurations, the recommendations are based mainly on test results. Consequently, they must be restricted to joints whose geometry closely matches that of the tested joints. This leads to many seemingly arbitrary geometric limitations, and little guidance is provided for the design of joints that may not meet these limitations. An illustration of this is the wide-beam joint discussed in Section 11.2f.

Good physical models are available for many aspects of reinforced concrete behavior—for example, for predicting the flexural strength of a beam or the strength of an eccentrically loaded column—but no clear physical model is evident in the

FIGURE 11.12
Strut-and-tie model for behavior of a beam-column joint.

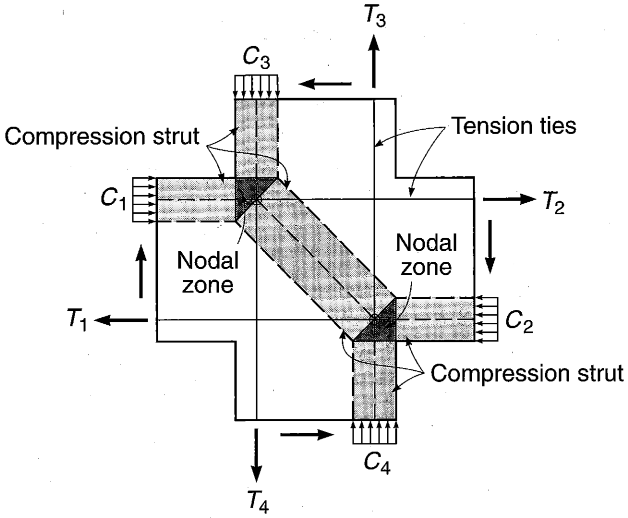

Committee 352 recommendations for the behavior of a joint. For this reason, among others, increasing attention is being given to the strut-and-tie models, described in Chapter 10, as a basis for the design of D-regions in joints.

The essential features of a strut-and-tie model of joint behavior may be understood with reference to Fig. 11.12, which shows a joint of a frame subject to lateral loading, with clockwise moments from the beams equilibrated by counterclockwise moments from the columns. The line of action of the horizontal forces C_1 and T_2 intersects that of the vertical forces C_3 and T_4 at a *nodal zone*, where the resultant force is equilibrated by a diagonal *compression strut* within the joint. At the lower end of the strut, the diagonal compression equilibrates the resultant of the horizontal forces T_1 and C_2 and the vertical forces T_3 and C_4. The tension bars must be well anchored by extension into and through the joint, or in the case of discontinuous bars (such as the top beam steel in an exterior joint) by hooks. The concrete within the nodal zone is subjected to a biaxial or, in many cases, a triaxial state of stress.

With this simple model, the flow of forces in a joint is easily visualized, satisfaction of the requirements of equilibrium is confirmed, and the need for proper anchorage of bars is emphasized. In a complete strut-and-tie model analysis, through proper attention to deformations within the joint, serviceability is ensured through control of cracking.

According to the strut-and-tie model, the main function of the column ties required within the joint region by conventional design procedures, in addition to preventing outward buckling of the vertical column bars, is to confine the concrete in the compression strut, thereby improving both its strength and ductility, and to control the cracking that may occur owing to diagonal tension perpendicular to the axis of the compression strut. The main load is carried by the uniaxially loaded struts and ties.

The strut-and-tie model not only provides valuable insights into the behavior of ordinary beam-column joints but also represents an important tool for the design of joints that fall outside of the limited range of those considered in Ref. 11.6. In the sections of this chapter that follow, a number of types of joints will be considered that occur commonly in reinforced concrete structures, for which the strut-and-tie models provide essential aid in developing proper bar details.

11.4 BEAM-TO-GIRDER JOINTS

Commonly in concrete construction, secondary floor beams are supported by primary girders, as shown in Fig. 11.13*a* and *b*. It is often assumed that the reaction from the floor beam is more or less uniformly distributed through the depth of the interface between beam and girder. This incorrect assumption is perhaps encouraged by the ACI Code "$V_c + V_s$" approach to shear design, which makes use of a nominal average shear stress in the concrete, $v_c = V_c/b_w d$, suggesting a uniform distribution of shear stress through the beam web.

The actual behavior of a diagonally cracked beam, as indicated by tests, is quite different, and the flow of forces can be represented in somewhat simplified form by the truss model of the beam shown in Fig. 11.13*c* (Ref. 11.7). The main reaction is delivered from beam to girder by a diagonal compression strut *mn*, which applies its thrust near the bottom of the carrying girder. Failure to provide for this thrust may result in splitting off the concrete at the bottom of the girder followed by collapse of the beam. A graphic example of lack of support for diagonal compression at the junction of a beam and its supporting girder is shown in Fig. 11.14.

Proper detailing of steel in the region of such a joint requires the use of well-anchored "hanger" stirrups in the girder, as shown in Fig. 11.13*a* and *b*, to provide for the downward thrust of the compression strut at the end of the beam (Refs. 11.8 and 11.9). These stirrups serve as tension ties to transmit the reaction of the beam to the compression zone of the girder, where it can be equilibrated by diagonal compression struts in the girder. The hanger stirrups, which are required *in addition* to the normal girder stirrups required for shear, can be designed based on equilibrating part or all of the reaction from the beam, with the hanger stirrups assumed to be stressed to their yield stress f_y at the factored load stage.

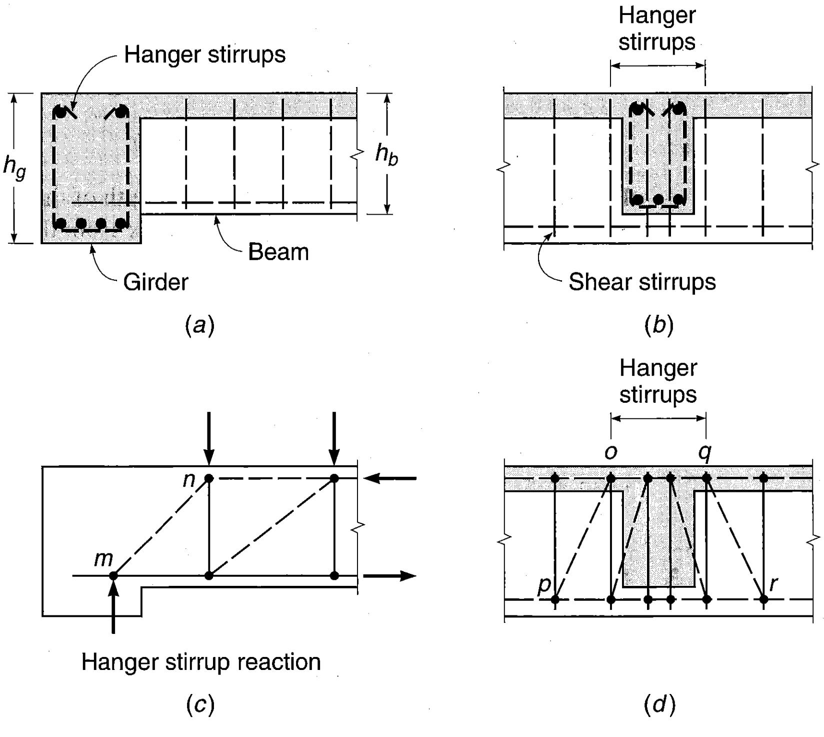

FIGURE 11.13
Main girder supporting secondary beam: (*a*) cross section through girder showing hanger stirrups; (*b*) cross section through beam; (*c*) truss model showing transfer of beam load to girder at load near ultimate; (*d*) truss model showing transfer of load into the girder.

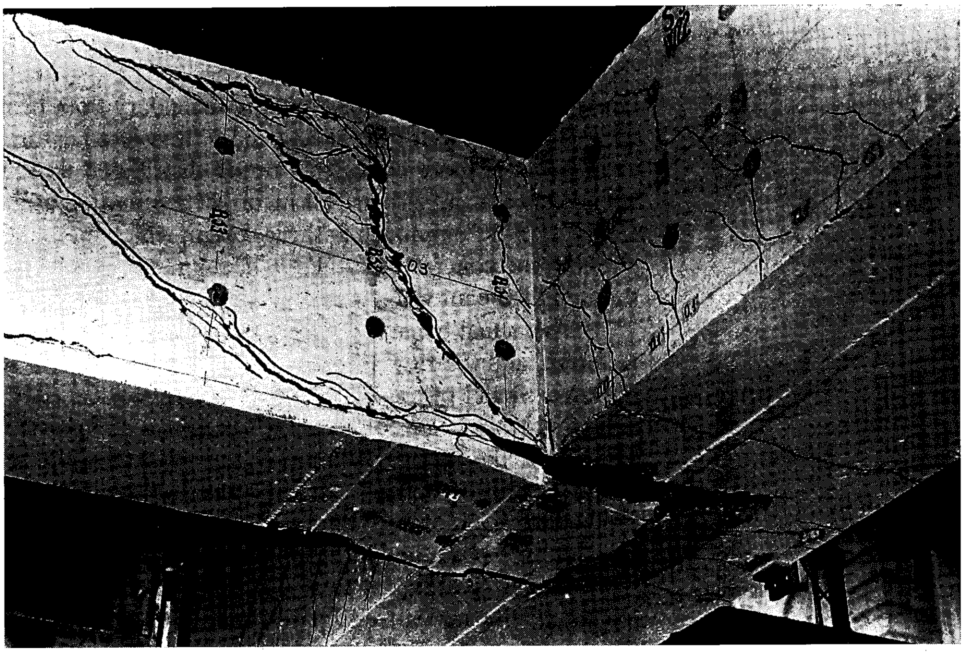

FIGURE 11.14
Failure due to lack of support for diagonal compression in beam-girder joint. (*Courtesy of M. P. Collins, University of Toronto.*)

The strut-and-tie model allows visualization of the transfer of the beam load along the girder as seen in Fig. 11.13*d*. The compression struts *op* and *qr* complete the shear transfer into the girder. The orientation of these compression struts depends on the location of the beam relative to the girder end.

If the beam and girder are the same depth, the hangers should take the full reaction. However, if the beam depth is much less than that of the girder, hangers may prove unnecessary. It is suggested in Ref. 11.10 that hanger stirrups be placed to resist a downward force of V_s^*, where

$$V_s^* = \frac{h_b}{h_g} V \tag{11.5}$$

Here h_b is the depth of the beam, h_g is the depth of the carrying girder, as indicated by Fig. 11.13, and V is the end reaction received from the beam.

Hangers will also be unnecessary if the factored beam shear is less than ϕV_c (as is usually the case for one-way joists, for example), because in such a case diagonal cracks would not form in the supported member. The predictions of the truss model would thus not be valid, and the reaction would be more nearly uniform through the depth.

The hanger stirrups should pass around the main flexural reinforcement of the girder, as shown in Fig. 11.13. If the beam and girder have the same depth, the main flexural bars in the girder should pass below those entering the connection from the beam to provide the best possible reaction platform for the diagonal compression strut.

11.5 LEDGE GIRDERS

Frequently in precast concrete construction, an L or inverted T girder is used to provide a seat, or ledge, to support precast beams framing into the carrying girder from the perpendicular direction. Typical ledge girder cross sections are shown in Fig. 11.15.

FIGURE 11.15
Ledge girders carrying precast T beams: (*a*) L girder providing exterior support for T beam; (*b*) inverted T girder carrying two T beam reactions.

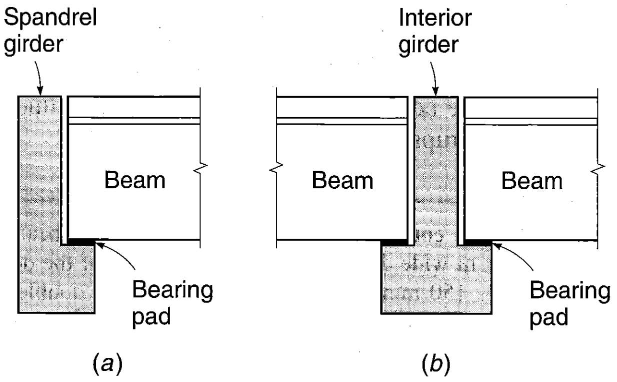
Spandrel girder
Beam
Bearing pad
(a)
Interior girder
Beam
Beam
Bearing pad
(b)

The end reaction of the beams introduces a heavy concentrated load near the bottom of such girders, requiring special reinforcement in the projecting ledge and in the girder web.

The design of such reinforcement is facilitated through use of a strut-and-tie model, as illustrated in Fig. 11.16. The downward reaction of the supported beam creates a compression fan in the ledge that distributes the reaction along a length greater than that of the bearing plate, as shown in Fig. 11.16*b*. The horizontal components of the fan are equilibrated by a compression strut along the lower flange of the girder.

In the cross section view of Fig. 11.16*a*, the downward thrust under the bearing plate is equilibrated by a diagonal compression strut, with the outward thrust at the top of the strut causing tension in the upper horizontal leg of closed hoop stirrups in the lower part of the girder. In many cases, a short structural steel angle is used just under the bearing plate, and the main tie at the top of the ledge is welded to the angle to ensure positive anchorage. At the bottom of the diagonal strut, the horizontal

FIGURE 11.16
Strut-and-tie model for behavior of inverted T ledge girder: (*a*) girder cross section; (*b*) side elevation.

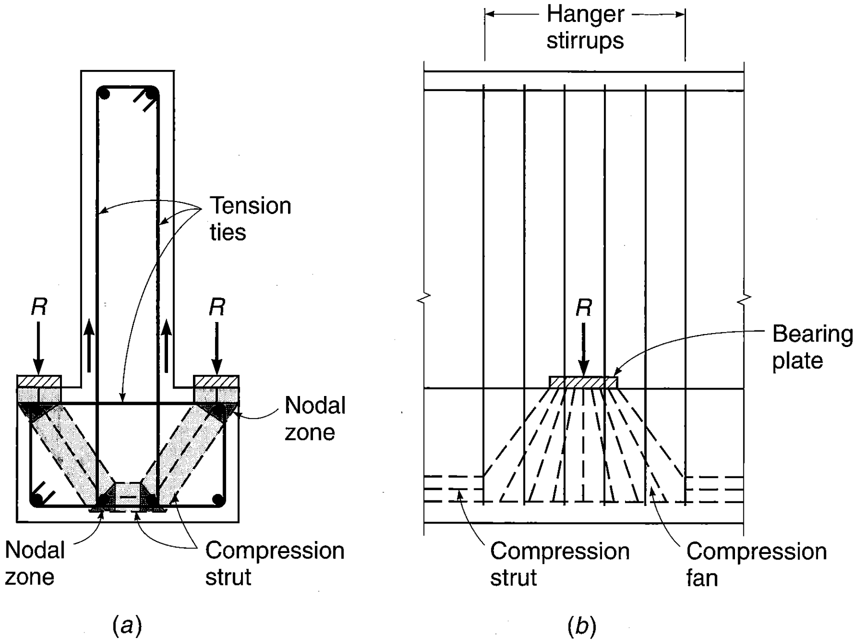
Tension ties
R
R
Nodal zone
Nodal zone
Compression strut
(a)
Hanger stirrups
R
Bearing plate
Compression strut
Compression fan
(b)

component of thrust is equilibrated by the opposing thrust from the other side, and the vertical component causes tension in stirrups that extend to the top of the girder. These stirrups are used in addition to those required for girder shear. Proper anchorage at the nodes is ensured by passing longitudinal bars inside the bends of both sets of stirrups.

EXAMPLE 11.4

Inverted T beam connection design. The inverted T beam shown in Fig. 11.17*a* supports 12 m long, 3.6 m wide double T beams. The width of the double T stem is 120 mm and the bearing plate is 150 mm long. The dead load of the double T is 3.4 kN/m^2, including self-weight, and the beam carries a live load of 1.9 kN/m^2. A horizontal force is taken equal to 20 percent of the vertical reaction. Design the reinforcement in the inverted T at the double T bearing point. Material properties are $f'_c = 42$ MPa and $f_y = 420$ MPa.

SOLUTION. The factored loads on the beam stem for a 1.8-m tributary width are

$$q_u = 1.2 \times 3.4 + 1.6 \times 1.9 = 7.12 \text{ kN/m}^2$$

$$R_u = 7.12 \text{ kN/m}^2 \times 1.8 \text{ m} \times 12 \text{ m}/2 = 77 \text{ kN}$$

and

$$T_u = 0.2 \times 77 = 15.4 \text{ kN}$$

The bearing area under the double T leg is 150 mm × 120 mm = 18,000 mm^2, giving a nodal bearing stress of

$$f_n = \frac{77}{18000} = 4.3 \text{ MPa}$$

which is well below the nominal capacity of the nodes and bottle-shaped or rectangular struts. The low stress is used to demonstrate an alternative solution methodology. By using the low stress, the node and strut capacities are adequate by inspection; however, the size of strut *cd* must be confirmed. Solving for the geometry and forces in Fig. 11.17*b*, $T_{ab} = 69$ kN, $T_{df} = 76$ kN, and strut *cd* carries $F_{cd} = 54$ kN. The thickness of the strut is assumed as 120 mm, the same as the bearing plate. Therefore, the width of strut *cd* is

$$w_{cd} = \frac{54}{4.27 \times 120} = 105 \text{ mm}$$

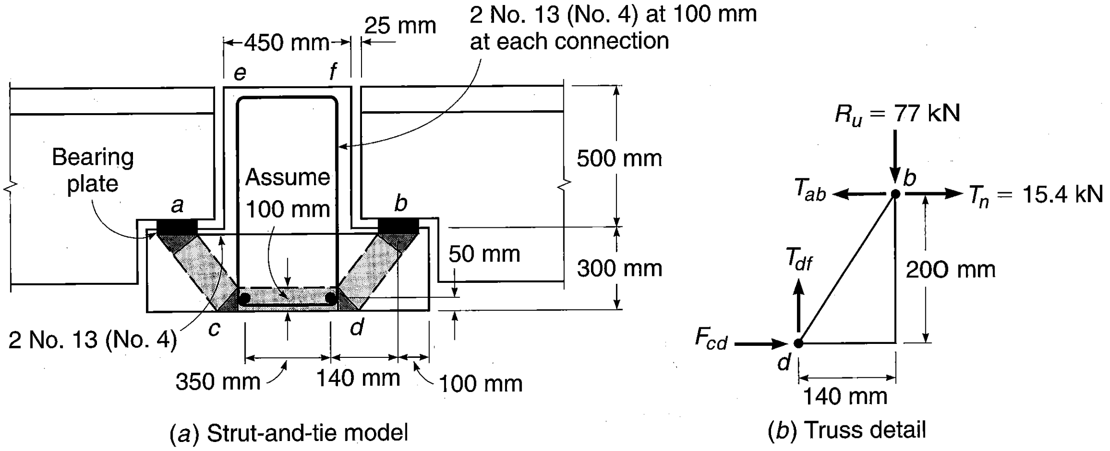

(*a*) Strut-and-tie model

(*b*) Truss detail

FIGURE 11.17
Strut-and-tie model for Example 11.4.

This is slightly more than the 100 mm assumed. A minor modification to the bearing stress would make this acceptable; therefore, the design continues with the selected geometry. The required area of steel for tie *ab* is

$$A_{ts} = \frac{T_{ab}}{\phi f_y} = \frac{69 \times 10^3}{0.75 \times 420} = 219 \text{ mm}^2$$

which is satisfied by using two No. 13 (No. 4) bars welded to each bearing plate. For tie *df*,

$$A_{ts} = \frac{T_{df}}{\phi f_y} = \frac{77 \times 10^3}{0.75 \times 420} = 244 \text{ mm}^2$$

which is also met using two No. 13 (No. 4) closed stirrups at 100 mm on center at each load point.

11.6 CORNERS AND T JOINTS

In many common types of reinforced concrete structures, moments and other forces must be transmitted around corners. Some examples, shown in Fig. 11.18, include gable frames, retaining walls, liquid storage tanks, and large box culverts. Reinforcement detailing at the corners is rarely obvious. A comprehensive experimental study of such joints by Nilsson and Losberg (Ref. 11.3) showed that many commonly used joint details will transmit only a small fraction of their assumed strength. Ideally, the joint should resist a moment at least as large as the calculated failure moment of the members framing into it (i.e., the *joint efficiency* should be at least 100 percent). Tests have shown that, for common reinforcing details, joint efficiency may be as low as 30 percent.

Corner joints may be subjected to opening moments, causing flexural tension on the inside of the joint, or closing moments, causing tension on the outside. Generally, the first case is the more difficult to detail properly.

Consider, for example, a corner joint subjected to opening moments, such as an exterior corner of the liquid storage tank shown in the plan view in Fig. 11.18*d*.

FIGURE 11.18
Structures with corners subject to opening or closing moments: (*a*) gable frame; (*b*) earth-retaining wall; (*c*) liquid storage tank; (*d*) plan view of multicell liquid storage tank; (*e*) large box culvert.

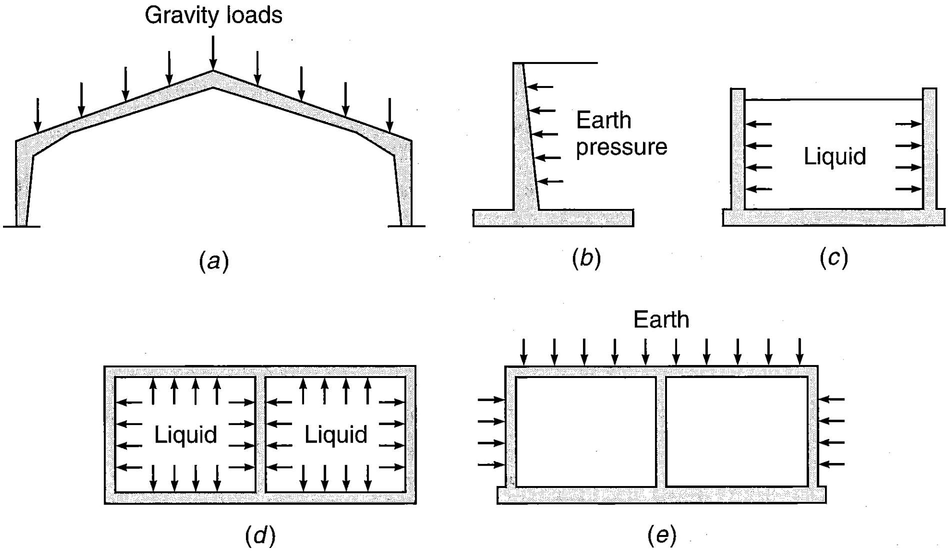

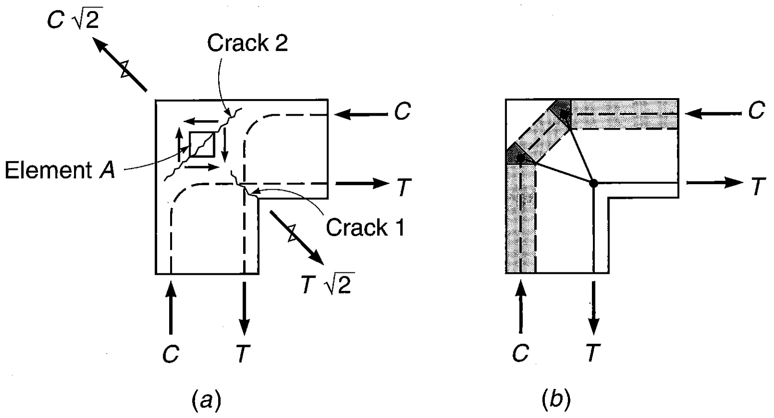

FIGURE 11.19
Corner joint subject to opening moments: (*a*) cracking in an improperly designed joint; (*b*) strut-and-tie model of joint behavior.

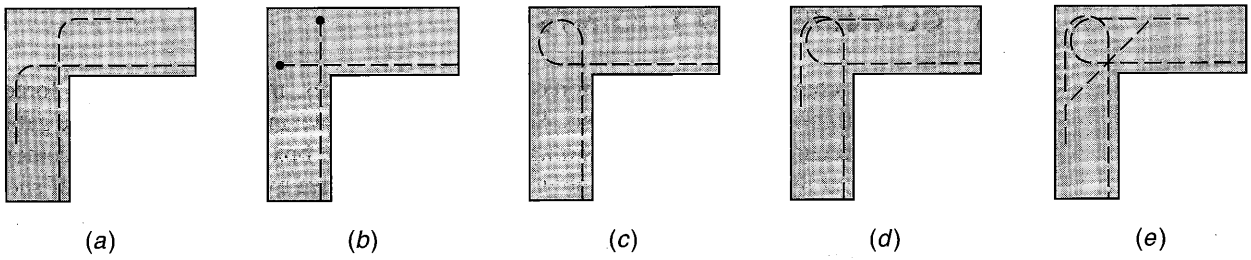

FIGURE 11.20
Efficiencies of corner joints subject to opening moments for various reinforcing details: (*a*) 32 percent; (*b*) 68 percent; (*c*) 77 percent; (*d*) 87 percent; (*e*) 115 percent. (*After Ref. 11.3.*)

Figure 11.19*a* shows the system of forces acting on such a corner. The reinforcing bar pattern shown is *not* recommended. Formation of crack 1, radiating inward from the corner, is perhaps obvious. Crack 2, which may lead to splitting off the outside corner, may not be so obvious. However, the resultant of the two compressive forces C, having a magnitude $C\sqrt{2}$, is equilibrated by the resultant tension $T\sqrt{2}$. These two forces, one applied near the outer corner and one near the inner corner, require high tensile stress between the two, leading to formation of crack 2 as shown. The same conclusion is reached considering a small concrete element A in the corner. It is subjected to the shearing forces shown as a result of the forces C and T from the entering members. The resultant of these shearing stresses is 45° principal tension across the corner, confirming formation of crack 2.

One may, at first, be tempted to add an L-shaped bar around the outside of the corner in an attempt to confine the outer concrete. Such a bar would serve no purpose, however, because the bar would be in compression and may actually assist in pushing the corner off. The strut-and-tie model of Fig. 11.19*b* provides valuable insight into the needed reinforcement, indicating that, in addition to well-anchored tensile bars to transmit the forces T into the joint, some form of radial reinforcement is required to permit the compressive forces C to "turn the corner."

Test results for a large number of joints with alternative bar details are reported in Ref. 11.3. Comparative efficiencies for some specific details, relating the maximum moment transmitted by the corner joint to the flexural capacity of the entering members, are summarized in Fig. 11.20. In all cases, the reinforcement ratio of the entering

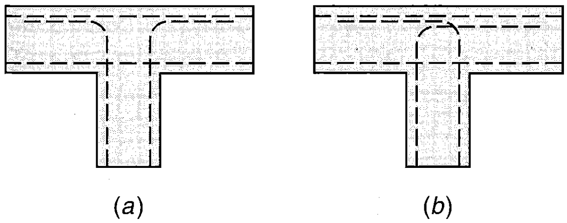

FIGURE 11.21
Comparative efficiencies of T joints subject to bending moment: (*a*) 24 to 40 percent depending on reinforcement ratio; (*b*) 82 to 110 percent depending on reinforcement ratio. (*After Ref. 11.3.*)

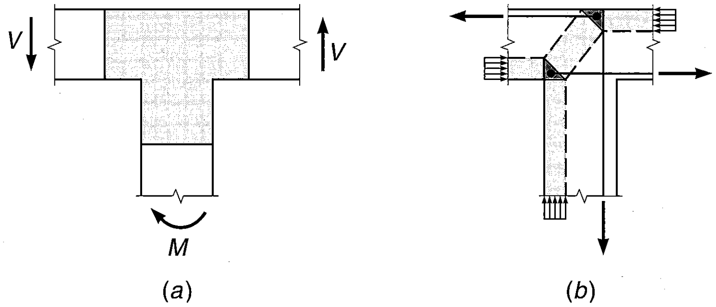

FIGURE 11.22
T joint behavior subjected to moment: (*a*) bending moment and resulting shear forces; (*b*) strut-and-tie model.

members is 0.75 percent. Figure 11.20*a* is a simple detail, probably often used, but it provides joint efficiency of only 32 percent. The details in Fig. 11.20*b*, reinforced with bent bars in the form of hairpins with the plane of the hooks parallel to the inside face of the joint, provide efficiency of 68 percent. In Fig. 11.20*c*, the main reinforcement is simply looped and continued out the other leg of the joint, resulting in an efficiency of 77 percent. The somewhat similar detail shown in Fig. 11.20*d*, in which the bars entering the joint are terminated with separate loops, gives an efficiency of 87 percent. The best performance results from the detail shown in Fig. 11.20*e*—the same as in Fig. 11.20*d* except for the addition of a diagonal bar. This improves joint efficiency to 115 percent, so that the joint is actually stronger than the design strength of the members framing into it. It was determined experimentally that the area of the diagonal bar should be about one-half that of the main reinforcement.

The joints between the vertical wall and horizontal base slab of retaining walls (see Fig. 11.18*b*) are also subjected to opening moments. Tests of such joints confirm the benefit of placing a diagonal bar similar to Fig. 11.20*e*. Retaining wall bar details will be discussed further in Chapter 17.

T joints also may be subjected to bending moments, such as if only one cell of the multiple-cell liquid storage tank of Fig. 11.18*d* were filled. Tests of such joints, reported in Ref. 11.3, again indicate the importance of proper detailing. The reinforcing bar arrangement shown in Fig. 11.21*a*, which is sometimes seen, permits a joint efficiency of only 24 to 40 percent, but the simple rearrangement shown in Fig. 11.21*b* improves the efficiency to between 82 and 110 percent. In both cases, efficiency depends upon the main reinforcement ratio in the entering members, with highest efficiency corresponding to the lowest tensile reinforcement ratio.

A strut-and-tie model for the T joint confirms the research results presented above. Figure 11.22*a* shows that a clockwise moment applied to the stem of the T is resisted by shear forces at the inflection points of the T top. The strut-and-tie model in Fig. 11.22*b* clearly shows that the stem reinforcement must hook to the left for the joint to be effective, just as shown in Fig. 11.21*b*.

Joints subjected to closing moments, with main reinforcement passing around the corner close to the outside face, cause few detailing problems because the main tension steel from the entering members can be carried around the outside of the corner. There is, however, a risk of splitting the concrete in the plane of the bend, or concrete crushing inside the bend. The efficiency of such joints can be improved by increasing the bend radius of the bar.

11.7 BRACKETS AND CORBELS

Brackets such as shown in Fig. 11.23*a* are widely used in precast construction for supporting precast beams at the columns. When they project from a wall, rather than from a column, they are properly called corbels, although the two terms are often used interchangeably. Brackets are designed mainly to provide for the vertical reaction V_u at the end of the supported beam, but unless special precautions are taken to avoid horizontal forces caused by restrained shrinkage, creep (in the case of prestressed beams), or temperature change, they must also resist a horizontal force N_{uc}.

Steel bearing plates or angles are generally used on the top surface of the brackets, as shown, to provide a uniform contact surface and to distribute the reaction. A corresponding steel bearing plate or angle is usually provided at the lower corner of the supported member. If the two plates are welded together, horizontal forces clearly must be allowed for in the design. Even with Teflon or elastomeric bearing pads, frictional forces will develop due to volumetric change.

The structural performance of a bracket can be visualized easily by means of the strut-and-tie model shown in Fig. 11.23*b*. The downward thrust of the load V_u is equilibrated by the vertical component of the reaction from the diagonal compression strut that carries the load down into the column. The outward thrust at the top of the strut is balanced by the tension in the horizontal tie bars across the top of the bracket; these also take the tension, if any, imparted by the horizontal force N_{uc}. At the left end of the horizontal tie, the tension is equilibrated by the horizontal component of thrust from the second compression strut shown. The vertical

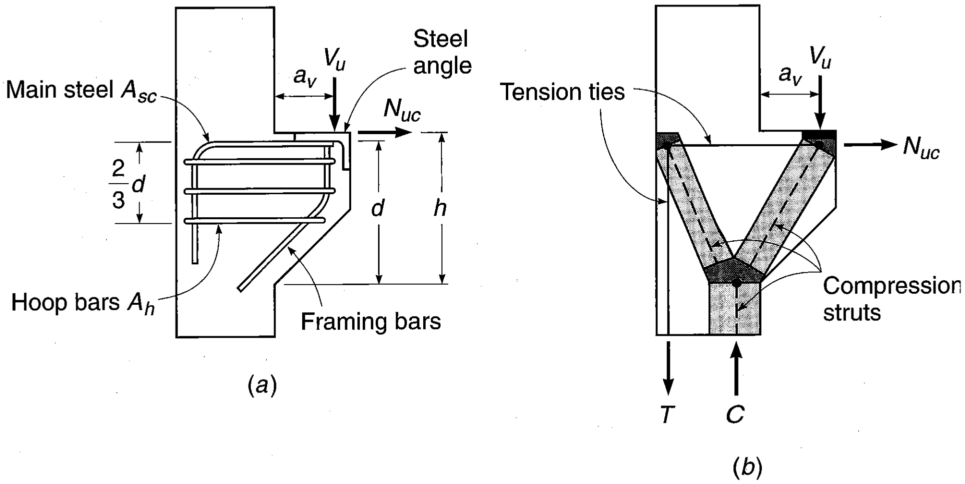

FIGURE 11.23
Typical reinforced concrete bracket: (*a*) loads and reinforcement; (*b*) strut-and-tie model for internal forces.

component of this thrust requires the tensile force shown acting downward at the left side of the supporting column.

The steel required, according to the strut-and-tie model, is shown in Fig. 11.23*a*. The main bars A_{sc} must be carefully anchored because they need to develop their full yield strength f_y directly under the load V_u, and for this reason they are usually welded to the underside of the bearing angle and a 90° hook is provided for anchorage at the left side. Closed hoop bars with area A_h confine the concrete in the two compression struts and resist a tendency for splitting in a direction parallel to the thrust. The framing bars shown are usually of about the same diameter as the stirrups and serve mainly to improve the stirrup anchorage at the outer face of the bracket.

The bracket may also be considered as a very short cantilevered beam, with flexural tension at the column face resisted by the top bars A_{sc}. Either concept will result in about the same area of main reinforcement.

A second possible mode of failure is by direct shear along a plane more or less flush with the vertical face of the main part of the column. Shear-friction reinforcement crossing such a crack (see Section 4.9) would include the area A_{sc} previously placed in the top tie and the area A_h from the hoops below it. Other failure modes include flexural tension failure, with yielding of the top bars followed by crushing of the concrete at the bottom of the bracket; crushing of the concrete under the bearing angle (particularly if end rotation of the supported beam causes the force V_u to be applied too close to the outer corner of the bracket); and direct tension failure, if the horizontal force N_{uc} is larger than anticipated.

The provisions of ACI Code 11.8 for the design of brackets and corbels have been developed mainly based on tests (Refs. 11.9, 11.11, and 11.12) and relate to the flexural model of bracket behavior. They apply to brackets and corbels with a shear span ratio a_v/d of 1.0 or less (see Fig. 11.23*a*). Brackets and corbels with a_v/d less than 2 may be designed using strut-and-tie models, as described in Chapter 10. The distance d is measured at the column face, and the depth at the outside edge of the bearing area must not be less than $0.5d$. The usual design basis is employed, i.e., $M_u \leq \phi M_n$ and $V_u \leq \phi V_n$, and for brackets and corbels (for which shear dominates the design), ϕ is to be taken equal to 0.75 for all strength calculations, including flexure and direct tension as well as shear.

The section at the face of the supporting column must simultaneously resist the shear V_u, the moment $M_u = V_u a_v + N_{uc}(h - d)$, and the horizontal tension N_{uc}. Unless special precautions are taken, a horizontal tension not less than 20 percent of the vertical reaction must be assumed to act. This tensile force is to be regarded as live load, and a load factor of 1.6 should be applied.

An amount of steel A_f to resist the moment M_u can be found by the usual methods for flexural design. Thus,

$$A_f = \frac{M_u}{\phi f_y(d - a/2)} \tag{11.6}$$

where $a = A_f f_y / 0.85 f'_c b$. An additional area of steel A_n must be provided to resist the tensile component of force:

$$A_n = \frac{N_{uc}}{\phi f_y} \tag{11.7}$$

The total area required *for flexure and direct tension* at the top of the bracket is thus

$$A_{sc} \geq A_f + A_n \tag{11.8}$$

Design for shear is based on the shear-friction method of Section 4.9, and the total shear-friction reinforcement A_{vf} is found by

$$A_{vf} = \frac{V_u}{\phi \mu f_y} \tag{11.9}$$

where the friction factor μ for monolithic construction is 1.4λ, where $\lambda = 1.0$ for normalweight concrete and 0.75 for both sand-lightweight and all-lightweight concrete, in accordance with ACI Code 11.6. The value of $V_n = V_u/\phi$ must not exceed the smallest of $0.2f'_c b_w d$, $(480 + 0.08f'_c)b_w d$, and $1600 b_w d$ at the support face for normalweight concrete or the smaller of $(0.2 - 0.07a_v/d)f'_c b_w d$ and $(800 - 280a_v/d)b_w d$ for lightweight concrete. Then, according to ACI Code 11.8, the total area required *for shear plus direct tension* at the top of the bracket is

$$A_{sc} \geq \frac{2}{3} A_{vf} + A_n \tag{11.10}$$

with the remaining part of A_{vf} placed in form of closed hoops having area A_h in the lower part of the bracket, as shown in Fig. 11.23*a*.

Thus, the total steel area A_{sc} required at the top of the bracket is equal to the larger of the values given by Eq. (11.8) or (11.10). An additional restriction, that A_{sc} not be less than $0.04(f'_c/f_y)bd$, is intended to avoid the possibility of sudden failure upon formation of a flexural tensile crack at the top of the bracket.

According to the ACI Code, closed hoop stirrups having area A_h (see Fig. 11.23*a*) not less than $0.5(A_{sc} - A_n)$ must be provided and be uniformly distributed within two-thirds of the effective depth adjacent to and parallel to A_{sc}. This requirement is more clearly stated as follows:

$$A_h \geq 0.5A_f \qquad \text{and} \qquad \geq \frac{1}{3} A_{vf} \tag{11.11}$$

EXAMPLE 11.5 **Design of column bracket.** A column bracket having the general features shown in Fig. 11.24 is to be designed to carry the end reaction from a long-span precast girder. Vertical reactions from service dead and live loads are 110 and 225 kN, respectively, applied at $a_v = 140$ mm from the column face. A steel bearing plate will be provided for the girder, which will rest directly on a 125 × 75 × 10 mm steel angle anchored at the outer corner of the bracket. Bracket reinforcement will include main steel A_{sc} welded to the underside of the steel angle, closed hoop stirrups having total area A_h distributed appropriately through the bracket depth, and framing bars in a vertical plane near the outer face. Select appropriate concrete dimensions, and design and detail all reinforcement. Material strengths are $f'_c = 35$ MPa and $f_y = 420$ MPa.

SOLUTION. The vertical factored load to be carried is

$$V_u = 1.2 \times 110 + 1.6 \times 225 = 492 \text{ kN}$$

In the absence of a roller or low-friction support pad, a horizontal tensile force of

$$N_{uc} = 0.20 \times 492 = 98 \text{ kN}$$

will be included. According to the shear friction provisions of the ACI Code, the nominal shear strength V_n must not exceed $0.2f'_c bd$, $(3.3 + 0.08f'_c)bd$, or $11bd$. With $f'_c = 35$ MPa, the second limit controls. Then, with $V_u = \phi V_n$ and with the column width $b = 300$ mm,

$$492 \times 10^3 = 0.75 \times 6.1 \times 300d$$

FIGURE 11.24
Column bracket design example.

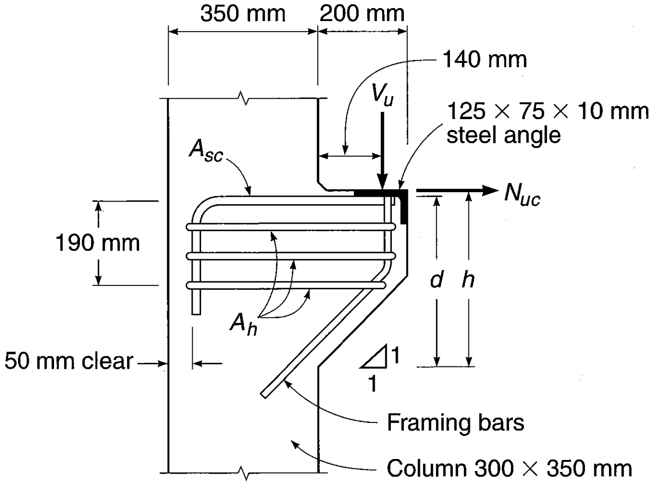

from which $d = 358$ mm. Estimating 25 mm from the center of the main steel to the top surface of the bracket, a total depth $h = 400$ mm will be selected, with d approximately equal to 375 mm, the exact value depending on the bar diameter chosen for A_{sc}. If a 45° slope is used, as indicated in Fig. 11.24, the bracket depth at the outside of the bearing area will be 200 mm. This is not less than $0.5d = 187$ mm, as required. For the bracket geometry selected, $a_v/d = 140/375 = 0.37$. This does not exceed the 1.0 limit imposed by the ACI Code.

The total shear friction steel is found from Eq. (11.9):

$$A_{vf} = \frac{V_u}{\phi \mu f_y} = \frac{492 \times 10^3}{0.75 \times 1.4 \times 420} = 1116 \text{ mm}^2$$

The bending moment to be resisted is

$$\begin{aligned} M_u &= V_u a_v + N_{uc}(h - d) \\ &= 492 \times 0.14 + 98 \times 0.025 = 71 \text{ kN-m} \end{aligned}$$

The depth of the flexural compression stress block will be estimated to be 50 mm, so, from Eq. (11.6),

$$A_f = \frac{M_u}{\phi f_y(d - a/2)} = \frac{71 \times 10^6}{0.75 \times 420(375 - 50/2)} = 644 \text{ mm}^2$$

Checking the stress block depth gives

$$a = \frac{A_f f_y}{0.85 f_c' b} = \frac{644 \times 420}{0.85 \times 35 \times 300} = 30 \text{ mm}$$

so the revised steel area is

$$A_f = \frac{71 \times 10^6}{0.75 \times 420(375 - 30/2)} = 626 \text{ mm}^2$$

The tensile force of 98 kN requires an additional steel area, from Eq. (11.7), of

$$A_n = \frac{N_{uc}}{\phi f_y} = \frac{98 \times 10^3}{0.75 \times 420} = 311 \text{ mm}^2$$

Thus, from Eqs. (11.8) and (11.10), respectively, the total steel area at the top of the bracket must not be less than

$$A_{sc} \geq A_f + A_n = 626 + 311 = 937 \text{ mm}^2$$

or less than

$$A_{sc} \geq \tfrac{2}{3} A_{vf} + A_n = \tfrac{2}{3} \times 1116 + 311 = 1055 \text{ mm}^2$$

The second requirement controls here. The minimum steel requirement of

$$A_{sc,\min} = 0.04 \frac{f'_c}{f_y} bd = 0.04 \times \frac{35}{420} \times 300 \times 400 = 400 \text{ mm}^2$$

is seen not to control. A total of three No. 22 (No. 7) bars, providing $A_{sc} = 1161$ mm^2, will be used.

Closed hoop steel having a total area A_h not less than $0.5(A_{sc} - A_n)$ must be provided. Thus,

$$A_h \geq 0.5A_f = 0.5 \times 644 = 322 \text{ mm}^2$$

and

$$A_h \geq 0.5 \times \tfrac{2}{3} A_{vf} = \tfrac{1}{3} \times 1116 = 372 \text{ mm}^2$$

The second requirement controls. Three No. 10 (No. 3) closed hoops will be provided, giving total area $A_h = 426$ mm^2. These must be placed within $\tfrac{2}{3}$ of the effective depth of the main steel. A spacing of 63 mm will be satisfactory, as indicated in Fig. 11.24. A pair of No. 10 (No. 3) framing bars will be added at the inside corner of the hoops to improve anchorage, as shown.

Anchorage of the No. 22 (No. 7) bars will be provided at the right end by welding to the underside of the steel angle and at the left end by a standard 90° bend (see Fig. 5.10). The basic development length for hooked bars (Table 5.3) is

$$l_{dh} = \left(\frac{0.24\psi_e f_y}{\lambda\sqrt{f'_c}}\right) d_b = \left(\frac{0.24 \times 1 \times 420}{1 \times \sqrt{35}}\right) 22.2 = 378 \text{ mm}$$

Two modification factors apply here. The first is 0.7, provided at least 50 mm cover is maintained at the end of the hook, and the second is (required A_s)/(provided A_s) = 1055/1161 = 0.91. Thus, the required development length past the face of the column is

$$l_{dh} = 378 \times 0.7 \times 0.91 = 241 \text{ mm}$$

This requirement is easily met. The hook extension will be $12d_b = 12 \times 22.2 = 266$ mm. For the hoop bars, a standard 35° hook, as shown in Fig. 5.9*b*, will be used.

REFERENCES

11.1. "Reinforced Concrete Design Includes Approval of Details," CRSI Engineering Practice Committee, *Concr. Int.*, vol. 10, no. 1, 1988, pp. 21–22.

11.2. *ACI Detailing Manual*, ACI Special Publication SP66, American Concrete Institute, Farmington Hills, MI, 2004.

11.3. I. H. E. Nilsson and A. Losberg, "Reinforced Concrete Corners and Joints Subjected to Bending Moment," *J. Struct. Div.*, ASCE, vol. 102, no. ST6, 1976, pp. 1229–1254.

11.4. D. F. Meinheit and J. O. Jirsa, "Shear Strength of Reinforced Concrete Beam-Column Connections," *J. Struct. Div.*, ASCE, vol. 107, no. ST11, 1981, pp. 2227–2244.

11.5. J. G. L. Marques and J. O. Jirsa, "A Study of Hooked Bar Anchorages in Beam-Column Joints," *J. ACI*, vol. 72, no. 5, 1975, pp. 198–209.

11.6. ACI-ASCE Committee 352, Recommendations for Design of Beam-Column Joints in Monolithic Reinforced Concrete Structures (ACI 352R-02), American Concrete Institute, Farmington Hills, MI, 2002.

11.7. N. S. Anderson and J. A. Ramirez, "Detailing of Stirrup Reinforcement," *ACI Struct. J.*, vol. 86, no. 5, 1989, pp. 507–515.

11.8. R. Park and T. Pauley, *Reinforced Concrete Structures*, John Wiley, New York, 1975.

11.9. L. B. Kriz and C. H. Raths, "Connections in Precast Concrete Structures—Strength of Corbels," *J. Prestressed Concr. Inst.*, vol. 10, no. 1, 1965, pp. 16–47.

11.10. A. H. Mattock and J. F. Shen, "Joints Between Reinforced Concrete Members of Similar Depth," *ACI Struct. J.*, vol. 89, no. 3, 1992, pp. 290–295.

11.11. A. H. Mattock, K. C. Chen, and K. Soongswang, "The Behavior of Reinforced Concrete Corbels," *J. Prestressed Concr. Inst.*, vol. 21, no. 2, 1976, pp. 52–77.

11.12. A. H. Mattock, "Design Proposals for Reinforced Concrete Corbels," *J. Prestressed Concr. Inst.*, vol. 21, no. 3, 1976, pp. 18–24.

PROBLEMS

11.1. An interior Type 1 joint, which is to be considered a part of the primary lateral load–resisting system, is to be designed. The 400 mm square column, with main steel consisting of four No. 36 (No. 11) bars, is intersected by two 300 × 450 mm beams in the X direction, reinforced with three No. 32 (No. 10) top bars and three No. 25 (No. 8) bottom bars. In the Y direction, there are two 300 × 550 mm girders, reinforced with three No. 36 (No. 11) top bars and three No. 29 (No. 9) bottom bars. Concrete cover is 63 mm to the center of the bars, except for the top steel in the girders, which is carried just under the top steel of the beams. Design and detail the joint, using $f'_c = 28$ MPa and $f_y = 420$ MPa. Specify placement of all bars and cutoff points.

11.2. A typical exterior joint of the building of Problem 11.1 is identical to the interior joint except that the 300 × 450 mm beam occurs on one side of the column only; the girders frame into two opposite faces, as before. All reinforcement is the same as for the joint of Problem 11.1. Design and detail the joint, specifying bar placement, cutoff points, and details such as bar hook dimensions.

11.3. The precast columns of a proposed parking garage will incorporate symmetrical brackets to carry the end reactions of short girders that, in turn, carry long-span precast, prestressed double T floor units. The girder reactions will be applied 150 mm from the column face, as shown in Fig. P11.3, and a total width of bracket of 225 mm must be provided for proper bearing. Column width in the perpendicular direction is 500 mm. Service load reactions applied at the top face of the brackets are 200 kN dead load and 160 kN live load. Select all unspecified concrete dimensions and design and detail the reinforcement. A corner angle is suggested at the outer top edge of the bracket. Column material strengths are $f'_c = 42$ MPa and $f_y = 420$ MPa.

FIGURE P11.3

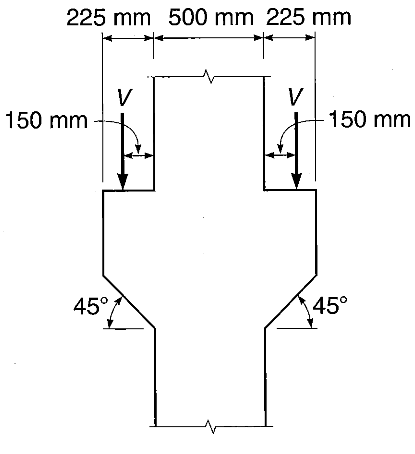

11.4. The stem of a 18 m long, 2.4 m wide simply supported single T beam rests on the ledge of the inverted T beam shown in Fig. P11.4. The T beam has a bearing area 150 mm thick and 100 mm parallel to the axis of the T. The applied service load is 4.0 kN/m^2 dead load, including self-weight, and 2.4 kN/m^2 live load. Design the connection detail under the stem using $f_c' = 35$ MPa and $f_y = 420$ MPa.

FIGURE P11.4

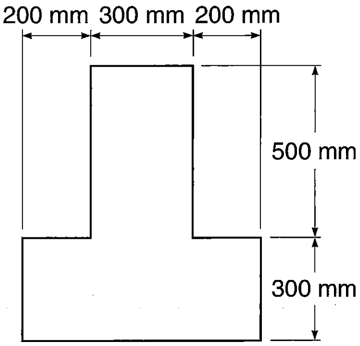

12 Analysis of Indeterminate Beams and Frames

12.1 CONTINUITY

The individual members that compose a steel or timber structure are fabricated or cut separately and joined together by rivets, bolts, welds, or nails. Unless the joints are specially designed for rigidity, they are too flexible to transfer moments of significant magnitude from one member to another. In contrast, in reinforced concrete structures, as much of the concrete as is practical is placed in one single operation. Reinforcing steel is not terminated at the ends of a member but is extended through the joints into adjacent members. At construction joints, special care is taken to bond the new concrete to the old by carefully cleaning the latter, by extending the reinforcement through the joint, and by other means. As a result, reinforced concrete structures usually represent monolithic, or continuous, units. A load applied at one location causes deformation and stress at all other locations. Even in precast concrete construction, which resembles steel construction in that individual members are brought to the job site and joined in the field, connections are often designed to provide for the transfer of moment as well as shear and axial load, producing at least partial continuity.

The effect of continuity is most simply illustrated by a continuous beam, such as shown in Fig. 12.1*a*. With simple spans, such as provided in many types of steel construction, only the loaded member *CD* would deform, and all other members of the structure would remain straight. But with continuity from one member to the next through the support regions, as in a reinforced concrete structure, the distortion caused by a load on one single span is seen to spread to all other spans, although the magnitude of deformation decreases with increasing distance from the loaded member. All members of the six-span structure are subject to curvature, and thus also to bending moment, as a result of loading span *CD*.

Similarly, for the rigid-jointed frame of Fig. 12.1*b*, the distortion caused by a load on the single member *GH* spreads to all beams and all columns, although, as before, the effect decreases with increasing distance from the load. All members are subject to bending moment, even though they may carry no transverse load.

If horizontal forces, such as forces caused by wind or seismic action, act on a frame, it deforms as illustrated by Fig. 12.1*c*. Here, too, all members of the frame distort, even though the forces act only on the left side; the amount of distortion is seen to be the same for all corresponding members, regardless of their distance from the points of loading, in contrast to the case of vertical loading. A member such as *EH*, even without a directly applied transverse load, will experience deformations and associated bending moment.

In *statically determinate structures,* such as simple-span beams, the deflected shape and the moments and shears depend only on the type and magnitude of the loads

FIGURE 12.1
Deflected shape of continuous beams and frames.

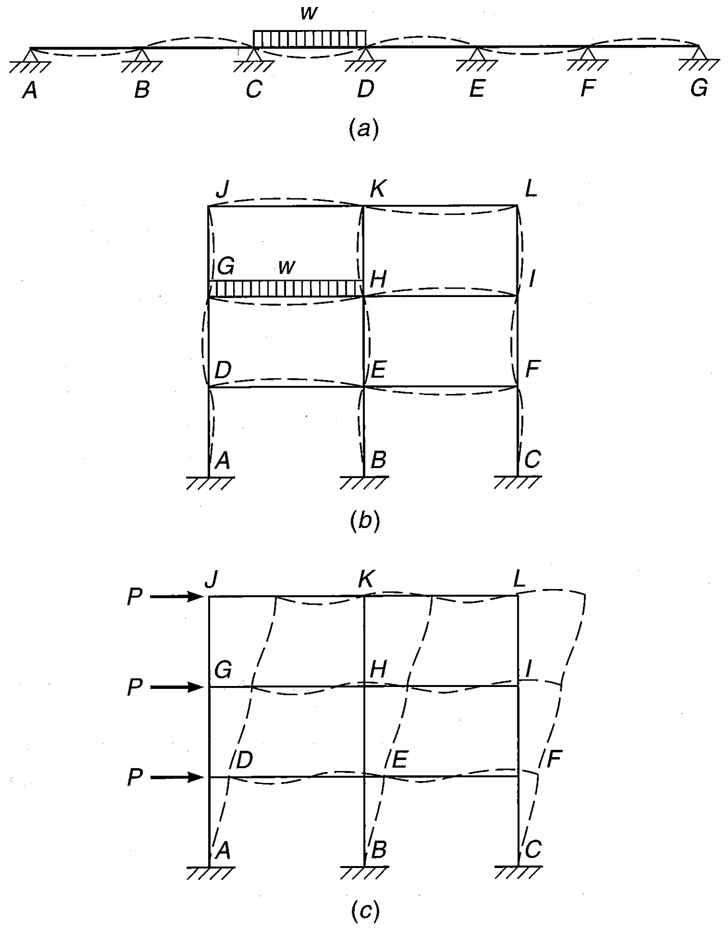

and the dimensions of the member. In contrast, inspection of the *statically indeterminate structures* in Fig. 12.1 shows that the deflection curve of any member depends not only on the loads but also on the joint rotations, whose magnitudes in turn depend on the distortion of adjacent, rigidly connected members. For a rigid joint such as joint H in the frame shown in Fig. 12.1*b* or *c*, all the rotations at the near ends of all members framing into that joint must be the same. For a correct design of continuous beams and frames, it is evidently necessary to determine moments, shears, and thrusts considering the effect of continuity at the joints.

The determination of these internal forces in continuously reinforced concrete structures is usually based on *elastic analysis* of the structure at factored loads with methods that will be described in Sections 12.2 through 12.5. Such analysis requires knowledge of the cross-sectional dimensions of the members. Member dimensions are initially estimated during preliminary design, which is described in Section 12.6 along with guidelines for establishing member proportions. For checking the results of more exact analysis, the approximate methods of Section 12.7 are useful. For many structures, a full elastic analysis is not justified, and the ACI coefficient method of analysis described in Section 12.8 provides an adequate basis for design moments and shears.

Before failure, reinforced concrete sections are usually capable of considerable inelastic rotation at nearly constant moment, as was described in Section 6.9. This permits a *redistribution of elastic moments* and provides the basis for *plastic analysis* of beams, frames, and slabs. Plastic analysis will be developed in Section 12.9 for beams and frames and in Chapters 14 and 15 for slabs.

12.2 LOADING

The individual members of a structural frame must be designed for the worst combination of loads that can reasonably be expected to occur during its useful life. Internal moments, shears, and thrusts are brought about by the combined effect of dead and live loads, plus other loads, such as wind and earthquake, as discussed in Section 1.7. While dead loads are constant, live loads such as floor loads from human occupancy can be placed in various ways, some of which will result in larger effects than others. In addition, the various combinations of factored loads specified in Table 1.2 must be used to determine the load cases that govern member design. The subject of load placement will be addressed first.

a. Placement of Loads

In Fig. 12.2*a* only span *CD* is loaded by live load. The distortions of the various frame members are seen to be largest in, and immediately adjacent to, the loaded span and to decrease rapidly with increasing distance from the load. Since bending moments are proportional to curvatures, the moments in more remote members are correspondingly smaller than those in, or close to, the loaded span. However, the loading shown in Fig. 12.2*a* does not produce the maximum possible positive moment in *CD*. In fact,

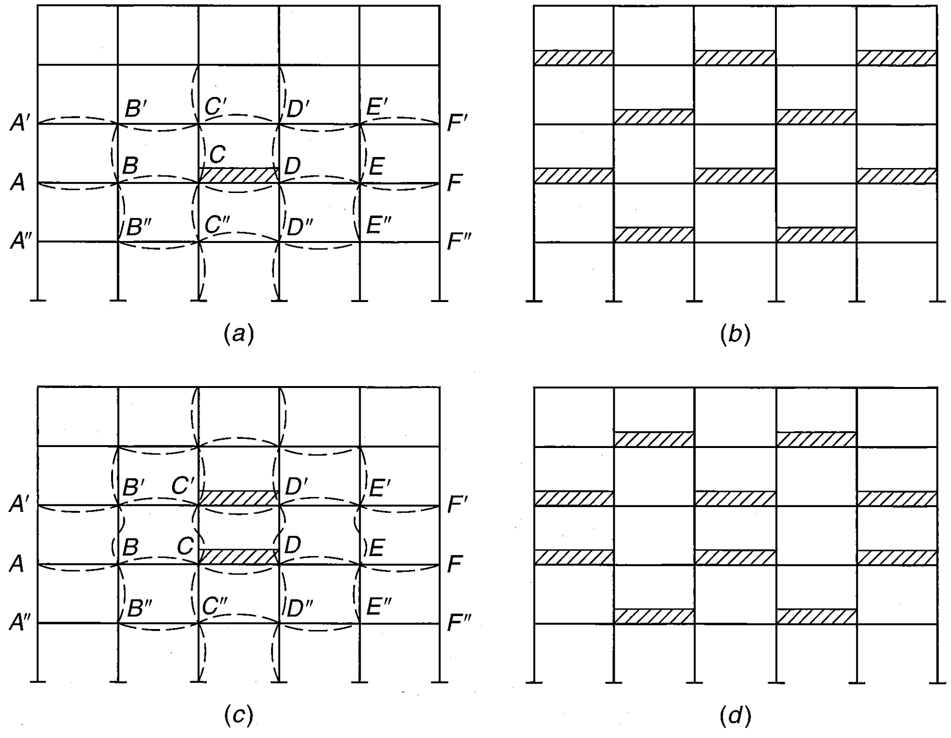

(*a*) (*b*)

(*c*) (*d*)

FIGURE 12.2
Alternate live loadings for maximum effects.

if additional live load were placed on span *AB,* this span would bend down, *BC* would bend up, and *CD* itself would bend down in the same manner, although to a lesser degree, as it is bent by its own load. Hence, the positive moment in *CD* is increased if *AB* and, by the same reasoning, *EF* are loaded simultaneously. By expanding the same reasoning to the other members of the frame, one can easily see that the checkerboard pattern of live load shown in Fig. 12.2*b* produces the largest possible positive moments, not only in *CD,* but in all loaded spans. Hence, two such checkerboard patterns are required to obtain the maximum positive moments in all spans.

In addition to maximum span moments, it is often necessary to investigate minimum span moments. Dead load, acting as it does on all spans, usually produces only positive span moments. However, live load, placed as in Fig. 12.2*a,* and even more so in Fig. 12.2*b,* is seen to bend the unloaded spans upward, i.e., to produce negative moments in the span. If these negative live load moments are larger than the generally positive dead load moments, a given girder, depending on load position, may be subject at one time to positive span moments and at another to negative span moments. It must be designed to withstand both types of moments; i.e., it must be furnished with tensile steel at both top and bottom. Thus, the loading of Fig. 12.2*b,* in addition to giving maximum span moments in the loaded spans, gives minimum span moments in the unloaded spans.

Maximum negative moments at the supports of the girders are obtained, on the other hand, if loads are placed on the two spans adjacent to the particular support and in a corresponding pattern on the more remote girders. A separate loading scheme of this type is then required for each support for which maximum negative moments are to be computed.

In each column, the largest moments occur at the top or bottom. While the loading shown in Fig. 12.2*c* results in large moments at the ends of columns *CC′* and *DD′*, the reader can easily be convinced that these moments are further augmented if additional loads are placed as shown in Fig. 12.2*d.*

It is seen from this brief discussion that to calculate the maximum possible moments at all critical points of a frame, live load must be placed in a great variety of different schemes. In most practical cases, however, consideration of the relative magnitude of effects will permit limitation of analysis to a small number of significant cases.

b. Load Combinations

The ACI Code requires that structures be designed for a number of load combinations, as discussed in Section 1.7. Thus, for example, factored load combinations might include (1) dead plus live load; (2) dead plus fluid plus temperature plus live plus soil plus snow load; (3) three possible combinations that include dead, live, and wind load; and (4) two combinations that include dead load, live load, and earthquake load, with some of the combinations including snow, rain, soil, and roof live load. While each of the combinations may be considered as an individual loading condition, experience has shown that the most efficient technique involves separate analyses for each of the basic loads without load factors, that is, a full analysis for unfactored dead load only, separate analyses for the various live load distributions described in Section 12.2*a,* and separate analyses for each of the other loads (wind, snow, etc.). Once the separate analyses are completed, it is a simple matter to combine the results using the appropriate load factor for each type of load. This procedure is most advantageous because, for example, live load may require a load factor of 1.6 for one combination, a value of 1.0 for another, and a value of 0.5 for yet another. Once the forces have been calculated for each combination, the combination of loads that governs for each member can usually be identified by inspection.

12.3 SIMPLIFICATIONS IN FRAME ANALYSIS

Considering the complexity of many practical building frames and the need to account for the possibility of alternative loadings, there is evidently a need to simplify. This can be done by means of certain approximations that allow the determination of moments with reasonable accuracy while substantially reducing the amount of computation.

Numerous trial computations have shown that, for building frames with a reasonably regular outline, not involving unusual asymmetry of loading or shape, the influence of sidesway caused by vertical loads can be neglected. In that case, moments due to vertical loads are determined with sufficient accuracy by dividing the entire frame into simpler subframes. Each of these consists of one continuous beam, plus the top and bottom columns framing into that particular beam. Placing the live loads on the beam in the most unfavorable manner permits sufficiently accurate determination of all beam moments, as well as the moments at the top ends of the bottom columns and the bottom ends of the top columns. For this partial structure, the far ends of the columns are considered fixed, except for such first-floor or basement columns where soil and foundation conditions dictate the assumption of hinged ends. Such an approach is explicitly permitted by ACI Code 8.11, which specifies the following for floor and roof members:

1. The live load may be considered to be applied only to the floor or roof under consideration, and the far ends of columns built integrally with the structure may be considered fixed.
2. The arrangement of live load may be limited to combinations of (*a*) factored dead load on all spans with full factored live load on two adjacent spans, and (*b*) factored dead load on all spans with full factored live load on alternate spans.

When investigating the maximum negative moment at any joint, negligible error will result if the joints second removed in each direction are considered to be completely fixed. Similarly, in determining maximum or minimum span moments, the joints at the far ends of the adjacent spans may be considered fixed. Thus, individual portions of a frame of many members may be investigated separately.

Figure 12.3 demonstrates the application of the ACI Code requirements for live load on a three-span subframe. The loading in Fig. 12.3*a* results in maximum positive moments in the exterior spans, the minimum positive moment in the center span, and the maximum negative moments at the interior faces of the exterior columns. The loading shown in Fig. 12.3*b* results in the maximum positive moment in the center span and minimum positive moments in the exterior spans. The loading in Fig. 12.3*c* results in maximum negative moment at both faces of the interior columns. Since the structure is symmetrical, values of moment and shear obtained for the loading shown in Fig. 12.3*c* apply to the right side of the structure as well as the left. Due to the simplicity of this structure, joints away from the spans of interest are not treated as fixed.

Moments and shears used for design are determined by combining the moment and shear diagrams for the individual load cases to obtain the maximum values along each span length. The resulting envelope moment and shear diagrams are shown in Fig. 12.3*d* and *e*, respectively. The moment and shear envelopes (note the range of

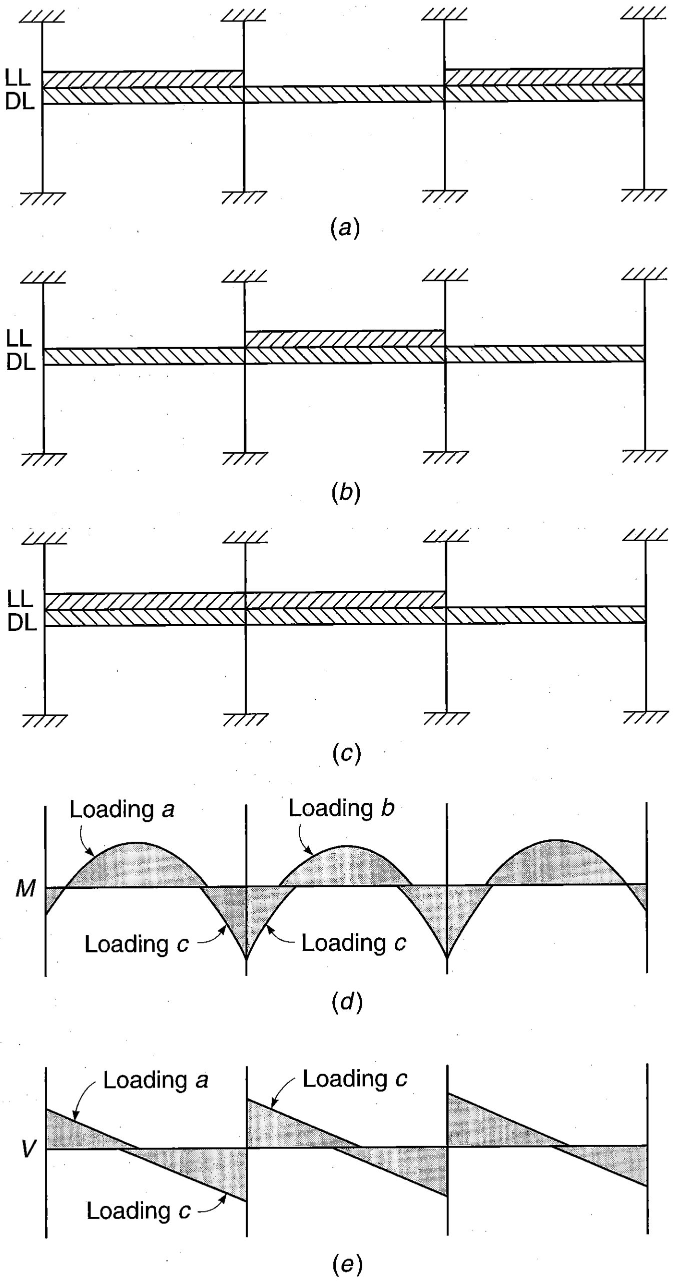

FIGURE 12.3
Subframe loading as required by ACI Code 8.9: Loading for (*a*) maximum positive moments in the exterior spans, the minimum positive moment in the center span, and the maximum negative moments at the interior faces of the exterior columns; (*b*) maximum positive moment in the center span and minimum positive moments in the exterior spans; and (*c*) maximum negative moment at both faces of the interior columns; (*d*) envelope moment diagram; (*e*) envelope shear diagram. (DL and LL represent factored dead and live loads, respectively.)

positions for points of inflection and points of zero shear) are used not only to design the critical sections but to determine cutoff points for flexural reinforcement and requirements for shear reinforcement.

In regard to columns, ACI Code 8.10 indicates

1. Columns shall be designed to resist the axial forces from factored loads on all floors or roof and the maximum moment from factored loads on a single adjacent span of the floor or roof under consideration. The loading condition giving the maximum ratio of moment to axial load shall also be considered.

2. In frames or continuous construction, consideration shall be given to the effect of unbalanced floor or roof loads on both exterior and interior columns and of eccentric loading due to other causes.
3. In computing moments in columns due to gravity loading, the far ends of columns built integrally with the structure may be considered fixed.
4. The resistance to moments at any floor or roof level shall be provided by distributing the moment between columns immediately above and below the given floor in proportion to the relative column stiffness and conditions of restraint.

Although it is not addressed in the ACI Code, axial loads on columns are usually determined based on the column tributary areas, which are defined based on the midspan of flexural members framing into each column. The axial load from the tributary area is used in design, with the exception of first interior columns, which are typically designed for an extra 10 percent axial load to account for the higher shear expected in the flexural members framing into the exterior face of first interior columns. The use of this procedure to determine axial loads due to gravity is conservative (note that the total vertical load exceeds the factored loads on the structure) and is adequately close to the values that would be obtained from a more detailed frame analysis.

12.4 METHODS FOR ELASTIC ANALYSIS

Many methods have been developed over the years for the elastic analysis of continuous beams and frames. The so-called classical methods (Ref. 12.1), such as application of the theorem of three moments, the method of least work (Castigliano's second theorem), and the general method of consistent deformation, will prove useful only in the analysis of continuous beams having few spans or of very simple frames, and are, in fact, rarely used. For the cases generally encountered in practice, such methods prove exceedingly tedious, and alternative approaches are preferred.

For many years moment distribution (Ref. 12.1) provided the basic analytical tool for the analysis of indeterminate concrete beams and frames, originally with the aid of the slide rule and later with handheld programmable calculators. For relatively small problems, moment distribution may still provide the most rapid results, and it is often used in current practice, for example, in the Equivalent Frame Method of design for slabs described in Section 13.9. However, with the widespread availability of computers, manual methods have been replaced largely by matrix analysis, which provides rapid solutions with a high degree of accuracy (Refs. 12.2 and 12.3).

Approximate methods of analysis, based either on careful sketches of the shape of the deformed structure under load or on moment coefficients, still provide a means for rapid estimation of internal forces and moments (Ref. 12.4). Such estimates are useful in preliminary design and in checking more exact solutions for gross errors that might result from input errors. In structures of minor importance, approximations may even provide the basis for final design.

In view of the number of excellent texts now available that treat methods of analysis (Refs. 12.1 to 12.4 to name just a few), the present discussion will be confined to an evaluation of the usefulness of several of the more important of these, with particular reference to the analysis of reinforced concrete structures. Certain idealizations and approximations that facilitate the solution in practical cases will be described in more detail.

a. Moment Distribution

In 1932, Hardy Cross developed the method of moment distribution to solve problems in frame analysis that involve many unknown joint displacements and rotations. For the next three decades, moment distribution provided the standard means in engineering offices for the analysis of indeterminate frames. Even now, it serves as the basic analytical tool if computer facilities are not available.

In the moment distribution method (Ref. 12.1), the fixed-end moments for each member are modified in a series of cycles, each converging on the precise final result, to account for rotation and translation of the joints. The resulting series can be terminated whenever one reaches the degree of accuracy required. After member end moments are obtained, all member stress resultants can be obtained from the laws of statics.

It has been found by comparative analyses that, except in unusual cases, building-frame moments found by modifying fixed-end moments by only two cycles of moment distribution will be sufficiently accurate for design purposes (Ref. 12.5).

b. Matrix Analysis

Use of matrix theory makes it possible to reduce the detailed numerical operations required in the analysis of an indeterminate structure to systematic processes of matrix manipulation that can be performed automatically and rapidly by computer. Such methods permit the rapid solution of problems involving large numbers of unknowns. As a consequence, less reliance is placed on special techniques limited to certain types of problems, and powerful methods of general applicability have emerged, such as the direct stiffness method (Refs. 12.2 and 12.3). By such means, an "exact" determination of internal forces throughout an entire building frame can be obtained quickly and at small expense. Three-dimensional frame analysis is possible where required. A large number of alternative loadings can be considered, including dynamic loads.

Some engineering firms prefer to write and maintain their own programs for structural analysis particularly suited to their needs. However, most make use of readily available programs that can be used for a broad range of problems. Input—including loads, material properties, structural geometry, and member dimensions—is provided by the user, often in an interactive mode. Output includes joint displacements and rotations, plus moment, shear, and thrust at critical sections throughout the structure. Most of these programs perform analysis of two- or three-dimensional framed structures subject to static or dynamic loads, shear walls, and other elements in a small fraction of the time formerly required, providing results to a high degree of accuracy.

12.5 IDEALIZATION OF THE STRUCTURE

It is seldom possible for the engineer to analyze an actual complex redundant structure. Almost without exception, certain idealizations must be made in devising an analytical model, so that the analysis will be practically possible. Thus, three-dimensional members are represented by straight lines, generally coincident with the actual centroidal axis. Supports are idealized as rollers, hinges, or rigid joints. Loads actually distributed over a finite area are assumed to be point loads. In three-dimensional framed structures, analysis is often limited to plane frames, each of which is assumed to act independently.

In the idealization of reinforced concrete frames, certain questions require special comment. The most important of these pertain to effective span lengths, effective moments of inertia, and conditions of support.

a. Effective Span Length

In elastic frame analysis, a structure is usually represented by a simple line diagram, based dimensionally on the centerline distances between columns and between floor beams. Actually, the depths of beams and the widths of columns (in the plane of the frame) amount to sizable fractions of the respective lengths of these members; their clear lengths are therefore considerably smaller than their centerline distances between joints.

It is evident that the usual assumption in frame analysis that the members are prismatic, with constant moment of inertia between centerlines, is not strictly correct. A beam intersecting a column may be prismatic up to the column face, but from that point to the column centerline it has a greatly increased depth, with a moment of inertia that could be considered infinite compared with that of the remainder of the span. A similar variation in width and moment of inertia is obtained for the columns. Thus, to be strictly correct, the actual variation in member depth should be considered in the analysis. Qualitatively, this would increase beam support moments somewhat and decrease span moments. In addition, it is apparent that the critical section for design for negative bending would be at the face of the support, and not at the centerline, since for all practical purposes an unlimited effective depth is obtained in the beam across the width of the support.

It will be observed that, in the case of the columns, the moment gradient is not very steep, so that the difference between centerline moment and the moment at the top or bottom face of the beam is small and in most cases can be disregarded. However, the slope of the moment diagram for the beam is usually quite steep in the region of the support, and there will be a substantial difference between the support centerline moment and face moment. If the former were used in proportioning the member, an unnecessarily large section would result. It is desirable, then, to reduce support moments found by elastic analysis to account for the finite width of the supports.

In Fig. 12.4, the change in moment between the support centerline and the support face will be equal to the area under the shear diagram between those two points. For knife edge supports, this shear area is seen to be very nearly equal to $VaL/2$. Actually, however, the reaction is distributed in some unknown way across the width of the support. This will have the effect of modifying the shear diagram as shown by the dashed line; it has been proposed that the reduced area be taken as equal to $VaL/3$. The fact that the reaction is distributed will modify the moment diagram as well as the shear diagram, causing a slight rounding of the negative moment peak, as shown in the figure, and the reduction of $VaL/3$ is properly applied to the moment diagram after the peak has been rounded. This will give nearly the same face moment as would be obtained by deducting the amount $VaL/2$ from the peak moment.

Another effect is present, however: the modification of the moment diagram due to the increased moment of inertia of the beam at the column. This effect is similar to that of a haunch, and it will mean slightly increased negative moment and slightly decreased positive moment. For ordinary values of the ratio a, this shift in the moment curve will be on the order of $VaL/6$. Thus, it is convenient simply to deduct the amount $VaL/3$ from the unrounded peak moment obtained from elastic analysis. This allows for (1) the actual rounding of the shear diagram and the negative moment peak due to

FIGURE 12.4
Reduction of negative and positive moments in a frame.

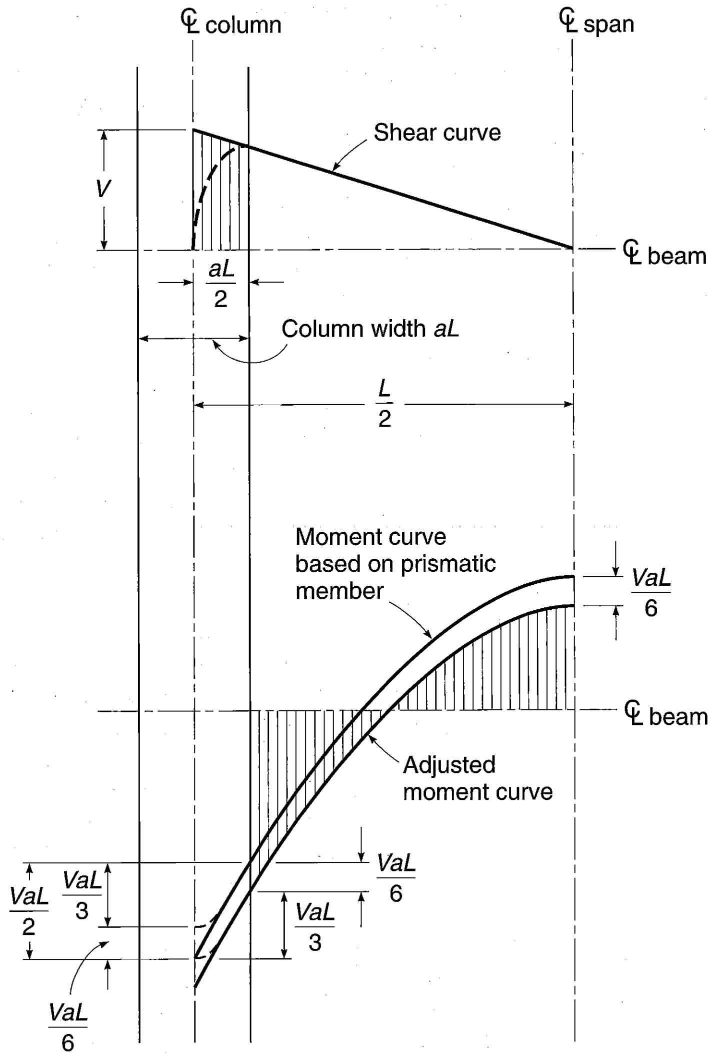
℄ column
℄ span
Shear curve
V
℄ beam
$\frac{aL}{2}$
Column width aL
$\frac{L}{2}$
Moment curve based on prismatic member
$\frac{VaL}{6}$
℄ beam
Adjusted moment curve
$\frac{VaL}{6}$
$\frac{VaL}{3}$
$\frac{VaL}{2}$
$\frac{VaL}{3}$
$\frac{VaL}{6}$

the distributed reaction and (2) the downward shift of the moment curve due to the haunch effect at the supports. The consistent reduction in positive moment of $VaL/6$ is illustrated in Fig. 12.4.

With this said, there are two other approaches that are often used by structural designers. The first is to analyze the structure based on the simple line diagram and to reduce the moment from the column centerline to the face of the support by $VaL/2$ without adjusting for the higher effective stiffness within the thickness width of the column. The moment diagram, although somewhat less realistic than represented by the lower curve in Fig. 12.4, still satisfies statics and requires less flexural reinforcement at the face of the support. As a consequence, there is less congestion in the beam-column joint, a location where it is often difficult to place concrete because of the high quantity of reinforcing steel from the flexural members framing into the column (usually from two different directions) and from the column itself. The somewhat higher percentage of reinforcement required at midspan usually causes little difficulty in concrete placement. The second approach involves representing the portion of the "beam" within the width of the column as a rigid link that connects the column centerline with the clear span of the flexural member. The portion of the column within the depth of the beam can also be represented using a rigid link. Such a model will produce moment diagrams similar to the lower curve in Fig. 12.4, without additional analysis. The second approach is both realistic and easy to implement in matrix analysis programs.

It should be noted that there are certain conditions of support for which no reduction in negative moment is justified. For example, when a continuous beam is carried by a girder of approximately the same depth, the negative moment in the beam at the centerline of the girder should be used to design the negative reinforcing steel.

b. Moments of Inertia

Selection of reasonable values for moments of inertia of beams and columns for use in the frame analysis is far from a simple matter. The design of beams and columns is based on cracked section theory, i.e., on the supposition that tension concrete is ineffective. It might seem, therefore, that moments of inertia to be used should be determined in the same manner, i.e., based on the cracked transformed section, in this way accounting for the effects of cracking and presence of reinforcement. Things are not this simple, unfortunately.

Consider first the influence of cracking. For typical members, the moment of inertia of a cracked beam section is about one-half that of the uncracked gross concrete section. However, the extent of cracking depends on the magnitude of the moments relative to the cracking moment. In beams, no flexural cracks would be found near the inflection points. Columns, typically, are mostly uncracked, except for those having relatively large eccentricity of loading. A fundamental question, too, is the load level to consider for the analysis. Elements that are subject to cracking will have more extensive cracks near ultimate load than at service load. Compression members will be unaffected in this respect. Thus, the relative stiffness depends on load level.

A further complication results from the fact that the effective cross section of beams varies along a span. In the positive bending region, a beam usually has a T section. For typical T beams, with flange width about 4 to 6 times web width and flange thickness from 0.2 to 0.4 times the total depth, the gross moment of inertia will be about 2 times that of the rectangular web with width b_w and depth h. However, in the negative bending region near the supports, the bottom of the section is in compression. The T flange is cracked, and the effective cross section is therefore rectangular.

The amount and arrangement of reinforcement are also influential. In beams, if bottom bars are continued through the supports, as is often done, this steel acts as compression reinforcement and stiffens the section. In columns, reinforcement ratios are generally much higher than in beams, adding to the stiffness.

Given these complications, it is clear that some simplifications are necessary. It is helpful to note that, in most cases, it is only the *ratio* of member stiffnesses that influences the final result, not the absolute value of the stiffnesses. The stiffness ratios may be but little affected by different assumptions in computing moment of inertia if there is consistency for all members.

In practice, it is generally sufficiently accurate to base stiffness calculations for frame analysis on the gross concrete cross section of the columns. In continuous T beams, cracking will reduce the moment of inertia to about one-half that of the uncracked section. Thus, the effect of the flanges and the effect of cracking may nearly cancel in the positive bending region. In the negative moment regions there are no flanges; however, if bottom bars continue through the supports to serve as compression steel, the added stiffness tends to compensate for lack of compression flange. Thus, for beams, generally a constant moment of inertia can be used, based on the rectangular cross-sectional area $b_w h$.

ACI Code 8.7.1 states that *any* set of reasonable assumptions may be used for computing relative stiffnesses, provided that the assumptions adopted are consistent throughout the analysis. ACI Commentary 8.7.1 notes that *relative* values of stiffness are important and that two common assumptions are to use gross EI values for all members or to use one-half of the gross EI of the beam stem for beams and the gross EI for the columns. Additional guidance is given in ACI Code 10.10.4, which specifies the section properties to be used for frames subject to sidesway. Thirty-five percent of the *gross* moment of inertia is used for beams and 70 percent for columns. This differs from the guidance provided in ACI Commentary 8.7.1 but, except for a factor of 0.70, matches the guidance provided in the earlier discussion.

c. Conditions of Support

For purposes of analysis, many structures can be divided into a number of two-dimensional frames. Even for such cases, however, there are situations in which it is impossible to predict with accuracy what the conditions of restraint might be at the ends of a span; yet moments are frequently affected to a considerable degree by the choice made. In many other cases, it is necessary to recognize that structures may be three-dimensional. The rotational restraint at a joint may be influenced or even governed by the characteristics of members framing into that joint at right angles. Adjacent members or frames parallel to the one under primary consideration may likewise influence its performance.

If floor beams are cast monolithically with reinforced concrete walls (frequently the case when first-floor beams are carried on foundation walls), the moment of inertia of the wall about an axis parallel to its face may be so large that the beam end could be considered completely fixed for all practical purposes. If the wall is relatively thin or the beam particularly massive, the moment of inertia of each should be calculated, that of the wall being equal to $bt^3/12$, where t is the wall thickness and b the wall width tributary to one beam.

If the outer ends of concrete beams rest on masonry walls, as is sometimes the case, an assumption of zero rotational restraint (i.e., hinged support) is probably closest to the actual case.

For columns supported on relatively small footings, which in turn rest on compressible soil, a hinged end is generally assumed, since such soils offer but little resistance to rotation of the footing. If, on the other hand, the footings rest on solid rock, or if a cluster of piles is used with their upper portion encased by a concrete cap, the effect is to provide almost complete fixity for the supported column, and this should be assumed in the analysis. Columns supported by a continuous foundation mat should likewise be assumed fixed at their lower ends.

If members framing into a joint in a direction perpendicular to the plane of the frame under analysis have sufficient torsional stiffness, and if their far ends are fixed or nearly so, their effect on joint rigidity should be included in the computations. The torsional stiffness of a member of length L is given by the expression GJ/L, where G is the shear modulus of elasticity of concrete (approximately to $E_c/2.2$) and J is the torsional stiffness factor of the member. For beams with rectangular cross sections or with sections made up of rectangular elements, J can be taken equal to $\Sigma(hb^3/3 - b^4/5)$, in which h and b are the cross-sectional dimensions of each rectangular element, b being the lesser dimension in each case. In moment

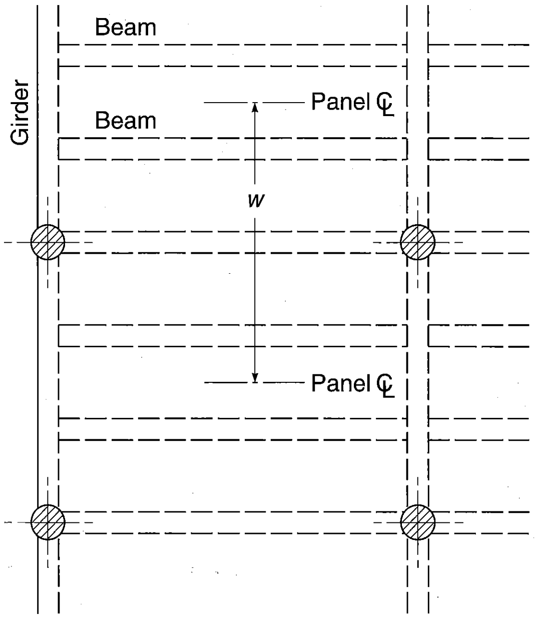

FIGURE 12.5
Slab, beam, and girder floor system.

distribution, when the effect of torsional rigidity is included, it is important that the absolute flexural stiffness $4EI/L$ be used rather than relative I/L values.

A common situation in beam-and-girder floors and concrete joist floors is illustrated in Fig. 12.5. The sketch shows a beam-and-girder floor system in which longitudinal beams are placed at the third points of each bay, supported by transverse girders, in addition to the longitudinal beams supported directly by the columns. If the transverse girders are quite stiff, it is apparent that the flexural stiffness of all beams in the width w should be balanced against the stiffness of one set of columns in the longitudinal bent. If, on the other hand, the girders have little torsional stiffness, there would be ample justification for making two separate longitudinal analyses, one for the beams supported directly by the columns, in which the rotational resistance of the columns would be considered, and a second for the beams framing into the girders, in which case hinged supports would be assumed. In most cases, it would be sufficiently accurate to consider the girders stiff torsionally and to add directly the stiffness of all beams tributary to a single column. This has the added advantage that all longitudinal beams will have the same cross-sectional dimensions and the same reinforcing steel, which will greatly facilitate construction. Plastic redistribution of loads upon overloading would generally ensure nearly equal restraint moments on all beams before collapse as assumed in design. Torsional moments should not be neglected in designing the girders.

12.6 PRELIMINARY DESIGN AND GUIDELINES FOR PROPORTIONING MEMBERS

In making an elastic analysis of a structural framework, it is necessary to know at the outset the cross-sectional dimensions of the members, so that moments of inertia and stiffnesses can be calculated. Yet the determination of these same cross-sectional dimensions is the precise purpose of the elastic analysis. In terms of load, the dead load on a structure is often dominated by the weight of the slab. Obviously, a preliminary estimate of member sizes must be one of the first steps in the analysis. Subsequently, with the results of the analysis at hand, members are proportioned, and the resulting dimensions compared with those previously assumed. If necessary, the assumed section properties are modified, and the analysis is repeated. Since the procedure may become quite laborious, it is obviously advantageous to make the best possible original estimate of member sizes, in the hope of avoiding repetition of the analysis.

In this connection, it is worth repeating that in the ordinary frame analysis, one is concerned with relative stiffnesses only, not the absolute stiffnesses. If, in the original estimate of member sizes, the stiffnesses of all beams and columns are overestimated or underestimated by about the same amount, correction of these estimated sizes after the first analysis will have little or no effect. Consequently, no revision of the analysis would be required. If, on the other hand, a nonuniform error in estimation is made, and relative stiffnesses differ from assumed values by more than about 30 percent, a new analysis should be made.

The experienced designer can estimate member sizes with surprising accuracy. Those with little or no experience must rely on trial calculations or arbitrary rules, modified to suit particular situations. In building frames, the depth of one-way slabs (discussed at greater length in Chapter 13) is often controlled by either deflection requirements or the negative moments at the faces of the supporting beams. Minimum depth criteria are reflected in Table 13.1, and negative moments at the face of the support can be estimated using coefficients described in Section 12.8. A practical minimum thickness of 100 mm is often used, except for joist construction meeting the requirements of ACI Code 8.13 (see Section 18.2d).

Beam sizes are usually governed by the negative moments and the shears at the supports, where their effective section is rectangular. Moments can be approximated by the fixed-end moments for the particular span, or by using the ACI moment coefficients (see Section 12.8). In most cases, shears will not differ greatly from simple beam shears. Alternatively, many designers prefer to estimate the depth of beams at 60 to 65 mm per meter of span, with the width equal to about one-half the depth.

For most construction, wide, relatively shallow beams and girders are preferred to obtain minimum floor depths, and using the same depth for all flexural members allows the use of simple, low-cost forming systems. Such designs can significantly reduce forming costs, while incurring only small additional costs for concrete and reinforcing steel. It is often wise to check the reinforcement ratio ρ based on the assumed moments to help maintain overall economy. A value of $\rho \approx 0.012$ in preliminary design will give $\rho \approx 0.01$ in a final design, if a more exact analysis is used. Obviously, member dimensions are subject to modification, depending on the type and magnitude of the loads, methods of design, and material strength.

Column sizes are governed primarily by axial loads, which can be estimated quickly, although the presence of moments in the columns is cause for some increase of the area as determined by axial loads. For interior columns, in which unbalanced moments will not be large, a 10 percent increase may be sufficient, while for exterior columns, particularly for upper stories, an increase of 50 percent in area may be appropriate. In deciding on these estimated increases, the following factors should be considered. Moments are larger in exterior than in interior columns, since in the latter dead load moments from adjacent spans will largely balance, in contrast to the case in exterior columns. In addition, the influence of moments, compared with that of axial loads, is larger in upper-floor than in lower-floor columns, because the moments are usually of about the same magnitude, while the axial loads are larger in the latter than in the former.

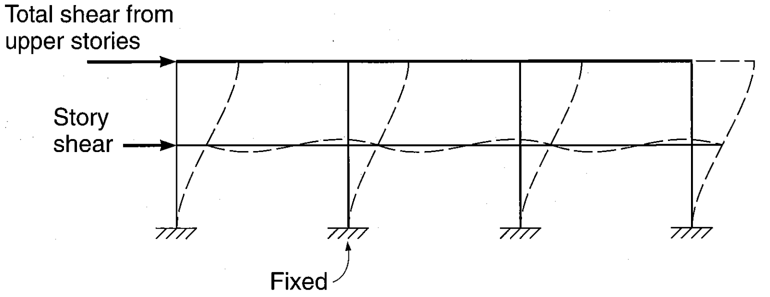

FIGURE 12.6
Subframe for estimating moments in lower-story columns of lateral load–resisting frames.

For minimum forming costs, it is highly desirable to use the same column dimensions throughout the height of a building. This can be accomplished by using higher-strength concrete on the lower stories (for high-rise buildings, this should be the highest-strength concrete available) and reducing concrete strength in upper stories, as appropriate. For columns in *laterally braced frames*, the preliminary design of the lower-story columns may be based on zero eccentricity using $0.80\phi P_o = P_u$. A total reinforcement ratio $\rho_g \approx 0.02$ should be used for the column with the highest axial load. With a value of $\rho_g \approx 0.01$ for the column with the lowest axial load on higher stories, the column size is maintained, reducing f_c' when ρ_g drops below 1 percent. Although ACI Code 10.9.1 limits ρ_g to a range of 1 to 8 percent, the effective minimum value of ρ_g is 0.005 based on ACI Code 10.8.4, which allows the minimum reinforcement to be calculated based on a reduced effective area A_g not less than one-half the total area (this provision cannot be used in regions of high seismic risk). For columns in lateral load–resisting frames, a subframe may be used to estimate the factored bending moments due to lateral load on the lower-story columns. The subframe illustrated in Fig. 12.6 consists of the lower two stories in the structure, with the appropriate level of fixity at the base. The upper flexural members in the subframe are treated as rigid. Factored lateral loads are applied to the structure. The subframe can be analyzed using matrix analysis or the portal frame method described in Section 12.7. Judicious consideration of factors such as those just discussed, along with simple models, as appropriate, will enable a designer to produce a reasonably accurate preliminary design, which in most cases will permit a satisfactory analysis to be made on the first trial.

12.7 APPROXIMATE ANALYSIS

In spite of the development of refined methods for the analysis of beams and frames, increasing attention is being paid to various approximate methods of analysis (Ref. 12.4). There are several reasons for this. Prior to performing a complete analysis of an indeterminate structure, it is necessary to estimate the proportions of its members to determine their relative stiffness, upon which the analysis depends. These dimensions can be obtained on the basis of approximate analysis. Also, even with the availability of computers, most engineers find it desirable to make a rough check of results, using approximate means, to detect gross errors. Further, for structures of minor importance, it is often satisfactory to design on the basis of results obtained by rough calculation. For these reasons, many engineers at some stage in the design process estimate the values of moments, shears, and thrusts at critical locations, using approximate sketches of the structure deflected by its loads.

Provided that points of inflection (locations in members at which the bending moment is zero and there is a reversal of curvature of the elastic curve) can be located accurately, the stress resultants for a framed structure can usually be found on the basis of static equilibrium alone. Each portion of the structure must be in equilibrium under the application of its external loads and the internal stress resultants.

For the fixed-end beam in Fig. 12.7*a*, for example, the points of inflection under uniformly distributed load are known to be located $0.211l$ from the ends of the span. Since the moment at these points is zero, imaginary hinges can be placed there without modifying the member behavior. The individual segments between hinges can be analyzed by statics, as shown in Fig. 12.7*b*. Starting with the center segment, shears equal to $0.289wl$ must act at the hinges. These, together with the transverse load, produce a midspan moment of $0.0417wl^2$. Proceeding next to the outer segments, a downward load is applied at the hinge representing the shear from the center segment. This, together with the applied load, produces support moments of $0.0833wl^2$. Note that, for this example, since the correct position of the inflection points was known at the start,

FIGURE 12.7
Analysis of fixed-end beam by locating inflection points.

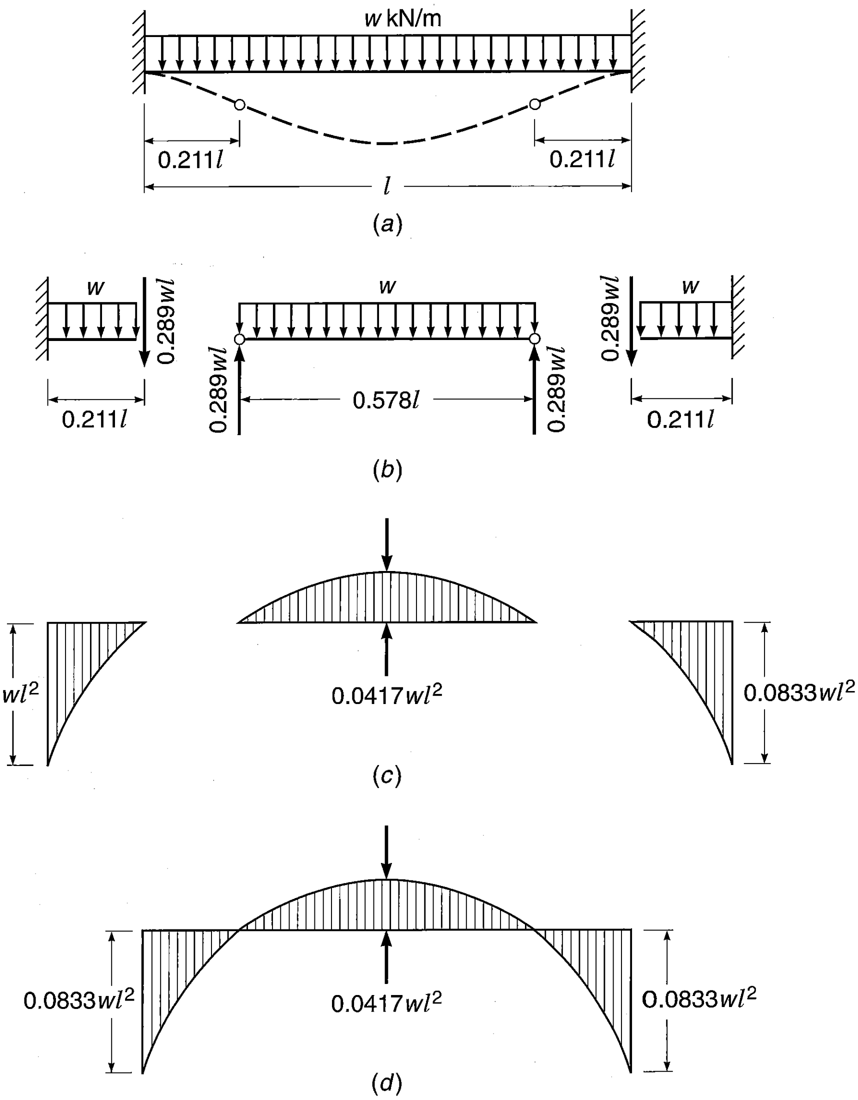

FIGURE 12.8
Approximate analysis of rigid frame.

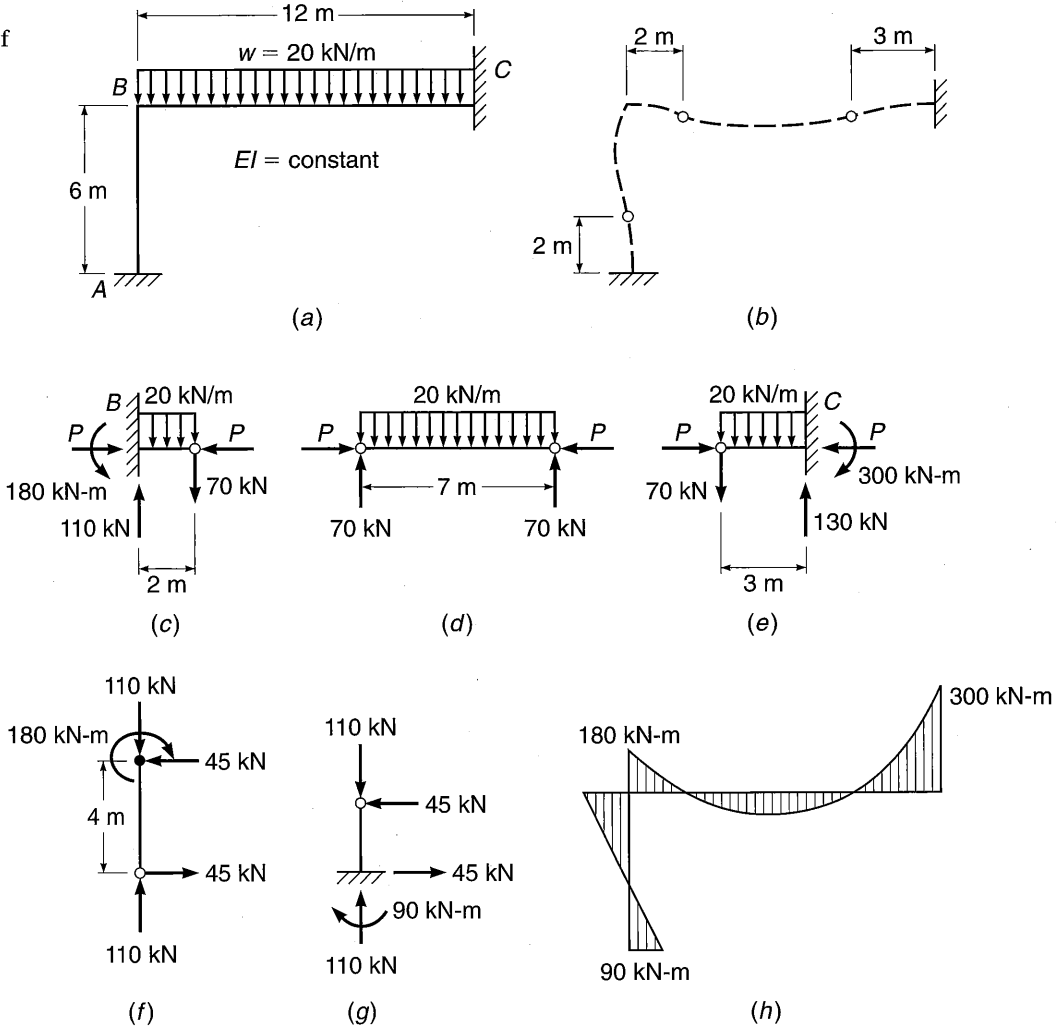
12 m
w = 20 kN/m
B
C
EI = constant
6 m
A
(a)
2 m
3 m
2 m
(b)
B
20 kN/m
P
P
180 kN-m
110 kN
70 kN
2 m
(c)
20 kN/m
P
P
7 m
70 kN
70 kN
(d)
20 kN/m
C
P
P
70 kN
300 kN-m
130 kN
3 m
(e)
110 kN
180 kN-m
45 kN
4 m
45 kN
110 kN
(f)
110 kN
45 kN
45 kN
90 kN-m
110 kN
(g)
300 kN-m
180 kN-m
90 kN-m
(h)

the resulting moment diagram of Fig. 12.7*c* agrees exactly with the true moment diagram for a fixed-end beam shown in Fig. 12.7*d*. In more practical cases, inflection points must be estimated, and the results obtained will only approximate the true values.

The use of approximate analysis in determining stress resultants in frames is illustrated by Fig. 12.8. Figure 12.8*a* shows the geometry and loading of a two-member rigid frame. In Fig. 12.8*b* an exaggerated sketch of the probable deflected shape is given, together with the estimated location of points of inflection. On this basis, the central portion of the girder is analyzed by statics, as shown in Fig. 12.8*d*, to obtain girder shears at the inflection points of 70 kN, acting with an axial load P (still not determined). Similarly, the requirements of statics applied to the outer segments of the girder in Fig. 12.8*c* and *e* give vertical shears of 110 and 130 kN at B and C, respectively, and end moments of 180 and 300 kN-m at the same locations. Proceeding then to the upper segment of the column, shown in Fig. 12.8*f*, with known axial load of 110 kN and top moment of 180 kN-m acting, a horizontal shear of 45 kN at the inflection point is required for equilibrium. Finally, static analysis of the lower part of the column indicates a requirement of 90 kN-m moment at A, as shown in Fig. 12.8*g*. The value of P equal to 45 kN is obtained by summing horizontal forces at joint B.

The moment diagram resulting from approximate analysis is shown in Fig. 12.8*h*. For comparison, an exact analysis of the frame indicates member end moments of 80 kN-m at *A*, 160 kN-m at *B*, and 280 kN-m at *C*. The results of the approximate analysis would be satisfactory for design in many cases; if a more exact analysis is to be made, a valuable check is available on the magnitude of results.

A specialization of the approximate method described, known as the *portal method*, is commonly used to estimate the effects of sidesway due to lateral forces acting on multistory building frames. For such frames, it is usual to assume that horizontal loads are applied at the joints only. If this is true, moments in all members vary linearly and, except in hinged members, have opposite signs close to the midpoint of each member.

For a simple rectangular portal frame having three members, the shear forces are the same in both legs and are each equal to one-half the external horizontal load. If one of the legs is more rigid than the other, it will require a larger horizontal force to displace it horizontally the same amount as the more flexible leg. Consequently, the portion of the total shear resisted by the stiffer column is larger than that of the more flexible column.

In multistory building frames, moments and forces in the girders and columns of each individual story are distributed in substantially the same manner as just discussed for single-story frames. The portal method of computing approximate moments, shears, and axial forces from horizontal loads is, therefore, based on the following three simple propositions:

1. The total horizontal shear in all columns of a given story is equal and opposite to the sum of all horizontal loads acting above that story.
2. The horizontal shear is the same in both exterior columns; the horizontal shear in each interior column is twice that in an exterior column.
3. The inflection points of all members, columns and girders, are located midway between joints.

Although the last of these propositions is commonly applied to all columns, including those of the bottom floor, the authors prefer to deal with the latter separately, depending on conditions of foundation. If the actual conditions are such as practically to prevent rotation (foundation on rock, massive pile foundations, etc.), the inflection points of the bottom columns are above midpoint and may be assumed to be at a distance $2h/3$ from the bottom. If little resistance is offered to rotation, e.g., for relatively small footings on compressible soil, the inflection point is located closer to the bottom and may be assumed to be at a distance $h/3$ from the bottom, or even lower. (With ideal hinges, the inflection point is at the hinge, i.e., at the very bottom.) Since shears and corresponding moments are largest in the bottom story, a judicious evaluation of foundation conditions as they affect the location of inflection points is of considerable importance.

The first of the three cited propositions follows from the requirement that horizontal forces be in equilibrium at any level. The second takes account of the fact that in building frames interior columns are generally more rigid than exterior ones because (1) the larger axial loads require a larger cross section and (2) exterior columns are restrained from joint rotation only by one abutting girder, while interior columns are so restrained by two such members. The third proposition is very nearly true because, except for the top and bottom columns and, to a minor degree, for the exterior girders, each member in a building frame is restrained about equally at both ends. For this reason, members deflect under horizontal loads in an antisymmetrical manner, with the inflection point at midlength.

The actual computations in this method are extremely simple. Once column shears are determined from propositions 1 and 2 and inflection points located from proposition 3, all moments, shears, and forces are simply computed by statics. The process is illustrated in Fig. 12.9*a*.

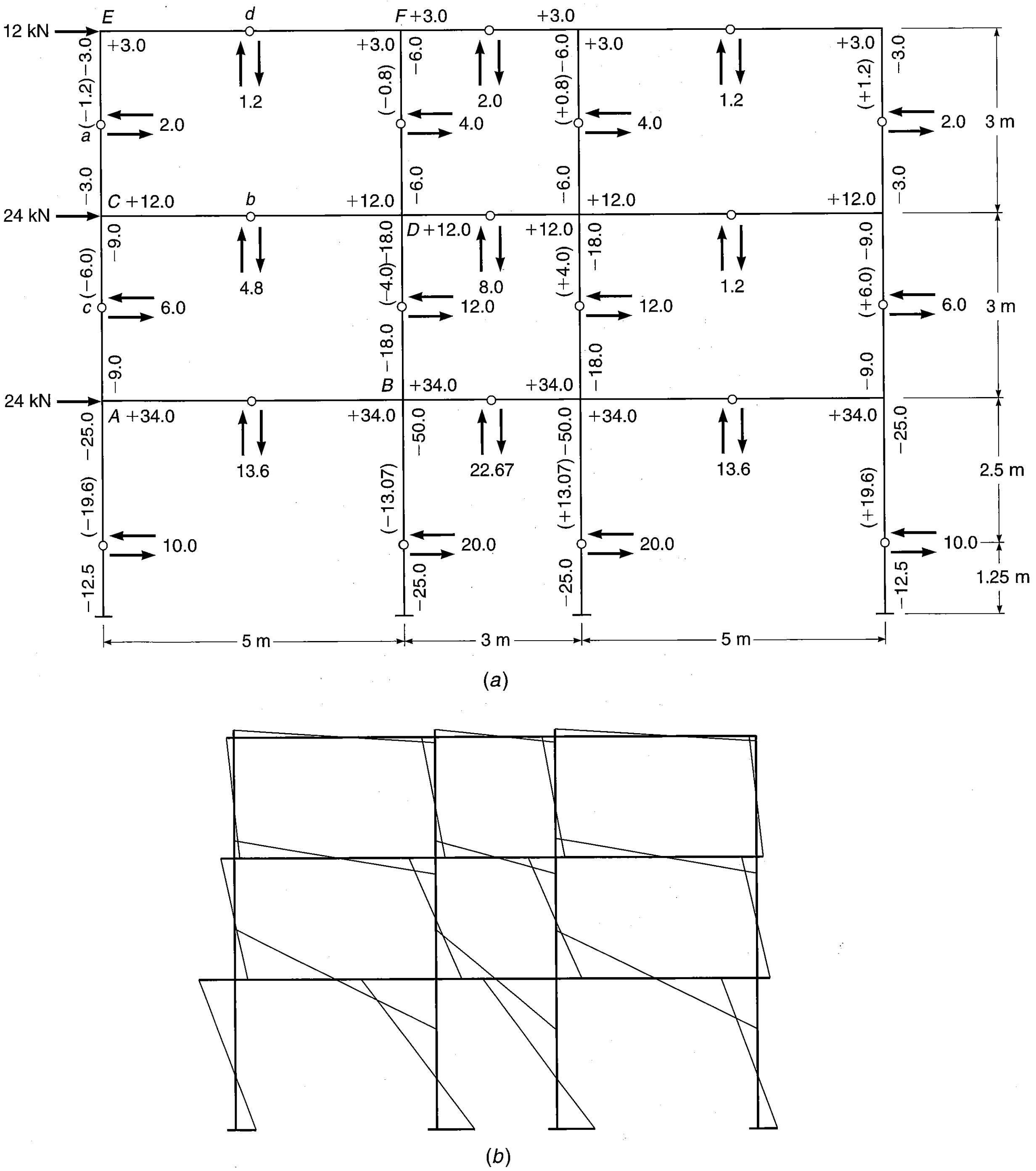
12 kN
24 kN
24 kN
E
d
F +3.0
+3.0
+3.0
(−1.2) −3.0
a
2.0
1.2
(−0.8)
−6.0
2.0
4.0
(+0.8) −6.0
4.0
1.2
(+1.2)
−3.0
2.0
3 m
C +12.0
b
+12.0
D +12.0
+12.0
(−6.0) −9.0
c
6.0
4.8
(−4.0) −18.0
8.0
12.0
(+4.0) −18.0
12.0
1.2
(+6.0) −9.0
6.0
3 m
A +34.0
B
+34.0
+34.0
(−19.6) −25.0
10.0
13.6
(−13.07)
−50.0
22.67
20.0
(+13.07) −50.0
20.0
13.6
(+19.6)
−25.0
2.5 m
10.0
1.25 m
−12.5
−25.0
−25.0
−12.5
5 m
3 m
5 m
(a)
(b)

FIGURE 12.9
Portal method for determining moments from wind load in a building frame: (*a*) moments, shears, and thrusts; (*b*) variations of moments.

Consider joints *C* and *D*. The total shear in the second story is $12 + 24 = 36$ kN. According to proposition 2, the shear in each exterior column is $36/6 = 6$ kN, and in each interior column $2 \times 6 = 12$ kN. The shears in the other floors, obtained in the same manner, act at the hinges as shown. Consider the equilibrium of the rigid structure between hinges *a, b,* and *c*; the column moments, 3.0 and 9.0 kN-m, respectively, are obtained directly by multiplying the shears by their lever arms, 1.5 m. The girder moment at *C*, to produce equilibrium, is equal and opposite to the sum of the column moments. The shear in the girder is obtained by recognizing that its moment (i.e., shear times one-half the girder span) must be equal to the girder moment at *C*. Hence, this shear is $12.0/2.5 = 4.8$ kN. The moment at end *D* is equal to that at *C*, since the inflection point is at midspan. At *D*, column moments are computed in the same manner from the known column shears and lever arms. The sum of the two girder moments, to produce equilibrium, must be equal and opposite to the sum of the two column moments, from which the girder moment to the right of *D* is $18.0 + 6.0 - 12.0 = 12.0$ kN-m. Axial forces in the columns also follow from statics. Thus, for the rigid body *aEd,* a vertical shear of 1.2 kN is seen to act upward at *d.* To equilibrate it, a tensile force of -1.2 kN is required in the column *CE.* In the rigid body *abc*, an upward shear of 4.8 kN at *b* is added to the previous upward tension of 1.2 kN at *a.* To equilibrate these two forces, a tension force of -6.0 kN is required in column *AC.* If the equilibrium of all other partial structures between hinges is considered in a similar manner, all moments, forces, and shears are rapidly determined.

In the present case, relatively flexible foundations were assumed, and the location of the lowermost inflection points was estimated to be at $h/3$ from the bottom. The general character of the resulting moment distribution is shown in Fig. 12.9*b.*

12.8 ACI MOMENT COEFFICIENTS

ACI Code 8.3 includes expressions that may be used for the approximate calculation of maximum moments and shears in continuous beams and one-way slabs. The expressions for moment take the form of a coefficient multiplied by $w_u l_n^2$, where w_u is the total factored load per unit length on the span and l_n is the clear span from face to face of supports for positive moment, or the average of the two adjacent clear spans for negative moment. Shear is taken equal to a coefficient multiplied by $w_u l_n/2$. The coefficients, found in ACI Code 8.3.3, are shown in Table 12.1 and summarized in Fig. 12.10.

The ACI moment coefficients were derived by elastic analysis, considering alternative placement of live load to yield maximum negative or positive moments at the critical sections, as was described in Section 12.2. They are applicable within the following limitations:

1. There are two or more spans.
2. Spans are approximately equal, with the longer of two adjacent spans not greater than the shorter by more than 20 percent.
3. Loads are uniformly distributed.
4. The unfactored live load does not exceed 3 times the unfactored dead load.
5. Members are prismatic.

As discussed in Section 12.3 for more general loading conditions, the alternative loading patterns considered in applying the Code moment coefficients result in an envelope of maximum moments, as illustrated in Fig. 12.11 for one span of a continuous

TABLE 12.1
Moment and shear values using ACI coefficients[†]

Positive moment	
End spans	
If discontinuous end is unrestrained	$\frac{1}{11} w_u l_n^2$
If discontinuous end is integral with the support	$\frac{1}{14} w_u l_n^2$
Interior spans	$\frac{1}{16} w_u l_n^2$
Negative moment at exterior face of first interior support	
Two spans	$\frac{1}{9} w_u l_n^2$
More than two spans	$\frac{1}{10} w_u l_n^2$
Negative moment at other faces of interior supports	$\frac{1}{11} w_u l_n^2$
Negative moment at face of all supports for (1) slabs with spans not exceeding 3 m and (2) beams and girders where ratio of sum of column stiffness to beam stiffness exceeds 8 at each end of the span	$\frac{1}{12} w_u l_n^2$
Negative moment at interior faces of exterior supports for members built integrally with their supports	
Where the support is a spandrel beam or girder	$\frac{1}{24} w_u l_n^2$
Where the support is a column	$\frac{1}{16} w_u l_n^2$
Shear in end members at first interior support	$1.15 \frac{w_u l_n}{2}$
Shear at all other supports	$\frac{w_u l_n}{2}$

[†] w_u = total factored load per unit length of beam or per unit area of slab.
l_n = clear span for positive moment and shear and the average of the two adjacent clear spans for negative moment.

frame. For maximum positive moment, that span would carry dead and live loads, while adjacent spans would carry dead load only, producing the diagram of Fig. 12.11*a*. For maximum negative moment at the left support, dead and live loads would be placed on the given span and that to the left, while the adjacent span on the right would carry only dead load, with the result shown in Fig. 12.11*b*. Figure 12.11*c* shows the corresponding results for maximum moment at the right support.

The composite moment diagram formed from the controlling portions of those just developed (Fig. 12.11*d*) provides the basis for design of the span. As observed in Section 12.3, there are a range of positions for the points of inflection resulting from alternate loadings. The extreme locations, required to determine bar cutoff points, can be found with the aid of Graph A.3 of Appendix A. In the region of the inflection point, it is evident from Fig. 12.11*d* that there may be a reversal of moments for alternative load patterns. However, within the stated limits for use of the coefficients, there should be no reversal of moments at the critical design sections near midspan or at the support faces.

Comparison of the moments found using the ACI coefficients with those calculated by more exact analysis will usually indicate that the coefficient moments are quite conservative. Actual elastic moments may be considerably smaller. Consequently, in many reinforced concrete structures, significant economy can be achieved by making a more precise analysis. This is mandatory for beams and slabs with spans differing by more than 20 percent, sustaining loads that are not uniformly distributed, or carrying live loads greater than 3 times the dead load.

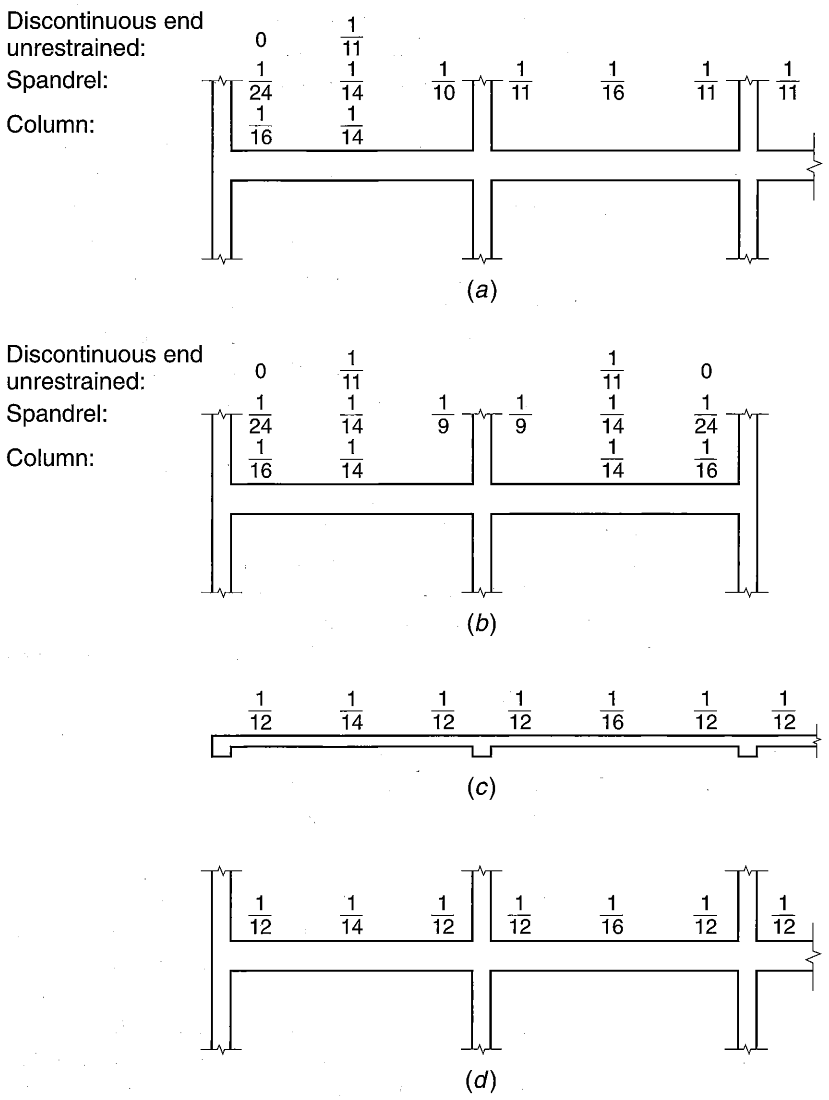
Discontinuous end unrestrained:
0
1/11
Spandrel:
1/24
1/14
1/10
1/11
1/16
1/11
1/11
Column:
1/16
1/14
(a)
Discontinuous end unrestrained:
0
1/11
1/11
0
Spandrel:
1/24
1/14
1/9
1/9
1/14
1/24
Column:
1/16
1/14
1/14
1/16
(b)
1/12
1/14
1/12
1/12
1/16
1/12
1/12
(c)
1/12
1/14
1/12
1/12
1/16
1/12
1/12
(d)

FIGURE 12.10
Summary of ACI moment coefficients: (*a*) beams with more than two spans; (*b*) beams with two spans only; (*c*) slabs with spans not exceeding 3 m; (*d*) beams in which the sum of column stiffnesses exceeds 8 times the sum of beam stiffnesses at each end of the span.

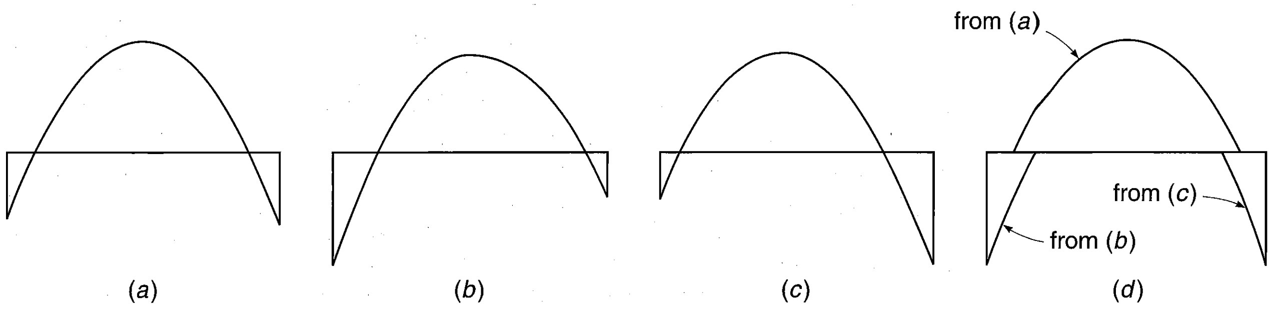
from (a)
from (c)
from (b)
(a)
(b)
(c)
(d)

FIGURE 12.11
Maximum moment diagrams and moment envelope for a continuous beam: (*a*) maximum positive moment; (*b*) maximum negative moment at left end; (*c*) maximum negative moment at right end; (*d*) composite moment envelope.

Because the load patterns in a continuous frame that produce critical moments in the columns are different from those for maximum negative moments in the beams, column moments must be found separately. According to ACI Code 8.10, columns must be designed to resist the axial load from factored dead and live loads on all floors above and on the roof plus the maximum moment from factored loads on a single adjacent span of the floor or roof under consideration. In addition, because of the characteristic shape of the column strength interaction diagram (see Chapter 8), it is necessary to consider the case that gives the maximum ratio of moment to axial load. In multistory structures, this results from a checkerboard loading pattern (see Fig. 12.2*d*), which gives maximum column moments but at a less-than-maximum axial force. As a simplification, in computing moments resulting from gravity loads, the far ends of the columns may be considered fixed. The moment found at a column-beam joint for a given loading is to be assigned to the column above and the column below in proportion to the relative column stiffness and conditions of restraint.

The shears at the ends of the spans in a continuous frame are modified from the value of $w_u l_n/2$ for a simply supported beam because of the usually unbalanced end moments. For interior spans, within the limits of the ACI coefficient method, this effect will seldom exceed about 8 percent, and it may be neglected, as suggested in Table 12.1. However, for end spans, at the face of the first interior support, the additional shear is significant, and a 15 percent increase above the simple beam shear is indicated in Table 12.1. The corresponding reduction in shear at the face of the exterior support is conservatively neglected.

12.9 LIMIT ANALYSIS

a. Introduction

Most reinforced concrete structures are designed for moments, shears, and axial forces found by elastic theory with methods such as those described in Sections 12.1 through 12.8. On the other hand, the actual proportioning of members is done by strength methods, with the recognition that inelastic section and member response would result upon overloading. Factored loads are used in the elastic analysis to find moments in a continuous beam, for example, after which the critical beam sections are designed with the knowledge that the steel would be well into the yield range and the concrete stress distribution very nonlinear before final collapse. Clearly this is an inconsistent approach to the total analysis-design process, although it can be shown to be both safe and conservative. A beam or frame so analyzed and designed will not fail at a load lower than the value calculated in this way.[†]

On the other hand, it is known that a continuous beam or frame normally will not fail when the nominal moment capacity of just one critical section is reached. A *plastic hinge* will form at that section, permitting large rotation to occur at essentially constant resisting moment and thus transferring load to other locations along the span where the limiting resistance has not yet been reached. Normally in a continuous beam or frame, excess capacity will exist at those other locations because they would have been reinforced for moments resulting from different load distributions selected to produce maximum moments at those other locations.

As loading is further increased, additional plastic hinges may form at other locations along the span and eventually result in collapse of the structure, but only

---

[†] See the discussion of upper and lower bound theorems of the theory of plasticity, Section 14.2, for an elaboration on this point.

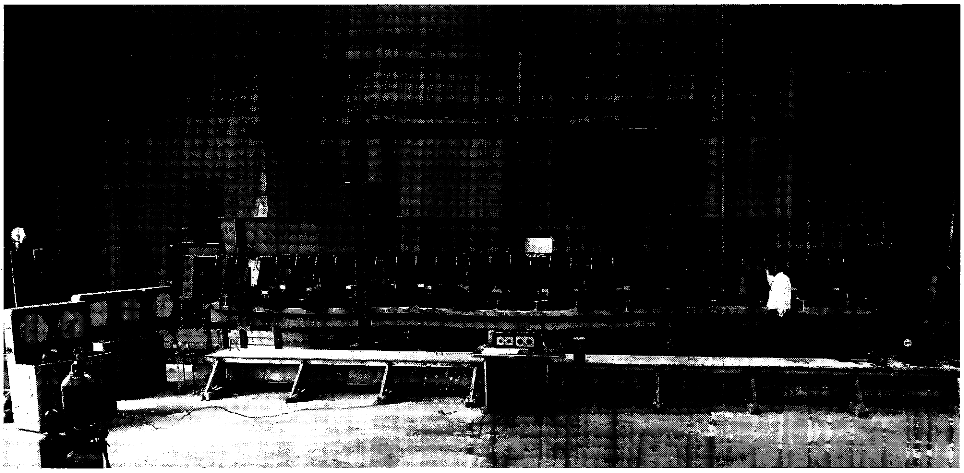

FIGURE 12.12
Three-span continuous beam after the formation of plastic hinges at the interior supports.

after a significant *redistribution of moments* has occurred. The ratio of negative to positive moments found from elastic analysis is no longer correct, for example, and the true ratio after redistribution depends upon the flexural strengths actually provided at the hinging sections.

Recognition of redistribution of moments can be important because it permits a more realistic appraisal of the actual load-carrying capacity of a structure, thus leading to improved economy. In addition, it permits the designer to modify, within limits, the moment diagrams for which members are to be designed. Certain sections can be deliberately underreinforced if moment resistance at adjacent critical sections is increased correspondingly. Adjustment of design moments in this way enables the designer to reduce the congestion of reinforcement that often occurs in high-moment areas, such as at the beam-column joints.

The formation of plastic hinges is well established by tests such as that pictured in Fig. 12.12. The three-span continuous beam illustrates the inelastic response typical of heavily overloaded members. It was reinforced in such a way that plastic hinges would form at the interior support sections before the limit capacity of sections elsewhere was reached. The beam continued to carry increasing load well beyond the load that produced first yielding at the supports. The extreme deflections and sharp changes in slope of the member axis that are seen here were obtained only slightly before final collapse.

The *inconsistency* of the present approach to the total analysis-design process, the possibility of using the *reserve strength* of concrete structures resulting from moment redistribution, and the opportunity to *reduce steel congestion* in critical regions have motivated considerable interest in limit analysis for reinforced concrete based on the concepts just described. For beams and frames, ACI Code 8.4 permits limited redistribution of moments, depending upon the strain in the tensile steel ϵ_t. For slabs, which generally use very low reinforcement ratios and consequently have great ductility, plastic design methods are especially suitable.

b. Plastic Hinges and Collapse Mechanisms

If a short segment of a reinforced concrete beam is subjected to a bending moment, curvature of the beam axis will result, and there will be a corresponding rotation of one face of the segment with respect to the other. It is convenient to express this in terms of an angular change per unit length of the member. The relation between moment and angle change per unit length of beam, or curvature, at a reinforced concrete beam section subject to tensile cracking was developed in Section 6.9. Methods were presented there by which the theoretical moment-curvature graph might be drawn for a given beam cross section, as in Fig. 6.17.

The actual moment-curvature relationship measured in beam tests differs somewhat from that shown in Fig. 6.17, mainly because, from tests, curvatures are calculated from average strains measured over a finite gage length, usually about equal to the effective depth of the beam. In particular, the sharp increase in curvature upon concrete cracking shown in Fig. 6.17 is not often seen because the crack occurs at only one discrete location along the gage length. Elsewhere, the uncracked concrete shares in resisting flexural tension, resulting in what is known as *tension stiffening.* This tends to reduce curvature. Furthermore, the exact shape of the moment-curvature relation depends strongly upon the reinforcement ratio as well as upon the exact stress-strain curves for the concrete and steel.

Figure 12.13 shows a somewhat simplified moment-curvature diagram for an actual concrete beam section having a tensile reinforcement ratio equal to about one-half the balanced value. The diagram is linear up to the cracking moment M_{cr}, after which a nearly straight line of somewhat flatter slope is obtained. At the moment

FIGURE 12.13
Plastic hinge characteristics in a reinforced concrete member: (*a*) typical moment-curvature diagram; (*b*) strains and stresses at start of yielding; (*c*) strains and stresses at incipient failure.

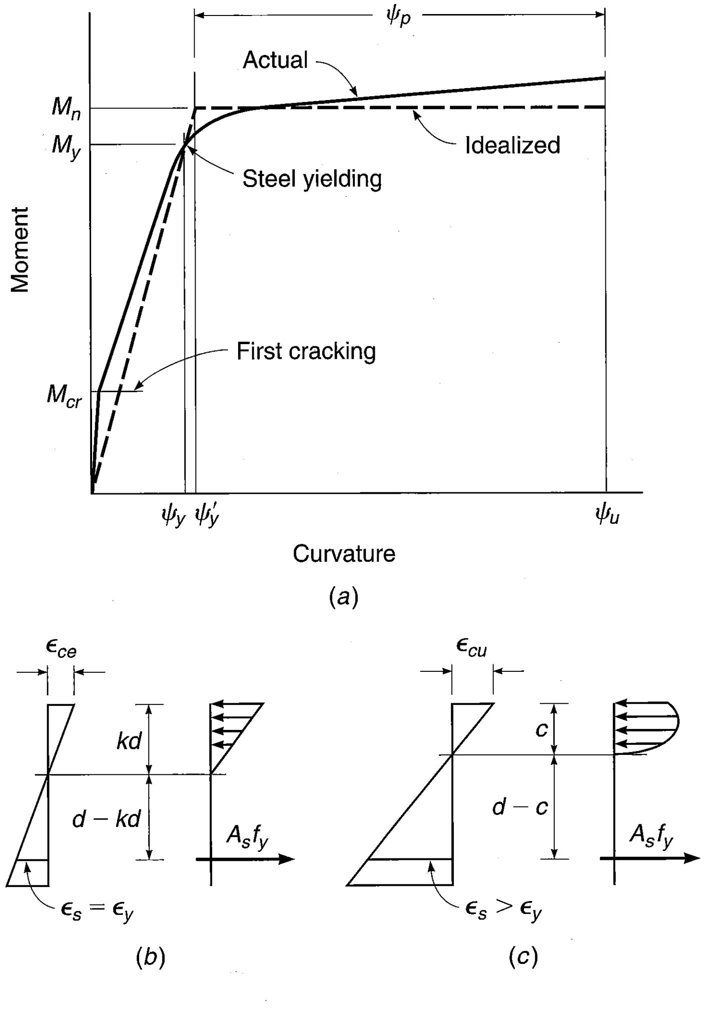

that initiates yielding M_y, the curvature starts to increase disproportionately. Further increase in applied moment causes extensive inelastic rotation until, eventually, the compressive strain limit of the concrete is reached at the ultimate rotation ψ_u. The maximum moment is often somewhat above the calculated flexural strength M_n, due largely to strain hardening of the reinforcement.

The effect of inelastic concrete response prior to steel yielding is small for typically underreinforced sections, as is indicated in Fig. 6.17, and the yield moment can be calculated based on the elastic concrete stress distribution shown in Fig. 12.13*b*:

$$M_y = A_s f_y \left(d - \frac{kd}{3} \right) \tag{12.1}$$

where *kd* is the distance from the compression face to the cracked elastic neutral axis (see Section 3.3b). The nominal moment capacity M_n, based on Fig. 12.13*c*, is calculated by the usual expression

$$M_n = A_s f_y \left(d - \frac{a}{2} \right) = A_s f_y \left(d - \frac{\beta_1 c}{2} \right) \tag{12.2}$$

For purposes of limit analysis, the M–ψ curve is usually idealized, as shown by the dashed line in Fig. 12.13*a*. The slope of the elastic portion of the curve is obtained with satisfactory accuracy using the moment of inertia of the cracked transformed section. After the nominal moment M_n is reached, continued plastic rotation is assumed to occur with no change in applied moment. The elastic curve of the beam will show an abrupt change in slope at such a section. The beam behaves as if there were a hinge at that point. However, the hinge will not be "friction-free," but will have a constant resistance to rotation.

If such a plastic hinge forms in a determinate structure, as shown in Fig. 12.14, uncontrolled deflection takes place, and the structure will collapse. The resulting system is referred to as a *mechanism,* an analogy to linkage systems in mechanics. Generalizing, one can say that a statically determinate system requires the formation of only one plastic hinge to become a mechanism.

This is not so for indeterminate structures. In this case, stability may be maintained even though hinges have formed at several cross sections. The formation of such hinges in indeterminate structures permits a redistribution of moments within the beam or frame. It will be assumed for simplicity that the indeterminate beam of Fig. 12.15*a* is symmetrically reinforced, so that the negative bending capacity is the same as the positive. Let the load P be increased gradually until the elastic moment at the fixed support, $\frac{3}{16}PL$, is just equal to the plastic moment capacity of the section M_n. This load is

$$P = P_{el} = \frac{16}{3}\frac{M_n}{L} = 5.33\frac{M_n}{L} \tag{a}$$

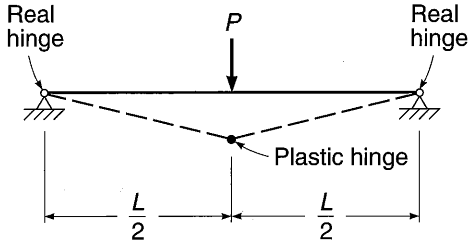

FIGURE 12.14
Statically indeterminate member after the formation of plastic hinge.

FIGURE 12.15
Indeterminate beam with plastic hinges at support and midspan.

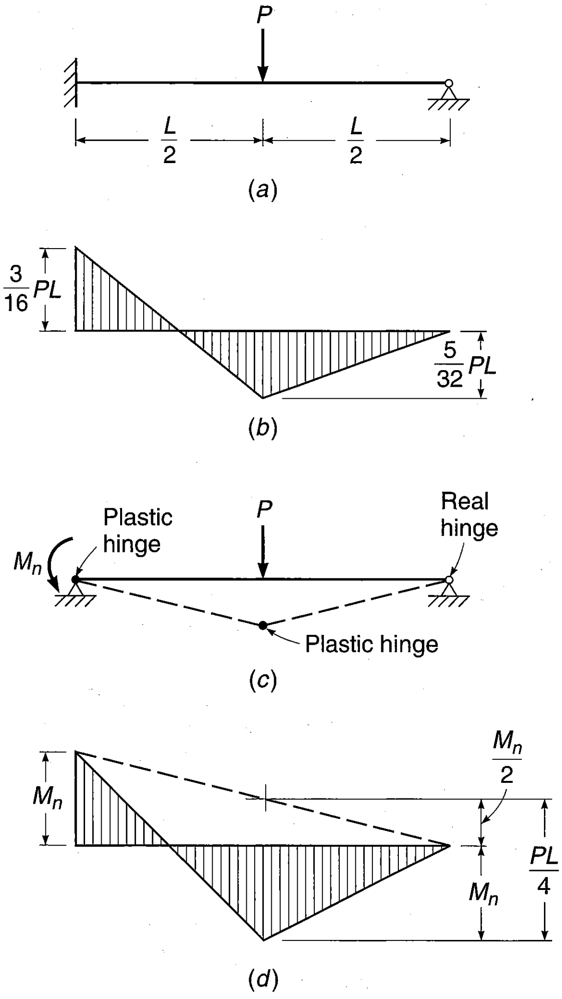

At this load, the positive moment under the load is $\frac{5}{32}PL$, as shown in Fig. 12.15*b*. The beam still responds elastically everywhere but at the left support. At that point the actual fixed support can be replaced for purposes of analysis with a plastic hinge offering a known resisting moment M_n. Because a redundant reaction has been replaced by a known moment, the beam is now determinate.

The load can be increased further until the moment under the load also becomes equal to M_n, at which load the second hinge forms. The structure is converted into a mechanism, as shown in Fig. 12.15*c*, and collapse occurs. The moment diagram at collapse load is shown in Fig. 12.15*d*.

The magnitude of load causing collapse is easily calculated from the geometry of Fig. 12.15*d:*

$$M_n + \frac{M_n}{2} = \frac{PL}{4}$$

from which

$$P = P_n = \frac{6M_n}{L} \tag{b}$$

By comparison of Eqs. (*b*) and (*a*), it is evident that an increase in P of 12.5 percent is possible, beyond the load that caused the formation of the first plastic hinge, before the beam will actually collapse. Due to the formation of plastic hinges, a redistribution of moments has occurred such that, at failure, the ratio between the positive moment and negative moment is equal to that assumed in reinforcing the structure.

c. Rotation Requirement

It may be evident that there is a direct relation between the amount of redistribution desired and the amount of inelastic rotation at the critical sections of a beam required to produce the desired redistribution. In general, the greater the modification of the elastic moment ratio, the greater the required rotation capacity to accomplish that change. To illustrate, if the beam of Fig. 12.15*a* had been reinforced according to the elastic moment diagram of Fig. 12.15*b*, no inelastic-rotation capacity at all would be required. The beam would, at least in theory, yield simultaneously at the left support and at midspan. On the other hand, if the reinforcement at the left support had been deliberately reduced (and the midspan reinforcement correspondingly increased), inelastic rotation at the support would be required before the strength at midspan could be realized.

The amount of rotation required at plastic hinges for any assumed moment diagram can be found by considering the requirements of compatibility. The member must be bent, under the combined effects of elastic moment and plastic hinges, so that the correct boundary conditions are satisfied at the supports. Usually, zero support deflection is to be maintained. Moment-area and conjugate-beam principles are useful in quantitative determination of rotation requirements (Ref. 12.6). In deflection calculations, it is convenient to assume that plastic hinging occurs at a point, rather than being distributed over a finite *hinging length,* as is actually the case. Consequently, in loading the conjugate beam with unit rotations, plastic hinges are represented as concentrated loads.

Calculation of rotation requirements will be illustrated by the two-span continuous beam shown in Fig. 12.16*a*. The elastic moment diagram resulting from a single concentrated load is shown in Fig. 12.16*b*. The moment at support B is $0.096Pl$, while that under the load is $0.182Pl$. If the deflection of the beam at support C were calculated using the unit rotations equal to M/EI, based on this elastic moment diagram, a zero result would be obtained.

Figure 12.16*c* shows an alternative, statically admissible moment diagram that was obtained by arbitrarily increasing the support moment from $0.096Pl$ to $0.150Pl$. If the beam deflection at C were calculated using this moment diagram as a basis, a nonzero value would be obtained. This indicates the necessity for inelastic rotation at one or more points to maintain geometric compatibility at the right support.

If the beam were reinforced according to Fig. 12.16*c*, increasing loads would produce the first plastic hinge at D, where the beam has been deliberately made understrength. Continued loading would eventually result in formation of the second plastic hinge at B, creating a mechanism and leading to collapse of the structure.

Limit analysis requires calculation of rotation at all plastic hinges up to, but not including, the last hinge that triggers actual collapse. Figure 12.16*d* shows the M/EI load to be imposed on the conjugate beam of Fig. 12.16*e*. Also shown is the concentrated angle change θ_d, which is to be evaluated. Starting with the left span,

FIGURE 12.16
Moment redistribution in a two-span beam: (*a*) loaded beam; (*b*) elastic moments; (*c*) modified moments; (*d*) M/EI loads; (*e*) conjugate beam; (*f*) deflection curve.

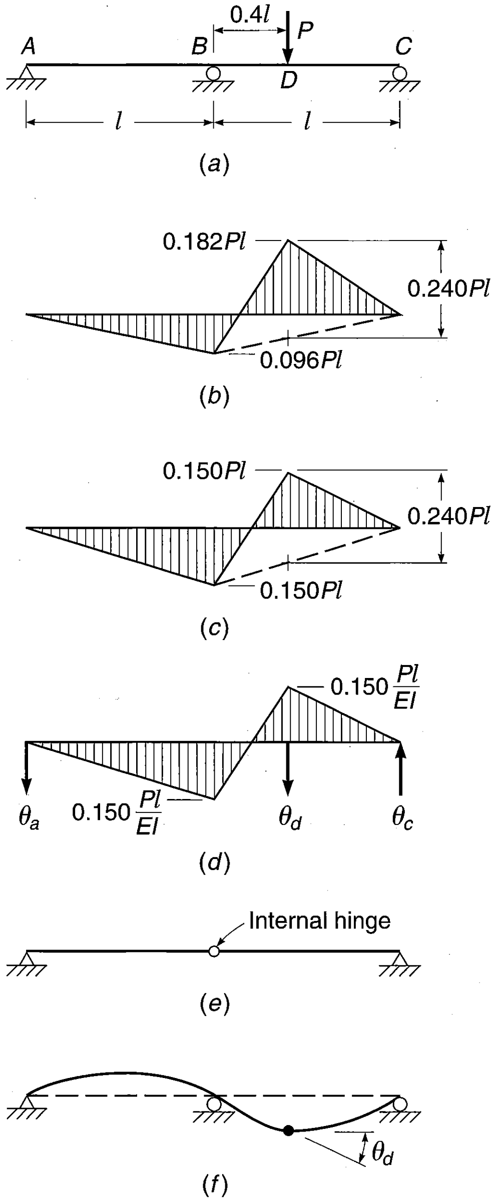
0.4l
P
A
B
C
D
l
l
(a)
0.182Pl
0.240Pl
0.096Pl
(b)
0.150Pl
0.240Pl
0.150Pl
(c)
0.150 Pl/EI
θa
0.150 Pl/EI
θd
θc
(d)
Internal hinge
(e)
θd
(f)

taking moments of the M/EI loads about the internal hinge of the conjugate beam at B, one obtains the left reaction of the conjugate beam (equal to the slope of the real beam):

$$\theta_a = 0.025\frac{Pl^2}{EI}$$

With that reaction known, moments are taken about the support C of the conjugate beam and set equal to zero to obtain

$$\theta_d = 0.060\frac{Pl^2}{EI}$$

This represents the necessary discontinuity in the slope of the elastic curve shown in Fig. 12.16*f* to restore the beam to zero deflection at the right support. The beam must be capable of developing at least that amount of plastic rotation if the modified moment diagram assumed in Fig. 12.16*c* is to be valid.

d. Rotation Capacity

The capacity of concrete structures to absorb inelastic rotations at plastic-hinge locations is not unlimited. The designer adopting full limit analysis in concrete must calculate not only the amount of rotation required at critical sections to achieve the assumed degree of moment redistribution but also the rotation capacity of the members at those sections to ensure that it is adequate.

Curvature at initiation of yielding is easily calculated from the elastic strain distribution shown in Fig. 12.13*b*.

$$\psi_y = \frac{\epsilon_y}{d(1-k)} \tag{12.3}$$

in which the ratio k establishing the depth of the elastic neutral axis is found from Eq. (3.12). The curvature corresponding to the nominal moment can be obtained from the geometry of Fig. 12.13*c*:

$$\psi_u = \frac{\epsilon_{cu}}{c} \tag{12.4}$$

Although it is customary in flexural strength analysis to adopt $\epsilon_{cu} = 0.003$, for purposes of limit analysis a more refined value is needed. Extensive experimental studies (Refs. 12.7 and 12.8) indicate that the ultimate strain capacity of concrete is strongly influenced by the beam width b, by the moment gradient, and by the presence of additional reinforcement in the form of compression steel and confining steel (i.e., web reinforcement). The last parameter is conveniently introduced by means of a reinforcement ratio ρ'', defined as the ratio of the volume of one stirrup plus its tributary compressive steel volume to the concrete volume tributary to one stirrup. On the basis of empirical studies, the ultimate flexural strain at a plastic hinge is

$$\epsilon_{cu} = 0.003 + 0.02\frac{b}{z} + \left(\frac{\rho'' f_y}{14.5}\right)^2 \tag{12.5}$$

where z is the distance between points of maximum and zero moment. Based on Eqs. (12.3) to (12.5), the inelastic curvature for the idealized relation shown in Fig. 12.13*a* is

$$\psi_p = \psi_u - \psi_y\frac{M_n}{M_y} \tag{12.6}$$

This plastic rotation is not confined to one cross section but is distributed over a finite length referred to as the *hinging length.* The experimental studies upon which Eq. (12.5) is based measured strains and rotations in a length equal to the effective depth d of the test members. Consequently, ϵ_{cu} is an *average* value of ultimate strain over a finite length, and ψ_p, given by Eq. (12.6), is an *average* value of curvature. The total inelastic rotation θ_p can be found by multiplying the average curvature by the hinging length:

$$\theta_p = \left(\psi_u - \psi_y\frac{M_n}{M_y}\right)l_p \tag{12.7}$$

On the basis of current evidence, it appears that the hinging length l_p in support regions, on either side of the support, can be approximated by the expression

$$l_p = 0.5d + 0.05z \tag{12.8}$$

in which z is the distance from the point of maximum moment to the nearest point of zero moment.

e. Moment Redistribution under the ACI Code

Full use of the plastic capacity of reinforced concrete beams and frames requires an extensive analysis of all possible mechanisms and an investigation of rotation requirements and capacities at all proposed hinge locations. The increase in design time may not be justified by the gains obtained. On the other hand, a restricted amount of redistribution of elastic moments can safely be made without complete analysis, yet may be sufficient to obtain most of the advantages of limit analysis.

A limited amount of redistribution is permitted by ACI Code 8.4, depending upon a rough measure of available ductility, without explicit calculation of rotation requirements and capacities. The net tensile strain in the extreme tension steel at nominal strength ϵ_t, given in Eq. (3.29), is used as an indicator of rotation capacity. Accordingly, ACI Code 8.4 provides as follows:

> Except where approximate values for moments are used, it shall be permitted to decrease factored moments calculated by elastic theory at sections of maximum negative or maximum positive moment in any span of continuous flexural members for any assumed loading arrangement by not more than $1000\epsilon_t$ percent, with a maximum of 20 percent. Redistribution of moments shall be made only when ϵ_t is equal to or greater than 0.0075 at the section at which moment is reduced. The reduced moment shall be used for calculating redistributed moments at all other sections within the spans. Static equilibrium shall be maintained after redistribution of moments for each loading arrangement.

Redistribution for values of $\epsilon_t < 0.0075$ is conservatively prohibited. The ACI Code provisions are shown graphically in Fig. 12.17. The value of ρ corresponding to a given value of ϵ_t, and thus a given percentage change in moment, can be calculated using Eq. (3.30*a*) from Section 3.4d.

To demonstrate the advantage of moment redistribution when alternative loadings are involved, consider the concrete beam of Fig. 12.18. A three-span continuous beam is shown, with dead load of 10 kN/m and live load of 20 kN/m. To obtain maximum moments at all critical design sections, it is necessary to consider three alternative loadings. Case *a,* with live and dead load over exterior spans and dead load only over the interior span, will produce the maximum positive moment in the exterior spans. Case *b,* with dead load on exterior spans and dead and live load on the interior span, will produce the maximum positive moment in the interior span. The maximum negative moment over the interior support is obtained by placing dead and live load on the two adjacent spans and dead load only on the far exterior span, as shown in case *c*.

It will be assumed for simplicity that a 10 percent adjustment of maximum negative and positive moments is permitted throughout, provided that other span moments are modified accordingly. An overall reduction in design moments through the entire three-span beam may be possible. Case *a,* for example, produces an elastic

FIGURE 12.17
Allowable moment redistribution under the ACI Code.

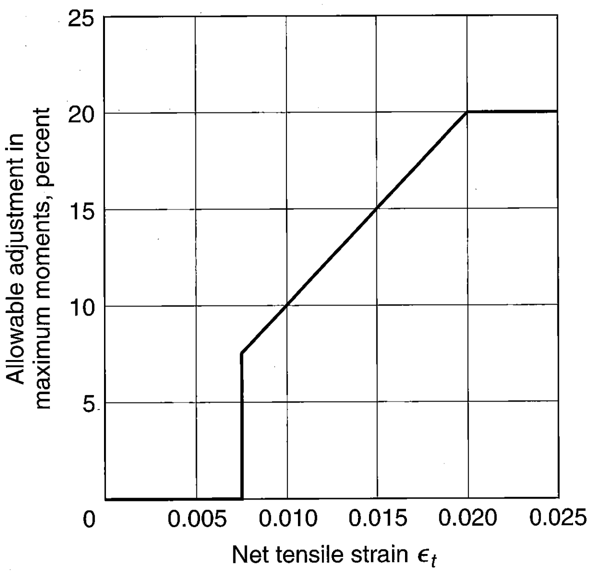

maximum span moment in the exterior spans of 99 kN-m. Corresponding to this is an elastic negative moment of 72 kN-m at the interior support. Adjusting the maximum positive moment downward by 10 percent, one obtains a positive moment of 89 kN-m, which results in an upward adjustment of the support moment to 90 kN-m.

Now consider case *b*. By a similar redistribution of moments, a reduced middle-span moment of 57 kN-m is accompanied by an increase in the support moment from 72 to 79 kN-m.

The moment obtained at the first interior support for loading case *c* can be decreased by 10 percent to 108 kN-m. To limit the increase in the controlling span moment of the interior span, the right interior support moment is not decreased. The positive moments in the left exterior span and in the interior span corresponding to the modified moment at the left interior support are 81 and 51 kN-m, respectively.

It will be observed that the reduction obtained for the span moments in cases *a* and *b* was achieved at the expense of increasing the moment at the first interior support. However, the increased support moment in each case was less than the moment for which that support would have to be designed based on the loading *c*, which produced the maximum support moment. Similarly, the reduction in support moment in case *c* was taken at the expense of an increase in span moments in the two adjacent spans. However, in each case the increased span moments were less than the maximum span moments obtained for other loading conditions. The final design moments at all critical sections are underlined in Fig. 12.18. It can be seen, then, that the net result is a reduction in design moments over the entire beam. This modification of moments does not mean a reduction in safety factor below that implied in code safety provisions; rather, it means a reduction of the *excess* strength that would otherwise be present in the structure because of the actual redistribution of moments that would occur before failure. It reflects the fact that the maximum design moments are obtained from alternative load patterns, which could not exist concurrently. The end result is a more realistic appraisal of the actual collapse load of the indeterminate structure.

FIGURE 12.18
Redistribution of moments in a three-span continuous beam. The final design moments are underlined.

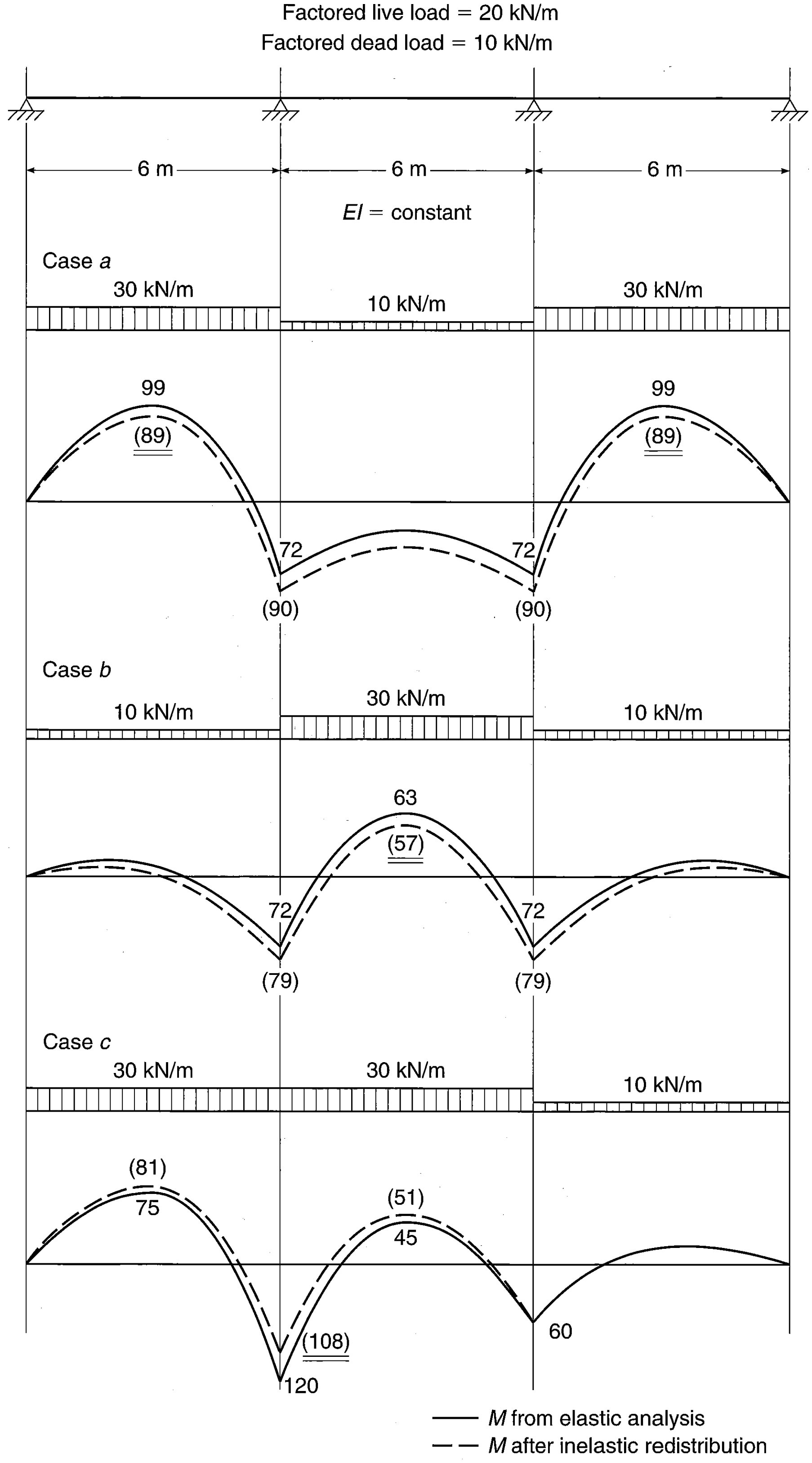
Factored live load = 20 kN/m
Factored dead load = 10 kN/m
6 m
6 m
6 m
EI = constant
Case a
30 kN/m
10 kN/m
30 kN/m
99
(89)
99
(89)
72
72
(90)
(90)
Case b
10 kN/m
30 kN/m
10 kN/m
63
(57)
72
72
(79)
(79)
Case c
30 kN/m
30 kN/m
10 kN/m
(81)
75
(51)
45
(108)
120
60
M from elastic analysis
M after inelastic redistribution

12.10 CONCLUSION

The problems associated with analysis of reinforced concrete structures are many. The engineer not only must accept the uncertainties of load placement, magnitude, and duration typical of any structural analysis, but also must cope with other complications that are unique to reinforced concrete. These are mainly associated with estimation of moment of inertia of the reinforced concrete sections and with the influence of concrete creep. They may be summarized briefly as follows: (1) effective moments of inertia change depending on the sign of the bending moment; (2) moments of inertia depend not only on the effective concrete section, but also on the steel, a part of which may be discontinuous; (3) moments of inertia depend on cracking, which is both location-dependent and load-dependent; and (4) the concrete is subject to creep under sustained loads, reducing its effective modulus. In addition, joint restraints and conditions of support for complex structures are seldom completely in accordance with the idealization. The student may well despair of accurate calculation of the internal forces for which the members of a reinforced concrete frame must be designed.

It may be reassuring to know that reinforced concrete has a remarkable capacity to adapt to the assumptions of the designer. This has been pointed out by a number of outstanding engineers. *Luigi Nervi,* the renowned Italian architect-engineer, has stated it eloquently as follows:

> Mainly because of plastic flow, a concrete structure tries with admirable docility to adapt itself to our calculations—which do not always represent the most logical and spontaneous answer to the request of the forces at play—and even tries to correct our deficiencies and errors. Sections and regions too highly stressed yield and channel some of their loads to other sections or regions, which accept this additional task with commendable spirit of collaboration, within the limits of their own strength.[†]

Hardy Cross, best known for his development of the moment distribution method of analysis (see Section 12.4), noted the beneficial effects of concrete creep, by which a structure can adapt to support settlements, which, on the basis of elastic analysis, cause forces and movements sufficient to fail the structure. *Halvard Birkeland,* one of the pioneers in the development of prestressed concrete in the United States, referred to the "wisdom of the structure," noting that ". . . the structure, in many instances, will accept our rash assumptions and our imperfect mathematical models . . . the structure will exhaust all means of standing before it decides to fall."[‡]

Thus it may be of some comfort to know that *a reinforced concrete structure will tend to act as the engineer has assumed it will act.* Reasonable assumptions in the analysis may safely be made. But corollary to this important principle is the acceptance of its limits: *the general pattern of forces and moments must be recognized, and at least one reasonable load path provided.* Too great a deviation from the actual distribution of internal forces can result in serviceability problems associated with cracking and deflection, and can even result in premature failure. It is for this reason that methods of limit analysis for reinforced concrete include restrictions on the amount of redistribution of elastic moments (see Section 12.9). But it is reassuring to know that if good judgment is used in assigning internal forces to critical sections, the *wisdom of the structure* will prevail.

[†] P. L. Nervi, *Structures,* F. W. Dodge Corp., New York, 1956.

[‡] H. L. Birkeland, "The Wisdom of the Structure," *J. ACI,* April 1978, pp. 105–111.

REFERENCES

12.1. J. C. McCormac, *Structural Analysis Using Classical and Matrix Methods*, 4th ed., Wiley, Hoboken, New Jersey, 2007.

12.2. W. McGuire, R. H. Gallagher, and R. D. Ziemian, *Matrix Structural Analysis, with MASTAN2,* 2nd ed., McGraw-Hill, New York, 1999.

12.3. M. Paz and W. Leigh, *Integrated Matrix Structural Analysis for Structures,* Kluwer, Boston, 2001.

12.4. K. M. Leet, C.-M. Uang, and A. Gilbert, *Fundamentals of Structural Analysis,* 3rd ed., McGraw-Hill, New York, 2008.

12.5. *Continuity in Concrete Building Frames,* 4th ed., Portland Cement Association, Skokie, IL, 1959.

12.6. G. C. Ernst, "A Brief for Limit Design," *Trans. ASCE,* vol. 121, 1956, pp. 605–632.

12.7. A. H. Mattock, "Rotation Capacity of Hinging Regions in Reinforced Concrete Frames," *Proc. Int. Symp. Flexural Mech. Reinforced Concrete,* ACI Publication SP-12, 1964.

12.8. J. S. Ford, D. C. Chang, and J. E. Breen, "Design Indications from Tests of Unbraced Multipanel Concrete Frames," *Concr. Intl.,* vol. 3, no. 3, 1981, pp. 37–47.

PROBLEMS

12.1. Complete the preliminary design of the four-story heavy storage facility shown in Fig. P12.1. The floor live load is 12 kN/m^2, the roof live load is 0.6 kN/m^2, and the dead load on all floors and the roof consists of the structure self-weight plus 5 kN/m^2 for utilities. The building is enclosed in a self-supporting curtain wall that also carries the lateral load on the structure. Beams are spaced at 3.5 m; girders are spaced at 8 m. The minimum clear space between floors is 3.35 m, and the floor depth should not exceed 750 mm. The column cross sections should be maintained from floor to floor. Use f_y = 420 MPa and f_c' = 28 MPa for the floors. Concrete with f_c' up to 56 MPa is available for the columns. The preliminary design should include the initial dimensions of the structural slab, beams, girders, and columns for a typical floor.

FIGURE P12.1

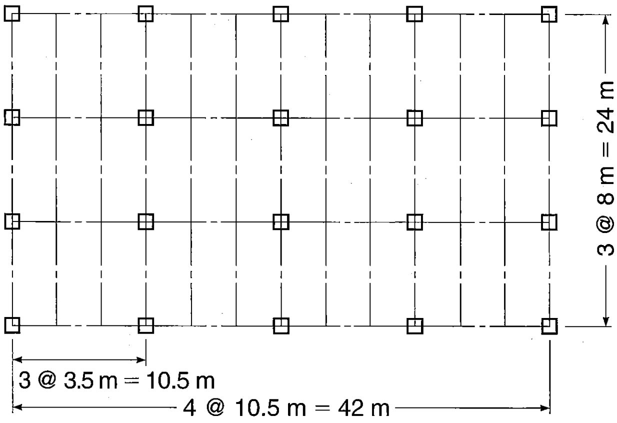

12.2. A concrete beam with b = 300 mm, h = 670 mm, and d = 600 mm, having a span of 7.3 m, can be considered fully fixed at the left support and supported vertically but with no rotational restraint (e.g., roller) at the right end. It is reinforced for positive bending with a combination of bars giving A_s = 1580 mm^2, and for negative bending at the left support with A_s = 1858 mm^2. Positive bars are carried 150 mm into the face of the left support, according to the ACI Code requirements, but lack the embedded length to be considered effective as compression steel. No. 10 (No. 3) closed hoop stirrups are provided at 225 mm spacing over the full span. The factored load consists of a single concentrated force of 280 kN at midspan. Self-weight of the beam may be neglected in the calculations. Calculate the rotation requirement at the first plastic hinge to form (*a*) if the beam is reinforced according to the description above; (*b*) if, to reduce bar congestion at the left support, that steel area is reduced by 12.5 percent, with an appropriate increase in the positive steel area; and (*c*) if the steel area at the left support is reduced by 25 percent, compared with the original description, with an appropriate increase in the positive steel area. Also calculate the rotation capacity of the critical section, for comparison with the requirements of (*a*), (*b*), and (*c*). Comment on your results and compare with the approach to moment redistribution presented in the ACI Code. Material strengths are $f_y = 420$ MPa and $f_c' = 28$ MPa.

12.3. A 12-span continuous reinforced concrete T beam is to carry a calculated dead load of 13 kN/m including self-weight, plus a service live load of 20 kN/m on uniform spans measuring 8.1 m between centers of supporting columns (7.6 m clear spans). The slab thickness is 150 mm, and the effective flange width is 1900 mm. Web proportions are $b_w = 0.6d$, and the maximum reinforcement ratio will be set at 0.011. All columns will be 450 mm square. Material strengths are $f_c' = 28$ MPa and $f_y = 420$ MPa.

(*a*) Find the factored moments for the exterior and first interior span based on the ACI Code moment coefficients of Table 12.1.

(*b*) Find the factored moments in the exterior and first interior span by elastic frame analysis, assuming the floor-to-floor height to be 3 m. Note that alternative live loadings should be considered (see Section 12.2a) and that moments can be reduced to account for the support width (see Section 12.5a). Compare your results with those obtained using the ACI moment coefficients.

(*c*) Adjust the factored negative and positive moments, taking advantage of the redistribution provisions of the ACI Code. Assume that a 10 percent minimum redistribution is possible.

(*d*) Design the exterior and first interior spans for flexure and shear, finding concrete dimensions and bar requirements, basing your design on the assumptions and modified moments in part (*c*).

12.4. A continuous reinforced concrete frame consists of a two-span rectangular beam *ABC*, with center-to-center spans *AB* and *BC* of 7.3 m. Columns measuring 350 mm square are provided at *A*, *B*, and *C*. The columns may be considered fully fixed at the floors above and below for purposes of analysis. The beam will carry a service live load of 17.5 kN/m and a calculated dead load of 14.5 kN/m, including self-weight. Floor-to-floor height is 3.65 m. Material strengths are $f_y = 420$ MPa and $f_c' = 28$ MPa.

(*a*) Carry out an elastic analysis of the two-span frame, considering alternate live loadings to maximize the bending moment at all critical sections. Design the beams, using a maximum reinforcement ratio of 0.012 and $d = 2b$. Find the required concrete section and required steel areas at positive and negative bending sections. Select the reinforcement. Cutoff points can be determined according to Fig. 5.20*a*. Note that negative design moments are at the face of supports, not support centerlines.

(*b*) Take maximum advantage of the redistribution provisions of ACI Code 8.4 (see Section 12.9e) to reduce design moments at all critical sections, and redesign the steel for the beams. Keep the concrete section unchanged. Select reinforcement and determine cutoff points.

(*c*) Comment on your two designs with regard to the amount of steel required and the possible congestion of steel at the critical bending sections. You may assume that the shear reinforcement is unchanged in the redesigned beam.

12.5. Complete the preliminary design of the four-story library building shown in Fig. P12.5, using a beam-girder (or joist-girder) floor system. The first floor (slab-on-grade) is supported on drilled piers and serves as the reading and library services area. The upper three floors serve as stack areas (see Table 1.1). The out-to-out building dimensions are 27 × 45 m, exclusive of the exterior facade. Columns should be spaced at approximately 9 m in each direction. The minimum clear space between floors is 3.65 m, and the floor depth should not exceed 600 mm. Assume a load of 3.35 kN/m^2 on the roof for the mechanical penthouse and a snow load of 0.95 kN/m^2. The building is enclosed in a self-supporting curtain wall that also carries the lateral load on the structure. The column cross sections should be maintained from floor to floor. Use $f_y =$ 420 MPa and $f_c' = 28$ MPa for the floors. Concrete with f_c' up to 56 MPa is available for the columns. The preliminary design should include the initial dimensions of the structural slab, beams, girders, and columns for a typical floor.

FIGURE P12.5

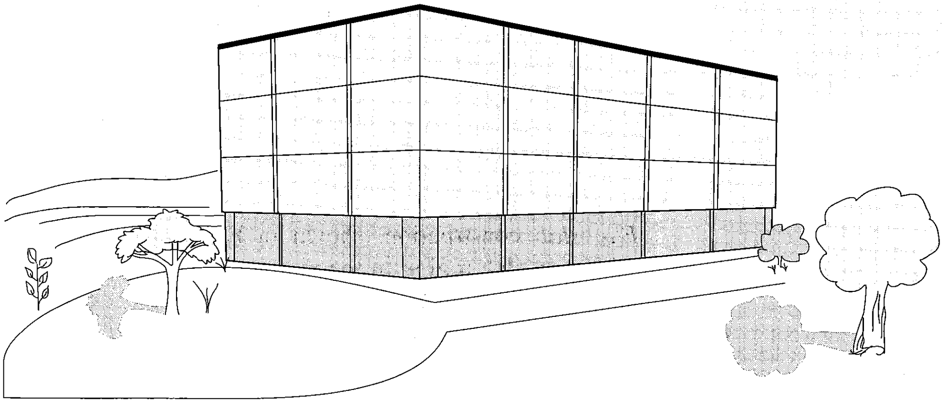

13

Analysis and Design of Slabs

13.1 TYPES OF SLABS

In reinforced concrete construction, slabs are used to provide flat, useful surfaces. A reinforced concrete slab is a broad, flat plate, usually horizontal, with top and bottom surfaces parallel or nearly so. It may be supported by reinforced concrete beams (and is usually cast monolithically with such beams), by masonry or reinforced concrete walls, by structural steel members, directly by columns, or continuously by the ground.

Slabs may be supported on two opposite sides only, as shown in Fig. 13.1*a*, in which case the structural action of the slab is essentially *one-way*, the loads being carried by the slab in the direction perpendicular to the supporting beams. There may be beams on all four sides, as shown in Fig. 13.1*b*, so that *two-way* slab action is obtained. Intermediate beams, as shown in Fig. 13.1*c*, may be provided. If the ratio of length to width of one slab panel is larger than about 2, most of the load is carried in the short direction to the supporting beams and one-way action is obtained in effect, even though supports are provided on all sides.

Concrete slabs in some cases may be carried directly by columns, as shown in Fig. 13.1*d*, without the use of beams or girders. Such slabs are described as *flat plates* and are commonly used where spans are not large and loads not particularly heavy. *Flat slab* construction, shown in Fig. 13.1*e*, is also beamless but incorporates a thickened slab region in the vicinity of the column and often employs flared column tops. Both are devices to reduce stresses due to shear and negative bending around the columns. They are referred to as *drop panels* and *column capitals*, respectively. Closely related to the flat plate slab is the two-way joist, also known as a *grid* or *waffle slab*, shown in Fig. 13.1*f*. To reduce the dead load of solid-slab construction, voids are formed in a rectilinear pattern through use of metal or fiberglass form inserts. A two-way ribbed construction results. Usually inserts are omitted near the columns, so a solid slab is formed to resist moments and shears better in these areas.

In addition to the column-supported types of construction shown in Fig. 13.1, many slabs are supported continuously on the ground, as for highways, airport runways, and warehouse floors. In such cases, a well-compacted layer of crushed stone or gravel is usually provided to ensure uniform support and to allow for proper subgrade drainage.[†]

Reinforcing steel for slabs is primarily parallel to the slab surfaces. Straight bar reinforcement is generally used, although in continuous slabs bottom bars are sometimes bent up to serve as negative reinforcement over the supports. Welded wire reinforcement

---

[†] Design guidance for slabs-on-ground, including the effects of deformation of both the slab and the subgrade, can be found in *Design of Slabs-on-Ground* reported by ACI Committee 360 (Ref. 13.1).

FIGURE 13.1
Types of structural slabs.

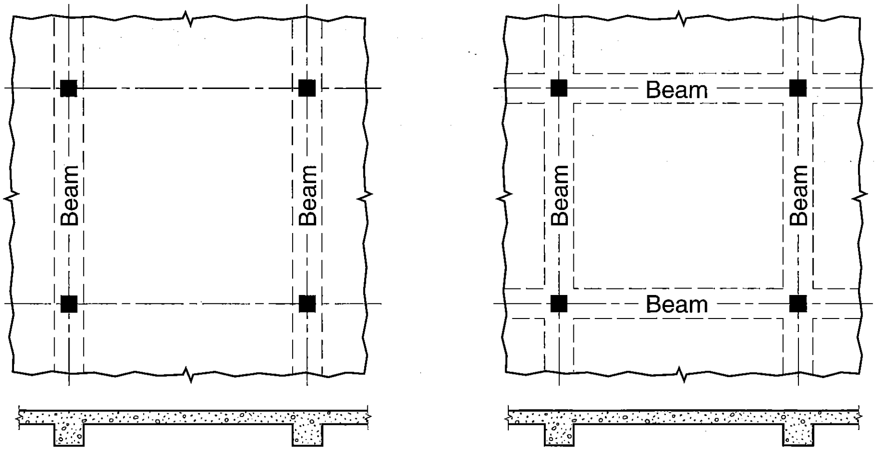
Beam
Beam
Beam
Beam
Beam
Beam

(*a*) One-way slab (*b*) Two-way slab

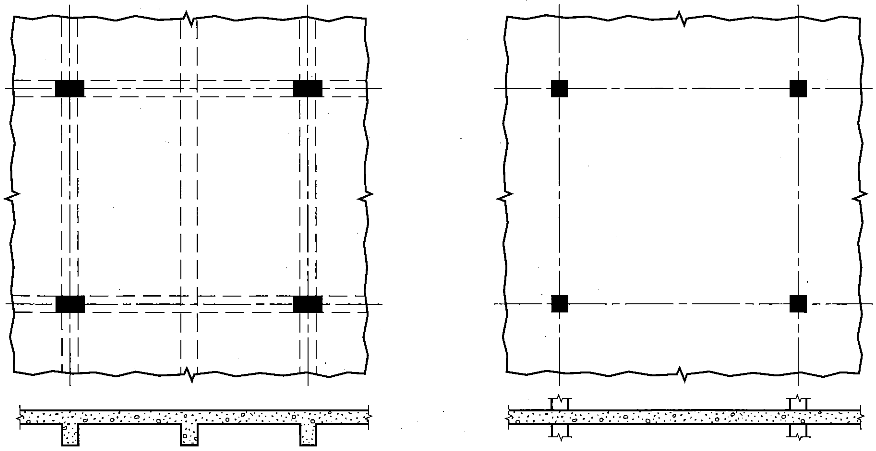

(*c*) One-way slab (*d*) Flat plate

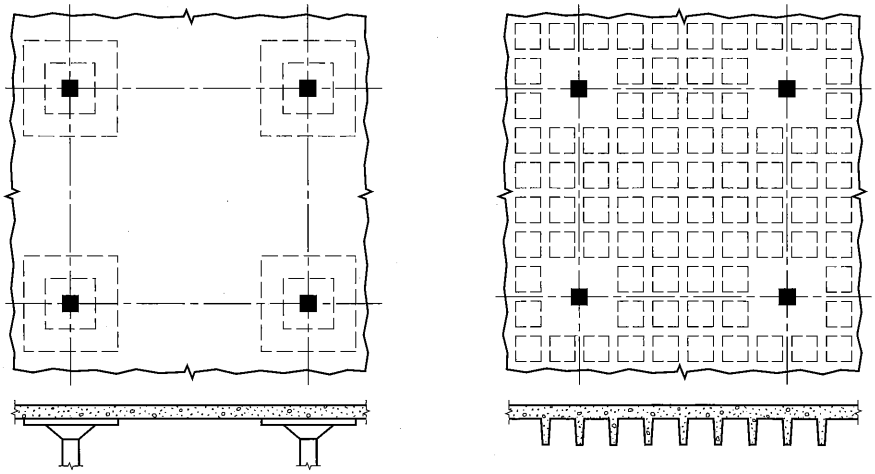

(*e*) Flat slab (*f*) Grid or waffle slab is commonly employed for slabs on the ground. Bar mats are available for the heavier reinforcement sometimes needed in highway slabs and airport runways. Slabs may also be prestressed using high tensile strength strands.

Reinforced concrete slabs of the types shown in Fig. 13.1 are usually designed for loads assumed to be uniformly distributed over one entire slab panel, bounded by supporting beams or column centerlines. Minor concentrated loads can be accommodated through two-way action of the reinforcement (two-way flexural steel for two-way slab systems or one-way flexural steel plus lateral distribution steel for one-way systems). Heavy concentrated loads generally require supporting beams.

One-way and two-way edge-supported slabs, such as shown in Fig. 13.1*a*, *b*, and *c*, will be discussed in Sections 13.2 to 13.4. Two-way beamless systems, such as shown in Fig. 13.1*d*, *e*, and *f*, as well as two-way edge-supported slabs (Fig. 13.1*b*), will be treated in Sections 13.5 to 13.13. Special methods based on limit analysis at the overload state, applicable to all types of slabs, will be presented in Chapters 14 and 15.

13.2 DESIGN OF ONE-WAY SLABS

The structural action of a one-way slab may be visualized in terms of the deformed shape of the loaded surface. Figure 13.2 shows a rectangular slab, simply supported along its two opposite long edges and free of any support along the two opposite short edges. If a uniformly distributed load is applied to the surface, the deflected shape will be as shown by the solid lines. Curvatures, and consequently bending moments, are the same in all strips s spanning in the short direction between supported edges, whereas there is no curvature, hence no bending moment, in the long strips l parallel to the supported edges. The surface is approximately cylindrical.

For purposes of analysis and design, a unit strip of such a slab cut out at right angles to the supporting beams, as shown in Fig. 13.3, may be considered as a rectangular beam of unit width, with a depth h equal to the thickness of the slab and a span l_a equal to the distance between supported edges. This strip can then be analyzed by the methods that were used for rectangular beams, the bending moment being computed for the strip of unit width. The load per unit area on the slab becomes the load per unit length on the slab strip. Since all of the load on the slab must be transmitted to the two supporting beams, it follows that all of the reinforcement should be placed at right

FIGURE 13.2
Deflected shape of uniformly loaded one-way slab.

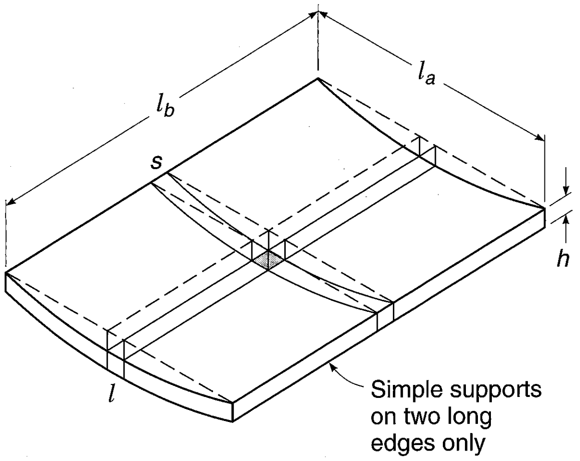

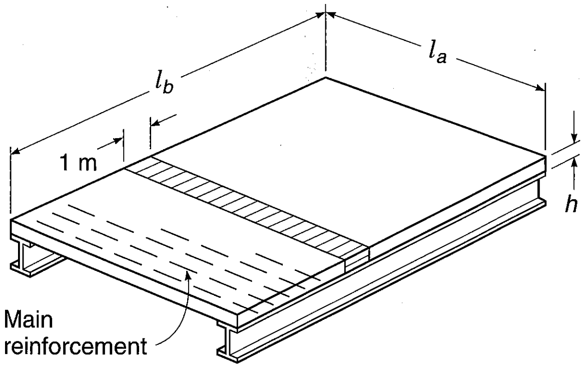

FIGURE 13.3
Unit strip basis for flexural design.

angles to these beams, with the exception of any bars that may be placed in the other direction to control shrinkage and temperature cracking. A one-way slab, thus, consists of a set of rectangular beams side by side.

This simplified analysis, which assumes Poisson's ratio to be zero, is slightly conservative. Actually, flexural compression in the concrete in the direction of l_a will result in lateral expansion in the direction of l_b unless the compressed concrete is restrained. In a one-way slab, this lateral expansion is resisted by adjacent slab strips, which tend to expand also. The result is a slight strengthening and stiffening in the span direction, but this effect is small and can be disregarded.

The reinforcement ratio for a slab can be determined by dividing the area of one bar by the area of concrete between two successive bars, the latter area being the product of the depth to the center of the bars and the distance between them, center to center. The reinforcement ratio can also be determined by dividing the average area of steel per meter of width by the effective area of concrete in a 1-m strip. The average area of steel per meter of width is equal to the area of one bar times the average number of bars in a 1-m strip, and the effective area of concrete in a 1-m strip is equal to 1000 mm times the effective depth d in mm.

To illustrate the latter method of obtaining the reinforcement ratio ρ, assume a 125 mm slab with an effective depth of 100 mm, with No. 13 (No. 4) bars spaced 110 mm center to center. The average number of bars in a 1-m strip of slab is 1000/110 = 9.1 bars, and the average steel area in a 1-m strip is $9.1 \times 129 = 1174$ mm^2. Hence $\rho = 1174/(1000 \times 100) = 0.0117$. By the other method,

$$\rho = \frac{129}{110 \times 100} = 0.0117$$

The spacing of bars that is necessary to furnish a given area of steel per meter of width is obtained by dividing the number of bars required to furnish this area into 1000 mm. For example, to furnish an average area of 973 mm^2/m, with No. 13 (No. 4) bars, requires $973/129 = 7.5$ bars per meter; the bars must be spaced not more than $1000/7.5 = 133$ mm center to center. The determination of slab steel areas for various combinations of bars and spacings is facilitated by Table A.3 of Appendix A.

Factored moments and shears in one-way slabs can be found either by elastic analysis or through the use of the same coefficients as used for beams (see Chapter 12). If the slab rests freely on its supports, the span length may be taken equal to the clear span plus the depth of the slab but need not exceed the distance between centers of supports, according to ACI Code 8.9.1. In general, center-to-center distances should be used in continuous slab analysis, but a reduction is allowed in negative moments to

TABLE 13.1
Minimum thickness *h* of nonprestressed one-way slabs

Simply supported	$l/20$
One end continuous	$l/24$
Both ends continuous	$l/28$
Cantilever	$l/10$

account for support width as discussed in Chapter 12. For slabs with clear spans not more than 3 m that are built integrally with their supports, ACI Code 8.9.4 permits analysis as a continuous slab on knife edge supports with spans equal to the clear spans and the width of the beams otherwise neglected. If moment and shear coefficients are used, computations should be based on clear spans.

One-way slabs are normally designed with tensile reinforcement ratios well below the maximum practical value of $\rho_{0.005}$. Typical reinforcement ratios range from about 0.004 to 0.008. This is partially for reasons of economy, because the saving in steel associated with increasing the effective depth more than compensates for the cost of the additional concrete, and partially because very thin slabs with high reinforcement ratios would be likely to permit large deflections. Thus, flexural design may start with selecting a relatively low reinforcement ratio, say about $0.3\rho_{0.005}$, setting $M_u = \phi M_n$ in Eq. (3.38), and solving for the required effective depth d, given that $b = 1$ m for the unit strip. Alternatively, Table A.5 or Graph A.1 of Appendix A may be used. Table A.9 is also useful. The required steel area per 1 m strip $A_s = \rho bd$ is then easily found.

ACI Code 9.5.2 specifies the minimum thickness in Table 13.1 for nonprestressed slabs of normalweight concrete ($w_c = 24$ kN/m^3, 2325 kg/m^3) using Grade 60 reinforcement, provided that the slab is not supporting or attached to construction that is likely to be damaged by large deflections. Lesser thicknesses may be used if calculation of deflections indicates no adverse effects. For concretes having unit weight w_c in the range from 14 to 18 kN/m^3 (1440 to 1840 kg/m^3), the tabulated values should be multiplied by $1.65 - 0.003w_c$, but not less than 1.09. For reinforcement having a yield stress f_y other than 420 MPa, the tabulated values should be multiplied by $0.4 + f_y/700$. Slab deflections may be calculated, if required, by the same methods as for beams (see Section 6.7).

Shear will seldom control the design of one-way slabs, particularly if low tensile reinforcement ratios are used. It will be found that the shear capacity of the concrete ϕV_c will, almost without exception, be well above the required shear strength V_u at factored loads.

The total slab thickness h is usually rounded to the next higher 10 mm. Best economy is often achieved when the slab thickness is selected to match nominal lumber dimensions. The concrete protection below the reinforcement should follow the requirements of ACI Code 7.7.1, calling for 20 mm below the bottom of the steel (see Fig. 3.13*b*). In a typical slab, 25 mm below the center of the steel may be assumed. The lateral spacing of the bars, except those used only to control shrinkage and temperature cracks (see Section 13.3), should not exceed 3 times the thickness h or 450 mm, whichever is less, according to ACI Code 7.6.5. Generally, bar size should be selected so that the actual spacing is not less than about 1.5 times the slab thickness, to avoid excessive cost for bar fabrication and handling. Also, to reduce cost, straight bars are usually used for slab reinforcement, cut off where permitted as described for beams in Section 5.10.

13.3 TEMPERATURE AND SHRINKAGE REINFORCEMENT

Concrete shrinks as it dries out, as was pointed out in Section 2.11. It is advisable to minimize such shrinkage by using concretes with the smallest possible amounts of water and cement compatible with other requirements, such as strength and workability, and by thorough moist-curing of sufficient duration. However, no matter what precautions are taken, a certain amount of shrinkage is usually unavoidable. If a slab of moderate dimensions rests freely on its supports, it can contract to accommodate the shortening of its length produced by shrinkage. Usually, however, slabs and other members are joined rigidly to other parts of the structure and cannot contract freely. This results in tension stresses known as *shrinkage stresses*. A decrease in temperature relative to that at which the slab was cast, particularly in outdoor structures such as bridges, may have an effect similar to shrinkage. That is, the slab tends to contract and if restrained from doing so becomes subject to tensile stresses.

Since concrete is weak in tension, these temperature and shrinkage stresses are likely to result in cracking. Cracks of this nature are not detrimental, provided their size is limited to what are known as *hairline cracks*. This can be achieved by placing reinforcement in the slab to counteract contraction and distribute the cracks uniformly. As the concrete tends to shrink, such reinforcement resists the contraction and consequently becomes subject to compression. The total shrinkage in a slab so reinforced is less than that in one without reinforcement; in addition, whatever cracks do occur will be of smaller width and more evenly distributed by virtue of the reinforcement.

In one-way slabs, the reinforcement provided for resisting the bending moments has the desired effect of reducing shrinkage and distributing cracks. However, as contraction takes place equally in all directions, it is necessary to provide special reinforcement for shrinkage and temperature contraction in the direction perpendicular to the main reinforcement. This added steel is known as *temperature* or *shrinkage reinforcement*, or *distribution steel.*

Reinforcement for shrinkage and temperature stresses normal to the principal reinforcement should be provided in a structural slab in which the principal reinforcement extends in one direction only. ACI Code 7.12.2 specifies the minimum ratios of reinforcement area to *gross concrete area* (i.e., based on the total depth of the slab) shown in Table 13.2, but in no case may such reinforcing bars be placed farther apart than 5 times the slab thickness or more than 450 mm. In no case is the reinforcement ratio to be less than 0.0014.

The steel required by the ACI Code for shrinkage and temperature crack control also represents the minimum permissible reinforcement in the span direction of one-way slabs; the usual minimums for flexural steel do not apply.

TABLE 13.2
Minimum ratios of temperature and shrinkage reinforcement in slabs based on gross concrete area

Slabs where Grade 40 or 50 deformed bars are used	0.0020
Slabs where Grade 60 deformed bars or welded wire fabric (smooth or deformed) is used	0.0018
Slabs where reinforcement with yield strength exceeding 420 MPa measured at yield strain of 0.35 percent is used	$\dfrac{0.0018 \times 420}{f_y}$

EXAMPLE 13.1

One-way slab design. A reinforced concrete slab is built integrally with its supports and consists of two equal spans, each with a clear span of 4.5 m. The service live load is 4.8 kN/m^2, and 28 MPa concrete is specified for use with steel with a yield stress equal to 420 MPa. Design the slab, following the provisions of the ACI Code.

Solution. The thickness of the slab is first estimated, based on the minimum thickness from Table 13.1: $l/28 = 4500/28 = 161$ mm. A trial thickness of 160 mm will be used, for which the weight is $24 \times 0.160 = 3.84$ kN/m^2. The specified live load and computed dead load are multiplied by the ACI load factors:

$$\begin{aligned} \text{Dead load} &= 3.84 \times 1.2 = 4.61 \text{ kN/m}^2 \\ \text{Live load} &= 4.80 \times 1.6 = \underline{7.68 \text{ kN/m}^2} \\ \text{Total} &= 12.29 \text{ kN/m}^2 \end{aligned}$$

For this case, factored moments at critical sections may be found using the ACI moment coefficients (see Table 12.1):

$$\begin{aligned} &\text{At interior support:} && -M = \tfrac{1}{9} \times 12.29 \times 4.5^2 = 27.7 \text{ kN-m/m} \\ &\text{At midspan:} && +M = \tfrac{1}{14} \times 12.29 \times 4.5^2 = 17.8 \text{ kN-m/m} \\ &\text{At exterior support:} && -M = \tfrac{1}{24} \times 12.29 \times 4.5^2 = 10.4 \text{ kN-m/m} \end{aligned}$$

The maximum practical reinforcement ratio is, according to Eq. (3.30d),

$$\rho_{0.005} = (0.85^2)\frac{28}{420}\frac{0.003}{0.003 + 0.005} = 0.0181$$

If this value of ρ were actually used, the minimum required effective depth, controlled by negative moment at the interior support, would be found from Eq. (3.38) to be

$$\begin{aligned} d^2 &= \frac{M_u}{\phi \rho f_y b(1 - 0.59\rho f_y/f'_c)} \\ &= \frac{27.7 \times 10^6}{0.90 \times 0.0181 \times 420 \times 1000[1 - 0.59 \times 0.0181 \times (420/28)]} = 4821 \text{ mm}^2 \\ d &= 69.4 \text{ mm}^{\dagger} \end{aligned}$$

This is less than the effective depth of $160 - 25 = 135$ mm resulting from application of Code restrictions, and the latter figure will be adopted. At the interior support, if the stress-block depth $a = 25$ mm, the area of steel required per meter of width in the top of the slab is [Eq. (3.37)]

$$A_s = \frac{M_u}{\phi f_y(d - a/2)} = \frac{27.7 \times 10^6}{0.90 \times 420 \times (135 - 25/2)} = 598 \text{ mm}^2/\text{m}$$

Checking the assumed depth a by Eq. (3.32), one gets

$$a = \frac{A_s f_y}{0.85 f'_c b} = \frac{598 \times 420}{0.85 \times 28 \times 1000} = 10.6 \text{ mm}$$

A second trial will be made with $a = 10.6$ mm. Then

$$A_s = \frac{27.7 \times 10^6}{0.90 \times 420 \times (135 - 10.6/2)} = 565 \text{ mm}^2/\text{m}$$

for which $a = 10.6 \times 565/598 = 10.0$ mm. No further revision is necessary. At other critical-moment sections, it will be satisfactory to use the same lever arm to determine steel areas, and

---

† The depth is more easily found using Graph A.1 of Appendix A. For $\rho = \rho_{0.005}$, $M_u/\phi bd^2 = 6.38$, from which $d = 69.4$ mm. Table A.5a may also be used.

$$\text{At midspan:} \qquad A_s = \frac{17.8 \times 10^6}{0.9 \times 420 \times (135 - 10/2)} = 362 \text{ mm}^2/\text{m}$$

$$\text{At exterior support:} \qquad A_s = \frac{10.4 \times 10^6}{0.9 \times 420 \times (135 - 10/2)} = 212 \text{ mm}^2/\text{m}$$

The minimum reinforcement is that required for control of shrinkage and temperature cracking. This is

$$A_s = 0.0018 \times 1000 \times 160 = 288 \text{ mm}^2$$

per meter strip. This requires a small increase in the amount of steel used at the exterior support.

The factored shear force at a distance d from the face of the interior support is

$$V_u = 1.15 \times \frac{12.29 \times 4.5}{2} - 12.29 \times 0.135 = 30.1 \text{ kN}$$

By Eq. (4.12*b*), the nominal shear strength of the concrete slab is

$$V_n = V_c = 0.17\lambda\sqrt{f_c'}\,bd = 0.17 \times 1\sqrt{28} \times 1000 \times 135 \times 10^{-3} = 121.4 \text{ kN}$$

Thus, the design strength of the concrete slab $\phi V_c = 0.75 \times 121.4 = 91.1$ kN is well above the required strength in shear of $V_u = 30.3$ kN.

The required tensile steel areas may be provided in a variety of ways, but whatever the selection, due consideration must be given to the actual placing of the steel during construction. The arrangement should be such that the steel can be placed rapidly with the minimum of labor costs even though some excess steel is necessary to achieve this end.

Two possible arrangements are shown in Fig. 13.4. In Fig. 13.4*a*, bent bars are used, while in Fig. 13.4*b* all bars are straight.

FIGURE 13.4
One-way slab design example.

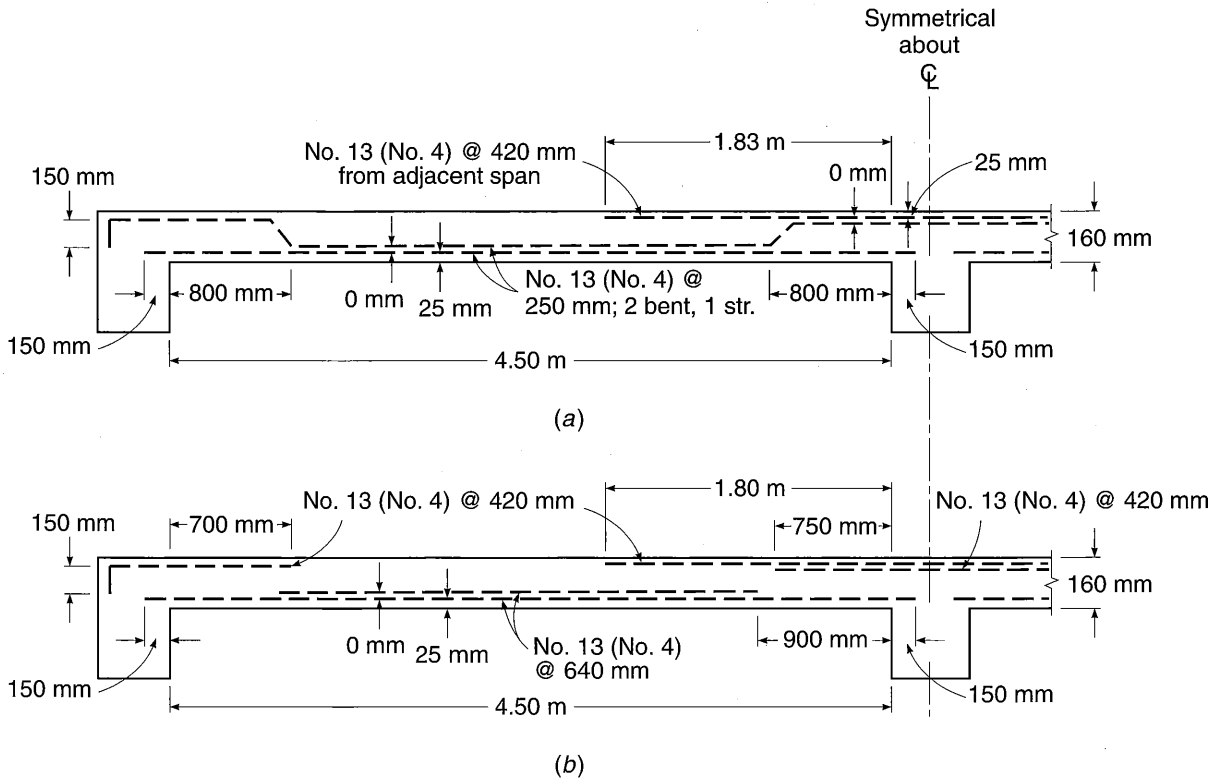
Symmetrical about ℄
No. 13 (No. 4) @ 420 mm from adjacent span
1.83 m
0 mm
25 mm
150 mm
160 mm
800 mm
0 mm
25 mm
No. 13 (No. 4) @ 250 mm; 2 bent, 1 str.
800 mm
150 mm
150 mm
4.50 m
(a)
No. 13 (No. 4) @ 420 mm
1.80 m
No. 13 (No. 4) @ 420 mm
150 mm
700 mm
750 mm
160 mm
0 mm
25 mm
No. 13 (No. 4) @ 640 mm
900 mm
150 mm
150 mm
4.50 m
(b)

In the arrangement of Fig. 13.4*a*, No. 13 (No. 4) bars at 250 mm furnish 516 mm^2/m of steel at midspan, about 40 percent more than required. If two-thirds of these bars are bent upward for negative reinforcement over the interior support, the average spacing of such bent bars at the interior support will be $250 \times 3/2 = 375$ mm. Since an identical pattern of bars is bent upward from the other side of the support, the effective spacing of the No. 13 (No. 4) bars over the interior support is 188 mm. This pattern satisfies the required steel area of 565 mm^2/m width of slab over the support. The bars bent at the interior support will also be bent upward for negative reinforcement at the exterior support, providing reinforcement equivalent to No. 13 (No. 4) bars at 375 mm, or 344 mm^2 of steel.

Note that it is not necessary to achieve uniform spacing of reinforcement in slabs, and that the steel provided can be calculated safely on the basis of average spacing, as in the example. Care should be taken to satisfy requirements for both minimum and maximum spacing of principal reinforcement, however.

The locations of bend and cutoff points shown in Fig. 13.4*a* were obtained using Graph A.3 of Appendix A, as explained in Section 5.10 and Table A.10 (see also Fig. 5.19).

The arrangement shown in Fig. 13.4*b* uses only straight bars. Although it is satisfactory according to the ACI Code (since the shear stress does not exceed two-thirds of that permitted), cutting off the shorter positive and negative bars as shown leads to an undesirable condition at the ends of those bars, where there will be concentrations of stress in the concrete. The design would be improved if the negative bars were cut off 900 mm from the face of the interior support rather than 750 mm as shown, and if the positive steel were cut off at 650 mm rather than at 900 mm. This would result in an overlap of approximately $2d$ of the cut positive and negative bars. Figure 5.20*a* suggests a somewhat simpler arrangement that would also prove satisfactory.

The required area of steel to be placed normal to the main reinforcement for purposes of temperature and shrinkage crack control is 288 mm^2. This will be provided by No. 13 (No. 4) bars at 400 mm spacing, placed directly on top of the main reinforcement in the positive-moment region and below the main steel in the negative-moment zone.

13.4 BEHAVIOR OF TWO-WAY EDGE-SUPPORTED SLABS

The slabs discussed in Sections 13.2 and 13.3 deform under load into an approximately cylindrical surface. The main structural action is one-way in such cases, in the direction normal to supports on two opposite edges of a rectangular panel. In many cases, however, rectangular slabs are of such proportions and are supported in such a way that two-way action results. When loaded, such slabs bend into a dished surface rather than a cylindrical one. This means that at any point the slab is curved in both principal directions, and since bending moments are proportional to curvatures, moments also exist in both directions. To resist these moments, the slab must be reinforced in both directions, by at least two layers of bars perpendicular, respectively, to two pairs of edges. The slab must be designed to take a proportionate share of the load in each direction.

Types of reinforced concrete construction that are characterized by two-way action include slabs supported by walls or beams on all sides (Fig. 13.1*b*), flat plates (Fig. 13.1*d*), flat slabs (Fig. 13.1*e*), and waffle slabs (Fig. 13.1*f*).

The simplest type of two-way slab action is that represented by Fig. 13.1*b*, where the slab, or slab panel, is supported along its four edges by relatively deep, stiff, monolithic concrete beams or by walls or steel girders. If the concrete edge beams are shallow or are omitted altogether, as they are for flat plates and flat slabs, deformation of the floor system along the column lines significantly alters the distribution of

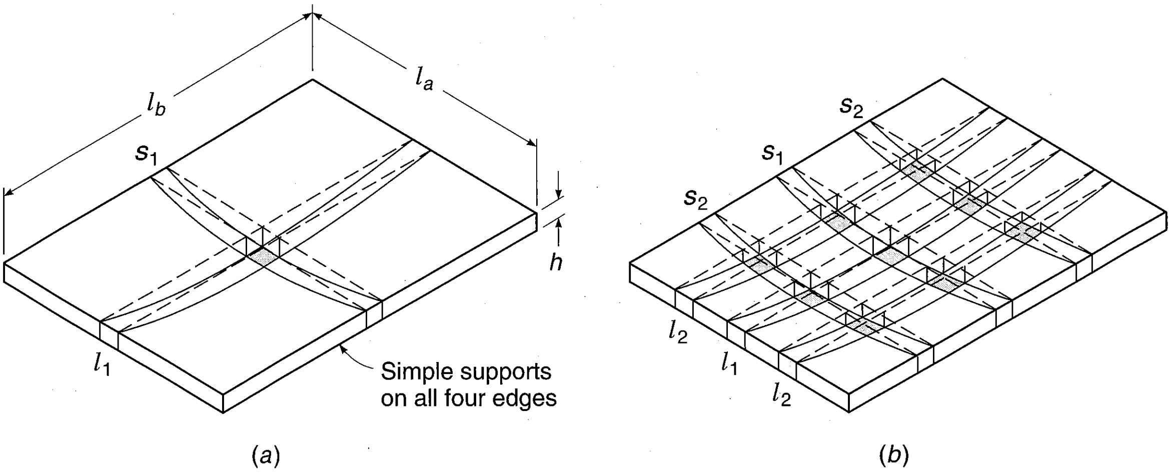

FIGURE 13.5
Two-way slab on simple edge supports: (*a*) bending of center strips of slab; (*b*) grid model of slab.

moments in the slab panel itself (Ref. 13.2). Two-way systems of this type are considered separately, beginning in Section 13.5. The present discussion pertains to the former type, in which edge supports are stiff enough to be considered unyielding.

Such a slab is shown in Fig. 13.5*a*. To visualize its flexural performance, it is convenient to think of it as consisting of two sets of parallel strips, in each of the two directions, intersecting each other. Evidently, part of the load is carried by one set and transmitted to one pair of edge supports, and the remainder by the other.

Figure 13.5*a* shows the two center strips of a rectangular plate with short span l_a and long span l_b. If the uniform load is q per square meter of slab, each of the two strips acts approximately as a simple beam, uniformly loaded by its share of q. Because these imaginary strips actually are part of the same monolithic slab, their deflections at the intersection point must be the same. Equating the center deflections of the short and long strips gives

$$\frac{5q_a l_a^4}{384EI} = \frac{5q_b l_b^4}{384EI} \tag{a}$$

where q_a is the share of the load q carried in the short direction and q_b is the share of the load q carried in the long direction. Consequently,

$$\frac{q_a}{q_b} = \frac{l_b^4}{l_a^4} \tag{b}$$

One sees that the larger share of the load is carried in the short direction, the ratio of the two portions of the total load being inversely proportional to the fourth power of the ratio of the spans.

This result is approximate because the actual behavior of a slab is more complex than that of the two intersecting strips. An understanding of the behavior of the slab itself can be gained from Fig. 13.5*b*, which shows a slab model consisting of two sets of three strips each. It is seen that the two central strips s_1 and l_1 bend in a manner similar to that shown in Fig. 13.5*a*. The outer strips s_2 and l_2, however, are not only bent but also twisted. Consider, for instance, one of the intersections of s_2 with l_2. It is seen that at the intersection the exterior edge of strip l_2 is at a higher elevation than the interior edge, while at the nearby end of strip l_2 both edges are at the same elevation; the strip is twisted. This twisting results in torsional stresses and torsional moments that are seen to be most pronounced near the corners. Consequently, the total load on the slab is carried not only by the bending moments in two directions but also by the twisting moments. For this reason, bending moments in elastic slabs are smaller than would be computed for sets of unconnected strips loaded by q_a and q_b. For instance, for a simply supported square slab, $q_a = q_b = q/2$. If only bending were present, the maximum moment in each strip would be

$$\frac{(q/2)l^2}{8} = 0.0625ql^2 \tag{c}$$

The exact theory of bending of elastic plates shows that actually the maximum moment in such a square slab is only $0.048ql^2$, so that in this case the twisting moments relieve the bending moments by about 25 percent.

The largest moment occurs where the curvature is sharpest. Figure 13.5*b* shows this to be the case at midspan of the short strip s_1. Suppose the load is increased until this location is overstressed, so that the steel at the middle of strip s_1 is yielding. If the strip were an isolated beam, it would now fail. Considering the slab as a whole, however, one sees that no immediate failure will occur. The neighboring strips (those parallel as well as those perpendicular to s_1), being actually monolithic with it, will take over any additional load that strip s_1 can no longer carry until they, in turn, start yielding. This inelastic redistribution will continue until in a rather large area in the central portion of the slab all the steel in both directions is yielding. Only then will the entire slab fail. From this reasoning, which is confirmed by tests, it follows that slabs need not be designed for the absolute maximum moment in each of the two directions (such as $0.048ql^2$ in the example given in the previous paragraph), but only for a smaller average moment in each of the two directions in the central portion of the slab. For instance, one of the several analytical methods in general use permits a square slab to be designed for a moment of $0.036ql^2$. By comparison with the actual elastic maximum moment $0.048ql^2$, it is seen that, owing to inelastic redistribution, a moment reduction of 25 percent is provided.

The largest moment in the slab occurs at midspan of the short strip s_1 of Fig. 13.5*b*. It is evident that the curvature, and hence the moment, in the short strip s_2 is less than at the corresponding location of strip s_1. Consequently, a variation of short-span moment occurs in the long direction of the span. This variation is shown qualitatively in Fig. 13.6. The short-span moment diagram in Fig. 13.6*a* is valid only along the center strip at 1-1. Elsewhere, the maximum-moment value is less, as shown. Other moment ordinates are reduced proportionately. Similarly, the long-span moment diagram in Fig. 13.6 applies only at the longitudinal centerline of the slab; elsewhere, ordinates are reduced according to the variation shown. These variations in maximum moment across the width and length of a rectangular slab are accounted for in an approximate way in most practical design methods by designing for a reduced moment in the outer quarters of the slab span in each direction.

It should be noted that only slabs with side ratios less than about 2 need be treated as two-way slabs. From Eq. (*b*) above, it is seen that for a slab of this proportion, the share of the load carried in the long direction is only on the order of one-sixteenth of that in the short direction. Such a slab acts almost as if it were spanning in the short direction only. Consequently, rectangular slab panels with an aspect ratio of 2 or more may be reinforced for one-way action, with the main steel perpendicular to the long edges.

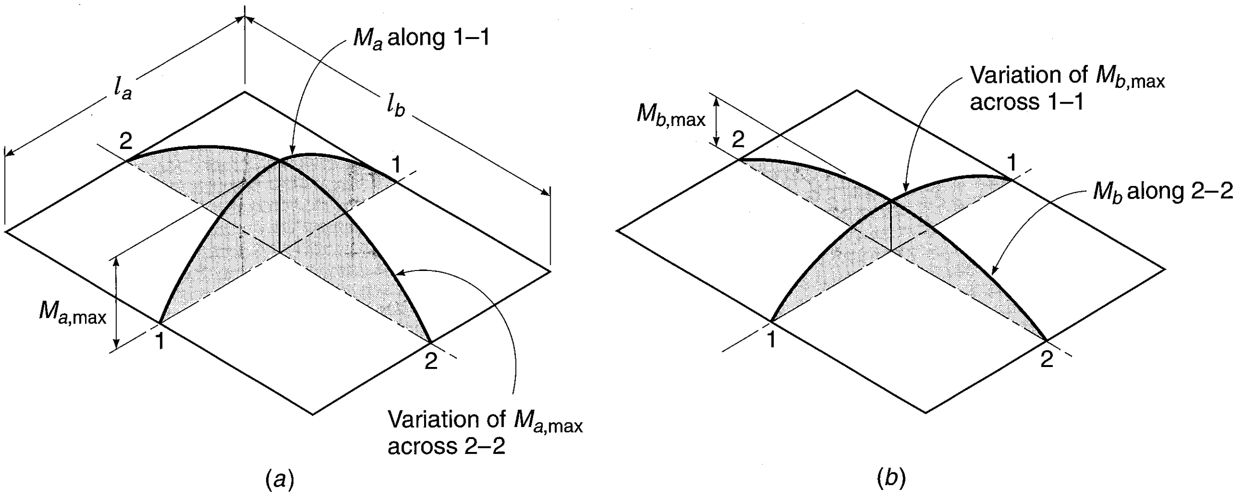

FIGURE 13.6
Moments and moment variations in a uniformly loaded slab with simple supports on four sides.

Consistent with the assumptions of the analysis of two-way edge-supported slabs, the main flexural reinforcement is placed in an orthogonal pattern, with reinforcing bars parallel and perpendicular to the supported edges. As the positive steel is placed in two layers, the effective depth d for the upper layer is smaller than that for the lower layer by one bar diameter. Because the moments in the long direction are the smaller ones, it is economical to place the steel in that direction on top of the bars in the short direction. The stacking problem does not exist for negative reinforcement perpendicular to the supporting edge beams except at the corners, where moments are small.

Either straight bars, cut off where they are no longer required, or bent bars may be used for two-way slabs, but economy of bar fabrication and placement will generally favor all straight bars. The precise locations of inflection points (or lines of inflection) are not easily determined, because they depend upon the side ratio, the ratio of live to dead load, and continuity conditions at the edges. The standard cutoff and bend points for beams, summarized in Fig. 5.21, may be used for edge-supported slabs as well.

According to ACI Code 13.3.1, the minimum reinforcement in each direction for two-way slabs is that required for shrinkage and temperature crack control, as given in Table 13.2. For two-way systems, the spacing of flexural reinforcement at critical sections must not exceed 2 times the slab thickness h.

The twisting moments discussed earlier are usually of consequence only at exterior corners of a two-way slab system, where they tend to crack the slab at the bottom along the panel diagonal, and at the top perpendicular to the panel diagonal. Special reinforcement should be provided at exterior corners in both the bottom and top of the slab, for a distance in each direction from the corner equal to one-fifth the longer span of the corner panel, as shown in Fig. 13.7. The reinforcement at the top of the slab should be parallel to the diagonal from the corner, while that at the bottom should be perpendicular to the diagonal. Alternatively, either layer of steel may be placed in two bands parallel to the sides of the slab. The positive and negative reinforcement, in any case, should be of a size and spacing equivalent to

FIGURE 13.7
Special reinforcement at exterior corners of a beam-supported two-way slab.

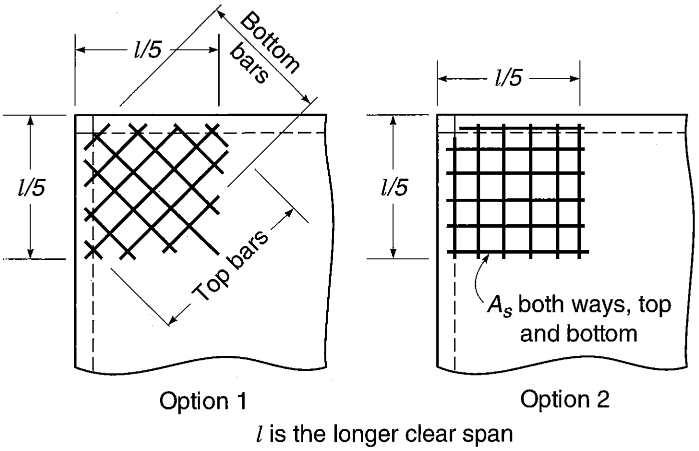

that required for the maximum positive moment (per meter of width) in the panel, according to ACI Code 13.3.6.

13.5 TWO-WAY COLUMN-SUPPORTED SLABS

When two-way slabs are supported by relatively shallow, flexible beams (Fig. 13.1*b*), or if column-line beams are omitted altogether, as for flat plates (Fig. 13.1*d*), flat slabs (Fig. 13.1*e*), or two-way joist systems (Fig. 13.1*f*), then a number of new considerations are introduced. Figure 13.8*a* shows a portion of a floor system in which a rectangular slab panel is supported by relatively shallow beams on four sides. The beams, in turn, are carried by columns at the intersection of their centerlines. If a surface load q is applied, that load is shared between imaginary slab strips l_a in the short direction and l_b in the long direction, as described in Section 13.4. The portion of the load that is carried by the long strips l_b is delivered to the beams B1 spanning in the short direction of the panel. The portion carried by the beams B1 plus that carried directly in the short direction by the slab strips l_a sums up to 100 percent of the load applied to the panel. Similarly, the short-direction slab strips l_a deliver a part of the load to long-direction beams B2. That load, plus the load carried directly in the long direction by the slab, includes 100 percent of the applied load. It is clearly a requirement of statics that, for column-supported construction, *100 percent of the applied load must be carried in each direction*, jointly by the slab and its supporting beams (Ref. 13.3).

A similar situation is obtained in the flat plate floor shown in Fig. 13.8*b*. In this case beams are omitted. However, broad strips of the slab centered on the column lines in each direction serve the same function as the beams of Fig. 13.8*a*; for this case, also, the full load must be carried in each direction. The presence of drop panels or column capitals (Fig. 13.1*e*) in the double-hatched zone near the columns does not modify this requirement of statics.

Figure 13.9*a* shows a flat plate floor supported by columns at *A, B, C*, and *D*. Figure 13.9*b* shows the moment diagram for the direction of span l_1. In this direction, the slab may be considered as a broad, flat beam of width l_2. Accordingly, the load per meter of span is ql_2. In any span of a continuous beam, the sum of the midspan positive

FIGURE 13.8
Column-supported two-way slabs: (*a*) two-way slab with beams; (*b*) two-way slab without beams.

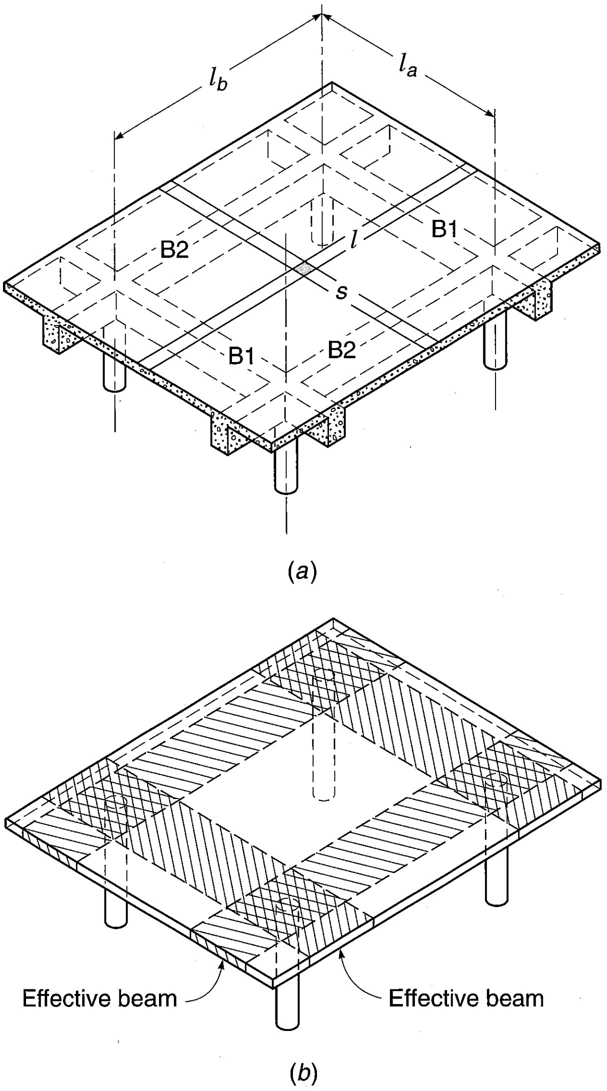

moment and the average of the negative moments at adjacent supports is equal to the midspan positive moment of a corresponding simply supported beam. In terms of the slab, this requirement of statics may be written

$$\tfrac{1}{2}(M_{ab} + M_{cd}) + M_{ef} = \tfrac{1}{8}ql_2l_1^2 \tag{a}$$

A similar requirement exists in the perpendicular direction, leading to the relation

$$\tfrac{1}{2}(M_{ac} + M_{bd}) + M_{gh} = \tfrac{1}{8}ql_1l_2^2 \tag{b}$$

These results disclose nothing about the relative magnitudes of the support moments and span moments. The proportion of the total static moment that exists at each critical section can be found from an elastic analysis that considers the relative span lengths in adjacent panels, the loading pattern, and the relative stiffness of the

FIGURE 13.9
Moment variation in column-supported two-way slabs: (*a*) critical-moment sections; (*b*) moment variation along a span; (*c*) moment variation across the width of critical sections.

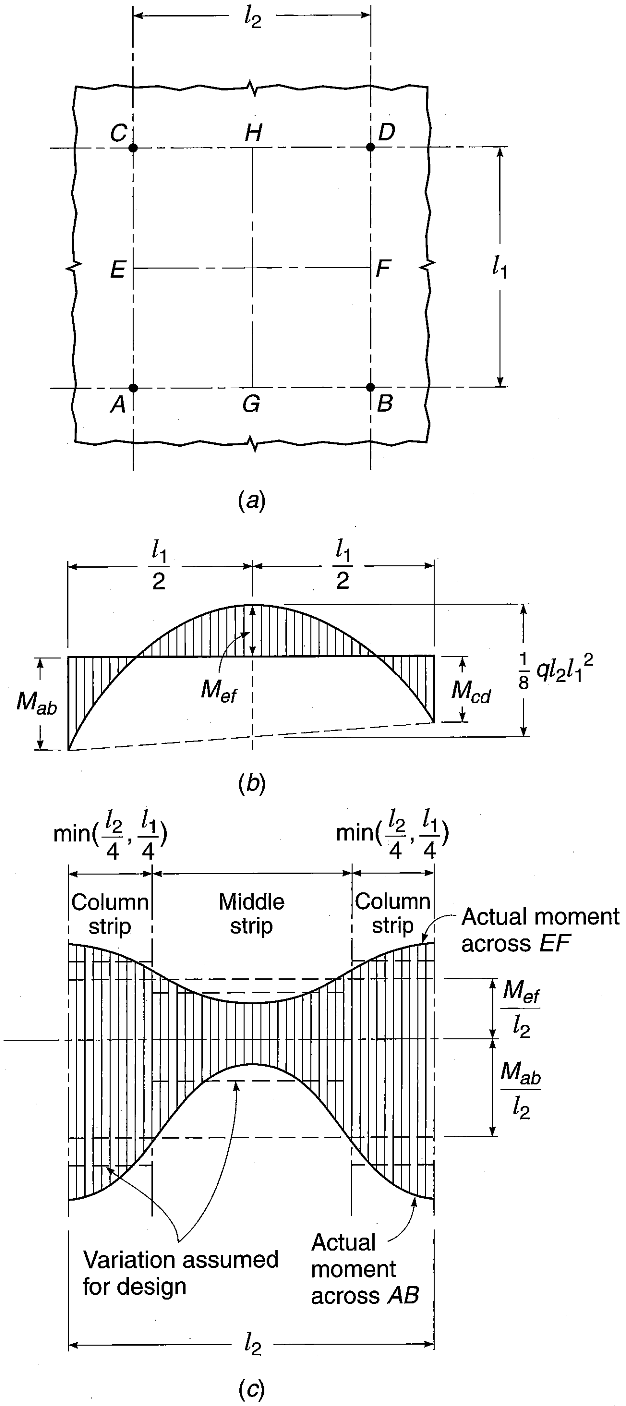

l_2
C
H
D
E
F
l_1
A
G
B
(a)
$\frac{l_1}{2}$
$\frac{l_1}{2}$
M_{ab}
M_{ef}
M_{cd}
$\frac{1}{8}ql_2l_1^2$
(b)
$\min(\frac{l_2}{4}, \frac{l_1}{4})$
$\min(\frac{l_2}{4}, \frac{l_1}{4})$
Column strip
Middle strip
Column strip
Actual moment across EF
$\frac{M_{ef}}{l_2}$
$\frac{M_{ab}}{l_2}$
Variation assumed for design
Actual moment across AB
l_2
(c)

supporting beams, if any, and that of the columns. Alternatively, empirical methods that have been found to be reliable under restricted conditions may be adopted.

The moments across the width of critical sections such as *AB* or *EF* are not constant but vary as shown qualitatively in Fig. 13.9*c*. The exact variation depends on the presence or absence of beams on the column lines, the existence of drop panels

FIGURE 13.10
Portion of slab to be included with beam.

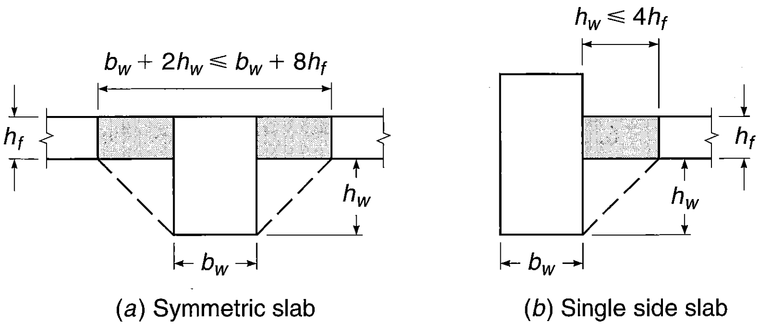

(*a*) Symmetric slab

(*b*) Single side slab

and column capitals, as well as on the intensity of the load. For design purposes, it is convenient to divide each panel as shown in Fig. 13.9*c* into column strips, having a width of one-fourth the panel width, on each side of the column centerlines, and middle strips in the one-half panel width between two column strips. Moments may be considered constant within the bounds of a middle strip or column strip, as shown, unless beams are present on the column lines. In the latter case, while the beam must have the same curvature as the adjacent slab strip, the beam moment will be larger in proportion to its greater stiffness, producing a discontinuity in the moment-variation curve at the lateral face of the beam. Since the total moment must be the same as before, according to statics, the slab moments must be correspondingly less.

Chapter 13 of the ACI Code deals in a unified way with all such two-way systems. Its provisions apply to slabs supported by beams and to flat slabs and flat plates, as well as to two-way joist slabs. While permitting design "by any procedure satisfying the conditions of equilibrium and geometrical compatibility," specific reference is made to two alternative approaches: a semiempirical *direct design method* and an approximate elastic analysis known as the *equivalent frame method.*

In either case, a typical panel is divided, for purposes of design, into *column strips* and *middle strips*. A column strip is defined as a strip of slab having a width on each side of the column centerline equal to one-fourth the smaller of the panel dimensions l_1 and l_2. Such a strip includes column-line beams, if present. A middle strip is a design strip bounded by two column strips. In all cases, l_1 is defined as the span in the direction of the moment analysis and l_2 as the span in the lateral direction measured center to center of the support. In the case of monolithic construction, beams are defined to include that part of the slab on each side of the beam extending a distance equal to the projection of the beam above or below the slab h_w (whichever is greater) but not greater than 4 times the slab thickness (see Fig. 13.10).

13.6 DIRECT DESIGN METHOD FOR COLUMN-SUPPORTED SLABS

Moments in two-way slabs can be found using the semiempirical direct design method, subject to the following restrictions:

1. There must be a minimum of three continuous spans in each direction.
2. The panels must be rectangular, with the ratio of the longer to the shorter spans within a panel not greater than 2.
3. The successive span lengths in each direction must not differ by more than one-third of the longer span.

4. Columns may be offset a maximum of 10 percent of the span in the direction of the offset from either axis between centerlines of successive columns.
5. Loads must be due to gravity only, and the unfactored live load must not exceed 2 times the unfactored dead load.
6. If beams are used on the column lines, the relative stiffness of the beams in the two perpendicular directions, given by the ratio $\alpha_{f1}l_2^2/\alpha_{f2}l_1^2$, must be between 0.2 and 5.0 (see definitions below).

a. Total Static Moment at Factored Loads

For purposes of calculating the total static moment M_o in a panel, the clear span l_n in the direction of moments is used. The *clear span* is defined to extend from face to face of the columns, capitals, brackets, or walls but is not to be less than $0.65l_1$. The total factored moment in a span, for a strip bounded laterally by the centerline of the panel on each side of the centerline of supports, is

$$M_o = \frac{q_u l_2 l_n^2}{8} \tag{13.1}$$

b. Assignment of Moments to Critical Sections

For interior spans, the total static moment is apportioned between the critical positive and negative bending sections according to the following ratios:

$$\text{Negative factored moment: Neg } M_u = 0.65M_o \tag{13.2}$$

$$\text{Positive factored moment: Pos } M_u = 0.35M_o \tag{13.3}$$

as illustrated by Fig. 13.11. The critical section for negative bending is taken at the face of rectangular supports, or at the face of an equivalent square support having the same cross-sectional area as a round support.

In the case of end spans, the apportionment of the total static moment among the three critical moment sections (interior negative, positive, and exterior negative, as illustrated by Fig. 13.11) depends upon the flexural restraint provided for the slab by the exterior column or the exterior wall, as the case may be, and depends also upon

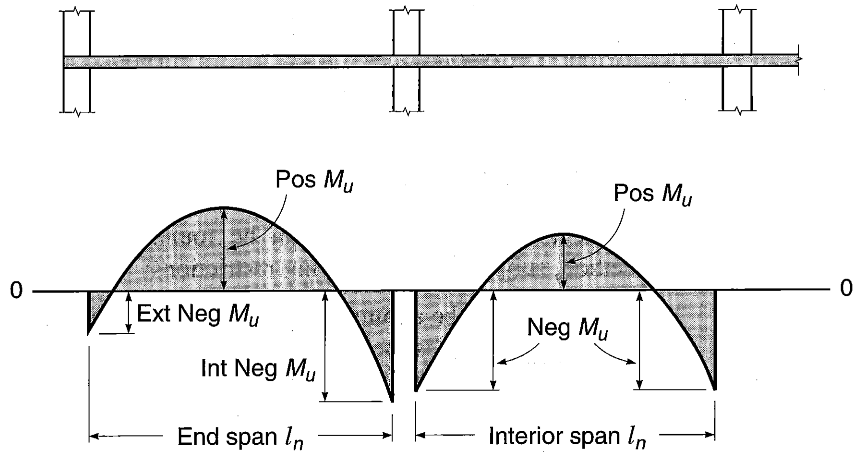

FIGURE 13.11
Distribution of total static moment M_o to critical sections for positive and negative bending.

the presence or absence of beams on the column lines. ACI Code 13.6.3 specifies five alternative sets of moment distribution coefficients for end spans, as shown in Table 13.3 and illustrated in Fig. 13.12.

TABLE 13.3
Distribution factors applied to static moment M_o for positive and negative moments in end span

	(*a*)	(*b*)	(*c*)	(*d*)	(*e*)
	Exterior Edge Unrestrained	Slab with Beams between All Supports	Slab without Beams between Interior Supports		Exterior Edge Fully Restrained
			Without Edge Beam	With Edge Beam	
Interior negative moment	0.75	0.70	0.70	0.70	0.65
Positive moment	0.63	0.57	0.52	0.50	0.35
Exterior negative moment	0	0.16	0.26	0.30	0.65

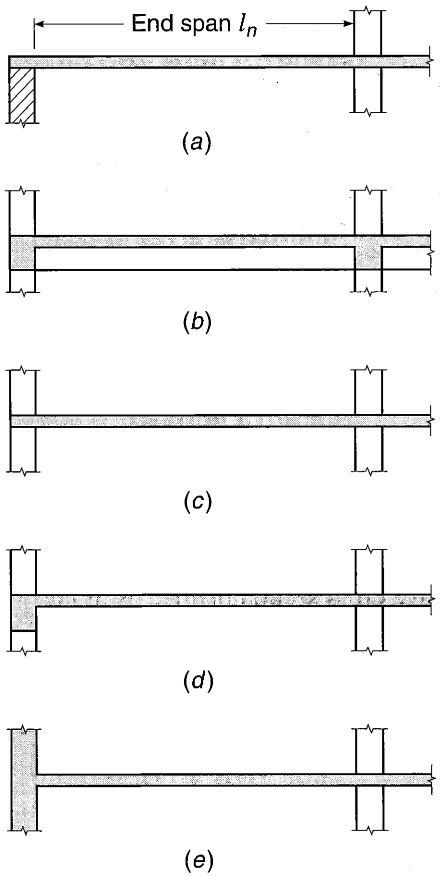

FIGURE 13.12
Conditions of edge restraint considered in distributing total static moment M_o to critical sections in an end span: (*a*) exterior edge unrestrained, e.g., supported by a masonry wall; (*b*) slab with beams between all supports; (*c*) slab without beams, i.e., flat plate; (*d*) slab without beams between interior supports but with edge beam; (*e*) exterior edge fully restrained, e.g., by monolithic concrete wall.

In case *a*, the exterior edge has no moment restraint, such as would be the condition with a masonry wall, which provides vertical support but no rotational restraint. Case *b* represents a two-way slab with beams on all sides of the panels. Case *c* is a flat plate, with no beams at all, while case *d* is a flat plate in which a beam is provided along the exterior edge. Finally, case *e* represents a fully restrained edge, such as that obtained if the slab is monolithic with a very stiff reinforced concrete wall. The appropriate coefficients for each case are given in Table 13.3 and are based on three-dimensional elastic analysis modified to some extent in the light of tests and practical experience (Refs. 13.4 to 13.11).

At interior supports, negative moments may differ for spans framing into the common support. In such a case, the slab should be designed to resist the larger of the two moments, unless a special analysis based on relative stiffnesses is made to distribute the unbalanced moment (see Chapter 12). Edge beams if they are used, or the edge of the slab if they are not, must be designed to resist in torsion their share of the exterior negative moment indicated by Table 13.3 (see Chapter 7).

c. Lateral Distribution of Moments

Having distributed the moment M_o to the positive and negative-moment sections as just described, the designer still must distribute these design moments across the width of the critical sections. For design purposes, as discussed in Section 13.5, it is convenient to consider the moments constant within the bounds of a middle strip or column strip unless there is a beam present on the column line. In the latter case, because of its greater stiffness, the beam will tend to take a larger share of the column-strip moment than the adjacent slab. The distribution of total negative or positive moment between slab middle strips, slab column strips, and beams depends upon the ratio l_2/l_1, the relative stiffness of the beam and the slab, and the degree of torsional restraint provided by the edge beam.

A convenient parameter defining the relative stiffness of the beam and slab spanning in either direction is

$$\alpha_f = \frac{E_{cb} I_b}{E_{cs} I_s} \tag{13.4}$$

in which E_{cb} and E_{cs} are the moduli of elasticity of the beam and slab concrete (usually the same) and I_b and I_s are the moments of inertia of the effective beam and the slab. Subscripted parameters α_{f1} and α_{f2} are used to identify α computed for the directions of l_1 and l_2, respectively.

The flexural stiffnesses of the beam and slab may be based on the gross concrete section, neglecting reinforcement and possible cracking, and variations due to column capitals and drop panels may be neglected. For the beam, if present, I_b is based on the effective cross section defined as in Fig. 13.10. For the slab, I_s is taken equal to $bh^3/12$, where b in this case is the width between panel centerlines on each side of the beam.

The relative restraint provided by the torsional resistance of the effective transverse edge beam is reflected by the parameter β_t, defined as

$$\beta_t = \frac{E_{cb} C}{2E_{cs} I_s} \tag{13.5}$$

where I_s, as before, is calculated for the slab spanning in direction l_1 and having width bounded by panel centerlines in the l_2 direction. The constant C pertains to the torsional rigidity of the effective transverse beam, which is defined according to ACI Code 13.7.5 as the largest of the following:

1. A portion of the slab having a width equal to that of the column, bracket, or capital in the direction in which moments are taken
2. The portion of the slab specified in 1 plus that part of any transverse beam above and below the slab
3. The transverse beam defined as in Fig. 13.10

The constant C is calculated by dividing the section into its component rectangles, each having smaller dimension x and larger dimension y, and summing the contributions of all the parts by means of the equation

$$C = \sum \left(1 - 0.63\,\frac{x}{y}\right)\frac{x^3y}{3} \tag{13.6}$$

The subdivision can be done in such a way as to maximize C.

With these parameters defined, ACI Code 13.6.4 distributes the negative and positive moments between column strips and middle strips, assigning to the column strips the percentages of positive and negative moments shown in Table 13.4. Linear interpolations are to be made between the values shown.

Implementation of these provisions is facilitated by the interpolation charts of Graph A.4 of Appendix A. Interior negative and positive-moment percentages can be read directly from the charts for known values of l_2/l_1 and $\alpha_{f1}l_2/l_1$. For exterior negative moment, the parameter β_t requires an additional interpolation, facilitated by the auxiliary diagram on the right side of the charts. To illustrate its use for

TABLE 13.4
Column-strip moment, percent of total moment at critical section

		l_2/l_1		
		0.5	**1.0**	**2.0**
Interior negative moment				
$\alpha_{f1}l_2/l_1 = 0$		75	75	75
$\alpha_{f1}l_2/l_1 \geq 1.0$		90	75	45
Exterior negative moment				
$\alpha_{f1}l_2/l_1 = 0$	$\beta_t = 0$	100	100	100
	$\beta_t \geq 2.5$	75	75	75
$\alpha_{f1}l_2/l_1 \geq 1.0$	$\beta_t = 0$	100	100	100
	$\beta_t \geq 2.5$	90	75	45
Positive moment				
$\alpha_{f1}l_2/l_1 = 0$		60	60	60
$\alpha_{f1}l_2/l_1 \geq 1.0$		90	75	45

$l_2/l_1 = 1.55$ and $\alpha_{f1}l_2/l_1 = 0.6$, the dotted line indicates moment percentages of 100 for $\beta_t = 0$ and 65 for $\beta_t = 2.5$. Projecting to the right as indicated by the arrow to find the appropriate vertical scale of 2.5 divisions for an intermediate value of β_t, say 1.0, then upward and finally to the left, one reads the corresponding percentage of 86 on the main chart.

The column-line beam spanning in the direction l_1 is to be proportioned to resist 85 percent of the column-strip moment if $\alpha_{f1}l_2/l_1$ is equal to or greater than 1.0. For values between 1 and 0, the proportion to be resisted by the beam may be obtained by linear interpolation. Concentrated or linear loads applied directly to such a beam should be accounted for separately.

The portion of the moment not resisted by the column strip is proportionately assigned to the adjacent half-middle strips. Each middle strip is designed to resist the sum of the moments assigned to its two half-middle strips. A middle strip adjacent and parallel to a wall is designed for twice the moment assigned to the half-middle strip corresponding to the first row of interior supports.

d. Shear in Slab Systems with Beams

Special attention must be given to providing the proper resistance to shear, as well as to moment, when designing by the direct method. According to ACI Code 13.6.8, beams with $\alpha_{f1}l_2/l_1 \geq 1.0$ must be proportioned to resist the shear caused by loads on a tributary area defined as shown in Fig. 13.13. For values of $\alpha_{f1}l_2/l_1$ between 1 and 0, the proportion of load carried by beam shear is found by linear interpolation. The remaining fraction of the load on the shaded area is assumed to be transmitted directly by the slab to the columns at the four corners of the panel, and the shear stress in the slab computed accordingly (see Section 13.10).

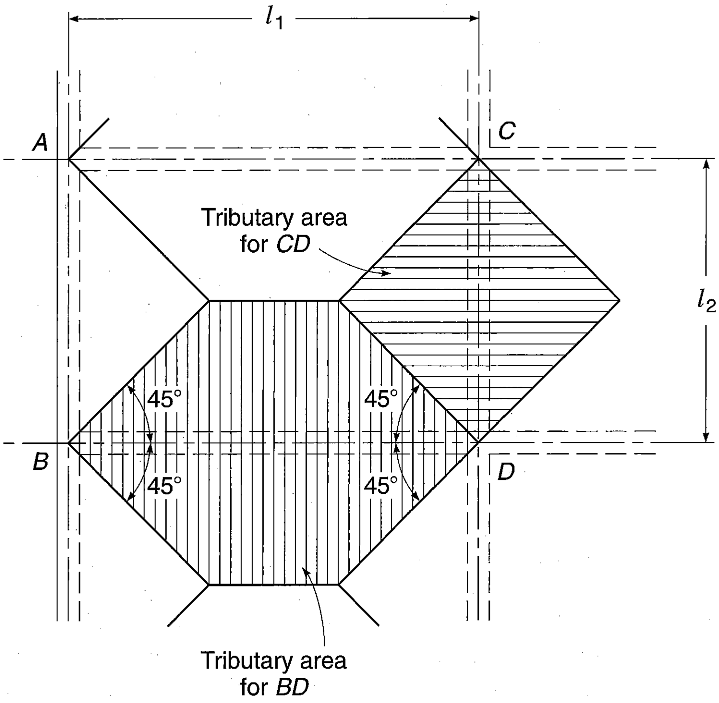

FIGURE 13.13
Tributary areas for shear calculation.

e. Design of Columns

Columns in two-way construction must be designed to resist the moments found from analysis of the slab-beam system. The column supporting an edge beam must provide a resisting moment equal to the moment applied from the edge of the slab (see Table 13.4). At interior locations, slab negative moments are found, assuming that dead and full live loads act. For the column design, a more severe loading results from partial removal of the live load. Accordingly, ACI Code 13.6.9 requires that interior columns resist a moment

$$M_u = 0.07\left[(q_{Du} + 0.5q_{Lu})l_2 l_n^2 - q'_{Du} l'_2 (l'_n)^2\right] \qquad (13.7)$$

In Eq. (13.7), q_{Du} and q_{Lu} are, respectively, the factored dead and live loads per unit area. The primed quantities refer to the shorter of the two adjacent spans (assumed to carry dead load only), and the unprimed quantities refer to the longer span (assumed to carry dead load and half live load). In all cases, the moment is distributed to the upper and lower columns in proportion to their relative flexural stiffness.

13.7 FLEXURAL REINFORCEMENT FOR COLUMN-SUPPORTED SLABS

Consistent with the assumptions made in analysis, flexural reinforcement in two-way slab systems is placed in an orthogonal grid, with bars parallel to the sides of the panels. Bar diameters and spacings may be found as described in Section 13.2. Straight bars are generally used throughout, although in some cases positive-moment steel is bent up where no longer needed, to provide for part or all of the negative requirement. To provide for local concentrated loads, as well as to ensure that tensile cracks are narrow and well distributed, a maximum bar spacing at critical sections of 2 times the total slab thickness is specified by ACI Code 13.3.2 for two-way slabs. At least the minimum steel required for temperature and shrinkage crack control (see Section 13.3) must be provided. For protection of the steel against damage from fire or corrosion, at least 20 mm concrete cover must be maintained.

Because of the stacking that results when bars are placed in perpendicular layers, the inner steel will have an effective depth 1 bar diameter less than the outer steel. For flat plates and flat slabs, the stacking problem relates to middle-strip positive steel and column-strip negative bars. In two-way slabs with beams on the column lines, stacking occurs for the middle-strip positive steel, and in the column strips is important mainly for the column-line beams, because slab moments are usually very small in the region where column strips intersect.

In the discussion of the stacking problem for two-way slabs supported by walls or stiff edge beams, in Section 13.4 it was pointed out that, because curvatures and moments in the short direction are greater than in the long direction of a rectangular panel, short-direction bars are normally placed closer to the top or bottom surface of the slab, with the larger effective depth *d*, and long-direction bars are placed inside these, with the smaller *d*. For two-way beamless flat plates, or slabs with relatively flexible edge beams, things are not so simple.

Consider a rectangular interior panel of a flat plate floor. If the slab column strips provided unyielding supports for the middle strips spanning in the perpendicular direction, the short-direction middle-strip curvatures and moments would be the larger. In fact, the column strips deflect downward under load, and this softening of the effective support greatly reduces curvatures and moments in the supported middle strip.

For the entire panel, including both middle strips and column strips in each direction, the moments in the long direction will be larger than those in the short direction, as is easily confirmed by calculating the static moment M_o in each direction for a rectangular panel. Noting that the apportioning of M_o first to negative and positive-moment sections, and then laterally to column and middle strips, is done by applying exactly the same ratios in each direction to the corresponding section, it is clear that the middle-strip positive moments (for example) are larger in the long direction than the short direction, exactly the opposite of the situation for the slab with stiff edge beams. In the column strips, positive and negative moments are larger in the long than in the short direction. On this basis, the designer is led to place the long-direction negative and positive bars, in both middle and column strips, closer to the top or bottom surface of the slab, respectively, with the larger effective depth.

If column-line beams are added, and if their stiffness is progressively increased for comparative purposes, it will be found that the short-direction slab moments gradually become dominant, although the long-direction beams carry larger moments than the short-direction beams. This will be clear from a careful study of Table 13.4.

The situation is further complicated by the influence of the ratio of short to long side dimensions of a panel, and by the influence of varying conditions of edge restraint (e.g., corner vs. typical exterior vs. interior panel). The best guide in specifying steel placement order in areas where stacking occurs is the relative magnitudes of design moments obtained from analysis for a particular case, with maximum d provided for the bars resisting the largest moment. No firm rules can be given. For square slab panels, many designers calculate the required steel area based on the average effective depth, thus obtaining the same bar size and spacing in each direction. This is slightly conservative for the outer layer and slightly unconservative for the inner steel. Redistribution of loads and moments before failure would provide for the resulting differences in capacities in the two directions.

Reinforcement cutoff points could be calculated from moment envelopes if available; however, when the direct design method is used, moment envelopes and lines of inflection are not found explicitly. In such a case (and often when the equivalent frame method of Section 13.9 is used as well), standard bar cutoff points from Fig. 13.14 are used, as recommended in the ACI Code.

ACI Code 13.3.8.5 requires that all bottom bars within the column strip in each direction be continuous or spliced with Class B splices (see Section 5.13a) or mechanical or welded splices located as shown in Fig. 13.14. At least two of the column strip bars in each direction must pass within the column core and must be anchored at exterior supports. The continuous column strip bottom steel is intended to provide some residual ability to carry load to adjacent supports by catenary action if a single support should be damaged or destroyed. The two continuous bars through the column can be considered to be "integrity steel" and are provided to give the slab some residual capacity following a single punching shear failure.

The need for special reinforcement at the exterior corners of two-way beam-supported slabs was described in Section 13.4, and typical corner reinforcement is shown in Fig. 13.7. According to ACI Code 13.3.6, such reinforcement is required for slabs with beams between supporting columns if the value of α_f given by Eq. (13.3) is greater than 1.0.

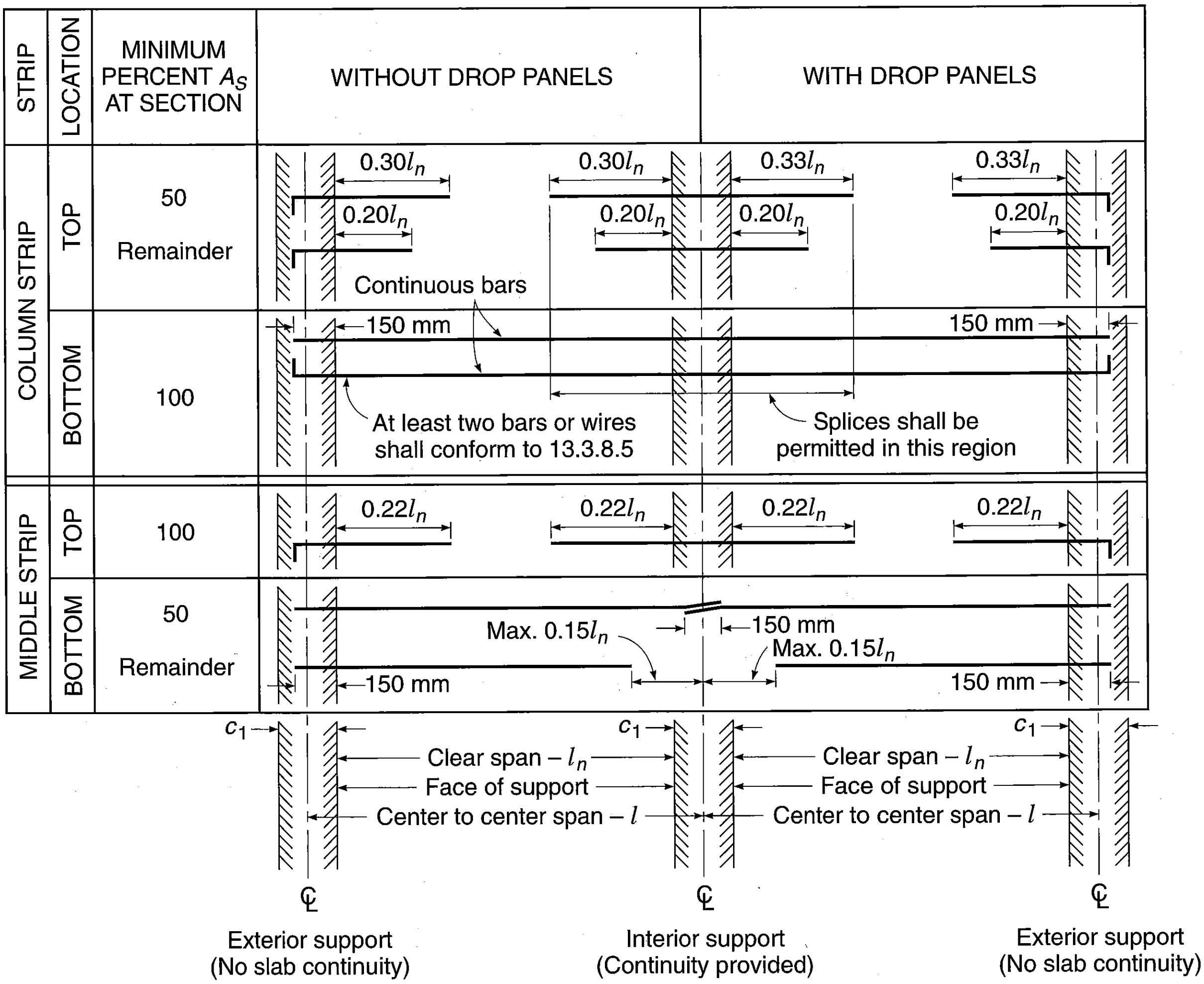
STRIP
LOCATION
MINIMUM PERCENT A_s AT SECTION
WITHOUT DROP PANELS
WITH DROP PANELS
COLUMN STRIP
TOP
50
Remainder
BOTTOM
100
MIDDLE STRIP
TOP
100
BOTTOM
50
Remainder
$0.30l_n$
$0.30l_n$
$0.33l_n$
$0.33l_n$
$0.20l_n$
$0.20l_n$
$0.20l_n$
$0.20l_n$
Continuous bars
150 mm
150 mm
At least two bars or wires shall conform to 13.3.8.5
Splices shall be permitted in this region
$0.22l_n$
$0.22l_n$
$0.22l_n$
$0.22l_n$
Max. $0.15l_n$
150 mm
Max. $0.15l_n$
150 mm
150 mm
c_1
c_1
c_1
Clear span – l_n
Face of support
Center to center span – l
Clear span – l_n
Face of support
Center to center span – l
℄
℄
℄
Exterior support (No slab continuity)
Interior support (Continuity provided)
Exterior support (No slab continuity)

FIGURE 13.14
Minimum length of slab reinforcement in a slab without beams.

13.8 DEPTH LIMITATIONS OF THE ACI CODE

To ensure that slab deflections in service will not be troublesome, the best approach is to compute deflections for the total load or load component of interest and to compare the computed deflections with limiting values. Methods have been developed that are both simple and acceptably accurate for predicting deflections of two-way slabs. A method for calculating the deflection of two-way column-supported slabs will be found in Section 13.13.

Alternatively, deflection control can be achieved indirectly by adhering to more or less arbitrary limitations on minimum slab thickness, limitations developed from review of test data and study of the observed deflections of actual structures. As a result of efforts to improve the accuracy and generality of the limiting equations, they have become increasingly complex.

TABLE 13.5
Minimum thickness of slabs without interior beams

	Without Drop Panels			With Drop Panels		
Yield Stress f_y, MPa	Exterior Panels		Interior Panels	Exterior Panels		Interior Panels
	Without Edge Beams	With Edge Beams[a]		Without Edge Beams	With Edge Beams[a]	
280	$l_n/33$	$l_n/36$	$l_n/36$	$l_n/36$	$l_n/40$	$l_n/40$
420	$l_n/30$	$l_n/33$	$l_n/33$	$l_n/33$	$l_n/36$	$l_n/36$
520	$l_n/28$	$l_n/31$	$l_n/31$	$l_n/31$	$l_n/34$	$l_n/34$

[a] Slabs with beams along exterior edges. The value of α_f for the edge beam shall not be less than 0.8.

ACI Code 9.5.3 establishes minimum thicknesses for two-way construction designed according to the methods of ACI Code Chapter 13, i.e., for slabs designed by either the equivalent frame method or the direct design method. Simplified criteria are included pertaining to slabs without interior beams (flat plates and flat slabs with or without edge beams), while more complicated limit equations are to be applied to slabs with beams spanning between the supports on all sides. In both cases, minimum thicknesses less than the specified value may be used if calculated deflections are within Code-specified limits, as quoted in Table 6.2.

a. Slabs without Interior Beams

The minimum thickness of two-way slabs without interior beams, according to ACI Code 9.5.3.2, must not be less than provided by Table 13.5. Edge beams, often provided even for two-way slabs otherwise without beams to improve moment and shear transfer at the exterior supports, permit a reduction in minimum thickness of about 10 percent in exterior panels. In all cases, the minimum thickness of slabs without interior beams must not be less than the following:

For slabs without drop panels	125 mm
For slabs with drop panels	100 mm

b. Slabs with Beams on All Sides

The parameter used to define the relative stiffness of the beam and slab spanning in either direction is α_f, calculated from Eq. (13.4) of Section 13.6c. Then α_{fm} is defined as the average value of α_f for all beams on the edges of a given panel. According to ACI Code 9.5.3.3, for α_{fm} equal to or less than 0.2, the minimum thicknesses of Table 13.5 shall apply.

For α_{fm} greater than 0.2 but not greater than 2.0, the slab thickness must not be less than

$$h = \frac{l_n(0.8 + f_y/1400)}{36 + 5\beta(\alpha_{fm} - 0.2)} \tag{13.8a}$$

and not less than 125 mm.

For α_{fm} greater than 2.0, the thickness must not be less than

$$h = \frac{l_n(0.8 + f_y/1400)}{36 + 9\beta} \tag{13.8b}$$

and not less than 90 mm,

where l_n = clear span in long direction, mm
α_{fm} = average value of α_f for all beams on edges of a panel [see Eq. (13.4)]
β = ratio of clear span in long direction to clear span in short direction

At discontinuous edges, an edge beam must be provided with a stiffness ratio α_f not less than 0.8; otherwise the minimum thickness provided by Eq. (13.8*a*) or (13.8*b*) must be increased by at least 10 percent in the panel with the discontinuous edge.

In all cases, slab thickness less than the stated minimum may be used if it can be shown by computation that deflections will not exceed the limit values of Table 6.2.

Equations (13.8*a*) and (13.8*b*) can be restated in the general form

$$h = \frac{l_n(0.8 + f_y/1400)}{F} \tag{13.8c}$$

where F is the value of the denominator in each case. Figure 13.15 shows the value of F as a function of α_{fm}, for comparative purposes, for three panel aspect ratios β:

1. Square panel, with $\beta = 1.0$
2. Rectangular panel, with $\beta = 1.5$
3. Rectangular panel, with $\beta = 2.0$, the upper limit of applicability of Eqs. (13.8*a*) and (13.8*b*)

Note that, for α_{fm} less than 0.2, column-line beams have little effect, and minimum thickness is given by Table 13.5. For stiff, relatively deep edge beams, with α_{fm} of 2 or greater, Eq. (13.8*b*) governs. Equation (13.8*a*) provides a transition for slabs with shallow column-line beams having α_{fm} in the range from 0.2 to 2.0.

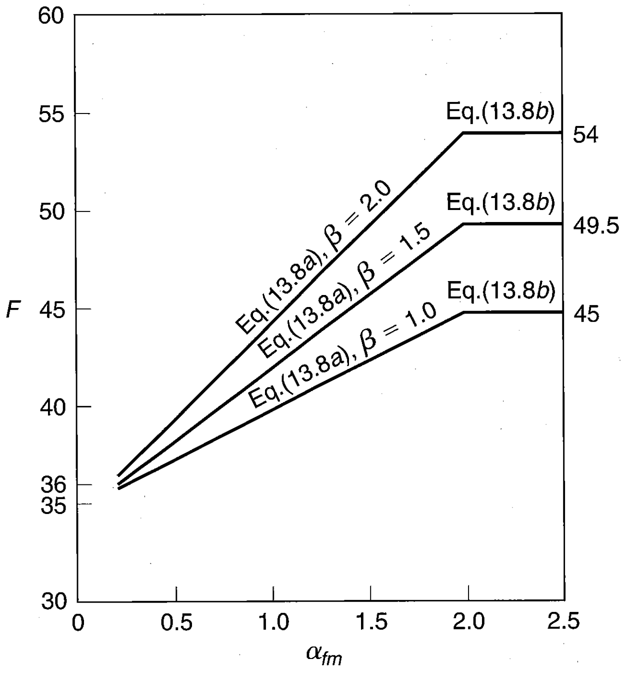

FIGURE 13.15
Parameter F governing minimum thickness of two-way slabs; minimum thickness $h = l_n(0.8 + f_y/1400)/F$.

EXAMPLE 13.2

Design of two-way slab with edge beams.[†] A two-way reinforced concrete building floor system is composed of slab panels measuring 6 × 7.5 m in plan, supported by shallow column-line beams cast monolithically with the slab, as shown in Fig. 13.16. Using concrete with $f'_c = 28$ MPa and steel with $f_y = 420$ MPa, design a typical exterior panel to carry a service live load of 7.0 kN/m^2 in addition to the self-weight of the floor.

Solution. The floor system satisfies all limitations stated in Section 13.6, and the ACI direct design method will be used. For illustrative purposes, only a typical exterior panel, as shown in Fig. 13.16, will be designed. The depth limitations of Section 13.8 will be used as a guide to the desirable slab thickness. To use Eqs. (13.8*a*) and (13.8*b*), a trial value of $h = 180$ mm will be introduced, and beam dimensions 350 × 500 mm will be assumed, as shown in Fig. 13.16. The effective flange projection beyond the face of the beam webs is the lesser of $4h_f$ or h_w, and in the present case is 320 mm. The moment of inertia of the T beams will be estimated as multiples of that of the rectangular portion as follows:

For the edge beams: $I = \frac{1}{12} \times 350 \times 500^3 \times 1.5 = 5.47 \times 10^9 \text{ mm}^4$

For the interior beams: $I = \frac{1}{12} \times 350 \times 500^3 \times 2 = 7.29 \times 10^9 \text{ mm}^4$

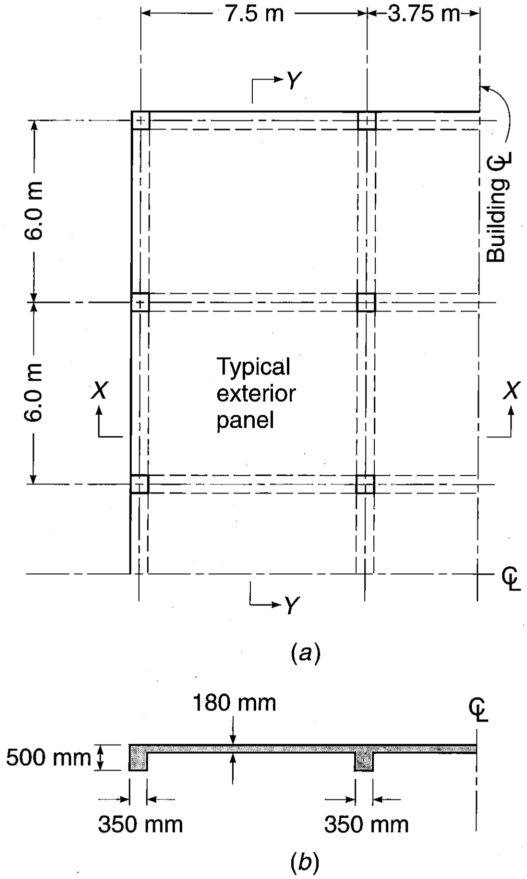

FIGURE 13.16
Two-way slab floor with beams on column lines:
(*a*) partial floor plan;
(*b*) section *X*-*X* (section *Y*-*Y* similar).

[†] The design of a two-way slab without beams, i.e., a flat plate floor system, which may also be done by the direct design method if the restrictions of Section 13.6 are met, will be illustrated by an example in Section 13.7.

For the slab strips:

For the 3.92 m edge width: $I = \frac{1}{12} \times 3920 \times 180^3 = 1.91 \times 10^9 \text{ mm}^4$
For the 6.0 m width: $I = \frac{1}{12} \times 6000 \times 180^3 = 2.92 \times 10^9 \text{ mm}^4$
For the 7.5 m width: $I = \frac{1}{12} \times 7500 \times 180^3 = 3.65 \times 10^9 \text{ mm}^4$

Thus, for the edge beam $\alpha_f = 5.47/1.91 = 2.8$, for the two 7.5 m long beams $\alpha_f = 7.29/2.92 = 2.5$, and for the 6.0 m long beam $\alpha_f = 7.29/3.65 = 2.0$, producing an average value $\alpha_{fm} = 2.4$. The ratio of long to short clear spans is $\beta = 7.15/5.65 = 1.27$. Then the minimum thickness is not to be less than that given by Eq. (13.8*b*):

$$h = \frac{6000(0.8 + 420/1400)}{36 + 9 \times 1.27} = 139 \text{ mm}$$

The 90 mm limitation of Section 13.8 clearly does not control in this case, and the 180 mm depth tentatively adopted will provide the basis of further calculation.

For a 180 mm slab, the dead load is $24 \times 0.18 = 4.3$ kN/m^2. Applying the usual load factors to obtain design load gives

$$q = 1.2 \times 4.3 + 1.6 \times 7.0 = 16.4 \text{ kN/m}^2$$

For the *short-span direction*, for the slab-beam strip centered on the interior column line, the total static design moment is

$$M_o = \tfrac{1}{8} \times 16.4 \times 7.5 \times 5.65^2 = 491 \text{ kN-m}$$

This is distributed as follows:

$$\text{Negative design moment} = 491 \times 0.65 = 319 \text{ kN-m}$$

$$\text{Positive design moment} = 491 \times 0.35 = 172 \text{ kN-m}$$

The column strip has a width of $2 \times 6.0/4 = 3.0$ m. With $l_2/l_1 = 7.5/6.0 = 1.25$ and $\alpha_{f1}l_2/l_1 = 2.0 \times 7.5/6.0 = 2.5$, Graph A.4 of Appendix A indicates that 68 percent of the negative moment, or 217 kN-m, is taken by the column strip, of which 85 percent, or 184 kN-m, is taken by the beam and 33 kN-m by the slab. The remaining 102 kN-m is allotted to the slab middle strip. Graph A.4 also indicates that 68 percent of the positive moment, or 117 kN-m, is taken by the column strip, of which 85 percent, or 99 kN-m, is assigned to the beam and 18 kN-m to the slab. The remaining 55 kN-m is taken by the slab middle strip.

A similar analysis is performed for the slab-beam strip at the edge of the building, based on a total static design moment of

$$M_o = \tfrac{1}{8} \times 16.4 \times 3.92 \times 5.65^2 = 257 \text{ kN-m}$$

of which 65 percent is assigned to the negative and 35 percent to the positive bending sections as before. In this case, $\alpha_{f1}l_2/l_1 = 2.8 \times 7.5/6.0 = 3.5$. The distribution factor for column-strip moment, from Graph A.4, is 68 percent for positive and negative moments as before, and again 85 percent of the column-strip moments is assigned to the beams.

In summary, the short-direction moments, in kN-m, are as follows:

	Beam Moment	Column-Strip Slab Moment	Middle-Strip Slab Moment
Interior slab-beam strip—6.0 m span			
Negative	184	33	102
Positive	99	18	55
Exterior slab-beam strip—6.0 m span			
Negative	97	17	53
Positive	52	9	29

The total static design moment in the *long direction* of the exterior panel is

$$M_o = \tfrac{1}{8} \times 16.4 \times 6.0 \times 7.15^2 = 629 \text{ kN-m}$$

This will be apportioned to the negative and positive moment sections according to Table 13.3, and distributed laterally across the width of critical moment sections with the aid of Graph A.4. The moment ratios to be applied to obtain exterior negative, positive, and interior negative moments are, respectively, 0.16, 0.57, and 0.70. The torsional constant for the edge beam is found from Eq. (13.6) for a 350 × 500 mm rectangular shape with a 180 × 320 mm projecting flange:

$$C = \left(1 - 0.63\frac{350}{500}\right)\frac{350^3 \times 500}{3} + \left(1 - 0.63\frac{180}{320}\right)\frac{180^3 \times 320}{3} = 4.40 \times 10^9\ \text{mm}^4$$

With $l_2/l_1 = 0.80$, $\alpha_{f1}l_2/l_1 = 2.4 \times 6.0/7.5 = 1.9$, and from Eq. (13.5), $\beta_t = 4.40/(2 \times 2.92) = 0.75$, Graph A.4 indicates that the column strip will take 91 percent of the exterior negative moment, 81 percent of the positive moment, and 81 percent of the interior negative moment. As before, the column-line beam will account for 85 percent of the column-strip moment. The results of applying these moment ratios are as follows:

	Beam Moment	**Column-Strip Slab Moment**	**Middle-Strip Slab Moment**
Exterior negative—7.5 m span	78	14	9
Positive—7.5 m span	247	44	68
Interior negative—7.5 m span	303	53	84

It is convenient to tabulate the design of the slab reinforcement, as shown in Table 13.6. In the 7.5 m direction, the two half-column strips may be combined for purposes of calculation into one strip of 2.65 m width. In the 6.0 m direction, the exterior half-column strip and the interior half-column strip will normally differ and are treated separately. Factored moments from the previous distributions are summarized in column 3 of the table.

The short-direction positive steel will be placed first, followed by the long-direction positive bars. If 20 mm clear distance below the steel is allowed and use of No. 13 (No. 4) bars is anticipated, the effective depth in the short direction will be 150 mm, while that in the long direction will be 140 mm. A similar situation occurs for the top steel.

After calculating the design moment per meter strip of slab (column 6), find the minimum effective slab depth required for flexure. For the material strengths to be used, the maximum practical reinforcement ratio is $\rho_{0.005} = 0.0181$. For this ratio,

$$d^2 = \frac{M_u}{\phi\rho f_y b(1 - 0.59\rho f_y/f_c')}$$

$$= \frac{M_u}{0.90 \times 0.0181 \times 420(1 - 0.59 \times 0.0181 \times 420/28)} = \frac{M_u}{5.75}$$

Hence $d = \sqrt{M_u/5.75}$. Thus, the following minimum effective depths are needed:

In 7.5 m direction: $d = \sqrt{\dfrac{23000}{5.75}} = 63.3$ mm

In 6.0 m direction: $d = \sqrt{\dfrac{22700}{5.75}} = 62.8$ mm

both well below the depth dictated by deflection requirements. An underreinforced slab results. The required reinforcement ratios (column 7) are conveniently found from Table A.5 with $R = M_u/\phi bd^2$ or from Table A.9. Note that a minimum steel area equal to 0.0018 times the gross concrete area must be provided for control of temperature and shrinkage cracking. For a 1 m slab strip, the corresponding area is $0.0018 \times 180 \times 1000 = 324\ \text{mm}^2$. Expressed in terms of minimum reinforcement ratio for actual effective depths, this gives

TABLE 13.6
Design of slab reinforcement

(1)	(2) Location	(3) M_u, kN-m	(4) b, m	(5) d, mm	(6) M_u/b, kN-m/m	(7) ρ	(8) A_s, mm^2	(9) Number of No. 13 (No. 4) Bars
7.5 m span Two half-column strips	Exterior negative	14	2.65	140	5.3	0.0023[a]	853	7
	Positive	44	2.65	140	16.6	0.0023	853	7
	Interior negative	53	2.65	140	20.0	0.0028	1039	9
Middle strip	Exterior negative	9	3.0	140	3.0	0.0023[a]	966	9[b]
	Positive	68	3.0	140	22.6	0.0031	1302	11
	Interior negative	84	3.0	140	28.0	0.0039	1638	13
6.0 m span Exterior half-column strip	Negative	17	1.325	150	12.8	0.0021[a]	417	4
	Positive	9	1.325	150	6.8	0.0021[a]	417	4
Middle strip	Negative	102	4.5	150	22.7	0.0032	2160	17
	Positive	55	4.5	150	12.2	0.0021[a]	1418	13[b]
Interior half-column strip	Negative	17	1.325	150	12.8	0.0021[a]	417	4
	Positive	9	1.325	150	6.8	0.0021[a]	417	4

[a] Reinforcement ratio controlled by shrinkage and temperature requirements.
[b] Number of bars controlled by maximum spacing requirements.

In 7.5 m direction: $$\rho_{\min} = \frac{324}{140 \times 1000} = 0.0023$$

In 6.0 m direction: $$\rho_{\min} = \frac{324}{150 \times 1000} = 0.0022$$

This requirement controls at the locations indicated in Table 13.6.

The total steel area in each band is easily found from the reinforcement ratio and is given in column 8. Finally, with the aid of Table A.2, the required number of bars is obtained. Note that in two locations, the number of bars used is dictated by the maximum spacing requirement of 2 × 180 = 360 mm.

The shear capacity of the slab is checked on the basis of the tributary areas shown in Fig. 13.13. At a distance d from the face of the long beam,

$$V_u = 16.4\left(3.0 - \frac{0.35}{2} - 0.15\right) = 43.9 \text{ kN/m}$$

The design shear strength of the slab is

$$\begin{aligned}\phi V_c &= 0.75 \times 0.17\sqrt{28} \times 1000 \times 150 \\ &= 101 \text{ kN/m}\end{aligned}$$

well above the shear applied at factored loads.

Each beam must be designed for its share of the total static moment, as found in the above calculations, as well as the moment due to its own weight; this moment may be distributed to positive and negative bending sections, using the same ratios used for the static moments due to slab loads. Beam shear design should be based on the loads from the tributary areas shown in Fig. 13.13. Since no new concepts would be introduced, the design of the beams will not be presented here.

Since 0.85 × 91 = 77 percent of the exterior negative moment in the long direction is carried directly to the column by the column-line beam in this example, torsional stresses in the spandrel beam are very low and may be disregarded. In other circumstances, the spandrel beams would be designed for torsion following the methods of Chapter 7.

13.9 EQUIVALENT FRAME METHOD

a. Basis of Analysis

The direct design method for two-way slabs described in Section 13.6 is useful if each of the six restrictions on geometry and load is satisfied by the proposed structure. Otherwise, a more general method is needed. One such method, proposed by Peabody in 1948 (Ref. 13.12), was incorporated in subsequent editions of the ACI Code as *design by elastic analysis*. The method was greatly expanded and refined based on research in the 1960s (Refs. 13.13 and 13.14), and it appears in Chapter 13 of the current ACI Code as the *equivalent frame method.*

It will be evident that the equivalent frame method was derived with the assumption that the analysis would be done using the moment distribution method (see Chapter 12). If analysis is done by computer using a standard frame analysis program, special modeling devices are necessary. This point will be discussed further in Section 13.9e.

By the equivalent frame method, the structure is divided, for analysis, into continuous frames centered on the column lines and extending both longitudinally and transversely, as shown by the shaded strips in Fig. 13.17. Each frame is composed of a row of columns and a broad continuous beam. The beam, or slab beam, includes the portion of the slab bounded by panel centerlines on either side of the columns, together with column-line beams or drop panels, if used. For vertical loading, each floor with its columns may be analyzed separately, with the columns assumed to be fixed at the floors above and below. In calculating bending moment at a support, it is convenient and sufficiently accurate to assume that the continuous frame is completely fixed at the support two panels removed from the given support, provided the frame continues past that point.

b. Moment of Inertia of Slab Beam

Moments of inertia used for analysis may be based on the concrete cross section, neglecting reinforcement, but variations in cross section along the member axis should be accounted for.

FIGURE 13.17
Building idealization for equivalent frame analysis.

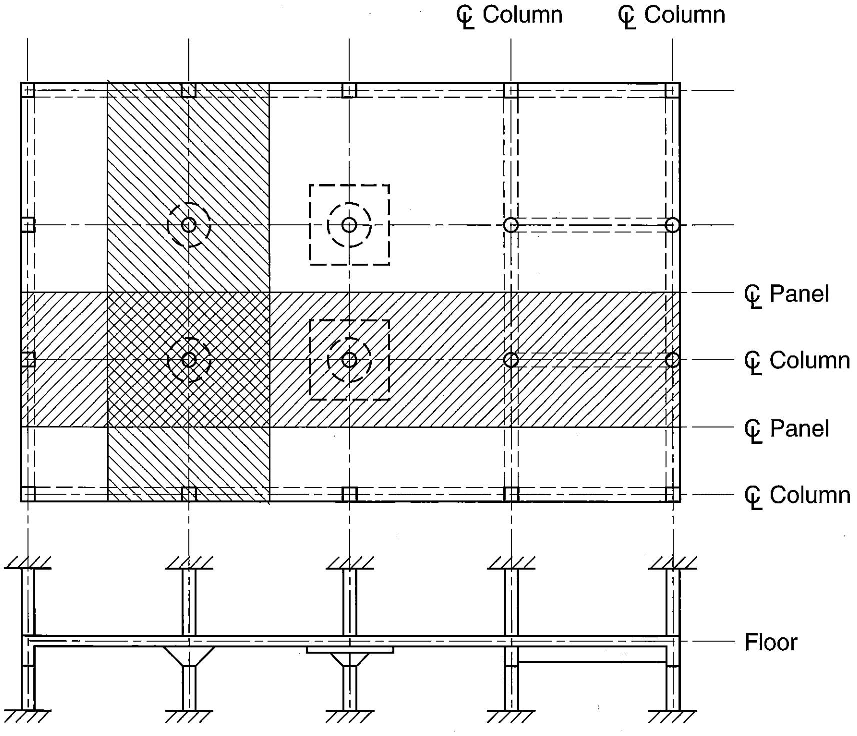

For the beam strips, the first change from the midspan moment of inertia normally occurs at the edge of drop panels, if they are used. The next occurs at the edge of the column or column capital. While the stiffness of the slab strip could be considered infinite within the bounds of the column or capital, at locations close to the panel centerlines (at each edge of the slab strip), the stiffness is much less. According to ACI Code 13.7.3, from the center of the column to the face of the column or capital, the moment of inertia of the slab is taken equal to the value at the face of the column or capital, divided by the quantity $(1 - c_2/l_2)^2$, where c_2 and l_2 are the size of the column or capital and the panel width, respectively, both measured transverse to the direction in which moments are being determined.

Accounting for these changes in moments of inertia results in a member, for analysis, in which the moment of inertia varies in a stepwise manner. The stiffness factors, carryover factors, and uniform-load fixed-end moment factors needed for moment distribution analysis (see Chapter 12) are given in Table A.13*a* of Appendix A for a slab without drop panels and in Table A.13*b* for a slab with drop panels with a depth equal to 1.25 times the slab depth and a total length equal to one-third the span length.

c. The Equivalent Column

In the equivalent frame method of analysis, the columns are considered to be attached to the continuous slab beam by torsional members that are transverse to the direction of the span for which moments are being found; the torsional member extends to the panel centerlines bounding each side of the slab beam under study. Torsional deformation of these transverse supporting members reduces the effective flexural stiffness provided by

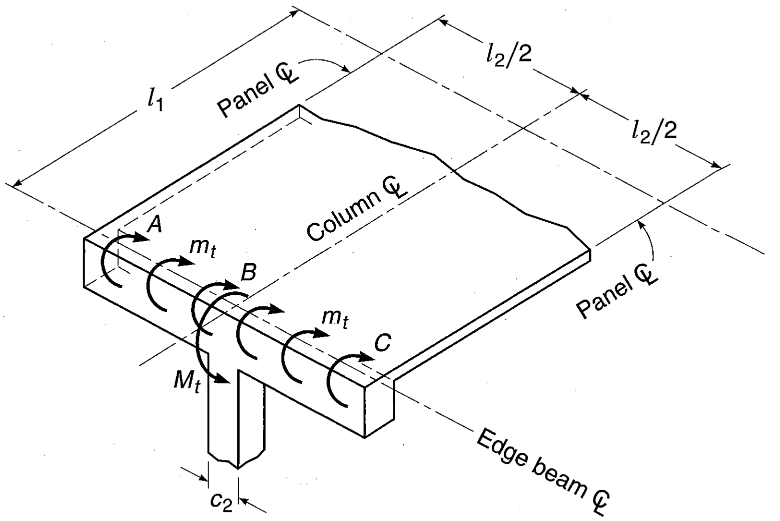

FIGURE 13.18
Torsion at a transverse supporting member illustrating the basis of the equivalent column.

the actual column at the support. This effect is accounted for in the analysis by use of what is termed an *equivalent column* having stiffness less than that of the actual column.

The action of a column and the transverse torsional member is easily explained with reference to Fig. 13.18, which shows, for illustration, the column and transverse beam at the exterior support of a continuous slab-beam strip. From Fig. 13.18, it is clear that the rotational restraint provided at the end of the slab spanning in the direction l_1 is influenced not only by the flexural stiffness of the column but also by the torsional stiffness of the edge beam *AC*. With distributed torque m_t applied by the slab and resisting torque M_t provided by the column, the edge-beam sections at *A* and *C* will rotate to a greater degree than the section at *B*, owing to torsional deformation of the edge beam. To allow for this effect, the actual column and beam are replaced by an equivalent column, so defined that the total flexibility (inverse of stiffness) of the equivalent column is the sum of the flexibilities of the actual column and beam. Thus,

$$\frac{1}{K_{ec}} = \frac{1}{\Sigma K_c} + \frac{1}{K_t} \tag{13.9}$$

where K_{ec} = flexural stiffness of equivalent column
K_c = flexural stiffness of actual column
K_t = torsional stiffness of edge beam

all expressed in terms of moment per unit rotation. In computing K_c, the moment of inertia of the actual column is assumed to be infinite from the top of the slab to the bottom of the slab beam, and I_g is based on the gross concrete section elsewhere along the length. Stiffness factors for such a case are given in Table A.13*c*.

The effective cross section of the transverse torsional member, which may or may not include a beam web projecting below the slab, as shown in Fig. 13.18, is the same as defined earlier in Section 13.6c. The torsional constant *C* is calculated by Eq. (13.6) based on the effective cross section so determined. The torsional stiffness K_t can then be calculated by the expression

$$K_t = \sum \frac{9E_{cs}C}{l_2(1 - c_2/l_2)^3} \tag{13.10}$$

where E_{cs} = modulus of elasticity of slab concrete
c_2 = size of rectangular column, capital, or bracket in direction l_2
C = cross-sectional constant [see Eq. (13.6)]

The summation applies to the typical case in which there are slab beams (with or without edge beams) on both sides of the column. The length l_2 is measured center to center of the supports and thus may have different values in each of the summation terms in Eq. (13.10), if the transverse spans are unequal.

If a panel contains a beam parallel to the direction in which moments are being determined, the value of K_t obtained from Eq. (13.10) leads to values of K_{ec} that are too low. Accordingly, in such cases, the value of K_t found by Eq. (13.10) should be multiplied by the ratio of the moment of inertia of the slab with such a beam to the moment of inertia of the slab without it.

The concept of the equivalent column, illustrated with respect to an exterior column, is employed at *all* supporting columns for each continuous slab beam, according to the equivalent frame method.

d. Moment Analysis

With the effective stiffness of the slab-beam strip and the supports found as described, the analysis of the equivalent frame can proceed by moment distribution (see Chapter 12).

In keeping with the requirements of statics (see Section 13.5), equivalent beam strips in each direction must each carry 100 percent of the load. If the unfactored live load does not exceed three-quarters of the unfactored dead load, maximum moment may be assumed to occur at all critical sections when the full factored live load (plus factored dead load) is on the entire slab, according to ACI Code 13.7.6. Otherwise pattern loadings must be used to maximize positive and negative moments. Maximum positive moment is calculated with three-quarters factored live load on the panel and on alternate panels, while maximum negative moment at a support is calculated with three-quarters factored live load on the adjacent panels only. Use of three-quarters live load rather than the full value recognizes that maximum positive and negative moments cannot occur simultaneously (since they are found from different loadings) and that redistribution of moments to less highly stressed sections will take place before failure of the structure occurs. Factored moments must not be taken less than those corresponding to full factored live load on all panels, however.

Negative moments obtained from that analysis apply at the centerlines of supports. Since the support is not a knife edge but a rather broad band of slab spanning in the transverse direction, some reduction in the negative design moment is proper (see also Section 12.5a). At interior supports, the critical section for negative bending, in both column and middle strips, may be taken at the face of the supporting column or capital, but in no case at a distance greater than $0.175l_1$ from the center of the column, according to ACI Code 13.7.7. To avoid excessive reduction of negative moment at the exterior supports (where the distance to the point of inflection is small) for the case where columns are provided with capitals, the critical section for negative bending in the direction perpendicular to an edge should be taken at a distance from the face of support not greater than one-half the projection of the capital beyond the face of the support.

With positive and negative design moments obtained as just described, it still remains to distribute these moments across the widths of the critical sections. For design purposes, the total strip width is divided into column strip and adjacent half-middle strips, defined previously in Section 13.5, and moments are assumed constant within the bounds of each. The distribution of moments to column and middle strips is done using the same percentages given in connection with the direct design method. These are summarized in Table 13.4 and by the interpolation charts of Graph A.4 of Appendix A.

The distribution of moments and shears to column-line beams, if present, is in accordance with the procedures of the direct design method also. Restriction 6 of Section 13.6, pertaining to the relative stiffness of column-line beams in the two directions, applies here also if these distribution ratios are used.

EXAMPLE 13.3

Design of flat plate floor by equivalent frame method. An office building is planned using a flat plate floor system with the column layout as shown in Fig. 13.19. No beams, drop panels, or column capitals are permitted. Specified live load is 4.9 kN/m^2, and dead load will include the weight of the slab plus an allowance of 1.0 kN/m^2 for finish floor plus suspended loads. The columns will be 450 mm square, and the floor-to-floor height of the structure will be 3.6 m. Design the interior panel C, using material strengths f_y = 420 MPa and f'_c = 28 MPa. Straight-bar reinforcement will be used.

Solution. Minimum thickness h for a flat plate, according to the ACI Code, may be found from Table 13.5.† For the present example, the minimum h for the exterior panel is

$$h = \frac{6250}{30} = 208 \text{ mm}$$

FIGURE 13.19
Two-way flat plate floor.

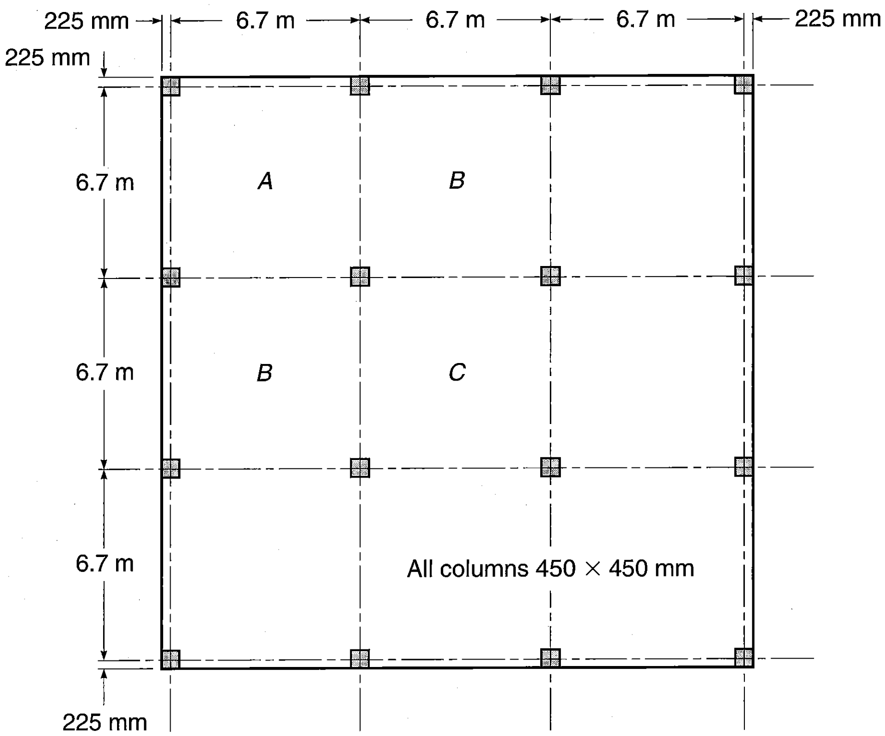

---

† In many flat plate floors, the minimum slab thickness is controlled by requirements for shear transfer at the supporting columns, and h is determined either to avoid supplementary shear reinforcement or to limit the excess shear to a reasonable margin above that which can be carried by the concrete. Design for shear in flat plates and flat slabs will be treated in Section 13.10.

This will be rounded upward for practical reasons, with calculations based on a trial thickness of 210 mm for all panels. Thus the dead load of the slab is $24 \times 0.21 = 5.0$ kN/m^2, to which the superimposed dead load of 1.0 kN/m^2 must be added. The factored design loads are

$$1.2q_d = 1.2(5.0 + 1.0) = 7.2 \text{ kN/m}^2$$

$$1.6q_l = 1.6 \times 4.9 = 7.8 \text{ kN/m}^2$$

The structure is identical in each direction, permitting the design for one direction to be used for both (an average effective depth to the tensile steel will be used in the calculations). While the restrictions of Section 13.6 are met and the direct design method of analysis is permissible, the equivalent frame method will be adopted to demonstrate its features. Moments will be found by the method of moment distribution.

For flat plate structures, it is usually acceptable to calculate stiffnesses as if all members were prismatic, neglecting the increase in stiffness within the joint region, as it generally has negligible effect on design moments and shears. Then, for the slab spans,

$$K_s = \frac{4E_cI_c}{l}$$

$$= \frac{4E_c(6700 \times 210^3)}{12 \times 6700} = 3.08 \times 10^6 E_c$$

and the column stiffnesses are

$$K_c = \frac{4E_c(450 \times 450^3)}{12 \times 3600} = 3.80 \times 10^6 E_c$$

Calculation of the equivalent column stiffness requires consideration of the torsional deformation of the transverse strip of slab that functions as the supporting beam. Applying the criteria of the ACI Code establishes that the effective torsional member has width 450 mm and depth 210 mm. For this section, the torsional constant C from Eq. (13.6) is

$$C = \left(1 - 0.63\frac{210}{450}\right)210^3 \times \frac{450}{3} = 981 \times 10^6 \text{ mm}^4$$

and the torsional stiffness, from Eq. (13.10), is

$$K_t = \frac{9E_c \times 981 \times 10^6}{6700(1 - 450/6700)} = 1.62 \times 10^6 E_c$$

From Eq. (13.9), accounting for two columns and two torsional members at each joint,

$$\frac{1}{K_{ec}} = \frac{1}{2 \times 3.8E_c} + \frac{1}{2 \times 1.62E_c}$$

from which $K_{ec} = 2.27 \times 10^6 E_c$. Distribution factors at each joint are then calculated in the usual way.

For the present example, the ratio of service live load to dead load is $4.9/6.0 = 0.82$, and because this exceeds 0.75, according to ACI Code 13.7.6 maximum positive and negative moments must be found based on pattern loadings, with full factored dead load in place and three-quarters factored live load positioned to cause the maximum effect. In addition, the design moments must not be less than those produced by full factored live and dead loads on all panels. Thus three load cases must be considered: (*a*) full factored dead and live load, 15.0 kN/m^2, on all panels; (*b*) factored dead load of 7.2 kN/m^2 on all spans plus three-quarters factored live load, 5.9 kN/m^2, on panel *C*; and (*c*) full factored dead load on all spans and three-quarters live load on first and second spans. Fixed-end moments and final moments obtained from moment distribution are summarized in Table 13.7. The results indicate that load case *a* controls the slab design in the support region, while load case *b* controls at the midspan of panel *C*. Moment diagrams for the two controlling cases are shown in Fig. 13.20*a*. According to the ACI Code the critical section at interior supports may be taken at the face of supports, but not greater than $0.175l_1$ from the column centerline. The former criterion controls here, and the negative design

TABLE 13.7
Moments in flat plate floor, kN-m

Panel	B		C		B	
Joint	**1**	**2**	**2**	**3**	**3**	**4**
(*a*) 15.0 kN/m² all panels						
Fixed-end moments	+376	−376	+376	−376	+376	−376
Final moments	+171	−443	+407	−407	+443	−171
Span moment in *C*			157			
(*b*) 7.2 kN/m² panels *B* and 13.1 kN/m² panel *C*						
Fixed-end moments	+180	−180	+328	−328	+180	−180
Final moments	+67	−270	+304	−304	+270	−67
Span moment in *C*			188			
(*c*) 13.1 kN/m² panels *B* (left) and *C* and 7.2 kN/m² panel *B* (right)						
Fixed-end moments	+328	−328	+328	−328	+180	−180
Final moments	+144	−394	+374	−282	+257	−69
Span moment in *C*			165			

FIGURE 13.20
Design moments and shears for flat plate floor interior panel *C*: (*a*) moments; (*b*) shears.

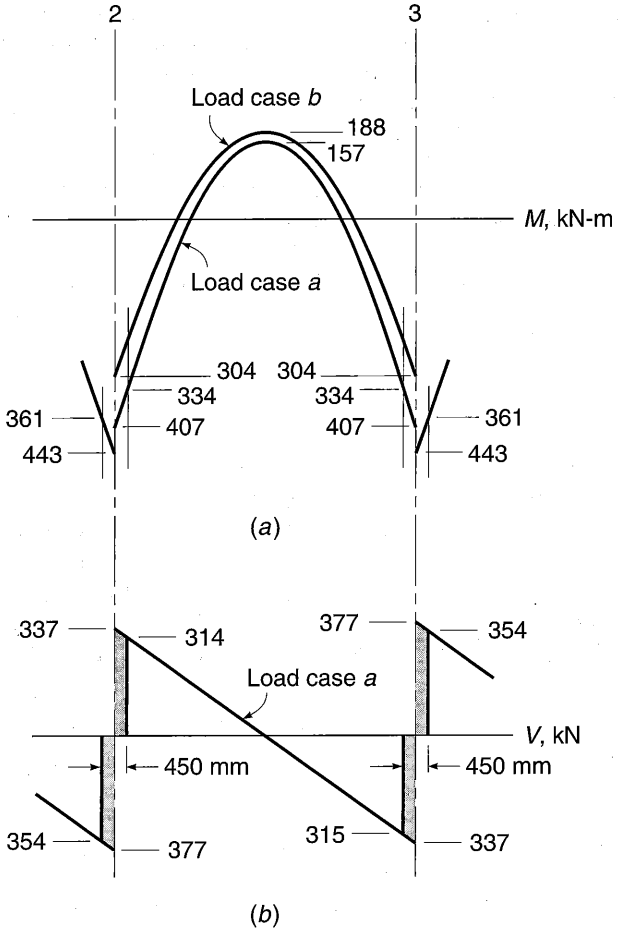
2
3
Load case *b*
188
157
M, kN-m
Load case *a*
304
304
334
334
361
407
407
361
443
443
(*a*)
337
314
377
354
Load case *a*
V, kN
450 mm
450 mm
354
377
315
337
(*b*)

TABLE 13.8
Design of flat plate reinforcement

(1)	(2) Location	(3) M_u, kN-m	(4) b, m	(5) d, mm	(6) M_u/b, kN-m/m	(7) ρ	(8) A_s, mm^2	(9) Number and Size of Bars
Column strip	Negative	271	3.35	175	80.9	0.0075	4397	16 No. 19 (No. 6)
	Positive	113	3.35	175	33.7	0.0030	1759	9 No. 16 (No. 5)
Two half-middle strips	Negative	90	3.35	175	26.9	0.0024	1407	8 No. 16 (No. 5)[a]
	Positive	75	3.35	175	22.4	0.0020	1173	8 No. 16 (No. 5)[a]

[a] Number of bars controlled by maximum spacing requirement.

moment is calculated by subtracting the area under the shear diagram between the centerline and face of support, for load case *a*, from the negative moment at the support centerline. The shear diagram for load case *a* is given in Fig. 13.20*b*, with the adjusted design moments shown in Fig. 13.20*a*.

Because the effective depth for all panels will be the same, and because the negative steel for panel *C* will continue through the support region to become the negative steel for panels *B*, the larger negative moment found for the panels *B* will control. Accordingly, the design negative moment is 361 kN-m and the design positive moment is 188 kN-m.†

Moments will be distributed laterally across the slab width according to Table 13.4, which indicates that 75 percent of the negative moment will be assigned to the column strip and 60 percent of the positive moment assigned to the column strip. The design of the slab reinforcement is summarized in Table 13.8.

Other important aspects of the design of flat plates include design for punching shear at the columns, which may require supplementary shear reinforcement, and transfer of unbalanced moments to the columns, which may require additional flexural bars in the negative bending region of the column strips or adjustment of spacing of negative steel. These considerations are of special importance at exterior columns and corner columns, such as shown in Fig. 13.19. Shear and moment transfer at the columns will be discussed in Sections 13.10 and 13.11, respectively.

e. Equivalent Frame Analysis by Computer

It is clear that the equivalent frame method, as described in the ACI Code and the ACI Code Commentary, is oriented toward analysis using the method of moment distribution. Presently, most offices make use of computers, and frame analysis is done using general-purpose programs based on the direct stiffness method. Plane frame analysis programs can be used for slab analysis based on the concepts of the equivalent frame method, but the frame must be specially modeled. Variable moments of inertia along the axis of slab-beams and columns require nodal points (continuous joints) between sections where I is to be considered constant (i.e., in the slab at the junction of slab and drop panel, drop panel and capital, and in the columns at the bottom of the capitals). In addition, it is necessary to compute K_{ec} for each column and then to compute the equivalent value of the moment of inertia for the column.

---

† When slab systems that meet the restrictions of the direct design method are designed by the equivalent frame method, according to ACI Code 13.7.7 the resulting design moments may be reduced proportionately so that the sum of the positive and average negative moments in a span is no greater than M_o calculated for the direct design method according to Eq. (13.1). There is no theoretical basis for this. The reduction is less than 5 percent in the present example, and it will not be included in the design calculations.

Alternately, a three-dimensional frame analysis may be used, in which the torsional properties of the transverse supporting beams may be included directly. A third option is to make use of specially written computer programs, the most widely used being pcaSlab, developed by the Portland Cement Association (Skokie, Illinois).

13.10 SHEAR DESIGN IN FLAT PLATES AND FLAT SLABS

When two-way slabs are supported directly by columns, as in flat slabs and flat plates, or when slabs carry concentrated loads, as in footings, shear near the columns is of critical importance. Tests of flat plate structures indicate that, in most practical cases, the capacity is governed by shear (Ref. 13.15).

a. Slabs without Special Shear Reinforcement

Two kinds of shear may be critical in the design of flat slabs, flat plates, or footings. The first is the familiar beam-type shear leading to diagonal tension failure. Applicable particularly to long narrow slabs or footings, this analysis considers the slab to act as a wide beam, spanning between supports provided by the perpendicular column strips. A potential diagonal crack extends in a plane across the entire width l_2 of the slab. The critical section is taken a distance d from the face of the column or capital. As for beams, the design shear strength ϕV_c must be at least equal to the required strength V_u at factored loads. The nominal shear strength V_c should be calculated by either Eq. (4.12*a*) or Eq. (4.12*b*), with b_w equal to the panel width l_2 in this case.

Alternatively, failure may occur by *punching shear*, with the potential diagonal crack following the surface of a truncated cone or pyramid around the column, capital, or drop panel, as shown in Fig. 13.21*a*. The failure surface extends from the bottom of the slab, at the support, diagonally upward to the top surface. The angle of inclination with the horizontal θ (see Fig. 13.21*b*) depends upon the nature and amount of reinforcement in the slab. It may range between about 20 and 45°. The

FIGURE 13.21
Failure surface defined by punching shear.

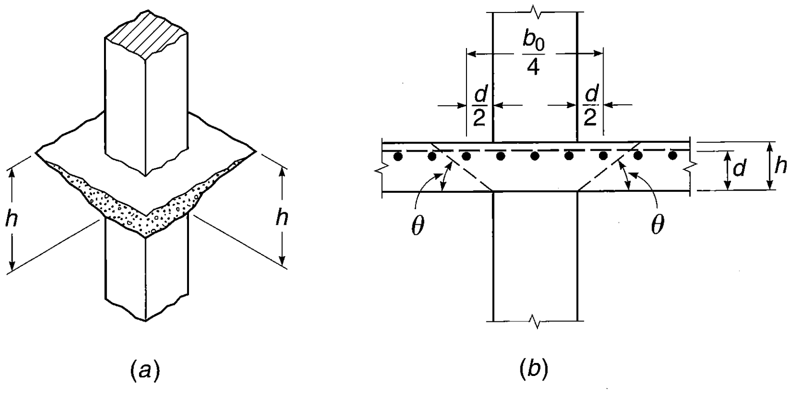

critical section for shear is taken perpendicular to the plane of the slab and a distance $d/2$ from the periphery of the support, as shown. The shear force V_u to be resisted can be calculated as the total factored load on the area bounded by panel centerlines around the column less the load applied within the area defined by the critical shear perimeter, unless significant moments must be transferred from the slab to the column (see Section 13.11).

At such a section, in addition to the shearing stresses and horizontal compressive stresses due to negative bending moment, vertical or somewhat inclined compressive stress is present, owing to the reaction of the column. The simultaneous presence of vertical and horizontal compression increases the shear strength of the concrete. For slabs supported by columns having a ratio of long to short sides not greater than 2, tests indicate that the nominal shear strength may be taken equal to

$$V_c = 0.33\lambda\sqrt{f'_c}b_od \qquad (13.11a)$$

according to ACI Code 11.11.2, where b_o = the perimeter along the critical section, and λ is the lightweight concrete factor (see Section 4.5*a*).

However, for slabs supported by very rectangular columns, the shear strength predicted by Eq. (13.11*a*) has been found to be unconservative. According to tests reported in Ref. 13.16, the value of V_c approaches $2\lambda\sqrt{f'_c}b_od$ as β, the ratio of long to short sides of the column, becomes very large. Reflecting these test data, ACI Code 11.11.2 states further that V_c in punching shear shall not be taken greater than

$$V_c = \left(0.16 + \frac{0.33}{\beta}\right)\lambda\sqrt{f'_c}b_od \qquad (13.11b)$$

The variation of the shear strength coefficient, as governed by Eqs. (13.11*a*) and (13.11*b*), is shown in Fig. 13.22 as a function of β.

Further tests, reported in Ref. 13.17, have shown that the shear strength V_c decreases as the ratio of critical perimeter to slab depth b_o/d increases. Accordingly, ACI Code 11.11.2 states that V_c in punching shear must not be taken greater than

$$V_c = 0.083\left(\frac{\alpha_s d}{b_o} + 2\right)\lambda\sqrt{f'_c}b_od \qquad (13.11c)$$

where α_s is 40 for interior columns, 30 for edge columns, and 20 for corner columns, i.e., columns having critical sections with 4, 3, or 2 sides, respectively.

FIGURE 13.22
Shear strength coefficient for flat plates as a function of ratio β of long side to short side of support.

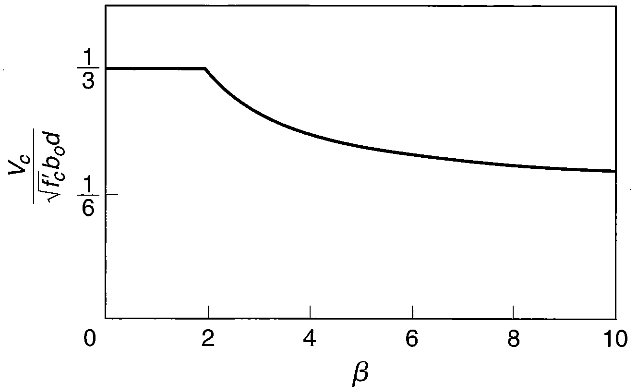

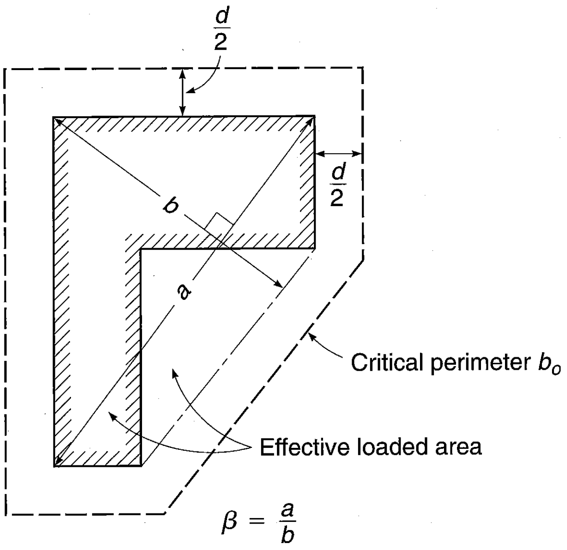

FIGURE 13.23
Punching shear for columns of irregular shape.

Thus, according to the ACI Code, the punching shear strength of slabs and footings is to be taken as the smallest of the values of V_c given by Eqs. (13.11*a*), (13.11*b*), and (13.11*c*). The design strength is taken as ϕV_c as usual, where $\phi = 0.75$ for shear. The basic requirement is then $V_u \leq \phi V_c$.

For columns with nonrectangular cross sections the ACI Code indicates that the perimeter b_o must be of minimum length, but need not approach closer than $d/2$ to the perimeter of the reaction area. The manner of defining the critical perimeter b_o and the ratio β for such irregular support configurations is illustrated in Fig. 13.23.

b. Types of Shear Reinforcement

Special shear reinforcement is often used at the supports for flat plates, and sometimes for flat slabs as well. It may take several forms. A few common types are shown in Fig. 13.24.

The *shearheads* shown in Fig. 13.24*a* and *c* consist of standard structural steel shapes embedded in the slab and projecting beyond the column. They serve to increase the effective perimeter b_o of the critical section for shear. In addition, they may contribute to the negative bending resistance of the slab. The reinforcement shown in Fig. 13.24*a* is particularly suited for use with concrete columns. It consists of short lengths of I or wide-flange beams, cut and welded at the crossing point so that the arms are continuous through the column. Normal negative slab reinforcement passes over the top of the structural steel, while bottom bars are stopped short of the shearhead. Column bars pass vertically at the corners of the column. The effectiveness of this type of shearhead has been documented by tests by Corley and Hawkins (Ref. 13.18). The channel frame in Fig. 13.24*c* is very similar in its action, but is adapted for use with steel columns. The bent-bar arrangement in Fig. 13.24*b* is suited for use with concrete columns. The bars are usually bent at 45° across the potential diagonal tension crack, and extend along the bottom of the slab a distance sufficient to develop their strength by bond. The flanged collar in Fig. 13.24*d* is designed mainly for use with lift-slab construction (see Chapter 18). It consists of a flat bottom plate with vertical stiffening ribs. It may incorporate sockets for lifting rods, and usually is

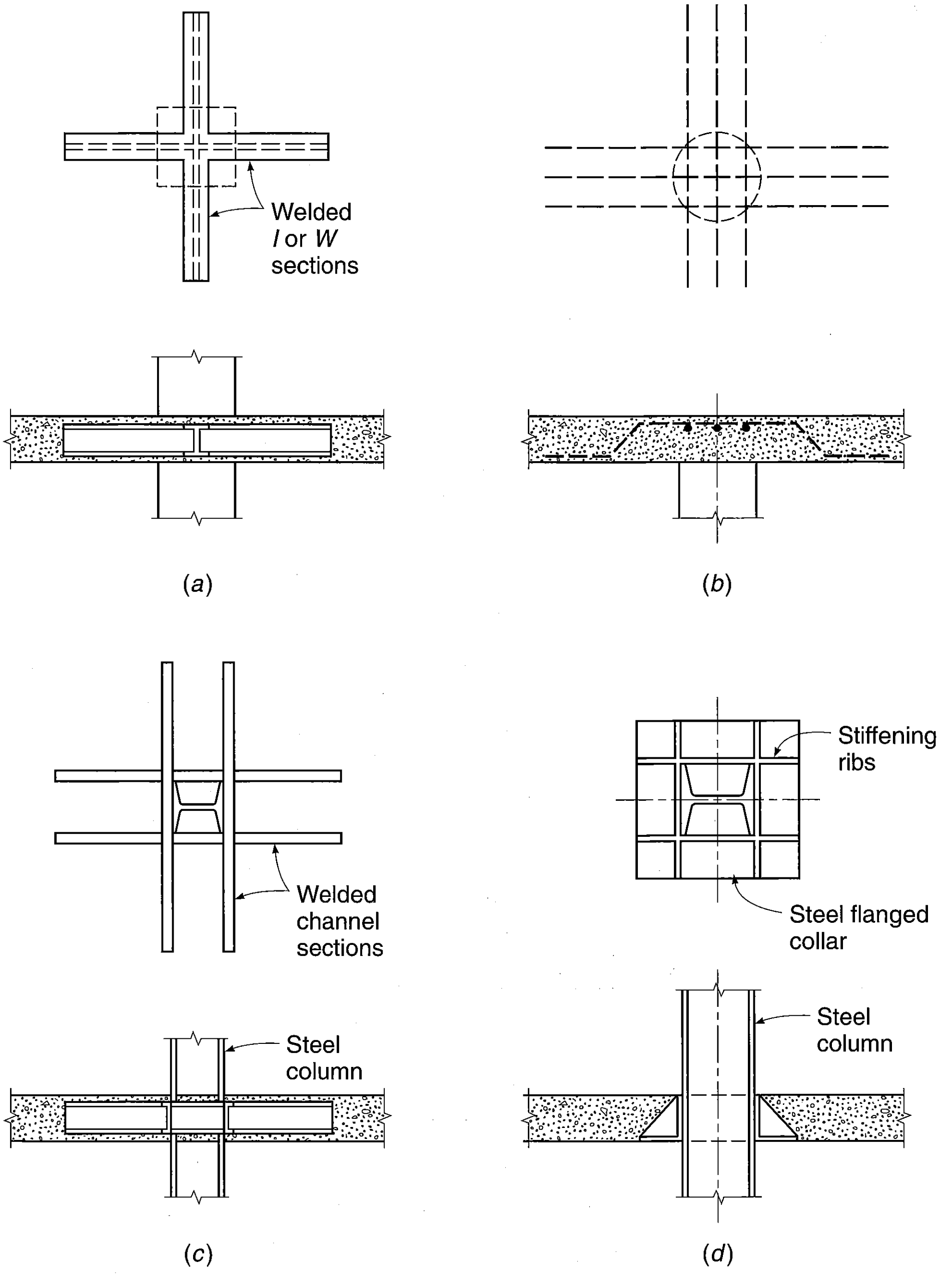
Welded
I or *W*
sections
(*a*)
(*b*)
Welded
channel
sections
Steel
column
(*c*)
Stiffening
ribs
Steel flanged
collar
Steel
column
(*d*)

FIGURE 13.24
Shear reinforcement for flat plates (*continued on next page*).

used in conjunction with shear pads welded directly to the column surfaces below the collar to transfer the vertical reaction.

Another type of shear reinforcement is illustrated in Fig. 13.24*e*, where vertical stirrups have been used in conjunction with supplementary horizontal bars radiating outward in two perpendicular directions from the support, to form what are termed *integral beams* contained entirely within the slab thickness. These beams act in the same general way as the shearheads shown in Fig. 13.24*a* and *c*. Adequate anchorage of the stirrups is difficult in slabs thinner than about 250 mm. ACI Code 11.11.3 requires the slab effective depth *d* to be at least 150 mm, but not less than 16 times the

FIGURE 13.24
(*continued*)

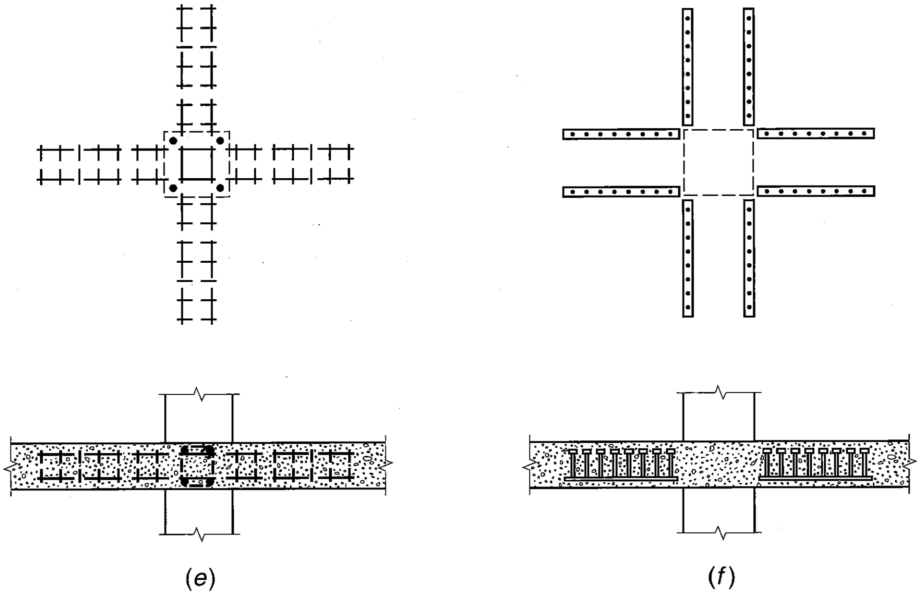

diameter of the shear reinforcement. In all cases, closed hoop stirrups should be used, with a large-diameter horizontal bar at each bend point, and the stirrups must be terminated with a standard hook (Ref. 13.19).

Headed shear stud reinforcement, shown in Fig. 13.24*f*, is governed by ACI Code 11.11.5. This consists of large-head studs welded to steel strips. The strips are supported on wire chairs during construction to maintain the required concrete cover to the bottom of the slab below the strip, and the usual cover is maintained over the top of the head. Because of the positive anchorage provided by the stud head and the steel strip, these devices are more effective, according to tests, than either the bent-bar or integral beam reinforcement (Refs. 13.20 and 13.21). In addition, they can be placed more easily, with less interference with other reinforcement, than other types of shear steel.

c. Design of Bent-Bar Reinforcement

If shear reinforcement in the form of bars is used (Fig. 13.24*b*), the limit value of nominal shear strength V_n, calculated at the critical section $d/2$ from the support face, may be increased to $0.5\sqrt{f_c'}\,b_o d$ according to ACI Code 11.11.3. The shear resistance of the concrete V_c is reduced to $0.17\lambda\sqrt{f_c'}\,b_o d$, and reinforcement must provide for the excess shear above ϕV_c. The total bar area A_v crossing the critical section at slope angle α is easily obtained by equating the vertical component of the steel force to the excess shear force to be accommodated:

$$\phi A_v f_y \sin\alpha = V_u - \phi V_c$$

Where inclined shear reinforcement is all bent at the same distance from a support, $V_s = A_v f_y \sin\alpha$ is not to exceed $0.25\sqrt{f'}\,b_o d$, according to ACI Code 11.4.7. The required area of reinforcement for shear is found by transposing the preceding equation:

$$A_v = \frac{V_u - \phi V_c}{\phi f_y \sin\alpha} \tag{13.12}$$

Successive sections at increasing distances from the support must be investigated and reinforcement provided where V_u exceeds ϕV_c as given by Eq. (13.11).† Only the center three-quarters of the inclined portion of the bent bars can be considered effective in resisting shear, and full development length must be provided past the location of peak stress in the steel, which is assumed to be at slab middepth $d/2$.

EXAMPLE 13.4

Design of bar reinforcement for punching shear. A flat plate floor has thickness $h = 190$ mm and is supported by 450 mm square columns spaced 6 m on centers each way. The floor will carry a total factored load of 14.0 kN/m^2. Check the adequacy of the slab in resisting punching shear at a typical interior column, and provide shear reinforcement, if needed, using bent bars similar to Fig. 13.24*b*. An average effective depth $d = 150$ mm may be used. Material strengths are $f_y = 420$ MPa and $f'_c = 28$ MPa.

Solution. The first critical section for punching shear is a distance $d/2 = 75$ mm from the column face, providing a shear perimeter $b_o = 600 \times 4 = 2400$ mm. Based on the tributary area of loaded floor, the factored shear is

$$V_u = 14.0(6^2 - 0.6^2) = 487 \text{ kN}$$

and if no shear reinforcement is used, the design strength of the slab, controlled by Eq. (13.11*a*), is

$$\phi V_c = 0.75 \times 0.33\sqrt{28} \times 2400 \times 150 \times 10^{-3} = 471 \text{ kN}$$

confirming that shear reinforcement is required. Bars bent at 45° will be used in two directions, as shown in Fig. 13.25. When shear strength is provided by a combination of reinforcement and concrete, the concrete contribution is reduced to

$$\phi V_c = 0.75 \times 0.17\sqrt{28} \times 2400 \times 150 \times 10^{-3} = 243 \text{ kN}$$

and so the shear V_s to be resisted by the reinforcement is

$$V_s = \frac{V_u - \phi V_c}{\phi} = \frac{487 - 243}{0.75} = 325 \text{ kN}$$

This is below the maximum permissible value of $0.25\sqrt{28} \times 2400 \times 150 \times 10^{-3} = 476$ kN. The required bar area is then found from Eq. (13.12) to be

$$A_v = \frac{325 \times 10^3}{420 \times 0.707} = 1094 \text{ mm}^2$$

A total of four bars will be used (two in each direction), and with eight legs crossing the critical section, the necessary area per bar is $1094/8 = 137$ mm^2. No. 16 (No. 5) bars will be used as shown in Fig. 13.25. The upper limit of $V_n = 0.5\sqrt{f'_c}b_od$ is automatically satisfied in this case, given the more stringent limit on V_s.

---

† ACI Code 11.11.3 and ACI Commentary 11.11.3 are ambiguous regarding the value of V_c to be used for flat plate slabs beyond the region where shear reinforcement is required. In general, for slabs where shear reinforcement is not required, V_c is calculated from Eqs. (13.11*a*) to (13.11*c*), with V_c in most cases equal to $0.17\lambda\sqrt{f'_c}\, b_od$. When shear reinforcement is provided, the limiting shear may be increased to a maximum of $0.5\sqrt{f'_c}b_od$; however, the shear reinforcement must be designed to carry all shear in excess of ϕV_c with $V_c = 0.17\lambda\sqrt{f'_c}\, b_od$. This seems to imply that the reduction in V_c to one-half its normal value applies only where there is a sharing of the force between concrete and steel reinforcement and that, in the region where shear reinforcement is *not* required, the full concrete contribution of $0.33\lambda\sqrt{f'_c}\, b_od$ can be used. The examples that follow have been prepared on that basis. The alternative interpretation is that if shear reinforcement is required at the column, then the concrete contribution is reduced to $0.17\lambda\sqrt{f'_c}\, b_od$ throughout the slab. This more conservative interpretation could be adopted in many cases without significant cost increase, because of the rapid increase in V_c with increasing distance from the column resulting from the increase in concrete shear perimeter b_o, as well as the reduction in net shear force V_u.

FIGURE 13.25
Bar reinforcement for punching shear in flat plate slab.

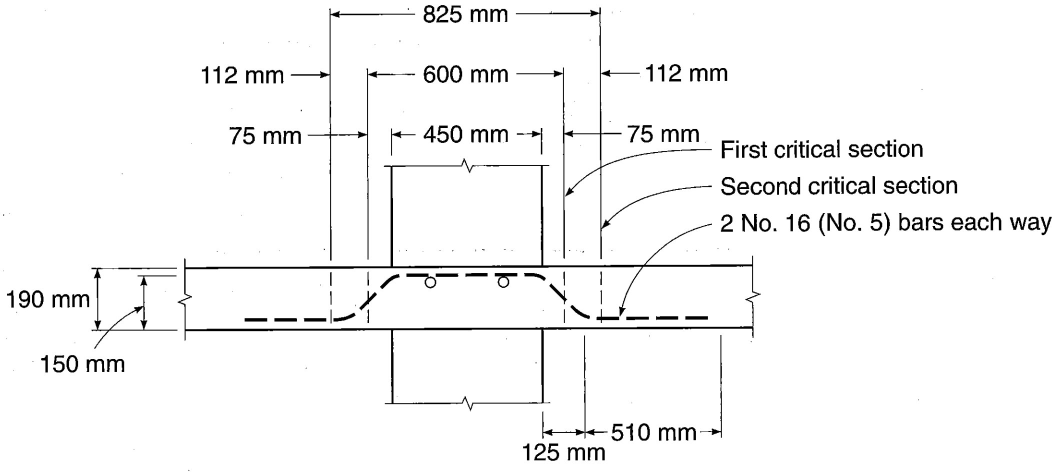

With bars bent at 45° and effective through the center three-fourths of the inclined length, the next critical section is approximately $\frac{3}{4}$ times the effective depth, or 112 mm, past the first, as shown, giving a shear perimeter of 825 × 4 = 3300 mm. The factored shear at that critical section is

$$V_u = 14.0(6^2 - 0.825^2) = 494 \text{ kN}$$

and the design capacity of the concrete is

$$\phi V_c = 0.75 \times 0.33 \times 1\sqrt{28} \times 3300 \times 150 \times 10^{-3} = 648 \text{ kN}$$

confirming that no additional bent bars are needed. The No. 16 (No. 5) bars will be extended along the bottom of the slab the full development length of 510 mm, as shown in Fig. 13.25.

d. Design of Integral Beams with Vertical Stirrups

The bent-bar shear reinforcement cages of Section 13.10c may lead to troublesome congestion of reinforcement in the column-slab joint region. Shear reinforcement using vertical stirrups in *integral beams,* as shown in Fig. 13.24*e,* avoids much of this difficulty.

The first critical section for shear design in the slab is taken at $d/2$ from the column face, as usual, and the stirrups, if needed, are extended outward from the column in four directions for the typical interior case (three or two directions for exterior or corner columns, respectively), until the concrete alone can carry the shear, with $V_c = 0.33\lambda\sqrt{f_c'}b_o d$ at the second critical section.[†] Within the region adjacent to the column, where shear resistance is provided by a combination of concrete and steel, the nominal shear strength V_n must not exceed $0.5\sqrt{f_c'}b_o d$, according to ACI Code 11.11.3. In this region, the concrete contribution is reduced to $V_c = 0.17\lambda\sqrt{f_c'}b_o d$. The second critical section crosses each integral beam at a distance $d/2$ measured outward from the last stirrup and is located so that its perimeter b_o is a minimum (i.e., for the typical case, defined by 45° lines between the integral beams). The required spacing of the vertical stirrups s is found using Eq. (4.14*a*), but must not exceed $d/2$, with the first line of stirrups not more than $d/2$ from the column face. The spacing of the stirrup legs (measured parallel to the face of the column) in the first line of shear reinforcement must not exceed $2d$.

[†] Neither the ACI Code nor the ACI Commentary makes clear whether Eqs. (13.11*b*) and (13.11*c*) are to be applied at successive critical sections past the first, immediately adjacent to the column. The research on which these equations were based considered only the first critical section at the column. Except in extreme cases, the aspect ratio of the column, in Eq. (13.11*b*), seems less relevant with increasing distance from the column; however, the b_o/d ratio, in Eq. (13.11*c*), may be influential, and that equation might conservatively be applied.

The problem of anchorage of the shear reinforcement in shallow flat plates is critical, and closed hoop stirrups, terminating in standard hooks, always should be provided with interior corner bars to improve pullout resistance.

EXAMPLE 13.5

Design of an integral beam with vertical stirrups. The flat plate slab with 190 mm total thickness and 150 mm effective depth shown in Fig. 13.26 is carried by 300 mm square columns 4.6 m on centers in each direction. A factored load of 534 kN must be transmitted from the slab to a typical interior column. Concrete and steel strengths used are, respectively, $f'_c = 28$ MPa and $f_y = 420$ MPa. Determine if shear reinforcement is required for the slab; and if so, design integral beams with stirrups to carry the excess shear.

Solution. The design shear strength of the concrete alone at the critical section $d/2$ from the face of the column, by the controlling Eq. (13.11*a*), is

$$\phi V_c = 0.75 \times 0.33 \times 1\sqrt{28} \times 1800 \times 150 \times 10^{-3} = 354 \text{ kN}$$

This is less than $V_u = 534$ kN, indicating that shear reinforcement is required. The effective depth $d = 150$ mm just satisfies the minimum allowed to use stirrup reinforcement, as described in Section 13.10b. In this case, the maximum design strength allowed by the ACI Code is

$$\phi V_n = 0.75 \times 0.5\sqrt{28} \times 1800 \times 150 \times 10^{-3} = 536 \text{ kN}$$

FIGURE 13.26
Vertical stirrup shear reinforcement for slab in Example 13.5.

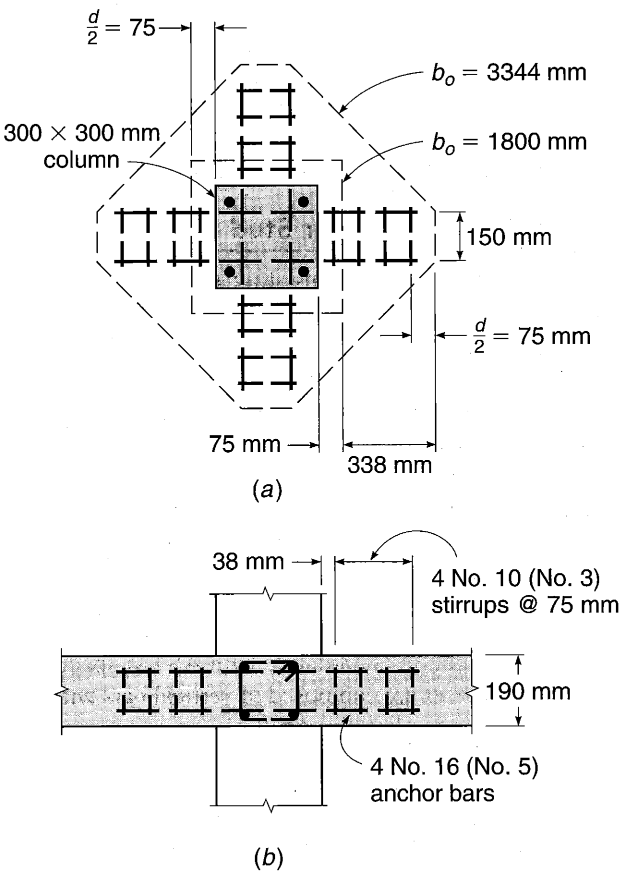

satisfactorily above the actual V_u. When shear is resisted by combined action of concrete and bar reinforcement, the concrete contribution is reduced to

$$\phi V_c = 0.75 \times 0.17 \times \sqrt{28} \times 1800 \times 150 \times 10^{-3} = 182 \text{ kN}$$

The No. 10 (No. 3) vertical closed hoop stirrups will be used since d must be ≥ 16 times the stirrup diameter ($d/16 = 9.4$ mm) and arranged along four integral beams as shown in Fig. 13.26. Thus, the A_v provided is $4 \times 2 \times 71 = 568 \text{ mm}^2$ at the first critical section, a distance $d/2$ from the column face, and the required spacing can be found from Eq. (4.14*a*):

$$s = \frac{\phi A_v f_y d}{V_u - \phi V_c} = \frac{0.75 \times 568 \times 420 \times 150}{(534 - 182) \times 10^3} = 76.2 \text{ mm}$$

However, the maximum spacing of $d/2 = 75$ mm controls here, and No. 10 (No. 3) stirrups at a constant spacing of 75 mm will be used. In other cases, stirrup spacing might be increased with distance from the column, as excess shear is less, although this would complicate placement of the reinforcement and generally save little steel.

The required perimeter of the second critical section, at which the concrete alone can carry the shear, is found from the controlling Eq. (13.11*a*) as follows:

$$\phi V_c = 0.75 \times 0.33\sqrt{28} \times b_o \times 150 \times 10^{-3} = 534 \text{ kN}$$

from which the minimum perimeter $b_o = 2718$ mm. Using this value of b_o in Eq. (13.11*c*) gives $\phi V_c = 535$ kN; thus, Eq. (13.11*a*) governs. It is easily confirmed that $b_o = 2718$ mm requires a minimum projection of the critical section past the face of the column of 299 mm. Four stirrups at a constant 75 mm spacing will be sufficient, the first placed at $s/2 = 38 \text{ mm} \leq d/2 = 75$ mm from the column face, as indicated in Fig. 13.26. This provides a perimeter b_o at the second critical section of $(413\sqrt{2} + 150)4 = 2936$ mm, exceeding the requirement.

Four longitudinal No. 16 (No. 5) bars will be provided inside the corners of each closed hoop stirrup, as shown, to provide for proper anchorage of the shear reinforcement.

Note that the approach taken here is somewhat conservative because the portion of the slab load applied inside the perimeter of the critical section does not act on that section and can thus be subtracted from the factored load of 534 kN.

e. Design of Headed Shear Stud Reinforcement

Slab shear reinforcement consisting of integral beams with stirrups, as described in Section 13.10d, is probably the most widely used type at present. However, the cage that is formed by the stirrups and longitudinal anchor bars may be difficult to install. Also, the slab-column joint region is somewhat congested, with top and bottom slab steel running in two perpendicular directions, with vertical bars in the column, and with the stirrups. Congestion can become critical when the slab has openings, which are frequently required, at or near the column faces.

Shear stud reinforcing strips, as shown in Fig. 13.24*f* and in Fig. 13.27*a* and *b*, are widely used in Germany, Switzerland, and Canada (Refs. 13.20 and 13.21). Their use in the United States has increased and design guidelines, based on extensive testing (Refs. 13.22 and 13.23), are incorporated in ACI Code 11.11.5. The studs have a minimum yield strength f_{yt} of 350 MPa and are available in diameters of 9.5, 12.7, 15.6 and 19.0 mm, in accordance with ASTM specification A1044.

These devices are composed of vertical bars with anchor heads at their top, welded to a steel strip at the bottom. Multiple strips are arranged in two perpendicular directions for square and rectangular columns or usually in radial directions for circular columns. They are secured in position in the forms before the top and bottom flexural steel is in place. The steel strip rests on bar chairs to maintain the needed concrete cover below the steel and is held in position by nails through holes in the strip.

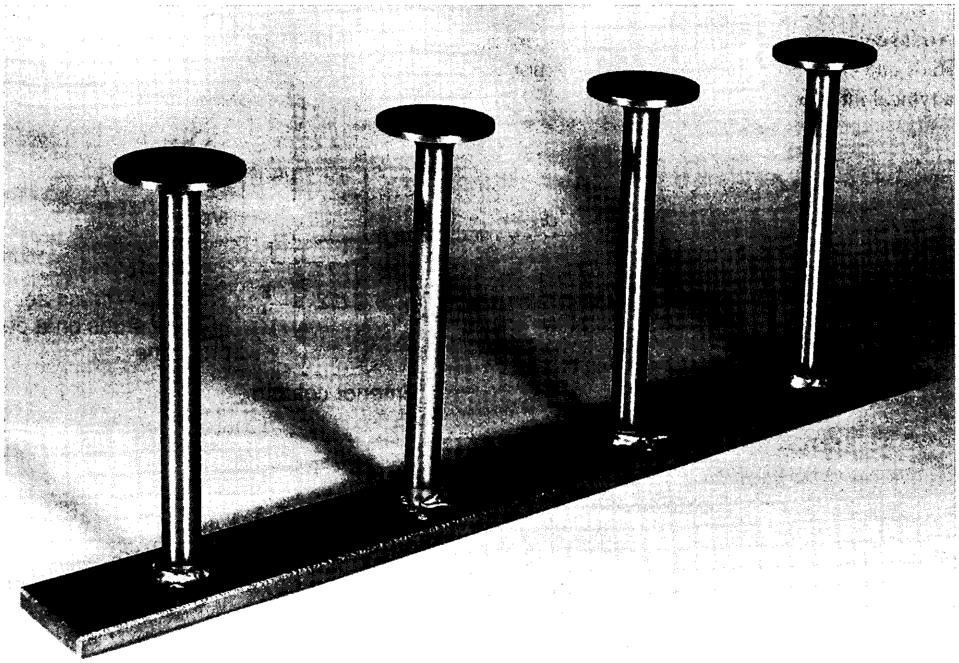

FIGURE 13.27*a*
Shear stud reinforcement for concrete slabs: shear stud assembly. (*Courtesy of Amin Ghali and Walter H. Dilger.*)

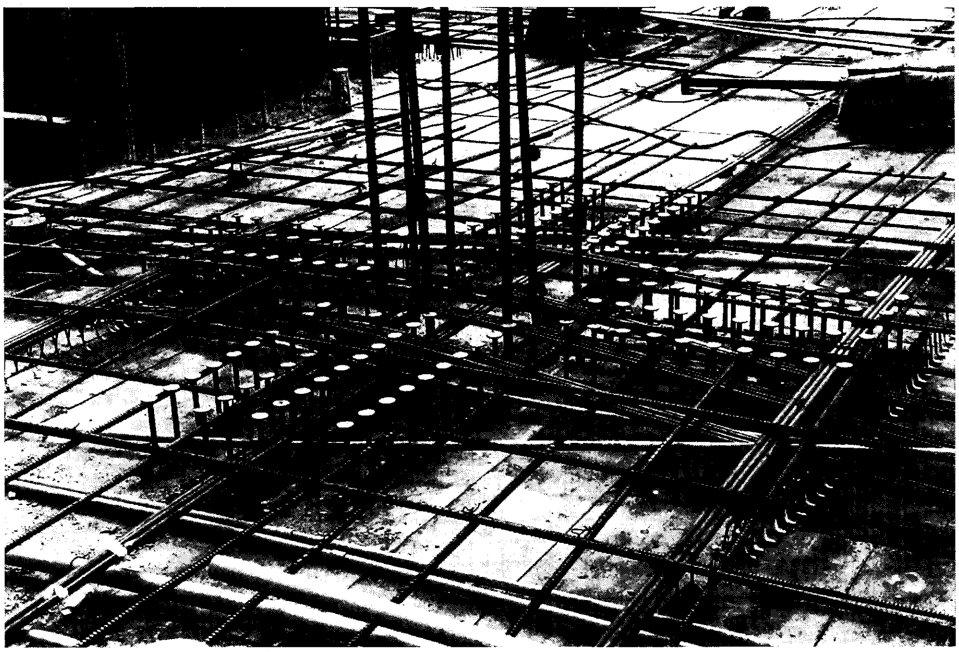

FIGURE 13.27*b*
Shear stud reinforcements for concrete slabs: shear reinforcement installed in forms for prestressed concrete slab. (*Courtesy of Amin Ghali and Walter H. Dilger.*)

Headed shear studs are placed perpendicular to the plane of the slab. The overall height of the shear stud assembly may not be less than the thickness of the member less the sum of (1) the concrete cover over the top reinforcement, (2) the concrete cover on the base rail, and (3) one-half the diameter of the tension flexural reinforcement. Two critical shear sections exist. The first is located a distance $d/2$ from the face of the column, and the second is located a distance $d/2$ from the outermost peripheral line of studs, as shown in Fig. 13.28 for a typical interior column. As with the integral beams with vertical

FIGURE 13.28
Arrangement of headed shear studs and critical sections for a typical interior column.

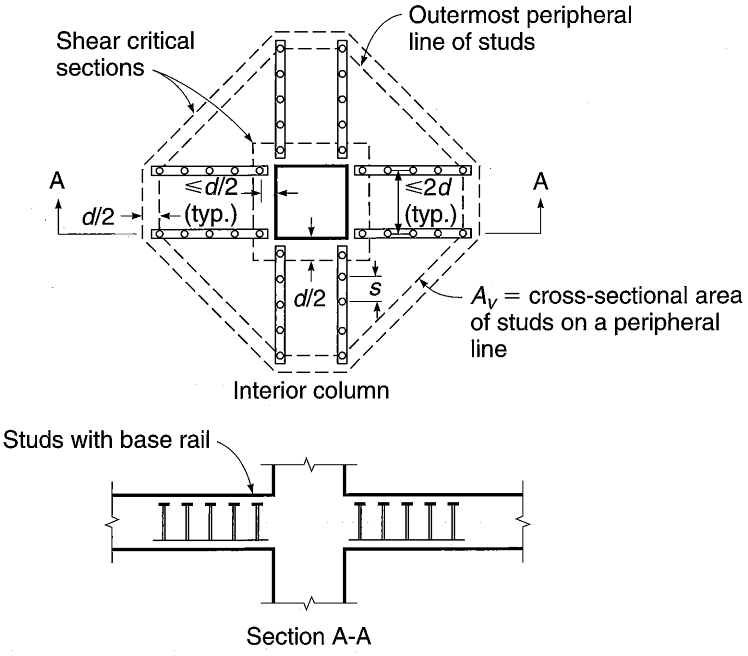

stirrups described in Section 13.10d, the studs are extended outward from the column until the concrete alone can carry the shear; but in the case of slabs reinforced with headed shear studs, the shear stress due to the factored shear force and any unbalanced moment (see Section 13.11) may not exceed $0.17\phi\lambda\sqrt{f_c'}$ on the second critical section.

The nominal shear capacity of the headed shear stud assembly V_n is the sum of the concrete contribution V_c and the shear stud contribution V_s. In the region adjacent to the column, the concrete contribution V_c is reduced to $0.25\lambda\sqrt{f_c'}b_o d$, and the total nominal capacity V_n may not exceed $0.67\sqrt{f_c'}b_o d$. The shear stud contribution is $A_v f_{yt} d/s$, where A_v is the area of the studs on a peripheral line and s is the spacing between the peripheral lines, as shown in Fig. 13.28. The value of the shear stud contribution, expressed as a stress on the critical section as $A_v f_{yt}/b_o s$, must be at least $0.17\sqrt{f_c'}$ in accordance with ACI Code 11.11.5.

The spacing of the studs between the column face and the first peripheral line of studs should not exceed $d/2$, and the spacing of the concentric peripheral lines of studs s should be based on the combined effects of shear and any unbalanced moment on the critical section adjacent to the column face and should not exceed $0.75d$ when the shear stress due to factored loads is less than or equal to $0.5\phi\sqrt{f_c'}$ or $0.5d$ when the shear stress exceeds $0.5\phi\sqrt{f_c'}$. Lastly, the spacing between the shear stud rails should not exceed $2d$.

EXAMPLE 13.6

Design of headed stud reinforcement. Repeat Example 13.5, using headed stud reinforcement. The No. 16 (No. 5) bars will be used as negative flexural reinforcement. The yield strength is f_{yt} = 350 MPa for studs.

Solution. The minimum height of the shear stud assembly equals the thickness of the slab less the cover over the rail, the cover over the reinforcement, and one-half the reinforcement bar diameter. Thus, from Fig 13.29*b* the minimum height is

$$190 - 20 - 20 - 0.5 \times 15.9 = 142 \text{ mm}$$

FIGURE 13.29
Headed shear stud arrangement and detail of structural depth requirements for Example 13.6.

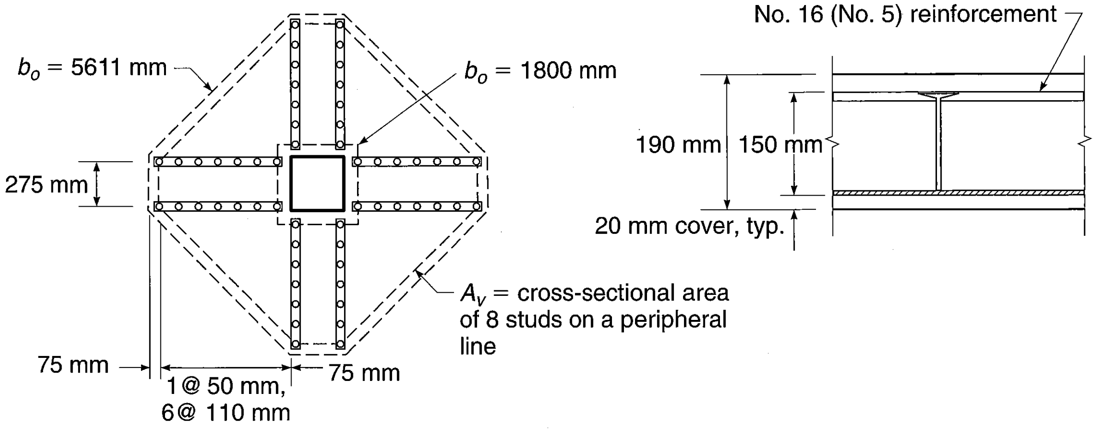

(*a*) (*b*)

A stud height of 150 mm will be used, which is consistent with the effective depth and exceeds the minimum requirement. As in Example 13.5, the design shear strength of the concrete alone at the critical section from the face of the column based on an effective depth of 150 mm, by the controlling Eq. (13.11*a*), is

$$\phi V_c = 0.75 \times 0.33 \times 1\sqrt{28} \times 1800 \times 150 \times 10^{-3} = 354 \text{ kN}$$

which is less than $V_u = 534$ kN, indicating that shear reinforcement is required. The maximum design strength allowed by the ACI Code when headed stud reinforcement is used is

$$\phi V_n = 0.75 \times 0.67\sqrt{28} \times 1800 \times 150 \times 10^{-3} = 718 \text{ kN}$$

which is satisfactorily above the actual V_u. The maximum concrete strength allowed by ACI in conjunction with headed shear studs is

$$\phi V_c = 0.75 \times 0.25 \times 1\sqrt{28} \times 1800 \times 150 \times 10^{-3} = 268 \text{ kN}$$

The maximum spacing between the stud rails must be less than $2d$, so two lines of studs are needed for a 300 mm square column; a center-to-center spacing of 275 mm will be used. The shear stress in the slab at the first critical section is approximately $0.37\sqrt{f'_c}$, which is below $\phi 0.5\sqrt{f'_c} = 0.38\sqrt{f'_c}$, giving a maximum stud spacing of $0.75d$. A spacing of 110 mm, equal to the maximum, is selected. The area of the studs is found from Eq. (4.14*a*):

$$A_v = \frac{(V_u - \phi V_c)s}{\phi f_{yt} d} = \frac{(534 - 268)110 \times 10^3}{0.75 \times 350 \times 150} = 743 \text{ mm}^2$$

A peripheral line of studs contains 8 studs, requiring a cross-sectional area of 93 mm^2 per stud, so 12.7 mm diameter studs with a cross-sectional area of 126 mm^2 per stud are selected.

The required perimeter of the second critical section, at which the concrete alone can carry the shear, is based on a maximum shear stress of $0.17\phi\lambda\sqrt{f'_c}$. Thus,

$$\phi V_c = 0.75 \times 0.17 \times 1\sqrt{28} \times b_o \times 150 \times 10^{-3} = 534 \text{ kN}$$

from which the minimum perimeter $b_o = 5606$ mm. The first stud is placed at $d/2$ or 50 mm from the column face. Six more studs at a spacing of 110 mm provide a minimum perimeter of 5611 mm, as shown in Fig. 13.29*a*.

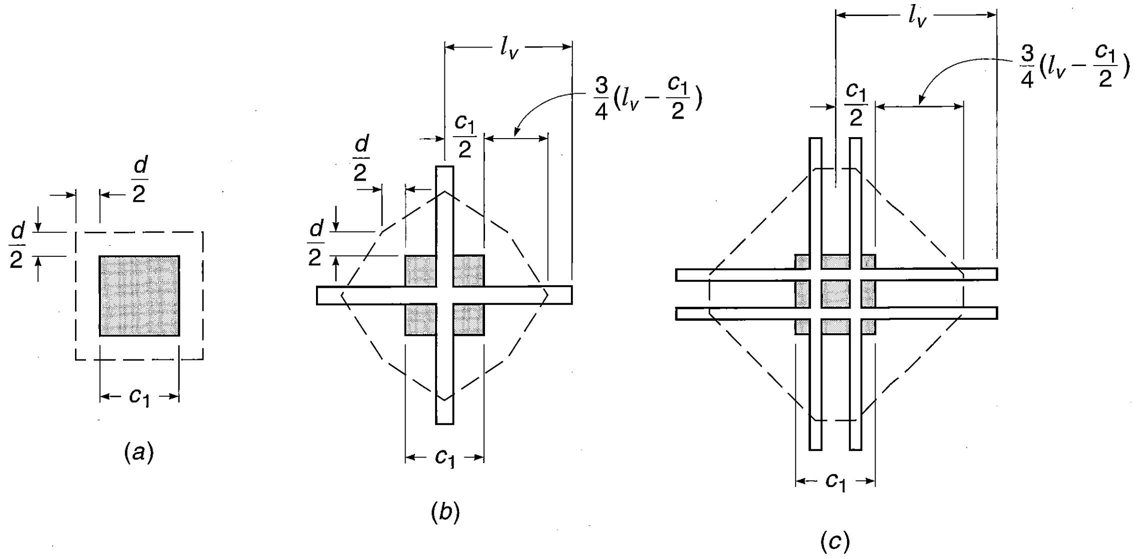

FIGURE 13.30
Critical sections for shear for flat plates: (*a*) no shearhead; (*b*) small shearhead; (*c*) large shearhead.

f. Design of Shearhead Reinforcement

If embedded structural steel shapes are used, as shown in Fig. 13.24*a* and *c*, the limiting value of V_n may be increased to $0.58\sqrt{f'_c}b_od$. As with the techniques described in Sections 13.10c, d, and e, such a shearhead, provided it is sufficiently stiff and strong, has the effect of moving the critical section out away from the column, as shown in Fig. 13.30. According to ACI Code 11.11.4, this critical section crosses each arm of the shearhead at a distance equal to three-quarters of the projection beyond the face of the support, and is defined so that the perimeter is a minimum. It need not approach closer than $d/2$ to the face of the support.

Moving the critical section out in this way provides the double benefit of increasing the effective perimeter b_o and decreasing the total shear force for which the slab must be designed. The nominal shear V_n at the new critical section must not be taken greater than $0.33\sqrt{f'_c}b_od$, according to ACI Code 11.11.4.

Tests reported in Ref. 13.18 indicate that throughout most of the length of a shearhead arm the shear is constant, and, further, that the part of the total shear carried by the shearhead arm is proportional to α_v, its relative flexural stiffness, compared with that of the surrounding concrete section:

$$\alpha_v = \frac{E_sI_s}{E_cI_c} \tag{13.13}$$

The concrete section is taken with an effective width of $c_2 + d$, where c_2 is the width of the support measured perpendicular to the arm direction. Properties are calculated for the cracked, transformed section, including the shearhead. The observation that shear is essentially constant, at least up to the diagonal cracking load, implies that the reaction is concentrated largely at the end of the arm. Thus, if the total shear at the support is V and if the shearhead has n identical arms (generally $n = 4$ for shearheads at interior columns), the constant shear force in each arm is equal to α_vV/n.

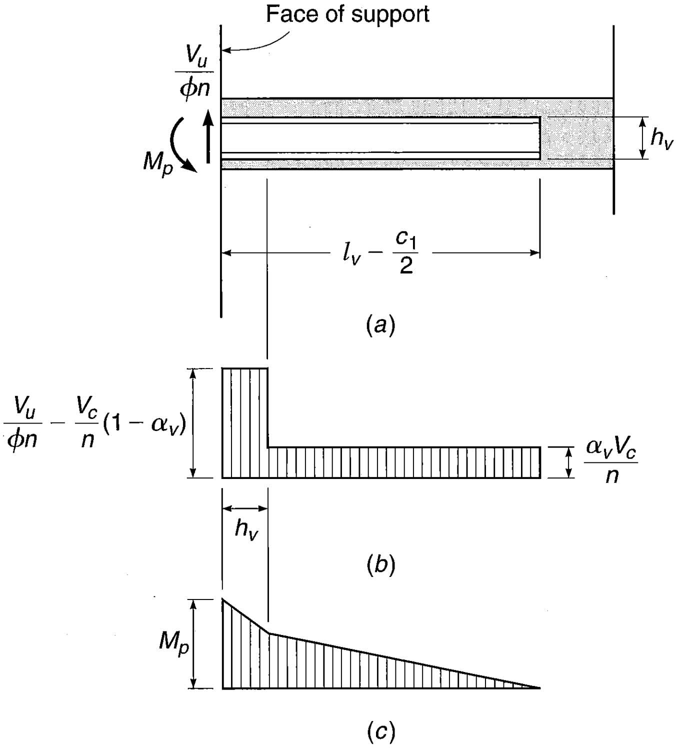

FIGURE 13.31
Stress resultants in shearhead arm: (*a*) shearhead arm; (*b*) shear; (*c*) moment.

If the load is increased past that which causes diagonal cracking immediately around the column, tests indicate that the increased shear above the cracking shear V_c is carried mostly by the steel shearhead, and that the shear force in the projecting arm within a distance from the column face equal to h_v, the depth of the arm, assumes a nearly constant value greater than $\alpha_v V/n$. This increased value is very nearly equal to the total shear per arm $V_u/\phi n$ minus the shear carried by the partially cracked concrete. The latter term is equal to $(V_c/n)(1 - \alpha_v)$; hence, the idealized shear diagram shown in Fig. 13.31*b* is obtained.

The moment diagram of Fig. 13.31*c* is obtained by integration of the shear diagram. If V_c is equal to $V_n/2 = V_u/2\phi$, as tests indicate for shearheads of common proportions, it is easily confirmed that the plastic moment M_p at the face of the support, for which the shearhead arm must be proportioned, is

$$M_p = \frac{V_u}{2\phi n}\left[h_v + \alpha_v\left(l_v - \frac{c_1}{2}\right)\right] \tag{13.14}$$

in which $\phi = 0.90$, the capacity reduction factor for tension-controlled members.

According to ACI Code 11.11.4, the value of α_v must be at least equal to 0.15; more flexible shearheads have proved ineffective. The compression flange must not be more than $0.3d$ from the bottom surface of the slab, and the steel shapes used must not be deeper than 70 times the web thickness.

For flexural design of the slab, moments found at the support centerline by the equivalent frame method are reduced to moments at the support face, assumed to be the critical section for moment. By the direct design method, support-face moments are calculated directly through the use of the clear-span distance. If shearheads are used, they have the effect of reducing the design moment in the column strips still further by increasing the effective support width. This reduction is proportional to the share of the load carried by the shearhead and to its size, and can be estimated conservatively (see Fig. 13.31*b* and *c*) by the expression

$$M_v = \frac{\phi \alpha_v V_u}{2n}\left(l_v - \frac{c_1}{2}\right) \tag{13.15}$$

where $\phi = 0.90$. According to ACI Code 11.11.4, the reduction may not be greater than 30 percent of the total design moment for the slab column strip, or greater than the change in column-strip moment over the distance l_v, or greater than M_p given by Eq. (13.14).

Limited test information pertaining to shearheads at a slab edge indicates that behavior may be substantially different due to torsional and other effects. If shearheads are to be used at an edge or corner column, special attention must be given to anchorage of the embedded steel within the column. The use of edge beams or a cantilevered slab edge may be preferred.

EXAMPLE 13.7 **Design of shearhead reinforcement.** A flat plate slab 190 mm thick is supported by 250 mm square columns and is reinforced for negative bending with No. 16 (No. 5) bars 125 mm on centers in each direction, with an average effective depth d of 150 mm. The concrete strength f'_c is 21 MPa. The slab must transfer a factored shear V_u of 475 kN to the column. What special slab reinforcement is required, if any, at the column to transfer the factored shear?

Solution. The nominal shear strength at the critical section $d/2$ from the face of the column is found from Eq. (13.11*a*) to be

$$V_c = 0.33\sqrt{21} \times 1600 \times 150 \times 10^{-3} = 363 \text{ kN}$$

and $\phi V_c = 0.75 \times 363 = 272$ kN. This is less than $V_u = 475$ kN, indicating that shear reinforcement is necessary. A shearhead similar to Fig. 13.24*a* will be used, fabricated from I-beam sections with $f_y = 345$ MPa. Maintaining 20 mm clearance below such steel, bar clearance at the top of the slab permits use of an I beam with a 115 mm depth; a nominal 100 mm section will be used. With such reinforcement, the upper limit of shear V_n on the critical section is $0.58\sqrt{21} \times 1600 \times 150 \times 10^{-3} = 638$ kN, and $\phi V_n = 0.75 \times 638 = 478$ kN, above the value of V_u to be resisted. The required perimeter b_o can be found by setting $V_u = \phi V_c$, where V_c is given by Eq. (13.11*a*):

$$b_o = \frac{V_u}{0.33\phi\sqrt{f'_c}d} = \frac{475 \times 10^3}{0.33 \times 0.75\sqrt{21} \times 150} = 2792 \text{ mm}$$

(Note that the actual shear force to be transferred at the critical section is slightly less than 475 kN because a part of the floor load is within the effective perimeter b_o; however, the difference is small except for very large shearheads.) The required projecting length l_v of the shearhead arm is found from geometry, with b_o expressed in terms of l_v.

$$b_o = 4\sqrt{2}\left[\frac{c_1}{2} + \frac{3}{4}\left(l_v - \frac{c_1}{2}\right)\right] = 2792 \text{ mm}$$

from which $l_v = 615$ mm. To determine the required plastic section modulus for the shear arm, it is necessary to assume a trial value of the relative stiffness α_v. After selecting 0.25 for trial, the required moment capacity is found from Eq. (13.14):

$$M_p = \frac{475}{8 \times 0.90}[100 + 0.25(615 - 125)] \times 10^{-3} = 14.7 \text{ kN-m}$$

A standard I beam S100 × 11.5, with yield stress of 345 MPa, provides 19.5 kN-m resistance and will tentatively be adopted. The E_sI_s value provided by the beam is 506×10^9 mm^2-N. The

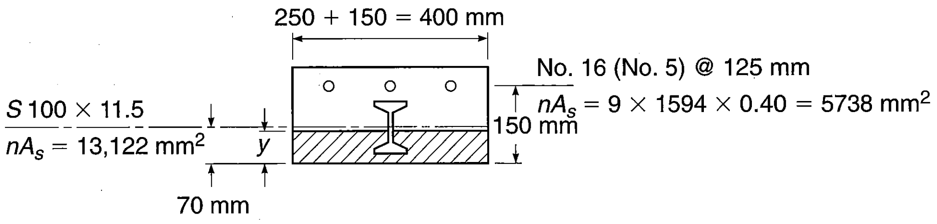
250 + 150 = 400 mm
No. 16 (No. 5) @ 125 mm
$nA_s = 9 \times 1594 \times 0.40 = 5738\ \text{mm}^2$
150 mm
$S\,100 \times 11.5$
$nA_s = 13{,}122\ \text{mm}^2$
y
70 mm

FIGURE 13.32
Effective section of slab.

effective cross section of the slab strip is shown in Fig. 13.32. Taking moments of the composite cracked section about the bottom surface to locate the neutral axis gives

$$y = \frac{5738 \times 150 + 13{,}122 \times 70 + 200y^2}{5738 + 13{,}122 + 400y}$$

from which $y = 58.3$ mm. The moment of inertia of the composite section is

$$I_c = \tfrac{1}{3}400 \times 58.3^3 + 5738 \times 91.7^2 + 9 \times 2.53 \times 10^6 + 1458 \times 11.7^2 = 97.6 \times 10^6\ \text{mm}^4$$

the flexural stiffness of the effective composite slab strip is

$$E_c I_c = 21.5 \times 10^3 \times 97.6 \times 10^6 = 2098 \times 10^9\ \text{mm}^2\text{-N}$$

and, from Eq. (13.13),

$$\alpha_v = \frac{506}{2098} = 0.24$$

This is greater than the specified minimum of 0.15 and close to the 0.25 value assumed earlier. The revised value of M_p is

$$M_p = \frac{475}{8 \times 0.90}[100 + 0.24(615 - 125)] \times 10^{-3} = 14.4\ \text{kN-m}$$

The 100 mm beam is adequate. The calculated length l_v of 615 mm will be retained. The reduction in column-strip moment in the slab may be based on this actual length. From Eq. (13.15),

$$M_v = \frac{0.90 \times 0.24 \times 475 \times 10^{-3}}{8}(615 - 125) = 6.28\ \text{kN-m}$$

This value is less than M_p, as required by specification, and must also be less than 30 percent of the design negative moment in the column strip and less than the change in the column-strip moment in the distance l_v.

13.11 TRANSFER OF MOMENTS AT COLUMNS

The analysis for punching shear in flat plates and flat slabs presented in Section 13.10 assumed that the shear force V_u was resisted by shearing stresses uniformly distributed around the perimeter b_o of the critical section, a distance $d/2$ from the face of the supporting column. The nominal shear strength V_c was given by Eqs. (13.11*a*), (13.11*b*), and (13.11*c*).

If significant moments are to be transferred from the slab to the columns, as would result from unbalanced gravity loads on either side of a column or from horizontal loading due to wind or seismic effects, the shear stress on the critical section is no longer uniformly distributed.

FIGURE 13.33
Transfer of moment from slab to column: (*a*) forces resulting from vertical load and unbalanced moment; (*b*) critical section for an interior column; (*c*) shear stress distribution for an interior column; (*d*) critical section for an edge column; (*e*) shear stress distribution for an edge column.

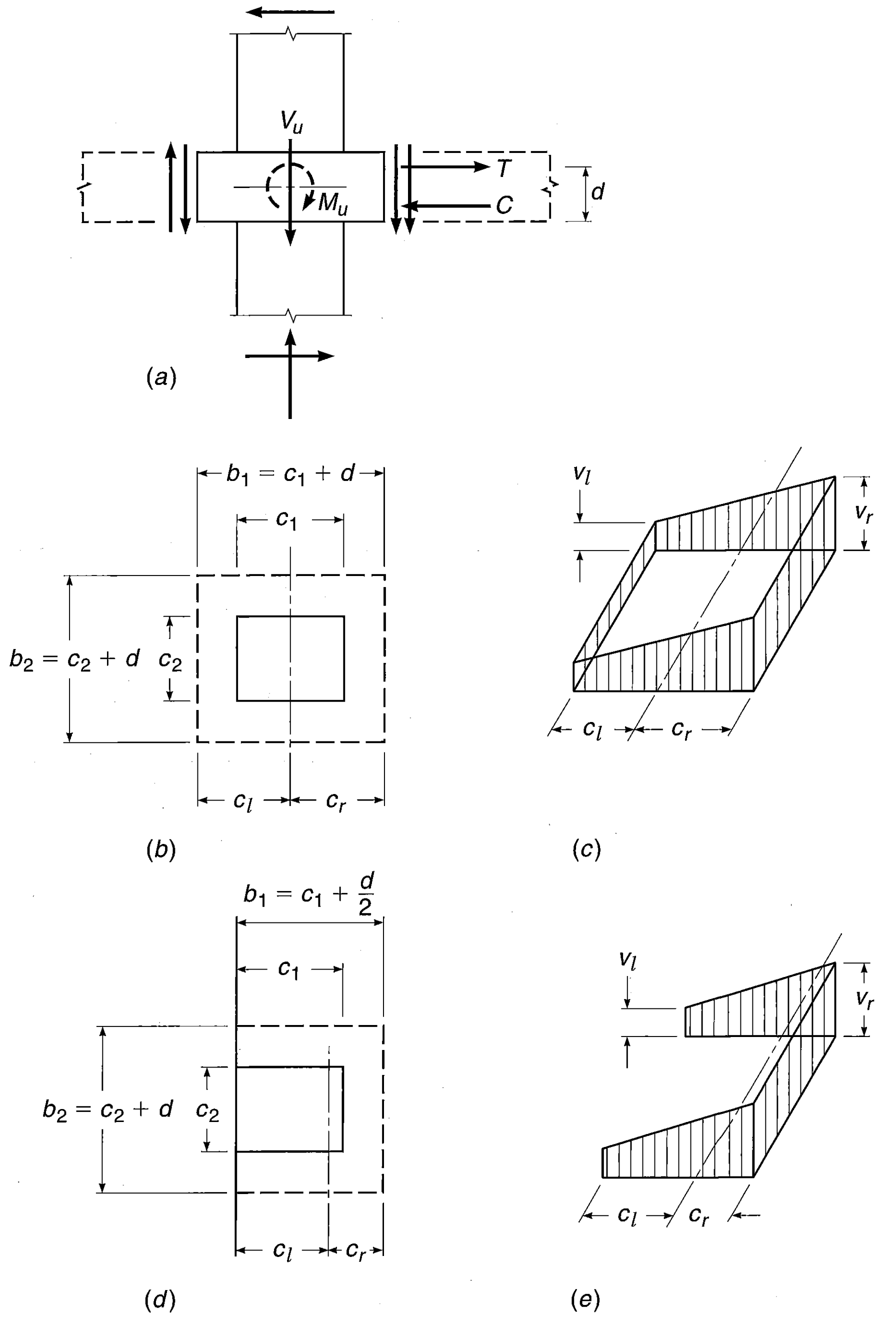

The situation can be modeled as shown in Fig. 13.33*a*. Here V_u represents the total vertical reaction to be transferred to the column, and M_u represents the unbalanced moment to be transferred, both at factored loads. The vertical force V_u causes shear stress distributed more or less uniformly around the perimeter of the critical section as assumed earlier, represented by the inner pair of vertical arrows, acting downward. The unbalanced moment M_u causes additional loading on the joint, represented by the outer pair of vertical arrows, which add to the shear stresses otherwise present on the right side, in the sketch, and subtract on the left side.

Tests indicate that for square columns about 60 percent of the unbalanced moment is transferred by flexure (forces T and C in Fig. 13.33*a*) and about 40 percent by shear stresses on the faces of the critical section (Ref. 13.24). For rectangular columns, it is reasonable to suppose that the portion transferred by flexure increases as the width of the critical section that resists the moment increases, i.e., as $c_2 + d$ becomes larger relative to $c_1 + d$ in Fig. 13.33*b*. According to ACI Code 13.5.3, the moment considered to be transferred by flexure is

$$M_{ub} = \gamma_f M_u \tag{13.16a}$$

where

$$\gamma_f = \frac{1}{1 + \frac{2}{3}\sqrt{b_1/b_2}} \tag{13.16b}$$

and b_1 = width of critical section for shear measured in direction of span for which moments are determined

b_2 = width of critical section for shear measured in direction perpendicular to b_1

The value of γ_f may be modified if certain conditions are met: For unbalanced moments about an axis parallel to the edge of exterior supports, γ_f may be increased to 1.0, provided that the factored shear V_u at the edge support does not exceed $0.75\phi V_c$ or at a corner support does not exceed $0.5\phi V_c$. For unbalanced moments at interior supports and about an axis perpendicular to the edge at exterior supports, γ_f may be increased up to 1.25 times the value in Eq. (13.16*b*), provided that $V_u \le 0.4\phi V_c$. In all of these cases, the net tensile strain ϵ_t calculated for the section within $1.5h$ on either side of the column or column capital must be at least 0.010.

The moment assumed to be transferred by shear, by ACI Code 11.11.7, is

$$M_{ub} = (1 - \gamma_f)M_u = \gamma_v M_u \tag{13.16c}$$

It is seen that for a square column Eqs. (13.16*a*), (13.16*b*), and (13.16*c*) indicate that 60 percent of the unbalanced moment is transferred by flexure and 40 percent by shear, in accordance with the available data. If b_2 is very large relative to b_1, nearly all of the moment is transferred by flexure.

The moment M_{ub} can be accommodated by concentrating a suitable fraction of the slab column-strip reinforcement near the column. According to ACI Code 13.5.3, this steel must be placed within a width between lines $1.5h$ on each side of the column or capital, where h is the total thickness of the slab or drop panel.

The moment M_{uv}, together with the vertical reaction delivered to the column, causes shear stresses assumed to vary linearly with distance from the centroid of the critical section, as indicated for an interior column by Fig. 13.33*c*. The stresses can be calculated from

$$v_l = \frac{V_u}{A_c} - \frac{M_{uv}c_l}{J_c} \tag{13.17a}$$

$$v_r = \frac{V_u}{A_c} + \frac{M_{uv}c_r}{J_c} \tag{13.17b}$$

where A_c = area of critical section = $2d[(c_1 + d) + (c_2 + d)]$

c_l, c_r = distances from centroid of critical section to left and right faces of section, respectively

J_c = property of critical section analogous to polar moment of inertia

For an interior column, the quantity J_c is

$$J_c = \frac{2d(c_1 + d)^3}{12} + \frac{2(c_1 + d)d^3}{12} + 2d(c_2 + d)\left(\frac{c_1 + d}{2}\right)^2 \qquad (13.18)$$

Note the implication, in the use of the parameter J_c in the form of a polar moment of inertia, that shear stresses indicated on the near and far faces of the critical section in Fig. 13.33*c* have horizontal as well as vertical components.

According to ACI Code 11.11.7, the maximum shear stress calculated by Eq. (13.17) must not exceed ϕv_n. For slabs without shear reinforcement, $\phi v_n = \phi V_c / b_o d$, where V_c is the smallest value given by Eqs. (13.11*a*), (13.11*b*), or (13.11*c*). For slabs with shear reinforcement other than shearheads, $\phi v_n = \phi(V_c + V_s)/b_o d$, where V_c and V_s are as established in Section 13.10c, d, or e. Where shearhead reinforcement (see Section 13.10f) is used, the sum of the shear stresses due to vertical load on the second critical section, near the end of the shearhead arms, and the shear stresses resulting from moment transfer about the centroid of the first critical section $d/2$ from the support faces must not exceed $0.33\phi\lambda\sqrt{f'_c}$. In support of the last calculation, ACI Commentary 11.11.7.3 notes that tests indicate the first critical section is appropriate for calculation of stresses caused by transfer of moments even when shearheads are used. Even though the critical sections for direct shear transfer and shear due to moment transfer differ, they coincide or are in close proximity at the column corners where failures initiate, and it is conservative to take the maximum shear as the sum of the two components.

Equations similar to those above can be derived for the edge columns shown in Fig. 13.33*d* and *e* or for a corner column. Although the centroidal distances c_l and c_r are equal for the interior column, this is not true for the edge column of Fig. 13.33*d* or for a corner column.

According to ACI Code 13.6.3.6, when the direct design method is used, the moment to be transferred between the slab and an edge column by shear is to be taken equal to $0.30M_o$, where M_o is found from Eq. (13.1). This is intended to compensate for assigning a high proportion of the static moment to the positive and interior negative moment regions according to Table 13.3, and to ensure that adequate shear strength is provided between the slab and the edge column, where unbalanced moment is high and the critical section width is reduced.

The application of moment to a column from a slab or beam introduces shear to the column also, as is clear from Fig. 13.33*a*. This shear must be considered in the design of lateral column reinforcement.

As pointed out in Section 13.10, most flat plate structures, if they are overloaded, fail in the region close to the column, where large shear and bending forces must be transferred. There has been much research aimed at developing improved design details for this region. The design engineer should consult Refs. 13.24 through 13.26 for additional specific information.

13.12 OPENINGS IN SLABS

Almost invariably, slab systems must include openings. These may be of substantial size, as required by stairways and elevator shafts, or they may be of smaller dimensions, such as those needed to accommodate heating, plumbing, and ventilating risers; floor and roof drains; and access hatches.

Relatively small openings usually are not detrimental in *beam-supported slabs*. As a general rule, the equivalent of the interrupted reinforcement should be added at the sides of the opening. Additional diagonal bars should be included at the corners to control the cracking that will almost inevitably occur there. The importance of small openings in *slabs supported directly by columns* (flat slabs and flat plates) depends upon the location of the opening with respect to the columns. From a structural point of view, they are best located away from the columns, preferably in the area common to the slab middle strips. Unfortunately, architectural and functional considerations usually cause them to be located close to the columns. In this case, the reduction in effective shear perimeter is the major concern, because such floors are usually shear-critical.

According to ACI Code 11.11.6, if the opening is close to the column (within 10 slab thicknesses or within the column strips), then that part of b_o included within the radial lines projecting from the opening to the centroid of the column should be considered ineffective. This is shown in Fig. 13.34, along with the effect of free edges on the perimeter of the critical section. If sheatheads (see Section 13.10f) are used under such circumstances, the reduction in width of the critical section is found in the same way, except that only one-half the perimeter included within the radial lines need be deducted.

With regard to flexural requirements, the total amount of steel required by calculation must be provided regardless of openings. Any steel interrupted by holes should be matched with an equivalent amount of supplementary reinforcement on either side, properly lapped to transfer stress by bond. Concrete compression area to provide the required strength must be maintained; usually this would be restrictive only

FIGURE 13.34
Effect of openings and free edges on the determination of the perimeter of the critical section for shear b_o.

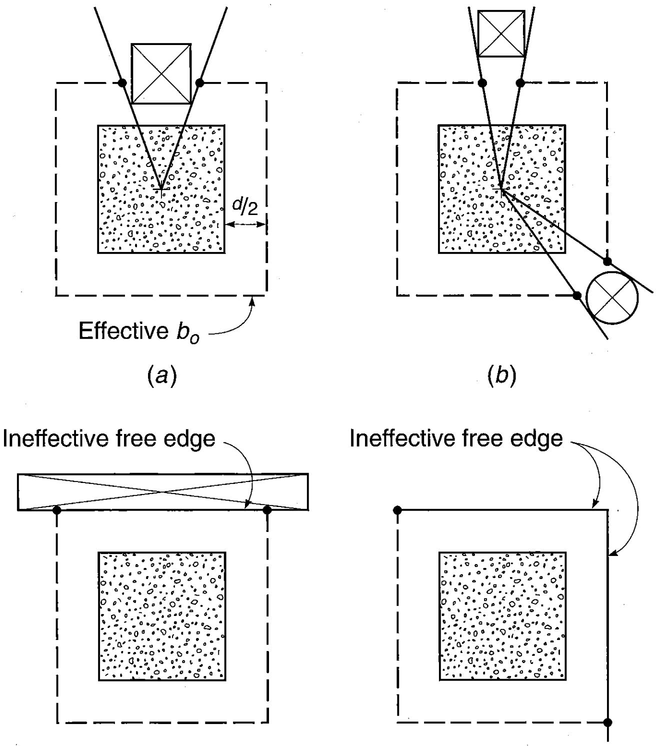

near the columns. According to ACI Code 13.4.2, openings of any size may be located in the area common to intersecting middle strips. In the area common to intersecting column strips, not more than one-eighth of the width of the column strip in either span can be interrupted by openings. In the area common to one middle strip and one column strip, not more than one-quarter of the reinforcement in either strip may be interrupted by the opening.

ACI Code 13.4.1 permits openings of *any* size if it can be shown by analysis that the strength of the slab is at least equal to that required and that all serviceability conditions, i.e., cracking and deflection limits, are met. The *strip method* of analysis and design for openings in slabs, by which specially reinforced integral beams, or *strong bands*, of depth equal to the slab depth are used to frame the openings, will be described in detail in Chapter 15. Very large openings should preferably be framed by beams or slab bands of increased depth to restore, as nearly as possible, the continuity of the slab. The beams must be designed to carry a portion of the floor load, in addition to loads applied directly by partition walls, elevator support beams, or stair slabs.

13.13 DEFLECTION CALCULATIONS

The deflection of a uniformly loaded flat plate, flat slab, or two-way slab supported by beams on column lines can be calculated by an equivalent frame method that corresponds with the method for moment analysis described in Section 13.9 (Ref. 13.27). The definition of column and middle strips, the longitudinal and transverse moment distribution coefficients, and many other details are the same as for the moment analysis. Following the calculation of deflections by this means, they can be compared directly with limiting values like those of Table 6.2, which are applicable to slabs as well as to beams, according to the ACI Code.

A slab region bounded by column centerlines is shown in Fig. 13.35. While no column-line beams, drop panels, or column capitals are shown, the presence of any of these introduces no fundamental complication.

The deflection calculation considers the deformation of such a typical region in one direction at a time, after which the contributions from each direction are added to obtain the total deflection at any point of interest.

In reference to Fig. 13.35*a*, the slab is considered to act as a broad, shallow beam of width equal to the panel dimension l_y and having the span l_x. Initially the slab is considered to rest on unyielding support lines at $x = 0$ and $x = l_x$. Because of variation of moment as well as flexural stiffness across the width of the slab, not all unit strips in the X direction will deform identically. Typically the slab curvature in the middle-strip region will be less than that in the region of the column strips because the middle-strip moments are less. The result is as indicated in Fig. 13.35*a*.

Next the slab is analyzed for bending in the Y direction (Fig. 13.35*b*). Once again the effect of transverse variation of bending moment and flexural rigidity is seen.

The actual deformed shape of the panel is represented in Fig. 13.35*c*. The midpanel deflection is the sum of the midspan deflection of the column strip in one direction and that of the middle strip in the other direction; i.e.,

$$\Delta_{\max} = \Delta_{cx} + \Delta_{my} \tag{13.19a}$$

or

$$\Delta_{\max} = \Delta_{cy} + \Delta_{mx} \tag{13.19b}$$

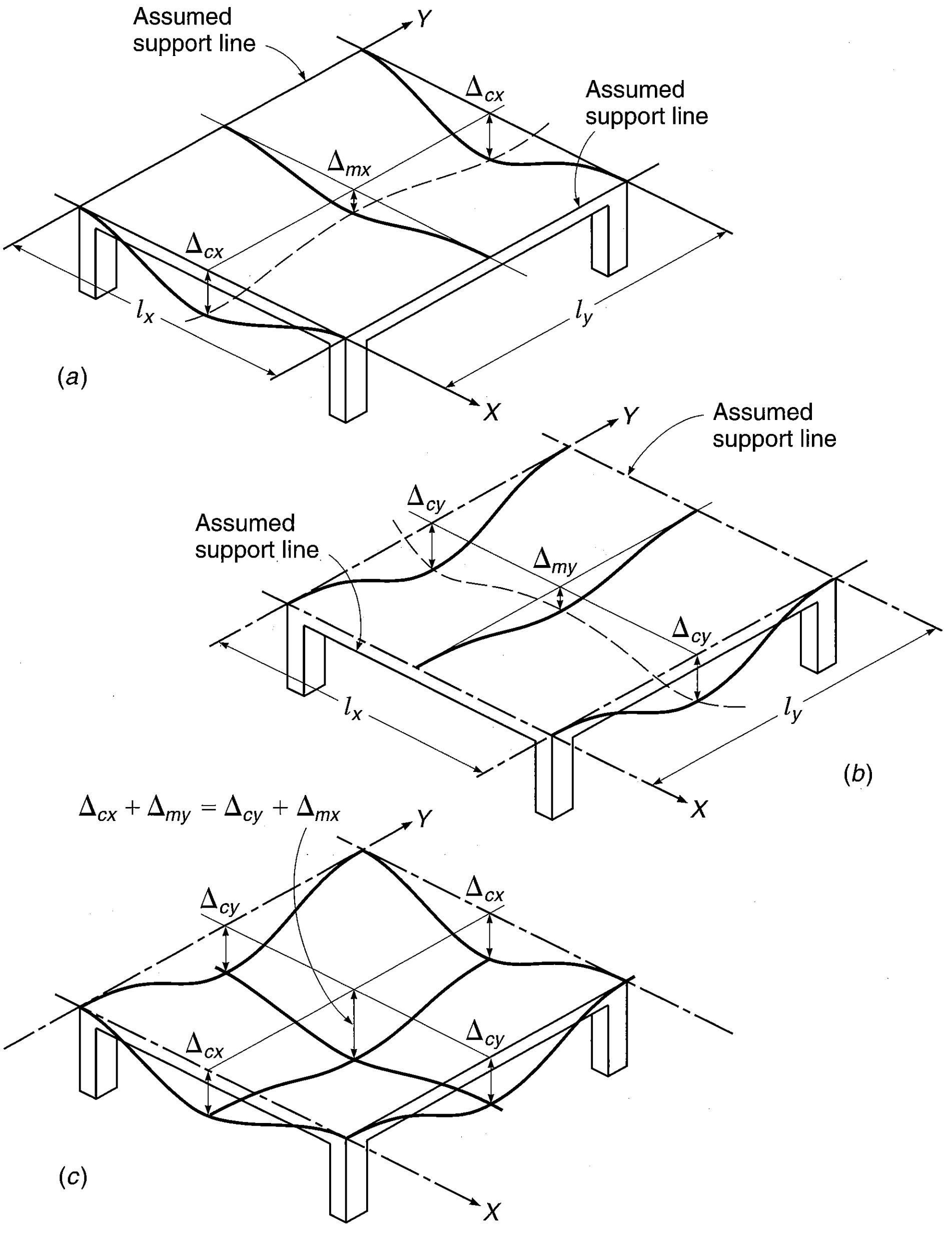
Assumed support line
Y
Δ_{cx}
Assumed support line
Δ_{mx}
Δ_{cx}
l_x
l_y
(a)
X
Y
Assumed support line
Δ_{cy}
Assumed support line
Δ_{my}
Δ_{cy}
l_x
l_y
(b)
X
$\Delta_{cx} + \Delta_{my} = \Delta_{cy} + \Delta_{mx}$
Y
Δ_{cy}
Δ_{cx}
Δ_{cx}
Δ_{cy}
(c)
X

FIGURE 13.35
Basis of equivalent frame method for deflection analysis: (*a*) *X* direction bending; (*b*) *Y* direction bending; (*c*) combined bending.

In calculations of the deformation of the slab panel in either direction, it is convenient first to assume that it deforms into a cylindrical surface, as it would if the bending moment at all sections were uniformly distributed across the panel width and if lateral bending of the panel were suppressed. The supports are considered to be fully fixed against both rotation and vertical displacement at this stage. Thus, a *reference deflection* is computed:

$$\Delta_{f,\mathrm{ref}} = \frac{wl^4}{384E_cI_{\mathrm{frame}}} \tag{13.20}$$

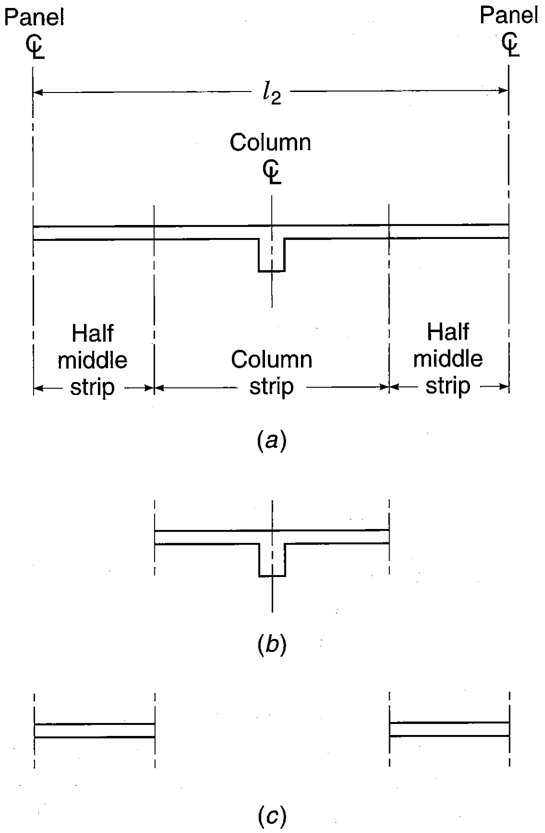

FIGURE 13.36
Effective cross sections for deflection calculations: (*a*) full-width frame; (*b*) column strip; (*c*) middle strips.

where w is the load per meter along the span of length l and I_{frame} is the moment of inertia of the full-width panel (Fig. 13.36*a*) including the contribution of the column-line beam or drop panels and column capitals if present.

The effect of the actual moment variation across the width of the panel and the variation of stiffness due to beams, variable slab depth, etc., are accounted for by multiplying the reference deflection by the ratio of M/EI for the respective strips to that of the full-width frame:

$$\Delta_{f,\text{col}} = \Delta_{f,\text{ref}} \frac{M_{\text{col}}}{M_{\text{frame}}} \frac{E_c I_{\text{frame}}}{E_c I_{\text{col}}} \tag{13.21a}$$

$$\Delta_{f,\text{mid}} = \Delta_{f,\text{ref}} \frac{M_{\text{mid}}}{M_{\text{frame}}} \frac{E_c I_{\text{frame}}}{E_c I_{\text{mid}}} \tag{13.21b}$$

The subscripts relate the deflection Δ, the bending moment M, or the moment of inertia I to the full-width frame, column strip, or middle strip, as shown in Fig. 13.36*a, b,* and *c*, respectively.

The moment ratios $M_{\text{col}}/M_{\text{frame}}$ and $M_{\text{mid}}/M_{\text{frame}}$ are identical to the lateral moment distribution factors already found for the flexural analysis (see Table 13.4). A minor complication results from the fact that the lateral distribution of bending moments, according to the ACI Code, is not the same at the negative and positive-moment sections. However, it appears consistent with the degree of accuracy usually required, as well as consistent with deflection methods endorsed elsewhere in the ACI Code, to use a simple average of lateral distribution coefficients for the negative and positive portions of each strip.

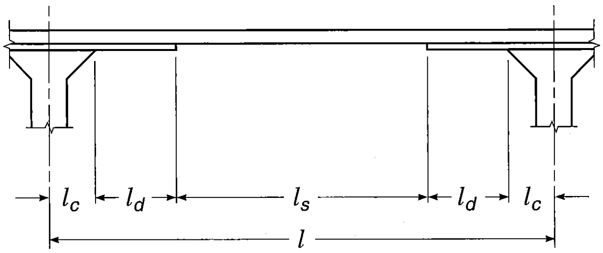

FIGURE 13.37
Flat slab span with variable moment of inertia.

The presence of drop panels or column capitals in the column strip of a flat slab floor requires consideration of the variation of the moment of inertia in the span direction (see Fig. 13.37). It is suggested in Ref. 13.28 that a weighted average moment of inertia be used in such cases:

$$I_{\text{av}} = 2\frac{l_c}{l}I_c + 2\frac{l_d}{l}I_d + \frac{l_s}{l}I_s \tag{13.22}$$

where I_c = moment of inertia of slab including both drop panel and capital
I_d = moment of inertia of slab with drop panel only
I_s = moment of inertia of slab alone

Span distances are defined in Fig. 13.37.

Next it is necessary to correct for the rotations of the equivalent frame at the supports, which until now were considered fully fixed. If the ends of the columns are considered fixed at the floor above and floor below, as usual for frame analysis, the rotation of the column at the floor divided by the stiffness of the equivalent column is

$$\theta = \frac{M_{\text{net}}}{K_{ec}} \tag{13.23}$$

where θ = angle change, radians
M_{net} = difference in floor moments to left and right of column
K_{ec} = stiffness of equivalent column (see Section 13.9c)

In some cases, the connection between the floor slab and column transmits negligible moment, as for lift slabs; thus $K_{ec} = 0$. The flexural analysis will indicate that the net moment is zero. The support rotation can be found in such cases by applying the moment-area theorems, taking moments of the M/EI area about the far end of the span and dividing by the span length.

Once the rotation at each end is known, the associated midspan deflection of the equivalent frame can be calculated. It is easily confirmed that the midspan deflection of a member experiencing an end rotation of θ rad, the far end being fixed, is

$$\Delta_\theta = \frac{\theta l}{8} \tag{13.24}$$

Thus the total deflection at midspan of the column strip or middle strip is the sum of the three parts

$$\Delta_{\text{col}} = \Delta_{f,\text{col}} + \Delta_{\theta l} + \Delta_{\theta r} \tag{13.25a}$$

$$\Delta_{\text{mid}} = \Delta_{f,\text{mid}} + \Delta_{\theta l} + \Delta_{\theta r} \tag{13.25b}$$

where the subscripts l and r refer to the left and right ends of the span, respectively.

The calculations described are repeated for the equivalent frame in the second direction of the structure, and the total deflection at midpanel is obtained by summing the column-strip deflection in one direction and the middle-strip deflection in the other, as indicated by Eqs. (13.19).

The midpanel deflection should be the same whether calculated by Eq. (13.19*a*) or Eq. (13.19*b*). Actually, a difference will usually be obtained because of the approximate nature of the calculations. For very rectangular panels, the main contribution to midpanel deflection is that of the long-direction column strip. Consequently, the midpanel deflection is best found by summing the deflections of the long-direction column strip and the short-direction middle strip. However, for exterior panels, the important contribution is from the column strips perpendicular to the discontinuous edge, even though the long side of the panel may be parallel to that edge.

In slabs, as in beams, the effect of concrete cracking is to reduce the flexural stiffness. According to ACI Code 9.5.3, the effective moment of inertia given by Eq. (6.8) is applicable to slabs as well as beams, although other values may be used if results are in reasonable agreement with tests. In most cases, two-way slabs will be essentially uncracked at service loads, and it is satisfactory to base deflection calculations on the uncracked moment of inertia I_g (see Ref. 13.27 for comparison with tests). In Ref. 13.29, Branson suggests the following refinements: (1) for slabs without beams, use I_g for all dead load deflections; for dead plus live load deflections, use I_g for middle strips and I_e for column strips; (2) for slabs with beams, use I_g for all dead load deflections; for dead plus live load deflections, use I_g for column strips and I_e for middle strips. For continuous spans, I_e can be based on the midspan positive moment without serious error.

The deflections calculated using the procedure described are short-term deflections. Long-term slab deflections can be calculated by multiplying the short-term deflections by the factor λ_Δ of Eq. (6.11), as for beams. Because compression steel is seldom used in slabs, a multiplier of 2.0 results. Test evidence and experience with actual structures indicate that this may seriously underestimate long-term slab deflections, and multipliers for long-term deflection from 2.5 to 4.0 have been recommended (Refs. 13.29 to 13.31). A multiplier of 3.0 gives acceptable results in most cases.

It should be recognized that the prediction of slab deflections, both initial elastic and long-term, is complicated by the many uncertainties associated with actual building construction. Loading history, particularly during construction, has a profound effect on final deflections (Ref. 13.32). Construction loads can equal or exceed the service live load. Such loads may include the weight of stacked building material and usually include the weight of slabs above the one cast earlier, applied through shoring and reshoring to the lower slab. Because construction loads are applied to immature concrete in the slabs, the immediate elastic deflections are large, and, upon removal of the construction loads, elastic recovery is less than the initial elastic deflection because E_c increases with age. Cracking resulting from construction loading does not disappear with removal of the temporary load and may result in live load deflections greater than expected. Creep during construction loading may be greater than expected because of the early age of the concrete when loaded. Shrinkage deflections of thin slabs are often of the same order of magnitude as the elastic deflections, and some cases must be calculated separately.

It is important to recognize that both initial and time-dependent slab deflections are subject to a high degree of variability. Calculated deflections are an estimate, at best, and considerable deviation from calculated values is to be expected in actual structures.

EXAMPLE 13.8

Calculation of deflections. Find the deflections at the center of the typical exterior panel of the two-way floor designed in Example 13.2 due to dead and live loads. The live load may be considered a short-term load and will be distributed uniformly over all panels. The floor will support nonstructural elements that are likely to be damaged by large deflections. Take E_c = 25,000 MPa.

Solution. The elastic deflection due to the self-weight of 4.2 kN/m^2 will be found, after which the additional long-term dead load deflection can be found by applying the factor $\lambda = 3.0$, and the short-term live load deflection due to 6.9 kN/m^2 by direct proportion.

The effective concrete cross sections, upon which moment of inertia calculations will be based, are shown in Fig. 13.38 for the full-width frame, the column strip, and the middle strips, for the short-span and long-span directions. Note that the width of the column strip in both directions is based on the shorter panel span, according to the ACI Code. The values of moment of inertia are as follows:

	Short Direction	Long Direction
I_{frame}	10.9×10^9 mm^4	10.1×10^9 mm^4
I_{col}	8.2×10^9 mm^4	8.2×10^9 mm^4
I_{mid}	2.0×10^9 mm^4	1.34×10^9 mm^4

First calculating the deflections of the floor in the *short-span direction* of the panel, from Eq. (13.20) the reference deflection is

$$\Delta_{f,\text{ref}} = \frac{4.2 \times 10^{-3} \times 7500 \times 6000^4}{384 \times 25 \times 10^3 \times 10.9 \times 10^9} = 0.39 \text{ mm}$$

(Note that the centerline span distance is used here, although clear span was used in the moment analysis to approximate the moment reduction due to support width, according to ACI Code procedures.) From the moment analysis in the short-span direction, it was concluded that

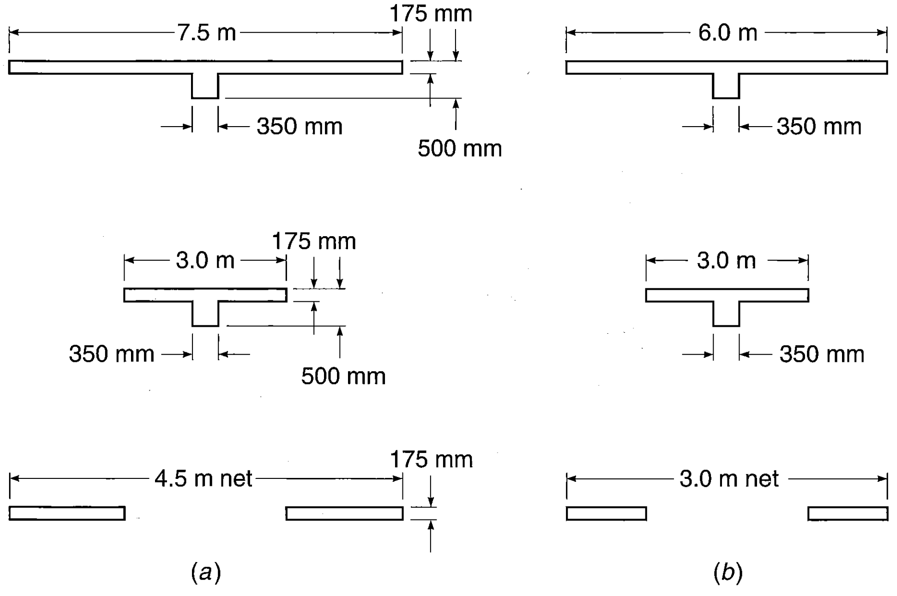

FIGURE 13.38
Cross-sectional dimensions for deflection example: (*a*) short-span direction frame, column strip, and middle strip; (*b*) long-span direction frame, column strip, and middle strip.

68 percent of the moment at both negative and positive sections was taken by the column strip and 32 percent by the middle strips. Accordingly, from Eqs. (13.21*a*) and (13.21*b*),

$$\Delta_{f,\mathrm{col}} = 0.39 \times 0.68 \times \frac{10.9}{8.2} = 0.35 \text{ mm}$$

$$\Delta_{f,\mathrm{mid}} = 0.39 \times 0.32 \times \frac{10.9}{2.0} = 0.68 \text{ mm}$$

For the panel under investigation, which is fully continuous over both supports in the short direction, it may be assumed that support rotations are negligible; consequently, $\Delta_{\theta t}$ and $\Delta_{\theta r} = 0$, and from Eqs. (13.25*a*) and (13.25*b*),

$$\Delta_{\mathrm{col}} = 0.35 \text{ mm}$$

$$\Delta_{\mathrm{mid}} = 0.68 \text{ mm}$$

Now calculating the deformations in the *long direction* of the panel gives the reference deflection

$$\Delta_{f,\mathrm{ref}} = \frac{4.2 \times 10^{-3} \times 6000 \times 7500^4}{384 \times 25 \times 10^3 \times 10.9 \times 10^9} = 0.76 \text{ mm}$$

From the moment analysis it was found that the column strip would take 91 percent of the exterior negative moment, 81 percent of the positive moment, and 81 percent of the interior negative moment. Thus the average lateral distribution factor for the column strip is

$$\left(\frac{0.91 + 0.81}{2} + 0.81\right)\frac{1}{2} = 0.84$$

or 84 percent, while the middle strips are assigned 16 percent. Then from Eqs. (13.21*a*) and (13.21*b*),

$$\Delta_{f,\mathrm{col}} = 0.76 \times 0.84 \times \frac{10.8}{8.2} = 0.84 \text{ mm}$$

$$\Delta_{f,\mathrm{mid}} = 0.76 \times 0.16 \times \frac{10.8}{8.2} = 1.07 \text{ mm}$$

While rotation at the interior column may be considered negligible, rotation at the exterior column cannot. For the dead load of the slab, the full static moment is

$$M_o = \tfrac{1}{8} \times 4.2 \times 6 \times 7.5^2 = 177 \text{ kN-m}$$

It was found that 16 percent of the static moment, or 28.3 kN-m, should be assigned to the exterior support section. The resulting rotation is found from Eq. (13.23). It is easily confirmed that the stiffness of the equivalent column (see Section 13.9c) is $2.64 \times 25 \times 10^9$ kN-m/rad; hence

$$\theta = \frac{28.3 \times 10^6}{2.64 \times 25 \times 10^9} = 0.00043 \text{ rad}$$

From Eq. (13.24), the corresponding midpanel deflection component is

$$\Delta_{\theta l} = \frac{0.00043 \times 7500}{8} = 0.40 \text{ mm}$$

Thus, from Eqs. (13.25*a*) and (13.25*b*), the deflections of the column and middle strips in the long direction are

$$\Delta_{\mathrm{col}} = 0.84 + 0.40 = 1.24 \text{ mm}$$

$$\Delta_{\mathrm{mid}} = 1.07 + 0.40 = 1.47 \text{ mm}$$

and from Eq. (13.19*a*) the short-term midpanel deflection due to self-weight is

$$\Delta_{\max} = 1.24 + 0.68 = 1.92 \text{ mm}$$

The long-term deflection due to dead load is 3.0 × 1.92 = 5.76 mm, and the short-term live load deflection is 1.92 × 6.9/4.2 = 3.15 mm.

The ACI limiting value for the present case is found to be 1/480 times the span, or 6000/480 = 12.5 mm, based on the sum of the long-time deflection due to sustained load and the immediate deflection due to live load. The sum of these deflection components in the present case is

$$\Delta_{\max} = 5.76 + 3.15 = 8.91 \text{ mm}$$

well below the permissible value.

13.14 ANALYSIS FOR HORIZONTAL LOADS

Either the direct design method or the equivalent frame method, described in the preceding sections of this chapter, may be used for the analysis of two-way slab systems for gravity loads, according to ACI Code 13.5.1. However, the ACI Code provisions are not meant to apply to the analysis of buildings subject to lateral loads, such as loads caused by wind or earthquake. For lateral load analysis, the designer may select any method that is shown to satisfy equilibrium and geometric compatibility, and to give results that are in reasonable agreement with available test data. The results of the lateral load analysis may then be combined with those from the vertical load analysis, according to ACI Code 13.5.1.

Plane frame analysis, with the building assumed to consist of parallel frames each bounded laterally by the panel centerlines on either side of the column lines, has often been used in analyzing unbraced buildings for horizontal loads, as well as vertical. For vertical load analysis by the equivalent frame method, a single floor is usually studied as a substructure with attached columns assumed fully fixed at the floors above and below, but for horizontal frame analysis the equivalent frame includes all floors and columns, extending from the bottom to the top of the structure.

The main difficulty in equivalent frame analysis for horizontal loads lies in modeling the stiffness of the region at the beam-column (or slab-beam-column) connections. Transfer of forces in this region involves bending, torsion, shear, and axial load, and is further complicated by the effects of concrete cracking in reducing stiffness, and reinforcement in increasing it. Frame moments are greatly influenced by horizontal displacements at the floors, and a conservatively low value of stiffness should be used to ensure that a reasonable estimate of drift is included in the analysis.

While a completely satisfactory basis for modeling the beam-column joint stiffness has not been developed, at least two methods have been used in practice (Ref. 13.33). The first is based on an equivalent beam width αl_2, less than the actual width, to reduce the stiffness of the slab for purposes of analysis. Figure 13.39*a* shows a plate fixed at the far edge and supported by a column of width c_2 at the near side. If a rotation θ is imposed at the column, the plate rotation along the axis A will vary as shown by Fig. 13.39*a*, from θ at the column to smaller values away from the column. An equivalent width factor α is obtained from the requirement that the stiffness of a prismatic beam of width αl_2 must equal the stiffness of the plate of width l_2. This equality is obtained if the areas under the two rotation diagrams of Fig. 13.39*b* are equal. Thus the frame analysis is based on a reduced slab (or slab-beam) stiffness found using αl_2

FIGURE 13.39
Equivalent beam width for horizontal load analysis.

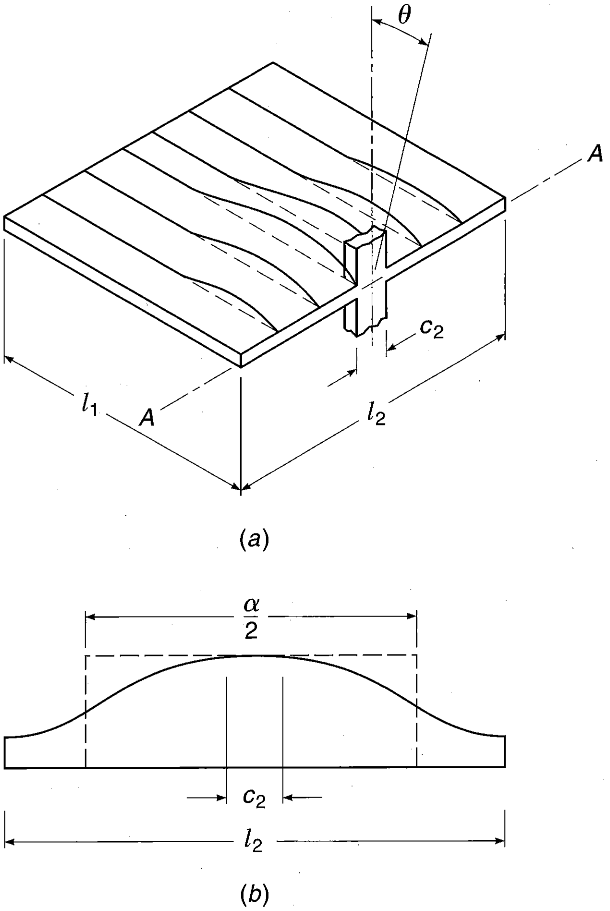

rather than l_2. Comparative studies indicate that, for flat plate floors, a value for α between 0.25 and 0.50 may be used (Ref. 13.33).

Alternatively, the beam-column stiffness can be modeled based on a transverse torsional member corresponding to that used in deriving the stiffness of the equivalent column for the vertical load analysis of two-way slabs by the equivalent frame method (see Section 13.9c). Rotational stiffness of the joint is a function of the flexural stiffness of the columns framing into the joint from above and below and the torsional stiffness of the transverse strip of slab or slab beam at the column. The equivalent column stiffness is found from Eq. (13.9) and the torsional stiffness from Eq. (13.10), as before.

Finally, for frames in which two-way systems act as primary members resisting lateral loads, ACI Code 13.3.8 requires that the lengths of reinforcement be determined by analysis because the lengths shown in Fig. 13.14 may not be adequate. The values in Fig. 13.14, however, are retained as minimum values.

REFERENCES

13.1. ACI Committee 360, *Design of Slabs-on-Ground* (ACI 360R-06), American Concrete Institute, Farmington Hills, MI, 2006.
13.2. W. L. Gamble, "Moments in Beam-Supported Slabs," *J. ACI,* vol. 69, no. 3, 1972, pp. 149–157.

13.3. J. R. Nichols, "Statical Limitations upon the Steel Requirement in Reinforced Concrete Flat Slab Floors," *Trans. ASCE*, vol. 77, 1914, pp. 1670–1736.

13.4. D. S. Hatcher, M. A. Sozen, and C. P. Siess, "Test of a Reinforced Concrete Flat Plate," *J. Struct. Div.,* ASCE, vol. 91, no. ST5, 1965, pp. 205–231.

13.5. S. A. Guralnick and R. W. LaFraugh, "Laboratory Study of a Forty-Five Foot Square Flat Plate Structure," *J. ACI*, vol. 60, no. 9, 1963, pp. 1107–1185.

13.6. D. S. Hatcher, M. A. Sozen, and C. P. Siess, "Test of a Reinforced Concrete Flat Slab," *J. Struct. Div.,* ASCE, vol. 95, no. ST6, 1969, pp. 1051–1072.

13.7. J. O. Jirsa, M. A. Sozen, and C. P. Siess, "Test of a Flat Slab Reinforced with Welded Wire Fabric," *J. Struct. Div.,* ASCE, vol. 92, no. ST3, 1966, pp. 199–224.

13.8. W. L. Gamble, M. A. Sozen, and C. P. Siess, "Tests of a Two-Way Reinforced Concrete Floor Slab," *J. Struct. Div.,* ASCE, vol. 95, no. ST6, 1969, pp. 1073–1096.

13.9. M. D. Vanderbilt, M. A. Sozen, and C. P. Siess, "Test of a Modified Reinforced Concrete Two-Way Slab," *J. Struct. Div.,* ASCE, vol. 95, no. ST6, 1969, pp. 1097–1116.

13.10. W. L. Gamble, "Moments in Beam-Supported Slabs," *J. ACI*, vol. 69, no. 3, 1972, pp. 149–157.

13.11. J. O. Jirsa, M. A. Sozen, and C. P. Siess, "Pattern Loadings on Reinforced Concrete Floor Slabs," *J. Struct. Div.,* ASCE, vol. 95, no. ST6, 1969, pp. 1117–1137.

13.12. D. Peabody, Jr., "Continuous Frame Analysis of Flat Slabs," *J. Boston Society Civ. Eng.*, January 1948.

13.13. W. G. Corley, M. A. Sozen, and C. P. Siess, "The Equivalent Frame Method for Reinforced Concrete Slabs," Univ. Ill. Dept. Civ. Eng. Struct. Res. Series 218, June 1961.

13.14. W. G. Corley and J. O. Jirsa, "Equivalent Frame Analysis for Slab Design," *J. ACI*, vol. 67, no. 11, 1970, pp. 875–884.

13.15. ASCE-ACI Task Committee 426, "The Shear Strength of Reinforced Concrete Members—Slabs," *J. Struct. Div.,* ASCE, vol. 100, no. ST8, 1974, pp. 1543–1591.

13.16. N. M. Hawkins, H. B. Fallsen, and R. C. Hinojosa, "Influence of Column Rectangularity on the Behavior of Flat Plate Structures," in *Cracking, Deflection, and Ultimate Load of Concrete Slab Systems*, ACI Publication SP-30, 1971, p. 127.

13.17. M. D. Vanderbilt, "Shear Strength of Continuous Plates," *J. Struct. Div.,* ASCE, vol. 98, no. ST5, 1972, pp. 961–973.

13.18. W. G. Corley and N. M. Hawkins, "Shearhead Reinforcement for Slabs," *J. ACI*, vol. 65, no. 10, 1968, pp. 811–824.

13.19. N. W. Hawkins, D. Mitchell, and S. N. Hanna, "Effects of Shear Reinforcement on the Reversed Cyclic Loading Behavior of Flat Plate Structures," *Can. J. Civ. Eng.*, vol. 2, no. 4, 1975, pp. 572–582.

13.20. A. Ghali, "An Efficient Solution to Punching of Slabs," *Concr. Intl.*, vol. 11, no. 6, 1989, pp. 50–54.

13.21. A. A. Elgabry and A. Ghali, "Design of Stud-Shear Reinforcement for Slabs," *ACI Struct. J.*, vol. 87, no. 3, 1990, pp. 350–361.

13.22. A. S. Mokhtar, A. Ghali, and W. Dilger, "Stud Shear Reinforcement for Flat Concrete Plates," *J. ACI*, vol. 82, no. 5, 1985, pp. 676–683.

13.23. A. A. Elgabry and A. Ghali, "Tests on Concrete Slab-Column Connections with Stud Shear Reinforcement Subjected to Shear-Moment Transfer," *ACI Struct. J.*, vol. 84, no. 5, 1987, pp. 433–442.

13.24. N. M. Hawkins, A. Bao, and J. Yamazaki, "Moment Transfer from Concrete Slabs to Columns," *ACI Struct. J.*, vol. 86, no. 6, 1989, pp. 705–716.

13.25. "Recommendations for Design of Slab-Column Connections in Monolithic Reinforced Concrete Structures," reported by ACI-ASCE Committee 352, *ACI Struct. J.*, vol. 85, no. 6, 1988, pp. 675–696.

13.26. J. P. Moehle, M. E. Kreger, and R. Leon, "Background to Recommendations for Design of Reinforced Concrete Slab-Column Connections," *ACI Struct. J.*, vol. 85, no. 6, 1988, pp. 636–644.

13.27. A. H. Nilson and D. B. Walters, "Deflection of Two-Way Floor Systems by the Equivalent Frame Method," *J. ACI*, vol. 72, no. 5, May 1975, pp. 210–218.

13.28. E. S. Hoffman, D. P. Gustafson, and A. J. Gouwens, *Structural Design Guide to the ACI Building Code*, 4th ed., Kluwer Academic Publishers, Boston, 1998.

13.29. D. E. Branson, *Deformation of Concrete Structures*, McGraw-Hill, New York, 1977.

13.30. P. J. Taylor and J. L. Heiman, "Long-Term Deflection of Reinforced Concrete Flat Slabs and Plates," *J. ACI*, vol. 74, no. 11, 1977, pp. 556–561.

13.31. C. J. Graham and A. Scanlon, "Long-Time Multipliers for Estimating Two-Way Slab Deflections," *J. ACI*, vol. 83, no. 6, 1986, pp. 899–908.

13.32. N. J. Gardner and A. Scanlon, "Long-Term Deflections of Two-Way Slabs," *Concr. Intl.*, vol. 12, no. 1, 1990, pp. 63–67.

13.33. M. D. Vanderbilt and W. G. Corley, "Frame Analysis of Concrete Buildings," *Concr. Intl.*, vol. 5, no. 12, 1983, pp. 33–43.

PROBLEMS

13.1. A footbridge is to be built, consisting of a one-way solid slab spanning 5 m between masonry abutments, as shown in Fig. P13.1. A service live load of 5 kN/m^2 must be carried. In addition, a 9 kN concentrated load, assumed to be uniformly distributed across the bridge width, may act at any location on the span. A 50 mm asphalt wearing surface will be used, weighing 1 kN/m^2. Precast concrete curbs are attached so as to be nonstructural. Prepare a design for the slab, using material strengths $f_y = 420$ MPa and $f_c' = 28$ MPa, and summarize your results in the form of a sketch showing all concrete dimensions and reinforcement.

FIGURE P13.1

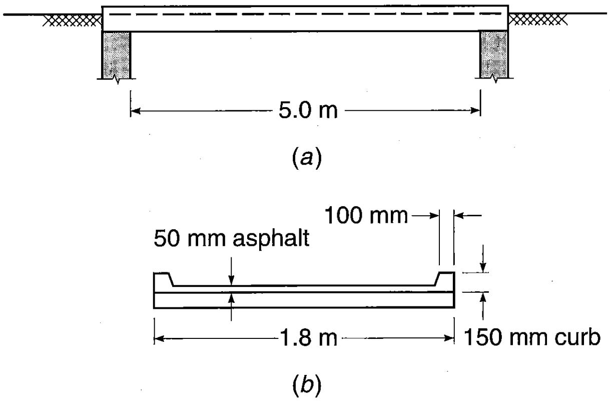

13.2. A reinforced concrete building floor system consists of a continuous one-way slab built monolithically with its supporting beams, as shown in cross section in Fig. P13.2. Service live load will be 6 kN/m^2. Dead loads include a 0.5 kN/m^2 allowance for nonstructural lightweight concrete floor fill and surface, and a 0.5 kN/m^2 allowance for suspended loads, plus the self-weight of the floor. Using ACI coefficients from Chapter 12, calculate the design moments and shears and design the slab, using a maximum tensile reinforcement ratio of 0.006. Use all straight bar reinforcement. One-half of the positive-moment bars will be discontinued where no longer required; the other half will be continued into the supporting beams as specified by the ACI Code. All negative steel will be discontinued at the same distance from the support face in each case. Summarize your design with a sketch showing concrete dimensions, and size, spacing, and cutoff points for all reinforcement. Material strengths are $f_y = 420$ MPa and $f_c' = 21$ MPa.

FIGURE P13.2

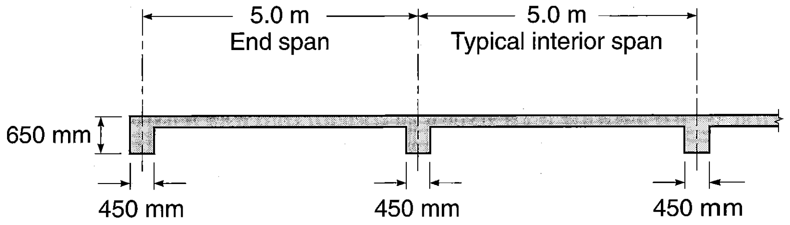

13.3. For the one-way slab floor in Problem 13.2, calculate the immediate and long-term deflection due to dead loads. Assume that all dead loads are applied when the construction shoring is removed. Also determine the deflection due to application of the full-service live load. Assuming that sensitive equipment will be installed 6 months after the shoring is removed, calculate the relevant deflection components and compare the total with maximum values recommended in the ACI Code.

13.4. A monolithic reinforced concrete floor consists of rectangular bays measuring 6.4 × 8.0 m, as shown in Fig. P13.4. The floor is designed to carry a service live load of 6.0 kN/m^2 uniformly distributed over its surface in addition to its own weight, using a concrete strength of 35 MPa and reinforcement having f_y = 420 MPa. Design a typical interior panel using the ACI direct design method of Sections 13.6 through 13.8.

FIGURE P13.4

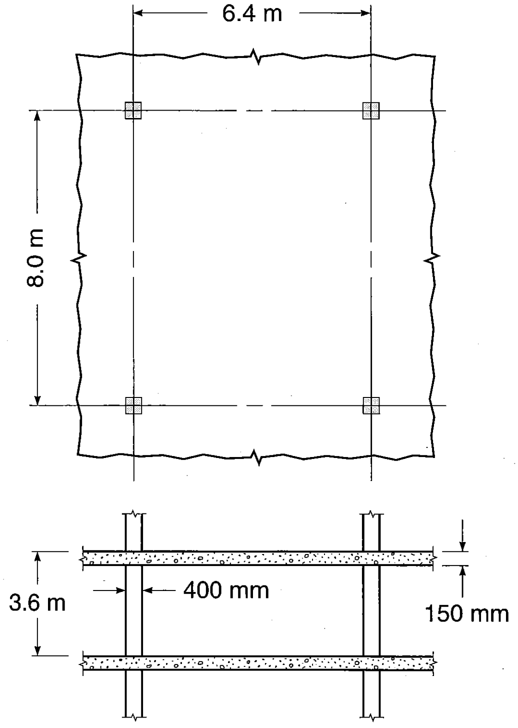

13.5. Redesign the typical exterior panel of the floor of Example 13.2 as a part of a flat plate structure, with no beams between interior columns but with beams provided along the outside edge to stiffen the slab. No drop panels or column capitals are permitted, but shear reinforcement similar to Fig. 13.24*b* may be incorporated if necessary. Column size is 500 × 500 mm, and the floor-to-floor height is 3.6 m. Use either the direct design method or the equivalent frame method. Summarize your design by means of a sketch showing plan and typical cross sections.

13.6. For the four-story structure shown in Figure P13.6, (*a*) select the slab thickness, (*b*) design the highlighted floor slab panel using the equivalent frame method,

FIGURE P13.6

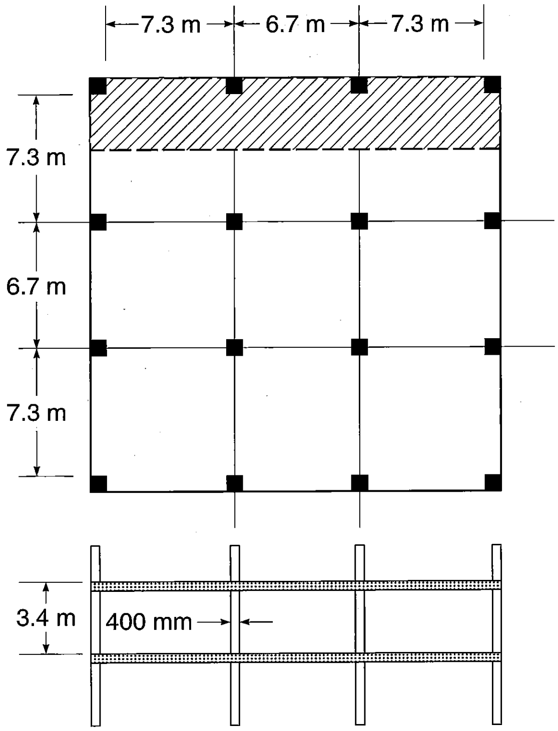

(*c*) prepare sketches of the steel layout, and (*d*) comment on your selection of the original thickness and what effect using shear studs might have on the design. Material strengths are f_y = 420 MPa and f'_c = 28 MPa. Building loads are the superimposed dead load of 1.4 kN/m^2 and live load of 2.5 kN/m^2.

13.7. A multistory commercial building is to be designed as a flat plate system with floors of uniform thickness having no beams or drop panels. Columns are laid out on a uniform 6 m spacing in each direction and have a 400 mm square section and a vertical dimension 3.0 m from floor to floor. Specified service live load is 5.0 kN/m^2 including partition allowance. Using the direct design method, design a typical interior panel, determining the required floor thickness, size and spacing of reinforcing bars, and bar details including cutoff points. To simplify construction, the reinforcement in each direction will be the same; use an average effective depth in the calculations. Use all straight bars. For moderate spans such as this, it has been determined that supplementary shear reinforcement would not be economical, although column capitals may be used if needed. Thus, slab thickness may be based on Eqs. (13.11*a*), (13.11*b*), and (13.11*c*); or column capital dimensions can be selected using those equations if slab thickness is based on the equations in Section 13.8. Material strengths are f_y = 420 MPa and f'_c = 28 MPa.

13.8. Prepare alternative designs for shear reinforcement at the supports of the slab described in Example 13.7, (*a*) using bent-bar reinforcement similar to Fig. 13.24*b*, (*b*) using integral beams with vertical stirrups similar to Fig. 13.24*e*, and (*c*) using headed shear stud reinforcement similar to Fig. 13.24*f*.

13.9. Prepare an alternative design for shear reinforcement at the supports of the slab described in Example 13.4, using a shearhead similar to Fig. 13.24*a*.

As an alternative to shear reinforcement of any kind, calculate the smallest acceptable dimensions for a 45° column capital (see Fig. 13.1*e*) that would permit the concrete slab to resist the entire shear force. Drop panels are not permitted.

13.10. Figure P13.10 shows a flat plate floor designed to carry a factored load of 15.5 kN/m². The total slab thickness h = 190 mm and the average effective depth d = 150 mm. Material strengths are f_y = 420 MPa and f_c' = 28 MPa. The design for punching shear at a typical interior column B2 provided the basis for Example 13.4. To provide a full perimeter b_o at the exterior column B1, the slab is cantilevered past the columns as shown. A total shear force V_u = 470 kN must be transmitted to the column, along with a bending moment M_u = 160 kN-m about an axis parallel to the edge of the slab. Check for punching shear at column B1 and, if ACI Code restrictions are not met, suggest appropriate modifications in the proposed design. Edge beams are not permitted.

FIGURE P13.10

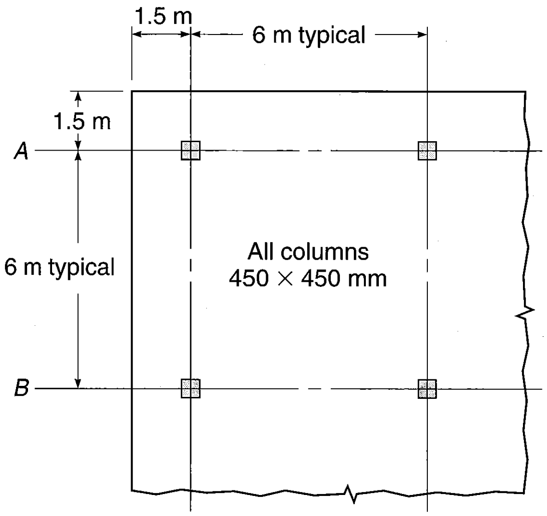

13.11. For the flat plate floor in Example 13.3, find the following deflection components at the center of panel C: (a) immediate deflection due to total dead load; (b) additional dead load deflection after a long period of time, due to total dead load; (c) immediate deflection due to three-quarters full live load. The moment of inertia of the cross concrete sections I_g may be used for all calculations. It may be assumed that maximum deflection will be obtained for the same loading pattern that would produce maximum positive moment in the panel. Check predicted deflection against ACI limitations, assuming that nonstructural attached elements would be damaged by excessive deflections.

13.12. A parking garage is to be designed using a two-way flat slab on the column lines, as shown in Fig. P13.12. A live load of 5 kN/m² is specified. Find the required slab thickness, using a reinforcement ratio of approximately 0.005, and design the reinforcement for a typical corner panel A, edge panel B, and interior panel C. Check shear capacity. Detail the reinforcement, showing size, spacing, and length. All straight bars will be used. Material strengths will be f_y = 420 MPa and f_c' = 35 MPa. Specify the design method selected and comment on your results.

FIGURE P13.12

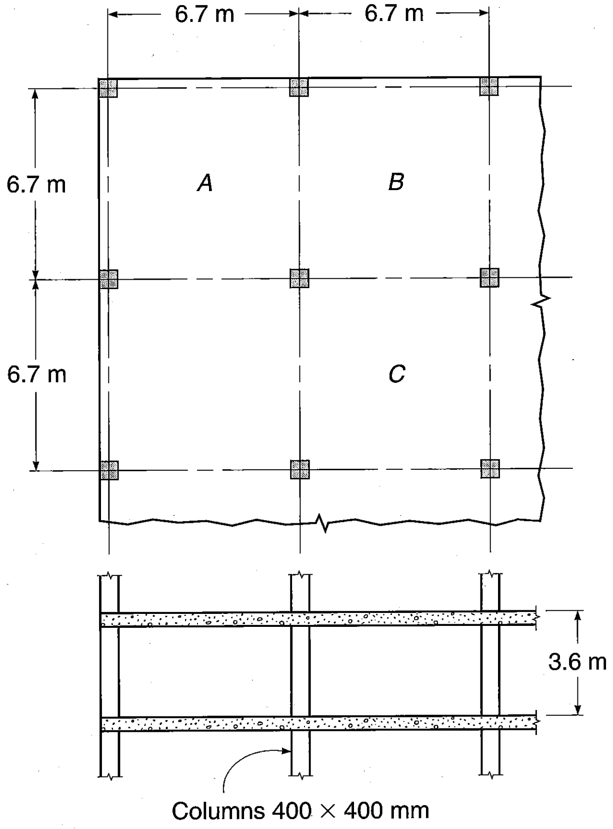

13.13. For the typical interior panel C of the parking garage in Problem 13.12, (a) compute the immediate and long-term deflections due to dead load and (b) compute the deflection due to the full-service live load. Compare with ACI Code maximum permissible values, given that there are no elements attached that would be damaged by large deflections.

14

Yield Line Analysis for Slabs

14.1 INTRODUCTION

Most concrete slabs are designed for moments found by the methods described in Chapter 13. These methods are based essentially upon elastic theory. On the other hand, reinforcement for slabs is calculated by strength methods that account for the actual inelastic behavior of members at the factored load stage. A corresponding contradiction exists in the process by which beams and frames are analyzed and designed, as was discussed in Section 12.9, and the concept of limit, or plastic, analysis of reinforced concrete was introduced. Limit analysis not only eliminates the inconsistency of combining elastic analysis with inelastic design, but also accounts for the reserve strength characteristic of most reinforced concrete structures and permits, within limits, an arbitrary readjustment of moments found by elastic analysis to arrive at design moments that permit more practical reinforcing arrangements.

For slabs, there is still another good reason for interest in limit analysis. The elasticity-based methods of Chapter 13 are restricted in important ways. Slab panels must be square or rectangular. They must be supported along two opposite sides (one-way slabs), two pairs of opposite sides (two-way edge-supported slabs), or by a fairly regular array of columns (flat plates and related forms). Loads must be uniformly distributed, at least within the bounds of any single panel. There can be no large openings. But in practice, many slabs do not meet these restrictions. Answers are needed, for example, for round or triangular slabs, slabs with large openings, slabs supported on two or three edges only, and slabs carrying concentrated loads. Limit analysis provides a powerful and versatile tool for treating such problems.

It was evident from the discussion of Section 12.9 that full plastic analysis of a continuous reinforced concrete beam or frame would be tedious and time-consuming because of the need to calculate the rotation requirement at all plastic hinges and to check rotation capacity at each hinge to ensure that it is adequate. Consequently, for beams and frames, the very simplified approach to plastic moment redistribution of ACI Code 8.4 is used. However, for slabs, which typically have tensile reinforcement ratios much below the balanced value and consequently have large rotation capacity, it can be safely assumed that the necessary ductility is present. Practical methods for the plastic analysis of slabs are thus possible and have been developed. *Yield line theory*, presented in this chapter, is one of these. Although the ACI Code contains no specific provisions for limit or plastic analysis of slabs, ACI Code 1.4 permits use of "any system of design or construction," the adequacy of which has been shown by successful use, analysis, or tests, and ACI Commentary 13.5.1 refers specifically to yield line analysis as an acceptable approach.

Yield line analysis for slabs was first proposed by Ingerslev (Ref. 14.1) and was greatly extended by Johansen (Refs. 14.2 and 14.3). Early publications were mainly in Danish, and it was not until Hognestad's English language summary (Ref. 14.4) of Johansen's work that the method received wide attention. Since that time, a number of important publications on the method have appeared (Refs. 14.5 through 14.15). A particularly useful and comprehensive treatment will be found in Ref. 14.15.

The *plastic hinge* was introduced in Section 12.9 as a location along a member in a continuous beam or frame at which, upon overloading, there would be large inelastic rotation at essentially a constant resisting moment. For slabs, the corresponding mechanism is the *yield line*. For the overloaded slab, the resisting moment per unit length measured along a yield line is constant as inelastic rotation occurs; the yield line serves as an axis of rotation for the slab segment.

Figure 14.1*a* shows a simply supported, uniformly loaded reinforced concrete slab. It will be assumed to be underreinforced (as are almost all slabs), with $\rho < \rho_{0.005}$. The elastic moment diagram is shown in Fig. 14.1*b*. As the load is increased, when the applied moment becomes equal to the flexural capacity of the slab cross section, the tensile steel starts to yield along the transverse line of maximum moment.

Upon yielding, the curvature of the slab at the yielding section increases sharply, and deflection increases disproportionately. The elastic curvatures along the slab span are small compared with the curvature resulting from plastic deformation at the yield line, and it is acceptable to consider that the slab segments between the yield line and supports remain rigid, with all the curvature occurring at the yield line, as shown in Fig. 14.1*c*. The "hinge" that forms at the yield line rotates with essentially constant resistance, according to the relation shown earlier in Fig. 12.13*a*. The resistance per unit width of slab is the nominal flexural strength of the slab; that is, $m_p = m_n$, where m_n is calculated by the usual equations. For design purposes, m_p would be taken equal to ϕm_n, with ϕ typically equal to 0.90, since ρ is well below $\rho_{0.005}$ for most slabs.

FIGURE 14.1
Simply supported, uniformly loaded one-way slab.

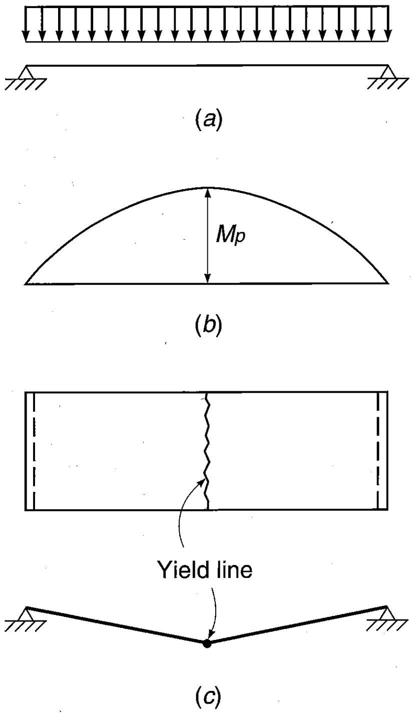

FIGURE 14.2
Fixed-end, uniformly loaded one-way slab.

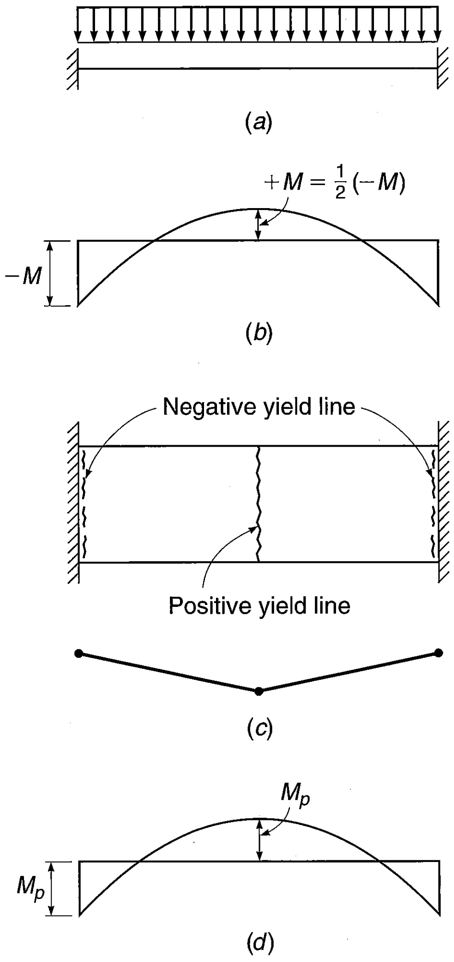

For a statically determinate slab like that in Fig. 14.1, the formation of one yield line results in collapse. A "mechanism" forms; i.e., the segments of the slab between the hinge and the supports are able to move without an increase in load. Indeterminate structures, however, can usually sustain their loads without collapse even after the formation of one or more yield lines. When it is loaded uniformly, the fixed-fixed slab in Fig. 14.2*a*, assumed here to be equally reinforced for positive and negative moments, will have an elastic distribution of moments, as shown in Fig. 14.2*b*. As the load is gradually increased, the more highly stressed sections at the support start yielding. Rotations occur at the support line hinges, but restraining moments of constant value m_p continue to act. The load can be increased further, until the moment at midspan becomes equal to the moment capacity there, and a third yield line forms, as shown in Fig. 14.2*c*. The slab is now a mechanism, large deflections occur, and collapse takes place.

The moment diagram just before failure is shown in Fig. 14.2*d*. Note that the ratio of elastic positive to negative moments of 1:2 no longer holds. Due to inelastic deformation, the ratio of these moments just before collapse is 1:1 for this particular structure. Redistribution of moments was discussed earlier in Section 12.9, and it was pointed out that the moment ratios at the collapse stage depend upon the reinforcement provided, not upon the results of elastic analysis.

14.2 UPPER AND LOWER BOUND THEOREMS

Plastic analysis methods such as the yield line theory derive from the general theory of structural plasticity, which states that the collapse load of a structure lies between two limits, an upper bound and a lower bound of the true collapse load. These limits can be found by well-established methods. A full solution by the theory of plasticity would attempt to make the lower and upper bounds converge to a single correct solution.

The lower bound theorem and the upper bound theorem, when applied to slabs, can be stated as follows:

> **Lower bound theorem:** If, for a given external load, it is possible to find a distribution of moments that satisfies equilibrium requirements, with the moment not exceeding the yield moment at any location, and if the boundary conditions are satisfied, then the given load is a lower bound of the true carrying capacity.
>
> **Upper bound theorem:** If, for a small increment of displacement, the internal work done by the slab, assuming that the moment at every plastic hinge is equal to the yield moment and that boundary conditions are satisfied, is equal to the external work done by the given load for that same small increment of displacement, then that load is an upper bound of the true carrying capacity.

If the lower bound conditions are satisfied, the slab can certainly carry the given load, although a higher load may be carried if internal redistributions of moment occur. If the upper bound conditions are satisfied, a load greater than the given load will certainly cause failure, although a lower load may produce collapse if the selected failure mechanism is incorrect in any sense.

In practice, in the plastic analysis of structures, one works with either the lower bound theorem or the upper bound theorem, not both, and precautions are taken to ensure that the predicted failure load at least closely approaches the correct value.

The yield line method of analysis for slabs is an upper bound method, and consequently, the failure load calculated for a slab with known flexural resistances may be higher than the true value. This is certainly a concern, as the designer would naturally prefer to be correct, or at least on the safe side. However, procedures can be incorporated in yield line analysis to help ensure that the calculated capacity is correct. Such procedures will be illustrated by the examples in Sections 14.4 and 14.5.

14.3 RULES FOR YIELD LINES

The location and orientation of the yield line were evident for the simple slab in Fig. 14.1. Similarly, the yield lines were easily established for the one-way indeterminate slab in Fig. 14.2. For other cases, it is helpful to have a set of guidelines for drawing yield lines and locating axes of rotation. When a slab is on the verge of collapse because of the existence of a sufficient number of real or plastic hinges to form a mechanism, axes of rotation will be located along the lines of support or over point supports such as columns. The slab segments can be considered to rotate as rigid bodies in space about these axes of rotation. The yield line between any two adjacent slab segments is a straight line, being the intersection of two essentially plane surfaces. Because the yield line (as a line of intersection of two planes) contains all points common to these two planes, it must contain the point of intersection (if any) of the two axes of rotation, which is also common to the two planes. That is, the yield line (or yield line extended) must pass through the point of intersection of the axes of rotation of the two adjacent slab segments.

The terms *positive yield line* and *negative yield line* are used to distinguish between those associated with tension at the bottom and tension at the top of the slab, respectively.

Guidelines for establishing axes of rotation and yield lines are summarized as follows:

1. Yield lines are straight lines because they represent the intersection of two planes.
2. Yield lines represent axes of rotation.
3. The supported edges of the slab will also establish axes of rotation. If the edge is fixed, a negative yield line may form, providing constant resistance to rotation. If the edge is simply supported, the axis of rotation provides zero restraint.
4. An axis of rotation will pass over any column support. Its orientation depends on other considerations.
5. Yield lines form under concentrated loads, radiating outward from the point of application.
6. A yield line between two slab segments must pass through the point of intersection of the axes of rotation of the adjacent slab segments.

In Fig. 14.3, which shows a slab simply supported along its four sides, rotation of slab segments *A* and *B* is about *ab* and *cd*, respectively. The yield line *ef* between these two segments is a straight line passing through *f*, the point of intersection of the axes of rotation.

Illustrations are given in Fig. 14.4 of the application of the guidelines to the establishment of yield line locations and failure mechanisms for a number of slabs with various support conditions. Figure 14.4*a* shows a slab continuous over parallel supports. Axes of rotation are situated along the supports (negative yield lines) and near midspan, parallel to the supports (positive yield line). The particular location of the positive yield line in this case and the other cases in Fig. 14.4 depends upon the distribution of loading and the reinforcement of the slab. Methods for determining its location will be discussed later.

For the continuous slab on nonparallel supports, shown in Fig. 14.4*b*, the midspan yield line (extended) must pass through the intersection of the axes of rotation over the supports. In Fig. 14.4*c* there are axes of rotation over all four simple supports. Positive yield lines form along the lines of intersection of the rotating segments of the slab. A rectangular two-way slab on simple supports is shown in Fig. 14.4*d*. The diagonal yield lines must pass through the corners, while the central yield line is

FIGURE 14.3
Two-way slab with simply supported edges.

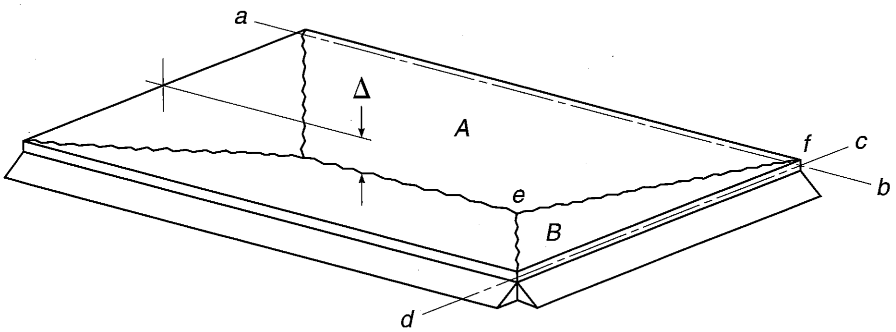

FIGURE 14.4
Typical yield line patterns.

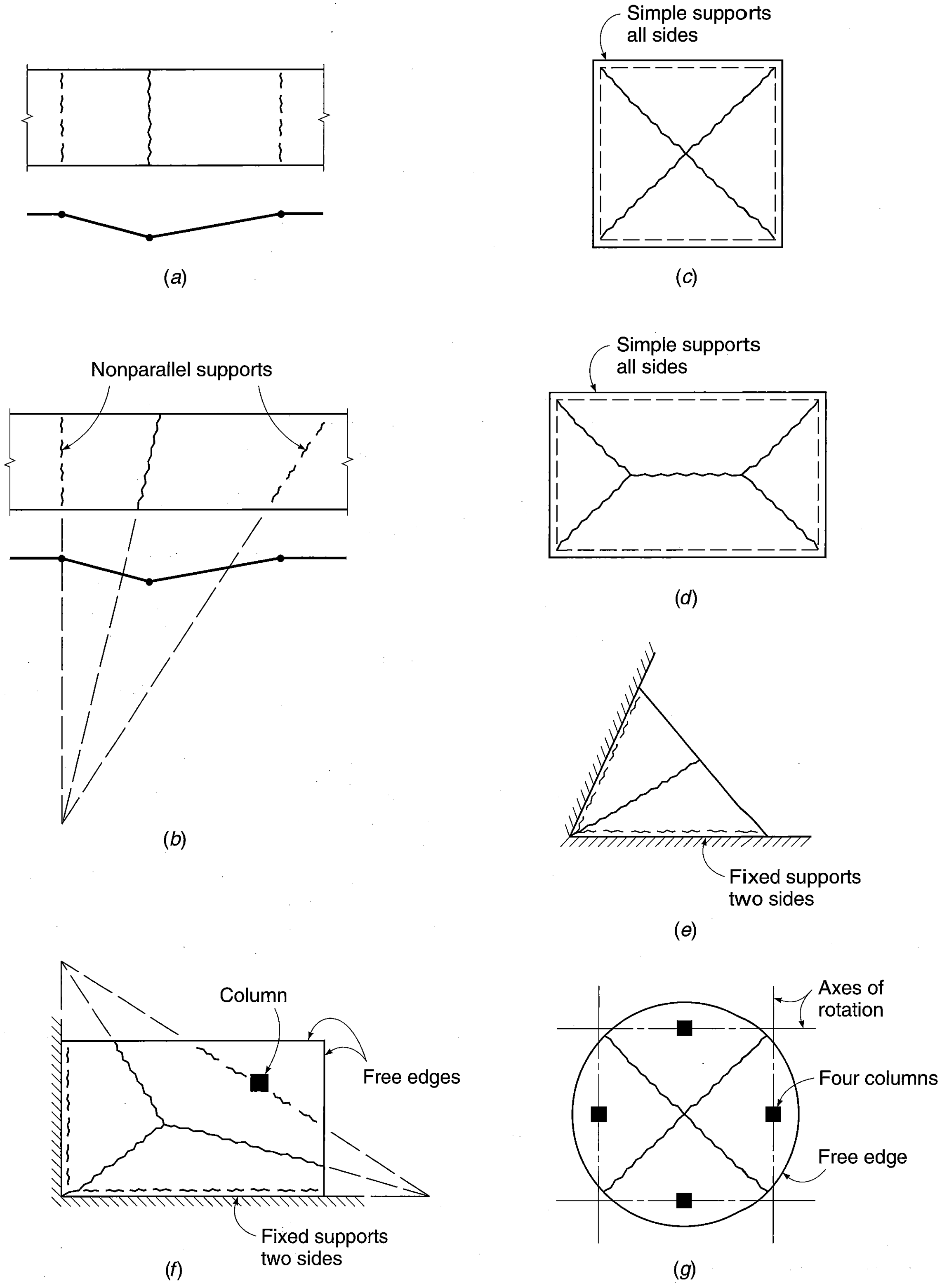
Simple supports all sides
(a)
(c)
Nonparallel supports
Simple supports all sides
(d)
(b)
Fixed supports two sides
(e)
Column
Free edges
Fixed supports two sides
(f)
Axes of rotation
Four columns
Free edge
(g)

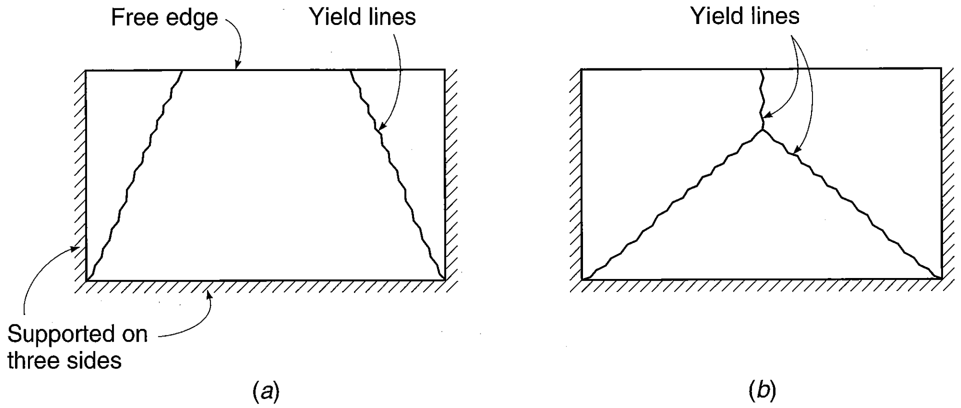

FIGURE 14.5
Alternative mechanisms for a slab supported on three sides.

parallel to the two long sides (axes of rotation along opposite supports intersect at infinity in this case).

With this background, the reader should have no difficulty in applying the guidelines to the slabs in Fig. 14.4*e* to *g* to confirm the general pattern of yield lines shown. Many other examples will be found in Refs. 14.1 to 14.15.

Once the general pattern of yielding and rotation has been established by applying the guidelines just stated, the specific location and orientation of the axes of rotation and the failure load for the slab can be established by either of two methods. The first will be referred to as the *method of segment equilibrium* and will be presented in Section 14.4. It requires consideration of the equilibrium of the individual slab segments forming the collapse mechanism and leads to a set of simultaneous equations permitting solution for the unknown geometric parameters and for the relation between load capacity and resisting moments. The second, the *method of virtual work*, will be described in Section 14.5. This method is based on equating the internal work done at the plastic hinges with the external work done by the loads as the predefined failure mechanism is given a small virtual displacement.

It should be emphasized that *either method of yield line analysis is an upper bound approach* in the sense that the true collapse load will never be higher, but may be lower, than the load predicted. For either method, the solution has two essential parts: (1) establishing the correct failure pattern and (2) finding the geometric parameters that define the exact location and orientation of the yield lines and solving for the relation between applied load and resisting moments. Either method can be developed in such a way as to lead to the correct solution for the mechanism chosen for study, but the true failure load will be found only if the correct mechanism has been selected.

For example, the rectangular slab in Fig. 14.5, supported along only three sides and free along the fourth, may fail by either of the two mechanisms shown. An analysis based on yield pattern *a* may indicate a slab capacity higher than one based on pattern *b*, or vice versa. It is necessary to investigate *all possible mechanisms* for any slab to confirm that the correct solution, giving the lowest failure load, has been found.†

---

† The importance of this point was underscored by Professor Arne Hillerborg, of Lund Institute of Technology, Sweden, in a letter to the editor of the ACI publication *Concr. Intl*, vol. 13, no. 5, 1991. Professor Hillerborg noted that, in reality, there are two additional yield line patterns for a slab such as shown in Fig. 14.5. For a particular set of dimensions and reinforcement, both of these gave a lower failure load than did the mechanism shown in Fig. 14.5*a*.

The method of segment equilibrium should not be confused with a true equilibrium method such as the strip method described in Chapter 15. A true equilibrium method is a lower bound method of analysis; i.e., it will always give a *lower bound* of the true capacity of the slab.

14.4 ANALYSIS BY SEGMENT EQUILIBRIUM

Once the general pattern of yielding and rotation has been established by applying the guidelines of Section 14.3, the location and orientation of axes of rotation and the failure load for the slab can be established based on the equilibrium of the various segments of the slab. Each segment, studied as a free body, must be in equilibrium under the action of the applied loads, the moments along the yield lines, and the reactions or shear along the support lines. Because the yield moments are principal moments, twisting moments are zero along the yield lines, and in most cases the shearing forces are also zero. Only the unit moment m generally is considered in writing equilibrium equations.

EXAMPLE 14.1

Segment equilibrium analysis of one-way slab. The method will be demonstrated first with respect to the one-way, uniformly loaded, continuous slab of Fig. 14.6*a*. The slab has a 3 m span and is reinforced to provide a resistance to positive bending ϕm_n = 22 kN-m/m through the span. In addition, negative steel over the supports provides moment capacities of 22 kN-m/m at A and 33 kN-m/m at C. Determine the load capacity of the slab.

Solution. The number of equilibrium equations required will depend upon the number of unknowns. One unknown is always the relation between the resisting moments of the slab and the load. Other unknowns are needed to define the locations of yield lines. In the present instance, one additional equation will suffice to define the distance of the yield line from the

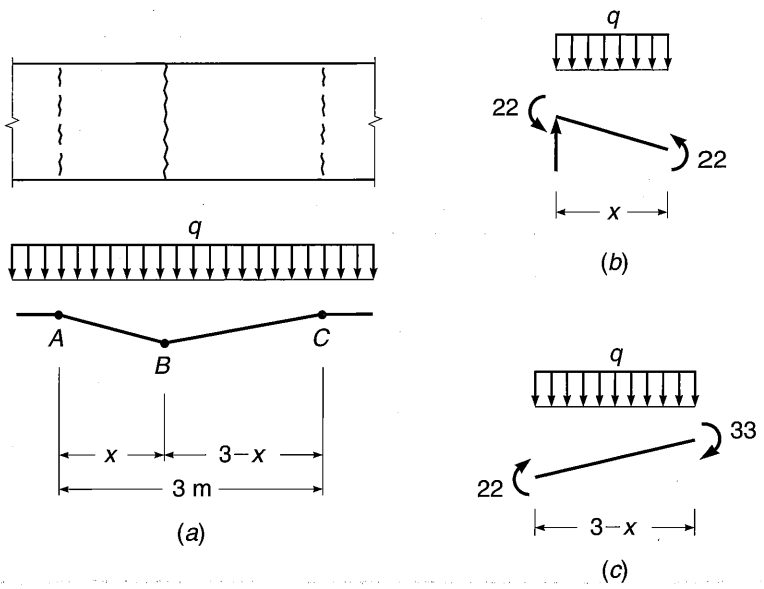

FIGURE 14.6
Analysis of a one-way slab by segment equilibrium equations.

supports. Taking the left segment of the slab as a free body and writing the equation for moment equilibrium about the left support line (see Fig. 14.6*b*) lead to

$$\frac{qx^2}{2} - 44.0 = 0 \qquad (a)$$

Similarly, for the right slab segment,

$$\frac{q}{2}(3 - x)^2 - 55 = 0 \qquad (b)$$

Solving Eqs. (*a*) and (*b*) simultaneously for q and x results in

$$q = 43.6 \text{ kN/m}^2 \qquad x = 1.42 \text{ m}$$

If a slab is reinforced in orthogonal directions so that the resisting moment is the same in these two directions, the moment capacity of the slab will be the same along any other line, regardless of direction. Such a slab is said to be *isotropically* reinforced. If, however, the strengths are different in two perpendicular directions, the slab is called *orthogonally anisotropic*, or simply *orthotropic*. Only isotropic slabs will be discussed in this section. Orthotropic reinforcement, which is very common in practice, will be discussed in Section 14.6.

It is convenient in yield line analysis to represent moments with vectors. The standard convention, in which the moment acts in a clockwise direction when viewed along the vector arrow, will be followed. Treatment of moments as vector quantities will be illustrated by the following example:

EXAMPLE 14.2

Segment equilibrium analysis of square slab. A square slab is simply supported along all sides and is to be isotropically reinforced. Determine the resisting moment $m = \phi m_n$ per linear meter required just to sustain a uniformly distributed factored load of q kN/m^2.

Solution. Conditions of symmetry indicate the yield line pattern shown in Fig. 14.7*a*. Considering the moment equilibrium of any one of the identical slab segments about its support (see Fig. 14.7*b*), one obtains

$$\frac{qL^2}{4}\,\frac{L}{6} - 2\frac{mL}{\sqrt{2}}\,\frac{1}{\sqrt{2}} = 0$$

$$m = \frac{qL^2}{24}$$

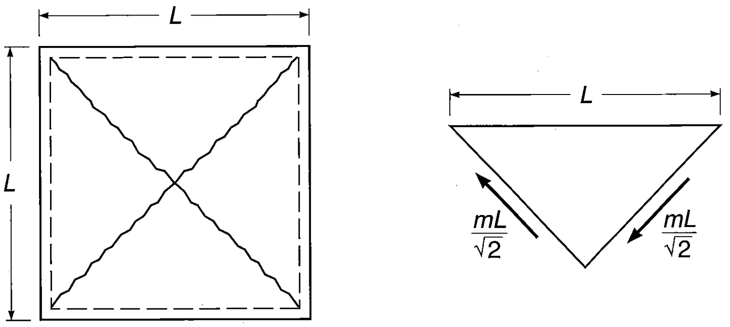

(*a*) (*b*)

FIGURE 14.7
Analysis of a square two-way slab by segment equilibrium equations.

In both examples just given, the resisting moment was constant along any particular yield line; i.e., the reinforcing bars were of constant diameter and equally spaced along a given yield line. On the other hand, it will be recalled that, by the elastic methods of slab analysis presented in Chapter 13, reinforcing bars generally have a different spacing and may be of different diameter in middle strips compared with column or edge strips. A slab designed by elastic methods, leading to such variations, can easily be analyzed for strength by the yield line method. It is merely necessary to subdivide a yield line into its component parts, within any one of which the resisting moment per unit length of hinge is constant. Either the equilibrium equations of this section or the work equations of Section 14.5 can be modified in this way.

14.5 ANALYSIS BY VIRTUAL WORK

Alternative to the method of Section 14.4 is a method of analysis using the principle of virtual work. Since the moments and loads are in equilibrium when the yield line pattern has formed, an infinitesimal increase in load will cause the structure to deflect further. The external work done by the loads to cause a small arbitrary virtual deflection must equal the internal work done as the slab rotates at the yield lines to accommodate this deflection. The slab is therefore given a virtual displacement, and the corresponding rotations at the various yield lines can be calculated. By equating internal and external work, the relation between the applied loads and the resisting moments of the slab is obtained. Elastic rotations and deflections are not considered when writing the work equations, as they are very small compared with the plastic deformations.

a. External Work Done by Loads

An external load acting on a slab segment, as a small virtual displacement is imposed, does work equal to the product of its constant magnitude and the distance through which the point of application of the load moves. If the load is distributed over a length or an area, rather than concentrated, the work can be calculated as the product of the total load and the displacement of the point of application of its resultant.

Figure 14.8 illustrates the basis for external work calculation for several types of loads. If a square slab carrying a single concentrated load at its center (Fig. 14.8*a*) is given a virtual displacement defined by a unit value under the load, the external work is

$$W_e = P \times 1 \tag{a}$$

If the slab shown in Fig. 14.8*b*, supported along three sides and free along the fourth, is loaded with a line load w per unit length along the free edge, and if that edge is given a virtual displacement having unit value along the central part, the external work is

$$W_e = (2wa) \times \frac{1}{2} + wb = w(a + b) \tag{b}$$

When a distributed load q per unit area acts on a triangular segment defined by a hinge and yield lines, such as Fig. 14.8*c*,

$$W_e = \frac{qab}{2} \times \frac{1}{3} = \frac{qab}{6} \tag{c}$$

FIGURE 14.8
External work basis for various types of loads.

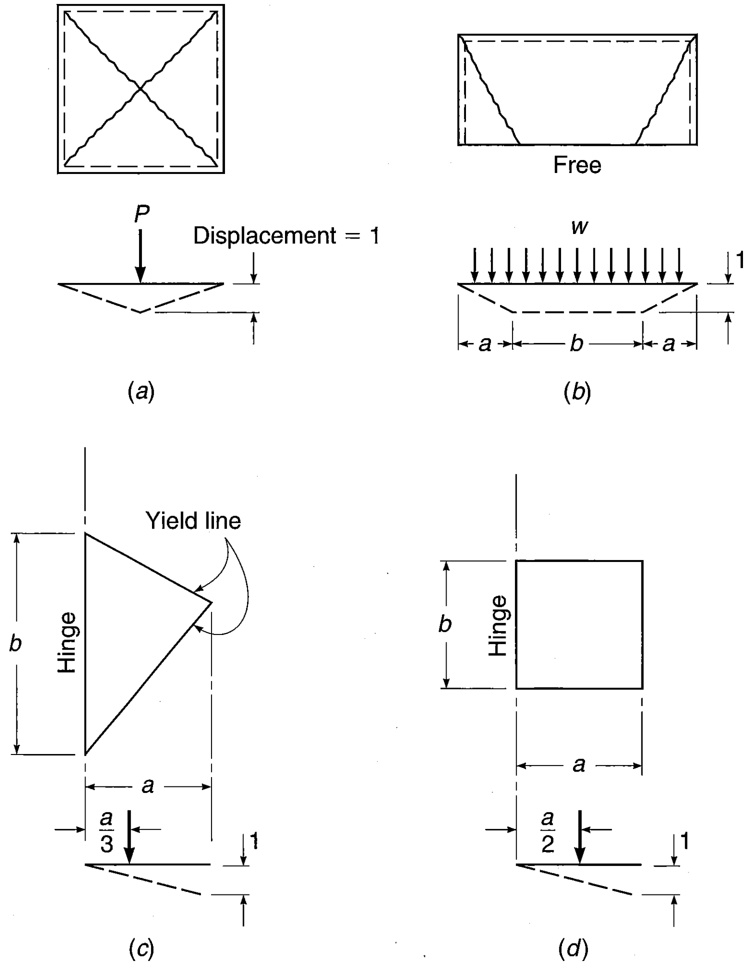

while for the rectangular slab segment shown in Fig. 14.8*d*, carrying a distributed load q per unit area, the external work is

$$W_e = \frac{qab}{2} \qquad (d)$$

More complicated trapezoidal shapes may always be subdivided into component triangles and rectangles. The total external work is then calculated by summing the work done by loads on the individual parts of the failure mechanism, with all displacements keyed to a unit value assigned somewhere in the system. There is no difficulty in combining the work done by concentrated loads, line loads, and distributed loads, if these act in combination.

b. Internal Work Done by Resisting Moments

The internal work done during the assigned virtual displacement is found by summing the products of yield moment m per unit length of hinge times the plastic rotation θ at the respective yield lines, consistent with the virtual displacement. If the resisting moment m is constant along a yield line of length l, and if a rotation θ is experienced, the internal work is

$$W_i = ml\theta \tag{e}$$

If the resisting moment varies, as would be the case if bar size or spacing were not constant along the yield line, the yield line is divided into n segments, within each one of which the moment is constant. The internal work is then

$$W_i = (m_1l_1 + m_2l_2 + \cdots + m_nl_n)\theta \tag{f}$$

For the entire system, the total internal work done is the sum of the contributions from all yield lines. In all cases, the internal work contributed is positive, regardless of the sign of m, because the rotation is in the same direction as the moment. External work, on the other hand, may be either positive or negative, depending on the direction of the displacement of the point of application of the force resultant.

EXAMPLE 14.3

Virtual work analysis of one-way slab. Determine the load capacity of the one-way uniformly loaded continuous slab shown in Fig. 14.9, using the method of virtual work. The resisting moments of the slab are 22, 22, and 33 kN-m/m at A, B, and C, respectively.

Solution. A unit deflection is given to the slab at B. Then the external work done by the load is the sum of the loads times their displacements and is equal to

$$\frac{qx}{2} + \frac{q}{2}(3 - x)$$

The rotations at the hinges are calculated in terms of the unit deflection (Fig. 14.9) and are

$$\theta_A = \theta_{B1} = \frac{1}{x} \qquad \theta_{B2} = \theta_C = \frac{1}{3 - x}$$

The internal work is the sum of the moments times their corresponding rotation angles:

$$22 \times \frac{1}{x} \times 2 + 22 \times \frac{1}{3 - x} + 33 \times \frac{1}{3 - x}$$

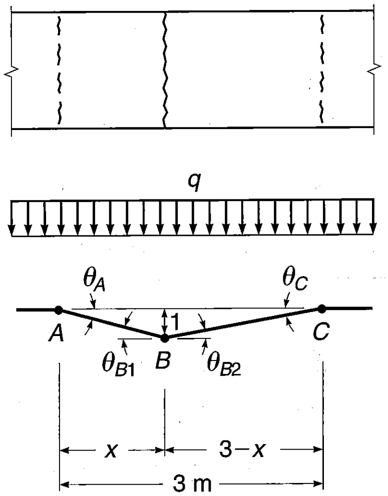

FIGURE 14.9
Virtual work analysis of one-way slab.

Equating the external and internal work gives

$$\frac{qx}{2} + 22q - \frac{qx}{2} = \frac{44}{x} + \frac{22}{3 - x} + \frac{33}{3 - x}$$

$$5q = \frac{44}{x} + \frac{110}{2(3 - x)}$$

$$q = \frac{2}{x} + \frac{5}{2(3 - x)}$$

To determine the minimum value of w, this expression is differentiated with respect to x and set equal to zero:

$$\frac{dq}{dx} = -\frac{2}{x^2} + \frac{5}{2(3 - x)^2} = 0$$

from which

$$x = 1.42 \text{ m}$$

Substituting this value in the preceding expression for w, one obtains

$$q = 43.6 \text{ kN/m}^2$$

as before.

In many cases, particularly those with yield lines established by several unknown dimensions (such as Fig. 14.4*f*), direct solution by virtual work would become quite tedious. The ordinary derivatives in Example 14.3 would be replaced by several partial derivatives, producing a set of equations to be solved simultaneously. In such cases it is often more convenient to select an arbitrary succession of possible yield line locations, solve the resulting mechanisms for the unknown load (or unknown moment), and determine the correct minimum load (or maximum moment) by trial.

EXAMPLE 14.4

Virtual work analysis of rectangular slab. The two-way slab shown in Fig. 14.10 is simply supported on all four sides and carries a uniformly distributed load of q kN/m^2. Determine the required moment resistance for the slab, which is to be isotropically reinforced.

Solution. Positive yield lines will form in the pattern shown in Fig. 14.10*a*, with the dimension a unknown. The correct dimension a will be such as to maximize the moment resistance required to support the load q. The values of a and m will be found by trial.

In Fig. 14.10*a* the length of the diagonal yield line is $\sqrt{2.25 + a^2}$. From similar triangles,

$$b = 1.5\,\frac{\sqrt{2.25 + a^2}}{a} \qquad c = a\,\frac{\sqrt{2.25 + a^2}}{1.5}$$

Then the rotation of the plastic hinge at the diagonal yield line corresponding to a unit deflection at the center of the slab (see Fig. 14.10*b*) is

$$\theta_1 = \frac{1}{b} + \frac{1}{c} = \frac{a}{1.5\sqrt{2.25 + a^2}} + \frac{1.5}{a\sqrt{2.25 + a^2}} = \frac{1}{\sqrt{2.25 + a^2}}\left(\frac{a}{1.5} + \frac{1.5}{a}\right)$$

The rotation of the yield line parallel to the long edges of the slab (see Fig. 14.10*c*) is

$$\theta_2 = \frac{1}{1.5} + \frac{1}{1.5} = 1.33$$

FIGURE 14.10
Virtual work analysis for rectangular two-way slab.

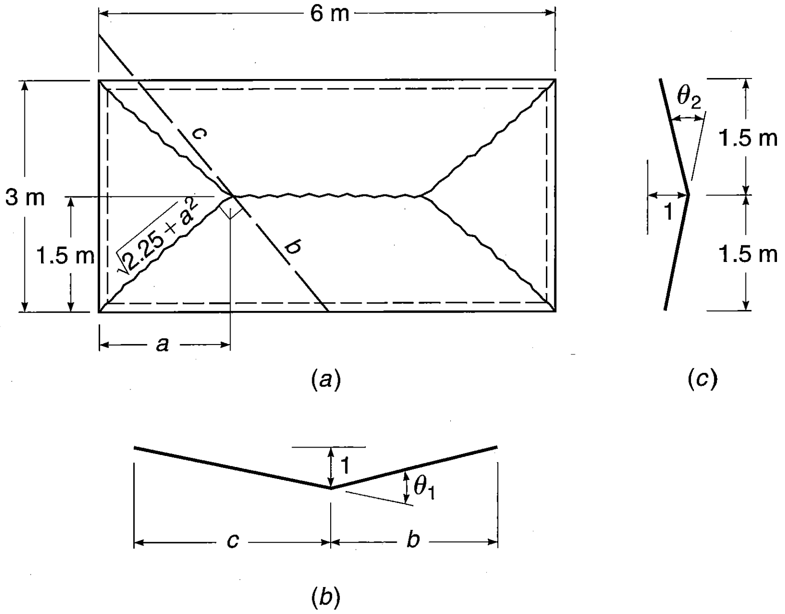

(a)

(c)

(b)

For a first trial, let $a = 1.8$ m. Then the length of the diagonal yield line is

$$\sqrt{2.25 + 3.24} = 2.34 \text{ m}$$

The rotation at the diagonal yield line is

$$\theta_1 = \frac{1}{2.34}\left(\frac{1.8}{1.5} + \frac{1.5}{1.8}\right) = 0.868$$

At the central yield line, it is $\theta_2 = 1.33$. The internal work done as the incremental deflection is applied is

$$W_i = (m \times 2.34 \times 0.868 \times 4) + (m \times 2.4 \times 1.33) = 11.32m$$

The external work done during the same deflection is

$$W_e = (3 \times 1.8 \times \tfrac{1}{2}q \times \tfrac{1}{3} \times 2) + (2.4 \times 1.5q \times \tfrac{1}{2} \times 2) + (3.6 \times 1.5 \times \tfrac{1}{2}q \times \tfrac{1}{3} \times 2) = 7.2q$$

Equating W_i and W_e, one obtains

$$m = \frac{7.2q}{11.32} = 0.635q$$

Successive trials for different values of a result in the following data:

a	W_i	W_e	m
1.8	$11.32m$	$7.20q$	$0.635q$
2.0	$11.00m$	$7.00q$	$0.636q$
2.2	$10.73m$	$6.80q$	$0.634q$
2.4	$10.50m$	$6.60q$	$0.629q$

It is evident that the yield line pattern defined by $a = 2.0$ m is critical. The required resisting moment for the given slab is $0.636q$.

14.6 ORTHOTROPIC REINFORCEMENT AND SKEWED YIELD LINES

Generally slab reinforcement is placed orthogonally, i.e., in two perpendicular directions. The same reinforcement is often provided in each direction, but the effective depths will be different. In many practical cases, economical designs are obtained using reinforcement having different bar areas or different spacings in each direction. In such cases, the slab will have different moment capacities in the two orthogonal directions and is said to be orthogonally anisotropic, or simply orthotropic.

Often yield lines will form at an angle with the directions established by the reinforcement; this was so in many of the examples considered earlier. For yield line analysis, it is necessary to calculate the resisting moment, per unit length, along such skewed yield lines. This requires calculation of the contribution to resistance from each of the two sets of bars.

Figure 14.11*a* shows an orthogonal grid of reinforcement, with angle α between the yield line and the X direction bars. Bars in the X direction are at spacing v and have moment resistance m_y per unit length about the Y axis, while bars in the Y direction are at spacing u and have moment resistance m_x per unit length about the X axis. The resisting moment per unit length for the bars in the Y and X directions will be determined separately, with reference to Fig. 14.11*b* and *c*, respectively.

For the Y direction bars, the resisting moment *per bar* about the X axis is $m_x u$, and the component of that resistance about the α axis is $m_x u \cos\alpha$. The resisting moment per unit length along the α axis provided by the Y direction bars is therefore

$$m_{\alpha y} = \frac{m_x u \cos\alpha}{u/\cos\alpha} = m_x \cos^2\alpha \qquad (a)$$

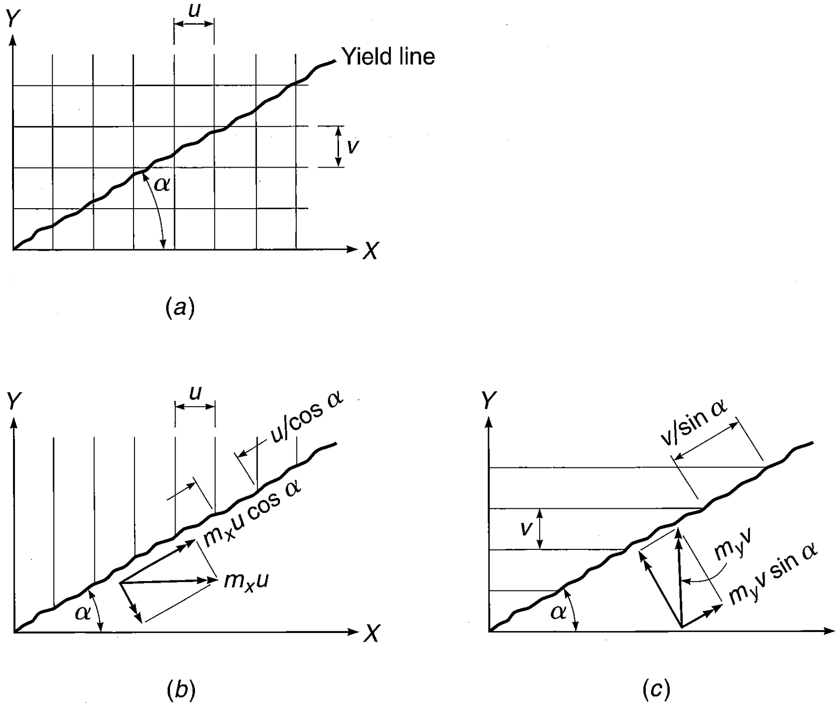

(*a*)

(*b*)

(*c*)

FIGURE 14.11
Yield line skewed with orthotropic reinforcement: (*a*) orthogonal grid and yield line; (*b*) *Y* direction bars; (*c*) *X* direction bars.

For the bars in the X direction, the resisting moment per bar about the Y axis is $m_y v$, and the component of that resistance about the α axis is $m_y v \sin \alpha$. Thus the resisting moment per unit length along the α axis provided by the X direction bars is

$$m_{\alpha x} = \frac{m_y v \sin \alpha}{v/\sin \alpha} = m_y \sin^2 \alpha \qquad (b)$$

Thus, for the combined sets of bars, the resisting moment per unit length measured along the α axis is given by the sum of the resistances from Eqs. (*a*) and (*b*):

$$m_\alpha = m_x \cos^2 \alpha + m_y \sin^2 \alpha \qquad (14.1)$$

For the special case where $m_x = m_y = m$, with the same reinforcement provided in each direction,

$$m_\alpha = m(\cos^2 \alpha + \sin^2 \alpha) = m \qquad (14.2)$$

The slab is said to be *isotropically reinforced*, with the same resistance per unit length regardless of the orientation of the yield line.

The analysis just presented neglects any consideration of strain compatibility along the yield line, and assumes that the displacements at the level of the steel during yielding, which are essentially perpendicular to the yield line, are sufficient to produce yielding in both sets of bars. This is reasonably in accordance with test data, except for values of α close to 0 to 90°. For such cases, it would be conservative to neglect the contribution of the bars nearly parallel to the yield line.

It has been shown that the analysis of an orthotropic slab can be simplified to that of a related isotropic slab, referred to as the *affine slab*, provided that the ratio of negative to positive reinforcement areas is the same in both directions. The horizontal dimensions and slab loads must be modified to permit this transformation. Details will be found in Refs. 14.1 to 14.5.

EXAMPLE 14.5

Resisting moment along a skewed yield line. The balcony slab in Fig. 14.12 has fixed supports along two adjacent sides and is unsupported along the third side. It is reinforced for positive bending with No. 16 (No. 5) bars at 250 mm spacing and 140 mm effective depth,

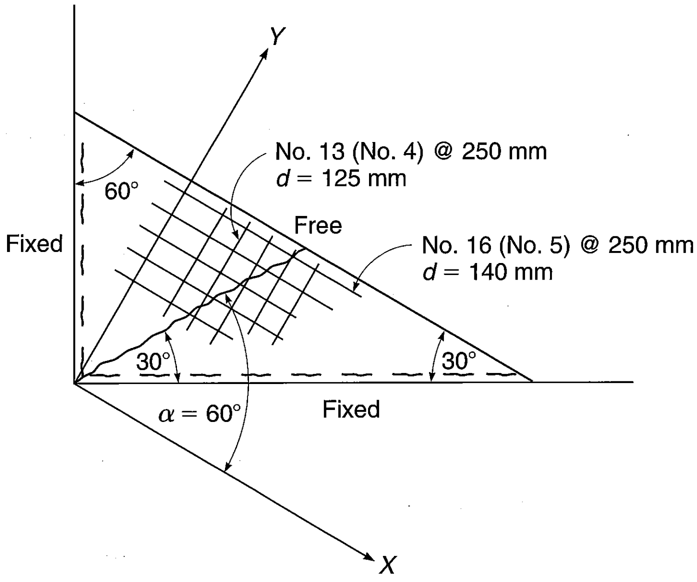

FIGURE 14.12
Skewed yield line example.

parallel to the free edge, and No. 13 (No. 4) bars at 250 mm spacing and 125 mm effective depth perpendicular to that edge. Concrete strength and steel yield stress are 28 MPa and 420 MPa, respectively. One possible failure mechanism includes a positive yield line at 30° with the long edge, as shown. Find the total resisting moment along the positive yield line provided by the two sets of bars.

Solution. It is easily confirmed that the resisting moment about the X axis provided by the Y direction bars is $m_x = 23.5$ kN-m/m, and the resisting moment about the Y axis provided by the X direction bars is $m_y = 40.0$ kN-m/m (both with $\phi = 0.90$ included). The yield line makes an angle of 60° with the X axis bars. With $\cos \alpha = 0.500$ and $\sin \alpha = 0.866$, from Eq. (14.1) the resisting moment along the α axis is

$$m_\alpha = 23.5 \times 0.500^2 + 40.0 \times 0.866^2 = 35.9 \text{ kN-m/m}$$

14.7 SPECIAL CONDITIONS AT EDGES AND CORNERS

Certain simplifications were made in defining yield line patterns in some of the preceding examples, in the vicinity of edges and corners. In some cases, such as Fig. 14.4*b* and *f*, positive yield lines were shown intersecting an edge at an angle. Actually, at a free or simply supported edge, both bending and twisting moments should theoretically be zero. The principal stress directions are parallel and perpendicular to the edge, and consequently the yield lines should enter an edge perpendicular to it. Tests confirm that this is the case, but the yield lines generally turn only quite close to the edge, the distance t in Fig. 14.13 being small compared to the dimensions of the slab (Ref. 14.4).

Referring to Fig. 14.13, the actual yield line of *a* can be simplified by extending the yield line in a straight line to the edge, as in *b*, if a pair of concentrated shearing forces m_t is introduced at the corners of the slab segments. The force m_t acting downward at the acute corner (circled cross) and the force m_t acting upward at the obtuse corner (circled dot) together are the static equivalent of twisting moments and shearing forces near the edge. It is shown in Ref. 14.4 that the magnitude of the fictitious shearing forces m_t is given by the expression

$$m_t = m \cot \alpha \tag{14.3}$$

where m is the resisting moment per unit length along the yield line and α is the acute angle between the simplified yield line and the edge of the slab.

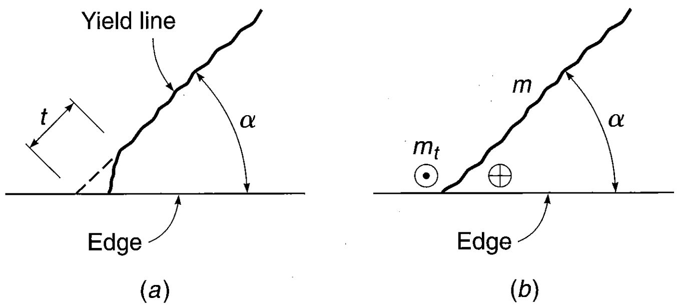

(*a*) (*b*)

FIGURE 14.13
Conditions at edge of slab:
(*a*) actual yield line;
(*b*) simplified yield line.

FIGURE 14.14
Corner conditions.

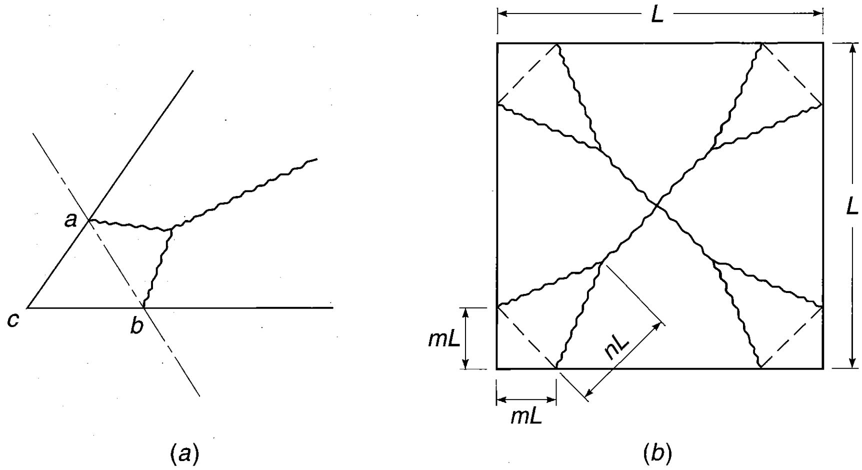

(*a*) (*b*)

It should be noted that while the fictitious forces enter the solution by the equilibrium method, the virtual work solution is not affected because the net work done by the pair of equal and opposite forces moving through the identical virtual displacement is zero.

Also, in the preceding examples, it was assumed that yield lines enter the corners between the two intersecting sides. An alternative possibility is that the yield line forks before it reaches the corner, forming what is known as a *corner lever*, shown in Fig. 14.14*a*.

If the corner is not held down, the triangular element *abc* will pivot about the axis *ab* and lift off the supports. The development of such a corner lever is clearly shown in Fig. 14.15. The photograph shows a model reinforced concrete slab that was tested under uniformly distributed load. The edges were simply supported and were

FIGURE 14.15
Development of corner levers in a simply supported, uniformly loaded slab.

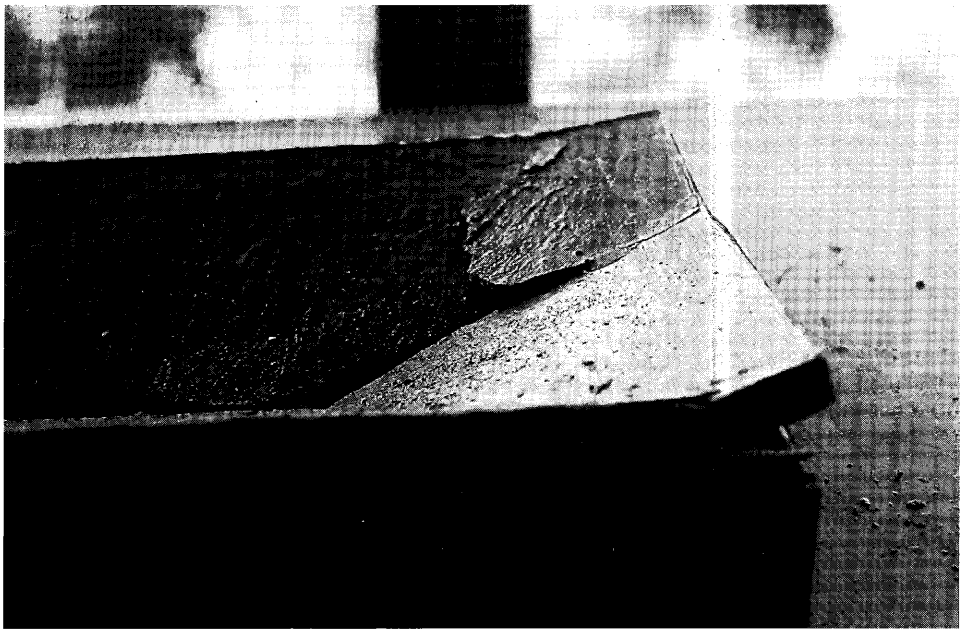

not restrained against upward movement. If the corner is held down, a similar situation occurs, except that the line *ab* becomes a yield line. If cracking at the corners of such a slab is to be controlled, top steel more or less perpendicular to the line *ab* must be provided. The direction taken by the positive yield lines near the corner indicates the desirability of supplementary bottom-slab reinforcement at the corners, placed approximately parallel to the line *ab* (see Section 13.4).

Although yield line patterns with corner levers are generally more critical than those without, they are often neglected in yield line analysis. The analysis becomes considerably more complicated if the possibility of corner levers is introduced, and the error made by neglecting them is usually small.

To illustrate, the uniformly loaded square slab of Example 14.2, when analyzed for the assumed yield pattern shown in Fig. 14.7, required a moment capacity of $qL^2/24$. The actual yield line pattern at failure is probably as shown in Fig. 14.14*b*. Since two additional parameters m and n have necessarily been introduced to define the yield line pattern, a total of three equations of equilibrium is now necessary. These equations are obtained by summing moments and vertical forces on the segments of the slab. Such an analysis results in a required resisting moment of $qL^2/22$, an increase of about 9 percent compared with the results of an analysis neglecting corner levers. The influence of such corner effects may be considerably larger when the corner angle is less than 90°.

14.8 FAN PATTERNS AT CONCENTRATED LOADS

If a concentrated load acts on a reinforced concrete slab at an interior location, away from any edge or corner, a negative yield line will form in a more or less circular pattern, as in Fig. 14.16*a*, with positive yield lines radiating outward from the load point.

FIGURE 14.16
Yield fan geometry at concentrated load: (*a*) yield fan; (*b*) moment vectors acting on fan segment; (*c*) resultant of positive-moment vectors; (*d*) edge view of fan segment.

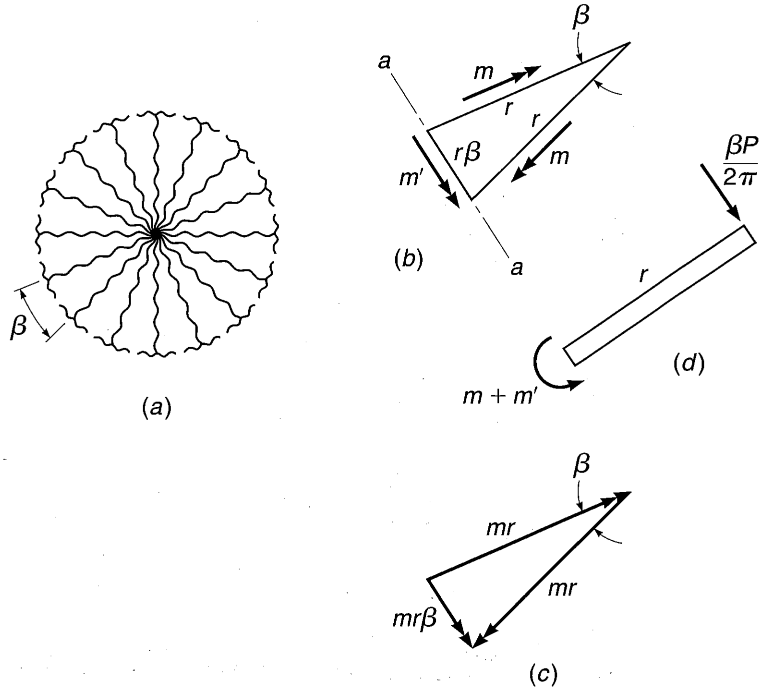

If the positive resisting moment per unit length is m and the negative resisting moment m', the moments per unit length acting along the edges of a single element of the fan, having a central angle β and radius r, are as shown in Fig. 14.16*b*. For small values of the angle β, the arc along the negative yield line can be represented as a straight line of length $r\beta$.

Figure 14.16*c* shows the moment resultant obtained by vector addition of the positive moments mr acting along the radial edges of the fan segment. The vector sum is equal to $mr\beta$, acting along the length $r\beta$, and the resultant positive moment, per unit length, is therefore m. This acts in the same direction as the negative moment m', as shown in Fig. 14.16*d*. Figure 14.16*d* also shows the fractional part of the total load P that acts on the fan segment.

Taking moments about the axis $a - a$ gives

$$(m + m')r\beta - \frac{\beta Pr}{2\pi} = 0$$

from which

$$P = 2\pi(m + m') \tag{14.4}$$

The collapse load P is seen to be independent of the fan radius r. Thus, with only a concentrated load acting, a complete fan of any radius could form with no change in collapse load.

It follows that Eq. (14.4) also gives the collapse load for a fixed-edge slab of any shape, carrying only a concentrated load P. The only necessary condition is that the boundary must be capable of a restraining moment equal to m' at all points. Finally, Eq. (14.4) is useful in establishing whether flexural failure will occur before a punching shear failure under a concentrated load.

Other load cases of practical interest, including a concentrated load near or at a free edge, and a concentrated corner load, are treated in Ref. 14.5. Loads distributed over small areas and load combinations are discussed in Ref. 14.12.

14.9 LIMITATIONS OF YIELD LINE THEORY

The usefulness of yield line theory should be apparent from the preceding sections. In general, elastic solutions are available only for restricted conditions, usually uniformly loaded rectangular slabs and slab systems. They do not account for the effects of inelastic action, except empirically. By yield line analysis, a rational determination of flexural strength may be had for slabs of any shape, supported in a variety of ways, with concentrated loads as well as distributed and partially distributed loads. The effects of holes of any size can be included. It is thus seen to be a powerful analytical tool for the structural engineer.

On the other hand, as an upper bound method, it will predict a collapse load that may be greater than the true collapse load. The actual capacity will be less than predicted if the selected mechanism is not the controlling one or if the specific locations of yield lines are not exactly correct. Most engineers would prefer an approach that would be in error, if at all, on the safe side. In this respect, the strip method of Chapter 15 is distinctly superior.

Beyond this, it should be evident that yield line theory provides, in essence, a method for determining the capacity of trial designs, arrived at by some other means, rather than for determining the amount and spacing of reinforcement. It is not, strictly speaking, a design method. To illustrate, yield line theory provides no inducement for the designer to place steel at anything other than a uniform lateral spacing along a yield line. It is necessary to consider the results of elastic analysis of a flat plate, for example, to recognize that reinforcement in that case should be placed in strong bands across the columns.

In applying yield line analysis to slabs, it must be remembered that the analysis is predicated upon available rotation capacity at the yield lines. If the slab reinforcement happens to correspond closely to the elastic distribution of moments in the slab, little rotation is required. If, on the other hand, there is a marked difference, it is possible that the required rotation will exceed the available rotation capacity, in which case the slab will fail prematurely. However, in general, because slabs are typically rather lightly reinforced, they will have adequate rotation capacity to attain the collapse loads predicted by yield line analysis.

It should also be borne in mind that the yield line analysis focuses entirely on the flexural capacity of the slab. It is presumed that earlier failure will not occur due to shear or torsion and that cracking and deflections at service load will not be excessive. ACI Code 13.5.1 calls attention specifically to the need to meet "all serviceability conditions, including limits on deflections," and ACI Commentary 13.5.1 calls attention to the need for "evaluation of the stress conditions around the supports in relation to shear and torsion as well as flexure."

REFERENCES

14.1. A. Ingerslev, "The Strength of Rectangular Slabs," *J. Inst. Struct. Eng.*, London, vol. 1, no. 1, 1923, pp. 3–14.

14.2. K. W. Johansen, *Brutlinieteorier*, Jul. Gjellerups Forlag, Copenhagen, 1943 (see also *Yield Line Theory*, English translation, Cement and Concrete Association, London, 1962).

14.3. K. W. Johansen, *Pladeformler*, 2nd ed., Polyteknisk Forening, Copenhagen, 1949 (see also *Yield Line Formulae for Slabs*, English translation, Cement and Concrete Association, London, 1972).

14.4. E. Hognestad, "Yield Line Theory for the Ultimate Flexural Strength of Reinforced Concrete Slabs," *J. ACI*, vol. 24, no. 7, 1953, pp. 637–656.

14.5. L. L. Jones and R. H. Wood, *Yield Line Analysis of Slabs*, American Elsevier, New York, 1967.

14.6. R. Taylor, D. R. H. Maher, and B. Hayes, "Effect of the Arrangement of Reinforcement on the Behavior of Reinforced Concrete Slabs," *Mag. Concr. Res.*, vol. 18, no. 55, 1966, pp. 85–94.

14.7. R. Lenschow and M. A. Sozen, "A Yield Criterion for Reinforced Concrete Slabs," *J. ACI*, vol. 64, no. 5, 1967, pp. 266–273.

14.8. S. H. Simmonds and A. Ghali, "Yield Line Design of Slabs," *J. Struct. Div.*, ASCE, vol. 102, no. ST1, 1976, pp. 109–123.

14.9. K. H. Chu and R. B. Singh, "Yield Analysis of Balcony Floor Slabs," *J. ACI*, vol. 63, no. 5, 1966, pp. 571–586.

14.10. E. C. Demsky and D. S. Hatcher, "Yield Line Analysis of Slabs Supported on Three Sides," *J. ACI*, vol. 66, no. 9, 1969, pp. 741–744.

14.11. A. Zaslavsky and C. H. Avraham, "Yield Line Design of Rectangular Reinforced Concrete Balconies," *J. ACI*, vol. 67, no. 1, 1970, pp. 53–56.

14.12. H. Gesund, "Limit Design of Slabs for Concentrated Loads," *J. Struct. Div.*, ASCE, vol. 107, no. ST9, 1981, pp. 1839–1856.

14.13. A. Zaslavsky, "Yield Line Analysis of Rectangular Slabs with Central Openings," *J. ACI*, vol. 64, no. 12, 1967, pp. 838–844.

14.14. S. Islam and R. Park, "Yield Line Analysis of Two-Way Reinforced Concrete Slabs with Openings," *J. Inst. Struct. Eng.*, vol. 49, no. 6, 1971, pp. 269–276.

14.15. R. Park and W. L. Gamble, *Reinforced Concrete Slabs*, 2nd ed., John Wiley & Sons, New York, 1999.

PROBLEMS

14.1. A square slab measuring 3 m on each side is simply supported on three sides and unsupported along the fourth. It is reinforced for positive bending with an isotropic mat of steel providing resistance ϕm_n of 9.5 kN-m/m in each of the two principal directions. Determine the uniformly distributed load that would cause flexural failure, using the method of virtual work.

14.2. The triangular slab shown in Fig. P14.2 has fixed supports along the two perpendicular edges and is free of any support along the diagonal edge. Negative reinforcement perpendicular to the supported edges provides design strength $\phi m_n = 18$ kN-m/m. The slab is reinforced for positive bending by an orthogonal grid providing resistance $\phi m_n = 12$ kN-m/m in all directions. Find the total factored load w_u that will produce flexural failure. A virtual work solution is suggested.

FIGURE P14.2

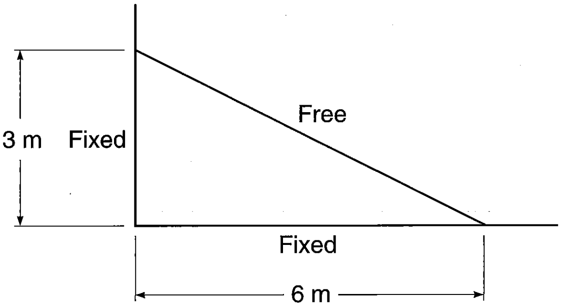

14.3. The one-way reinforced concrete slab shown in Fig. P14.3 spans 6 m. It is simply supported at its left edge, fully fixed at its right edge, and free of support along the two long sides. Reinforcement provides design strength ϕm_n = 22 kN-m/m in positive bending and $\phi m_n = 33$ kN-m/m in negative bending at the right edge. Using the equilibrium method, find the factored load q_u uniformly distributed over the surface that would cause flexural failure.

FIGURE P14.3

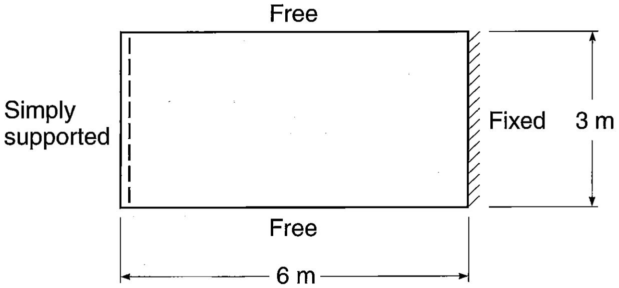

14.4. Solve Problem 14.3 using the method of virtual work.

14.5. The triangular slab shown in Fig. P14.5 is to serve as weather protection over a loading dock. Support conditions are essentially fixed along AB and BC, and AC is a free edge. In addition to self-weight, a superimposed dead load of 0.7 kN/m^2 and service live load of 2 kN/m^2 must be provided for. Material strengths are $f'_c = 28$ MPa and $f_y = 420$ MPa. Using yield line analysis, find the required slab thickness h and find the reinforcement required at critical sections. Neglect corner pivots. Use a maximum reinforcement ratio of 0.005. Select bar sizes and spacings, and provide a sketch summarizing important aspects of the design. Make an approximate, conservative check of safety against shear failure for the design. Also include a conservative estimate of the deflection near the center of edge AC due to a full live load.

FIGURE P14.5

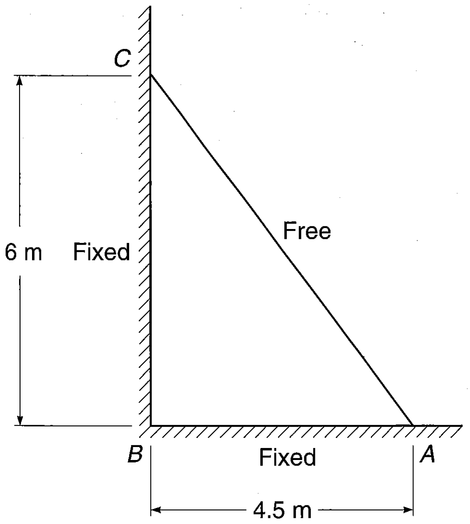

14.6. The square concrete slab shown in Fig. P14.6 is supported by monolithic concrete walls providing full vertical and rotational restraint along two adjacent edges, and by a 150 mm diameter steel pipe column, near the outer corner, that offers negligible rotational restraint. It is reinforced for positive bending by an orthogonal grid of bars parallel to the walls, providing design moment capacity $\phi m_n = 28.9$ kN-m/m in all directions. Negative reinforcement perpendicular to the walls and negative bars at the outer corner parallel to the slab diagonal provide $\phi m_n = 39.6$ kN-m/m. Neglecting corner pivots, find the total factored uniformly distributed load q_u that will initiate flexural failure. Solution by the method of virtual work is recommended, with collapse geometry established by successive trials. Yield line lengths and perpendicular distances are most easily found graphically. Include a check of the shear capacity of the slab, using approximate methods. The steel column is capped with a 300 × 300 mm plate providing bearing.

FIGURE P14.6

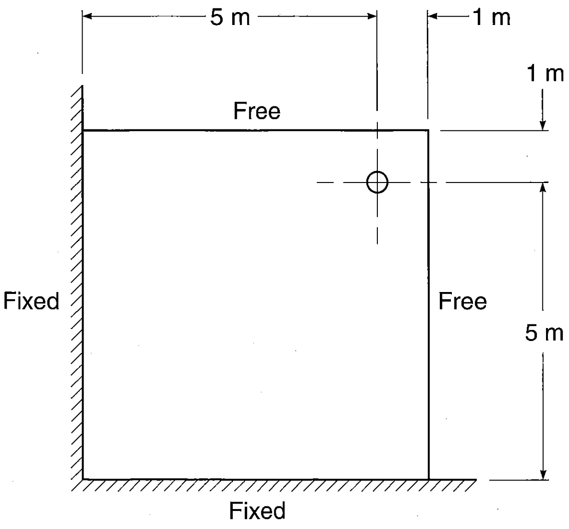

14.7. The square slab shown in Fig. P14.7 is supported by, and is monolithic with, a reinforced concrete wall along the edge *CD* that provides full fixity, and also is supported by a masonry wall along *AB* that provides a simply supported line. It is carry a factored load $q_u = 14$ kN/m^2 including its self-weight. Assuming a uniform 150 mm slab thickness, find the required reinforcement. Include a sketch summarizing details of your design, indicating placement and length of all reinforcing bars. Also check the shear capacity of the structure, making whatever assumptions appear reasonable and necessary. Use $f_c' = 28$ MPa and $f_y = 420$ MPa.

FIGURE P14.7

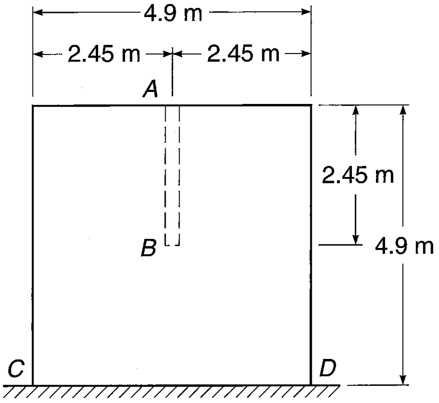

14.8. The slab of Fig. P14.8 is supported by three fixed edges but has no support along one long side. It has a uniform thickness of 175 mm, resulting in effective depths in the long direction of 150 mm and in the short direction of 136 mm. Bottom reinforcement consists of No. 13 (No. 4) bars at 350 mm centers in each direction, continued to the supports and the free edge. Top negative steel along the supported edges consists of No. 13 (No. 4) bars at 300 mm on centers, except that in a 600 mm wide "strong band" parallel and adjacent to the free edge, four No. 16 (No. 5) bars are used. All negative bars extend past the points of inflection, as required by ACI Code. Material strengths are $f_c' = 28$ MPa and $f_y = 420$ MPa. Using the yield line method, determine the factored load q_u that can be carried.

FIGURE P14.8

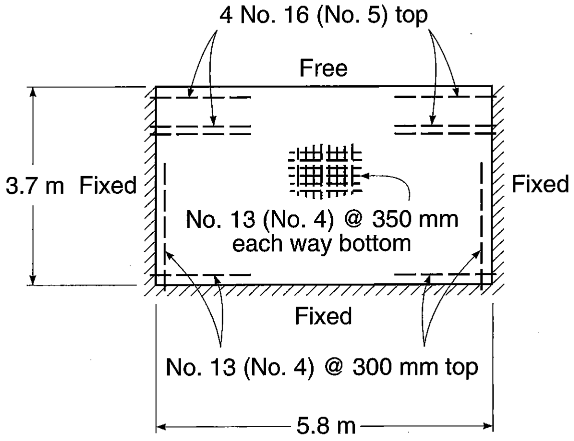
4 No. 16 (No. 5) top
Free
3.7 m
Fixed
Fixed
No. 13 (No. 4) @ 350 mm each way bottom
Fixed
No. 13 (No. 4) @ 300 mm top
5.8 m

14.9. Using virtual work and yield line theory, compute the flexural collapse load of the one-way slab in Example 13.1. Assume that all straight bars are used, according to Fig. 13.4*b*. Compare the calculated collapse load with the original factored design load, and comment on differences.

14.10. Using virtual work and yield line theory, compute the flexural collapse load of the two-way column-supported flat plate of Example 13.3. To simplify the calculations, assume that all positive moment bars are carried to the edges of the panels, not cut off in the span. Consider all possible failure mechanisms, including a circular fan around the column. Neglect corner effects. Compare the calculated collapse load with the original factored design load and comment on differences.

15

Strip Method for Slabs

15.1 INTRODUCTION

In Section 14.2, the upper and lower bound theorems of the theory of plasticity were presented, and it was pointed out that the yield line method of slab analysis was an *upper bound approach* to determining the flexural strength of slabs. An upper bound analysis, if in error, will be so on the unsafe side. The actual carrying capacity will be less than, or at best equal to, the capacity predicted, which is certainly a cause for concern in design. Also, when applying the yield line method, it is necessary to assume that the distribution of reinforcement is known over the whole slab. It follows that the yield line approach is a tool to *analyze* the capacity of a given slab and can be used for *design* only in an iterative sense, for calculating the capacities of trial designs with varying reinforcement until a satisfactory arrangement is found.

These circumstances motivated Hillerborg to develop what is known as the *strip method* for slab design, his first results being published in Swedish in 1956 (Ref. 15.1). In contrast to yield line analysis, the strip method is a *lower bound approach*, based on satisfaction of equilibrium requirements everywhere in the slab. By the strip method (sometimes referred to as the *equilibrium theory*), a moment field is first determined that fulfills equilibrium requirements, after which the reinforcement in the slab at each point is designed for this moment field. If a distribution of moments can be found that satisfies both equilibrium and boundary conditions for a given external loading, and if the yield moment capacity of the slab is nowhere exceeded, then the given external loading will represent a lower bound of the true carrying capacity.

The strip method gives results on the safe side, which is certainly preferable in practice, and differences from the true carrying capacity will never impair safety. The strip method is a *design* method, by which the needed reinforcement can be calculated. It encourages the designer to vary the reinforcement in a logical way, leading to an economical arrangement of steel, as well as a safe design. It is generally simple to use, even for slabs with holes or irregular boundaries.

In his original work in 1956, Hillerborg set forth the basic principles for edge-supported slabs and introduced the expression *strip method* (Ref. 15.1). He later expanded the method to include the practical design of slabs on columns and L-shaped slabs (Refs. 15.2 and 15.3). The first treatment of the subject in English was by Crawford (Ref. 15.4). In 1964, Blakey translated the earlier Hillerborg work into English (Ref. 15.5). Important contributions, particularly regarding continuity conditions, have been made by Kemp (Refs. 15.6 and 15.7) and Wood and Armer (Refs. 15.8, 15.9, and 15.10). Load tests of slabs designed by the strip method were carried out by Armer (Ref. 15.11) and confirmed that the method produces safe and satisfactory designs. In 1975, Hillerborg produced Ref. 15.12 "for the practical designer, helping him in the simplest possible way to produce safe designs for most of the slabs that he will meet in practice, including slabs that are irregular in plan or that carry unevenly distributed loads." Subsequently, he published a paper in which he summarized what has become known as the *advanced strip method*, pertaining to the design of slabs supported on columns, reentrant corners, or interior walls (Ref. 15.13). Useful summaries of both the simple and advanced strip methods will be found in Refs. 15.14 and 15.15.

The strip method is appealing not only because it is safe, economical, and versatile over a broad range of applications, but also because it formalizes procedures followed instinctively by competent designers in placing reinforcement in the best possible position. In contrast with the yield line method, which provides no inducement to vary bar spacing, the strip method encourages the use of strong bands of steel where needed, such as around openings or over columns, improving economy and reducing the likelihood of excessive cracking or large deflections under service loading.

15.2 BASIC PRINCIPLES

The governing equilibrium equation for a small slab element having sides dx and dy is

$$\frac{\partial^2 m_x}{\partial x^2} + \frac{\partial^2 m_y}{\partial y^2} - 2\frac{\partial^2 m_{xy}}{\partial x \partial y} = -q \tag{15.1}$$

where q = external load per unit area
m_x, m_y = bending moments per unit width in X and Y directions, respectively
m_{xy} = twisting moment (Ref. 15.16)

According to the lower bound theorem, any combination of m_x, m_y, and m_{xy} that satisfies the equilibrium equation at all points in the slab and that meets boundary conditions is a valid solution, provided that the reinforcement is placed to carry these moments.

The basis for the simple strip method is that the torsional moment is chosen equal to zero; no load is assumed to be resisted by the twisting strength of the slab. Therefore, if the reinforcement is parallel to the axes in a rectilinear coordinate system,

$$m_{xy} = 0$$

The equilibrium equation then reduces to

$$\frac{\partial^2 m_x}{\partial x^2} + \frac{\partial^2 m_y}{\partial y^2} = -q \tag{15.2}$$

This equation can be split conveniently into two parts, representing twistless beam strip action

$$\frac{\partial^2 m_x}{\partial x^2} = -kq \tag{15.3a}$$

and

$$\frac{\partial^2 m_y}{\partial y^2} = -(1-k)q \tag{15.3b}$$

where the proportion of load taken by the strips is k in the X direction and $1 - k$ in the Y direction. In many regions in slabs, the value of k will be either 0 or 1. With $k = 0$, all of the load is dispersed by strips in the Y direction; with $k = 1$, all of the load is carried in the X direction. In other regions, it may be reasonable to assume that the load is divided equally in the two directions (i.e., $k = 0.5$).

15.3 CHOICE OF LOAD DISTRIBUTION

Theoretically, the load q can be divided arbitrarily between the X and Y directions. Different divisions will, of course, lead to different patterns of reinforcement, and not all will be equally appropriate. The desired goal is to arrive at an arrangement of steel that is safe and economical and that will avoid problems at the service load level associated with excessive cracking or deflections. In general, the designer may be guided by knowledge of the general distribution of elastic moments.

To see an example of the strip method and to illustrate the choices open to the designer, consider the square, simply supported slab shown in Fig. 15.1, with side length a and a uniformly distributed factored load q per unit area.

The simplest load distribution is obtained by setting $k = 0.5$ over the entire slab, as shown in Fig. 15.1. The load on all strips in each direction is then $q/2$, as illustrated by the load dispersion arrows of Fig. 15.1a. This gives maximum moments

$$m_x = m_y = \frac{qa^2}{16} \tag{15.4}$$

over the whole slab, as shown in Fig. 15.1c, with a uniform lateral distribution across the width of the critical section, as in Fig. 15.1d.

FIGURE 15.1
Square slab with load shared equally in two directions.

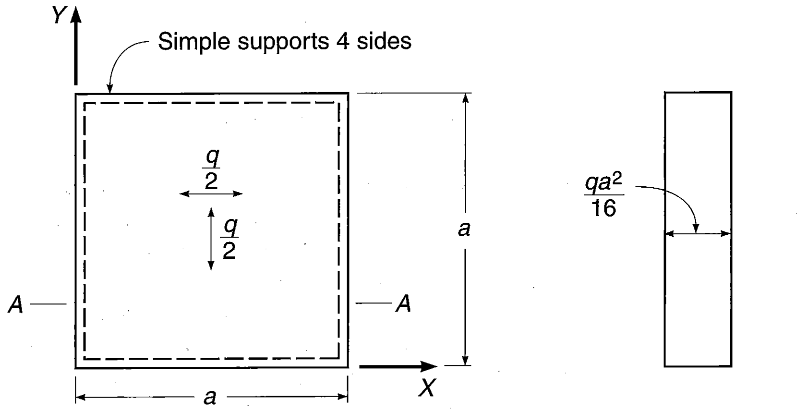

(a) Plan view

(d) m_x across $x = \frac{a}{2}$

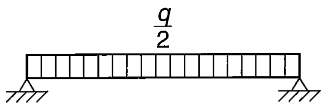

(b) q_x along A–A

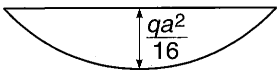

(c) m_x along A–A

FIGURE 15.2
Square slab with load dispersion lines following diagonals.

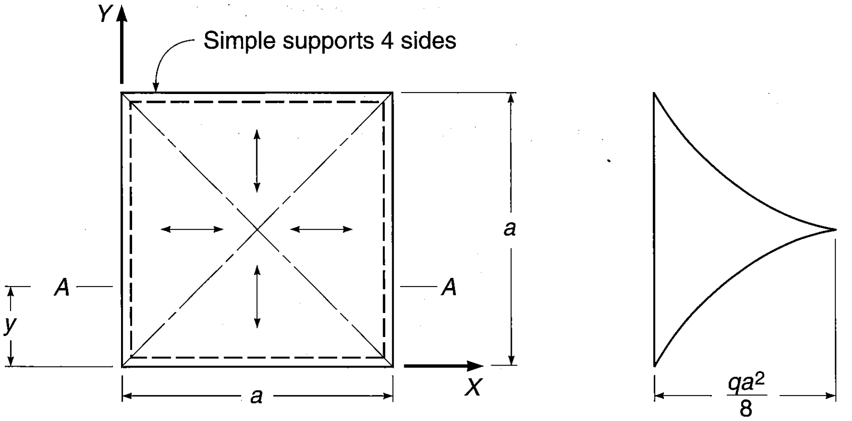

(a) Plan view

(d) m_x across $x = \frac{a}{2}$

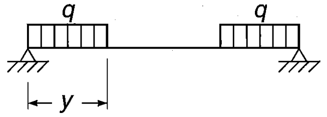

(b) q_x along A–A

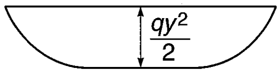

(c) m_x along A–A

This would not represent an economical or serviceable solution because it is recognized that curvatures, hence moments, must be greater in the strips near the middle of the slab than near the edges in the direction parallel to the edge (see Fig. 13.5). If the slab were reinforced according to this solution, extensive redistribution of moments would be required, certainly accompanied by much cracking in the highly stressed regions near the middle of the slab.

An alternative, more reasonable distribution is shown in Fig. 15.2. Here the regions of different load dispersion, separated by the dash-dotted "discontinuity lines," follow the diagonals, and all of the load on any region is carried in the direction giving the shortest distance to the nearest support. The solution proceeds, giving k values of either 0 or 1, depending on the region, with load transmitted in the directions indicated by the arrows of Fig. 15.2a. For a strip A–A at a distance $y \leq a/2$ from the X axis, the moment is

$$m_x = \frac{qy^2}{2} \tag{15.5}$$

The load acting on a strip A–A is shown in Fig. 15.2b, and the resulting diagram of moment m_x is given in Fig. 15.2c. The lateral variation of m_x across the width of the slab is as shown in Fig. 15.2d.

The lateral distribution of moments shown in Fig. 15.2d would theoretically require a continuously variable bar spacing, obviously an impracticality. One way of using the distribution in Fig. 15.2, which is considerably more economical than that in Fig. 15.1, would be to reinforce for the *average* moment over a certain width, approximating the actual lateral variation shown in Fig. 15.2*d* in a stepwise manner. Hillerborg notes that this is not strictly in accordance with the equilibrium theory and that the design is no longer certainly on the safe side, but other conservative assumptions, e.g., neglect of membrane strength in the slab and neglect of strain hardening of the reinforcement, would surely compensate for the slight reduction in safety margin.

A third alternative distribution is shown in Fig. 15.3. Here the division is made so that the load is carried to the nearest support, as before, but load near the diagonals has been divided, with one-half taken in each direction. Thus, k is given values of 0 or 1

FIGURE 15.3
Square slab with load near diagonals shared equally in two directions.

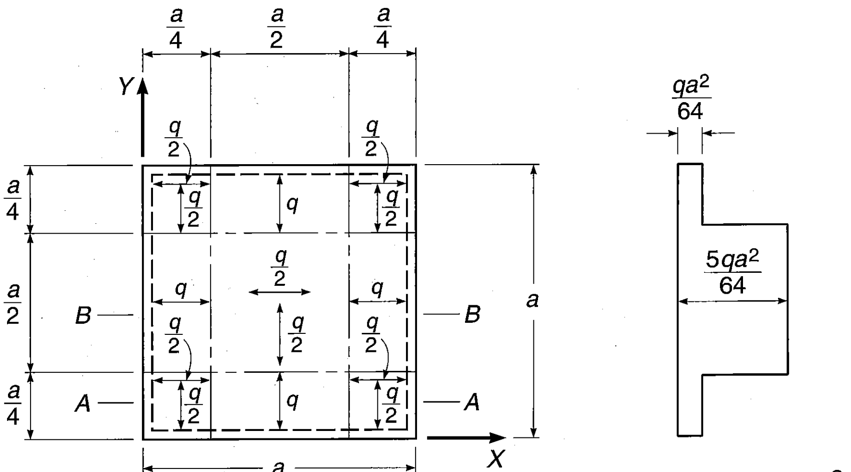
$\frac{a}{4}$
$\frac{a}{2}$
$\frac{a}{4}$
Y
X
$\frac{q}{2}$
q
$\frac{q}{2}$
B
A
a
$\frac{qa^2}{64}$
$\frac{5qa^2}{64}$

(*a*) Plan view

(*d*) m_x across $x = \frac{a}{2}$

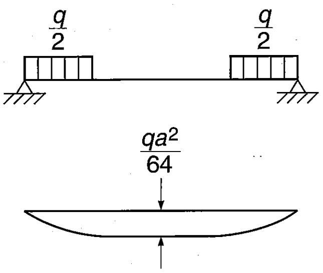
$\frac{q}{2}$
$\frac{q}{2}$
$\frac{qa^2}{64}$

(*b*) q_x and m_x along *A–A*

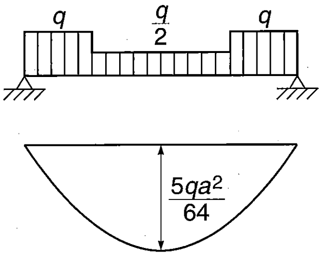
q
$\frac{q}{2}$
q
$\frac{5qa^2}{64}$

(*c*) q_x and m_x along *B–B*

along the middle edges and a value of 0.5 in the corners and center of the slab, with load dispersion in the directions indicated by the arrows shown in Fig. 15.3*a*. Two different strip loadings are now identified. For an *X* direction strip along section *A–A*, the maximum moment is

$$m_x = \frac{q}{2} \times \frac{a}{4} \times \frac{a}{8} = \frac{qa^2}{64} \tag{15.6a}$$

and for a strip along section *B–B*, the maximum moment is

$$m_x = q \times \frac{a}{4} \times \frac{a}{8} + \frac{q}{2} \times \frac{a}{4} \times \frac{3a}{8} = \frac{5qa^2}{64} \tag{15.6b}$$

The variation of m_x along the line $x = a/2$ is shown in Fig. 15.3*d*. This design leads to a practical arrangement of reinforcement, one with constant spacing through the center strip of width $a/2$ and a wider spacing through the outer strips, where the elastic curvatures and moments are known to be less. The averaging of moments necessitated in the second solution is avoided here, and the third solution is fully consistent with the equilibrium theory.

Comparing the three solutions just presented shows that the first would be unsatisfactory, as noted earlier, because it would require great redistribution of moments to achieve, possibly accompanied by excessive cracking and large deflections. The second, with discontinuity lines following the slab diagonals, has the advantage that the reinforcement more nearly matches the elastic distribution of moments, but it either leads to an impractical reinforcing pattern or requires an averaging of moments in bands that involves a deviation from strict equilibrium theory. The third solution, with discontinuity lines parallel to the edges, does not require moment averaging and leads to a practical reinforcing arrangement, so it will often be preferred.

The three examples also illustrate the simple way in which moments in the slab can be found by the strip method, based on familiar beam analysis. It is important to note, too, that the load on the supporting beams is easily found because it can be computed from the end reactions of the slab beam strips in all cases. This information is not available from solutions such as those obtained by the yield line theory.

15.4 RECTANGULAR SLABS

With rectangular slabs, it is reasonable to assume that, throughout most of the area, the load will be carried in the short direction, consistent with elastic theory (see Section 13.4). In addition, it is important to take into account the fact that because of their length, longitudinal reinforcing bars will be more expensive than transverse bars of the same size and spacing. For a uniformly loaded rectangular slab on simple supports, Hillerborg presents one possible division, as shown in Fig. 15.4, with discontinuity lines originating from the slab corners at an angle depending on the ratio of short to long sides of the slab. All of the load in each region is assumed to be carried in the directions indicated by the arrows.

Instead of the solution of Fig. 15.4, which requires continuously varying reinforcement to be strictly correct, Hillerborg suggests that the load can be distributed as shown in Fig. 15.5, with discontinuity lines parallel to the sides of the slab. For such cases, it is reasonable to take edge bands of width equal to one-fourth the short span dimension. Here the load in the corners is divided equally in the *X* and *Y* directions as shown, while elsewhere all of the load is carried in the direction indicated by the arrows.

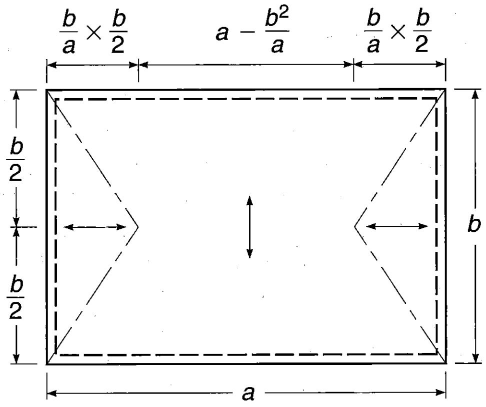

$\frac{b}{a} \times \frac{b}{2}$
$a - \frac{b^2}{a}$
$\frac{b}{a} \times \frac{b}{2}$
$\frac{b}{2}$
$\frac{b}{2}$
b
a

FIGURE 15.4
Rectangular slab with discontinuity lines originating at the corners.

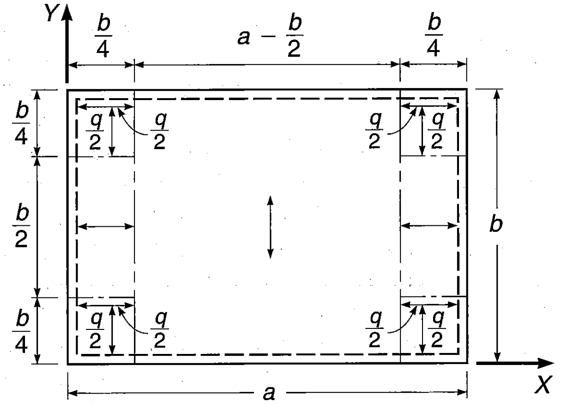

Y
$\frac{b}{4}$
$a - \frac{b}{2}$
$\frac{b}{4}$
$\frac{b}{4}$
$\frac{b}{2}$
$\frac{b}{4}$
$\frac{q}{2}$
b
a
X

FIGURE 15.5
Discontinuity lines parallel to the sides for a rectangular slab.

The second, preferred arrangement, shown in Fig. 15.5, gives slab moments as follows:

In the X direction:

Side strips: $$m_x = \frac{q}{2} \times \frac{b}{4} \times \frac{b}{8} = \frac{qb^2}{64} \tag{15.7a}$$

Middle strips: $$m_x = q \times \frac{b}{4} \times \frac{b}{8} = \frac{qb^2}{32} \tag{15.7b}$$

In the Y direction:

Side strips: $$m_y = \frac{qb^2}{64} \tag{15.8a}$$

Middle strips: $$m_y = \frac{qb^2}{8} \tag{15.8b}$$

This distribution, requiring no averaging of moments across band widths, is always on the safe side and is both simple and economical.

15.5 FIXED EDGES AND CONTINUITY

Designing by the strip method has been shown to provide a large amount of flexibility in assigning load to various regions of slabs. This same flexibility extends to the assignment of moments between negative and positive bending sections of slabs that are fixed or continuous over their supported edges. Some attention should be paid to elastic moment ratios to avoid problems with cracking and deflection at service loads. However, the redistribution that can be achieved in slabs, which are typically rather lightly reinforced and, thus, have large plastic rotation capacities when overloaded, permits considerable arbitrary readjustment of the ratio of negative to positive moments in a strip.

This is illustrated by Fig. 15.6, which shows a slab strip carrying loads only near the supports and unloaded in the central region, such as often occurs in designing by the strip method. It is convenient if the unloaded region is subject to a constant moment (and zero shear), because this simplifies the selection of positive reinforcement. The sum of the absolute values of positive span moment and negative end moment at the left or right end, shown as m_l and m_r in Fig. 15.6, depends only on the conditions at the respective end and is numerically equal to the negative moment if the strip carries the load as a cantilever. Thus, in determining moments for design, one calculates the "cantilever" moments, selects the span moment, and determines the corresponding support moments. Hillerborg notes that, as a general rule for fixed edges, the support moment should be about 1.5 to 2.5 times the span moment in the same strip. Higher values should be chosen for longitudinal strips that are largely unloaded, and in such cases a ratio of support to span moment of 3 to 4 may be used. However, little will be gained by using such a high ratio if the positive moment steel is controlled by minimum requirements of the ACI Code.

For slab strips with one end fixed and one end simply supported, the dual goals of constant moment in the unloaded central region and a suitable ratio of negative to positive moments govern the location to be chosen for the discontinuity lines. Figure 15.7*a* shows a uniformly loaded rectangular slab having two adjacent edges fixed and the other two edges simply supported. Note that although the middle strips have the same width as those of Fig. 15.5, the discontinuity lines are shifted to account for the greater stiffness of the strips with fixed ends. Their location is defined by a coefficient α, with a value clearly less than 0.5 for the slab shown, its exact value yet to be determined. It will be seen that the selection of α relates directly to the ratio of negative to positive moments in the strips.

The moment curve of Fig. 15.7*b* is chosen so that moment is constant over the unloaded part, i.e., shearing force is zero. With constant moment, the positive steel can be fully stressed over most of the strip. The maximum positive moment in the *X* direction middle strip is then

$$m_{xf} = \frac{\alpha q b}{2} \times \frac{\alpha b}{4} = \alpha^2 \frac{q b^2}{8} \tag{15.9}$$

FIGURE 15.6
Slab strip with central region unloaded.

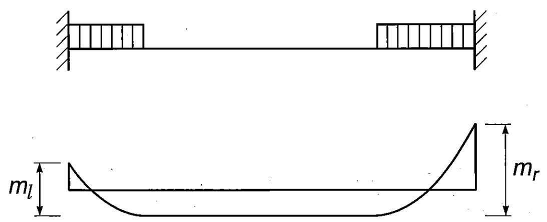

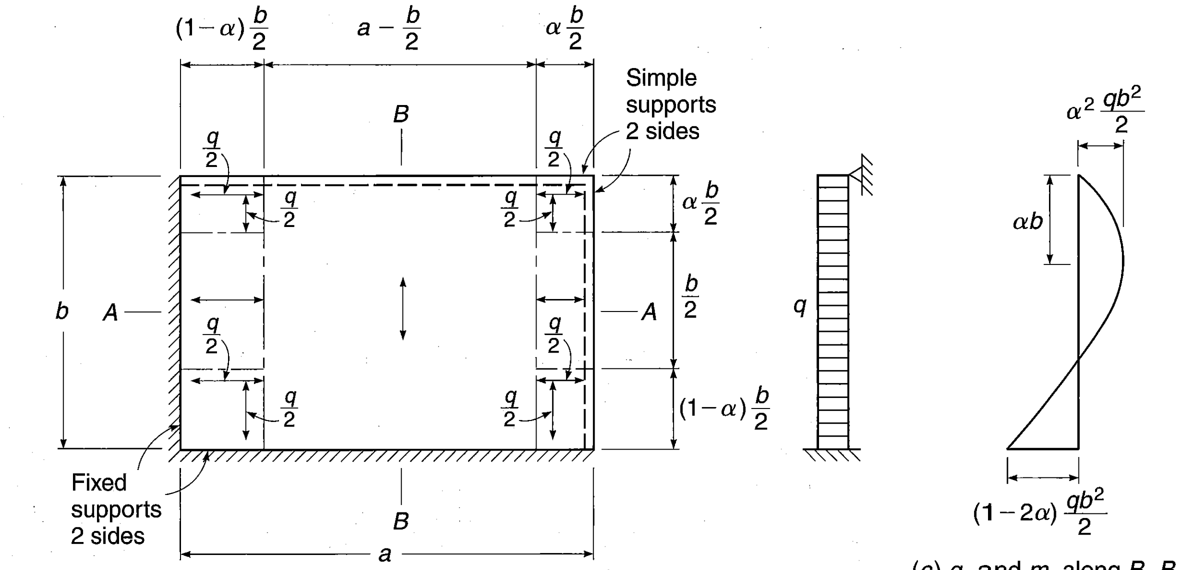
$(1-\alpha)\frac{b}{2}$
$a-\frac{b}{2}$
$\alpha\frac{b}{2}$
Simple supports 2 sides
B
$\frac{q}{2}$
b
A
A
$\alpha\frac{b}{2}$
$\frac{b}{2}$
$(1-\alpha)\frac{b}{2}$
Fixed supports 2 sides
B
a
q
$\alpha^2\frac{qb^2}{2}$
αb
$(1-2\alpha)\frac{qb^2}{2}$

(*a*) Plan view

(*c*) q_y and m_y along *B–B*

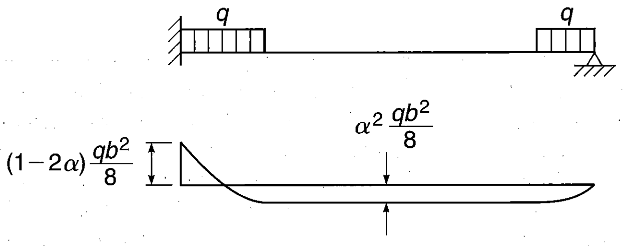
q
q
$\alpha^2\frac{qb^2}{8}$
$(1-2\alpha)\frac{qb^2}{8}$

(*b*) q_x and m_x along *A–A*

FIGURE 15.7
Rectangular slab with two edges fixed and two edges simply supported.

The cantilever moment at the left support is

$$m_x = (1-\alpha)\frac{qb}{2}(1-\alpha)\frac{b}{4} = (1-\alpha)^2\frac{qb^2}{8} \tag{15.10}$$

and so the negative moment at the left support is

$$m_{xs} = (1-\alpha)^2\frac{qb^2}{8} - \alpha^2\frac{qb^2}{8} = (1-2\alpha)\frac{qb^2}{8} \tag{15.11}$$

For reference, the ratio of negative to positive moments in the *X* direction middle strip is

$$\frac{m_{xs}}{m_{xf}} = \frac{1-2\alpha}{\alpha^2} \tag{15.12}$$

The moments in the *X* direction edge strips are one-half of those in the middle strips because the load is one-half as great.

It is reasonable to choose the same ratio between support and span moments in the *Y* direction as in the *X* direction. Accordingly, the distance from the right support, Fig. 15.7c, to the maximum positive moment section is chosen as ab. It follows that the maximum positive moment is

$$m_{yf} = \alpha qb \times \frac{\alpha b}{2} = \alpha^2 \frac{qb^2}{2} \tag{15.13}$$

Applying the same methods as used for the X direction shows that the negative support moment in the Y direction middle strips is

$$m_{ys} = (1 - 2\alpha)\frac{qb^2}{2} \tag{15.14}$$

It is easily confirmed that the moments in the Y direction edge strips are just one-eighth of those in the Y direction middle strip.

With the above expressions, all of the moments in the slab can be found once a suitable value for α is chosen. From Eq. (15.12), it can be confirmed that values of α from 0.35 to 0.39 give corresponding ratios of negative to positive moments from 2.45 to 1.45, the range recommended by Hillerborg. For example, if it is decided that support moments are to be twice the span moments, the value of α should be 0.366, and the negative and positive moments in the central strip in the Y direction are, respectively, $0.134qb^2$ and $0.067qb^2$. In the middle strip in the X direction, moments are one-fourth those values; and in the edge strips in both directions, they are one-eighth of those values.

EXAMPLE 15.1

Rectangular slab with fixed edges. Figure 15.8 shows a typical interior panel of a slab floor in which support is provided by beams on all column lines. Normally proportioned beams will be stiff enough, both flexurally and torsionally, that the slab can be assumed fully restrained on all sides. Clear spans for the slab, face to face of beams, are 7.6 and 6.0 m, as shown. The floor must carry a service live load of 7.0 kN/m^2, using concrete with $f'_c = 21$ MPa and steel with $f_y = 420$ MPa. Find the moments at all critical sections, and determine the required slab thickness and reinforcement.

Solution. The minimum slab thickness required by the ACI Code can be found from Eq. (13.8b), with $l_n = 7.6$ m and $\beta = 1.25$:

$$h = \frac{7600 \times (0.8 + 420/1400)}{36 + 9 \times 1.25} = 176 \text{ mm}$$

A total thickness of 175 mm will be selected, for which $q_d = 24 \times 0.175 = 4.2$ kN/m^2. Applying the load factors of 1.2 and 1.6 to dead load and live load, respectively, determines that the total factored load for design is 16.2 kN/m^2. For strip analysis, discontinuity lines will be selected as shown in Fig. 15.8, with edge strips of width $b/4 = 7.6/4 = 1.9$ m. In the corners, the load is divided equally in the two directions; elsewhere, 100 percent of the load is assigned to the direction indicated by the arrows. A ratio of support moment to span moment of 2.0 will be used. Calculation of moments then proceeds as follows:

X direction middle strip:

Cantilever: $$m_x = \frac{qb^2}{32} = 16.2 \times \frac{6.0^2}{32} = 18.3 \text{ kN-m/m}$$

Negative: $$m_{xs} = 18.3 \times \frac{2}{3} = 12.2$$

Positive: $$m_{xf} = 18.3 \times \frac{1}{3} = 6.1$$

FIGURE 15.8
Design example: two-way slab with fixed edges.

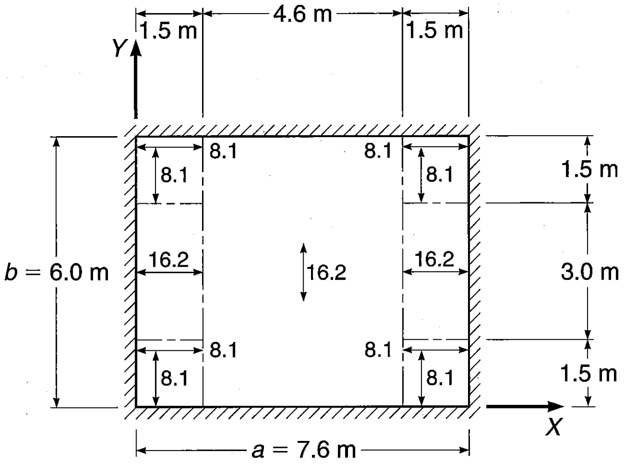
1.5 m
4.6 m
1.5 m
Y
8.1
8.1
8.1
8.1
16.2
16.2
16.2
8.1
8.1
8.1
8.1
1.5 m
3.0 m
1.5 m
b = 6.0 m
X
a = 7.6 m

(*a*) Plan view

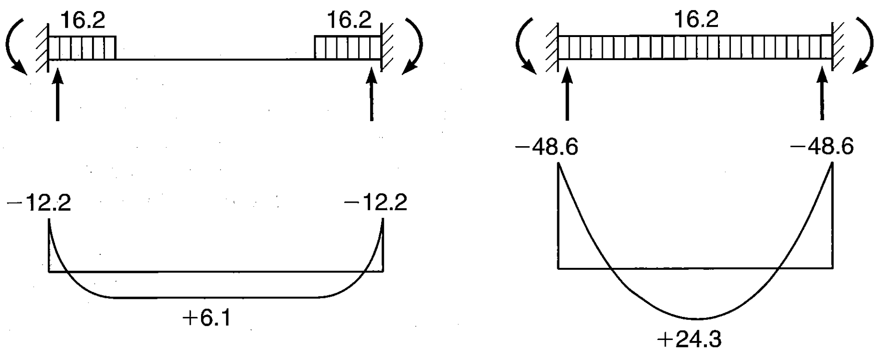
16.2
16.2
−12.2
−12.2
+6.1
16.2
−48.6
−48.6
+24.3

(*b*) *X* direction middle strip (*d*) *Y* direction middle strip

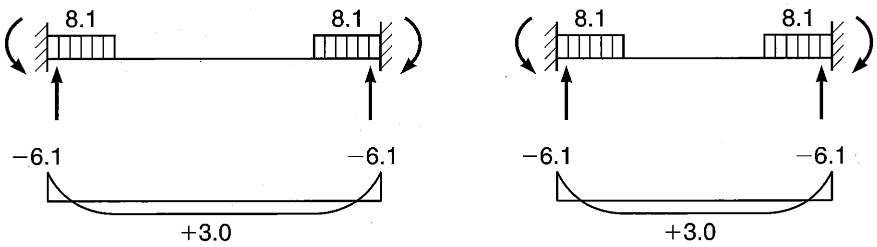
8.1
8.1
−6.1
−6.1
+3.0
8.1
8.1
−6.1
−6.1
+3.0

(*c*) *X* direction edge strip (*e*) *Y* direction edge strip

X direction edge strips:

Cantilever: $m_x = \dfrac{qb^2}{64} = 16.2 \times \dfrac{6.0^2}{64} = 9.11 \text{ kN-m/m}$

Negative: $m_{xs} = 9.14 \times \dfrac{2}{3} = 6.1$

Positive: $m_{xf} = 9.14 \times \dfrac{1}{3} = 3.0$

Y direction middle strip:

Cantilever: $m_y = \dfrac{qb^2}{8} = 16.2 \times \dfrac{6.0^2}{8} = 72.9 \text{ kN-m/m}$

Negative: $m_{ys} = 72.9 \times \dfrac{2}{3} = 48.6$

Positive: $m_{yf} = 72.9 \times \dfrac{1}{3} = 24.3$

Y direction edge strips:

Cantilever: $m_y = \dfrac{qb^2}{64} = 16.2 \times \dfrac{6.0^2}{64} = 9.1 \text{ kN-m/m}$

Negative: $m_{ys} = 9.1 \times \dfrac{2}{3} = 6.1$

Positive: $m_{yf} = 9.1 \times \dfrac{1}{3} = 3.0$

Strip loads and moment diagrams are as shown in Fig. 15.8. According to ACI Code 7.12, the minimum steel required for shrinkage and temperature crack control is $0.0018 \times 175 \times 1000 = 315 \text{ mm}^2/\text{m}$ strip. With a total depth of 175 mm, with 20 mm concrete cover, and with estimated bar diameters of 13 mm, the effective depth of the slab in the short direction will be 148 mm, and in the long direction, 135 mm. Accordingly, the flexural reinforcement ratio provided by the minimum steel acting at the smaller effective depth is

$$\rho_{\min} = \frac{315}{135 \times 1000} = 0.0023$$

From Table A.5a of Appendix A, $R = 0.94$, and the flexural design strength is

$$\phi m_n = \phi R b d^2 = 0.90 \times 0.94 \times 1000 \times 135^2 \times 10^{-6} = 15.4 \text{ kN-m/m}$$

Comparing this with the required moment resistance shows that the minimum steel will be adequate in the *X* direction in both middle and edge strips and in the *Y* direction edge strips. No. 10 (No. 3) bars at 225 mm spacing will provide the needed area. In the *Y* direction middle strip, for negative bending,

$$R = \frac{m_u}{\phi b d^2} = \frac{48.6 \times 10^6}{0.90 \times 1000 \times 148^2} = 2.46$$

and from Table A.5a, the required reinforcement ratio is 0.0064. The required steel is then

$$A_s = 0.0064 \times 1000 \times 148 = 947 \text{ mm}^2/\text{m}$$

This will be provided with No. 16 (No. 5) bars at 200 mm on centers. For positive bending,

$$R = \frac{24.3 \times 10^6}{0.90 \times 1000 \times 148^2} = 1.23$$

for which $\rho = 0.0030$, and the required positive steel area per strip is

$$A_s = 0.0030 \times 1000 \times 148 = 444 \text{ mm}^2/\text{m}$$

to be provided by No. 13 (No. 4) bars on 250 mm centers. Note that all bar spacings are less than $2h = 2 \times 175 = 350$ mm, as required by the Code, and that the reinforcement ratios are well below the value for a tension-controlled section of 0.0135.

Negative bar cutoff points can easily be calculated from the moment diagrams. For the X direction middle strip, the point of inflection a distance x from the left edge is found as follows:

$$24.3x - 12.2 - 16.2\left(\frac{x^2}{2}\right) = 0$$

$$x = 0.553 \text{ m}$$

According to the Code, the negative bars must be continued at least d or $12d_b$ beyond that point, nominally requiring a 150 mm extension in this case. Thus, the negative bars will be cut off 553 + 150 = 703 mm, say 750 mm, from the face of support. The same result is obtained for the X direction edge strips and the Y direction edge strips. For the Y direction middle strip, the distance $y = 1.27$ m from face of support to inflection point is found in a similar manner. In this case, with No. 10 (No. 5) bars used, the required extension is 190 mm, giving a total length past the face of supports of 1270 + 190 = 1460 mm or 1.50 m. All positive bars will be carried 150 mm into the face of the supporting beams.

15.6 UNSUPPORTED EDGES

The slabs considered in the preceding sections, together with the supporting beams, could also have been designed by the methods of Chapter 13. The real power of the strip method becomes evident when dealing with nonstandard problems, such as slabs with an unsupported edge, slabs with holes, or slabs with reentrant corners (L-shaped slabs).

For a slab with one edge unsupported, for example, a reasonable basis for analysis by the simple strip method is that a strip along the unsupported edge takes a greater load per unit area than the actual unit load acting, i.e., that the strip along the unsupported edge acts as a support for the strips at right angles. Such strips have been referred to by Wood and Armer as *strong bands* (Ref. 15.8). A strong band is, in effect, an integral beam, usually having the same total depth as the remainder of the slab but containing a concentration of reinforcement. The strip may be made deeper than the rest of the slab to increase its carrying capacity, but this will not usually be necessary.

Figure 15.9*a* shows a rectangular slab carrying a uniformly distributed factored load q per unit area, with fixed edges along three sides and no support along one short side. Discontinuity lines are chosen as shown. The load on a unit middle strip in the X direction, shown in Fig. 15.9*b*, includes the downward load q in the region adjacent to the fixed left edge and the upward reaction kq in the region adjacent to the free edge. Summing moments about the left end, with moments positive clockwise and with the unknown support moment denoted m_{xs}, gives

$$m_{xs} + \frac{qb^2}{32} - \frac{kqb}{4}\left(a - \frac{b}{8}\right) = 0$$

from which

$$k = \frac{1 + 32m_{xs}/qb^2}{8(a/b) - 1} \tag{15.15}$$

Thus, k can be calculated after the support moment is selected.

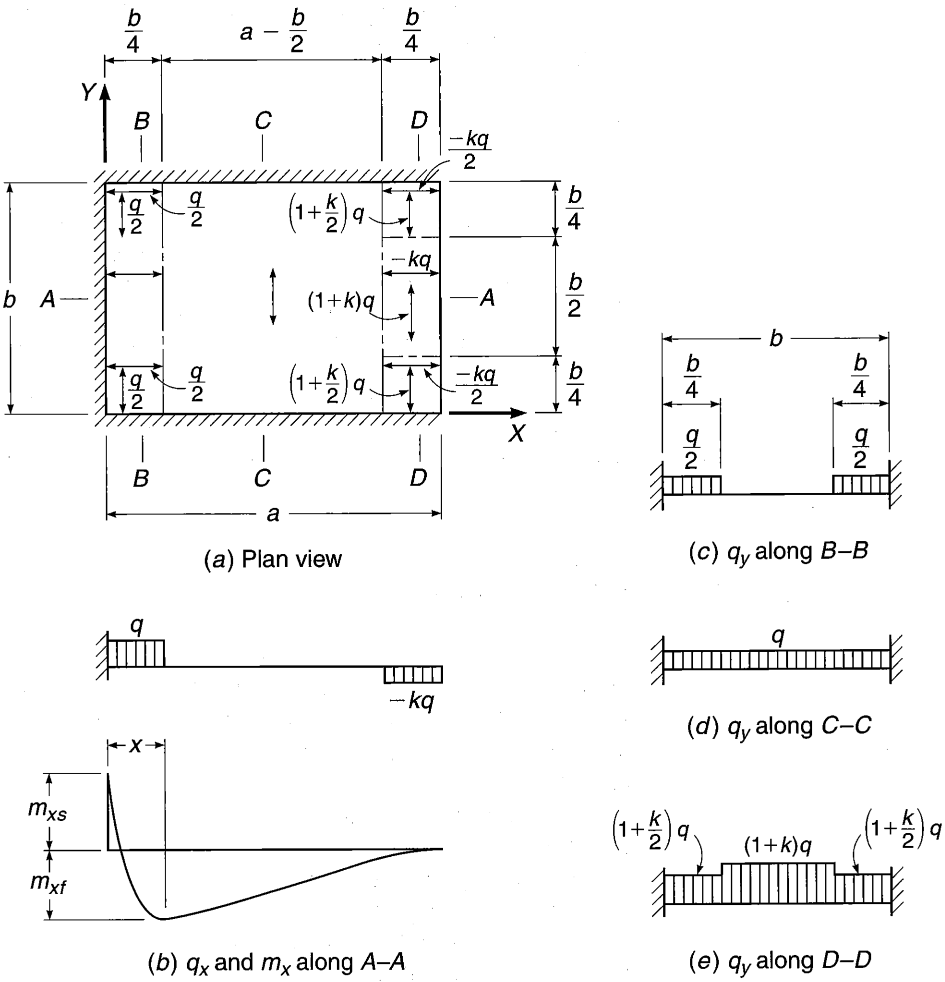
b/4
a − b/2
b/4
Y
B
C
D
−kq/2
q/2
q/2
(1 + k/2)q
−kq
b
A
(1 + k)q
A
b/4
b/2
b/4
q/2
q/2
(1 + k/2)q
−kq/2
X
B
C
D
a
b
b/4
b/4
q/2
q/2
q
−kq
q
x
m_{xs}
m_{xf}
(1 + k/2)q
(1 + k)q
(1 + k/2)q

FIGURE 15.9
Slab with free edge along short side.

(a) Plan view

(c) q_y along B–B

(d) q_y along C–C

(b) q_x and m_x along A–A

(e) q_y along D–D

The appropriate value of m_{xs} to be used in Eq. (15.15) will depend on the shape of the slab. If a is large relative to b, the strong band in the Y direction at the edge will be relatively stiff, and the moment at the left support in the X direction strips will approach the elastic value for a propped cantilever. If the slab is nearly square, the deflection of the strong band will tend to increase the support moment; a value about one-half the free cantilever moment might be selected (Ref. 15.14).

Once m_{xs} is selected and k is known, it is easily shown that the maximum span moment occurs when

$$x = (1 - k)\frac{b}{4}$$

It has a value

$$m_{xf} = \frac{kqb^2}{32}\left(\frac{8a}{b} - 3 + k\right) \tag{15.16}$$

The moments in the X direction edge strips are one-half of those in the middle strip. In the Y direction middle strip, Fig. 15.9*d*, the cantilever moment is $qb^2/8$. Adopting a ratio of support to span moment of 2 results in support and span moments, respectively, of

$$m_{ys} = \frac{qb^2}{12} \tag{15.17a}$$

$$m_{yf} = \frac{qb^2}{24} \tag{15.17b}$$

Moments in the Y direction strip adjacent to the fixed edge, Fig. 15.9*c*, will be one-eighth of those values. In the Y direction strip along the free edge, Fig. 15.9*e*, moments can, with slight conservatism, be made equal to $(1 + k)$ times those in the Y direction middle strip.

If the unsupported edge is in the long-span direction, then a significant fraction of the load in the slab central region will be carried in the direction perpendicular to the long edges, and the simple distribution shown in Fig. 15.10*a* is more suitable. A strong band along the free edge serves as an integral edge beam, with width βb normally chosen as low as possible considering limitations on tensile reinforcement ratio in the strong band.

For a Y direction strip, with moments positive clockwise,

$$m_{ys} + \frac{1}{2} k_1 q(1 - \beta)^2 b^2 - k_2 q \beta b^2 (1 - \beta/2) = 0$$

FIGURE 15.10
Slab with free edge in long-span direction.

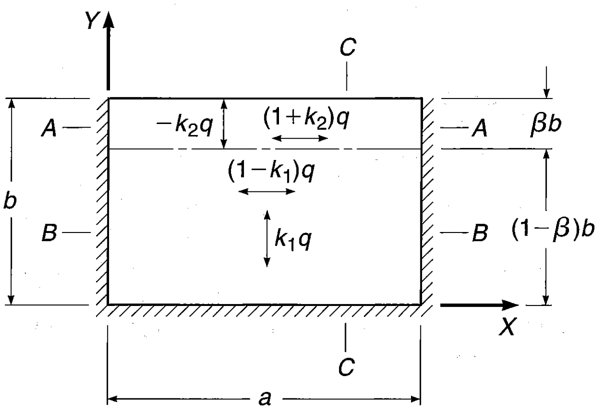

(*a*) Plan view

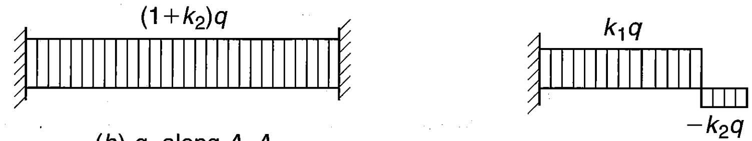

(*b*) q_x along *A–A*

(*d*) q_y along *C–C*

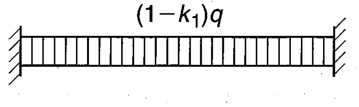

(*c*) q_x along *B–B*

from which

$$k_2 = \frac{k_1(1-\beta)^2 + 2m_{ys}/qb^2}{\beta(2-\beta)} \tag{15.18}$$

The value of k_1 may be selected so as to make use of the minimum steel in the X direction required by ACI Code 7.12. In choosing m_{ys} to be used in Eq. (15.18) for calculating k_2, one should again recognize that the deflection of the strong band along the free edge will tend to increase the Y direction moment at the supported edge above the propped cantilever value based on zero deflection. A value for m_{ys} of about one-half the free cantilever moment may be appropriate in typical cases. A high ratio of a/b will permit greater deflection of the free edge through the central region, tending to increase the support moment, and a low ratio will restrict deflection, reducing the support moment.

EXAMPLE 15.2

Rectangular slab with long edge unsupported. The 3.7 × 5.8 m slab shown in Fig. 15.11*a*, with three fixed edges and one long edge unsupported, must carry a uniformly distributed service live load of 6.0 kN/m^2; $f'_c = 28$ MPa, and $f_y = 420$ MPa. Select an appropriate slab thickness, determine all factored moments in the slab, and select reinforcing bars and spacings for the slab.

SOLUTION. The minimum thickness requirements of the ACI Code do not really apply to the type of slab considered here. However, Table 13.5, which controls for beamless flat plates, can be applied conservatively because although the present slab is beamless along the free edge, it has infinitely stiff supports on the other three edges. From that table, with $l_n = 5.8$ m,

$$h = \frac{5800}{33} = 176 \text{ mm}$$

A total thickness of 175 mm will be selected. The slab dead load is $24 \times 0.175 = 4.2$ kN/m^2, and the total factored design load is $1.2 \times 4.2 + 1.6 \times 6.0 = 14.6$ kN/m^2.

A strong band 600 mm wide will be provided for support along the free edge. In the main slab, a value $k_1 = 0.45$ will be selected, resulting in a slab load in the Y direction of $0.45 \times 14.6 = 6.6$ kN/m^2 and in the X direction of $0.55 \times 14.6 = 8.0$ kN/m^2.

First, with regard to the Y direction slab strips, the negative moment at the supported edge will be chosen as one-half the free cantilever value, which in turn will be approximated based on 6.6 kN/m^2 over a 3.4 m distance from the support face to the center of the strong band. The restraining moment is thus

$$m_{ys} = \frac{1}{2} \times \frac{6.6 \times 3.4^2}{2} = 19.1 \text{ kN-m/m}$$

Then, from Eq. (15.18)

$$k_2 = \frac{0.45(3.1/3.7)^2 - 2 \times 19.1/(14.6 \times 3.7^2)}{(0.6/3.7)(2 - 0.6/3.7)} = 0.419$$

Thus, an uplift of $0.419 \times 14.6 = 6.1$ kN/m^2 will be provided for the Y direction strips by the strong band, as shown in Fig. 15.11*d*. For this loading, the negative moment at the left support is

$$m_{ys} = 6.6 \times \frac{3.1^2}{2} - 6.1 \times 0.60 \times 3.4 = 19.3 \text{ kN-m/m}$$

The difference from the original value of 19.1 kN-m/m is caused by numerical rounding of the load terms. The statically consistent value of 19.3 kN-m/m will be used for design. The maximum positive moment in the Y direction strips will be located at the point of zero shear.

FIGURE 15.11
Design example: slab with long edge unsupported.

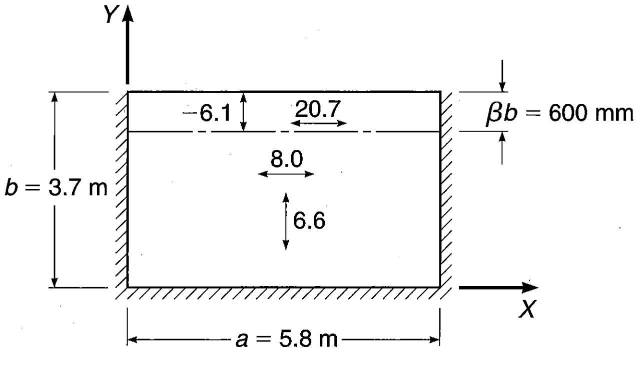
Y
−6.1
20.7
βb = 600 mm
8.0
b = 3.7 m
6.6
X
a = 5.8 m

(*a*) Plan view

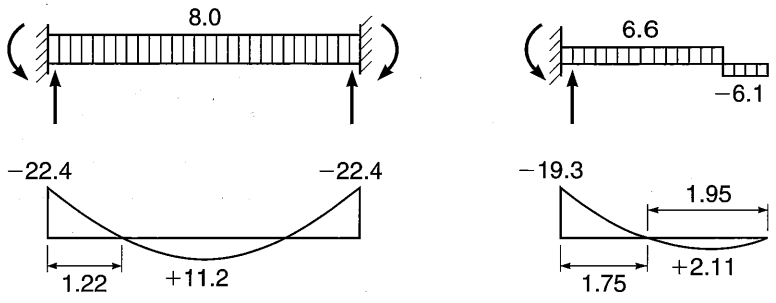
8.0
−22.4
−22.4
1.22
+11.2
6.6
−6.1
−19.3
1.95
1.75
+2.11

(*b*) *X* direction strip

(*d*) *Y* direction strip

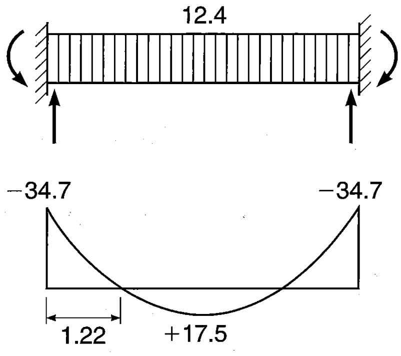
12.4
−34.7
−34.7
1.22
+17.5

(*c*) Strong band

With y_1 as the distance of that point from the free edge to the zero shear location, and with reference to Fig. 15.11*d*,

$$6.1 \times 0.60 - 6.6(y_1 - 0.60) = 0$$

from which $y_1 = 1.15$ m. The maximum positive moment, found at that location, is

$$m_{yf} = 6.1 \times 0.60(1.15 - 0.30) - 6.6 \times \frac{0.55^2}{2} = 2.11 \text{ kN-m/m}$$

For later reference in cutting off bars, the point of inflection is located a distance y_2 from the free edge:

$$6.1 \times 0.60(y_2 - 0.30) - \frac{6.6}{2}(y_2 - 0.60)^2 = 0$$

FIGURE 15.11
(*Continued*)

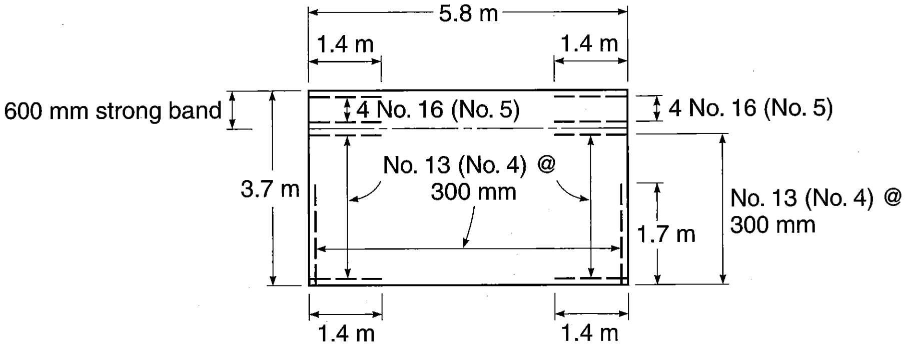

(*e*) Top bars

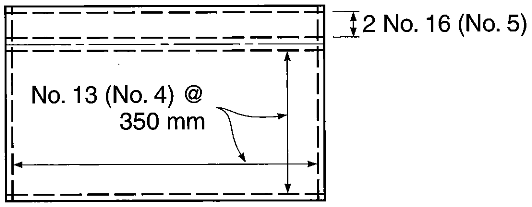

(*f*) Bottom bars

resulting in $y_2 = 1.95$ m.

For the X direction slab strips, the cantilever moment is

$$\text{Cantilever:} \qquad m_x = \frac{8.0 \times 5.8^2}{8} = 33.6 \text{ kN-m/m}$$

A ratio of negative to positive moments of 2.0 will be chosen here, resulting in negative and positive moments, respectively, of

$$\text{Negative:} \qquad m_{xs} = 33.6 \times \frac{2}{3} = 22.4 \text{ kN-m/m}$$

$$\text{Positive:} \qquad m_{xf} = 33.6 \times \frac{1}{3} = 11.2 \text{ kN-m/m}$$

as shown in Fig. 15.11*b*.

The unit load on the strong band in the X direction is

$$(1 + k_2)q = (1 + 0.419) \times 14.6 = 20.7 \text{ kN/m}^2$$

so for the 600 mm wide band the load per meter is $0.60 \times 20.7 = 12.4$ kN/m^2, as indicated in Fig. 15.11*c*. The cantilever, negative, and positive strong band moments are, respectively,

$$\text{Cantilever:} \qquad M_x = 12.4 \times 5.8^2/8 = 52.1 \text{ kN-m}$$

$$\text{Negative:} \qquad M_{xs} = 52.1 \times \frac{2}{3} = 34.7 \text{ kN-m}$$

$$\text{Positive:} \qquad M_{xf} = 52.1 \times \frac{1}{3} = 17.4 \text{ kN-m}$$

With a negative moment of -34.7 kN-m and a support reaction of $12.4 \times 5.8/2 = 36.0$ kN, the point of inflection in the strong band is found as follows:

$$-34.7 + 36.0x - \frac{12.4x^2}{2} = 0$$

giving $x = 1.22$ m. The inflection point in the X direction slab strips will be at the same location.

In designing the slab steel in the X direction, one notes that the minimum steel required by the ACI Code is $0.0018 \times 175 \times 1000 = 315$ mm^2/m. The effective slab depth in the X direction, assuming 13 mm diameter bars with 20 mm cover, is $175 - 33 = 148$ mm. The corresponding flexural reinforcement ratio in the X direction is $\rho = 315/(1000 \times 148) = 0.0021$. From Table A.5a, $R = 0.86$, and the design strength is

$$\phi m_n = \phi R b d^2 = 0.90 \times 0.86 \times 1000 \times 148^2 \times 10^{-6} = 17.0 \text{ kN-m/m}$$

It is seen that the minimum slab steel required by the Code will provide for the positive bending moment of 11.2 kN-m/m. The requirement of 315 mm^2/m could be met by No. 10 (No. 3) bars at 225 mm spacing, but to reduce placement costs, No. 13 (No. 4) bars at the maximum permitted spacing of $2h = 350$ mm will be selected, providing 369 mm^2/m. The X direction negative moment of 22.4 kN/m requires

$$R = \frac{m_u}{\phi b d^2} = \frac{22.4 \times 10^6}{0.90 \times 1000 \times 148^2} = 1.14$$

and Table A.5a indicates that the required $\rho = 0.0028$. Thus, the negative bar requirement is $A_s = 0.0028 \times 1000 \times 148 = 414$ mm^2/m. This will be provided by No. 13 (No. 4) bars at 300 mm spacing, continued $1220 + 150 = 1370$ mm, or say 1.4 m, from the support face.

In the Y direction, the effective depth will be one bar diameter less than in the X direction, or 135 mm. Thus, the flexural reinforcement ratio provided by the shrinkage and temperature steel is $\rho = 315/(1000 \times 135) = 0.0023$. This results in $R = 0.95$, so the design strength is

$$\phi m_n = 0.90 \times 0.95 \times 1.0 \times 135^2 \times 10^{-3} = 15.6 \text{ kN-m/m}$$

well above the requirement for positive bending of 2.11 kN-m/m. No. 13 (No. 4) bars at 350 mm will be satisfactory for positive steel in this direction also. For the negative moment of 19.1 kN-m/m,

$$R = \frac{19.3 \times 10^6}{0.90 \times 1000 \times 135^2} = 1.18$$

and from Table A.5a, the required $\rho = 0.0029$. The corresponding steel requirement is $0.0029 \times 1000 \times 135 = 392$ mm^2/m. No. 13 (No. 4) bars at 300 mm will be used, and they will be extended $1540 + 150 = 1690$ mm, or say 1.7 m, past the support face.

In the strong band, the positive moment of 17.4 kN-m requires

$$R = \frac{17.4 \times 10^6}{0.90 \times 1000 \times 148^2} = 1.47$$

The corresponding reinforcement ratio is 0.0036, and the required bar area is $0.0036 \times 1000 \times 148 = 320$ mm^2. This can be provided by two No. 16 (No. 5) bars. For the negative moment of 34.7 kN-m,

$$R = \frac{34.7 \times 10^6}{0.90 \times 600 \times 148^2} = 2.93$$

resulting in $\rho = 0.0075$, and required steel equal to $0.0075 \times 600 \times 148 = 666$ mm^2. Four No. 16 (No. 5) bars, providing an area of 796 mm^2, will be used, and they will be cut off $1220 + 150 = 1370$ mm, or say 1.4 m, from the support face.

The final arrangement of bar reinforcement is shown in Fig. 15.11*e* and *f*. Negative bar cutoff locations are as indicated, and development by embedded lengths into the supports will be provided. All positive bars in the slab and strong band will be carried 150 mm into the support faces.

A design problem commonly met in practice is that of a slab supported along three edges and unsupported along the fourth, with a distributed load that increases linearly from zero along the free edge to a maximum at the opposite supported edge. Examples include the wall of a rectangular tank subjected to liquid pressure and earth-retaining walls with buttresses or counterforts (see Section 17.1).

Figure 15.12 shows such a slab, with load of intensity q_0 at the long, supported edge, reducing to zero at the free edge. In the main part of the slab, a constant load k_2q_0 is carried in the X direction, as shown in Fig. 15.12*c*; thus, a constant load k_2q_0 is deducted from the linear varying load in the Y direction, as shown in Fig. 15.12*d*. Along the free edge, a strong band of width βb is provided, carrying a load k_1q_0, as in Fig. 15.12*a*, and so providing an uplift load equal to that amount at the end of the Y direction strip in Fig. 15.12*d*. The choice of k_1 and k_2 depends on the ratio of a/b. If this ratio is high, k_2 should be chosen with regard to the minimum slab reinforcement required by the ACI Code. The value of k_1 is then calculated by statics, based on a selected value of the restraining moment at the fixed edge, say one-half of the free cantilever value. In many cases it will be convenient to let k_1 equal k_2. Then it is the support moment that follows from statics. The value of β is selected as low as possible considering the upper limit on tensile reinforcement ratio in the strong band imposed by the Code for beams. The strong band is designed for a load of intensity k_1q_0 distributed uniformly over its width βb.

FIGURE 15.12
Slab with one free edge and linearly varying load.

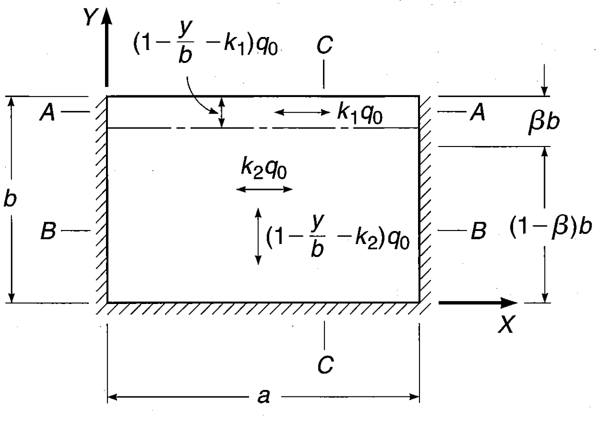

(*a*) Plan view

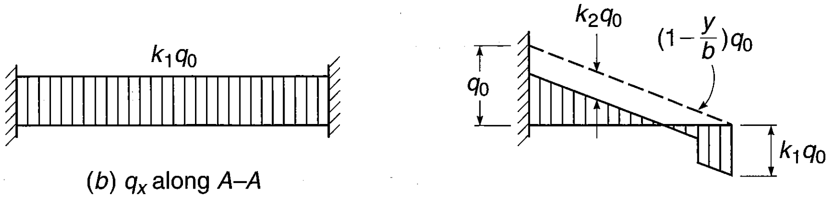

(*b*) q_x along *A–A*

(*d*) m_y along *C–C*

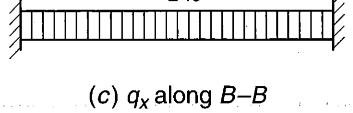

(*c*) q_x along *B–B*

15.7 SLABS WITH HOLES

Slabs with small openings can usually be designed as if there were no openings, replacing the interrupted steel with bands of reinforcing bars of equivalent area on either side of the opening in each direction (see Section 13.12). Slabs with larger openings must be treated more rigorously. The strip method offers a rational and safe basis for design in such cases. Integral load-carrying beams are provided along the edges of the opening, usually having the same depth as the remainder of the slab but with extra reinforcement, to pick up the load from the affected regions and transmit it to the supports. In general, these integral beams should be chosen so as to carry the loads most directly to the supported edges of the slab. The width of the strong bands should be selected so that the reinforcement ratios ρ are at or below the value required to produce a tension-controlled member (i.e., $\epsilon_t \geq 0.005$ and $\phi = 0.90$). Doing so will ensure ductile behavior of the slab.

Use of the strip method for analysis and design of a slab with a large central hole will be illustrated by the following example.

EXAMPLE 15.3

Rectangular slab with central opening. Figure 15.13*a* shows a 4.8 × 8.5 m slab with fixed supports along all four sides. A central opening 1.2 × 2.5 m must be accommodated. Estimated slab thickness, from Eq. (13.8*b*), is 175 mm. The slab is to carry a uniformly distributed factored load of 14.5 kN/m^2, including self-weight. Devise an appropriate system of strong bands to reinforce the opening, and determine moments to be resisted at all critical sections of the slab.

Solution. The basic pattern of discontinuity lines and load dispersion will be selected according to Fig. 15.5. Edge strips are defined having width 4.8/4 = 1.2 m. In the corners, the load is equally divided in the two directions. In the central region, 100 percent of the load is assigned to the *Y* direction, while along the central part of the short edges, 100 percent of the load is carried in the *X* direction. Moments for this "basic case" without the hole will be calculated and later used as a guide in selecting moments for the actual slab with hole. A ratio of

FIGURE 15.13
Design example: slab with central hole. All dimensions in m.

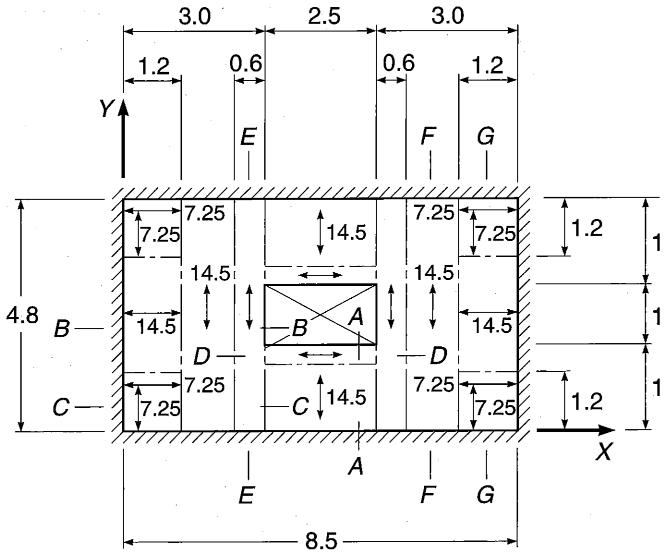

(*a*) Plan view

support to span moments of 2.0 will be used generally, as for the previous examples. Moments for the slab, neglecting the hole, would then be as follows:

X direction middle strips:

Cantilever: $$m_x = \frac{qb^2}{32} = 14.5 \times \frac{4.8^2}{32} = 10.4 \text{ kN-m/m}$$

Negative: $$m_{xs} = 10.4 \times \frac{2}{3} = 6.9$$

Positive: $$m_{xf} = 10.4 \times \frac{1}{3} = 3.5$$

X direction edge-strip moments are one-half of the middle-strip moments.

Y direction middle strips:

Cantilever: $$m_y = \frac{qb^2}{8} = 14.5 \times \frac{4.8^2}{8} = 41.8 \text{ kN-m/m}$$

Negative: $$m_{ys} = 41.8 \times \frac{2}{3} = 27.9$$

Positive: $$m_{yf} = 41.8 \times \frac{1}{3} = 13.9$$

Y direction edge-strip moments are one-half of the middle-strip moments.

Because of the hole, certain strips lack support at one end. To support them, 300 mm wide strong bands will be provided in the *X* direction at the long edges of the hole and 600 mm wide strong bands in the *Y* direction on each side of the hole. The *Y* direction bands will provide for the reactions of the *X* direction bands. With the distribution of loads shown in Fig. 15.13*a*, strip reactions and moments are found as follows:

Strip *A–A*
It may at first be assumed that propped cantilever action is obtained, with the restraint moment along the slab edge taken as 27.9 kN-m/m, the same as for the basic case. Summing moments about the left end of the loaded strip then results in

$$q_1 = \frac{14.5 \times 1.8 \times 0.9 - 27.9}{0.3 \times 1.65} = -8.9 \text{ kN/m}^2$$

The negative value indicates that the cantilever strips are serving as supports for strip *D–D*, and in turn for the strong bands in the *Y* direction, which is hardly a reasonable assumption. Instead, a discontinuity line will be assumed 1.5 m from the support, as shown in Fig. 15.13*b*, terminating the cantilever and leaving the 300 mm strip *D–D* along the edge of the opening in the *X* direction to carry its own load. It follows that the support moment in the cantilever strip is

Negative: $$m_{ys} = 14.5 \times 1.5 \times 0.75 = 16.3 \text{ kN-m/m}$$

Strip *B–B*
The restraint moment at the supported edge will be taken to be the same as the basic case, i.e., 6.9 kN-m/m. Summing moments about the left end of the strip of Fig. 15.13*c* then results in an uplift reaction at the right end, to be provided by strip *E–E*, of

$$q_2 = \frac{14.5 \times 1.2 \times 0.6 - 6.9}{0.6 \times 2.7} = 2.2 \text{ kN/m}^2$$

FIGURE 15.13
(*Continued*)

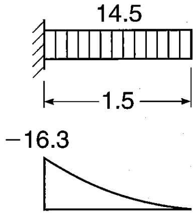

(*b*) Strip *A–A*

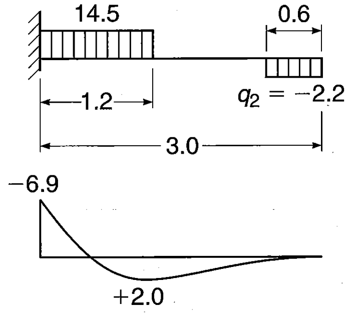

(*c*) Strip *B–B*

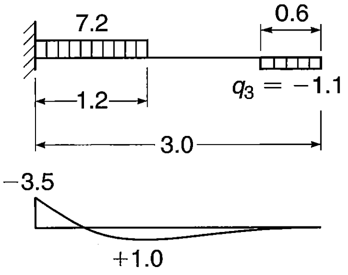

(*d*) Strip *C–C*

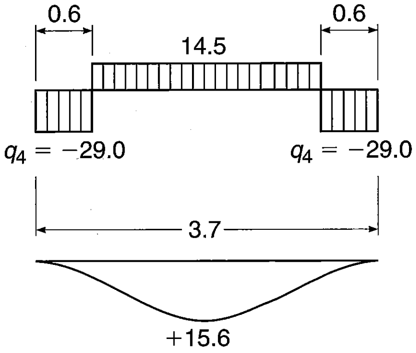

(*e*) Strip *D–D*

The left reaction is easily found to be 16.08 kN, and the point of zero shear is 1.11 m from the left support. The maximum positive moment, at that point, is

$$\text{Positive:} \qquad m_{xf} = 16.08 \times 1.11 - 6.9 - 14.5\,\frac{1.11^2}{2} = 2.0 \text{ kN-m/m}$$

Strip *C–C*
Negative and positive moments and the reaction to be provided by strip *E–E*, as shown in Fig. 15.13*d*, are all one-half the corresponding values for strip *B–B*.

Strip *D–D*
The 300 mm wide strip carries 14.5 kN/m^2 in the X direction with reactions provided by the strong bands *E–E*, as shown in Fig. 15.13*e*. The maximum positive moment is

$$m_{xf} = 29.0 \times 0.6 \times 1.55 - 14.5 \times 1.25 \times 1.25/2 = 15.6 \text{ kN-m/m}$$

Strip *E–E*
In reference to Fig. 15.13*f*, the strong bands in the Y direction carry the directly applied load of 14.5 kN/m^2 plus the 2.2 kN/m^2 load from strip *B–B*, the 1.1 kN/m^2 load from strip *C–C*, and the 29.0 kN/m^2 end reaction from strip *D–D*. For strip *E–E* the cantilever, negative, and positive moments are

Cantilever:

$$m_y = 14.5 \times 2.4 \times 1.2 + 1.1 \times 1.2 \times 0.6 + 2.2 \times 1.2 \times 1.8 + 29.0 \times 0.3 \times 1.65$$

$$= 61.7 \text{ kN-m/m}$$

$$\text{Negative:} \qquad m_{ys} = 61.7 \times \frac{2}{3} = 41.1$$

$$\text{Positive:} \qquad m_{yf} = 61.7 \times \frac{1}{3} = 20.6$$

FIGURE 15.13
(*Continued*)

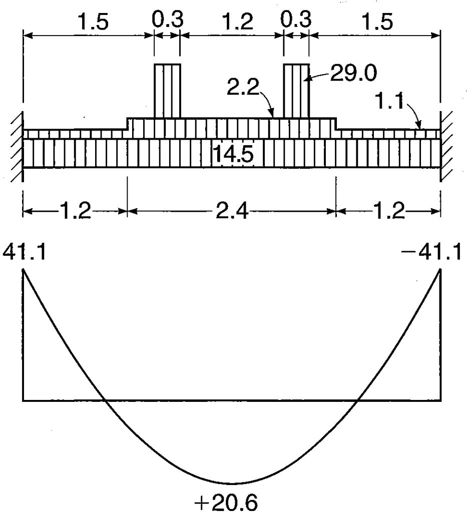

1.5
0.3
1.2
0.3
1.5
2.2
29.0
1.1
14.5
1.2
2.4
1.2
−41.1
−41.1
+20.6

(*f*) Strip *E–E*

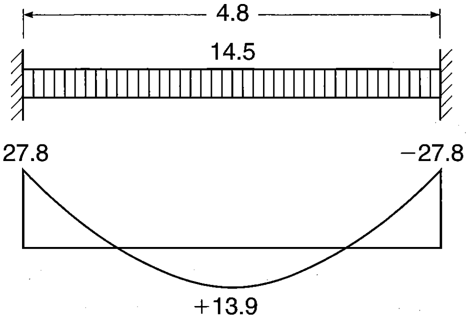

4.8
14.5
−27.8
−27.8
+13.9

(*g*) Strip *F–F*

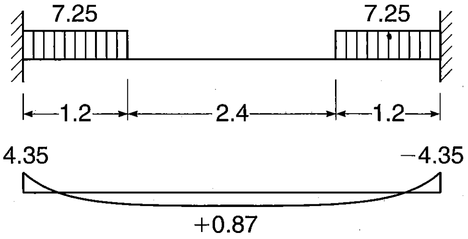

7.25
7.25
1.2
2.4
1.2
−4.35
−4.35
+0.87

(*h*) Strip *G–G*

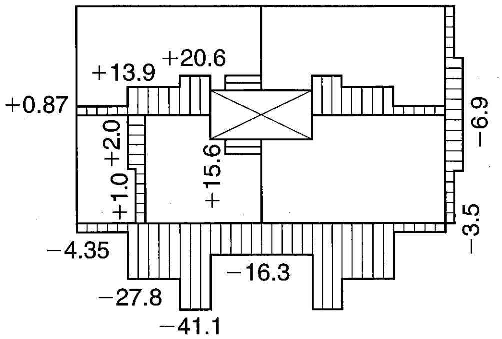

+13.9
+20.6
+0.87
+2.0
+1.0
+15.6
−6.9
−3.5
−4.35
−16.3
−27.8
−41.1

(*i*) Factored moments – symmetrical about both axes

It should be emphasized that the loads shown are kN/m^2 and would be multiplied by 0.6 to obtain loads per meter acting on the strong bands. Correspondingly, the moments just obtained are per meter width and must be multiplied by 0.6 to give the support and span moments for the 600 mm wide strong band.

Strip *F–F*
The moments for the *Y* direction middle strip of the basic case may be used without change; thus, in Fig. 15.13*g*,

Negative: $m_{ys} = 27.8$ kN-m/m

Positive: $m_{yf} = 13.9$

Strip *G–G*
Moments for the *Y* direction edge strips of the basic case are used without change, resulting in

Negative: $m_{ys} = 4.35$ kN-m/m

Positive: $m_{yf} = 0.87$

as shown in Fig. 15.13*h*.

The final distribution of moments across the negative and positive critical sections of the slab is shown in Fig. 15.13*i*. The selection of reinforcing bars and determination of cutoff points would follow the same methods as presented in Examples 15.1 and 15.2 and will not be given here. Reinforcing bar ratios needed in the strong bands are well below the maximum permitted for the 175 mm slab depth.

It should be noted that strips *B–B, C–C,* and *D–D* have been designed as if they were simply supported at the strong band *E–E.* To avoid undesirably wide cracks where these strips pass over the strong band, nominal negative reinforcement should be added in this region. Positive bars should be extended fully into the strong bands.

15.8 ADVANCED STRIP METHOD

The simple strip method described in the earlier sections of this chapter is not directly suitable for the design of slabs supported by columns (e.g., flat plates) or slabs supported at reentrant corners.[†] For such cases, Hillerborg introduced the advanced strip method (Refs. 15.2, 15.5, 15.12, and 15.13).

Fundamental to the advanced strip method is the corner-supported element, such as that shown shaded in Fig. 15.14*a*. The corner-supported element is a rectangular region of the slab with the following properties:

1. The edges are parallel to the reinforcement directions.
2. It carries a uniform load q per unit area.
3. It is supported at only one corner.
4. No shear forces act along the edges.
5. No twisting moments act along the edges.
6. All bending moments acting along an edge have the same sign or are zero.
7. The bending moments along the edges are the factored moments used to design the reinforcing bars.

[†] However, Wood and Armer, in Ref. 15.8, suggest that beamless slabs with column supports can be solved by the simple strip method through the use of strong bands between columns or between columns and exterior walls.

FIGURE 15.14
Slab with central supporting column.

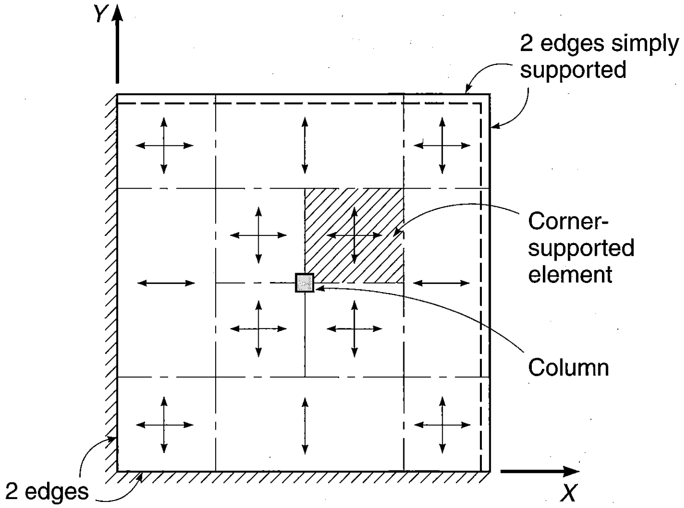

(*a*) Plan view

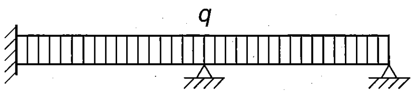

(*b*) Loads

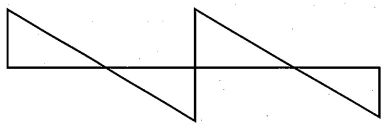

(*c*) Shears

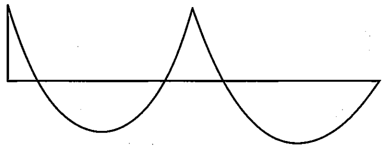

(*d*) Moments

A uniformly loaded strip in the X direction, shown in Fig. 15.14*b*, will thus have shear and moment diagrams as shown in Fig. 15.14*c* and *d*, respectively. Maximum moments are located at the lines of zero shear. The outer edges of the corner-supported element are defined at the lines of zero shear in both the X and Y directions.

A typical corner-supported element, with an assumed distribution of moments along the edges, is shown in Fig. 15.15. It will be assumed that the bending moment is constant along each half of each edge. The vertical reaction is found by summing vertical forces:

$$R = qab \tag{15.19}$$

and moment equilibrium about the Y axis gives

$$m_{xfm} - m_{xsm} = \frac{qa^2}{2} \tag{15.20}$$

FIGURE 15.15
Corner-supported element.

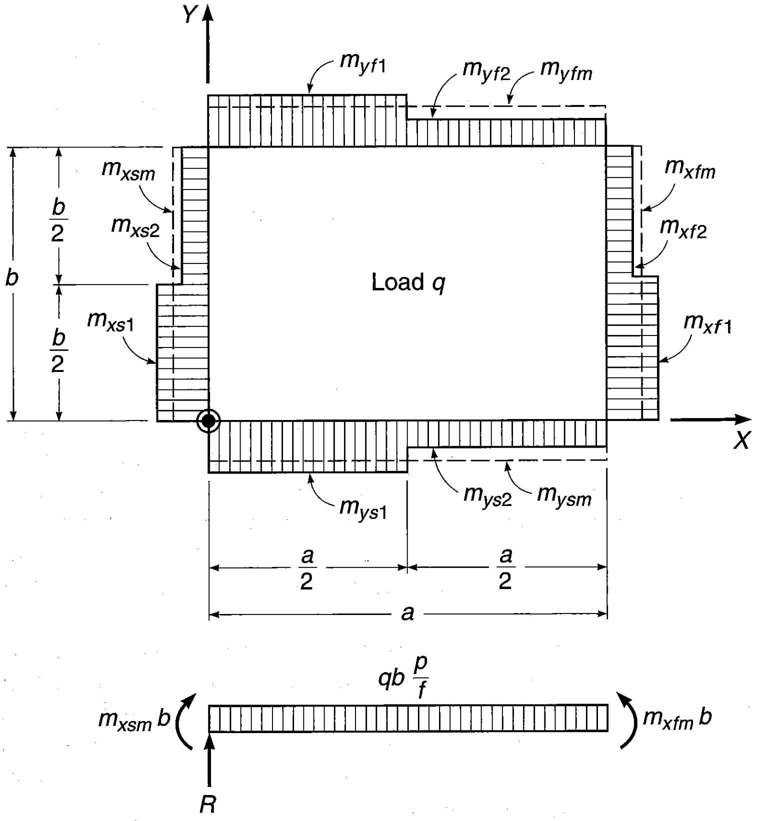

where m_{xfm} and m_{xsm} are the mean span and support moments per unit width, and the beam sign convention is followed. Similarly,

$$m_{yfm} - m_{ysm} = \frac{qb^2}{2} \tag{15.21}$$

The last two equations are identical with the condition for a corresponding part of a simple strip—Eq. (15.20) spanning in the X direction and Eq. (15.21) in the Y direction—supported at the axis and carrying the load qb or qa per meter. So if the corner-supported element forms a part of a strip, that part should carry 100 percent of the load q in each direction. (This requirement was discussed earlier in Chapter 13 and is simply a requirement of static equilibrium.)

The distribution of moments within the boundaries of a corner-supported element is complex. With the load on the element carried by a single vertical reaction at one corner, strong twisting moments must be present within the element; this contrasts with the assumptions of the simple strip method used previously.

The moment field within a corner-supported element and its edge moments have been explored in great detail in Ref. 15.12. It is essential that the edge moments, given in Fig. 15.15, are used to design the reinforcing bars (i.e., that nowhere within the element will a bar be subjected to a greater moment than at the edges). To meet this requirement, a limitation must be put on the moment distribution along the edges. Based on his studies (Ref. 15.12), Hillerborg has recommended the following restriction on edge moments:

$$m_{xf2} - m_{xs2} = \alpha\,\frac{qa^2}{2} \tag{15.22a}$$

with

$$0.25 \leq \alpha \leq 0.7 \tag{15.22b}$$

where m_{xf2} and m_{xs2} are the positive and negative X direction moments, respectively, in the outer half of the element, as shown in Fig. 15.15. The corresponding restriction applies in the Y direction. He notes further that for most practical applications, the edge moment distribution shown in Fig. 15.16 is appropriate, with

$$m_{xf1} = m_{xf2} = m_{xfm} \tag{15.23}$$

$$m_{xs2} = 0 \tag{15.24a}$$

$$m_{xs1} = 2m_{xsm} \tag{15.24b}$$

(Alternatively, it is suggested in Ref. 15.14 that negative support moments across the column line be taken at $1.5m_{xsm}$ in the half-element width by the column and at $0.5m_{xsm}$ in the remaining outside half-element width.) Positive reinforcement in the span should be carried through the whole corner-supported element. The negative reinforcement corresponding to $m_{xs1} - m_{xs2}$ in Fig. 15.15 must be extended at least $0.6a$ from the support. The remaining negative steel, if any, should be carried through the whole corner-supported element. The corresponding restrictions apply in the Y direction.

In practical applications, corner-supported elements are combined with each other and with parts of one-way strips, as shown in Fig. 15.14, to form a system of strips. In this system, each strip carries the total load q, as discussed earlier. In laying out the elements and strips, the concentrated corner support for the element may be assumed to be at the center of the supporting column, as shown in Fig. 15.14, unless supports are of significant size. In that case, the corner support may be taken at the corner of the column, and an ordinary simple strip may be included that spans between the column faces, along the edge of the corner-supported elements. Note in the figure that the corner regions of the slab are not included in the main strips that

FIGURE 15.16
Recommended distribution of moments for typical corner-supported element.

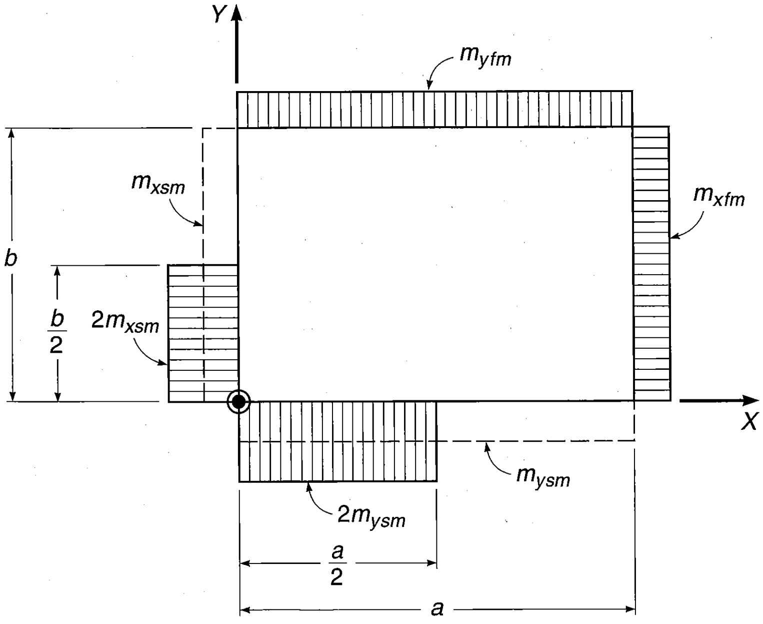

include the corner-supported elements. These may safely be designed for one-third of the corresponding moments in the main strips (Ref. 15.13).

EXAMPLE 15.4 **Edge-supported flat plate with central column.** Figure 15.17*a* illustrates a flat plate with overall dimensions 10.4 × 10.4 m, with fixed supports along the left and lower edges in the sketch, hinged supports at the right and upper edges, and a single central column 400 mm square. It must carry a service live load of 2.0 kN/m^2 over its entire surface plus its own weight and an additional superimposed dead load of 0.3 kN/m^2. Find the moments at all critical sections, and determine the required slab thickness and reinforcement. Material strengths are specified at $f_y = 420$ MPa and $f_c' = 28$ MPa.

Solution. A trial slab depth will be chosen based on Table 13.5, which governs for flat plates. It will be conservative for the present case, where continuous support is provided along the outer edges.

$$h = \frac{5200}{33} = 158 \text{ mm}$$

A thickness of 160 mm will be selected tentatively, for which the self-weight is 24 × 0.16 = 3.8 kN/m^2. The total factored load to be carried is thus

$$q_u = 1.2(3.8 + 0.3) + 1.6 \times 2.0 = 8.2 \text{ kN/m}^2$$

The average strip moments in the X direction in the central region caused by the load of 8.2 kN/m^2 are found by elastic theory and are shown in Fig. 15.17*c*. The analysis in the Y direction is identical. The points of zero shear (and maximum moments) are located 2.79 m to the left of the column and 3.16 m to the right, as indicated. These dimensions determine the size of the four corner-supported elements.

Moments in the slab are then determined according to the preceding recommendations. At the fixed edge along the left side of the main strips, the moment m_{xs} is simply the moment

FIGURE 15.17
Design example: edge-supported flat plate with central column.

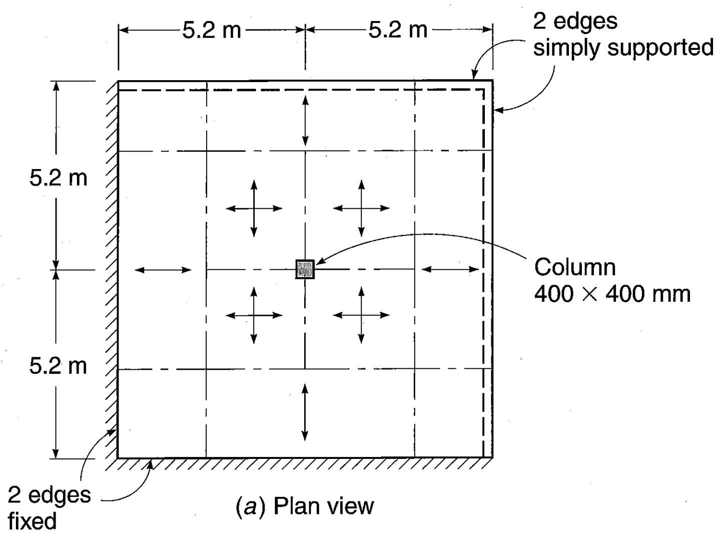

(*a*) Plan view

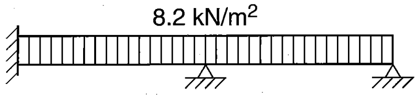

(*b*) Strip load

FIGURE 15.17
(Continued)

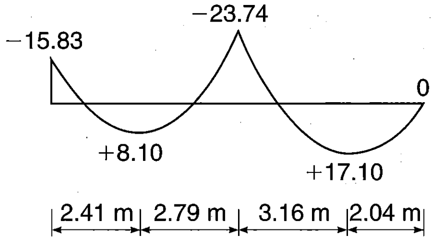

(*c*) Moments m_x, kN-m/m

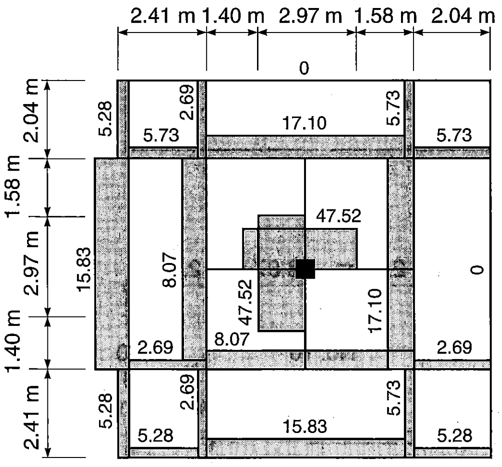
2.41 m
1.40 m
2.97 m
1.58 m
2.04 m
0
2.04 m
1.58 m
2.97 m
1.40 m
2.41 m
5.28
2.69
5.73
17.10
5.73
5.73
47.52
15.83
8.07
0
47.52
17.10
2.69
8.07
2.69
5.28
2.69
5.73
15.83
5.28
5.28

(*d*) Factored moments per 1 meter strip

per meter strip from the elastic analysis, 15.83 kN-m/m. At the left edge of the corner-supported element in the left span,

$$m_{xf1} = m_{xf2} = m_{xfm} = 8.07 \text{ kN-m/m}$$

Along the centerline of the slab, over the column, following the recommendations shown in Fig. 15.16,

$$m_{xs2} = 0$$

$$m_{xs1} = 2m_{xsm} = 47.52 \text{ kN-m/m}$$

At the right edge of the corner-supported element in the right span,

$$m_{xf1} = m_{xf2} = m_{xfm} = 17.10 \text{ kN-m/m}$$

At the outer, hinge-supported edge, all moments are zero. Make a check of the α values, using Eq. (15.22*b*), and note from Eq. (15.20) that $qa^2/2 = m_{xfm} - m_{xsm}$. Thus, in the left span,

$$\alpha = \frac{m_{xf2} - m_{xs2}}{qa^2/2} = \frac{8.07 - 0}{8.07 + 23.76} = 0.25$$

and in the right span,

$$\alpha = \frac{17.10 - 0}{17.10 + 23.76} = 0.42$$

Because both values are within the range of 0.25 to 0.75, the proposed distribution of moments is satisfactory. If the first value had been below the lower limit of 0.25, the negative moment in the column half-strip might have been reduced from 47.52 kN-m/m, and the negative moment

FIGURE 15.17
(*Continued*)

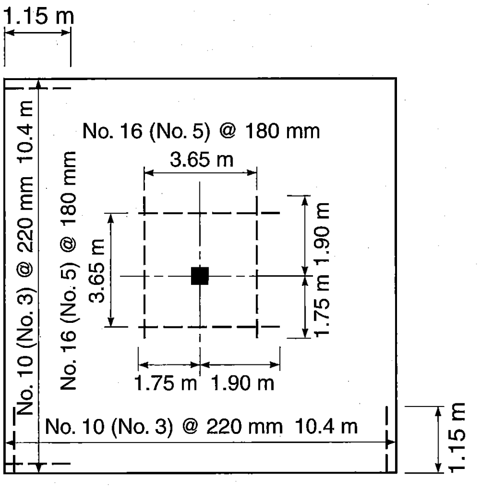
1.15 m
No. 16 (No. 5) @ 180 mm
3.65 m
No. 10 (No. 3) @ 220 mm 10.4 m
No. 16 (No. 5) @ 180 mm
3.65 m
1.90 m
1.75 m
1.75 m
1.90 m
No. 10 (No. 3) @ 220 mm 10.4 m
1.15 m

(*e*) Top steel

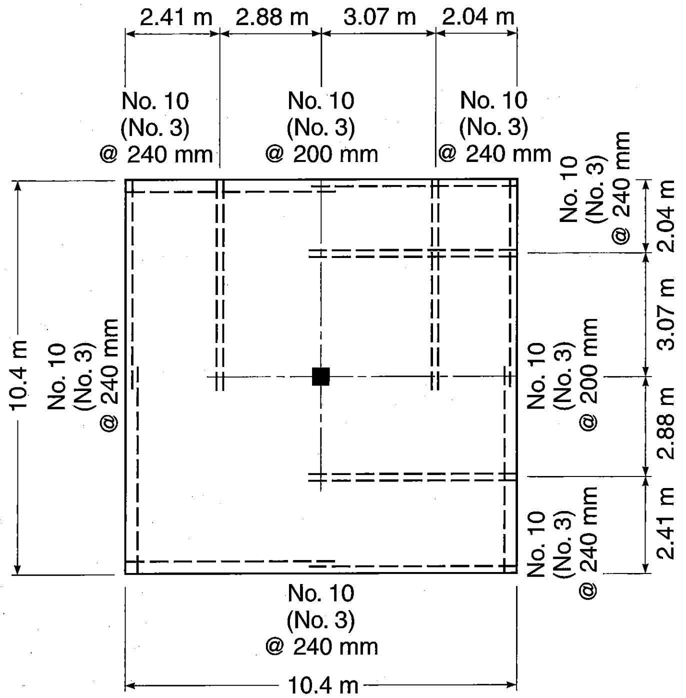
2.41 m
2.88 m
3.07 m
2.04 m
No. 10 (No. 3) @ 240 mm
No. 10 (No. 3) @ 200 mm
No. 10 (No. 3) @ 240 mm
No. 10 (No. 3) @ 240 mm
2.04 m
3.07 m
No. 10 (No. 3) @ 200 mm
2.88 m
No. 10 (No. 3) @ 240 mm
2.41 m
10.4 m
No. 10 (No. 3) @ 240 mm
No. 10 (No. 3) @ 240 mm
10.4 m

(*f*) Bottom steel

in the adjacent half-strip might have been increased above the 0 value used. Alternatively, the total negative moment over the column might have been somewhat decreased, with a corresponding increase in span moments.

Moments in the *Y* direction correspond throughout, and all results are summarized in Fig. 15.17*d*. Moments in the strips adjacent to the supported edges are set equal to one-third of those in the adjacent main strips.

With moments per meter strip known at all critical sections, the required reinforcement is easily found. With a 20 mm concrete cover and 13 mm bar diameter, in general the effective depth of the slab will be 134 mm. Where bar stacking occurs—i.e., over the central column and near the intersection of the two fixed edges—an average effective depth equal to 128 mm will be used. This will result in reinforcement identical in the two directions and will simplify construction.

For the 160 mm thick slab, minimum steel for shrinkage and temperature crack control is $0.0018 \times 1000 \times 160 = 288\ \text{mm}^2/\text{m}$ strip, which will be provided by No. 10 (No. 3) bars at 240 mm spacing. The corresponding flexural reinforcement ratio is

$$\rho_{\min} = \frac{288}{134 \times 1000} = 0.0021$$

Interpolating from Table A.5a of Appendix A makes $R = 0.87$, and the design strength is

$$\phi m_n = \phi R b d^2 = 0.90 \times 0.87 \times 1000 \times 134^2 \times 10^{-6} = 14.1\ \text{kN-m/m}$$

In comparison with the required strengths summarized in Fig. 15.17*d*, this will be adequate everywhere except for particular regions as follows:

Negative steel over column:

$$R = \frac{m_u}{\phi b d^2} = \frac{47.52 \times 10^6}{0.90 \times 1000 \times 128^2} = 3.22$$

for which $\rho = 0.0083$ (from Table A.5a), and $A_s = 0.0083 \times 1000 \times 128 = 1064\ \text{mm}^2/\text{m}$. This will be provided using No. 16 (No. 5) bars at 180 mm spacing. They will be continued a distance $0.6 \times 2.79 = 1.67$ m, say 1.75 m, to the left of the column centerline, and $0.6 \times 3.16 = 1.90$ m, to the right.

Negative steel along fixed edges:

$$R = \frac{15.83 \times 10^6}{0.90 \times 1000 \times 134^2} = 0.98$$

for which $\rho = 0.0024$ and $A_s = 0.0024 \times 1000 \times 134 = 322\ \text{mm}^2/\text{m}$. No. 10 (No. 3) bars at 220 mm spacing will be adequate. The point of inflection for the slab in this region is easily found to be 1.01 m from the fixed edge. The negative bars will be extended 134 mm beyond that point, resulting in a cutoff 1.15 mm, from the support face.

Positive steel in outer spans:

$$R = \frac{17.10 \times 10^6}{0.90 \times 1000 \times 134^2} = 1.06$$

resulting in $\rho = 0.0025$ and $A_s = 0.0025 \times 1000 \times 134 = 335\ \text{mm}^2/\text{m}$. No. 10 (No. 3) bars at 200 mm spacing will be used. In all cases, the maximum spacing of $2h = 320$ mm is satisfied. That maximum would preclude the economical use of larger-diameter bars.

Bar size and spacing and cutoff points for the top and bottom steel are summarized in Fig. 15.17*e* and *f*, respectively.

Finally, the load carried by the central column is

$$P = 8.2 \times 5.95 \times 5.95 = 290\ \text{kN}$$

Investigating punching shear at a critical section taken $d/2$ from the face of the 400 mm column, with reference to Eq. (13.11*a*) and with $b_o = 4 \times (400 + 128) = 2112$ mm, gives

$$\phi V_c = 0.33\phi\sqrt{f'_c}\, b_o d = 0.33 \times 0.75\sqrt{28} \times 2112 \times 129 \times 10^{-3} = 354\ \text{kN}$$

This is well above the applied shear of 290 kN, confirming that the slab thickness is adequate and that no shear reinforcement is required.

15.9 COMPARISONS OF METHODS FOR SLAB ANALYSIS AND DESIGN

The conventional methods of slab analysis and design, as described in Chapter 13 and as treated in Chapter 13 of the ACI Code, are limited to applications in which slab panels are supported on opposite sides or on all four sides by beams or walls or to the case of flat plates and related forms supported by a relatively regular array of columns. In all cases, slab panels must be square or rectangular, loads must be uniformly distributed within each panel, and slabs must be free of significant holes.

Both the yield line theory and the strip method offer the designer rational methods for slab analysis and design over a much broader range, including the following:

1. Boundaries of any shape, including rectangular, triangular, circular, and L-shaped boundaries with reentrant corners
2. Supported or unsupported edges, skewed supports, column supports, or various combinations of these conditions
3. Uniformly distributed loads, loads distributed over partial panel areas, linear varying distributed loads, line loads, and concentrated loads
4. Slabs with significant holes

The most important difference between the strip method and the yield line method is the fact that the strip method produces results that are always on the safe side, but yield line analysis may result in unsafe designs. A slab designed by the strip method may possibly carry a higher load than estimated, through internal force redistributions, before collapse; a slab analyzed by yield line procedures may fail at a lower load than anticipated if an incorrect mechanism has been selected as the basis or if the defining dimensions are incorrect.

Beyond this, it should be realized that the strip method is a tool for *design*, by which the slab thickness and reinforcing bar size and distribution may be selected to resist the specified loads. In contrast, the yield line theory offers only a means for *analyzing the capacity of a given slab*, with known reinforcement. According to the yield line approach, the design process is actually a matter of reviewing the capacities of a number of trial designs and alternative reinforcing patterns. All possible yield line patterns must be investigated and specific dimensions varied to be sure that the correct solution has been found. Except for simple cases, this is likely to be a time-consuming process.

Neither the strip method nor the yield line approach provides any information regarding cracking or deflections at service load. Both focus attention strictly on flexural strength. However, by the strip method, if care is taken at least to approximate the elastic distribution of moments, little difficulty should be experienced with excessive cracking. The methods for deflection prediction presented in Section 13.13 can, without difficulty, be adapted for use with the strip method, because the concepts are fully compatible.

With regard to economy of reinforcement, it might be supposed that use of the strip method, which always leads to designs on the safe side, might result in more expensive structures than the yield line theory. Comparisons, however, indicate that in most cases this is not so (Refs. 15.8 and 15.12). Through proper use of the strip method, reinforcing bars are placed in a nonuniform way in the slab (e.g., in strong bands around openings) where they are used to best effect; yield line methods, on the other hand, often lead to uniform bar spacings, which may mean that individual bars are used inefficiently.

Many tests have been conducted on slabs designed by the strip method (Ref. 15.11; also, see the summary in Ref. 15.12). These tests included square slabs, rectangular slabs, slabs with both fixed and simply supported edges, slabs supported directly by columns, and slabs with large openings. The conclusions drawn determine that the strip method provides for safe design with respect to nominal strength and that at service load, behavior with respect to cracking and deflections is generally satisfactory. The method has been widely and successfully used in the Scandinavian countries since the 1960s.

REFERENCES

15.1. A. Hillerborg, "Equilibrium Theory for Reinforced Concrete Slabs" (in Swedish), *Betong*, vol. 41, no. 4, 1956, pp. 171–182.

15.2. A. Hillerborg, *Strip Method for Slabs on Columns, L-Shaped Plates, Etc.* (in Swedish), Svenska Riksbyggen, Stockholm, 1959.

15.3. A. Hillerborg, "A Plastic Theory for the Design of Reinforced Concrete Slabs," *Proc. Sixth Congr.*, International Association for Bridge and Structural Engineering, Stockholm, 1960.

15.4. R. E. Crawford, *Limit Design of Reinforced Concrete Slabs*, thesis submitted to University of Illinois for the degree of Ph.D., Urbana, IL, 1962.

15.5. F. A. Blakey, *Strip Method for Slabs on Columns, L-Shaped Plates, Etc.* (translation of Ref. 15.2), Commonwealth Scientific and Industrial Research Organization, Melbourne, 1964.

15.6. K. O. Kemp, "A Lower Bound Solution to the Collapse of an Orthotropically Reinforced Slab on Simple Supports," *Mag. Concr. Res.*, vol. 14, no. 41, 1962, pp. 79–84.

15.7. K. O. Kemp, "Continuity Conditions in the Strip Method of Slab Design," *Proc. Inst. Civ. Eng.*, vol. 45, 1970, p. 283 (supplement paper 7268s).

15.8. R. H. Wood and G. S. T. Armer, "The Theory of the Strip Method for the Design of Slabs," *Proc. Inst. Civ. Eng.*, vol. 41, 1968, pp. 285–311.

15.9. R. H. Wood, "The Reinforcement of Slabs in Accordance with a Predetermined Field of Moments," *Concrete*, vol. 2, no. 2, 1968, pp. 69–76.

15.10. G. S. T. Armer, "The Strip Method: A New Approach to the Design of Slabs," *Concrete*, vol. 2, no. 9, 1968, pp. 358–363.

15.11. G. S. T. Armer, "Ultimate Load Tests of Slabs Designed by the Strip Method," *Proc. Inst. Civ. Eng.*, vol. 41, 1968, pp. 313–331.

15.12. A. Hillerborg, *Strip Method of Design*, Viewpoint Publications, Cement and Concrete Association, Wexham Springs, Slough, England, 1975.

15.13. A. Hillerborg, "The Advanced Strip Method—a Simple Design Tool," *Mag. Concr. Res.*, vol. 34, no. 121, 1982, pp. 175–181.

15.14. R. Park and W. L. Gamble, *Reinforced Concrete Slabs,* 2nd ed. (Chapter 6), John Wiley, New York, 2000, pp. 232–302.

15.15. A. Hillerborg, *Strip Method Design Handbook*, E & FN Spon/Chapman & Hill, London, 1996.

15.16. S. Timoshenko and S. Woinowsky-Krieger, *Theory of Plates and Shells*, 2nd ed., McGraw-Hill, New York, 1959.

PROBLEMS

Note: For all the following problems, use material strengths $f_y = 420$ MPa and $f'_c = 28$ MPa. All ACI Code requirements for minimum steel, maximum spacings, bar cutoff, and special corner reinforcement are applicable.

15.1. The square slab of Fig. P15.1 is simply supported by masonry walls along all four sides. It is to carry a service live load of 4.8 kN/m^2 in addition to its self-weight. Specify a suitable load distribution; determine moments at all controlling sections; and select the slab thickness, reinforcing bars, and spacing.

FIGURE P15.1

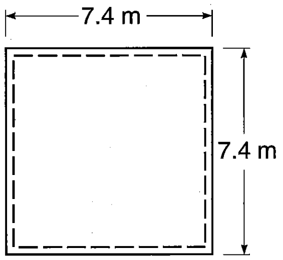

15.2. The rectangular slab shown in Fig. P15.2 is a typical interior panel of a large floor system having beams on all column lines. Columns and beams are sufficiently stiff that the slab can be considered fully restrained along all sides. A live load of 4.8 kN/m^2 and a superimposed dead load of 1.4 kN/m^2 must be carried in addition to the slab self-weight. Determine the required slab thickness, and specify all reinforcing bars and spacings. Cutoff points for negative bars should be specified; all positive steel may be carried into the supporting beams. Take support moments to be 2 times the span moments in the strips.

FIGURE P15.2

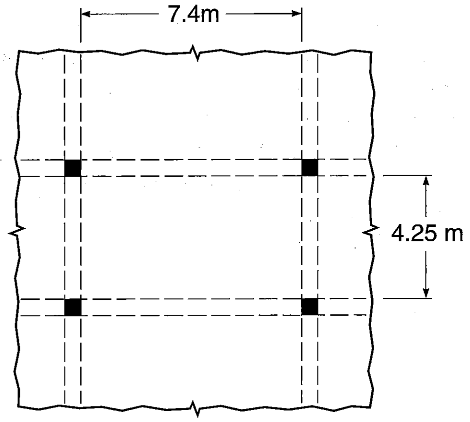

15.3. The slab of Fig. P15.3 may be considered fully fixed along three edges, but it is without support along the fourth, long side. It must carry a uniformly distributed live load of 4.0 kN/m^2 plus an external dead load of 2.0 kN/m^2. Specify a suitable slab depth, and determine reinforcement and cutoff points.

FIGURE P15.3

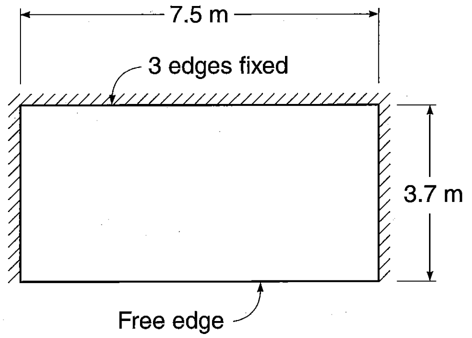

15.4. Figure P15.4 shows a counterfort retaining wall (see Section 17.9) consisting of a base slab and a main vertical wall of constant thickness retaining the earth. Counterfort walls spaced at 5.8 m on centers along the wall provide additional

FIGURE P15.4

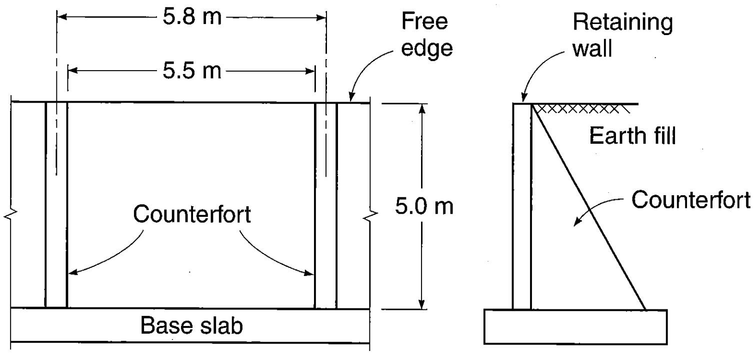
5.8 m
5.5 m
Free edge
Retaining wall
Earth fill
Counterfort
Counterfort
5.0 m
Base slab

support for the main slab. Each section of the main wall, which is 5 m high and 5.4 m long, may be considered fully fixed at its base and also along its two vertical sides (because of full continuity and identical loadings on all such panels). The top of the main wall is without support. The horizontal earth pressure varies from 0 at the top of the wall to 28 kN/m^2 at the top of the base slab. Determine a suitable thickness for the main wall, and select reinforcing bars and spacing.

15.5. The triangular slab shown in Fig. P15.5, providing cover over a loading dock, is fully fixed along two adjacent sides and free of support along the diagonal edge. A uniform snow load of 3.0 kN/m^2 is anticipated. Dead load of 0.5 kN/m^2 will act, in addition to self-weight. Determine the required slab depth and specify all reinforcement. (*Hint:* The main bottom reinforcement should be parallel to the free edge, and the negative reinforcement should be perpendicular to the supported edges.)

FIGURE P15.5

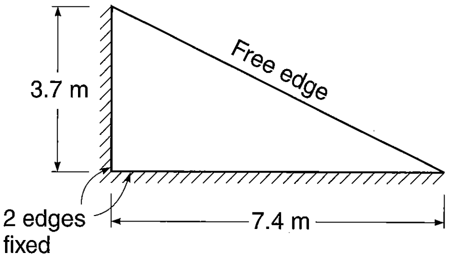
3.7 m
Free edge
2 edges fixed
7.4 m

15.6. Figure P15.6 shows a rectangular slab with a large opening near one corner. It is simply supported along one long side and the adjacent short side, and the two

FIGURE P15.6

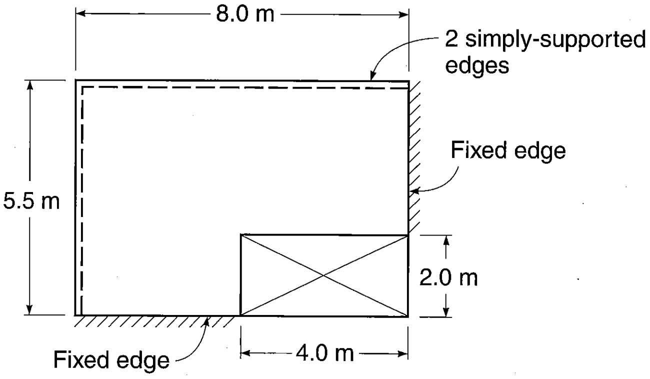
8.0 m
2 simply-supported edges
Fixed edge
5.5 m
2.0 m
Fixed edge
4.0 m

edges adjacent to the opening are fully fixed. A factored load of 12.0 kN/m^2 must be carried. Find the required slab thickness, and specify all reinforcement.

15.7. The roof deck slab of Fig. P15.7 is intended to carry a total factored load, including self-weight, of 8.0 kN/m^2. It will have fixed supports along the two long sides and one short side, but the fourth edge must be free of any support. Two 400 mm square columns will be located as shown.

(*a*) Determine an acceptable slab thickness.
(*b*) Select appropriate load dispersion lines.
(*c*) Determine moments at all critical sections.
(*d*) Specify bar sizes, spacings, and cutoff points.
(*e*) Check controlling sections in the slab for shear strength.

FIGURE P15.7

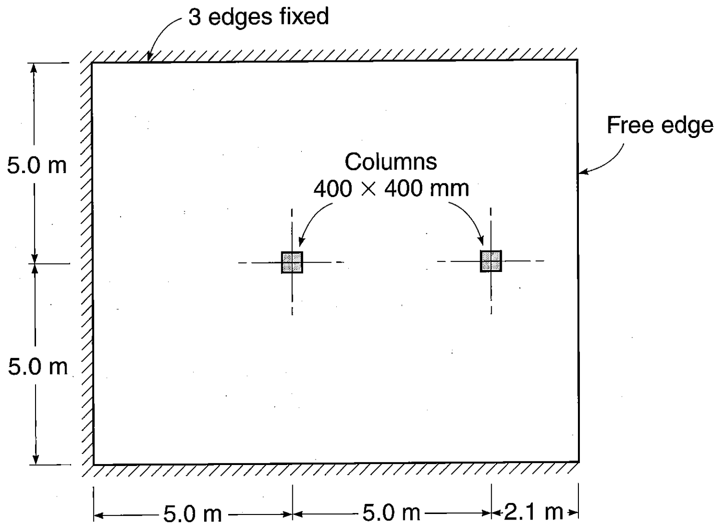

16

Footings and Foundations

16.1 TYPES AND FUNCTIONS

The substructure, or foundation, is the part of a structure that is usually placed below the surface of the ground and that transmits the load to the underlying soil or rock. All soils compress noticeably when loaded and cause the supported structure to settle. The two essential requirements in the design of foundations are that the total settlement of the structure be limited to a tolerably small amount and that differential settlement of the various parts of the structure be eliminated as nearly as possible. With respect to possible structural damage, the elimination of differential settlement, i.e., different amounts of settlement within the same structure, is even more important than limitations on uniform overall settlement.

To limit settlements as indicated, it is necessary (1) to transmit the load of the structure to a soil stratum of sufficient strength and (2) to spread the load over a sufficiently large area of that stratum to minimize bearing pressure. If adequate soil is not found immediately below the structure, it becomes necessary to use deep foundations such as piles or caissons to transmit the load to deeper, firmer layers. If satisfactory soil directly underlies the structure, it is merely necessary to spread the load, by footings or other means. Such substructures are known as *spread* foundations, and it is mainly this type that will be discussed. Information on the more special types of deep foundations can be found in texts on foundation engineering, e.g., Refs. 16.1 to 16.4.

16.2 SPREAD FOOTINGS

Spread footings can be classified as wall and column footings. The horizontal outlines of the most common types are given in Fig. 16.1. A wall footing is simply a strip of reinforced concrete, wider than the wall, that distributes its pressure. Single-column footings are usually square, sometimes rectangular, and represent the simplest and most economical type. Their use under exterior columns meets with difficulties if property rights prevent the use of footings projecting beyond the exterior walls. In this case, combined footings or strap footings are used that enable one to design a footing that will not project beyond the wall column. Combined footings under two or more columns are also used under closely spaced, heavily loaded interior columns where single footings, if they were provided, would completely or nearly merge.

Such individual or combined column footings are the most frequently used types of spread foundations on soils of reasonable bearing capacity. If the soil is weak and/or column loads are great, the required footing areas become so large as to be uneconomical. In this case, unless a deep foundation is called for by soil conditions, a mat

FIGURE 16.1
Types of spread footing.

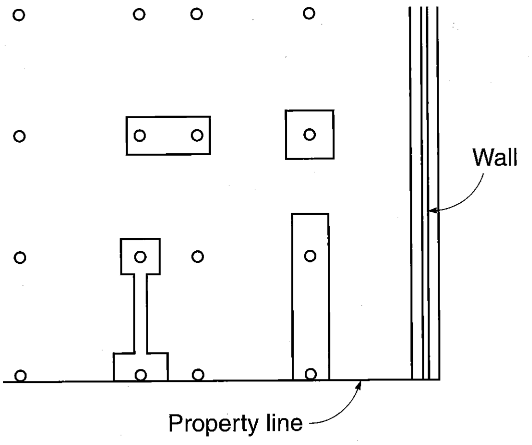

or raft foundation is resorted to. This consists of a solid reinforced concrete slab that extends under the entire building and, consequently, distributes the load of the structure over the maximum available area. Such a foundation, in view of its own rigidity, also minimizes differential settlement. It consists, in its simplest form, of a concrete slab reinforced in both directions. A form that provides more rigidity consists of an inverted girder floor. Girders are located in the column lines in each direction, and the slab is provided with two-way reinforcement, spanning between girders. Inverted flat slabs, with capitals at the bottoms of the columns, are also used for mat foundations.

16.3 DESIGN FACTORS

In ordinary construction, the load on a wall or column is transmitted vertically to the footing, which in turn is supported by the upward pressure of the soil on which it rests. If the load is symmetrical with respect to the bearing area, the bearing pressure is assumed to be uniformly distributed (Fig. 16.2*a*). It is known that this is only approximately true. Under footings resting on coarse-grained soils, the pressure is larger at the center of the footing and decreases toward the perimeter (Fig. 16.2*b*). This is so because the individual grains in such soils are somewhat mobile, so that the soil located close to the perimeter can shift very slightly outward in the direction of lower soil stresses. In contrast, in clay soils pressures are higher near the edge than at the center of the footing, since in such soils the load produces a shear resistance around the perimeter that adds to the upward pressure (Fig. 16.2*c*). It is customary to disregard these nonuniformities (1) because their numerical amount is uncertain and highly

FIGURE 16.2
Bearing pressure distribution: (*a*) as assumed; (*b*) actual, for granular soils; (*c*) actual, for cohesive soils.

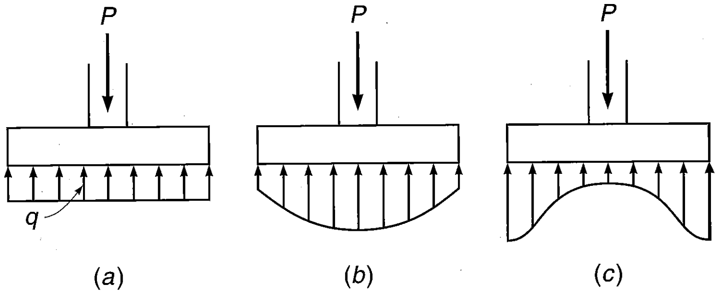

variable, depending on types of soil, and (2) because their influence on the magnitudes of bending moments and shearing forces in the footing is relatively small.

On compressible soils, footings should be loaded concentrically to avoid tilting, which will result if bearing pressures are significantly larger under one side of the footing than under the opposite side. This means that single footings should be placed concentrically under the columns and wall footings concentrically under the walls and that, for combined footings, the centroid of the footing area should coincide with the resultant of the column loads. Eccentrically loaded footings can be used on highly compacted soils and on rock. It follows that one should count on rotational restraint of the column by a single footing only when such favorable soil conditions are present and when the footing is designed for both the column load and the restraining moment. Even then, less than full fixity should be assumed, except for footings on rock.

The accurate determination of stresses in foundation elements of all kinds is difficult, partly because of the uncertainties in determining the actual distribution of upward pressures but also because the structural elements themselves represent relatively massive blocks or thick slabs subject to heavy concentrated loads from the structure above. Design procedures for single-column footings are based largely on the results of experimental investigations by Talbot (Ref. 16.5) and Richart (Ref. 16.6). These tests and the recommendations resulting from them have been reevaluated in the light of more recent research, particularly that focusing on shear and diagonal tension (Refs. 16.7 to 16.9). Combined footings and mat foundations also can be designed by simplified methods, although increasing use is made of more sophisticated tools, such as finite element analysis and strut-and-tie models (Ref. 16.10).

16.4 LOADS, BEARING PRESSURES, AND FOOTING SIZE

Footing sizes are determined for *unfactored* service loads and *allowable* soil pressures, in contrast to the strength design of reinforced concrete members, which uses factored loads and factored nominal strengths. This is because, for footing design, safety is provided by overall safety factors, in contrast to the separate load and strength reduction factors used to dimension members.

Allowable bearing pressures are established from principles of soil mechanics, on the basis of load tests and other experimental determinations (see, for example, Refs. 16.1 to 16.4). Allowable bearing pressures q_a under service loads are usually based on a safety factor of 2.5 to 3.0 against exceeding the bearing capacity of the particular soil and to keep settlements within tolerable limits. Many local building codes contain allowable bearing pressures for the types of soils and soil conditions found in the particular locality.

For concentrically loaded footings, the required area is determined from

$$A_{\text{req}} = \frac{D + L}{q_a} \tag{16.1}$$

In addition, most building codes, including the *International Building Code* (IBC) (Ref. 16.11), which is used throughout the United States, permit a 33 percent increase in the allowable pressure when the effects of wind W or earthquake E are included, if specific loading combinations are used for foundation design. For example,

$$A_{\text{req}} = \frac{D + L + \omega W}{1.33 q_a} \quad \text{or} \quad A_{\text{req}} = \frac{D + L + S + E/1.4}{1.33 q_a} \tag{16.2}$$

where $\omega = 1.3$ if the wind load is calculated based on ASCE/SEI 7 (Ref. 16.12) and 1.0 otherwise, and the 1.4 factor that divides E recognizes that a load factor of 1.0 is used for earthquake loads in strength design.

The required footing area A_{req} is the larger of those determined by Eqs. (16.1) and (16.2). The loads in the numerators of Eqs. (16.1) and (16.2) must be calculated at the level of the base of the footing, i.e., at the contact plane between soil and footing. This means that the weight of the footing and surcharge (i.e., fill and possible liquid pressure on top of the footing) must be included. Wind loads and other lateral loads cause a tendency to overturn. In checking for overturning of a foundation, only those live loads that contribute to overturning should be included, and dead loads that stabilize against overturning should be multiplied by 0.9. A safety factor of at least 1.5 should be maintained against overturning, unless otherwise specified by the local building code (Ref. 16.8).

A footing is eccentrically loaded if the supported column is not concentric with the footing area or if the column transmits at its juncture with the footing not only a vertical load but also a bending moment. In either case, the load effects at the footing base can be represented by the vertical load P and a bending moment M. The resulting bearing pressures are again assumed to be linearly distributed. As long as the resulting eccentricity $e = M/P$ does not exceed the kern distance k of the footing area, the usual flexure formula

$$q_{\substack{\max \\ \min}} = \frac{P}{A} \pm \frac{Mc}{I} \tag{16.3}$$

permits the determination of the bearing pressures at the two extreme edges, as shown in Fig. 16.3*a*. The footing area is found by trial and error from the condition $q_{\max} \le q_a$. If the eccentricity falls outside the kern, Eq. (16.3) gives a negative value (tension) for q along one edge of the footing. Because no tension can be transmitted at the contact area between soil and footing, Eq. (16.3) is no longer valid and bearing pressures are distributed as shown in Fig. 16.3*b*. For rectangular footings of size $l \times b$, the maximum pressure can be found from

$$q_{\max} = \frac{2P}{3bm} \tag{16.4}$$

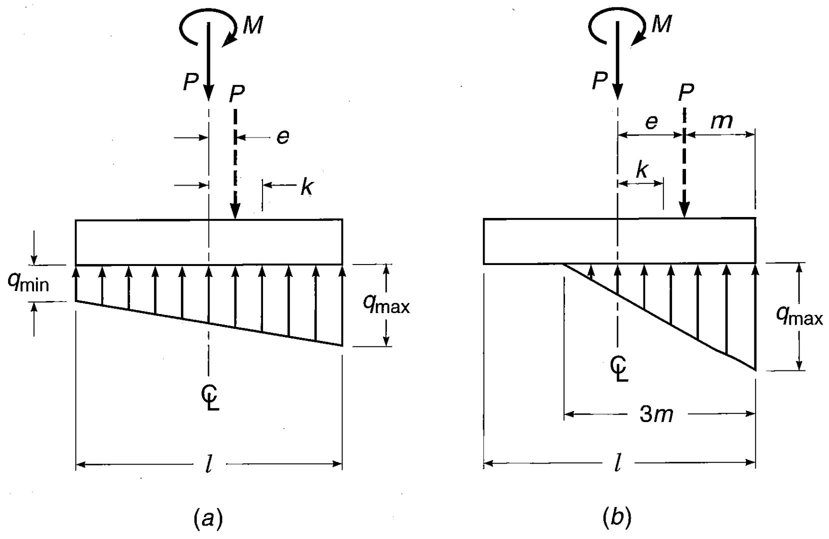

FIGURE 16.3
Assumed bearing pressures under eccentrically loaded footing.

which, again, must be no larger than the allowable pressure q_a. For nonrectangular footing areas of various configurations, kern distances and other aids for calculating bearing pressures can be found in Refs. 16.1 and 16.8 and elsewhere.

Once the required footing area has been determined, the footing must then be designed to develop the necessary strength to resist all moments, shears, and other internal actions caused by the applied loads. For this purpose, the load factors of ACI Code 9.2 apply to footings as to all other structural components. Correspondingly, for strength design, the footing is dimensioned for the effects of the load combinations in Table 1.2. The most common is

$$U = 1.2D + 1.6L$$

or if wind effects are to be included,

$$U = 1.2D + 1.6W + 1.0L + 0.5L_r$$

In seismic zones, earthquake forces E must be considered according to Table 1.2. The requirement that

$$U = 0.9D + 1.6W$$

will hardly ever govern the strength design of a footing, but will affect overturning and stability. Lateral earth pressure H and fluid pressure F must be included if present.

These factored loads must be counteracted and equilibrated by corresponding bearing pressures in the soil. Consequently, once the footing area is determined, the bearing pressures are recalculated for the factored loads for purposes of strength computations. These are fictitious pressures that are needed only to determine the factored loads for use in design. To distinguish them from the actual pressures q under service loads, the soil pressures that equilibrate the factored loads U will be designated q_u.

16.5 WALL FOOTINGS

The simple principles of beam action apply to wall footings with only minor modifications. Figure 16.4 shows a wall footing with the forces acting on it. If bending moments were computed from these forces, the maximum moment would be found to occur at the middle of the width. Actually, the very large rigidity of the wall modifies this situation, and the tests cited in Section 16.3 show that, for footings under concrete walls, it is satisfactory to compute the moment at the face of the wall (section 1-1). Tension cracks in these tests formed at the locations shown in Fig. 16.4, i.e., under the face of the wall rather than in the middle. For footings supporting masonry walls, the maximum moment is computed midway between the middle and the face of the wall, because masonry is generally less rigid than concrete. The maximum bending moment in footings under concrete walls is therefore given by

$$M_u = \frac{1}{8} q_u(b - a)^2 \tag{16.5}$$

For determining shear stresses, the vertical shear force is computed on section 2-2, located, as in beams, at a distance d from the face of the wall. Thus,

$$V_u = q_u\left(\frac{b - a}{2} - d\right) \tag{16.6}$$

The calculation of development length is based on the section of maximum moment, i.e., section 1-1.

FIGURE 16.4
Wall footing.

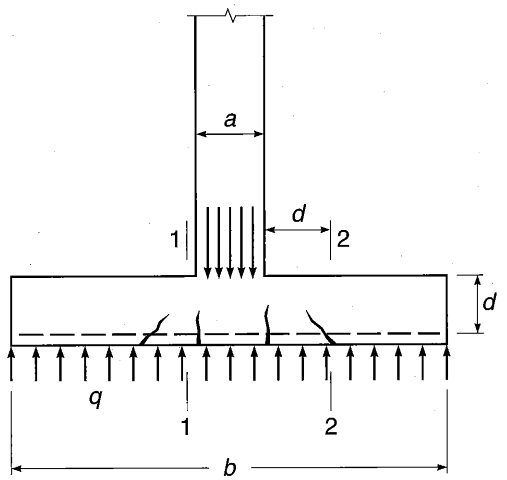

EXAMPLE 16.1

Design of wall footing. A 400 mm concrete wall supports a dead load $D = 200$ kN/m and a live load $L = 150$ kN/m. The allowable bearing pressure is $q_a = 215$ kN/m^2 at the level of the bottom of the footing, which is 1.3 m below grade. Design a footing for this wall using 28 MPa concrete and Grade 420 steel.

Solution. With a 300 mm thick footing, the footing weight per square meter is 7.2 kN/m^2, and the weight of the 1 m fill on top of the footing is $1 \times 16 = 16$ kN/m^2. Consequently, the portion of the allowable bearing pressure that is available or effective for carrying the wall load is

$$q_e = 215 - (7.2 + 16) = 192 \text{ kN/m}^2$$

The required width of the footing is therefore $b = 350/192 = 1.82$ m. A 1.9 m wide footing will be assumed.

The bearing pressure for strength design of the footing, caused by the factored loads, is

$$q_u = \frac{1.2 \times 200 + 1.6 \times 150}{1.9} = 253 \text{ kN/m}^2$$

From this, the factored moment at the face of the wall, section 1-1, for strength design is

$$M_u = \frac{1}{8} \times 253(1.9 - 0.4)^2 = 71.2 \text{ kN-m/m}$$

and assuming $d = 220$ mm, the shear at section 2-2 is

$$V_u = 253\left[\frac{1}{2}(1.9 - 0.4) - 0.22\right] = 134 \text{ kN/m}$$

Shear usually governs the depth of footings, particularly since the use of shear reinforcements in footings is generally avoided as uneconomical. The design shear strength per foot [see Eq. (4.12*b*)] is

$$\phi V_c = \phi(0.17\lambda\sqrt{f_c'}bd) = 0.75(0.17 \times 1\sqrt{28} \times 1000d) \times 10^{-3} = 0.675d \text{ kN/m}$$

from which

$$d = \frac{134}{0.675} = 199 \text{ mm}$$

Since ACI Code 7.7.1 calls for a 75 mm clear cover on bars, a 300 mm thick footing will be selected, giving $d = 218$ mm. This is sufficiently close to the assumed values, and the calculations need not be revised.

To determine the required steel area, $M_u/\phi bd^2 = 71.2 \times 10^6/(0.90 \times 1000 \times 218^2) = 1.66$ is used to enter Graph A.1b of Appendix A. For this value, the curve 420/28 gives the reinforcement ratio $\rho = 0.0041$. The required steel area is then $A_s = 0.0041 \times 1000 \times 218 = 894$ mm²/m. No. 16 (No. 5), 200 mm on centers, furnish $A_s = 995$ mm. The required development length according to Table A.10 of Appendix A is 604 mm. This length is to be furnished from section 1-1 outward. The length of each bar, if end cover is 75 mm, is $1.90 - 0.15 = 1.75$ m, and the actual development length from section 1-1 to the nearby end is $\frac{1}{2}(1750 - 400) = 675$ mm, which is more than the required development length.

Longitudinal shrinkage and temperature reinforcement, according to ACI Code 7.12, must be at least $0.0018 \times 1000 \times 300 = 540$ mm²/m. No. 16 (No. 5) bars on 350 mm centers will furnish 569 mm²/m.

16.6 COLUMN FOOTINGS

In plan, single-column footings are usually square. Rectangular footings are used if space restrictions dictate this choice or if the supported columns have a strongly elongated rectangular cross section. In the simplest form, they consist of a single slab (Fig. 16.5*a*). Another type is that shown in Fig. 16.5*b*, where a pedestal or cap is interposed between the column and the footing slab; the pedestal provides for a more favorable transfer of load and in many cases is required to provide the necessary development length for dowels. This form is also known as a *stepped* footing. All parts of a stepped footing must be cast at one time to provide monolithic action. Sometimes sloped footings like those shown in Fig. 16.5*c* are used. They require less concrete than stepped footings, but the additional labor necessary to produce the sloping surfaces (formwork, etc.) usually makes stepped footings more economical. In general, single-slab footings (Fig. 16.5*a*) are most economical for thicknesses up to 0.9 m.

Single-column footings can be represented as cantilevers projecting out from the column in both directions and loaded upward by the soil pressure. Corresponding tension stresses are caused in both of these directions at the bottom surface. Such footings are, therefore, reinforced by two layers of steel, perpendicular to each other and parallel to the edges.

The required bearing area is obtained by dividing the total load, including the weight of the footing, by the selected bearing pressure. Weights of footings, at this stage, must be estimated and usually amount to 4 to 8 percent of the column load, the former value applying to the stronger types of soils.

In computing bending moments and shears, only the upward pressure q_u that is caused by the factored column loads is considered. The weight of the footing proper

FIGURE 16.5
Types of single-column footings.

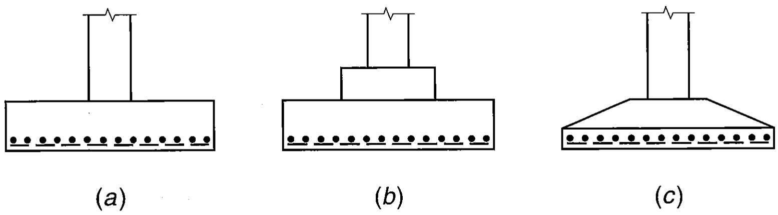

does not cause moments or shears, just as no moments or shears are present in a book lying flat on a table.

a. Shear

Once the required footing area A_{req} has been established from the allowable bearing pressure q_a and the most unfavorable combination of service loads, including weight of footing and overlying fill (and such surcharge as may be present), the thickness h of the footing must be determined. In single footings, the effective depth d is mostly governed by shear. Since such footings are subject to two-way action, i.e., bending in both major directions, their performance in shear is much like that of flat slabs in the vicinity of columns (see Section 13.10). However, in contrast to two-way floor and roof slabs, it is generally not economical in footings to use shear reinforcement. For this reason, only the design of footings in which all shear is carried by the concrete will be discussed here. For the rare cases where the thickness is restricted so that shear reinforcement must be used, the information in Section 13.10 about slabs applies also to footings.

Two different types of shear strength are distinguished in footings: two-way, or punching, shear and one-way, or beam, shear.

A column supported by the slab shown in Fig. 16.6 tends to punch through that slab because of the shear stresses that act in the footing around the perimeter of the column. At the same time, the concentrated compressive stresses from the column spread out into the footing so that the concrete adjacent to the column is in vertical or slightly inclined compression, in addition to shear. As a consequence, if failure occurs, the fracture takes the form of the truncated pyramid shown in Fig. 16.6 (or of a truncated cone for a round column), with sides sloping outward at an angle approaching 45°. The average shear stress in the concrete that fails in this manner can be taken as that acting on vertical planes laid through the footing around the column on a perimeter a distance $d/2$ from the faces of the column (vertical section through *abcd* in Fig. 16.7). The concrete subject to this shear stress v_{u1} is also in vertical compression from the stresses spreading out from the column, and in horizontal compression in both major directions because of the biaxial bending moments in the footing. This triaxiality of stress increases

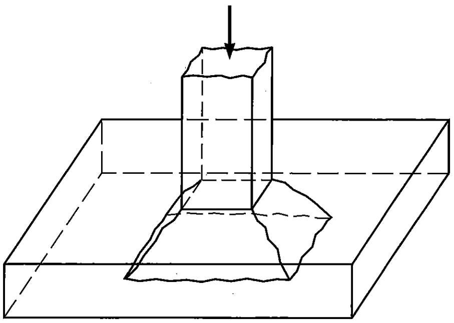

FIGURE 16.6
Punching-shear failure in single footing.

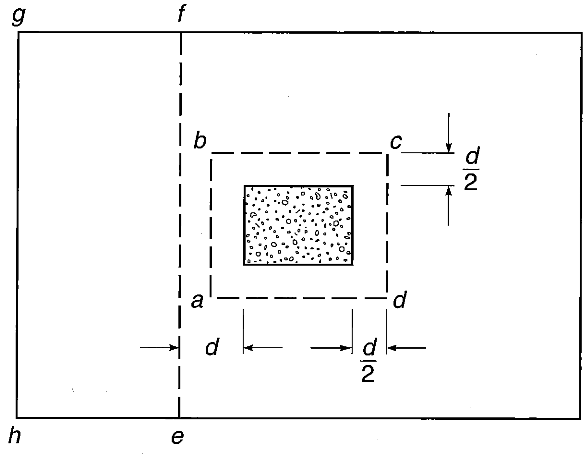

FIGURE 16.7
Critical sections for shear.

the shear strength of the concrete. Tests of footings and of flat slabs have shown, correspondingly, that for punching-type failures the shear stress computed on the critical perimeter area is larger than in one-way action (e.g., beams).

As discussed in Section 13.10, the ACI Code equations (13.11*a,b,c*) give the nominal punching-shear strength on this perimeter:

$$V_c = 0.33\lambda\sqrt{f_c'}\,b_o d \tag{16.7a}$$

except for columns of elongated cross section, for which

$$V_c = 0.17\left(1 + \frac{2}{\beta}\right)\lambda\sqrt{f_c'}\,b_o d \tag{16.7b}$$

For cases in which the ratio of critical perimeter to slab depth b_o/d is very large,

$$V_c = 0.83\left(\frac{\alpha_s d}{b_o} + 2\right)\lambda\sqrt{f_c'}\,b_o d \tag{16.7c}$$

where b_o is the perimeter *abcd* in Fig. 16.7; $\beta = a/b$ is the ratio of the long to short sides of the column cross section; and α_s is 40 for interior loading, 30 for edge loading, and 20 for corner loading of a footing. The punching-shear strength of the footing is to be taken as the smallest of the values given by Eqs. (16.7*a*), (16.7*b*), and (16.7*c*); and the design strength is ϕV_c, as usual, where $\phi = 0.75$ for shear.

The application of Eqs. (16.7) to punching shear in footings under columns with other than a rectangular cross section is shown in Fig. 13.23. For such situations, ACI Code 11.11.1 indicates that the perimeter b_o must be of minimum length but need not approach closer than $d/2$ to the perimeter of the actual loaded area. The manner of defining a and b for such irregular loaded areas is also shown in Fig. 13.23. If a moment is transferred from the column to the footing, the criteria discussed in Section 13.11 for the transfer of moment by bending and shear at slab-column connections must be satisfied.

Shear failures can also occur, as in beams or one-way slabs, at a section a distance d from the face of the column, such as section *ef* of Fig. 16.7. Just as in beams and one-way slabs, the nominal shear strength is given by Eq. (4.12*a*), that is,

$$V_c = \left(0.16\lambda\sqrt{f_c'} + 17\rho\frac{V_u d}{M_u}\right)bd \le 0.29\lambda\sqrt{f_c'}\,bd \tag{16.8a}$$

where b = width of footing at distance d from face of column
= *ef* in Fig. 16.7
V_u = total factored shear force on that section
= q_u times footing area outside that section (area *efgh* in Fig. 16.7)
M_u = moment of V_u about *ef*

In footing design, the simpler and somewhat more conservative Eq. (4.12*b*) is generally used, i.e.,

$$V_c = 0.17\lambda\sqrt{f_c'}\,bd \tag{16.8b}$$

The required depth of footing d is then calculated from the usual equation

$$V_u \le \phi V_c \tag{16.9}$$

applied separately in connection with Eqs. (16.7) and (16.8). For Eq. (16.7), $V_u = V_{u1}$ is the total upward pressure caused by q_u on the area outside the perimeter *abcd* in Fig. 16.7. For Eq. (16.8), $V_u = V_{u2}$ is the total upward pressure on the area *efgh* outside the section *ef* in Fig. 16.7. The required depth is then the larger of those calculated from either Eq. (16.7) or (16.8). For shear, $\phi = 0.75$.

Although the lightweight concrete factor λ appears in Eqs. (16.7) and (16.8), normalweight concrete ($\lambda = 1$) is almost universally used in foundations.

b. Bearing: Transfer of Forces at Base of Column

When a column rests on a footing or pedestal, it transfers its load to only a part of the total area of the supporting member. The adjacent footing concrete provides lateral support to the directly loaded part of the concrete. This causes triaxial compressive stresses that increase the strength of the concrete that is loaded directly under the column. Based on tests, ACI Code 10.14.1 provides that when the supporting area is wider than the loaded area on all sides, the design bearing strength is

$$\phi P_n = \phi(0.85 f_c' A_1)\sqrt{\frac{A_2}{A_1}} \le \phi(0.85 f_c' A_1) \times 2 \tag{16.10}$$

For bearing on concrete, $\phi = 0.65$, f_c' is the specified compressive strength of the footing concrete, which frequently is less than that of the column, and A_1 is the loaded area. A_2 is the area of the lower base of the largest frustum of a pyramid, cone, or tapered wedge contained wholly within the support and having for its upper base the loaded area and having side slopes of 1 vertical to 2 horizontal. The meaning of this definition of A_2 may be clarified by Fig. 16.8. For the somewhat unusual case shown, where the top of the support is stepped, a step that is deeper or closer to the loaded area than that shown may result in reduction in the value of A_2. A footing for which the top surface is sloped away from the loaded area more steeply than 1 to 2 will result in a value of A_2 equal to A_1. In most usual cases, for which the top of the footing is flat and the sides are vertical, A_2 is simply the maximum area of the portion of the supporting surface that is geometrically similar to, and concentric with, the loaded area.

FIGURE 16.8
Definition of areas A_1 and A_2.

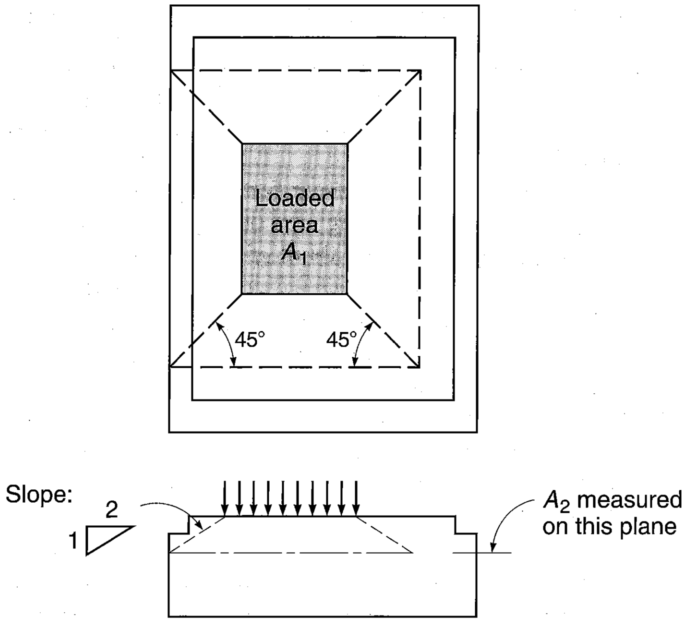

All axial forces and bending moments that act at the bottom section of a column must be transferred to the footing at the bearing surface by compression in the concrete and by reinforcement. With respect to the reinforcement, this may be done either by extending the column bars into the footing or by providing dowels that are embedded in the footing and project above it. In the latter case, the column bars merely rest on the footing and in most cases are tied to dowels. This results in a simpler construction procedure than extending the column bars into the footing. To ensure the integrity of the junction between column and footing, ACI Code 15.8.2 requires that the minimum area of reinforcement that crosses the bearing surface (dowels or column bars) be 0.005 times the gross area of the supported column. The length of the dowels or bars of diameter d_b must be sufficient on both sides of the bearing surface to provide the required development length for compression bars (see Section 5.8), that is, $l_{dc} \geq (0.24f_y/\lambda\sqrt{f_c'})d_b$ and $\geq 0.043f_yd_b$. In addition, if dowels are used, the lapped length must be at least that required for a lap splice in compression (see Section 5.11b); i.e., the length of lap must not be less than the usual development length in compression and must not be less than $0.071f_yd_b$. Where bars of different sizes are lap-spliced, the splice length should be the larger of the development length of the larger bar or the splice length of the smaller bar, according to the ACI Code.

The two largest bar sizes, Nos. 43 (No. 14) and 57 (No. 18), are frequently used in columns with large axial forces. Under normal circumstances, the ACI Code specifically prohibits the lap splicing of these bars because tests have shown that welded splices or other positive connections are necessary to develop these heavy bars fully. A specific exception, however, is made for dowels for Nos. 43 (No. 14) and 57 (No. 18) column bars. Relying on long-standing successful use, ACI Code 12.16.2 permits these heavy bars to be spliced to dowels of lesser diameter [i.e., No. 36 (No. 11) or smaller], provided that the dowels have a development length into the column corresponding to that of the column bar [i.e., Nos. 43 or 57 (Nos. 14 or 18), as the case may be] and into the footing as prescribed for the particular dowel size [i.e., No. 36 (No. 11) or smaller, as the case may be].

c. Bending Moments, Reinforcement, and Bond

If a vertical section is passed through a footing, the bending moment that is caused in the section by the net upward soil pressure (i.e., factored column load divided by bearing area) is obtained from simple statics. Figure 16.9 shows such a section *cd* located along the face of the column. The bending moment about *cd* is that caused by the upward pressure q_u on the area to one side of the section, i.e., the area *abcd*. The reinforcement perpendicular to that section, i.e., the bars running in the long direction, is calculated from this bending moment. Likewise, the moment about section *ef* is caused by the pressure q_u on the area *befg*, and the reinforcement in the short direction, i.e., perpendicular to *ef*, is calculated for this bending moment. In footings that support reinforced concrete columns, the critical section *cd* or *ef* for bending is located at the face of the column, as shown in Fig. 16.10*a*, according to ACI Code 15.4.2.

In footings supporting masonry columns, the critical section *cd* or *ef* is located halfway between the centerline and the face of the column, as shown in Fig. 16.10*b*; and in footings supporting steel columns, the critical section *cd* or *ef* is located halfway between the face of the steel column and the edge of the steel base plate, as shown in Fig. 16.10*c*.

In footings with *pedestals*, the width resisting compression in sections *cd* and *ef* is that of the pedestal; the corresponding depth is the sum of the thickness of pedestal

FIGURE 16.9
Critical sections for bending and bond.

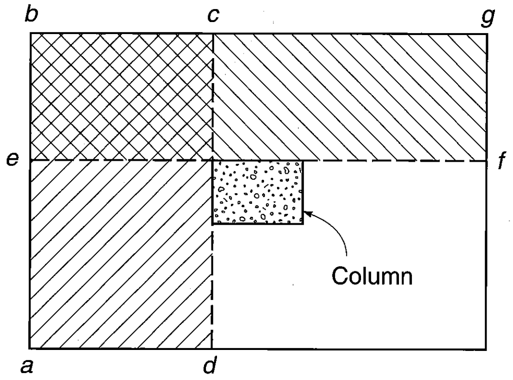

FIGURE 16.10
Critical sections *cd* or *ef* for concrete, masonry, and steel columns.

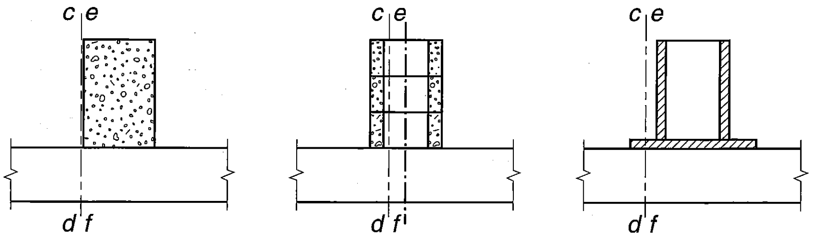

(*a*) Face of concrete column

(*b*) Halfway between centerline and face of masonry wall or column

(*c*) Halfway between face of steel column and edge of steel base plate

and footing. Further sections parallel to *cd* and *ef* are passed at the edge of the pedestal, and the moments are determined in the same manner, to check the strength at locations in which the depth is that of the footing only.

For footings with relatively small pedestals, the latter are often discounted in moment and shear computation, and bending is checked at the face of the column, with width and depth equal to that of the footing proper.

In *square footings*, the reinforcement is uniformly distributed over the width of the footing in each of the two layers; i.e., the spacing of the bars is constant. The moments for which the two layers are designed are the same. However, the effective depth d for the upper layer is less by 1 bar diameter than that of the lower layer. Consequently, the required A_s is larger for the upper layer. Instead of using different spacings or different bar diameters in each of the two layers, it is customary to determine A_s based on average depth and to use the same arrangement of reinforcement for both layers.

In *rectangular footings*, the reinforcement *in the long direction* is again uniformly distributed over the pertinent (shorter) width. In locating the bars in the short direction, one has to consider that the support provided to the footing by the column is concentrated near the middle. Consequently, the curvature of the footing is sharpest, i.e., the moment per meter largest, immediately under the column, and it decreases in the long direction with increasing distance from the column. For this reason, a larger steel area per longitudinal meter is needed in the central portion than near the far ends of the footing. ACI Code 15.4.4, therefore, provides the following:

> For reinforcement in the short direction, a portion of the total reinforcement $\gamma_s A_s$ shall be distributed uniformly over a band width (centered on the centerline of the column or pedestal) equal to the length of the short side of the footing. The remainder of the

reinforcement required in the short direction $(1 - \gamma_s)A_s$ shall be distributed uniformly outside the center band width of the footing

$$\gamma_s = \frac{\text{reinforcement in band width}}{\text{total reinforcement in short direction}} = \frac{2}{\beta + 1} \tag{16.11}$$

where β is the ratio of the long side to the short side of the footing.

According to the ACI Code 10.5.4, the usual minimum flexural reinforcement ratios of Section 3.4e need not be applied to either slabs or footings. Instead, the minimum steel requirements for shrinkage and temperature crack control for structural slabs are to be imposed, as given in Table 13.2. The maximum spacing of bars in the direction of the span is reduced to the lesser of 3 times the footing thickness h and 450 mm, rather than $5h$ as is normal for shrinkage and temperature steel. These requirements for minimum steel and maximum spacing are to be applied to mat foundations as well as individual footings.

Earlier editions of the ACI Code, through 1989, were somewhat ambiguous as to whether or not minimum steel requirements for flexural members were to be applied to slabs and footings. For slabs, the argument was presented that an overload would be distributed laterally and that a sudden failure is therefore less likely than for beams; therefore the usual requirement could be relaxed. Although that reasoning may apply to highly indeterminate building floors, the possibility for redistribution in a footing is much more limited. Because of this, and because of the importance of a footing to the safety of the structure, many engineers apply the minimum flexural reinforcement ratio of Eq. (3.41) to footings as well as beams. This seems prudent, and the following design examples use the more conservative minimum flexural steel requirements of Eq. (3.41).

The critical sections for development length of footing bars are the same as those for bending. Development length may also have to be checked at all vertical planes in which changes of section or of reinforcement occur, as at the edges of pedestals or where part of the reinforcement may be terminated.

EXAMPLE 16.2

Design of a square footing. A column 450 mm square, with $f'_c = 28$ MPa, reinforced with eight No. 25 (No. 8) bars of $f_y = 420$ MPa, supports a dead load of 1000 kN and a live load of 800 kN. The soil (fill) has a unit weight of 16 kN/m^3. The allowable soil pressure q_a is 250 kN/m^2. Design a square footing with base 1.5 m below grade, using $f'_c = 28$ MPa and $f_y = 420$ MPa.

Solution. Since the space between the bottom of the footing and the surface will be occupied partly by concrete and partly by soil (fill), an average unit weight of 20 kN/m^3 will be assumed. The pressure of this material at the 1.5 m depth is $1.5 \times 20 = 30$ kN/m^2, leaving a bearing pressure of $q_e = 250 - 30 = 220$ kN/m^2 available to carry the column service load. Hence, the required footing area $A_{\text{req}} = (1000 + 800)/220 = 8.18$ m^2. A base 2.85 m square is selected, furnishing a footing area of 8.12 m^2, which differs from the required area by about 1 percent.

For strength design, the upward pressure caused by the factored column loads is $q_u = (1.2 \times 1000 + 1.6 \times 800)/2.85^2 = 305$ kN/m^2.

The footing depth in square footings is usually determined based on two-way or punching shear on the critical perimeter *abcd* in Fig. 16.11. Trial calculations suggest $d = 475$ mm. Hence, the length of the critical perimeter is

$$b_o = 4(450 + d) = 3700 \text{ mm}$$

The shear force acting on this perimeter, being equal to the total upward pressure minus that acting within the perimeter *abcd*, is

$$V_{u1} = 305[2.85^2 - 0.925^2] = 2216 \text{ kN}$$

FIGURE 16.11
Critical sections for Example 16.2.

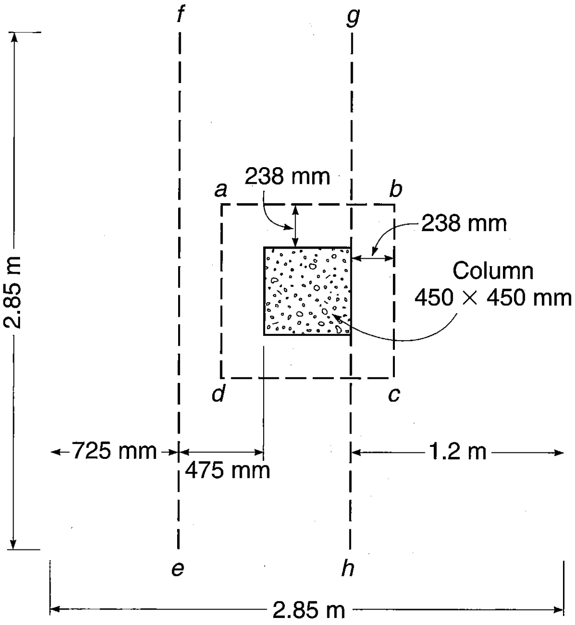

The corresponding nominal shear strength [Eq. (13.11*a*)] is

$$V_c = 0.33 \times 1\sqrt{28} \times 3700 \times 475 \times 10^{-3} = 3069 \text{ kN}$$

and

$$\phi V_c = 0.75 \times 3069 = 2302 \text{ kN}$$

Since the design strength exceeds the factored shear V_{u1}, the depth $d = 475$ mm is adequate for punching shear. The selected value $d = 475$ mm will now be checked for one-way or beam shear on section *ef*. The factored shear force acting on that section is

$$V_{u2} = 305 \times 0.725 \times 2.85 = 630 \text{ kN}$$

and the nominal shear strength is

$$V_c = 0.17 \times 1\sqrt{28} \times 2850 \times 475 \times 10^{-3} = 1218 \text{ kN}$$

The design shear strength $0.75 \times 1218 = 914$ kN is larger than the factored shear V_{u2}, so that $d = 475$ mm is also adequate for one-way shear.

The bending moment on section *gh* of Fig. 16.11 is

$$M_u = 305 \times 2.85\left(\frac{1.2^2}{2}\right) = 626 \text{ kN-m}$$

Because the depth required for shear is greatly in excess of that required for bending, the reinforcement ratio will be low and the corresponding depth of the rectangular stress block small. If $a = 50$ mm, the required steel area is

$$A_s = \frac{626 \times 10^6}{0.90 \times 420(475 - 50/2)} = 3680 \text{ mm}^2$$

FIGURE 16.12
Footing in Example 16.2.

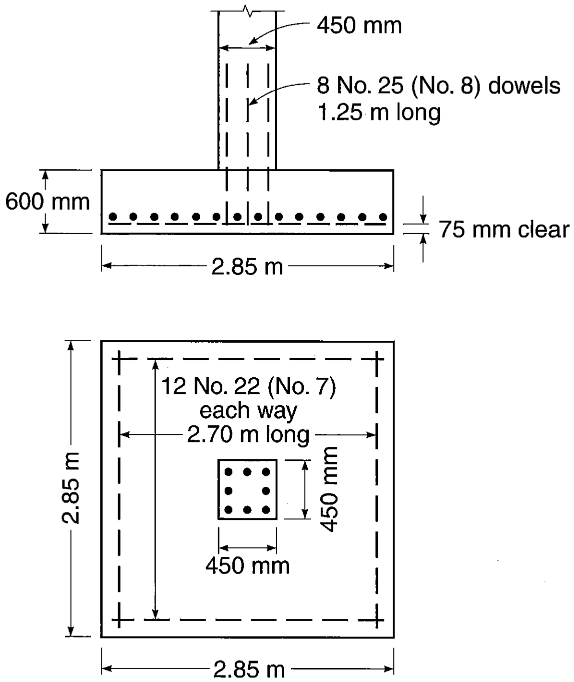

Checking the minimum reinforcement ratio using Eq. (3.41) results in

$$A_{s,\min} = \frac{0.25\sqrt{28}}{420} \times 2850 \times 475 = 4264 \text{ mm}^2$$

but not less than

$$A_{s,\min} = \frac{1.4}{420} \times 2850 \times 475 = 4513 \text{ mm}^2$$

The controlling value of 4513 mm^2 is larger than the 3680 mm^2 calculated for bending. Twelve No. 22 (No. 7) bars furnishing 4644 mm^2 will be used in each direction. The required development length beyond section *gh* is found from Table A.10 to be 1.04 m, which is more than adequately met by the actual length of bars beyond section *gh*, namely, $1.2 - 0.075 = 1.12$ m.

Checking for transfer of forces at the base of the column shows that the footing concrete, which has the same f'_c as the column concrete and for which the strength is enhanced according to Eq. (16.10), is clearly capable of carrying that part of the column load transmitted by the column concrete. The force in the column carried by the steel will be transmitted to the footing using dowels to match the column bars. These must extend into the footing the full development length in compression, which is found from Table A.11 of Appendix A to be 480 mm for No. 25 (No. 8) bars. This is accommodated in a footing with $d = 480$ mm. Above the top surface of the footing, the No. 25 (No. 8) dowels must extend into the column that same development length, but not less than the requirement for a lapped splice in compression (see Section 5.13b). The minimum lap splice length for the No. 25 (No. 8) bars is $0.071 \times 420 \times 25.4 = 757$ mm, which is seen to control here. Thus the bars will be carried 760 mm into the column, requiring a total dowel length of 1.24 m. This will be rounded upward for practical reasons to 1.25 m, as shown in Fig. 16.12. It is easily confirmed that the minimum dowel steel requirement of $0.005 \times 450 \times 450 = 1013$ mm^2 does not control here.

For concrete in contact with ground, a minimum cover of 75 mm is required for corrosion protection. With $d = 475$ mm, measured from the top of the footing to the center of the upper layer of bars, the total thickness of the footing that is required to provide 75 mm clear cover for the lower steel layer is

$$h = 480 + 1.5 \times 22.2 + 75 = 588 \text{ mm}$$

The footing, with 600 mm thickness, is shown in Fig. 16.12.

16.7 COMBINED FOOTINGS

Spread footings that support more than one column or wall are known as *combined footings*. They can be divided into two categories: those that support two columns and those that support more than two (generally large numbers of) columns.

Examples of the first type, i.e., two-column footings, are shown in Fig. 16.1. In buildings where the allowable soil pressure is large enough for single footings to be adequate for most columns, two-column footings are seen to become necessary in two situations: (1) if columns are so close to the property line that single-column footings cannot be made without projecting beyond that line, and (2) if some adjacent columns are so close to each other that their footings would merge. Both situations are shown in Fig. 16.1.

When the bearing capacity of the subsoil is low so that large bearing areas become necessary, individual footings are replaced by *continuous strip footings* that support more than two columns and usually all columns in a row. Sometimes such strips are arranged in both directions, in which case a *grid foundation* is obtained, as shown in Fig. 16.13. Strip footings can be made to develop a much larger bearing area much more economically than can be done by single footings because the individual strips represent continuous beams whose moments are much smaller than the cantilever moments in large single footings that project far out from the column in all four directions.

FIGURE 16.13
Grid foundation.

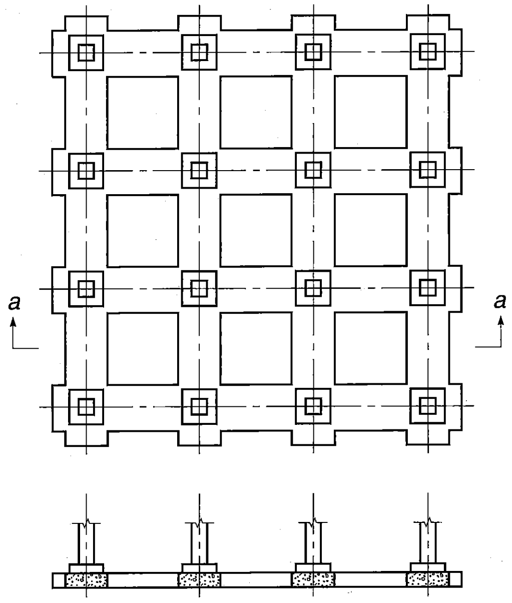

FIGURE 16.14
Mat foundation.

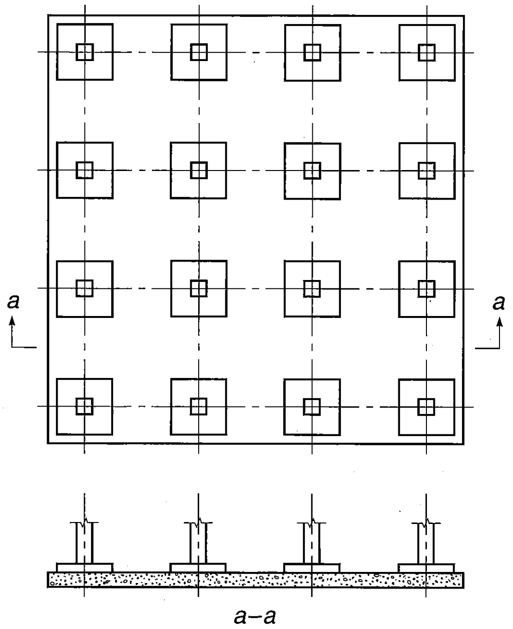

In many cases, the strips are made to merge, resulting in a mat foundation, as shown in Fig. 16.14. That is, the foundation consists of a solid reinforced concrete slab under the entire building. In structural action, such a mat is very similar to a flat slab or a flat plate, upside down, i.e., loaded upward by the bearing pressure and downward by the concentrated column reactions. The mat foundation evidently develops the maximum available bearing area under the building. If the soil's capacity is so low that even this large bearing area is insufficient, some form of deep foundation, such as piles or caissons, must be used. These are discussed in texts on foundation design and fall outside the scope of the present volume.

Mat foundations may be designed with the column pedestals, as shown in Figs. 16.13 and 16.14, or without them, depending on whether they are necessary for shear strength and the development length of dowels.

Apart from developing large bearing areas, another advantage of strip and mat foundations is that their continuity and rigidity help in reducing differential settlements of individual columns relative to each other, which may otherwise be caused by local variations in the quality of subsoil, or other causes. For this purpose, continuous foundations are frequently used in situations where the superstructure or the type of occupancy provides unusual sensitivity to differential settlement.

Much useful and important design information pertaining to combined footings and mats is found in Refs. 16.10 and 16.13.

16.8 TWO-COLUMN FOOTINGS

It is desirable to design combined footings so that the centroid of the footing area coincides with the resultant of the two column loads. This produces uniform bearing pressure over the entire area and forestalls a tendency for the footings to tilt. In plan, such footings are rectangular, trapezoidal, or T-shaped, the details of the shape being arranged to produce coincidence of centroid and resultant. The simple relationships

FIGURE 16.15
Two-column footing.
(*Adapted from Ref. 16.8.*)

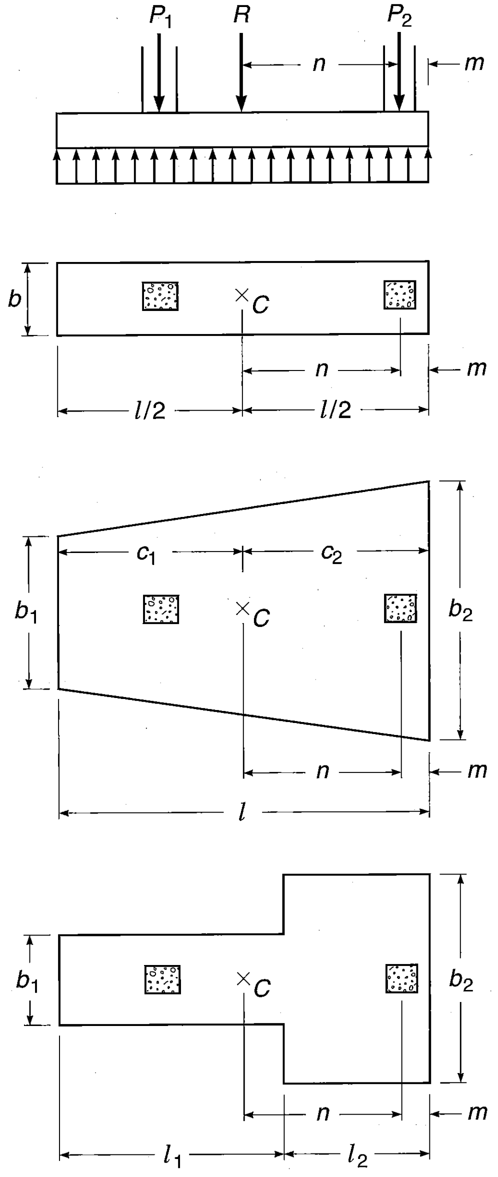

$$l = 2(m+n)$$

$$b = \frac{R}{q_e l}$$

$$\frac{b_2}{b_1} = \frac{3(n+m) - l}{2l - 3(n+m)}$$

$$(b_1+b_2) = \frac{2R}{q_e l}$$

$$c_1 = \frac{l(b_1+2b_2)}{3(b_1+b_2)}$$

$$c_2 = \frac{l(2b_1+b_2)}{3(b_1+b_2)}$$

$$b_1 = \frac{R}{q_e} = \left[\frac{2(n+m) - l_2}{l_1(l_1+l_2)}\right]$$

$$b_2 = \frac{R}{l_2 q_e} - \frac{l_1 b_1}{l_2}$$

$$l_1 b_1 + l_2 b_2 = \frac{R}{q_e}$$

shown in Fig. 16.15 facilitate the determination of the shape of the bearing area (from Ref. 16.8). In general, the distances *m* and *n* are given, the former being the distance from the center of the exterior column to the property line and the latter the distance from that column to the resultant of both column loads.

Another expedient that is used if a single footing cannot be centered under an exterior column is to place the exterior column footing eccentrically and to connect it with the nearest interior column footing by a beam or strap. This strap, being counterweighted by the interior column load, resists the tilting tendency of the eccentric exterior footing and equalizes the pressure under it. Such foundations are known as *strap, cantilever*, or *connected footings*.

The two examples that follow demonstrate some of the peculiarities of the design of two-column footings.

EXAMPLE 16.3

Design of a combined footing supporting one exterior and one interior column. An exterior 600 × 450 mm column with $D = 750$ kN, $L = 600$ kN, and an interior 600 × 600 mm column with $D = 1100$ kN, $L = 900$ kN are to be supported on a combined rectangular footing whose outer end cannot protrude beyond the outer face of the exterior column (see Fig. 16.1). The distance center to center of columns is 5.5 m, and the allowable bearing pressure of the soil is 300 kN/m^2. The bottom of the footing is 1.8 m below grade, and a surcharge of 5 kN/m^2 is specified on the surface. Design the footing for $f'_c = 21$ MPa and $f_y = 420$ MPa.

Solution. The space between the bottom of the footing and the surface will be occupied partly by concrete (footing, concrete floor) and partly by backfill. An average unit weight of 20 kN/m^3 can be assumed. Hence, the effective portion of the allowable bearing pressure that is available for carrying the column loads is $q_e = q_a -$ (weight of fill and concrete + surcharge) = $300 - (1.8 \times 20 + 5) = 259$ kN/m^2. Then the required area A_{req} = sum of column loads/$q_e = 3350/259 = 12.9$ m^2. The resultant of the column loads is located from the center of the exterior column a distance $2000 \times 5.5/3350 = 3.38$ m. Hence, the length of the footing must be $2(3.28 + 0.225) = 7.02$ m. A length of 7.02 m is selected. The required width is then $12.9/7.02 = 1.84$ m. A width of 1.85 m is selected (see Fig. 16.16).

Longitudinally, the footing represents a beam, loaded from below, spanning between columns and cantilevering beyond the interior column. Since this beam is considerably wider than the columns, the column loads are distributed crosswise by transverse beams, one under each column. In the present relatively narrow and long footing, it will be found that the required minimum depth for the transverse beams is smaller than is required for the footing in the longitudinal direction. These "beams," therefore, are not really distinct members but merely represent transverse strips in the main body of the footing, reinforced so that they are capable of resisting the transverse bending moments and the corresponding shears. It then

FIGURE 16.16
Combined footing in Example 16.3.

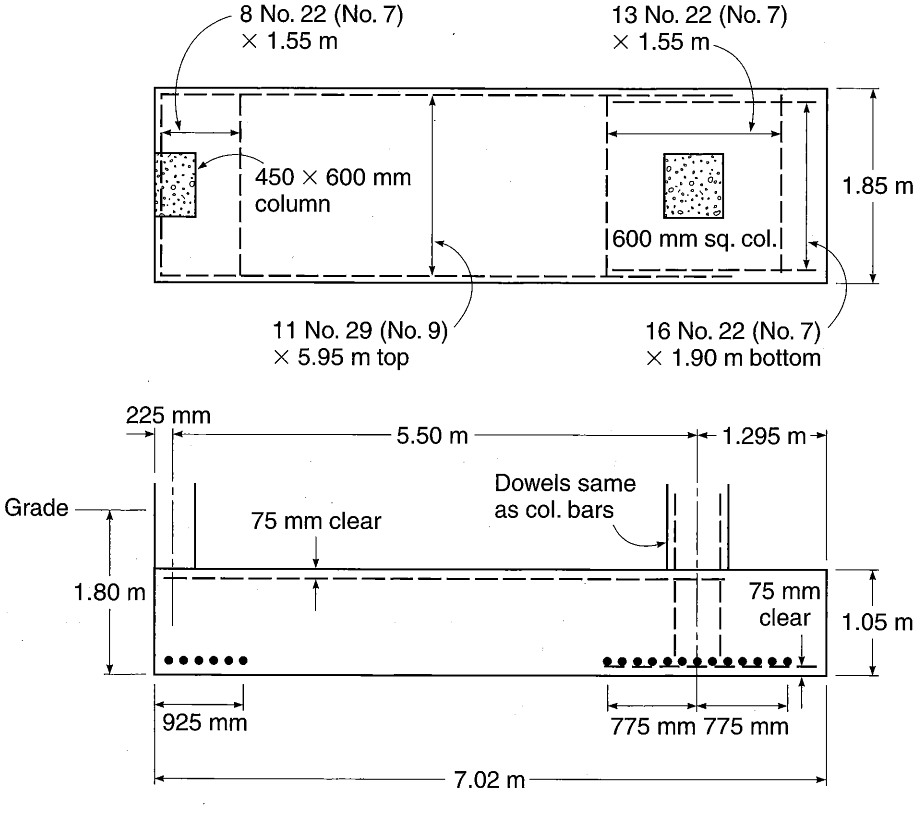

becomes necessary to decide how large the effective width of this transverse beam can be assumed to be. Obviously, the strip directly under the column does not deflect independently and is strengthened by the adjacent parts of the footing. The effective width of the transverse beams is therefore evidently larger than that of the column. In the absence of definite rules for this case, or of research results on which to base such rules, the authors recommend conservatively that the load be assumed to spread outward from the column into the footing at a slope of 2 vertical to 1 horizontal. This means that the effective width of the transverse beam is assumed to be equal to the width of the column plus $d/2$ on either side of the column, d being the effective depth of the footing.

Strength design in longitudinal direction
The net upward pressure caused by the factored column loads is

$$q_u = \frac{1.2(750 + 1100) + 1.6(600 + 900)}{7.02 \times 1.85} = 355.7 \text{ kN/m}^2$$

Then the net upward pressure per linear meter in the longitudinal direction is $355.7 \times 1.85 = 658$ kN/m. The maximum negative moment between the columns occurs at the section of zero shear. Let x be the distance from the outer edge of the exterior column to this section. Then (see Fig. 16.17)

$$V_u = 658x - 1860 = 0$$

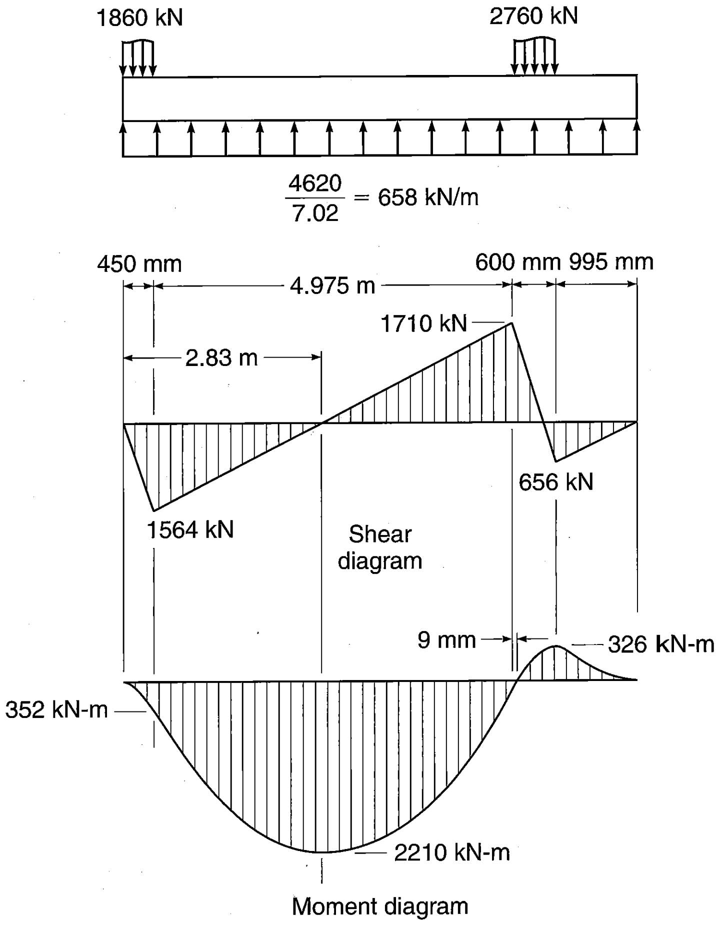

FIGURE 16.17
Moment and shear diagrams for footing in Example 16.3.

results in $x = 2.83$ m. The moment at this section is

$$M_u = \left[658\,\frac{2.83^2}{2} - 1860(2.83 - 0.225)\right] = -2210\text{ kN-m}$$

The moment at the right edge of the interior column is

$$M_u = 658\left(\frac{0.995^2}{2}\right) = 326\text{ kN-m}$$

and the details of the moment diagram are as shown in Fig. 16.17. Try $d = 950$ mm.

From the shear diagram in Fig. 16.17, it is seen that the critical section for flexural shear occurs at a distance d to the left of the left face of the interior column. At that point, the factored shear is

$$V_u = 1710 - 658 \times 0.950 = 1085\text{ kN-m}$$

and the design shear strength

$$\phi V_c = 0.75 \times 0.17 \times 1\sqrt{21} \times 1850 \times 950 \times 10^{-3} = 1127\text{ kN} > V_u$$

indicating that $d = 950$ mm is adequate.

Additionally, as in single footings, punching shear should be checked on a perimeter section a distance $d/2$ around the column, on which the nominal shear stress $v_c = 0.33 \times 1\sqrt{21} = 1.51$ MPa. Of the two columns, the exterior one with a three-sided perimeter a distance $d/2$ from the column is more critical in regard to this punching shear. The perimeter is

$$b_o = 2\left(0.45 + \frac{0.95}{2}\right) + (0.60 + 0.95) = 3.40\text{ m}$$

and the shear force, being the column load minus the soil pressure within the perimeter, is

$$V_u = 1860 - 0.925 \times 1.55(355.7) = 1350\text{ kN}$$

On the other hand, the design shear strength on the perimeter section is

$$\phi V_c = 0.75 \times 1.51 \times 3400 \times 950 \times 10^{-3} = 3678\text{ kN}$$

considerably larger than the factored shear V_u.

With $d = 950$ mm, and with 90 mm cover from the center of the bars to the top surface of the footing, the total thickness is 1040 mm.

To determine the required steel area, $M_u/\phi bd^2 = 2{,}210 \times 10^6/(0.9 \times 1850 \times 950^2) = 1.47$ is used to enter Graph A.1*b* of Appendix A. For this value, the curve 420/21 gives the reinforcement ratio $\rho = 0.0037$. The required steel area is $A_s = 0.0037 \times 950 \times 1850 = 6503\text{ mm}^2$. Eleven No. 29 (No. 9) bars furnish 7095 mm^2. The required development length is found to be 1.84 m. From Fig. 16.17, the distance from the point of maximum moment to the nearer left end of the bars is seen to be $2.83 - 0.75 = 2.08$ m, much larger than the required minimum development length. The selected reinforcement is therefore adequate for both bending and bond.

For the portion of the longitudinal beam that cantilevers beyond the interior column, the minimum required steel area controls. Here,

$$A_{s,\min} = \frac{0.25\sqrt{21}}{420} \times 1850 \times 950 = 4794\text{ mm}^2$$

but not less than

$$A_{s,\min} = \frac{1.4}{420} \times 1850 \times 950 = 5858\text{ mm}^2$$

Sixteen No. 22 (No. 7) bars with $A_s = 6192\text{ mm}^2$ are selected; their development length is computed and for bottom bars is found satisfactory.

Design of transverse beam under interior column

The width of the transverse beam under the interior column can now be established as previously suggested and is $600 + 2(d/2) = 600 + 2 \times (950/2) = 1550$ mm. The net upward load per linear foot of the transverse beam is $2760/1.85 = 1492$ kN/m. The moment at the edge of the interior column is

$$M_u = 1492\left(\frac{0.625^2}{2}\right) = 291 \text{ kN-m}$$

Since the transverse bars are placed on top of the longitudinal bars (see Fig. 16.16), the actual value of d furnished is $950 - 25 = 925$ mm. The minimum required steel area controls; i.e.,

$$A_s = \frac{1.4}{420} 1550 \times 925 = 4779 \text{ mm}^2$$

Thirteen No. 22 (No. 7) bars are selected and placed within the 1.55 m effective width of the transverse beam.

Punching shear at the perimeter a distance $d/2$ from the column has been checked before. The critical section for regular flexural shear, at a distance d from the face of the column, lies beyond the edge of the footing, and therefore no further check on shear is needed.

The design of the transverse beam under the exterior column is the same as the design of that under the interior column, except that the effective width is 925 mm. The details of the calculations are not shown. It can be easily checked that eight No. 22 (No. 7) bars, placed within the 925 mm effective width, satisfy all requirements. Design details are shown in Fig. 16.16.

EXAMPLE 16.4

Design of a strap footing. In a strap or connected footing, the exterior footing is placed eccentrically under its column so that it does not project beyond the property line. Such an eccentric position would result in a strongly uneven distribution of bearing pressure, which could lead to tilting of the footing. To counteract this eccentricity, the footing is connected by a beam or strap to the nearest interior footing.

Both footings are so proportioned that under service load the pressure under each of them is uniform and the same under both footings. To achieve this, it is necessary, as in other combined footings, that the centroid of the combined area for the two footings coincide with the resultant of the column loads. The resulting forces are shown schematically in Fig. 16.18. They consist of the loads P_e and P_i of the exterior and interior columns, respectively, and of the net upward pressure q, which is uniform and equal under both footings. The resultants R_e and R_i of these upward pressures are also shown. Since the interior footing is concentric with the interior column, R_i and P_i are collinear. This is not the case for the exterior forces R_e and P_e where the resulting couple just balances the effect of the eccentricity of the column relative to the center

FIGURE 16.18
Forces and reactions on the strap footing in Example 16.4.

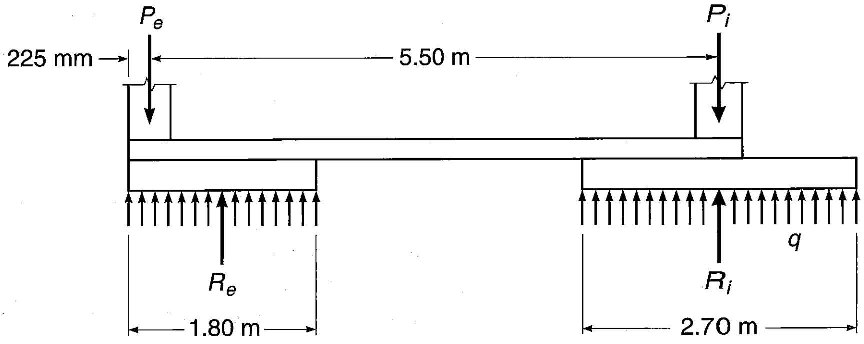

FIGURE 16.19
Strap footing in Example 16.4.

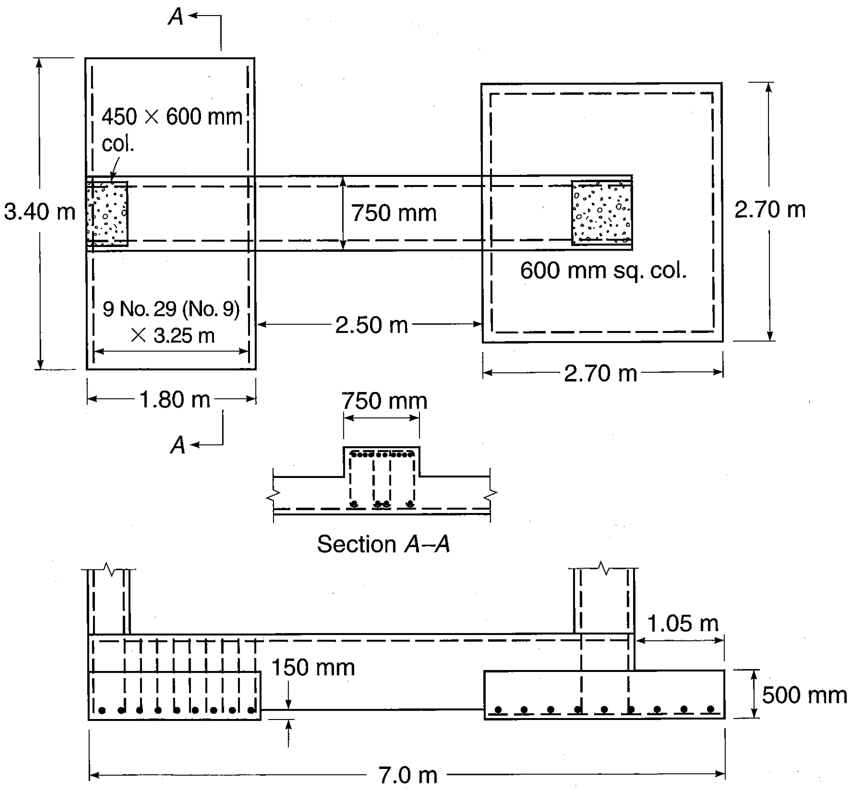

of the footing. The strap proper is generally constructed so that it will not bear on the soil. This can be achieved by providing formwork not only for the sides but also for the bottom face and by withdrawing it before backfilling.

To illustrate this design, the columns in Example 16.3 will now be supported on a strap footing. Its general shape, plus dimensions as determined only subsequently by calculations, is seen in Fig. 16.19. With an allowable bearing pressure of $q_a = 300$ kN/m^2 and a depth of 1.8 m to the bottom of the footing as before, the bearing pressure available for carrying the external loads applied to the footing is $q_e = 259$ kN/m^2, as in Example 16.3. These external loads, for the strap footing, consist of the column loads and of the weight plus fill and surcharge of that part of the strap that is located between the footings. (The portion of the strap located directly on top of the footing displaces a corresponding amount of fill and therefore is already accounted for in the determination of the available bearing pressure q.) If the bottom of the strap is 150 mm above the bottom of the footings to prevent bearing on soil, the total depth to grade is 1.65 m. If the strap width is estimated to be 750 mm, its estimated weight plus fill and surcharge is $0.75 \times 1.65 \times 20 + 5 \times 0.75 = 28.5$ kN/m. If the gap between footings is estimated to be 2.5 m, the total weight of the strap is 71.3 kN. Hence, for purposes of determining the required footing area, 36 kN will be added to the dead load of each column. The required total area of both footings is then $(3300 + 71)/2.59 = 13.0$ m^2. The distance of the resultant of the two column loads plus the strap load from the axis of the exterior column, with sufficient accuracy, is $(2000 + 71/2) \times 5.5/3371 = 3.32$ m, or 3.54 m from the outer edge, almost identical to that calculated for Example 16.3. Trial calculations show that a rectangular footing 1.8×3.4 m under the exterior column and a square footing 2.7×2.7 m under the interior column have a combined area of 13.4 m^2 and a distance from the outer edge to the centroid of the combined areas of $(1.8 \times 3.4 \times 0.9 + 2.7 \times 2.7 \times 5.73)/13.4 = 3.53$ m, which is almost exactly equal to the previously calculated distance to the resultant of the external forces.

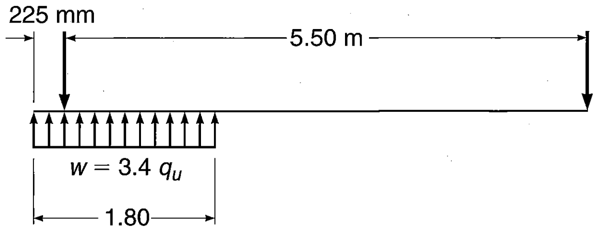

FIGURE 16.20
Forces acting on strap in Example 16.4.

For *strength calculations*, the bearing pressure caused by the factored external loads, including that of the strap with its fill and surcharge, is

$$q_u = \frac{1.2(750 + 1100 + 71) + 1.6(600 + 900)}{13.0} = 362 \text{ kN/m}^2$$

Design of footings

The exterior footing performs exactly like a wall footing with a length of 1.8 m. Even though the column is located at its edge, the balancing action of the strap results in uniform bearing pressure, the downward load being transmitted to the footing uniformly by the strap. Hence, the design is carried out exactly as it is for a wall footing (see Section 16.5).

The interior footing, even though it merges in part with the strap, can safely be designed as an independent, square single-column footing (see Section 16.6). The main difference is that, because of the presence of the strap, punching shear cannot occur along the truncated pyramid surface shown in Fig. 16.6. For this reason, two-way or punching shear, according to Eq. (16.7), should be checked along a perimeter section located at a distance $d/2$ outward from the longitudinal edges of the strap and from the free face of the column, d being the effective depth of the footing. Flexural or one-way shear, as usual, is checked at a section a distance d from the face of the column.

Design of strap

Even though the strap is in fact monolithic with the interior footing, the effect on the strap of the soil pressure under this footing can safely be neglected because the footing has been designed to withstand the entire upward pressure as if the strap were absent. In contrast, because the exterior footing has been designed as a wall footing that receives its load from the strap, the upward pressure from the wall footing becomes a load that must be resisted by the strap. With this simplification of the actually somewhat more complex situation, the strap represents a single-span beam loaded upward by the bearing pressure under the exterior footing and supported by downward reactions at the centerlines of the two columns (Fig. 16.20). A width of 750 mm is selected. For a column width of 600 mm, this permits beam and column bars to be placed without interference where the two members meet and allows the column forms to be supported on the top surface of the strap. The maximum moment, as determined by equating the shear force to zero, occurs close to the inner edge of the exterior footing. Shear forces are large in the vicinity of the exterior column. Stirrup design is completed using a strut-and-tie model. The footing is drawn approximately to scale in Fig. 16.19, which also shows the general arrangement of the reinforcement in the footings and the strap.

16.9 STRIP, GRID, AND MAT FOUNDATIONS

As mentioned in Section 16.7, continuous foundations are often used to support heavily loaded columns, especially when a structure is located on relatively weak or uneven soil. The foundation may consist of a *continuous strip footing* supporting all columns in a given row, or of two sets of such strip footings intersecting at right angles so that they form one continuous *grid foundation* (Fig. 16.13). For even larger loads or weaker soils, the strips are made to merge, resulting in a *mat foundation* (Fig. 16.14).

For the design of such continuous foundations, it is essential that reasonably realistic assumptions be made regarding the distribution of bearing pressures that act as upward loads on the foundation. For compressible soils, it can be assumed, as a first approximation, that the deformation or settlement of the soil at a given location and the bearing pressure at that location are proportional to each other. If columns are spaced at moderate distances and if the strip, grid, or mat foundation is quite rigid, the settlements in all portions of the foundation will be substantially the same. This means that the bearing pressure, also known as *subgrade reaction*, will be the same, provided that the centroid of the foundation coincides with the resultant of the loads. If they do not coincide, then for such rigid foundations the subgrade reaction can be assumed to vary linearly. Bearing pressures can be calculated based on statics, as discussed for single footings (see Fig. 16.3). In this case, all loads, the downward column loads as well as the upward-bearing pressures, are known. Hence, moments and shear forces in the foundation can be found by statics alone. Once these are determined, the design of strip and grid foundations is similar to that of inverted continuous beams, and that of mat foundations to that of inverted flat slabs or plates.

On the other hand, if the foundation is relatively flexible and the column spacing large, settlements will no longer be uniform or linear. For one thing, the more heavily loaded columns will cause larger settlements, and thereby larger subgrade reactions, than the lighter ones. Also, since the continuous strip or slab midway between columns will deflect upward relative to the nearby columns, the soil settlement, and thereby the subgrade reaction, will be smaller midway between columns than directly at the columns. This is shown schematically for a strip footing in Fig. 16.21; the subgrade reaction can no longer be assumed to be uniform. Mat foundations likewise require

FIGURE 16.21

Strip footing. (*Adapted from Ref. 16.8.*)

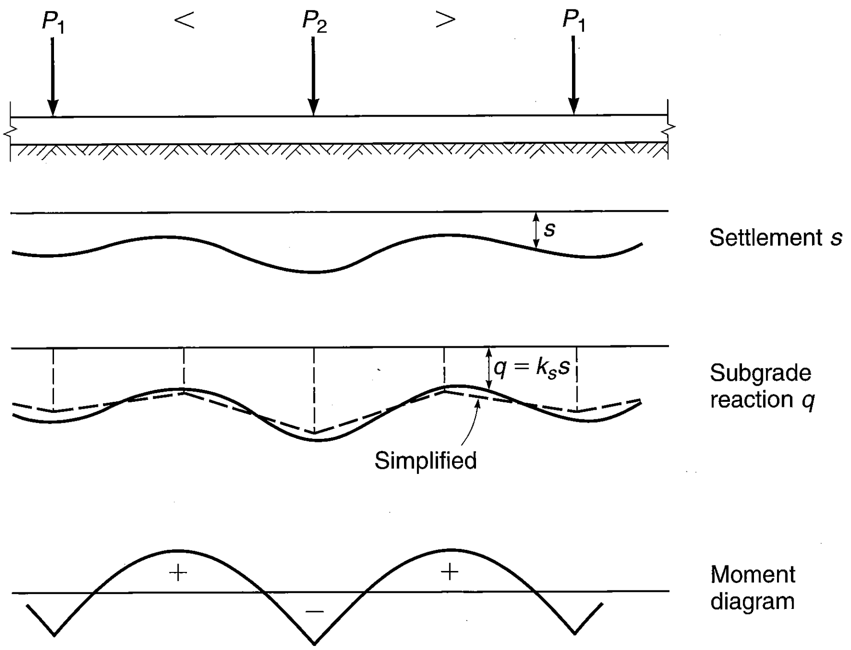

different approaches, depending on whether they can be assumed to be rigid when calculating the soil reaction.

Criteria have been established as a measure of the relative stiffness of the structure versus the stiffness of the soil (Refs. 16.10 and 16.13). If the relative stiffness is low, the foundation should be designed as a flexible member with a nonlinear upward reaction from the soil. For strip footings, a reasonably accurate but fairly complex analysis can be done using the theory of beams on elastic foundations (Ref. 16.14). Kramrisch (Ref. 16.8) has suggested simplified procedures, based on the assumption that contact pressures vary linearly between load points, as shown in Fig. 16.21.

For nonrigid mat foundations, great advances in analysis have been made using finite element methods, which can account specifically for the stiffnesses of both the structure and the soil. There are a large number of commercially available programs (e.g., pcaMats, Portland Cement Association, Skokie, Illinois) based on the finite element method, permitting quick modeling and analysis of combined footings, strip footings, and mat foundations.

16.10 PILE CAPS

If the bearing capacity of the upper soil layers is insufficient for a spread foundation, but firmer strata are available at greater depth, piles are used to transfer the loads to these deeper strata. Piles are generally arranged in groups or clusters, one under each column. The group is capped by a spread footing or cap that distributes the column load to all piles in the group. These pile caps are in most ways very similar to footings on soil, except for two features. For one, reactions on caps act as concentrated loads at the individual piles, rather than as distributed pressures. For another, if the total of all pile reactions in a cluster is divided by the area of the footing to obtain an equivalent uniform pressure (for purposes of comparison only), it is found that this equivalent pressure is considerably higher in pile caps than for spread footings. This means that moments, and particularly shears, are also correspondingly larger, which requires greater footing depths than for a spread footing of similar horizontal dimensions. To spread the load evenly to all piles, it is in any event advisable to provide ample rigidity, i.e., depth, for pile caps.

Allowable bearing capacities of piles R_a are obtained from soil exploration, pile-driving energy, and test loadings, and their determination is not within the scope of the present book (see Refs. 16.1 to 16.4). As in spread footings, the effective portion of R_a available to resist the unfactored column loads is the allowable pile reaction less the weight of footing, backfill, and surcharge per pile. That is,

$$R_e = R_a - W_f \tag{16.12}$$

where W_f is the total weight of footing, fill, and surcharge divided by the number of piles.

Once the available or effective pile reaction R_e is determined, the number of piles in a concentrically loaded cluster is the integer next larger than

$$n = \frac{D + L}{R_e}$$

As far as the effects of wind, earthquake moments at the foot of the columns, and safety against overturning are concerned, design considerations are the same as described in

Section 16.4 for spread footings. These effects generally produce an eccentrically loaded pile cluster in which different piles carry different loads. The number and location of piles in such a cluster are determined by successive approximations based on the requirement that the load on the most heavily loaded pile not exceed the allowable pile reaction R_a. With a linear distribution of pile loads due to bending, the maximum pile reaction is

$$R_{\max} = \frac{P}{n} + \frac{M}{I_{pg}/c} \tag{16.13}$$

where P is the maximum load (including weight of cap, backfill, etc.) and M the moment to be resisted by the pile group, both referred to the bottom of the cap; I_{pg} is the moment of inertia of the entire pile group about the centroidal axis about which bending occurs; and c is the distance from that axis to the extreme pile. $I_{pg} = \Sigma_1^n(1 \times y_i^2)$; i.e., it is the moment of inertia of n piles, each counting as one unit and located a distance y_i from the described centroidal axis.

Piles are generally arranged in tight patterns, which minimizes the cost of the caps, but they cannot be placed closer than conditions of driving and of undisturbed carrying capacity will permit. A spacing of about 3 times the butt (top) diameter of the pile but no less than 750 mm is customary. Commonly, piles with allowable reactions of 270 to 620 kN are spaced at 0.90 m (Ref. 16.8).

The *design* of footings on piles is similar to that of single-column footings. One approach is to design the cap for the pile reactions calculated for the factored column loads. For a concentrically loaded cluster, this would give $R_u = (1.2D + 1.6L)/n$. However, since the number of piles was taken as the next-larger integral according to Eq. (16.13), determining R_u in this manner can lead to a design where the strength of the cap is less than the capacity of the pile group. It is therefore recommended that the pile reaction for strength design be taken as

$$R_u = R_e \times \text{average load factor} \tag{16.14}$$

where the average load factor $= (1.2D + 1.6L)/(D + L)$. In this manner, the cap is designed to be capable of developing the full allowable capacity of the pile group. Details of a typical pile cap are shown in Fig. 16.22.

As in single-column spread footings, the depth of the pile cap is usually governed by shear. ACI Code 15.5.3 specifies that when the distance between the axis of a pile and the axis of a column is more than 2 times the distance from the top of the pile cap and the top of the pile, shear design must follow the procedures for flat slabs and footings, as described in Section 16.6a. For closer spacings between piles and columns, the Code specifies either the use of the procedures described in Section 16.6a or the use of a three-dimensional strut-and-tie model (ACI Code Appendix A) based on the principles described in Chapter 10. In the latter case, the struts must be designed as bottle-shaped without transverse reinforcement (Table 10.1) because of the difficulty of providing such reinforcement in a pile cap. The use of strut-and-tie models to design pile caps is discussed in Ref. 16.15.

When the procedures for flat slabs and footings are used, both punching or two-way shear and flexural or one-way shear need to be considered. The critical sections are the same as given in Section 16.6a. The difference is that shear in caps is caused by concentrated pile reactions rather than by distributed bearing pressures. This poses the question of how to calculate shear if the critical section intersects the circumference of one or more piles. For this case ACI Code 15.5.4 accounts for the fact that a

FIGURE 16.22
Typical single-column footing on piles (pile cap).

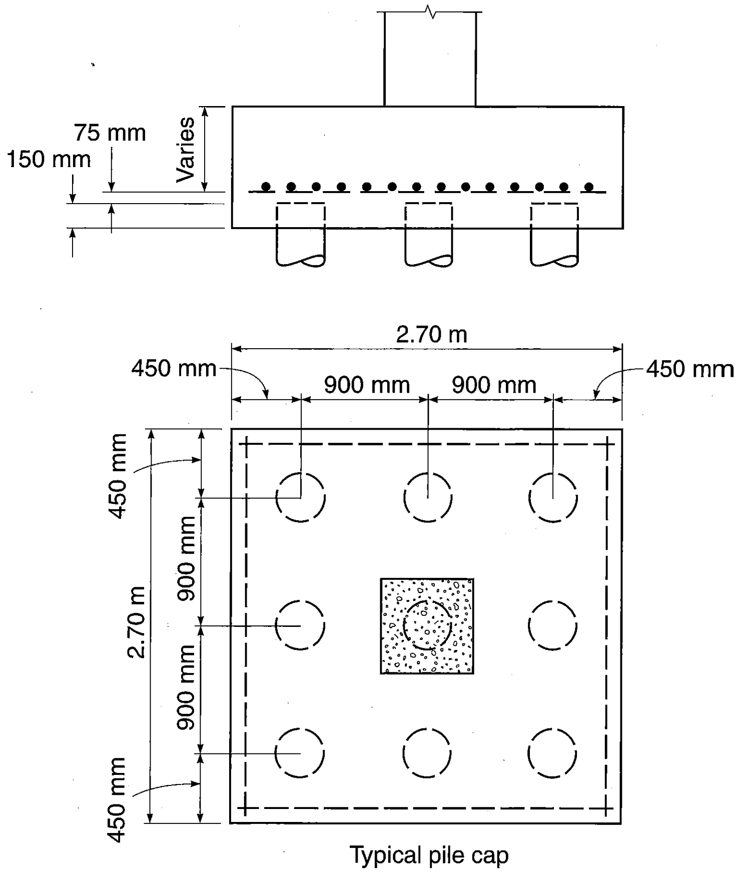

pile reaction is not really a point load, but is distributed over the pile-bearing area. Correspondingly, for piles with diameters d_{pile}, it stipulates as follows:

> Computation of shear on any section through a footing on piles shall be in accordance with the following:
>
> (*a*) The entire reaction from any pile whose center is located $d_{\text{pile}}/2$ or more outside this section shall be considered as producing shear on that section.
>
> (*b*) The reaction from any pile whose center is located $d_{\text{pile}}/2$ or more inside the section shall be considered as producing no shear on that section.
>
> (*c*) For intermediate positions of the pile center, the portion of the pile reaction to be considered as producing shear on the section shall be based on straight-line interpolation between the full value at $d_{\text{pile}}/2$ outside the section and zero at $d_{\text{pile}}/2$ inside the section.

In addition to checking two-way and one-way shear, as just discussed, punching shear must also be investigated for the individual pile. Particularly in caps on a small number of heavily loaded piles, it is this possibility of a pile punching upward through the cap that may govern the required depth. The critical perimeter for this action, again, is located at a distance $d/2$ outside the upper edge of the pile. However, for relatively deep caps and closely spaced piles, critical perimeters around adjacent piles may overlap. In this case, fracture, if any, would undoubtedly occur along an

FIGURE 16.23
Critical section for punching shear with closely spaced piles.

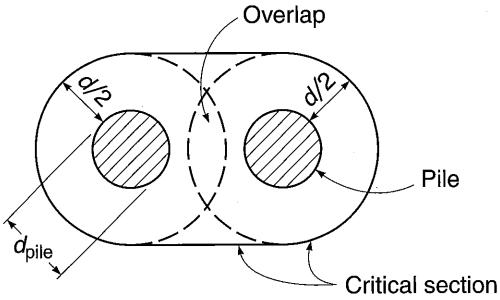

outward-slanting surface around both adjacent piles. For such situations the critical perimeter is so located that its length is a minimum, as shown for two adjacent piles in Fig. 16.23.

REFERENCES

16.1. R. B. Peck, W. E. Hanson, and T. H. Thornburn, *Foundation Engineering*, 2nd ed., John Wiley & Sons, New York, 1974.
16.2. K. Terzaghi, R. B. Peck, and G. Mesri, *Soil Mechanics in Engineering Practice*, 3rd ed., John Wiley & Sons, New York, 1996.
16.3. J. E. Bowles, *Foundation Analysis and Design*, 5th ed., McGraw-Hill, New York, 1996.
16.4. H.-Y. Fang, *Foundation Engineering Handbook*, 2nd ed., Van Nostrand Reinhold, New York, 1991.
16.5. A. N. Talbot, "Reinforced Concrete Wall Footings and Column Footings," *Univ. Ill. Eng. Exp. Stn. Bull.* 67, 1913.
16.6. F. E. Richart, "Reinforced Concrete Wall and Column Footings," *J. ACI*, vol. 45, 1948, pp. 97 and 237.
16.7. E. Hognestad, "Shearing Strength of Reinforced Column Footings," *J. ACI*, vol. 50, 1953, p. 189.
16.8. F. Kramrisch, "Footings," chap. 5 in M. Fintel (ed.), *Handbook of Concrete Engineering*, 2nd ed., Van Nostrand Reinhold, New York, 1985.
16.9. ASCE–ACI Committee 426, "The Shear Strength of Reinforced Concrete Members—Slabs," *J. Struct. Div.*, ASCE, vol. 100, no. ST8, 1974, pp. 1543–1591.
16.10. ACI Committee 336, *Suggested Analysis and Design Procedures for Combined Footings and Mats* (Reapproved 2002), ACI 326.2R-88, American Concrete Institute, Farmington Hills, MI, 2002.
16.11. *International Building Code*, International Code Council, Washington, DC, 2006.
16.12. *Minimum Design Loads for Buildings and Other Structures*, ASCE /SEI 7-05, American Society of Civil Engineers, Reston, VA, 2005.
16.13. *Design and Performance of Mat Foundations—State of the Art Review,* SP-152, American Concrete Institute, Detroit, MI, 1995.
16.14. M. Hetenyi, *Beams on Elastic Foundations*, Univ. of Michigan Press, Ann Arbor, 1946.
16.15. P. Adebar, D. Kuchma, and M. P. Collins, "Strut-and-Tie Models for the Design of Pile Caps—An Experimental Study," *ACI Struct. J.*, vol. 87, no. 1, 1990, pp. 81–92.

PROBLEMS

16.1. A continuous strip footing is to be located concentrically under a 300 mm wall that delivers service loads $D = 360$ kN/m and $L = 220$ kN/m to the top of the footing. The bottom of the footing will be 1.2 m below the final ground surface. The soil has a density of 20 kN/m^3 and allowable bearing capacity of 380 kN/m^2. Material strengths are $f_c' = 21$ MPa and $f_y = 420$ MPa. Find (*a*) the required width of the footing, (*b*) the required effective and total depths, based on shear, and (*c*) the required flexural steel area.

16.2. An interior column for a tall concrete structure carries total service loads $D = 2200$ kN and $L = 2300$ kN. The column is 550 × 550 mm in cross section and is reinforced with 12 No. 36 (No. 11) bars centered 75 mm from the column faces (equal number of bars each face). For the column, $f_c' = 28$ MPa and $f_y = 420$ MPa. The column will be supported on a square footing, with the bottom of the footing 1.8 m below grade. Design the footing, determining all concrete dimensions and amount and placement of all reinforcement, including length and placement of dowel steel. No shear reinforcement is permitted. The allowable soil bearing pressure is 380 kN/m^2. Material strengths for the footing are $f_c' = 21$ MPa and $f_y = 420$ MPa.

16.3. Design a single-column footing (including dowels) to support a 275 mm square column reinforced with eight No. 29 (No. 9) bars centered 65 mm from the column faces (equal number of bars on each face). The unfactored axial dead load = 600 kN, and the unfactored axial live load = 550 kN. For the column, $f_c' = 28$ MPa and $f_y = 420$ MPa. The base of the footing will be 0.9 m below grade. The allowable soil bearing pressure is 150 kN/m^2. Material strengths for the footing are $f_c' = 21$ MPa and $f_y = 420$ MPa.

16.4. Two interior columns for a high-rise concrete structure are spaced 4.6 m apart, and each carries service loads $D = 2200$ kN and $L = 2300$ kN. The columns are to be 550 mm square in cross section, and will each be reinforced with 12 No. 36 (No. 11) bars centered 75 mm from the column faces, with an equal number of bars at each face. For the columns, $f_c' = 28$ MPa and $f_y = 420$ MPa. The columns will be supported on a rectangular combined footing with a long-side dimension twice that of the short side. The allowable soil bearing pressure is 380 kN/m^2. The bottom of the footing will be 1.8 m below grade. Design the footing for these columns, using $f_c' = 21$ MPa and $f_y = 420$ MPa. Specify all reinforcement, including length and placement of footing bars and dowel steel.

16.5. A pile cap is to be designed to distribute a concentric force from a single column to a nine-pile group, with geometry as shown in Fig. 16.22. The cap will carry calculated dead and service live loads of 1250 kN and 2500 kN, respectively, from a 475 mm square concrete column reinforced with six No. 43 (No. 14) bars. The permissible load per pile at service load is 450 kN, and the pile diameter is 400 mm. Find the required effective and total depths of the pile cap and the required reinforcement. Check all relevant aspects of the design, including the development length for the reinforcement and transfer of forces at the base of the column. Material strengths for the column are $f_c' = 28$ MPa and $f_y = 420$ MPa, and for the pile cap are $f_c' = 21$ MPa and $f_y = 420$ MPa.

16.6. Complete the design of the strap footing in Example 16.4 and determine all dimensions and reinforcement. Compare the total volume of concrete in the strap footing in Example 16.4 with that of the rectangular combined footing in Example 16.3. It will be found that the strap footing is significantly more economical in terms of material (although forming would be more costly). This economy of material would increase with increasing distance between the columns.

17

Retaining Walls

17.1 FUNCTION AND TYPES OF RETAINING WALLS

Retaining walls are used to hold back masses of earth or other loose material where conditions make it impossible to let those masses assume their natural slopes. Such conditions occur when the width of an excavation, cut, or embankment is restricted by conditions of ownership, use of the structure, or economy. For example, in railway or highway construction the width of the right of way is fixed, and the cut or embankment must be contained within that width. Similarly, the basement walls of buildings must be located within the property and must retain the soil surrounding the basement.

Freestanding retaining walls, as distinct from those that form parts of structures, such as basement walls, are of various types, the most common of which are shown in Fig. 17.1. The gravity wall (Fig. 17.1*a*) retains the earth entirely by its own weight and generally contains no reinforcement. The reinforced concrete cantilever wall (Fig. 17.1*b*) consists of the vertical arm that retains the earth and is held in position by a footing or base slab. In this case, the weight of the fill on top of the heel, in addition to the weight of the wall, contributes to the stability of the structure. Since the arm represents a vertical cantilever, its required thickness increases rapidly with increasing height. To reduce the bending moments in vertical walls of great height, counterforts are used spaced at distances from each other equal to or slightly larger than one-half of the height (Fig. 17.1*c*). Property rights or other restrictions sometimes make it necessary to place the wall at the forward edge of the base slab, i.e., to omit the toe. Whenever it is possible, toe extensions of one-third to one-fourth of the width of the base provide a more economical solution.

Which of the three types of walls is appropriate in a given case depends on a variety of conditions, such as local availability and price of construction materials and property rights. In general, gravity walls are economical only for relatively low walls, possibly up to about 3 m. Cantilever walls are economical for heights from 3 to 6 m, while counterforts are used for greater heights.

17.2 EARTH PRESSURE

In terms of physical behavior, soils and other granular masses occupy a position intermediate between liquids and solids. If sand is poured from a dump truck, it flows, but, unlike a frictionless liquid, it will not assume a horizontal surface. It maintains itself in a stable heap with sides reaching an *angle of repose*, the tangent of which is roughly equal to the coefficient of intergranular friction. If a pit is dug in clay soil, its sides can

FIGURE 17.1
Types of retaining walls and back drains: (*a*) gravity wall; (*b*) cantilever wall; (*c*) counterfort wall.

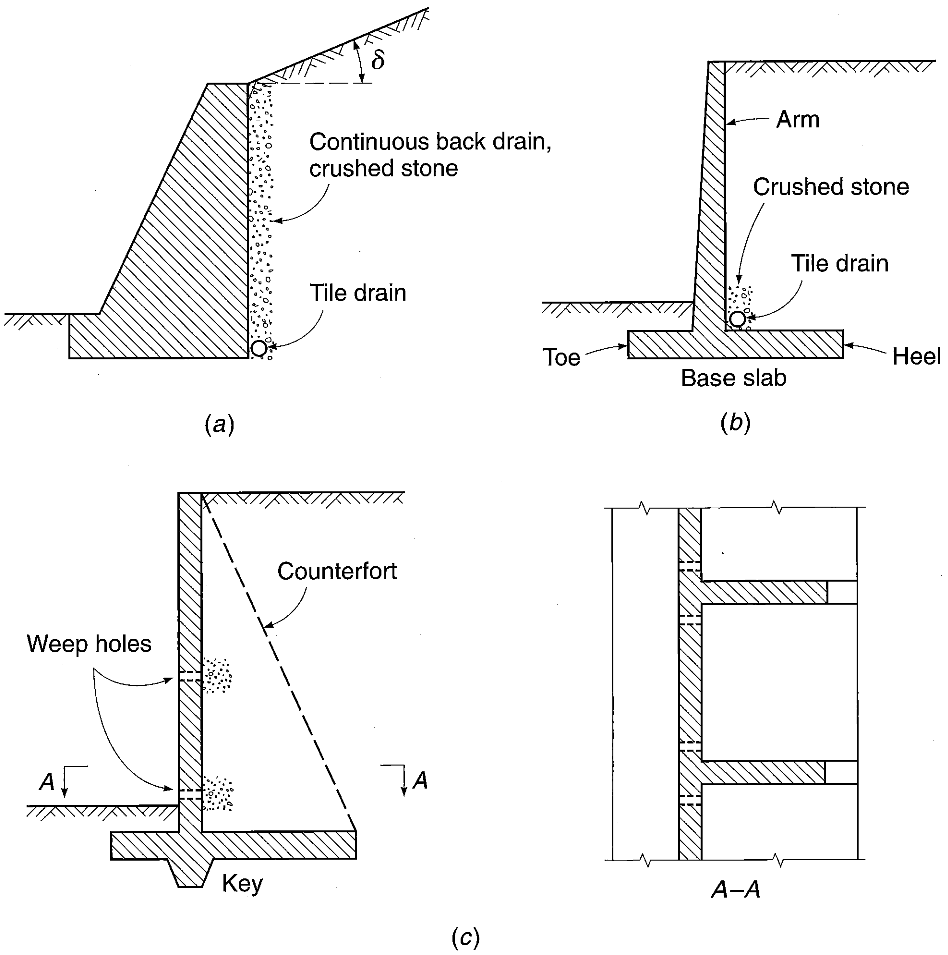

usually be made vertical over considerable depths without support; i.e., the clay will behave as a solid and will retain the shape it is given. If, however, the pit is flooded, the sides will give way, and in many cases the saturated clay will be converted nearly into a true liquid. The clay is capable of maintaining its shape by means of its internal cohesion, but flooding reduces that cohesion greatly, often to zero.

If a wall is built in contact with a solid, such as a rock face, no pressure is exerted on it. If, on the other hand, a wall retains a liquid, as in a reservoir, it is subject at any level to the hydrostatic pressure $w_w h$, where w_w is the unit weight of the liquid and h is the distance from the surface. If a vertical wall retains soil, the earth pressure similarly increases proportionally to the depth, but its magnitude is

$$p_h = K_0 w h \tag{17.1}$$

where w is the unit weight of the soil and K_0 is a constant known as the *coefficient of earth pressure at rest*. The value of K_0 depends not only on the nature of the backfill but also on the method of depositing and compacting it. It has been determined experimentally that, for uncompacted noncohesive soils such as sands and gravels, K_0 ranges between 0.4 and 0.5, while it may be as high as 0.8 for the same soils in a highly compacted state (Refs. 17.1 through 17.3). For cohesive soils, K_0 may be on the order of 0.7 to 1.0. Clean sands and gravels are considered superior to all other soils

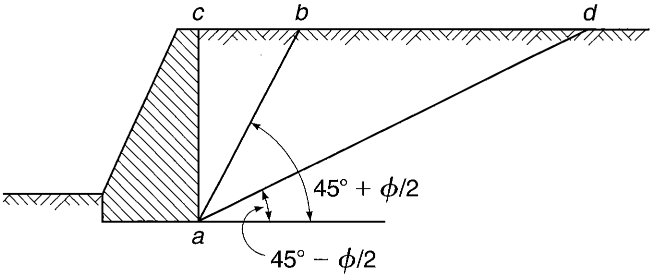

FIGURE 17.2
Basis of active and passive earth pressure determination.

because they are free-draining and are not susceptible to frost action and because they do not become less stable with the passage of time. For this reason, noncohesive backfills are usually specified.

Usually, walls move slightly under the action of the earth pressure. Since walls are constructed of elastic material, they deflect under the action of the pressure, and because they generally rest on compressible soils, they tilt and shift away from the fill. (For this reason, the wall is often constructed with a slight batter toward the fill on the exposed face so that, if and when such tilting takes place, the tilt does not appear evident to the observer.) Even if this movement at the top of the wall is only a fraction of a percent of the wall height ($\frac{1}{2}$ to $\frac{1}{10}$ percent according to Ref. 17.2), the rest pressure is materially decreased by it.

If the wall moves away from the fill, a sliding plane *ab* (Fig. 17.2) forms in the soil mass, and the wedge *abc*, sliding along that plane, exerts pressure against the wall. Here the angle ϕ is known as the *angle of internal friction*; i.e., its tangent is equal to the coefficient of intergranular friction, which can be determined by appropriate laboratory tests. The corresponding pressure is known as the *active earth pressure*. If, on the other hand, the wall is pushed against the fill, a sliding plane *ad* is formed, and the wedge *acd* is pushed upward by the wall along that plane. The pressure that this larger wedge exerts against the wall is known as the *passive earth pressure*. (This latter case will also occur at the left face of the gravity wall in Fig. 17.1*a* when this wall yields slightly to the left under the pressure of the fill.)

The magnitude of these pressures has been analyzed by Rankine, Coulomb, and others. If the soil surface makes an angle δ with the horizontal (Fig. 17.1*a*), then, according to Rankine, the *coefficient for active earth pressure* is

$$K_a = \cos\delta \frac{\cos\delta - \sqrt{\cos^2\delta - \cos^2\phi}}{\cos\delta + \sqrt{\cos^2\delta - \cos^2\phi}} \tag{17.2}$$

and the *coefficient for passive pressure* is

$$K_p = \cos\delta \frac{\cos\delta + \sqrt{\cos^2\delta - \cos^2\phi}}{\cos\delta - \sqrt{\cos^2\delta - \cos^2\phi}} \tag{17.3}$$

K_a and K_p replace K_0 in Eq. (17.1) to determine soil pressure p_h under active and passive conditions, respectively.

For the frequent case of a horizontal surface, that is, $\delta = 0$ (Fig. 17.2), for active pressure,

$$K_{ah} = \frac{1 - \sin\phi}{1 + \sin\phi} \tag{17.4}$$

and for passive pressure,

$$K_{ph} = \frac{1 + \sin \phi}{1 - \sin \phi} \tag{17.5}$$

Rankine's theory is valid only for noncohesive soils such as sand and gravel but, with corresponding adjustments, can also be used successfully for cohesive clay soils.

From Eqs. (17.1) through (17.5), it is seen that the earth pressure at a given depth h depends on the inclination of the surface δ, the unit weight w, and the angle of friction ϕ. The first two of these are easily determined, while little agreement has yet been reached as to the proper values of ϕ. For the ideal case of a dry, noncohesive fill, ϕ could be determined by laboratory tests and then used in the formulas. This is impossible for clays, only part of whose resistance is furnished by intergranular friction, while the rest is due to internal cohesion. For this reason, their actual ϕ values are often increased by an arbitrary amount to account implicitly for the added cohesion. However, this is often unsafe since, as was shown by the example of the flooded pit, cohesion may vanish almost completely due to saturation and inundation.

In addition, fills behind retaining walls are rarely uniform, and, what is more important, they are rarely dry. Proper drainage of the fill is vitally important to reduce pressures (see Section 17.6), but even in a well-drained fill, the pressure will temporarily increase during heavy storms or sudden thaws. This is so because even though the drainage may successfully remove the water as fast as it appears, its movement through the fill toward the drains causes additional pressure (seepage pressure). In addition, frost action and other influences may temporarily increase its value over that of the theoretical active pressure. Many walls that were designed without regard to these factors have failed, been displaced, or cracked.

It is good practice, therefore, to select conservative values for ϕ, considerably smaller than the actual test values, in all cases except where extraordinary and usually expensive precautions are taken to keep the fill dry under all conditions. An example of recommended earth pressure values, which are quite conservative, though based on extensive research and practical experience, can be found in Ref. 17.2. Less conservative values are often used in practical designs, but these should be employed (1) with caution in view of the fact that occasional trouble has been encountered with walls so designed and (2) preferably with the advice of a geotechnical engineer.

Table 17.1 gives representative values for w and ϕ often used in engineering practice. (Note that the ϕ values do not account for probable additional pressures due to porewater, seepage, frost, etc.) The table also contains values for the coefficient of

TABLE 17.1
Unit weights w, effective angles of internal friction ϕ, and coefficients of friction with concrete f

Soil	Unit Weight w, kN/m^3	ϕ, deg	f
1. Sand or gravel without fine particles, highly permeable	17–19	33–40	0.5–0.6
2. Sand or gravel with silt mixture, low permeability	19–21	25–35	0.4–0.5
3. Silty sand, sand and gravel with high clay content	17–19	23–30	0.3–0.4
4. Medium or stiff clay	16–19	25–35[a]	0.2–0.4
5. Soft clay, silt	14–17	20–25[a]	0.2–0.3

[a] For saturated conditions, ϕ for clays and silts may be close to zero.

friction f between concrete and various soils. The values of ϕ for soils 3 through 5 may be quite unconservative; under saturated conditions, clays and silts may become entirely liquid (that is, $\phi = 0$). Soils of type 1 or 2 should be used as backfill for retaining walls wherever possible.

17.3 EARTH PRESSURE FOR COMMON CONDITIONS OF LOADING

In computing earth pressures on walls, three common conditions of loading are most often met: (1) horizontal surface of fill at the top of the wall, (2) inclined surface of fill sloping up and back from the top of the wall, and (3) horizontal surface of fill carrying a uniformly distributed additional load (surcharge), such as from goods in a storage yard or traffic on a road.

The increase in pressure caused by uniform surcharge s (case 3) is computed by converting its load into an equivalent, imaginary height of earth h' above the top of the wall such that

$$h' = \frac{s}{w} \tag{17.6}$$

and measuring the depth to a given point on the wall from this imaginary surface. This amounts to replacing h with $h + h'$ in Eq. (17.1).

The distributions of pressure for cases 1 to 3 are shown in Fig. 17.3. The total earth thrust P per linear meter of wall is equal to the area under the pressure distribution figure, and its line of action passes through the centroid of the pressure. Figure 17.3 gives information, computed in this manner, on magnitude, point of action, and direction of P for these three cases.

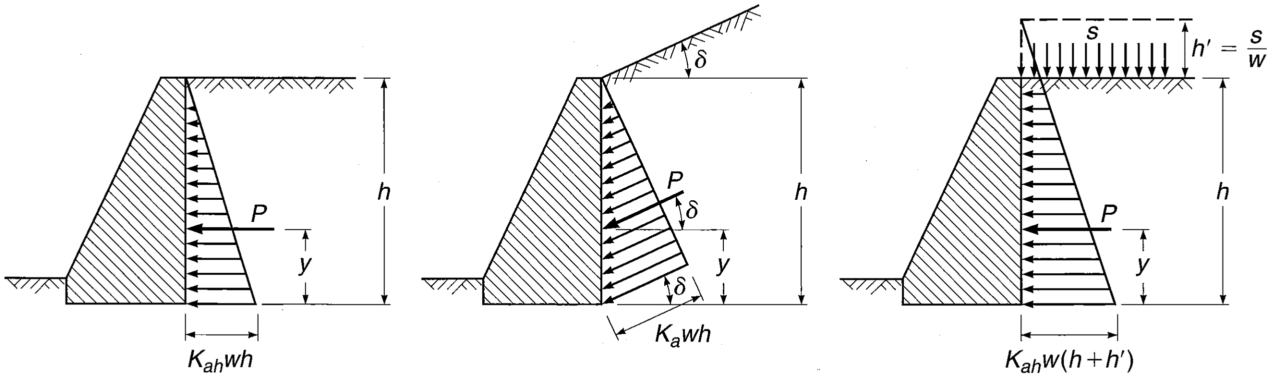

$y = \frac{h}{3}$

$P = \frac{1}{2}K_{ah}wh^2$

(*a*)

$y = \frac{h}{3}$ $P = \frac{1}{2}K_a wh^2$

For $\delta = \phi$, $K_a = \cos\phi$

(*b*)

$y = \frac{h^2 + 3hh'}{3(h+2h')}$

$P = \frac{1}{2}K_{ah}wh(h+2h')$

(*c*)

FIGURE 17.3
Earth pressures for (*a*) horizontal surface; (*b*) sloping surface; (*c*) horizontal surface with surcharge s.

Occasionally retaining walls must be built for conditions in which the groundwater level is above the base of the wall, either permanently or seasonally. In that case, the pressure of the soil *above* groundwater is determined as usual. The part of the wall *below* groundwater is subject to the sum of the water pressure and the earth pressure. The former is equal to the full hydrostatic pressure $p_w = w_w h_w$, where w_w and h_w are, respectively, the unit weight of water and the distance from the groundwater level to the point on the wall. The additional pressure of the soil below the groundwater level is computed from Eq. (17.1), where, however, for the portion of the soil below water, w is replaced with $w - w_w$, while h, as usual, is measured from the soil surface. That is, for submerged soil, buoyancy reduces the effective weight in the indicated manner. Pressures of this magnitude, which are considerably larger than those of drained soil, will also occur temporarily after heavy rainstorms or thaws in walls without provision for drainage, or if drains have become clogged.

The seeming simplicity of the determination of earth pressure, as indicated here, should not lull the designer into a false sense of security and certainty. No theory is more accurate than the assumptions on which it is based. Actual soil pressures are affected by irregularities of soil properties, porewater and drainage conditions, and climatic and other factors that cannot be expressed in formulas. This situation, on the one hand, indicates that involved refinements of theoretical earth pressure determinations, as sometimes attempted, are of little practical value. On the other hand, the design of a retaining wall is seldom a routine procedure, since the local conditions that affect pressures and safety vary from one locality to another.

17.4 EXTERNAL STABILITY

A wall may fail in two different ways: (1) its individual parts may not be strong enough to resist the acting forces, such as when a vertical cantilever wall is cracked by the earth pressure acting on it; and (2) the wall as a whole may be bodily displaced by the earth pressure, without breaking up internally. To design against the first possibility requires the determination of the necessary dimensions, thicknesses, and reinforcement to resist the moments and shears; this procedure, then, is in no way different from that of determining required dimensions and reinforcement of other types of concrete structures. The usual load factors and strength reduction factors of the ACI Code may be applied (see Section 17.5).

To safeguard the wall against bodily displacements, i.e., to ensure its external stability, requires special consideration. Consistent with current practice in geotechnical engineering, the stability investigation is based on actual earth pressures (as nearly as they may be determined) and on computed or estimated service dead and live loads, all without load factors. Computed bearing pressures are compared with allowable values, and overall factors of safety evaluated by comparing resisting forces to maximum loads acting under service conditions.

A wall, such as that in Fig. 17.4, together with the soil mass *ijkl* that rests on the base slab, may be bodily displaced by the earth thrust P that acts on the plane *ak* by *sliding* along the plane *ab*. Such sliding is resisted by the friction between the soil and footing along the same plane. To forestall motion, the forces that resist sliding must exceed those that tend to produce sliding; a factor of safety of 1.5 is generally assumed satisfactory in this connection.

In Fig. 17.4, the force that tends to produce sliding is the horizontal component P_h of the total earth thrust P. The resisting friction force is fR_v, where f is the coefficient of friction between the concrete and soil (see Table 17.1) and R_v is the vertical

FIGURE 17.4
External stability of a cantilever wall.

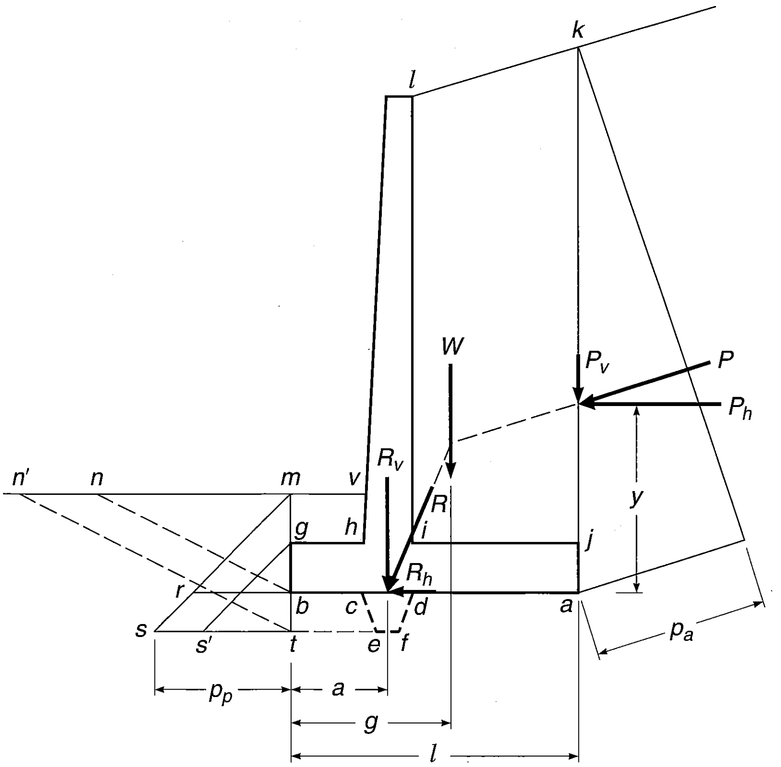

component of the total resultant R; that is, $R_v = W + P_v$ (W = weight of wall plus soil resting on the footing, P_v = vertical component of P). Hence, to provide sufficient safety,

$$f(W + P_v) \geq 1.5P_h \tag{17.7}$$

Actually, for the wall to slide to the left, it must push with it the earth *nmb*, which gives rise to the passive earth pressure indicated by the triangle *rmb*. This passive pressure represents a further resisting force that could be added to the left side of Eq. (17.7). However, this should be done only if the proper functioning of this added resistance is ensured. For that purpose, the fill *ghmv* must be placed before the backfill *ijkl* is put in place and must be secure against later removal by scour or other means throughout the lifetime of the wall. If these conditions are not met, it is better not to count on the additional resistance of the passive pressure.

If the required sliding resistance cannot be developed by these means, a key wall *cdef* can be used to increase horizontal resistance. In this case, sliding, if it occurs, takes place along the planes *ad* and *tf*. While along *ad* and *ef*, the friction coefficient f applies, sliding along *te* occurs within the soil mass. The coefficient of friction that applies in this portion is consequently tan ϕ, where the value of ϕ may be taken from the next to last column in Table 17.1. In this situation sliding of the front soil occurs upward along *tn'* so that if the front fill is secure, the corresponding resistance from passive soil pressure is represented by the pressure triangle *stm*. If doubt exists as to the reliability of the fill above the toe, the free surface should more conservatively be assumed at the top level of the footing, in which case the passive pressure is represented by the triangle *s'tg*.

Next, it is necessary to ensure that the pressure under the footing not exceed the *permissible bearing pressure* for the particular soil. Let a (Fig. 17.4) be the distance from the front edge b to the intersection of the resultant with the base plane, and let R_v be the vertical component of R. (This intersection need not be located beneath the vertical arm, as shown, even though an economical wall generally results if it is so located.) Then the base plane ab, 1 m wide longitudinally, is subject to a normal force R_v and to a moment about the centroid $(l/2 - a)R_v$. When these values are substituted in the usual formula for bending plus axial force

$$q_{\substack{\max\\ \min}} = \frac{N}{A} \pm \frac{Mc}{I} \tag{17.8}$$

it will be found that if the resultant is located within the middle third ($a > l/3$), compression will act throughout the section, and the maximum and minimum pressures can be computed from the equations in Fig. 17.5a. If the resultant is located just at the edge of the middle third ($a = l/3$), the pressure distribution is as shown in Fig. 17.5b, and Eq. (17.8) results in the formula given there.

FIGURE 17.5
Bearing pressures for different locations of resultant.

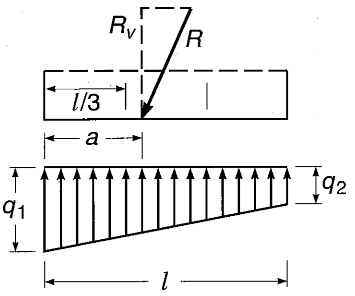

$$q_1 = (4l - 6a)\frac{R_v}{l^2}$$

$$q_2 = (6a - 2l)\frac{R_v}{l^2}$$

$$\text{when } a = \frac{l}{2},\ q_1 = q_2 = \frac{R_v}{l}$$

(a) Resultant in middle third

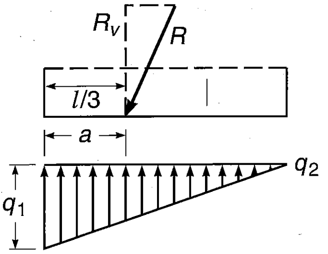

$$q_1 = \frac{2R_v}{l}$$

$$q_2 = 0$$

(b) Resultant at edge of middle third

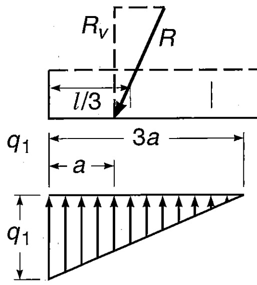

$$q_1 = \frac{2R_v}{3a}$$

(c) Resultant outside middle third

If the resultant were located outside the middle third ($a < l/3$), Eq. (17.8) would indicate tension at and near point a. Obviously, tension cannot be developed between soil and a concrete footing that merely rests on it. Hence, in this case the pressure distribution of Fig. 17.5*c* will develop, which implies a slight lifting off the soil of the rear part of the footing. Equilibrium requires that R_v pass through the centroid of the pressure distribution triangle, from which the formula for q_1 for this case can easily be derived.

It is good practice, in general, to have the resultant located within the middle third. This not only will reduce the magnitude of the maximum bearing pressure but also will prevent too large a nonuniformity of pressure. If the wall is founded on a highly compressible soil, such as certain clays, a pressure distribution as in Fig. 17.5*b* will result in a much larger settlement of the toe than of the heel, with a corresponding tilting of the wall. In a foundation on such a soil, the resultant, therefore, should strike at or very near the center of the footing. If the foundation is on very incompressible soil, such as well-compacted gravel or rock, the resultant can be allowed to fall outside the middle third (Fig. 17.5*c*).

A third mode of failure is the possibility of the wall *overturning* bodily around the front edge b (Fig. 17.4). For this to occur, the overturning moment yP_h about point b would have to be larger than the restoring moment $Wg + P_y l$ in Fig. 17.4, which is the same as saying that the resultant would have to strike outside the edge b. If, as is mostly the case, the resultant strikes within the middle third, adequate safety against overturning exists, and no special check need be made. If the resultant is located outside the middle third, a factor of safety of at least 1.5 should be maintained against overturning; i.e., the restoring moment should be at least 1.5 times the overturning moment.

17.5 BASIS OF STRUCTURAL DESIGN

In the investigation of a retaining wall for external stability, described in Section 17.4, it is the current practice to base the calculations on actual earth pressures, and on computed or estimated service dead and live loads, all with load factors of 1.0 (i.e., without load increase to account for a hypothetical overload condition). Computed soil bearing pressures, for service load conditions, are compared with allowable values set suitably lower than ultimate bearing values. Factors of safety against overturning and sliding are established, based on service load conditions.

On the other hand, the structural design of a retaining wall should be consistent with methods used for all other types of members, and thus should be based on factored loads in recognition of the possibility of an increase above service loading. ACI Code load factors relating to structural design of retaining walls are summarized as follows:

1. If resistance to earth pressure H is included in the design, together with dead loads D and live loads L, the required strength U shall be at least equal to

$$U = 1.2D + 1.6L + 1.6H$$

2. Where D or L reduce the effect of H, the required strength U shall be at least equal to

$$U = 0.9D + 1.6H$$

3. For any combination of D, L, and H, the required strength shall not be less than

$$U = 1.2D + 1.6L$$

While the ACI Code approach to load factor design is logical and relatively easy to apply to members in buildings, its application to structures that are to resist earth pressures is not so easy. Many alternative combinations of factored dead and live loads and lateral pressures are possible. Dead loads such as the weight of the concrete should be multiplied by 0.9 where they reduce design moments, such as for the toe slab of a cantilevered retaining wall, but should be multiplied by 1.2 where they increase moments, such as for the heel slab. The vertical load of the earth over the heel should be multiplied by 1.6. Obviously, no two factored load states could be obtained concurrently. For each combination of factored loads, different reactive soil pressures will be produced under the structure, requiring a new determination of those pressures for each alternative combination. Furthermore, there is no reason to believe that soil pressure would continue to be linearly distributed at the overload stage, or would increase in direct proportion to the load increase; knowledge of soil pressure distributions at incipient failure is incomplete. Necessarily, a somewhat simplified view of load factor design must be adopted in designing retaining walls.

Following the ACI Code, lateral earth pressures are multiplied by a load factor of 1.6. In general, the reactive pressure of the soil under the structure at the factored load stage is taken equal to 1.6 times the soil pressure found for service load conditions in the stability analysis.[†] For cantilever retaining walls, the calculated dead load of the toe slab, which causes moments acting in the opposite sense to those produced by the upward soil reaction, is multiplied by a factor of 0.9. For the heel slab, the required moment capacity is based on the dead load of the heel slab itself and is multiplied by 1.2, while the downward load of the earth is multiplied by 1.6. Surcharge, if present, is treated as live load with a load factor of 1.6. The upward pressure of the soil under the heel slab is taken equal to zero, recognizing that for the severe overload stage a nonlinear pressure distribution will probably be obtained, with most of the reaction concentrated near the toe. Similar assumptions appear to be reasonable in designing counterfort walls.

In accordance with ACI Code 14.1.2, cantilever retaining walls are designed following the flexural design provisions covered in Chapter 3, with minimum horizontal reinforcement provided in accordance with ACI Code 14.3.3, which stipulates a minimum ratio of

> 0.0020 for deformed bars not larger than No. 16 (No. 5) with a specified yield strength not less than 420 MPa; or 0.0025 for other deformed bars; or 0.0020 for welded wire reinforcement not larger than MW200 or MD200.

17.6 DRAINAGE AND OTHER DETAILS

Such failures or damage to retaining walls as have occasionally occurred were due, in most cases, to one of two causes: overloading of the soil under the wall with consequent forward tipping or insufficient drainage of the backfill. In the latter case, hydrostatic pressure from porewater accumulated during or after rainstorms greatly increases the thrust on the wall; in addition, in subfreezing weather, ice pressure of considerable magnitude can develop in such poorly drained soils. The two causes are often interconnected, since large thrusts correspondingly increase the bearing pressure under the footing.

[†] These reactions are caused by the assumed factored load condition and have no direct relationship to ultimate soil bearing values or pressure distributions.

Allowable bearing pressures should be selected with great care. It is necessary, for this purpose, to investigate not only the type of soil immediately underlying the footing, but also the deeper layers. Unless reliable information is available at the site, subsurface borings should be made to a depth at least equal to the height of the wall. The foundation must be laid below *frost depth*, which amounts to 1.2 to 1.5 m and more in the northern states, to ensure against heaving by the freezing of soils containing moisture.

Drainage can be provided in various ways. *Weep holes* consisting of 150 or 200 mm pipe embedded in the wall, as shown in Fig. 17.1*c*, are usually spaced horizontally at 1.5 to 3 m. In addition to the bottom row, additional rows should be provided in walls of substantial height. To facilitate drainage and prevent clogging, 0.03 m^3 or more of crushed stone is placed at the rear end of each weeper. Care must be taken that the outflow from the weep holes is carried off safely so as not to seep into and soften the soil underneath the wall. To prevent this, instead of weepers, *longitudinal drains* embedded in crushed stone or gravel can be provided along the rear face of the wall (Fig. 17.1*b*) at one or more levels; the drains discharge at the ends of the wall or at a few intermediate points. The most efficient drainage is provided by a *continuous backdrain* consisting of a layer of gravel or crushed stone covering the entire rear face of the wall (Fig. 17.1*a*), with discharge at the ends. Such drainage is expensive, however, unless appropriate material is cheaply available at the site. Wherever possible, the surface of the fill should be covered with a layer of low permeability and, in the case of a horizontal surface, should be laid with a slight slope away from the wall toward a gutter or other drainage.

In long walls, provision must be made against damage caused by *expansion* or *contraction* from temperate changes and shrinkage. The AASHTO *LRFD Bridge Design Specifications* require that for gravity walls, as well as reinforced concrete walls, expansion joints be placed at intervals of 30 m or less, and contraction joints at not more than 10 m (Ref. 17.4). The same specifications provide that, in reinforced concrete walls, temperature reinforcement equal to $0.0018bh$ in both the vertical and horizontal directions be distributed uniformly on the exposed (including end) surfaces. This AASHTO requirement is expressed as an area of reinforcement per meter on each face equal to

$$A_s \geq \frac{750bh}{2(b+h)f_y} \tag{17.9a}$$

$$233 \leq A_s \leq 1270 \text{ mm}^2/\text{m} \tag{17.9b}$$

where b = least width of the component, h = least thickness of the component, and f_y = yield strength of the bars, expressed in MPa, ≤ 520 MPa. Similar provisions are found in Ref. 17.5.

17.7 EXAMPLE: DESIGN OF A GRAVITY RETAINING WALL

A gravity wall is to retain a bank 3.5 m high whose horizontal surface is subject to a live load surcharge of 20 kN/m^2. The soil is a sand and gravel mixture with a rather moderate amount of fine, silty particles. It can, therefore, be assumed to be in class 2 of Table 17.1 with the following characteristics: unit weight $w = 20$ kN/m^3, $\phi = 30°$ (with adequate drainage to be provided), and base friction coefficient $f = 0.5$. With $\sin 30° = 0.5$, from Eqs. (17.4) and (17.5), the soil pressure coefficients are $K_{ah} = 0.333$ and $K_{ph} = 3.0$. The allowable bearing pressure is assumed to be 380 kN/m^2. This coarse-grained soil has little compressibility, so that the resultant can be allowed to strike near the outer-third point (see Section 17.4). The weight of the concrete is $w_c = 24$ kN/m^3.

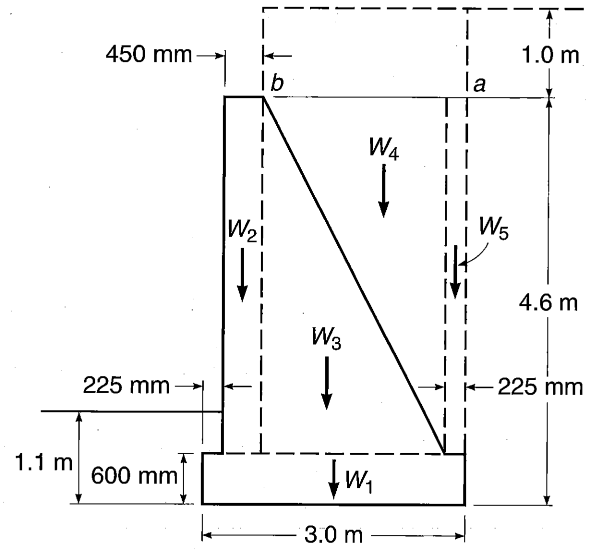

FIGURE 17.6
Gravity retaining wall.

The optimum design of any retaining wall is a matter of successive approximation. Reasonable dimensions are assumed based on experience, and the various conditions of stability are checked for these dimensions. On the basis of a first trial, dimensions are readjusted, and one or two additional trials usually result in a favorable design. In the following, only the final design is analyzed in detail. The final dimensions are shown in Fig. 17.6.

The equivalent height of surcharge is $h' = 20/20 = 1.0$ m. From Fig. 17.3*c* the total earth thrust is

$$P = \tfrac{1}{2} \times 0.333 \times 20 \times 4.6 \times 6.6 = 101 \text{ kN/m}$$

and its distance from the base is $y = (4.6^2 + 3 \times 4.6 \times 1)/(3 \times 6.6) = 1.77$ m. Hence, the overturning moment $M_o = 101 \times 1.77 = 179$ kN-m/m. To compute the weight W and its restoring moment M_r about the edge of the toe, individual weights are taken, as shown in Fig. 17.6. With x representing the distance of the line of action of each subweight from the front edge, the following computation results:

Component Weights	W, kN/m	x, m	$M_r = xW$, kN-m/m
W_1: $3 \times 0.6 \times 24$	43.2	1.5	64.8
W_2: $0.45 \times 4 \times 24$	43.2	0.45	19.4
W_3: $2.1/2 \times 4 \times 24$	100.8	1.38	139.1
W_4: $2.1/2 \times 4 \times 20$	84.0	2.08	174.7
W_5: $0.225 \times 4 \times 20$	18.0	2.89	52.0
Total	289.2		450.0

The distance of the resultant from the front edge is

$$a = \frac{450 - 179}{289.2} = 0.937 \text{ m}$$

which is just outside the middle third. The safety factor against overturning, $450/179 = 2.51$, is ample. From Fig. 17.5*c* the maximum soil pressure is $q = (2 \times 289.2)/(3 \times 0.937) = 206 \text{ kN/m}^2$.

These computations were made for the case in which the surcharge extends only to the rear edge of the wall, point *a* of Fig. 17.6. If the surcharge extends forward to point *b*, the following modifications are obtained:

$$W = 289.2 + 20 \times 2.32 = 335.6 \text{ kN/m}$$

$$M_r = 450.0 + 20 \times 2.32 \times 1.84 = 535.4 \text{ kN/m}$$

$$a = \frac{535.4 - 179}{335.6} = 1.06 \text{ m}$$

This is inside the middle third, and from Fig. 17.5*a*, the maximum bearing pressure is

$$q_1 = \frac{(4 \times 3 - 6 \times 1.06)335.6}{3^2} = 210 \text{ kN/m}^2$$

The situation most conducive to sliding occurs when the surcharge extends only to point *a*, since additional surcharge between *a* and *b* would increase the total weight and the corresponding resisting friction. The friction force is

$$F = 0.5 \times 289.2 = 144.6 \text{ kN/m}$$

Additionally, sliding is resisted by the passive earth pressure on the front of the wall. Although the base plane is 1.1 m below grade, the top layer of soil cannot be relied upon to furnish passive pressure, since it is frequently loosened by roots and the like, or it could be scoured out by cloudbursts. For this reason, the top 450 mm will be discounted in computing the passive pressure, which then becomes

$$P_p = \tfrac{1}{2}wh^2K_{ph} = \tfrac{1}{2} \times 20 \times 0.65^2 \times 3.0 = 12.7 \text{ kN/m}$$

The safety factor against sliding, $(144.6 + 12.7)/101 = 1.56$, is but slightly larger than the required value 1.5, indicating a favorable design. Ignoring the passive pressure gives a safety factor of 1.43, which is below the acceptable value.

17.8 EXAMPLE: DESIGN OF A CANTILEVER RETAINING WALL

A cantilever wall is to be designed for the situation of the gravity wall in Section 17.7. Concrete with $f'_c = 30$ MPa and steel with $f_y = 420$ MPa will be used.

a. Preliminary Design

To facilitate computation of weights for checking the stability of the wall, it is advantageous first to ascertain the thickness of the arm and the footing.[†] For this purpose the thickness of the footing is roughly estimated, and then the required thickness of the arm is determined at its bottom section. With the bottom of the footing at 1.05 m below grade and an estimated footing thickness of 450 mm, the free height of the arm is 4.15 m. Hence, with respect to the bottom of the arm (see Fig. 17.3*c*),

$$P = \tfrac{1}{2} \times 0.333 \times 20 \times 4.15 \times 6.15 = 85 \text{ kN/m}$$

$$y = \frac{4.15^2 + 12.45}{3 \times 6.15} = 1.61 \text{ m}$$

$$M_u = 1.6 \times 85 \times 1.61 = 219 \text{ kN-m/m}$$

[†] Valuable guidance is provided for the designer in tabulated designs such as those found in Ref. 17.6 and by the sample calculations in Ref. 17.7.

For the given grades of concrete and steel, the maximum practical reinforcement ratio $\rho_{0.005} = 0.0191$. For economy and ease of bar placement, a ratio of about 40 percent of the maximum, or 0.008, will be used. Then from Graph A.1*b* of Appendix A,

$$\frac{M_u}{\phi b d^2} = 3.14$$

For a unit length of the wall ($b = 1000$ mm), with $\phi = 0.90$, the required effective depth is

$$d = \sqrt{\frac{219 \times 10^6}{0.9 \times 3.14 \times 1000}} = 278 \text{ mm}$$

A protective cover of 50 mm is required for concrete exposed to earth. Thus, estimating the bar diameter to be 25 mm, the minimum required thickness of the arm at the base is 341 mm. This will be increased to 400 mm, because the cost of the extra concrete in such structures is usually more than balanced by the simultaneous saving in steel and ease of concrete placement. The arm is then checked for shear at a distance $d = 337$ mm above the base, or 3.81 m below the top of the wall:

$$P = \tfrac{1}{2} \times 0.333 \times 20 \times 3.81 \times 5.81 = 73.7 \text{ kN/m}$$

$$V_u = 1.6 \times 73.7 = 118 \text{ kN/m}$$

$$\begin{aligned}\phi V_c &= \phi 0.17 \lambda \sqrt{f'_c}\, bd \\ &= 0.75 \times 0.17 \times 1 \times \sqrt{30} \times 1000 \times 337 \\ &= 253 \text{ kN/m}\end{aligned}$$

confirming that the arm is more than adequate to resist the factored shear force.

The thickness of the base is usually the same as or slightly larger than that at the bottom of the arm. Hence, the estimated 450 mm need not be revised. Since the moment in the arm decreases with increasing distance from the base and is zero at the top, the arm thickness at the top will be made 200 mm. It is now necessary to assume lengths of heel and toe slabs and to check the stability for these assumed dimensions. Intermediate trials are omitted here, and the final dimensions are shown in Fig. 17.7*a*. Trial computations have shown that safety against sliding can be achieved only by an excessively long heel or by a key. The latter, requiring the smaller concrete volume, has been adopted.

b. Stability Investigation

Weights and moments about the front edge are as follows:

Component Weights	*W*, kN/m	*x*, m	M_r, kN-m/m
W_1: $0.20 \times 4.15 \times 24$	19.9	1.25	24.9
W_2: $0.20 \times 4.15 \times 24/2$	10.0	1.42	14.2
W_3: $2.95 \times 0.45 \times 24$	31.9	1.48	47.2
W_4: $0.4 \times 0.375 \times 24$	3.6	1.35	4.9
W_5: $1.15 \times 0.65 \times 20$	15.0	0.57	8.6
W_6: $0.2 \times 4.15 \times 20/2$	8.3	1.48	12.3
W_7: $1.4 \times 4.15 \times 20$	116.2	2.25	201.5
Total	204.9		373.6

FIGURE 17.7
Cantilever retaining wall: (*a*) cross section; (*b*) bearing pressure with surcharge to *a*; (*c*) bearing pressure with surcharge to *b*; (*d*) reinforcement; (*e*) moment variation with height.

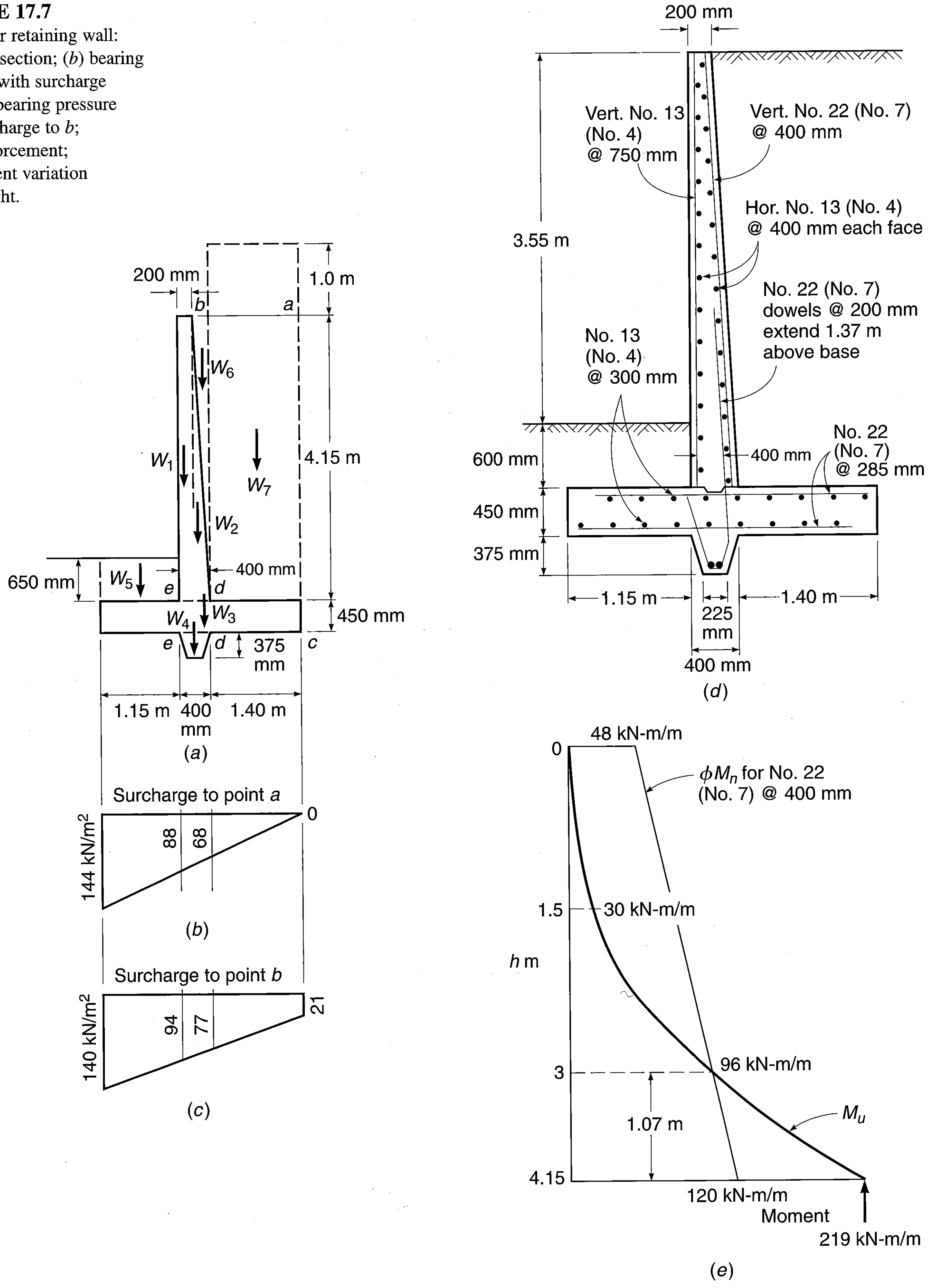
200 mm
b
a
1.0 m
W6
W1
W7
4.15 m
W2
400 mm
650 mm
W5
e
d
W4
W3
450 mm
e
d
375 mm
c
1.15 m
400 mm
1.40 m
(a)
Surcharge to point a
144 kN/m2
88
68
0
(b)
Surcharge to point b
140 kN/m2
94
77
21
(c)
200 mm
Vert. No. 13 (No. 4) @ 750 mm
Vert. No. 22 (No. 7) @ 400 mm
Hor. No. 13 (No. 4) @ 400 mm each face
3.55 m
No. 22 (No. 7) dowels @ 200 mm extend 1.37 m above base
No. 13 (No. 4) @ 300 mm
No. 22 (No. 7) @ 285 mm
600 mm
400 mm
450 mm
375 mm
1.15 m
225 mm
1.40 m
400 mm
(d)
48 kN-m/m
0
ϕMn for No. 22 (No. 7) @ 400 mm
1.5
30 kN-m/m
h m
3
96 kN-m/m
1.07 m
Mu
4.15
120 kN-m/m
Moment
219 kN-m/m
(e)

The total soil pressure on the plane *ac* is the same as for the gravity wall designed in Section 17.7; that is, $P = 101$ kN, and the overturning moment is

$$M_o = 179 \text{ kN-m/m}$$

The distance of the resultant from the front edge is

$$a = \frac{373.6 - 179}{204.9} = 0.950 \text{ m}$$

which locates the resultant barely outside of the middle third. The corresponding maximum soil pressure at the toe, from Fig. 17.5*c*, is

$$q_1 = \frac{2 \times 204.9}{3 \times 0.950} = 144 \text{ kN/m}^2$$

The factor of safety against overturning, $373.6/179 = 2.09$, is ample.

To check the safety against sliding, remember (Section 17.4) that if sliding occurs, it proceeds between concrete and soil along the heel and key (i.e., length *ae* in Fig. 17.4), but takes place within the soil in front of the key (i.e., along length *te* in Fig. 17.4). Consequently, the coefficient of friction that applies for the former length is $f = 0.5$, while for the latter it is equal to the internal soil friction, i.e., $\tan 30° = 0.577$.

The bearing pressure distribution is shown in Fig. 17.7*b*. Since the resultant is at a distance $a = 0.950$ m from the front, i.e., nearly at the middle third, it is assumed that the bearing pressure becomes zero exactly at the edge of the heel, as shown in Fig. 17.7*b*.

The resisting force is then computed as the sum of the friction forces of the rear and front portion, plus the passive soil pressure in front of the wall. For the latter, as in Section 17.7, the top 450 mm layer of soil will be discounted as unreliable. Hence,

Friction, toe:	$(144 + 88) \times 0.5 \times 1.15 \times 0.577 =$	77 kN/m
Friction, heel and key:	$88 \times 0.5 \times 1.8 \times 0.5 =$	40 kN/m
Passive earth pressure:	$0.5 \times 20 \times 1.03^2 \times 3 =$	32 kN/m
Total resistance to sliding:		= 149 kN/m

The factor of safety against sliding, $149/101 = 1.48$, is only 1.3 percent below the recommended value of 1.5 and can be regarded as adequate.

The computations hold for the case in which the surcharge extends from the right to point *a* above the edge of the heel. The other case of load distribution, in which the surcharge is placed over the entire surface of the fill up to point *b*, evidently does not change the earth pressure on the plane *ac*. It does, however, add to the sum of the vertical forces and increases both the restoring moment M_r and the friction along the base. Consequently, the danger of sliding or overturning is greater when the surcharge extends only to *a*, for which situation these two cases have been checked and found adequate. In view of the added vertical load, however, the bearing pressure is largest when the surface is loaded to *b*. For this case,

$$W = 204.9 + 20 \times 1.6 = 236.9 \text{ kN/m}$$

$$M_r = 373.6 + 20 \times 1.6 \times 2.15 = 442.4 \text{ kN/m}$$

$$a = \frac{442.4 - 179}{236.9} = 1.11 \text{ m}$$

which places the resultant inside the middle third. Hence, from Fig. 17.5*a*,

$$q_1 = (4 \times 2.95 - 6 \times 1.11)\frac{236.9}{2.95^2} = 140 \text{ kN/m}^2$$

$$q_2 = (6 \times 1.11 - 2 \times 2.95)\frac{236.9}{2.95^2} = 21 \text{ kN/m}^2$$

which are far below the allowable pressure of 380 kN/m^2. The corresponding bearing pressure distribution is shown in Fig. 17.7*c*.

The external stability of the wall has now been ascertained, and it remains to determine the required reinforcement and to check internal resistances.

c. Arm and Key

The moment at the bottom section of the arm has previously been determined as $M_u =$ 219 kN-m/m, and a wall thickness of 400 mm at the bottom and 200 mm at the top has been selected. With a concrete cover of 50 mm clear, $d = 400 - 50 - 13 = 337$ mm. Then

$$\frac{M_u}{\phi b d^2} = \frac{219 \times 10^6}{0.9 \times 1000 \times 337^2} = 2.14$$

Interpolating from Graph A.1*b* of Appendix A, with $f_y = 420$ MPa and $f'_c = 30$ MPa, the required reinforcement ratio ρ is 0.0054 and $A_s = 0.0054 \times 1000 \times 337 = 1820$ mm^2/m. The required area of steel is provided by No. 22 (No. 7) bars at 200 mm on centers.

The bending moment in the arm decreases rapidly with increasing distance from the bottom. For this reason, only part of the main reinforcement is needed at higher elevations, and alternate bars will be discontinued where no longer needed. To determine the cutoff point, the moment diagram for the arm has been drawn by computing bending moments at two intermediate levels, 3 and 1.5 m from the top. These two moments, determined in the same manner as that at the base of the arm, were found to be 96 kN-m/m and 30 kN-m/m, respectively. The resisting moment provided by alternate bars, i.e., by No. 22 (No. 7) bars at 400 mm center to center, at the bottom of the arm is

$$\phi M_n = 0.9 \times 968 \times 420(337 - 8) \times 10^{-6} = 120 \text{ kN-m/m}$$

At the top, $d = 200 - 65 = 135$, and the resisting moment of the same bars is only $\phi M_n = 120(135/337) = 48$ kN-m/m. Hence, the straight line drawn in Fig. 17.7*e* indicates the resisting moment provided at any elevation by one-half the number of main bars. The intersection of this line with the moment diagram at a distance of 1.07 m from the bottom represents the point above which alternate bars are no longer needed. ACI Code 12.10.3 specifies that any bar shall be extended beyond the point at which it is no longer needed to carry flexural stress for a distance equal to d or 12 bar diameters, whichever is greater. In the arm, at a distance of 1.07 m from the bottom, $d = 284$ mm, while 12 bar diameters for No. 22 (No. 7) bars are equal to 266 mm. Hence, one-half the bars can be discontinued 300 mm above the point where no longer needed, or a distance of 1.37 m above the base. This exceeds the required development length of 1001 mm above the base.

To facilitate construction, the footing is placed first, and a construction joint is provided at the base of the arm, as shown in Fig. 17.7*d*. The main bars of the arm, therefore, end at the top of the base slab, and dowels are placed in the latter to be spliced with them; the integrity of the arm depends entirely on the strength of the splices used for these tension bars. Splicing all tension bars in one section by simple contact splices can easily lead to splitting of the concrete owing to the stress concentrations at the ends of the spliced bars. One way to avoid this difficulty is to weld all splices; this will entail considerable extra cost.

In this particular wall, another way of placing the reinforcing offers a more economical solution. Because alternate bars in the arm can be discontinued at a distance of 1.37 m above the base, the dowels will be carried up 1.37 m from the top of the base. These need not be spliced at all, because above that level only alternate No. 22 (No. 7) bars, 400 mm on centers, are needed. These latter bars are placed full length over the entire height of the arm and are spliced at the bottom with alternate shorter dowels. By this means, only 50 percent of the bars needed at the bottom of the arm are spliced; this is not objectionable.

For splices of deformed bars in tension, at sections where the ratio of steel provided to steel required is less than 2 and where no more than 50 percent of the steel is spliced, the ACI Code requires a Class B splice with a length equal to 1.3 times the development length of the bar (see Section 5.13a). The development length of the No. 22 (No. 7) bars for the given material strengths is 1001 mm, and so the required splice length is $1.3 \times 1.001 = 1.3$ m, which is less than the 1.37 m available.

According to the ACI Code, main flexural reinforcement is not to be terminated in a tension zone unless one of three conditions is satisfied: (1) shear at the cutoff point does not exceed two-thirds that permitted, (2) certain excess shear reinforcement is provided, or (3) the continuing reinforcement provides double the area required for flexure at the cutoff point and the factored shear does not exceed three-fourths of the design shear. It is easily confirmed that the shear 1.37 m above the base is well below two-thirds the value that can be carried by the concrete; thus main bars can be terminated as planned.

Prior to completing the design of the arm, the minimum tensile reinforcement ratio specified by the ACI Code must be checked. The actual ratio provided by the No. 22 (No. 7) bars at 400 mm spacing, with $d = 270$ mm just above the cutoff point, is 0.0036, about 10 percent above the minimum value of $0.25\sqrt{30}/420 = 0.0033$. Thus, the spacing of the No. 22 (No. 7) bars, 200 mm, giving a spacing of 400 mm above the cutoff is satisfactory. A final ACI Code requirement is that the maximum spacing of the primary flexural reinforcement exceed neither 3 times the wall thickness nor 450 mm; these restrictions are satisfied as well.

Since the dowels had to be extended at least partly into the key to produce the necessary length of embedment, they were bent as shown to provide both reinforcement for the key and anchorage for the arm reinforcement. The exact force that the key must resist is difficult to determine, since probably the major part of the force acting on the portion of the soil in front of the key is transmitted to it through friction along the base of the footing. The relatively strong reinforcement of the key by means of the extended dowels is considered sufficient to prevent separation from the footing.

The sloping sides of the key were provided to facilitate excavation without loosening the adjacent soil. This is necessary to ensure proper functioning of the key.

In addition to the main steel in the stem, reinforcement must be provided in the horizontal direction to control shrinkage and temperature cracking, in accordance with ACI Code 14.3.3. Calculations will be based on the average wall thickness of 300 mm. The required steel area is 0.0020 times the gross concrete area. No. 13 (No. 4) bars 400 mm on centers, each face, will be used, as shown in Fig. 17.7*d*. Although not required by the Code for cantilever retaining walls, vertical steel equal to 0.0012 times the gross concrete area will also be provided (to limit horizontal surface cracking), with at least one-half of this value provided on the exposed face, as specified for other walls under ACI Code 14.3.2. No. 13 (No. 4) bars 750 mm on centers will satisfy this requirement.

d. Toe Slab

The toe slab acts as a cantilever projecting outward from the face of the stem. It must resist the upward pressures shown in Fig. 17.7*b* or *c* and the downward load of the toe slab itself, each multiplied by appropriate load factors. The downward load of the earth fill over the toe will be neglected because it is subject to possible erosion or removal. A load factor of 1.6 will be applied to the service load bearing pressures. Comparison of the pressures of Fig. 17.7*b* and *c* indicates that for the toe slab, the more severe loading case results from surcharge to *b*. Because the self-weight of the toe slab tends to reduce design moments and shears, it will be multiplied by a load factor of 0.9. Thus the factored load moment at the outer face of the stem is

$$\begin{aligned} M_u &= 1.6\left(\frac{140}{2} \times 1.15^2 \times \frac{2}{3} + \frac{94}{2} \times 1.15^2 \times \frac{1}{3}\right) - 0.9\left(24 \times 0.45 \times 1.15^2 \times \frac{1}{2}\right) \\ &= 125 \text{ kN-m/m} \end{aligned}$$

For concrete cast against and permanently exposed to earth, a minimum protective cover for steel of 75 mm is required; if the bar diameter is about 25 mm, the effective depth will be 450 − 75 − 13 = 362 mm. Thus, for a 1 m strip of toe slab,

$$\frac{M_u}{\phi b d^2} = \frac{125 \times 10^6}{0.90 \times 1000 \times 362^2} = 1.06$$

Graph A.1*b* of Appendix A shows that, for this value, the required reinforcement ratio would be below the minimum of $0.25\sqrt{30}/420 = 0.0033$. A somewhat thinner base slab appears possible. However, moments in the heel slab are yet to be investigated, as well as shears in both the toe and heel, and the trial depth of 450 mm will be retained tentatively. The required flexural steel

$$A_s = 0.0033 \times 1000 \times 362 = 1195 \text{ mm}^2\text{/m}$$

is provided by No. 22 (No. 7) bars 300 mm on centers. The required length of embedment for these bars past the exterior face of the stem is the full development length of 1001 mm. Thus, they will be continued 1 m past the face of the wall, as shown in Fig. 17.7*d*.

Shear will be checked at a distance $d = 362$ mm from the face of the stem (788 mm from the end of the toe), according to the usual ACI Code procedures. The service load bearing pressure at that location (with reference to Fig. 17.7*c*) is 108 kN/m², and the factored load shear is

$$\begin{aligned} V_u &= 1.6(140 \times \tfrac{1}{2} \times 0.788 + 108 \times \tfrac{1}{2} \times 0.788) - 0.9(24 \times 0.45 \times 0.788) \\ &= 149 \text{ kN/m} \end{aligned}$$

The design shear strength of the concrete is

$$\phi V_c = 0.17 \times 0.75\sqrt{30} \times 1000 \times 362 \times 10^{-3} = 253 \text{ kN/m}$$

well above the required value V_u.

e. Heel Slab

The heel slab, too, acts as a cantilever, projecting in this case from the back face of the stem and loaded by surcharge, earth fill, and its own weight. The upward reaction of the soil will be neglected here, for reasons given earlier. Applying appropriate load factors, the moment to be resisted is

$$\begin{aligned} M_u &= 1.2 \times 24 \times 0.45 \times 1.40^2 \times \tfrac{1}{2} + 1.6(20 \times 1.4^2 \times \tfrac{1}{2} + 83 \times 1.4^2 \times \tfrac{1}{2}) \\ &= 187 \text{ kN-m/m} \end{aligned}$$

The effective depth will be 450 − 50 − 13 = 387 mm. Thus,

$$\frac{M_u}{\phi b d^2} = \frac{187 \times 10^6}{0.90 \times 1000 \times 387^2} = 1.39$$

Interpolating from Graph A.1*b*, the required reinforcement ratio is 0.0035, just above the minimum value of 0.0033. The required steel area will again be provided using No. 22 (No. 7) bars, but the spacing will need to be 285 mm. For simplicity of layout, all footing bars, including those in the toe slab, will be placed at 285 mm, as shown in Fig. 17.7*d*. The bars just designed in the heel slab are classed as top bars, as they have more than 300 mm of concrete below; thus the required length of embedment to the left of the inside face of the stem is 1.001 × 1.3 = 1.3 m.

According to normal ACI Code procedures, the first critical section for shear would be a distance *d* from the face of support. However, the justification for this provision of the ACI Code is the presence, in the usual case, of vertical compressive stress near a support which tends to decrease the likelihood of shear failure in that region. However, the cantilevered heel slab is essentially hung from the bottom of the stem by the flexural tensile steel in the stem, and the concrete compression normally found near a support is absent here. Consequently, the critical section for shear in the heel slab will be taken at the back face of the stem. At that location,

$$\begin{aligned} V_u &= 1.2(10.8 \times 1.4) + 1.6(103 \times 1.4) \\ &= 249 \text{ kN/m} \end{aligned}$$

The design shear strength provided by the concrete is the same as for the toe slab:

$$\phi V_c = 0.17 \times 0.75\sqrt{30} \times 1000 \times 387 \times 10^{-3} = 270 \text{ kN/m}$$

Because this is only 8 percent in excess of the required value V_u, no reduction in thickness of the base slab, considered earlier, will be made.

The base slab is well below grade and will not be subjected to the extremes of temperature that will be imposed on the stem concrete. Consequently, crack control steel in the direction perpendicular to the main reinforcement is not a major consideration. No. 13 (No. 4) bars 300 mm on centers will be provided, at one face only, placed as shown in Fig. 17.7*d*. These bars serve chiefly as spacers for the main flexural reinforcement.

17.9 COUNTERFORT RETAINING WALLS

The external stability of a counterfort retaining wall is determined in the same manner as in the examples of Sections 17.7 and 17.8. The toe slab represents a cantilever built in along the front face of the wall, loaded upward by the bearing pressure, exactly as in the cantilever wall described in Section 17.8. Reinforcement is provided by bars *a* in Fig. 17.8.

FIGURE 17.8
Details of counterfort retaining wall.

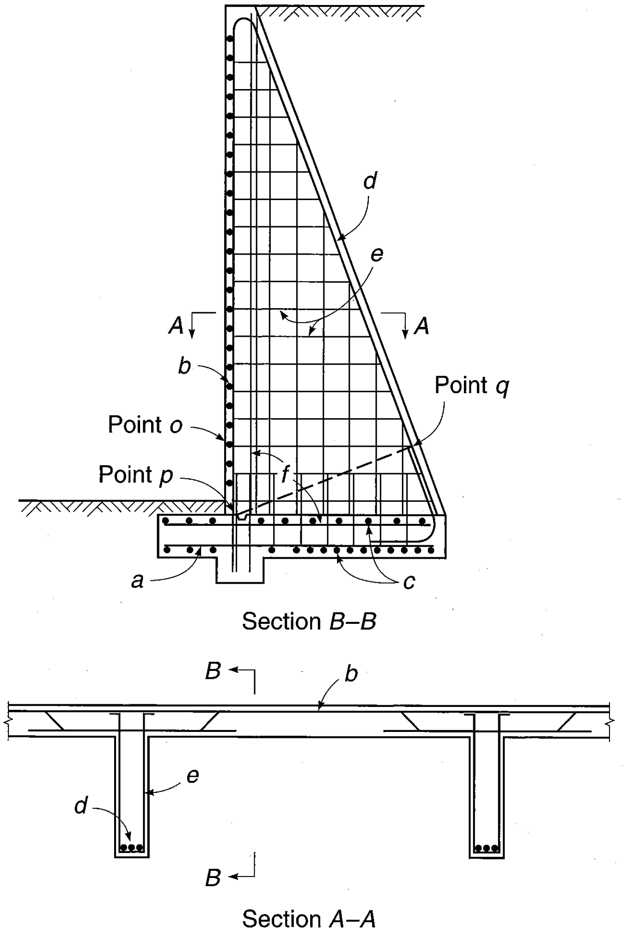

Section *B–B*

Section *A–A*

A panel of the vertical wall between two counterforts is a slab acted upon by horizontal earth pressure and supported along three sides, i.e., at the two counterforts and the base slab, while the fourth side, the top edge, is not supported. The earth pressure increases with distance from the free surface. The determination of moments and shears in such a slab supported on three sides and nonuniformly loaded is rather involved. It is customary in the design of such walls to disregard the support of the vertical wall by the base slab and to design it as if it were a continuous slab spanning horizontally between counterforts. This procedure is conservative, because the moments obtained by this approximation are larger than those corresponding to the actual conditions of support, particularly in the lower part of the wall. Hence, for very large installations, significant savings may be achieved by a more accurate analysis. The best computational tool for this is the Hillerborg *strip method*, a plasticity-based theory for design of slabs described in detail in Chapter 15. Alternatively, results of elastic analysis are tabulated for a range of variables in Ref. 17.8.

Slab moments are determined for strips 1 m wide spanning horizontally, usually for the strip at the bottom of the wall and for three or four equally spaced additional strips at higher elevations. The earth pressure on the different strips decreases with increasing elevation and is determined using Eq. (17.1). Moment values for the bottom strips may be reduced to account for the fact that additional support is provided by the base slab. Horizontal bars *b* (Fig. 17.8) are provided, as required, with increased spacing or decreased diameter corresponding to the smaller moments. Alternate bars are bent to provide for the negative moments in the wall at the counterforts, or additional straight bars are used as negative reinforcement, as shown in Section *A–A* of Fig. 17.8.

The heel slab is supported, as is the wall slab, i.e., by the counterforts and at the wall. It is loaded downward by the weight of the fill resting on it, its own weight, and such surcharge as there may be. This load is partially counteracted by the upward bearing pressure on the underside of the heel. As in the vertical wall, a simplified analysis consists in neglecting the influence of the support along the third side and in determining moments and shears for strips parallel to the wall, each strip representing a continuous beam supported at the counterforts. For a horizontal soil surface, the downward load is constant for the entire heel, whereas the upward load from the bearing pressure is usually smallest at the rear edge and increases frontward. For this reason, the span moments are positive (compression on top) and the support moments negative in the rear portion of the heel. Near the wall, the bearing pressure often exceeds the vertical weights, resulting in a net upward load. The signs of the moments are correspondingly reversed, and steel must be placed accordingly. Bars *c* are provided for these moments.

The counterforts are wedge-shaped cantilevers built in at the bottom in the base slab. They support the wall slab and, therefore, are loaded by the total soil pressure over a length equal to the distance center to center between counterforts. They act as a T beam of which the wall slab is the flange and the counterfort the stem. The maximum bending moment is that of the total earth pressure, taken about the bottom of the wall slab. This moment is held in equilibrium by the force in the bars *d*, and hence, the effective depth for bending is the perpendicular distance *pq* from the center of bars *d* to the center of the bottom section of the wall slab. Since the moment decreases rapidly in the upper parts of the counterfort, part of the bars *d* can be discontinued.

In regard to shear, the authors suggest the horizontal section *oq* as a conservative location for checking adequacy. Modification of the customary shear computation is required for wedge-shaped members (see Section 4.7). Usually concrete alone is sufficient to carry the shear, although bars *e* act as stirrups and can be used for resisting excess shear.

The main purpose of bars *e* is to counteract the pull of the wall slab, and they are thus designed for the full reaction of this slab.

The remaining bars of Fig. 17.8 serve as shrinkage reinforcement, except that bars *f* have an important additional function. It will be recalled that the wall and heel slabs are supported on three sides. Even though they were designed as if supported only by the counterforts, they develop moments where they join. The resulting tension in and near the reentrant corner should be provided for by bars *f*.

The question of reinforcing bar details, always important, is particularly so for corners subject to substantial bending moments, such as are present for both cantilever and counterfort retaining walls. Valuable suggestions are found in Ref. 17.9.

17.10 PRECAST RETAINING WALLS

Largely because of the high cost of forming cast-in-place retaining walls, there has been increasing use in recent years of various forms of precast concrete walls. Sections can be mass produced under controlled factory conditions using standardized forms, with excellent quality control. On-site construction time is greatly reduced, and

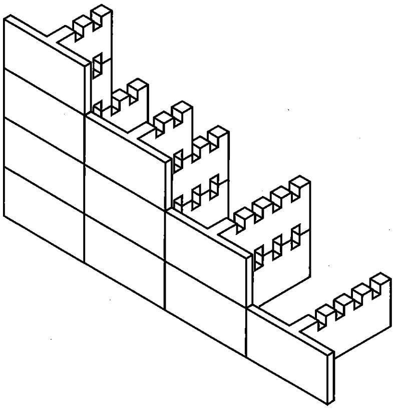

FIGURE 17.9
Precast T-Wall® retaining wall system. (*Courtesy Concrete Systems Inc., Hudson, New Hampshire.*)

generally only a small crew using light equipment is required. Weather becomes much less of a factor in completion of the work than for cast-in-place walls.

One type of precast wall is shown in Fig. 17.9. Precast T sections are used, each 0.75 m high and 1.5 m wide, with T stems varying according to requirements from 1.25 m to 6 m. Individual units are stacked, using shear keys in the space created where teeth of a top and bottom unit come together, at approximately a 2 m spacing perpendicular to the face of the wall. Calculations for stability against sliding and overturning and for bearing pressures are the same as for cast-in-place cantilever or counterfort walls, with stability provided by the combined weight of the concrete wall and compacted select backfill. Such walls can be constructed with vertical face or battered section, with heights up to 8 m.

Walls of the type shown have been used for highways, parking lots, commercial and industrial sites, bank stabilization, wing walls, and similar purposes.

REFERENCES

17.1. R. B. Peck, W. E. Hanson, and T. H. Thornburn, *Foundation Engineering*, 2nd ed., John Wiley & Sons, Inc., New York, 1974.

17.2. K. Terzaghi, R. B. Peck, and G. Mesri, *Soil Mechanics in Engineering Practice*, 3rd ed., John Wiley & Sons, Inc., New York, 1996.

17.3. W. C. Huntington, *Earth Pressures and Retaining Walls*, John Wiley & Sons, Inc., New York, 1957.

17.4. *AASHTO LRFD Bridge Design Specifications,* 4th ed., American Association of State Highway and Transportation Officials (AASHTO), Washington, DC, 2008.

17.5. *Manual for Railway Engineering*, American Railway Engineering and Maintenance of Way Association (AREMA), Landover, MD, 2008.

17.6. *CRSI Design Handbook*, 10th ed., Concrete Reinforcing Steel Institute, Shaumburg, IL, 2008.

17.7. M. Fintel, *Handbook of Concrete Engineering*, 2nd ed., Van Nostrand Reinhold Co., New York, 1985.

17.8. *Rectangular Concrete Tanks,* Publication No. IS003, Portland Cement Association, Skokie, IL, 1998.

17.9. I. H. E. Nilsson and A. Losberg, "Reinforced Concrete Corners and Joints Subjected to Bending Moment," *J. Struct. Div.,* ASCE, vol. 102, no. ST6, 1976, pp. 1229–1254.

PROBLEMS

17.1. A cantilever retaining wall is to be designed with geometry as indicated in Fig. P17.1. Backfill material will be well-drained gravel having unit weight $w = 20$ kN/m^3, internal friction angle $\phi = 33°$, and friction factor against the concrete base $f = 0.55$. Backfill placed in front of the toe will have the same properties and will be well compacted. The final grade behind the wall will be level with the top of the wall, with no surcharge. At the lower level, it will be 1 m above the top of the base slab. To improve sliding resistance, a key will be used, tentatively projecting to a depth 1.2 m below the top of the base slab. (This dimension may be modified if necessary.)

(*a*) Based on a stability investigation, select wall geometry suitable for the specified conditions. For a first trial, place the outer face of the wall $\frac{1}{3}$ the width of the base slab back from the toe.

(*b*) Prepare the complete structural design, specifying size, placement, and cutoff points for all reinforcement. Materials have strengths $f'_c = 28$ MPa and $f_y = 420$ MPa. Allowable soil bearing pressure is 240 kN/m^2.

FIGURE P17.1

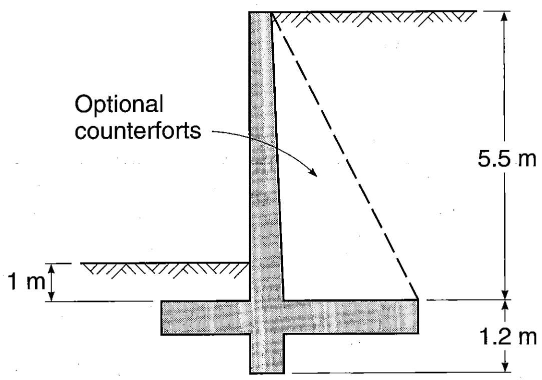

17.2. Redesign the wall of Problem 17.1 as a counterfort retaining wall. Counterforts are tentatively spaced 3.5 m on centers, although this may be modified if desirable. Include all reinforcement details, including reinforcement in the counterforts.

18

Concrete Building Systems

18.1 INTRODUCTION

Most of the material in the preceding chapters has pertained to the design of reinforced concrete *structural elements*, e.g., slabs, columns, beams, and footings. These elements are combined in various ways to create *structural systems* for buildings and other construction. An important part of the total responsibility of the structural engineer is to select, from many alternatives, the best structural system for the given conditions. The wise choice of structural system is far more important, in its effect on overall economy and serviceability, than refinements in proportioning the individual members. Close cooperation with the architect in the early stages of a project is essential in developing a structure that not only meets functional and esthetic requirements but exploits to the fullest the special advantages of reinforced concrete, which include the following:

Versatility of form. Usually placed in the structure in the fluid state, the material is readily adaptable to a wide variety of architectural and functional requirements.

Durability. With proper concrete protection of the steel reinforcement, the structure will have long life, even under highly adverse climatic or environmental conditions.

Fire resistance. With proper protection for the reinforcement, a reinforced concrete structure provides the maximum in fire protection.†

Speed of construction. In terms of the entire period, from the date of approval of the contract drawings to the date of completion, a concrete building can often be completed in less time than a steel structure. Although the field erection of a steel building is more rapid, this phase must necessarily be preceded by prefabrication of all parts in the shop.

Cost. In many cases the first cost of a concrete structure is less than that of a comparable steel structure. In almost every case, maintenance costs are less.

Availability of labor and material. It is always possible to make use of local sources of labor, and in many inaccessible areas, a nearby source of good aggregate can be found, so that only the cement and reinforcement need to be brought in from a remote source.

Two record-setting examples of good building design in concrete are shown in Figs. 18.1 and 18.2.

---

† Code requirements for fire protection are presented in Ref. 18.1.

FIGURE 18.1
View of 311 South Wacker Drive under construction. When completed, it was the world's tallest concrete building, with total height of 288 m. (*Courtesy of Portland Cement Association.*)

18.2 FLOOR AND ROOF SYSTEMS

The types of concrete floor and roof systems are so numerous as to defy concise classification. In steel construction, the designer usually is limited to using structural shapes that have been standardized in form and size by the relatively few producers in the field. In reinforced concrete, on the other hand, the engineer has almost complete control over the form of the structural parts of a building. In addition, many small producers of reinforced concrete structural elements and accessories can compete profitably in this field, since plant and equipment requirements are not excessive. This has resulted in the development of a wide variety of concrete systems. Only the more common types can be mentioned in this text.

In general, reinforced concrete floor and roof systems can be classified as one-way systems, in which the main reinforcement in each structural element runs in one direction only, and two-way systems, in which the main reinforcement in at least one of the structural elements runs in perpendicular directions. Systems of each type can be identified in the following list:

(a) One-way slab supported by monolithic concrete beams
(b) One-way slab supported by steel beams (shear connectors are used for composite action in the direction of the beam span)

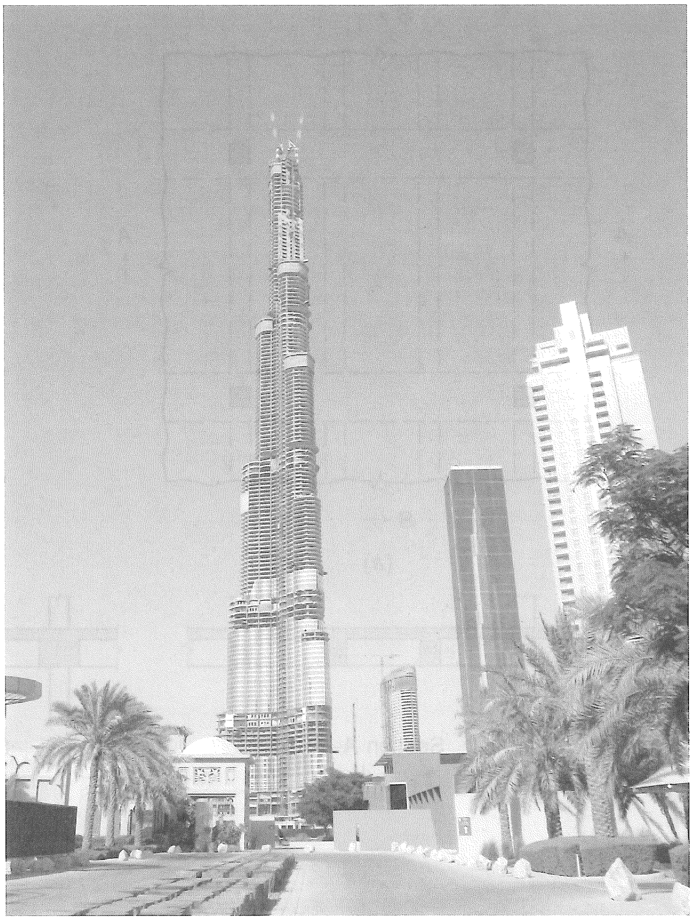

FIGURE 18.2
The Burj Khalifa (formerly known as the Burj Dubai), shown under construction, is the current record holder, not only as the tallest reinforced concrete building, but also as the tallest structure of any type in the world, with a total height in excess of 790 m. (*Burj Khalifa, designed by and copyright to Skidmore, Owings and Merrill LLP.*)

(c) One-way slab with cold-formed steel decking as form and reinforcement
(d) One-way joist floor (also known as ribbed slab)
(e) Two-way slab supported by edge beams for each panel
(f) Flat slabs, with column capitals or drop panels or both, but without beams
(g) Flat plates, without beams and with no drop panels or column capitals
(h) Two-way joist floors, with or without beams on the column lines

Each of these types will be described briefly in the following sections. Additional information will be found in Refs. 18.2 to 18.4. In addition to the cast-in-place floor and roof systems described in this section, a great variety of precast concrete systems have been devised. Some of these will be described in Section 18.5.

a. Monolithic Beam-and-Girder Floors

A beam-and-girder floor consists of a series of parallel beams supported at their extremities by girders, which in turn frame into concrete columns placed at more or less regular intervals over the entire floor area, as shown in Fig. 18.3. This framework is covered by a one-way reinforced concrete slab, the load from which is transmitted first to the beams and then to the girders and columns. The beams are usually spaced so that they come at the midpoints, at the third points, or at the quarter points of the

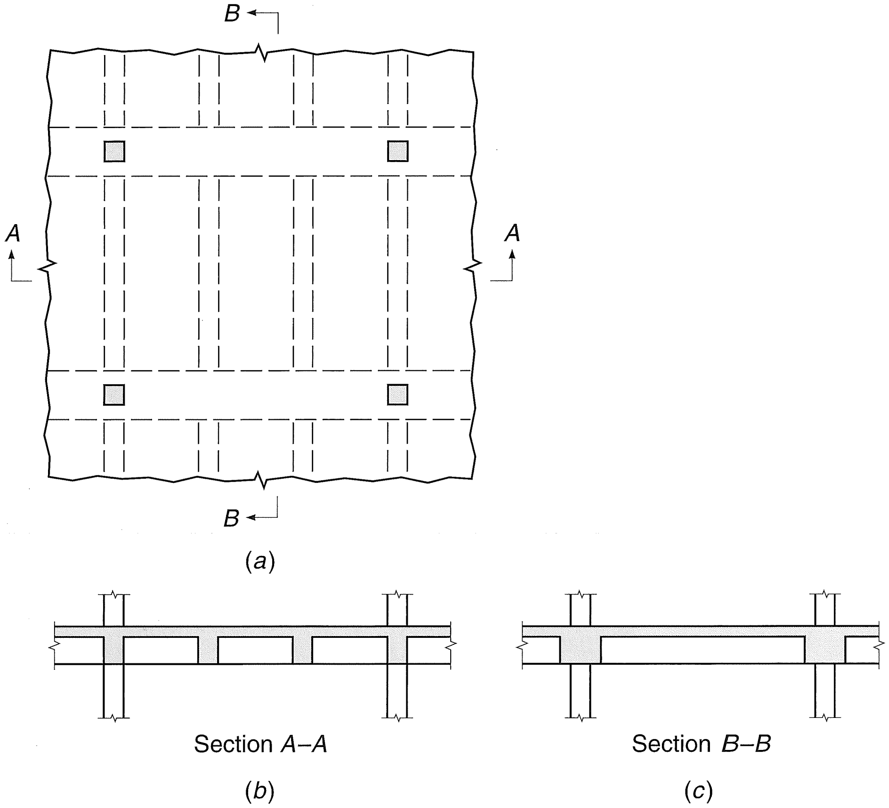

FIGURE 18.3
Framing of beam-and-girder floor: (*a*) plan view; (*b*) section through beams; (*c*) section through girders.

girders. The arrangement of beams and spacing of columns should be determined by economical and practical considerations. These will be affected by the use to which the building is to be put, the size and shape of the ground area, and the load that must be carried. A comparison of a number of trial designs and estimates should be made if the size of the building warrants, and the most satisfactory arrangement selected. If the spans in one direction are not long, say 6 m or less, the beams may be omitted altogether, and the slab, spanning in one direction, can be carried directly by girders spanning in the perpendicular direction on the column lines. Since the slabs, beams, and girders are built monolithically, the beams and girders are designed as T beams and advantage is taken of continuity.

Beam-and-girder floors are adapted to any loads and to any spans that might be encountered in ordinary building construction. The normal maximum spread in live load values is from 2 to 20 kN/m^2, and the normal range in column spacings is from 5 to 10 m.

The design and detailing of the joints where beams or girders frame into building columns should be given careful consideration, particularly for designs in which substantial horizontal loads are to be resisted by frame action of the building. In this case, the column region, within the depth of the beams framing into it, is subjected to significant horizontal shears as well as to axial and flexural loads. Special horizontal column ties must be included to avoid uncontrolled diagonal cracking and disintegration of the concrete, particularly if the joint is subjected to load reversals. Specific recommendations for the design of beam-column joints are found in Chapter 11 and

Ref. 18.5. Joint design for buildings that resist seismic forces is subject to special ACI Code provisions (see Chapter 20).

In normal beam-and-girder construction, the depth of the beams may be as much as 3 times the web width. Improved economy, however, is achieved by using beams with webs that are generally wider and shallower, coupled with girders that have the same depth as the beams. The resulting girders, more often than not, have webs that are wider than their effective depths. Although the flexural steel in the members is increased because of the reduced effective depth compared with deeper members, the increases in material costs are more than paid for by savings in forming costs (one depth for all members) and easier construction (wider beams are easier to cast than narrow beams). Another key advantage is the reduced construction depth, which permits a reduction in the overall height of the building.

For light loads, a floor system has been developed in which the beams are omitted in one direction, the one-way slab being carried directly by column-line beams that are very broad and shallow, as shown in Fig. 18.4. These beams, supported directly by the columns, become little more than a thickened portion of the slab. This type of construction, in fact, is known as *banded slab construction,* and there are a number of advantages associated with its use, over and above those associated with shallow beam-and-girder construction. In the direction of the slab span, a haunched member is present, in effect, with the maximum effective depth at the location of greatest negative moment, across the support lines. Negative moments are small at the edge of the haunch, but the depth becomes less, and positive slab moments are reduced as well. The increased flexural steel in the beam (slab-band) resulting from the reduced effective depth is often outweighed by savings in the slab steel. Along with reduced construction depth, banded slab construction allows greater flexibility in locating columns, which may be displaced some distance from the centerline of the slab-band without significantly changing the structural action of the floor. Formwork is simplified because of the reduction in the number of framing members. For such systems, special attention should be given to design details at the beam-column joint. Transverse top steel may be required to distribute the column reaction over the width of the slab-band. In addition, punching shear failure is possible; this may be investigated using the same methods presented earlier for flat plates (see Section 13.10).

b. Composite Construction with Steel Beams

One-way reinforced concrete slabs are also frequently used in buildings for which the columns, beams, and girders consist of structural steel. The slab is normally designed for full continuity over the supporting beams, and the usual methods are followed. The spacing of the beams is usually 1.8 to 2.4 m.

To provide composite action, shear connectors are welded to the top of the steel beam and are embedded in the concrete slab, as shown in Fig. 18.5*a*. By preventing longitudinal slip between the slab and steel beam in the direction of the beam axis, the combined member is both stronger and stiffer than if composite action were not developed. Thus, for given loads and deflection limits, smaller and lighter steel beams can be used.

Composite floors may also use encased beams, as shown in Fig. 18.5*b*, offering the advantage of full fireproofing of the steel, but at the cost of more complicated formwork and possible difficulty in placing the concrete around and under the steel member. Such fully encased beams do not require shear connectors as a rule.

FIGURE 18.4
Banded slab floor system.

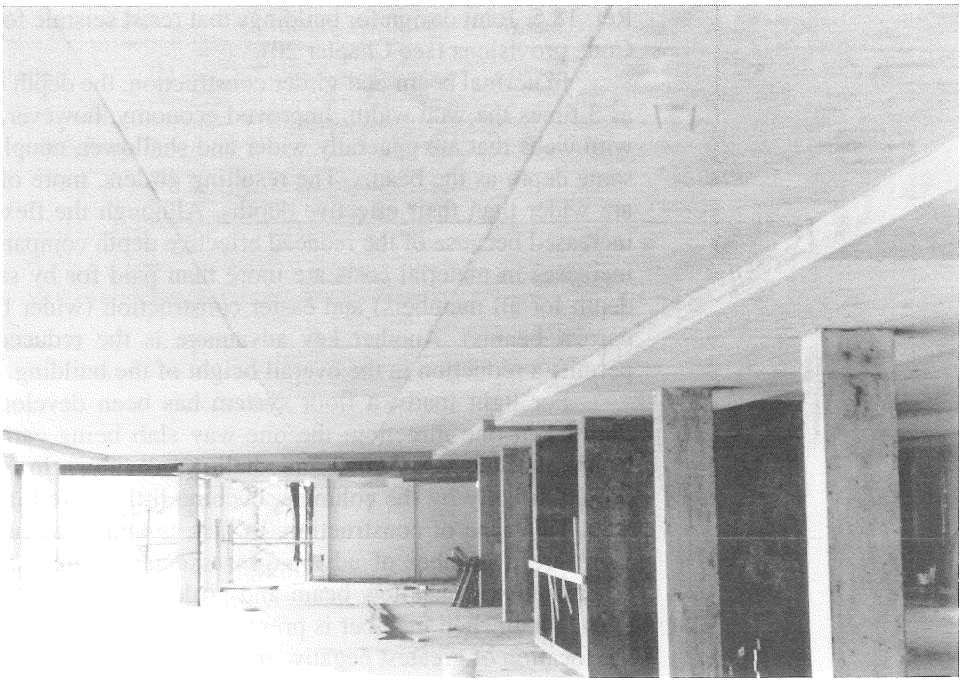

(*a*) Interior slab band

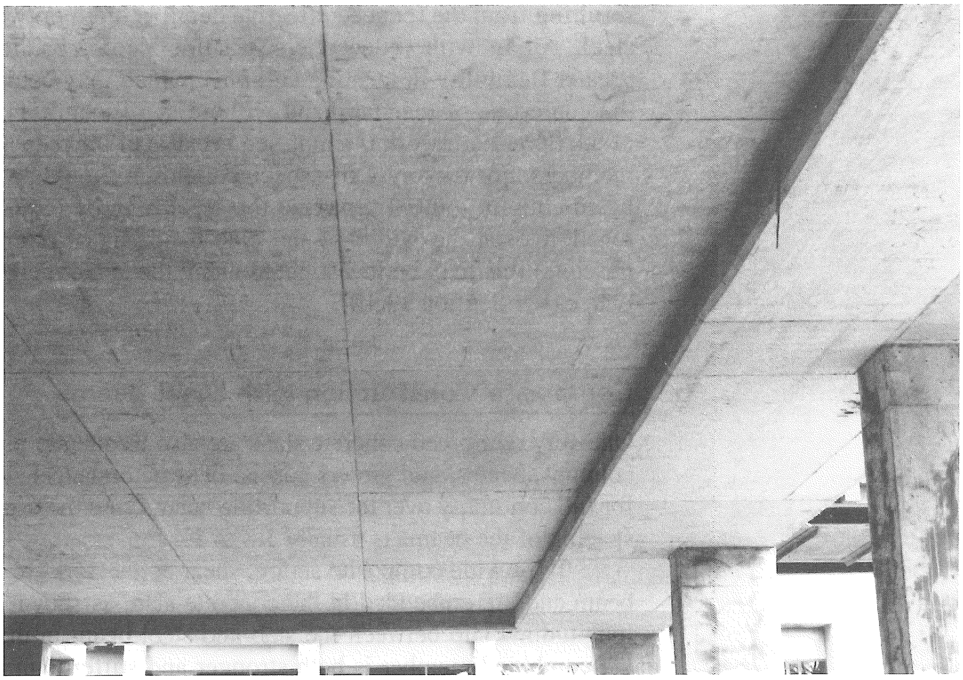

(*b*) Edge band at exterior column

c. Steel Deck Reinforced Composite Slabs

It is nearly standard practice to use stay-in-place light-gage cold-formed steel deck panels in composite floor construction. As shown in Fig. 18.5*c*, the steel deck serves as a stay-in-place form and, with suitable detailing, the slab becomes composite with

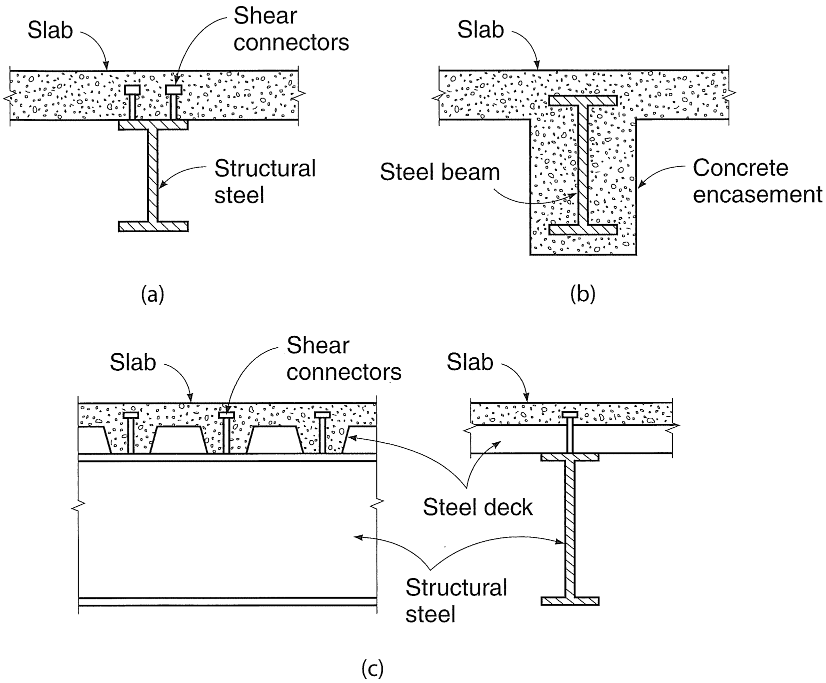

FIGURE 18.5
Composite beam-and-slab floor.

the steel deck, serving as the main tensile flexural steel. Suitable for relatively light floor loading and short spans, composite steel deck reinforced slabs are found in office buildings and apartment buildings, with column-line girders and beams in the perpendicular direction subdividing panels into spans up to about 3.6 m. Temporary shoring may be used at the midspan or third point of the panels to avoid excessive stresses and deflections while the concrete is placed, when the steel deck panel alone must carry the load.

d. One-Way Joist Floors

A one-way joist floor consists of a series of small, closely spaced reinforced concrete T beams, framing into monolithically cast concrete girders, which are in turn carried by the building columns. The T beams, called *joists*, are formed by creating void spaces in what otherwise would be a solid slab. Usually these voids are formed using special steel pans, as shown in Fig. 18.6. Concrete is cast between the forms to create ribs, and placed to a depth over the top of the forms so as to create a thin monolithic slab that becomes the T beam flange.

Since the strength of concrete in tension is small and is commonly neglected in design, elimination of much of the tension concrete in a slab by the use of pan forms results in a saving of weight with little change in the structural characteristics of the slab. Ribbed floors are economical for buildings, such as apartment houses, hotels, and hospitals, where the live loads are fairly small and the spans comparatively long. They are not suitable for heavy construction such as in warehouses, printing plants, and heavy manufacturing buildings.

In U.S. practice, standard forms for the void spaces between ribs are either 508 or 762 mm wide and 203, 254, 305, 356, 406, or 508 mm deep. They are tapered in cross section, as shown in Fig. 18.7, generally at a slope of 1 to 12, to facilitate

FIGURE 18.6
Steel forms for one-way joist floor.

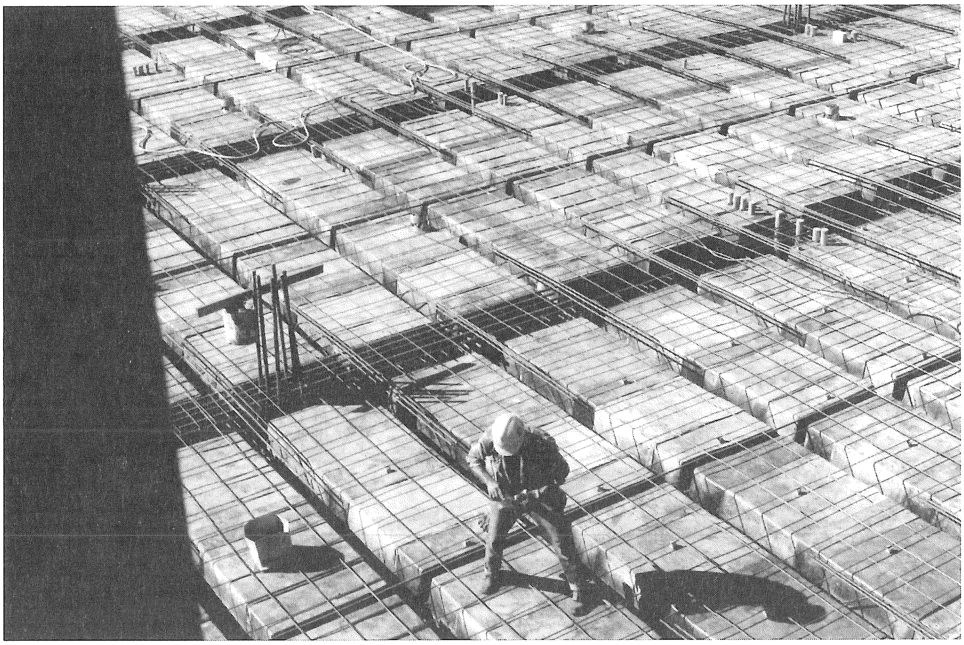

removal. Any joist width can be obtained by varying the width of the soffit (bottom) form. Tapered end pans are used where it is desired to obtain a wider joist near the end supports, such as may be required for high shear or negative bending moment. After the concrete has hardened, the steel pans are removed for reuse.

According to ACI Code 8.13.2, ribs must not be less than 100 mm wide and may not have a depth greater than 3.5 times the minimum web width. (For easier bar placement and placement of concrete, a minimum web width of 125 mm is desirable.) The clear spacing between ribs (determined by the pan width) must not exceed 750 mm. The slab thickness over the top of the pans must not be less than one-twelfth of the clear distance between ribs, nor less than 50 mm, according to ACI Code 8.13.6. Table 18.1 gives unit weights, in terms of kN/m^2 of floor surface, for common combinations of joist width and depth, slab thickness, and form width.

Reinforcement for the joists usually consists of two bars in the positive bending region, with one bar discontinued where no longer needed or bent up to provide

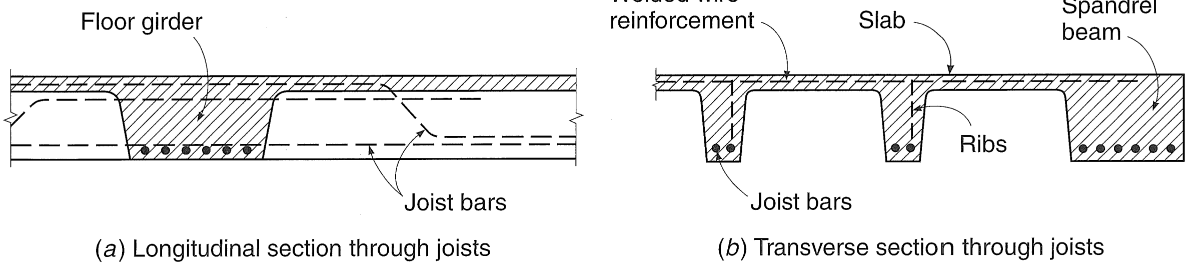

(*a*) Longitudinal section through joists

(*b*) Transverse section through joists

FIGURE 18.7
One-way joist floor cross sections: (*a*) cross section through supporting girder showing ends of joists; (*b*) cross section through typical joists.

TABLE 18.1
Weight of one-way joist floor systems (U.S. practice)

76 mm Top Slab			114 mm Top Slab		
Depth of Pan Form, mm	Width of Joist + Pan Form, mm	Weight, kN/m²	Depth of Pan Form, mm	Width of Joist + Pan Form, mm	Weight, kN/m²
203	127 + 508	2.87	203	127 + 508	3.78
203	127 + 762	2.59	203	127 + 762	3.45
254	127 + 508	3.21	254	127 + 508	4.07
254	127 + 762	2.78	254	127 + 762	3.69
305	127 + 508	3.54	305	127 + 508	4.41
305	127 + 762	3.02	305	127 + 762	3.93
356	127 + 762	3.26	356	127 + 762	4.17
356	152 + 762	3.45	356	152 + 762	4.36
406	152 + 762	3.74	406	152 + 762	4.65
406	178 + 762	3.98	406	178 + 762	4.84
508	152 + 762	4.36	508	152 + 762	5.22
508	178 + 762	4.60	508	178 + 762	5.51

Source: Adapted from Ref. 18.3.

a part of the negative steel requirement over the supporting girders. Straight top bars are added over the support to provide for the negative bending moment. According to ACI Code 7.13.2, at least one bottom bar must be continuous over the support, or at noncontinuous supports, terminated with a standard hook or headed bar, as a measure to improve structural integrity in the event of major structural damage.

ACI Code 7.7.1 permits a reduced concrete cover of 20 mm to be used for joist construction, just as for slabs. The thin slab (top flange) is reinforced mainly for temperature and shrinkage stresses, using welded wire reinforcement or small bars placed at right angles to the joists. The area of this reinforcement is usually 0.18 percent of the gross cross section of the concrete slab.

One-way joists are generally proportioned with the concrete providing all of the shear strength, with no stirrups used. A 10 percent increase in V_c above the value given by Eq. (4.12*a*) or (4.12*b*) is permitted for joist construction, according to ACI Code 8.13.8, based on the possibility of redistribution of local overloads to adjacent joists. Tests have shown that while local redistribution does occur, the shear strength of the full system (all joists acting together) is enhanced by less than 10 percent (Ref. 18.6).

The joists and the supporting girders are placed monolithically. Like the joists, the girders are designed as T beams. The shape of the girder cross section depends on the shape of the end pans that form the joists, as shown in Fig. 18.7*a*. If the girders are deeper than the joists, the thin concrete slab directly over the top of the pans is often neglected in the girder design. The girder width can be adjusted, as needed, by varying the placement of the end pans. The width of the web below the bottom of the joists must be at least 75 mm narrower than the flange (on either side) to allow for pan removal.

A type of one-way joist floor system has evolved known as a *joist-band system* in which the joists are supported by broad girders having the same total depth as the joists, as illustrated in Fig. 18.7. Separate beam forms are eliminated, and the same deck forms the soffit of both the joists and the girders. The simplified formwork, faster construction, level ceiling with no obstructing beams, and reduced overall height of walls, columns, and vertical utilities combine to achieve an overall reduction in cost in most cases.

In one-way joist floors, the thickness of the slab is often controlled by fire resistance requirements. For a rating of 2 hours, for example, the slab must be about 110 mm thick (Ref. 18.1). If 508 or 762 mm pan forms are used, slab span is small and slab strength is underutilized. This has led to what is known as the *wide module joist system*, or *skip joist system* (Ref. 18.7). Such floors generally have 300 to 400 mm wide ribs that are 1.5 to 1.8 m on centers, with a 110 mm top slab. These floors not only provide more efficient use of concrete in the slab, but also require less formwork labor. By ACI Code 8.13.4, wide module joist ribs must be designed as ordinary T beams, because the clear spacing between ribs exceeds the 750 mm maximum for joist construction, and the special ACI Code provisions for joists do not apply. Concrete cover for reinforcement is as required for beams, not joists, and the 10 percent increase in V_c does not apply. Often the joists in wide module systems are carried by wide beams on the column lines, the depth of which is the same as that of the joists, to form a joist-band system equivalent to that described earlier.

Useful design information pertaining to one-way joist floors, including extensive load tables, will be found in the *CRSI Design Handbook* (Ref. 18.3). Suggested bar details and typical design drawings are found in the *ACI Detailing Manual* (Ref. 18.4).

e. Two-Way Edge-Supported Slabs

Two-way solid slabs supported by beams on the column lines on all sides of each slab panel have been discussed in detail in Chapter 13. The perimeter beams are usually concrete cast monolithically with the slab, although they may also be structural steel, often encased in concrete for composite action and for improved fire resistance. For monolithic concrete, both the beams and the slabs are designed using the direct design method or the equivalent frame method described in Chapter 13.

Two-way solid slab systems are suitable for intermediate to heavy loads on spans up to about 9 m. This range corresponds closely to that for beamless slabs with drop panels and column capitals, described in the following section. The latter are often preferred because of the complete elimination of obstructing beams below the slab.

For lighter loads and shorter spans, a two-way solid slab system has evolved in which the column-line beams are wide and shallow, such that a cross section through the floor in either direction resembles the slab-band shown earlier in Fig. 18.4. The result is a two-way slab-band floor that, from below, appears as a paneled ceiling. Advantages are similar to those given earlier for one-way slab-band floors and for joist-band systems.

f. Beamless Flat Slabs with Drop Panels or Column Capitals

By suitably proportioning and reinforcing the slab, it is possible to eliminate supporting beams altogether. The slab is supported directly on the columns. In a rectangular or square region centered on the columns, the slab may be thickened and the column tops flared, as shown in Fig. 18.8. The thickened slab is termed a *drop panel*, and the column flare is referred to as a *column capital*. Both of these serve a double purpose: they increase the shear strength of the floor system in the critical region around the column, and they provide increased effective depth for the flexural steel in the region

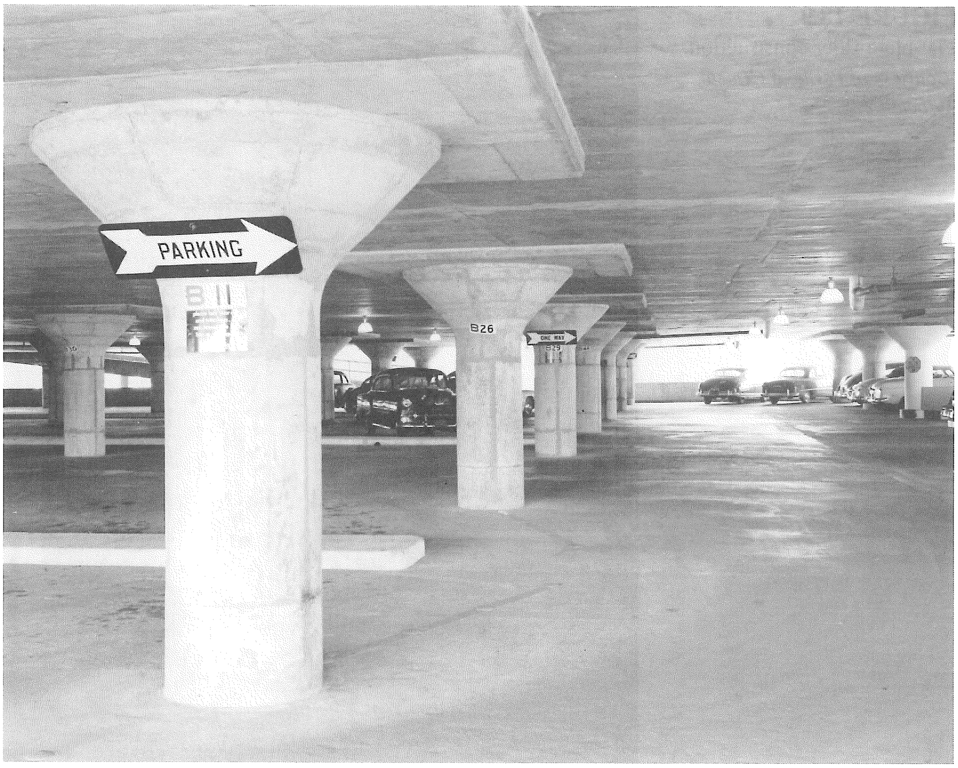

FIGURE 18.8
Flat slab garage floor with both drop panels and column capitals. (*Courtesy of Portland Cement Association.*)

of high negative bending moment over the support. Beamless systems with drop panels or column capitals or both are termed *flat slab systems* (although almost all slabs in structural engineering practice are "flat" in the usual sense of the word), and are differentiated from flat plate systems, with absolutely no projections below the slab, which are described in the following section.

In general, flat slab construction is economical for live loads of 4.8 kN/m^2 or more and for spans up to about 9 m. It is widely used for storage warehouses, parking garages, and below-grade structures carrying heavy earth-fill loads, for example. For lighter loads such as in apartment houses, hotels, and office buildings, flat plates (Section 18.2g) or some form of joist construction (Sections 18.2d and h) will usually prove less expensive. For spans longer than about 9 m, beams and girders are used because of the greater stiffness of that form of construction.

Flat slabs may be designed by the direct design method or the equivalent frame method, both described in detail in Chapter 13, or the strip method described in Chapter 15.

g. Flat Plate Slabs

A flat plate floor is essentially a flat slab floor with the drop panels and column capitals omitted, so that a floor of uniform thickness is carried directly by prismatic columns. Flat plate floors have been found to be economical and otherwise advantageous for such uses as apartment buildings, as shown in Fig. 18.9, where the spans are moderate (up to about 9 m) and loads relatively light. Prestressed concrete (Chapter 19) flat plate construction for residential and light commercial buildings has

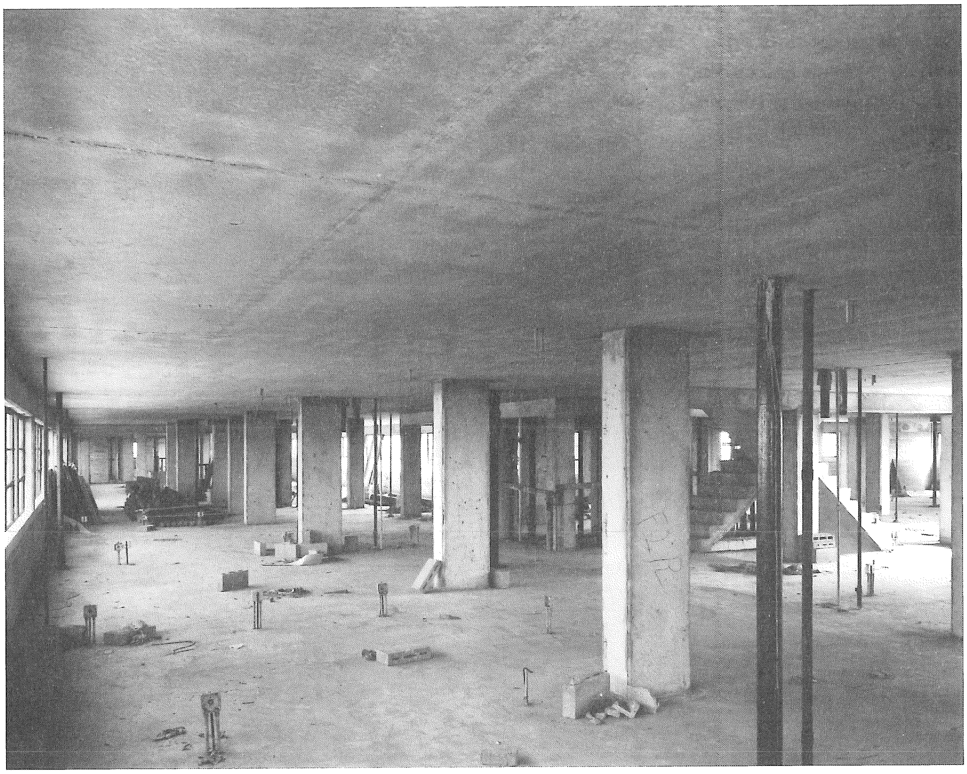

FIGURE 18.9
Flat plate floor construction. (*Courtesy of Portland Cement Association.*)

spans up to 12 m. The construction depth for each floor is held to the absolute minimum, with resultant savings in the overall height of the building. The smooth underside of the slab can be painted directly and left exposed for ceiling, or plaster can be applied to the concrete. Minimum construction time and low labor costs result from the very simple formwork.

Certain problems associated with flat plate construction require special attention. Shear stresses near the columns may be very high, requiring the use of special types of slab reinforcement there. The transfer of moments from slab to columns may further increase these shear stresses and requires concentration of negative flexural steel in the region close to the columns. Both these problems are treated in detail in Chapter 13. At the exterior columns, where such shear and moment transfer may cause particular difficulty, the design is much improved by extending the slab past the column in a short cantilever.

Some flat plate buildings are constructed by the lift slab method, shown in Fig. 18.10. A casting bed (often doubling as the ground-floor slab) is placed, steel columns are erected and braced, and at ground level successive slabs, which will later become the upper floors, are cast. A membrane or sprayed parting agent is laid down between successive pours so that each slab can be lifted in its turn, starting with the top. Jacks placed atop the columns are connected to threaded rods extending down the faces of the columns and connecting, in turn, to lifting collars embedded in the slabs, as shown in Fig. 13.24*d*. When a slab is in its final position, shear plates are welded to the column below the lifting collar, or other devices are used to transfer the vertical slab reaction. Lifting collars such as those shown in Fig. 13.24*d*, in addition to providing anchorage for the lifting rods, serve to increase the effective size of the support for the slab and consequently improve the shear strength of the

FIGURE 18.10
Lift slab construction used with flat plate floors; student dormitory at Clemson University, South Carolina.

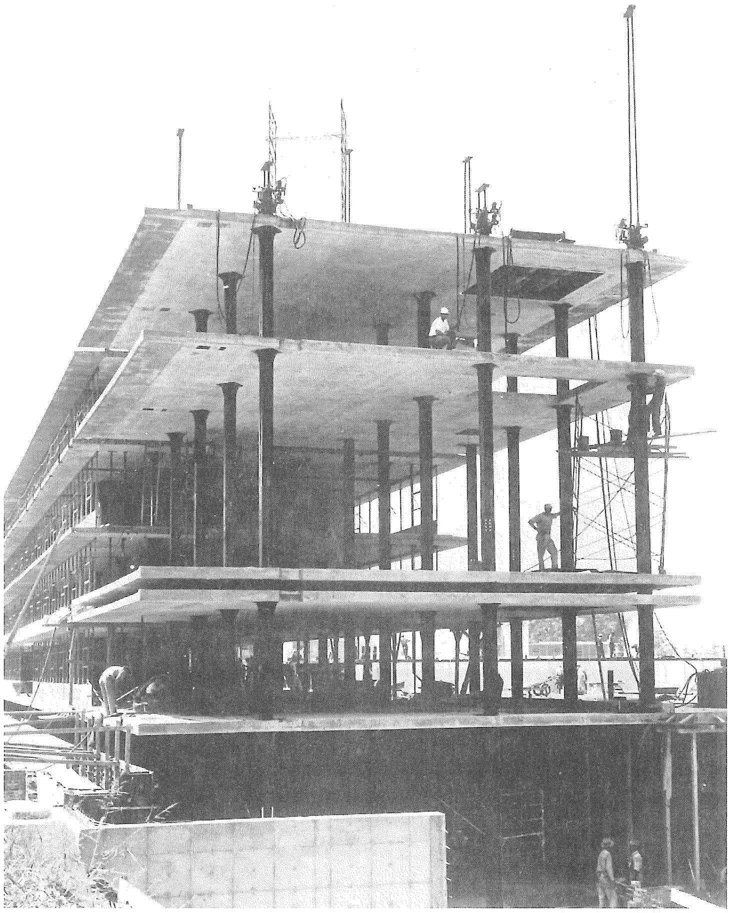

slab. The successful erection of structures using the lift slab method requires precise control of the lifting operation at all times, because even slight differences in level of the support collars may drastically change moments and shears in the slab, possibly leading to reversal of loading. Catastrophic accidents have resulted from failure to observe proper care in lifting or to provide adequate lateral bracing for the columns (Ref. 18.8). As a result of these accidents, this method of construction is used only by specialized contractors.

h. Two-Way Joist Floors

As in one-way floor systems, the dead weight of two-way slabs can be reduced considerably by creating void spaces in what would otherwise be a solid slab. For the most part, the concrete removed is in tension and ineffective, so the lighter floor has virtually the same structural characteristics as the corresponding solid floor. Voids are usually formed using dome-shaped steel pans that are removed for reuse after the slab has hardened. Forms are placed on a plywood platform as shown in Fig. 18.11. Note in the figure that domes have been omitted near the columns to obtain a solid slab in the region of negative bending moment and high shear. The lower flange of each dome contacts that of the adjacent dome, so that the concrete

FIGURE 18.11
Two-way joist floor under construction with steel dome forms. *(Courtesy of Ceco Corporation.)*

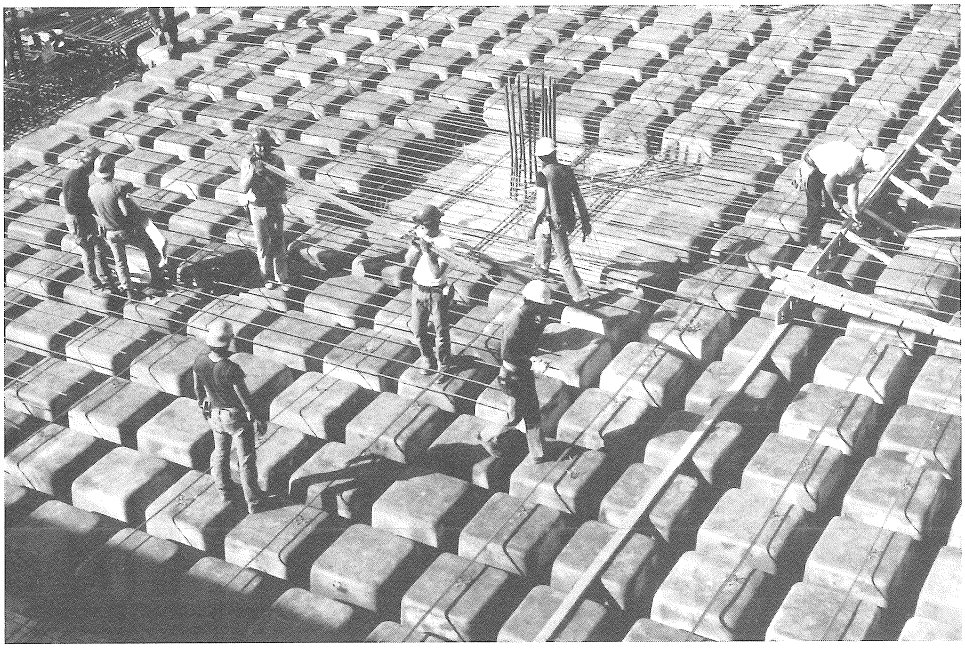

FIGURE 18.12
Regency House Apartments, San Antonio, with cantilevered two-way joist slab plus integral beams on column lines.

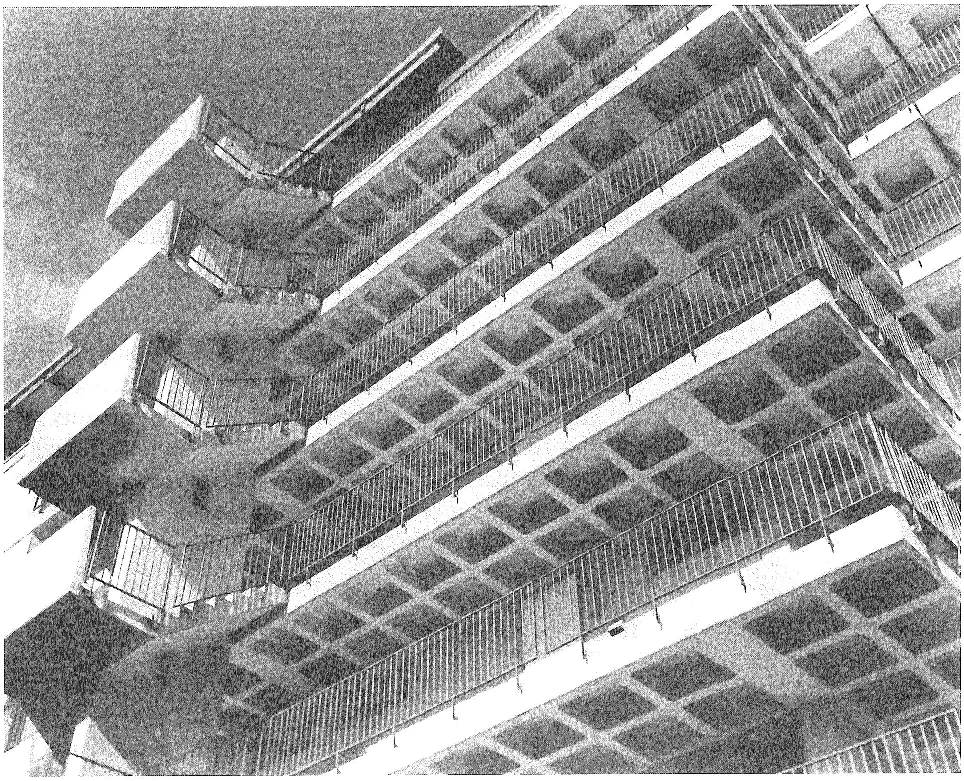

is cast entirely against a metal surface, resulting in an excellent finished appearance of the slab. A wafflelike appearance (these slabs are sometimes called waffle slabs) is imparted to the underside of the slab, which can be featured to architectural advantage, as shown in Fig. 18.12.

TABLE 18.2
Equivalent slab thickness and weight of two-way joist floor systems (U.S. practice)

	76 mm Top Slab		114 mm Top Slab	
Depth of Pan Form, mm	Equivalent Uniform Thickness, mm	Weight, kN/m²	Equivalent Uniform Thickness, mm	Weight, kN/m²
914 mm Module (762 mm pans plus 152 mm ribs)				
203	145	3.40	183	4.31
254	163	3.83	201	4.72
305	183	4.31	221	5.22
356	203	4.79	241	5.70
406	226	5.32	262	6.18
508	269	6.32	307	7.23
610 mm Module (483 mm pans plus 127 mm ribs)				
203	160	3.78	198	4.69
254	185	4.36	223	5.27
305	208	4.93	249	5.84
356	236	5.56	272	6.42
508	262	6.18	300	7.09

Source: Adapted from Ref. 18.3.

Two-way joist floors are designed following the usual procedures for two-way solid slab systems, as presented in Chapter 13, with the solid regions at the columns considered as drop panels. Joists in each direction are divided into column strip joists and middle strip joists, the former including all joists that frame into the solid head. Each joist rib usually includes two bars for positive-moment resistance, and one may be discontinued where no longer required. Negative steel is provided by separate straight bars running in each direction over the columns.

In design calculations, the self-weight of two-way joist floors is considered to be uniformly distributed, based on an equivalent slab of uniform thickness having the same volume of concrete as the actual ribbed slab. Equivalent thicknesses and weights are given in Table 18.2 for standard 762 and 483 mm pans of various depths and for either a 76 mm top slab or 114 mm top slab, based on normalweight concrete (2400 kg/m^3, 23.6 kN/m^3).

18.3 PANEL, CURTAIN, AND BEARING WALLS

As a general rule, the exterior walls of a reinforced concrete building are supported at each floor by the skeleton framework, their only function being to enclose the building. Such walls are called *panel walls*. They may be made of concrete (often precast), concrete block, brick, tile blocks, or insulated metal panels. The latter may be faced with aluminum, stainless steel, or a porcelain-enamel finish over steel, backed by insulating material and an inner surface sheathing. The thickness of each of these types of panel walls will vary according to the material, type of construction, climatological conditions, and the building requirements governing the particular locality in which the construction takes place.

The pressure of the wind is usually the only load that is considered in determining the structural thickness of a wall panel, although in some cases exterior walls are used as diaphragms to transmit forces caused by horizontal loads down to the building foundations.

Curtain walls are similar to panel walls except that they are not supported at each story by the frame of the building, but are self-supporting. However, they are often anchored to the building frame at each floor to provide lateral support.

A *bearing wall* may be defined as one that carries any vertical load in addition to its own weight. Such walls may be constructed of stone masonry, brick, concrete block, or reinforced concrete. Occasional projections or pilasters add to the strength of the wall and are often used at points of load concentration. In small commercial buildings, bearing walls may be used with economy and expediency. In larger commercial and manufacturing buildings, when the element of time is an important factor, the delay necessary for the erection of the bearing wall and the attendant increased cost of construction often dictate the use of some other arrangement.

18.4 SHEAR WALLS

Horizontal forces acting on buildings, e.g., those due to wind or seismic action, can be resisted by different means. Rigid-frame resistance of the structure, augmented by the contribution of ordinary masonry walls and partitions, can provide for wind loads in many cases. However, when heavy horizontal loading is likely, such as would result from an earthquake, reinforced concrete shear walls are used. These may be added solely to resist horizontal forces, or concrete walls enclosing stairways or elevator shafts may also serve as shear walls.

Figure 18.13 shows a building with wind or seismic forces represented by arrows acting on the edge of each floor or roof. The horizontal surfaces act as deep beams to transmit loads to vertical resisting elements A and B. These shear walls, in turn, act as cantilever beams fixed at their base to carry loads down to the foundation. They are

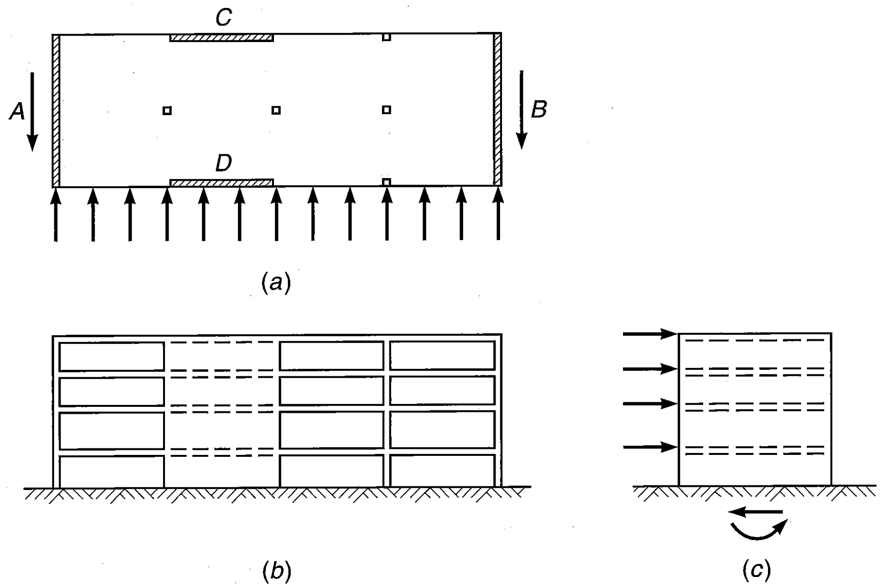

FIGURE 18.13
Building with shear walls subject to horizontal loads: (*a*) typical floor; (*b*) front elevation; (*c*) end elevation.

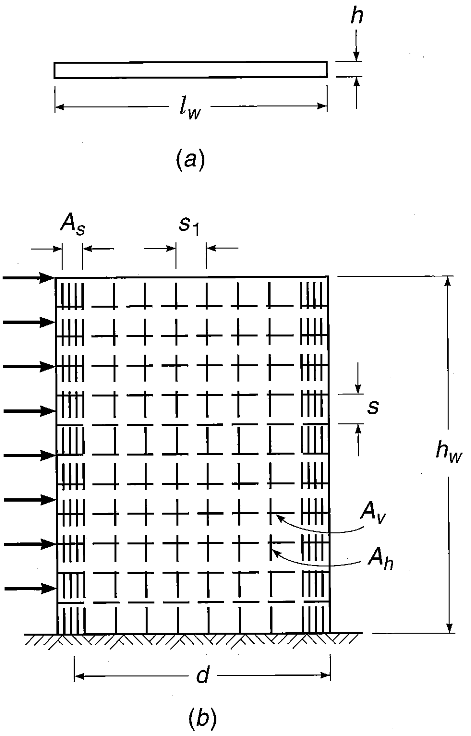

FIGURE 18.14
Geometry and reinforcement of a typical shear wall: (*a*) cross section; (*b*) elevation.

subjected to (1) a variable shear, which reaches a maximum at the base; (2) a bending moment, which tends to cause vertical tension near the loaded edge and compression at the far edge; and (3) a vertical compression due to ordinary gravity loading from the structure. For the building shown, additional shear walls *C* and *D* are provided to resist loads acting in the long direction of the structure.

Shear is apt to be critical for walls with a relatively low ratio of height to length. High shear walls are controlled mainly by flexural requirements.

Figure 18.14 shows a typical shear wall with height h_w, length l_w, and thickness *h*. It is assumed to be fixed at its base and loaded horizontally along its left edge. Vertical flexural reinforcement of area A_s is provided at the left edge, with its centroid a distance *d* from the extreme compression face. To allow for reversal of load, identical reinforcement is provided along the right edge. Horizontal shear reinforcement with area A_v at spacing *s* is provided, as well as vertical shear reinforcement with area A_h at spacing s_1. Such distributed steel is normally placed in two layers, parallel to the faces of the wall.

The design basis for shear walls, according to ACI Code 11.9, is of the same general form as that used for ordinary beams:

$$V_u \le \phi V_n \tag{18.1}$$

where

$$V_n = V_c + V_s \tag{18.2}$$

Based on tests (Refs. 18.9 and 18.10), an upper limit has been established on the nominal shear strength of walls:

$$V_n \le 0.83\sqrt{f_c'}\,hd \tag{18.3}$$

In this and all other equations pertaining to the design of shear walls, the distance d is taken equal to $0.8l_w$. A larger value of d, equal to the distance from the extreme compression face to the center of force of all reinforcement in tension, may be used when determined by a strain compatibility analysis.

The value of V_c, the nominal shear strength provided by the concrete, may be based on the usual equations for beams, according to ACI Code 11.9.5. For walls subject to vertical compression,

$$V_c = 0.17\lambda\sqrt{f_c'}\,hd \tag{18.4}$$

and for walls subject to vertical tension N_u,

$$V_c = 0.17\left(1 + \frac{0.29\,N_u}{A_g}\right)\lambda\sqrt{f_c'}\,hd \tag{18.5}$$

where λ is the lightweight concrete strength modification factor (see Section 4.5a). Here, N_u is the factored axial load in Newtons, taken negative for tension, and A_g is the gross area of horizontal concrete section in square millimeters. Alternately, the value of V_c may be based on a more detailed calculation, as the lesser of

$$V_c = 0.27\lambda\sqrt{f_c'}\,hd + \frac{N_u d}{4l_w} \tag{18.6}$$

or

$$V_c = \left[0.05\lambda\sqrt{f_c'} + \frac{l_w(0.1\lambda\sqrt{f_c'} + 0.2N_u/l_w h)}{M_u/V_u - l_w/2}\right]hd \tag{18.7}$$

where N_u is negative for tension as before. Equation (18.6) corresponds to the occurrence of a principal tensile stress of approximately $0.33\sqrt{f_c'}$ at the centroid of the shear-wall cross section. Equation (18.7) corresponds approximately to the occurrence of a flexural tensile stress of $0.5\sqrt{f_c'}$ at a section $l_w/2$ above the section being investigated. Thus, the two equations predict, respectively, web-shear cracking and flexure-shear cracking. When the quantity $M_u/V_u - l_w/2$ is negative, Eq. (18.7) is inapplicable. According to the ACI Code, horizontal sections located closer to the wall base than a distance $l_w/2$ or $h_w/2$, whichever is less, may be designed for the same V_c as that computed at a distance $l_w/2$ or $h_w/2$.

When the factored shear force V_u does not exceed $\phi V_c/2$, a wall may be reinforced according to minimum requirements. When V_u exceeds $\phi V_c/2$, reinforcement for shear is to be provided according to the following requirements.

The nominal shear strength V_s provided by the horizontal wall steel is determined on the same basis as for ordinary beams:

$$V_s = \frac{A_v f_y d}{s} \tag{18.8}$$

where A_v = area of horizontal shear reinforcement within vertical distance s, mm^2
s = vertical distance between horizontal reinforcement, mm
f_y = yield strength of reinforcement, MPa

Substituting Eq. (18.8) into Eq. (18.2), then combining with Eq. (18.1), one obtains the equation for the required area of horizontal shear reinforcement within a distance s:

$$A_v = \frac{(V_u - \phi V_c)s}{\phi f_y d} \tag{18.9}$$

The minimum permitted ratio of horizontal shear steel to gross concrete area of vertical section is

$$\rho_t = 0.0025 \tag{18.10}$$

and the maximum spacing s is not to exceed $l_w/5$, $3h$, or 450 mm.

Test results indicate that for low shear walls, vertical distributed reinforcement is needed as well as horizontal reinforcement. Code provisions require vertical steel of area A_h within a spacing s_1, such that the ratio of vertical steel to gross concrete area of horizontal section will be not less than

$$\rho_l = 0.0025 + 0.5\left(2.5 - \frac{h_w}{l_w}\right)(\rho_t - 0.0025) \tag{18.11}$$

nor less than 0.0025. However, the vertical reinforcement ratio need not be greater than the required horizontal reinforcement ratio. The spacing of the vertical bars is not to exceed $l_w/3$, $3h$, or 450 mm.

Walls may be subject to flexural tension due to overturning moment, even when the vertical compression from gravity loads is superimposed. In many but not all cases, vertical steel is provided, concentrated near the wall edges, as shown in Fig. 18.14. The required steel area can be found by the usual methods for beams.

The dual function of the floors and roofs in buildings with shear walls should be noted. In addition to resisting gravity loads, they must act as deep beams spanning between shear-resisting elements. Because of their proportions, both shearing and flexural stresses are usually quite low. According to ACI Code 9.2.1, the load factor for live load drops to 1.0 when wind or earthquake effects are combined with the effects of gravity loads. Consequently, floor and roof reinforcement designed for gravity loads can usually serve as reinforcement for horizontal beam action also, with no increase in bar areas.

ACI Code 11.9.1 permits walls with height-to-length ratios not exceeding 2.0 to be designed using strut-and-tie models (Chapter 10). The minimum shear reinforcement criteria of Eqs. (18.9) through (18.11) and the maximum spacing limits for s and s_1 must be satisfied.

There are special considerations and requirements for the design of reinforced concrete walls in structures designed to resist forces associated with seismic motion. These are based on design for energy dissipation in the nonlinear range of response. This subject will be treated separately, in Chapter 20.

18.5 PRECAST CONCRETE FOR BUILDINGS

The earlier sections in this chapter have emphasized cast-in-place reinforced concrete structures. Construction of these structures requires a significant amount of skilled on-site labor. There is, however, another class of concrete construction for which the members are manufactured off site in precasting yards, under factory conditions, and subsequently assembled on site, a process that provides significant advantages in terms of economy and speed of construction.

Precast concrete construction involves the mass production of repetitive and often standardized units: columns, beams, floor and roof elements, and wall panels. On large jobs, precasting yards are sometimes constructed on or adjacent to the site. More frequently, these yards are stationary regional enterprises that supply precast members to sizable areas within reasonable shipping distances, on the order of 300 km.

Advantages of precast construction include less labor per unit because of mechanized series production; use of unskilled local labor, in contrast to skilled mobile construction labor; shorter construction time because site labor primarily involves only foundation construction and connecting the precast units; better quality control and higher concrete strength that are achievable under factory conditions; and greater independence of construction from weather and season. Disadvantages are the greater cost of transporting precast units, as compared with transporting materials, and the additional technical problems and costs of site connections of precast elements.

Precast construction is used in all major types of structures: industrial buildings, residential and office buildings, halls of sizable span, bridges, stadiums, and prisons. Precast members frequently are prestressed in the casting yard. In the context of the present chapter, it is irrelevant whether a precast member is also prestressed. Discussion is focused on types of precast members and precast structures and on methods of connection; these are essentially independent of whether the desired strength of the member was achieved with ordinary reinforcement or by prestressing. A broader discussion of precast construction, which includes planning, design, materials, manufacturing, handling, construction, and inspection, will be found in Refs. 18.11 and 18.12. ACI Code Chapter 16 is dedicated to precast concrete.

a. Types of Precast Members

A number of types of precast units are in common use. Though most are not formally standardized, they are widely available, with minor local variations. At the same time, the precasting process is sufficiently adaptable for special shapes developed for particular projects to be produced economically, provided that the number of repetitive units is sufficiently large. This is particularly important for exterior wall panels, which permit a wide variety of architectural treatments.

Wall panels are made in a considerable variety of shapes, depending on architectural requirements. The most frequent four shapes are shown in Fig. 18.15. These units are produced in one to four-story-high sections and up to 2.4 m in width. They are used either as curtain walls attached to columns and beams or as bearing walls. To improve thermal insulation, sandwich panels are used that consist of an insulation core (e.g., foam glass, glass fiber, or expanded plastic) between two layers of normalweight or lightweight concrete. The two layers must be adequately interconnected through the core to act as one unit. A variety of surface finishes can be produced through the use of special exposed aggregates or of colored cement, sometimes employed in combination. The special design problems that arise in load-bearing wall panels, such as tilt-up construction, are discussed in Ref. 18.13.

Stresses in wall panels are frequently more severe in handling and during erection than in the finished structure, and the design must provide for these temporary conditions. Also, control of cracking is of greater importance in wall panels than in other precast units, for appearance more than for safety. To control cracking, the maximum tensile stress in the concrete, calculated by straight-line theory, should not exceed the modulus of rupture of the particular concrete with an adequate margin of safety. ACI Committee 533 (Ref. 18.14) recommends that tensile stresses for normalweight concrete be limited to $0.42\sqrt{f_c'}$ under the effects of form removal, handling, transportation, impact, and live load. Maximum tensile stresses equal to 75 and 85 percent of this value are recommended for all-lightweight and sand-lightweight concrete, respectively. A wealth of information on precast wall panels is found in Refs. 18.12 and 18.14.

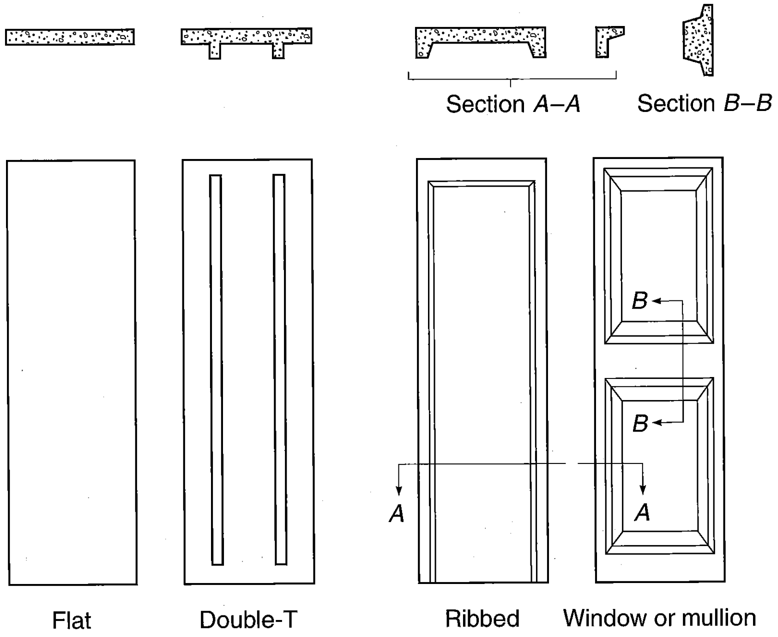
Section A–A
Section B–B
B
B
A
A
Flat
Double-T
Ribbed
Window or mullion

FIGURE 18.15
Precast concrete wall panels.

Roof and floor elements are made in a wide variety of shapes adapted to specific conditions, such as span lengths, magnitude of loads, desired fire ratings, and appearance. Figure 18.16 shows typical examples of the most common shapes, arranged in approximate order of increasing span length, even though the spans covered by the various configurations overlap widely.

Flat slabs (Fig. 18.16*a*) are usually 100 mm thick, although they are used as thin as 65 mm when continuous over several spans, and are produced in widths of 1.2 to 2.4 m and in lengths up to 11 m. Depending on the magnitude of loads and on deflection limitations, they are used over roof and floor spans ranging from 1.2 to

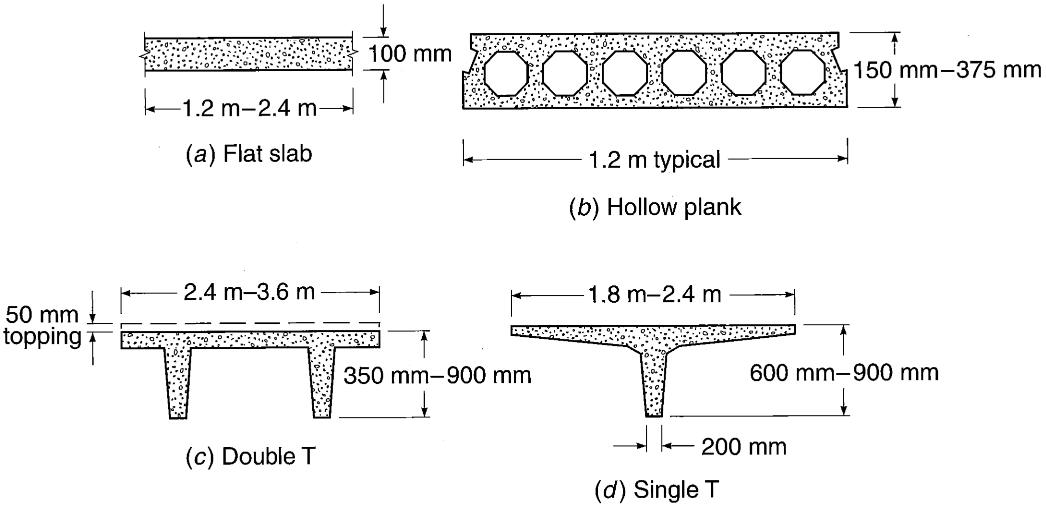
100 mm
1.2 m–2.4 m
(a) Flat slab
150 mm–375 mm
1.2 m typical
(b) Hollow plank
50 mm topping
2.4 m–3.6 m
350 mm–900 mm
(c) Double T
1.8 m–2.4 m
600 mm–900 mm
200 mm
(d) Single T

FIGURE 18.16
Precast floor and roof elements.

about 6.7 m. For lower weight and better insulation and to cover longer spans, *hollow-core planks* (Fig. 18.16*b*) with a variety of shapes are used. Some of these are made by extrusion in special machines. Depths range from 150 to 375 mm, with widths of 0.9 or 1.2 m. Again depending on load and deflection requirements, they are used on roof spans from about 5 to 10 m and on floor spans from 3.7 to 7.9 m, which can be augmented to about 9 m if a 50 mm topping is applied to act monolithically with the hollow plank.

For longer spans, *double T* members (Fig. 18.16*c*) are the most widely used shapes. Usual depths are from 350 to 900 mm. They are used on roof spans up to 37 m. When used as floor members, a concrete topping of at least 50 mm is usually applied to act monolithically with the precast members for spans up to about 15 m, depending on load and deflection requirements. Finally, *single T* members are available in dimensions shown in Fig. 18.16*d*, mostly used for roof spans up to 30 m and more.

For all of these units, the member itself or its flange constitutes the roof or floor slab. If the floor or roof proper is made of other material (e.g., plywood, gypsum, and plank), it can be supported on *precast joists* in a variety of shapes for spans from about 4.5 to 18 m. Reference 18.12 addresses the design of both reinforced and prestressed concrete floor and roof units.

The shape of *precast beams* depends chiefly on the manner of framing. If floor and roof members are supported on top of the beams, these are mostly rectangular in shape (Fig. 18.17*a*). To reduce total depth of floor and roof construction, the tops of beams are often made flush with the top surface of the floor elements. To provide bearing, the beams are then constructed as ledger beams (Fig. 18.17*b*) or L beams (Fig. 18.17*c*). Although these shapes pertain to building construction,

FIGURE 18.17
Precast beams and girders.

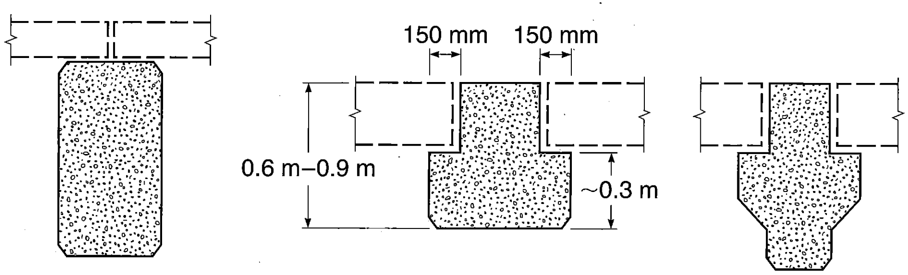

(*a*) Rectangular beam (*b*) Ledger beams

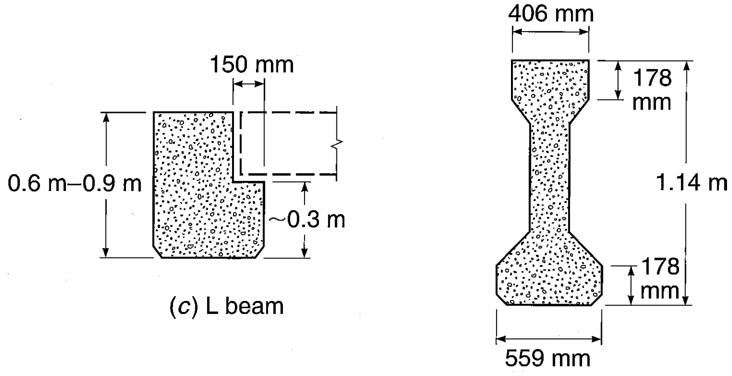

(*c*) L beam

(*d*) AASHTO bridge girder

FIGURE 18.18
Precast concrete columns.

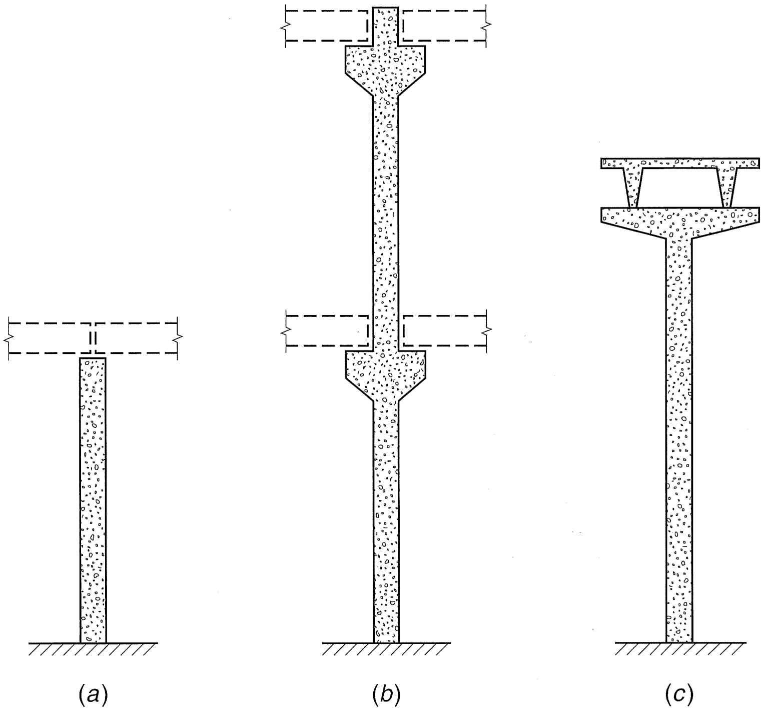

precast beams or girders are also frequently used in highway bridges. As an example, Fig. 18.17*d* shows one of the various AASHTO bridge girders, so named because they were developed by the American Association of State Highway and Transportation Officials.

If *precast columns* of single-story height are used so that the beams rest on top of the columns, simple prismatic columns are employed, which are available in sizes from about 300 × 300 to 600 × 600 mm (Fig. 18.18*a*). In this case, the beams are usually made continuous over the columns. Alternatively, in multistory construction, the columns can be made continuous for up to about six stories. In this case, integral brackets are frequently used to provide a bearing for the beams, as shown in Fig. 18.18*b* (see also Section 18.6b). Occasionally, T columns are used for direct support of double T floor members without the use of intermediate beams (Fig. 18.18*c*).

Figures 18.19 to 18.27 illustrate some of the many ways in which precast members have been used. Figure 18.19 shows a floor slab element being placed on precast columns with integral column capitals. The entire building, including elevator and stair shafts, is precast concrete. The photograph in Fig. 18.20 was taken in a precasting yard producing a variety of L, T, and rectangular shapes. Figure 18.21 shows symmetrical precast I beams, such as are used both for buildings and bridges. The projecting stirrup bars along the top flange will provide secure interlock between the precast beams and a cast-in-place slab added later, ensuring composite action. Figure 18.22 shows a multistory parking garage in which three-story precast columns support L-section and inverted T-section girders. The girders, in turn, carry 18 m span prestressed single T beams, which provide the deck surface.

Figure 18.23 demonstrates that unusual architectural designs can be realized in precast concrete, as in this all-precast administration building. Wall panels are used to

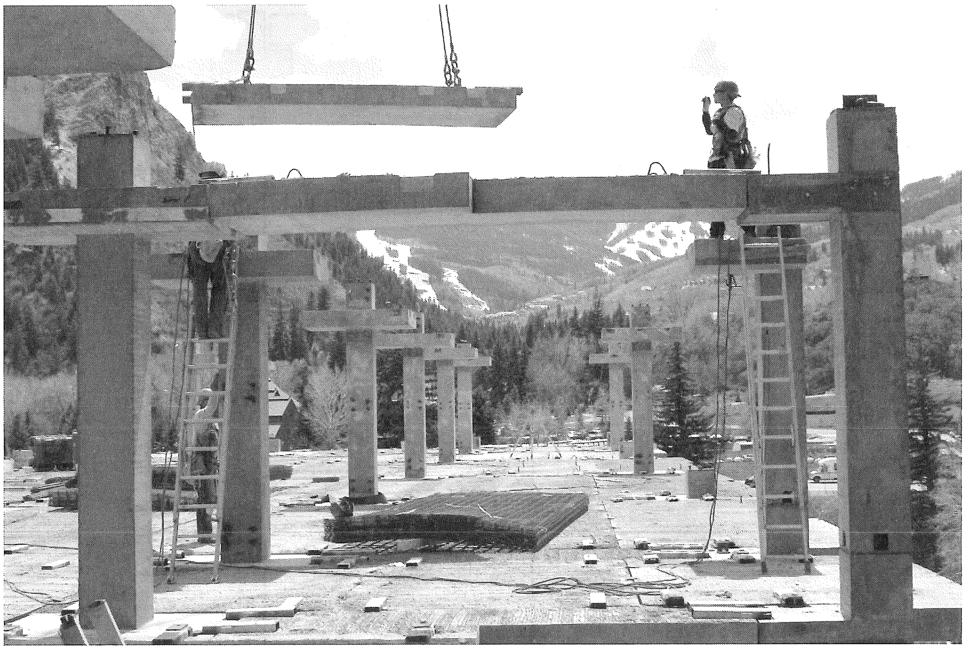

FIGURE 18.19
Precast slab element with precast columns, beams, and lateral framing.

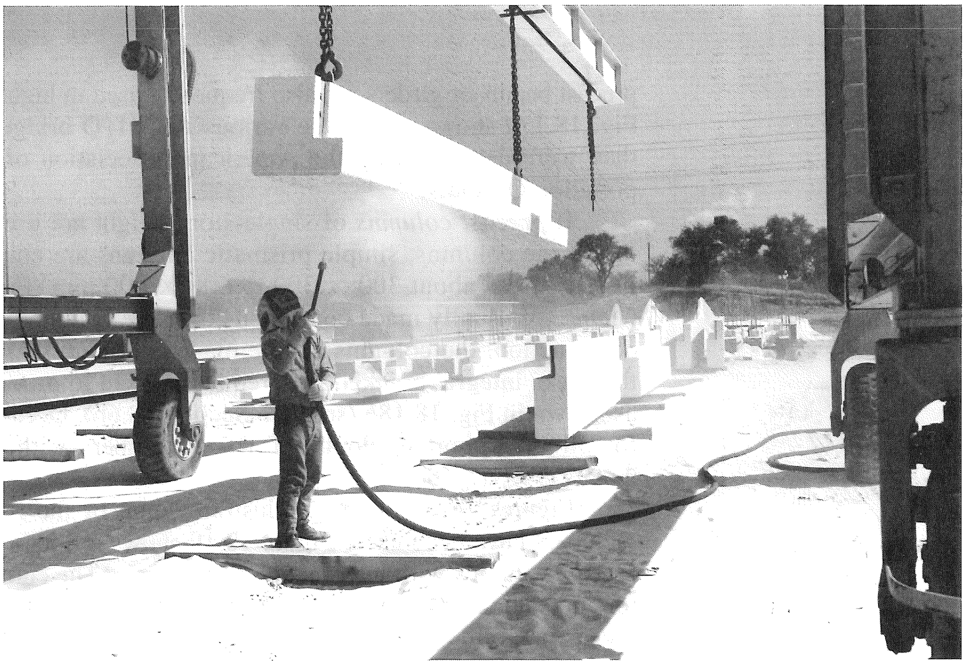

FIGURE 18.20
Sand-blasted architectural finish applied to a precast L beam.

produce a curved facade. Wedge-shaped repetitive floor units span freely from the exterior facade to the interior curved beam and column framework. In the insurance building shown in Fig. 18.24, 1.118 m deep precast girders span 30 m between exterior walls supported on four points each and provide six floors of office space entirely free of

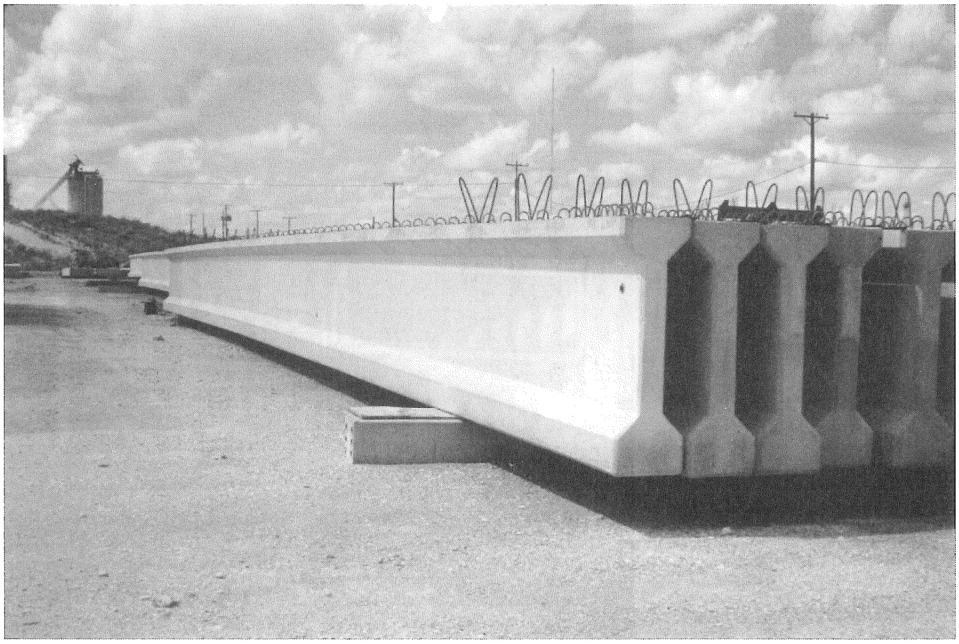

FIGURE 18.21
Precast I beams designed for composite action with a deck slab to be cast in place.

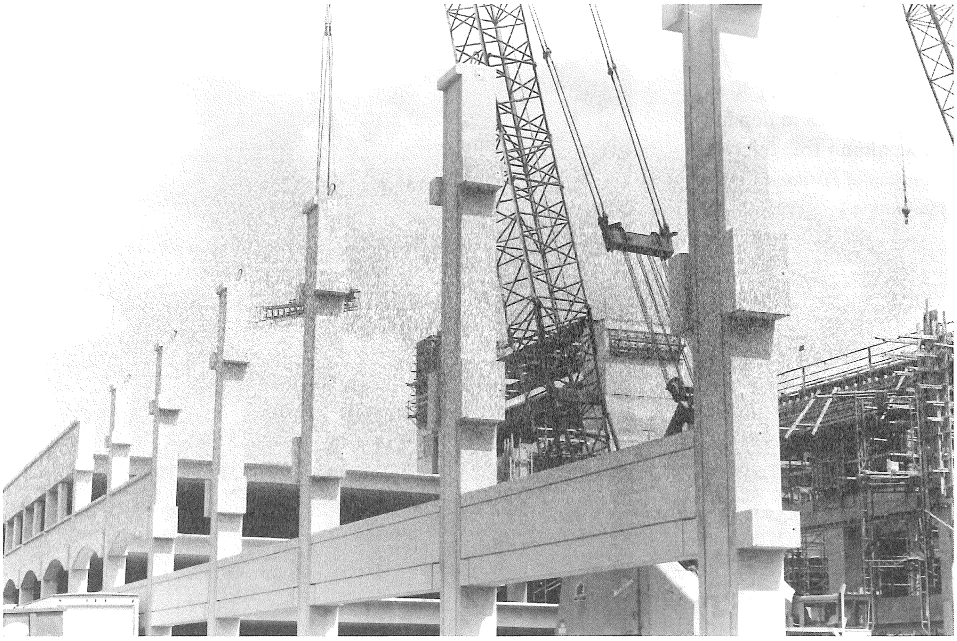

FIGURE 18.22
Precast parking garage at Cornell University.

interior supports. The convention headquarters of Fig. 18.25 combines cast-in-place frames and floor slabs with precast double T roof beams and precast wall panels of special design. Figure 18.26 shows a 21-story hotel under construction, which, except for the service units, consists entirely of box-shaped, room-sized modules completely prefabricated and stacked on top of each other. Abroad, such precast modules, with

FIGURE 18.23
All precast administration building. (*Courtesy of Portland Cement Association.*)

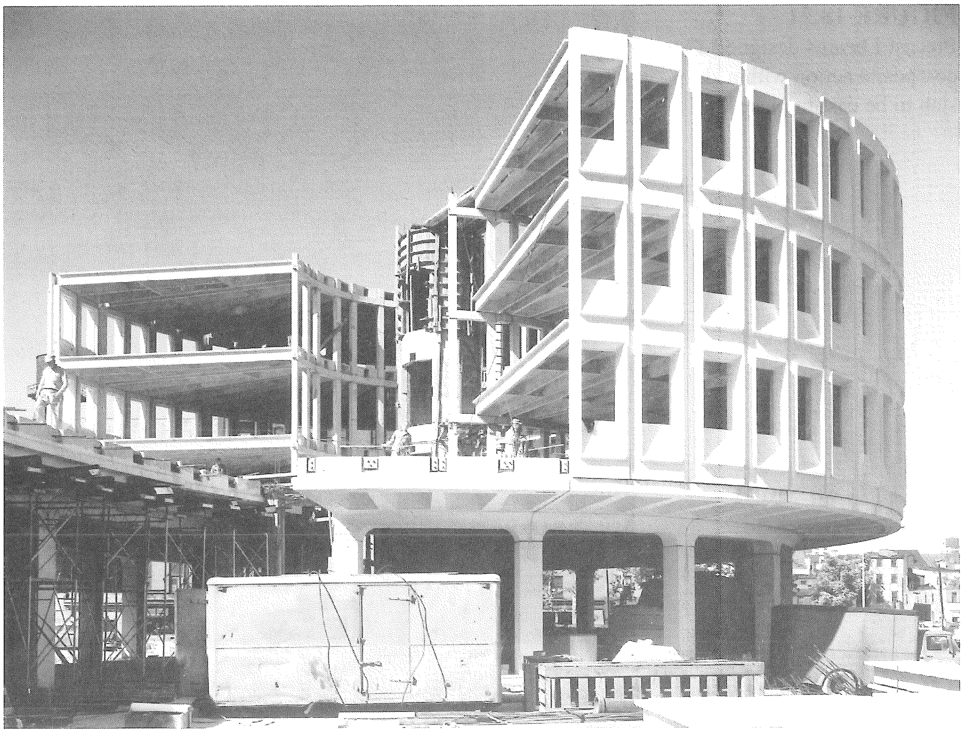

FIGURE 18.24
Precast girders with 30 m span and 1.118 m depth for a column-free interior. (*Courtesy of Portland Cement Association.*)

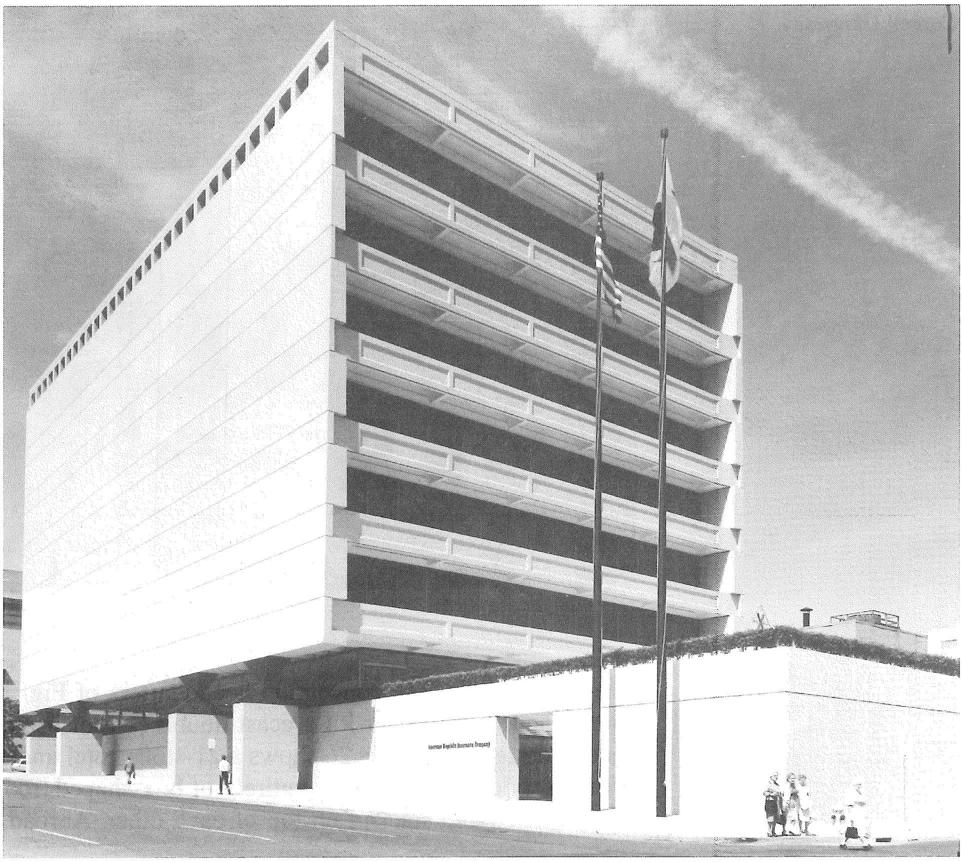

FIGURE 18.25
Precast roof and wall panels combined with cast-in-place frames and floor slabs. (*Courtesy of Portland Cement Association.*)

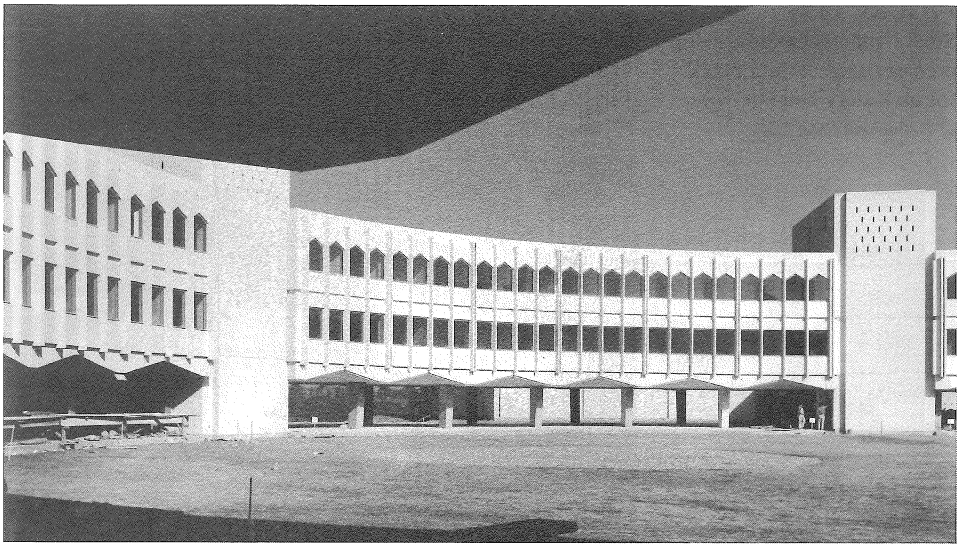

FIGURE 18.26
Precast room-sized modules for a 21-story hotel. (*Courtesy of Portland Cement Association.*)

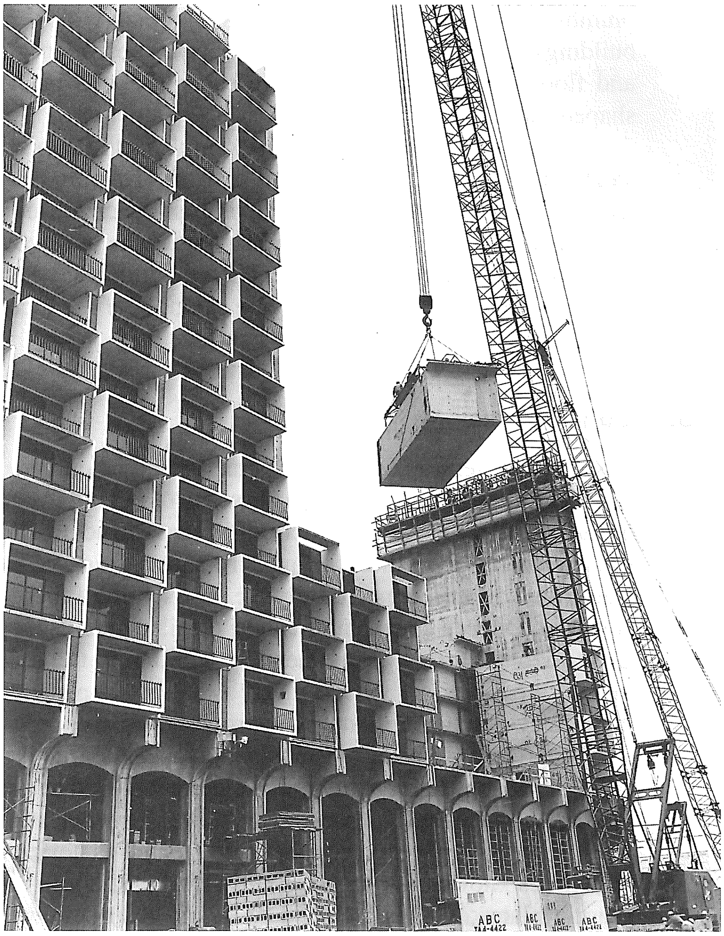

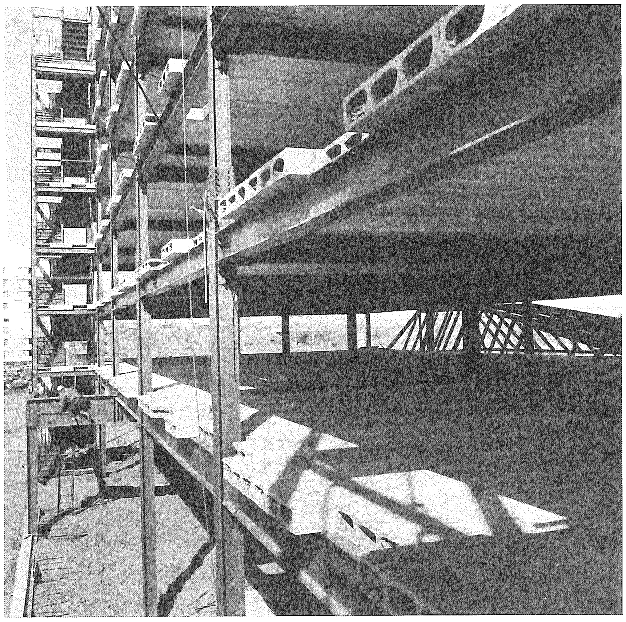

FIGURE 18.27
Steel framing combined with precast concrete floor planks for an 8-story hotel. (*Courtesy of Bethlehem Steel Co.*)

plumbing, wiring, and heating preinstalled, are widely used for multistory apartment buildings as an alternative to making similar apartment structures in precast wall, roof, and floor panels, which are more easily shipped but less easily erected than box-shaped modules.

Finally, Fig. 18.27 shows an example of the frequent combined use of structural steel with precast concrete. In this case, the framing of an eight-story hotel was done using bolted structural steel, while precast concrete floor and roof planks and precast wall panels were used for all other main structural components. This type of construction is economical for 6 to 12-story buildings, where it provides savings in both cost and construction time. It is one example of the increasingly important combined use of various structural materials and methods.

b. Connections

Cast-in-place reinforced concrete structures, by their very nature, tend to be monolithic and continuous. Connections, in the sense of joining two hitherto separate pieces, rarely occur in that type of construction. Precast structures, on the other hand, resemble steel construction in that the final structure consists of large numbers of prefabricated elements that are connected on site to form the finished structure. In both types of construction, such connections can be detailed to transmit gravity forces only, or gravity and horizontal forces, or moments in addition to these forces. In the last case, a continuous structure is obtained much as in cast-in-place construction, and connections that achieve such continuity by appropriate use of special hardware, reinforcing steel, and concrete to transmit all tension, compression, and shear stresses are sometimes called *hard* connections. In contrast, connections that transmit reactions in one direction only, analogous to rockers or rollers in steel structures, but permit a limited amount of motion to relieve other forces, such as horizontal reaction components, are sometimes known as *soft* connections (Ref. 18.15). In almost all precast connections, bearing plates or pads are used to ensure distribution and reasonable uniformity of bearing pressures. Bearing plates are made of steel, while bearing pads are made of materials such as chloroprene, fiber-reinforced polymers, and Teflon. If bearing plates are used, and the plates on two members are suitably joined by welding or other means, a hard connection is obtained in the sense that horizontal, as well as vertical, forces are transmitted. On the other hand, bearing pads transmit gravity loads but can permit sizable horizontal deformations and, thus, relieve horizontal forces.

Precast concrete structures are subject to dimensional changes from creep, shrinkage, and relaxation of prestress in addition to temperature, while in steel structures only temperature changes produce dimensional variations. In the early development of precast construction, there was a tendency to use soft connections extensively to permit these dimensional changes to occur without causing restraint forces in the members, and particularly in the connections. Subsequent experience, however, has shown that the resulting structures possess insufficient stability against lateral forces, such as high wind and, particularly, earthquake effects. Therefore, current practice emphasizes the use of hard connections that provide a high degree of continuity (Refs. 18.12 and 18.16). When designing hard connections, provisions must be made to resist the restraint forces that are caused by the previously described volume changes (Ref. 18.12). Considerable information concerning this and other matters relating to connections is found in Refs. 18.12 and 18.16.

Bearing stresses on plain concrete are limited by ACI Code 10.14.1 to $0.85\phi f'_c$, except when the supporting area is wider on all sides than the loaded area A_1. In such a case this value of the permissible bearing stress may be multiplied by $\sqrt{A_2/A_1}$ but not more than 2.0, where A_2 is the maximum portion of the supporting surface that is geometrically similar to and concentric with the loading area (see Section 16.6b).

In the design of connections, it is prudent to use load factors that exceed those required for the connected members. This is so because connections are generally subject to high stress concentrations that preclude the development of much ductility. In contrast, the members connected are likely to possess considerable ductility if designed by usual ACI Code procedures and will give warning of impending collapse if overloading should take place. In addition, imperfections in connection geometry may cause large changes in the magnitude of stresses compared with those assumed in the design.

In designing members according to the ACI Code, load factors of 1.2 and 1.6 are applied to dead and live loads, D and L respectively, to determine the required strength. When volume change effects T are considered, they are normally treated as dead load, and the factored load U is calculated from the equation $U = 1.2(D + T) + 1.6L$.

A wide variety of connection details for precast concrete building components have evolved, only a few of which will be shown here as more or less representative connections. Many additional possibilities are described fully in Refs. 18.12 and 18.16.

Column base connections are generally accomplished using steel base plates that are anchored into the precast column. Figure 18.28*a* shows a column base detail with projecting base plate. Four anchor bolts are used, with double nuts facilitating erection and leveling of the column. Typically a minimum of 50 mm of nonshrink grout is used between the top of the pier, footing, or wall and the bottom of the steel base plate. Column reinforcement is welded to the top face of the base plate. Tests have confirmed that such column connections can transmit the full moment for which the column is designed, if properly detailed.

An alternative base detail is shown in Fig. 18.28*b*, with the dimensions of the base plate the same as, or slightly smaller than, the outside column dimensions. Anchor bolt pockets are provided, either centered on the column faces as shown or located at the corners. Bolt pockets are grouted after the nuts are tightened. Column

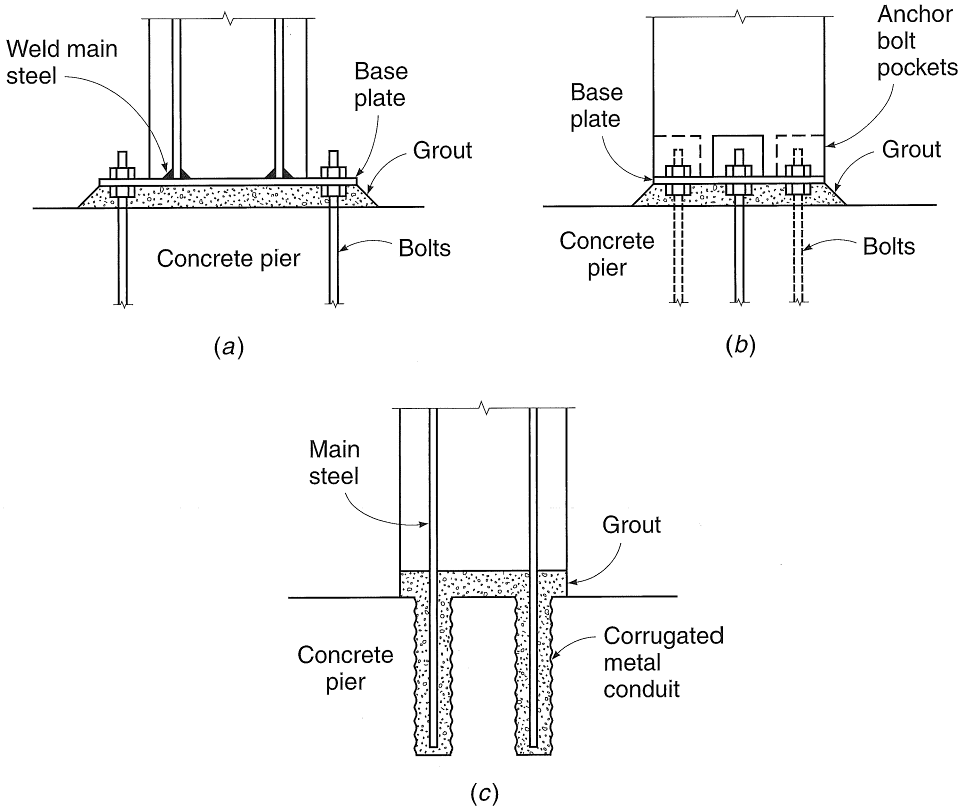

FIGURE 18.28
Column base connections.

bars, not shown here, would be welded to the top face of the base plate as before. Figure 18.29 shows the base plate detail, similar to Fig. 18.28*b*, that was used for the precast three-story columns in the parking garage shown in Fig. 18.22.

In Fig. 18.28*c*, the main column bars project from the ends of the precast member a sufficient distance to develop their strength by bond. The projecting bars are inserted into grout-filled holes cast in the foundation when it is placed.

In all of the cases shown, confining steel should be provided around the anchor bolts in the form of closed ties. A minimum of four No. 10 (No. 3) ties is recommended, placed on 75 mm centers near the top surface of the pier or wall. Tie reinforcement in the columns should be provided as usual.

Figure 18.30 shows several *beam-to-column* connections. In all cases, rectangular beams are shown, but similar details apply to I or T beams. The figure shows only the basic geometry; and auxiliary reinforcement, anchors, and ties are omitted for the sake of clarity.

Figure 18.30*a* shows a joint detail with a concealed haunch. Well-anchored bearing angles are provided at the column seat and beam end. This type of connection may be used to provide vertical and horizontal reaction components, and with the addition of post-tensioned prestressing, will provide moment resistance as well.

Figure 18.30*b* shows a typical bracket, common for industrial construction where the projecting bracket is not objectionable. The seat angle is welded to reinforcing bars anchored in the column. A steel bearing plate is used at the bottom of the beam and anchored into the concrete.

The embedded steel shape in Fig. 18.30*c* is used when it is necessary to avoid projections beyond the face of the column or below the bottom of the beam. A socket

FIGURE 18.29
Detail at base of precast column of Cornell University parking garage shown in Fig. 18.22.

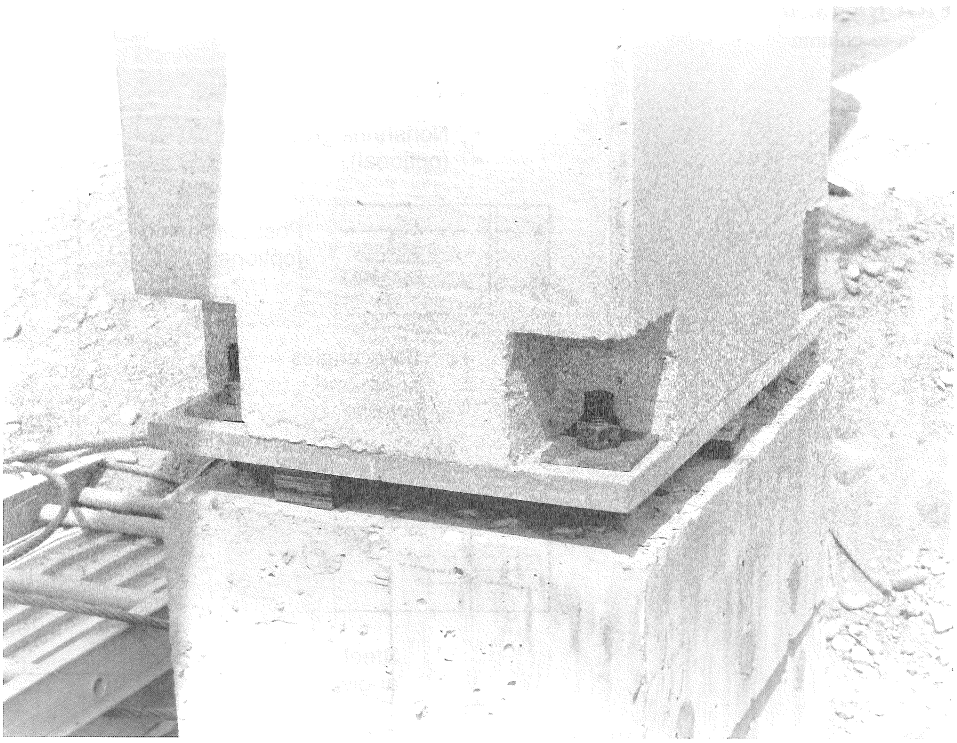

is formed in casting the beam, with steel angle or plate at its top, to receive the beam stub. A steel connection can also be used in place of the bracket shown in Fig. 18.30*b*.

Finally, Fig. 18.30*d* shows a doweled connection with bars projecting from the column into holes formed in the beam ends. These are grouted after the beams are in position. This connection is popular in precast concrete construction but has little flexural capacity (Ref. 18.17).

Figure 18.31 shows several typical *column-to-column* connections. Figure 18.31*a* shows a detail using anchor bolt pockets and a double-nut system for leveling the upper column. Bolts can also be located at the center of the column faces, as shown in Fig. 18.28*b*. The detail shown in Fig. 18.31*b* permits the main steel to be lap-spliced with that in the column below. One of the many possibilities for splicing a column through a continuous beam is shown in Fig. 18.31*c*. Main reinforcing bars in both upper and lower columns should be welded to steel cap and base plates to transfer their load, and anchor bolts should be designed with the same consideration. Closely spaced ties must be provided in the columns and in this case in the beam as well, to transfer the load between columns.

Slab-to-beam connections generally use some variation of the detail shown in Fig. 18.32. Support is provided by an L beam (Fig. 18.32*a*) or an inverted T beam (Fig. 18.32*b*) that is flush with the top of the precast floor planks. The detail shown is sufficient if no mechanical tie is required between the precast parts. Where a positive connection is required, steel plates are set into the top of the members, suitably anchored, and short connecting plates are welded so as to attach the built-in plates.

Basic tools for the design of precast concrete connections are the *shear friction design method* described in detail in Chapter 4 and the *strut-and-tie model* described in Chapter 10. Example 4.6 (Section 4.9) demonstrated the use of the shear-friction

FIGURE 18.30
Beam-to-column connections.

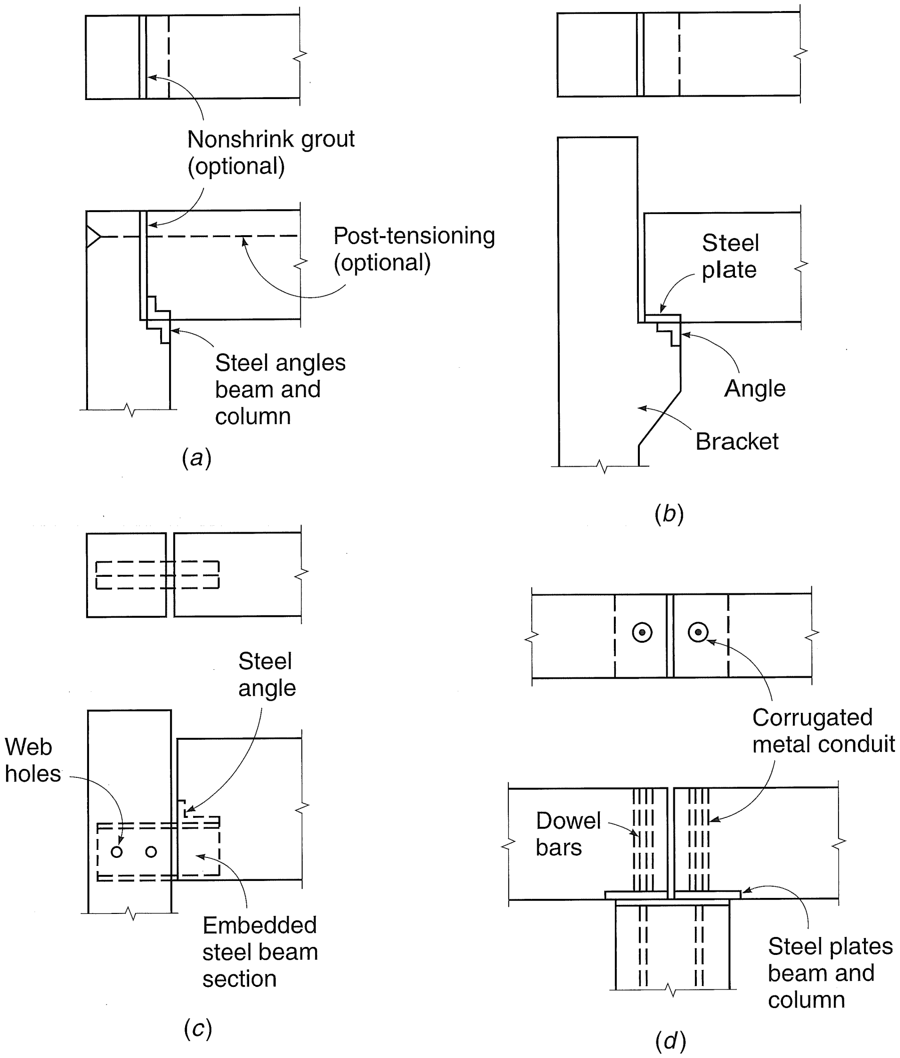
Nonshrink grout (optional)
Post-tensioning (optional)
Steel angles beam and column
(a)
Steel plate
Angle
Bracket
(b)
Steel angle
Web holes
Embedded steel beam section
(c)
Corrugated metal conduit
Dowel bars
Steel plates beam and column
(d)

approach to determining the reinforcement for the end-bearing region of a precast concrete girder. The use of both the shear-friction method and a strut-and-tie model for joint behavior was shown in Section 11.7, and Example 11.5 presented the detailed design of a bracket for a precast concrete column. Additional design information pertaining to precast concrete connection design will be found in Refs. 18.12, 18.15, and 18.16.

c. Structural Integrity

Precast concrete structures normally lack the joint continuity and high degree of redundancy characteristic of monolithic, cast-in-place reinforced concrete construction. Progressive collapse in the event of abnormal loading, in which the failure of one element leads to the collapse of another, then another, can produce catastrophic results. For this reason, the structural integrity of precast concrete structures is specifically addressed in ACI Code 16.5. ACI Code 16.5.1 does not permit the use of “soft” connections that rely solely on friction caused by gravity forces. Full moment-resisting

FIGURE 18.31
Column-to-column connections.

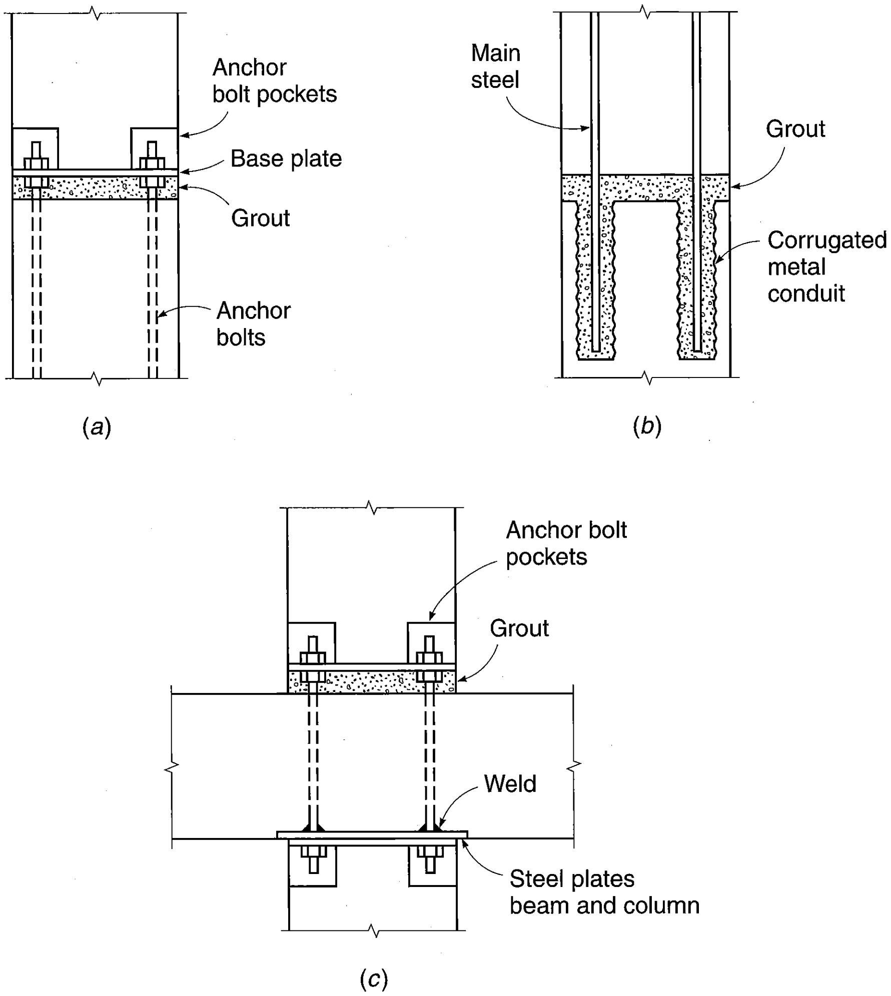
Anchor bolt pockets
Base plate
Grout
Anchor bolts
(a)
Main steel
Grout
Corrugated metal conduit
(b)
Anchor bolt pockets
Grout
Weld
Steel plates beam and column
(c)

FIGURE 18.32
Slab-to-beam connections.

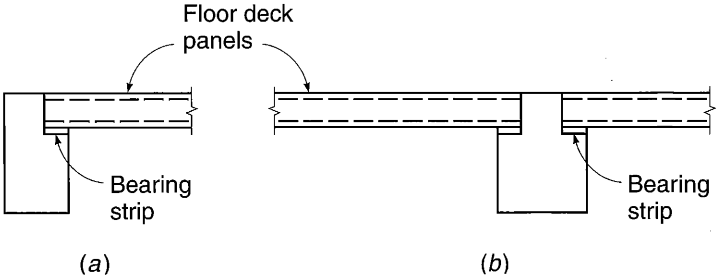
Floor deck panels
Bearing strip
Bearing strip
(a)
(b)

connections are unusual, but some positive means of connecting members to their supports, with due regard to the need to accommodate dimensional changes associated with creep, shrinkage, and temperature effects, is strongly recommended.

In addition, experience with precast structures has shown that the introduction of special reinforcement in the form of tension ties, though adding little to the cost of construction, can contribute greatly to maintaining structural integrity in the event of extraordinary loading, such as loads caused by extreme winds, earthquake, or explosion. This tension reinforcement is best arranged in a three-dimensional grid, usually on the column lines, tying the floors together vertically and in both horizontal directions. For precast concrete construction, ACI Code 7.13.3 and 16.5.1 require that tension ties be provided in the transverse, longitudinal, and vertical directions of the structure and around its perimeter. Specific details vary widely. Although no specific guidance is offered in either the ACI Code or Commentary regarding steel placement or design forces, valuable suggestions will be found in Refs. 18.11, 18.12, and 18.16.

18.6 ENGINEERING DRAWINGS FOR BUILDINGS

Design information is conveyed to the builder mainly by engineering drawings. Their preparation is therefore a matter of the utmost importance, and they should be carefully checked by the design engineer to ensure that concrete dimensions and reinforcement agree with the calculations.

Engineering drawings for buildings usually consist of a plan view of each floor showing overall dimensions and locating the main structural elements, cross-sectional views through typical members, and beam and slab schedules that give detailed information on the concrete dimensions and reinforcement in tabular form. Sectional views are usually drawn to a larger scale than the plan and serve to locate the steel and establish cutoff and bend points as well as to define the shape of the member. Usually a separate drawing is included that gives, in the form of schedules and cross sections, the details of columns and footings.

The contract documents, including the plans, specifications, and cost estimates, provide detailed descriptions of the material strengths. Additionally, many building officials, particularly in active seismic regions, require a description of the structural framing system, lateral load-resisting system, and design live loads to be included on the structural drawings. Typical concrete design drawings and details will be found in Ref. 18.4.

REFERENCES

18.1. ACI Committee 216, *Code Requirements for Determining Fire Resistance of Concrete and Masonry Construction Assemblies*, ACI 216.1-07, American Concrete Institute, Farmington Hills, MI, 2007.

18.2. E. S. Hoffman, D. P. Gustafson, and A. J. Gouwens, *Structural Design Guide for the ACI Building Code*, Kluwer Academic Publishers, Boston, 1998.

18.3. *CRSI Design Handbook*, 10th ed., Concrete Reinforcing Steel Institute, Schaumburg, IL, 2008.

18.4. *ACI Detailing Manual*, ACI Special Publication SP-66, American Concrete Institute, Farmington Hills, MI, 1994.

18.5. ACI Committee 352, *Recommendations for Design of Beam-Column Joints in Monolithic Reinforced Concrete Structures,* ACI 352R-02, American Concrete Institute, Farmington Hills, MI, 2002.

18.6. S. Ravikumar, D. Darwin, S. L. McCabe, and G. P. Pasley, "Shear Strength of Continuous Lightly Reinforced Concrete Joist Systems," *SM Report* No. 37, University of Kansas Center for Research, Lawrence, March 1994.

18.7. L. E. Svab and R. E. Jurewicz, "Wide Module Concrete Joist Construction," *Concr. Intl.*, vol. 12, no. 11, 1990, pp. 39–42.

18.8. C. F. Scribner and C. G. Culver, "Investigation of the Collapse of L'Ambiance Plaza," *J. Perform. Construct. Facil.* ASCE, vol. 2, no. 2, 1988, pp. 58–79.

18.9. A. E. Cardenas, J. M. Hanson, W. G. Corley, and E. Hognestad, "Design Provisions for Shear Walls," *J. ACI*, vol. 70, no. 3, 1973, pp. 221–230.

18.10. A. E. Cardenas and D. D. Magura, "Strength of High-Rise Shear Walls: Rectangular Cross Section," pp. 119–150 in *Response of Multistory Structures to Lateral Forces*, SP-36, American Concrete Institute, Farmington Hills, MI, 1973.

18.11. ACI Committee 550, "Design Recommendations for Precast Concrete Structures," ACI 550R-96, *Manual of Concrete Practice*, Part 6, American Concrete Institute, Farmington Hills, MI, 2008.
18.12. *PCI Design Handbook*, 6th ed., Precast/Prestressed Concrete Institute, Chicago, 2004.
18.13. K. M. Kripanarayanan and M. Fintel, "Analysis and Design of Slender Tilt-Up Reinforced Concrete Wall Panels," *J. ACI*, vol. 71, no. 1, 1974, pp. 20–28.
18.14. ACI Committee 533, "Guide for Precast Concrete Wall Panels," ACI 533R-93, *Manual of Concrete Practice*, Part 6, American Concrete Institute, Farmington Hills, MI, 2008.
18.15. P. W. Birkland and H. W. Birkland, "Connections in Precast Concrete Construction," *J. ACI*, vol. 63, no. 3, 1966, pp. 345–368.
18.16. PCI Committee on Connection Details, *Design and Typical Details of Connections for Precast and Prestressed Concrete,* MNL-123-88, Precast/Prestressed Concrete Institute, Chicago, 1988.
18.17. C. W. Dolan, J. F. Stanton, and R. G. Anderson, "Moment Resistant Connections and Simple Connections," *J. Precast/Prestressed Concr. Inst.*, vol. 32, no. 2, 1987, pp. 62–74.

19 Prestressed Concrete

19.1 INTRODUCTION

Modern structural engineering tends to progress toward more economical structures through gradually improved methods of design and the use of higher-strength materials. This results in a reduction of cross-sectional dimensions and consequent weight savings. Such developments are particularly important in the field of reinforced concrete, where the dead load represents a substantial part of the total load. Also, in multistory buildings, any saving in depth of members, multiplied by the number of stories, can represent a substantial saving in total height, load on foundations, length of heating and electrical ducts, plumbing risers, and wall and partition surfaces.

Significant savings can be achieved by using high-strength concrete and steel in conjunction with present-day design methods, which permit an accurate appraisal of member strength. However, there are limitations to this development, due mainly to the interrelated problems of cracking and deflection at service loads. The efficient use of high-strength steel is limited by the fact that the amount of cracking (width and number of cracks) is proportional to the strain, and therefore the stress, in the steel. Although a moderate amount of cracking is normally not objectionable in structural concrete, excessive cracking is undesirable in that it exposes the reinforcement to corrosion, it may be visually offensive, and it may trigger a premature failure by diagonal tension. The use of high-strength materials is further limited by deflection considerations, particularly when refined analysis is used. The slender members that result may permit deflections that are functionally or visually unacceptable. This is further aggravated by cracking, which reduces the flexural stiffness of members.

These limiting features of ordinary reinforced concrete have been largely overcome by the development of prestressed concrete. A prestressed concrete member can be defined as one in which there have been introduced internal stresses of such magnitude and distribution that the stresses resulting from the given external loading are counteracted to a desired degree. Concrete is basically a compressive material, with its strength in tension being relatively low. Prestressing applies a precompression to the member that reduces or eliminates undesirable tensile stresses that would otherwise be present. Cracking under service loads can be minimized or even avoided entirely. Deflections may be limited to an acceptable value; in fact, members can be designed to have zero deflection under the combined effects of service load and prestress force. Deflection and crack control, achieved through prestressing, permit the engineer to make use of efficient and economical high-strength steels in the form of strands, wires, or bars, in conjunction with concretes of much higher strength than normal. Thus, prestressing results in the overall improvement in performance of structural concrete used for ordinary loads and spans and extends the range of application far beyond the limits for ordinary reinforced concrete, not only leading to much longer spans than previously thought possible, but also permitting innovative new structural forms to be employed.

19.2 EFFECTS OF PRESTRESSING

There are at least three ways to look at the prestressing of concrete: (a) as a method of achieving *concrete stress control,* by which the concrete is precompressed so that tension normally resulting from the applied loads is reduced or eliminated, (b) as a means for introducing *equivalent loads* on the concrete member so that the effects of the applied loads are counteracted to the desired degree, and (c) as a *special variation of reinforced concrete* in which prestrained high-strength steel is used, usually in conjunction with high-strength concrete. Each of these viewpoints is useful in the analysis and design of prestressed concrete structures, and they will be illustrated in the following paragraphs.

a. Concrete Stress Control by Prestressing

Many important features of prestressed concrete can be demonstrated by simple examples. Consider first the plain, unreinforced concrete beam with a rectangular cross section shown in Fig. 19.1*a*. It carries a single concentrated load at the center of its span. (The self-weight of the member will be neglected here.) As the load W is gradually applied, longitudinal flexural stresses are induced. If the concrete is stressed only within its elastic range, the flexural stress distribution at midspan will be linear, as shown.

At a relatively low load, the tensile stress in the concrete at the bottom of the beam will reach the tensile strength of the concrete f_r, and a crack will form. Because no restraint is provided against upward extension of the crack, the beam will collapse without further increase of load.

Now consider an otherwise identical beam, shown in Fig. 19.1*b*, in which a longitudinal axial force P is introduced prior to the vertical loading. The longitudinal prestressing force will produce a uniform axial compression $f_c = P/A_c$, where A_c is the cross-sectional area of the concrete. The force can be adjusted in magnitude so that when the transverse load Q is applied, the superposition of stresses due to P and Q will result in zero tensile stress at the bottom of the beam as shown. Tensile stress in the concrete may be eliminated in this way or reduced to a specified amount.

It would be more logical to apply the prestressing force near the bottom of the beam, to compensate more effectively for the load-induced tension. A possible design specification, for example, might be to introduce the maximum compression at the bottom of the beam without causing tension at the top, when only the prestressing force acts. It is easily shown that, for a beam with a rectangular cross section, the point of application of the prestressing force should be at the lower third point of the section depth to achieve this. The force P, with the same value as before, but applied with eccentricity $e = h/6$ relative to the concrete centroid, will produce a longitudinal compressive stress distribution varying linearly from zero at the top surface to a maximum of $2f_c = P/A_c + Pec_2/I_c$ at the bottom, where f_c is the concrete stress at the concrete centroid, c_2 is the distance from the concrete centroid to the bottom

FIGURE 19.1
Alternative schemes for prestressing a rectangular concrete beam: (*a*) plain concrete beam; (*b*) axially prestressed beam; (*c*) eccentrically prestressed beam; (*d*) beam with variable eccentricity; (*e*) balanced load stage for beam with variable eccentricity.

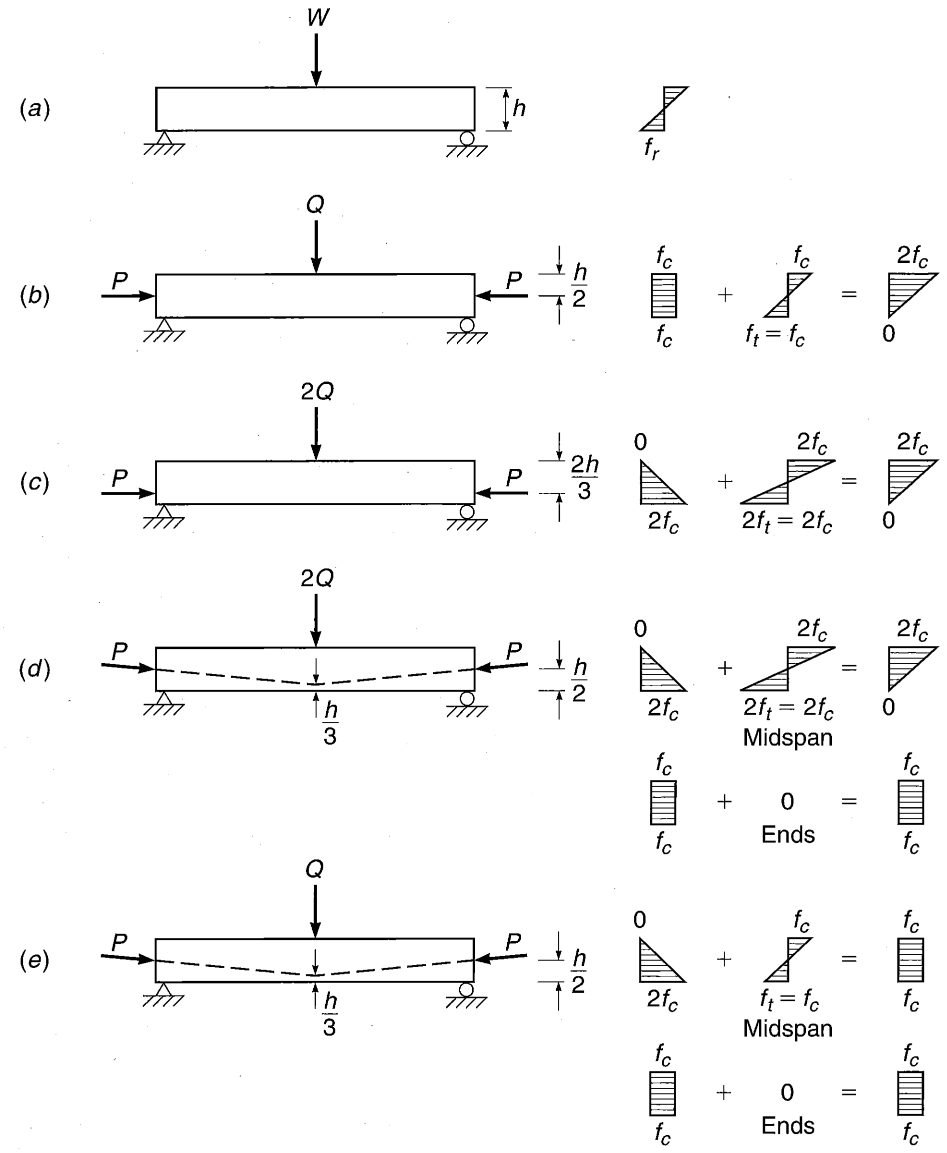
W
(a)
h
fr
Q
(b)
P
P
h/2
fc
fc
+
fc
ft = fc
=
2fc
0
2Q
(c)
P
P
2h/3
0
2fc
+
2fc
2ft = 2fc
=
2fc
0
2Q
(d)
P
P
h/3
h/2
0
2fc
+
2fc
2ft = 2fc
Midspan
=
2fc
0
fc
fc
+
0
Ends
=
fc
fc
Q
(e)
P
P
h/3
h/2
0
2fc
+
fc
ft = fc
Midspan
=
fc
fc
fc
fc
+
0
Ends
=
fc
fc

of the beam, and I_c is the moment of inertia of the cross section. This is shown in Fig. 19.1*c*. The stress at the bottom will be exactly twice the value produced before by axial prestressing.

Consequently, the transverse load can now be twice as great as before, or $2Q$, and still cause no tensile stress. In fact, the final stress distribution resulting from the superposition of load and prestressing force in Fig. 19.1*c* is identical to that of Fig. 19.1*b*, with the same prestressing force, although the load is twice as great. The advantage of eccentric prestressing is obvious.

The methods by which concrete members are prestressed will be discussed in Section 19.3. For present purposes, it is sufficient to know that one practical method of prestressing uses high-strength steel tendons passing through a conduit embedded in the concrete beam. The tendon is anchored, under high tension, at both ends of the beam, thereby causing a longitudinal compressive stress in the concrete. The prestress force of Fig. 19.1*b* and *c* could easily have been applied in this way.

A significant improvement can be made, however, by using a prestressing tendon with variable eccentricity with respect to the concrete centroid, as shown in Fig. 19.1*d*. The load $2Q$ produces a bending moment that varies linearly along the span, from zero at the supports to maximum at midspan. Intuitively, one suspects that the best arrangement of prestressing would produce a *countermoment* that acts in the opposite sense to the load-induced moment and that would vary in the same way. This would be achieved by giving the tendon an eccentricity that varies linearly, from zero at the supports to maximum at midspan. This is shown in Fig. 19.1*d*. The stresses at midspan are the same as those in Fig. 19.1*c*, both when the load $2Q$ acts and when it does not. At the supports, where only the prestress force with zero eccentricity acts, a uniform compression stress f_c is obtained as shown.

For each characteristic load distribution, there is a *best tendon profile* that produces a prestress moment diagram that corresponds to that of the applied load. If the prestress countermoment is made exactly equal and opposite to the load-induced moment, the result is a beam that is subject only to uniform axial compressive stress in the concrete all along the span. Such a beam would be free of flexural cracking, and theoretically it would not be deflected up or down when that particular load is in place, compared to its position as originally cast. Such a result would be obtained for a load of $\frac{1}{2} \times 2Q = Q$, as shown in Fig. 19.1*e*, for example.

Some important conclusions can be drawn from these simple examples as follows:

1. Prestressing can control or even eliminate concrete tensile stress for specified loads.
2. Eccentric prestress is usually much more efficient than concentric prestress.
3. Variable eccentricity is usually preferable to constant eccentricity, from the viewpoints of both stress control and deflection control.

b. Equivalent Loads

The effect of a change in the vertical alignment of a prestressing tendon is to produce a vertical force on the concrete beam. That force, together with the prestressing force acting at the ends of the beam through the tendon anchorages, can be looked upon as a system of external loads.

In Fig. 19.2*a*, for example, a tendon that applies force P at the centroid of the concrete section at the ends of a beam and that has a uniform slope at angle θ between the ends and midspan introduces a transverse force $2P \sin \theta$ at the point of change of slope at midspan. At the anchorages, the vertical component of the prestressing force is $P \sin \theta$ and the horizontal component is $P \cos \theta$. The horizontal component is very nearly equal to P for the usual flat slope angles. The moment diagram for the beam of Fig. 19.2*a* is seen to have the same form as that for any center-loaded simple span.

The beam of Fig. 19.2*b*, with a curved tendon, is subject to a vertical upward load from the tendon as well as the forces P at each end. The exact distribution of the load depends on the profile of the tendon. A tendon with a parabolic profile, for example, will produce a uniformly distributed load. In this case, the moment diagram will be parabolic, as it is for a uniformly loaded simple span.

If a straight tendon is used with constant eccentricity, as shown in Fig. 19.2*c*, there are no vertical forces on the concrete, but the beam is subject to a moment Pe at each end, as well as the axial force P, and a diagram of constant moment results.

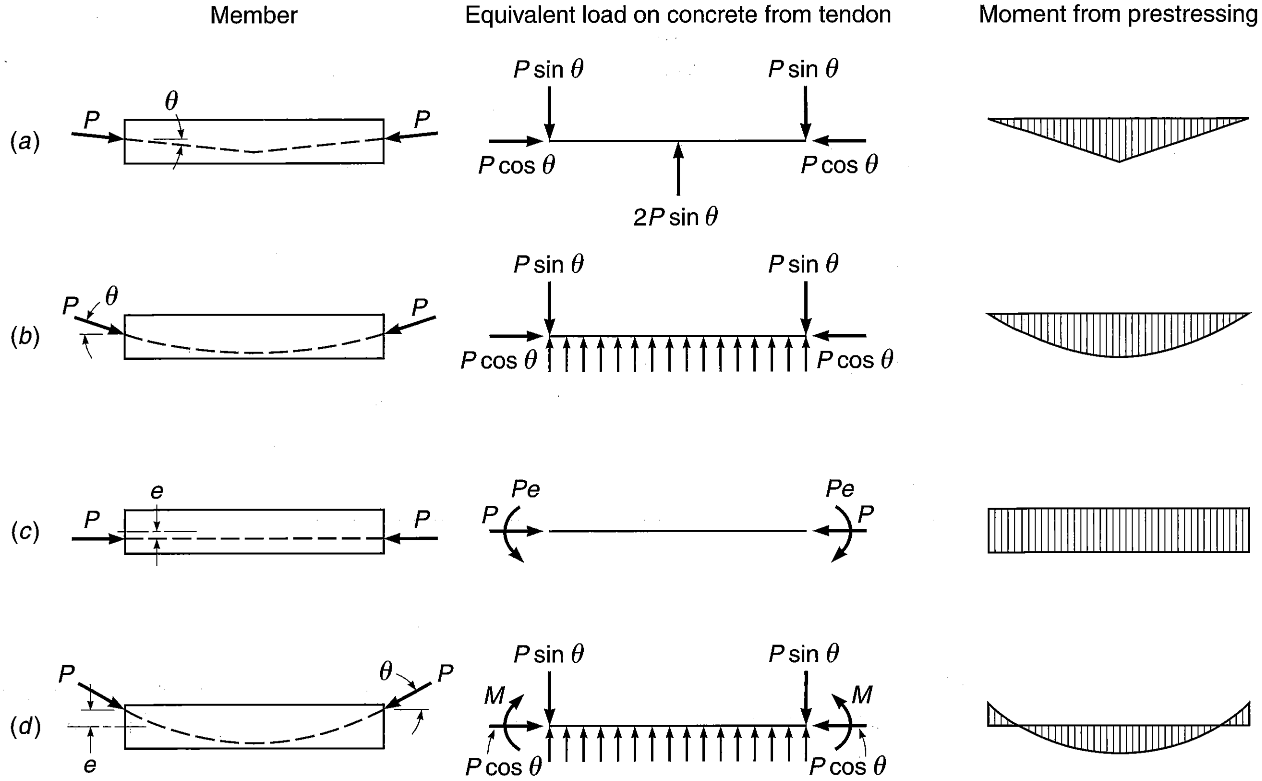
Member
Equivalent load on concrete from tendon
Moment from prestressing
(a)
P
θ
P
P sin θ
P sin θ
P cos θ
P cos θ
2P sin θ
(b)
P
θ
P
P sin θ
P sin θ
P cos θ
P cos θ
(c)
e
P
P
Pe
Pe
P
P
(d)
P
θ
P
e
P sin θ
P sin θ
M
M
P cos θ
P cos θ

FIGURE 19.2
Equivalent loads and moments produced by prestressing tendons.

The end moment must also be accounted for in the beam shown in Fig. 19.2*d*, in which a parabolic tendon is used that does not pass through the concrete centroid at the ends of the span. In this case, a uniformly distributed upward load plus end anchorage forces are produced, as shown in Fig. 19.2*b*, but in addition, the end moments $M = Pe \cos \theta$ must be accounted for.

It may be evident that for any arrangement of applied loads, a tendon profile can be selected so that the equivalent loads acting on the beam from the tendon are just equal and opposite to the applied loads. The result would be a state of pure compressive stress in the concrete, as discussed in somewhat different terms in reference to stress control and Fig. 19.1*e*. An advantage of the equivalent load concept is that it leads the designer to select what is probably the best tendon profile for a particular loading.

c. Prestressed Concrete as a Variation of Reinforced Concrete

In the descriptions of the effects of prestressing in Sections 19.2a and b, it was implied that the prestress force remained constant as the vertical load was introduced, that the concrete responded elastically, and that no concrete cracking occurred. These conditions may prevail up to about the service load level, but if the loads should be increased much beyond that, flexural tensile stresses will eventually exceed the modulus of rupture and cracks will form. Loads, however, can usually be increased much beyond the cracking load in well-designed prestressed beams, and

FIGURE 19.3
Prestressed concrete beam at load near flexural failure: (*a*) beam with factored load applied; (*b*) equilibrium of forces on left half of beam.

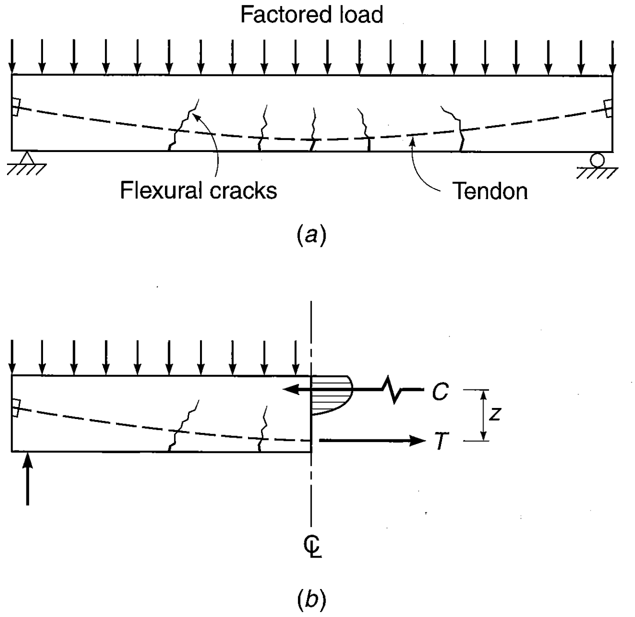

depending on the level of prestress, the beam response at service load may vary from uncracked, to minor cracking, to fully cracked, as occurs for an ordinary reinforced concrete beam.

Eventually both the steel and concrete at the cracked section will be stressed into the inelastic range. The condition at incipient failure is shown in Fig. 19.3, which shows a beam carrying a *factored load* equal to some multiple of the expected service load. The beam undoubtedly would be in a partially cracked state; a possible pattern of flexural cracking is shown in Fig. 19.3*a*.

At the maximum moment section, only the concrete in compression is effective, and all of the tension is taken by the steel. The external moment from the applied loads is resisted by the internal force couple $Cz = Tz$. The behavior at this stage is almost identical to that of an ordinary reinforced concrete beam at overload. The main difference is that the very high strength steel used must be *prestrained* before loads are applied to the beam; otherwise, the high steel stresses would produce excessive concrete cracking and large beam deflections.

Each of the three viewpoints described—concrete stress control, equivalent loads, and reinforced concrete using prestrained steel—is useful in the analysis and design of prestressed concrete beams, and none of the three is sufficient in itself. Neither an elastic stress analysis nor an equivalent load analysis provides information about strength or safety margin. However, the stress analysis is helpful in predicting the extent of cracking, and the equivalent load analysis is often the best way to calculate deflections. Strength analysis is essential to evaluate safety against collapse, but it tells nothing about cracking or deflections of the beam under service conditions.

19.3 SOURCES OF PRESTRESS FORCE

Prestress can be applied to a concrete member in many ways. Perhaps the most obvious method of precompressing is to use jacks reacting against abutments, as shown in Fig. 19.4*a*. Such a scheme has been employed for large projects. Many variations are

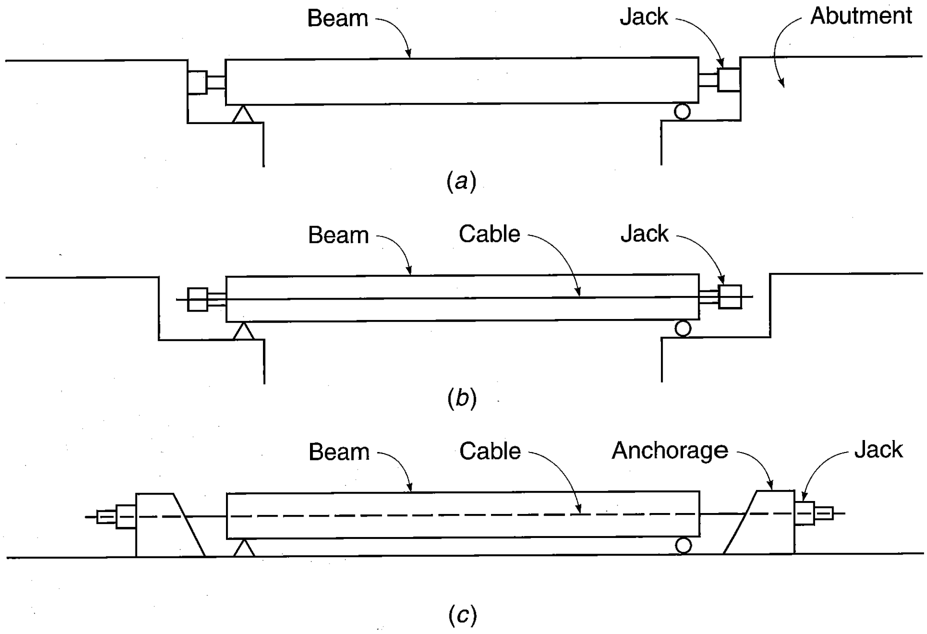

FIGURE 19.4
Prestressing methods: (*a*) post-tensioning by jacking against abutments; (*b*) post-tensioning with jacks reacting against beam; (*c*) pretensioning with tendon stressed between fixed external anchorages.

possible, including replacing the jacks with compression struts after the desired stress in the concrete is obtained or using inexpensive jacks that remain in place in the structure, in some cases with a cement grout used as the hydraulic fluid. The principal difficulty associated with such a system is that even a slight movement of the abutments will drastically reduce the prestress force.

In most cases, the same result is more conveniently obtained by tying the jack bases together with wires or cables, as shown in Fig. 19.4*b*. These wires or cables may be external, located on each side of the beam; more usually they are passed through a hollow conduit embedded in the concrete beam. Usually, one end of the prestressing tendon is anchored, and all of the force is applied at the other end. After reaching the desired prestress force, the tendon is wedged against the concrete and the jacking equipment is removed for reuse. In this type of prestressing, the entire system is self-contained and is independent of relative displacement of the supports.

Another method of prestressing that is widely used is illustrated by Fig. 19.4*c*. The prestressing strands are tensioned between massive abutments in a casting yard prior to placing the concrete in the beam forms. The concrete is placed around the tensioned strands, and after the concrete has attained sufficient strength, the jacking pressure is released. This transfers the prestressing force to the concrete by bond and friction along the strands, chiefly at the outer ends.

It is essential, in all three cases shown in Fig. 19.4, that the beam be supported in such a way as to permit the member to shorten axially without restraint so that the prestressing force can be transferred to the concrete.

Other means for introducing the desired prestressing force have been attempted on an experimental basis. Thermal prestressing can be achieved by preheating the steel by electrical or other means. Anchored against the ends of the concrete beam while in the extended state, the steel cools and tends to contract. The prestress force is developed through the restrained contraction. The use of expanding cement in concrete members has been tried with varying success. The volumetric expansion, restrained by steel strands or by fixed abutments, produces the prestress force.

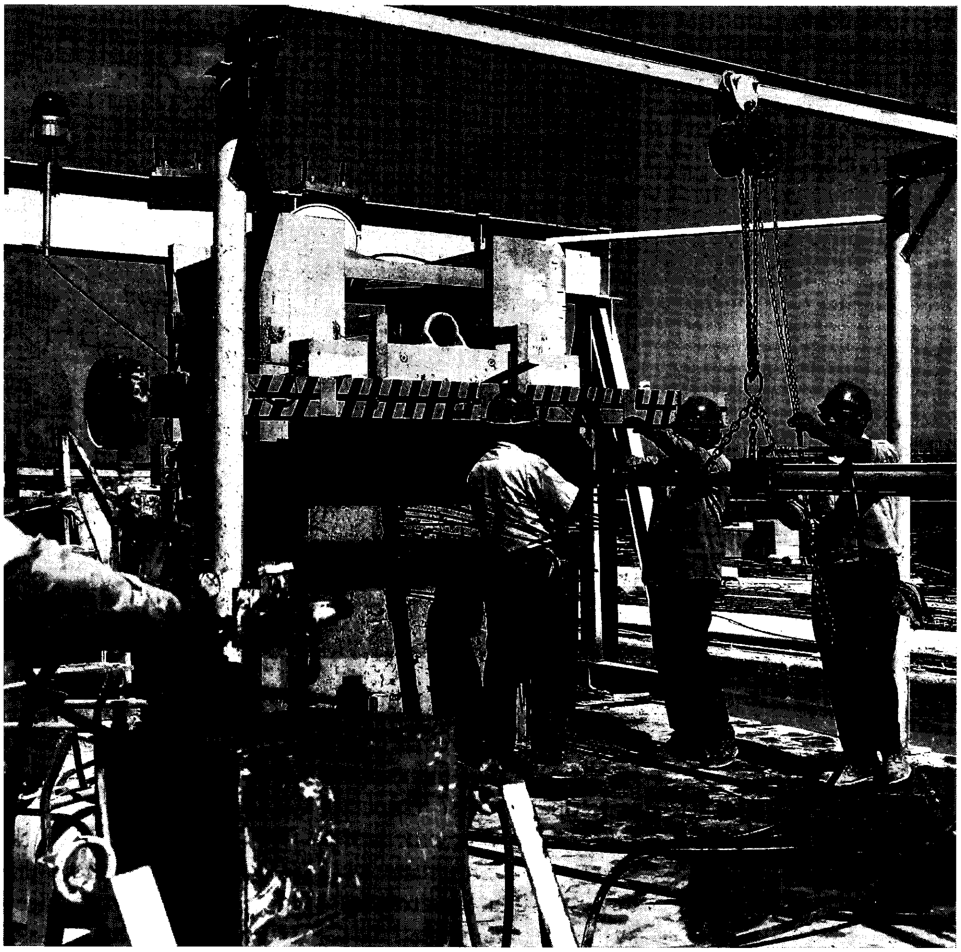

FIGURE 19.5
Massive strand jacking abutment at the end of a long pretensioning bed. (*Courtesy of Concrete Technology Corporation.*)

Most of the patented systems for applying prestress in current use are variations of those shown in Fig. 19.4*b* and *c*. Such systems can generally be classified as *pretensioning* or *post-tensioning* systems. In the case of pretensioning, the tendons are stressed before the concrete is placed, as in Fig. 19.4*c*. This system is well suited for mass production, since casting beds can be made several hundred meters long, the entire length cast at once, and individual beams fabricated to the desired length in a single casting. Figure 19.5 shows workers using a hydraulic jack to tension strands at the anchorage of a long pretensioning bed. Although each tendon is individually stressed in this case, large capacity jacks are often used to tension all strands simultaneously.

In post-tensioned construction, shown in Fig. 19.4*b*, the tendons are tensioned after the concrete is placed and has gained its strength. Usually, a hollow conduit or sleeve is provided in the beam, through which the tendon is passed. In some cases, tendons are placed in the interior of hollow box-section beams. The jacking force is usually applied against the ends of the hardened concrete, eliminating the need for massive abutments. In Fig. 19.6, six tendons, each consisting of many individual strands, are being post-tensioned sequentially using a portable hydraulic jack.

A large number of particular systems, steel elements, jacks, and anchorage fittings have been developed in this country and abroad, many of which differ from each other only in minor details (Refs. 19.1 to 19.8). As far as the designer of prestressed

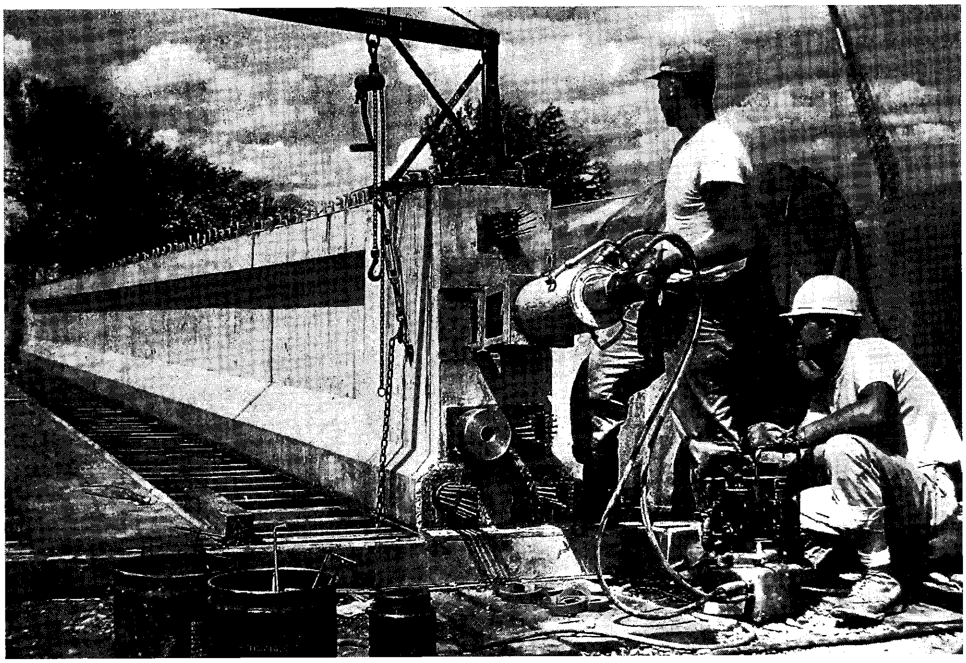

FIGURE 19.6
Post-tensioning a bridge girder using a portable jack to stress multistrand tendons. (*Courtesy of Concrete Technology Corporation.*)

concrete structures is concerned, it is unnecessary and perhaps even undesirable to specify in detail the technique that is to be followed and the equipment to be used. It is frequently best to specify only the magnitude and line of action of the prestress force. The contractor is then free, in bidding the work, to receive quotations from several different prestressing subcontractors, with resultant cost savings. It is evident, however, that the designer must have some knowledge of the details of the various systems contemplated for use, so that in selecting cross-sectional dimensions, any one of several systems can be accommodated.

19.4 PRESTRESSING STEELS

Early attempts at prestressing concrete were unsuccessful because steel with ordinary structural strength was used. The low prestress obtainable in such rods was quickly lost due to shrinkage and creep in the concrete.

Such changes in length of concrete have much less effect on prestress force if that force is obtained using highly stressed steel wires or cables. In Fig. 19.7*a*, a concrete member of length L is prestressed using steel bars with ordinary strength stressed to 160 MPa. With E_s = 200,000 MPa, the unit strain ϵ_s required to produce the desired stress in the steel of 160 MPa is

$$\epsilon_s = \frac{\Delta L}{L} = \frac{f_s}{E_s} = \frac{160}{200{,}000} = 8.0 \times 10^{-4}$$

However, the long-term strain in the concrete due to shrinkage and creep alone, if the prestress force were maintained over a long period, would be on the order of 8.0×10^{-4} and would be sufficient to completely relieve the steel of all stress.

Alternatively, suppose that the beam is prestressed using high-strength steel stressed to 1000 MPa. The elastic modulus of steel does not vary greatly, and the same

FIGURE 19.7
Loss of prestress due to concrete shrinkage and creep.

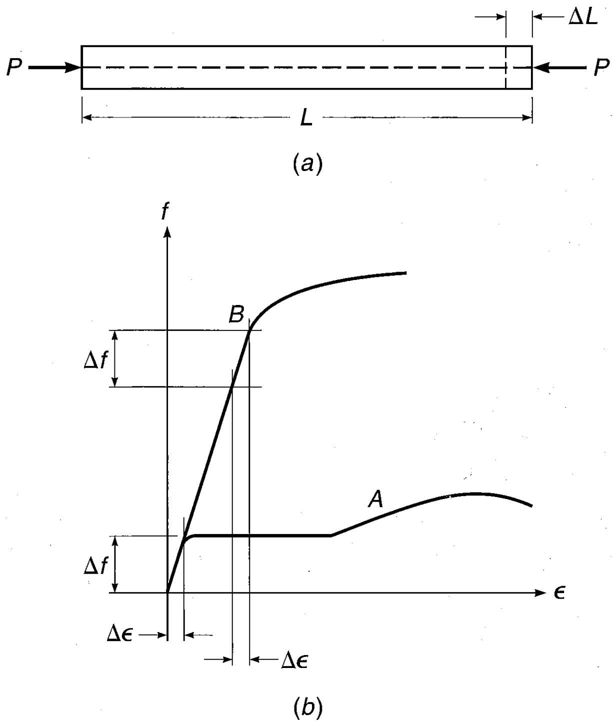

value of 200,000 MPa will be assumed here. Then in this case, the unit strain required to produce the desired stress in the steel is

$$\epsilon_s = \frac{1000}{200{,}000} = 50.0 \times 10^{-4}$$

If shrinkage and creep strain are the same as before, the net strain in the steel after these losses is

$$\epsilon_{s,\text{net}} = (50.0 - 8.0) \times 10^{-4} = 42.0 \times 10^{-4}$$

and the corresponding stress after losses is

$$f_s = \epsilon_{s,\text{net}} E_s = (42.0 \times 10^{-4})(200{,}000) = 840 \text{ MPa}$$

This represents a stress loss of about 15 percent, compared with 100 percent loss in the beam using ordinary steel. It is apparent that the amount of stress lost because of shrinkage and creep is independent of the original stress in the steel. Therefore, the higher the original stress, the lower the percentage loss. This is illustrated graphically by the stress-strain curves of Fig. 19.7*b*. Curve *A* is representative of ordinary reinforcing bars, with a yield stress of 420 MPa, while curve *B* represents high tensile steel, with a tensile strength of 1860 MPa. The stress change Δf resulting from a certain change in strain $\Delta\epsilon$ is seen to have much less effect when high steel stress levels are attained. Prestressing of concrete is therefore practical only when steels of very high strength are used.

Prestressing steel is most commonly used in the form of individual wires, stranded cable (strands) made up of seven wires, and alloy-steel bars. The physical properties of these have been discussed in Section 2.16, and typical stress-strain curves appear in Fig. 2.16. Virtually all strands in use are low-relaxation (Section 2.16c).

TABLE 19.1
Maximum permissible stresses in prestressing steel

1. Due to tendon jacking force but not greater than the lesser of $0.80f_{pu}$ and the maximum value recommended by the manufacturer of the prestressing steel or anchorage devices	$0.94f_{py}$
2. Immediately after prestress transfer but not greater than $0.74f_{pu}$	$0.82f_{py}$
3. Post-tensioning tendons, at anchorage devices and couplers, immediately after tendon anchorage	$0.70f_{pu}$

The tensile stress permitted by ACI Code 18.5 in prestressing wires, strands, or bars is dependent upon the stage of loading. When the jacking force is first applied, a maximum stress of $0.80f_{pu}$ or $0.94f_{py}$ is allowed, whichever is smaller, where f_{pu} is the tensile strength of the steel and f_{py} is the yield strength. Immediately after transfer of prestress force to the concrete, the permissible stress is $0.74f_{pu}$ or $0.82f_{py}$, whichever is smaller (except at post-tensioning anchorages where the stress is limited to $0.70f_{pu}$). The justification for a higher allowable stress during the stretching operation is that the steel stress is known quite precisely at this stage. Hydraulic jacking pressure and total steel strain are quantities that are easily measured, and quality control specifications require correlation of load and deflection at jacking (Ref. 19.9). In addition, if an accidentally deficient tendon should break, it can be replaced; in effect, the tensioning operation is a performance test of the material. The lower values of allowable stress apply after elastic shortening of the concrete, frictional loss, and anchorage slip have taken place. The steel stress is further reduced during the life of the member due to shrinkage and creep in the concrete and relaxation in the steel. ACI allowable stresses in prestressing steels are summarized in Table 19.1.

The strength and other characteristics of prestressing wire, strands, and bars vary somewhat between manufacturers, as do methods of grouping tendons and anchoring them. Typical information is given for illustration in Table A.15 of Appendix A and in Refs. 19.1 to 19.8.

19.5 CONCRETE FOR PRESTRESSED CONSTRUCTION

Ordinarily, concrete of substantially higher compressive strength is used for prestressed structures than for those constructed of ordinary reinforced concrete. Most prestressed construction in the United States at present is designed for a compressive strength above 35 MPa. There are several reasons for this:

1. High-strength concrete normally has a higher modulus of elasticity (see Fig. 2.3). This means a reduction in initial elastic strain under application of prestress force and a reduction in creep strain, which is approximately proportional to elastic strain. This results in a reduction in loss of prestress.
2. In post-tensioned construction, high bearing stresses result at the ends of beams where the prestressing force is transferred from the tendons to anchorage fittings, which bear directly against the concrete. This problem can be met by increasing the size of the anchorage fitting or by increasing the bearing capacity of the concrete by increasing its compressive strength. The latter is usually more economical.
3. In pretensioned construction, where transfer by bond is customary, the use of high-strength concrete will permit the development of higher bond stresses.

TABLE 19.2
Permissible stresses in concrete in prestressed flexural members

	Class		
Condition	**U**	**T**	**C***
a. Extreme fiber stress in compression immediately after transfer (except as in b)	$0.60f'_{ci}$	$0.60f'_{ci}$	$0.60f'_{ci}$
b. Extreme fiber stress in compression at ends of simply supported members	$0.70f'_{ci}$	$0.70f'_{ci}$	$0.70f'_{ci}$
c. Extreme fiber stress in tension immediately after transfer (except as in d)	$0.25\sqrt{f'_{ci}}$	$0.25\sqrt{f'_{ci}}$	$0.25\sqrt{f'_{ci}}$
d. Extreme fiber stress in tension immediately after transfer at the end of simply supported members[†]	$0.5\sqrt{f'_{ci}}$	$0.5\sqrt{f'_{ci}}$	$0.5\sqrt{f'_{ci}}$
e. Extreme fiber stress in compression due to prestress plus sustained load	$0.45f'_c$	$0.45f'_c$	—
f. Extreme fiber stress in compression due to prestress plus total load	$0.60f'_c$	$0.60f'_c$	—
g. Extreme fiber stress in tension f_t in precompressed tensile zone under service load	$\leq 0.62\sqrt{f'_c}$	$>0.62\sqrt{f'_c}$ and $\leq 1.0\sqrt{f'_c}$	—

* There are no service stress requirements for Class C.

[†] When computed tensile stresses exceed these values, bonded auxiliary prestressed or nonprestressed reinforcement shall be provided in the tensile zone to resist the total tensile force in the concrete computed with the assumption of an uncracked section.

4. A substantial part of the prestressed construction in the United States is precast, with the concrete mixed, placed, and cured under carefully controlled conditions that facilitate obtaining higher strengths.

The strain characteristics of concrete under short-term and sustained loads assume an even greater importance in prestressed structures than in reinforced concrete structures because of the influence of strain on loss of prestress force. Strains due to stress, together with volume changes due to shrinkage and temperature changes, may have considerable influence on prestressed structures. In this connection, it is suggested that the reader review Sections 2.8 to 2.11, which discuss in some detail the compressive and tensile strengths of concrete under short-term and sustained loads and the changes in concrete volume that occur due to shrinkage and temperature change.

As for prestressing steels, the allowable stresses in the concrete, according to ACI Code 18.4, depend upon the stage of loading and the behavior expected of the member. ACI Code 18.3.3 defines three classifications of behavior, depending on the extreme fiber stress f_t at service load in the precompressed tensile zone. The three classifications are U, T, and C. Class U flexural members are assumed to behave as uncracked members. Class T members represent a transition between uncracked and cracked flexural members, while Class C members are assumed to behave as cracked flexural members. Permissible stresses for these three classifications are given in Table 19.2.

In Table 19.2, f'_{ci} is the compressive strength of the concrete at the time of initial prestress, and f'_c the specified compressive strength of the concrete. In parts e and f of Table 19.2, *sustained load* is any part of the service load that will be sustained for a sufficient period of time to cause significant time-dependent deflections, whereas *total load* refers to the total service load, a part of which may be transient or temporary live load. Thus, sustained load would include dead load and may or may not include service live load, depending on its duration. If the live load duration is short or intermittent, the higher limit of part f is permitted.

Two-way slabs are designated as Class U flexural members with f_t limited to values $\leq 0.5\sqrt{f'_c}$. Class C flexural members have no service level stress requirements but must satisfy strength and serviceability requirements. Service load stress calculations are computed based on uncracked section properties for Class U and T flexural members and on the cracked section properties for Class C members.

19.6 ELASTIC FLEXURAL ANALYSIS

It has been noted earlier in this text that the design of concrete structures may be based either on providing sufficient strength, which would be used fully only if the expected loads were increased by an overload factor, or on keeping material stresses within permissible limits when actual service loads act. In the case of ordinary reinforced concrete members, strength design is used. Members are proportioned on the basis of strength requirements and then checked for satisfactory service load behavior, notably with respect to deflection and cracking. The design is then modified if necessary.

Class C members are principally designed based on strength. Class U and T members, however, are proportioned so that stresses in the concrete and steel at actual service loads are within permissible limits. These limits are a fractional part of the actual capacities of the materials. There is some logic to this approach, since an important objective of prestressing is to improve the performance of members at service loads. Consequently, service load requirements often control the amount of prestress force used in Class U and Class T members. Design based on service loads may usually be carried out assuming elastic behavior of both the concrete and the steel, since stresses are relatively low in each.

Regardless of the starting point chosen for the design, a structural member must be satisfactory at all stages of its loading history. Accordingly, prestressed members proportioned on the basis of permissible stresses must also be checked to ensure that sufficient strength is provided should overloads occur, and deflection and cracking under service loads should be investigated. Consistent with most U.S. practice, in this text the design of prestressed concrete beams will start with a consideration of stress limits, after which strength and other properties will be checked.

It is convenient to think of prestressing forces as a system of external forces acting on a concrete member, which must be in equilibrium under the action of those forces. Figure 19.8*a* shows a simple-span prestressed beam with curved tendons, typical of many post-tensioned members. The portion of the beam to the left of a vertical cutting plane *x-x* is taken as a free body, with forces acting as shown in Fig. 19.8*b*. The force P at the left end is exerted on the concrete through the tendon anchorage, while the force P at the cutting plane *x-x* results from combined shear and normal stresses acting at the concrete surface at that location. The direction of P is tangent to the curve of the tendon at each location. Note the presence of the force N, acting on the concrete from the tendon, due to tendon curvature. This force will be distributed in some manner along the length of the tendon, the exact distribution depending upon the tendon profile. Its resultant and the direction in which the resultant acts can be found from the force diagram of Fig. 19.8*c*.

It is convenient when working with the prestressing force P to divide it into its components in the horizontal and vertical directions. The horizontal component (Fig. 19.8*d*) is $H = P \cos \theta$, and the vertical component is $V = H \tan \theta = P \sin \theta$, where θ is the angle of inclination of the tendon centroid at the particular section. Since the slope angle is normally quite small, the cosine of θ is very close to unity and it is sufficient for most calculations to take $H = P$.

The magnitude of the prestress force is not constant. The *jacking force* P_j is immediately reduced to what is termed the *initial prestress force* P_i because of elastic shortening of the concrete upon transfer, slip of the tendon as the force is transferred

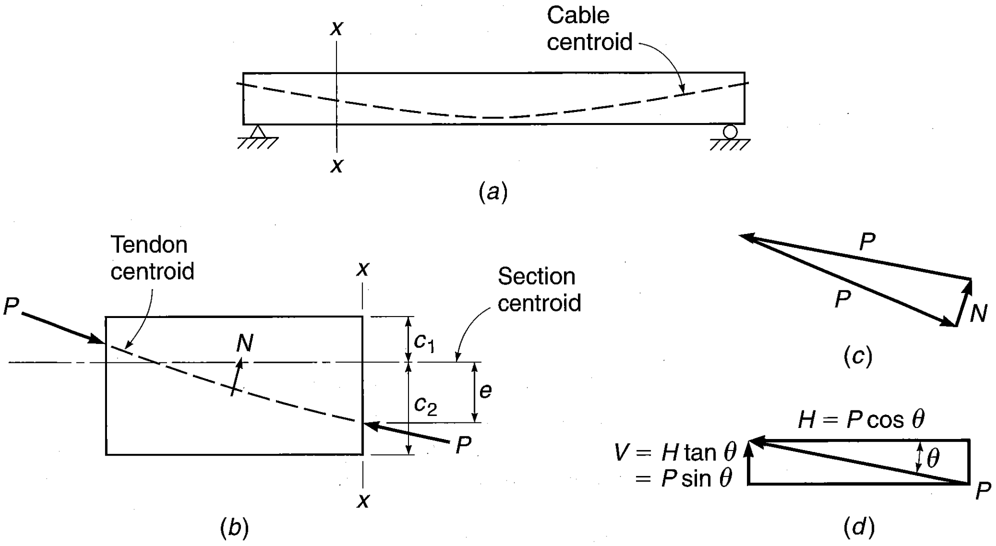

FIGURE 19.8
Prestressing forces acting on concrete.

from the jacks to the beam ends, and loss due to friction between the tendon and the concrete (post-tensioning) or between the tendon and cable alignment devices (pretensioning). There is a further reduction of force from P_i to the *effective prestress* P_e, occurring over a long period of time at a gradually decreasing rate, because of concrete creep under the sustained prestress force, concrete shrinkage, and relaxation of stress in the steel. Methods for predicting losses will be discussed in Section 19.13. Of primary interest to the designer are the initial prestress P_i immediately after transfer and the final or effective prestress P_e after all losses.

In developing elastic equations for flexural stress, the effects of prestress force, self-weight moment, and dead and live load moments are calculated separately, and the separate stresses are superimposed. When the initial prestress force P_i is applied with an eccentricity e below the centroid of the cross section with area A_c and top and bottom fiber distances c_1 and c_2, respectively, it causes the compressive stress $-P_i/A_c$ and the bending stresses $+P_iec_1/I_c$ and $-P_iec_2/I_c$ in the top and bottom fibers, respectively (compressive stresses are designated as negative, tensile stresses as positive), as shown in Fig. 19.9*a*. Then, at the top fiber, the stress is

$$f_1 = -\frac{P_i}{A_c} + \frac{P_iec_1}{I_c} = -\frac{P_i}{A_c}\left(1 - \frac{ec_1}{r^2}\right) \tag{19.1a}$$

and at the bottom fiber

$$f_2 = -\frac{P_i}{A_c} - \frac{P_iec_2}{I_c} = -\frac{P_i}{A_c}\left(1 + \frac{ec_2}{r^2}\right) \tag{19.1b}$$

where r is the radius of gyration of the concrete section. Normally, as the eccentric prestress force is applied, the beam deflects upward. The beam self-weight w_o then causes additional moment M_o to act, and the net top and bottom fiber stresses become

$$f_1 = -\frac{P_i}{A_c}\left(1 - \frac{ec_1}{r^2}\right) - \frac{M_oc_1}{I_c} \tag{19.2a}$$

$$f_2 = -\frac{P_i}{A_c}\left(1 + \frac{ec_2}{r^2}\right) + \frac{M_oc_2}{I_c} \tag{19.2b}$$

FIGURE 19.9
Concrete stress distributions in beams: (*a*) effect of prestress; (*b*) effect of prestress plus self-weight of beam; (*c*) effect of prestress, self-weight, and external dead and live service loads.

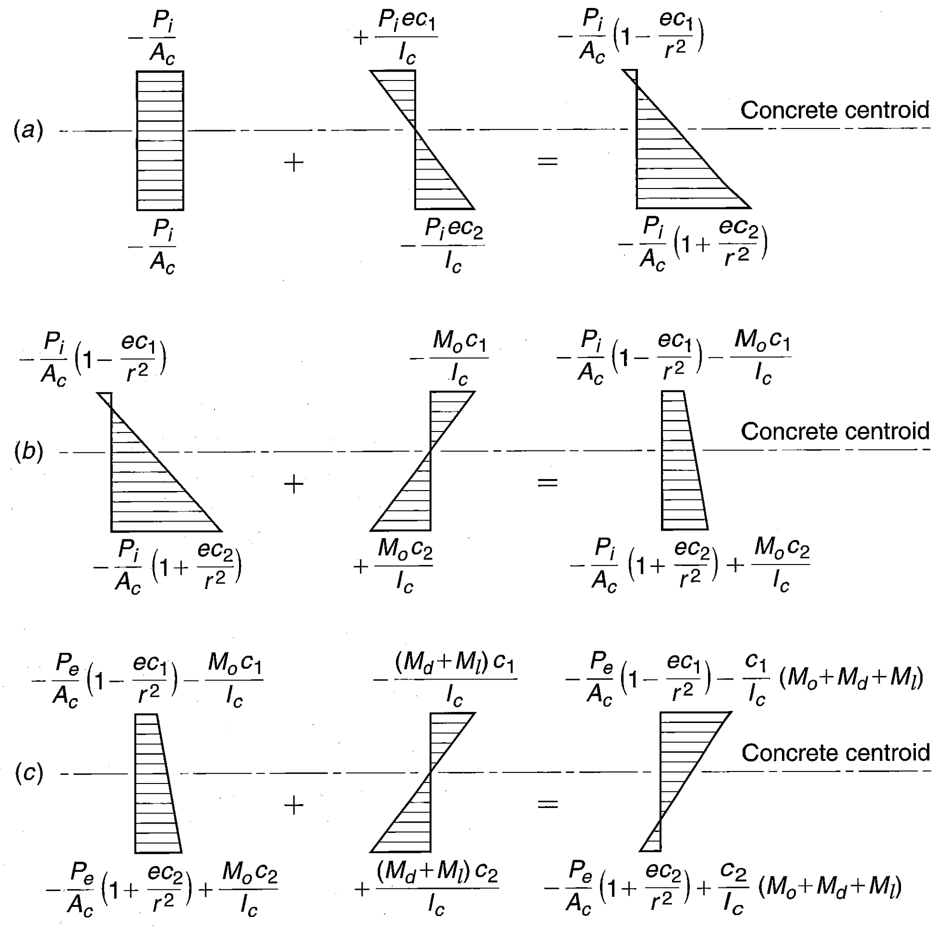
$-\frac{P_i}{A_c}$
$+\frac{P_i e c_1}{I_c}$
$-\frac{P_i}{A_c}\left(1-\frac{ec_1}{r^2}\right)$
Concrete centroid
(a)
+
=
$-\frac{P_i}{A_c}$
$-\frac{P_i e c_2}{I_c}$
$-\frac{P_i}{A_c}\left(1+\frac{ec_2}{r^2}\right)$
$-\frac{P_i}{A_c}\left(1-\frac{ec_1}{r^2}\right)$
$-\frac{M_o c_1}{I_c}$
$-\frac{P_i}{A_c}\left(1-\frac{ec_1}{r^2}\right)-\frac{M_o c_1}{I_c}$
Concrete centroid
(b)
+
=
$-\frac{P_i}{A_c}\left(1+\frac{ec_2}{r^2}\right)$
$+\frac{M_o c_2}{I_c}$
$-\frac{P_i}{A_c}\left(1+\frac{ec_2}{r^2}\right)+\frac{M_o c_2}{I_c}$
$-\frac{P_e}{A_c}\left(1-\frac{ec_1}{r^2}\right)-\frac{M_o c_1}{I_c}$
$-\frac{(M_d+M_l)c_1}{I_c}$
$-\frac{P_e}{A_c}\left(1-\frac{ec_1}{r^2}\right)-\frac{c_1}{I_c}(M_o+M_d+M_l)$
Concrete centroid
(c)
+
=
$-\frac{P_e}{A_c}\left(1+\frac{ec_2}{r^2}\right)+\frac{M_o c_2}{I_c}$
$+\frac{(M_d+M_l)c_2}{I_c}$
$-\frac{P_e}{A_c}\left(1+\frac{ec_2}{r^2}\right)+\frac{c_2}{I_c}(M_o+M_d+M_l)$

as shown in Fig. 19.9*b*. At this stage, time-dependent losses due to shrinkage, creep, and relaxation commence, and the prestressing force gradually decreases from P_i to P_e. It is usually acceptable to assume that all such losses occur prior to the application of service loads, since the concrete stresses at service loads will be critical after losses, not before. Accordingly, the stresses in the top and bottom fiber, with P_e and beam load acting, become

$$f_1 = -\frac{P_e}{A_c}\left(1 - \frac{ec_1}{r^2}\right) - \frac{M_o c_1}{I_c} \tag{19.3a}$$

$$f_2 = -\frac{P_e}{A_c}\left(1 + \frac{ec_2}{r^2}\right) + \frac{M_o c_2}{I_c} \tag{19.3b}$$

When full service loads (dead load in addition to self-weight of the beam, plus service live load) are applied, the stresses are

$$f_1 = -\frac{P_e}{A_c}\left(1 - \frac{ec_1}{r^2}\right) - \frac{(M_o + M_d + M_l)c_1}{I_c} \tag{19.4a}$$

$$f_2 = -\frac{P_e}{A_c}\left(1 + \frac{ec_2}{r^2}\right) + \frac{(M_o + M_d + M_l)c_2}{I_c} \tag{19.4b}$$

as shown in Fig. 19.9*c*.

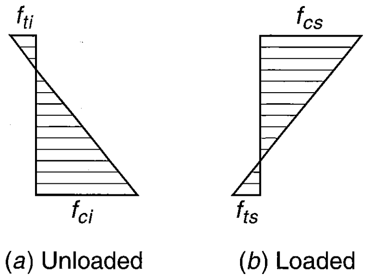

(*a*) Unloaded (*b*) Loaded

FIGURE 19.10
Stress limits: (*a*) unloaded beam, with initial prestress plus self-weight; (*b*) loaded beam, with effective prestress, self-weight, and full service load.

It is necessary, in reviewing the adequacy of a beam (or in designing a beam on the basis of permissible stresses), that the stresses in the extreme fibers remain within specified limits under any combination of loadings that can occur. Normally, the stresses at the section of maximum moment, in a properly designed beam, must stay within the limit states defined by the distributions shown in Fig. 19.10 as the beam passes from the unloaded stage (P_i plus self-weight) to the loaded stage (P_e plus full service loads). In the figure, f_{ci} and f_{ti} are the permissible compressive and tensile stresses, respectively, in the concrete immediately after transfer, and f_{cs} and f_{ts} are the permissible compressive and tensile stresses at service loads (see Table 19.2).

In calculating the section properties A_c, I_c, etc., to be used in the above equations, it is relevant that, in post-tensioned construction, the tendons are usually grouted in the conduits after tensioning. Before grouting, stresses should be based on the net section with holes deducted. After grouting, the transformed section should be used with holes considered filled with concrete and with the steel replaced with an equivalent area of concrete. However, it is satisfactory, unless the holes are quite large, to compute section properties on the basis of the gross concrete section. Similarly, while in pretensioned beams the properties of the transformed section should be used, it makes little difference if calculations are based on properties of the gross concrete section.†

It is useful to establish the location of the upper and lower *kern points* of a cross section. These are defined as the limiting points inside which the prestress force resultant may be applied without causing tension anywhere in the cross section. Their locations are obtained by writing the expression for the tensile fiber stress due to application of an eccentric prestress force acting alone and setting this expression equal to zero to solve for the required eccentricity. In Fig. 19.11, to locate the upper kern-point distance k_1 from the neutral axis, let the prestress force resultant P act at that point. Then the bottom fiber stress is

$$f_2 = -\frac{P}{A_c}\left(1 + \frac{ec_2}{r^2}\right) = 0$$

Thus, with

$$1 + \frac{ec_2}{r^2} = 0$$

one obtains the corresponding eccentricity

$$e = k_1 = -\frac{r^2}{c_2} \tag{19.5a}$$

---

† ACI Code 18.2.6 contains the following provision: "In computing section properties prior to bonding of prestressing steel, the effect of loss of area due to open ducts shall be considered." It is noted in ACI Commentary 18.2.6 that "If the effect of the open duct area on design is deemed negligible, section properties may be based on total area. In post-tensioned members after grouting and in pretensioned members, section properties may be based on effective sections using transformed areas of bonded prestressing steel and nonprestressed gross sections, or net sections."

FIGURE 19.11
Location of kern points.

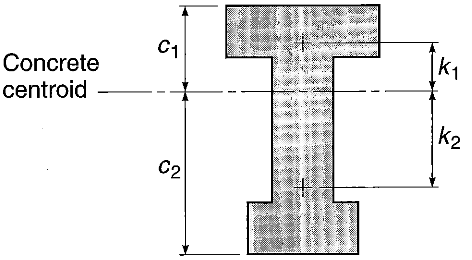

Similarly, the lower kern-point distance k_2 is

$$k_2 = \frac{r^2}{c_1} \tag{19.5b}$$

The region between these two limiting points is known as the *kern*, or in some cases the *core*, of the section.

EXAMPLE 19.1

Pretensioned I beam with constant eccentricity. A simply supported symmetrical I beam shown in cross section in Fig. 19.12*a* will be used on a 12.2 m simple span. It has the following section properties

Moment of inertia: $I_c = 4.69 \times 10^9\ \text{mm}^4$
Concrete area: $A_c = 110 \times 10^3\ \text{mm}^2$
Radius of gyration: $r^2 = 42.6 \times 10^3\ \text{mm}^2$
Section modulus: $S = 15.63 \times 10^6\ \text{mm}^3$
Self-weight: $w_o = 2.64\ \text{kN/m}$

and is to carry a superimposed dead plus live load (considered "sustained," not short-term) of 11 kN/m in addition to its own weight. The beam will be pretensioned with multiple seven-wire strands with the centroid at a constant eccentricity of 198 mm. The prestress force P_i immediately after transfer will be 703 kN; after time-dependent losses, the force will reduce to $P_e = 596$ kN. The specified compressive strength of the concrete $f'_c = 35$ MPa, and at the time of prestressing the strength will be $f'_{ci} = 26$ MPa. Calculate the concrete flexural stresses at the midspan section of the beam at the time of transfer, and after all losses with full service load in place. Compare with ACI allowable stresses for a Class U member.

SOLUTION. Stresses in the concrete along the length of the beam resulting from the initial prestress force of 703 kN may be found by Eqs. (19.1*a*) and (19.1*b*):

$$f_1 = -\frac{703 \times 10^3}{110 \times 10^3}\left(1 - \frac{198 \times 300}{42.6 \times 10^3}\right) = +2.52\ \text{MPa}$$

$$f_2 = -\frac{703 \times 10^3}{110 \times 10^3}\left(1 + \frac{198 \times 300}{42.6 \times 10^3}\right) = -15.30\ \text{MPa}$$

The self-weight of the beam causes the immediate superposition of a moment at midspan of

$$M_o = 2.64 \times \frac{12.2^2}{8} = 49.1\ \text{kN-m}$$

and corresponding stresses of $M_o/S = 49.1/15.63 = 3.14$ MPa, so that the net stresses at the top and bottom of the concrete section at midspan due to initial prestress and self-weight, from Eqs. (19.2*a*) and (19.2*b*), are

$$f_1 = +2.52 - 3.14 = -0.62\ \text{MPa}$$

$$f_2 = -15.30 + 3.14 = -12.16\ \text{MPa}$$

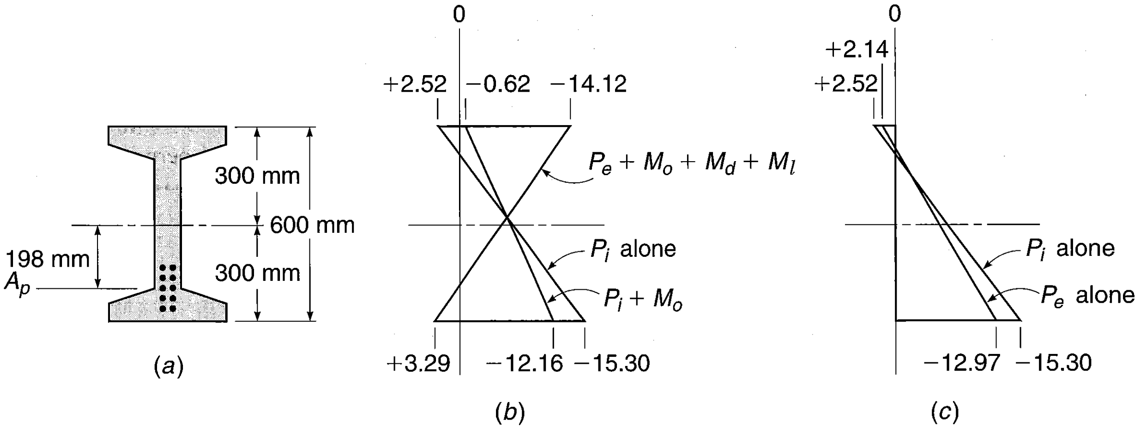

FIGURE 19.12
Pretensioned I beam. Design example: (*a*) cross section, (*b*) stresses at midspan (MPa), (*c*) stresses at ends (MPa).

After losses, the prestress force is reduced to 596 kN, and the concrete stresses at midspan due to that force plus self-weight are

$$f_1 = +2.52 \times \frac{596}{703} - 3.14 = -1.00 \text{ MPa}$$

$$f_2 = -15.30 \times \frac{596}{703} + 3.14 = -9.83 \text{ MPa}$$

and stresses at the end of the beam are

$$f_1 = +2.52\left(\frac{596}{703}\right) = 2.14$$

$$f_2 = -15.30\left(\frac{596}{703}\right) = -12.97$$

The superimposed load of 11 kN/m produces a midspan moment of $M_d + M_l = 11.0 \times 12.2^2/8 =$ 205 kN-m and the corresponding stresses of $205 \times 10^6/(15.63 \times 10^6) = 13.12$ MPa in compression and tension at the top and bottom of the beam, respectively. Thus, the service load stresses at the top and bottom faces at midspan are

$$f_1 = -1.00 - 13.12 = -14.12 \text{ MPa}$$

$$f_2 = -9.83 + 13.12 = 3.29 \text{ MPa}$$

Concrete stresses at midspan are shown in Fig. 19.12*b* and at the beam end in Fig. 19.12*c*. According to the ACI Code (see Table 19.2), the stresses permitted in the concrete are

$$\text{Tension at transfer: } f_{ti} = 0.25\sqrt{26} = +1.27 \text{ MPa}$$

$$\text{Compression at transfer: } f_{ci} = -0.60 \times 26 = -15.60 \text{ MPa}$$

$$\text{Tension at service load: } f_{ts} = 0.6\sqrt{35} = +3.55 \text{ MPa}$$

$$\text{Compression at service load: } f_{cs} = -0.45 \times 35 = -15.75 \text{ MPa}$$

At the initial stage, with prestress plus self-weight in place, the actual compressive stress of 12.16 MPa is well below the limit of 15.75 MPa, and no tension acts at the top, although 1.27 MPa is allowed. While more prestress force or more eccentricity might be suggested to more fully utilize the section, to attempt to do so in this beam, with constant eccentricity, would violate limits at the support, where self-weight moment is zero. It is apparent that at the supports, the initial prestress force acting alone produces tension of 2.52 MPa at the top of the beam (Fig. 19.12*c*), barely below the value of $0.5\sqrt{26} = 2.55$ MPa permitted at the beam end, so very little improvement can be made. The compressive stress at the supports is -15.30 MPa, well below the magnitude of the permitted value of $0.70f'_{ci} = -18.20$ MPa. Finally, at full service load, the tension of 3.29 MPa is under the allowed 3.55 MPa, and compression of 14.12 MPa is well below the permitted 15.75 MPa.

19.7 FLEXURAL STRENGTH

In an ordinary reinforced concrete beam, the stress in the tensile steel and the compressive force in the concrete increase in proportion to the applied moment up to and somewhat beyond service load, with the distance between the two internal stress resultants remaining essentially constant. In contrast to this behavior, in a prestressed beam, increased moment is resisted by a proportionate increase in the distance between the compressive and tensile resultant forces, the compressive resultant moving upward as the load is increased. The magnitude of the internal forces remains nearly constant up to, and usually somewhat beyond, service loads.

This situation changes drastically upon flexural tensile cracking of the prestressed beam. When the concrete cracks, there is a sudden increase in the stress in the steel as the tension that was formerly carried by the concrete is transferred to it. After cracking, the prestressed beam behaves essentially as an ordinary reinforced concrete beam. The compressive resultant cannot continue to move upward indefinitely, and increasing moment must be accompanied by a nearly proportionate increase in steel stress and compressive force. The strength of a prestressed beam can, therefore, be predicted by the same methods developed for ordinary reinforced concrete beams, with modifications to account for (a) the different shape of the stress-strain curve for prestressing steel, as compared with that for ordinary reinforcement, and (b) the tensile strain already present in the prestressing steel before the beam is loaded.

Highly accurate predictions of the flexural strength of prestressed beams can be made based on a *strain compatibility analysis* that accounts for these factors in a rational and explicit way (Ref. 19.1). For ordinary design purposes, certain approximate relationships have been derived. ACI Code 18.7 and the accompanying ACI Commentary 18.7 include approximate equations for flexural strength that will be summarized in the following paragraphs.

a. Stress in the Prestressed Steel at Flexural Failure

When a prestressed concrete beam fails in flexure, the prestressing steel is at a stress f_{ps} that is higher than the effective prestress f_{pe} but below the tensile strength f_{pu}. If the effective prestress $f_{pe} = P_e/A_{ps}$ is not less than $0.50f_{pu}$, ACI Code 18.7.2 permits use of certain approximate equations for f_{ps}. These equations appear quite complex as they are presented in the ACI Code, mainly because they are written in general form to account for differences in type of prestressing steel and to apply to beams in which nonprestressed bar reinforcement may be included in the flexural tension zone or the compression region or both. Separate equations are given for members with bonded tendons and unbonded tendons because, in the latter case, the increase in steel stress at the maximum moment section as the beam is overloaded is much less than if the steel were bonded throughout its length.

For the basic case, in which the prestressed steel provides all of the flexural reinforcement, the ACI Code equations can be stated in simplified form as follows:

1. For members with bonded tendons:

$$f_{ps} = f_{pu}\left(1 - \frac{\gamma_p}{\beta_1}\frac{\rho_p f_{pu}}{f'_c}\right) \tag{19.6}$$

   where $\rho_p = A_{ps}/bd_p$, d_p = effective depth to the prestressing steel centroid, b = width of compression face, β_1 = the familiar relations between stress block depth and depth to the neutral axis [Eq. (3.26)], and γ_p is a factor that depends on the type of prestressing steel used, as follows:

$$\gamma_p = \begin{cases} 0.55 & \text{for } f_{py}/f_{pu} \geq 0.80 \text{ (typical high-strength bars)} \\ 0.40 & \text{for } f_{py}/f_{pu} \geq 0.85 \text{ (typical ordinary strand)} \\ 0.28 & \text{for } f_{py}/f_{pu} \geq 0.90 \text{ (typical low-relaxation strand)} \end{cases}$$

2. For members with unbonded tendons and with a span-depth ratio of 35 or less (this includes most beams),

$$f_{ps} = f_{pe} + 70 + \frac{f'_c}{100\rho_p} \tag{19.7}$$

   but not greater than f_{py} and not greater than f_{pe} + 420 MPa.

3. For members with unbonded tendons and with span-depth ratio greater than 35 (applying to many slabs),

$$f_{ps} = f_{pe} + 70 + \frac{f'_c}{300\rho_p} \tag{19.8}$$

   but not greater than f_{py} and not greater than f_{pe} + 210 MPa.

b. Nominal Flexural Strength and Design Strength

With the stress in the prestressed tensile steel when the member fails in flexure established by Eq. (19.6), (19.7), or (19.8), the nominal flexural strength can be calculated by methods and equations that correspond directly with those used for ordinary reinforced concrete beams. For rectangular cross sections, or flanged sections such as I or T beams in which the stress block depth is equal to or less than the average flange thickness, the nominal flexural strength is

$$M_n = A_{ps}f_{ps}\left(d_p - \frac{a}{2}\right) \tag{19.9}$$

where

$$a = \frac{A_{ps}f_{ps}}{0.85f'_c b} \tag{19.10}$$

Equations (19.9) and (19.10) can be combined as follows:

$$M_n = \rho_p f_{ps} b d_p^2\left(1 - 0.588\,\frac{\rho_p f_{ps}}{f'_c}\right) \tag{19.11}$$

In all cases, the *flexural design strength* is taken equal to ϕM_n, where ϕ is the strength reduction factor for flexure (see Section 19.7c).

If the stress block depth exceeds the average flange thickness, the method for calculating flexural strength is exactly analogous to that used for ordinary reinforced concrete I and T beams. The total prestressed tensile steel area is divided into two parts for computational purposes. The first part A_{pf}, acting at the stress f_{ps}, provides a tensile force to balance the compression in the overhanging parts of the flange. Thus,

$$A_{pf} = 0.85 \frac{f'_c}{f_{ps}}(b - b_w)h_f \tag{19.12}$$

The remaining prestressed steel area

$$A_{pw} = A_{ps} - A_{pf} \tag{19.13}$$

provides tension to balance the compression in the web. The total resisting moment is the sum of the contributions of the two force couples:

$$M_n = A_{pw}f_{ps}\left(d_p - \frac{a}{2}\right) + A_{pf}f_{ps}\left(d_p - \frac{h_f}{2}\right) \tag{19.14a}$$

or

$$M_n = A_{pw}f_{ps}\left(d_p - \frac{a}{2}\right) + 0.85f'_c(b - b_w)h_f\left(d_p - \frac{h_f}{2}\right) \tag{19.14b}$$

where

$$a = \frac{A_{pw}f_{ps}}{0.85f'_c b_w} \tag{19.15}$$

As before, the design strength is taken as ϕM_n, where ϕ is typically 0.90, as discussed in Section 19.7c.

If, after a prestressed beam is designed by elastic methods at service loads, it has inadequate strength to provide the required safety margin under factored load, nonprestressed reinforcement can be added on the tension side and will work in combination with the prestressing steel to provide the needed strength. Such nonprestressed steel, with area A_s, can be assumed to act at its yield stress f_y, to contribute a tension force at the nominal moment of $A_s f_y$. The reader should consult ACI Code 18.7 and ACI Commentary 18.7 for equations for prestressed steel stress at failure and for flexural strength, which are direct extensions of those given above.

c. Limits for Reinforcement

The ACI Code classifies prestressed concrete flexural members as tension-controlled or compression-controlled based on the net tensile strain ϵ_t in the same manner as done for ordinary reinforced concrete beams. Section 3.4d describes the strain distributions and the variation of strength reduction factors associated with limitations on the net tensile strain. Recall that the net tensile strain excludes strains due to creep, shrinkage, temperature, and effective prestress. To maintain a strength reduction factor ϕ of 0.90 and ensure that if flexural failure were to occur, it would be a ductile failure, a net tensile strain of at least 0.005 is required. Due to the complexity of computing net tensile strain in prestressed members, it is easier to perform the check using the c/d_t ratio. From Fig. 3.10a, this simplifies to

$$\frac{c}{d_t} \leq 0.375 \tag{19.16}$$

where d_t is the distance from the extreme compressive fiber to the extreme tensile steel. In many cases, d_t will be the same as d_p, the distance from the extreme compressive fiber to the centroid of the prestressed reinforcement. However, when supplemental nonprestressed steel is used or the prestressing strands are distributed through the depth of the section, d_t will be greater than d_p. If the prestressed beam does not meet the requirements of Eq. (19.16), it may no longer be considered as tension-controlled, and the strength reduction factor ϕ must be determined as shown in Fig. 3.9. If $c/d_t \geq 0.60$, corresponding to $\epsilon_t \leq 0.002$, the section is considered to be *overreinforced*, and alternative equations must be derived for computing the flexural strength (see Ref. 19.1).

It will be recalled that a *minimum tensile reinforcement ratio* is required for ordinary reinforced concrete beams, so that the beams will be safe from sudden failure upon the formation of flexural cracks. Because of the same concern, ACI Code 18.8.2 requires that the total tensile reinforcement in members with bonded prestressed reinforcement be adequate to support a factored load of at least 1.2 times the cracking load of the beam, calculated on the basis of a modulus of rupture of $0.62\sqrt{f_c'}$. A similar requirement is not placed on members with unbonded prestressed reinforcement. Unlike members with bonded reinforcement, which are subject to tendon failure when the concrete cracks and the tensile force in the concrete is suddenly transferred to the bonded steel, abrupt failure does not occur in beams with unbonded tendons because the reinforcement can undergo slip, which distributes the increased strain along the length of the tendon, lowering the magnitude of the increased stress in the tendon.

d. Minimum Bonded Reinforcement

To control cracking in beams and one-way prestressed slabs with *unbonded tendons*, some bonded reinforcement must be added in the form of nonprestressed reinforcing bars, uniformly distributed over the tension zone as close as permissible to the extreme tension fiber. According to ACI Code 18.9.2, the minimum amount of such reinforcement is

$$A_s = 0.004A_{ct} \tag{19.17}$$

where A_{ct} is the area of that part of the cross section between the flexural tension face and the centroid of the gross concrete cross section. ACI Code 18.9.3 provides exceptions for two-way slabs with very low tensile stresses.

EXAMPLE 19.2 **Flexural strength of pretensioned I beam.** The prestressed I beam shown in cross section in Fig. 19.13 is pretensioned using five low relaxation stress-relieved Grade 1860 12.7 mm diameter strands, carrying effective prestress f_{pe} = 1100 MPa. Concrete strength is f_c' = 28 MPa. Calculate the design strength of the beam.

Solution. The effective prestress in the strands of 1100 MPa is well above 0.50 × 1860 = 930 MPa, confirming that the approximate ACI equations are applicable. The tensile reinforcement ratio is

$$\rho_p = \frac{49.4}{300 \times 430} = 0.0038$$

and the steel stress f_{ps} when the beam fails in flexure is found from Eq. (19.6) to be

$$f_{ps} = f_{pu}\left(1 - \frac{\gamma_p}{\beta_1}\frac{\rho_p f_{pu}}{f_c'}\right) = 1860\left(1 - \frac{0.28}{0.85}\frac{0.0038 \times 1860}{28}\right) = 1705 \text{ MPa}$$

FIGURE 19.13
Post-tensioned beam of Example 19.2.

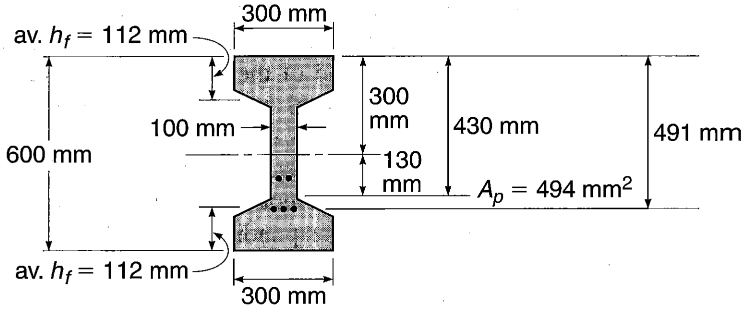

Next, it is necessary to check whether the stress block depth is greater or less than the average flange thickness of 112 mm. On the assumption that it is not greater than the flange thickness, Eq. (19.10) is used:

$$a = \frac{A_p f_{ps}}{0.85 f'_c b} = \frac{494 \times 1705}{0.85 \times 28 \times 300} = 118 \text{ mm}$$

It is concluded from this trial calculation that a actually exceeds h_f, so the trial calculation is not valid and equations for flanged members must be used. The steel that acts with the overhanging flanges is found from Eq. (19.12) to be

$$A_{pf} = \frac{0.85 \times 28(300 - 100)112}{1705} = 313 \text{ mm}^2$$

and from Eq. (19.13), the steel acting with the web is

$$A_{pw} = 494 - 313 = 181 \text{ mm}^2$$

The actual stress block depth is now found from Eq. (19.15):

$$a = \frac{181 \times 1705}{0.85 \times 28 \times 100} = 130 \text{ mm}$$

$$c = \frac{a}{\beta_1} = \frac{130}{0.85} = 153$$

A check should now be made to determine if the beam can be considered tension-controlled. As shown in Fig. 19.13, d_t = 491 mm. From Eq. (19.16),

$$\frac{c}{d_t} = \frac{153}{491} = 0.312$$

This is less than 0.375 for $\epsilon_t \geq 0.005$, confirming that this can be considered to be a tension-controlled prestressed beam, and $\phi = 0.90$. The nominal flexural strength, from Eq. (19.14*b*), is

$$M_n = 180 \times 1705(430 - 130/2) + 0.85 \times 28(300 - 100) \times 112(430 - 112/2)$$
$$= 311 \times 10^6 \text{ N-mm} = 311 \text{ kN-m}$$

and, finally, the design strength is ϕM_n = 280 kN-m.

19.8 PARTIAL PRESTRESSING

Early in the development of prestressed concrete, the goal of prestressing was the complete elimination of concrete tensile stress at service load. This kind of design, in which the service load tensile stress limit $f_{ts} = 0$, is often referred to as *full prestressing*.

While full prestressing offers many advantages over nonprestressed construction, some problems can arise. Heavily prestressed beams, particularly those for which full live load is seldom in place, may have excessively large upward deflection, or camber, which will increase with time because of concrete creep under the eccentric prestress force. Fully prestressed beams may also have a tendency for severe longitudinal shortening, causing large restraint forces unless special provision is made to permit free movement at one end of each span. If shortening is permitted to occur freely, prestress losses due to elastic and creep deformation may be large. Furthermore, if heavily prestressed beams are overloaded to failure, they may fail in a sudden and brittle mode, with little warning before collapse.

Today there is general recognition of the advantages of *partial prestressing*, in which flexural tensile stress and some limited cracking are permitted under full service load. That full load may be infrequently applied. Typically, many beams carry only dead load much of the time, or dead load plus only part of the service live load. Under these conditions, a partially prestressed beam would normally not be subject to flexural tension, and cracks that form occasionally, when the full live load is in place, would close completely when that live load is removed. Controlled cracks prove no more objectionable in prestressed concrete structures than in reinforced concrete structures. With partial prestressing, excessive camber and troublesome axial shortening are avoided. Should overloading occur, there will be ample warning of distress, with extensive cracking and large deflections (Refs. 19.10 to 19.13).

Although the amount of prestressing steel may be reduced in partially prestressed beams compared with fully prestressed beams, a proper safety margin must still be maintained, and to achieve the necessary flexural strength, partially prestressed beams may require additional tensile reinforcement. In fact, partially prestressed beams are often defined as beams in which (1) flexural cracking is permitted at full service load and (2) the main flexural tension reinforcement includes both prestressed and nonprestressed steel. Analysis indicates, and tests confirm, that such nonprestressed steel is fully stressed to f_y at flexural failure.

The ACI Code does not specifically mention partial prestressing but does include the concept explicitly in the classification of flexural members. Class T flexural members require service level stress checks and have maximum allowable tensile stresses above the modulus of rupture. Class C flexural members do not require stress checks at service load but do require crack control checks (Section 19.18). The designations of Class T and Class C flexural members bring the ACI Code into closer agreement with European practice (Refs. 19.13 to 19.15).

The three classes of prestressed flexural members, U, T, and C, provide the designer with considerable flexibility in achieving economical designs. To attain the required strength, supplemental reinforcement in the form of nonprestressed ordinary steel or unstressed prestressing strand may be required. Reinforcing bars are less expensive than high-strength prestressing steel. Strand, however, at twice the cost of ordinary reinforcement, provides 3 times the strength. Labor costs for bar placement are generally similar to those for placing unstressed strand on site. Similarly, the addition of a small number of strands in a plant prestressing bed is often more economical than adding reinforcing bars. The designer may select the service level performance strategy best suited for the project. A criterion that includes no tensile stress under dead load and a tensile stress less than the modulus of rupture at the service live load is possible with Class U and T flexural members, while Class C members use prestressing primarily for deflection control.

The choice of a suitable degree of prestress is governed by a number of factors. These include the nature of the loading (for example, highway or railroad bridges, and storage warehouses), the ratio of live to dead load, the frequency of occurrence of the full service load, and the presence of a corrosive environment.

19.9 FLEXURAL DESIGN BASED ON CONCRETE STRESS LIMITS

As in reinforced concrete, problems in prestressed concrete can be separated generally as analysis problems or design problems. For the former, with the applied loads, the concrete cross section, steel area, and the amount and point of application of the prestress force known, Eqs. (19.1) to (19.4) permit the direct calculation of the resulting concrete stresses. The equations in Section 19.7 will predict the flexural strength. However, if the dimensions of a concrete section, the steel area and centroid location, and the amount of prestress are to be found—given the loads, limiting stresses, and required strength—the problem is complicated by the many interrelated variables.

There are at least three practical approaches to the flexural design of a prestressed concrete member. Some engineers prefer to assume a concrete section, calculate the required prestress force and eccentricities for what will probably be the controlling load stage, then check the stresses at all stages using the preceding equations, and finally check the flexural strength. The trial section is then revised if necessary. If a beam is to be chosen from a limited number of standard shapes, as is often the case for shorter spans and ordinary loads, this procedure is probably best. For longer spans or when customized shapes are used, a more efficient member may result by designing the cross section so that the specified concrete stress limits of Table 19.2 are closely matched. This cross section, close to "ideal" from the limit stress viewpoint, may then be modified to meet functional requirements (e.g., providing a broad top flange for a bridge deck) or to meet strength requirements, if necessary. Equations facilitating this approach will be developed in this section. A third method of design is based on load balancing, using the concept of equivalent loads (see Section 19.2b). A trial section is chosen, after which the prestress force and tendon profile are selected to provide uplift forces as to just balance a specified load. Modifications may then be made, if needed, to satisfy stress limits or strength requirements. This third approach will be developed in Section 19.12.

Notation is established pertaining to the allowable concrete stresses at limiting stages as follows:

f_{ci} = allowable compressive stress immediately after transfer

f_{ti} = allowable tensile stress immediately after transfer

f_{cs} = allowable compressive stress at service load, after all losses

f_{ts} = allowable tensile stress at service load, after all losses

The values of these limit stresses are normally set by specification (see Table 19.2).

a. Beams with Variable Eccentricity

For a typical Class U or T beam in which the tendon eccentricity is permitted to vary along the span, flexural stress distributions in the concrete at the maximum moment section are shown in Fig. 19.14*a*. The eccentric prestress force, having an initial value of P_i, produces the linear stress distribution (1). Because of the upward camber of the beam as that force is applied, the self-weight of the member is immediately introduced, the flexural stresses resulting from the moment M_o are superimposed, and the

FIGURE 19.14
Flexural stress distributions for beams with variable eccentricity: (*a*) maximum moment section; (*b*) support section.

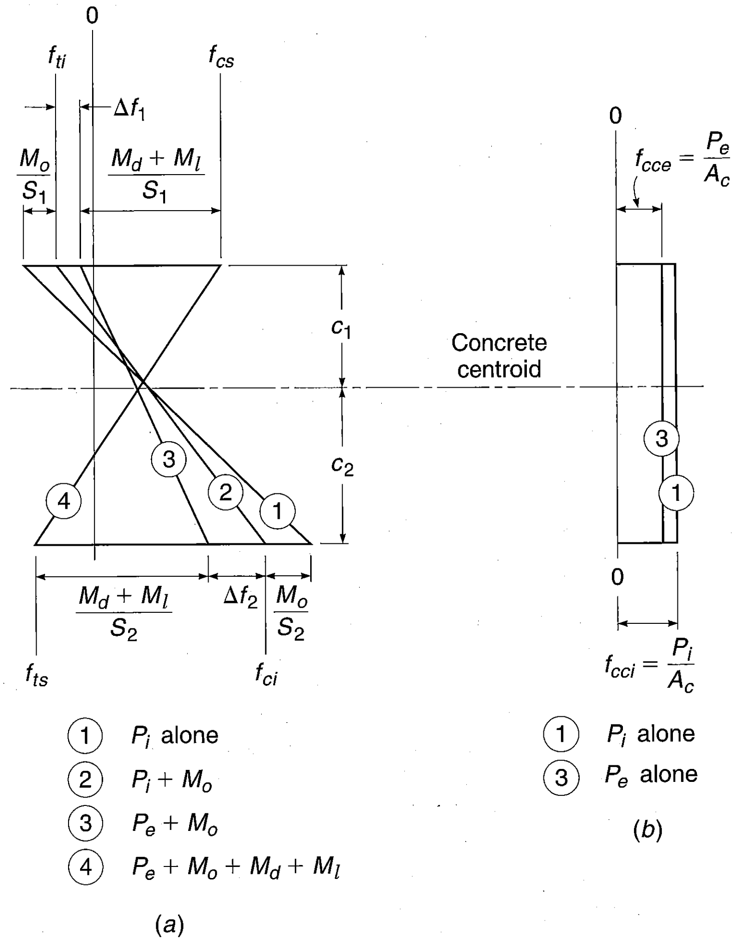
0
f_{ti}
f_{cs}
Δf_1
$\frac{M_o}{S_1}$
$\frac{M_d + M_l}{S_1}$
c_1
c_2
Concrete centroid
$\frac{M_d + M_l}{S_2}$
Δf_2
$\frac{M_o}{S_2}$
f_{ts}
f_{ci}
① P_i alone
② $P_i + M_o$
③ $P_e + M_o$
④ $P_e + M_o + M_d + M_l$
(*a*)
0
$f_{cce} = \frac{P_e}{A_c}$
0
$f_{cci} = \frac{P_i}{A_c}$
① P_i alone
③ P_e alone
(*b*)

distribution (2) is the first that is actually attained. At this stage, the tension at the top surface is not to exceed f_{ti}, and the compression at the bottom surface is not to exceed f_{ci}, as shown in Fig. 19.14*a*.

It will be assumed that all the losses occur at this stage, and that the stress distribution changes to distribution (3). The losses produce a reduction of tension in the amount Δf_1 at the top surface and a reduction of compression in the amount Δf_2 at the bottom surface.

As the superimposed dead load moment M_d and the service live load moment M_l are introduced, the associated flexural stresses, when superimposed on stresses already present, produce distribution (4). At this stage, the tension at the bottom surface must not be greater than f_{ts}, and the compression at the top of the section must not exceed f_{cs} as shown.

The requirements for the sections moduli S_1 and S_2 with respect to the top and bottom surfaces, respectively, are

$$S_1 \geq \frac{M_d + M_l}{f_{1r}} \tag{a}$$

$$S_2 \geq \frac{M_d + M_l}{f_{2r}} \tag{b}$$

where the available stress ranges f_{1r} and f_{2r} at the top and bottom face can be calculated from the specified stress limits f_{ti}, f_{cs}, f_{ts}, and f_{ci}, once the stress changes Δf_1 and Δf_2, associated with prestress loss are known.

The effectiveness ratio R accounts for the loss of prestress and is defined as

$$R = \frac{P_e}{P_i} \tag{19.18}$$

Thus, the loss in prestress force is

$$P_i - P_e = (1 - R)P_i \tag{19.19}$$

The changes in stress at the top and bottom faces, Δf_1 and Δf_2, as losses occur, are equal to $(1 - R)$ times the corresponding stresses due to the initial prestress force P_i *acting alone*:

$$\Delta f_1 = (1 - R)\left(f_{ti} + \frac{M_o}{S_1}\right) \tag{c}$$

$$\Delta f_2 = (1 - R)\left(-f_{ci} + \frac{M_o}{S_2}\right) \tag{d}$$

where Δf_1 is a reduction of tension at the top surface and Δf_2 is a reduction of compression at the bottom surface.† Thus, the stress ranges available as the superimposed load moments $M_d + M_l$ are applied are

$$\begin{aligned} f_{1r} &= f_{ti} - \Delta f_1 - f_{cs} \\ &= Rf_{ti} - (1 - R)\frac{M_o}{S_1} - f_{cs} \end{aligned} \tag{e}$$

and

$$\begin{aligned} f_{2r} &= f_{ts} - f_{ci} - \Delta f_2 \\ &= f_{ts} - Rf_{ci} - (1 - R)\frac{M_o}{S_2} \end{aligned} \tag{f}$$

The minimum acceptable value of S_1 is thus established:

$$S_1 \geq \frac{M_d + M_l}{Rf_{ti} - (1 - R)M_o/S_1 - f_{cs}}$$

or

$$S_1 \geq \frac{(1 - R)M_o + M_d + M_l}{Rf_{ti} - f_{cs}} \tag{19.20}$$

Similarly, the minimum value of S_2 is

$$S_2 \geq \frac{(1 - R)M_o + M_d + M_l}{f_{ts} - Rf_{ci}} \tag{19.21}$$

---

† Note that the stress limits such as f_{ti} and other specific points along the stress axis are considered signed quantities, whereas stress changes such as M_o/S_1 and Δf_2 are taken as absolute values.

The cross section must be selected to provide at least these values of S_1 and S_2. Furthermore, since $I_c = S_1c_1 = S_2c_2$, the centroidal axis must be located such that

$$\frac{c_1}{c_2} = \frac{S_2}{S_1} \tag{g}$$

or in terms of the total section depth $h = c_1 + c_2$

$$\frac{c_1}{h} = \frac{S_2}{S_1 + S_2} \tag{19.22}$$

From Fig. 19.14*a*, the concrete centroidal stress under initial conditions f_{cci} is given by

$$f_{cci} = f_{ti} - \frac{c_1}{h}\left(f_{ti} - f_{ci}\right) \tag{19.23}$$

The initial prestress force is easily obtained by multiplying the value of the concrete centroidal stress by the concrete cross-sectional area A_c.

$$P_i = A_c f_{cci} \tag{19.24}$$

The eccentricity of the prestress force may be found by considering the flexural stresses that must be imparted by the bending moment P_ie. With reference to Fig. 19.14, the flexural stress at the top surface of the beam resulting from the eccentric prestress force alone is

$$\frac{P_ie}{S_1} = \left(f_{ti} - f_{cci}\right) + \frac{M_o}{S_1} \tag{h}$$

from which the required eccentricity is

$$e = \left(f_{ti} - f_{cci}\right)\frac{S_1}{P_i} + \frac{M_o}{P_i} \tag{19.25}$$

Summarizing the design process to determine the best cross section and the required prestress force and eccentricity based on stress limitations: the required section moduli with respect to the top and bottom surfaces of the member are found from Eqs. (19.20) and (19.21) with the centroidal axis located using Eq. (19.22). Concrete dimensions are chosen to satisfy these requirements as nearly as possible. The concrete centroidal stress for this ideal section is given by Eq. (19.23), the desired initial prestress force by Eq. (19.24), and its eccentricity by Eq. (19.25).

In practical situations, very seldom will the concrete section chosen have exactly the required values of S_1 and S_2 as found by this method, nor will the concrete centroid be exactly at the theoretically ideal level. Rounding concrete dimensions upward, providing broad flanges for functional reasons, or using standardized cross-sectional shapes will result in a member whose section properties will exceed the minimum requirements. In such a case, the stresses in the concrete as the member passes from the unloaded stage to the full service load stage will stay within the allowable limits, but the limit stresses will not be obtained exactly. An infinite number of combinations of prestress force and eccentricity will satisfy the requirements. Usually, the design requiring the lowest value of prestress force, and the largest practical eccentricity, will be the most economical.

The total eccentricity in Eq. (19.25) includes the term M_o/P_i. As long as the beam is deep enough to allow this full eccentricity, the girder dead load moment is carried with no additional penalty in terms of prestress force, section, or stress range. This ability to carry the beam dead load "free" is a major contribution of variable eccentricity.

The stress distributions shown in Fig. 19.14*a*, on which the design equations are based, apply at the maximum moment section of the member. Elsewhere, M_o is less, and, consequently, the prestress eccentricity or the force must be reduced if the stress limits f_{ti} and f_{ci} are not to be exceeded. In many cases, tendon eccentricity is reduced to zero at the support sections, where all moments due to transverse load are zero. In this case, the stress distributions of Fig. 19.14*b* are obtained. The stress in the concrete is uniformly equal to the centroidal value f_{cci} under conditions of initial prestress and f_{cce} after losses.

EXAMPLE 19.3

Design of beam with variable eccentricity tendons. A post-tensioned prestressed concrete beam is to carry an intermittent live load of 14.5 kN/m and superimposed dead load of 7.5 kN/m, in addition to its own weight, on a 12 m simple span. Normal-density concrete will be used with design strength $f_c' = 42$ MPa. It is estimated that, at the time of transfer, the concrete will have attained 70 percent of f_c', or 29 MPa. Time-dependent losses may be assumed to be 15 percent of the initial prestress, giving an effectiveness ratio of 0.85. Determine the required concrete dimensions, magnitude of prestress force, and eccentricity of the steel centroid based on ACI stress limitations for a Class U beam, as given in Sections 19.4 and 19.5.

Solution. Referring to Table 19.2, the stress limits are

$$f_{ci} = -0.60 \times 29 = -17.40 \text{ MPa}$$

$$f_{ti} = 0.25\sqrt{29} = +1.35 \text{ MPa}$$

$$f_{cs} = -0.60 \times 42 = -25.20 \text{ MPa}$$

$$f_{ts} = 0.62\sqrt{42} = 4.02 \text{ MPa}$$

The self-weight of the girder will be estimated at 3.6 kN/m. The service moments due to transverse loading are

$$M_o = \frac{1}{8} \times 3.6 \times 12^2 = 65 \text{ kN-m}$$

$$M_d + M_l = \frac{1}{8} \times 22 \times 12^2 = 396 \text{ kN-m}$$

The required section moduli with respect to the top and bottom surfaces of the concrete beam are found from Eqs. (19.20) and (19.21).

$$S_1 \geq \frac{(1 - R)M_o + M_d + M_l}{Rf_{ti} - f_{cs}} = \frac{(0.15 \times 65 + 396)10^6}{0.85 \times 1.35 + 25.20} = 15.4 \times 10^6 \text{ mm}^3$$

$$S_2 \geq \frac{(1 - R)M_o + M_d + M_l}{f_{ts} - Rf_{ci}} = \frac{(0.15 \times 65 + 396)10^6}{4.02 + 0.85 \times 17.40} = 21.6 \times 10^6 \text{ mm}^3$$

The values obtained for S_1 and S_2 suggest that an asymmetrical section is most appropriate. However, a symmetrical section is selected for simplicity and to ensure sufficient compression area for flexural strength. The 700 mm deep I section shown in Fig. 19.15*a* will meet the requirements and has the following properties:

$$I_c = 7.78 \times 10^9 \text{ mm}^4$$

$$S = 22.2 \times 10^6 \text{ mm}^3$$

$$A_c = 150 \times 10^3 \text{ mm}^2$$

$$r^2 = 51.9 \times 10^3 \text{ mm}^2$$

$$w_o = 3.6 \text{ kN/m (as assumed)}$$

FIGURE 19.15
Design example of beam with variable eccentricity of tendons: (*a*) cross section dimensions (mm); (*b*) concrete stresses at midspan (MPa).

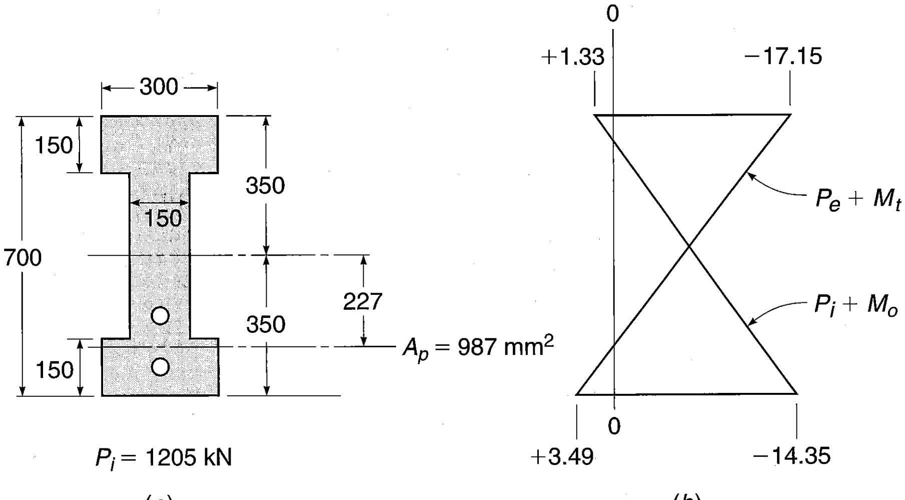

Next, the concrete centroidal stress is found from Eq. (19.23):

$$f_{cci} = f_{ti} - \frac{c_1}{h}(f_{ti} - f_{ci}) = 1.35 - \frac{1}{2}(1.35 + 17.40) = -8.03 \text{ MPa}$$

and from Eq. (19.24) the initial prestress force is

$$P_i = A_c f_{cci} = 150 \times 10^3 \times 8.03 = 1.205 \times 10^6 \text{ N} = 1205 \text{ kN}$$

From Eq. (19.25), the required tendon eccentricity at the maximum moment section of the beam is

$$e = (f_{ti} - f_{cci})\frac{S_1}{P_i} + \frac{M_o}{P_i} = (1.35 + 8.03)\,\frac{22.2 \times 10^6}{1205 \times 10^3} + \frac{65 \times 10^6}{1205 \times 10^3}$$

$$= 227 \text{ mm}$$

Elsewhere along the span, the eccentricity will be reduced so that the concrete stress limits will not be violated.

The required initial prestress force of 1205 kN will be provided using tendons consisting of 12.7 mm diameter Grade 1860 low-relaxation strands (see Section 2.16). The minimum tensile strength is $f_{pu} = 1860$ MPa, and the yield strength may be taken as $f_{py} = 0.90 \times 1860 = 1674$ MPa. According to the ACI Code (see Section 19.4), the permissible stress in the strand immediately after transfer must not exceed $0.82f_{py} = 1373$ MPa or $0.74\,f_{pu} = 1376$ MPa. The first criterion controls. The required area of prestressing steel is

$$A_{ps} = \frac{1205}{1373} = 878 \text{ mm}^2$$

The cross-sectional area of one 12.7 mm diameter strand is 98.7 mm²; hence, the number of strands required is

$$\text{Number of strands} = \frac{878}{98.7} = 8.9$$

Two five-strand tendons will be used, as shown in Fig. 19.15*a*, each stressed to 602.5 kN immediately following transfer.

It is good practice to check the calculations by confirming that stress limits are not exceeded at critical load stages. The top and bottom surface concrete stresses produced, in this case, by the separate loadings are

$$P_i: \quad f_1 = -\frac{1205 \times 10^3}{150 \times 10^3}\left(1 - \frac{227 \times 350}{51.9 \times 10^3}\right) = +4.26 \text{ MPa}$$

$$f_2 = -\frac{1205 \times 10^3}{150 \times 10^3}\left(1 + \frac{227 \times 350}{51.9 \times 10^3}\right) = -20.33 \text{ MPa}$$

$$P_e: \quad f_1 = 0.85 \times 4.26 = +3.62 \text{ MPa}$$

$$f_2 = 0.85(-20.33) = -17.28 \text{ MPa}$$

$$M_o: \quad f_1 = -\frac{65 \times 10^6}{22.2 \times 10^6} = -2.93 \text{ MPa}$$

$$f_2 = +2.93 \text{ MPa}$$

$$M_d + M_l: \quad f_1 = -\frac{396 \times 10^6}{22.2 \times 10^6} = -17.84 \text{ MPa}$$

$$f_2 = +17.84 \text{ MPa}$$

Thus, when the initial prestress force of 1205 kN is applied and the beam self-weight acts, the top and bottom stresses in the concrete at midspan are, respectively,

$$f_1 = +4.26 - 2.93 = +1.33 \text{ MPa}$$

$$f_2 = -17.28 + 2.93 = -14.35 \text{ MPa}$$

When the prestress force has decreased to its effective value of 1024 kN and the full service load is applied, the concrete stresses are

$$f_1 = +3.62 - 2.93 - 17.84 = -17.15 \text{ MPa}$$

$$f_2 = -17.28 + 2.93 + 17.84 = 3.49 \text{ MPa}$$

These stress distributions are shown in Fig. 19.15*b*. Comparison with the specified limit stresses confirms that the design is satisfactory.

b. Beams with Constant Eccentricity

The design method presented in the previous section was based on stress conditions at the maximum moment section of a beam, with the maximum value of moment M_o resulting from the self-weight immediately being superimposed. If P_i and e were to be held constant along the span, as is often convenient in pretensioned prestressed construction, then the stress limits f_{ti} and f_{ci} would be exceeded elsewhere along the span, where M_o is less than its maximum value. To avoid this condition, the constant eccentricity must be less than that given by Eq. (19.25). Its maximum value is given by conditions at the support of a simple span, where M_o is zero.

Figure 19.16 shows the flexural stress distributions at the support and midspan sections for a beam with constant eccentricity. In this case, the stress limits f_{ti} and f_{ci} are not to be violated when the eccentric prestress moment acts alone, as at the supports. The stress changes Δf_1 and Δf_2 as losses occur are equal to $(1 - R)$ times the top and bottom surface stresses, respectively, due to initial prestress alone:

$$\Delta f_1 = (1 - R)(f_{ti}) \qquad (a)$$

$$\Delta f_2 = (1 - R)(-f_{ci}) \qquad (b)$$

FIGURE 19.16
Flexural stress distributions for beam with constant eccentricity of tendons: (*a*) maximum moment section; (*b*) support section.

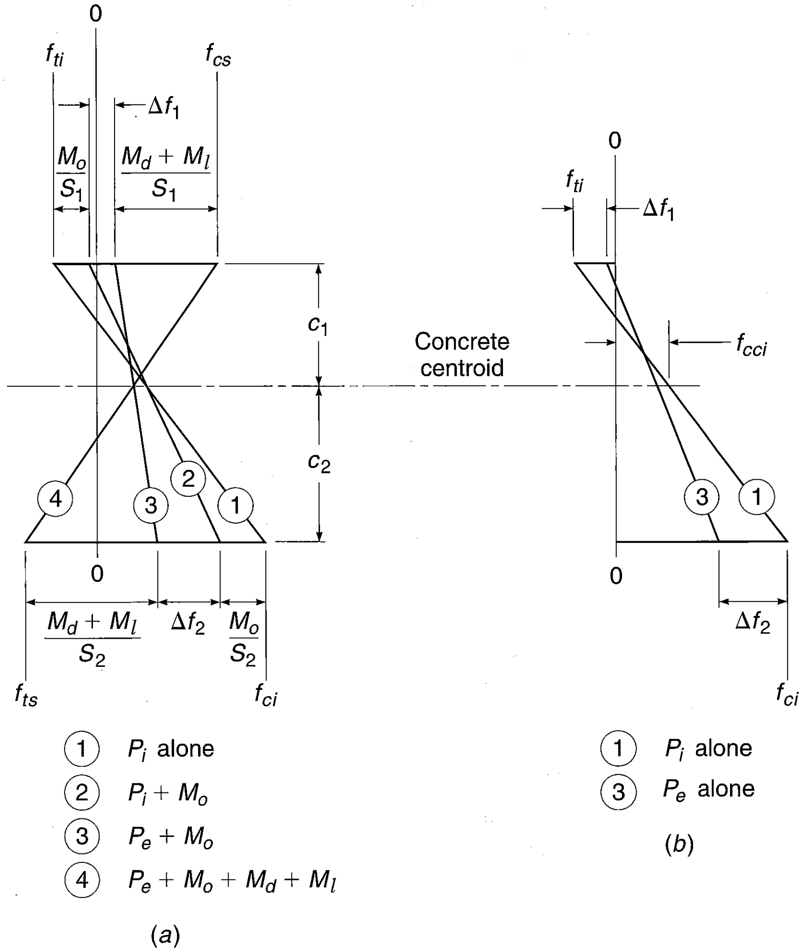
0
f_{ti}
f_{cs}
Δf_1
$\frac{M_o}{S_1}$
$\frac{M_d + M_l}{S_1}$
c_1
c_2
Concrete centroid
④
③
②
①
0
$\frac{M_d + M_l}{S_2}$
Δf_2
$\frac{M_o}{S_2}$
f_{ts}
f_{ci}
① P_i alone
② $P_i + M_o$
③ $P_e + M_o$
④ $P_e + M_o + M_d + M_l$
0
f_{ti}
Δf_1
f_{cci}
③
①
0
Δf_2
f_{ci}
① P_i alone
③ P_e alone
(*a*)

(*b*)

In this case, the available stress ranges between limit stresses must provide for the effect of M_o as well as M_d and M_l, as seen from Fig. 19.16*a*, and are

$$\begin{aligned} f_{1r} &= f_{ti} - \Delta f_1 - f_{cs} \\ &= Rf_{ti} - f_{cs} \qquad (c) \\ f_{2r} &= f_{ts} - f_{ci} - \Delta f_2 \\ &= f_{ts} - Rf_{ci} \qquad (d) \end{aligned}$$

and the requirements on the section moduli are that

$$S_1 \geq \frac{M_o + M_d + M_l}{Rf_{ti} - f_{cs}} \tag{19.26}$$

$$S_2 \geq \frac{M_o + M_d + M_l}{f_{ts} - Rf_{ci}} \tag{19.27}$$

The concrete centroidal stress may be found by Eq. (19.23) and the initial prestress force by Eq. (19.24) as before. However, the expression for required eccentricity differs. In this case, referring to Fig. 19.16*b*,

$$\frac{P_i e}{S_1} = f_{ti} - f_{cci} \qquad (e)$$

from which the required eccentricity is

$$e = (f_{ti} - f_{cci})\frac{S_1}{P_i} \tag{19.28}$$

A significant difference between beams with variable eccentricity and those with constant eccentricity will be noted by comparing Eqs. (19.20) and (19.21) with the corresponding Eqs. (19.26) and (19.27). In the first case, the section modulus requirement is governed mainly by the superimposed load moments M_d and M_l. Almost all of the self-weight is carried "free," that is, without increasing section modulus or prestress force, by the simple expedient of increasing the eccentricity along the span by the amount M_o/P_i. In the second case, the eccentricity is controlled by conditions at the supports, where M_o is zero, and the full moment M_o due to self-weight must be included in determining section moduli. Nevertheless, beams with constant eccentricity are often used for practical reasons.

EXAMPLE 19.4

Design of beam with constant eccentricity tendons. The beam in the preceding example is to be redesigned using straight tendons with constant eccentricity. All other design criteria are the same as before. At the supports, a temporary concrete tensile stress $f_{ti} = 0.5\sqrt{f'_{ci}} = 2.69$ MPa and a compressive stress $f_{ci} = 0.7f'_{ci} = 20.30$ MPa are permitted.

SOLUTION. Anticipating a somewhat less efficient beam, the dead load estimate will be increased to 4.0 kN/m in this case. The resulting moment M_o is 72 kN-m. The moment due to superimposed dead load and live load is 396 kN-m as before.

Using Eqs. (19.26) and (19.27), the requirements for section moduli based on the midspan allowable stresses are

$$S_1 \geq \frac{M_o + M_d + M_l}{Rf_{ti} - f_{cs}} = \frac{(72 + 396)10^6}{0.85 \times 2.69 + 25.20} = 17.0 \times 10^6 \text{ mm}^3$$

$$S_2 \geq \frac{M_o + M_d + M_l}{f_{ts} - Rf_{ci}} = \frac{(72 + 396)10^6}{4.02 + 0.85 \times 20.30} = 22.0 \times 10^3 \text{ mm}^2$$

Once again, a symmetrical section will be chosen. Flange dimensions and web width will be kept unchanged compared with the previous example, but in this case a beam depth of 750 mm is required. The dimensions of the cross section are shown in Fig. 19.17*a*. The following properties are obtained:

$$I_c = 9.41 \times 10^9 \text{ mm}^4$$

$$S = 25.1 \times 10^6 \text{ mm}^3$$

$$A_c = 157.5 \times 10^3 \text{ mm}^2$$

$$r^2 = 59.7 \times 10^3 \text{ mm}^2$$

$$w_o = 3.78 \text{ kN/m (close to the assumed value)}$$

The concrete centroidal stress, from Eq. (19.23), is

$$f_{cci} = f_{ti} - \frac{c_1}{h}(f_{ti} - f_{ci}) = 2.69 - \frac{1}{2}(2.69 + 20.30) = -8.81 \text{ MPa}$$

and from Eq. (19.24), the initial prestress force is

$$P_i = A_c f_{cci} = 157.5 \times 8.81 = 1388 \text{ kN}$$

From Eq. (19.28), the required constant eccentricity is

$$e = (f_{ti} - f_{cci})\frac{S_1}{P_i} = (2.69 + 8.81)\frac{25.1 \times 10^6}{1388 \times 10^3} = 208 \text{ mm}$$

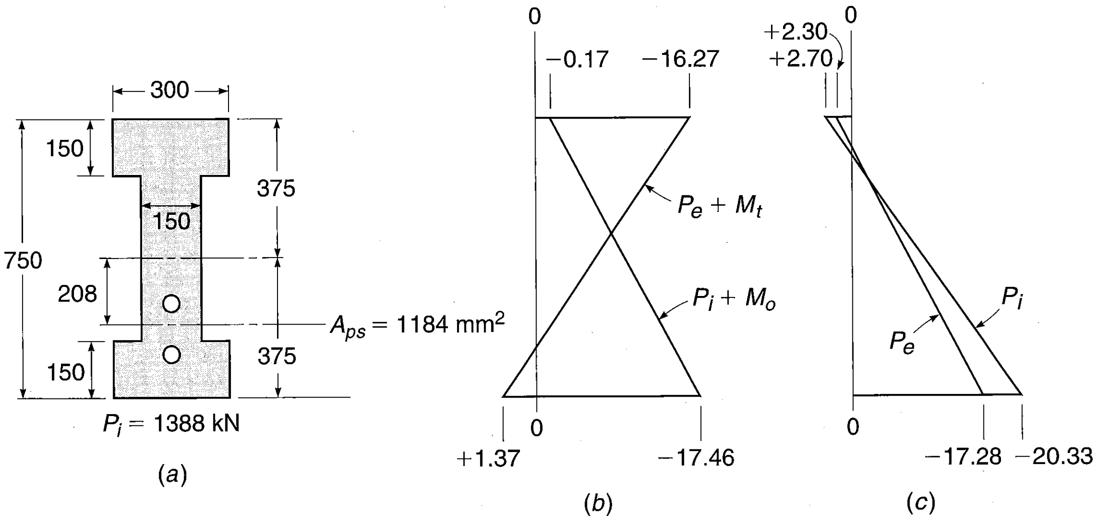

FIGURE 19.17

Design example of beam with constant eccentricity of tendons: (*a*) cross section dimensions (mm); (*b*) stresses at midspan (MPa); (*c*) stresses at supports (MPa).

Again, two tendons will be used to provide the required prestress force, each composed of multiple 12.7 mm diameter Grade 1860 low-relaxation strands. With the maximum permissible stress in the stranded cable just after transfer of 1373 MPa, the total required steel area is

$$A_{ps} = \frac{1388 \times 10^3}{1373} = 1011 \text{ mm}^2$$

A total of 12 strands is required. Two identical six-strand tendons with a total area of 1184 mm² will be used and stressed to a total of 1388 kN.

The calculations will be checked by verifying the concrete stresses at the top and bottom of the beam for the critical load stages. The component stress contributions are

$$P_i: \quad f_1 = -\frac{1388 \times 10^3}{157.5}\left(1 - \frac{208 \times 375}{59.7 \times 10^3}\right) = +2.70 \text{ MPa}$$

$$f_2 = -\frac{1388 \times 10^3}{157.5}\left(1 + \frac{208 \times 375}{59.7 \times 10^3}\right) = -20.33 \text{ MPa}$$

$$P_e: \quad f_1 = 0.85 \times 2.70 = +2.30 \text{ MPa}$$

$$f_2 = 0.85(-20.33) = -17.28 \text{ MPa}$$

$$M_o: \quad f_1 = -\frac{72 \times 10^6}{25.1 \times 10^6} = -2.87 \text{ MPa}$$

$$f_2 = +2.87 \text{ MPa}$$

$$M_d + M_l: \quad f_1 = -\frac{396 \times 10^6}{25.1 \times 10^6} = -15.78 \text{ MPa}$$

$$f_2 = +15.78 \text{ MPa}$$

Superimposing the appropriate stress contributions, the stress distributions in the concrete at midspan and at the supports are obtained, as shown in Fig. 19.17*b* and *c*, respectively. When the initial prestress force of 1388 kN acts alone, as at the supports, the stresses at the top and bottom surfaces are

$$f_1 = +2.70 \text{ MPa}$$

$$f_2 = -20.33 \text{ MPa}$$

After losses, the prestress force is reduced to 1180 kN and the support stresses are reduced accordingly. At midspan, the beam weight is immediately superimposed, and stresses resulting from P_i plus M_o are

$$f_1 = +2.70 - 2.87 = -0.17 \text{ MPa}$$

$$f_2 = -20.33 + 2.9 = -17.46 \text{ MPa}$$

When the full service load acts, together with P_e, the midspan stresses are

$$f_1 = +2.30 - 2.87 - 15.78 = -16.27 \text{ MPa}$$

$$f_2 = -17.28 + 2.87 + 15.78 = +1.37 \text{ MPa}$$

If we check against the specified limiting stresses, it is evident that the design is satisfactory in this respect at the critical load stages and locations.

19.10 SHAPE SELECTION

One of the special features of prestressed concrete design is the freedom to select cross-section proportions and dimensions to suit the special requirements of the job at hand. The member depth can be changed, the web thickness modified, and the flange widths and thicknesses varied independently to produce a beam with nearly ideal proportions for a given case.

Several common precast shapes are shown in Fig. 19.18. Some of these are standardized and mass-produced, employing reusable steel or fiberglass forms. Others are individually proportioned for large and important works. The double T (Fig. 19.18*a*) is probably the most widely used cross section in U.S. prestressed construction. A flat surface is provided, 1 to 4 m wide. Slab thicknesses and web depths vary, depending upon requirements. Spans to 18 m are not unusual. The single T (Fig. 19.18*b*) is more appropriate for longer spans, to 36 m, and heavier loads. The I and bulb

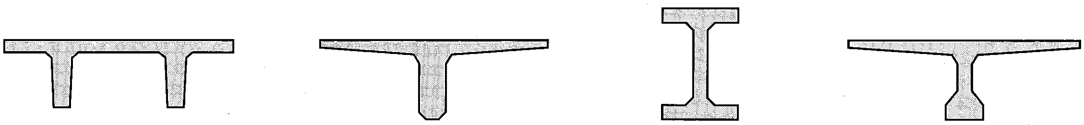

(*a*) Double T (*b*) Single T (*c*) I Girder (*d*) Bulb T

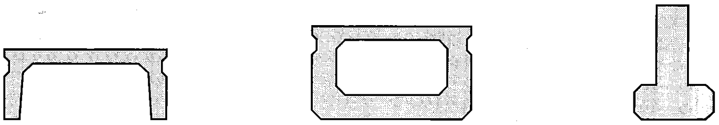

(*e*) Channel slab (*f*) Box girder (*g*) Inverted T

FIGURE 19.18
Typical beam cross sections.

T sections (Fig. 19.18*c* and *d*) are widely used for bridge spans and roof girders up to about 45 m, while the channel slab (Fig. 19.18*e*) is suitable for floors in the intermediate span range. The box girder (Fig. 19.18*f*) is advantageous for bridges of intermediate and major span. The inverted T section (Fig. 19.18*g*) provides a bearing ledge to carry the ends of precast deck members spanning in the perpendicular direction. Local precasting plants can provide catalogs of available shapes. This information is also available in the *PCI Design Handbook* (Ref. 19.8).

As indicated, the cross section may be symmetrical or unsymmetrical. An unsymmetrical section is a good choice (1) if the available stress ranges f_{1r} and f_{2r} at the top and bottom surfaces are not the same; (2) if the beam must provide a flat, useful surface as well as offering load-carrying capacity; (3) if the beam is to become a part of composite construction, with a cast-in-place slab acting together with a precast web; or (4) if the beam must provide support surfaces, such as shown in Fig. 19.18*g*. In addition, T sections provide increased flexural strength, since the internal arm of the resisting couple at maximum design load is greater than for rectangular sections.

Generally speaking, I, T, and box sections with relatively thin webs and flanges are more efficient than members with thicker parts. However, several factors limit the gain in efficiency that may be obtained in this way. These include the instability of very thin overhanging compression parts, the vulnerability of thin parts to breakage in handling (in the case of precast construction), and the practical difficulty of placing concrete in very thin elements. The designer must also recognize the need to provide adequate spacing and concrete protection for tendons and anchorages, the importance of construction depth limitations, and the need for lateral stability if the beam is not braced by other members against buckling (Ref. 19.16).

19.11 TENDON PROFILES

The equations developed in Section 19.9a for members with variable tendon eccentricity establish the requirements for section modulus, prestress force, and eccentricity at the maximum moment section of the member. Elsewhere along the span, the eccentricity of the steel must be reduced if the concrete stress limits for the unloaded stage are not to be exceeded. (Alternatively, the section must be increased, as demonstrated in Section 19.9b.) Conversely, there is a minimum eccentricity, or upper limit for the steel centroid, such that the limiting concrete stresses are not exceeded when the beam is in the full service load stage.

Limiting locations for the prestressing steel centroid at any point along the span can be established using Eqs. (19.2) and (19.4), which give the values of concrete stress at the top and bottom of the beam in the unloaded and service load stages, respectively. The stresses produced for those load stages should be compared with the limiting stresses applicable in a particular case, such as the ACI stress limits of Table 19.2. This permits a solution for tendon eccentricity e as a function of distance x along the span.

To indicate that both eccentricity e and moments M_o or M_t are functions of distance x from the support, they will be written as $e(x)$ and $M_o(x)$ or $M_t(x)$, respectively. In writing statements of inequality, it is convenient to designate tensile stress as larger than zero and compressive stress as smaller than zero. Thus, $+3.1 > -9.3$ and $-4.1 > -7.8$, for example.

Considering first the unloaded stage, the tensile stress at the top of the beam must not exceed f_{ti}. From Eq. (19.2*a*),

$$f_{ti} \geq -\frac{P_i}{A_c}\left[1 - \frac{e(x)c_1}{r^2}\right] - \frac{M_o(x)}{S_1} \qquad (a)$$

Solving for the maximum eccentricity gives

$$e(x) \leq \frac{f_{ti}S_1}{P_i} + \frac{S_1}{A_c} + \frac{M_o(x)}{P_i} \tag{19.29}$$

At the bottom of the unloaded beam, the stress must not exceed the limiting initial compression. From Eq. (19.2*b*),

$$f_{ci} \leq -\frac{P_i}{A_c}\left[1 + \frac{e(x)c_2}{r^2}\right] + \frac{M_o(x)}{S_2} \tag{b}$$

Hence, the second lower limit for the steel centroid is

$$e(x) \leq -\frac{f_{ci}S_2}{P_i} - \frac{S_2}{A_c} + \frac{M_o(x)}{P_i} \tag{19.30}$$

Now considering the member in the fully loaded stage, the upper limit values for the eccentricity may be found. From Eq. (19.4*a*),

$$f_{cs} \leq -\frac{P_e}{A_c}\left[1 - \frac{e(x)c_1}{r^2}\right] - \frac{M_t(x)}{S_1} \tag{c}$$

from which

$$e(x) \geq \frac{f_{cs}S_1}{P_e} + \frac{S_1}{A_c} + \frac{M_t(x)}{P_e} \tag{19.31}$$

and using Eq. (19.4*b*)

$$f_{ts} \geq -\frac{P_e}{A_c}\left[1 + \frac{e(x)c_2}{r^2}\right] + \frac{M_t(x)}{S_2} \tag{d}$$

from which

$$e(x) \geq -\frac{f_{ts}S_2}{P_e} - \frac{S_2}{A_c} + \frac{M_t(x)}{P_e} \tag{19.32}$$

Using Eqs. (19.29) and (19.30), the lower limit of tendon eccentricity is established at successive points along the span. Then, using Eqs. (19.31) and (19.32), the corresponding upper limit is established. This upper limit may well be negative, indicating that the tendon centroid may be above the concrete centroid at that location.

It is often convenient to plot the envelope of acceptable tendon profiles, as done in Fig. 19.19, for a typical case in which both dead and live loads are uniformly distributed. Any tendon centroid falling completely within the shaded zone would be satisfactory from the point of view of concrete stress limits. It should be emphasized that it is only the tendon centroid that must be within the shaded zone; individual cables are often outside of it.

The tendon profile actually used is often a parabolic curve or a catenary in the case of post-tensioned beams. The duct containing the prestressing steel is draped to the desired shape and held in that position by wiring it to the transverse web reinforcement, after which the concrete may be placed. In pretensioned beams, *deflected tendons* are often used. The cables are held down at midspan, at the third points, or at the quarter points of the span and held up at the ends, so that a smooth curve is approximated to a greater or lesser degree.

In practical cases, it is often not necessary to make a centroid zone diagram, such as is shown in Fig. 19.19. By placing the centroid at its known location at midspan, at or

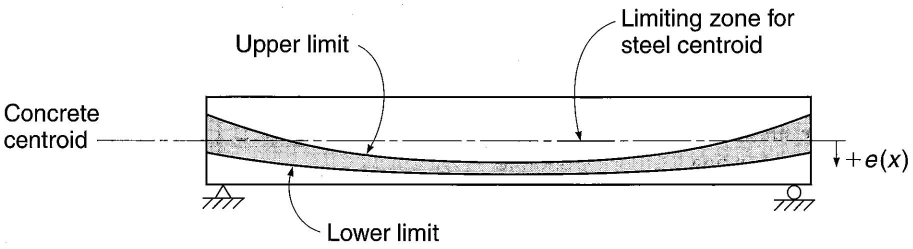

FIGURE 19.19
Typical limiting zone for centroid of prestressing steel.

close to the concrete centroid at the supports, and with a near-parabolic shape between those control points, satisfaction of the limiting stress requirements is ensured. With nonprismatic beams, beams in which a curved concrete centroidal axis is employed, or with continuous beams, diagrams such as Fig. 19.19 are a great aid.

19.12 FLEXURAL DESIGN BASED ON LOAD BALANCING

It was pointed out in Section 19.2b that the effect of a change in the alignment of a prestressing tendon in a beam is to produce a vertical force on the beam at that location. Prestressing a member with curved or deflected tendons thus has the effect of introducing a set of equivalent loads, and these may be treated just as any other loads in finding moments or deflections. Each particular tendon profile produces its own unique set of equivalent forces. Typical tendon profiles, with corresponding equivalent loads and moment diagrams, were illustrated in Fig. 19.2. Both Fig. 19.2 and Section 19.2b should be reviewed carefully.

The equivalent load concept offers an alternative approach to the determination of required prestress force and eccentricity. The prestress force and tendon profile can be established so that external loads that will act are exactly counteracted by the vertical forces resulting from prestressing. The net result, for that particular set of external loads, is that the beam is subjected only to axial compression and no bending moment. The selection of the load to be balanced is left to the judgment of the designer. Often the balanced load chosen is the sum of the self-weight and superimposed dead load.

The design approach described in this section was introduced in the United States by T. Y. Lin in 1963 and is known as the *load-balancing method.* The fundamentals will be illustrated in the context of the simply supported, uniformly loaded beam shown in Fig. 19.20*a*. The beam is to be designed for a balanced load consisting of its own weight w_o, the superimposed dead load w_d, and some fractional part of the live load, denoted by $k_b w_l$. Since the external load is uniformly distributed, it is reasonable to adopt a tendon having a parabolic shape. It is easily shown that a parabolic tendon will produce a uniformly distributed upward load equal to

$$w_p = \frac{8Py}{l^2} \tag{19.33}$$

where P = magnitude of prestress force
y = maximum sag of tendon measured with respect to the chord between its endpoints
l = span length

FIGURE 19.20
Load balancing for uniformly loaded beam: (*a*) external and equivalent loads; (*b*) concrete stresses resulting from axial and bending effects of prestress plus bending resulting from balanced external load; (*c*) concrete stresses resulting when load $k_b w_l$ is removed.

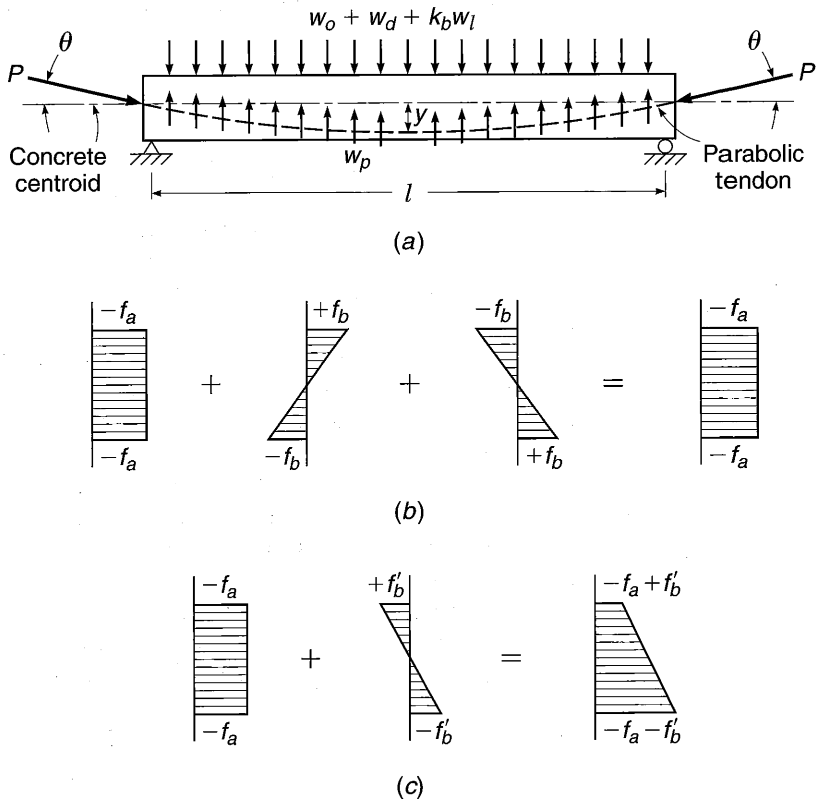

If the downward load exactly equals the upward load from the tendon, these two loads cancel and no bending stress is produced, as shown in Fig. 19.20*b*. The bending stresses due to prestress eccentricity are equal and opposite to the bending stresses resulting from the external load. The net resulting stress is uniform compression f_a equal to that produced by the axial force $P \cos \theta$. Excluding consideration of time-dependent effects, the beam would show no vertical deflection.

If the live load is removed or increased, then bending stresses and deflections will result because of the *unbalanced* portion of the load. Stresses resulting from this differential loading must be calculated and superimposed on the axial compression to obtain the net stresses for the unbalanced state. Referring to Fig. 19.20*c*, the bending stresses f_b' resulting from removal of the partial live loading are superimposed on the uniform compressive stress f_a, resulting from the combination of eccentric prestress force and full balanced load to produce the final stress distribution shown.

Loads other than uniformly distributed would lead naturally to the selection of other tendon configurations. For example, if the external load consisted of a single concentration at midspan, a deflected tendon such as that of Fig. 19.2*a* would be chosen, with maximum eccentricity at midspan, varying linearly to zero eccentricity at the supports. A third-point loading would lead the designer to select a tendon deflected at the third points. A uniformly loaded cantilever beam would best be stressed using a tendon in which the eccentricity varied parabolically, from zero at the free end to y at the fixed support, in which case the upward reaction of the tendon would be

$$w_p = \frac{2Py}{l^2} \tag{19.34}$$

It should be clear that, for simple spans designed by the load-balancing concept, it is necessary for the tendon to have zero eccentricity at the supports because the moment due to superimposed loads is zero there. Any tendon eccentricity would produce an unbalanced moment (in itself an equivalent load) equal to the horizontal component of the prestress force times its eccentricity. At the simply supported ends, the requirement of zero eccentricity must be retained.

In practice, the load-balancing method of design starts with selection of a trial beam cross section, based on experience and judgment. An appropriate span-depth ratio is often applied. The tendon profile is selected using the maximum available eccentricity, and the prestress force is calculated. The trial design may then be checked to ensure that concrete stresses are within the allowable limits should the live load be totally absent or fully in place, when bending stresses will be superimposed on the axial compressive stresses. There is no assurance that the section will be adequate for these load stages, or that adequate strength will be provided should the member be overloaded. Revision may be necessary.

It should further be observed that obtaining a uniform compressive concrete stress at the balanced load stage does not ensure that the member will have zero deflection at this stage. The reason is that the uniform stress distribution is made up of two parts: that from the eccentric prestress force and that from the external loads. The prestress force varies with time because of shrinkage, creep, and relaxation, changing the vertical deflection associated with the prestress force. Concurrently, the beam will experience creep deflection under the combined effects of the diminishing prestress force and the external loads, a part of which may be sustained and a part of which may be short-term. However, if load balancing is carried out based on the effective prestress force P_e plus self-weight and external dead load only, the result may be near-zero deflection for that combination.

The load-balancing method provides the engineer with a useful tool. For simple spans, it leads the designer to choose a sensible tendon profile and focuses attention very early on the matter of deflection. But the most important advantages become evident in the design of indeterminate prestressed members, including both continuous beams and two-way slabs. For such cases, at least for one unique loading, the member carries only axial compression but no bending. This greatly simplifies the analysis.

EXAMPLE 19.5

Beam design initiating with load balancing. A post-tensioned beam is to be designed to carry a uniformly distributed load over a 9 m span, as shown in Fig. 19.21. In addition to its own weight, it must carry a dead load of 2.0 kN/m and a service live load of 9.0 kN/m. Concrete strength of 28 MPa will be attained at 28 days; at the time of transfer of the prestress force, the strength will be 21 MPa. Prestress loss may be assumed at 20 percent of P_i. On the basis that about one-quarter of the live load will be sustained over a substantial time period, k_b of 0.25 will be used in determining the balanced load.

Solution. On the basis of an arbitrarily chosen span-depth ratio of 18, a 500 mm deep, 250 mm wide trial section is selected. The calculated self-weight of the beam is 3.0 kN/m, and the selected load to be balanced is

$$w_{\text{bal}} = w_o + w_d + k_b w_l = 3.0 + 2.0 + 2.25 = 7.25 \text{ kN/m}$$

Based on a minimum concrete cover from the steel centroid to the bottom face of the beam of 100 mm, the maximum eccentricity that can be used for the 500 mm trial section is 150 mm. A parabolic tendon will be used to produce a uniformly distributed upward tendon load. To equilibrate the sustained downward loading, the prestress force P_e after losses, from Eq. (19.33), should be

$$P_e = \frac{w_{\text{bal}} l^2}{8y} = \frac{7.25 \times 9^2}{8 \times 0.15} = 489 \text{ kN}$$

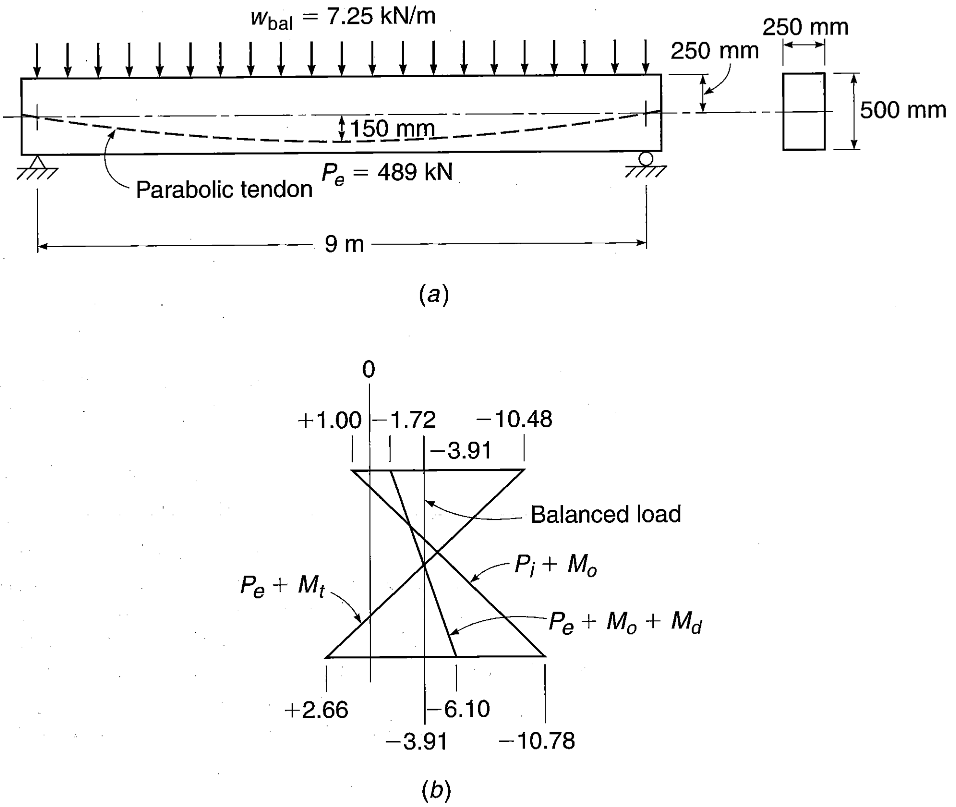
$w_{\text{bal}} = 7.25$ kN/m
250 mm
250 mm
500 mm
150 mm
$P_e = 489$ kN
Parabolic tendon
9 m
(a)
0
+1.00
−1.72
−10.48
−3.91
Balanced load
$P_i + M_o$
$P_e + M_t$
$P_e + M_o + M_d$
+2.66
−6.10
−3.91
−10.78
(b)

FIGURE 19.21
Example of design by load balancing: (*a*) beam profile and cross section; (*b*) flexural stresses at maximum moment section (MPa).

and the corresponding initial prestress force is

$$P_i = \frac{P_e}{R} = \frac{489}{0.8} = 611 \text{ kN}$$

For the balanced load stage, the concrete will be subjected to a uniform compressive stress of

$$f_{\text{bal}} = \frac{489 \times 10^3}{250 \times 500} = 3.91 \text{ MPa}$$

as shown in Fig. 19.21*b*. Should the partial live load of 2.25 kN/m be removed, the stresses to be superimposed on f_{bal} result from a net *upward* load of 2.25 kN/m. The section modulus for the trial beam is 10.4×10^6 mm^3 and

$$M_{\text{unbal}} = 2.25 \times \frac{9^2}{8} = 22.8 \text{ kN-m}$$

Hence, the unbalanced bending stresses at the top and bottom faces are

$$f_{\text{unbal}} = \frac{22.8 \times 10^6}{10.4 \times 10^6} = 2.91 \text{ MPa}$$

Thus, the net stresses are

$$f_1 = -3.91 + 2.19 = -1.72 \text{ MPa}$$
$$f_2 = -3.91 - 2.19 = -6.10 \text{ MPa}$$

Similarly, if the *full* live load should act, the stresses to be superimposed are those resulting from a net *downward* load of 6.75 kN/m. The resulting stresses in the concrete at full service load are

$$f_1 = -3.91 - 6.57 = -10.48 \text{ MPa}$$
$$f_2 = -3.91 + 6.57 = +2.66 \text{ MPa}$$

Stresses in the concrete with live load absent and live load fully in place are shown in Fig. 19.21*b*.

It is also necessary to investigate the stresses in the initial unloaded stage, when the member is subjected to P_i plus moment due to its own weight.

$$M_o = 3.0 \times \frac{9^2}{8} = 30.4 \text{ kN-m}$$

Hence, in the initial stage:

$$f_1 = -\frac{611 \times 10^3}{125 \times 10^3}\left(1 - \frac{150 \times 250}{20.8 \times 10^3}\right) - \frac{30.4 \times 10^6}{10.4 \times 10^6} = +1.00 \text{ MPa}$$

$$f_2 = -\frac{611 \times 10^3}{125 \times 10^3}\left(1 + \frac{150 \times 250}{20.8 \times 10^3}\right) + \frac{30.4 \times 10^6}{10.4 \times 10^6} = -10.78 \text{ MPa}$$

The stresses in the unloaded and full service load stages must be checked against these permitted by the ACI Code. With $f'_c = 28$ MPa and $f'_{ci} = 21$ MPa, the stresses permitted for a Class U member are

$$f_{ti} = +1.15 \text{ MPa} \qquad f_{ts} = +3.28 \text{ MPa}$$
$$f_{ci} = -12.6 \text{ MPa} \qquad f_{cs} = -16.80 \text{ MPa}$$

The actual stresses, shown in Fig. 19.21*b*, are within these limits and acceptably close, and no revision will be made in the trial 250 × 500 mm cross section on the basis of stress limits.

The flexural strength of the members must now be checked, to ensure that an adequate margin of safety against collapse has been provided. The required P_i of 611 kN will be provided using Grade 270 strand, with $f_{pu} = 1860$ MPa and $f_{py} = 1674$ MPa. Referring to Section 19.4, the initial stress immediately after transfer must not exceed $0.74 \times 1860 = 1376$ MPa, or $0.82 \times 1674 = 1373$ MPa, which controls in this case. Accordingly, the required area of tendon steel is

$$A_{ps} = 611 \times 10^3/1373 = 445 \text{ mm}^2$$

This will be provided using five 12.7 mm strands, giving an actual area of 494 mm^2 (Table A.15). The resulting stresses at the initial and final stages are

$$f_{pi} = \frac{611 \times 10^3}{494} = 1237 \text{ MPa}$$

$$f_{pe} = \frac{489 \times 10^3}{494} = 990 \text{ MPa}$$

Using the ACI approximate equation for steel stress at failure [see Eq. (19.6)], with $\rho_p = 494/(400 \times 250) = 0.0049$, and $\gamma_p = 0.40$ for the ordinary Grade 1860 tendons, the stress f_{ps} is given by

$$\begin{aligned} f_{ps} &= f_{pu}\left(1 - \frac{\gamma_p}{\beta_1}\frac{\rho_p f_{pu}}{f'_c}\right) \\ &= 1860\left(1 - \frac{0.40}{0.85}\frac{0.0049 \times 1860}{28}\right) \\ &= 1537 \text{ MPa} \end{aligned}$$

Then

$$\begin{aligned} a &= \frac{A_{ps} f_{ps}}{0.85 f'_c b} \\ &= \frac{494 \times 1537}{0.85 \times 28 \times 250} = 128 \text{ mm} \end{aligned}$$

$$c = \frac{128}{0.85} = 151$$

$$\frac{c}{d_t} = \frac{151}{400} = 0.378$$

This exceeds $c/d_t = 0.375$, reducing ϕ to 0.89. The nominal flexural strength is

$$M_n = A_{ps}f_{ps}\left(d - \frac{a}{2}\right) = 494 \times 1537\left(400 - \frac{128}{2}\right) \times 10^{-6}$$
$$= 255 \text{ kN-m}$$

and the design strength with $\phi = 0.89$ is

$$\phi M_n = 0.89 \times 255 = 227 \text{ kN-m}$$

It will be recalled that the ACI load factors with respect to dead and live loads are, respectively, 1.2 and 1.6. Calculating the factored load,

$$w_u = 1.2(3.0 + 2.0) + 1.6(9.0) = 20.4 \text{ kN/m}$$

$$M_u = \frac{20.4 \times 9^2}{8} = 207 \text{ kN-m}$$

Thus, $\phi M_n > M_u$, and the design is judged satisfactory.

19.13 LOSS OF PRESTRESS

As discussed in Section 19.6, the initial prestress force P_i immediately after transfer is less than the jacking force P_j because of elastic shortening of the concrete, slip at the anchorages, and frictional losses along the tendons. The force is reduced further, after a period of many months or even years, due to length changes resulting from shrinkage and creep of the concrete and relaxation of the highly stressed steel; eventually it attains its effective value P_e. In the preceding sections of this chapter, losses were accounted for, making use of an assumed effectiveness ratio $R = P_e/P_i$. Losses have no effect on the nominal strength of a member with bonded tendons, but overestimation or underestimation of losses may have a pronounced effect on service conditions including camber, deflection, and cracking.

The estimation of losses can be made on several different levels. Lump-sum losses, used in the early development of prestressed concrete, are now considered obsolete. Values of R based on detailed calculations and verified in field applications are used in design offices, as are tables of individual loss contributions. For cases where greater accuracy is required, it is necessary to estimate the separate losses, taking account of the conditions of member geometry, material properties, and construction methods that apply. Accuracy of loss estimation can be improved still further by accounting for the interdependence of time-dependent losses, using the summation of losses in a sequence of discrete time steps. These methods will be discussed briefly in the following paragraphs.

a. Lump-Sum Estimates of Losses

It was recognized very early in the development of prestressed concrete that there was a need for approximate expressions to be used to estimate prestress losses in design. Many thousands of successful prestressed structures have been built based on such estimates, and where member sizes, spans, materials, construction procedures, prestress forces, and environmental conditions are not out of the ordinary, this approach is satisfactory. For such conditions, the American Association of State Highway and Transportation Officials (AASHTO, Ref. 19.17) has recommended

TABLE 19.3
Estimate of prestress losses

Type of Beam Section	Level	Wires or Strands with f_{pu} = 1620, 1725, 1860 MPa[a]
Rectangular beams, solid slabs	Upper bound	228 MPa
	Average	208 MPa
Box girder	Upper bound	173 MPa
	Average	158 MPa
I girder	Average	$230[1 - 0.15(f_c' - 41)/41] + 41$
Single T, double T, hollow core and voided slab	Upper bound	$270[1 - 0.15(f_c' - 41)/41] + 41$
	Average	$230[1 - 0.15(f_c' - 41)/41] + 41$

[a] Values are for fully prestressed beams; reductions are allowed for partial prestress.
Losses due to friction are excluded. Friction losses should be computed according to Section 19.13b.
For low-relaxation strands, the values specified may be reduced by 28 MPa for box girders; 42 MPa for rectangular beams, solid slabs, and I girders; and 56 MPa for single T's, double T's, hollow core and voided slabs.

Source: Adapted from Ref. 19.17.

the values in Table 19.3 for preliminary design or for certain controlled precasting conditions. It should be noted that losses due to friction must be added to these values for post-tensioned members. These may be calculated separately by the equations of Section 19.13b below.

The AASHTO recommended losses of Table 19.3 include losses due to elastic shortening, creep, shrinkage, and relaxation (see Section 19.13b). Thus for comparison with R values for estimating losses, such as were employed for the preceding examples, which included only the time-dependent losses due to shrinkage, creep, and relaxation, elastic shortening losses should be estimated by the methods discussed in Section 19.13b and deducted from the total.

b. Estimate of Separate Losses

A separate estimate of individual losses is made for most designs and specifically required when using the ACI Code. Such an analysis is complicated by the interdependence of time-dependent losses. For example, the relaxation of stress in the tendons is affected by length changes due to creep of concrete. Rate of creep, in turn, is altered by change in tendon stress. In the following six subsections, losses are treated as if they occurred independently, although certain arbitrary adjustments are included to account for the interdependence of time-dependent losses. If greater refinement is necessary, a step-by-step approach like that mentioned in Section 19.13c may be used (see also Refs. 19.8, 19.18, and 19.19).

(1) SLIP AT THE ANCHORAGES As the load is transferred to the anchorage device in post-tensioned construction, a slight inward movement of the tendon will occur as the wedges seat themselves and as the anchorage itself deforms under stress. The amount of movement will vary greatly, depending on the type of anchorage and on construction techniques. The amount of movement due to seating and stress deformation associated with any particular type of anchorage is best established by test. Once this amount ΔL is determined, the stress loss is easily calculated from

$$\Delta f_{s,\text{slip}} = \frac{\Delta L}{L} E_s \tag{19.35}$$

It is significant to note that the amount of slip is nearly independent of the cable length. For this reason, the stress loss will be large for short tendons and relatively small for long tendons. The practical consequence of this is that it is most difficult to post-tension short tendons with any degree of accuracy.

(2) ELASTIC SHORTENING OF THE CONCRETE In pretensioned members, as the tendon force is transferred from the fixed abutments to the concrete beam, elastic instantaneous compressive strain will take place in the concrete, tending to reduce the stress in the bonded prestressing steel. The steel stress loss is

$$\Delta f_{s,\text{elastic}} = E_s \frac{f_c}{E_c} = nf_c \tag{19.36}$$

where f_c is the concrete stress at the level of the steel centroid immediately after prestress is applied:

$$f_c = -\frac{P_i}{A_c}\left(1 + \frac{e^2}{r^2}\right) + \frac{M_o e}{I_c} \tag{19.37}$$

If the tendons are placed with significantly different effective depths, the stress loss in each should be calculated separately.

In computing f_c by Eq. (19.37), the prestress force used should be that after the losses being calculated have occurred. It is usually adequate to estimate this as about 10 percent less than P_j.

In post-tensioned members, if all of the strands are tensioned at one time, there will be no loss due to elastic shortening, because this shortening will occur as the jacking force is applied and before the prestressing force is measured. On the other hand, if various strands are tensioned sequentially, the stress loss in each strand will vary, being a maximum in the first strand tensioned and zero in the last strand. In most cases, it is sufficiently accurate to calculate the loss in the first strand and to apply one-half that value to all strands.

(3) FRICTIONAL LOSSES Losses due to friction, as the tendon is stressed in post-tensioned members, are usually separated for convenience into two parts: curvature friction and wobble friction. The first is due to intentional bends in the tendon profile as specified and the second to the unintentional variation of the tendon from its intended profile. It is apparent that even a "straight" tendon duct will have some unintentional misalignment so that wobble friction must always be considered in post-tensioned work. Usually, curvature friction must be considered as well. The force at the jacking end of the tendon P_o, required to produce the force P_x at any point x along the tendon, can be found from the expression

$$P_o = P_x e^{Kl_x + \mu\alpha} \tag{19.38a}$$

where e = base of natural logarithms
l_x = tendon length from jacking end to point x
α = angular change of tendon from jacking end to point x, rad
K = wobble friction coefficient, N/N per m
μ = curvature friction coefficient

There has been much research on frictional losses in prestressed construction, particularly with regard to the values of K and μ. These vary appreciably, depending on construction methods and materials used. The values in Table 19.4, from ACI Commentary R18.6, may be used as a guide.

TABLE 19.4
Friction coefficients for post-tensioned tendons

Type of Tendon	Wobble Coefficient K, per m	Curvature Coefficient μ
Grouted tendons in metal sheathing		
Wire tendons	0.0033–0.0049	0.15–0.25
High-strength bars	0.0003–0.0020	0.08–0.30
Seven-wire strand	0.0016–0.0066	0.15–0.25
Unbonded tendons		
Mastic-coated wire tendons	0.0033–0.0066	0.05–0.15
Mastic-coated seven-wire strand	0.0033–0.0066	0.05–0.15
Pregreased wire tendons	0.0010–0.0066	0.05–0.15
Pregreased seven-wire strand	0.0010–0.0066	0.05–0.15

If one accepts the approximation that the normal pressure on the duct causing the frictional force results from the undiminished initial tension all the way around the curve, the following simplified expression for loss in tension is obtained:

$$P_o = P_x(1 + Kl_x + \mu\alpha) \tag{19.38b}$$

where α is the angle between the tangents at the ends. The ACI Code permits the use of the simplified form, if the value of $Kl_x + \mu\alpha$ is not greater than 0.3.

The loss of prestress for the entire tendon length can be computed by segments, with each segment assumed to consist of either a circular arc or a length of tangent.

(4) CREEP OF CONCRETE Shortening of concrete under sustained load has been discussed in Section 2.8. It can be expressed in terms of the creep coefficient C_c. Creep shortening may be several times the initial elastic shortening, and it is evident that it will result in loss of prestress force. The stress loss can be calculated from

$$\Delta f_{s,\text{creep}} = C_c n f_c \tag{19.39}$$

Ultimate values of C_c for different concrete strengths for average conditions of humidity C_{cu} are given in Table 2.2.

In Eq. (19.39), the concrete stress f_c to be used is that at the level of the steel centroid, when the eccentric prestress force plus all sustained loads are acting. Equation (19.37) can be used, except that the moment M_o should be replaced by the moment due to *all* dead loads plus that due to any portion of the live load that may be considered sustained.

It should be noted that the prestress force causing creep is not constant but diminishes with the passage of time due to relaxation of the steel, shrinkage of the concrete, and length changes associated with creep itself. To account for this, it is recommended that the prestress force causing creep be assumed at 10 percent less than the initial value P_i.

(5) SHRINKAGE OF CONCRETE It is apparent that a decrease in the length of a member due to shrinkage of the concrete will be just as detrimental as length changes due to stress, creep, or other causes. As discussed in Section 2.11, the shrinkage strain ϵ_{sh} may vary between about 0.0004 and 0.0008. A typical value of 0.0006 may be used in lieu of specific data. The steel stress loss resulting from shrinkage is

$$\Delta f_{s,\text{shrink}} = \epsilon_{sh} E_s \tag{19.40}$$

Only that part of the shrinkage that occurs after transfer of prestress force to the concrete need be considered. For pretensioned members, transfer commonly takes place just 18 hours after placing the concrete, and nearly all the shrinkage takes place after that time. However, post-tensioned members are seldom stressed at an age earlier than 7 days and often much later than that. About 15 percent of ultimate shrinkage may occur within 7 days, under typical conditions, and about 40 percent by the age of 28 days.

(6) RELAXATION OF STEEL The phenomenon of relaxation, similar to creep, was discussed in Section 2.16c. Loss of stress due to relaxation will vary depending upon the stress in the steel, and may be estimated using Eqs. (2.11) and (2.12). To allow for the gradual reduction of steel stress resulting from the combined effects of creep, shrinkage, and relaxation, the relaxation calculation can be based on a prestress force 10 percent less than P_i.

It is interesting to observe that the largest part of the relaxation loss occurs shortly after the steel is stretched. For stresses of $0.80f_{pu}$ and higher, even a very short period of loading will produce substantial relaxation, and this in turn will reduce the relaxation that will occur later at a lower stress level. The relaxation rate can thus be artificially accelerated by temporary overtensioning. This technique is the basis for producing low-relaxation steel.

c. Loss Estimation by the Time-Step Method

The loss calculations of the preceding paragraphs recognized the interdependence of creep, shrinkage, and relaxation losses in an approximate way, by an arbitrary reduction of 10 percent of the initial prestress force P_i to obtain the force for which creep and relaxation losses were calculated. For cases requiring greater accuracy, losses can be calculated for discrete time steps over the period of interest. The prestress force causing losses during any time step is taken equal to the value at the end of the preceding time step, accounting for losses due to all causes up to that time. Accuracy can be improved to any desired degree by reducing the length and increasing the number of time steps.

A step-by-step method developed by the Committee on Prestress Losses of the Prestressed Concrete Institute uses only a small number of time steps and is adequate for ordinary cases (Ref. 19.18).

19.14 SHEAR, DIAGONAL TENSION, AND WEB REINFORCEMENT

In prestressed concrete beams at service load, there are two factors that greatly reduce the intensity of diagonal tensile stresses, compared with stresses that would exist if no prestress force were present. The first of these results from the combination of longitudinal compressive stress and shearing stress. An ordinary tensile reinforced concrete beam under load is shown in Fig. 19.22*a*. The stresses acting on a small element of the beam taken near the neutral axis and near the support are shown in (*b*). It is found by means of Mohr's circle of stress (*c*) that the principal stresses act at 45° to the axis of the beam (*d*) and are numerically equal to the shear stress intensity; thus

$$t_1 = t_2 = v \tag{a}$$

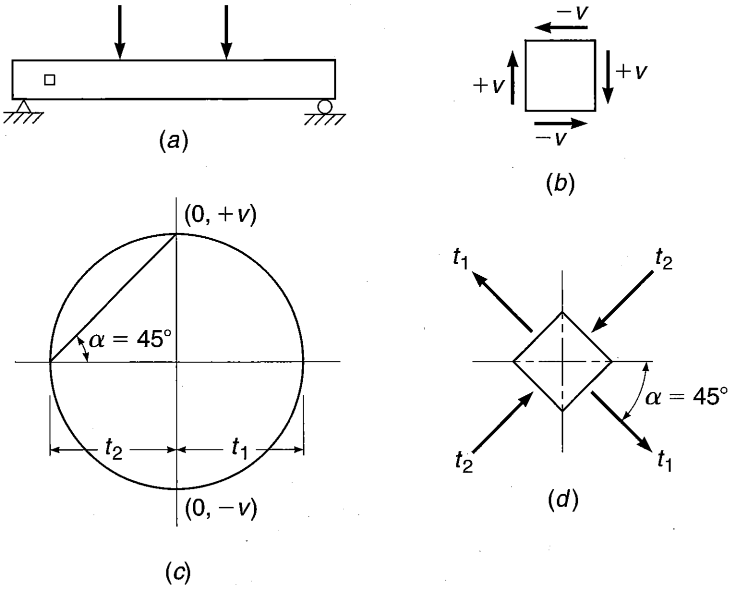
(a)
−v
+v
+v
−v
(b)
(0, +v)
α = 45°
t2
t1
(0, −v)
(c)
t1
t2
α = 45°
t2
t1
(d)

FIGURE 19.22
Principal stress analysis for an ordinary reinforced concrete beam.

Now suppose that the same beam, with the same loads, is subjected to a precompression stress in the amount *c*, as shown in Fig. 19.23*a* and *b*. From Mohr's circle (Fig. 19.23*c*), the principal tensile stress is

$$t_1 = -\frac{c}{2} + \sqrt{v^2 + \left(\frac{c}{2}\right)^2} \qquad (b)$$

and the direction of the principal tension with respect to the beam axis is

$$\tan 2\alpha = \frac{2v}{c} \qquad (c)$$

as shown in Fig. 19.23*d*.

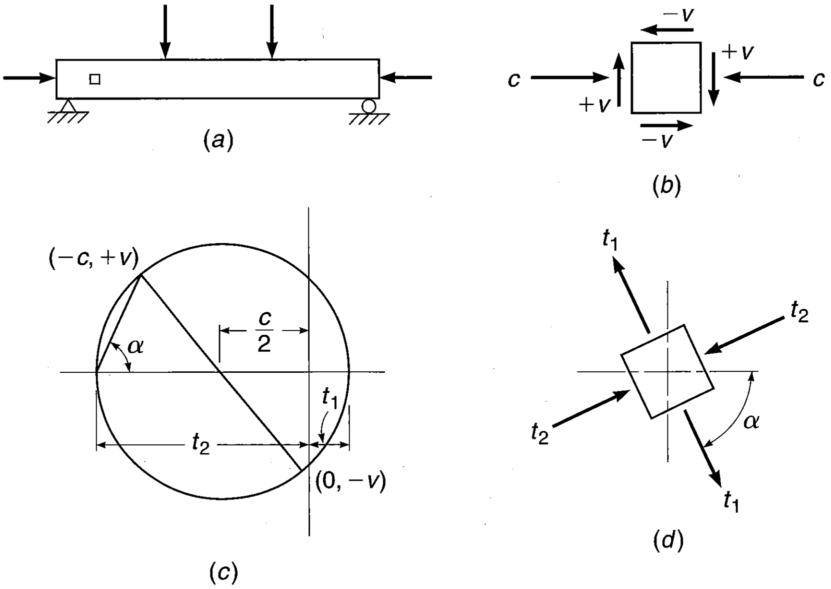
(a)
−v
c
+v
+v
c
−v
(b)
(−c, +v)
α
c/2
t1
t2
(0, −v)
(c)
t1
t2
t2
α
t1
(d)

FIGURE 19.23
Principal stress analysis for a prestressed concrete beam.

Comparison of Eq. (*a*) with Eq. (*b*) and Fig. 19.22*c* with Fig. 19.23*c* shows that, with the same shear stress intensity, the principal tension in the prestressed beam is much reduced.

The second factor working to reduce the intensity of the diagonal tension at service loads results from the slope of the tendons. Normally, this slope is such as to produce a shear due to the prestress force that is opposite in direction to the load-imposed shear. The magnitude of this *countershear* is $V_p = P_e \sin\theta$, where θ is the slope of the tendon at the section considered (see Fig. 19.8).

It is important to note, however, that in spite of these characteristics of prestressed beams at service loads, an investigation of diagonal tensile stresses at service loads does not ensure an adequate margin of safety against failure. In Fig. 19.23*c*, it is evident that a relatively small decrease in compressive stress and increase in shear stress, which may occur when the beam is overloaded, will produce a disproportionately large increase in the resulting principal tension. In addition to this effect, if the countershear of inclined tendons is used to reduce design shear, its contribution does not increase directly with load, but much more slowly (see Section 19.7). Consequently, a small increase in total shear may produce a large increase in the net shear for which the beam must be designed. For these two reasons, it is necessary to base design for diagonal tension in prestressed beams on conditions at factored load rather than at service load. The study of principal stresses in the uncracked prestressed beam is significant only in predicting the load at which the first diagonal crack forms.

At loads near failure, a prestressed beam is usually extensively cracked and behaves much like an ordinary reinforced concrete beam. Accordingly, many of the procedures and equations developed in Section 4.5 for the design of web reinforcement for nonprestressed beams can be applied to prestressed beams also. Shear design is based on the relation

$$V_u \le \phi V_n \tag{19.41}$$

where V_u is the total shear force applied to the section at factored loads and V_n is the nominal shear strength, equal to the sum of the contributions of the concrete V_c and web reinforcement V_s:

$$V_n = V_c + V_s \tag{19.42}$$

The strength reduction factor ϕ is equal to 0.75 for shear.

In computing the factored load shear V_u, the first critical section is assumed to be at a distance $h/2$ from the face of a support, and sections located a distance less than $h/2$ are designed for the shear computed at $h/2$.

The shear force V_c resisted by the concrete after cracking has occurred is taken equal to the shear that causes the first diagonal crack. Two types of diagonal cracks have been observed in tests of prestressed concrete beams:

1. **Flexure-shear cracks,** occurring at nominal shear V_{ci}, start as nearly vertical flexural cracks at the tension face of the beam, then spread diagonally upward (under the influence of diagonal tension) toward the compression face. These are common in beams with a low value of prestress force.
2. **Web-shear cracks,** occurring at nominal shear V_{cw}, start in the web due to high diagonal tension, then spread diagonally both upward and downward. These are often found in beams with thin webs with high prestress force.

On the basis of extensive tests, it was established that the shear causing flexure shear cracking can be found using the expression

$$V_{ci} = 0.05\sqrt{f'_c}\,b_w d_p + V_{cr,o+d+l} \tag{a}$$

where $V_{cr,o+d+l}$ is the shear force, due to total load, at which the flexural crack forms at the section considered, and $0.05\sqrt{f'_c}b_w d_p$ represents an additional shear force required to transform the flexural crack into an inclined crack.

While self-weight is generally uniformly distributed, the superimposed dead and live loads may have any distribution. Consequently, it is convenient to separate the total shear into V_o caused by the beam self-weight (without load factor) and V_{cr}, the additional shear force, due to superimposed dead and live loads, corresponding to flexural cracking. Thus,

$$V_{ci} = 0.05\sqrt{f'_c}b_w d_p + V_o + V_{cr} \tag{b}$$

The shear V_{cr} due to superimposed loads can then be found conveniently from

$$V_{cr} = \frac{V_{d+l}}{M_{d+l}} M_{cre} \tag{c}$$

where V_{d+l}/M_{d+l}, the ratio of superimposed dead and live load shear to moment, remains constant as the load increases to the cracking load, and

$$M_{cre} = \frac{I_c}{y_t}\,(0.5\lambda\sqrt{f'_c} + f_{pe} - f_o) \tag{19.43}$$

where y_t = distance from concrete centroid to tension face
f_{pe} = compressive stress at tension face resulting from effective prestress force alone
f_o = stress due to beam self-weight (unfactored) at extreme fiber of section where tensile stress is caused by externally applied dead and live loads[†]

The first term inside the parentheses is a conservative estimate of the modulus of rupture. The bottom-fiber stress due to self-weight is subtracted here because self-weight is considered separately in Eq. (*b*). Thus, Eq. (*b*) becomes

$$V_{ci} = 0.05\lambda\sqrt{f'_c}b_w d_p + V_o + \frac{V_{d+l}}{M_{d+l}} M_{cre} \tag{19.44}$$

Tests indicate that V_{ci} need not be taken less than $0.14\lambda\sqrt{f'_c}b_w d_p$. The value of d_p need not be taken less than $0.80h$ for this and all other equations relating to shear, according to the ACI Code, unless specifically noted otherwise. Additionally, the values V_{d+l} and M_{d+l} should be computed for the load combination causing the maximum moment in the section. Because V_{d+l} is the incremental load above the beam self-weight, the ACI Code uses the notation $V_i M_{cre}/M_{\max}$, noting that M_{cre} comes from Eq. (19.43).

The shear force causing web-shear cracking can be found from an exact principal stress calculation, in which the principal tensile stress is set equal to the direct tensile capacity of the concrete (conservatively taken equal to $0.33\lambda\sqrt{f'_c}$ according to the ACI Code). Alternatively, the ACI Code permits use of the approximate expression

$$V_{cw} = (0.29\lambda\sqrt{f'_c} + 0.3f_{pc})b_w d_p + V_p \tag{19.45}$$

in which f_{pc} is the compressive stress in the concrete, after losses, at the centroid of the concrete section (or at the junction of the web and the flange when the centroid lies in the flange) and V_p is the vertical component of the effective prestress force. In a pretensioned beam, the $0.3f_{pc}$ contribution to V_{cw} should be adjusted from zero at the beam end to its full value one transfer length (see Section 19.15b) in from the end of the beam.

[†] All stresses are used with absolute value here, consistent with ACI convention.

After V_{ci} and V_{cw} have been calculated, then V_c, the shear resistance provided by the concrete, is taken equal to the smaller of the two values.

Calculating M_{cre}, V_{ci}, and V_{cw} for a prestressed beam is a tedious matter because many of the parameters vary along the member axis. For hand calculations, the required quantities may be found at discrete intervals along the span, such as at $l/2$, $l/3$, $l/6$, and at $h/2$ from the support face, and stirrups spaced accordingly, or computer spreadsheets may be used.

To shorten the calculation required, the ACI Code includes, as a conservative alternative to the above procedure, an equation for finding the concrete shear resistance V_c directly:

$$V_c = \left(0.05\lambda\sqrt{f'_c} + 4.8\,\frac{V_u d_p}{M_u}\right) b_w d \tag{19.46}$$

in which M_u is the bending moment occurring simultaneously with shear force V_u, but $V_u d_p/M_u$ is not to be taken greater than 1.0, and d is the effective depth including prestressed and nonprestressed reinforcement. When this equation is used, V_c need not be taken less than $0.17\lambda\sqrt{f'_c}b_w d_p$ and must not be taken greater than $0.42\lambda\sqrt{f'_c}b_w d_p$. While Eq. (19.46) is temptingly easy to use and may be adequate for uniformly loaded members of minor importance, its use is apt to result in highly uneconomical designs for I beams with medium and long spans and for composite construction (Ref. 19.20).

When shear reinforcement perpendicular to the axis of the beam is used, its contribution to shear strength of a prestressed beam is

$$V_s = \frac{A_v f_{yt} d}{s} \tag{19.47}$$

the same as for a nonprestressed member. According to the ACI Code, the value of V_s must not be taken greater than $0.66\sqrt{f'_c}b_w d$.

The total nominal shear strength V_n is found by summing the contributions of the concrete and steel, as indicated by Eq. (19.42):

$$V_n = V_c + \frac{A_v f_{yt} d}{s} \tag{19.48}$$

Then, from Eq. (19.41),

$$V_u = \phi V_n = \phi(V_c + V_s)$$

from which

$$V_u = \phi\left(V_c + \frac{A_v f_{yt} d}{s}\right) \tag{19.49}$$

The required cross-sectional area of one stirrup A_v can be calculated by suitable transposition of Eq. (19.49).

$$A_v = \frac{(V_u - \phi V_c)s}{\phi f_{yt} d} \tag{19.50}$$

Normally, in practical design, the engineer will select a trial stirrup size, for which the required spacing is found. Thus, a more convenient form of the last equation is

$$s = \frac{\phi A_v f_{yt} d}{V_u - \phi V_c} \tag{19.51}$$

A minimum area of shear reinforcement is required in all prestressed concrete members where the total factored shear force is greater than one-half the design shear strength provided by the concrete ϕV_c. Exceptions are made for slabs and footings, concrete-joist floor construction, and certain very shallow beams, according to the ACI Code. The minimum area of shear reinforcement to be provided in all other cases is equal to the smaller of

$$A_{v,\min} = 0.062\sqrt{f_c'}\,\frac{b_w s}{f_{yt}} \le 0.35\,\frac{b_w s}{f_{yt}} \tag{19.52}$$

and

$$A_{v,\min} = \frac{A_{ps}}{80}\,\frac{f_{pu}}{f_{yt}}\,\frac{s}{d}\sqrt{\frac{d}{b_w}} \tag{19.53}$$

in which A_{ps} is the cross-sectional area of the prestressing steel, f_{pu} is the tensile strength of the prestressing steel, and all other terms are as defined above.

The ACI Code contains certain restrictions on the maximum spacing of web reinforcement to ensure that any potential diagonal crack will be crossed by at least a minimum amount of web steel. For prestressed members, this maximum spacing is not to exceed the smaller of $0.75h$ or 600 mm. If the value V_s exceeds $0.33\sqrt{f_c'}\,b_w d_p$, these limits are reduced by one-half.

EXAMPLE 19.6 The unsymmetrical I beam shown in Fig. 19.24 carries an effective prestress force of 1280 kN and supports a superimposed dead load of 5 kN/m and service live load of 13 kN/m, in addition to its own weight of 3.6 kN/m, on a 15 m simple span. At the maximum moment section, the effective depth to the main steel is 612 mm (eccentricity 293 mm). The strands are deflected upward starting 4.5 m from the support, and eccentricity is reduced linearly to zero at the support. If concrete with $f_c' = 35$ MPa and stirrups with $f_{yt} = 420$ MPa are used, and if the prestressed strands have strength $f_{pu} = 1860$ MPa, what is the required stirrup spacing at a point 3 m from the support?

SOLUTION. For a cross section with the given dimensions, it is easily confirmed that $I_c = 9.45 \times 10^9$ mm^4, $A_c = 153 \times 10^3$ mm^2, and $r^2 = I_c/A_c = 61.8 \times 10^3$ mm^2. At a distance 3 m from the support centerline, the tendon eccentricity is

$$e = 293 \times \frac{3}{4.5} = 195 \text{ mm}$$

FIGURE 19.24
Post-tensioned beam in Example 19.6.

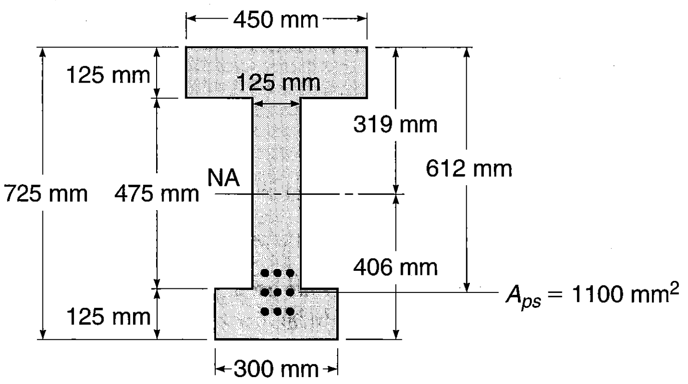

corresponding to an effective depth d from the compression face of 514 mm. According to the ACI Code, the larger value of $d = 0.80 \times 725 = 580$ mm will be used. Calculation of V_{ci} is based on Eqs. (19.43) and (19.44). The bottom-fiber stress due to effective prestress acting alone is

$$f_{pe} = f_{2pe} = -\frac{P_e}{A_c}\left(1 + \frac{ec_2}{r^2}\right) = -\frac{1280 \times 10^3}{153 \times 10^3}\left(1 + \frac{195 \times 406}{61.8 \times 10^3}\right) = -19.08 \text{ MPa}$$

The moment and shear at the section due to beam load alone are, respectively,

$$M_{o,10} = \frac{w_o x}{2}(l - x) = \frac{3.6 \times 3}{2}(15 - 3) = 64.8 \text{ kN-m}$$

$$V_{o,10} = w_o\left(\frac{l}{2} - x\right) = 3.6\left(\frac{15}{2} - 3\right) = 16.2 \text{ kN}$$

and the bottom-fiber stress due to this load is

$$f_{2o} = \frac{64.8 \times 406}{9.45 \times 10^9} = 2.78 \text{ MPa}$$

Then, from Eq. (19.43),

$$M_{cre} = \frac{9.45 \times 10^9(2.96 + 19.08 - 2.78)}{406} \times 10^{-6} = 448 \text{ kN-m}$$

The ratio of superimposed load shear to moment at the section is

$$\frac{V_{d+l}}{M_{d+l}} = \frac{l - 2x}{x(l - x)} = \frac{15 - 2 \times 3}{3(15 - 3)} = 0.25 \text{ m}^{-1}$$

Equation (19.44) is then used to determine the shear force at which flexure-shear cracks can be expected to form.

$$V_{ci} = [0.05 \times 1\sqrt{35}(125 \times 580) \times 10^{-3} + 16.2 + 0.25 \times 448] = 150 \text{ kN}$$

The lower limit of $0.14 \times 1\sqrt{35}(125 \times 580) \times 10^{-3} = 60$ kN does not control.

Calculation of V_{cw} is based on Eq. (19.45). The slope θ of the tendons at the section under consideration is such that $\sin\theta \approx \tan\theta = 293/4500 = 0.065$. Consequently, the vertical component of the effective prestress force is $V_p = 0.065 \times 1280 = 83.2$ kN. The concrete compressive stress at the section centroid is

$$f_{pc} = \frac{1280 \times 10^3}{153 \times 10^3} = 8.37 \text{ MPa}$$

Equation (19.45) can now be used to find the shear at which web-shear cracks should occur.

$$V_{cw} = [(0.29 \times 1\sqrt{35} + 0.3 \times 8.37)125 \times 580 \times 10^{-3} + 83.2] = 390 \text{ kN}$$

Thus, in the present case,

$$V_c = V_{ci} = 150 \text{ kN}$$

At the section considered, the total shear force at factored loads is

$$V_u = 1.2 \times 8.6 \times 4.5 + 1.6 \times 13.0 \times 4.5 = 140 \text{ kN}$$

When No. 10 (No. 3) U stirrups are used, for which $A_v = 2 \times 71 = 142 \text{ mm}^2$, the required spacing is found from Eq. (19.51) to be

$$s = \frac{0.75 \times 142 \times 420 \times 580}{(140 - 0.75 \times 150) \times 10^3} = 943 \text{ mm}$$

Equation (19.53) is then applied to establish a maximum spacing criterion.

$$142 = \frac{1100}{80} \times \frac{1860}{420} \times \frac{s}{580}\sqrt{\frac{580}{125}} = 0.226s$$

$$s = 628 \text{ mm}$$

The other criteria for maximum spacing, $\frac{3}{4} \times 725 = 544$ mm and 600 mm, however, control here. Open U stirrups will be used, at a spacing of 540 mm.

For comparison, the concrete shear will be calculated on the basis of Eq. (19.46). The ratio V_u/M_u is 0.25, and

$$V_c = (0.05 \times 1\sqrt{35} + 4.8 \times 0.25 \times 0.58)(125 \times 580)10^{-3} = 71.9 \text{ kN}$$

The lower and upper limits, $0.17 \times 1\sqrt{35}(125 \times 580) \times 10^{-3} = 72.9$ kN and $0.42 \times 1\sqrt{35}(125 \times 580) \times 10^{-3} = 180$ kN, do not control. Thus, on the basis of V_c obtained from Eq. (19.46), the required spacing of No. 10 (No. 3) U stirrups is

$$s = \frac{0.75 \times 142 \times 420 \times 580}{(140 - 0.75 \times 71.9) \times 10^3} = 351 \text{ mm}$$

For the present case, an I-section beam of intermediate span, nearly 2 times the web steel is required at the location investigated if the alternative expression giving V_c directly is used.

19.15 BOND STRESS, TRANSFER LENGTH, AND DEVELOPMENT LENGTH

There are two separate sources of bond stress in prestressed concrete beams: (1) flexural bond, which exists in pretensioned construction between the tendons and the concrete and in grouted post-tensioned construction between the tendons and the grout, and between the conduit (if any) and concrete; and (2) prestress transfer bond, generally applicable to pretensioned members only.

a. Flexural Bond

Flexural bond stresses arise due to the change in tension along the tendon resulting from differences in bending moment at adjacent sections. They are proportional to the rate of change of bending moment, hence to the shear force, at a given location along the span. Provided the concrete member is uncracked, flexural bond stress is very low. After cracking, it is higher by an order of magnitude. However, flexural bond stress need not be considered in designing prestressed concrete beams, provided that adequate end anchorage is furnished for the tendon, in the form of either mechanical anchorage (post-tensioning) or strand embedment (pretensioning).

b. Transfer Length and Development Length

For pretensioned beams, when the external jacking force is released, the prestressing force is transferred from the steel to the concrete near the ends of the member by bond, over a distance which is known as the *transfer length.* The transfer length depends upon a number of factors, including the steel stress, the configuration of the steel cross section (e.g., strands vs. wires), the condition of the surface of the steel, and the suddenness with which the jacking force is released. Based on tests of seven-wire prestressing strand (Ref. 19.21), the effective prestress f_{pe} in the steel may be assumed to act at a transfer length from the end of the member equal to

$$l_t = \frac{f_{pe}}{21} d_b \tag{a}$$

where l_t = transfer length, mm
d_b = nominal strand diameter, mm
f_{pe} = effective prestress, MPa

The same tests indicate that the additional distance past the original transfer length necessary to develop the failure strength of the steel is closely represented by the expression

$$l_t' = \left(\frac{f_{ps} - f_{pe}}{7}\right) d_b \tag{b}$$

where the quantity in parentheses is the stress increment above the effective prestress level, in MPa units, to reach the calculated steel stress at failure f_{ps}. Thus the total development length at failure is

$$l_d = l_t + l_t' \tag{c}$$

or

$$l_d = \left(\frac{3f_{ps} - 2f_{pe}}{21}\right) d_b \tag{19.54}$$

The ACI Code does not require that flexural bond stress be checked in either pretensioned or post-tensioned members, but for pretensioned strand it is required that the full development length, given by Eq. (19.54), be provided beyond the critical bending section. Investigation may be limited to those cross sections nearest each end of the member that are required to develop their full flexural strength under the specified factored load.

The development length of prestressing strand affects both shear and flexural strength at the end of pretensioned beams. The prestress component of the concrete shear contribution in Eq. (19.45) is usually considered to vary linearly from zero at the beam end to its full value of $0.3f_{pc}$ at the end of the transfer length l_t, according to ACI Commentary 12.9; and the flexural strength reduction factor $\phi = 0.75$ from the end of the member to the end of the transfer length and then varies linearly from 0.75 to 0.9 from the end of the transfer length to the end of the development length l_d, according to ACI Code 9.3.2.7. These reductions are especially relevant if concentrated loads are applied between the beam end and the end of the development length.

19.16 ANCHORAGE ZONE DESIGN

In prestressed concrete beams, the prestressing force is introduced as a load concentration acting over a relatively small fraction of the total member depth. For post-tensioned beams with mechanical anchorage, the load is applied at the end face, while for pretensioned beams it is introduced somewhat more gradually over the transfer length. In either case, the compressive stress distribution in the concrete becomes linear, conforming to that dictated by the overall eccentricity of the applied forces, only after a distance from the end roughly equal to the depth of the beam.

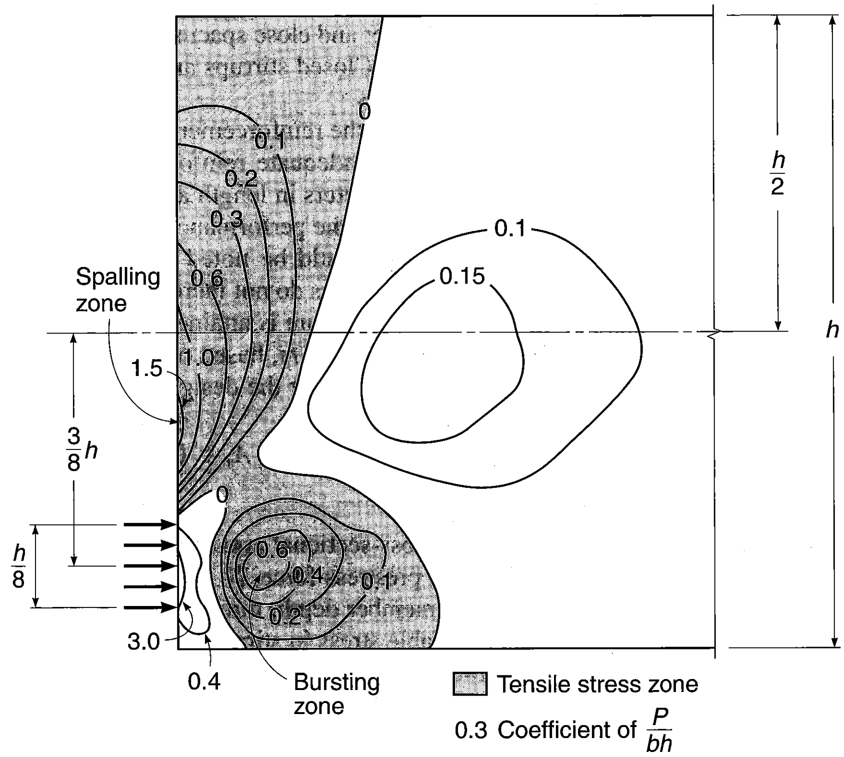
0
0.1
0.2
0.3
0.6
1.0
1.5
Spalling zone
0.1
0.15
$\frac{h}{2}$
h
$\frac{3}{8}h$
$\frac{h}{8}$
0
0.6
0.4
0.1
0.2
3.0
0.4
Bursting zone
Tensile stress zone
0.3 Coefficient of $\frac{P}{bh}$

FIGURE 19.25
Contours of equal vertical stress. (*Adapted from Ref. 19.16.*)

This transition of longitudinal compressive stress, from concentrated to linearly distributed, produces transverse (vertical) tensile stresses that may lead to longitudinal cracking of the member. The pattern and magnitude of the concrete stresses depend on the location and distribution of the concentrated forces applied by the tendons. Numerous studies have been made using the methods of classical elasticity, photoelasticity, and finite element analysis, and typical results are given in Fig. 19.25. Here the beam is loaded uniformly over a height equal to $h/8$ at an eccentricity of $3h/8$. Contour lines are drawn through points of equal vertical tension, with coefficients expressing the ratio of vertical stress to average longitudinal compression. Typically, there are high *bursting stresses* along the axis of the load a short distance inside the end zone and high *spalling stresses* at the loaded face.

In many post-tensioned prestressed I beams, solid end blocks are provided, as shown in Fig. 19.26. While these are often necessary to accommodate end-anchorage hardware and supplemental reinforcement, they are of little use in reducing transverse tension or avoiding cracking.

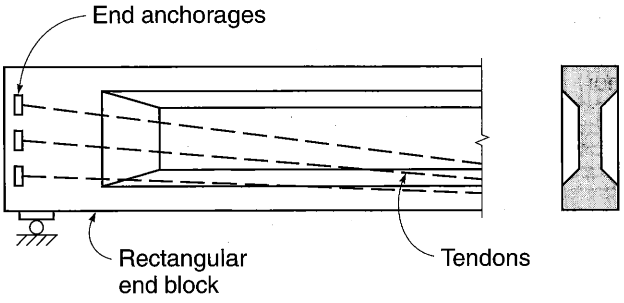
End anchorages
Rectangular end block
Tendons

FIGURE 19.26
Post-tensioned I beam with rectangular end block.

Steel reinforcement for end-zone stresses may be in the form of vertical bars of relatively small diameter and close spacing and should be well anchored at the top and bottom of the member. Closed stirrups are commonly used, with auxiliary horizontal bars inside the 90° bends.

Rational design of the reinforcement for end zones must recognize that horizontal cracking is likely. If adequate reinforcement is provided, so that the cracks are restricted to a few millimeters in length and to 0.25 mm or less in width, these cracks will not be detrimental to the performance of the beam either at service load or at the factored load stage. It should be noted that end-zone stresses in pretensioned and bonded post-tensioned beams do not increase in proportion to loads. The failure stress f_{ps} in the tendon at beam failure is attained only at the maximum moment section.

For *pretensioned members*, based on tests reported in Ref. 19.22, a very simple equation has been proposed for the design of end-zone reinforcement:

$$A_t = 0.021 \frac{P_i h}{f_s l_t} \tag{19.55}$$

where A_t = total cross-sectional area of stirrups necessary, mm^2
P_i = initial prestress force, N
h = total member depth, mm
f_s = allowable stress in stirrups, MPa
l_t = transfer length, mm

An allowable stress f_s = 140 MPa has been found in tests to produce acceptably small crack widths. The required reinforcement having total area A_t should be distributed over a length equal to $h/5$ measured from the end face of the beam, and for most efficient crack control the first stirrup should be placed as close to the end face as practical. It is recommended in Ref. 19.22 that vertical reinforcement according to Eq. (19.55) be provided for *all* pretensioned members, unless tests or experience indicates that cracking does not occur at service or overload stages.

For post-tensioned members, the end region is divided into two zones, local and general, as shown in Fig. 19.27*a*. The *local zone* is a rectangular prism immediately surrounding the anchorage device and any confining reinforcement around the device. The *general zone* consists of a region that is approximately one structural depth h from the end of the beam and includes the local zone. For internal anchors, such as used in slabs, the general zone extends a distance h ahead of and behind the anchorage hardware. Stresses in the local zone are determined based on tests. The post-tensioning supplier specifies the reinforcement details for the local zone.

FIGURE 19.27
Post-tensioned end block: (*a*) local and general zone; (*b*) strut-and-tie model.

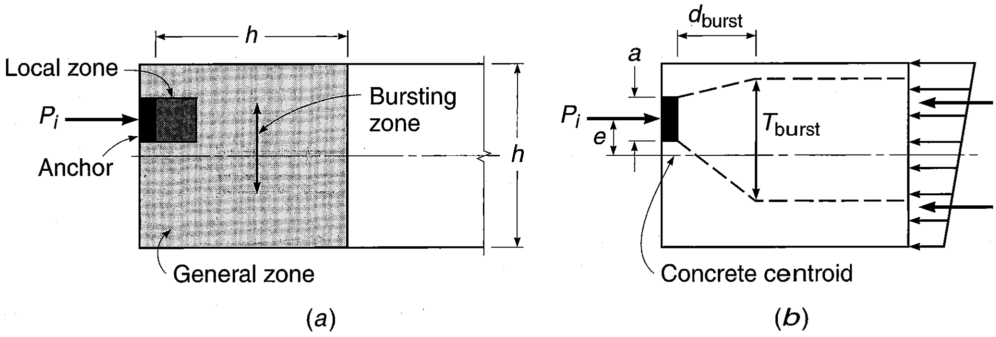

Stress variations in the general zone are nonlinear and are characterized by a transition from the local zone to an assumed uniform stress gradient a distance h from the anchor. Reinforcement in the general zone may be designed by one of three methods. These methods include equilibrium-based plasticity models, such as the strut-and-tie model, linear stress analysis such as finite element analysis, and simplified elasticity solutions similar to the photoelastic model shown graphically in Fig. 19.25 or elasticity analyses described in Ref. 19.23. Simplified equations are not permitted for nonrectangular cross sections, where multiple anchorages are used (unless closely spaced), or where discontinuities disrupt the force flow path.

Strut-and-tie design approaches for highway girder anchorages are detailed in the *AASHTO LRFD Bridge Design Specifications* (Refs. 19.17 and 19.23). An abbreviated version of the AASHTO Specifications is incorporated in ACI Commentary R18.13. ACI Code 18.15 requires that complex, multistrand anchorage systems conform to the full AASHTO Specifications.

For the common case of a rectangular end block and simple anchorage (Fig. 19.27*b*), ACI Commentary 18.13 offers simplified equations based on test results and strut-and-tie modeling. The magnitude of the bursting force T_{burst} and the location of its centroid distance from the front of the anchor d_{burst} may be calculated as

$$T_{\text{burst}} = 0.25\Sigma P_{pu}\left(1 - \frac{h_{\text{anc}}}{h}\right) \tag{19.56}$$

and

$$d_{\text{burst}} = 0.5(h - 2e_{\text{anc}}) \tag{19.57}$$

where ΣP_{pu} = sum of total factored post-tensioning force
e_{anc} = absolute value of eccentricity of anchorage device to centroid of concrete section
h = depth of cross section
h_{anc} = depth of anchorage device

The use of the factored post-tensioning force P_{pu} recognizes that the tendon force is acting as a load. Hence, the maximum jacking stress $0.80f_{pu}$ is multiplied by a load factor of 1.2 to calculate P_{pu}.

$$P_{pu} = 1.2(0.80f_{pu})A_{ps} = 0.96f_{pu}A_{ps} \tag{19.58}$$

Transverse reinforcement with total area $A_s = T_{\text{burst}}/\phi f_y$ is added in a region that is centered on the location d_{burst} to carry the bursting force.

In cases where the simplified equations do not apply, a strut-and-tie model (Chapter 10) or finite element analysis may be required to design the bursting zone.

EXAMPLE 19.7

Design of end-zone reinforcement for post-tensioned beam. End-zone reinforcement is to be designed for the rectangular post-tensioned beam shown in Fig. 19.28. The initial prestress force P_i of 1100 kN is applied by two closely spaced tendons having a combined eccentricity of 200 mm. Material properties are f'_{ci} = 29 MPa and f_y = 420 MPa.

SOLUTION. The rectangular section and the closely spaced anchorage devices allow the use of the simplified ACI equations.

$$d_{\text{burst}} = 0.5(h - 2e_{\text{anc}}) = 0.5(750 - 2 \times 200) = 175 \text{ mm}$$

FIGURE 19.28
Design of post-tensioned anchor zone: (*a*) section at end anchors; (*b*) end zone reinforcement.

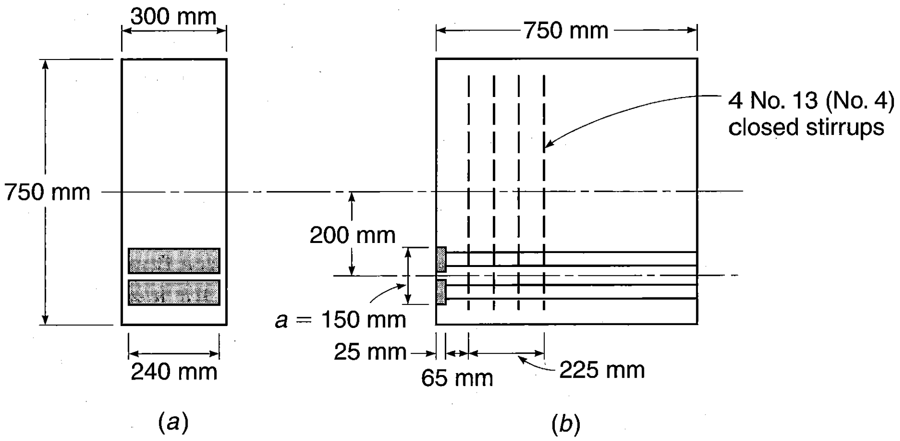

The initial prestressing force is 1100 kN, which corresponds to a tendon stress level of $0.82 f_{py}$. The maximum jacking stress level in the tendons is $0.94 f_{py}$, or $0.80 f_{pu}$. In this example, only the initial prestress is provided. Hence, the factored tendon force is calculated as

$$P_{pu} = 1.2\left(\frac{0.94}{0.82}\right)1100 = 1513 \text{ kN}$$

for which

$$T_{\text{burst}} = 0.25\Sigma P_{pu}\left(1 - \frac{h_{\text{anc}}}{h}\right) = 0.25 \times 1513\left(1 - \frac{150}{750}\right) = 303 \text{ kN}$$

The area of steel needed to resist T_{burst} is

$$A_s = \frac{T_{\text{burst}}}{\phi f_y} = \frac{303 \times 10^3}{0.85 \times 420} = 849 \text{ mm}^2$$

Using No. 13 (No. 4) closed stirrups with an area of 2×129 mm^2 gives

$$n = \frac{849}{2 \times 129} = 3.3 \text{ stirrups}$$

Four No. 13 (No. 4) closed stirrups will be used. The first stirrup will be placed 65 mm from the anchor plate, and the other three stirrups will be placed 75 mm on center, as shown in Fig. 19.28*b*, centering the stirrups a distance d_{burst} from the anchor plate. The closed stirrups ensure that anchorage requirements are satisfied. Details of the reinforcement in the local zone are not shown.

19.17 DEFLECTION

Deflection of the slender, relatively flexible beams that are made possible by prestressing must be predicted with care. Many members, satisfactory in all other respects, have proved to be unserviceable because of excessive deformation. In some cases, the absolute amount of deflection is excessive. Often, it is the differential deformation between adjacent members (e.g., precast roof-deck units) that causes problems. More often than not, any difficulties that occur are associated with upward deflection due to the sustained prestress load. Such difficulties are easily avoided by proper consideration in design.

When the prestress force is first applied, a beam will normally camber upward. With the passage of time, concrete shrinkage and creep will cause a gradual reduction of prestress force. In spite of this, the upward deflection usually will increase, due to the differential creep, affecting the highly stressed bottom fibers more than the top. With the application of superimposed dead and live loads, this upward deflection will be partially or completely overcome, and zero or downward deflection obtained. Clearly, in computing deformation, careful attention must be paid to both the age of the concrete at the time of load application and the duration of the loading.

The prediction of deflection can be approached at any of several levels of accuracy, depending upon the nature and importance of the work. In some cases, it is sufficient to place limitations on the span-depth ratio, based on past experience. Generally, deflections must be calculated. (Calculation is required for *all* prestressed members, according to ACI Code 9.5.4.) The approximate method described here will be found sufficiently accurate for most purposes. In special circumstances, where it is important to obtain the best possible information on deflection at all important load stages, such as for long-span bridges, the only satisfactory approach is to use a summation procedure based on incremental deflection at discrete time steps, as described in Refs. 19.1, 19.8, 19.24, and 19.25. In this way, the time-dependent changes in prestress force, material properties, and loading can be accounted for to the desired degree of accuracy.

Normally, the deflections of primary interest are those at the initial stage, when the beam is acted upon by the initial prestress force P_i and its own weight, and one or more combinations of load in service, when the prestress force is reduced by losses to the effective value P_e. Deflections are modified by creep under the sustained prestress force and due to all other sustained loads.

The short-term deflection Δ_{pi} due to the initial prestress force P_i can be found based on the variation of prestress moment along the span, making use of moment-area principles and superposition. For statically determinate beams, the ordinates of the moment diagram resulting from the eccentric prestress force are directly proportional to the eccentricity of the steel centroid line with respect to the concrete centroid. For indeterminate beams, eccentricity should be measured to the thrust line rather than to the steel centroid (see Ref. 19.1). In either case, the effect of prestress can also be regarded in terms of equivalent loads and deflections found using familiar deflection equations.

The downward deflection Δ_o due to girder self-weight, which is usually uniformly distributed, is easily found by conventional means. Thus, the net deflection obtained immediately upon prestressing is

$$\Delta = -\Delta_{pi} + \Delta_o \tag{19.59}$$

where the negative sign indicates upward displacement.

Long-term deflections due to prestress occur as that force is gradually reducing from P_i to P_e. This can be accounted for in an approximate way by assuming that creep occurs under a constant prestress force equal to the average of the initial and final values. Corresponding to this assumption, the total deflection resulting from prestress alone is

$$\Delta = -\Delta_{pe} - \frac{\Delta_{pi} + \Delta_{pe}}{2} C_c \tag{19.60}$$

where

$$\Delta_{pe} = \Delta_{pi} \frac{P_e}{P_i}$$

TABLE 19.5
Deflection and crack width requirements for prestressed concrete members

	Class		
Condition	**U**	**T**	**C**
Assumed behavior	Uncracked	Transition between cracked and uncracked	Cracked
Deflection calculation basis	Gross section	Cracked section—bilinear behavior	Cracked section—bilinear behavior

and C_c is set equal to the ultimate creep coefficient C_u for the concrete (see Table 2.1).

The long-term deflection due to self-weight is also increased by creep and can be obtained by applying the creep coefficient directly to the instantaneous value. Thus, the total member deflection, after losses and creep deflections, when effective prestress and self-weight act, is

$$\Delta = -\Delta_{pe} - \frac{\Delta_{pi} + \Delta_{pe}}{2} C_c + \Delta_o(1 + C_c) \tag{19.61}$$

The deflection due to superimposed loads can now be added, with the creep coefficient introduced to account for the long-term effect of the sustained loads, to obtain the net deflection at full service loading:

$$\Delta = -\Delta_{pe} - \frac{\Delta_{pi} + \Delta_{pe}}{2} C_c + (\Delta_o + \Delta_d)(1 + C_c) + \Delta_l \tag{19.62}$$

where Δ_d and Δ_l are the immediate deflections due to superimposed dead and live loads, respectively.

The selection of section properties for the calculation of deflections is dependent upon the cracking in the section. Table 19.5 defines the appropriate section properties and deflection calculation methodology for Class U, T, and C members (Refs. 19.1, 19.23, and 19.24). Bilinear behavior in Table 19.5 implies that deflections based on loads up to the cracking moment are based on the gross section, and deflections on loads greater than the cracking load are based on the effective cracked section properties (Ref. 19.8).

EXAMPLE 19.8

The 12 m simply supported T beam shown in Fig. 19.29 is prestressed with a force of 1400 kN, using a parabolic tendon with an eccentricity of 75 mm above the concrete centroid at the supports and 195 mm below the centroid at midspan. After time-dependent losses have occurred, this prestress is reduced to 1190 kN. In addition to its own weight of 4.8 kN/m, the girder must carry a short-term superimposed live load of 13.0 kN/m. Estimate the deflection at all critical stages of loading. The creep coefficient $C_c = 2.0$, $E_c = 28{,}000$ MPa, and modulus of rupture = 3.6 MPa.

SOLUTION. It is easily confirmed that the stress in the bottom fiber when the beam carries the maximum load to be considered is 1.0 MPa compression, meeting the requirements for a

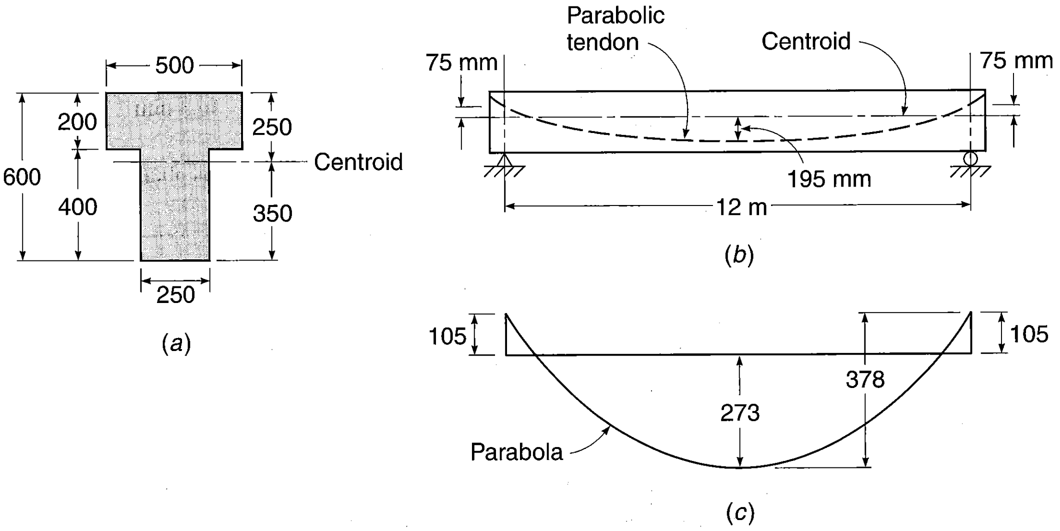

FIGURE 19.29
T beam of Example 19.8: (*a*) cross section (mm); (*b*) tendon profile; (*c*) moment from initial prestressing force (kN-m).

Class U member. All deflection calculations can, therefore, be based on the moment of inertia of the gross concrete section $I_c = 6.172 \times 10^9$ mm^4. It is convenient to calculate the deflection due to prestress and that due to girder load separately, superimposing the results later. For the eccentricities of the tendon profile shown in Fig. 19.29*b*, the application of $P_i = 1400$ kN causes the moments shown in Fig. 19.29*c*. Applying the second moment-area theorem by taking moments of the M/EI diagram between midspan and the support, about the support, produces the vertical displacement between those two points as follows:

$$\Delta_{pi} = \frac{[-(378 \times 6 \times \frac{2}{3} \times 6 \times \frac{5}{8}) + 105 \times 6^2/2] \times 10^{12}}{28{,}000 \times 6.172 \times 10^9} = -21.9 \text{ mm}$$

the minus sign indicating upward deflection due to initial prestress alone. The downward deflection due to the self-weight of the girder is calculated by the well-known equation

$$\Delta_o = \frac{5wl^4}{384EI} = \frac{5 \times 4.8 \times 12^4 \times 10^{12}}{384 \times 28{,}000 \times 6.172 \times 10^9} = +7.5 \text{ mm}$$

When these two results are superimposed, the net upward deflection when initial prestress and girder load act together is

$$-\Delta_{pi} + \Delta_o = -21.9 + 7.5 = -14.4 \text{ mm}$$

Shrinkage and creep of the concrete cause a gradual reduction of prestress force from $P_i = 1400$ kN to $P_e = 1190$ kN and reduce the bending moment due to prestress proportionately. Concrete creep, however, acts to increase both the upward deflection component due to the prestress force and the downward deflection component due to the girder load. The net deflection after these changes take place is found using Eq. (19.60), with $\Delta_{pe} = -21.9(1190/1400) = -18.6$ mm:

$$\begin{aligned}\Delta &= -18.6 - \frac{21.9 + 18.6}{2} \times 2.0 + 7.5(1 + 2.0)\\ &= -18.6 - 40.5 + 22.5 = -36.6 \text{ mm}\end{aligned}$$

In spite of prestress loss, the upward deflection is considerably larger than before. Finally, as the 13.0 kN/m short-term superimposed load is applied, the net deflection is

$$\Delta = -36.6 + 7.5\left(\frac{13.0}{4.8}\right) = -16.3 \text{ mm}$$

Thus, a net upward deflection of about 1/750 times the span is obtained when the member carries its full superimposed load.

19.18 CRACK CONTROL FOR CLASS C FLEXURAL MEMBERS

The service level stress limitations for Class U and T flexural members are sufficient to control cracking at service loads. Class C flexural members must satisfy the crack control provisions for ordinary reinforced concrete members, modified by ACI Code 18.4.4. These requirements take the form of limitations on tendon spacing and on the change in stress in the prestressing tendon under service load.

For Class C prestressed flexural members not subjected to fatigue or aggressive exposure, the spacing of bonded reinforcement nearest the extreme tension face may not exceed that given for nonprestressed concrete in Section 6.3. Aggressive conditions occur where the tendons may be exposed to chemical attack and include seawater and corrosive industrial environments. In these situations, the designer should increase the concrete cover or reduce the tensile stresses, based on professional judgment, commensurate with the exposure risk.

The spacing requirements for reinforcement in Class C members may be satisfied by using nonprestressed bonded tendons. The spacing between bonded tendons, however, may not exceed two-thirds of the maximum spacing for nonprestressed reinforcement given in Eq. (6.3). When both conventional reinforcement and bonded tendons are used to meet the spacing requirements, the spacing between a tendon and a bar may not exceed five-sixths of that permitted in Eq. (6.3). When applying Eq. (6.3), Δf_{ps} is substituted for f_s, where Δf_{ps} is the difference between the tendon stress at service loads based on a cracked section and the decompression stress f_{dc}, which is equal to the stress in the tendon when concrete stress at the level of the tendon is zero. ACI Code 18.4.4 permits f_{dc} to be taken as the effective prestress f_{pe}. The magnitude of Δf_{ps} is limited to a maximum of 250 MPa. When Δf_{ps} is less than 140 MPa, the reduced spacing requirements need not be applied. If the effective depth of the member exceeds 900 mm, additional skin reinforcement along the sides of the member web, as described in Section 6.3, is required to prevent excessive surface crack widths above the main flexural reinforcement.

REFERENCES

19.1. A. H. Nilson, *Design of Prestressed Concrete*, 2nd ed., John Wiley, New York, 1987.

19.2. A. E. Naaman, *Prestressed Concrete Analysis and Design: Fundamentals*, 2nd ed., TechnoPress 3000, Ann Arbor, Michigan, 2004.

19.3. T. Y. Lin and N. H. Burns, *Design of Prestressed Concrete Structures*, 3rd ed., John Wiley, New York, 1981.

19.4. J. R. Libby, *Modern Prestressed Concrete*, 3rd ed., Van Nostrand Reinhold, New York, 1984.

19.5. E. G. Nawy, *Prestressed Concrete*, 5th ed., Prentice-Hall, Englewood Cliffs, NJ, 2005.

19.6. M. P. Collins and D. Mitchell, *Prestressed Concrete Structures*, Prentice-Hall, Englewood Cliffs, NJ, 1991.

19.7. *Post-Tensioning Manual*, 6th ed., Post-Tensioning Institute, Phoenix, AZ, 2006.

19.8. *PCI Design Handbook*, 6th ed., Precast/Prestressed Concrete Institute, Chicago, IL, 2004.

19.9. *Quality Control for Plants and Production of Structural Precast and Prestressed Concrete Products*, MNL 116-99, Precast/Prestressed Concrete Institute, Chicago, IL, 1999.
19.10. P. W. Abeles, "Design of Partially Prestressed Concrete Beams," *J. ACI*, vol. 64, no. 10, 1967, pp. 669–677.
19.11. A. H. Nilson, "Discussion of 'Design of Partially Prestressed Concrete Beams' by P. W. Abeles" (Ref. 19.10), *J. ACI*, vol. 65, no. 4, 1968, pp. 345–347.
19.12. P. W. Abeles and B. K. Bardhan-Roy, *Prestressed Concrete Designer's Handbook*, 3rd ed., Cement and Concrete Association, London, 1981.
19.13. ACI Committee 423, *State-of-the-Art Report on Partially Prestressed Concrete* (ACI 423.5R-99), American Concrete Institute, Farmington Hills, MI, 1999.
19.14. CEB-FIP Joint Committee, "International Recommendations for the Design and Construction of Prestressed Concrete Structures," Cement and Concrete Association, London, 1970.
19.15. *Code of Practice for the Structural Use of Concrete*, CP110, British Standards Institution, London, 1972.
19.16. Y. Guyon, *Limit State Design of Prestressed Concrete*, vols. 1 and 2, John Wiley, New York, 1972.
19.17. *AASHTO LRFD Bridge Design Specifications*, 4th ed., American Association of State Highway and Bridge Officials, Washington, DC, 2008.
19.18. PCI Committee on Prestress Losses, "Recommendations for Estimating Prestress Losses," *J. Prestressed Concr. Inst.*, vol. 20, no. 4, 1975, pp. 43–75.
19.19. P. Zia, H. K. Preston, N. L. Scott, and E. B. Workman, "Estimating Prestress Losses," *Concr. Intl.*, vol. 1, no. 6, 1979, pp. 32–38.
19.20. J. G. MacGregor and J. M. Hanson, "Proposed Changes in Shear Provisions for Reinforced and Prestressed Concrete Beams," *J. ACI*, vol. 66, no. 4, 1969, pp. 276–288.
19.21. N. W. Hanson and P. W. Kaar, "Flexural Bond Tests of Pretensioned Prestressed Beams," *J. ACI*, vol. 30, no. 7, 1959, pp. 783–802.
19.22. W. T. Marshall and A. H. Mattock, "Control of Horizontal Cracking in the Ends of Pretensioned Prestressed Concrete Girders," *J. Prestressed Concr. Inst.*, vol. 5, no. 5, 1962, pp. 56–74.
19.23. J. E. Breen, O. Burdet, C. Roberts, D. Sanders, G. Wollman, and B. Falconer, "Anchorage Zone Reinforcement for Post-Tension Concrete Girders," NCHRP Report 356, Transportation Research Board, National Academy Press, Washington, DC, 1994.
19.24. ACI Committee 435, "Deflection of Prestressed Concrete Members," *J. ACI*, vol. 60, no. 12, 1963, pp. 1697–1728.
19.25. D. E. Branson, *Deformation of Concrete Structures*, McGraw-Hill, New York, 1977.

PROBLEMS

19.1. A rectangular concrete beam with width $b = 275$ mm and total depth $h = 700$ mm is post-tensioned using a single parabolic tendon with an eccentricity of 195 mm at midspan and 0 mm at the simple supports. The initial prestress force $P_i = 1440$ kN, and the effectiveness ratio $R = 0.84$. The member is to carry superimposed dead and live loads of 4.4 and 14.2 kN/m, respectively, uniformly distributed over the 12 m span. Specified concrete strength $f_c' = 35$ MPa, and at the time of transfer $f_{ci}' = 28$ MPa. Determine the flexural stress distributions in the concrete at midspan (*a*) for initial conditions before application of superimposed load and (*b*) at full service load. Compare with the ACI limit stresses for Class U members.

19.2. A pretensioned prestressed beam has a rectangular cross section of 150 mm width and 500 mm total depth. It is built using normal-density concrete with a specified strength $f_c' = 28$ MPa and a strength at transfer of $f_{ci}' = 21$ MPa. Stress limits are as follows: $f_{ti} = 1.15$ MPa, $f_{ci} = -12.60$ MPa, $f_{ts} = 3.28$ MPa, and $f_{cs} = -12.60$ MPa. The effectiveness ratio R may be assumed equal to 0.80. For these conditions, find the initial prestress force P_i and eccentricity e to maximize the superimposed load moment $M_d + M_l$ that can be carried without exceeding the stress limits. What uniformly distributed load can be carried on a 9 m simple span? What tendon profile would you recommend?

19.3. A pretensioned beam is to carry a superimposed dead load of 8.8 kN/m and service live load of 17.5 kN/m on a 17 m simple span. A symmetrical I section with $b = 0.5h$ will be used. Flange thickness $h_f = 0.2h$ and web width

$b_w = 0.4b$. The member will be prestressed using Grade 1860 strands. Time-dependent losses are estimated at 20 percent of P_i. Normal-density concrete will be used, with $f'_c = 35$ MPa and $f'_{ci} = 21$ MPa.

(*a*) Using straight strands, find the required concrete dimensions, prestress force, and eccentricity. Select an appropriate number and size of tendons, and show by sketch their placement in the section.

(*b*) Revise the design of part (*a*) using tendons harped at the third points of the span, with eccentricity reduced to zero at the supports.

(*c*) Comment on your results. In both cases, ACI stress limits are to be applied. You may assume that deflections are not critical and that the beam is Class T at full service load.

19.4. The hollow core section shown in Fig. P19.4 is prestressed with four 12.7 mm diameter, 1860 MPa low-relaxation strands and is simply supported on masonry walls with a span length of 6 m, center to center of the supports. In addition to its self-weight, the section carries a superimposed live load of 11 kN/m^2. Material properties are $f'_c = 35$ MPa and $f'_{ci} = 24$ MPa. Determine (*a*) if service load stresses in the section are suitable for a Class U flexural member using $R = 0.82$ and (*b*) if the section has sufficient capacity for the specified loads.

FIGURE P19.4

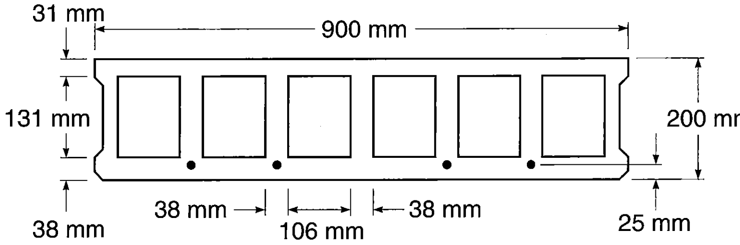

Section Properties

$A = 96.3 \times 10^3$ mm^2

$I = 478 \times 10^6$ mm^4

$b_w = 266$ mm

$c_2 = 97.3$ mm

$S_1 = 4.65 \times 10^6$ mm^3

$S_2 = 4.91 \times 10^6$ mm^3

Self-weight = 2.48 kN/m^2

19.5. For the beam in Problem 19.4, make a detailed computation of the losses in the prestressing force. Compare your results to the assumed value of $R = 0.82$.

19.6. Establish the required spacing of No. 10 (No. 3) stirrups at a beam cross section subject to factored load shear V_u of 158 kN and moment M_u of 643 kN-m. Web width $b_w = 125$ mm, effective depth $d = 600$ mm, and total depth $h = 750$ mm. The concrete shear contribution may be based on the approximate relationship of Eq. (19.46). Use $f_y = 420$ MPa for stirrup steel, and take $f'_c = 35$ MPa.

19.7. A symmetrical prestressed I beam having total depth 1.2 m, flange width 600 mm, flange thickness 240 mm, and web thickness 240 mm is to span 21 m. It is post-tensioned using 18 Grade 1860 12.7 mm diameter low-relaxation strands in a single tendon having a parabolic profile, with $e = 450$ mm at midspan and 0 mm at the supports. (The curve can be approximated by a circular arc for loss calculations.) The jacking force $P_j = 2750$ kN. Calculate losses due to slip, elastic shortening, friction, creep, shrinkage, and relaxation. Express your results in tabular form both numerically and as percentages of initial prestress P_i. Creep effects may be assumed to occur under the combination of prestress force plus self-weight. The beam is prestressed when the concrete is aged 7 days. Anchorage slip = 6.3 mm, coefficient of strand friction = 0.20, coefficient of wobble friction = 0.0033, creep coefficient = 2.35. Member properties are as follows: $A_c = 460.6 \times 10^3$ mm^2, $I_c = 75.0 \times 10^9$ mm^4, $c_1 = c_2 = 600$ mm, $f'_c = 35$ MPa, $E_c = 27{,}800$ MPa, $E_s = 186{,}000$ MPa, $w_c = 24$ kN/m^3, and $C_c = 2.65$.

19.8. The concrete T beam shown in Fig. P19.8 is post-tensioned at an initial force $P_i = 1020$ kN, which reduces after 1 year to an effective value $P_e = 815$ kN. In addition to its own weight, the beam will carry a superimposed short-term live load of 100 kN at midspan. Using the approximate method described in Section 19.17, find (*a*) the initial deflection of the unloaded girder and (*b*) the deflection at the age of 1 year of the loaded girder. The following data are given: $A_c = 281 \times 10^3$ mm^2, $c_1 = 200$ mm, $I_c = 9.61 \times 10^9$ mm^4, $E_c =$ 24,500 MPa, $C_c = 2.5$.

FIGURE P19.8

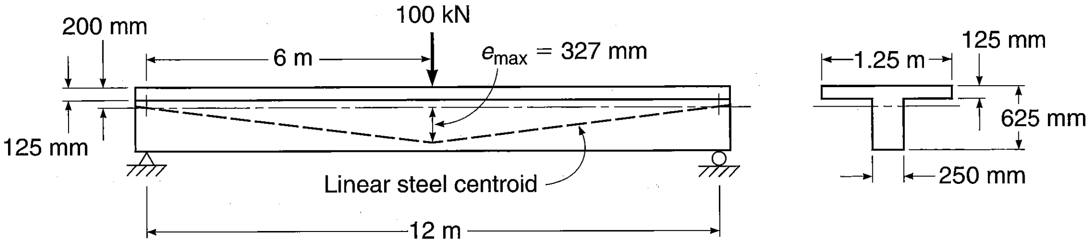
200 mm
125 mm
100 kN
6 m
e_{max} = 327 mm
Linear steel centroid
12 m
1.25 m
125 mm
625 mm
250 mm

20 Seismic Design

20.1 INTRODUCTION

Earthquakes result from the sudden movement of tectonic plates in the earth's crust. The movement takes place at fault lines, and the energy released is transmitted through the earth in the form of waves that cause ground motion many miles from the epicenter. Regions adjacent to active fault lines are the most prone to experience earthquakes. The map in Fig. 20.1 shows the *maximum considered ground motion* for the contiguous 48 states. The mapped values, expressed as a percent of gravity, represent the expected peak acceleration of a single-degree-of-freedom system with a 0.2 sec period and 5 percent of critical damping. Known as the *0.2 sec spectral response acceleration* S_s (subscript *s* for *short* period), it is used, along with the 1.0 sec spectral response acceleration S_1 (mapped in a similar manner), to establish the loading criteria for seismic design. Accelerations S_s and S_1 are based on historical records and local geology. For most of the country, they represent earthquake ground motion with a "likelihood of exceedance of 2 percent in 50 years," a value that is equivalent to a return period of about 2500 years (Ref. 20.1).

As experienced by structures, earthquakes consist of random horizontal and vertical movements of the earth's surface. As the ground moves, inertia tends to keep structures in place (Fig. 20.2), resulting in the imposition of displacements and forces that can have catastrophic results. The purpose of seismic design is to proportion structures so that they can withstand the displacements and the forces induced by the ground motion.

Historically in North America, seismic design has emphasized the effects of horizontal ground motion because the horizontal components of an earthquake usually exceed the vertical component and because structures are usually much stiffer and stronger in response to vertical loads than they are in response to horizontal loads. Experience has shown that the horizontal components are the most destructive. For structural design, the intensity of an earthquake is usually described in terms of the peak ground acceleration as a fraction of the acceleration of gravity, i.e., $0.1g$, $0.2g$, or $0.3g$. Although peak acceleration is an important design parameter, the frequency characteristics and duration of an earthquake are also important; the closer the frequency of the earthquake motion is to the natural frequency of a structure and the longer the duration of the earthquake, the greater the potential for damage.

Based on elastic behavior, structures subjected to a major earthquake would be required to undergo large displacements. However, North American practice (Ref. 20.2) requires that structures be designed for only a fraction of the forces associated with those displacements. The relatively low design forces are justified by the observations that buildings designed for low forces have behaved satisfactorily and that structures

FIGURE 20.1 Map showing maximum considered earthquake ground motion, 0.2 sec spectral response acceleration (5 percent of critical damping), for the contiguous United States. (*United States Geological Survey.*)

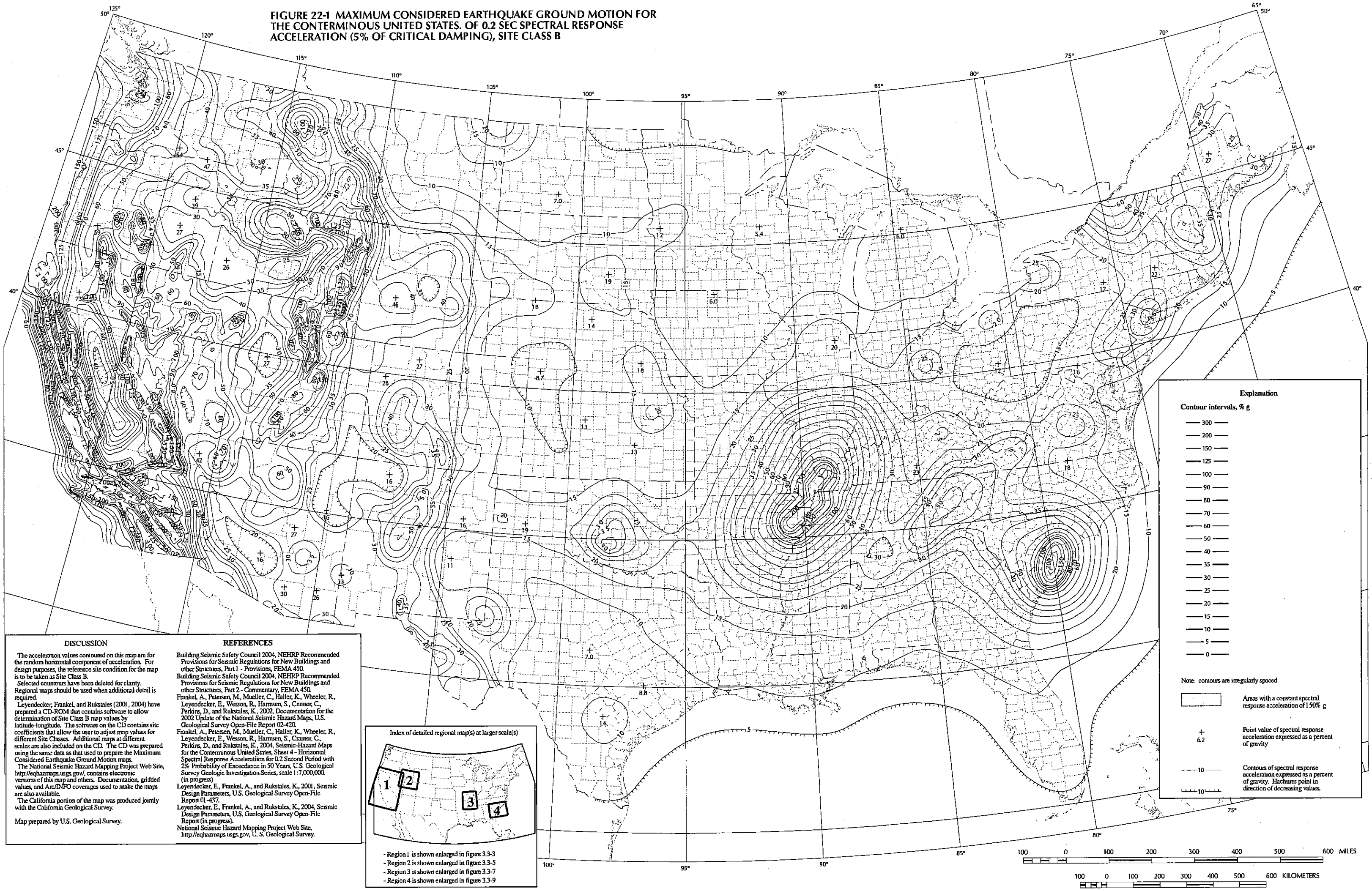

FIGURE 22-1 MAXIMUM CONSIDERED EARTHQUAKE GROUND MOTION FOR THE CONTERMINOUS UNITED STATES. OF 0.2 SEC SPECTRAL RESPONSE ACCELERATION (5% OF CRITICAL DAMPING), SITE CLASS B

Explanation
Contour intervals, % g
300
200
150
125
100
90
80
70
60
50
40
35
30
25
20
15
10
5
0
Note: contours are irregularly spaced
Areas with a constant spectral response acceleration of 150% g
6.2
Point value of spectral response acceleration expressed as a percent of gravity
10
Contours of spectral response acceleration expressed as a percent of gravity. Hachures point in direction of decreasing values.
100 0 100 200 300 400 500 600 MILES
100 0 100 200 300 400 500 600 KILOMETERS
Index of detailed regional map(s) at larger scale(s)
1
2
3
4

- Region 1 is shown enlarged in figure 3.3-3
- Region 2 is shown enlarged in figure 3.3-5
- Region 3 is shown enlarged in figure 3.3-7
- Region 4 is shown enlarged in figure 3.3-9

DISCUSSION

The acceleration values contoured on this map are for the random horizontal component of acceleration. For design purposes, the reference site condition for the map is to be taken as Site Class B.

Selected countours have been deleted for clarity. Regional maps should be used when additional detail is required.

Leyendecker, Frankel, and Rukstales (2001, 2004) have prepared a CD-ROM that contains software to allow determination of Site Class B map values by latitude-longitude. The software on the CD contains site coefficients that allow the user to adjust map values for different Site Classes. Additional maps at different scales are also included on the CD. The CD was prepared using the same data as that used to prepare the Maximum Considered Earthquake Ground Motion maps.

The National Seismic Hazard Mapping Project Web Site, http://eqhazmaps.usgs.gov/, contains electronic versions of this map and others. Documentation, gridded values, and Arc/INFO coverages used to make the maps are also available.

The California portion of the map was produced jointly with the California Geological Survey.

Map prepared by U.S. Geological Survey.

REFERENCES

Building Seismic Safety Council 2004, NEHRP Recommended Provisions for Seismic Regulations for New Buildings and other Structures, Part 1 - Provisions, FEMA 450.

Building Seismic Safety Council 2004, NEHRP Recommended Provisions for Seismic Regulations for New Buildings and other Structures, Part 2 - Commentary, FEMA 450.

Frankel, A., Petersen, M., Mueller, C., Haller, K., Wheeler, R., Leyendecker, E., Wesson, R., Harmsen, S., Cramer, C., Perkins, D., and Rukstales, K., 2002, Documentation for the 2002 Update of the National Seismic Hazard Maps, U.S. Geological Survey Open-File Report 02-420.

Frankel, A., Petersen, M., Mueller, C., Haller, K., Wheeler, R., Leyendecker, E., Wesson, R., Harmsen, S., Cramer, C., Perkins, D., and Rukstales, K., 2004, Seismic-Hazard Maps for the Conterminous United States, Sheet 4 - Horizontal Spectral Response Acceleratiion for 0.2 Second Period with 2% Probability of Exceedance in 50 Years, U.S. Geological Survey Geologic Investigation Series, scale 1:7,000,000 (in progress)

Leyendecker, E., Frankel, A., and Rukstales, K., 2001, Seismic Design Parameters, U.S. Geological Survey Open-File Report 01-437.

Leyendecker, E., Frankel, A., and Rukstales, K., 2004, Seismic Design Parameters, U.S. Geological Survey Open-File Report (in progress).

National Seismic Hazard Mapping Project Web Site, http://eqhazmaps.usgs.gov, U. S. Geological Survey.

FIGURE 20.2
Structure subjected to ground motion.

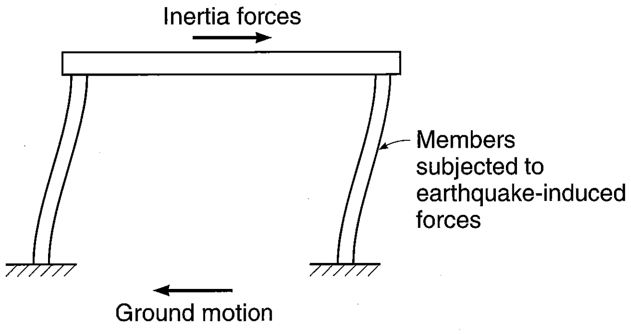

dissipate significant energy as the materials yield and behave inelastically. This nonlinear behavior, however, usually translates into increased displacements, which may require significant ductility and result in major nonstructural damage. Displacements may also be of such a magnitude that the strength of the structure is affected by stability considerations, such as discussed for slender columns in Chapter 9.

Designers of structures that may be subjected to earthquakes, therefore, are faced with a choice: (1) providing adequate stiffness and strength to limit the response of structures to the elastic range or (2) providing lower-strength structures, with presumably lower initial costs, that have the ability to withstand large inelastic deformations while maintaining their load-carrying capability.

20.2 STRUCTURAL RESPONSE

The safety of a structure subjected to seismic loading rests on the designer's understanding of the response of the structure to ground motion. For many years, the goal of earthquake design in North America has been to construct buildings that will withstand *moderate earthquakes without damage and severe earthquakes without collapse*. Building codes have undergone regular modification as major earthquakes have exposed weaknesses in existing design criteria.

Design for earthquakes differs from design for gravity and wind loads in the relatively greater sensitivity of earthquake-induced forces to the geometry of the structure. Without careful design, forces and displacements can be concentrated in portions of a structure that are not capable of providing adequate strength or ductility. Steps to strengthen a member for one type of loading may actually increase the forces in the member and change the mode of failure from ductile to brittle.

a. Structural Considerations

The closer the frequency of the ground motion is to one of the natural frequencies of a structure, the greater the likelihood of the structure experiencing resonance, resulting in an increase in both displacement and damage. Therefore, earthquake response depends strongly on the geometric properties of a structure, especially height. Tall buildings respond more strongly to long-period (low-frequency) ground motion, while short buildings respond more strongly to short-period (high-frequency) ground motion. Figure 20.3 shows the shapes for the principal modes of vibration of a three-story frame structure. The relative contribution of each mode to the lateral displacement of the structure depends on the frequency characteristics of the ground motion. The first mode (Fig. 20.3*a*) usually provides the greatest contribution to lateral displacement.

FIGURE 20.3
Modal shapes for a three-story building: (*a*) first mode; (*b*) second mode; (*c*) third mode. (*Adapted from Ref. 20.3.*)

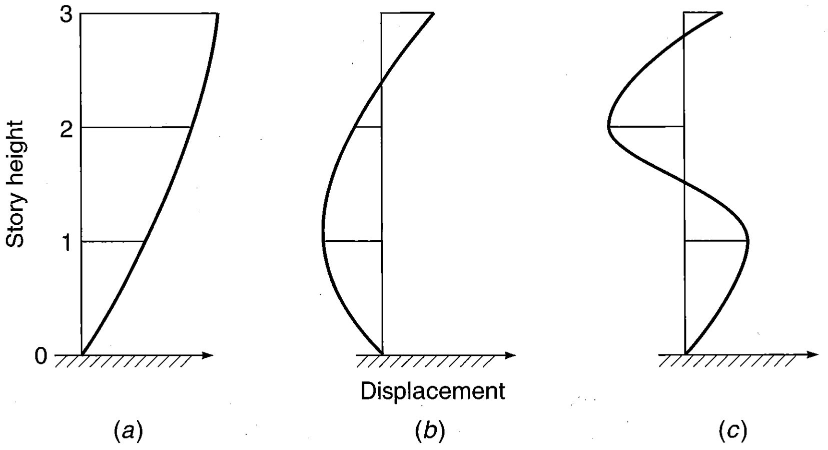

FIGURE 20.4
Soft first story supporting a stiff upper structure.

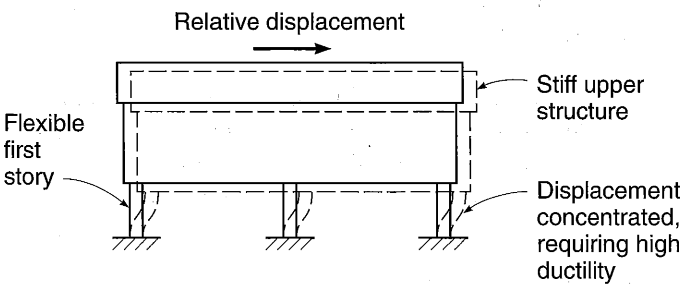

The taller a structure, the more susceptible it is to the effects of higher modes of vibration, which are generally additive to the effects of the lower modes and tend to have the greatest influence on the upper stories. Under any circumstances, the longer the duration of an earthquake, the greater the potential for damage.

The configuration of a structure also has a major effect on its response to an earthquake. Structures with a discontinuity in stiffness or geometry can be subjected to undesirably high displacements or forces. For example, the discontinuance of shear walls, infill walls, or even cladding at a particular story level, such as shown in Fig. 20.4, will have the result of concentrating the displacement in the open, or "soft," story. The high displacement will, in turn, require a large amount of ductility if the structure is not to fail. Such a design is not recommended, and the stiffening members should be continued to the foundation. The problems associated with a soft story are illustrated in Fig. 20.5, which shows the Olive View Hospital following the 1971 San Fernando earthquake. The high ductility "demand" could not be satisfied by the column at the right, with low amounts of transverse reinforcement. Even the columns at center, with significant transverse reinforcement, performed poorly because the transverse reinforcement was not continued into the joint, resulting in the formation of hinges at the column ends. Figure 20.6 illustrates structures with vertical geometric and plan irregularities, which result in torsion induced by ground motion.

Within a structure, stiffer members tend to pick up a greater portion of the load. When a frame is combined with a shear wall, this can have the positive effect of reducing the displacements of the structure and decreasing both structural and nonstructural damage. However, when the effects of higher stiffness members, such as masonry infill walls, are not considered in the design, unexpected and often undesirable results can occur.

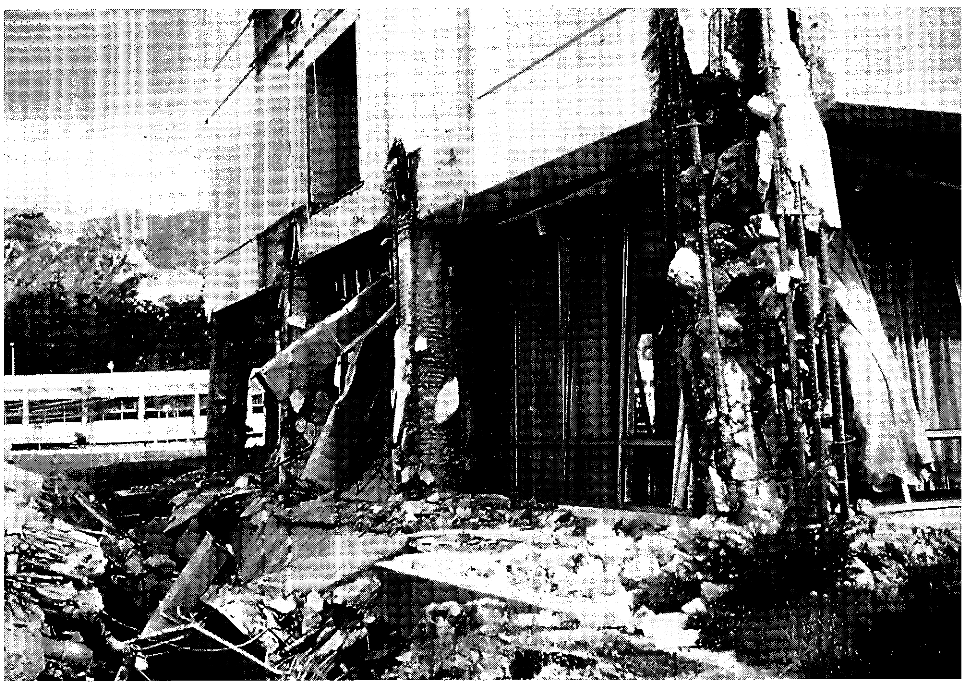

FIGURE 20.5
Damage to soft story columns in the Olive View Hospital as a result of the 1971 San Fernando earthquake. (*Photograph by James L. Stratta. Courtesy of the Federal Emergency Management Agency.*)

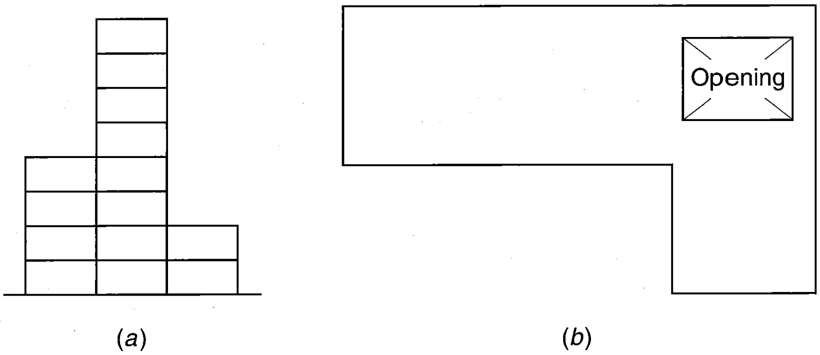

FIGURE 20.6
Structures with (*a*) vertical geometric and (*b*) plan irregularities. (*Adapted from Ref. 20.3.*)

Finally, any discussion of structural considerations would be incomplete without emphasizing the need to provide adequate separation between structures. Lateral displacements can result in structures coming in contact during an earthquake, resulting in major damage due to hammering, as shown in Fig. 20.7. Spacing requirements to ensure that adjacent structures do not come into contact as the result of earthquake-induced motion are specified in Ref. 20.2.

b. Member Considerations

Members designed for seismic loading must perform in a ductile fashion and dissipate energy in a manner that does not compromise the strength of the structure. Both the overall design and the structural details must be considered to meet this goal.

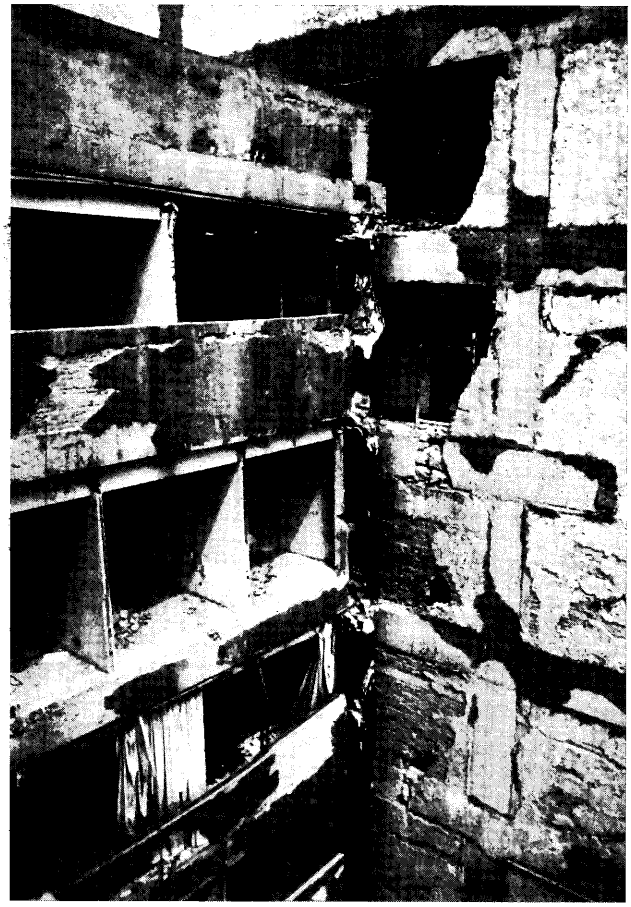

FIGURE 20.7
Damage caused by hammering for buildings with inadequate separation in the 1985 Mexico City earthquake. (*Photograph by Jack Moehle.*)

The principal method of ensuring ductility in members subject to shear and bending is to provide confinement for the concrete. This is accomplished through the use of closed *hoops* or spiral reinforcement, which enclose the core of beams and columns. Specific criteria are discussed in Sections 20.4, 20.5, and 20.6. When confinement is provided, beams and columns can undergo nonlinear cyclic bending while maintaining their flexural strength and without deteriorating due to diagonal tension cracking. The formation of *ductile hinges* allows reinforced concrete frames to dissipate energy.

Successful seismic design of frames requires that the structures be proportioned so that hinges occur at locations that least compromise strength. For a frame undergoing lateral displacement, such as shown in Fig. 20.8*a*, the flexural capacity of the members at a joint (Fig. 20.8*b*) should be such that the columns are stronger than the beams. In this way, hinges will form in the beams rather than the columns, minimizing the portion of the structure affected by nonlinear behavior and maintaining the overall vertical load capacity. For these reasons, the "weak beam–strong column" approach is used to design reinforced concrete frames subject to seismic loading.

When hinges form in a beam, or in extreme cases within a column, the moments at the end of the member, which are governed by flexural strength, determine the shear

FIGURE 20.8
Frame subjected to lateral loading: (*a*) deflected shape; (*b*) moments acting on beam-column joint; (*c*) deflected shape and forces acting on a beam; (*d*) forces acting on faces of a joint due to lateral load.

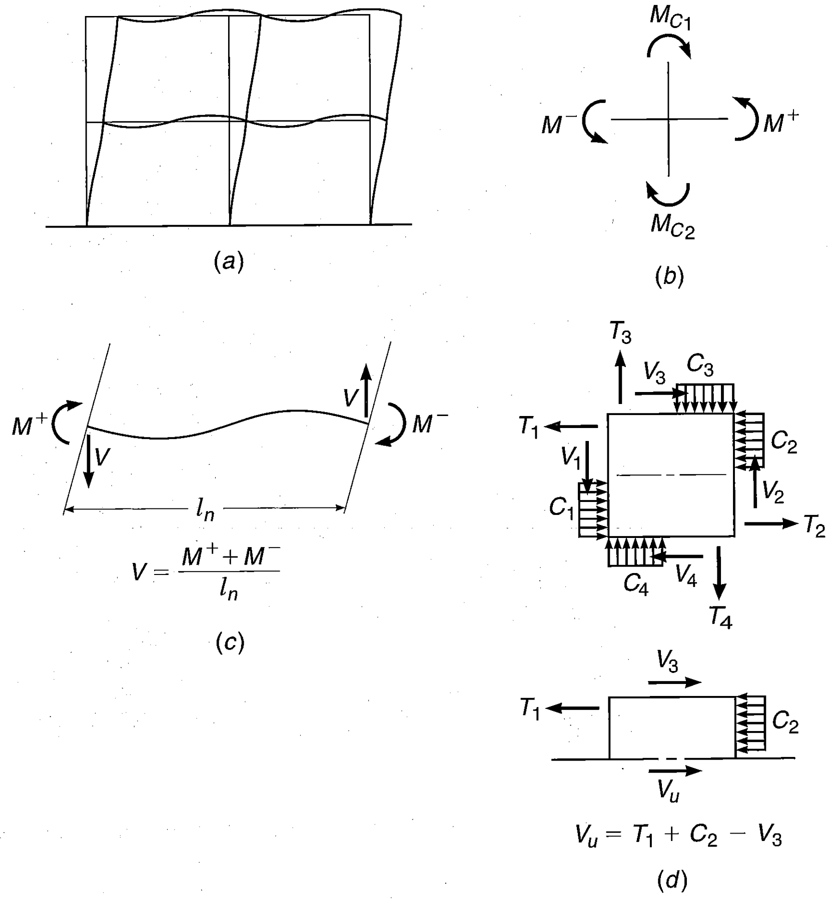

that must be carried, as illustrated in Fig. 20.8*c*. The shear V corresponding to a flexural failure at both ends of a beam or column is

$$V = \frac{M^+ + M^-}{l_n} \tag{20.1}$$

where M^+ and M^- = flexural capacities at the ends of the member
l_n = clear span between supports

The member must be checked for adequacy under the shear V in addition to shear resulting from dead and live gravity loads. Transverse reinforcement is added, as required. For members with inadequate shear capacity, the response will be dominated by the formation of diagonal cracks, rather than ductile hinges, resulting in a substantial reduction in the energy dissipation capacity of the member.

If short members are used in a frame, the members may be unintentionally strong in flexure compared to their shear capacity. An example would be columns in a structure with deep spandrel beams or with "nonstructural" walls with openings that expose a portion of the columns to the full lateral load. As a result, the exposed region, called a *captive column*, responds by undergoing a shear failure, as shown in Fig. 20.9.

The lateral displacement of a frame places beam-column joints under high shear stresses because of the change from positive to negative bending in the flexural members from one side of the joint to the other, as shown in Fig. 20.8*d*. The joint must

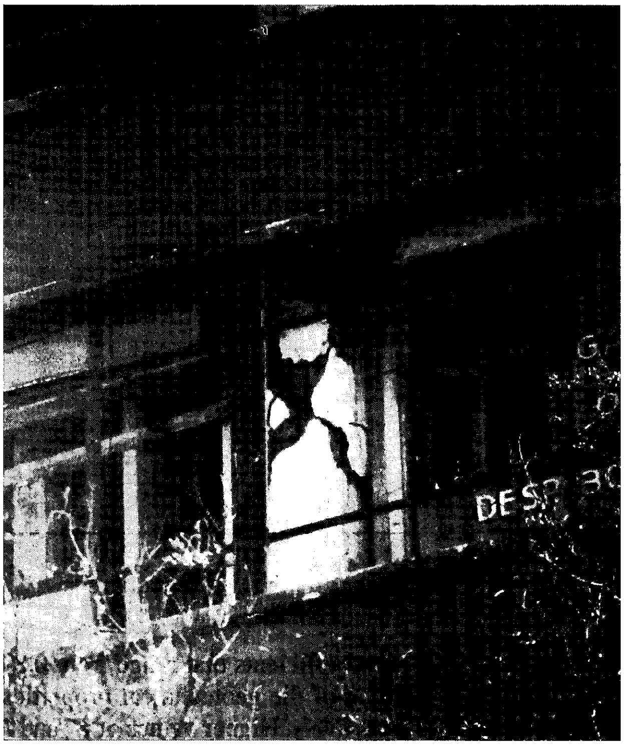

FIGURE 20.9
Shear failure in a captive column without adequate transverse reinforcement. (*Photograph by Jack Moehle.*)

be able to withstand the high shear stresses and allow for a change in bar stress from tension to compression between the faces of the joint. Such a transfer of shear and bond is often made difficult by congestion of reinforcement through the joint. Thus, designers must ensure that joints not only have adequate strength but are also constructable. Two-way systems without beams are especially vulnerable because of low ductility at the slab-column intersection.

Additional discussion of seismic design can be found in Refs. 20.3 to 20.7.

20.3 SEISMIC LOADING CRITERIA

In the United States, the design criteria for earthquake loading are based on design procedures developed by the Building Seismic Safety Council (Ref. 20.1) and incorporated in *Minimum Design Loads for Buildings and Other Structures* (ASCE/SEI 7) (Ref. 20.2). The values of the spectral response accelerations S_s and S_1 are obtained from detailed maps produced by the United States Geological Survey[†] (e.g., Fig. 20.1) and included in ASCE/SEI 7. The values of S_s and S_1 are used to determine the spectral response accelerations S_{DS} and S_{D1} that are used in design.

$$S_{DS} = \frac{2}{3} F_a S_s \tag{20.2}$$

$$S_{D1} = \frac{2}{3} F_v S_1 \tag{20.3}$$

[†] A full set of maps is available at the United States Geological Survey website.

FIGURE 20.10
Design response spectrum.
(*Adapted from Ref. 20.2.*)

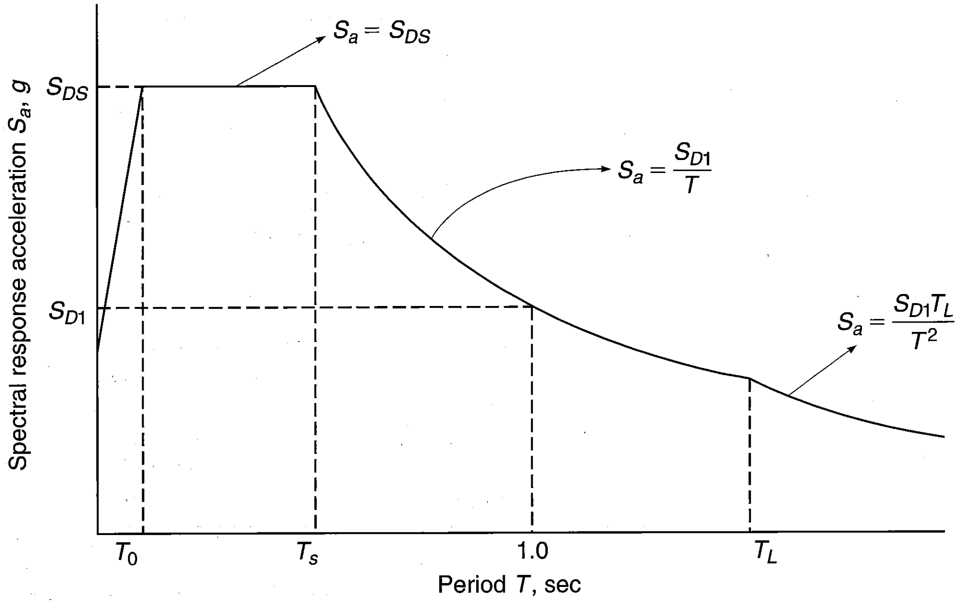

where F_a and F_v are site coefficients that range from 0.8 to 0.25 and from 0.8 to 0.35, respectively, as a function of the geotechnical properties of the building site and the values of S_s and S_1, respectively. Higher values of F_a and F_v are possible for some sites. The coefficients F_a and F_v increase in magnitude as site conditions change from hard rock to thick, soft clays and (for softer foundations) as the values of S_s and S_1 decrease.

Both S_{DS} and S_{D1} are used to construct the design response spectrum shown in Fig. 20.10, which relates the spectral response acceleration S_a, used to calculate the earthquake force, to the fundamental period of the structure T. In the spectrum, $T_0 = 0.2S_{D1}/S_{DS}$, $T_S = S_{D1}/S_{DS}$, and T_L is the site-specific *long-period transition period,* which, like S_s and S_1, is obtained from maps provided by the U.S. Geological Survey.

Structures are assigned to one of six *Seismic Design Categories* (SDCs) A through F as a function of (1) structure occupancy and use and (2) the values of S_{DS} and S_{D1}. Requirements for seismic design and detailing are minimal for SDCs A and B but become progressively more rigorous for SDCs C through F.

As presented in Table 1.2, earthquake loading is included in two combinations of factored load.

$$U = 1.2D + 1.0E + 1.0L + 0.2S \tag{20.4}$$

$$U = 0.9D + 1.0E + 1.6H \tag{20.5}$$

where D = dead load
E = earthquake load
H = weight or pressure from soil
L = live load
S = snow load

For SDC A, the earthquake load E is a horizontal load equal to 1 percent of the dead load D assigned to each floor. For SDCs B through F, the values of the earthquake load E used in Eqs. (20.4) and (20.5) are, respectively,

$$E = \rho Q_E + 0.2S_{DS}D \tag{20.6a}$$

$$E = \rho Q_E - 0.2S_{DS}D \tag{20.6b}$$

where Q_E = effect of horizontal seismic forces
ρ = reliability factor

The factor ρ is taken as 1.0 for structures assigned to SDCs B and C and as 1.3 for structures assigned to SDCs D though F, except for structures meeting specific criteria described in Ref. 20.2, in which case ρ may be taken as 1.0.

Combining Eq. (20.4) with Eq. (20.6*a*) and Eq. (20.5) with Eq. (20.6*b*) gives

$$U = (1.2 + 0.2S_{DS})D + \rho Q_E + 1.0L + 0.2S \tag{20.7}$$

$$U = (0.9 - 0.2S_{DS})D + \rho Q_E + 1.6H \tag{20.8}$$

Equations (20.4) and (20.6*a*) are used when dead load adds to the effects of horizontal ground motion, while Eqs. (20.5) and (20.6*b*) are used when dead load counteracts the effects of horizontal ground motion. Thus, the total load factor for dead load is greater than 1.2 in Eq. (20.7) and less than 0.9 in Eq. (20.8).

ASCE/SEI 7 specifies six procedures (if SDC A is included) for determining the horizontal earthquake load Q_E. These procedures include three progressively more detailed methods that represent earthquake loading through the use of equivalent static lateral loads, *modal response spectrum analysis, linear time-history analysis,* and *nonlinear time-history analysis.* The method selected depends on the seismic design category. All but the most basic reinforced concrete structures in Seismic Design Categories B through F must be designed using *equivalent lateral force analysis* (the most detailed of the three equivalent static lateral load procedures), modal response analysis, or time-history analysis. These procedures are discussed next.

a. Equivalent Lateral Force Procedure

According to ASCE/SEI 7 (Ref. 20.2), equivalent lateral force analysis may be applied to all structures with S_{DS} less than $0.33g$ and S_{D1} less than $0.133g$, as well as structures subjected to much higher design spectral response accelerations, if the structures meet certain requirements. More sophisticated dynamic analysis procedures must be used otherwise.

The equivalent lateral force procedure provides for the calculation of the total lateral force, defined as the design base shear V, which is then distributed over the height of the building. The design base shear V is calculated for a given direction of loading according to the equation

$$V = C_s W \tag{20.9}$$

where W is the total dead load plus applicable portions of other loads and

$$C_s = \frac{S_{DS}}{R/I} \tag{20.10}$$

which need not be greater than

$$C_s = \frac{S_{D1}}{T(R/I)} \qquad \text{for } T \le T_L \tag{20.11}$$

or

$$C_s = \frac{S_{D1}T_L}{T^2(R/I)} \qquad \text{for } T > T_L \tag{20.12}$$

but may not be less than

$$C_s = 0.44IS_{DS} \ge 0.01 \tag{20.13}$$

or where $S_1 \geq 0.6g$,

$$C_s = \frac{0.5S_1}{R/I} \tag{20.14}$$

where R = response modification factor (depends on structural system). Values of R for most reinforced concrete structures range from 4 to 8, based on ability of structural system to sustain earthquake loading and to dissipate energy
I = occupancy important factor = 1.0, 1.25, or 1.5, depending upon the occupancy and use of structure
T = fundamental period of structure

According to ASCE/SEI 7, the period T can be calculated based on an analysis that accounts for the structural properties and deformational characteristics of the elements within the structure. Approximate methods may also be used in which the fundamental period of the structure may be calculated as

$$T = C_t(3.28h_n)^x \tag{20.15}$$

where h_n = height above the base to the highest level of structure, m
C_t = 0.016 for reinforced concrete moment-resisting frames in which frames resist 100 percent of required seismic force and are not enclosed or adjoined by more rigid components that will prevent frame from deflecting when subjected to seismic forces, and 0.020 for all other reinforced concrete buildings
x = 0.90 for $C_t = 0.016$ and 0.75 for $C_t = 0.020$

Alternately, for structures not exceeding 12 stories in height, in which the lateral-force-resisting system consists of a moment-resisting frame and the story height is at least 3 m.

$$T = 0.1N \tag{20.16}$$

where N = number of stories.

For shear wall structures, ASCE/SEI 7 permits T to be approximated as

$$T = \frac{0.0062}{\sqrt{C_w}}h_n \tag{20.17}$$

where

$$C_w = \frac{100}{A_B}\sum_{i=1}^{n}\left(\frac{h_n}{h_i}\right)^2 \frac{A_i}{1 + 0.83(h_i/D_i)^2} \tag{20.18}$$

where A_B = base area of structure, m^2
A_i = area of shear wall, m^2
D_i = length of shear wall i, m
n = number of shear walls in building that are effective in resisting lateral forces in direction under consideration

The total base shear V is distributed over the height of the structure in accordance with Eq. (20.19).

$$F_x = \frac{w_x h_x^k}{\sum_{i=1}^{n} w_i k_i^k} V \tag{20.19}$$

FIGURE 20.11
Forces based on ASCE/SEI 7 (Ref. 20.2) equivalent lateral force procedure: (*a*) structure; (*b*) distribution of lateral forces over height; (*c*) story shears.

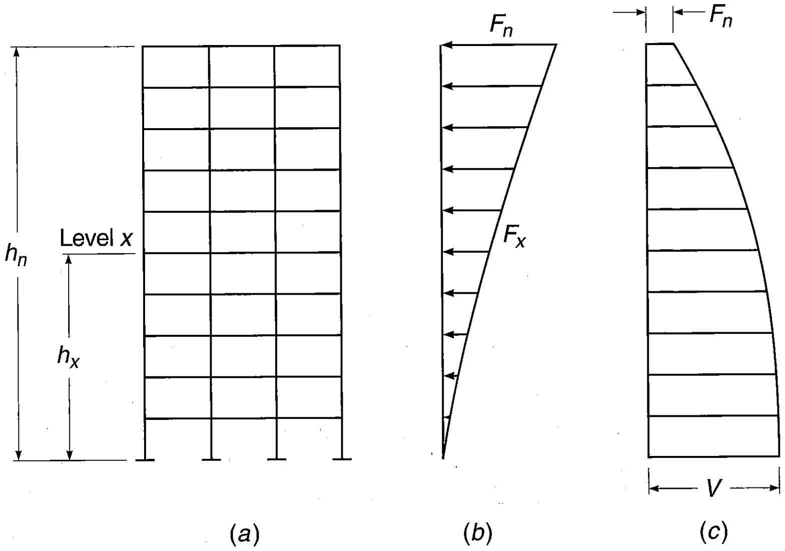

where F_x = lateral seismic force induced at level x
w_x, w_i = portion of W at level x and level i, respectively
h_x, h_i = height to level x and level i, respectively
k = exponent related to structural period, = 1 for $T \leq 0.5$ sec and = 2 for $T \geq 2.5$ sec. For $0.5 < T < 2.5$, k is determined by linear interpolation or set to a value of 2

The design shear at any story V_x equals the sum of the forces F_x at and above that story. For a 10-story building with a uniform mass distribution over the height and $T = 1.0$ sec, the lateral forces and story shears are distributed as shown in Fig. 20.11.

At each level, V_x is distributed in proportion to the stiffness of the elements in the vertical lateral-force-resisting system. To account for unintentional building irregularities that may cause a horizontal torsional moment, a minimum 5 percent eccentricity must be applied if the vertical lateral-force-resisting systems are connected by a floor system that is rigid in its own plane.

In addition to the criteria just described, ASCE/SEI 7 includes criteria to account for overturning effects and provides limits on story drift. P-Δ effects must be considered (as discussed in Chapter 9), and the effects of upward loads must be accounted for in the design of horizontal cantilever components and prestressed members.

b. Dynamic Lateral Force Procedures

ASCE/SEI 7 includes dynamic lateral force procedures that involve the use of (1) response spectra, which provide the earthquake-induced forces as a function of the natural periods of the structure, or (2) time-history analyses of the structural response based on a series of ground motion acceleration histories that are representative of ground motion expected at the site. Both procedures require the development of a mathematical model of the structure to represent the spatial distribution of mass and stiffness. Response spectra, such as shown in Fig. 20.10, are used to calculate peak forces for a "sufficient number of nodes to obtain the combined modal mass participation of at least 90 percent of the actual mass in each of two orthogonal directions"

(Ref. 20.2). Since these forces do not always act in the same direction, as shown in Fig. 20.3, the peak forces are averaged statistically, in most cases using the square root of the sum of the squares to obtain equivalent static lateral forces for use in design. In cases where the periods in the translational and torsional modes are closely spaced and result in significant cross correlation of the modes, the *complete quadratic combination* method is used (Ref. 20.8). When time-history analyses, which may include a linear or nonlinear representation of the structure, are used, design forces are obtained directly from the analyses. Both modal response spectrum and time-history procedures provide more realistic representations of the seismically induced forces in a structure than do equivalent lateral force analyses. The details of these methods are presented in Refs. 20.1 and 20.2.

20.4 ACI PROVISIONS FOR EARTHQUAKE-RESISTANT STRUCTURES

Criteria for seismic design are contained in Earthquake-Resistant Structures, Chapter 21 of the ACI Code (Ref. 20.9). The principal goal of the provisions is to ensure adequate toughness under inelastic displacement reversals brought on by earthquake loading. The provisions accomplish this goal by requiring the designer to provide for concrete confinement and inelastic rotation capacity. The provisions apply to frames, walls, coupling beams, diaphragms, and trusses in structures assigned to Seismic Design Categories D, E, and F, and to frames, including two-way slab systems, and precast walls in structures assigned to Seismic Design Category C. Structural systems in SDCs D, E, and F are referred to as *special,* while systems in SDC C are referred to as *intermediate.*

The requirements for frame structures assigned to SDC B, described as *ordinary moment frames,* are limited. Beams must have at least two longitudinal bars that are continuous along both the top and bottom faces of the beam and developed at the face of the supports; and columns with a clear height less than or equal to 5 times the column dimension in the direction of bending must be designed for shear, as required for intermediate frames (described in Section 20.8). There are no special requirements in ACI Code Chapter 20 for structures assigned to SDC A.

The ACI provisions are based on many of the observations made earlier in this chapter. The effect of nonstructural elements on overall structural response must be considered, as must the response of the nonstructural elements themselves. Structural elements that are not specifically proportioned to carry earthquake loads must also be considered.

The load factors used for earthquake loads are given in Eqs. (20.4) and (20.5). The strength reduction factors used for seismic design are the same as those used for nonseismic design (Table 1.3), with the additional requirements that $\phi = 0.60$ for shear, if the nominal shear capacity of a member is less than the shear based on the nominal flexural strength [see Eq. (20.1)], and $\phi = 0.85$ for shear in joints and diagonally reinforced coupling beams.

To ensure adequate ductility and toughness under inelastic rotation, ACI Code 21.1.4 sets a minimum concrete strength of 21 MPa. For lightweight aggregate concrete, an *upper limit* of 35 MPa is placed on concrete strength; this limit is based on a lack of experimental evidence for higher-strength lightweight concretes.

Under ACI Code 21.1.5, reinforcing steel must meet ASTM A706 (see Table 2.4). ASTM A706 specifies a Grade 420 steel with a maximum yield strength of 540 MPa

FIGURE 20.12
Example of transverse reinforcement in columns; consecutive crossties engaging the same longitudinal bars must have 90° hooks on opposite sides of columns. (*Adapted from Ref. 20.9.*)

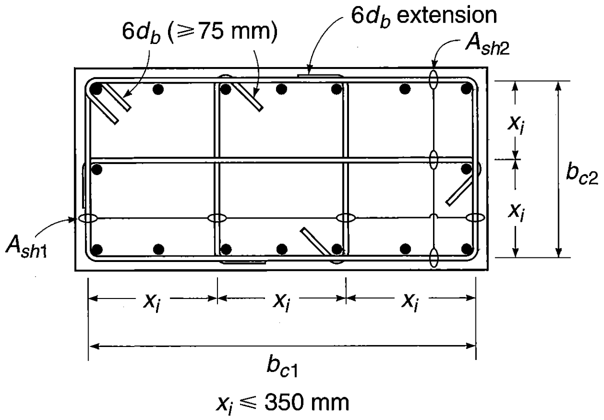

and a minimum tensile strength equal to 550 MPa. The actual tensile strength must be at least 1.25 times the actual yield strength. In addition to reinforcement manufactured under ASTM A706, the Code allows the use of Grades 40 and 60 reinforcement meeting the requirements of ASTM A615, provided that the actual yield strength does not exceed the specified yield by more than 125 MPa and that the actual tensile strength exceeds the actual yield strength by at least 25 percent. The upper limits on yield strength are used to limit the maximum moment capacity of the section because of the dependency of the earthquake-induced shear on the moment capacity [Eq. (20.1)]. The minimum ratio of tensile strength to yield strength helps provide adequate inelastic rotation capacity. Evidence reported in Ref. 20.10 indicates that an increase in the ratio of the ultimate moment to the yield moment results in an increase in the nonlinear deformation capacity of flexural members.

Confinement for concrete is provided by transverse reinforcement consisting of stirrups, hoops, and crossties. To ensure adequate anchorage, a *seismic hook* [with a bend not less than 135° and a 6 bar diameter (but not less than 75 mm) extension that engages the longitudinal reinforcement and projects into the interior of the stirrup or hoop] is used on stirrups, hoops, and crossties. *Hoops*, shown in Figs. 7.11*a*, *c–e* and 20.12, are closed ties that can be made up of several reinforcing elements, each having seismic hooks at both ends, or continuously wound ties with seismic hooks at both ends. A *crosstie* (see Fig. 20.12) is a continuous reinforcing bar with a seismic hook at one end and a hook with not less than a 90° bend and at least a 6 bar diameter extension at the other end. The hooks on crossties must engage peripheral longitudinal reinforcing bars.

In the following sections, ACI requirements for frames, walls, diaphragms, and trusses subject to seismic loading are discussed. Sections 20.5 and 20.6 describe the general design and detailing criteria for members in structures assigned to SDCs D, E, and F. Specific shear strength requirements are presented in Section 20.7. Section 20.8 describes requirements for frame structures assigned to SDC C.

20.5 ACI PROVISIONS FOR SPECIAL MOMENT FRAMES

ACI Code Chapter 21 addresses four member types in frame structures, termed *special moment frames*, subject to high seismic risk: flexural members, members subjected to bending and axial load, joints, and members not proportioned to resist earthquake forces. Two-way slabs without beams are prohibited as lateral-load-resisting systems in structures assigned to SDCs D, E, and F.

a. Flexural Members

Flexural members are defined by ACI Code 21.5.1 as structural members that resist earthquake-induced forces but have a factored axial compressive load P_u that does not exceed $A_g f'_c/10$, where A_g is the gross area of the cross section. The members must have a clear span-to-effective-depth ratio of at least 4 and a width b_w not less than $0.3h$ or 250 mm. The width b_w may not be wider than the support width c_2 plus a distance on either side of the support equal to the smaller of the width of the supporting member c_2 or 0.75 times the dimension of the supporting member in the direction of the span c_1, as shown in Fig. 20.13. The minimum clear span-to-depth ratio helps ensure that flexural rather than shear strength dominates member behavior under inelastic load reversals. Minimum web dimensions help provide adequate confinement for the concrete, whereas the width relative to the support (typically a column) is limited to provide adequate moment transfer between beams and columns.

In accordance with ACI Code 21.5.2, both top and bottom minimum flexural steel is required. $A_{s,\min}$ should not be less than given by Eq. (3.41) but need not be greater than four-thirds of that required by analysis, with a minimum of two reinforcing bars, top and bottom, throughout the member. In addition, the positive moment capacity at the face of columns must be at least one-half of the negative moment strength at the same location, and neither positive nor negative moment strength at any section in a member may be less than one-fourth of the maximum moment strength at either end of the member. These criteria are designed to provide for ductile behavior throughout the member, although the minimum of two reinforcing bars on the top and bottom is based principally on construction requirements. A maximum reinforcement ratio of 0.025 is set to limit problems with steel congestion and to ensure adequate member size for carrying shear that is governed by the flexural capacity of the member [Eq. (20.1)].

To obtain ductile performance, the location of lap splices is limited. They may not be used within joints, within twice the member depth from the face of a joint, or where analysis indicates that flexural yielding is caused by inelastic lateral displacements of the frame. Lap splices must be enclosed by hoops or spirals with a maximum spacing of one-fourth of the effective depth or 100 mm. Welded and mechanical connections may be used, provided that they are not used within a distance equal to twice the member depth from the face of a column or beam or sections where yielding of the reinforcement is likely to occur due to inelastic displacements under lateral load, in accordance with ACI Code 21.1.6 and 21.1.7.

Transverse reinforcement is required throughout flexural members in frames resisting earthquake-induced forces. According to ACI Code 21.5.3, transverse reinforcement in the form of hoops must be used over a length equal to twice the member depth measured from the face of the supporting member toward midspan, at both ends of the flexural member, and over lengths equal to twice the member depth on both sides of a section where flexural yielding is likely to occur in connection with inelastic lateral displacements of the frame. The first hoop must be located not more than 50 mm from the face of the supporting member, and the maximum spacing of the hoops must not exceed one-fourth of the effective depth, 8 times the diameter of the smallest longitudinal bar, 24 times the diameter of the hoop bars, or 300 mm.

FIGURE 20.13
Maximum effective width of wide beam and required transverse reinforcement.
(*Adapted from Ref. 20.9.*)

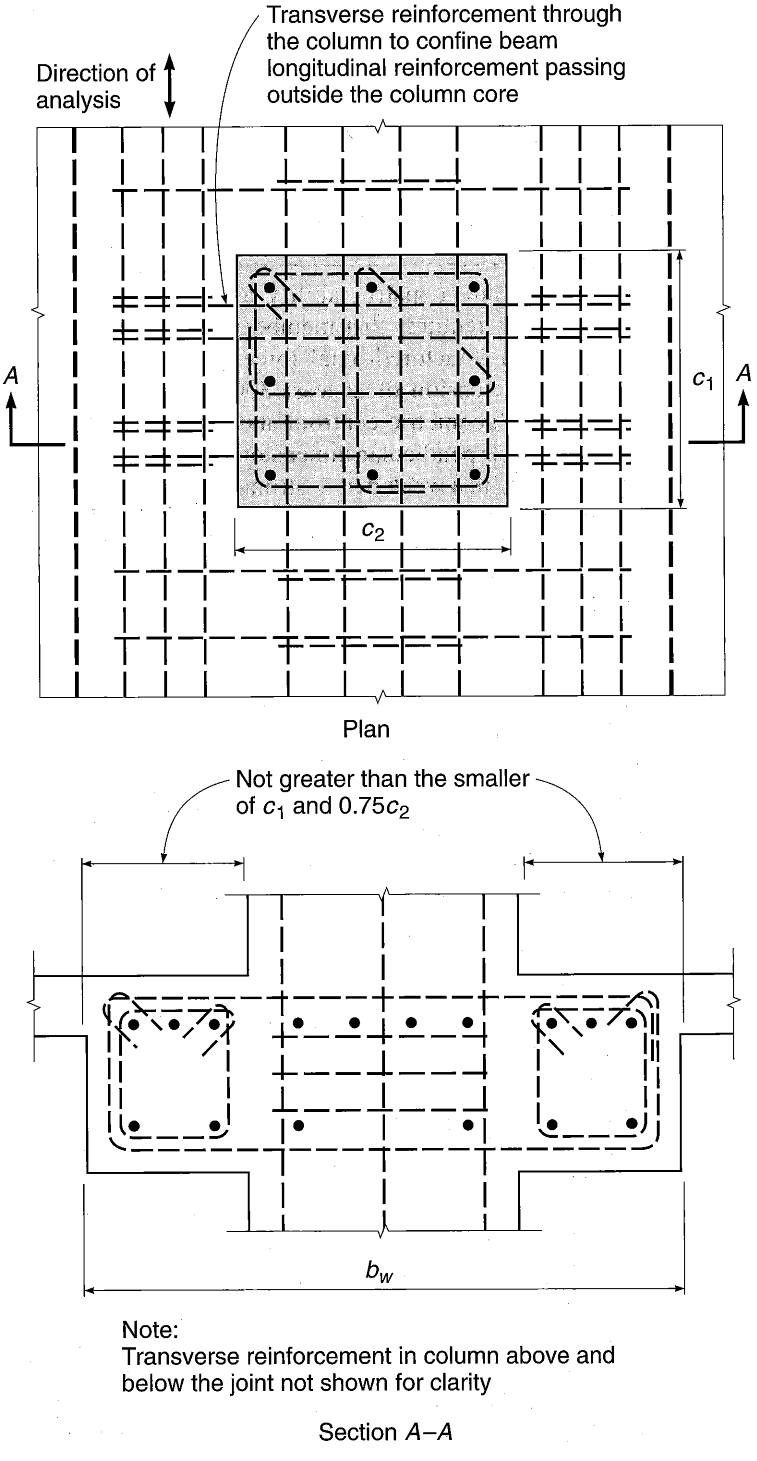
Transverse reinforcement through the column to confine beam longitudinal reinforcement passing outside the column core
Direction of analysis
A
A
c_1
c_2
Plan
Not greater than the smaller of c_1 and $0.75c_2$
b_w
Note:
Transverse reinforcement in column above and below the joint not shown for clarity
Section A–A

To provide adequate support for longitudinal bars on the perimeter of a flexural member when the bars are placed in compression due to inelastic rotation, ACI Code 21.5.3 requires that hoops be arranged so that every corner and alternate longitudinal bar is provided lateral support by ties, in accordance with ACI Code 7.10.5.3.

Arrangements meeting these criteria are illustrated in Fig. 8.3. Where hoops are not required, stirrups with seismic hooks at both ends must be provided throughout the member, with a maximum spacing of one-half of the effective depth. Hoops can be made up of a single reinforcing bar or two reinforcing bars consisting of a stirrup with seismic hooks at both ends and a crosstie. Examples of hoop reinforcement are presented in Figs. 7.11*a*, *c–e* and 20.12.

b. Members Subjected to Bending and Axial Load

To help ensure constructability and adequate confinement of the concrete, ACI Code 21.6.1 requires that members in frames designed to resist earthquake-induced forces, with a factored axial force exceeding $A_g f_c'/10$, have (1) a minimum cross-sectional dimension of at least 300 mm when measured on a straight line passing through the geometric centroid and (2) a ratio of the shortest cross-sectional dimension to the perpendicular dimension of at least 0.4.

To obtain a weak beam–strong column design, ACI Code 21.6.2 requires that the nominal flexural strengths of the columns framing into a joint exceed the nominal flexural strengths of the girders framing into the joint by at least 20 percent. This requirement is expressed as

$$\Sigma M_{nc} \geq \frac{6}{5} \Sigma M_{nb} \tag{20.20}$$

where ΣM_{nc} = sum of nominal flexural strengths of columns framing into joint, evaluated at the faces of the joint. Values of M_{nc} are based on the factored axial load, consistent with the direction of the lateral forces, resulting in the lowest flexural strength

ΣM_{nb} = sum of nominal flexural strengths of beams framing into joint, evaluated at the faces of the joint. In T-beam construction, where the slab is in tension under moment at the face of the joint, slab reinforcement within the effective flange width (see Section 3.8) is assumed to contribute to flexural strength if the slab reinforcement is developed at the critical section for flexure

As shown in Fig. 20.8*b*, the flexural strengths are summed so that the column moments oppose the beam moments. Equation (20.20) must be satisfied for beam moments acting both clockwise and counterclockwise on the joint.

If Eq. (20.20) is not satisfied for beam moments acting in both directions, the lateral strength and stiffness of the columns framing into the joint must be ignored when determining the strength and stiffness of the structures, and the columns must be designed under the provisions of ACI Code 21.13 for members that are not designated as part of the seismic-force-resisting system, as described in Section 20.5d. If the stiffness of the columns increases the design base shear or the effects of torsion, they must be included in the analysis, but still may not be considered as contributing to structural capacity.

In accordance with ACI Code 21.6.3, the column reinforcement ratio based on the gross section ρ_g must meet the requirement: $0.01 \leq \rho_g \leq 0.06$. Welded splices and mechanical connections in columns must satisfy the same requirements specified for flexural members, whereas lapped splices must be designed for tension and are permitted only within the center half of columns.

ACI Code 21.6.4 specifies the use of minimum transverse reinforcement over length l_o from each joint face and on both sides of any section where flexural yielding is likely because of inelastic lateral displacement of the frame. The length l_o may not be less than (1) the depth of the member at the joint face or at the section where flexural yielding is likely to occur, (2) one-sixth of the clear span of the member, or (3) 450 mm.

The transverse reinforcement may consist of single or overlapping spirals satisfying Eq. (8.5) and the provisions of ACI Code 7.10.4, circular hoops, or rectilinear hoops (Fig. 20.12) with or without crossties. The crossties may be the same size or smaller than the bars used for the hoops and may not be spaced more than 350 mm, as shown in Fig. 20.12.

A_{sh} is evaluated in both the 1 and 2 directions, as indicated in Fig. 20.12. In accordance with ACI Code 21.6.4, the spacing of transverse reinforcement within l_o may not exceed one-quarter of the minimum member dimension, 6 times the diameter of the longitudinal bar, or

$$s_o = 100 + \frac{350 - h_x}{3} \tag{20.21a}$$

$$100 \text{ mm} \leq s_o \leq 150 \text{ mm} \tag{20.21b}$$

where h_x is the maximum horizontal spacing of hoop or crosstie legs on all faces of the column (largest value of x_i in Fig. 20.12).

Minimum transverse reinforcement is specified in terms of the ratio of the volume of the transverse reinforcement to the volume of the core confined by the reinforcement (measured out-to-out of the confining steel) ρ_s for spirals or circular hoop reinforcement as

$$\rho_s = 0.12 \frac{f'_c}{f_{yt}} \tag{20.22}$$

but not less than specified in Eq. (8.5), where f_{yt} is the specified yield strength of transverse reinforcement.

To provide similar confinement using rectangular hoop reinforcement, ACI Code 21.6.4 requires a minimum total cross-sectional area of transverse reinforcement A_{sh} along the length of the longitudinal reinforcement that may not be less than

$$A_{sh} = 0.3 \frac{s b_c f'_c}{f_{yt}} \left(\frac{A_g}{A_{ch}} - 1 \right) \tag{20.23}$$

or

$$A_{sh} = 0.09 \frac{s b_c f'_c}{f_{yt}} \tag{20.24}$$

where A_{ch} = cross-sectional area of column core, measured out-to-out of transverse reinforcement
s = spacing of transverse reinforcement
b_c = cross-sectional dimension of column core, measured to outside edges of transverse reinforcement composing A_{sh}

For regions outside of l_o, when the minimum transverse reinforcement defined above is not provided, the spacing of spiral or hoop reinforcement may not exceed 6 times the diameter of the longitudinal column bars or 150 mm.

To account for the major ductility demands that are placed on columns that support rigid members (see Figs. 20.4 and 20.5), the Code specifies that, for such columns, the minimum transverse reinforcement requirements must be satisfied throughout the *full column height* and that the transverse reinforcement must extend into the discontinued stiff member for at least the development length of the largest longitudinal reinforcement for walls and at least 300 mm into foundations.

If the concrete cover outside the confining transverse reinforcement is greater than 100 mm, the Code requires the addition of transverse reinforcement with a cover of 100 mm or less to limit the potential hazard caused by spalling of the concrete shell away from the column.

EXAMPLE 20.1 **Relative flexural strengths of members at a joint and minimum transverse column reinforcement.** The exterior joint shown in Fig. 20.14 is part of a reinforced concrete frame designed to resist earthquake loads. A 150 mm slab, not shown, is reinforced with No. 16 (No. 5) bars spaced 250 mm center to center at the same level as the flexural steel in the beams. The member section dimensions and reinforcement are as shown. The frame story height is 3.65 m. Material strengths are $f'_c = 28$ MPa and $f_y = 420$ MPa. The maximum factored axial load on the upper column framing into the joint is 9523 kN, and the maximum factored axial load on the lower column is 9937 kN. Determine if the nominal flexural strengths of the columns exceed

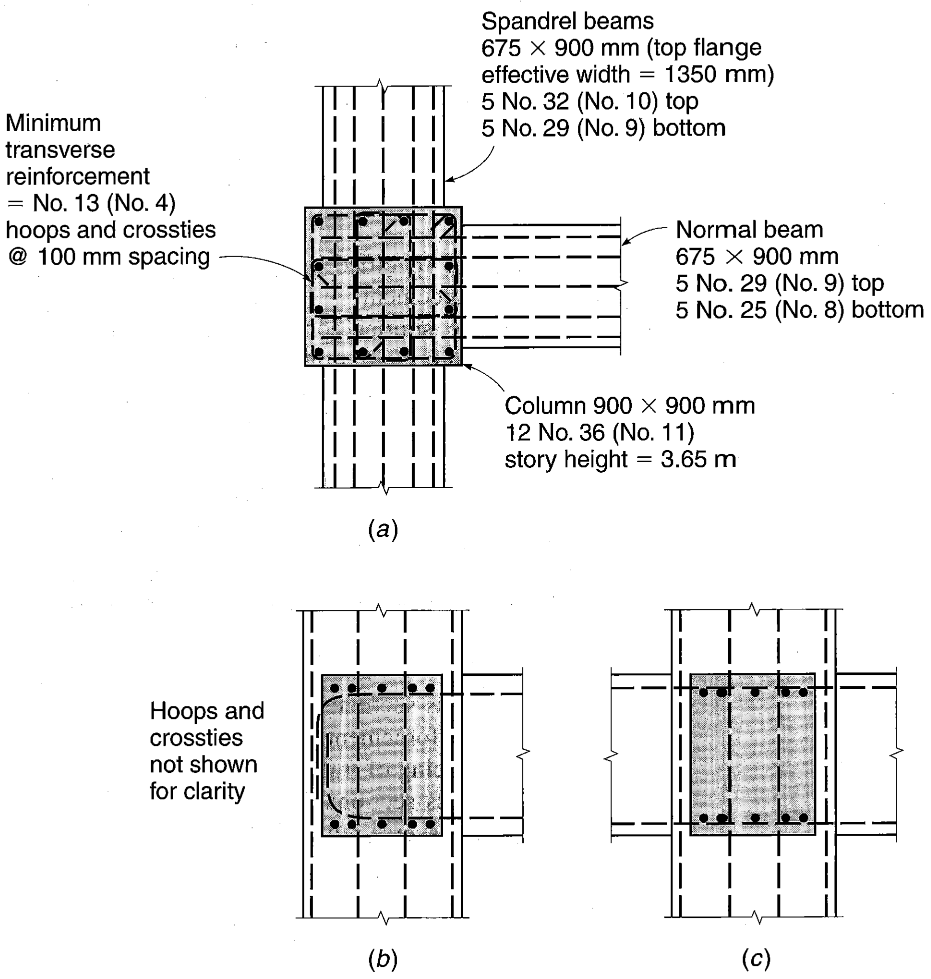
Spandrel beams
675 × 900 mm (top flange effective width = 1350 mm)
5 No. 32 (No. 10) top
5 No. 29 (No. 9) bottom
Minimum transverse reinforcement = No. 13 (No. 4) hoops and crossties @ 100 mm spacing
Normal beam
675 × 900 mm
5 No. 29 (No. 9) top
5 No. 25 (No. 8) bottom
Column 900 × 900 mm
12 No. 36 (No. 11)
story height = 3.65 m
(a)
Hoops and crossties not shown for clarity
(b)
(c)

FIGURE 20.14
Exterior beam-column joint for Examples 20.1 and 20.2: (*a*) plan view; (*b*) cross section through spandrel beam; (*c*) cross section through normal beam. Note that confining reinforcement is not shown, except for column hoops and crossties in (*a*).

those of the beams by at least 20 percent, as required by Eq. (20.20), and determine the minimum transverse reinforcement required over the length l_o in the columns.

Solution. Checking the relative flexural strengths in the frame of the spandrel beams will be sufficient, since this is clearly the controlling case for the joint. In addition, because the beam reinforcement is the same on both sides of the joint, a single comparison will suffice for both clockwise and counterclockwise beam moments.

The negative nominal flexural strength of the beam at the joint is governed by the top steel, which consists of five No. 32 (No. 10) bars in the beams plus four No. 16 (No. 5) bars in the slab within the effective width of the top flange, $A_s = 4095 + 796 = 4891 \text{ mm}^2$. The yield force in the steel is

$$A_s f_y = 4891 \times 420 = 2{,}054{,}220 \text{ N}$$

The effective depth is $d = 900 - 40 - 12.7 - 32.3/2 = 831$ mm, and with stress block depth $a = 2{,}054{,}220/(0.85 \times 28 \times 675) = 128$ mm, the nominal moment is

$$M_{nb} = \frac{2{,}054{,}220}{10^6}\left(831 - \frac{128}{2}\right) = 1576 \text{ kN-m}$$

The positive nominal flexural strength of the beam at the joint is determined by the bottom steel, five No. 29 (No. 9) bars, $A_s = 3225 \text{ mm}^2$. The yield force in the steel is

$$A_s f_y = 3225 \times 420 = 1{,}354{,}500 \text{ N}$$

The effective depth is $d = 900 - 40 - 12.7 - 28.7/2 = 833$ mm, and with stress block depth $a = 1{,}354{,}500/(0.85 \times 28 \times 1350) = 42$ mm, the nominal moment is

$$M_{nb} = \frac{1{,}354{,}500}{10^6}\left(833 - \frac{42}{2}\right) = 1100 \text{ kN-m}$$

The minimum nominal flexural strengths of the columns in this example depend on the maximum factored axial loads, which are 9523 and 9937 kN for the upper and lower columns, respectively. For the 900 × 900 mm columns, this gives

$$\frac{P_u}{f'_c A_g} = \frac{9526 \times 10^3}{28 \times 810{,}000} = 0.420 \qquad \text{upper column}$$

$$\frac{P_u}{f'_c A_g} = \frac{9937 \times 10^3}{28 \times 810{,}000} = 0.432 \qquad \text{lower column}$$

With total reinforcement of 12 No. 36 (No. 11) bars, $A_{st} = 12{,}072 \text{ mm}^2$ and the reinforcement ratio $\rho_g = 12{,}072/810{,}000 = 0.0149$. Using cover to the center of the bars of 75 mm, $\gamma = (900 - 150)/900 = 0.83$. Graphs A.7 and A.8 in Appendix A are appropriate for determining the flexural capacity.

For the upper column,

$$R_n = \frac{M_{nc}}{f'_c A_g h} = 0.168$$

$$M_{nc} = 0.168 \times 28 \times 810{,}000 \times 900 \times 10^{-6} = 3429 \text{ kN-m}$$

For the lower column,

$$R_n = \frac{M_{nc}}{f'_c A_g h} = 0.164$$

$$M_{nc} = 0.164 \times 28 \times 810{,}000 \times 900 \times 10^{-6} = 3348 \text{ kN-m}$$

Checking the relative flexural capacities,

$$\Sigma M_{nc} = 3429 + 3348 = 6777 \text{ kN-m}$$

$$\Sigma M_{nb} = 1576 + 1100 = 2676 \text{ kN-m}$$

By inspection, $\Sigma M_{nc} \geq \frac{6}{5}\, \Sigma M_{nb}$.

Minimum transverse reinforcement is required over a length l_o on either side of the joint. According to ACI Code 21.6.4, l_o is the greater of (1) the depth $h = 900$ mm, (2) one-sixth of the clear span $= (3650 - 900)/6 = 458$ mm, or (3) 450 mm. Since every corner and alternate longitudinal bar must have lateral support and because the spacing of crossties and legs of hoops is limited to a maximum of 350 mm within the plane of the transverse reinforcement, the scheme shown in Fig. 20.14*a* will be used, giving a maximum spacing of slightly less than 305 mm. The maximum spacing of transverse reinforcement *s* is limited to the smaller of one-quarter of the minimum member dimension $= 900/4 = 225$ mm, 6 times the diameter of the longitudinal bar, $6 \times 35.8 = 215$ mm, or

$$s_o = 100 + \frac{350 - 305}{3} = 115 \text{ mm}$$

with 100 mm $\leq s_o \leq$ 150 mm. A 100 mm spacing will be used.

Using No. 13 (No. 4) bars, the cross-sectional dimension of the column core, measured to the outside edges of the confining steel, is $b_c = 830$ mm, and the cross-sectional area of column core, also measured to the outside edges of the confining steel, is $A_{ch} = 830 \times 830 = 688{,}900 \text{ mm}^2$.

For $f_{yt} = 420$ MPa, the total area of transverse reinforcement with the 100 mm spacing is the larger of Eqs. (20.23) and (20.24).

$$A_{sh} = 0.3\, \frac{100 \times 830 \times 28}{420} \left(\frac{810{,}000}{688{,}900} - 1 \right) = 292 \text{ mm}^2$$

$$A_{sh} = 0.09\, \frac{100 \times 830 \times 28}{420} = 498 \text{ mm}^2$$

The requirement for 498 mm^2 is satisfied by four No. 13 (No. 4) bar legs.

c. Joints and Development of Reinforcement

The design of beam-column joints is discussed in Section 11.2. The forces acting on a joint subjected to lateral loads are illustrated in Fig. 11.4. The factored shear acting on a joint is

$$\begin{aligned} V_u &= T_1 + C_2 - V_{\text{col}} \\ &= T_1 + T_2 - V_{\text{col}} \end{aligned} \qquad (20.25)$$

where T_1 = tensile force in negative moment beam steel on one side of a joint
T_2 = tensile force in positive moment beam steel on one side of a joint
C_2 = compressive force counteracting T_2
V_{col} = shear in the column at top and bottom faces of the joint corresponding to the net moment in the joint and points of inflection at midheight of columns (see Fig. 11.5)

For seismic design, the forces T_1 and T_2 ($= C_2$) must be based on a stress in the flexural tension reinforcement of $1.25f_y$. In accordance with ACI Code 21.7.4, the nominal shear capacity of a joint depends on the degree of confinement provided by members framing into the joint.

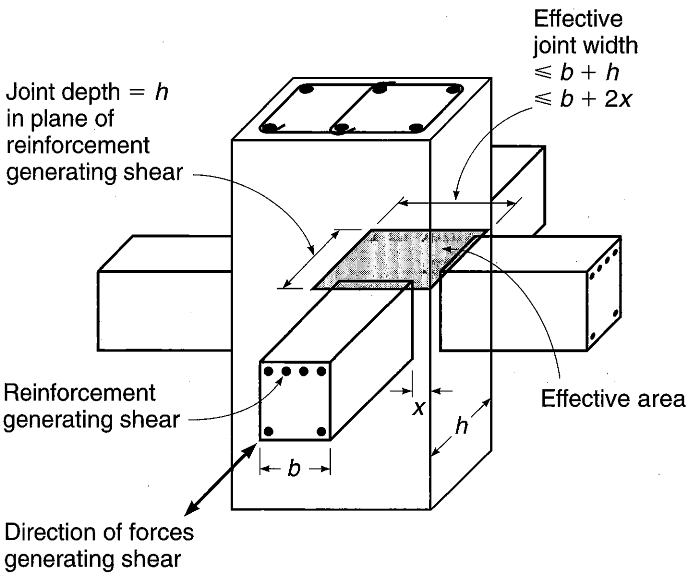
Effective joint width
$\leq b + h$
$\leq b + 2x$
Joint depth = h in plane of reinforcement generating shear
Reinforcement generating shear
Effective area
x
h
b
Direction of forces generating shear

FIGURE 20.15
Effective area of joint A_j, which must be considered separately for forces in each direction of framing. Note that the joint illustrated does not meet conditions necessary to be considered as confined because the forming members do not cover at least $\frac{3}{4}$ of each joint face. (*Adapted from Ref. 20.9.*)

For joints confined on all four faces	$1.7\sqrt{f'_c}A_j$
For joints confined on three faces or two opposite faces	$1.2\sqrt{f'_c}A_j$
For others	$1.0\sqrt{f'_c}A_j$

where A_j is the effective cross-sectional area of the joint in a plane parallel to the plane of reinforcement generating shear in the joint. The joint depth is the overall depth of the column. For beams framing into a support of larger width, the effective width of the joint is the smaller of (1) beam width plus joint depth or (2) twice the smaller perpendicular distance from the longitudinal axis of the beam to the column side. The effective area of a joint is illustrated in Fig. 20.15. The nominal shear strength for lightweight aggregate concrete is limited to three-quarters of the values given above.

To provide adequate confinement within a joint, the transverse reinforcement used in columns must be continued through the joint, in accordance with ACI Code 21.5.2. This reinforcement may be reduced by one-half within the depth of the shallowest framing member, and the spacing of spirals or hoops may be increased to 150 mm, if beams or girders frame into all four sides of the joint and the flexural members cover at least three-fourths of the column width.

For joints where the beam is wider than the column, transverse reinforcement, as required for columns (ACI Code 21.5.3), must be provided to confine the flexural steel in the beam, as shown in Fig. 20.13, unless confinement is provided by a transverse flexural member.

To provide adequate development of beam reinforcement passing through a joint, ACI Code 21.7.2 requires that the column dimension parallel to the beam reinforcement be at least 20 times the diameter of the largest longitudinal bar for normalweight concrete and 26 times the bar diameter for lightweight concrete. For beam longitudinal reinforcement that is terminated within a column, both hooked and straight reinforcement must be extended to the far face of the column core. The use of headed deformed reinforcement is not addressed. The reinforcement must be anchored in compression as described in Section 5.8 (ACI Code Chapter 12) and anchored in tension in accordance with ACI Code 21.7.5, which requires that the development length of bars with 90° hooks l_{dh} not be less than $8d_b$, 150 mm, or

$$l_{dh} = \frac{f_y d_b}{5.4\sqrt{f'_c}} \tag{20.26}$$

For lightweight aggregate concrete, these values are, respectively, $10d_b$, 190 mm, and 1.25 times the value in Eq. (20.26). The 90° hook must be located within the confined core of the column.

For straight bars anchored within a column core, the development length l_d of bottom bars must be at least 2.5 times the value required for hooks; l_d for top bars must be at least 3.25 times the length required for hooks.

According to ACI Code 21.7.5, straight bars that are terminated at a joint must pass through the confined core of a column or a boundary element (discussed in Section 20.6a). Because of the lower degree of confinement provided outside of the confined region, the Code requires that any portion of the straight embedment length that is not within the core be increased by a factor of 1.6. Thus, the required development length l_{dm} of a bar that is not entirely embedded in confined concrete is

$$l_{dm} = 1.6(l_d - l_{dc}) + l_{dc} \tag{20.27a}$$

$$l_{dm} = 1.6l_d - 0.6l_{dc} \tag{20.27b}$$

where l_d = required development length for a straight bar embedded in confined concrete

l_{dc} = length embedded in confined concrete

EXAMPLE 20.2 **Design of exterior joint.** Design the joint shown in Fig. 20.14.

Solution. As discussed in Chapter 11, a joint must be detailed so that the beam and column bars do not interfere with each other and so that placement and consolidation of the concrete are practical. Bar placement is shown in Fig. 20.14.

Development of the spandrel beam flexural steel within the joint is checked based on the requirement that the column dimension be at least 20 times the bar diameter of the largest bars. This requirement is met for the No. 32 (No. 10) bars used as top reinforcement.

$$20 \times 32.3 = 646 < 900 \text{ mm}$$

The flexural steel in the normal beam must be anchored within the core of the column based on Eq. (20.26), but not less than $8d_b$ or 150 mm. For the No. 29 (No. 9) top bars, Eq. (20.26) controls

$$l_{dh} = \frac{420 \times 28.7}{54\sqrt{28}} = 422 \text{ mm}$$

The same holds true for the No. 25 (No. 8) bottom bars, which must also be anchored in tension (ACI Code 12.11.2) because lateral loading will subject the beam to both positive and negative bending moments at the exterior joint.

$$l_{dh} = \frac{420 \times 25.4}{5.4\sqrt{28}} = 373 \text{ mm}$$

Since $3.25l_{dh}$ is not available for the top bars and $2.5l_{dh}$ is not available for the bottom bars, all flexural steel from the normal beam must be anchored using hooks, not straight reinforcement, extended to the far face of the column core, as shown in Fig. 20.14*b*.

FIGURE 20.16
Free-body diagrams in plane of spandrel beam for Example 20.2: (*a*) column and joint region; (*b*) forces acting on joint due to lateral load.

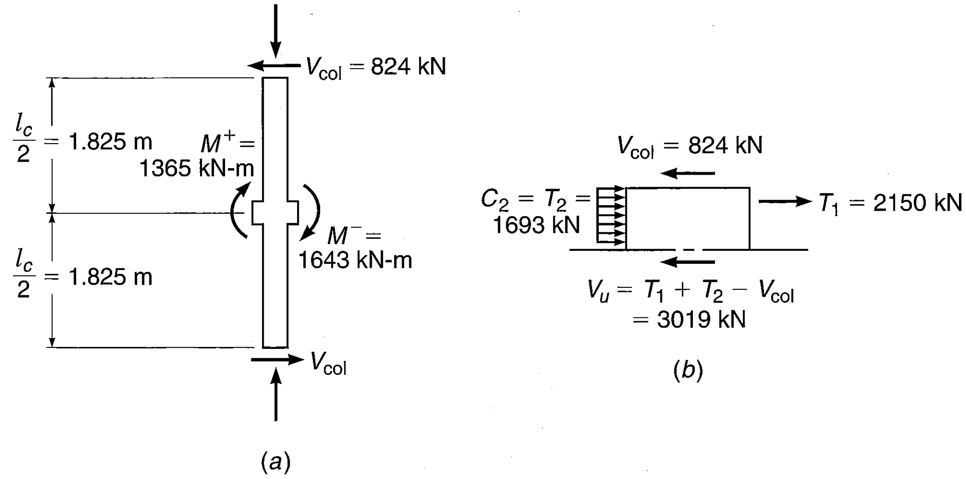

To check the shear strength of the joint, the shear forces acting on the joint must be calculated based on a stress of $1.25f_y$ in the flexural reinforcement. By inspection, shear in the plane of the spandrel beam will control.

The tensile force in the negative steel is

$$T_1 = 1.25 \times 4095 \times 420 = 2{,}150{,}000 \text{ N} = 2150 \text{ kN}$$

For an effective depth of 831 mm (Example 20.1) and a depth of stress block $a = 2{,}150{,}000/(0.85 \times 28 \times 675) = 134$ mm, the moment due to negative bending is

$$M^- = \frac{2{,}150{,}000}{10^6}\left(831 - \frac{134}{2}\right) = 1643 \text{ kN-m}$$

For positive bending on the other side of the column,

$$T_2 = 1.25 \times 3225 \times 420 = 1{,}693{,}000 \text{ N} = 1693 \text{ kN}$$

$$a = \frac{1{,}693{,}000}{0.85 \times 28 \times 1350} = 54 \text{ mm}$$

$$M^+ = \frac{1{,}693{,}000}{10^6}\left(833 - \frac{54}{2}\right) = 1365 \text{ kN-m}$$

The column shear corresponding to the sum of the moments M^+ and M^- and based on the free body of the column between assumed midheight inflection points, as shown in Fig. 20.16*a*, is $V_{col} = (1643 + 1365)/3.65 = 824$ kN. The shear forces acting on the joint are shown in Fig. 20.16*b*, and the factored joint shear is

$$V_u = T_1 + T_2 - V_{col} = 2150 + 1693 - 824 = 3019 \text{ kN}$$

For a joint confined on three faces with an effective cross-sectional area $A_j = 900 \times 900 = 810{,}000 \text{ mm}^2$, the nominal and design capacities of the joint are

$$V_n = 1.2\sqrt{f_c'}A_j = \frac{1.2\sqrt{28} \times 810{,}000}{1000} = 5143 \text{ kN}$$

$$\phi V_n = 0.85 \times 5143 = 4372 \text{ kN}$$

Since $\phi V_n > V_u$, the joint is satisfactory for shear.

Because the joint is not confined on all four sides, the transverse reinforcement in the column must be continued, unchanged, through the joint.

d. Members Not Designated as Part of Seismic-Force-Resisting System

Frame members in structures assigned to SDCs D, E, and F that are assumed not to contribute to the structure's ability to carry earthquake forces must still be able to support the factored gravity loads [see Eqs. (20.4) and (20.5)] for which they are designed as the structures undergo lateral displacement. To provide adequate strength and ductility, ACI Code 21.13.2 requires that these members be designed based on moments corresponding to the design displacement, which ACI Commentary 21.13 suggests should be based on models that will provide a conservatively large estimate of displacement. In this case, ACI Code 21.13.3 permits the load factor for live load L to be reduced to 0.5, except for garages, places of public assembly, and areas where $L > 4.8$ kN/m^2.

When the induced moments and shears, combined with the factored gravity moments and shears (see Table 1.2), do not exceed the design capacity of a frame member, ACI Code 21.13.3 requires that members with factored gravity axial forces below $A_g f'_c/10$ contain minimum longitudinal top and bottom reinforcement as provided in Eq. (3.41), a reinforcement ratio not greater than 0.025, and at least two continuous bars top and bottom. In addition, stirrups are required with a maximum spacing of $d/2$ throughout.

For members with factored gravity axial forces exceeding $A_g f'_c/10$, the longitudinal reinforcement must meet the requirements for columns proportioned for earthquake loads, and the transverse reinforcement must consist of hoops and crossties, as used in columns designed for seismic loading (as required by ACI Code 21.6.4.2). The maximum longitudinal spacing of the transverse reinforcement s_o may not be more than 6 times the diameter of the smallest longitudinal bar or 150 mm throughout the column height. In addition, the transverse reinforcement must carry shear induced by inelastic rotation at the ends of the member, as required by ACI Code 21.6.5 (discussed in Section 20.7). Members with factored gravity axial forces exceeding 35 percent of the axial capacity without eccentricity $0.35P_o$ must be designed with transverse reinforcement equal to at least one-half of that specified in ACI Code 21.6.4.4 [see Eqs. (20.21) through (20.24)].

If the induced moments or shears under the design lateral displacements exceed the design moment or shear strengths, or if such a calculation is not made, ACI Code 21.13.4 requires that the members meet the material criteria for concrete and steel in ACI Code 21.1.4 and 21.1.5 (see Section 20.4), along with criteria for mechanical and welded splices (ACI Code 21.1.6 and 21.1.7.1, respectively). For frame members with factored gravity axial loads below $A_g f'_c/10$, the minimum reinforcement criteria specified in ACI Code 21.5.2 must be met, along with the requirement that the shear capacity of the member be adequate to carry forces induced by flexural yielding under the criteria of ACI Code 21.5.4 [see Fig. 20.18 and Eq. (20.30) in Section 20.7]. In addition, stirrups may not be spaced at greater than $d/2$ throughout the length of the member. For members with factored gravity axial forces exceeding $A_g f'_c/10$, the longitudinal reinforcement ratio ρ_g must be within the range 0.01 to 0.06, and all requirements for transverse reinforcement and shear capacity specified for columns designed for earthquake-induced lateral loading must be satisfied. In addition, the transverse column reinforcement must be continued within the joints, as required by ACI Code 21.7.3.1 (see Section 20.5c) for frames in structures assigned to SDCs D, E, and F.

To reduce the potential for a punching shear failure for slab-column connections in two-way slabs without beams, ACI Code 21.13.6 requires that stirrups or headed studs satisfying the requirements of ACI Code 11.11.3 or 11.11.5, respectively (see Section 13.10), and providing V_s of at least $0.29\sqrt{f_c'}b_o d$ extend at least 4 times the slab thickness away from the face of the support, unless either (1) the requirements of ACI Code 11.11.7 are satisfied using the factored shear due to gravity load V_{ug} and the induced moment transferred between the slab and column under the design displacement, as described in Section 13.11, or (2) the design story drift ratio (relative lateral displacement under design load from the top to the bottom of a story divided by the height of the story) does not exceed the larger of 0.005 and $[0.035 - 0.05(V_{ug}/\phi V_c)]$. The design story drift ratio is equal to the larger of the design story drift ratios of the stories above and below the slab-column connection. V_c is defined by Eqs. (13.11*a*) through (13.11*c*), and V_{ug} is the factored shear force on the slab critical section for two-way action for the load combination $1.2D + 1.0L + 0.2S$. The load factor on the live load L may be reduced to 0.5, except for garages, places of public assembly, and cases in which L exceeds 4.8 kN/m^2.

20.6 ACI PROVISIONS FOR SPECIAL STRUCTURAL WALLS, COUPLING BEAMS, DIAPHRAGMS, AND TRUSSES

ACI Code Chapter 21 includes requirements for stiff structural systems and members that carry earthquake forces or distribute earthquake forces between portions of structures that carry earthquake forces. Structural walls, coupling beams, diaphragms, trusses, struts, ties, chords, and collector elements are in this category. The general requirements for these members are presented in this section. The requirements for shear design are presented in Section 20.7c.

a. Structural Walls

To ensure adequate ductility, ACI Code 21.9.2 requires that structural walls have minimum shear reinforcement ratios in both the longitudinal and transverse directions ρ_l and ρ_t of 0.0025 and a maximum reinforcement spacing of 450 mm. If the factored shear force assigned to a wall exceeds $0.17A_{cv}\lambda\sqrt{f_c'}$, where A_{cv} is the net area of the concrete section bounded by the web thickness and the length of the section in the direction of the factored shear force, at least two curtains of reinforcement must be used. If, however, the factored shear is not greater than $0.083A_{cv}\lambda\sqrt{f_c'}$, the minimum reinforcement criteria of ACI Code 14.3 govern.

Boundary elements are added along the edges of structural walls and diaphragms to increase strength and ductility. The elements include added longitudinal and transverse reinforcement and may lie entirely within the thickness of the wall or may require a larger cross section, as shown in Fig. 20.17. Under certain conditions, openings must be bordered by boundary elements. For walls that are continuous from the base of the structure to the top of a wall, compression zones must be reinforced with

FIGURE 20.17
Cross sections of structural walls with boundary elements.

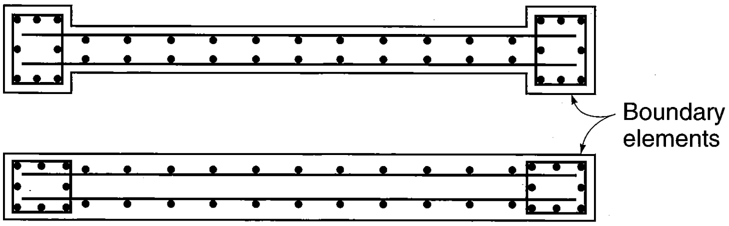

special boundary elements when the depth to the neutral axis c exceeds the value given in Eq. (20.28).

$$c \geq \frac{l_w}{600(\delta_u/h_w)} \tag{20.28}$$

where l_w and h_w are the length and width of the wall, respectively, and δ_u is the design displacement. In Eq. (20.28), δ_u/h_w is not taken greater than 0.007. When special boundary elements are required based on Eq. (20.28), the reinforcement in the boundary element must be extended vertically from the critical section a distance equal to the greater of l_w or $M_u/4V_u$.

Structural walls are also required to have boundary elements at boundaries and around openings where the maximum extreme fiber compressive stress under factored loads exceeds $0.2f'_c$. Stresses are calculated based on a linear elastic model using the gross cross section [$\sigma = (P/A) \pm (My/I)$]. The boundary elements may be discontinued once the calculated compressive stress drops below $0.15f'_c$. The confinement provided by the boundary element increases both the ductility of the wall and its ability to carry repeated cycles of loading. When required, the boundary element must extend horizontally from the extreme compressive fiber a distance not less than $c - 0.1l_w$ or $c/2$, whichever is greater, where c is the largest neutral axis depth calculated for the factored load and nominal moment capacity consistent with the displacement δ_u. When flanged sections are used, the boundary element is defined based on the effective flange width and extends at least 300 mm into the web. Transverse reinforcement within the boundary element must meet the requirements for columns in ACI Code 21.6.2 through 21.6.4 (discussed in Section 20.5b), but need not meet the requirements in Eq. (20.23), and the spacing limit for transverse reinforcement of one-quarter of the minimum member dimension in columns [described prior to Eq. (20.21) and specified in ACI Code 21.6.4.3(a)] is changed to one-third of the least dimension of the boundary element. The transverse reinforcement within a boundary element must extend into the support a distance equal to at least the development length of the largest longitudinal reinforcement, except where the boundary element terminates at a footing or mat, in which case the transverse reinforcement must extend at least 300 mm into the foundation. Horizontal reinforcement in the wall web must be anchored within the confined core of the boundary element, a requirement that usually requires standard 90° hooks or mechanical anchorage.

When boundary elements are not required and when the longitudinal reinforcement ratio in the wall boundary is greater than $2.8/f_y$, the transverse reinforcement at the boundary must consist of hoops or spirals at the wall boundary with crossties or legs that are not spaced more than 350 mm on center extending into the wall a distance of $c - 0.1l_w$ or $c/2$, whichever is greater, at a spacing of not greater than 200 mm. The transverse reinforcement in such cases must be anchored with a standard hook around the edge reinforcement, or the edge reinforcement must be enclosed in U stirrups of the same size and spacing as the transverse reinforcement. This requirement need not be met if the maximum shear force is less than $0.083A_{cv}\lambda\sqrt{f'_c}$.

b. Coupling Beams

Coupling beams connect structural walls, as shown in Fig. 20.18*a*. Under lateral loading, they can increase the stiffness of the structure and dissipate energy. Deeper coupling beams can be subjected to significant shear, which is carried effectively by diagonal reinforcement. According to ACI Code 21.9.7, coupling beams with clear span-to-total-depth ratios l_n/h of 4 or greater may be designed using the criteria for flexural members described in Section 20.5a. In this case, however, the limitations

FIGURE 20.18
Coupled shear walls and coupling beam. (*Parts b and c adapted from Ref. 20.9.*)

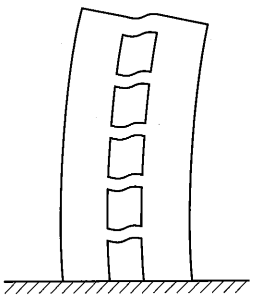

(*a*) Coupled shear walls

Note: For clarity, only part of the required reinforcement is shown on each side of the line of symmetry.

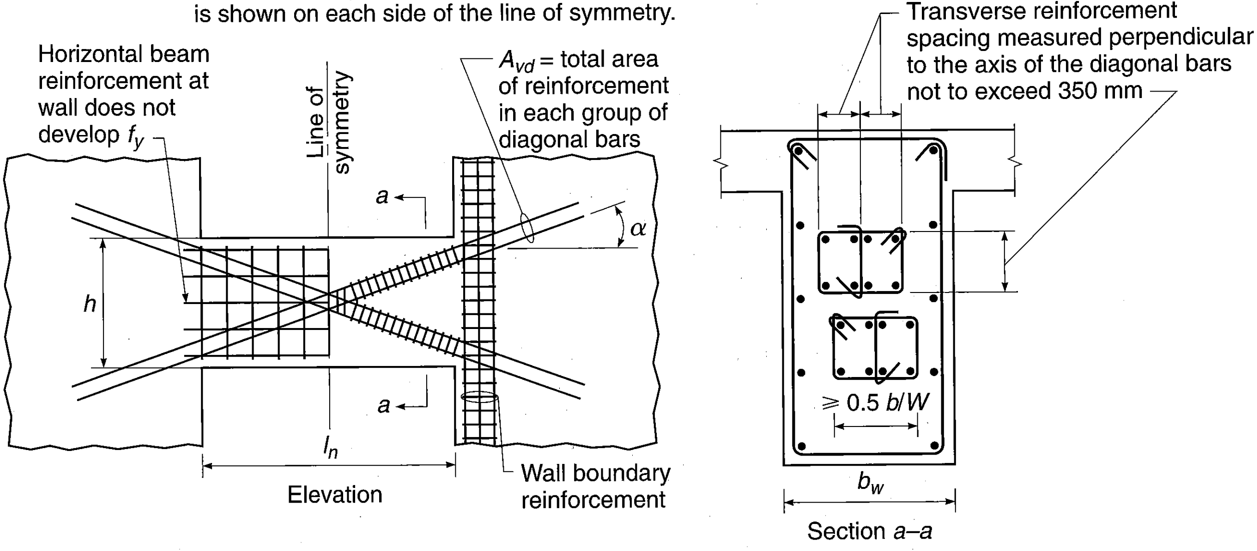

Horizontal beam reinforcement at wall does not develop f_y
Line of symmetry
A_{vd} = total area of reinforcement in each group of diagonal bars
Transverse reinforcement spacing measured perpendicular to the axis of the diagonal bars not to exceed 350 mm
a
α
h
a
l_n
Elevation
Wall boundary reinforcement
≥ 0.5 b/W
b_w
Section a–a

(*b*) Coupling beam with confinement of individual diagonals

Note: For clarity, only part of the required reinforcement is shown on each side of the line of symmetry.

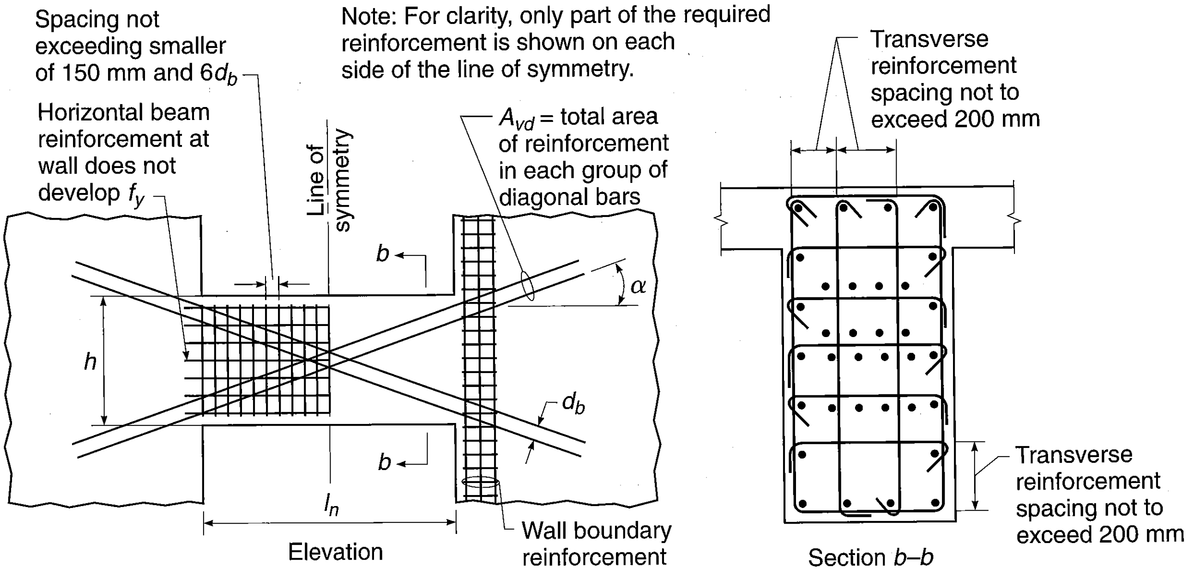

Spacing not exceeding smaller of 150 mm and $6d_b$
Horizontal beam reinforcement at wall does not develop f_y
Line of symmetry
A_{vd} = total area of reinforcement in each group of diagonal bars
Transverse reinforcement spacing not to exceed 200 mm
b
α
h
d_b
b
l_n
Elevation
Wall boundary reinforcement
Transverse reinforcement spacing not to exceed 200 mm
Section b–b

Note: Consecutive crossties engaging the same longitudinal bar have their 90-degree hooks on opposite sides of beam.

(*c*) Coupling beam with full confinement of diagonally reinforced concrete beam section on width-to-depth ratio and total width for flexural members need not be applied if it can be shown by analysis that the beam has adequate lateral stability. Coupling beams with l_n/h less than 2 and a factored shear $V_u > 0.33\lambda\sqrt{f_c'}A_{cw}$, where A_{cw} is the concrete area resisting shear, must be reinforced with two intersecting groups of diagonal reinforcement, as shown in Fig. 20.18*b* and *c*, unless it can be shown that the loss of stiffness and strength in the beams will not impair the vertical load-carrying capacity of the structure, egress from the structure, or the integrity of nonstructural components and their connections to the structure. Coupling beams with $2 \leq l_n/h < 4$ may be designed using the criteria for flexural members or may be reinforced using two intersecting groups of diagonally placed bars that are symmetrical about the midspan. Such reinforcement is not effective unless it is placed at a steep angle (Refs. 20.11 and 20.12) and thus is not permitted for coupling beams with $l_n/h \geq 4$. The criteria for shear reinforcement in coupling beams are discussed in Section 20.7c.

c. Structural Diaphragms

Floors and roofs serve as structural diaphragms in buildings. In addition to supporting vertical dead, live, and snow loads, they connect and transfer lateral forces between the members in the vertical lateral-force-resisting system and support other building elements, such as partitions, that may resist horizontal forces but do not act as part of the vertical lateral-force-resisting system. Floor and roof slabs that act as diaphragms may be monolithic with the other horizontal elements in the structures or may include a topping slab. ACI Code 21.11.6 requires that concrete slabs and composite topping slabs designed as structural diaphragms to transmit earthquake forces be at least 50 mm thick. Topping slabs placed over precast floor or roof elements that do not rely on composite action must be at least 65 mm thick.

d. Collector and Structural Truss Elements

To provide adequate confinement and ductility, collector elements, which act in tension or compression to transmit seismic forces between structural diaphragms and vertical load-carrying elements, with compressive stresses greater than $0.2f_c'$ must meet the same transverse reinforcement requirements as boundary elements in seismic-load-resisting frames, but over the full length of the elements. The special transverse reinforcement may be discontinued at a section where the calculated compressive stress is less than $0.15f_c'$ in accordance with ACI Code 21.11.7.5. Transverse reinforcement is also required for truss elements with compressive stresses greater than $0.2f_c'$, but in contrast with collector elements, must be continued over the full length of the element. For trusses, the requirements for columns in ACI Code 21.6.4.2 through 21.6.4.4 and 21.6.4.7 are used, as described in Section 20.5b. Compressive stresses in collector and truss elements are calculated for the factored forces using a linear elastic model and the gross section properties of the elements. Continuous reinforcement in stiff structural systems must be anchored and spliced to develop f_y in tension.

20.7 ACI PROVISIONS FOR SHEAR STRENGTH

a. Beams

A prime concern in the design of seismically loaded structures is the shear induced in members due to nonlinear behavior in flexure [Eq. (20.1)]. As discussed in Section 20.2, increasing the flexural strength of beams and columns may increase the shear in these

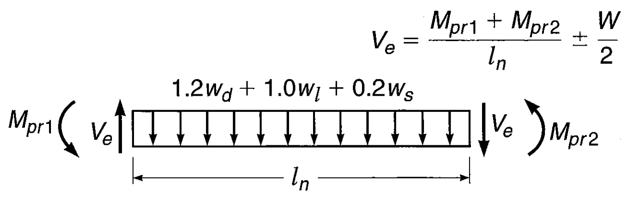
$V_e = \frac{M_{pr1} + M_{pr2}}{l_n} \pm \frac{W}{2}$
$1.2w_d + 1.0w_l + 0.2w_s$
M_{pr1}
V_e
V_e
M_{pr2}
l_n

FIGURE 20.19
Forces considered in the shear design of flexural members subjected to seismic loading. $W/2$ is the shear corresponding to gravity loads based on $1.2D + 1.0L + 0.2S$.

members if the structure is subjected to severe lateral loading. As a result, the ACI Code requires that beams and columns in frames that are part of the seismic-force-resisting system (including some members that are not designed to carry lateral loads) be designed for the combined effects of factored gravity load and shear induced by the formation of plastic hinges at the ends of the members.

For members with axial loads less than $A_g f'_c/10$, ACI Code 21.5.4 requires that the design shear force V_e be based on the factored tributary gravity load along the span plus shear induced by moments of opposite sign corresponding to the *probable flexural strength* M_{pr}. Loading corresponding to this case is shown in Fig. 20.19. The probable flexural strength M_{pr} is based on the reinforcing steel achieving a stress of $1.25f_y$.

$$M_{pr} = 1.25A_s f_y \left(d - \frac{a}{2}\right) \tag{20.29a}$$

where

$$a = \frac{1.25f_y A_s}{0.85f'_c b} \tag{20.29b}$$

The shear V_e is given by

$$V_e = \frac{M_{pr1} + M_{pr2}}{l_n} \pm \frac{w_u l_n}{2} \tag{20.30}$$

where M_{pr1} and M_{pr2} = probable moment strengths at two ends of member when moments are acting in the same sense
l_n = length of member between faces of supports
w_u = factored uniform gravity load based on $1.2D + 1.0L + 0.2S$

Equation (20.30) should be evaluated separately for moments at both ends acting in the clockwise and then counterclockwise directions.

To provide adequate ductility and concrete confinement, the transverse reinforcement over a length equal to twice the member depth from the face of the support, at both ends of the flexural member, must be designed based on a concrete shear capacity $V_c = 0$, when the earthquake-induced shear force in Eq. (20.30) $(M_{pr1} + M_{pr2})/l_n$ is one-half or more of the maximum required shear strength within that length and the factored axial compressive force in the member, including earthquake effects, is below $A_g f'_c/20$.

EXAMPLE 20.3

Beam shear design. A 450 mm wide by 600 mm deep reinforced concrete beam spans between two interior columns in a building frame designed for a region of high seismic risk. The clear span is 7.3 m and the reinforcement at the face of the support consists of four No. 32 (No. 10) top bars and four No. 25 (No. 8) bottom bars. The effective depth is 530 mm for both top and bottom steel. The maximum factored shear $w_u l_n/2 = (1.2w_d + 1.0w_l)l_n/2 = 138$ kN at

FIGURE 20.20
Configuration of hoop reinforcement for beam in Example 20.3.

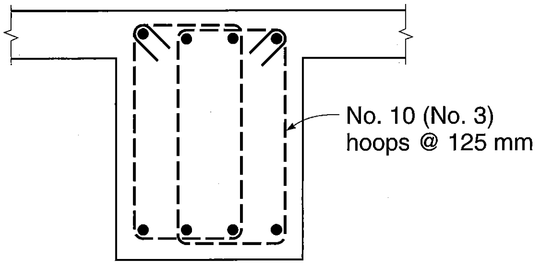

each end of the beam. Materials strengths are $f'_c = 35$ MPa and $f_y = 420$ MPa. Design the shear reinforcement for the regions adjacent to the column faces.

Solution. The probable moment strengths M_{pr} are based on a steel stress of $1.25f_y$. For negative bending, the area of steel is $A_s = 3276\text{ mm}^2$ at both ends of the beam, the stress block depth is $a = 1.25 \times 3276 \times 420/(0.85 \times 35 \times 450) = 128$ mm, and the probable strength is

$$M_{pr1} = \frac{1.25 \times 3276 \times 420}{10^6}\left(530 - \frac{128}{2}\right) = 801\text{ kN-m}$$

For positive bending, the area of steel is $A_s = 2040\text{ mm}^2$, the effective width is 2250 mm, the stress block depth $a = 1.25 \times 2040 \times 420/(0.85 \times 35 \times 2250) = 16$ mm, and the probable strength is

$$M_{pr2} = \frac{1.25 \times 2040 \times 420}{10^6}\left(530 - \frac{16}{2}\right) = 559\text{ kN-m}$$

As given in the problem statement, the effect of factored gravity loads $w_u l_n/2 = (1.2w_d + 1.0w_l)l_n/2 = 138$ kN giving a design shear force at each end of the beam, according to Eq. (20.30), of

$$V_e = \frac{801 + 559}{7.3} + 138 = 186 + 138 = 324\text{ kN}$$

Since the earthquake-induced force, 186 kN, is greater than one-half of the maximum required shear strength, the transverse hoop reinforcement must be designed to resist the full value of V_e (i.e., $\phi V_s \geq V_e$) over a length $2h = 1.2$ m from the face of the column, in accordance with ACI Code 21.3.3. The maximum spacing of the hoops s is based on the smaller of $d/4 = 132$ mm, $8d_b$ for the smallest longitudinal bars = 203 mm, or $24d_b$ for the hoop bars [assumed to be No. 10 (No. 3) bars] = 228 mm, or 300 mm. A spacing $s = 125$ mm will be used.

The area of shear reinforcement within a distance s is

$$A_v = \frac{(V_e/\phi)s}{f_{yt}d} = \frac{(324 \times 10^3/0.75)125}{420 \times 530} = 243\text{ mm}^2$$

Providing support for corner and alternate longitudinal bars, in accordance with ACI Code 21.5.3, leads to the use of overlapping hoop reinforcement, shown in Fig. 20.20, and a total area of transverse steel $A_v = 284\text{ mm}^2$.

The first hoop is placed 50 mm from the face of the column. The other hoops are spaced at 125 mm within 1.2 m from each column face. Transverse reinforcement for the balance of the beam is calculated based on the value of V_e at that location and a nonzero concrete contribution V_c. The stirrups must have seismic hooks and a maximum spacing of $d/2$.

b. Columns

In accordance with ACI Code 21.6.5, shear provisions similar to those used for beams to account for the formation of inelastic hinges must also be applied to members with

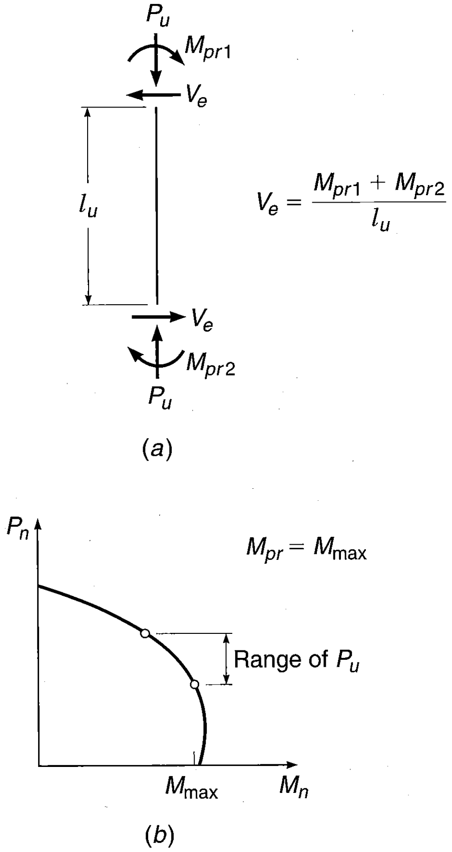

FIGURE 20.21
(*a*) Forces considered in the shear design of columns subjected to seismic loading. (*b*) Column interaction diagram used to determine maximum probable moment strengths. Note that M_{pr} for columns is usually governed by M_{pr} of the girders framing into a joint, rather than $M_{\max}$.

axial loads greater than $A_g f'_c/10$. In this case, the loading is illustrated in Fig. 20.21*a*, and the factored shear is

$$V_e = \frac{M_{pr1} + M_{pr2}}{l_u} \tag{20.31}$$

where l_u is the clear distance between beams, and M_{pr1} and M_{pr2} are based on a steel tensile strength of $1.25f_y$.

In Eq. (20.31), M_{pr1} and M_{pr2} are the maximum probable moment strengths for the range of factored axial loads to which the column will be subjected, as shown in Fig. 20.21*b*; V_e, however, need not be greater than a value based on M_{pr} for the transverse members framing into the joint. For most frames, the latter will control. Of course, V_e may not be less than that obtained from the analysis of the structure under factored loads.

The ACI Code requires that the transverse reinforcement in a column over a length l_o (the greater of the depth of the member at the joint face, one-sixth of the clear span, or 450 mm) from each joint face be proportioned to resist shear based on a concrete shear capacity $V_c = 0$ when (1) the earthquake-induced shear force is one-half or more of the maximum required shear strength within those lengths and (2) the factored axial compressive force, including earthquake effects, is less than $A_g f'_c/20$.

c. Walls, Coupling Beams, Diaphragms, and Trusses

According to ACI Code 21.9.3 and 21.11.9, the factored shear force V_u for walls, coupling beams, diaphragms, and trusses must be obtained from analysis based on the factored (including earthquake) loads.

In accordance with ACI Code 21.9.4, the nominal shear strength V_n of structural walls and diaphragms is taken as

$$V_n = A_{cv}(\alpha_c \lambda \sqrt{f'_c} + \rho_t f_y) \tag{20.32}$$

where A_{cv} = gross area of concrete section bounded by the web thickness and length of the section in the direction of shear force
ρ_t = ratio of distributed shear reinforcement on a plane perpendicular to the plane of A_{cv}
α_c = 0.25 for $h_w/l_w \leq 1.5$, = 0.17 for $h_w/l_w \geq 2.0$, and varies linearly for intermediate values of h_w/l_w

The values of h_w and l_w used to calculate α_c are the height and length, respectively, of the entire wall or diaphragm or segments of the wall or diaphragm. l_w is measured in the direction of the shear force. In applying Eq. (20.32), the ratio h_w/l_w is the larger of the ratios for the entire member or the segment of the member being considered. The use of α_c greater than 0.17 is based on the higher shear strength observed for walls with low aspect ratios.

As described in Section 20.6, ACI Code 21.9.2 requires that walls and diaphragms contain distributed shear reinforcement in two orthogonal directions in the plane of the member. For $h_w/l_w \leq 2.0$, the reinforcement ratio for steel crossing the plane of A_{cv}, ρ_l, must at least equal ρ_t. The nominal shear strength of all wall piers (vertical regions of a wall separated by openings) that together carry the lateral force is limited to a maximum value of $0.66A_{cv}\sqrt{f'_c}$, with no individual pier assumed to carry greater than $0.83A_{cw}\sqrt{f'_c}$, where A_{cv} is the total cross-sectional area and A_{cw} is the cross-sectional area of an individual pier. The nominal shear strength of horizontal wall segments (regions of a wall bounded by openings above and below) and coupling beams is limited to $0.83A_{cw}\sqrt{f'_c}$.

For coupling beams reinforced with two intersecting groups of diagonally placed bars symmetrical about the midspan (Fig. 20.18*b*), each group of the diagonally placed bars must consist of at least four bars provided in two or more layers and embedded into the wall not less than 1.25 times the development length required for f_y in tension. The nominal strength provided by the diagonal bars is given by

$$V_n = 2A_{vd} f_y \sin \alpha \leq 0.83\sqrt{f'_c}A_{cw} \tag{20.33}$$

where A_{vd} = total area of longitudinal reinforcement in an individual diagonal
A_{cw} = area of concrete section resisting shear
α = angle between diagonal reinforcement and longitudinal axis of coupling beam

The upper limit in Eq. (20.33) is a safe upper bound based on the experimental observation that coupling beams remain ductile at shear forces exceeding this value (Ref. 20.12).

ACI Code 21.9.7 allows two options for providing confinement for coupling beams. In the first, shown in Fig. 20.18*b*, each group of diagonal bars must be enclosed by transverse reinforcement having out-to-out dimensions not smaller than $0.5b_w$ in the direction parallel to b_w and $0.2b_w$ along the other sides (i.e., perpendicular to b_w). The transverse reinforcement must consist of hoops satisfying Eqs. (20.23) and (20.24), with a spacing measured parallel to the diagonal bars satisfying Eq. (20.21), but not exceeding 6 times the diameter of the diagonal bars, and have spacing of crossties or legs of hoops measured perpendicular to the diagonal bars not exceeding 350 mm. When computing A_g for use in Eqs. (8.5) and (21.23), the concrete cover required by ACI Code 7.7 (see Section 3.6a) is assumed on all four sides of each group of diagonal bars. The transverse reinforcement must be continued through the intersection of the diagonal bars. Additional longitudinal and transverse reinforcement must be distributed around the beam perimeter with a total area in each direction not less than $0.002b_w s$ and spacing not greater than 300 mm.

For the second option, shown in Fig. 20.18*c,* ACI Code 21.9.7 allows hoops to be provided for the entire beam cross section satisfying Eqs. (20.23) and (20.24) and extra confining transverse reinforcement, as required by ACI Code 21.6.4.7 when the cover exceeds 100 mm, with longitudinal spacing not exceeding the smaller of 150 mm and 6 times the diameter of the diagonal bars, and with spacing of crossties or legs of hoops both vertically and horizontally in the plane of the beam cross section not exceeding 200 mm. Each crosstie and each hoop leg must engage a longitudinal bar of equal or larger diameter.

According to ACI Code 21.11.9, the maximum nominal shear strength of diaphragms is

$$V_n = A_{cv}(0.17\lambda\sqrt{f_c'} + \rho_t f_y) \leq 0.66A_{cv}\sqrt{f_c'} \tag{20.34}$$

where A_{cv} is the gross area of the concrete bounded by the diaphragm thickness and length of the diaphragm in the direction of the shear force. Web reinforcement in the diaphragm is distributed uniformly in both directions.

20.8 ACI PROVISIONS FOR INTERMEDIATE MOMENT FRAMES

ACI Code 21.3 governs the design of frames in structures assigned to SDC C. The requirements include specified loading and detailing requirements. Unlike structures assigned to SDCs D, E, and F, two-way slab systems without beams are allowed to serve as lateral-load-resisting systems. Walls, diaphragms, and trusses in regions of moderate seismic risk are designed using the main part of the Code.

ACI Code 21.3.3 offers two options for the shear design of frame members. The first option is similar to that illustrated in Figs. 20.19 and 20.21 and Eqs. (20.30) and (20.31), with the exception that the probable strengths M_{pr} are replaced by the nominal strengths M_n. For beams, f_y is substituted for $1.25f_y$ in Eq. (20.29). For columns, the moments used at the top and bottom of the column [Fig. 20.21 and Eq. (20.31)] are based on the capacity of the column alone (not considering the moment capacity of the beams framing into the joints) under the factored axial load P_u that results in the maximum nominal moment capacity.

As an alternative to designing for shear induced by the formation of hinges at the ends of the members, ACI Code 21.3.3 allows shear design to be based on load combinations that include an earthquake effect that is twice that required by the governing building code. Thus, Eq. (20.4) becomes

$$U = 1.2D + 2.0E + 1.0L + 0.2S \tag{20.35}$$

For beams and columns, the Code prescribes detailing requirements that are not as stringent as those used in regions of high seismic risk, but that provide greater confinement and increased ductility compared to those used in structures not designed for earthquake loading. For beams, the positive-moment strength at the face of a joint must be at least one-third of the negative-moment strength at the joint, in accordance with ACI Code 21.3.4. Both the positive and negative-moment strength along the full length of a beam must be at least one-fifth of the maximum moment strength at the face of either joint. Hoops are required at both ends of beams over a length equal to twice the member depth; the first hoop must be placed within 50 mm of the face of the support, and the maximum spacing in this region may not exceed one-fourth of the effective depth, 8 times the diameter of the smallest longitudinal bar, 24 times the stirrup diameter, or 300 mm. The maximum stirrup spacing elsewhere in beams is one-half of the effective depth.

For columns, within length l_o from the joint face, the tie spacing s_o may not exceed 8 times the diameter of the smallest longitudinal bar, 24 times the diameter of the tie bar, one-half of the smallest cross-sectional dimension of the column, or 300 mm. The length l_o must be greater than one-sixth of the column clear span, the maximum cross-sectional dimension of the member, or 450 mm. The first tie must be located not more than $s_o/2$ from the joint face. Outside of l_o, the spacing of the transverse reinforcement must not exceed $d/2$ or 600 mm and must satisfy the requirements specified by ACI Code 7.10 for transverse reinforcement in columns. In accordance with ACI Code 21.3.5 and 11.10, lateral joint reinforcement with an area as specified in Eq. (4.13) must be provided within the column for a depth not less than the depth of the deepest flexural member framing into the joint.

Like columns in special moment frames, columns in intermediate moment frames must be designed to provide for ductile behavior when supporting discontinuous stiff members, such as walls. Columns in intermediate moment frames must contain transverse reinforcement with spacing s_o over the full height beneath the level at which the discontinuity occurs if the portion of factored axial compressive force in the columns related to earthquake effects exceeds $A_g f_c'/10$. This transverse reinforcement must extend above and below the columns into the discontinued stiff member for at least the development length of the largest longitudinal reinforcement for walls and at least 300 mm into foundations.

For two-way slabs without beams, ACI Code 21.3.6 requires design for earthquake effects using Eqs. (20.4) and (20.5). Under these loading conditions, the reinforcement provided to resist the unbalanced moment transferred between the slab and the column M_s (M_u in Section 13.11) must be placed within the column strip. Reinforcement to resist the fraction of the unbalanced moment M_s defined by Eq. (13.16*a*), $M_{ub} = \gamma_f M_u = \gamma_f M_s$, but not less than one-half of the reinforcement in the column strip at the support, must be concentrated near the column. This reinforcement is placed within an effective slab width located between lines $1.5h$ on either side of the column or column capital, where h is the total thickness of the slab or drop panel.

To ensure ductile behavior throughout two-way slabs without beams, at least one-quarter of the top reinforcement at the support in column strips must be continuous throughout the span, as must bottom reinforcement equal to at least one-third of the top reinforcement at the support in column strips. A minimum of one-half of all bottom reinforcement at midspan in both column and middle strips must be continuous and develop its yield strength at the face of the support. For discontinuous edges of the slab, both the top and bottom reinforcement must be developed at the face of the support. Finally, at critical sections for two-way shear at columns (Section 13.10a), V_u may not exceed $0.4\phi V_c$. The latter provision may be waived if the requirements of ACI Code 21.13.6 for slab-column connections in members not designated as part of the seismic-force-resisting system are met (see Section 20.5b).

REFERENCES

20.1 *2003 NEHRP Recommended Provisions for Seismic Regulations for New Buildings and Other Structures*, Part 1—Provisions, Part 2—Commentary, Building Seismic Safety Council, Washington, DC, 2003.

20.2 *Minimum Design Loads for Buildings and Other Structures,* ASCE/SEI 7-05, American Society of Civil Engineers, Reston, VA, 2005.

20.3 S. K. Ghosh, A. W. Domel, Jr., and D. A. Fanella, *Design of Concrete Buildings for Earthquake and Wind Forces*, 2nd ed., Portland Cement Association, Skokie, IL, and International Conference of Building Officials, Whittier, CA, 1995.

20.4 W.-F. Chen and C. Scrawthorn, eds., *Earthquake Engineering Handbook*, CRC Press, Boca Raton, FL, 2003.

20.5 T. Paulay and M. J. N. Priestly, *Seismic Design of Reinforced Concrete and Masonry Buildings*, John Wiley & Sons, Inc., New York, 1992.

20.6 G. G. Penelis and A. J. Kappos, *Earthquake-Resistant Concrete Structures*, E & FN Spon, New York, 1997.

20.7 *Concrete Structures in Earthquake Regions: Design & Analysis*, E. Booth, ed., Longman Scientific & Technical, Harlow, England, 1994.

20.8 *Seismic Analyisis of Safety-Related Nuclear Structures*, SEI/ASCE 4-98, American Society of Civil Engineers, Reston, VA, 2000.

20.9 *Building Code Requirements for Structural Concrete*, (ACI 318-08) *and Commentary*, American Concrete Institute, Farmington Hills, MI, 2008.

20.10 ACI Committee 352, *Recommendations for Design of Beam-Column Joints in Monolithic Reinforced Concrete Structures,* ACI 352R-02, American Concrete Institute, Farmington Hills, MI, 2008.

20.11 T. Paulay and J. R. Binney, "Diagonally Reinforced Coupling Beams of Shear Walls," in *Shear in Reinforced Concrete,* SP-42, American Concrete Institute, Detroit, MI, 1974, pp. 579–798.

20.12 G. B. Barney, K. N. Shiu, B. G. Rabbat, A. E. Fiorato, H. G. Russell, and W. G. Corley, *Behavior of Coupling Beams under Load Reversals* (RD068.01), Portland Cement Association, Skokie, IL, 1980.

PROBLEMS

20.1. An interior column joint in a reinforced concrete frame structure assigned to SDC D consists of 700 mm wide by 500 mm deep beams and 900 mm wide by 500 mm deep girders framing into a 700 × 700 mm column. The slab thickness is 125 mm, and the effective overhanging flange width on either side of the web of the flexural members is 1 m. Girder reinforcement at the joint consists of five No. 32 (No. 10) top bars and five No. 25 (No. 8) bottom bars. Beam reinforcement consists of four No. 32 (No. 10) top bars and four No. 25 (No. 8) bottom bars. As the flexural steel crosses the joint, the top and bottom girder bars rest on the respective top and bottom beam bars. Column reinforcement consists of 12 No. 29 (No. 9) bars evenly spaced around the perimeter of the column, similar to the placement shown in Fig. 20.14. Clear cover on the outermost main flexural and column longitudinal reinforcement is 50 mm. Assume No. 13 (No. 4) stirrups and ties. For earthquake loading, the maximum factored axial load on the upper column framing into the joint is 4731 kN, and the maximum factored axial load on the lower column is 4998 kN. For a frame story height of 4 m, determine if the nominal flexural strengths of the columns exceed those of the beams and girders by at least 20 percent, and determine the minimum transverse reinforcement required in the columns adjacent to the beams. Use $f_c' = 28$ MPa and $f_y = 420$ MPa.

20.2. Design the joint and the transverse column reinforcement for the members described in Problem 20.1. The factored shears due to earthquake load are 125 kN in the upper column and 134 kN in the lower column. Minimum factored axial loads are 90 and 108 kN below the forces specified in Problem 20.1 for the upper and lower columns, respectively.

20.3. In Example 20.1, the columns are spaced 8.5 m on center in the direction of the spandrel beams. The total dead load on the spandrel beam (including self-weight) is 29 kN/m and the total live load is 13.5 kN/m. Design the spandrel beam transverse reinforcement for a building subject to high seismic risk.

20.4. Repeat Problem 20.3 for an intermediate frame.

20.5. An interior column joint in a reinforced concrete frame structure assigned to SDC E consists of 500 mm wide by 700 mm deep beams and girders framing into 650 × 650 mm columns. The slab thickness is 100 mm, and the effective overhanging flange width on either side of the web of the flexural members is 800 mm. Girder and beam reinforcement at the joint consists of four No. 32 (No. 10) top bars and four No. 29 (No. 9) bottom bars. As the flexural steel crosses the joint, the top and bottom girder bars are outside the respective top and bottom beam bars. Column reinforcement consists of eight No. 43 (No. 14) bars evenly spaced around the perimeter of the column, similar to the placement shown in Fig. 11.10. Clear cover on the outermost main flexural and column longitudinal reinforcement is 50 mm. Assume No. 13 (No. 4) stirrups and ties. For earthquake loading, the maximum factored axial load on the upper column framing into the joint is 4740 kN, and the maximum factored axial load on the lower column is 5300 kN. The story height is 3.65 m, and the columns are spaced 7.3 m on center in the direction of the girders. Use $f'_c = 28$ MPa and $f_y = 420$ MPa.

(*a*) Determine if the nominal flexural strengths of the columns exceed those of the beams and girders by at least 20 percent, and determine the minimum transverse reinforcement required in the columns adjacent to the beams.

(*b*) The total dead load on the girder (including self-weight) is 41 kN/m, and the total live load is 19 kN/m. Design the girder transverse reinforcement.

APPENDIX

A

Design Aids

TABLE A.1
Designations, diameters, areas, and masses of standard bars

Bar No.			Cross-Sectional	Nominal Mass,
SI[a]	Inch-Pound[b]	Diameter, mm	Area, mm^2	kg/m
10	3	9.5	71	0.560
13	4	12.7	129	0.994
16	5	15.9	199	1.552
19	6	19.1	284	2.235
22	7	22.2	387	3.042
25	8	25.4	510	3.973
29	9	28.7	645	5.060
32	10	32.3	819	6.404
36	11	35.8	1,006	7.907
43	14	43.0	1,452	11.380
57	18	57.3	2,581	20.240

[a] Bar number approximates the number of millimeters included in the nominal diameter of the bar. Bars are marked with this designation. The nominal diameter of a deformed bar is equivalent to the diameter of a plain bar having the same mass per unit length as the deformed bar.

[b] Based on the number of eighths of an inch included in the nominal diameter of the bars.

TABLE A.2
Areas of groups of bars, mm²

Bar No.		Number of Bars											
SI	Inch-Pound	1	2	3	4	5	6	7	8	9	10	11	12
10	3	71	142	213	284	355	426	497	568	639	710	781	852
13	4	129	258	387	516	645	774	903	1,032	1,161	1,290	1,419	1,548
16	5	199	398	597	796	995	1,194	1,393	1,592	1,791	1,990	2,189	2,388
19	6	284	568	852	1,136	1,420	1,704	1,988	2,272	2,556	2,840	3,124	3,408
22	7	387	774	1,161	1,548	1,935	2,322	2,709	3,096	3,483	3,870	4,257	4,644
25	8	510	1,020	1,530	2,040	2,550	3,060	3,570	4,080	4,590	5,100	5,610	6,120
29	9	645	1,290	1,935	2,580	3,225	3,870	4,515	5,160	5,805	6,450	7,095	7,740
32	10	819	1,638	2,457	3,276	4,095	4,914	5,733	6,552	7,371	8,190	9,009	9,828
36	11	1,006	2,012	3,018	4,024	5,030	6,036	7,042	8,048	9,054	10,060	11,066	12,072
43	14	1,452	2,904	4,356	5,808	7,260	8,712	10,164	11,616	13,068	14,520	15,972	17,424
57	18	2,581	5,162	7,743	10,324	12,905	15,486	18,067	20,648	23,229	25,810	28,391	30,972

TABLE A.3
Areas of bars in slabs, mm²/m

		Bar No.								
Spacing,	SI:	10	13	16	19	22	25	29	32	36
mm	Inch-Pound:	3	4	5	6	7	8	9	10	11
75		947	1,720	2,653	3,787	5,160	6,800	8,600	10,920	13,413
80		888	1,613	2,488	3,550	4,838	6,375	8,063	10,238	12,575
90		789	1,433	2,211	3,156	4,300	5,667	7,167	9,100	11,178
100		710	1,290	1,990	2,840	3,870	5,100	6,450	8,190	10,060
110		645	1,173	1,809	2,582	3,518	4,636	5,864	7,445	9,145
120		592	1,075	1,658	2,367	3,225	4,250	5,375	6,825	8,383
130		546	992	1,531	2,185	2,977	3,923	4,962	6,300	7,738
140		507	921	1,421	2,029	2,764	3,643	4,607	5,850	7,186
150		473	860	1,327	1,893	2,580	3,400	4,300	5,460	6,707
160		444	806	1,244	1,775	2,419	3,188	4,031	5,119	6,288
170		418	759	1,171	1,671	2,276	3,000	3,794	4,818	5,918
180		394	717	1,106	1,578	2,150	2,833	3,583	4,550	5,589
190		374	679	1,047	1,495	2,037	2,684	3,395	4,311	5,295
200		355	645	995	1,420	1,935	2,550	3,225	4,095	5,030
225		316	573	884	1,262	1,720	2,267	2,867	3,640	4,471
250		284	516	796	1,136	1,548	2,040	2,580	3,276	4,024
300		237	430	663	947	1,290	1,700	2,150	2,730	3,353

TABLE A.4
Limiting steel reinforcement ratios for tension-controlled members

f_y, MPa	f'_c, MPa	β_1	$\rho_{0.005}$[a] $\epsilon_t = 0.005$[b]	$\rho_{0.004}$[a] $\epsilon_t = 0.004$[c]	$\rho_{\min} = \frac{1.4}{f_y}$	$\rho_{\min} = \frac{0.25\sqrt{f'_c}}{f_y}$
280	21	0.850	0.0203	0.0232	0.0050	0.0041
	28	0.850	0.0271	0.0310	0.0050	0.0047
	35	0.800	0.0319	0.0364	0.0050	0.0053
	42	0.750	0.0359	0.0410	0.0050	0.0058
	49	0.700	0.0390	0.0446	0.0050	0.0063
	56	0.650	0.0414	0.0474	0.0050	0.0067
	63	0.650	0.0466	0.0533	0.0050	0.0071
	70	0.650	0.0518	0.0592	0.0050	0.0075
350	21	0.850	0.0163	0.0186	0.0040	0.0033
	28	0.850	0.0217	0.0248	0.0040	0.0038
	35	0.800	0.0255	0.0291	0.0040	0.0042
	42	0.750	0.0287	0.0328	0.0040	0.0046
	49	0.700	0.0312	0.0357	0.0040	0.0050
	56	0.650	0.0332	0.0379	0.0040	0.0053
	63	0.650	0.0373	0.0426	0.0040	0.0057
	70	0.650	0.0414	0.0474	0.0040	0.0060
420	21	0.850	0.0135	0.0155	0.0033	0.0027
	28	0.850	0.0181	0.0206	0.0033	0.0031
	35	0.800	0.0213	0.0243	0.0033	0.0035
	42	0.750	0.0239	0.0273	0.0033	0.0039
	49	0.700	0.0260	0.0298	0.0033	0.0042
	56	0.650	0.0276	0.0316	0.0033	0.0045
	63	0.650	0.0311	0.0355	0.0033	0.0047
	70	0.650	0.0345	0.0395	0.0033	0.0050
520	21	0.850	0.0109	0.0125	0.0027	0.0022
	28	0.850	0.0146	0.0167	0.0027	0.0025
	35	0.800	0.0172	0.0196	0.0027	0.0028
	42	0.750	0.0193	0.0221	0.0027	0.0031
	49	0.700	0.0210	0.0240	0.0027	0.0034
	56	0.650	0.0223	0.0255	0.0027	0.0036
	63	0.650	0.0251	0.0287	0.0027	0.0038
	70	0.650	0.0279	0.0319	0.0027	0.0040

[a] $\rho = 0.85\beta_1 \frac{f'_c}{f_y} \frac{0.003}{0.003 + \epsilon_t}$

[b] $\frac{c}{d_t} = 0.375, \frac{a}{d_t} = 0.375\beta_1$

[c] $\frac{c}{d_t} = 0.429, \frac{a}{d_t} = 0.429\beta_1$

TABLE A.5a
Flexural resistance factor: $R = \rho f_y\left(1 - 0.588\,\frac{\rho f_y}{f'_c}\right)$MPa

	f_y = 280 MPa					f_y = 420 MPa				
	f'_c, MPa					f'_c, MPa				
ρ	21	28	35	42	49	21	28	35	42	49
0.0005	0.14	0.14	0.14	0.14	0.14	0.21	0.21	0.21	0.21	0.21
0.0010	0.28	0.28	0.28	0.28	0.28	0.42	0.42	0.42	0.42	0.42
0.0015	0.42	0.42	0.42	0.42	0.42	0.62	0.62	0.62	0.62	0.63
0.0020	0.55	0.55	0.55	0.56	0.56	0.82	0.83	0.83	0.83	0.83
0.0025	0.69	0.69	0.69	0.69	0.69	1.02	1.03	1.03	1.03	1.04
0.0030	0.82	0.83	0.83	0.83	0.83	1.22	1.23	1.23	1.24	1.24
0.0035	0.95	0.96	0.96	0.97	0.97	1.41	1.42	1.43	1.44	1.44
0.0040	1.08	1.09	1.10	1.10	1.10	1.60	1.62	1.63	1.64	1.65
0.0045	1.22	1.23	1.23	1.24	1.24	1.79	1.81	1.83	1.84	1.85
0.0050	1.35	1.36	1.37	1.37	1.38	1.98	2.01	2.03	2.04	2.05
0.0055	1.47	1.49	1.50	1.51	1.51	2.16	2.20	2.22	2.24	2.25
0.0060	1.60	1.62	1.63	1.64	1.65	2.34	2.39	2.41	2.43	2.44
0.0065	1.73	1.75	1.76	1.77	1.78	2.52	2.57	2.60	2.63	2.64
0.0070	1.85	1.88	1.90	1.91	1.91	2.70	2.76	2.79	2.82	2.84
0.0075	1.98	2.01	2.03	2.04	2.05	2.87	2.94	2.98	3.01	3.03
0.0080	2.10	2.13	2.16	2.17	2.18	3.04	3.12	3.17	3.20	3.22
0.0085	2.22	2.26	2.28	2.30	2.31	3.21	3.30	3.36	3.39	3.42
0.0090	2.34	2.39	2.41	2.43	2.44	3.38	3.48	3.54	3.58	3.61
0.0095	2.46	2.51	2.54	2.56	2.58	3.54	3.66	3.72	3.77	3.80
0.0100	2.58	2.64	2.67	2.69	2.71	3.71	3.83	3.90	3.95	3.99
0.0105	2.70	2.76	2.79	2.82	2.84	3.87	4.00	4.08	4.14	4.18
0.0110	2.81	2.88	2.92	2.95	2.97	4.02	4.17	4.26	4.32	4.36
0.0115	2.93	3.00	3.05	3.07	3.10	4.18	4.34	4.44	4.50	4.55
0.0120	3.04	3.12	3.17	3.20	3.22	4.33	4.51	4.61	4.68	4.74
0.0125	3.16	3.24	3.29	3.33	3.35	4.48	4.67	4.79	4.86	4.92
0.0130	3.27	3.36	3.42	3.45	3.48	4.63	4.83	4.96	5.04	5.10
0.0135	3.38	3.48	3.54	3.58	3.61	4.77	4.99	5.13	5.22	5.28
0.0140	3.49	3.60	3.66	3.70	3.74	4.91	5.15	5.30	5.40	5.47
0.0145	3.60	3.71	3.78	3.83	3.86	5.05	5.31	5.47	5.57	5.64
0.0150	3.71	3.83	3.90	3.95	3.99	5.19	5.47	5.63	5.74	5.82
0.0155	3.81	3.94	4.02	4.08	4.11	5.32	5.62	5.80	5.92	6.00
0.0160	3.92	4.06	4.14	4.20	4.24		5.77	5.96	6.09	6.18
0.0165	4.02	4.17	4.26	4.32	4.36		5.92	6.12	6.26	6.35
0.0170	4.13	4.28	4.38	4.44	4.49		6.07	6.28	6.43	6.53
0.0175	4.23	4.40	4.50	4.56	4.61		6.22	6.44	6.59	6.70
0.0180	4.33	4.51	4.61	4.68	4.74		6.36	6.60	6.76	6.87
0.0185	4.43	4.62	4.73	4.80	4.86		6.50	6.76	6.92	7.05
0.0190	4.53	4.73	4.84	4.92	4.98		6.64	6.91	7.09	7.22
0.0195	4.63	4.83	4.96	5.04	5.10		6.78	7.06	7.25	7.39
0.0200	4.72	4.94	5.07	5.16	5.22		6.92	7.21	7.41	7.55

TABLE A.5b
Flexural resistance factor: $R = \rho f_y\left(1 - 0.588\frac{\rho f_y}{f'_c}\right)$ MPa

	f_y = 280 MPa					f_y = 420 MPa				
	f'_c, MPa					f'_c, MPa				
ρ	21	28	35	42	49	21	28	35	42	49
0.003	0.82	0.83	0.83	0.83	0.83	1.22	1.23	1.23	1.24	1.24
0.004	1.08	1.09	1.10	1.10	1.10	1.60	1.62	1.63	1.64	1.65
0.005	1.35	1.36	1.37	1.37	1.38	1.98	2.01	2.03	2.04	2.05
0.006	1.60	1.62	1.63	1.64	1.65	2.34	2.39	2.41	2.43	2.44
0.007	1.85	1.88	1.90	1.91	1.91	2.70	2.76	2.79	2.82	2.84
0.008	2.10	2.13	2.16	2.17	2.18	3.04	3.12	3.17	3.20	3.22
0.009	2.34	2.39	2.41	2.43	2.44	3.38	3.48	3.54	3.58	3.61
0.010	2.58	2.64	2.67	2.69	2.71	3.71	3.83	3.90	3.95	3.99
0.011	2.81	2.88	2.92	2.95	2.97	4.02	4.17	4.26	4.32	4.36
0.012	3.04	3.12	3.17	3.20	3.22	4.33	4.51	4.61	4.68	4.74
0.013	3.27	3.36	3.42	3.45	3.48	4.63	4.83	4.96	5.04	5.10
0.014	3.49	3.60	3.66	3.70	3.74	4.91	5.15	5.30	5.40	5.47
0.015	3.71	3.83	3.90	3.95	3.99	5.19	5.47	5.63	5.74	5.82
0.016	3.92	4.06	4.14	4.20	4.24	5.46	5.77	5.96	6.09	6.18
0.017	4.13	4.28	4.38	4.44	4.49		6.07	6.28	6.43	6.53
0.018	4.33	4.51	4.61	4.68	4.74		6.36	6.60	6.76	6.87
0.019	4.53	4.73	4.84	4.92	4.98		6.64	6.91	7.09	7.22
0.020	4.72	4.94	5.07	5.16	5.22		6.92	7.21	7.41	7.55
0.021	4.91	5.15	5.30	5.40	5.47		7.19	7.51	7.73	7.89
0.022	5.10	5.36	5.52	5.63	5.70			7.81	8.04	8.22
0.023	5.28	5.57	5.74	5.86	5.94			8.09	8.35	8.54
0.024	5.46	5.77	5.96	6.09	6.18			8.37	8.66	8.86
0.025		5.97	6.18	6.31	6.41			8.65	8.96	9.18
0.026		6.17	6.39	6.54	6.64				9.25	9.49
0.027		6.36	6.60	6.76	6.87				9.54	9.80
0.028		6.55	6.81	6.98	7.10				9.82	10.10
0.029		6.74	7.01	7.20	7.33					10.40
0.030		6.92	7.21	7.41	7.55					10.69
0.031		7.10	7.41	7.63	7.78					
0.032			7.61	7.84	8.00					
0.033			7.81	8.04	8.22					
0.034			8.00	8.25	8.43					
0.035			8.19	8.46	8.65					
0.036			8.37	8.66	8.86					
0.037			8.56	8.86	9.07					
0.038				9.06	9.28					
0.039				9.25	9.49					
0.040				9.44	9.69					
0.041				9.63	9.90					

TABLE A.6

Parameters k and j for elastic, cracked section beam analysis, where $k = \sqrt{2\rho n + (\rho n)^2} - \rho n;\ j = 1 - \frac{1}{3}k$

	$n = 7$		$n = 8$		$n = 9$		$n = 10$	
ρ	k	j	k	j	k	j	k	j
0.0010	0.112	0.963	0.119	0.960	0.125	0.958	0.132	0.956
0.0020	0.154	0.949	0.164	0.945	0.173	0.942	0.180	0.940
0.0030	0.185	0.938	0.196	0.935	0.207	0.931	0.217	0.928
0.0040	0.210	0.930	0.223	0.926	0.235	0.922	0.246	0.918
0.0050	0.232	0.923	0.246	0.918	0.258	0.914	0.270	0.910
0.0054	0.240	0.920	0.254	0.915	0.267	0.911	0.279	0.907
0.0058	0.247	0.918	0.262	0.913	0.275	0.908	0.287	0.904
0.0062	0.254	0.915	0.269	0.910	0.283	0.906	0.296	0.901
0.0066	0.261	0.913	0.276	0.908	0.290	0.903	0.303	0.899
0.0070	0.268	0.911	0.283	0.906	0.298	0.901	0.311	0.896
0.0072	0.271	0.910	0.287	0.904	0.301	0.900	0.314	0.895
0.0074	0.274	0.909	0.290	0.903	0.304	0.899	0.318	0.894
0.0076	0.277	0.908	0.293	0.902	0.308	0.897	0.321	0.893
0.0078	0.280	0.907	0.296	0.901	0.311	0.896	0.325	0.892
0.0080	0.283	0.906	0.299	0.900	0.314	0.895	0.328	0.891
0.0082	0.286	0.905	0.303	0.899	0.317	0.894	0.331	0.890
0.0084	0.289	0.904	0.306	0.898	0.321	0.893	0.334	0.889
0.0086	0.292	0.903	0.308	0.897	0.324	0.892	0.338	0.887
0.0088	0.295	0.902	0.311	0.896	0.327	0.891	0.341	0.886
0.0090	0.298	0.901	0.314	0.895	0.330	0.890	0.344	0.885
0.0092	0.300	0.900	0.317	0.894	0.332	0.889	0.347	0.884
0.0094	0.303	0.899	0.320	0.893	0.335	0.888	0.350	0.883
0.0096	0.306	0.898	0.323	0.892	0.338	0.887	0.353	0.882
0.0098	0.308	0.897	0.325	0.892	0.341	0.886	0.355	0.882
0.0100	0.311	0.896	0.328	0.891	0.344	0.885	0.358	0.881
0.0104	0.316	0.895	0.333	0.889	0.349	0.884	0.364	0.879
0.0108	0.321	0.893	0.338	0.887	0.354	0.882	0.369	0.877
0.0112	0.325	0.892	0.343	0.886	0.359	0.880	0.374	0.875
0.0116	0.330	0.890	0.348	0.884	0.364	0.879	0.379	0.874
0.0120	0.334	0.889	0.353	0.882	0.369	0.877	0.384	0.872
0.0124	0.339	0.887	0.357	0.881	0.374	0.875	0.389	0.870
0.0128	0.343	0.886	0.362	0.879	0.378	0.874	0.394	0.867
0.0132	0.347	0.884	0.366	0.878	0.383	0.872	0.398	0.867
0.0136	0.351	0.883	0.370	0.877	0.387	0.871	0.403	0.866
0.0140	0.355	0.882	0.374	0.875	0.392	0.869	0.407	0.864
0.0144	0.359	0.880	0.378	0.874	0.396	0.868	0.412	0.863
0.0148	0.363	0.879	0.382	0.873	0.400	0.867	0.416	0.861
0.0152	0.367	0.878	0.386	0.871	0.404	0.865	0.420	0.860
0.0156	0.371	0.876	0.390	0.870	0.408	0.864	0.424	0.859
0.0160	0.374	0.875	0.394	0.869	0.412	0.863	0.428	0.857
0.0170	0.383	0.872	0.403	0.867	0.421	0.860	0.437	0.854
0.0180	0.392	0.869	0.412	0.863	0.430	0.857	0.446	0.851
0.0190	0.400	0.867	0.420	0.860	0.438	0.854	0.455	0.848
0.0200	0.407	0.864	0.428	0.857	0.446	0.851	0.463	0.846

TABLE A.7
Maximum number of bars as a single layer in beam stems

19 mm Maximum Aggregate Size, No. 13 (No. 4) Stirrups[a]

Bar No.		Beam Width b_w, mm											
SI	Inch-Pound	200	250	300	350	400	450	500	550	600	650	700	750
16	5	2	4	5	6	7	9	10	11	12	13	15	16
19	6	2	3	4	6	7	8	9	10	11	12	14	15
22	7	2	3	4	5	6	7	8	9	11	12	13	14
25	8	2	3	4	5	6	7	8	9	10	11	12	13
29	9	2	3	3	4	5	6	7	8	9	9	10	11
32	10	1	2	3	4	5	5	6	7	8	8	9	10
36	11	1	2	3	3	4	5	6	6	7	8	8	9
43	14	1	2	2	3	3	4	5	5	6	6	7	7
57	18	1	1	2	2	3	3	3	4	4	5	5	6

25 mm Maximum Aggregate Size, No. 13 (No. 4) Stirrups[a]

Bar No.		Beam Width b_w, mm											
SI	Inch-Pound	200	250	300	350	400	450	500	550	600	650	700	750
16	5	2	3	4	5	6	7	8	9	10	11	12	13
19	6	2	3	4	5	6	7	8	9	10	11	11	12
22	7	2	3	4	5	5	6	7	8	9	10	11	12
25	8	2	3	3	4	5	6	7	8	8	9	10	11
29	9	2	2	3	4	5	6	6	7	8	9	10	10
32	10	1	2	3	4	4	5	6	7	8	8	9	10
36	11	1	2	3	3	4	5	6	6	7	8	8	9

[a] Minimum concrete cover assumed to be 40 mm to the No. 13 (No. 4) stirrup.

TABLE A.8
Minimum number of bars as a single layer in beam stems governed by crack control requirements of the ACI Code

(*a*) 50 mm clear cover, sides and bottom

Minimum Number of Bars as a Single Layer of a Beam Stem

Bar No.		Beam Stem Width b_w, mm														
SI	Inch-Pound	200	250	300	350	400	450	500	550	600	650	700	750	800	850	900
10–43	3–14	1	1	2	2	3	3	3	3	3	4	4	4	4	4	5
57	18	1	1	2	2	2	3	3	3	3	3	4	4	4	4	4

(*b*) 40 mm clear cover, sides and bottom

Minimum Number of Bars as a Single Layer of a Beam Stem

Bar No.		Beam Stem Width b_w, mm														
SI	Inch-Pound	200	250	300	350	400	450	500	550	600	650	700	750	800	850	900
10–13	3–14	1	1	2	2	3	3	3	3	3	4	4	4	4	4	4
16–43	5–14	1	1	2	2	3	3	3	3	3	3	4	4	4	4	4
57	18	1	1	2	2	2	3	3	3	3	3	4	4	4	4	4

TABLE A.9

Design strength ϕM_n for slab sections 1 m wide, kN-m; $f_y = 420$ MPa; $\phi M_n = \phi f_y b d^2(1 - 0.59\rho f_y/f'_c)$

		Effective Depth *d*, mm									
f'_c, MPa	ρ	75	100	125	150	175	200	225	250	275	300
21	0.002	4.2	7.4	11.5	16.6	22.6	29.5	37.4	46.1	55.8	66.4
	0.003	6.2	10.9	17.1	24.6	33.5	43.8	55.4	68.4	82.7	98.4
	0.004	8.1	14.4	22.5	32.4	44.1	57.6	72.9	90.0	108.9	129.7
	0.005	10.0	17.8	27.8	40.0	54.5	71.1	90.0	111.2	134.5	160.1
	0.006	11.9	21.1	32.9	47.4	64.5	84.3	106.7	131.7	159.4	189.7
	0.007	13.7	24.3	37.9	54.6	74.3	97.1	122.9	151.7	183.6	218.5
	0.008	15.4	27.4	42.8	61.6	83.9	109.5	138.6	171.2	207.1	246.5
	0.009	17.1	30.4	47.5	68.4	93.1	121.6	153.9	190.0	230.0	273.7
	0.010	18.8	33.3	52.1	75.0	102.1	133.4	168.8	208.4	252.1	300.1
	0.011	20.4	36.2	56.5	81.4	110.8	144.7	183.2	226.1	273.6	325.6
28	0.002	4.2	7.4	11.6	16.7	22.7	29.7	37.6	46.4	56.2	66.8
	0.003	6.2	11.0	17.2	24.8	33.8	44.2	55.9	69.0	83.5	99.4
	0.004	8.2	14.6	22.8	32.8	44.7	58.3	73.8	91.2	110.3	131.3
	0.005	10.2	18.1	28.2	40.6	55.3	72.3	91.4	112.9	136.6	162.6
	0.006	12.1	21.5	33.6	48.3	65.8	85.9	108.7	134.2	162.4	193.3
	0.007	14.0	24.8	38.8	55.8	76.0	99.3	125.7	155.1	187.7	223.4
	0.008	15.8	28.1	43.9	63.2	86.1	112.4	142.3	175.6	212.5	252.9
	0.009	17.6	31.3	48.9	70.4	95.9	125.2	158.5	195.7	236.8	281.8
	0.010	19.4	34.5	53.8	77.5	105.5	137.8	174.4	215.3	260.6	310.1
	0.011	21.1	37.5	58.6	84.4	114.9	150.1	190.0	234.6	283.8	337.8
	0.012	22.8	40.5	63.3	91.2	124.2	162.2	205.2	253.4	306.6	364.9
	0.013	24.5	43.5	67.9	97.8	133.2	173.9	220.2	271.8	328.9	391.4
	0.014	26.1	46.4	72.4	104.3	142.0	185.5	234.7	289.8	350.6	417.3
	0.015	27.7	49.2	76.8	110.6	150.6	196.7	248.9	307.3	371.9	442.6
35	0.002	4.2	7.5	11.6	16.8	22.8	29.8	37.7	46.6	56.4	67.1
	0.003	6.2	11.1	17.3	25.0	34.0	44.4	56.2	69.4	83.9	99.9
	0.004	8.3	14.7	23.0	33.1	45.0	58.8	74.4	91.8	111.1	132.2
	0.005	10.3	18.2	28.5	41.0	55.8	72.9	92.3	113.9	137.9	164.1
	0.006	12.2	21.7	33.9	48.9	66.5	86.9	109.9	135.7	164.2	195.4
	0.007	14.1	25.1	39.3	56.6	77.0	100.6	127.3	157.2	190.2	226.3
	0.008	16.0	28.5	44.6	64.2	87.4	114.1	144.4	178.3	215.7	256.7
	0.009	17.9	31.9	49.8	71.7	97.5	127.4	161.3	199.1	240.9	286.7
	0.010	19.8	35.1	54.9	79.0	107.6	140.5	177.8	219.5	265.6	316.1
	0.011	21.6	38.3	59.9	86.3	117.4	153.4	194.1	239.6	290.0	345.1
	0.012	23.3	41.5	64.9	93.4	127.1	166.0	210.1	259.4	313.9	373.6
	0.013	25.1	44.6	69.7	100.4	136.6	178.5	225.9	278.9	337.4	401.6
	0.014	26.8	47.7	74.5	107.3	146.0	190.7	241.4	298.0	360.5	429.1
	0.015	28.5	50.7	79.2	114.0	155.2	202.7	256.6	316.7	383.3	456.1
	0.016	30.2	53.6	83.8	120.7	164.2	214.5	271.5	335.2	405.6	482.7
	0.017	31.8	56.5	88.3	127.2	173.1	226.1	286.2	353.3	427.5	508.7

TABLE A.10

Simplified tension development in bar diameters l_d/d_b for uncoated bars and normalweight concrete

		No. 19 (No. 6) and Smaller[a]			No. 22 (No. 7) and Larger		
		f'_c, MPa			f'_c, MPa		
	f_y, MPa	28	35	42	28	35	42
(1) Bottom bars							
Spacing, cover and ties as per Case *a* and *b*	280	25	23	21	31	28	25
	420	38	34	31	47	42	38
	520	47	42	38	58	52	47
Other cases	280	38	34	31	48	43	39
	420	57	51	46	72	65	59
	520	70	63	57	89	80	73
(2) Top bars							
Spacing, cover and ties as per Case *a* and *b*	280	33	29	27	40	36	33
	420	49	44	40	61	54	50
	520	61	54	50	75	67	61
Other cases	280	49	44	40	63	56	51
	420	74	66	60	94	84	77
	520	91	82	75	116	104	95

Case *a*: Clear spacing of bars being developed or spliced $\geq d_b$, clear cover $\geq d_b$, and stirrups or ties throughout l_d not less than the Code minimum.

Case *b*: Clear spacing of bars being developed or spliced $\geq 2d_b$, and clear cover not less than d_b.

[a] ACI Committee 408 recommends that the values indicated for bar sizes No. 22 (No. 7) and larger be used for all bar sizes.

TABLE A.11

Development length in compression, mm, for normalweight concrete

l_{dc} = greater of $(0.24f_y/\sqrt{f'_c})d_b$ or $0.043f_yd_b$ (Minimum of 200 mm in all cases)

			f'_c, MPa							
Bar No.			21		28		35		42	
SI	Inch-Pound	f_y, MPa	Basic l_{dc}	Confined	Basic l_{dc}	Confined	Basic l_{dc}	Confined	Basic l_{dc}	Confined
10	3	280	200	200	200	200	200	200	200	200
		420	210	200	200	200	200	200	200	200
		520	260	200	220	200	210	200	210	200
13	4	280	200	200	200	200	200	200	200	200
		420	280	210	240	200	230	200	230	200
		520	350	260	300	220	280	210	280	210
16	5	280	230	200	200	200	200	200	200	200
		420	350	260	300	230	290	220	290	220
		520	430	320	380	280	360	270	360	270
19	6	280	280	210	240	200	230	200	230	200
		420	420	320	360	270	340	260	340	260
		520	520	390	450	340	430	320	430	320
22	7	280	330	240	280	210	270	200	270	200
		420	490	370	420	320	400	300	400	300
		520	600	450	520	390	500	370	500	370
25	8	280	370	280	320	240	310	230	310	230
		420	560	420	480	360	460	340	460	340
		520	690	520	600	450	570	430	570	430
29	9	280	420	320	360	270	350	260	350	260
		420	630	470	550	410	520	390	520	390
		520	780	590	680	510	640	480	640	480
32	10	280	470	360	410	310	390	290	390	290
		420	710	530	620	460	580	440	580	440
		520	880	660	760	570	720	540	720	540
36	11	280	520	390	450	340	430	320	430	320
		420	790	590	680	510	650	480	650	480
		520	970	730	840	630	800	600	800	600
43	14	280	630	470	550	410	520	390	520	390
		420	950	710	820	610	780	580	780	580
		520	1,170	880	1,010	760	960	720	960	720
57	18	280	840	630	730	550	690	520	690	520
		420	1,260	950	1,090	820	1,030	780	1,030	780
		520	1,560	1,170	1,350	1,010	1,280	960	1,280	960

TABLE A.12
Common stock styles of welded wire reinforcement (WWR)

Steel Designation[a]	Steel Area, mm²/m Longitudinal	Steel Area, mm²/m Transverse	Weight (Approximate), kg per m²
	Rolls		
152 × 152 − MW9 × MW9	59.3	59.3	1.03
152 × 152 − MW13 × MW13	84.7	84.7	1.46
152 × 152 − MW19 × MW19	122.8	122.8	2.05
152 × 152 − MW26 × MW26	169.4	169.4	2.83
102 × 102 − MW9 × MW9	88.9	88.9	1.51
102 × 102 − MW13 × MW13	127.0	127.0	2.15
102 × 102 − MW19 × MW19	184.2	184.2	3.03
102 × 102 − MW26 × MW26	254.0	254.0	4.30
	Sheets		
152 × 152 − MW19 × MW19	122.8	122.8	2.05
152 × 152 − MW26 × MW26	169.4	169.4	2.83
152 × 152 − MW30 × MW30	199.0	199.0	3.32
102 × 102 − MW26 × MW26	254.0	254.0	4.30

[a] The designation MW indicates plain wire; WWR is also available as deformed wire, designated by MD.

TABLE A.13A

Coefficients for slabs with variable moment of inertia[a]

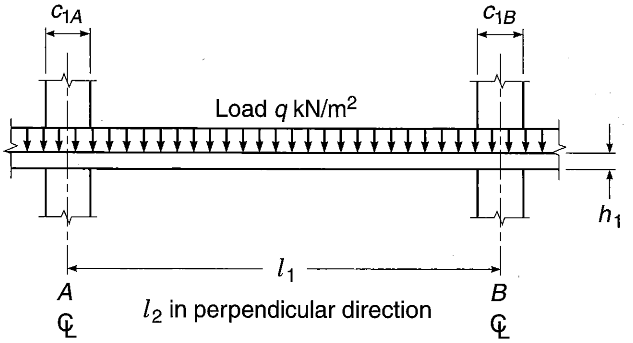

Column Dimension		Uniform Load FEM = Coeff.$(ql_2l_1^2)$		Stiffness Factor[b]		Carryover Factor	
c_{1A}/l_1	c_{1B}/l_1	M_{AB}	M_{BA}	k_{AB}	k_{BA}	COF_{AB}	COF_{BA}
0.00	0.00	0.083	0.083	4.00	4.00	0.500	0.500
	0.05	0.083	0.084	4.01	4.04	0.504	0.500
	0.10	0.082	0.086	4.03	4.15	0.513	0.499
	0.15	0.081	0.089	4.07	4.32	0.528	0.498
	0.20	0.079	0.093	4.12	4.56	0.548	0.495
	0.25	0.077	0.097	4.18	4.88	0.573	0.491
0.05	0.05	0.084	0.084	4.05	4.05	0.503	0.503
	0.10	0.083	0.086	4.07	4.15	0.513	0.503
	0.15	0.081	0.089	4.11	4.33	0.528	0.501
	0.20	0.080	0.092	4.16	4.58	0.548	0.499
	0.25	0.078	0.096	4.22	4.89	0.573	0.494
0.10	0.10	0.085	0.085	4.18	4.18	0.513	0.513
	0.15	0.083	0.088	4.22	4.36	0.528	0.511
	0.20	0.082	0.091	4.27	4.61	0.548	0.508
	0.25	0.080	0.095	4.34	4.93	0.573	0.504
0.15	0.15	0.086	0.086	4.40	4.40	0.526	0.526
	0.20	0.084	0.090	4.46	4.65	0.546	0.523
	0.25	0.083	0.094	4.53	4.98	0.571	0.519
0.20	0.20	0.088	0.088	4.72	4.72	0.543	0.543
	0.25	0.086	0.092	4.79	5.05	0.568	0.539
0.25	0.25	0.090	0.090	5.14	5.14	0.563	0.563

[a] Applicable when $c_1/l_1 = c_2/l_2$. For other relationships between these ratios, the constants will be slightly in error.

[b] Stiffness is $K_{AB} = k_{AB}E(l_2h_1^3/12l_1)$ and $K_{BA} = k_{BA}E(l_2h_1^3/12l_1)$.

TABLE A.13B

Coefficients for slabs with variable moment of inertia[a]

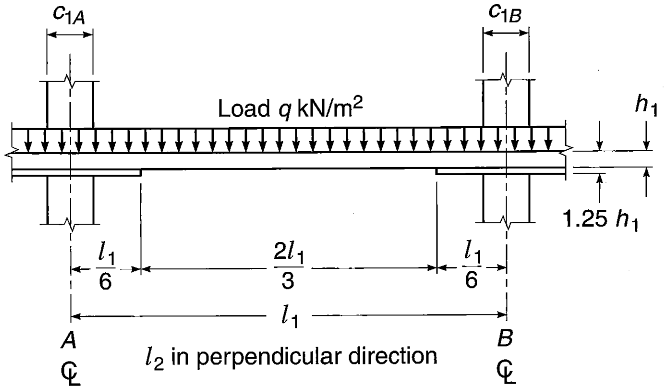

Column Dimension		Uniform Load FEM = Coeff.$(ql_2l_1^2)$		Stiffness Factor[b]		Carryover Factor	
c_{1A}/l_1	c_{1B}/l_1	M_{AB}	M_{BA}	k_{AB}	k_{BA}	COF_{AB}	COF_{BA}
0.00	0.00	0.088	0.088	4.78	4.78	0.541	0.541
	0.05	0.087	0.089	4.80	4.82	0.545	0.541
	0.10	0.087	0.090	4.83	4.94	0.553	0.541
	0.15	0.085	0.093	4.87	5.12	0.567	0.540
	0.20	0.084	0.096	4.93	5.36	0.585	0.537
	0.25	0.082	0.100	5.00	5.68	0.606	0.534
0.05	0.05	0.088	0.088	4.84	4.84	0.545	0.545
	0.10	0.087	0.090	4.87	4.95	0.553	0.544
	0.15	0.085	0.093	4.91	5.13	0.567	0.543
	0.20	0.084	0.096	4.97	5.38	0.584	0.541
	0.25	0.082	0.100	5.05	5.70	0.606	0.537
0.10	0.10	0.089	0.089	4.98	4.98	0.553	0.553
	0.15	0.088	0.092	5.03	5.16	0.566	0.551
	0.20	0.086	0.094	5.09	5.42	0.584	0.549
	0.25	0.084	0.099	5.17	5.74	0.606	0.546
0.15	0.15	0.090	0.090	5.22	5.22	0.565	0.565
	0.20	0.089	0.094	5.28	5.47	0.583	0.563
	0.25	0.087	0.097	5.37	5.80	0.604	0.559
0.20	0.20	0.092	0.092	5.55	5.55	0.580	0.580
	0.25	0.090	0.096	5.64	5.88	0.602	0.577
0.25	0.25	0.094	0.094	5.98	5.98	0.598	0.598

---

[a] Applicable when $c_1/l_1 = c_2/l_2$. For other relationships between these ratios, the constants will be slightly in error.

[b] Stiffness is $K_{AB} = k_{AB}E(l_2h_1^3/12l_1)$ and $K_{BA} = k_{BA}E(l_2h_1^3/12l_1)$.

TABLE A.13C
Stiffness factors for columns with variable moment of inertia[a]

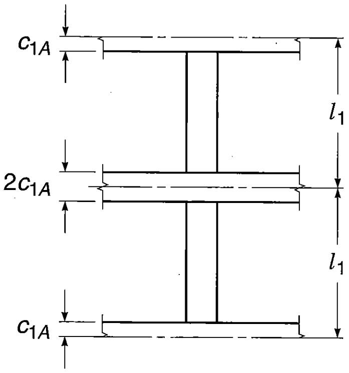

Slab Half-depth c_{1A}/l_1	Stiffness Factor k_{AB}	Slab Half-depth c_{1A}/l_1	Stiffness Factor k_{AB}
0.00	4.00	0.14	9.43
0.02	4.43	0.16	11.01
0.04	4.94	0.18	13.01
0.06	5.54	0.20	15.56
0.08	6.25	0.22	18.87
0.10	7.11	0.24	23.26
0.12	8.15		

[a] Adapted from S. H. Simmonds and J. Misic, "Design Factors for the Equivalent Frame Method," *J. ACI*, vol. 68, no. 11, 1971, pp. 825–831.

TABLE A.14
Size and pitch of spirals, ACI Code, mm

		f'_c, MPa			
Diameter of Column, mm	Out to Out of Spiral, mm	21	28	35	42
f_y = 420 MPa					
350, 375	270, 295	10–65	10–50	13–70	13–55
400–475	320–395	10–65	10–50	13–70	13–60
500	420	10–70	10–50	13–70	13–60
525–725	445–645	10–70	10–50	13–75	13–60
750	670	10–70	10–50	13–75	13–65
f_y = 550 MPa					
350–425	270–345	10–85	10–65	10–50	13–75
450, 475	370, 395	10–85	10–65	10–50	13–80
500–550	420–470	10–85	10–65	10–55	13–80
575–700	495–620	10–85	10–70	10–55	13–80
725, 750	645, 670	10–85	10–70	10–55	13–85

TABLE A.15
Properties of prestressing steels

Seven-wire Strand, $f_{pu} = 1{,}860$ MPa

Nominal Diameter mm	Area, mm^2	Mass, kg/m	$0.7f_{pu}A_{ps}$, kN	$0.74f_{pu}A_{ps}$, kN	$0.8f_{pu}A_{ps}$, kN	$f_{pu}A_{ps}$, kN
9.53	54.8	0.432	71.6	75.7	81.8	102.3
11.11	74.2	0.582	96.5	102.0	110.3	137.9
12.70	98.7	0.775	128.6	135.9	147.0	183.7
13.20	107.7	0.844	140.1	148.1	160.2	200.2
14.29	123.9	0.970	161.0	170.2	184.0	230.0
15.24	140.0	1.102	182.5	192.9	208.6	260.7
17.78	189.7	1.487	247.2	261.4	282.6	353.2

Prestressing Wire

Nominal Diameter mm	Area, mm^2	Mass, kg/m	f_{pu} MPa	$0.7f_{pu}A_{ps}$, kN	$0.8f_{pu}A_{ps}$, kN	$f_{pu}A_{ps}$, kN
4.88	18.7	0.432	1,725	22.6	25.8	32.3
4.98	19.5	0.582	1,725	23.5	26.9	33.6
6.35	31.7	0.775	1,655	36.7	41.9	52.4
7.01	38.6	0.844	1,620	43.8	50.0	62.5

Deformed Prestressing Bars

Nominal Diameter mm	Area, mm^2	Mass, kg/m	f_{pu} MPa	$0.7f_{pu}A_{ps}$, kN	$0.8f_{pu}A_{ps}$, kN	$f_{pu}A_{ps}$, kN
15	181	1.46	1,080	136.8	156.4	195.5
20	271	2.22	1,035	196.3	224.4	280.5
20	271	2.22	1,100	208.7	238.5	298.1
26	548	4.48	1,035	397.0	453.7	567.2
26	548	4.48	1,100	422.0	482.2	602.8
32	806	6.54	1,035	583.9	667.4	834.2
32	806	6.54	1,100	620.6	709.3	886.6
36	1,019	8.28	1,035	738.3	843.7	1,054.7
46	1,664	13.54	1,035	1,205.6	1,377.8	1,722.2
65	3,331	27.10	1,035	2,413.3	2,758.1	3,447.6

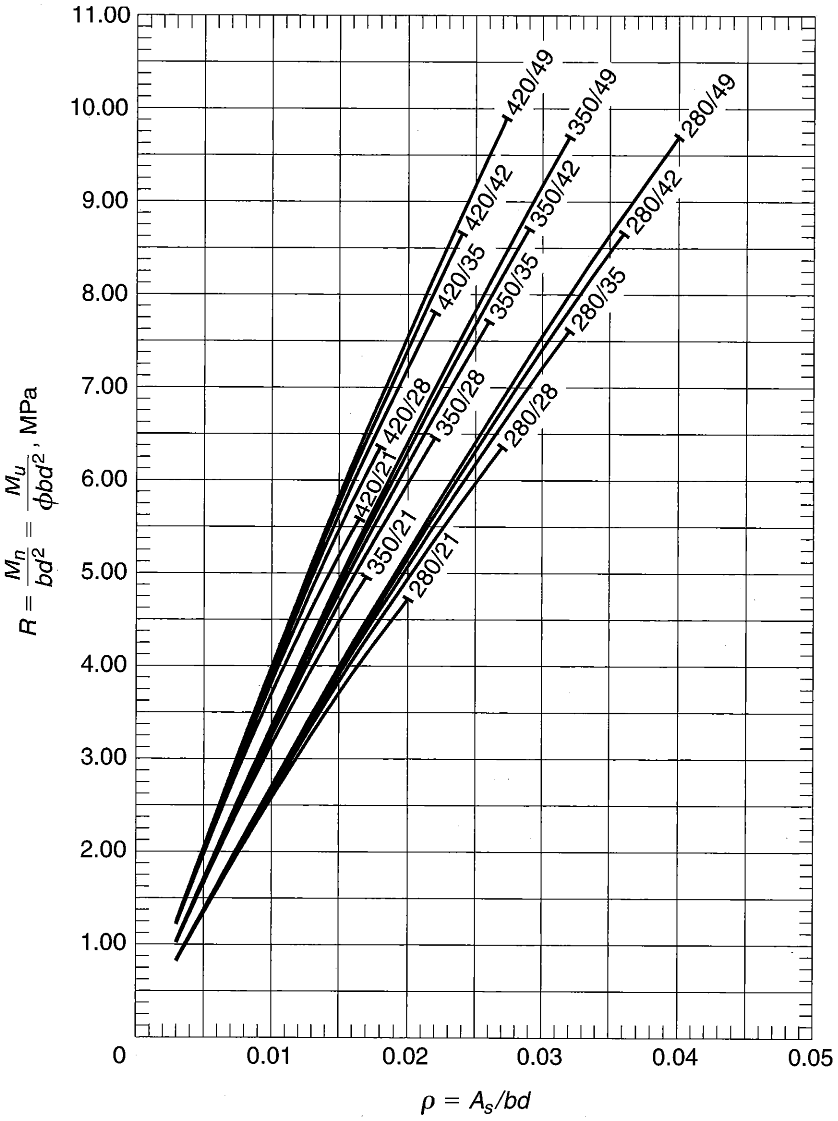

GRAPH A.1*a*
Moment capacity of rectangular sections.

GRAPH A.1*b*
Moment capacity of rectangular sections.

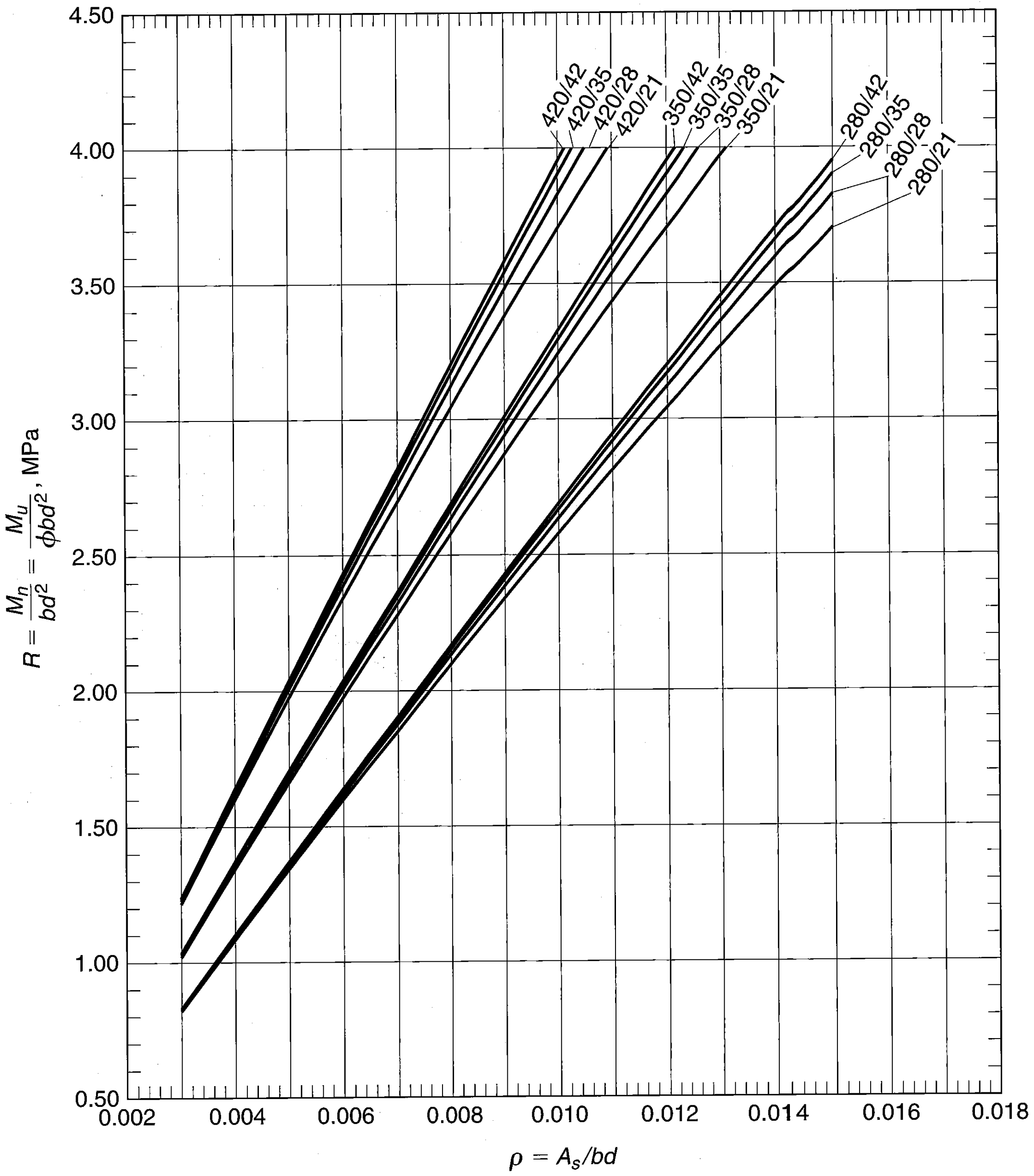

GRAPH A.2
Location of points where bars can be bent up or cut off for simply supported beams uniformly loaded.

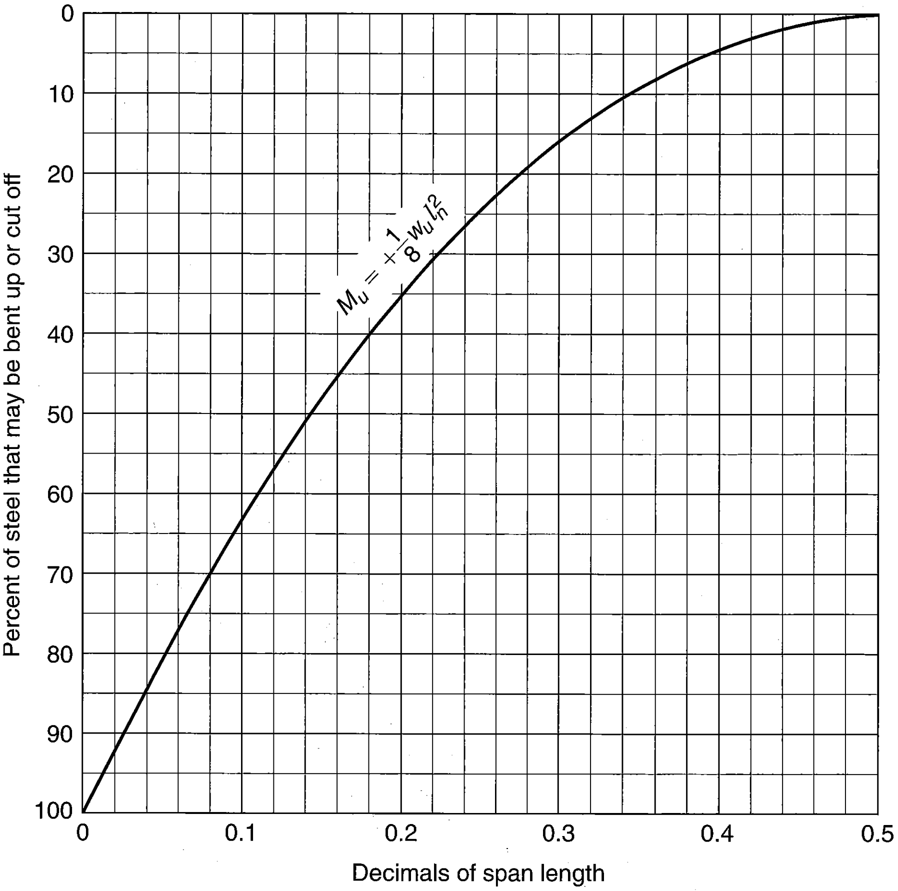

GRAPH A.3

Approximate locations of points where bars can be bent up or down or cut off for continuous beams uniformly loaded and built integrally with their supports according to the coefficients in the ACI Code.

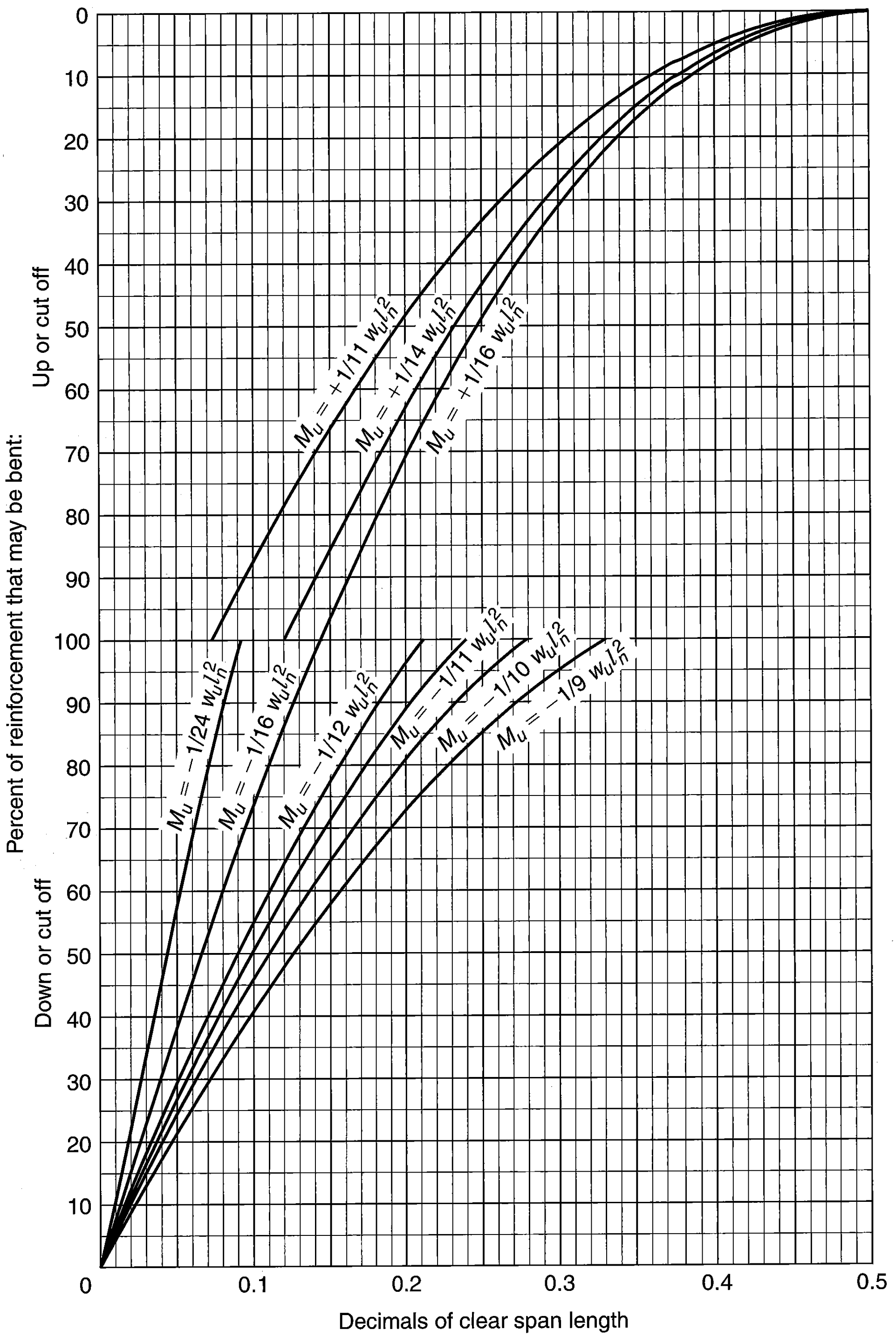

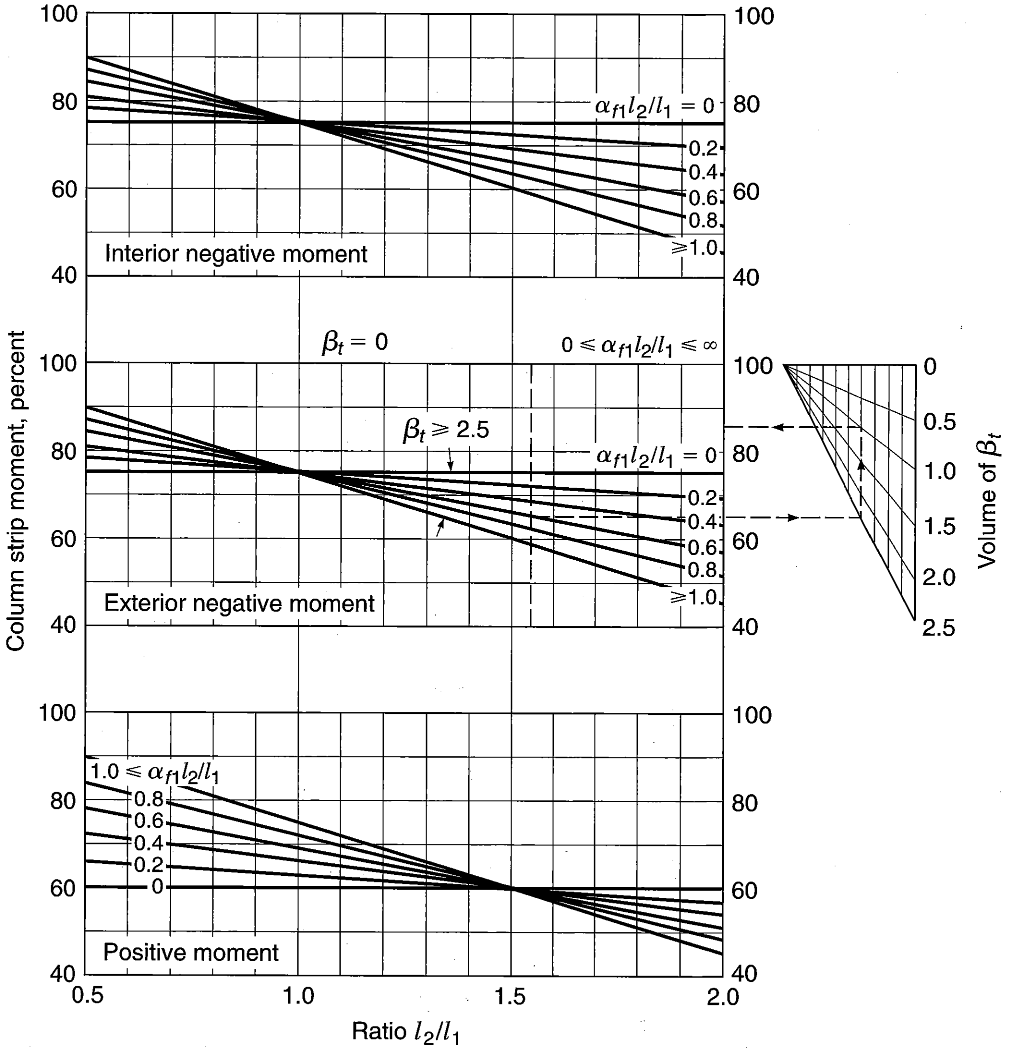

GRAPH A.4

Interpolation charts for lateral distribution of slab moments.

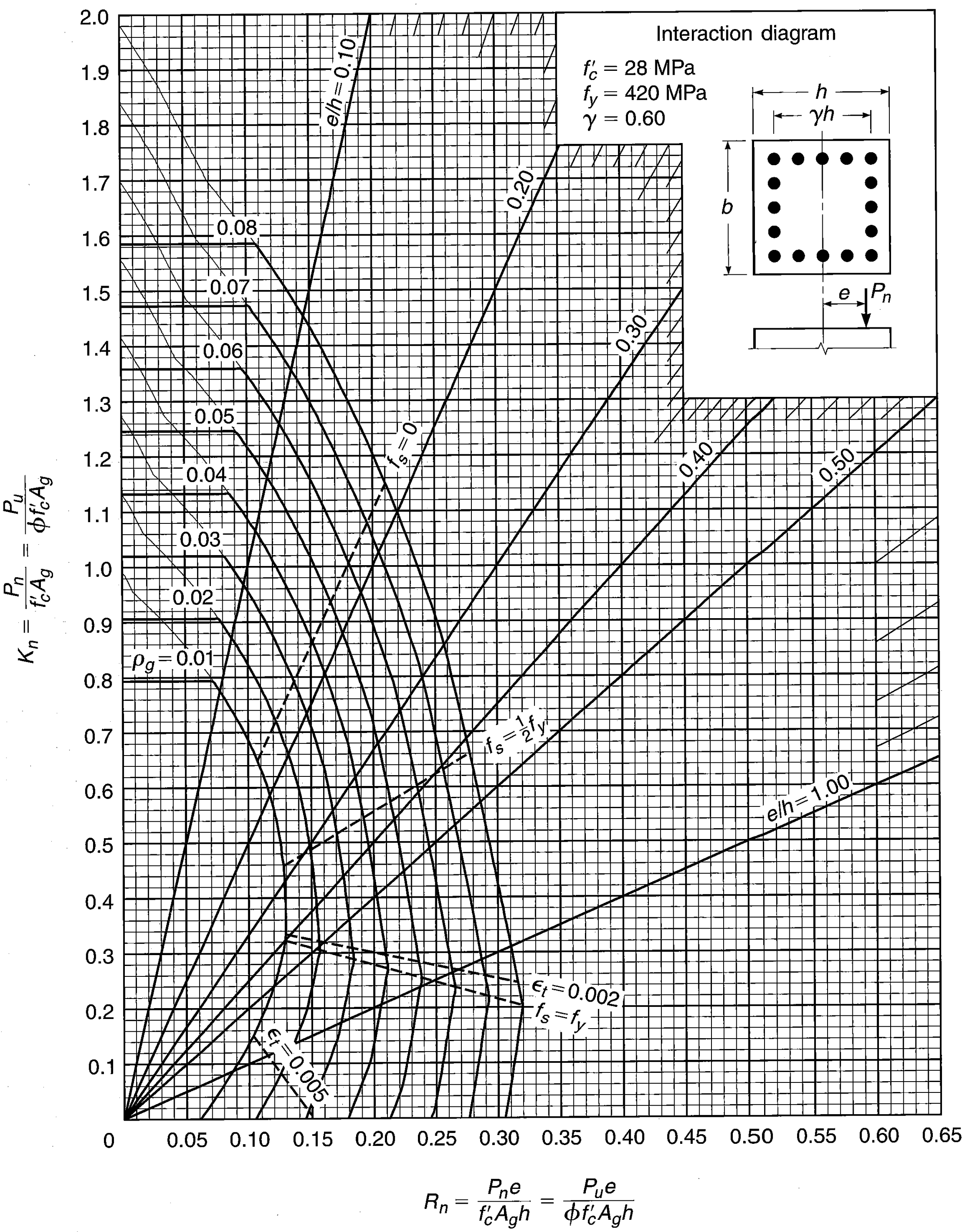

GRAPH A.5

Column strength interaction diagram for rectangular section with bars on four faces and $\gamma = 0.60$.

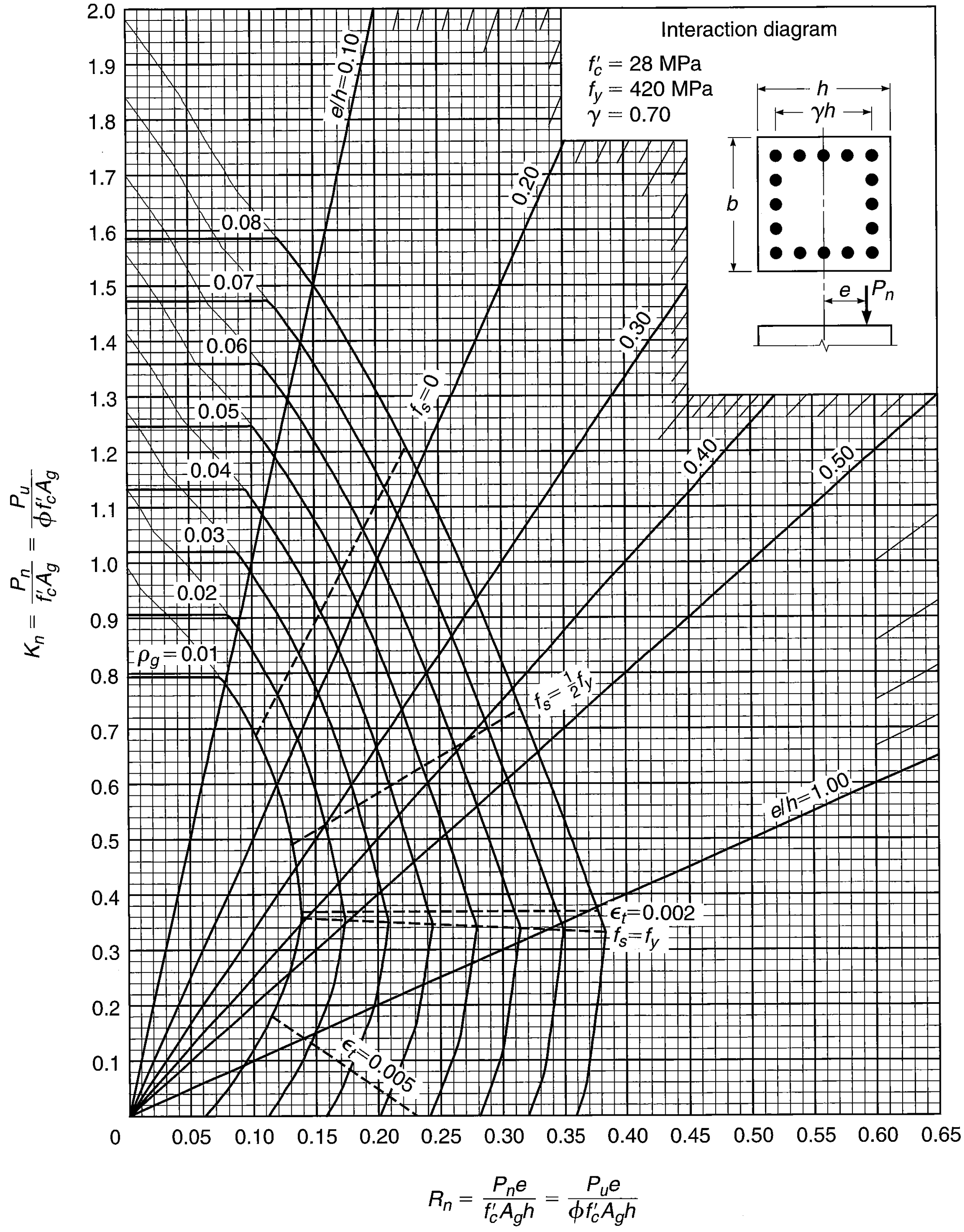

GRAPH A.6

Column strength interaction diagram for rectangular section with bars on four faces and $\gamma = 0.70$.

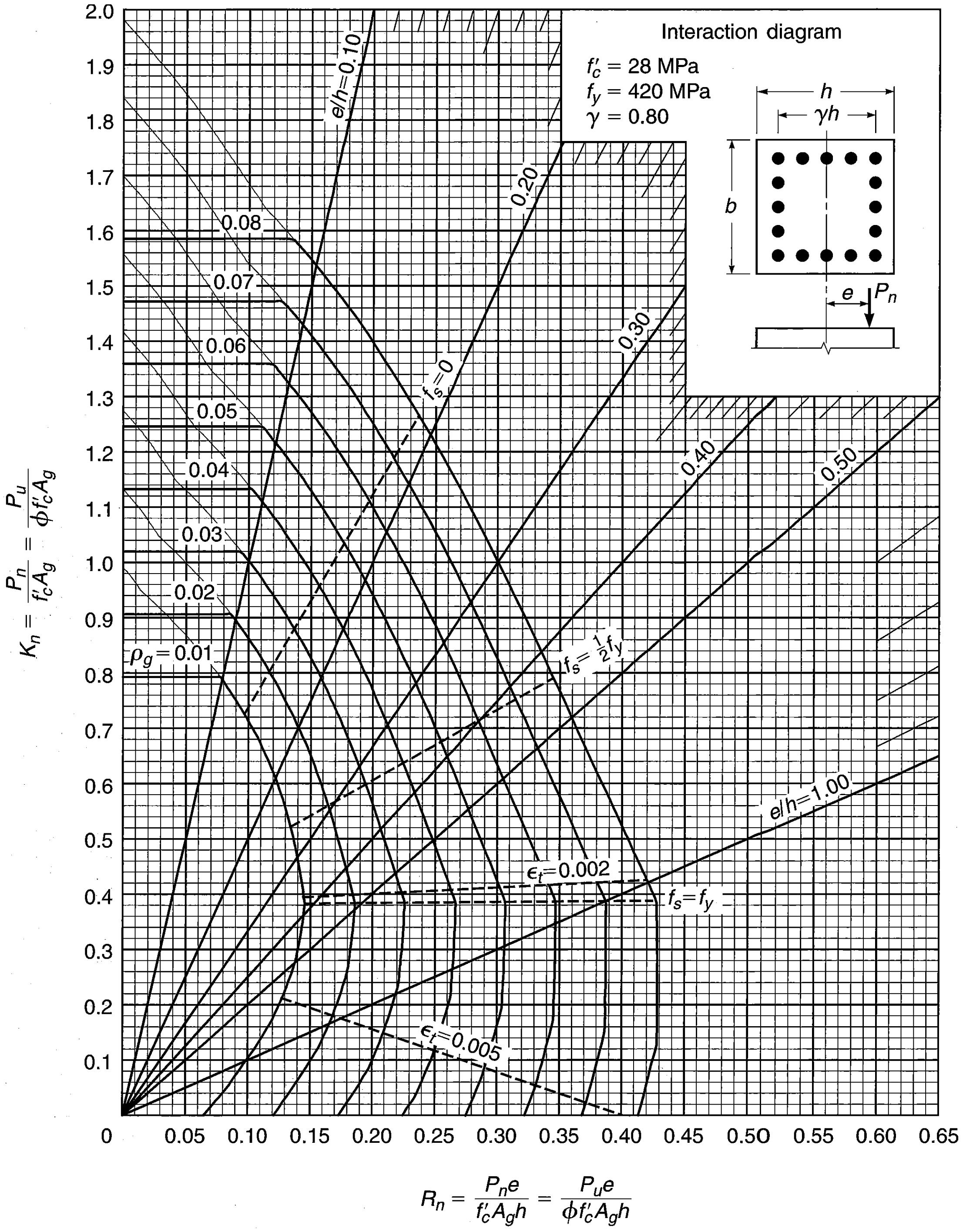

GRAPH A.7

Column strength interaction diagram for rectangular section with bars on four faces and $\gamma = 0.80$.

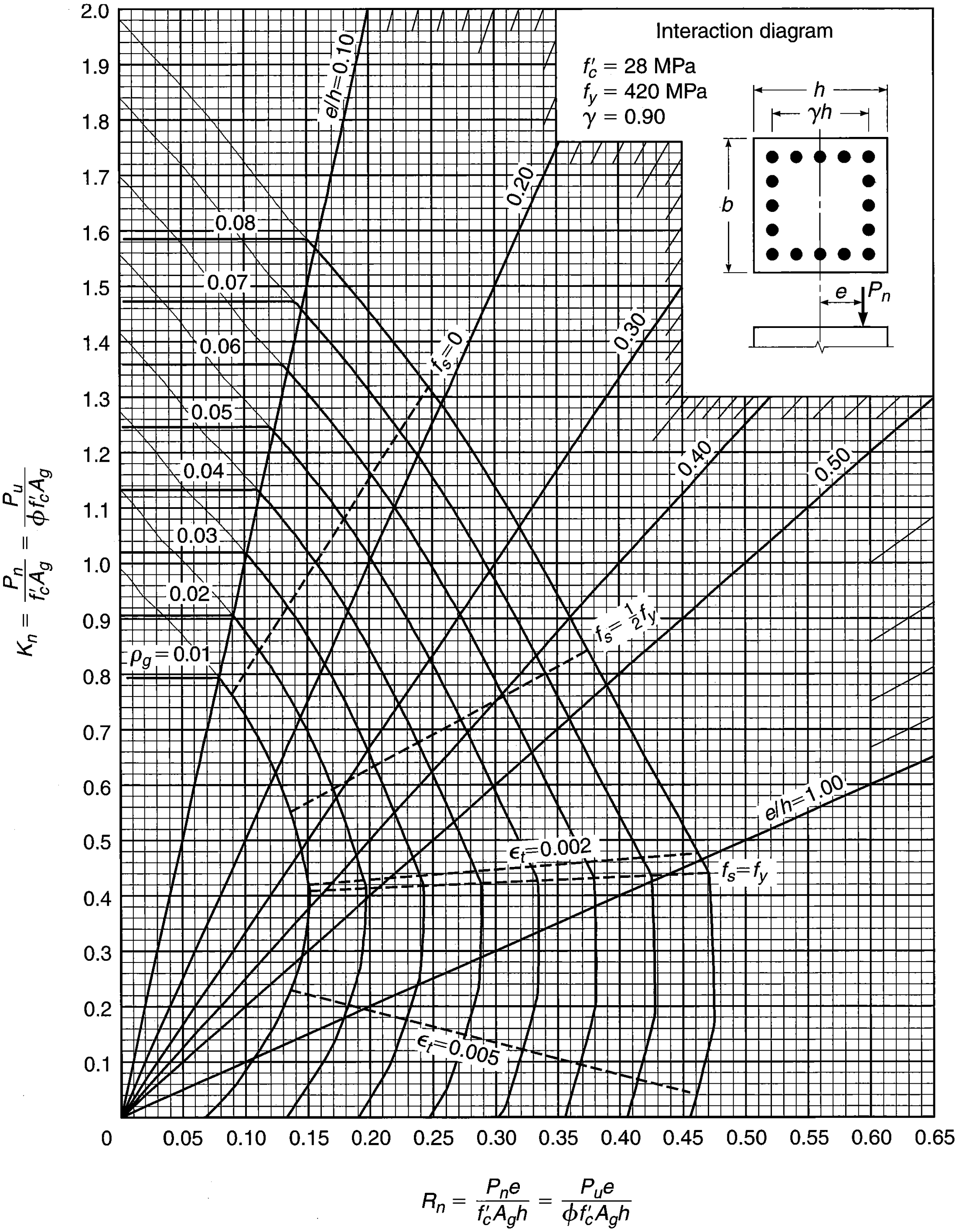

GRAPH A.8

Column strength interaction diagram for rectangular section with bars on four faces and $\gamma = 0.90$.

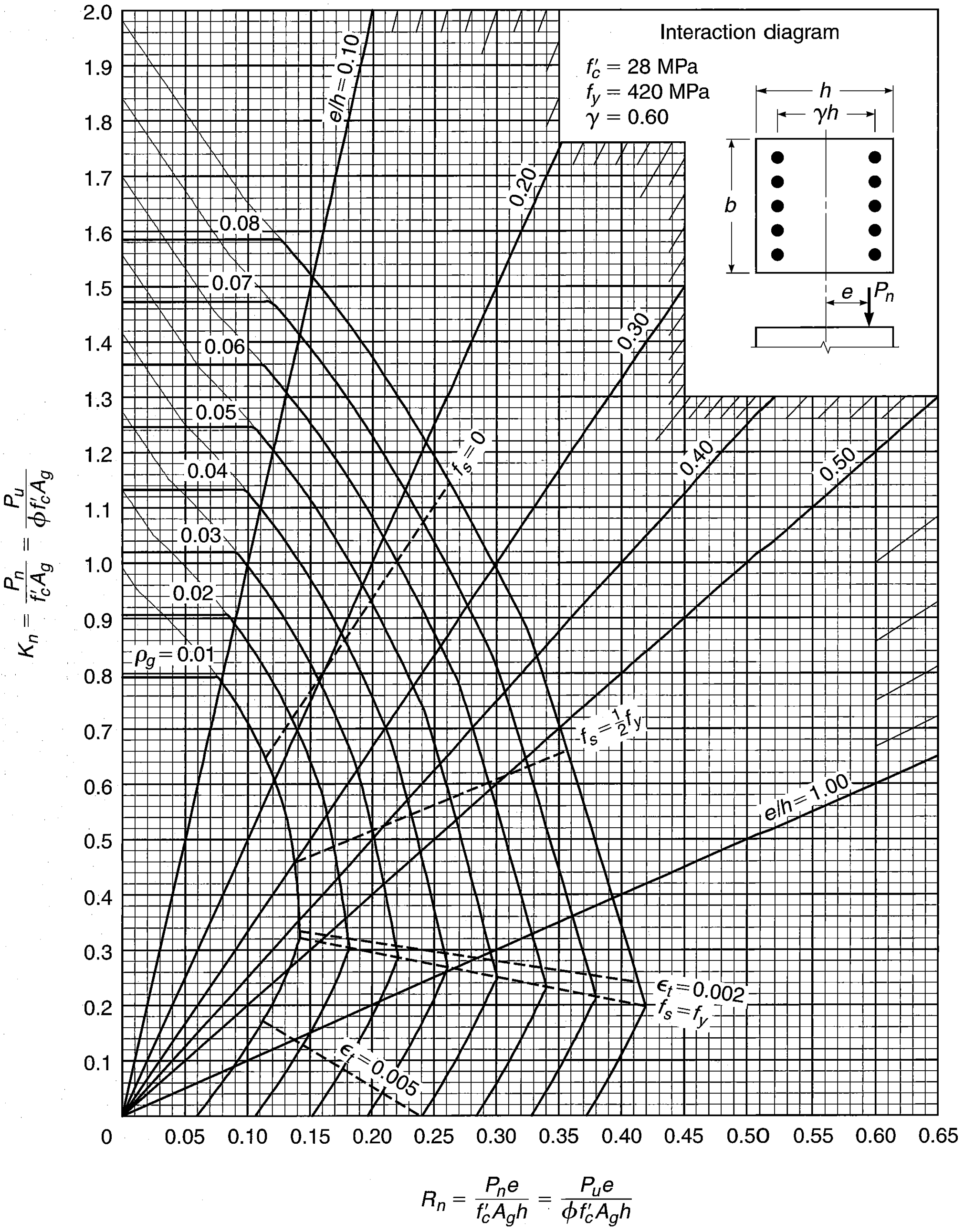

GRAPH A.9

Column strength interaction diagram for rectangular section with bars on end faces and γ = 0.60.

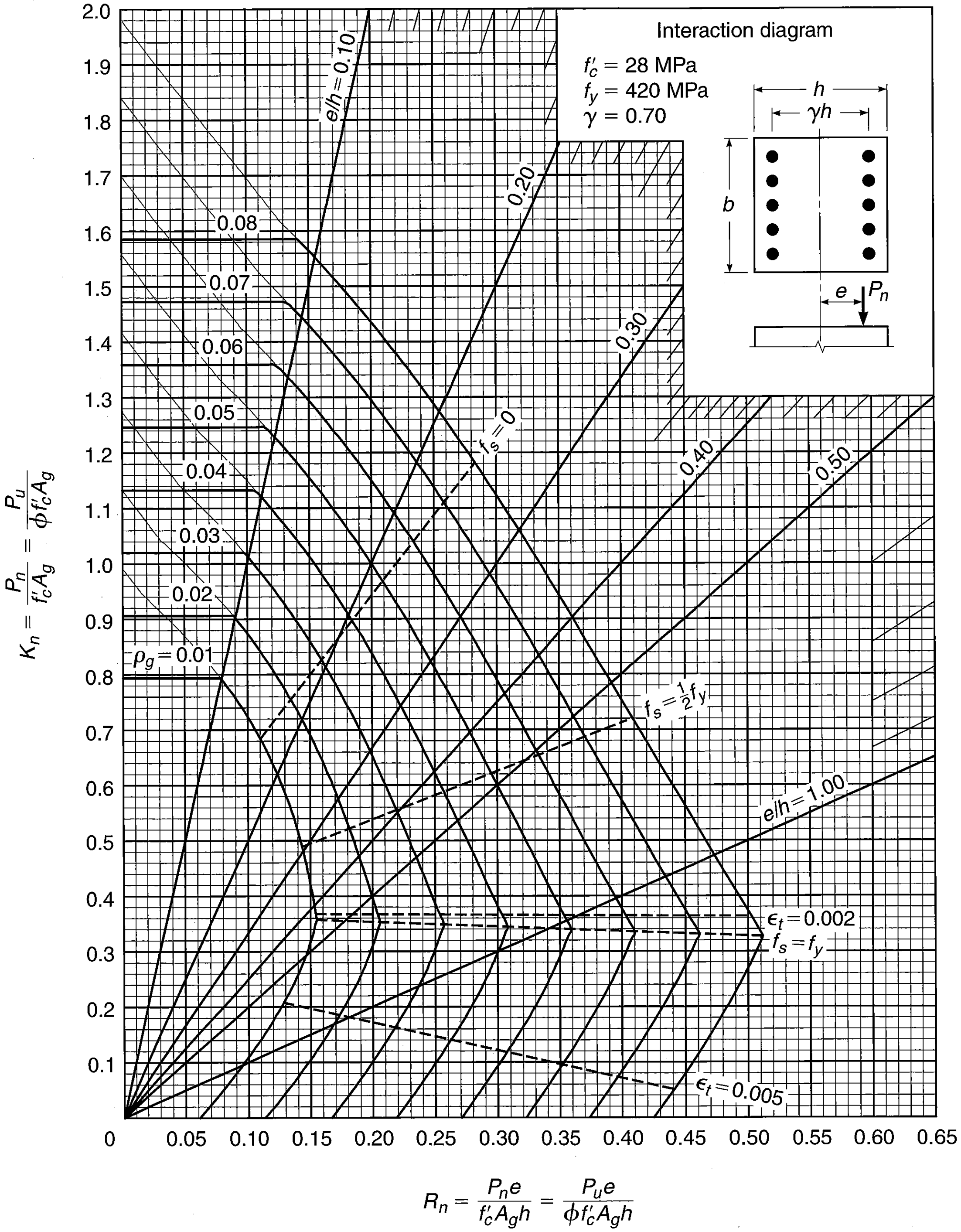

GRAPH A.10
Column strength interaction diagram for rectangular section with bars on end faces and $\gamma = 0.70$.

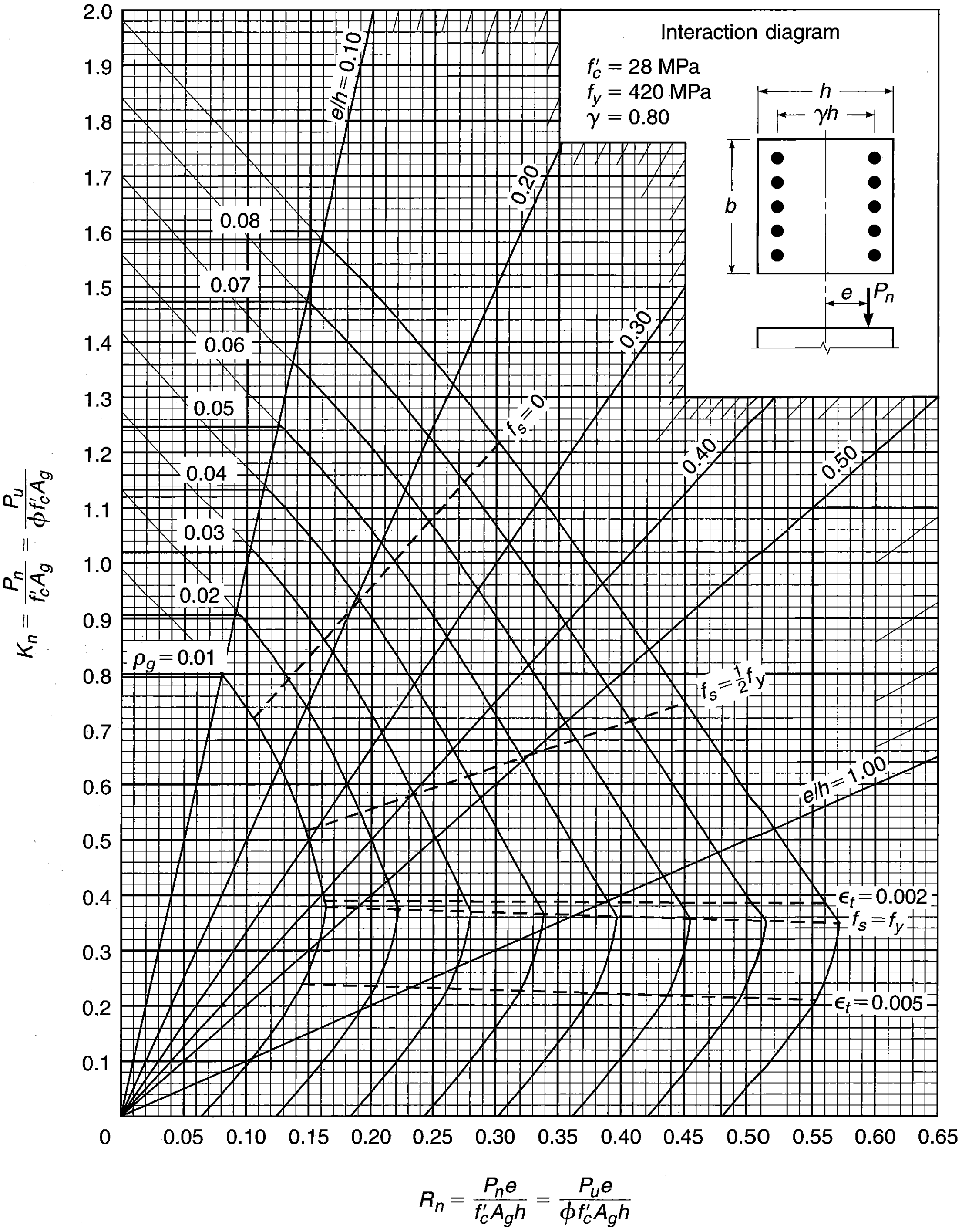

GRAPH A.11
Column strength interaction diagram for rectangular section with bars on end faces and $\gamma = 0.80$.

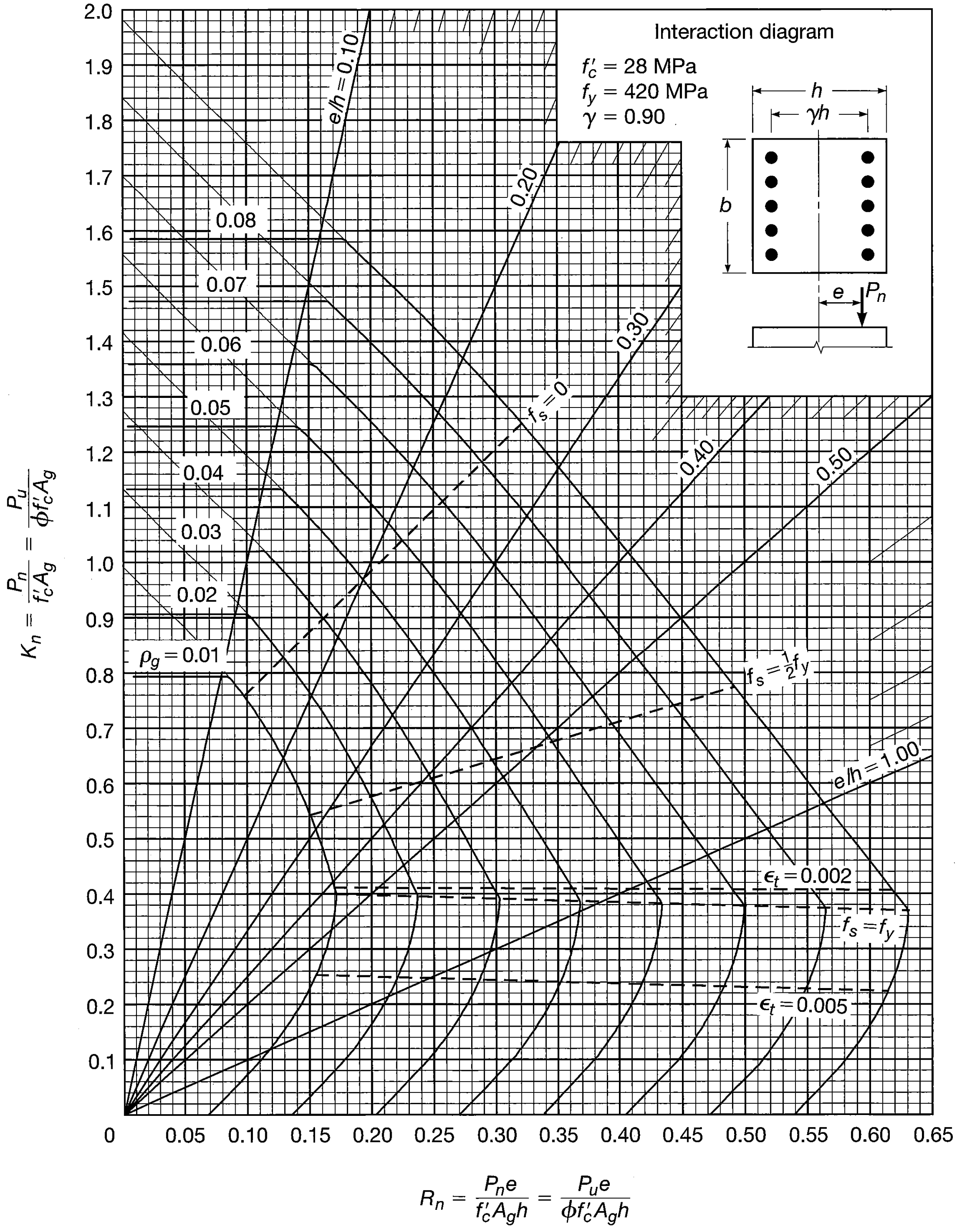

GRAPH A.12

Column strength interaction diagram for rectangular section with bars on end faces and $\gamma = 0.90$.

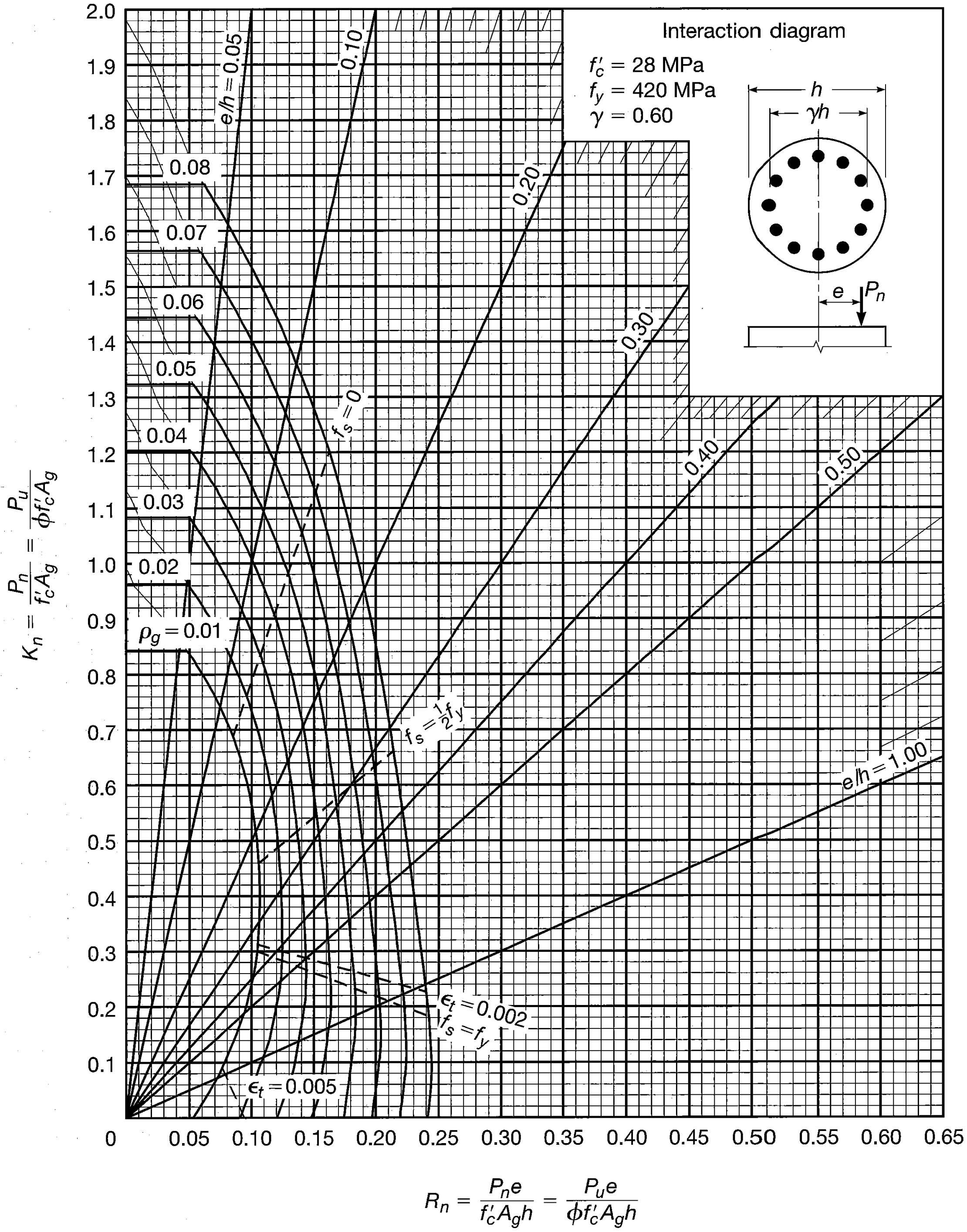

GRAPH A.13

Column strength interaction diagram for circular section with $\gamma = 0.60$.

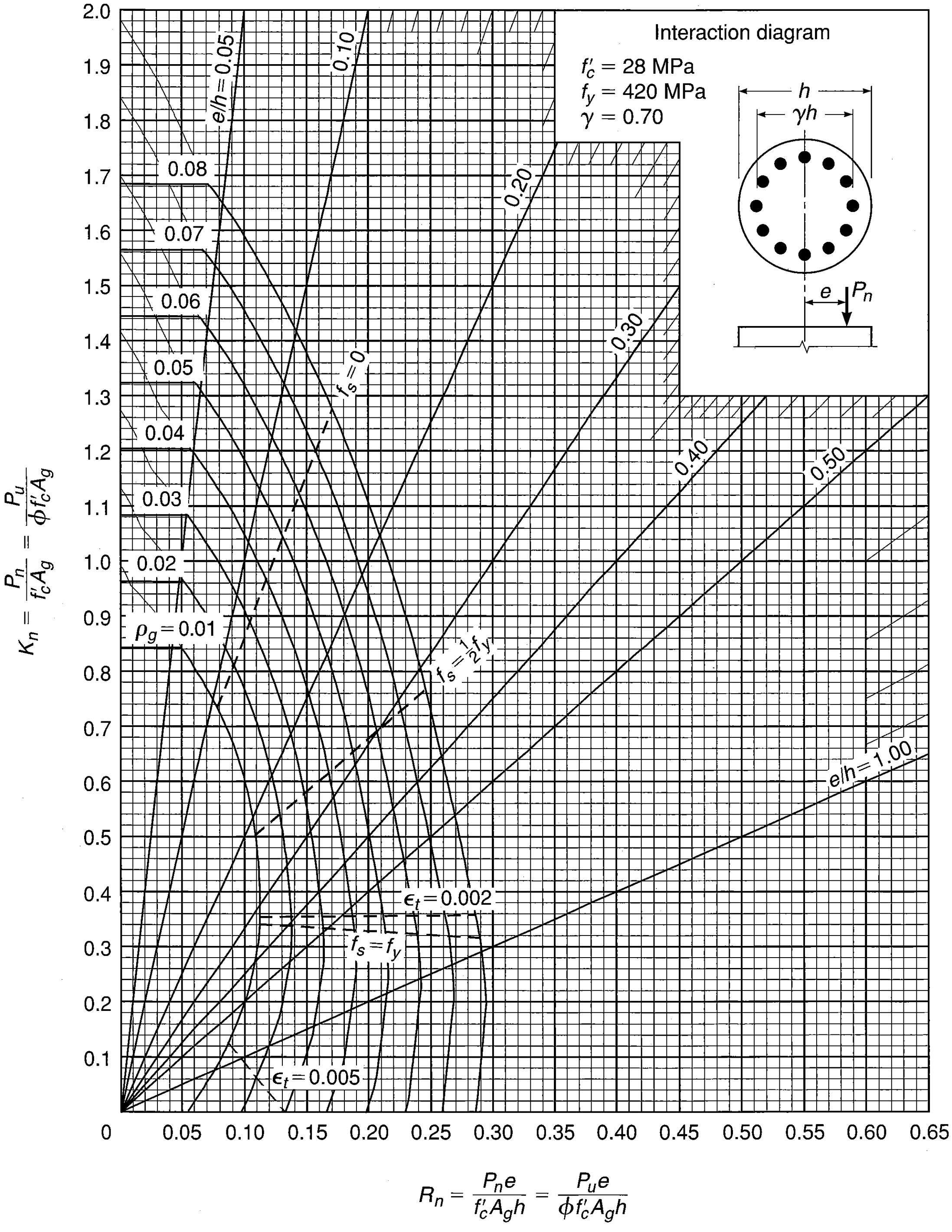

GRAPH A.14

Column strength interaction diagram for circular section with $\gamma = 0.70$.

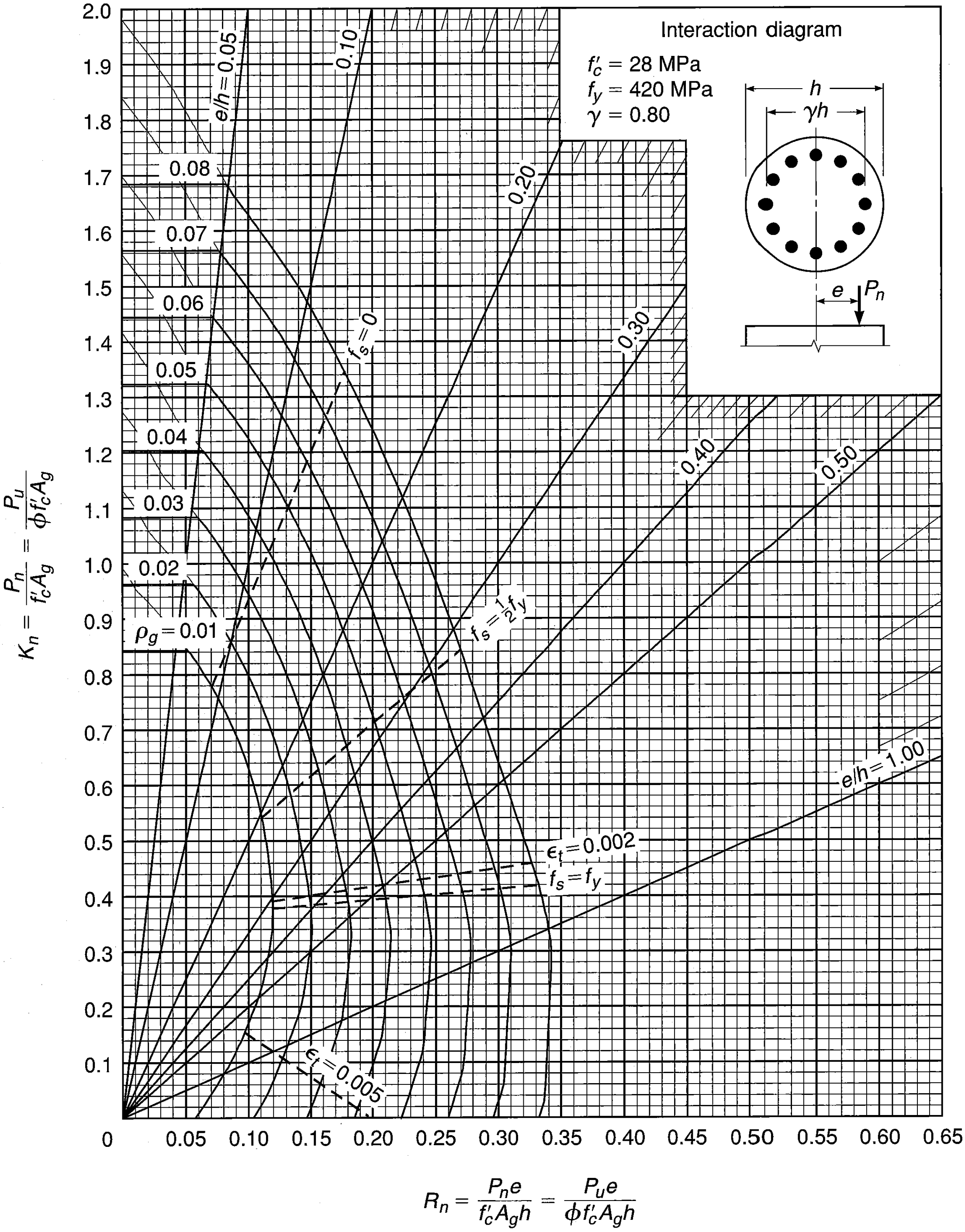

GRAPH A.15

Column strength interaction diagram for circular section with γ = 0.80.

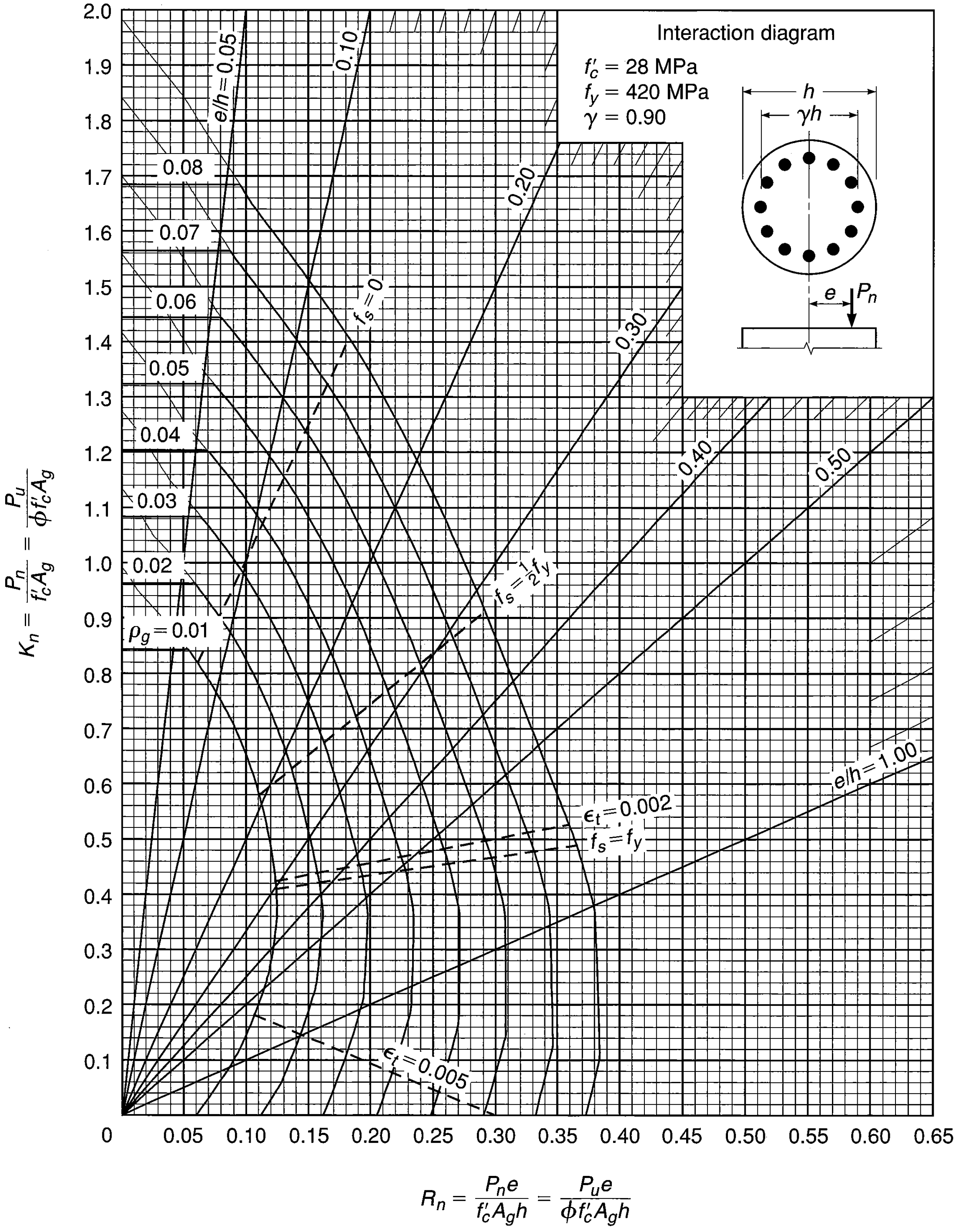

GRAPH A.16

Column strength interaction diagram for circular section with $\gamma = 0.90$.

APPENDIX

B

SI Conversion Factors: Inch-Pound Units to SI Units

Overall Geometry	
Spans	1 ft = 0.3048 m
Displacements	1 in. = 25.4 mm
Surface area	1 ft^2 = 0.0929 m^2
Volume	1 ft^3 = 0.0283 m^3
	1 yd^3 = 0.765 m^3
Structural Properties	
Cross-sectional dimensions	1 in. = 25.4 mm
Area	1 in^2 = 645.2 mm^2
Section modulus	1 in^3 = 16.39×10^3 mm^3
Moment of inertia	1 in^4 = 0.4162×10^6 mm^4
Material Properties	
Density	1 $\mathrm{lb/ft}^3$ = 16.03 $\mathrm{kg/m}^3$
Modulus and stress	1 $\mathrm{lb/in}^2$ = 0.006895 MPa
	1 $\mathrm{kip/in}^2$ = 6.895 MPa
Loadings	
Concentrated loads	1 lb = 4.448 N
	1 kip = 4.448 kN
Density	1 $\mathrm{lb/ft}^3$ = 0.1571 $\mathrm{kN/m}^3$
Linear loads	1 kip/ft = 14.59 kN/m
Surface loads	1 $\mathrm{lb/ft}^2$ = 0.0479 $\mathrm{kN/m}^2$
	1 $\mathrm{kip/ft}^2$ = 47.9 $\mathrm{kN/m}^2$
Stress and Moments	
Stress	1 $\mathrm{lb/in}^2$ = 0.006895 MPa
	1 $\mathrm{kip/in}^2$ = 6.895 MPa
Moment or torque	1 ft-lb = 1.356 N-m
	1 ft-kip = 1.356 kN-m

Index

A

AASHTO specifications, 10, 16, 26, 156, 165, 599, 711
Abeles, P. W., 711
Accelerators, 38
ACI
  Code, 16
  Code Commentary, 16
  load factors, 18
  moment coefficients, 406, 407
  safety provisions, 17
  strength reduction factors, 18
Adams, P. F., 328
Adebar, P., 165, 587
Admixtures, concrete, 38
Advanced strip method, 546
Aggregates, 29
  coarse, 30
  fine, 30
  heavyweight, 30
  lightweight, 30
Ahmad, S. H., 65, 165
Air entrainment, 38
Akiayma, Y., 165
Alcocer, S., 356
Alignment charts for columns, 316
Allowable stress design, 16
Analysis of continuous beams and frames, 387
  approximate, 401
  elastic, 393
  limit, 409
  portal method, 404
  preliminary, 399
  subframe, 391, 392
Anchorage
  headed bars, 185
  hooked, 181
  in joints, 365
  in nodal zones, 337, 342
  mechanical, 188
  web reinforcement, 189
  welded wire reinforcment, 190
Anchorage zone, prestress, 701
Anderson, N. S., 384
Anderson, R. G., 647
Approximate analysis, 401
Arches, concrete, 7
AREMA manual, 10, 16, 26
Armer, G. S. T., 555
ASCE Load Specification, 10, 11, 26, 749
ASTM specification, 28, 30, 37–39, 52, 55–57, 59–63, 185, 214
Avraham, C. H., 517
Axial compression, 20, 262, 299
Axial forces, effect on shear, 145
Axial tension, 25
Azizinamini, A., 65

B

B-regions, 332
Balanced steel ratio
  compression-reinforced beams, 101
  tension-reinforced beams, 82
Balanced strain condition
  beams, 82, 101
  columns, 273
Bao, A., 491
Bar designations, 55
Bardhan-Roy, B. K., 711
Barham, S., 64
Barney, G. B., 749
Bars, reinforcing
  cutoff and bend points, 192
  detailing, 194, 358
  selection of, 98
  spacing of, 98
  splices, 204
Beam-and-girder floors, 615
Beam-column joints, 359
Beams
  compression-reinforced, 99
  cracked elastic section analysis, 73
  deep, 346, 347
  doubly reinforced, 99
  overreinforced, 93
  proportions of, 98, 112, 399
  T section, 108
  tension-reinforced, 71, 80
  uncracked elastic section analysis, 72
  underreinforced, 83
Bearing walls, 627
Beaulieu, D., 328
Bending. *See* Flexure
Biaxial column bending, 285
  computer analysis, 291
  load contour method, 287
  reciprocal load method, 288
Biaxial strength of concrete, 48, 49
Binney, J. R., 749
Birkland, H. W., 165, 420, 647
Birkland, P. W., 165, 647
Blakey, F. A., 555
Blast-furnace slag, 39
Bond, 168. *See also* Development length
  compression, 191
  cracked section analysis, 169
  flexural, 170
  force distribution, 171

Bond—*Cont.*
  fundamentals, 168
  modification factors, 177, 178
  prestressed beams, 701
  strength, 172, 173
  tension, 177
Booth, E., 749
Bowles, J. E., 587
Brackets, 380
Brandtzaeg, A., 294
Branson, D., 45, 64, 238, 491, 711
Breen, J. E., 207, 208, 328, 421, 711
Bresler, B., 64, 164, 294
Brettmann, B. B., 207
Bridges, 6, 7
Broms, B., 238
Brown, R. L., 294
Browning, J., 65
Building Seismic Safety Council, 26, 721, 749
Building systems, 613
  beam-and-girder, 615
  composite, 617, 618
  flat plates, 623
  flat slabs, 622
  one-way joists, 619
  precast, 631
  steel-deck reinforced slabs, 618
  two-way joists, 625
  two-way slabs, 432, 622
Bundled reinforcement, 191
Burdett, O., 711
Burj Dubai, 52, 615
Burns, N. H., 710

C

c/d ratio, 85
Canadian National Standard, 153, 165
Cantilever retaining walls, 601
Capacity reduction factors, 19
Capell, H. T., 115
Capitals, column, 2, 4, 622
Captive column, 720
Cardenas, A. E., 646
Carino, N. J., 65
Carrasquillo, R. L., 64
Cement, 28
  composition, 29
  high early strength, 1, 29
  hydration of, 29
  portland, 28, 29
  types, 29
Chang, D. C., 328, 421
Chen, K. C., 385, 646
Chen, W. F., 749
Choi, O. C., 208
Chow, L., 356
Chu, K. H., 517
Clifton, J. E., 65, 207
Collins, M. P., 64, 153, 165, 258, 587, 710
Column footings, 565
Columns, 262
  ACI Code provisions, 281
  axially loaded, 20
  balanced failure, 273
  with bending, 269, 303
  biaxial bending of, 285
    computer analysis for, 291
    load contour method, 287
    reciprocal load method, 288
  captive, 720
  circular, 21, 279
  design aids, 282, 772
  distributed reinforcement, 276
  equivalent, 455
  Euler load, 300
  interaction diagrams, 270, 274, 772
  lateral reinforcement, 265
  rectangular, with bending, 269
  safety provisions, 281
  slender. *See* Slender columns
  spirally reinforced, 21, 265
  splices in, 206, 292
  tied, 21, 265
  transformed section, 23, 264
  unbraced frame analysis, 308, 320
  unsymmetrically reinforced, 278
Column-supported slabs, 436, 622
Combined footings, 574
Compacting of concrete, 33
Compatibility torsion, 241, 251
Compression, axial, 40
Compression field theory, 152
  design provisions, 156
  modified, 153
  shear, 152
Compression members, 262
Compression-reinforced beams, 99
Compression steel yield test, 101
Compression struts, 332
Concentrated loads on slabs, 515
Concrete
  admixtures, 1, 38
  biaxial strength, 48, 49
  compacting of, 33
  components, 1
  compression strength, 40
  consistency, 32
  creep, 43
  curing, 1, 33
  definition of, 1
  density, 30
  fatigue, 45
  heavyweight, 30
  high-strength, 52
  lightweight, 30
  long-term loading, 43
  mixing, 32
  modulus of elasticity, 41
  placing, 33
  Poisson's ratio, 42
  prestressed, 2, 648
  proportioning, 1, 31, 32
  protection for steel, 97
  quality control, 34
  short-term loading, 40
  shrinkage, 49
  strength: in combined stress, 48
    in compression, 40
    gain with age, 42
    required average strength, 36
    specified, 35
    in tension, 46
  stress-strain curves, 41, 43
  sustained load behavior, 43, 44
  thermal coefficient, 52
Connections of precast elements, 640
Continuity, 387
Conway, H. D., 356
Corbels, 380
Corley, W. G., 65, 491, 646, 749
Corner joints, 377
Corner-supported elements, 546
Counterfort retaining walls, 608
Coupling beams, 726, 739, 746
Cover requirements for bars, 97
Cracked section elastic analysis, 73

Cracking, 213
  ACI Code provisions, 216
  flexural, 213
  variables affecting, 214
  width of cracks, 214
Cracking torque, 244
Cranston, W. B., 328
Crawford, R. E., 555
Creep of concrete, 43
  coefficient, 44
  specific, 44
  time-variation of, 45
Cross, H., 394, 420
Culver, C. G., 646
Curing of concrete, 1, 33
Curtin Walls, 627
Curvature vs. moment, 234
Cutoff points for bars in beam, 192
Cylindrical shells, 3, 5

D

D-regions, 332, 338
Dapped beams, 353
Darwin, D., 64, 65, 207, 208, 646
Davis, H. E., 64
Debaiky, S. Y., 165
Deep beams, 339, 346
  ACI Code provision, 346
  reinforcement of, 346
  shear in, 346
Deflections, 219
  ACI Code provisions, 226
  continuous beams, 227
  control of, 219
  creep, 228
  effective moment of inertia for, 221
  elastic, 220, 224
  flat plates and flat slabs, 482
  immediate, 220, 227
  load-history effect, 225
  long-term multipliers, 223, 228
  permissible, 229
  prestressed concrete, 706
  shrinkage, 232
  sustained load, 223
  thermal, 232
  two-way edge-supported slabs, 432
Demsky, E. C., 517
dePaulo, N. I., 208
Depth, minimum
  beams and one-way slabs, 226, 428
  two-way slabs, 448
Design aids, 94, 282, 751
Design methods
  allowable stress, 16
  alternative basis, 18
  service load, 16
  strength, 15
Design response spectrum, 722
Detailing, joint, 358
Detwiler, G., 64
Development length, 172, 174
  ACI Code provisions, 177
  bundled bars, 191
  compression, 191
  headed bars, 185
  hooked bars, 182
  modification factors, 177, 178
  seismic design, 736
  stirrups, 189
  tension, 177
Diagonal cracking, 124, 128
Diagonal tension, 120
  homogeneous beams, 121
  prestressed concrete beams, 694
  reinforced concrete beams, 120, 124
Diaphragms, seismic, 739, 746
Dilger, W. H., 491
Direct design method for slabs, 439
  column design, 445
  lateral distribution of moments, 442
  minimum thickness, 448
  moments at critical sections, 440
  shear on supporting beams, 444
Discontinuity lines in slabs, 525
Discontinuity regions, 332
Distribution steel in slabs, 429
Dolan, C. W., 115, 647
Domel, A. W., 749
Donahey, R. C., 207
Drawings, typical engineering, 646
Ductile hinges, 719
Dumonteil, P., 328
Dynamic lateral force procedures, 725

E

Earth pressure on walls, 589
Earthquake design. *See* Seismic design
Eccentric columns, 269
Edge-supported slabs, 432, 442
Effective flange width, 108
Effective length of columns, 301, 315, 316
Effective moment of inertia, 221, 227
Effective span length, 395
Ehsani, M. R., 291, 294
Elastic analysis, 393
Elgabry, A. A., 491
Ellingwood, B., 26
Elmiema, E. I., 165
Elzanaty, A. H., 165
Engineering drawings, typical, 646
Epoxy-coated bars, 60, 176
Equilibrium method for slabs. *See* Strip method for slabs
Equilibrium torsion, 241, 251
Equivalent column, 455
Equivalent frame method for slabs, 454
  basis, 454
  by computer, 461
  deflection analysis, 482
  equivalent column, 455
  for horizontal loads, 489
  moment analysis, 457
  shear design, 462
Equivalent lateral force procedure, 723
Equivalent loads from prestress force, 651
Ernst, G. C., 421
Euler load, 300
Expansive cement, 52
Extended nodal zones, 336, 342

F

Factored loads, 18
Falconer, B., 711
Fallsen, H. B., 491
Fanella, D. A., 749
Fang, H. Y., 587

Fans, yield line, 515
Fatigue strength
  concrete, 45
  reinforcing bars, 59
FEMA provisions, 26
Ferguson, P. M., 207
Fintel, M., 611, 647
Fiorato, A. E., 65, 749
Flange width of T beams, 108
Flat plates, 2, 4, 424, 623
Flat slabs, 2, 4, 424, 622
Flexural bond, 168
Flexural resistance factor, 85
Flexure. *See also* beams
  assumptions, 67
  elastic cracked section analysis, 73
  elastic uncracked section analysis, 72
  flexural strength analysis, 75
  homogeneous beams, 67
Floor systems
  beam and girder, 2, 615
  edge-supported slab, 432, 622
  flat plates, 2, 4, 424, 623
  flat slabs, 2, 4, 424, 622
  grid slabs, 625
  lift slabs, 625
  one-way joists, 2, 3, 619
  precast, 633
  steel deck reinforced, 618
  two-way joists, 625
  two-way slabs, 432, 622
  waffle slabs, 625
Fly ash, 39, 52
Folded plates, 3, 5
Footings, 559
  column, 565
  combined, 574
  grid, 582
  loads on, 561
  mat, 575, 582
  pile cap, 584
  spread, 559
  strip, 582
  two-column, 575
  wall, 563
Ford, J. S., 328, 421
Foundations. *See* Footings
Fracture energy, 47, 175
Fracture mechanics, 47
Frame analysis, 387
  simplifications, 391
Frosch, R. J., 215, 238
Furlong, R. W., 328

G

Galambos, T. V., 327
Galvanized bars, 60
Gamble, W. L., 490, 491, 517, 555
Gardner, N. J., 491
Gebler, S. H., 65
Gere, J. M., 327
Gergely, P., 207, 215, 238
Gergely-Lutz equation, 215, 238
Gerstle, K. H., 65
Gesund, H., 517
Ghaffari, H. H., 208
Ghali, A., 491, 517
Ghoneim, M. G., 258
Ghosh, S. K., 65, 328, 749
Gilbert, A., 421
Gosain, N. K., 207
Goto, Y., 207
Gouwens, A., 294, 491, 646
Graham, C. J., 491
Gravity retaining walls, 599
Grid slabs, 625
Ground granulated blast-furnace slag, 39
Guralnick, S. A., 491
Gustafson, D. P., 491, 646
Guyon, Y., 711

H

Hage, S. E., 327, 328
Hamad, B. S., 208
Hammering, 718
Hanna, S. N., 491
Hansen, W., 65
Hanson, J. M., 65, 646, 711
Hanson, N. W., 711
Hanson, W. E., 587, 611
Hatcher, D. S., 491, 517
Hatfield, E., 65
Hawkins, N. M., 165, 491, 517
Hayes, B., 517
Headed deformed bars, 185
  development length, 185
  modification factors, 187
Headed shear studs, 470
  in slabs, 470
Heiman, J. L., 491
Helgason, T., 65
Hester, C. J., 208
Heteneyi, M., 587
High-strength concrete, 52
Hillerborg, A., 503, 555
Hillerborg method. *See* Strip method for slabs
Hilsdorf, H. K., 65
Hinojosa, R. C., 491
Hoffman, E. S., 491, 646
Hognestad, E., 115, 294, 517, 587, 646
Hooks, 181
  development length, 182
  modification factors, 184
  standard dimensions, 181
  for stirrups, 182
Hover, K. C., 64, 65, 238
Hsu, T. T. C., 64, 165, 258
Huntington, W. C., 611

I

Idealization of structure, 394
Idun, E. K., 207
Iguro, M., 165
Indeterminate beams and frames, 387
Inelastic moment redistribution, 409, 417
Inflection points for approximate analysis, 402
Ingerslev, A., 517
Integral beams in slabs, 468
Integrity, structural, 199, 644
Interaction diagrams
  for axial load plus bending, 270, 772
  for biaxial column bending, 285
  for biaxial strength of concrete, 48, 49
Intermediate moment frames, 747
International Building Code, 16, 26
Isenberg, J., 164
Islam, S., 517

J
Jeanty, P. R., 207
Jennewein, M., 165, 356
Jensen, E. A., 65
Jirsa, J. O., 207, 208, 384, 491
Johansen, K. W., 517
Joints, 358
  bar anchorage in, 365
  beam-column, 359
  beam-girder, 373
  classification of, 359
  loads and forces, 360
  reinforcement in, 364
  shear strength, 362
  strut-and-tie models, 371
  wide-beam, 369
Joist floors, 619, 625
Jones, L. L., 517
Jurewicz, R. E., 646

K
Kaar, R. H., 115, 238, 711
Kappos, A. J., 749
Kahn, L. F., 165
Kani, G. N. J., 165
Kelly, J. W., 64
Kemp, K. O., 555
Kerhkoff, B., 64
Khaloo, A. R., 165
Khuntia, M., 328
Klein G. J., 356
Kostmatka, S. A., 64
Kozul, R., 64
Kramrisch, F., 587
Kreger, M. E., 491
Kripanarayanan, K. M., 647
Kriz, L. B., 115, 294, 385
Kuchma, D., 64, 165, 587
Kupfer, H., 65

L
LaFraugh, R. W., 491
Lai, S. M. A., 327
Lampert, P., 258
Lateral ties in columns, 21, 265
Ledesma, A., 208
Lee, S. L., 115
Leet, K. M., 421
Leigh, W., 421
Lenschow, R., 517
Leon, R., 491
Libby, J. R., 711
Lift slabs, 626
Light-gage steel deck slabs, 618
Lightweight concrete, 30
Limit analysis, 409
Limit states design method, 80
Lin, T. Y., 672, 710
Lindquist, W. D., 65
Live loads
  buildings, 9, 10, 11
  placement, 389
Load balancing in prestressed beams, 685
Load combinations, 390
Load contour method for columns, 287
Load factors, ACI, 17, 18
Loads
  ASCE live loads, 10, 11, 26
  combinations, 18, 390
  dead, 8
  earth pressure, 589
  environmental, 10
  factored, 18
  live, 9–11
  placement of live loads, 9, 389
  seismic, 707
  snow, 10, 12
  variability of, 12
  wind, 11
Long-term loading, concrete, 43
Losberg, A., 384, 611
Loss of prestress force, 690
  lump sum estimate, 690
  separate losses, 691
  time-step method, 694
Lower bound theorem, 500
Luan, S., 64
Lutz, L. A., 207, 215, 238

M
MacGregor, J. G., 26, 152, 165, 258, 327, 328, 356, 711
Magura, D. D., 646
Maher, D. R. H., 517
Mains, R. M., 207
Malhotra, V. M., 64
Marques, G. L. J., 384
Marshall, W. T., 711
Marti, P., 152, 165, 356
Martinez, S., 64, 165, 294
Mast, R. F., 165
Materials, 28
Mathey, R. G., 207
Matrix analysis, 394
Mattock, A. H., 115, 165, 238, 258, 294, 385, 421, 711
McCabe, S. L., 208, 646
McCormac, J. C., 421
McGuire, W., 421
Meinheit, D. F., 384
Mesri, G., 587, 611
Microsilica. *See* Silica fume
Mindess, S., 64
Minimum depth of slabs, 428, 447
Minimum steel ratio in flexure, 87
Minimum web steel area, 139
Mirza, M. S., 207
Mirza, S. A., 26, 207
Mitchell, A. D., 165
Mitchell, D., 165, 207, 258, 491, 710
Mixing of concrete, 31
Modified compression field, 153
Modular ratio, 22
Modulus of elasticity
  of concrete, 41
  of prestressing steels, 63
  of reinforcing bars, 59
Modulus of rupture, 46
Moehle, J. P., 491
Mokhtar, A. S., 491
Moment coefficients, ACI, 406, 407
Moment vs. curvature in beams, 234
Moment distribution method, 394
Moment magnification in columns, 304, 305, 307, 312, 320
Moment of inertia, 311, 397
Moment redistribution, 410
  ACI Code provisions, 417
  in beams and frames, 412
  in slabs, 497, 499
Moment reduction in beams, 418
Moment transfer at columns, 477
Morsch, E., 165

N
Naaman, A. E., 64, 710
Nawy, E. G., 710
NEHRP recommendations, 26, 749
Nervi, L., 420
Net tensile strain, 83
Neutral axis in beams
  elastic, 73
  ultimate, 79
Neville, A. M., 64, 65
Ngab, A. S., 64
Nichols, J. R., 491
Nieves, J. M., 294
Nilson A. H., 64, 65, 164, 165, 207, 238, 294, 491, 710, 711
Nilsson, I. H. E., 384, 611
Nodal zones, 332, 335
  dimensions, 340
  extended, 336
  resolution of forces, 341
  strength, 345
Nodes, 335
Nowak, A. C., 26, 27
Nowak, L. C., 356

O
Oelhafen, V. H., 328
Okada, T., 165
Olive View Hospital, 718
One-way joists, 619
One-way slabs, 424
  distribution steel, 427
  minimum thickness, 428
  shrinkage reinforcement, 429
  temperature steel, 429
  typical steel ratios, 427
Openings in slabs, 480, 542
Orangun, C. O., 207
Overreinforced beams, 93

P
P-delta method, 304, 325, 725
Panarese, W. C., 64
Pannell, F. N., 294
Parra-Montesinos, G. J., 165, 356
Park, R., 384, 517, 555
Parme, A. L., 294
Partial prestressing, 670
Pasley, G. P., 646
Pattern loading of beams and frames, 389
Pauley, T., 384, 749
Paulson, K. A., 65, 238
Pavel, R., 65
Paz, M., 421
Peabody, D., Jr., 491
Peck, R. B., 587, 611
Penelis, G. G., 749
Peterman, R. J., 64
Pfrang, E. O., 328
Pickett, G., 65
Pile caps, 584
Plastic analysis, 409
Plastic centroid of columns, 278
Plastic hinges
  in beams and frames, 410
  in slabs, 498
Plasticity theory
  lower bound theorem, 500, 522
  upper bound theorem, 500, 522
Plasticizers, 39
Poisson's ratio, concrete, 42
Portal method, 404
Portland cement, 28
Post-tensioning, 654
Precast concrete, 631
  beams, 633
  brackets, 380
  building examples, 635
  columns, 635
  connections, 640
  corbels, 380
  double Ts, 631
  roof and floor units, 633
  single Ts, 633
  slabs, 633
  wall panels, 632
Preliminary design, 399
Preston, H. K., 711
Prestressed concrete, 648
  allowable stresses in concrete, 659
  allowable stresses in steel, 658
  anchorage zones, 702
  bond stresses, 701
  crack control, 710
  deflection, 706
  elastic analysis, 660
  equivalent loads, 651
  flexural design, 672, 685
  flexural strength, 666
  load balancing, 685
  loss of prestress force, 690
  partial prestressing, 670
  post-tensioning, 654
  pretensioning, 654
  shape selection, 682
  shear design, 694
  transfer length, 701
Prestressing steels, 61, 656
  allowable stresses, 658
  grades and strengths, 61
  relaxation of stress, 63
  stress-strain curves, 62
Pretensioning, 654
Priestly, M. J. N., 749
Proveda, A., 165

Q
Quality control, 34

R
Rabbat, B. G., 749
Ramamurthy, L. N., 294
Ramezanianpour, A. A., 64
Ramirez, J. A., 384
Raths, C. H., 385
Ravikumar, S., 646
Rebars. *See* Reinforcement
Reciprocal load analysis of columns, 288
Rectangular stress block, 80
Redistribution of moments, 410
  ACI Code method, 417
  in beams and frames, 412
  in slabs, 497, 499
Reinforcement, 54
  bar selection, 98
  bars, 55
  bend points, 193
  compression, 99
  cover requirements, 98, 217
  cutoff points, 183
  deformations, 55
  epoxy-coated, 60
  fatigue strength, 59

- galvanized, 60
- grades and strength, 56, 57
- maximum c/d ratio, 85
- maximum number of bars in beams, 99
- maximum reinforcement ratio, 84
- minimum number of bars in beams, 99
- minimum reinforcement ratio, 87
- modulus of elasticity, 59
- prestressed, 61, 656
- shear, 131
- slab, 445
- spacing requirements, 98, 216–218
- splices in, 204
- standard sizes, 55
- stress-strain curves, 59
- torsional, 252
- welded wire reinforcement, 61
- welding of, 56

Relaxation of prestressing steels, 63
Response spectrum, design, 722
Retaining walls, 589
- cantilever, 601
- counterfort, 608
- design basis, 597
- drainage for, 598
- gravity, 599
- stability analysis, 594
- structural design, 597

Retarders, set, 38
Richart, F. E., 294, 587
Ritter, W., 152, 165
Roberts, C., 711
Roller, J. J., 165
Rotation capacity at hinges, 416
Rotation requirement at hinges, 414
Rusch, H., 45, 64, 65, 115
Russell, H. G., 65, 165, 749

S

Safety
- ACI Code provisions, 17
- considerations, 12
- index, 15
- margin of, 14
- reduction factor, 15
- structural, 14, 34

Salamizavaregh, S., 208
Sanders, D., 711
Scanlon, A., 491
Schafer, K., 165, 356
Schlaich, J., 152, 165, 356
Scott, N. L., 711
Scrawthorn, C., 749
Scribner, C. F., 646
Secondary moments in columns, 299
Secondary torsion, 241, 251
Second order column analysis, 300, 325
Seismic design, 714
- ACI Code provisions, 726
  - beams, 728, 746
  - columns, 730
  - coupling beams, 739, 746
  - diaphragms, 739, 746
  - intermediate moment frames, 747
  - shear strength, 747
  - special moment frames, 727
  - walls, diaphragms, trusses, 739, 746
- hammering, 718
- joints, 734
- load factors, 18
- reinforcement for, 726

Seismic loading, 721
- base shears, 723
- criteria, 721
- design response spectrum, 722
- displacements, 716
- dynamic lateral forces, 725
- equivalent lateral forces, 723
- ground motion in the United States, 715
- member response, 718
- structural response, 716

Self-consolidating concrete, 39
Serviceability, 12, 213
Set retarders, 38
Shah, S. P., 64, 65
Shear, 120
- AASHTO provisions, 156
- ACI Code provisions, 136
- alternate models, 151
- and axial loads, 145
- compression field theory, 152
- deep beams, 347
- flat plate slabs, 462
- flat slabs, 462
- footings, 566
- headed shear studs in slabs, 474
- homogeneous beams, 72, 121
- joints, 355
- plus torsion, 249
- prestressed concrete beams, 694
- reinforced concrete beams, 120
- reinforcement: beams, 131
- seismic loading, 742, 747
- truss models for, 152
- varying-depth beams, 150
- walls, 629

Shear-friction method, 160
Shearheads in slabs, 465, 474
Shear studs in slabs, 466, 470
Shells
- cylindrical, 3, 5
- folded plate, 5
- spherical, 6

Shen, J. F., 385
Shioya, T., 165
Shiu, K. N., 749
Short-term loading, concrete, 40
Shrinkage-compensating concrete, 51
Shrinkage of concrete, 49
Shrinkage deflections, 232
Shrinkage reinforcement in slabs, 429
Siess, C. P., 65, 491
Silica fume, 39
Simmonds, S. H., 517
Singh, R. B., 517
Sivasundaram, V., 64
Skin reinforcement, 217
Slab-band floors, 617
Slabs
- column-supported, 436
- concentrated loads on, 515
- deflection of, 482
- direct design method, 439
- distribution steel, 429
- edge-supported, 432
- equivalent column, 455
- equivalent frame method, 454
- integral beam for shear, 468
- lateral distribution of moments, 442
- minimum thickness, 428, 447
- moments at critical sections, 440
- one-way, 426
- openings in, 480
- reinforcement for flexure, 427, 445

Slabs—*Cont.*
  shear in column-supported, 462
  static moment in, 437
  strip method (*see* Strip method for slabs)
  two-way edge supported, 432, 622
  types of, 424
  yield line theory. *See* Yield line analysis
Slag, 39
Slate, F. O., 64, 65, 165, 294
Slender columns, 299
  ACI Code provisions, 309
  in braced (nonsway) frames, 303, 308, 312
  defined, 299
  effective length factor, 301, 315, 316
  moment magnification factor, 304, 306, 307, 312, 320
  P-delta method, 304, 325, 735
  radius of gyration, 299
  second order analysis, 300, 325
  slenderness ratio, 299
  stability index, 310
  in unbraced (sway) frames, 308, 320
Slenderness ratio, 299, 300
Slump test, 32
Smadi, M. M., 64
Soongswang, K., 385, 646
South Wacker Drive Building, 51, 614
Sozen, M. A., 65, 491, 517
Space truss analogy, 247
Span length, 395
Special moment frames, 727
Specific creep, 44
Spectral response acceleration, 714, 721
Spirally reinforced columns, 21, 265
Spirals, column, 265
Splices in reinforcing bars, 204
  in columns, 205, 292
  compression, 205
  tension, 205
Split cylinder strength, 46
Spread footings, 559
Sprenger, H., 356
St. Venant, 332
Stability index, 310
Stability of retaining walls, 594
Stanton, J. F., 647
Static moment in slabs, 437
Steels
  prestressing, 61, 656
  reinforcing, 54
  welded wire reinforcement, 61
Stirrups, 131
  anchorage of, 181, 182
  forces in, 134
Strain limit in flexure, 71
Strength
  design, 15, 17
  nominal, 17
  reduction factors, 19, 84
  required, 17, 18
  variability of, 14, 84
Stress-strain curves
  concrete, 22, 41, 43
  in flexure, 73
  prestressing steels, 62
  reinforcing bars, 21, 22, 59
Strip method for slabs, 522
  advanced, 546
  basis, 523
  continuity, 529
  corner-supported elements, 548
  discontinuity lines, 525
  fixed edges, 529
  holes, 542
  load distributions, 524
  rectangular slabs, 527
  unsupported edges, 534
Structural integrity provisions, 199, 644
Structural systems, 2
Strut-and-tie method, 136, 332
  ACI provisions for, 342, 346
  B-regions, 332
  D-regions, 332, 338, 347
  dapped beam ends, 353
  deep beams, 346
  nodal zones, 335
Struts, 332,
  bottle-shaped, 334
  capacity of, 342, 343
  prismatic, 334
  rectangular, 334
Sturman, G. M., 65
Subframe, 391, 392
Superplasticizers, 39, 52
Support conditions, 398
Sustainable development, 40
Svab, L. E., 646
Systems, building, 613
Szerszen, M. M., 26, 27

T

T beams, 108
  effective flange width, 108
  maximum steel ratio, 111
  proportions, 112
  strength analysis, 109
T joints, 377
Talbot, A. N., 587
Tanks, 8
Tasuji, M. E., 65
Taylor, P. J., 491
Taylor, R., 517
Temperature reinforcement in slabs, 429
Tension
  axial, 25
  strength of concrete, 46
  ties, 332, 335, 345
Tension-controlled sections, 84, 753
Terzaghi, K., 587, 611
Thermal coefficient
  of concrete, 52
  of steel, 54
Thermal deflections, 232
Tholen, M. L., 207
Thompson, J. N., 207
Thompson, M. K., 208
Thornburn, T. H., 587, 611
Thurlimann, B., 258
Ties
  anchorage for, 341
  column, 265
  strength of, 345
  with struts, 335, 345
Timoshenko, S., 327, 555
Torsion, 241
  ACI Code provisions, 250
  compatibility, 241, 251
  cracking torque, 244
  equilibrium, 241, 251
  minimal, 251
  in plain concrete, 242
  plus shear, 249

  primary, 241, 251
  in reinforced concrete, 245
  reinforcement, 252
  secondary, 241, 251
  space truss analogy, 244, 247
  thin-walled tube analogy, 244
Transfer length in prestressed beams, 701
Transformed section
  for beams, 74
  for columns, 23, 264
Transmission of column loads through floors, 293
Treece, R. A., 208
Troxel, G. E., 64
Truss models, 338
  brackets, 380
  joint design, 371
  shear design, 152
Two-way edge-supported slabs
  behavior, 432
  reinforcement for flexure, 435

U

Uang, C. M., 421
Ultimate strain of concrete, 76
Uncracked elastic section analysis, 72
Underreinforced beams, 83
Upper bound theorem, 500
Uribe, C. M., 356
Utku, S., 409

V

Valley, M., 338
Vanderbilt, M. D., 491
Variable angle truss model, 152, 247
Variable depth beam shear, 150
Vecchio, F. J., 165
Virtual work analysis of slabs, 506

W

Wall footings, 563
Walls
  building, 628
  precast, 632
  retaining, 589
  seismic, 739
  shear, 628, 739
Walters, D. B., 491
Wang, P. T., 64
Water-cement ratio, 29, 31, 32
Water-cementitious material ratio, 40
Watstein, D., 207
Web reinforcement, 131
  anchorage, 189
  design of, 139, 140, 142
  inclined, 135
  minimum, 139
  vertical, 133
Welded wire reinforcement, 61
  development and anchorage, 190
Whiting, D., 65
Whitney, C. S., 115
Wide-beam joints, 369
Wight, J. K., 165, 356
Winter, G., 26, 65, 238, 356
Woinowsky-Krieger, S., 555
Wollman, G. 711
Wood, B. R., 328
Wood, R. H., 517, 555
Workman, E. B., 711

Y

Yamazaki, J., 491
Yield line analysis, 497
  corner effects, 513
  edge effects, 513
  equilibrium method, 504
  fans at concentrated loads, 515
  limitations, 516
  location of yield lines, 500
  skewed yield lines, 511
  virtual work method, 506
Young, J. F., 64
Yu, W. W., 238

Z

Zaslavsky, A., 517
Zia, P., 711
Ziehl, M., 208
Ziemian, R. D., 421
Zsutty, T. C., 165
Zuo, J., 64, 207, 208